

SPRINGER
REFERENCE

Franz J. Dahlkamp

Uranium Deposits of the World

Asia

Uranium Deposits of the World
Asia

Franz J. Dahlkamp

Uranium Deposits of the World

Asia

With 192 Figures and 28 Tables

Franz J. Dahlkamp
Oelbergstr. 10
53343 Wachtberg b. Bonn
Germany

A C.I.P. Catalog record for this book is available from the Library of Congress

ISBN: 978-3-540-78557-6

The entire set of four volumes is available under the following:

Print ISBN 978-3-540-78559-0

Electronic ISBN 978-3-540-78560-6

Print and electronic bundle ISBN 978-3-540-78556-9

This work is subject to copyright. All rights are reserved, whether the whole or part of the material is concerned, specifically the rights of translation, reprinting, reuse of illustrations, recitation, broadcasting, reproduction on microfilms or in other ways, and storage in data banks. Duplication of this publication or parts thereof is only permitted under the provisions of the German Copyright Law of September 9, 1965, in its current version, and permission for use must always be obtained from Springer-Verlag. Violations are liable for prosecution under the German Copyright Law.

© Springer-Verlag Berlin Heidelberg 2009

The use of registered names, trademarks, etc. in this publication does not imply, even in the absence of a specific statement, that such names are exempt from the relevant protective laws and regulations and therefore free for general use.

Springer is part of Springer Science+Business Media

springer.com

Printed on acid-free paper

SPIN: 11782711 2109 — 5 4 3 2 1 0

Acknowledgments

The author wishes to acknowledge the contributions of his many associates in the uranium industry, national and international institutions, and universities whose ideas, observations, and data through the years have directly or indirectly become a part of this report. Many of them are included in the list of selected references, but there are additional many more who contributed during discussions, field trips, and mine visits.

More specifically, the author is deeply indebted to those who gave freely of their time in the compilation and translation of data, and preparing and editing the manuscript, particularly A.V. Boitsov, Zhou Weixun, and T.C. Pool. Without the generous support by Alexander V. Boitsov and Zhou Weixun who spent their time over many years in selecting and translating literature on uranium deposits in Russia and all other CIS countries, and China, respectively, it would not have been possible to compile a presentation as comprehensive as given in this volume. Thomas C. Pool deserves my particular gratitude for undertaking the laborious and irksome endeavor to read, revise, and improve the entire text.

The author also is highly appreciative to the following individuals for discussions, providing information, reviewing and improving descriptions of individual deposits or districts: F. Barthel, J.R. Blaise, V.E. Boitsov, P. Bruneton, V.I. Kazansky, G. Ruhrmann, and M. Tauchid. Alexander V. Boitsov, Patrice Bruneton, Warren Finch, Jay McMurray, and Zhou Weixun critically assisted in refining the classification scheme or parts thereof for which they deserve my sincere gratitude. The contributions and comments of all these colleagues substantially improved the report, but may not necessarily endorse its contents.

A. Stasch and S. Kirchhofer skillfully prepared most figures of the manuscript.



Preface

An important prerequisite to the long-term use of nuclear energy is information on uranium ore deposits from which uranium can be economically exploited. Hence the basic purpose of this book is to present an overview of uranium geology, data characteristic for uranium districts and deposits in Asia, and a synthesis of these and additional data from uranium deposits worldwide in the form of a typological classification of uranium deposits. An additional goal is to provide access for the interested reader to the voluminous literature on uranium geology. Therefore a register of bibliography as global as possible, extending beyond the immediate need for this book, is provided.

The original concept of this work, which was to provide an encyclopedia of uranium deposits of the world in a single publication was soon doomed. The material grew out of all feasible proportions for a book of acceptable size and price as a wealth of data on uranium geology and related geosciences too vast for one volume became available during the past decades. So the original idea had to be abandoned in favor of a four- or five-volume publication covering the five continents. Each volume contains presentations of individual uranium districts, deposits and noteworthy occurrences organized by countries. For the sake of the comprehensiveness, not all the information could be distributed without some repetition.

These volumes were not originally designed as a product for its own sake. They evolved as a by-product during decades of active uranium exploration and were compiled thanks to a request by the Springer Publishing Company. Numerous publications as well as routine research work on identifying characteristic features and recognition criteria of uranium deposits, combined with associated modelling of types of deposits for reapplication in exploration, provided the data bank.

Finally, it was not so much the author's intention to present data and his own views on uranium geology and metallogenesis, but theories and models of other geoscientists who worked on any given deposit, in order to stimulate and encourage further research to achieve continuous progress in the understanding of uranium deposits and their metallogenesis.

Franz J. Dahlkamp



Table of Contents

Acknowledgments	v
Preface	vii
Remarks, Definitions, Units	xi
Part I Typology of Uranium Deposits	3
Part II Uranium in Asia – Overview	29
Chapter 1 China, Peoples Republic of.	31
Chapter 2 India	157
Chapter 3 Indonesia.	175
Chapter 4 Iran, Islamic Republic	177
Chapter 5 Japan	181
Chapter 6 Kazakhstan	191
Chapter 7 Kyrgyzstan	269
Chapter 8 Mongolia.	285
Chapter 9 Pakistan	313
Chapter 10 Russian Federation, Asian Territory.	321
Chapter 11 South Korea	391
Chapter 12 Tajikistan	393
Chapter 13 Turkey.	395
Chapter 14 Turkmenistan	397
Chapter 15 Uzbekistan	401
Chapter 16 Vietnam.	449
Chapter 17 Middle East Countries with Uraniferous Phosphorite	451
Bibliography.	453
Subject Index	469
Geographical Index.	481
U Minerals Index	493



Remarks, Definitions, Units

Organization of the Volume

The focus of this volume is on the characterization of uranium deposits in Asia presented in Part II. In spite of this emphasis, an abbreviated typology of uranium deposits on a worldwide basis was included as Part I, which describes the principal geological features, recognition criteria, and dimensions of identified types of deposits. This amendment was considered justified insofar as numerous publications and knowledge have become available since the publication of "Uranium Ore Deposits" (Dahlkamp 1993), which required a modification of some former views and hence an updating of the previous typology scheme.

Part II contains synoptic descriptions of uranium districts and deposits in Asian countries including metallogenetic concepts based on data and views of geoscientists who have actually worked on these deposits, which are not necessarily congruent with interpretations and definitions presented in Part I. Graphic presentations and tables had to be limited to the extent considered necessary to illustrate the principles of geological setting and configuration of deposits. However, quantity and quality of illustrations are variable depending on the availability and reliability of data in the source material.

Confidence of Data

Not all deposits are well researched and, on some, research data were not available. Some data are vague, if not biased or wrong. Other data are presented ambiguously, being easily misinterpreted. Interpretation of certain criteria may likewise be conflicting. Descriptions of the same district or deposit or specific features thereof by different authors are not necessarily unanimous and sometimes confusing, which, in some instances, may be due to the translation quality of the original text. Due to former and partly still existing secrecy conditions, in some former East Block countries (e.g. China and some CIS countries) published data particularly of resource and grade figures are not always congruent. In a number of cases resource figures do not coincide with independent calculations or are only given in a general way.

Concerning uranium metallogenesis, its principles are at present sufficiently well understood only for some types of deposits, whereas other types are understood to a lesser extent and in varying degrees and therefore permit space for speculation or geofantasy.

The attempt was made to reconcile conflicting data and deviating hypotheses as far as possible in order to give at least an idea of the overall geological situation and size of a district or deposit. It has to be admitted, however, that this demanding task was not always satisfactorily achieved. In any event, the various views are presented and in case the reader requires more precise information, the original literature should be reviewed or the original author(s) should be contacted for additional data.

Citing of Authors

All the country chapters include a reference list of authors whose data have been used directly or indirectly or who have contributed work to the country, district or deposit described in that particular chapter. This scheme was selected

- a to serve as a reference index on literature pertaining to the respective country, district or deposit. The list is restricted to respective principal uranium papers and to contributions to general geology with relevant or possible implications on uranium geology. Special publications not directly related to uranium geology, e.g., age dating of rocks, are cited in the text (titles of the papers can be found listed according to the author's name in the Bibliography);
- b to credit authors who have worked on the given district or deposit;
- c to reduce the immense repetition of authors' names to a bearable minimum within the text. In this kind of synoptically presentation, often using numerous papers on one single district or deposit, a complete citation of all authors would in many instances have required a list of names after a couple of sentences or a short section. Alternatively, numbers referring to authors and their papers could have been used. My preference is, however, to see the name of an author and not a colorless number, which, in addition, requires searching in the bibliography for the numbered individual. Although the selected system may not satisfy all authors who wish to see their names precisely repeated, they may forgive me for the sake of easier reading.

Bibliography

This section is organized in alphabetical order of authors and provides complete coverage of papers cited in the text and reference lists. Papers published since the final revision of the manuscript have been added in the bibliography but, for technical reasons, could be incorporated into the standing manuscript only in exceptional cases.

The attempt was made to provide a bibliography as complete as possible, but some papers will still be missing. This deficiency does not reflect my disregard of the respective contribution, but should rather be excused as an imperfection on my side. Proceedings of workshops, symposia, etc. were in many instances not published until several years later. Meanwhile, some authors had published the workshop data elsewhere or the data had been disseminated otherwise and hence the material may have had influenced and may have found access to publications of other workers prior to the printing of the original presentation. Consequently, publication years of reference data do not necessarily reflect the first presentation of results.

Geological, Mineralogical, Mining, and Related Terms

Connotation and spelling of geological and mineralogical terms are, in principle, understood as and based on those given by: Thrush and the Staff of the Bureau of Mines (eds), 1968, in "A Dictionary of Mining, Mineral, and Related Terms", U.S. Dept. of the Interior Washington, DC. Exceptions or additions to this are:

Clarke value (= background value): Mean content of a chemical element in the Earth's crust as a whole or in its particular segments and specific rocks (e.g. for granite).

Costs, expenditures: In U.S.\$ unless otherwise stated.

Deposit: This term is not restricted to economic U deposits but used in a broader sense to signify all U concentrations with U tenors distinctly elevated above common background U values of a corresponding (host) rock type.

Granite/granitoid, pegmatite/pegmatoid, etc.: The terms are used synonymously and not in their strict genetic sense. Various authors apply both words differently and the connotation is not always clear.

Mineralization, alteration, etc.: These terms are used in both connotations, to denote the process implied and the product of the process.

Monometallic mineralization/mineralogy (simple mineralization/ mineralogy): Denotes ore containing U only as recoverable element, although many other metals may be present but in trace or subeconomic quantities.

Polymetallic mineralization/polymetallic mineralogy (corresponds to complex mineralization/mineralogy of some authors): Denotes ore containing at least two different metals including U in economic or potentially economic amounts.

Uraninite/pitchblende: In this book *uraninite* is used for the macrocrystalline, more or less euhedral variety of UO_{2+x} , which typically occurs in rocks of higher P-T metamorphic grades (amphibolite grade and higher, contact-metamorphic), igneous rocks such as granite and pegmatite but also in vein and veinlike-type deposits.

Pitchblende is used for UO_{2+x} varieties of micro- or crypto-crystalline, colloform (colloformous, botryoidal, spherulitic) habit, which typically occur in low grade metamorphic and non-metamorphic rocks such as greenschist facies metasediments and more or less arenaceous sediments, and in most vein- and veinlike-type uranium deposits. It is understood that both varieties crystallize in the same crystallographic system, the cubic system, but have certain discriminating physico-chemical properties (for details see Fritsche et al. 1988, 2001 and Ramdohr 1980).

The term pitchblende was the first name used for black uranium oxide minerals back in 1565 and is widely used, particularly in Europe. Uraninite is a term commonly used for all kinds of uranium oxides in American literature. Worldwide, both terms are applied by a number of authors variably and in an overlapping way. The criteria used by various geoscientists to differentiate between uraninite and pitchblende are sometimes conflicting and can lead to confusion.

Secondary uranium minerals: This term, commonly referring to colored U minerals, was abandoned in favor of *hexavalent U (U^{6+}) minerals* to avoid confusion. "Secondary U minerals" are of primary origin in several deposits, e.g., in surficial deposits. Both terms, primary and secondary, have been restricted in this book to their strict genetic sense denoting primary or secondary origin of a given mineral.

Ore: Synonymous with (potentially) minable mineralization.

Regolith: refers to saprolite/paleosol. It is not used in the sense often applied in Canada, where weathered rocks are also called regolith. Herein, the term regolithic rock is preferred.

Resource/reserves, production, and grade figures are calculated in metric tons (t or tonnes) U and percent (%) U (respectively in ppm U for low grade values) and represent published data or best estimates based on published data and personal communication.

Terms Commonly Used in Russian Literature

Beresite: A metasomatic rock composed of quartz, sericite, carbonate, and pyrite.

Beresitization: A variety of phyllic alteration. This term as well as beresite originated from the Berezovskoye Au deposit in the Urals, Russia.

Geochemical specialization of rocks: Refers to a given rock or complex that contains a systematically higher content of one or more elements relative to other rocks or to the same rock occurring elsewhere.

Nenadkevite: Hydrous U, Th, REE silicate.

Rare metals: This term does not seem to be strictly defined. In a general way, a rare metal does not belong to ferrous, noble, base, or radioactive metals. In Russian publications Mo, Sn, W, Nb, Li, and other elements are commonly attributed to rare metals although they are not necessarily rare in nature.

Terminology of U Resources

OECD-NEA/IAEA replaced several of the category terms of resources in the 2005 Red Book, which they had used in their biannual Red Books through 2003. In this volume, the former terms were maintained in order to avoid a complete revision of the manuscript. For comparison, Table 0.1 provides a listing of the former and new resources terminology of OECD-NEA/IAEA combined with more or less equivalent categories used in several countries.

Resource/reserve definitions with respect to confidence classes and cost categories of an ore deposit cannot be achieved from purely geological parameters. Economic considerations have to be included. Demand for the commodity and related price/cost factors dictate whether a localized metal concentration is a deposit that can be profitably exploited presently or in the future, or whether it is a mineral occurrence of only scientific or academic interest. OECD-NEA/IAEA have accordingly established a cost category system that subdivides the various confidence resource classes into resources recoverable at <U.S.\$130 per kg U, <U.S.\$80 per kg U, and <U.S.\$40 per kg U, which was used as far as data were available.

Table 0.1.

Approximate correlation of terms used in resources classification systems of OECD-NEA/IAEA until 2003 and in 2005, and selected countries. (Note: The terms listed are not strictly comparable as the criteria used in the various systems are not identical. "Grey zones" in correlation are therefore unavoidable, particularly as the resources become less assured. Nonetheless, the chart presents a reasonable approximation of the comparability of terms.) (After OECD-NEA/IAEA 2005) (CIS: Russian Federation, Kazakhstan, Ukraine, Uzbekistan, etc., UNFC: United Nations International Framework Classification for Reserves/Resources-Solid Fuels and Mineral Commodities)

	Identified resources (known conventional resources)		Undiscovered resources (Undiscovered conventional resources)			
OECD-NEA/IAEA 2005 (OECD-NEA/IAEA <2003)	Reasonably assured (RAR)		Inferred (EAR-I)	Prognosticated (EAR-II)	Speculative (speculative)	
Australia	Demonstrated		Inferred	Undiscovered		
	Measured	Indicated				
Canada (NRCan)	Measured	Indicated	Inferred	Prognosticated	Speculative	
United States (DOE)	Reasonably assured		Estimated additional		Speculative	
CIS	A + B	C1	C2	P1	P2	P3
UNFC	G1		G1 + G2	G3	G4	

National Resource Data

In this book, national resource data were taken from the biannual OECD-NEA/IAEA Red Books. It should be noted, however, that national resource figures published in the Red Books are provided by government agencies. Some of these national authorities occasionally underestimate the real recovery costs. Therefore some of the national resource figures appear in, and consequently inflate to a certain extent, lower cost resource categories of the Red Book tables. On the other hand, changes in the market price of uranium may increase or decrease the figure of established economic resource quantities.

Terminology of Resources for Individual Deposits

Available resource figures for individual deposits or districts do not necessarily correspond to the OECD-NEA/IAEA nomenclature and categories since mining companies have not necessarily applied the terminology suggested by OECD-NEA/IAEA, or their published figures are not attributed to one or the other category. Hence in many cases it remains unclear whether in situ (geological) or recoverable (mining) reserves/resources are given, i.e., whether or not mining dilution and milling losses are included, whether the numbers refer to RAR to EAR categories or to any other equivalent category of reserves/resources (e.g., proven, probable, or possible reserves). Mining dilution can reduce recoverable reserves to less than 75% of the in situ tonnage and can downgrade the ore mined to 85% or less of the in situ grade. In addition, the cutoff grade for reserve/resource calculations are not always given. Depending on the cutoff grade used, reserve/resource figures can augment or decrease.

For this reason reserve, resource, and grade figures given for individual deposits or districts are, except for verifiable figures, best estimates of, but not always, in situ tonnages and grades based on various, not necessarily published, information. Also, the terms reserves and resources are not used in this volume in their strict sense but more synonymously. This means that, independent of their status of confidence, no great distinction is made between the terms “resources” (except for being used in rather undefined or not clearly defined cases) and “reserves” [more restricted to clearly defined (potentially) economic resources].

Abbreviations

a.o.	among others or and others
a.s.l.	above sea level
Ba (b.y.)	billion years = 1 000 Ma
EAR	estimated additional resources
ISL	In situ leaching method (also referred to as ISR In situ recovery method)
lb.	pound (7 000 grains = 16 ounces = 451 grams)
Ma (m.y.)	million years
RAR	reasonably assured resources
redox	reduction-oxidation (boundary)
REE	rare earth elements
sh.t.	short ton
t	metric ton(s) (tonnes)
U_{eq}	equivalent uranium measured by geophysics
U_{met}	metallic uranium or natural uranium

Conversion Factors

1 t	=	1	metric ton
1 t	=	1.1023 sh.t.	= 2 200 lbs
1 t U	=	1.18 t U ₃ O ₈	
1 t U	=	1.30 sh.t. U ₃ O ₈	= 2 600 lbs U ₃ O ₈
1 t U ₃ O ₈	=	0.848 t U	
1 t U ₃ O ₈	=	1.1 sh.t. U ₃ O ₈	= 2 200 lbs U ₃ O ₈
1 sh.t. U ₃ O ₈	=	0.769 t U	
1 sh.t. U ₃ O ₈	=	2 000 lbs U ₃ O ₈	
1% U ₃ O ₈	=	0.848% U	
1 \$/lb U ₃ O ₈	=	2.6 \$/kg U	
1 \$/kg U	=	0.3824 \$/lb	

Table of Contents

Acknowledgments	v
Preface	vii
Remarks, Definitions, Units	xi
Part I Typology of Uranium Deposits	3
Part II Uranium in Asia – Overview	29
Chapter 1 China, Peoples Republic of.	31
Chapter 2 India	157
Chapter 3 Indonesia.	175
Chapter 4 Iran, Islamic Republic	177
Chapter 5 Japan	181
Chapter 6 Kazakhstan	191
Chapter 7 Kyrgyzstan	269
Chapter 8 Mongolia.	285
Chapter 9 Pakistan	313
Chapter 10 Russian Federation, Asian Territory.	321
Chapter 11 South Korea	391
Chapter 12 Tajikistan	393
Chapter 13 Turkey.	395
Chapter 14 Turkmenistan	397
Chapter 15 Uzbekistan	401
Chapter 16 Vietnam.	449
Chapter 17 Middle East Countries with Uraniferous Phosphorite	451
Bibliography.	453
Subject Index	469
Geographical Index.	481
U Minerals Index	493

Part I



Typology of Uranium Deposits

Introduction

A variety of global and regional classification schemes for uranium deposits have been proposed in the past by a number of geoscientists including Heinrich (1958), Roubault (1958), Ruzicka (1971), Ziegler (1974), Mickle and Mathews (1978), Mathews et al. (1979), Nash et al. (1981), Barthel et al. (1986), Dahlkamp (1989, 1993), McKay and Miezitis (2001) mainly for deposits in the western hemisphere and by Kazansky and Laverov (1977), Boitsov (1989, 1996), Stoikov and Bojkov (1991), Petrov et al. (1995, 2000), Mashkovtsev et al. (1997), Terentiev and Naumov (1997), and others for deposits in CIS (former Soviet Union) and associated countries.

Although these classification schemes remain largely valid, more recent information on uranium deposits, particularly in the former eastern block countries and new research data on earlier established and defined types of uranium deposits justify a rearrangement and refinement of the classification scheme, which is presented further below in abbreviated form.

The classification chapter is not restricted to types of economic deposits but includes types with marginal to no economic potential as well. Knowledge of these types are thought to be equally important as economic types, particularly in exploration, in order to recognize and understand criteria typical for subeconomic mineralization ranging in size from small mineralogical showings to almost economic occurrences in order to comprehend somewhat similar economic deposits and their parameters.

While many authors in the western hemisphere prefer a descriptive, typological classification with emphasis on geological setting and ore characteristics, authors of the CIS (former Soviet Union) and associated countries as well as China based their deposit classification systems primarily on metallogenetic aspects (unfortunately often without furnishing type examples of deposits, which hampers the matching of deposit types of the two systems).

In many cases, however, open questions still remain with respect to the specific provenance of (1) ore forming uranium and related solutions, (2) conditions of uranium mobilization, transport, and redeposition, and (3) repetitive redistribution. For these academic as well as practical reasons such as exploration, a typology based primarily on descriptive data has been given preference in order to provide a synopsis of principal criteria of deposit types to the benefit of economic geologists. The criteria may serve to determine target types in virgin regions and also to evaluate the economic significance of interim exploration results through correlation with established U districts and/or deposits.

The terminology selected for types and subtypes refers primarily to the host environment or geotectonic setting of the discussed type. On this basis, twenty principal types of uranium

deposits are distinguished. They include some forty subtypes and classes. Subtypes and classes have certain mutual parameters permitting their attribution to a specific type, but they also exhibit distinctive features justifying an individual status.

Each type is introduced by a *type definition*, followed by *principal characteristics of subtypes* and *prominent classes*. Inevitably, this kind of organization involves overlap and repetition, which is considered minor in order to achieve a better type- and subtype-related comprehension and precision as well as avoidance of confusion. Metallogenetic aspects have not been addressed and the reader is referred to respective synoptic descriptions in Dahlkamp (1993) and publications by other authors or to the documentation of individual districts and deposits presented in this volume.

The description also includes selected references, though not exclusively, of authors who reviewed comprehensively the given type of deposit or districts thereof and list extensive bibliographies for further reference, or of authors describing in detail a specific deposit taken as type example.

Illustrations (► Figs. I.1–I.20) are added to furnish schematic presentations of the geological setting of the various types, subtypes, and classes of deposits.

Finally, definitions and type descriptions offered by the author in this chapter are his own interpretations, though strongly influenced by discussions with many colleagues, of data collected in the field and from pertinent literature study, but they must not necessarily represent the final and correct version. The reader is therefore strongly encouraged to study the literature cited as references to form his own opinion, which may be contrary to the one presented here.

Definitions

Deposit: In the following classification scheme this term is not restricted to economic U deposits but in a broader sense to signify all U concentrations with U tenors distinctly elevated above common background U values of a corresponding (host) rock type.

Resources of deposits: small = <5 000 t U; medium = 5 000–20 000 t U, large = >20 000 t U. *Ore grades* (given as average of deposits): low = <0.15% U, medium = 0.15–0.5% U, high = >0.5% U.

Resource, production, and grade figures of type examples are best estimates based on published data and personal communication.

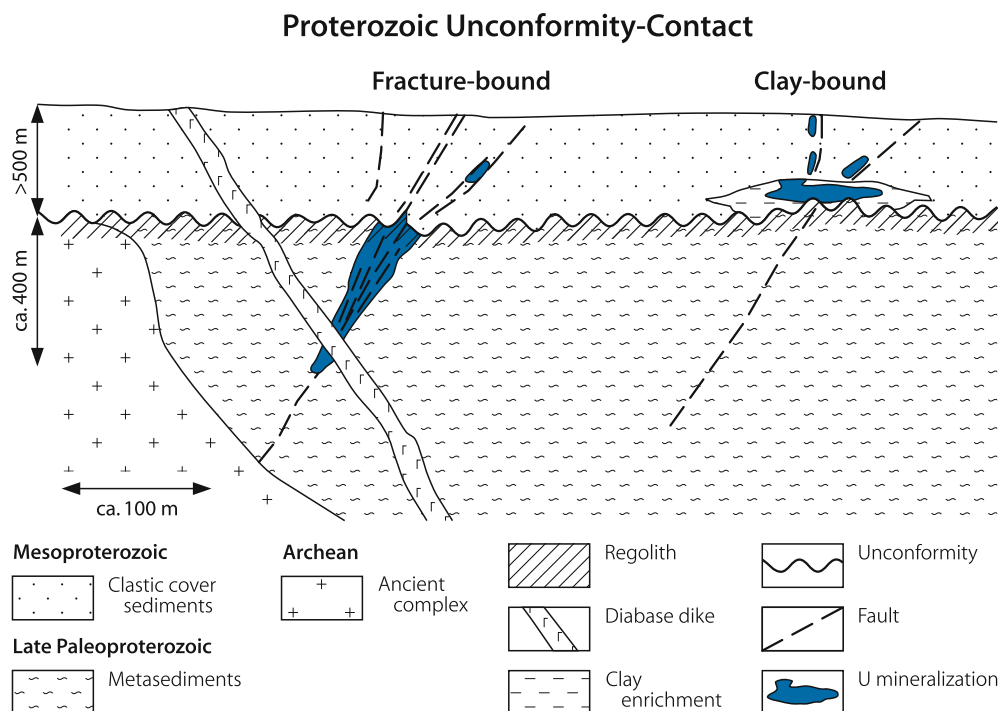
For more information see Sect. *Geological, Mineralogical, Mining, and Related Terms*.

Remarks

The formerly used “Vein Type” (which referred to granite-related and undifferentiated deposits) was abandoned as a principal deposit type since it causes confusion with other deposit types.

■ Fig. I.1.

U-deposit Type 1: unconformity-contact U deposits



Veins are not only associated with granites but also with volcanics or metasomatites, and they also occur in metasediments and sediments without any obvious link to a magmatic or metasomatic complex. Taking this into account, the term “vein” is now only used to describe the configuration of ore bodies in any respective geological environment as known from deposits grouped in types 4 to 7.

The term vein as used in types 4 to 7 deposits refers to true or classical veins composed of ore and gangue minerals that occur in the form of linear lenses, pockets, or disseminations in fissures, breccias, and stockworks in fractured rocks. Size and complexity of vein sets are variable. Distribution and intensity of mineralization are unpredictable. The bulk of vein material consists mainly of gangue while ore shoots occupy only from few percent to rarely 50% of the vein structure.

Principal uranium phases include pitchblende, uraninite, coffinite and/or alteration products thereof. Gangue minerals consist predominantly of quartz and/or carbonates. Uranium mineralization can be monometallic (without economic byproducts) or polymetallic (with at least one other metal as economic byproduct). The latter mainly includes Co, Ni, Bi, Ag, Cu, Pb, Zn, and/or Mo in the form of sulfides, arsenides, or sulfo-arsenides. Fe-sulfides or Fe-(hydro)-oxides are always present. Ore-related wall rock alteration is commonly restricted to a narrow margin (<1 m).

Type 1 Unconformity-Contact U Deposits (Fig. I.1)

Unconformity-contact deposits occur at and immediately above and below an unconformable contact that separates a crystalline

basement intensely altered by lateritic paleoweathering from overlying redbed-type sediments. All major deposits are of *Mesoproterozoic* age and represented by deposits in the Athabasca region, Canada. Some minor *Phanerozoic* deposits such as Le Roube are known from the southwestern Massif Central, France.

Subtype 1.1 Proterozoic Unconformity-Contact U Deposits (Athabasca Type)

Proterozoic unconformity-contact U deposits occur in a terrane of Lower Proterozoic metasediments with intercalated graphitic horizons that mantle Archean granite-gneiss domes. Middle Mesoproterozoic redbed-type arenaceous sediments rest upon this basement. The basement exhibits intense lateritic paleoweathering, and basement and overlying rocks show strong alteration effects associated with mineralized zones. Two varieties of deposits are known: (a) Clay-bound immediately overlying and (b) fracture-bound below the unconformity. Principal U minerals in both classes are pitchblende, uraninite, coffinite, minor brannerite, and some amorphous uranium-carbon material (carburan).

References general: Dahlkamp 1993; Jefferson et al. 2007; Jefferson and Delaney et al. 2007; Fogwill 1985; Hoeve and Quirt 1984; IAEA/Ferguson (ed) 1984; IAEA/UDEPO 2007; Lainé et al. (eds) 1985; Roy et al. 2006; Sibbald 1988; Sibbald and Petruk (eds) 1985; Sibbald and Quirt 1989; Thomas et al. 2000; Tremblay 1982.

a Clay-Bound

Clay-bound deposits are associated with massive clay and occur directly upon the Mesoproterozoic unconformity. Mineralization is commonly polymetallic composed of U with sulfides, arsenides, sulfo-arsenides, locally selenides and tellurides of Ni, Pb, and other metals; gangue minerals are mainly quartz and carbonates. The ore minerals range from disseminated to often massive in tabular to lenticular horizontal ore bodies in clay and argillic sandstone. Some mineralization extends along fractures into overlying sandstone and underlying metasediments. Resources range from small to very large and grades are very high (few 100 to >200 000 t U; 1–20% U).

Type examples: (a) Cigar Lake, Athabasca Basin, Canada (Resources: 135 000 t U, 15.3% U). *References:* Bruneton 1987, 1993; Fouques et al. 1986; (b) Key Lake, Athabasca Basin, Canada (Production 73 900 t U, 2.0% U). *References:* Ruhrmann 1986.

b Fracture-Bound

Fracture-bound deposits are hosted in metasediments immediately below the Mesoproterozoic unconformity. Mineralization is dominantly monometallic and occurs disseminated to massive in structures within Lower Proterozoic metasediments. Depths extension can be in excess of 400 m below the unconformity. Resources range from small to large and grades from medium to (rarely) high (few tens to 25 000 t U; 0.15–2% U).

Type example: Eagle Point, Athabasca Basin, Canada (Resources + Production: ~24 000 t U, 1.2% U). *References:* Eldorado Resources Ltd. 1987; Heine 1986.

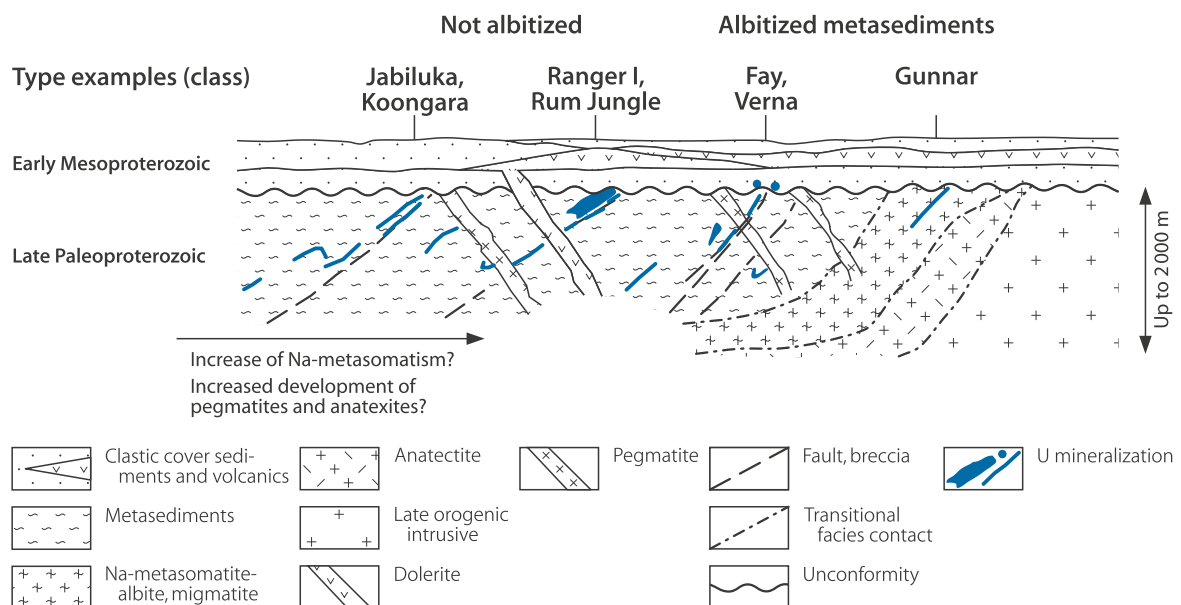
Subtype 1.2 Phanerozoic Unconformity U Deposits (Le Roubé Type)

Type examples are known from the SW Massif Central, France, in an environment of Permo-Carboniferous clastic sediments with some volcanic components resting upon the post-Hercynian unconformity on altered Upper Proterozoic to Lower Paleozoic schists and gneisses containing minor graphitic horizons. Host rocks exhibit various alteration phenomena including variable redox conditions in the cover sediments. U minerals occur as disseminations and fine veinlets forming small ore bodies along the post-Hercynian unconformity most commonly where the unconformity is transected by faults. Resources are small and grades low (few tens to ca. 2 000 t U, 0.1–0.15% U).

Type example: Le Roubé/Brousse-Broquiès Basin, Massif Central, France (Resources: ~2 000 t U, 0.1–0.15% U). *References:* George 1985; Schmitt and Clement 1986. (Remark: Although of minor economic significance, these deposits tend to indicate that unconformity related deposits could have formed at any time as long as the litho-stratigraphy, geotectonic, geochemical, and paleoclimatic conditions permitted the evolution of ore forming processes as known from the Athabasca region.)

Fig. I.2.

U-deposit Type 2: Proterozoic subunconformity-epimetamorphic U deposits Strata-structure bound in Late Paleoproterozoic metasediments (Alligator Rivers type)



Type 2 Proterozoic Subunconformity- Epimetamorphic U Deposits (Alligator Rivers Type) (Fig. I.2)

Deposits in the Alligator Rivers ore field, Australia, which provide the type example, are strata-structure bound in Paleoproterozoic metasediments. They abut against a Late Paleoproterozoic unconformity upon which clastic sediments rest (Kombolgie Formation). Mineralization is monometallic composed of pitchblende, uraninite, minor coffinite, brannerite, locally thucholite, associated with some Fe-, Pb-, Cu-sulfides and traces of other metals; hematite is relatively common. Gangue minerals include chlorite, quartz, sericite, and minor carbonates. The ore minerals occur as relatively continuous, peneconcordant, strata-bound fracture and breccia filling within distinct Lower Proterozoic metasediment horizons. Migmatitic-granitic complexes occur nearby. Wall rocks are strongly altered. In contrast to the Athabasca deposits (Type 1), deposits in the Alligator Rivers ore field occur under a Late Paleoproterozoic unconformity, and the basement was only moderately affected by paleoweathering. Deposits have large resources and low to medium grades.

Type example: Jabiluka/Alligator Rivers ore field, NT, Australia (Resources: 173 000 t U, 0.33% U). *References:* Binns et al. 1980; Ewers and Ferguson 1980; Ferguson and Goleby (eds) 1980; Hancock et al. 1990; Hegge et al. 1980; IAEA/Ferguson (ed) 1984; IAEA/UDEPO 2007; McKay and Miezitis 2001; Needham et al. 1988; Polito et al. 2005; Wilde 1988. (Note: Deposits in the Beaverlodge District, Saskatchewan, Canada, exhibit to some extent a similar geotectonic setting as deposits in the Alligator Rivers ore field. They also abut against a Late Paleoproterozoic unconformity and the basement was also only mildly affected by paleoweathering. The major difference is their distinct vein-type configuration and their lithological setting; they are hosted in albitized metasediments. As such, the Beaverlodge veins may be considered a subtype of subunconformity-epimetamorphic deposits but they may also

be attributed to undifferentiated (meta-)sediment hosted U vein deposits/Type 7.)

Type 3 Sandstone U Deposits (Fig. I.3)

Sandstone uranium deposits are confined to continental fluvial or marginal marine (mixed fluvial-marine) environments. Uranium occurs disseminated in reduced sandstones (\pm arkosic) that are mostly flat-lying ($<5^\circ$) unless affected by post-ore tilting and are interbedded with and bounded by less permeable sediments. Impermeable shale/mudstone units often overlie and underlie mineralized sandstone beds. Tuffaceous sediments may be (particularly at better grade deposits) but not always interbedded in the stratigraphic column.

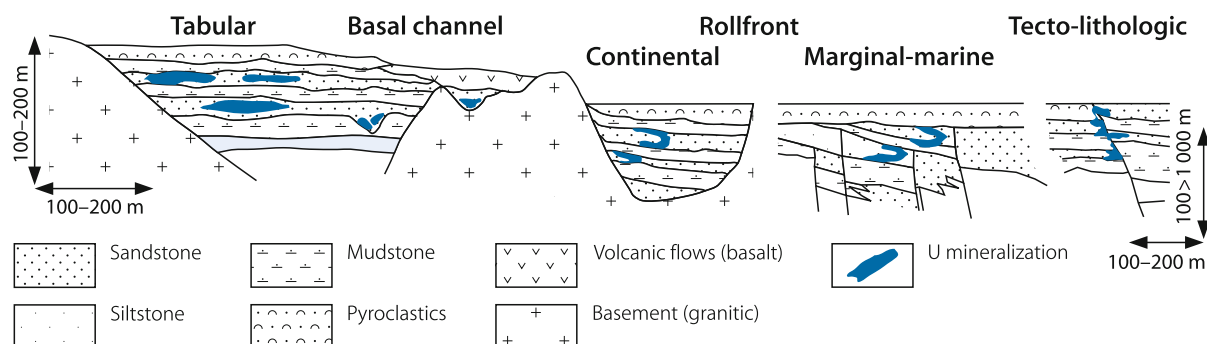
U precipitated most frequently at redox interfaces or by interaction with metals. Primary uranium minerals are generally of tetravalent U phases and consist dominantly of pitchblende and coffinite. Reducing conditions were provided by a variety of reducing agents including carbonaceous material (detrital plant debris, amorphous humate, marine algae), sulfides (pyrite, H_2S), hydrocarbons (petroleum, gas), and possibly intercalated mafic/ferro-magnesian minerals (e.g. chlorite). A distinction is made between *Phanerozoic* (post-Devonian) deposits (Ph) associated with terrestrial plant derived organics and (*b*) *Proterozoic* deposits (Pt) associated with marine, algae(?) derived organics.

Sandstone uranium deposits may be divided into four overall subtypes and further into classes that can be gradational into each other. Based on configuration and spatial relation to the depositional environment, rollfront and tabular subtypes in continental or marginal marine sediments are defined; and on distinct geomorphological setting into a basal channel subtype. In addition, the primary mineralization may be redistributed into secondary uranium "stack" ore bodies in the host sandstone defined as tectonic-lithologic subtype.

References general: Adams and Saucier 1981; Adams and Smith 1981; Granger and Finch 1988; Harshmann and Adams

Fig. I.3.

U-deposit Type 3: Sandstone U deposits, (Ph) Associated with organic material of terrestrial plant origin (Pt) Associated with organic material derived from algae



1981; IAEA (UDEPO) 2007; IAEA/Finch W (ed) 1985b; Karimov et al. 1996; Kazansky and Laverov (1977); Petrov et al. 1995; Thamm et al. 1981; Turner-Peterson et al. (eds) 1986.

Subtype 3.1 Rollfront U Deposits

(Russian terminology: *Exogenic infiltration; Strata-oxidation*)

Deposits consist of arcuate zones of uranium matrix impregnations that crosscut sandstone bedding extending from overlying to underlying less permeable horizons. The mineralized zones consist of elongate and sinuous bands approximately parallel to strata strike, and perpendicular to the direction of sedimentary deposition and groundwater flow. Redox interfaces control setting and configuration of these zones. The mineralized zones are convex down the hydrologic gradient. They exhibit diffuse boundaries with reduced sandstone on the down-gradient side and sharp contacts with oxidized sandstone on the up-gradient side (except in re-reduced sands; see *South Texas Subtype*).

Resources range from small to large and grades from low to medium (few 100 to several 1 000 t U, at grades averaging <0.05–0.25% U).

Further subdivision of rollfront deposits is based on emplacement either in intracratonic basins filled with continental alluvial/fluvial sediments or in mixed fluvial-marine sediments of coastal plains. Reductants may consist of detrital carbon, extrinsic hydrocarbons or H₂S, and/or Fe-sulfides that originated from influx of H₂S into the host sands.

a Continental Basin, U Associated with Intrinsic Reductant (Wyoming Type)

U occurs disseminated at the redox boundary at contact with detrital carbonaceous (generally plant) debris on the down-gradient side in arkosic and subarkosic sandstones deposited in intracratonic or intermontane basins in spatial proximity with rocks containing anomalous U concentrations such as tuffs or granites. Most deposits occur within interbedded sequences of fluvial sandstones and volcanic rich sediments. Up-gradient alteration is characterized by oxidation reflected by variable hematitization or bleaching whereas down-gradient sandstone is in reduced state. The shape of deposits is strongly controlled by the hydrology of the host rocks. Some deposits have long tabular limbs against overlying and/or underlying carbonaceous-rich clayey-silty sediments. Resources are small to large at medium grades (few tonnes to several 1 000 t U; 0.05–0.2% U).

Type example: Highland Mine (Cz)/Powder River Basin, Wyoming, USA (Resources + production: ~10 000 t U, 0.07–0.13% U). *References:* Crew 1981; Harshmann and Adams 1981.

b Continental to Marginal Marine, U Associated with Intrinsic Reductant (Chu-Sarysu Type)

Deposits are similar to rollfront deposits in continental basins but host lithologies correspond to a sequence of mixed continental and marginal marine origin. Resources are medium to large but grades generally low.

Type example: Inkay (Mz-Cz)/Chu-Sarysu Basin, Kazakhstan (Global resources: 330 000 t U including 55 000 t U at 0.06% U). *References:* Petrov et al. 1995.

c Marginal Marine; U Associated with Extrinsic Reductant (South Texas Type)

U is concentrated in roll-type deposits near faults and in contact with pyrite/marcasite-bearing sandstone on their down-gradient side. Sandstone on the up-gradient side of deposits is hematite and/or limonite-bearing except for certain deposits that occur totally within reduced, pyrite-bearing sandstone, which probably reflects the post-ore introduction of H₂S along faults. H₂S introduced before ore formation prepared the host for rollfront development. Host environments include point bars, lateral bars, and crevasse splays deposited in a fluvial environment, and barrier bars and offshore bars in a marine environment. Resources are small to medium and grades low to medium (<100 to several 1 000 t U; <0.05–0.25% U).

Type example: Rhodes Ranch (Cz)/McMullen County, South Texas Coastal Plains, USA (Resources + production: ~5 000 t U, 0.1–0.25% U). *References:* Adams and Smith 1981; Galloway 1985.

Subtype 3.2 Tabular/Peneconcordant U Deposits

(also referred to as *Peneconcordant* or *Blanket* deposits)

Tabular U deposits occur in extensive blanket sands formed in braided fluvial systems that unconformably overly or are eroded into underlying sedimentary or crystalline rocks. Mineralization consists of uranium matrix impregnation that generally forms irregularly shaped tabular or lenticular masses within selectively reduced sediments. The mineralized zones are, on a larger scale, oriented parallel (or peneconcordant) to the depositional trend but, on a small scale, they crosscut the bedding of the host sandstone. Uranium minerals occur as disseminations, sand grains coatings, fill of small interstices, and partial replacement of feldspar.

Further subdivision is based on uranium fixing agents such as (a) detrital plant debris or (b) amorphous organic material (e.g. humate) of intrinsic or extrinsic origin, respectively, or (c) metallic associations (e.g. vanadium) that occur in fluvial systems,

Individual deposits contain several hundreds of tonnes of U and up to 150 000 t U, at average grades ranging from 0.05 to 0.5% U, occasionally up to 1% U.

a Continental Fluvial, U Associated with Intrinsic Reductant (Arlit Type)

Tabular or lenticular U ore lodes are hosted in sediments rich in detrital carbonaceous matter (plant debris) of a continental paleoriver system composed of sandstone interbedded with claystone-shale beds. Uranium (with \pm V, Mo, Zn, and Zr) occurs as pitchblende and coffinite disseminated in reduced, pyritic sandstone and as finely disseminated argillic-organic U complexes in shale. Uranyl-vanadates prevail in oxidized zones. Resources are small to large and grades low to medium (<100 to 75 000 t U; 0.2–0.5% U).

Type example: Arlit (Pz)/Tim Mersoï Basin, Niger (Resources + production: ~60 000 t U, 0.2–0.3% U). *References:* James and Hamani 1999; Pagel et al. 2003.

b Continental Fluvial, U Associated with (Extrinsic) Humate/Bitumen (Grants Type)

U is associated with humate/bitumen derived from redistributed carbonaceous matter. Mineralization is of disseminated nature and occurs in lenses within continental sandstone. The host sandstone was deposited in a mid-fan environment within an extensive fluvial-lacustrine sedimentary system. Moderate quantities of pyroclastics are present. Sand-shale proportions are typically 3/2 to 4/1 (60–80% sandstone). Alteration includes destruction of ilmenite-magnetite and significant pyritization. Feldspar is moderately to strongly altered. Resources are medium to large and grades medium.

Type example: Ambrosia Lake District (Mz)/southern Grants Uranium Region, New Mexico, USA (Production: ~75 000 t U; 0.1–0.3% U). *References:* Adams and Saucier 1981; Granger and Finch 1988; Turner-Peterson et al. (eds) 1986.

c Continental Fluvial Vanadium-Uranium (Salt Wash Type)

U associated with vanadium ($V > U$) occurs in reduced fluvial sandstone within a sequence of continental “redbed” type sediments. This suite comprises thin but widespread units of selectively reduced sandstone with interbeds of grey clay and carbonaceous debris. The most favorable sandstones parallel an adjacent contact with red oxidized sandstone and are overlain, underlain, or interbedded with grey lacustrine clays. Altered, reduced sediments show ilmenite and magnetite destruction and significant concentrations of pyrite. U resources of

individual deposits are commonly small and U grades low to high but high vanadium contents often make these deposits viable exploitation targets (<1–2 000 t U, 12 500 t V_2O_5 ; <0.15–0.3 U, <1.5% V_2O_5).

Type example: C-JD-7 deposit (Mz)/Uravan Mineral Belt/Colorado Plateau, USA (Resources + production: 2 100 t U, 12 500 t V_2O_5 , 0.21% U, 1.25% V_2O_5). *Reference:* Thamm et al. 1981.

Subtype 3.3 Basal Channel U Deposits (Chinle Type)

(Russian terminology: *Exogenic infiltration; Valley or Paleovalley, or U-REE in erosive paleovalley*; subdivided into: (a) Valley on Plain, (b) Valley on Plateau)

Basal channel U deposits are defined by their pronounced geomorphological setting in (a) distinct fluvial paleochannels or (b) paleodrainage systems composed of bifurcating channels that are incised into unconformably underlying sedimentary or crystalline rocks. Ore hosting channels are from some 10 m to 1.5 km in width and filled with 10 m to 150 m thick permeable alluvial-fluvial sediments.

U (pitchblende, coffinite) is predominantly associated with detrital plant debris and occurs in ore bodies, which exhibit in plan view an elongated lens or ribbon-like configuration and in section a lenticular or more rarely roll shape. Resources of individual deposits are mostly small but with rare exception can reach as much as 20 000 t U. Grades range from 0.02 to 3% U.

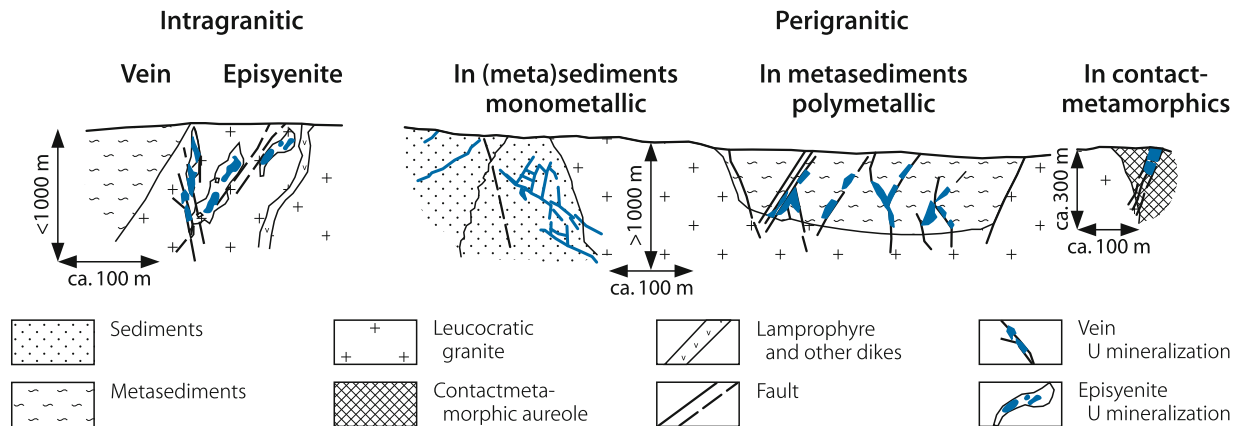
Type examples: (a) Monument Valley (Mz)/Colorado Plateau, USA (Production: 3 560 t U, 9 530 t V_2O_5 , 0.27% U, 0.94% V_2O_5). *References:* Chenoweth and Malan 1973; (b) Dalmatovskoye (Mz)/Transural (Resources 10 200 t U, 0.039% U); (c) Khiagda (Cz)/Vitim District, Russia (Resources: 15 500 t U, 0.05% U). *References:* Naumov et al. 2005; Boitsov 1999.

Subtype 3.4 Tectonic-Lithologic U Deposits

Tectonic-lithologic deposits are discordant to strata. They occur in permeable fault zones and adjacent sandstone beds in reducing environment created by hydrocarbons and/or detrital organic matter. Extrinsic uranium (liberated from sediments) may have precipitated (a) in fault zones from where it permeated tongue-like into permeable sand horizons or (b) intrinsic U was redistributed from tabular sandstone ore bodies into crosscutting faults to form locally rather thick ore bodies (termed *stack* deposits). Resources are small to medium and grades low to medium (few 100 to 10 000 t U or more, 0.1–0.4% U).

Fig. I.4.

U-deposit Type 4: granite-related U deposits (in veins, stockworks, and episyenites)



Type examples: (a) Ambrosia Lake District (Mz)/Grants Uranium Region, USA (Resources + production of individual ore lodes: up to several 100 t U, 0.1–0.4% U). *References:* Adams and Saucier 1981; Granger and Finch 1988; Turner-Peterson et al. (eds) 1986; (b) Mikouloungou/Franceville Basin (PC), Gabon (Resources: <math><10\,000\text{ t U}</math>, 0.25% U). *References:* Diouly-Osso and Chauvet 1979; Gauthier-Lafaye et al. 1980.

Type 4 Granite-Related U Deposits (in Veins, Stockworks, and Episyenites) (Fig. I.4)

Granite-related U deposits include: (1) true veins composed of ore and gangue minerals in granite or adjacent (meta-)sediments and (2) disseminated mineralization in granite internal episyenite bodies (a dequartzified, micaceous, vuggy alteration product of granite) that are often gradational into veins. In the Hercynian orogenic belt of Europe, these deposits are associated with large batholiths of peraluminous leucogranite modified by late magmatic and/or autometamorphic processes. U mineralization occurs within or at the contact or peripheral of the intrusion. Resources are small to large and grades low to high (<math><10</math> to $>25\,000\text{ t U}$, <math><0.1\text{--}0.6\%</math>, locally up to several percent U). Three subtypes of deposits are distinguished based on the spatial setting with respect to the granitic pluton and host rocks.

References general: IAEA/Fuchs H (ed) 1986; Kolektiv 1984, 2003; Petrov et al. 2000; Poty et al. 1986; Wismut 1999.

a Endo- and Contact-Granitic Deposits (Limousin-Vendée Type)

Endogranitic deposits are commonly monometallic and consist of (a) mostly discontinuous, linear ore bodies within

distinct veins or stockworks localized in fractured granite or (b) disseminations in pipes or columns of episyenite. *Contact-granitic veins* persist from inside the granite across and beyond the granite contact but also exist only in enclosing rocks in vicinity of the contact. Other features are similar to endogranitic veins. Depths extension of endo- and contact-granitic veins can be as much as 700 m while episyenite ore bodies are known to depths of almost 1 000 m (Bernardan, France).

Type example endogranitic vein deposits: Fanay-Les Sagnes/La Crouzille District, Massif Central, France (Production 4 500 t U, 0.18% U). *References:* Leroy 1978a,b.

Type example episyenite deposits: Bernardan/La Marche District; Massif Central, France (Production >7 300 t U, av. 0.57% U). *References:* Guiollard and Milville 2003; Leroy and Cathelineau 1982.

Type example contact-granitic deposits: L'Écarpière ore field/Vendée District, France (Production 4 100 t U, 0.1% U). *References:* Chapot et al. 1996.

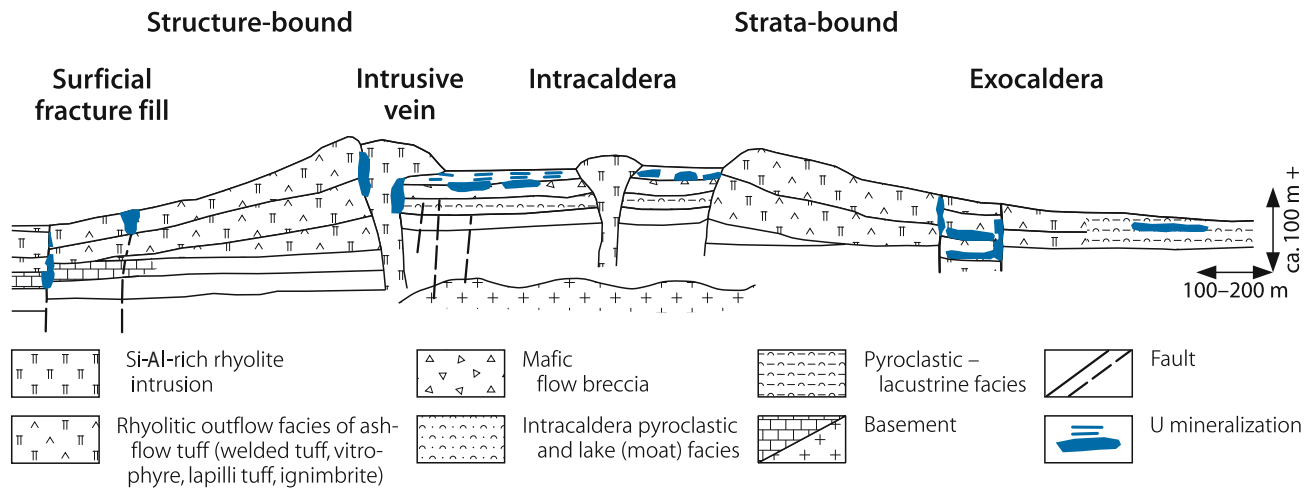
b Perigrantic Deposits in (Meta-)Sediments (Bohemien-Erzgebirge Type)

Perigrantic veins can be monometallic (essentially pitchblende and gangue minerals) or polymetallic (U, Co, Ni, Bi, Ag or other metals in economic quantities). The U and other elements are not genetically related. Both monometallic and polymetallic veins can persist as much as 2 000 m deep. Ore occupancy of host structures is generally low (5–30%).

Type example of monometallic veins: Příbram/Central Bohemian pluton, Czech Republic (Production: ~48 000 t U, 0.18% U). *References:* Komínek 1997; Kolektiv 1984, 2003; Petroš et al. 1986.

■ Fig. I.5.

U-deposit Type 5: volcanic U deposits (in veins, stockworks, and stratiform lodes)



Type example of polymetallic veins: Jáchymov, Erzgebirge, Czech Republic (Production: almost 10 000 t U, 0.1–1% U). *References:* Kolektiv 1984, 2003; Kominek and Veselý 1986.

c Perigranitic Deposits in Contact-Metamorphosed Rocks (Iberian Type)

Perigranitic deposits in the contact-metamorphic aureole of a granite intrusion have monometallic mineralization in the form of veinlets and disseminations in intensely fractured hornfels, speckled andalusite-cordierite schist, and similar rocks up to approximately 2 km wide around the granite. Host rocks are severely altered.

Type example: Nisa/Alto Alentejo District, Iberian Meseta, Portugal (Resources + production: 2 000 t U, 0.1% U). *Reference:* Basham and Matos Dias 1986.

Type 5 Volcanic U Deposits (in Veins, Stockworks, and Stratiform Lodes) (Fig. I.5)

(Russian terminology: *Endogenic hydrothermal; Molybdenum-uranium, Apatite-uranium, or Fluorite-uranium deposits, or Deposits in volcanic depressions*)

Volcanic U deposits occur mainly within or close to caldera complexes in the form of predominantly structure-bound and minor strata-bound mineralization in effusive and intrusive volcanic rocks.

Structure-bound mineralization includes (a) intrusive veins or stockworks in volcanic intrusions, diatremes, flows or bedded pyroclastic units and (b) surficial fracture fills in similar lithologies. *Strata-bound mineralization* consists of

disseminations and impregnations in permeable and/or reactive flows, flow breccias, tuffs, and intercalated pyroclastic and clastic sediments. Distinction of strata-bound mineralization is based on its (a) intracaldera or (b) exocaldera host environment, the latter is mixed with non-volcanic clastic sediments.

Uranium minerals (pitchblende, coffinite, U⁶⁺ minerals) preferentially associate with Mo-sulfides and pyrite. Other metallic minerals/elements include minor to traces of As, Bi, Hg, Li, Pb, Sb, Sn, W. Associated gangue minerals include fluorite, quartz, carbonates, baryte, jarosite.

Two principal subtypes are recognized: (1) Deposits indiscriminately hosted by mafic to felsic volcanic rocks in calderas underlain by granite, and (2) deposits associated with felsic volcanic complexes. Large deposits are confined to the *first variety*, e.g. at Strel'tsovsk, Russian Federation and Dornod, Mongolia. The *second variety* contains commonly small and low-grade deposits, e.g. in the Gan-Hang volcanic belt, SE China; at Michelin/Labrador, Canada; Nopal/Sierra de Peña Blanca, Mexico; and McDermitt, USA.

Subtype 1 deposits can have large resources and low to medium grades (several 10 000 t U, <0.25% U) whereas resources of Subtype 2 are commonly small (<1 000 t U) and grades very low to low (0.02–0.1% U).

References general: Dayvault et al. 1985; Goodell 1985; Ischukova 1997; Mashkovtsev et al. 2002; Petrov et al. 2000.

Note: (1) Most of the volcanic U occurrences also comply with criteria defining other types of deposits particularly of vein, surficial (fracture fill), and tabular sandstone types except for their singular volcanogenic relationship and mostly subeconomic magnitude. (2) Subtype 5.2 U concentrations, particularly in rhyolitic pyroclastics, may be more important as potential U sources for other types of deposits, particularly for those of sandstone type, than for consanguineous deposits.

Subtype 5.1 U Deposits Associated with Mafic-Felsic Volcanics in Calderas Underlain by Granite (Streltsovsk Type)

(Russian terminology: *Endogenic hydrothermal; Fluorite-uranium deposits associated with andesite-rhyolite in erosional-tectonic basins*)

Deposits consist of structurally controlled ore bodies contained in veins and intermittently at several levels in stratified mafic to felsic volcanic sheets intercalated with terrestrial sediments. Intense fracturing, and brecciation along steep and shallow dipping faults control location and dimension of ore bodies. Rocks along these structures exhibit polystage alterations. Some prominent veins persist to depths in excess of 1 100 m and extend into underlying granite and enclosed metamorphic xenoliths (Streltsovskoye-Antei, Argunskoye).

Mineralization is largely polymetallic. U is associated with Mo (>300 ppm) Fe, Pb sulfides, quartz, carbonates, phyllosilicates, locally albite and fluorite. The ore minerals form disseminated, banded, streaky, and massive ore in irregularly shaped (a) vein, stockwork, and (b) tabular-stratiform ore lodes of highly variable dimensions.

Resources range from small to large at low to medium grades (<1 000–70 000 t U, 0.07–0.25%).

a Vein-Stockwork Deposits (Streltsovskoye-Antei Type)

This mode of deposits is characterized by veins and/or stockworks that cut the caldera infill but also extend locally into the basement.

Type examples: (a) Streltsovskoye, (b) Antei (in granite)/Streltsovsk Caldera, Transbaykal, Russia (Resources + production: (a) 70 000 t U, 0.19% U; (b) 40 000 t U, 0.2% U). *Reference:* Ischukova 1997.

b Tabular-Stratiform U Deposits (Yubileinoe Type)

This mode of mineralization occurs at several stratigraphic levels controlled by peneconcordant, fractured intervals of the volcanic and sedimentary units.

Type example: Yubileinoe/Streltsovsk Caldera, Transbaykal, Russia (Resources + production: 10 000 t U, 0.19% U). *Reference:* Ischukova 1997.

Subtype 5.2 U Deposits Associated with Felsic Volcanic Complexes

a Structure-Bound/Veins-Stockworks (Nopal Type)

Deposits occur in rhyolitic ignimbrite, rhyolitic breccias, dacite flows, and granodiorite controlled by (a) intensely

altered, broken zones at crosscutting fault sets as exemplified by Nopal I (see below) in which U minerals occur as disseminations or coatings in a pipe-shaped body filled with silicified tectonic breccia; or (b) ring fracture systems with U impregnations, stringers, and veinlets that cut tectonic breccia and silica cemented rocks as typical for the Moonlight Mine (see below). Ore distribution is irregular changing from poor to locally rich sections. Most mineralization consists of uranyl-phosphates and -silicates, and limonite. Pitchblende associated with minor Fe-, Mo-, and other sulfides occurs in unoxidized environment. Resources are small and grades low to medium (<1 t to a few 100 t U, <0.1% to 0.5% U).

Type examples: (a) Nopal I/Sierra de Peña Blanca, Mexico (Resources + production: ~300 t U, 0.25% U). *References:* George-Aniel et al. 1991; Leroy et al. 1987; (b) Moonlight/McDermitt, USA (Production: <10 t U, <0.12% U). *Reference:* Dayvault et al. 1985.

b Structure-Bound/Surficial Veinlike (Cotaje Type)

Deposits occur near surface in zones of intensely broken and altered rhyolitic to rhyodacitic ignimbrite and tuff layers with intercalated volcanic breccias. Sooty pitchblende, coffinite, and uranyl phosphates associated with minor Mo, Fe, Pb, and Zn sulfides are irregularly distributed in narrow veins and disseminated throughout the cataclastic rock. Resources are small and grades low.

Type examples: Cotaje/Sevaruyo, Altiplano, Bolivia (Resources: 35 t U, 0.06% U). *References:* Leroy et al. 1985; Pardo-Leyton 1985.

c Diatreme Hosted (Maoyangtou Type)

U associated with other metals and commonly fluorite coats and fills fractures in cryptoexplosive breccia pipes. Resources are small and grades low.

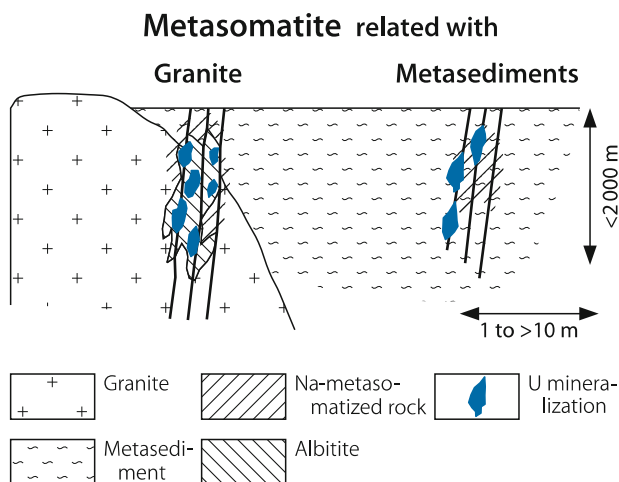
Type example: Maoyangtou/Wuyishan volcanic belt, Fujian Province, SE China (Resources: <100 t U, <0.1% U). *Reference:* Wang and Li 1996.

d Strata-Bound – Intracaldera (Aurora-Cottonwood Type)

Mineralization is hosted by mafic to intermediate tuffs, flows, and flow breccias overlain by tuffaceous lacustrine (moat) sediments. Disseminated pitchblende, coffinite, and locally uranyl phases associated with pyrite occur ± stratiform in almost completely altered porous intervals mainly along flow tops and brecciated

■ Fig. I.6.

U-deposit Type 6: metasomatite-related U deposits (in veins and stockworks)



layers, but also penetrate upwards and downwards into fracture zones. Resources range from few tens to several 1 000 t U, and grades from 0.02 to rarely 0.1% U.

Type examples: Aurora-Cottonwood Creek/Mc Dermitt, USA (Resources + production: ~7 000 t U, 0.04% U). *Reference:* Dayvault et al. 1985; Orajaka 1981.

e Strata-Bound – Exocaldera (Margaritas Type)

Mineralization consists of pitchblende and/or uranyl species associated with molybdenite, powellite, and locally pyrite, which occur erratically in fractures, joints, and voids of variably altered rhyolitic ash-flow tuff or peneconcordant in a sequence of pyroclastics interbedded with lacustrine or fluvial/alluvial sediments. Resources range from few tonnes to over 1 000 t U, at grades from 0.02 to rarely 0.2% U.

Type example: Margaritas/Peña Blanca, Mexico (Resources + production: ~2 000 t U, 0.1% U). *Reference:* Goodell 1985.

Type 6 Metasomatite-Related U Deposits (in Veins and Stockworks) (Fig. I.6)

Metasomatite U deposits are confined to areas of tectonomagmatic activity affected by intense Na- or Na- and carbonate-metasomatism that has produced albitized facies up to albitite, aegirinite, alkali-amphibole rocks, and carbonatic-ferruginous facies along deep rooted fault systems. Granite, gneiss, migmatite, or metasediments or metavolcanics are the parent lithologies. Deposits are structurally controlled by intersections, bifurcation, or abrupt bending of faults. Ore bodies are of variable shape and size composed of

disseminated grains and thin veinlets of ore minerals. Principal U phases are uraninite, U-Th-oxides, and U-Th-silicates. Two subtypes are defined on the basis of precursor rock facies: Metasomatized granite and metasomatized metasediments/metavolcanics. Resources range from small to large and grades from low to medium (<100 to >25 000 t U, <0.1–0.15% U).

References general: Avrashov/Bendix (ed) 1980; Belevtsev and Koval 1995; Collot 1981; Fritsche 1986; Kazanzky and Laverov 1977; Mineeva 1984.

Subtype 6.1 Metasomatized Granite (Kirovograd Type)

U minerals occur disseminated and in veinlets within intervals of closely spaced jointing, shearing, and brecciation in albitic aegirine granite, albitic arfvedsonite-aegirine granite, and albitite that occupy pre-metasomatic fault zones in anomalously uraniferous granite. Ore minerals include uraninite ± Th rich, uranothorianite, uranothorite, thorite, some brannerite, and coffinite associated with accessory Fe- and Pb-sulfides, REE minerals, apatite, and fluorite. Hematite and carbonates are locally abundant.

Deposits of the Kirovograd District have resources up to several 10 000 t U contained in discontinuous ore bodies to depths in excess of 1 000 m. In contrast, most deposits of this subtype elsewhere in the world are only few 100 m deep and have commonly resources from few tens to few thousands t U at grades averaging between <0.1 and rarely about 1% U.

Type examples: (a) Michurinskoye/Kirovograd District, Ukrainian Shield, Ukraine (Resources + production: ~27 000 t U, 0.1% U). *References:* Bakarzhiev et al. 1995a,b, 1997; Belevtsev and Koval 1995; Miguta and Tarkhanov 1998; Pavlenko 2005.

(b) Ross Adams/Bokan Mountain, Alaska, USA (Production: 750t U, 0.1–0.2% U). *References:* Collot 1981; Thompson et al. 1980, 1982.

Subtype 6.2 Metasomatized Metasediments/Metavolcanics (Zhelye Vody Type)

(Russian terminology: *Ferro-uranium formation* or *Iron-uranium formation associated with sodic and carbonate metasomatites*)

The Zhelye Vody District (type example) is in the Krivoy Rog Basin, a large synclinorium of Proterozoic carbonate, quartzite, schist, and ferruginous metasediments. These rocks are folded into large isoclinal folds with steep axes. Stocks and dikes of microcline granite have intruded along lineaments. Repeated brittle tectonism caused deep faulting and strong fracturing. Metasediments and granites are intensely altered along lineaments by early Fe-Mg-metasomatism (resulting in stratiform iron ore), followed by Na-metasomatism, carbonate-metasomatism, and finally silicification (secondary quartzites). U mineralization is restricted to fractured sections in Na- and carbonate-metasomatite zones in which it occurs in the form of lenses, shoots, and stratiform bodies with finely disseminated U minerals, and as veins. U minerals include uraninite, pitchblende, coffinite, brannerite, and nenadkevite associated with sulfides, apatite, malacon, and carbonate.

U mineralization at Zheltorechenskoye/Zhelye Vody persists to depths of some 2 000m. U-hosting metasomatites

decrease at depth below about 1 000m. Uraninite peters out synchronously at this depth and gives way to uraniferous malacon-apatite.

Type example: Zheltorechenskoye/Zhelye Vody District, Krivoy Rog Basin, Ukrainian Shield, Ukraine (Resources + production: estimated ~20 000 t U, 0.12% U). *Reference:* Bakarzhiev et al. 1995b; Belevtsev et al. 1984a.

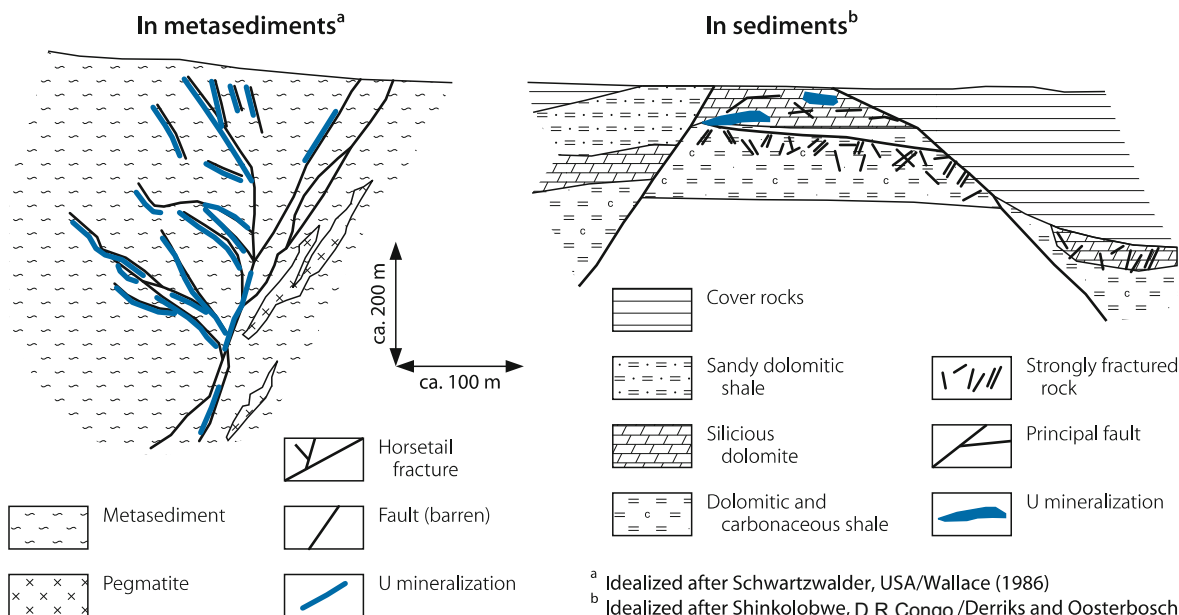
Type 7 Undifferentiated (Meta-)Sediment Hosted U Deposits (in Veins and Shear Zones) (Fig. 1.7)

Three varieties are recognized: Monometallic and polymetallic veins, and monometallic shear zone fillings. The two vein modes are similar in structural control, ore and gangue mineral association, and wall rock alteration to perigranitic monometallic and polymetallic veins in (meta-)sediments. Major differences include absence of granitic or other magmatic complexes and a relative continuity of mineralization. Resources are small to high and grades low to high (<10 to >25 000 t U, <0.1 to >1% U).

a Monometallic Veins (Schwartzwalder Type)

Uranium (mainly pitchblende, uraninite, coffinite) and gangue minerals with only traces of other metallic minerals form

Fig. 1.7. U-deposit Type 7: undifferentiated (meta-)sediment hosted U deposits (in veins and shear zones)



stringers, veinlets, and veins within larger tensional structures but particularly in horsetail fractures, which branch from the main lodes. Mineralization is relatively continuous although grades are highly variable. Resources are small to high and grades low to high (<100–20 000 t U, 0.1–0.5% U locally several percent U).

Type example: Schwartzwalder/Front Range, USA (Production: ~7 000 t U, 0.4% U). *Reference:* Wallace 1986.

b Polymetallic Veins, Stockworks (Shinkolobwe Type)

Uranium (pitchblende, uraninite, coffinite) associated with Co, Cu, Fe, Mo, Ni, Pb, Zn and gangue minerals occur in veins, stockworks, breccia matrix, as well as replacement masses and disseminated particles and aggregates in broken host rocks. Major faults are barren. Mineralization is fairly continuous but highly variable in grade and magnitude. At Shinkolobwe and other deposits in the Katanga copper belt of Congo and Zambia, ore distribution is discordant to strata but ore always occurs in beds underlying the cupriferous strata, which locally contain anomalous U concentrations, at the base of a thick sequence of sediments of shallow marine origin. Resources are small

to high and grades low to high (<100 to 25 000 t U, 0.1 to >1% U).

Type example: Shinkolobwe/Katanga Copper Belt, Democratic Republic of Congo (Resources + production: ~25 000 t U, 0.1 to >1% U). *Reference:* Derricks and Vaes 1956.

c Monometallic Shear Zone Fillings (Rožná Type)

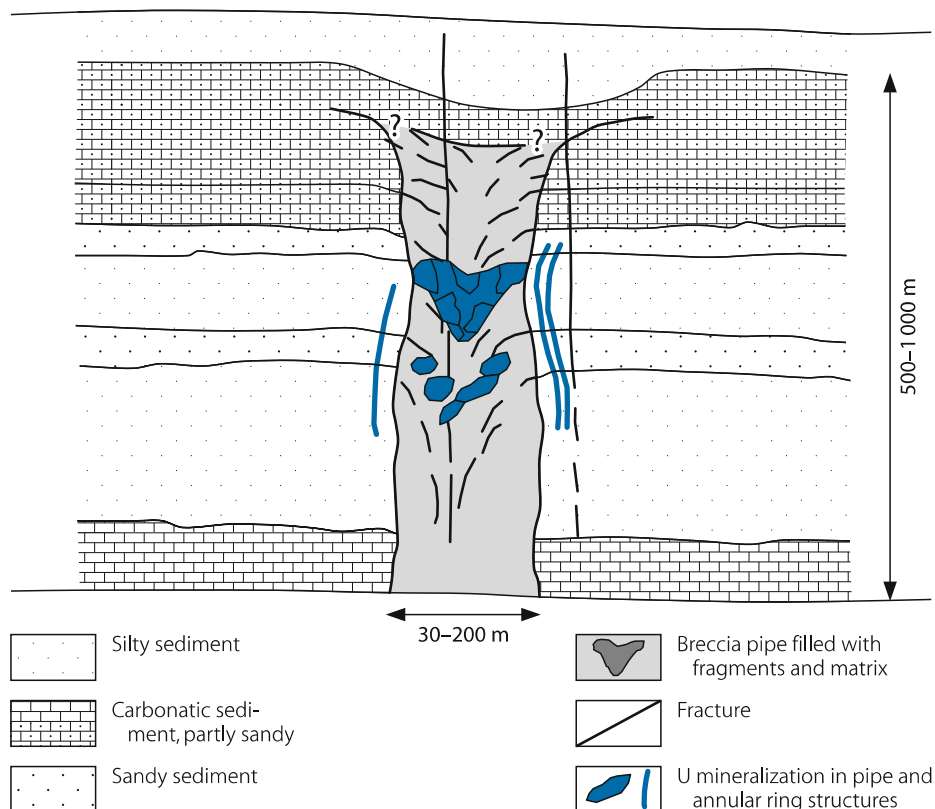
Ore bodies consist of stringers and disseminations of U phases (mainly pitchblende, coffinite) without or only minor gangue in small, narrow structures (fissures, joints, etc.) that group to lenticular ore shoots subparallel to the strike of the host strata. Prominent shear and breccia zones control position and dimension of ore shoots. Classical veins are rare.

Ore bodies comprise lower grade ore composed of U impregnations in a system of subparallel, anastomosing, and intersecting structures, which border and enclose variably fractured rock segments with better grade ore. Better grade ore shoots occur predominantly in the form of bundles of subparallel fracture fillings or network style mineralization.

Resources are small to medium and grades low (<20 000 t U, <0.1% U).

■ Fig. 1.8.

U-deposit Type 8: collapse breccia pipe U deposits (Arizona Strip type)



Type example: Rožná/Western Moravia, Czech Republic (Resources + production: ~20 000 t U, 0.1% U). *References:* Kolektiv 1984, 2003.

Type 8 Collapse Breccia Pipe U Deposits (Arizona Strip Type) (Fig. I.8)

Circular, vertical pipes (10–300 m in diameter, <1 000 m deep) filled with highly brecciated material constitute the host for mineralization. Pipe infill is composed of coarse fragments and fine matrix material that down-dropped by collapse of strata into a dissolution cavern in a basal soluble rock (limestone, gypsiferous rocks). Mineralization consists of U (pitchblende, coffinite, alteration products thereof) and various metallic minerals (Fe, Cu, Ni, Co, Mo, Pb, Zn, As, traces of Ag, Au, Hg, Sb, V) associated with a variety of gangue minerals. These minerals occur as veinlets in annular ring fractures surrounding the pipe, and as stringers and irregular impregnations of permeable (± sandy) matrix material within the pipe. A Fe-sulfide cap (80% sulfide) often tops the uppermost U mineralization in a pipe. Alteration is commonly weak and of

little extension into wall rocks. Resources of individual pipes are small and grades medium to high (few tonnes to ~2 000 t U, 0.2–1% U). Cu and Ag may locally be significant co-products.

Type examples: Hack Canyon Mines/Arizona Strip, Arizona, USA (Production: ~1 300 t U, 0.55% U). *References:* Carlisle 1983; Wenrich and Sutphin 1989, 1994.

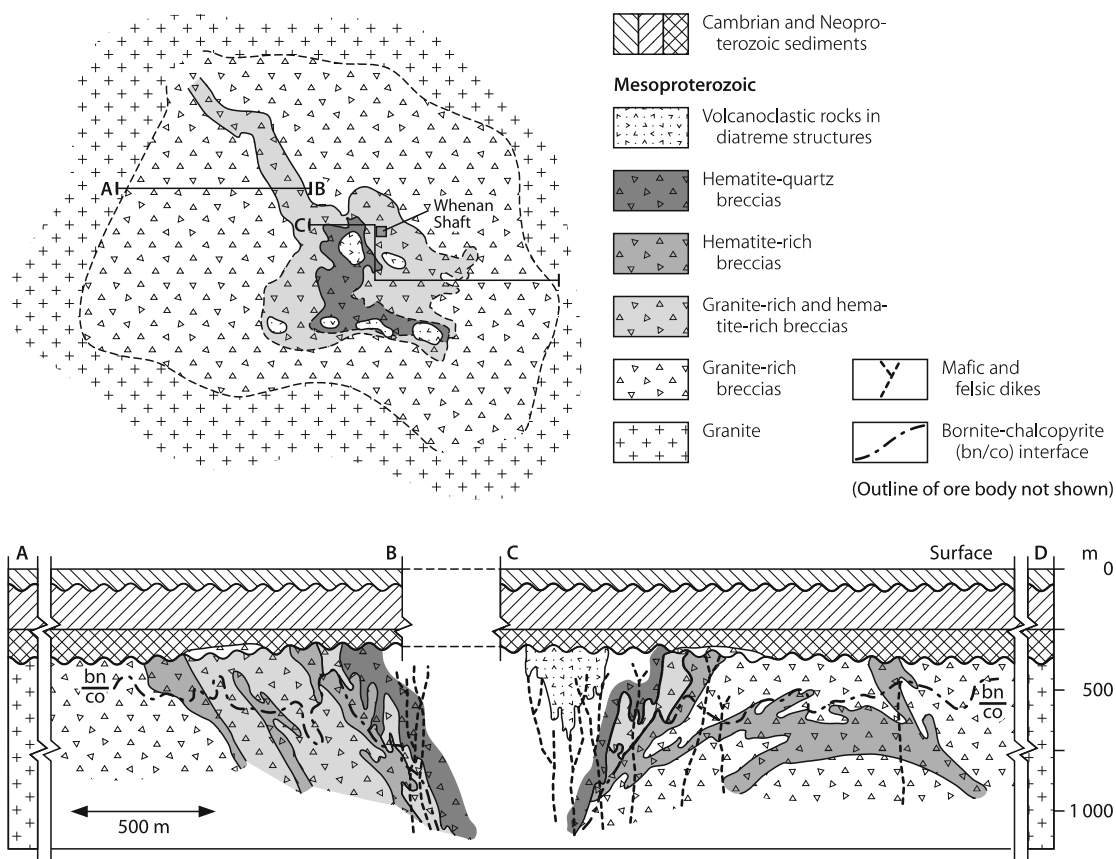
Type 9 Polymetallic Hematite-Breccia-Complex U Deposits (Olympic Dam Type) (Fig. I.9)

This type of deposits has been attributed to a broad category of worldwide known iron oxide-copper-gold deposits but Olympic Dam is the only known representative of this type with significant by-product U resources.

The Mesoproterozoic Olympic Dam deposit contains uranium in association with copper, gold, silver, and REE in a hematite-rich granite breccia complex. This breccia is within a granite intrusion that exhibits regional iron, potassium, and/or sodium metasomatism. The granite is part of a

Fig. I.9.

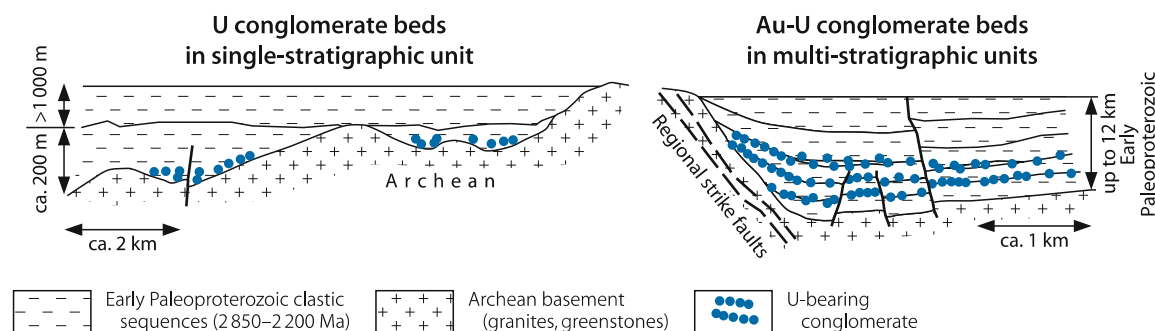
U-deposit Type 9: polymetallic hematite-breccia-complex U deposits (Olympic Dam type)



Idealized after Olympic Dam, Australia/McKay and Miezitis 2001 based on Reeve et al. (1990)

■ Fig. I.10.

U-deposit Type 10: Paleoproterozoic quartz-pebble conglomerate U deposits



suite of Mesoproterozoic plutonic intrusions and co-magmatic continental felsic volcanics. Neoproterozoic to Cambrian, flat-lying marine sediments of the Stuart Shelf, approximately 300 m thick, rest unconformably upon the breccia complex.

Hematite-rich and heterolithic hematitic breccias are the principal host for economic Cu-U mineralization. U minerals (fine-grained pitchblende, minor coffinite and brannerite) occur as disseminations, microveinlets, and aggregates intergrown with copper sulfides and breccia material, and partly as replacement of breccia constituents. Narrow, better grade uranium mineralization occurs preferentially in bornite-chalcocite ore in hematite breccias. High-grade U zones transgress locally the bornite-chalcopyrite interface. U is recovered as by-product of Cu, Au, Ag.

Type example: Olympic Dam/Gawler Craton-Stuart Shelf, S Australia (Resources + production: 1.4 million t U at 0.04% U, 42.7 million t Cu at 1.1% Cu, 1 905 t Au at 0.5 g t⁻¹, 2.9 g t⁻¹ Ag, approx. 0.2% La, 0.3% Ce). *References:* Reeve et al. 1990; McKay and Miezitis 2001; WMC 2004.

Type 10 Paleoproterozoic Quartz-Pebble Conglomerate U Deposits (● Fig. I.10)

(also referred to as *Oligomictic conglomerate* or *Lower Proterozoic conglomerate* or *Paleoconglomerate* or *Modified paleoconglomerate type*)

Quartz-pebble conglomerate U deposits are restricted to early Paleoproterozoic intracratonic basins (older than 2.3–2.4 Ga) downwarped into Archean basement that includes granites. Host rocks consist of typically trough cross-bedded, oligomictic quartz-pebble conglomerate layers with a pyritiferous matrix interbedded with quartzite and argillite beds. This suite

occurs as basal units in fluvial to deltaic braided stream systems.

Placer uraninite is the principal primary uranium phase. It is locally associated with gold, REE, and/or other detrital metallic oxide and sulfide minerals. The variable ore mineral assemblages are a function of different geological source provinces and hydrodynamic mineral separation during fluvial transport. Fluvial transport and accumulation of uraninite was conditioned by the reducing character of the early, oxygen-poor earth atmosphere prior to oxyatmoverion. Post-depositional redistribution and mineral crystallization mainly by diagenetic processes led to the formation of modified placers composed of a suite of authigenic ore and associated minerals such as brannerite, rutile, anatase, coffinite, pyrite, and others. Two economic subtypes are noticed: Monometallic and polymetallic (Au + U). Economic deposits are confined to the *Blind River-Elliot Lake* area, Canada, where predominantly monometallic uranium was formerly mined, and the *Witwatersrand Basin*, South Africa, where uranium is recovered as by-product of gold. Resources are large but grades low (several 100 000 t U; 0.01 to locally 0.12% U).

References general: Button and Adams 1981; Pretorius 1981; IAEA/Pretorius(ed) 1987.

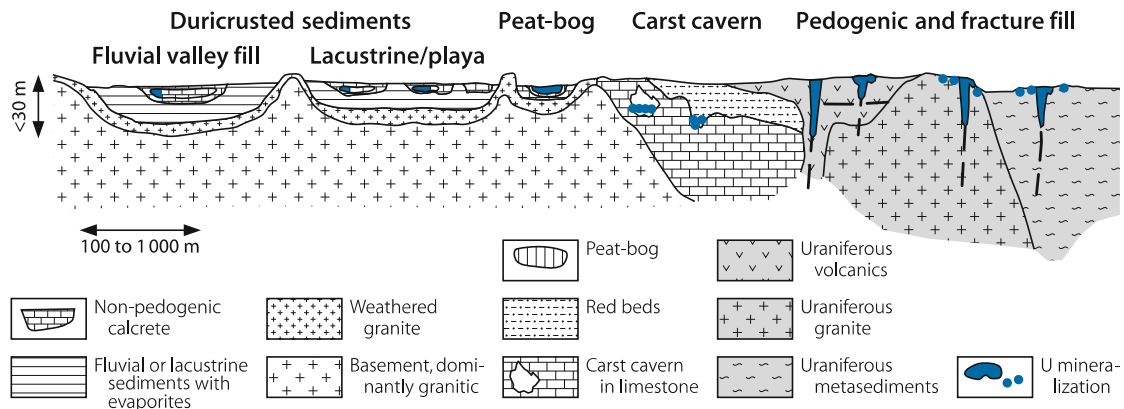
Subtype 10.1 Monometallic (or U-Dominant with REE) U Deposits (Elliot Lake Type)

Detrital heavy minerals (dominated by uraninite and REE minerals) and later formed authigenic phases occur as disseminated matrix components in pyritic (5–20 wt.-%), oligomictic quartz-pebble conglomerate horizons (termed reef), from 0.5 to >3.5 m thick. Quartzite units are interbedded with the conglomerate beds. This suite forms the basal section of a sequence, about 50 m thick, in paleovalleys scoured into Archean basement.

Uraninite, uranothorite, uranothorianite, monazite, and xenotime are the prevailing detrital minerals. Authigenic minerals

Fig. I.11.

U-deposit Type 11: surficial U deposits



include U-Ti-oxide phases (brannerite), coffinite, thucholite, and locally gummite.

Type example: Elliot Lake-Quirke Lake District/Ontario, Canada (Resources + production: >400 000 t U, 0.05–0.12% U; U was the primary commodity produced with occasional recovery of Th and some REE, particularly Y). *References:* Robertson 1989; Ruzicka 1988.

Subtype 10.2 Polymetallic Au with U Deposits (Witwatersrand Type)

Ore and associated minerals occur as detrital and redistributed matrix components in quartz-pebble conglomerate horizons in multi-stratigraphic cycles within six large fluvial-deltaic fans on the north and west side of the Witwatersrand Basin. Host rocks consist of pyritic, oligomictic quartz-pebble conglomerate beds, commonly only few cm to several tens of cm thick, interbedded with quartzite, arkose, shale, and volcanics. Carbonaceous material occurs in several horizons.

Detrital ore minerals include uraninite, uranotorite, native gold, and platinoid (Os, Ir, Ru, Pt) species. Postdepositional modification of the placers led to several generations with a multitude of authigenic ore and associated minerals including brannerite and thucholite.

Important concentrations of U ore are restricted to distinct narrow zones occupying ca. 2% of the entire Upper Witwatersrand System within a belt trending parallel to the former coastline.

Type example: Witwatersrand Basin, South Africa (Resources + production: >500 000 t U, av. 0.01–0.03% U, 5–12 ppm Au; recovery of U as by-product to Au except in a few mines, e.g. Africander/Vaal Reefs with 0.12% U and 1.1 ppm Au). *References:*

Anhaeuser and Maske (eds) 1986; Hallbauer 1986; Pretorius 1976a,b; von Backström 1975, 1976.

Type 11 Surficial U Deposits (Fig. I.11)

Surficial uranium deposits are broadly defined as young (Tertiary to Recent) near-surface uranium concentrations in rocks and soils. Uranium occurs almost exclusively as uranyl species present as impregnation and void filling or coating, or adsorbed on host constituents (organics, clay, etc.). Mineralization is strata-bound in selectively indurated sedimentary formations or unconsolidated sediments in surficial depressions, dissolution caverns, or structure-bound in high background U rocks. Based on host environment, four principal subtypes are recognized.

References general: Arakel 1988; Boyle 1984; Briot 1978; Butt et al. 1984; Carlisle 1983; Carlisle et al. 1978; Hambleton-Jones 1976, 1984; IAEA/Toens (ed) 1984; Mann and Deutscher 1978; Pagel 1984; Samama 1984.

Subtype 11.1 Duricrusted Sediments

(also referred to as *Calcrete, Silcrete, Groundwater-calcrete, or Valley-calcrete type*)
(Russian Terminology: *Exogenic infiltration; Ground-oxidation*)

In regions of arid to semi-arid climates, *nonpedogenic* calcrete, dolocrete, silcrete, or gypcrete that cement or replace young sediments along the groundwater table constitute the host for two modes of tabular U(-V) deposits in (a) fluvial, alluvial and eolian channel fills and (b) evaporative lacustrine playa facies.

a Fluvial Valley-Fill (Yeelirrie Type)

Mineralization in duricrusted valley sediments forms flat-lying lenses, up to few meters thick, with most of the mineralization emplaced immediately beneath the present water table. U minerals (carnotite, rarely other uranyl species) occur disseminated, as fracture coating and vug lining in earthy or porcellaneous calcrete etc., and as grain coating in clay-quartz sediments immediately below the calcrete. Resources are commonly small to medium and grades mostly low (<10–5 000 t U, 0.02–0.07% U) except for the type example deposit.

Type example: Yeelirrie/Yilgarn Block, Australia (Resources: 45 000 t U, 0.12% U). *Reference:* Cameron 1984.

b Lacustrine/Playa (Lake Maitland Type)

Mineralization is similar to (a) but hosted by duricrusted layers in shallow lake or playa sediments. Resources are small and grades low (<10 to 4 000 t U, <0.02–0.08% U, occasionally 0.15% U).

Type example: Lake Maitland/Yilgarn Block, Australia (Resources: 3 000 U, <0.06% U). *Reference:* Cavaney 1984.

Subtype 11.2 Peat-Bog (Flodelle Creek Type)

In humid climate regions, U is accumulated in vegetal organic and clay-rich shallow depressions (swamps, bogs, muskegs) composed of <65% vegetal organic matter, often peat, embedded in alluvial pelitic-psammitic sediments when these depressions are located in U source areas. No discrete U minerals occur. U is probably present as urano-organic complexes and/or adsorbed on organic material, clay, marl, or silt particles. Resources are

small and grades low (<1 to 50 t U, few 100 ppm U, rarely up to 0.2% U).

Type examples: Flodelle Creek, Stevens Co., NE Washington State, USA (Resources+production: ~50 t U, few 100 ppm U). *Reference:* Johnson et al. 1987; Otton et al. 1989.

Subtype 11.3 Karst Cavern (Pryor-Little Mtns. Type)

U mineralization is contained in the floor veneer of fallen blocks and insoluble residues of limestone embedded in loosely consolidated sand, silt, and clay in limestone caverns. Uranium minerals (tyuyamunite, metatyuyamunite) coat or fill fractures and solution voids, line rock components, and impregnate the matrix of the cavern fill. Resources are small but grades high (few tonnes to several 10 t U; 0.4 to >1% U, 0.6–4% V₂O₅).

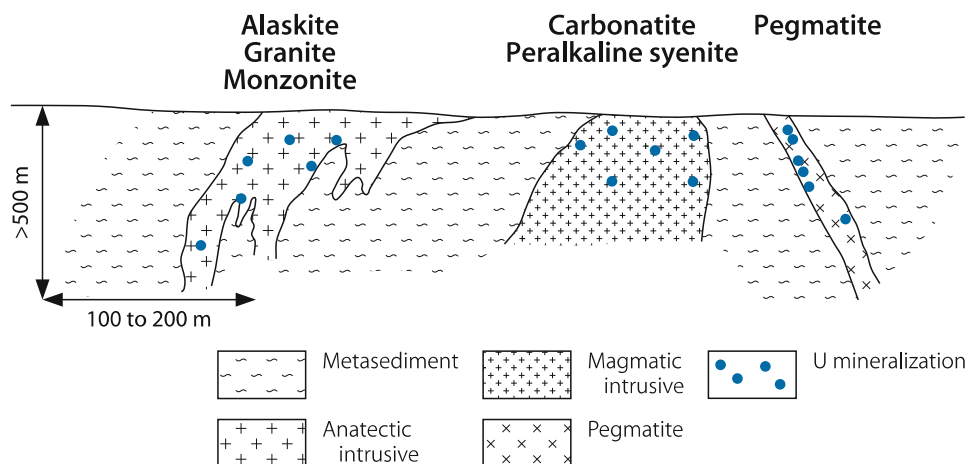
Type examples: (a) Pryor-Little Mtns/Montana-Wyoming, USA (Production 100 t U, 0.4–1.07% U, 0.6–4% V₂O₅). *Reference:* Bell 1963. (b) Tyuya-Myuyun/Osh Province, Kyrgyzstan (Resources+production: ~50 t U, 1.4% U, 3.8% V₂O₅, 3% CuO). *Reference:* Aleksandrov 1922; Kazansky 1970.

Subtype 11.4 Surficial Pedogenic and Structure Fill

This category comprises surface-bound U concentrations in soils and pedogenic encrustations (laterite/ferricrete, calcrete, silcrete, etc.), as well as dissemination, coating and filling of near-surface cataclastic zones (shears, fissures, joints) in rocks with anomalous U background tenors. Occurrences are commonly of minute to small size and low grade (<1 t U, <0.1% U) except a few cases.

■ Fig. I.12.

U-deposit Type 12: intrusive U deposits



Type examples: Daybreak Mine, Washington, USA (Production: 20 t U, 0.3% U). *References:* US-AEC 1959.

Type 12 Intrusive U Deposits (Fig. I.12)

Intrusive deposits consist of disseminated primary U minerals, dominantly uraninite, uranothorianite, and/or uranothorite in rocks of intrusive magmatic or anatectic origin. Five major subtypes are identified: alaskite, quartz-monzonite, carbonatite, peralkaline syenite, and pegmatite. The first four subtypes are all of very low grade (ca. 20–400 ppm U) but may contain large resources. Only pegmatite deposits may average up to 0.1% U but resources are generally low (few tonnes to few hundred tonnes U).

The only deposits mined in the western hemisphere are the Rössing alaskite, Namibia, and the Bancroft (Madawaska) pegmatite deposits, Canada. In addition, uranium was extracted as by-product from porphyry copper/quartz-monzonite deposits (Bingham, Twin Buttes) in the western USA, and from the Phalaborwa carbonatite, South Africa.

References general: Alexander 1986; Brynard and Andreoli 1988; Berning 1986; Camisani-Calzolari et al. 1985; Maurice (ed) 1982; Sørensen et al. 1974.

Subtype 12.1 Alaskite U Deposits (Rössing Type)

Alaskite U deposits are associated with alaskite bodies of variable shape and dimensions. Uranium minerals (uraninite, betafite, and alteration products thereof) occur as inclusions in quartz, feldspar, and biotite disseminated throughout the alaskite, and in interstices and microfractures. Resources can be large but grades are low.

Type example: Rössing, Namibia (Resources+production: >200 000 t U, 0.03–0.04% U). *References:* Berning 1986; Berning et al. 1976; Brynard and Andreoli 1988.

Subtype 12.2 Quartz-Monzonite/Copper-Porphyry Cu-U Deposits (Bingham Type)

This type of U concentration is associated with base (mainly Cu, Mo) and noble metals in highly differentiated quartz-monzonitic complexes (copper porphyries) altered by Mg- and K-metasomatism and late hydrothermal activity. No uranium mineral is listed but U may be present as disseminated uraninite or uranothorianite.

Type example: Bingham, Utah, USA (20–50 ppm U in Cu-Mo ore; U was extracted from leach containing 8–12 ppm U. Former

annual production of U as by-product is estimated at 60–80 t). *References:* John 1978; Lanier et al. 1978.

Subtype 12.3 Carbonatite Cu-U Deposits (Phalaborwa Type)

Differentiated, cupriferous carbonatite complexes contain increased U background concentrations in addition to other metals. At Phalaborwa, South Africa, the only deposit of this type mined, recoverable ore minerals (chalcopyrite, bornite, titaniferous magnetite, baddeleyite, uranothorianite) are widely disseminated or in veinlets throughout an almost vertical dipping carbonatite-phoscorite pipe. Resources are small and grades very low (<100 ppm U).

Type examples: Phalaborwa, South Africa (Resources+production: several 1 000 t U, 0.004% U, 0.51% Cu; recovery of U as by-product to Cu and other metals). *References:* Camisani-Calzolari et al. 1986; IAEA 1986a; Palabora Mining Co. 1976.

Subtype 12.4 Peralkaline Syenite U Deposits (Kvanefjeld Type)

Domes or stocks of differentiated agpaitic-peralkaline nepheline syenite contain disseminated U-Th minerals of refractory nature (steenstrupine, eudialyte, monazite) in late lujavrite facies with the best U-Th concentrations at or near the contact of intrusive apophyses and sheet-like lujavrite bodies. Resources are small to large and grades low (<500 ppm U).

Type examples: Kvanefjeld, Illimaussaq, Greenland (Resources: >25 000 t U, 0.03–0.04% U). *References:* Bohse et al. 1974; Kunzendorf et al. 1982; Sørensen et al. 1974.

Subtype 12.5 Pegmatite U Deposits (Bancroft Type)

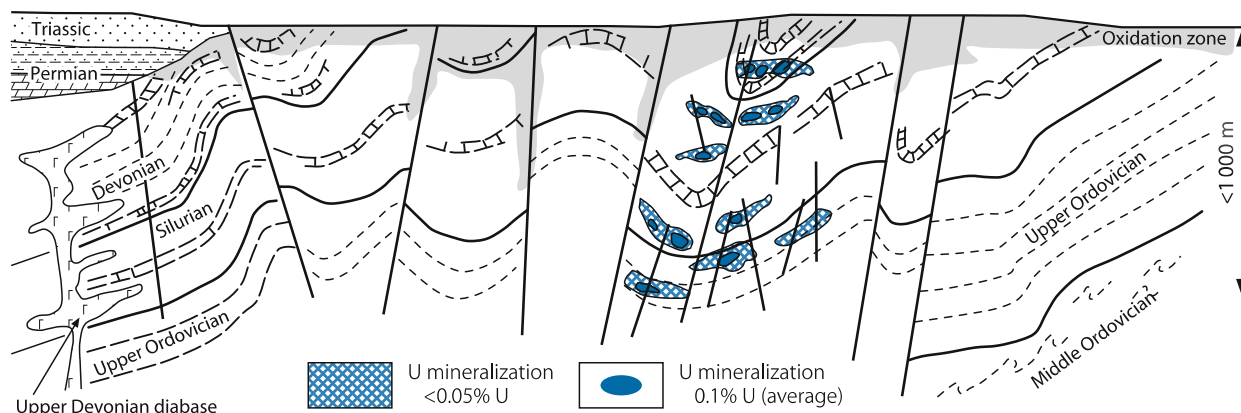
Granitic, rarely syenitic, pegmatite dikes may contain randomly distributed small U ore bodies. Uraninite, uranothorite, and alteration products thereof are the principal U phases.

Type examples: Madawaska/Bancroft District, Grenville orogenic belt, Canada (Production: ~200 t U, 0.05–0.15% U). *References:* Alexander 1986.

Another pegmatite variety, *rare metals pegmatite*, contain Sn, Ta, Nb, and Li mineralization with variable U, Th, and REE grades as known, e.g. from the Greenbushes and Wodgina pegmatites (West Australia). Although the U and Th contents of the Greenbushes pegmatites are very low (av. 6–20 ppm U, 3–25 ppm Th), mineral processing enrich U+ThO₂ combined up to 0.4% in

■ Fig. I.13.

U-deposit Type 13: uraniumiferous carbonaceous shale-related stockwork deposits (Ronneburg type)



Period		Lithology		U ore distribution
Triassic			Mudstone, anhydrite, dolomite, sandstone	
Permian				
Carboniferous	Lower		Alternating greywacke, shale	
	Upper		Limy schist, limestone, greywacke, spillite, tuff, tuffite	
Devonian	Middle		Shale, carbonaceous black shale	
	Lower		Shale, limestone, Tentokulite-shale	
	Upper		Upper Graptolite-shale	
Silurian	Upper		Limestone, dolomite (Ockerkalk)	
	Lower		Alternating shale, silicic shale, dolomite, phosphorite (Lower Graptolite-shale)	
Ordovician	Upper		Shale, carbonatic-sandy-carbonaceous, with sand-silt-limestone intercalations (Lederschiefer)	

Idealized after Ronneburg, Germany/Lange and Freyhof (1991)

tantalum concentrates and tin smelting of Greenbushes ore increases U+ThO₂ contents up to 1% in slags.

Type 13 Uraniferous Carbonaceous Shale-Related Stockwork Deposits (Ronneburg Type) (● Fig. I.13)

[Chinese terminology: *Carbonaceous-carbonate-siliceous-pelite* type, subdivided into pelite, carbonate, and silicite (or silicic breccia) subtypes; or – genetically – into (a) sedimentary-diagenetic, (b) phreatic infiltration (or leaching-accumulative), and (c) hydrothermal-reworked subtypes]

This type of uranium deposits consists of strata-controlled, structure-bound U concentrated in stockworks of microfractures

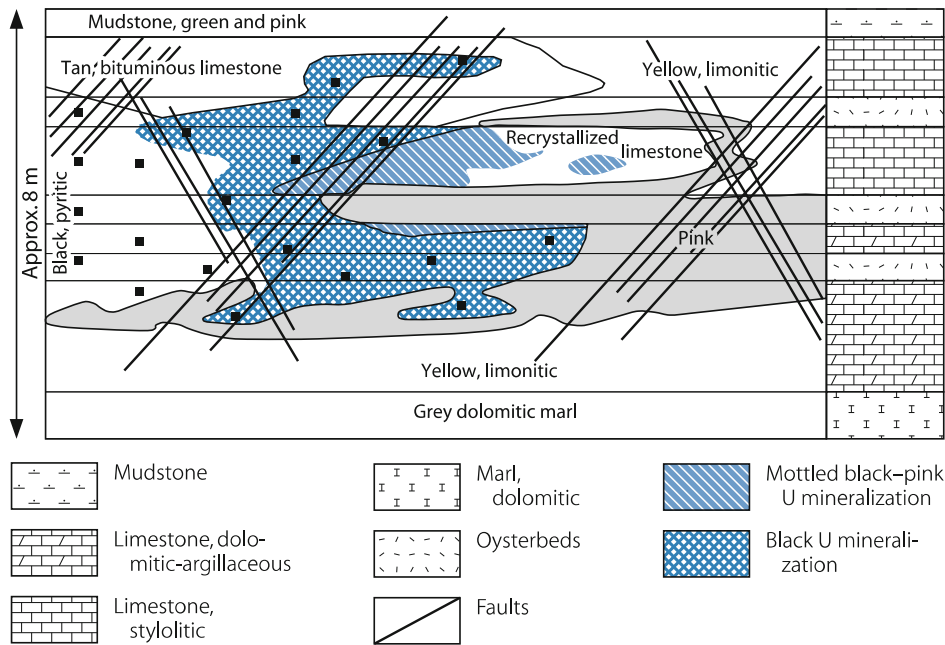
within or immediately adjacent to carbonaceous, pyritic (black) shale/pelite beds. Host rocks include argillaceous and siliceous black carbonaceous shales with more or less intercalations of calcareous (dolomitic) and phosphorite nodule beds, as well as carbonaceous sandy and carbonatic shales, and limestone-dolomite above and/or below the carbonaceous shale horizons. High organic carbon (up to 9% C), sulfide (up to 3.5% S), and anomalous trace element (U, Mo, Ni, V, As, Sb) contents are typical for the carbonaceous shale.

Mineralization is restricted to segments of intense microfracturing (fissures, joints, cleavages) controlled by major faults, thrusts, and their intersections. These microfracture systems form stockwork ore bodies within the cementation zone below a supergene oxidation profile. Weakly mineralized zones surround the stockwork ore bodies.

Ore minerals (pitchblende, rare coffinite, with subordinate sulfides, arsenides of various metals) fill and coat in unpredictable manner joints and cleavages and impregnate porous wall rocks for short distances from mineralized fractures. Ore-related

Fig. I.14.

U-deposit Type 14: uraniferous bituminous-cataclastic limestone deposits (Mailuu-Suu type)



Idealized after Mailuu-Suu, Kyrgyzstan/Roslyi (1975)

alteration is constraint to narrow aureoles of bleaching and hematitization around mineralized structures. Resources of individual deposits are small to large and grades low (<100 to several 10 000 t U, <0.05–0.15% U).

Type example: Gera-Ronneburg District/Thuringia, Germany (Resources+production: ~200 000 t U, 0.075–0.14% U). *References:* Lange and Freyhoff 1991; Wismut 1999.

Type 14 Uraniferous Bituminous-Cataclastic Limestone Deposits (Mailuu-Suu Type) (Fig. I.14)

(Russian terminology: *Exogenic epigenetic infiltration: Vanadium-uranium deposits in carbonate sediments*)

Uranium mineralization is structure-bound in organic-rich (bituminous/petroliferous) calcareous sediments (\pm impure limestone, dolomite, marlstone), sandwiched between arenaceous-argillaceous continental sediments. Repeated oxidation and reduction processes have altered the host rock.

The position and configuration of the ore zones and ore bodies are controlled by fractured intervals in intraformational folds and flexures. Uranium minerals (pitchblende, nivenite, coffinite, and U-V minerals e.g. montroseite) form lenticular and roll shaped ore bodies in which U minerals are irregularly distributed in stylolites, sutures, microfissures (which also contain solid bitumens), interstices between carbonate grains, and leached-

out voids. Associated elements include Fe, V, Mo, As, Ni, Co, Pb, and Cr.

Type example: Mailuu-Suu/Karamazar region, Kyrgyzstan (Production: estimated ~10 000 t U, 0.1–0.2% U). *References:* Roslyi 1975; Thoste 1999.

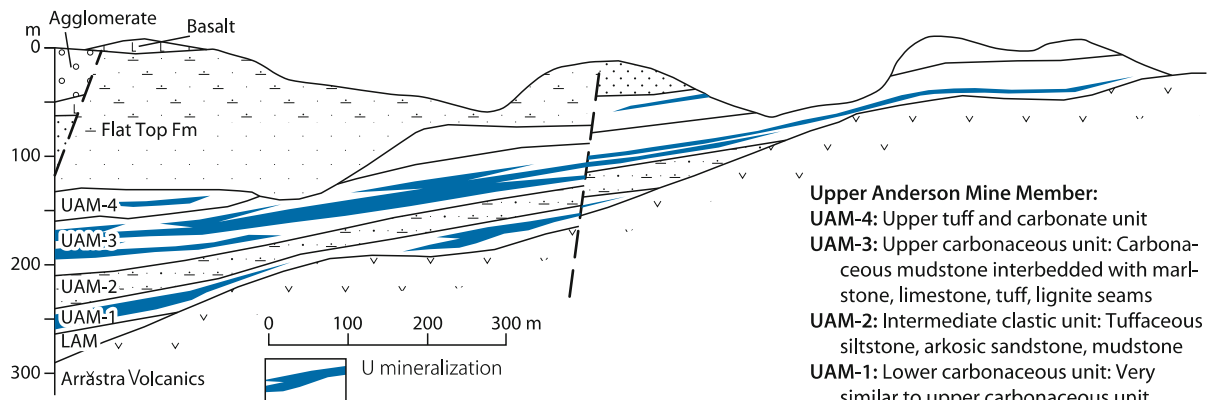
Type 15 Uraniferous Carbonaceous Lutite (Lacustrine) Deposits (Anderson Mine Type) (Fig. I.15)

This type, as exemplified by the Anderson Mine (see below), constitutes an intermediate member between lignite and sandstone-type U mineralization.

Carbonaceous lacustrine, locally paludal sediments with tuffaceous components provide the host rocks. They include carbonaceous lutite horizons with widespread, peneconcordant, low-grade U accumulations (<100 to 200 ppm U) associated with anomalous tenors of V, Mo, Li, F, B, Cu, and Ni. These low grade uraniferous horizons encompass irregular shaped zones with better grade mineralization of up to 0.3% U. Most of the mineralization is in thin-bedded, slightly silicified, pyritic, carbonaceous mudstone and siltstone, lignitic mudstone, and bioturbated marlstone in which ore minerals occur as fine disseminations in the matrix and discontinuous microveinlets or patches. Highest U concentrations occur in lignitic coal and as halos around root remains, often associated with framboidal pyrite. Principal U mineral is colloform coffinite that generally associates with carbonaceous matter and humate. Pitchblende is

■ Fig. I.15.

U-deposit Type 15: uraniferous carbonaceous lutite (lacustrine) deposits (Anderson Mine type)



Idealized after Anderson Mine, USA/Sherborne et al. 1979

Early to Middle Miocene

Flat Top Formation: Arkosic siltstone, sandstone, conglomerates interbedded with bentonitic/tuffaceous siltstone

Anderson Mine Formation: Tuffaceous, paludal, lacustrine sediments

Upper Anderson Mine Member:

UAM-4: Upper tuff and carbonate unit

UAM-3: Upper carbonaceous unit: Carbonaceous mudstone interbedded with marlstone, limestone, tuff, lignite seams

UAM-2: Intermediate clastic unit: Tuffaceous siltstone, arkosic sandstone, mudstone

UAM-1: Lower carbonaceous unit: Very similar to upper carbonaceous unit

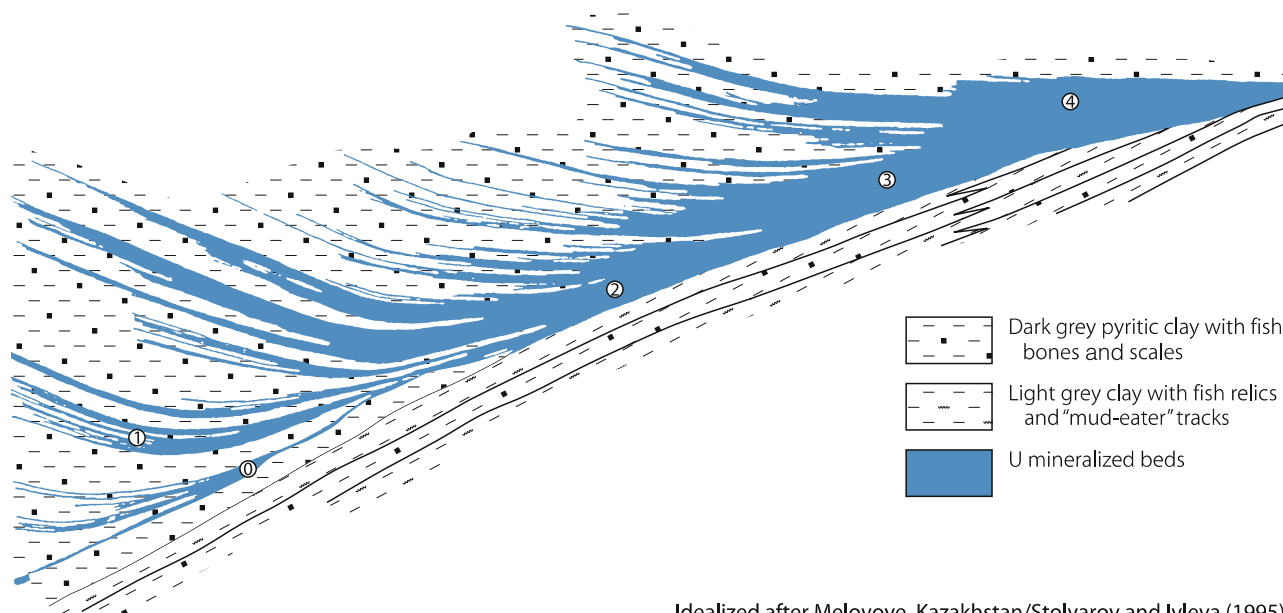
LAM: Lower Anderson Mine Member (Lower clastic unit): Arkosic and volcanic sandstone-conglomerate, reworked andesite lapilli bentonitic siltstones

Oligocene(?) to Eocene(?)

Arrastra Volcanics: Basalt, andesite, andesitic tuff, interstratified conglomerate

■ Fig. I.16.

U-deposit Type 16: uraniferous organic phosphorous deposits (Mangyshlak type)



Idealized after Melovoye, Kazakhstan/Stolyarov and Ivleva (1995)

rare. Elements enriched to various degrees in carbonaceous uranium ore include Mo, V, As, S, and in lesser amounts Ag, Au, B, Cu, Ga, Ge, Mn, and Ti.

Oxidized zones contain very fine carnotite as cement, fine coatings and coarse-fibrous fillings in fractures and along bedding planes, or with hematite in jasper pods. It also occurs as

uraniferous silica in massive jasper and in small silica veinlets. Oxidized mineralization is confined to fractured, highly silicified, oxidized mudstone, tuff, limestone, and marlstone with abundant megascopic plant debris.

Resources are small to medium and grades low (<10 to > 10 000 t U, <0.1–0.6% U).

Type example: Anderson Mine/Date Creek Basin, Arizona, USA (Resources: >12 000 t U, <0.06% U including 5 000 t U at 0.03–0.12% U, av. 0.06% U). *References:* Otton 1981, 1986; Sherborne et al. 1979.

Type 16 Uraniferous Organic Phosphorous Deposits (Mangyshlak Type) (Fig. I.16)

(Russian terminology: *Exogenic sedimentational-diagenetic; Rare-earth – uranium deposits in clays with fish remains*)

U-Sc-REE mineralization is bound to detritus of phosphatized fish remains in superjacent stacked clay beds enriched in fish bones, fish scales, and pyrite and melnicovite concretions. These mineralized beds are intercalated in a dark clay unit and occur in shallow (low energy) marine Tertiary basins in the northern Caspian Sea region/Kazakhstan-Russia. U resources are medium to large (<50 000 U) but grades are very low (av. 0.02–0.06% U, 0.5–2.1% total REE, 10–70 ppm Sc).

Type example: Melovoye/Karagiin OF, Pricaspian District, Mangyshlak Peninsula, W Kazakhstan [Remaining resources: 44 000 t U; mined ore averaged 0.042% U (fish bone concentrate 0.185% U, 30% P₂O₅), 0.178% REE (mainly Ce, La, Y, Nd), 0.06% Ni, 4.32% P₂O₅, 11.1% S (in pyrite)]. *References:* Abakumov 1995; Laverov et al. 1992b, c; Petrov et al. 1995; Stolyarov and Ivleva 1995.

Type 17 Uraniferous Mineralochemical Phosphorite Deposits (Idaho Phosphoria and Florida Land Pebble Types) (Fig. I.17)

Uraniferous phosphorite deposits consist of syndimentary, stratiform disseminated uranium in marine phosphorite of

continental-shelf origin. U is bound in cryptocrystalline fluor-carbonate apatite. Phosphorite deposits constitute large uranium resources, but at a very low grade (several million t U, av. <20 to 300 ppm U).

Two main varieties of uraniferous phosphorite are recognized: (a) bedded phosphorite (Idaho Phosphoria type) and (b) land pebble (Florida type). Both are of widespread extension (up to several 1 000's of km²) and exhibit a rather uniform U distribution throughout a given bed.

a Bedded Uraniferous Phosphorite

Bedded uraniferous phosphorite consists of phosphatic shale with oolitic, pisolitic, pelletal, and laminated textures interbedded with fine-grained miogeosynclinal facies (black shale, mudstone, chert, rare carbonate beds). Bedded phosphorites formed distal to shore-line and commonly contain a higher uranium content as nodular phosphorite.

Type example: Permian Phosphoria Formation/Montpelier, Idaho, USA (Resources: several million t U, 60–200 ppm U). *Reference:* McKelvey et al. 1956.

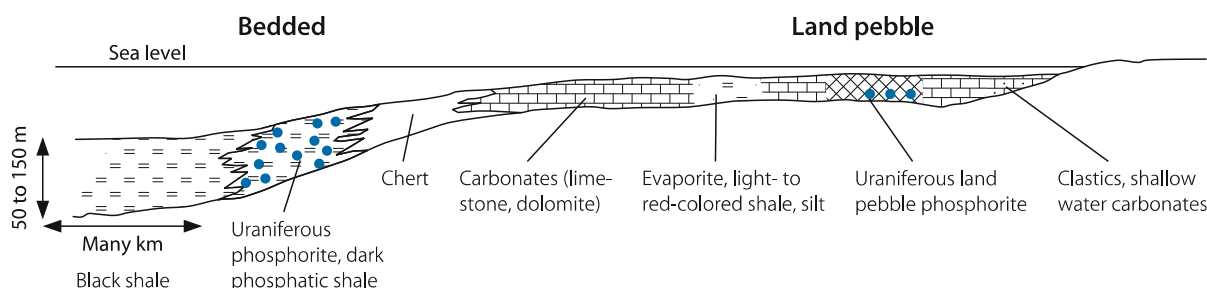
b Land-Pebble Phosphate

Land-pebble phosphate mineralization is composed of U enriched apatite pebbles within nodular phosphorite beds interbedded with fine- to medium-grained shallow marine facies (sand, clay) and carbonate beds. The “land pebbles” formed proximal to shore line by local reworking and leaching of nodular phosphorite leading to secondary U enrichment in the pebbles.

Type example: Pliocene Bone Valley Formation/Land Pebble District, central Florida, USA (Resources: >500 000 t U, grades average ca. 150 ppm U over <1–10 m thickness, and 2 500 km²). *Reference:* Altschuler et al. 1958.

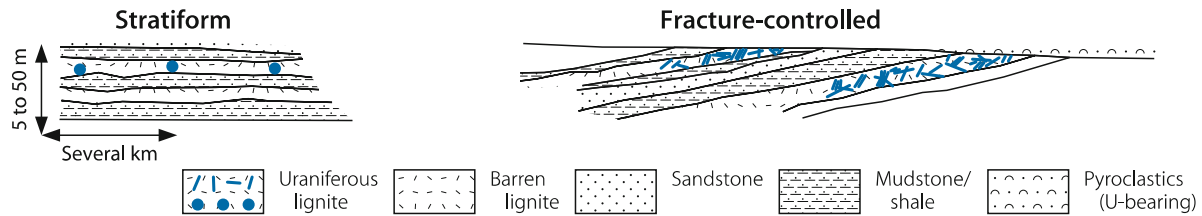
Fig. I.17.

U-deposit Type 17: uraniferous mineralochemical phosphorite deposits (Idaho Phosphoria and Florida Land Pebble types)



■ Fig. I.18.

U-deposit Type 18: uraniumiferous lignite/coal deposits (Cave Hills and Freital types)



Type 18 Uraniferous Lignite/Coal Deposits (Cave Hills and Freital Types) (Fig. I.18)

Uraniferous lignitic seams are interbedded with \pm carbonaceous clastic sediments in paludal, low-lying, poorly drained shallow depressions located either on coastal plains (paralic lignite) or within land-locked basins (limnic lignite). Uraniferous felsic pyroclastics (rhyolitic tuff, etc.) often overlie and/or are intercalated with the seams. Granite or other rocks with anomalous U contents are common near these basins.

Uranium occurs in lignite/coal mixed with mineral detritus (silt, clay), and in immediately adjacent carbonaceous mud and silt/sandstone beds. Pyrite and ash contents are high. U is largely adsorbed on carbonaceous matter or bound in uranyl-humate. Discrete U minerals can locally occur. A variety of metallic trace elements are commonly present.

U occurs in two modes: (a) as *stratiform-syngenetic*, uniformly disseminated mineralization and (b) as *mixed stratiform/fracture-controlled epigenetic*, spotty and irregularly distributed mineralization. Resources are commonly small (<5 000 t U). Grades of syngenetic U mineralization are very low (<150 ppm U) and of epigenetic deposits low to medium (0.03–0.15% U).

Type example of mixed stratiform-fracture-controlled mineralization: (a) Cave Hills-Slim Buttes/SW Williston Basin, S Dakota, USA (Production: 290 t U, <0.1% U). *Reference:* Denson and Gill 1965. (b) Freital-Gittersee/Döhlen Basin,

Saxony, Germany (Production 3 700 t U, 0.12% U). *References:* Wismut 1999.

Type 19 Uraniferous Stratiform Black Shale Deposits (Ranstad and Chattanooga Types) (Fig. I.19)

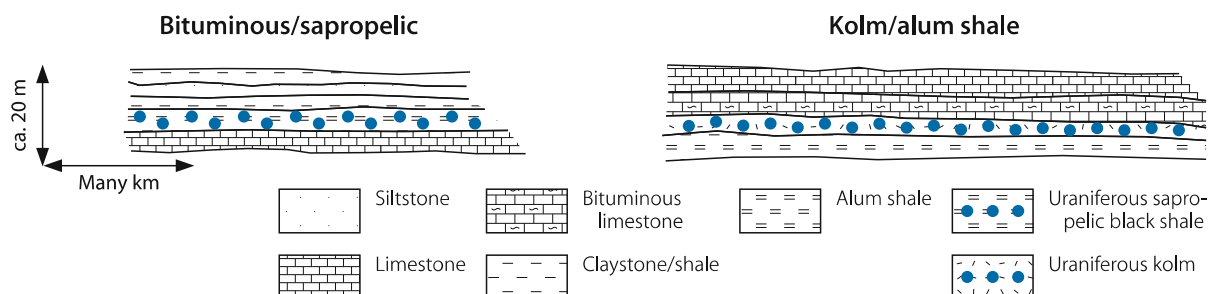
Stratiform black shale hosted uranium mineralization consists of syndepositional, uniformly disseminated uranium adsorbed on organic and clay particles in marine organic-rich, pyritic shale with thin coalified, phosphatic and/or silty intercalations. Discrete primary U minerals are absent. Other metals (Cu, Cr, Mo, Mn, REE, V, P) occur in small quantities. The organic matter is of sapropelic-bituminous or humic, coaly nature derived from planktonic marine algae and land plant (wood spores) debris. Limestone, sand/siltstone, and shale strata complete the stratigraphic sequence.

Mineralized black shale beds are of fairly uniform thickness (few meters to some 10 m), widespread extension (several 100s to 10 000s km²), and host enormous quantities of uranium but of very low U tenors. Better grades are confined to beds (dm to m thick) rich in organics, particularly humic-coaly material. If phosphate nodules are present, they normally contain more U than the surrounding shale. Resources are large and grades very low (several 100 000 t U to many million t U; 50–400 ppm U).

References general: Bell 1978; Carlsson and Nojd 1977; Kim 1988; Mutschler et al. 1976.

■ Fig. I.19.

U-deposit Type 19: uraniumiferous stratiform black shale deposits (Ranstad and Chattanooga types)



Quirt 1984; Hoeve and Sibbald 1978; Hoeve et al. 1980; IAEA 1986a; IAEA/Ferguson 1984; IAEA/Finch 1985b; IAEA/Fuchs 1986; IAEA/Pretorius 1987; IAEA/Toens 1984; IAEA/UDEPO 2007; Ischukova 1997; James and Hamani 1999; Jefferson et al. 2007; Jefferson and Delaney 2007; John 1978; Johnson et al. 1987; Jong Hwan Kim 1988; Karimov et al. 1996; Kazansky 1970; Kazanzky and Laverov 1977; Kolektiv 1984, 2003; Komínek 1997; Komínek and Veselý 1986; Kotzer and Kyser 1995; Lainé et al. 1985; Lange and Freyhoff 1991; Lanier et al. 1978; Laverov et al. 1992; Leroy and Cathelineau 1982; Leroy 1978a,b; Leroy et al. 1985, 1987; Mann and Deutscher 1978; Mashkovtsev et al. 1997, 2002; Mathews et al. 1979; Maurice 1982; McKay and Miezitis 2001; McKelvey et al. 1956; Mickle and Mathews 1978; Miguta and Tarkhanov 1998; Mineeva 1984; MSRandD 1978; Mutschler et al. 1976; Nash et al. 1981; Naumov et al. 2005; Needham et al.

1988; Orajaka 1981; Otton 1981, 1986; Pagel 1984; Pagel et al. 2003; Pardo-Leyton 1985; Pavlenko 2005; Perelman 1980; Petroš et al. 1986; Petrov et al. 1995, 2000; Phalaborwa Mining Co. 1976; Polito et al. 2005; Poty et al. 1986; Pretorius 1976a,b, 1981; Reeve et al. 1990; Robertson 1989; Roslyi 1975; Roubault 1958; Roy et al. 2006; Ruhrmann 1986; Ruzicka 1971, 1988; Samama 1984; Shcherbakov 1966; Schmitt and Clement 1986; Sherborne et al. 1979; Sibbald and Petruk 1985; Sibbald 1988; Sørensen et al. 1974; Stoikov and Bojkov 1991; Stolyarov and Ivleva 1995; Terentiev and Naumov 1997; Thamm et al. 1981; Thomas et al. 2000; Thompson et al. 1980, 1982; Thoste 1999; Tourigny et al. 2007; Tremblay 1982; Turner-Peterson et al. 1986; US-AEC 1959; von Backström 1975, 1976; Wallace 1986; Wang and Li 1996; Wenrich and Sutphin 1989, 1994; Wilde 1988; Wismut 1999; WMC Oct. 2004; Ziegler 1974.



Uranium in Asia – Overview

In 2004, uranium resources in Asian countries recoverable at less than U.S.\$130 per kg U amounted to some 850 000 t RAR and 450 000 t U inferred resources (= EAR-I) or 26% and 31%, respectively, of world total resources (3.3 million t U RAR, 1.45 million t U inferred resources) (U in phosphorite excluded) (OECD-NEA/IAEA 2005). The bulk of these resources occurs in Kazakhstan, Mongolia, Asian Russia, and Uzbekistan. These four countries host large minable deposits with resources in excess of 10 000 t U while China, India, Japan, Kyrgyzstan, Pakistan, Tajikistan, and Turkmenistan contain(ed) (partly exhausted) chiefly small to medium size deposits (<500 to 10 000 t U). Minor resources are also reported from Indonesia, Iran, South Korea, Turkey, and Vietnam.

In the past, uranium mining took place in China, India, Kazakhstan, Kyrgyzstan, Mongolia, Pakistan, Russia, Tajikistan, Turkmenistan, and Uzbekistan, where from 1945 to 2006 about 500 000 t U were produced, out of a world total in excess of 2.3 million t U in that period (OECD/NEA 2006). Iran and Japan produced some minor amounts mainly by test mining. Presently (2006) uranium mining is restricted to Kazakhstan, Asian Russia, Uzbekistan, China, India, and Pakistan, and probably Iran. The first six countries produced combined 10 000 t U in 2004 (= 25% of world U production), 90% of which derived from the first three countries.

Uranium deposits of sandstone and volcanic types constitute the largest uranium endowment in Asia. Other deposits are mainly of granite-related vein, carbonaceous shale-related stockwork, metasomatite, intrusive, bituminous-cataclastic limestone, organic phosphorous, and lignite/coal types.

Most major U deposits occur in an arcuate belt from the southern Ural mountains and Caspian Sea through central Asia into Transbaykalia, northern Mongolia, and northern China. This *Central Asian Mobile Belt* evolved from Late Paleozoic to Triassic between the Siberian Continental Block (or Platform) to the north and the Tarim-North China (Sino-Korean) Block to the south. Caledonian and Hercynian fold belts composed of Precambrian and Early (to Middle) Paleozoic rocks including Late Proterozoic granite occur between these blocks. Paleozoic igneous intrusions and extrusions include Caledonian granite, granodiorite, and granosyenite, and Hercynian leucogranite and alkaline granite as well as Middle to Late Paleozoic intermediate to felsic volcanics and pyroclastics.

Tectono-magmatic reactivation associated with igneous intrusions and volcanic extrusions affected this belt during the Mesozoic. Finally, Alpine orogenies generated the high ranges of the Tien Shan, Kunlun Shan, and Altai mountains that intervene or fringe this belt to the south. Intracratonic and intermontane Mesozoic to Cenozoic sedimentary basins cover parts of this belt.

Major U deposits of sandstone, volcanic, and other types are essentially related to the Mesozoic tectono-magmatic reactivation

as reflected by isotope ages of their uranium mineralization. An exception tends to be Late Caledonian *vein-type* mineralization in the Kokshetau region, northern Kazakhstan, that was, however, repeatedly modified, during Triassic-Jurassic and Tertiary times; and *carbonaceous shale-related stockwork* deposits in the Kyzylkum uplifts in Uzbekistan, which have roots in the Hercynian Orogeny but were regenerated during the Neogene-Quaternary as suggested by ages ranging from 400 Ma to Recent.

The Elkon District in eastern Siberia represents another district with *vein-type* U deposits. Located in the Precambrian Aldan Shield in southern Yakutia, this district contains brannerite and gold mineralization of only Mesozoic age in large rejuvenated Early Proterozoic faults.

Significant *sandstone-type* U deposits occur in intermittent intracratonic Cretaceous-Tertiary basins at the southern margin of the Turan Platform in Uzbekistan (Kyzylkum Basins) and Kazakhstan (Syr Darya-Chu Sarysu Basins). This southern chain of basins continues eastwards with the Ily Basin in SE Kazakhstan and the Yili, Junggar, and Turpan-Hami Basins in NW China. Similar basins with *sandstone-type* U deposits are known in the Eren and Ordos Basins, northern China, and in the Gobi Desert, south Mongolia. To the north of this zone, basal-channel sandstone-type U deposits are located in the Transural, West Siberian, and Yenisey regions at the southwestern and southern margin of the Jurassic West Siberian Basin and, further east, in intermontane basins in Transbaykalia in Russia.

Large *volcanic-type* U deposits occur in the Streltsovsk (Russia), and Mardai/Dornod (Mongolia) Districts in the Mongol-Argun intracontinental volcanic belt. Other districts with mostly small volcanic-type U deposits are in the Karakum (Turkmenistan), Pribalkhash (Kazakhstan), Karamazar (Uzbekistan-Tajikistan), and Transbaykalia (Russia) regions.

Bituminous-cataclastic limestone-type U deposits occur at the northern margin and *Karst-related pipe-type* U deposits occur at the southern margin of the Fergana Valley in Kyrgyzstan.

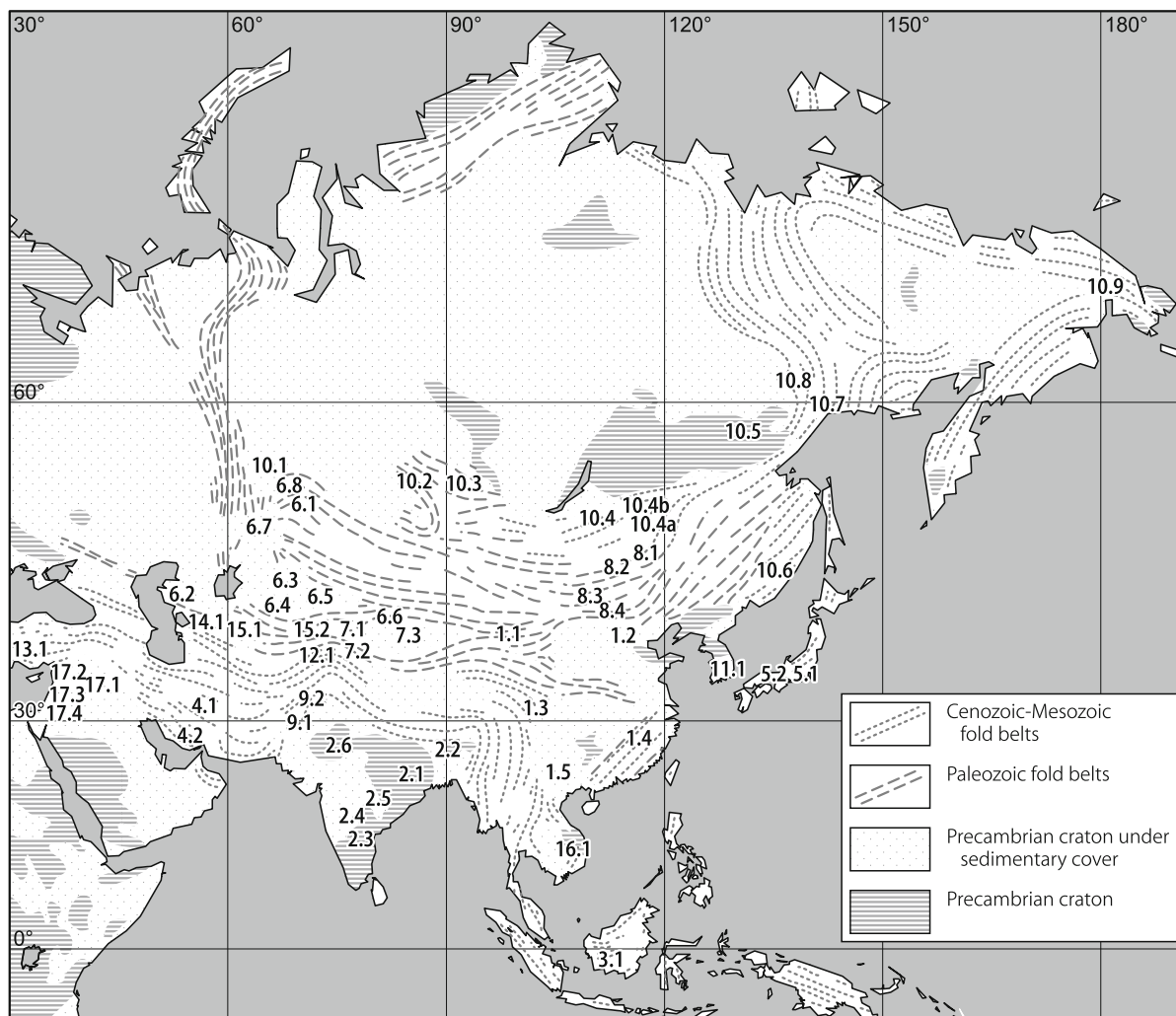
In contrast to the Central Asian region, major U deposits have not yet been discovered in *western, southern, and eastern Asia*. The most prominent U province is in South China. This region is well known not only for numerous uranium deposits, but also for deposits of Bi, Cu, Mo, Pb, REE, Sn, W, and Zn.

The South China U province overlaps the southeastern margin of the Yangtze Massif and the easterly adjacent Nanhua Mobile Zone (or South China Caledonian fold belt). This terrane evolved from the Caledonian Orogeny but was reactivated by intense Indosinian and Yanshanian tectono-magmatic activity associated with emplacement of granitic batholiths and intermediate to felsic volcanic activity. U deposits commonly comprise small *granite-related vein deposits* associated with Late Yanshanian granite, *volcanic deposits* that evolved from Late Jurassic and Early Cretaceous volcanism, and *black shale-related stockwork U types* (in China referred to as carbonate-siliceous-pelite type), which have roots in pre-Mesozoic events but which essentially formed during Yanshanian and Himalayan tectonism. Some minor sandstone-type U deposits are known from Late Cretaceous and Paleogene redbed basins.

Small *sandstone-type U deposits* have been identified in southwestern (West Yunnan U province) and northeastern

■ Fig. II-1.

Simplified geotectonic map indicating the location of uranium regions (numbers correlate with chapters in text). **China:** 1.1 Junggar-Tien Shan U province, 1.2 Yinshan-Liaohe U province, 1.3 Qilian-Qinling U province, 1.4 South China U province, 1.5 West Yunnan U province. **India:** 2.1 Singhbhum Belt, 2.2 Meghalaya Plateau, 2.3 Cuddapah Basin, 2.4 Bhima Basin, 2.5 Chattisgarh Basin, 2.6 Aravalli-Delhi Basins. **Indonesia:** 3.1 Kalan Dist. **Iran:** 4.1 Bafq reg., 4.2 Bandar Abbas reg. **Japan:** 5.1 Tono Dist., 5.2 Ningyo-Toge Dist. **Kazakhstan:** 6.1 Kokshetau reg., 6.2 Pricaspian (or Mangyshlak) reg., 6.3 Chu-Sarysu Basin, 6.4 Syr-Darya Basin, 6.5 Pribalkhash reg., 6.6 Ily reg., 6.7 Zhalanshiksky reg., 6.8 Turgai-Priyrtish reg. **Kyrgyzstan:** 7.1 Eastern Karamazar reg., 7.2 Tyuya-Muyun Dist., 7.3 Central Kyrgyzstan coal basins. **Mongolia:** 8.1 North Choibalsan reg., 8.2 Berkh reg., 8.3 Dornogovi reg., 8.4 Gobi-Tamtsag reg. **Pakistan:** 9.1 Sulaiman Range, 9.2 Bannu Basin. **Russia, Asian Territory:** 10.1 Transural reg., 10.2 West Siberian reg., 10.3 Yenisey reg., 10.4 Transbaykal reg. (10.4a Streltsovsk Dist., 10.4b Vitim Dist.), 10.5 Aldan Shield reg., 10.6 Far East reg., 10.7 Okhotsk reg., 10.8 Southern Kalyma River reg., 10.9 Chukotsky reg. **South Korea:** 11.1 Okchon reg. **Tajikistan:** 12.1 Kuramin Range. **Turkey:** 13.1 Menderes Massif. **Turkmenistan:** 14.1 Western Karakum reg. **Uzbekistan:** 15.1 Kyzylkum region, 15.2 Karamazar reg. **Vietnam:** 16.1 Nong Son Basin. Middle East countries with uraniferous phosphorite: 17.1 Iraq (Akashat area), 17.2 Syria (Palmyra reg.), 17.3 Israel (Negev Desert), 17.4 Jordan (western reg.)



China (Qinglong ore field, Yinshan-Liaohe U province), India (Meghalaya Plateau), Japan (Tono and Ningyo-Toge ore fields, Honshu island), Pakistan (Dera Ghazi Khan and Bannu Basin), and Vietnam (Nong Son Basin).

India reports a number of U occurrences of various types but only *vein-type U deposits* in the Singhbhum District; NE India, have seen production. Several sites with vein-type(?) mineralization are also identified on Kalimantan, Indonesia.

In *western Asia*, some minor deposits of *metasomatite type* exist in central Iran and of *sandstone type* in Turkey. A unique

U occurrence is located near Bandar Abbas, southwestern Iran, where U mineralization is associated with volcanic xenoliths or surficial sediments in a salt plug.

Uraniferous *phosphorite* exists in Iraq, Israel, Jordan, and Syria. These phosphorite deposits form part of the Mediterranean phosphorite belt, which extends from southwestern Turkey to Morocco. Other countries in Asia also contain phosphorite deposits but no figures are available on uranium contents or on uranium extraction, if any, from active phosphorite mines.

Chapter 1

China, Peoples Republic of

Uranium deposits are known from five uranium provinces and some separate areas (Fig. 1.1, and discussed below) but no complete uranium inventory of China is published since uranium resources are a state secret. Available information on resources is scanty, incomplete, and burdened with discrepancies. It is unclear whether reported figures document original resources or the resource status at a specific mining stage. Therefore, data on resources should be treated with caution. Taking this into account, available information suggests the following general picture of China's present resource situation (status 2002).

OECD-NEA/IAEA (2005) reports 85 000 t U (RAR and EAR-I) remaining resources. Resource figures are not classified by production costs hence, the resource fraction, which might be exploitable under any particular set of market economic conditions remains an open question.

Independent of deposits type, almost two thirds of China's uranium resources are of low to medium grade (about 0.05–0.2% U) and small tonnage, on the order of some hundreds to a few thousands tonnes of uranium, and rarely more. A few districts, however, may contain in excess of ten thousand tonnes of uranium as shown in Table 1.1. This situation is reflected by a distribution of deposit sizes in reference to the national resource quantity reported by Wang Jian and Dai Yuan Ning (1993). 31% of China's resources are in deposits containing less than 1 000 t U and 30% in deposits of 1 000–3 000 t U. Applying a grade attribution, 51.5% of the national resources are contained in ore grading from 0.1 to 0.2% U and 31.1% in ore with less than 0.1% U.

A distribution of uranium resources by deposit type shows that the bulk of the resources is contained in four types (Table 1.2): Granite-related deposits account for some 37% of the total resources, sandstone-type deposits for 24%, volcanic-related deposits for 19%, and carbonaceous-siliceous-pelite (C-Si-pelite)-type deposits for 16%. The remaining 4% are attributed to metasomatite, intrusive (pegmatite/pegmatitic granite, alkaline syenite), quartzite, and phosphorite hosted mineralization. (percentage figures from OECD-NEA/IAEA 2001).

As illustrated above, the largest fraction of China's uranium resources is still attributed to granite-related deposits. This relationship has probably changed in favor of sandstone deposits since important exploration progress has been achieved with the discovery of the Shihongtan deposit in the Turpan-Hami Basin, Xinjiang Uygur A.R. and deposits in the Zaohuohao/Dongsheng area, Ordos Basin, Inner Mongolia (according to information from the bimonthly magazine "Uranium Geology" published in Chinese with abstracts in English, sponsored by Uranium Geology Branch of the China Nuclear Society).

Uranium production figures were kept secret until 1990 and it can only be speculated that annual production varied mostly between 500 and over 1 000 t U in the 1970s and 1980s.

OECD-NEA/IAEA (2003, 2005) estimates that, since 1990, annual production rates varied between a maximum of 955 t U in 1992 and a minimum of 480 t U in 1994, and were on the order of 730 t U in the early 2000s. According to OECD-NEA/IAEA (2005) production totaled 28 419 t U through 2004.

Responsibility for the nuclear industry is vested in the state agency *China National Nuclear Corporation* (CNNC). CNNC was founded in 1988 and succeeded the former "Ministry of Nuclear Industry" that had previously replaced the "Second Ministry of Industry". CNNC reports to the "Council of State". Uranium exploration and mining are in the hands of two branches of CNNC, the *Bureau of Geology* (BOG) and the *Bureau of Uranium Mining and Metallurgy* (BOMM), respectively.

The following description is primarily based on Liu Xingzhong and Zhou Weixun (1990), Zhou Weixun (1997, 2000 and pers. commun. 2002), Zhou Weixun and Teng R (2003), Zhou Weixun et al. (2002, 2006a) amended by data from other sources mentioned.

Historical Review of Uranium in China

Little is recorded about uranium occurrences in China known prior to World War II. Systematic exploration for uranium got under way in 1955 under the direction of the Bureau of Geology (BOG) of the Second Ministry of Industry, and its successor, the Ministry of Nuclear Industry, initially with assistance and supervision of Soviet experts.

In hindsight, the uranium *exploration history* can be divided into four periods. From the mid 1950s through the mid 1960s, prospecting was carried out countrywide and was focused on detecting outcropping uranium deposits. These efforts met with success in 1955, when some lignite-type uranium deposits including Daladi and Mengqiguer (for types of deposits see Part I: *Typology of Uranium Deposits*) and later in the 1950s when the sandstone-type deposits 511 and 512 were discovered in Jurassic sediments in the intermontane Yili Basin in Xinjiang-Uygur Autonomous Region, NW China (Fig. 1.1). Subsequent discoveries in 1956 included the volcanic-type Baiyanghe deposit in Upper Paleozoic volcanics to the north of the Yili Basin, and the Pukuitang deposit in Cretaceous-Tertiary sandstones near Hengyang in Hunan Province, S China. In 1957, an endogranitic vein-type uranium deposit was found in what would become the Xiwang District (Jiangxi-Guangdong Provinces) in the Guidong granite massif located in the central part of the Nanling tectono-magmatic belt. Also in 1957, the first discovery of a volcanic-type deposit was made in what later became the Xiangshan District within the Gan Hang volcanic belt in the Jiangxi-Zhejiang Provinces, S China. Other discoveries of this period included Chenzhou (C-Si-pelite-type) and Dabu (sandstone-type) in Hunan Province, S China.

From the mid 1960s to the mid 1970s, exploration in the vicinities of established uranium occurrences and in formerly untouched regions with conceptually and technically more sophisticated methods resulted in the discovery of a number of deposits in South China including the C-Si-pelite-type Chanziping deposit, Guangxi A.R., and vein-type deposits associated

Fig. 1.1.

Generalized outline of uranium provinces and approximate location of reported U districts, basins and deposits in China (for details of South China see Fig. 1.27) (U provinces modified after Liu Xingzhong and Zhou Weixun 1990).

Deposit types: C-Si: pel carbonaceous siliceous pelite; grt granite-, metasom metasomate-, volc volcanic-related; intr intrusive; ss sandstone; ve vein. **J-T Junggar-Tianshan U Province** (Mesozoic basins: BB Burqin, JB Junggar, KD Kashi Depression, TB Tarim, T-HB Turpan-Hami, YB Yili); 1 U zone at south margin of Yili Basin; 2 U zone at north margin of Yili Basin; 3 Baiyanghe (volc), N Tien Shan; 4 Bashi Bulak (ss), KD; 5 Shihongtan (ss), T-HB. **Y-L Yinshan-Liaohu U Province** (LR Liaoning Region; Mesozoic basins: CB Chelaomiao, EB Eren (Erlian), GB Gangou, LB Liaohu, OB Ordos); 1 Benxi (metasom ve)/Lianshanguan Dome, LR; 2 Saima (intr, peralk syenite), LR; 3 Qinglong OF (ss, volc?), GB; 4 Guyuan-Duolun area (volc); 5 Nuheting and Subeng (ss), EB; 6 Bayantala Sag, EB; 7 Chelaomiao (deposit 110, ss), CB; 8 Dongsheng area (ss), OB. **Q-Q Qilian-Qinling U Province** (Fold belts: LFB Longshoushan Fold Belt, NQFB North Qinling Fold Belt, SQFB South Qinling Fold Belt); 1 Hongshiquan (intr, alaskite), LFB; 2 Jiling (metasom ve), LFB; 3 Lantian (grt ve), NQFB; 4 Chenjiazhuang/Danfeng area (intr, peg), NQFB; 5 Wudang-Huaiyong Massif (ss); 6 Lu Zong Volcanic Basin; 7 Ruergai District No. 512, deposit 512/Luojungou (C-Si-pel), SQFB; 8 Ruergai District No. 512, deposit 510/Larma (C-Si-pel/Au associated with U), SQFB. **W-Y West Yunnan U Province:** 1 Gaoligong region, Tengchong-Lianghe and Longchuanjiang basins (ss); 2 Lincang region, Bangmai Lincang, Mengwang basins (ss). **S-CH South China U Province** (details in Fig. 1.27). **DHE Da Hinggan-Ergun U Zone/Manzhouli area (volc)**

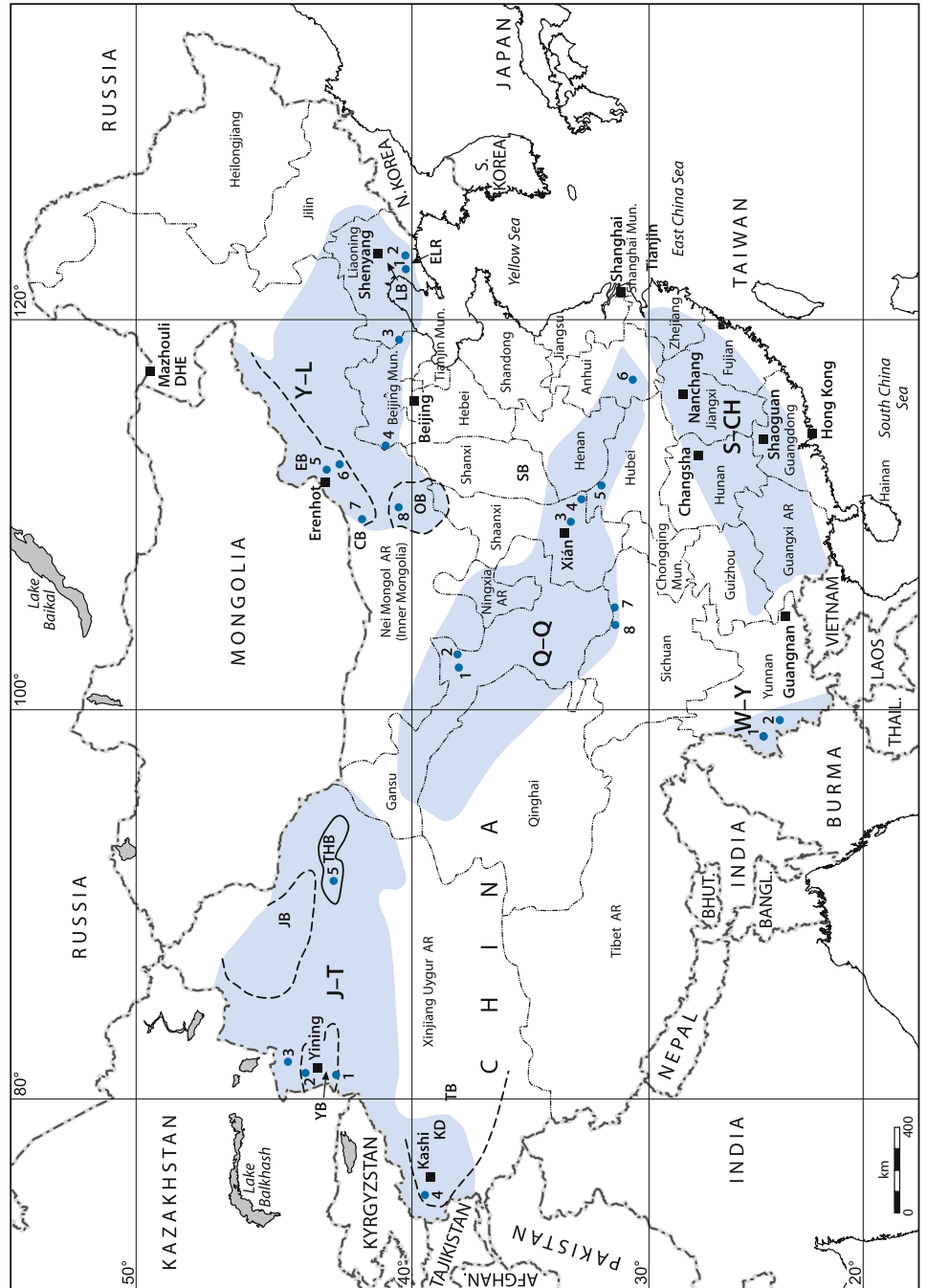


Table 1.1.

Status of in situ uranium resources of selected districts and deposits in China reported by OECD-NEA/IAEA (2005)

District/deposit, province	Deposit-type	Resources (t U)	Remarks/status
1 Junggar-Tien Shan Uranium Province			
Yili dep., Xinjiang Uygur AR	Sandstone	13 000	Active, ISL
Shihongtan dep., Xinjiang Uygur AR	Sandstone	3 000	
2 Yinshan-Liaohu Uranium Province			
Qinglong ore field, Hebei	Sandstone	8 000	Delayed
Zaohuohao, Inner Mongolia	Sandstone	5 000	
3 Qilian-Qinling Uranium Province			
Lantian dep., Guangxi	Granite	2 000	Active, UG
4 South China Uranium Province			
Xiangshan dist., Jiangxi	Volcanic	26 000	Active, UG
Xiazhuang dist., Guangdong	Granite	12 000	Active, UG
Chanziping dep., Guangxi	C-Si-pelite	5 000	Standby, UG
Chenxian dep., Hunan	C-Si-pelite	5 000	Standby
5 West Yunnan Uranium Belt			
Tengchong dep., Yunnan	Sandstone	6 000	Closed?
Subtotal		85 000	
Resources reported in various other reports			
Eren Basin, Inner Mong. AR	Sandstone	>10 000	Expl, ISL test
Benxi dep., Liaoning	Metasomatite	~1 000	Active, UG
Danfeng dep., Shaanxi	Intrusive	>1 000	Standby, UG

Note: There are more districts with resources but quantities are not available. It is also unknown just how much uranium has been extracted from the listed districts. By applying the estimated production amount of approximately 7 000 t U since beginning of 1991, the given reported resources should be reduced by this amount unless they are balanced by exactly this amount due to recent discoveries.

Remarks/status: ISL in situ leaching, UG underground, OP open pit.

Table 1.2.

China, percentage share of resources of types of deposits and common ranges of size and grade of individual deposits (Finch et al. 1993; OECD-NEA/IAEA 1997, 2001)

Type/subtype of deposit	Share of total resources (%)		Common ranges of deposits	
	1997	2001	Size (t U)	Grade (% U)
Granite	38.11	36.67	500–3 000	0.1–1
Volcanic	19.51	18.76	500–1 000	0.03–0.1
Sandstone	21.34	24.55	500–5 000 ^a	0.03–0.1
C-Si-pelite ^b	16.40	15.67	500–3 000	<0.1–1
Intrusive/pegmatite	3.05	2.88	500–3 000	<0.1–1
Intrusive/syenite ^c	0.61	0.58	500–3 000	<0.1–1
Metamorphite/quartzite	0.61	0.59		
Phosphate	0.31	0.30		

^a Locally >10 000 t U. ^b Carbonaceous-siliceous pelite. ^c Alkaline rock type.

with granites and volcanics in Jiangxi and Guangdong Provinces. Several sandstone-type deposits were found in Tertiary basins in Yunnan Province in what became the West Yunnan uranium belt. Discoveries in northeastern China included the sandstone-type deposits Qinglong, Hebei Province, and Jianchang, Liaoning Province, and some deposits associated with Silurian siliceous limestone of presumable C-Si-pelite-type in eastern Sichuan and Qinghai Provinces in central China.

From the mid 1970s into the 1980s, exploration focused on unexplored areas in the North China Platform (e.g. Erlian Basin,

Inner Mongolia Autonomous Republic, exploration started in 1980), and in northeast China where additional resources in volcanic- and sandstone-type deposits were discovered in the Yanliao metallogenetic belt. Additionally, new deposits were found in established uranium areas in southern China.

Since the 1980s, exploration efforts have been concentrated on finding new deposits with better economic characteristics in terms of grade, reserves or extraction amenability than those of most of the earlier established deposits. Success was achieved in the Eren (or Erlian) Basin where the sandstone-type deposits

Subeng and Nuheting were discovered in 1986 and 1990, respectively. From 1990 onwards, ISL amenable sandstone uranium deposits have become the prime target for exploration. Both, the Shihongtan deposit and the Dongsheng U area were discovered during this period.

The uranium *mining history* of China started with the development of the first uranium mines and mills in 1958. Operation of the Chenzhou and Dabu mines as well as of the Hengyang mill (all in Hunan Province) commenced in 1962 and 1963. Construction of the second group of production centers began in 1963 and included the #721 mill in the Fuzhou region, Jiangxi Province (also referred to as Fuzhou plant) and the mill and mine complex in the Yining area, Xinjiang-Uygur A.R. The Fuzhou mill became operational in 1966. Fuzhou received ore from volcanic-type uranium deposits in the Xiangshan District. Four of these mines went into production in 1965 and 1966. In 1976, the Yining plant began processing lignite-type ore from the Daladi and Mengqiguer deposits in the Yili Basin.

Almost twenty processing plants served by a number of mostly small mines had been active in China prior to the restructuring of the uranium industry in the course of the adjustment to a market oriented system in the 1980s. CNNC and its predecessors operated most of the plants but local governments also operated a few small ones. Since the 1980s, thirteen plants have been closed or put on standby.

Heap leaching has been tested at a number of uranium deposits since the early 1960s, and underground block leaching has been tried since 1969. It was not until the late 1980s, however, that commercial application of heap leaching was introduced at two granite-related deposits; first, in 1989, at the Chongyi mine, Jiangxi Province, and in 1993 at the Lantian mine, Shaanxi Province. At Lantian, uranium has also been recovered by underground block leaching since 1992.

Principal Characteristics and Distribution of Types of Uranium Deposits in China

A variety of types of uranium deposits have been identified in China, but the bulk of the minable reserves are confined to, and 95% of China's past uranium production derived from four prevailing types which are summarized below based on Finch et al. (1993), Liu Xingzhong and Zhou Weixun (1990), and Zhou Weixun (1997).

Granite-related deposits are subdivided into intracontact and exocontact subtypes, which correspond in western terminology to vein-type, intragranitic and perigranitic deposits, respectively. Deposits of this type are typically hydrothermal veins controlled by silicified fault and fracture zones. They generally occur within Mesozoic granite batholiths, and, in part, in sedimentary rocks within their exocontact aureole or adjacent basins. Pitchblende and minor coffinite are the principal U minerals. Gangue minerals include microquartz, fluorite, calcite, and clay minerals. Mineralizing events are dated at 87 Ma, 67 Ma, and 47 Ma ago. Granite-related deposits are commonly of small to medium size (<500 to 3 000 t U), low to medium grade (0.05–0.2% U) and

account for about 37% (OECD-NEA/IAEA 2001) and as such for the majority of China's U resources (▶ Table 1.2). The bulk of granite-related deposits occur in the Nanling tectono-magmatic zone and the central-south Jiangnan granite belt in south China. Some deposits are known from the Xi'an area in central China, the Lianshanguan Dome in northeast China, and the Lower Yangtze granite belt in southeast China.

Volcanic-related deposits consist of structure-bound and strata-bound mineralization controlled by volcanic systems and faults. At least three geostructural settings are distinguished: calderas, and downwarped and downfaulted volcanic basins. Host rocks are Mesozoic felsic volcanics and include subvolcanic bodies, lavas and pyroclastic rocks. Ore assemblages are of a complex nature and may be composed of U, Mo, Ag, and other metals. Mo and Ag are locally recovered as by-products to uranium. Deposits are commonly of small size (<500 to 1 000 t U) and low grade (0.03–0.1% U). Known volcanic uranium deposits account for almost 19% of China's uranium resources (▶ Table 1.2). While the quantity of neither uranium resources nor production is published, volcanic-type deposits are reported to be "one of the most important bases of uranium resources in China." Volcanic-related deposits are prominent in the eastern (Jiangxi-Zhejiang-Fujian) metallogenic zone in southeast China, here particularly in the Gan-Hang volcanic belt, and a few in the Wuyi volcanic belt. Some deposits are known from the Tien Shan mountains, northwest China, and the Qinglong area in the Daxing-anling-Yanshan volcanic belt in Hebei, and the Manzhouli area in Inner Mongolia, both in northeast China.

Sandstone-type deposits are subdivided into the rollfront subtype (in China referred to as interlayered oxidation-type) and basal channel or paleovalley subtype (referred to as phreatic oxidation type). Deposits occur in Mesozoic intermontane basins and in large basins downwarped into platforms. Basements and surroundings of uranium-bearing basins always contain granite and felsic volcanics. Host rocks are carbonaceous, partly arkosic sandstone and conglomerate with variable amounts of clay fractions. Lignite/coal seams and argillaceous horizons are commonly interbedded in the sedimentary sequence. Deposits are, on average, of small to medium size but can exceed 10 000 t U. Grades are low (0.03–0.1% U). Sandstone-type deposits account for 25% (the percentage may have increased recently) of China's uranium resources (▶ Table 1.2). Sandstone-type uranium deposits are reported from the Yili Basin and Kashi Depression/Tarim Basin in northwest China, Eren (Erlian) Basin in central north China, Jianchang and Qinglong Basins in northeast China, west Yunnan Basins in southwest China, and Hengyang and Jingan Basins in south China. Encouraging results have been achieved in the Turpan-Hami and Ordos Basins. Other basins with a potential for uranium deposits include the Junggar Basin in Xinjiang-Uygur A.R. and the Qaidam Basin in Qinghai Province.

Carbonate-siliceous-pelite-type deposits (in this article abbreviated to C-Si-pelite-type) correspond to a large part to the black shale-related stockwork type as defined in the introductory

chapter. Deposits of this type are strata-bound associated with carbonaceous, partly black shale-type (meta-)sediments of Upper Proterozoic and Paleozoic age in which or adjacent to which uranium occurs as structure controlled mineralization in fracture stockworks or, more rarely, in solution openings filled with collapse breccias in impure carbonatic rocks. Uranium mineralization consists predominantly of disseminated replacements confined to altered fracture zones. Ore genesis is thought to be by lexiviation and hydrothermal redistribution of uranium caused by remobilization events during the Mesozoic and Cenozoic eras. Host rocks are distinct sedimentary or slightly metamorphosed sedimentary lithologies composed of siliceous carbonate or pelite dominated facies both of which are enriched in carbonaceous matter. According to the prevailing lithology, four subtypes are distinguished by Zhou Weixun (1997): Sinian-Cambrian straticulate, Devonian-Carboniferous dark carbonate, Lower Permian silicolite, and Silurian silicolite-carbonate subtype. Deposits of the first three C-Si-pelite subtypes are typical for the western metallogenetic zone in south China where they occur in the Xuefeng-Jiuling region, also referred to as Xianggui foreland basin, and Xianggui (downwarped) Basin, Guangxi-Hunan-Jiangxi Provinces, and in the southwestern part of Guizhou Province. The fourth, Silurian silicolite-carbonate subtype, is represented by the Bentou deposit in the Xianggui Basin, S China and the Larma deposit in NE Sichuan Province, central China. Referring to C-Si-pelite deposits in south China, Min (1995) defines three genetic groups: sedimentary-diagenetic, leaching-accumulative, and hydrothermal-reworked. (for more details see Sect. 1.4.3: *Proterozoic-Paleozoic Terrane .../ Western U Metallogenetic Domain*). C-Si-pelite deposits are commonly of small to medium size, have low to medium grades (<0.1–0.2% U) and account for about 16% of China's uranium resources (Table 1.2).

Other types of deposits include metasomatite, intrusive (pegmatite/pegmatitic granite, peralkaline syenite), lignite, and phosphorite. *Metasomatite-type* deposits are known from the Lianshanguan Dome in northeast China, and from the eastern Longshoushan and North Qilian fold belts in central China. *Intrusive-type* mineralization of pegmatite subtype is reported from the currently (2003) mined Danfeng deposit in central China, and of the peralkaline syenite subtype from the Saima Complex in Liaoning Province, northeast China. Uraniferous *lignite* occurs in several Mesozoic sedimentary basins.

Description of Uranium Provinces, Regions and Districts in China

Most uranium-related publications provide generic geological and metallogenetic descriptions of uranium provinces and types of uranium mineralization. Comprehensive documentation of individual U deposits is scarce. Data on dimensions, grades, and resources are particularly scanty. Figure 1.1 shows the location of uranium provinces, principal districts, and deposits.

Five uranium provinces are recognized in China by Liu Xingzhong and Zhou Weixun (1990):

1. *Junggar-Tien Shan U province* (Xinjiang Uygur A.R.), NW China
2. *Yinshan-Liaohé U province* (Liaoning-Hebei-Inner Mongolia A.R.), N to NE China
3. *Qilian-Quinling U province* (Gansu-Shaanxi-Henan-Hubei), central China
4. *South China U province* (Zhejiang-Jiangxi-Hunan-Guangdong-Guangxi)
5. *West Yunnan U province (or belt)* (Yunnan), SW China

Additionally, some uranium deposits/occurrences are known from other parts of China. They include the Da Hinggan-Erguna zone in northeastern Inner Mongolia A.R. and the Ordos (or Shangangning) Basin in central north China.

1.1 Junggar-Tien Shan U Province, Xinjiang Uygur A.R., NW China

This uranium province covers an area of about 800 000 km² in northern and northwestern Xinjiang Uygur Autonomous Region where it encompasses the intermontane *Yili*, *Junggar*, *Turpan-Hami*, *Burqin*, and northwestern *Tarim* Basins and intervening ranges of the eastern *Tien Shan*. It extends eastwards to the Beishan Range, Gansu Province, and the Badain Jaran Desert, Inner Mongolia A.R. (Fig. 1.1). Established uranium deposits are mainly of sandstone- and lignite/coal-type along with some minor ones of volcanic-type.

Sources of information. Liu Xingzhong and Zhou Weixun 1990; Zhou Weixun 1997, 2000, and pers. commun. 2002; amended by data from other sources mentioned.

Regional Geology and Principal Characteristics of Mineralization

The Junggar-Tien Shan uranium province comprises Precambrian complexes amalgamated to fold belts by the Hercynian Orogeny, which was associated with continental, intermediate to felsic volcanism and intense uplift during the Permian to form the ancient Tien Shan Range. Subsequent erosion and deposition of clastic sediments rich in vegetal debris occurred in downwarped basins from the Early to Middle Jurassic and was followed, after a long hiatus, by sedimentation of continental variegated clastic rock series during the Late Cretaceous and Paleogene.

Uranium occurs in the form of volcanic-, coal-, and sandstone-type U deposits in the Junggar-Tien Shan U province.

Volcanic-type U mineralization is mainly structurally controlled and occurs at the contact between Lower Permian quartz porphyry and intrusive microgranitic porphyry; and to a minor degree in Upper Permian basalt and tuffaceous sandstone adjacent to Precambrian terrane. Wall rocks of the first variety are altered by marked hydromicazation and pink coloration. Veins and veinlets contain pitchblende as the principal U mineral

associated with sulfides, fluorite, and hydromica. U^{6+} minerals (silicates, hydro-oxides, phosphates) are well developed in oxidized intervals as are uraniferous Fe-Mn oxides in which Be content may be as high as 2.5% due to intermixed phenacite. The ore-forming event is dated at about 230 Ma, which corresponds to the post-orogenic tension episode at the end of the Permian.

Coal-type U mineralization is reported from the Yili Basin and is contained in coal seams interbedded with dark clastic sediments of Early-Middle Jurassic age. The coal seams consist of commonly thick and consistent durain with relatively high sulfur content. U mineralized sections are altered by goethitization, carbonatization, and sulfatization. Uranium is mostly adsorbed by organic gel, colloform pyrite, and clay minerals, but also occurs as pitchblende. Associated minerals include pyrite, marcasite, and native selenium. Most of the well-mineralized coal horizons are underlain by clay beds and covered by permeable sandstone. U-Pb isotope dating of pitchblende yields an age of 7.0–5.7 Ma that suggests an epigenetic infiltration of the uranium related to phreatic oxidation.

Sandstone-type U mineralization is known from the coal-bearing Early-Middle Jurassic dark clastic sediments and from Paleogene variegated clastic sediments. In *Early-Middle Jurassic* strata, U occurs in the form of more or less irregularly shaped rolls and lenses in sandstone sandwiched between impermeable clay- or siltstone horizons which fill channels of a braided delta system (at Kujiertai) and of a proximal braided channel zone (Shihongtan). Epigenetic alteration recolored the originally black sandstone to pink by hematitization, yellow by limonitization, or white by argillization. U occurs mainly in form of pitchblende, minor coffinite and brannerite; but also adsorbed on clay minerals, pyrite, and coal debris. Associated minerals include pyrite, clay minerals, and rare calcite, magnesite, and dolomite.

Zhou Weixun (2000) reports U-Pb ages of 24–19 Ma for sandstone hosted U mineralization in the Yili Basin while the pitchblende of deposits in the Turpan-Hami Basin gives 3 groups of ages at 104, 24, and 7 Ma. Xia Yuliang et al. (2002) obtained highly variable apparent ages for U mineralization in the Yili Basin ranging from 0.8 to 29.8 Ma but their samples contained very high contents of common lead, which hampers any realistic age determination. Based on U-Pb isochron calculations of samples from the Kujiertai deposit, these authors arrive at the conclusion that there must be two episodes of ore formation, at 12 ± 4 Ma and 1 Ma for U mineralization in carbonaceous mudstone and sandstone, respectively, in this deposit; and, based on sandstone samples with high U contents, at 5 ± 1 and 2 Ma in the Thajistan deposit.

Sandstone-type U mineralization in *Paleogene* strata is known from the Burqin and northern Junggar Basins where it preferentially occurs in the form of lens-shaped ore bodies in grey alluvial and fluvial sandstones that contain up to 0.03% organic carbon.

A critical ingredient for the metallogenesis of sandstone roll-type U deposits in Jurassic and Paleogene sediments in the

Junggar-Tien Shan U province tends to be the so-called sub-orogeny in Miocene time. This event caused vertical displacements between 200 and 1 000 m, the formation of artesian basins and, obviously in result, the development of an infiltration groundwater regime, which promoted strata oxidation and formation of roll-shaped ore bodies (Zhou Weixun 2000).

1.1.1 Yili Basin

The Mesozoic Yili Basin covers an area of 16 000 km² along the Yili River in northwestern Xinjiang Uygur A.R. from where it extends westward into the Ily Basin of Kazakhstan. Yining is the largest town in this area. Ranges of the eastern Tien Shan frame the basin to the north and south. U deposits are of sandstone- and lignite-type and occur in the southwestern part, close to the southern rim of the Yili Basin while some occurrences are situated at the northern margin of the basin (Fig. 1.2). Deposits include the rollfront *Kujiertai* (formerly referred to as Deposit 512) and *Thajistan* (511) deposits and the uraniferous lignite deposits *Mengqiguer* (510) and *Daladi* (509). The latter two were discovered in 1955 and mined in the 1960s; the ore was processed in a mill near Yining. Original in situ resources of explored sandstone-type uranium deposits are reportedly as much as 20 000 t U [OECD-NEA/IAEA (2005) reports 13 000 t U for “Yili deposit”].

Sources of information. Chen Zuyi and Huang Shijie 1993; Huang Shijie 1996; Li Shengxiang et al. 2002, 2005; Lin Shuangxin et al. 2002; Zhou Weixun 1997, 2000, pers. commun. 2002; Zhou Weixun et al. 2002; Zhou Wenbin et al. 2002.

1.1.1.1 Kujiertai (Deposit 512)

Kujiertai (also spelled Kujieertai) was discovered some 80 km SW of the town of Yining, close to the Kazakhstan border in the second half of the 1950s. OECD-NEA/IAEA (2000) reports 6 000 t U known in situ resources while Zhou Weixun (2000) notes explored resources to be in the 5 000–20 000 t U size class; as such Kujiertai is one of the largest known uranium deposits in China. Ore bodies are mainly of rollfront along with some tabular sandstone type and occur in three U-mineralized zones, *north*, *middle*, and *south*, within an area 12 km in length and 5 km in width. Exploitation by ISL techniques has been ongoing since 1993.

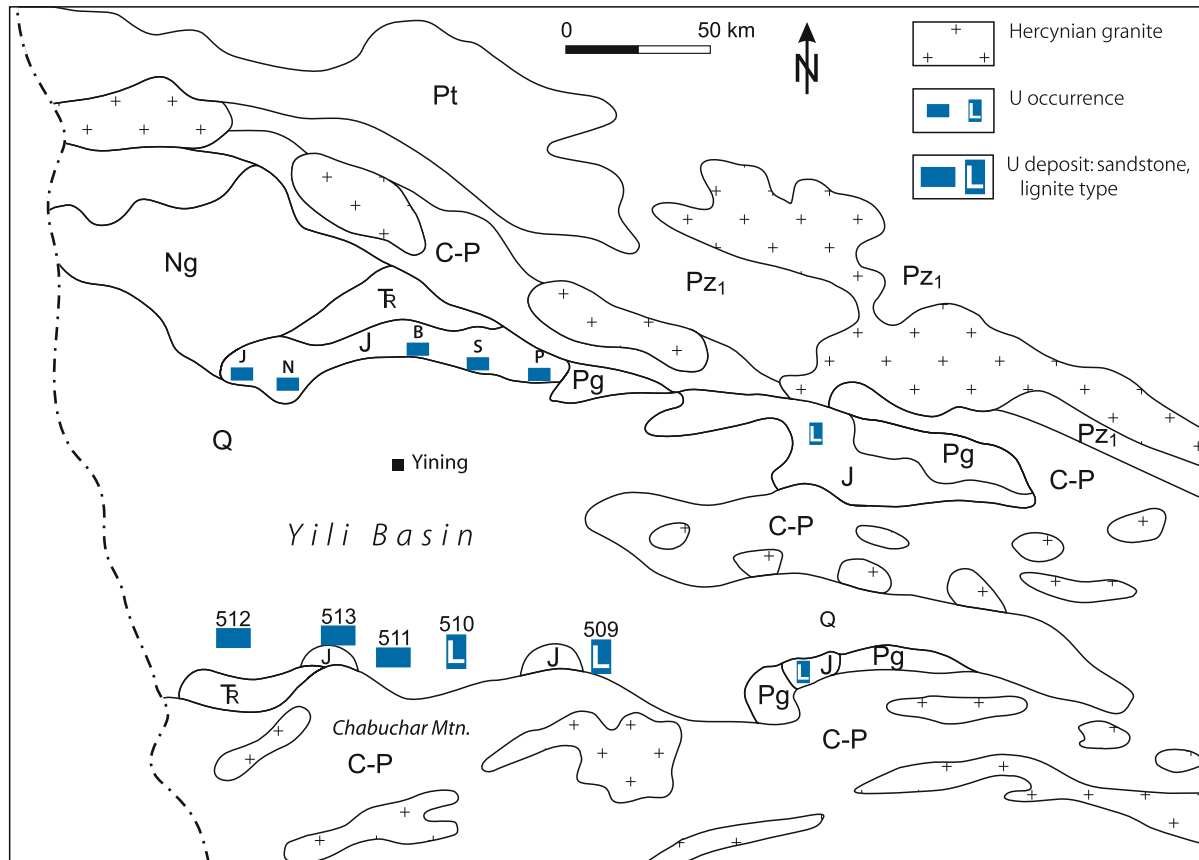
Sources of information. See previous chapter.

Geology and Mineralization

Mineralization occurs at the southern margin of the Mesozoic-Cenozoic intermontane Yili Basin. The basin is filled with continental sediments of Middle-Upper Triassic, Lower-Middle Jurassic, Cretaceous, and Tertiary age, upon which a Quaternary veneer rests. Table 1.3 provides a summary of litho-stratigraphic

Fig. 1.2.

Yili Basin, generalized geological map showing that sandstone-type uranium and uranium lignite deposits and occurrences are restricted to the margin of the intermontane Jurassic basin (after Chen Zuyi and Huang Shijie 1993). Q Quaternary, Ng Neogene, Pg Paleogene, J Jurassic (Lower-Middle. coal bearing), \bar{R} Triassic (Middle-Upper), C-P Carboniferous-Permian (predominantly intermediate-felsic volcanics), Pz₁ Lower Paleozoic, Pt Proterozoic. U deposits at southern margin of Yili Basin (from W to E): Deposit 512 Kujǐertai, 513 Wukulqi, 511 Thajistan, 510 Mengqiuer, 509 Daladi. U occurrences at northern margin of Yili Basin: J Jintsenzhi, N Nantaizhi, B Bilikatji, S Suli, P Pilijin



units combined with critical features involved in the evolution of the basin and ore formation.

The Jurassic unit is represented by the U-hosting Shuixigou Group that consists of eight sedimentary cycles and contains, basinwide, up to 13 superjacent coal seams. At Kujǐertai, the Shuixigou Group is 330–450 m thick (Fig. 1.3) and consists of arenaceous and argillaceous layers with four intercalated coal seams that form a 5–7° N dipping monocline.

Uranium ore bodies occur in sediments of a braided delta system of the 5th sedimentary cycle. The sequence has a sand/mud ratio of 1–2 and averages 1.12% organic carbon. Quartzose sandstone, feldspathic (kaolinized) sandstone with some volcanic debris, and sandy conglomerate of fluvial and deltaic provenance are the prevailing host rocks. Beds are from 10 to 25 m thick, have a hydraulic conductivity of 0.1–2.5 md⁻¹, and occur in a belt some 20 km in length along E-W strike and over 2 km in width.

Alteration is well developed and shows a downdip zoning grading from intensely altered, brown yellow sandstone with high hydrogoethite content; to weakly altered, yellow sandstone with about 6.5% hydrogoethite; into the redox front and related ore

bodies. Ore associated with hydrogoethite and pyrite is grey colored and turns to dark grey-in unaltered sandstone (Table 1.4).

Uranium occurs as pitchblende (about 80% of U minerals), coffinite (about 20%), rarely brannerite, or also as U-Ti-bearing magnetite and adsorbed on coal debris and pyrite. Pitchblende associates with pyrite. Additional elements include Se, Mo, Ge, Sc, Re, and V. Se is essentially bound in weakly altered sandstone while the other elements are concentrated together with uranium in the redox front.

Major ore bodies are of simple and complex crescent shape with two wings but there tends to be also some tabular U mineralization. Frontal parts of rolls are from about 50–150 m wide, from 5 to 12 m thick, and have grades averaging 0.05% U. Wings are from 200 to 400 m long in a south to north direction, from 1 to 2 m thick and average 0.03–0.1% U (Figs. 1.4, 1.5, 1.6).

A few tabular ore-bodies with a thickness of 0.5–2 m and grades of 0.05–0.1% U occur in sediments deposited in alluvial fans and braided fluvial systems of the 1st to 3rd cycles. These sediments have sand-mud ratios of 2–3 and contain 0.29% organic carbon.

■ Table 1.3.

Yili Basin, litho-stratigraphic units and related structural, paleoclimatic and U-metallogenic stages involved in the evolution of the basin (after Li Shengxiang et al. 2002)

Stratigraphy		Thickness (m)	Lithology	Structural stage	Paleoclimate	U-metallogenesis
Quaternary (Q)		80–220	Gravel, sand, silt and clay	Differential uplift and subsidence	Semi-arid to semi-humid	U redistribution and concentration by interlayer oxidation
Tertiary	Neogene (Ng)	519	Yellow conglomerate, brown calcareous mudstone	Weakly-compressional	Arid	
	Paleogene (Pg)	12–36	Brown-red sandy conglomerate with intercalated sandstone and mudstone			
Cretaceous	Upper Cretaceous (K ₂)	10–268	Red calcareous sandy conglomerate, muddy sandstone, mudstone		Uplift, erosion	
	J ₃ –K ₁					
Jurassic	Xishanyao Fm. (J ₂ x)	>102	Grey sandstone, siltstone, mudstone, coal seams	Weakly extensional	Humid	Syngenetic-diagenetic U concentration forming low-grade mineralization
	Sangonghe Fm. (J ₁ s)	46–82	Grey siltstone, mudstone, coal seams in upper section; pebbly and lithic sandstone, mudstone in lower section			
	Badaowan Fm. (J ₁ b)	110–611	Sandy conglomerate, lithic sandstone, mudstone, coal seams with basal conglomerate			
Triassic	Xiaoquangou Fm. (Tr ₂₋₃ x)	443	Interbedded siltstone, mudstone, fine-grained sandstone in upper section; sandy conglomerate, sandstone with intercalated siltstone and mudstone in lower section	Intensely extensional	Semi-arid to semi-humid	
	Upper Chuangfanggou Fm. (Tr ₁ ch)	785	Brown-red conglomerate, pebbly coarse-grained sandstone with intercalated fine-grained sandstone and mudstone		Arid	
Permian	Lower Chuangfanggou Fm. (P ₂ ch)	>1 000	Massive conglomerate with intercalated fine-grained sandstone and mudstone		Semi-arid	

A well field in the western section of Kujiertai exploits (status 2002) an ore body 5.3 km in E-W length. At the well field, the ore body is 0.5–12.3 m (av. 3.7 m) in thickness, 300–500 m in width, 100–240 m deep, and ranges in grade from 0.01% (cutoff grade) to 1.5% U averaging >0.03% U. The ore horizon dips 1–10° N and is overlain by a mudstone bed 20 m in thickness.

1.1.1.2 Wukulqi (513)

This deposit is located at the Wukulqi upwarp, about 20 km E of Kujiertai. U mineralization occurs in Cycle V of the Shuixigou Group and occupies a zone 5 km long, 20 m to 560 m wide, 3.18 m in average and 7.45 m in maximum thickness. Grades

vary between 0.013% and 0.075% U (BOG handout at IAEA conference in Beijing 2002). Resources are reportedly a few 1 000 t U (status 2002).

1.1.1.2 Thajistan (511)

Thajistan (Zajistan) is located in the Wukulqi upwarp area, about 30 km E of Kujiertai and contains on the order of 1 000 t U. Roll-shaped and tabular ore bodies occur in a pebbly sandstone horizon of Cycle V of the Shuixigou Group. The uraniumiferous horizon is underlain by mudstone and covered by mudstone with an intercalated coal seam. The mineralized zone is 3 km long, 50 m to 500 m wide, averages a thickness of 5.3 m, and has grades

Fig. 1.3.

Yili Basin, litho-stratigraphic section of the U mineralized interval in the Middle-Lower Jurassic Shuixigou Group at the southern margin of the basin (after Li Shuangxin et al. 2002 and Li Shengxiang et al. 2002). **Bedding:** *H* horizontal, *M* massive, *P* parallel, *W* wavy, *Wg* wedgelike. **D.E.** Depositional environment: *Af* alluvial fan, *Bs* proximal braided stream, *L-S* lacustrine and swamp, *D* lakeshore delta

Period	Formation	Cycle	Column	Bedding	Lithology	D.E.	U			
K		Thickness (m)		M	Yellow-brown sandy (calcareous) conglomerate					
J ₁₋₂ Shuixigou Group	J _{2x} Xishanyao	VIII ~30		H	Variegated mudstone and sandstone	D+L, S				
				M	Medium to coarse-grained sandstone					
		VII >40		H	Mudstone, siltstone and sandstone					
				P	Pebbly sandstone					
				H	Coal seam M ₁₀ Sandstone, siltstone					
				P	Pebbly sandstone					
		J _{1s} Sangonghe	VI ~30		H			Fine grained sandstone with intercalations of siltstone and mudstone	D	
					H			Pebbly sandstone		
				H	Coal seam M ₈ Siltstone and mudstone					
				Wg	Pebbly sandstone					
	V >80			W	Siltstone and muddy siltstone					
				H	Coal seam M ₅ Muddy siltstone					
				M	Sandy conglomerate and sandstone					
				W	Coal seam M ₃ Muddy siltstone and fine-grained sandstone					
	J _{1b} Badaowan	IV ~60		M	Sandy conglomerate and coarse-grained sandstone	Bs				
				H	Muddy siltstone and fine-grained sandstone					
III ~25			H	Muddy siltstone and fine-grained sandstone						
			M	Sandy conglomerate with intercalation of fine-grained sandstone						
II ~30		H	Muddy siltstone and fine-grained sandstone	Af						
		M	Sandy conglomerate and coarse-grained sandstone							
I ~25		H	Muddy siltstone and fine-grained sandstone	Af						
		M	Sandy conglomerate with intercalation of fine-grained sandstone							
Tr ₂₋₃										

Table 1.4.

Yili Basin, Kujiertai deposit, characteristic features across a U mineralized alteration zone. (K_p : U-Ra equilibrium coefficient) (after Li Shengxiang et al. 2002)

	Intensely oxidized zone	Weakly oxidized zone	Redox zone	Unaltered zone
Rock color	Maroon, yellow	Light yellow, greyish white	Grey, dark grey, black	Grey, dark grey
Fe minerals	Abundant hematite, limonite, no pyrite	Mostly limonite, less pyrite	Abundant pyrite, minor limonite	Abundant pyrite, no limonite
Organic matter	Absent	Minor	Abundant	Abundant
U (ppm)	28.7	18.3	1 996.4	27.5
ΔEh (mV)	18.9	25.4	41.1	37.9
$C_{org.}$ (%)	0.17	0.22	0.93	0.87
S_{total} (%)	0.05	0.16	0.28	0.20
FeO (%)	0.42	0.59	1.18	0.84
Fe_2O_3 (%)	3.05	0.81	0.67	0.49
Fe_2O_3/FeO	7.26	1.37	0.57	0.37
U^{6+}/U^{4+}	2.41	1.48	1.44	1.34
K_p	3.32	2.64	0.84	1.08
V (ppm)	108.6	82.9	104.5	101.4
Se (ppm)	1.98	17.52	136.61	2.45
Mo (ppm)	4.6	3.17	1.39	6.28

ranging from 0.01% to 0.07% U. The deposit is in many aspects similar to Kujiertai, such as host sediments (Shuixigou Group), ore composition, and kind of alterations; but in contrast to Kujiertai, the Shuixigou Group strata are deformed into a syncline with quite steep dip angles. In result, the form of redox fronts is more complex than at Kujiertai (Fig. 1.7). (BOG handout at IAEA conference in Beijing 2002).

1.1.1.4 Unnamed Deposit

Cycle VII of the Shuixigou Group contains two uranium zones. The zone in the upper section has a length of 1 km, a width from 20 m to 100 m wide, an average thickness of 4.67 m, and grades between 0.01% and 0.08% U; the lower zone is 2 km long, 75 m to 200 m wide, averages a thickness of 6.6 m, and grades ranging from 0.01% to 0.09% U (BOG handout at IAEA conference in Beijing 2002).

1.1.1.5 Mengqiguer (510)

Mengqiguer is located about 15 km to the east of Thajistan. Explored U resources are in the 500–1 500 t U size class and have grades of 0.03–0.1% U. The uraniumiferous coal strata belong to the upper Shuixigou Group; they were deposited in the transition zone between the fan-front of a braided river system and peat bogs. The host sediments form an imperfect box fold with the deposit located on the southern flank of a syncline.

1.1.1.6 Daladi (509)

Daladi is 30 km distant from Mengqiguer and 75 km from Kujiertai. Explored U resources are in the 500–1 500 t U size class and have grades of 0.1–0.3% U. Uraniferous coal seams

occur in the basal Shuixigou Group. The seams are intercalated with channel sandstone and conglomerate and were deposited in an alluvial fan. The strata are folded and the deposit occurs on the southern flank of a syncline that dips 30° N.

1.1.2 Junggar Basin

The Junggar Basin is situated in northern Xinjiang Uygur A.R. and bordered by the Altai Range to the N and NE, and the eastern Tien Shan to the SW. It covers about 130 000 km² and is filled with Mesozoic-Cenozoic sediments. Several U occurrences are known at the eastern margin such as Daqinggou in Lower-Middle Jurassic sediments, the western margin (Karamay, J_{1-2} and K_2), and the northern margin (E) but no sizable deposit has been identified as yet.

1.1.3 Turpan-Hami Basin

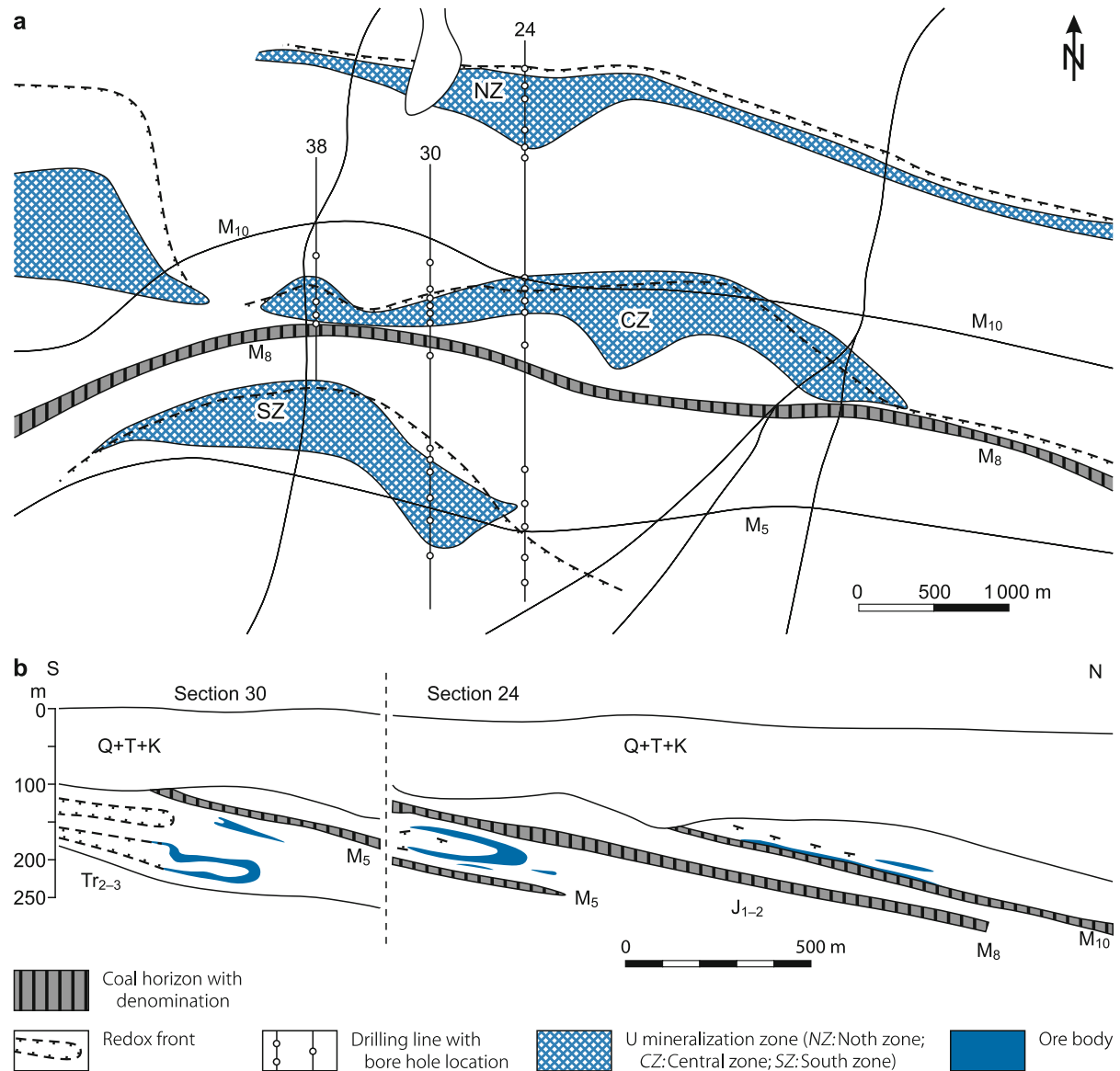
Situated to the SE of the Junggar Basin and separated from it by the Bogda Range, Tian Shan, the Turpan (also spelled Turfan)-Hami Basin is an E-W-elongated intermontane basin with a lowland at Aiding Lake 154.5 m below sea level. The basin covers about 48 000 km² and is subdivided into 3 segments: the Turpan Depression with 28 600 km² to the west, the Hami Depression with 19 300 km² to the east, and the intervening Liaodun Uplift. The Turpan Depression hosts the *Shihongtan* deposit.

1.1.3.1 Shihongtan

This deposit covers an area 20 km in length and 6 km in width in the western segment of the Aiding Slope that is situated 35 km SSW of Turpan City, Xinjiang A.R., at the SW margin of the

Fig. 1.4.

Yili Basin, Kuji'ertai (deposit 512, Yining Mine), generalized geological map and S-N sections (#24 and 30) with positioning of uranium mineralized zones and ore bodies in Jurassic sediments (after Gu Kangheng and Wang Baoqun 1996)



Turpan-Hami Basin (Fig. 1.8). Radioactive anomalies in coal were discovered in 1958; subsequent drilling in 1963–1964 led to a coal-type U deposit. A new drilling program started in 1997 and resulted in the discovery of the Shihongtan sandstone-type U deposit.

Sources of information. Huang Zhizhang et al. 2002; Peng Xinjian et al. 2002; Wang Jinping et al. 2002; Zhou Weixun et al. 2002.

Geology and Mineralization

Upper Permian to Tertiary sediments fill the Turpan-Hami Basin. Devonian to Early Permian rocks constitute the basement. Tertiary strata consist of diluvial, pink clay-sand and

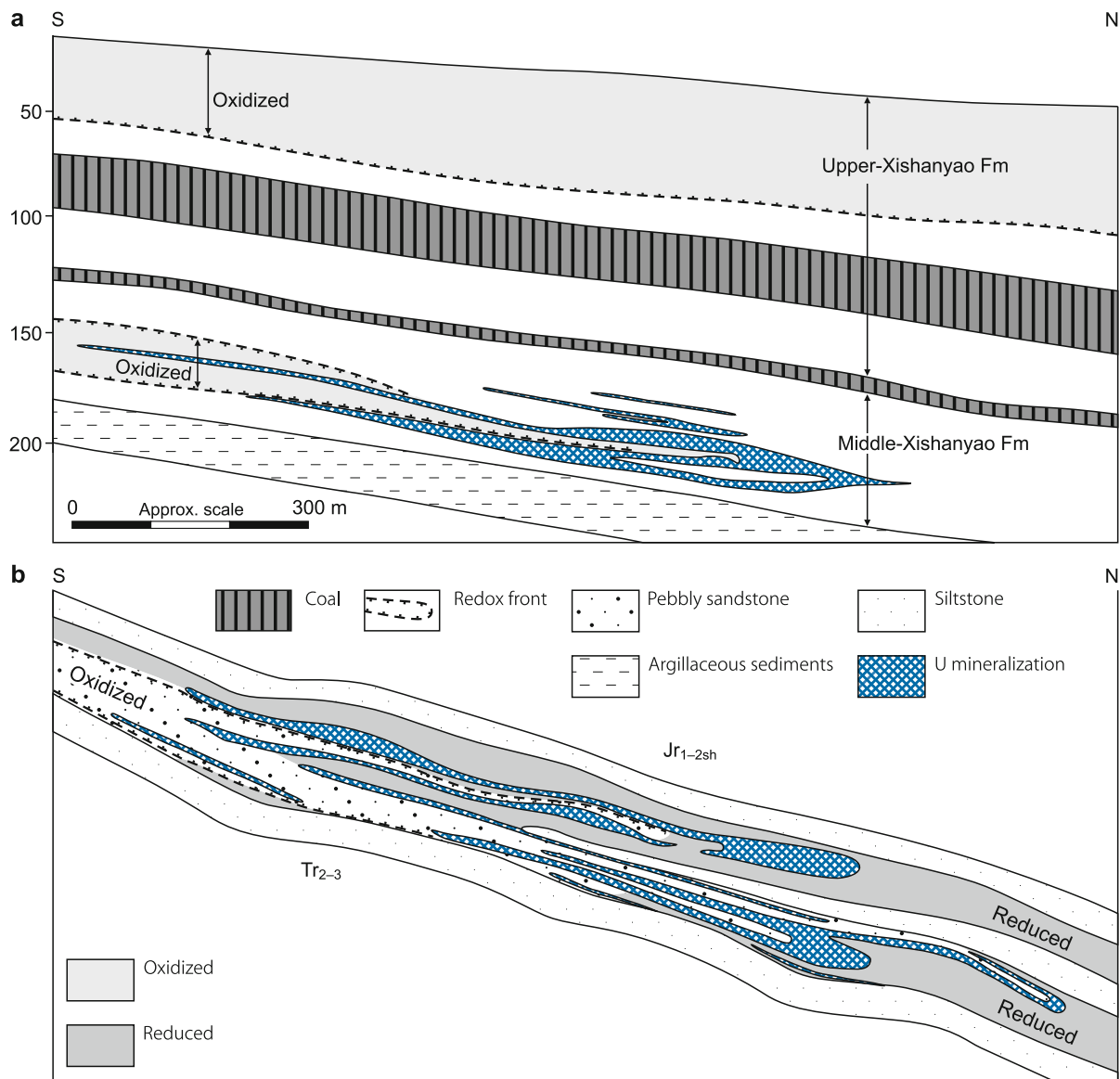
Quaternary deposits include gravel and eolian sediments from 5 to 50 m thick.

The U-hosting Lower-Middle Jurassic Shuixigou Group includes, from top to bottom, the Xishanyao (J_{2x}), Sangonghe (J_{1s}), and Badaowan (J_{1b}) Formations. These strata form an irregular monocline that dips 4–10° generally southwestwards but is distorted by a NNE-SSW elongated swell at which Shuixigou Group sediments outcrop at surface. Uranium is preferentially hosted by the Xishanyao Formation that is further subdivided into an upper member of rejuvenated braided fluvial origin, an intermediate member of a meandering fluvial-deltaic system, and a lower member derived from a braided fluvial system.

U mineralization extends intermittently for 20 km along a curvilinear NW-SE-oriented redox front in the lower member that trend northwards perpendicular to the long axis of the basin. Drill-indicated ore bodies occur on the eastern and

■ Fig. 1.5.

Yili Basin, Kujiertai, S-N cross-sections along **a** line 39 and **b** line 38, showing the irregular modes of roll and tabular U mineralization in Shuixigou Group Cycle V pebbly sandstone (after BOG handout at IAEA conference in Beijing 2002)



western flank of the Shihongtan swell in a zone of proximal braided fluvial sediments (► Fig. 1.9).

U is primarily hosted by unconsolidated, carbonaceous arkose and minor lithic sandstone lenses and beds intercalated with argillaceous lenses. Mineralized beds have variable contents of carbonate and pyrite averaging about 2% and 1%, respectively; they are altered by limonitization and hematitization updip from a redox front. The arenaceous aquifer system is from 23 to 60 m thick and sandwiched between clay/mud beds. Lignite seams occur in the hanging wall. Alteration is developed similarly to Kujiertai and exhibits a downdip zoning grading from (1) intensely altered, brown-yellowish sandstone with Fe^{3+}/Fe^{2+} ratios of >3.0 and 0.08% C_{org} to (2) weakly altered, light yellow and variegated pink sandstone with Fe^{3+}/Fe^{2+} ratios of $1.5-3.0$ and $0.08-0.72\%$ C_{org} ; to (3) deep grey to greyish white, mineralized sandstone with Fe^{3+}/Fe^{2+} ratios of

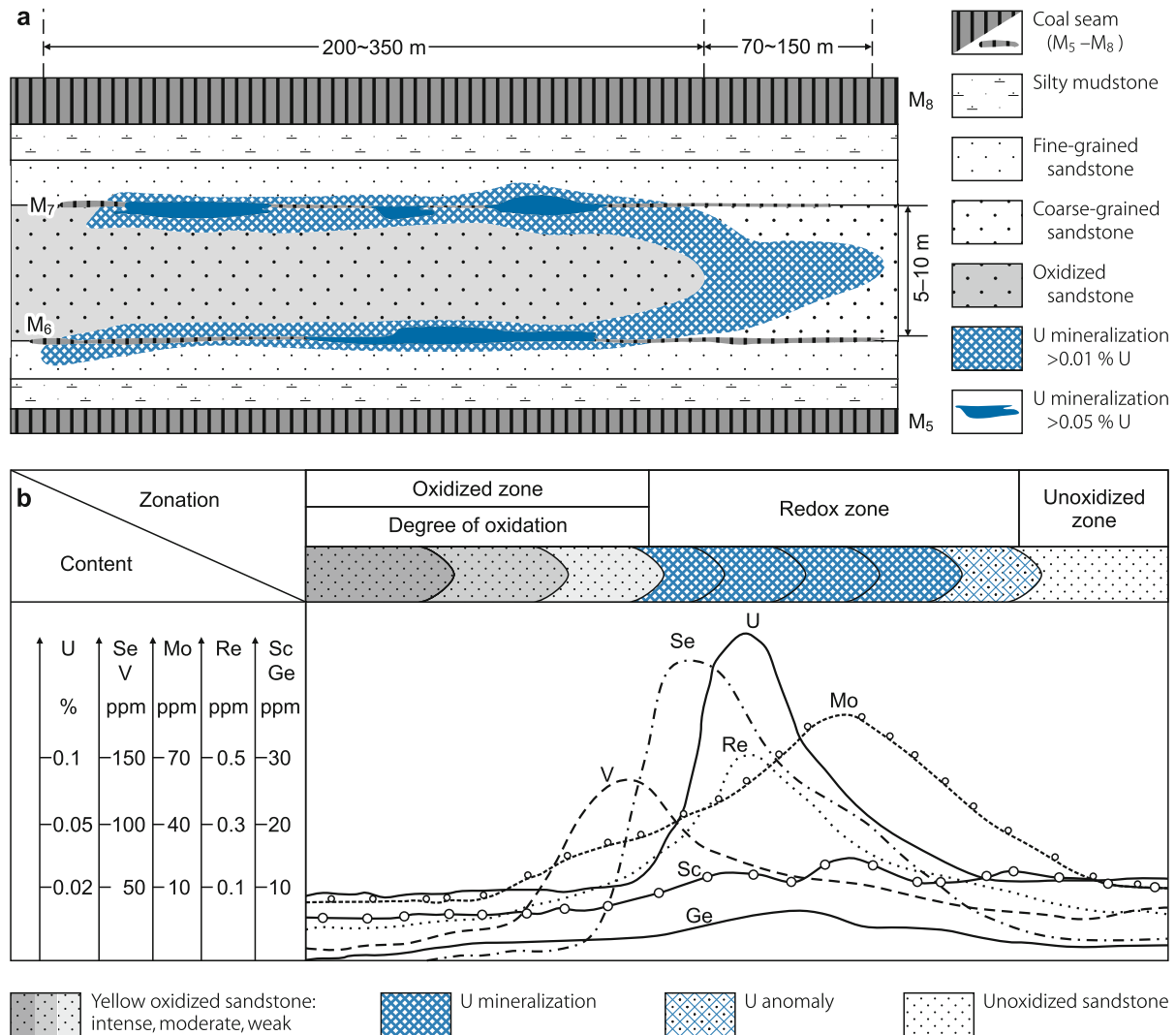
about 0.50 and 0.57% C_{org} at the redox front; and into (4) unaltered, grey sandstone with 0.26% C_{org} and Fe^{3+}/Fe^{2+} ratios of 0.34.

Uranium occurs in both mineral and adsorption form (about 50% each). Uranium minerals include pitchblende with minor coffinite and uraniferous Ti-Fe oxide. Associated elements and minerals include Mo, Se, Re, Ga, and Sc; and pyrite, kaolinite, illite, and chlorite, respectively. Pitchblende is commonly associated with pyrite, while coffinite is either associated with pitchblende and quartz or it coats pyrite. Uraniferous Ti-Fe oxide tends to be an alteration product of leucoxene or ilmenite. Adsorbed uranium is bound to clay minerals, powdery pyrite and carbonaceous debris.

Zhou Weixun (2000) reports ages of 104, 24, and 7 Ma for whole rock and ore samples corresponding to late Early Cretaceous, the end of Oligocene, and late Miocene, respectively.

Fig. 1.6.

Yili Basin, Kuji'ertai, **a** schematic cross-section illustrating typical uranium distribution in a roll-type ore body and **b** distribution and grades of U and associated elements across a redox front (after **a** Chen Zuyi and Huang Shijie 1993; **b** Lin Shuangxin et al. 2002)



Xia Yuliang et al. (2002) recalculated the ages by correcting the U-Ra equilibrium coefficient and arrived at two major ore forming episodes in the Shihongtan deposit at 48 ± 2 and 28 ± 4 Ma.

Ore bodies are of tabular and roll shape and occur at depths between 81 and 350 m. Rolls are about 4–8 m, exceptionally 20 m thick and 50–150 m long. Tabular ore bodies have a thickness of about 2–6 m and a length of 100–500 m. Grades vary between 0.012 and 0.2% and average 0.03% U.

1.1.4 Burqin Basin

This basin covers about 5 000 km² at the northwestern border of Xinjiang Uygur A.R. It extends along the Ertrix River westwards into the Zaisang Basin of Kazakhstan. Known U occurrences are hosted in Paleogene grey alluvial and fluvial sandstone that is considered to be indicative of a prospective district. However,

exploratory drilling has been dormant due to boggy surface conditions.

1.1.5 Kashi Depression/Northwest Tarim Basin

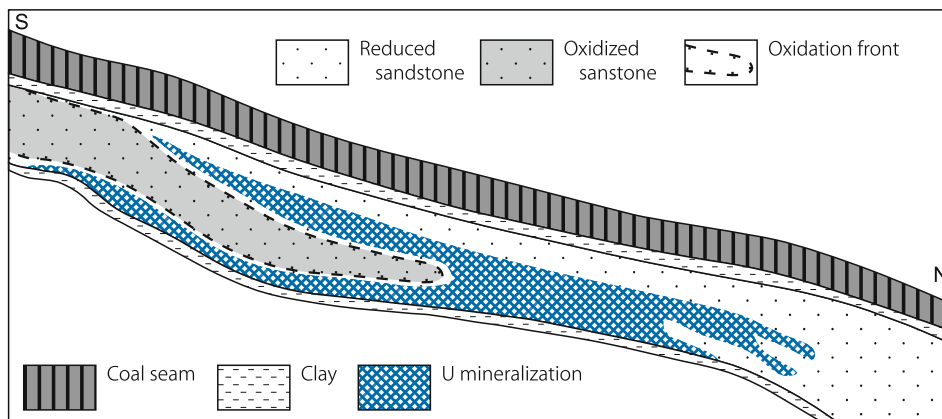
One sandstone-type U deposit, *Bashibulak*, is reported from the Mesozoic-Cenozoic Kashi Depression in western Xinjiang Uygur A.R., NW China. The Kashi Depression occupies the northwestern margin of the Tarim Basin and is bordered by ranges of the eastern Tien Shan to the north and Kunlun Shan to the southwest.

1.1.5.1 Bashibulak

This tabular sandstone-type U deposit is located in Wuqia County, to the west of the town of Kashi. Explored in situ

■ Fig. 1.7.

Yili Basin, Thajistan (#511) deposit, S-N cross-section along line 48 showing the irregular mode of roll and tabular U mineralization in Shuixigou Group Cycle V pebbly sandstone (after BOG handout at IAEA conference in Beijing 2002)



resources are on the order of 1 500–5 000 t U at grades between 0.03 and 0.1% U.

Source of information. Zhou Weixun 2000.

Uranium occurs in a Mesozoic-Cenozoic continental sedimentary sequence (150–800 m thick), which rests unconformably upon Proterozoic schist and quartzite and consists of the following litho-stratigraphic units – from top to bottom:

- Neogene, pink or variegated, gypsum-bearing clastic sediments
- Paleogene-Upper Cretaceous, grey, gypsiferous clastic and carbonate rocks
- Lower Cretaceous-Upper Jurassic, variegated clastic sediments; and
- Middle-Lower Jurassic, coal- and oil-bearing melanocratic clastic sediments

Mineralization is hosted by a NW-SE-striking, 30–40° SE-dipping Lower Cretaceous variegated clastic unit composed

of an upper sequence of pink sandstone, a middle sequence of bituminous conglomerate and sandstone with intercalated straculate pelite, and a lower sequence of pink sandstone and mudstone with intercalated green sandstone and conglomerate.

Ore bodies are of tabular and lenticular shape, from tens to hundreds of meters long and from a few to tens of meters thick, primarily contained in bituminous sandstone, conglomerate, locally in pelite of the middle sequence, and to a minor extent in the basal lower sequence.

1.1.6 North Tien Shan/Western Edge of Junggar Continental Block

1.1.6.1 Baiyanghe

Volcanic-type uranium mineralization is reported from Baiyanghe near the town of Karamay, Xinjiang-Uygur A.R., located in the northern branch of the Tien Shan. Explored in situ

■ Fig. 1.8.

Turpan-Hami Basin, schematic geological map with location of the Shihongtan U deposit (after Wang Jinping et al. 2002)

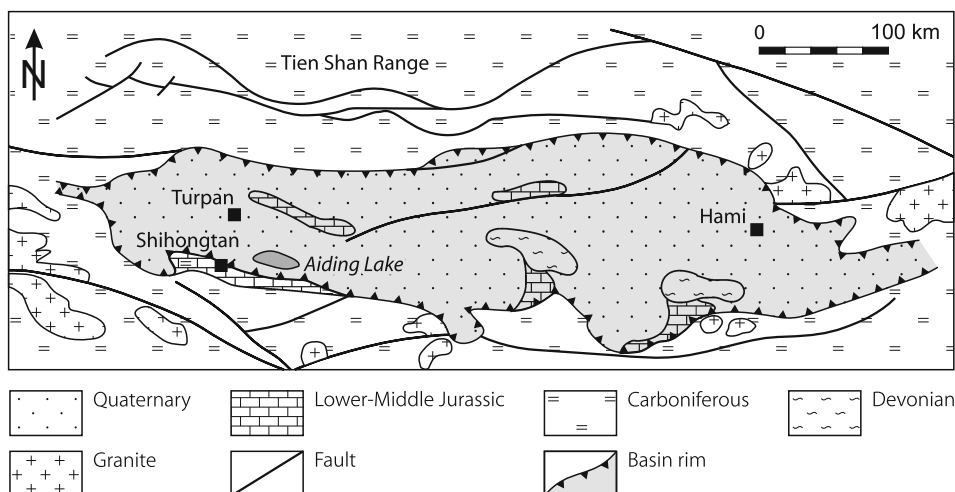
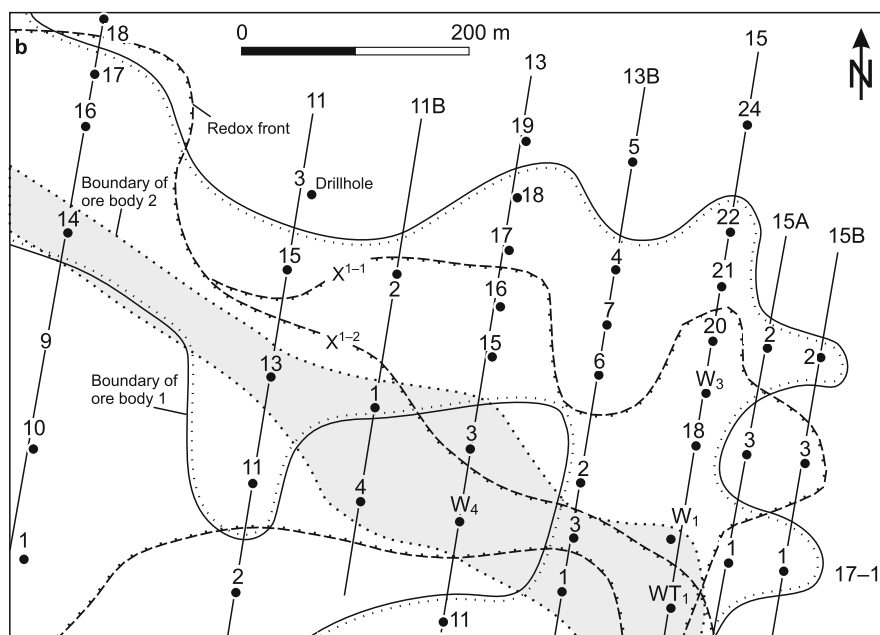
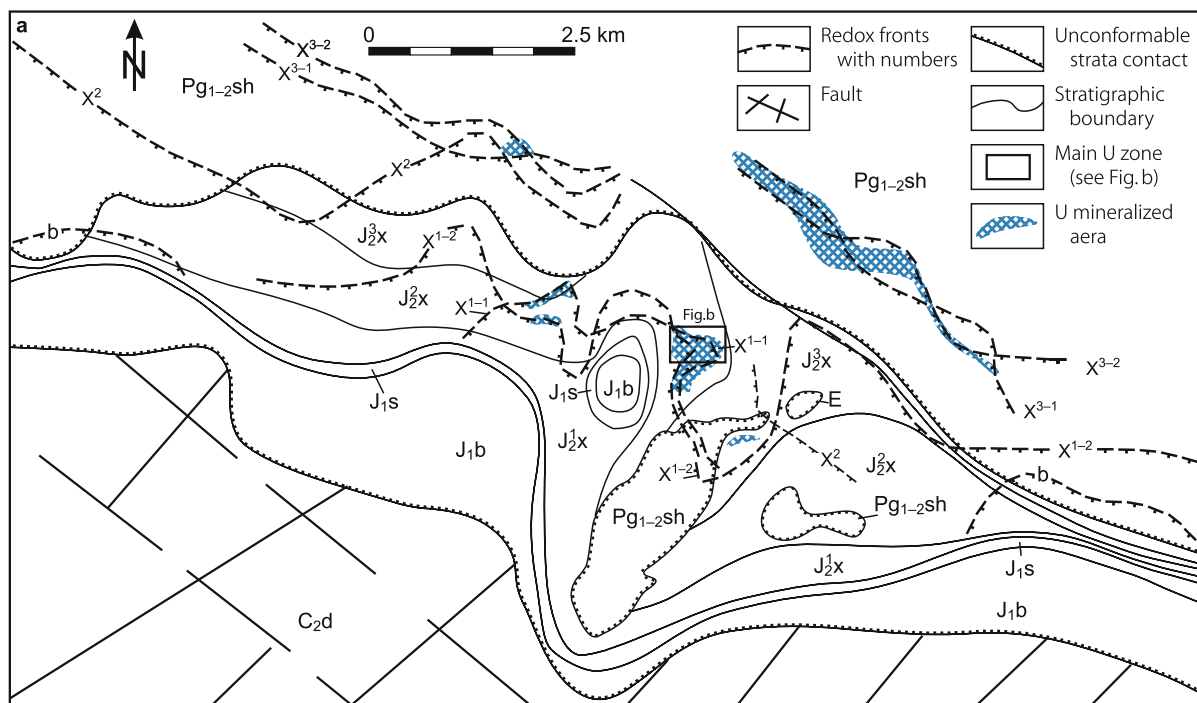


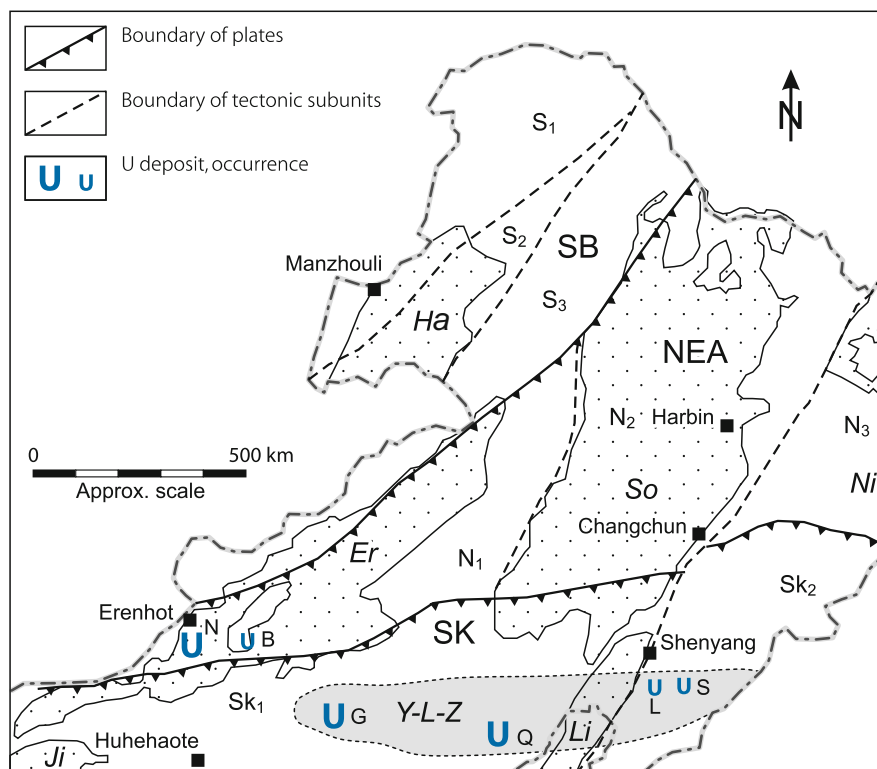
Fig. 1.9.

Turpan-Hami Basin, Shihongtan deposit. **a** Schematic stratigraphic map with surface projections of redox fronts and related U ore bodies. The two main ore bodies (shown in **b**) are on the eastern flank of a structural swell. *Pg₁₋₂sh* Shanshan Group: Paleogene brownish red sandy conglomerate, mudstone with gypsum. *J₁₋₂x* Shuixigou Group – *J₂x* Middle Jurassic Xishanyao Formation, 35–691 m thick: *J₂³x* Upper Member, 0–130 m thick: Greenish white and brownish yellow, medium- and coarse-grained sandstone with intercalations of conglomerate and grey mudstone with three interbedded coal seams, 12–14 m thick; *J₂²x* Middle Member, 130–140 m thick: Brownish yellow and greyish white, medium- to fine-grained sandstone and grey mudstone intercalated with conglomerate lenses and some thin coal seams at top; *J₂¹x* Lower Member, 35–85 m thick: Greyish white and brownish yellow sandy conglomerate, medium- and coarse-grained sandstone intercalated with thin-bedded mudstone and a coal seam on top; *J₁s* Sangonghe Formation, 11–15 m thick: Intercalated greyish green mudstone and greyish white sandstone with carbonaceous mudstone and thin-bedded coal layers and streaks; *J₁b* Badaowan Formation, 23–123 m thick: Greyish white sandstone and conglomerate intercalated with greyish green mudstone, containing a few coal layers and streaks; *C₂d* Dikaer Group: Greyish green, fine-grained sandstone, siltstone with intercalations of thin-bedded limestone, yellowish brown medium- to coarse-grained sandstone and bioclastic limestone. **b** Horizontal projection of redox fronts and related U ore bodies of the main segment of the deposit. The upper #1 ore body is at depths from 81 to 158 m and the lower ore body #2 at depths from 94 to 175 m. (After Zhou Weixun, pers. information 2006, based on Baoxia Li and Zhanshuang, 2003)



■ Fig. 1.10.

Yinshan-Liaohe U province in NE China, simplified structural map with location of U deposits and major occurrences as well as Mesozoic-Cenozoic continental basins (dotted) (Y-L-Z Yinshan-Liaoning metallogenic zone) (after Zhou Weixun 2000). **U deposits/occurrences:** B Bayantala (ss, basal channel), G Guyuan (volcanic, vein), L Liangshuguan (metasom, vein), N Nuheting (ss, tabular), Q Qinglong (ss, basal channel), S Saima (intrusive, alkaline syenite) **Tectonic units:** NEA Northeast Asian Plate, N₁ Xiwuzhumuxin Fold Belt (FB), N₂ Songnen Massif, N₃ Yichun-Yanshan Paleozoic FB; SB Siberian Plate, S₁ Ergun Early Paleozoic FB, S₂ Xiguitu Late Paleozoic FB, S₃ Hinggan Paleozoic FB; SK Sinokorean Plate, SK₁ Inner Mongolian-Yanshan Uplift, SK₂ East Liaoning Massif. **Mesozoic-Cenozoic basins:** Er Eren (Erlian), Ha Hailar, Ji Jilantai, Li Lower Liaohe, Ni Ningan, Sa Sanjiang, So Songliao



resources are in the 500–1 500 t U size class at grades between 0.1 and 0.3% U.

Source of information. Zhou Weixun 2000.

Country rocks include a Lower Permian pyroclastic unit that overlies Carboniferous rocks. Both are exposed on surface at the deposit except locally where they are covered by Paleogene sandy clay and pelitic conglomerate. The Lower Permian unit is composed of, from top to bottom: (a) basalt; (b) tuffite with intercalations of quartz porphyry and felsite; and (c) tuffite interbedded with quartz porphyry and tuff with intercalated tuffite and siliceous shale.

An Upper Permian tongue-like sill of microgranitic porphyry has intruded into the Paleozoic suite and controls the uranium mineralization. Ore bodies are from 30 to 60 m long and from 2 to 13 m thick. They occur fracture controlled at the contact and within microgranite porphyry bodies and extend as lenses and nests into surrounding quartz porphyry and tuff layers.

1.2 Yinshan-Liaohe U Province, NE China

The Yinshan-Liaohe U province extends in east-west direction across northeastern China from the East Liaoning Peninsula

through the Yanshan mountains and the Da (large) Hinggan Range and its southern extension into the Gobi Desert/eastern Inner Mongolian Plateau, including the Yinshan mountains (► Figs. 1.1, 1.10).

Geotectonically, this U province trends along the northern margin of the Precambrian North China Massif/Platform (Sino-Korean Paraplatform) and across the southern parts of three major, NE-SW-oriented geotectonic subdomains that encompass the U regions/districts mentioned (from east to west):

- the *Songnen-East Liaoning subdomain* consisting of pre-Cambrian Songnen and East Liaoning blocks amalgamated by Paleozoic fold belts with metasomatic vein-stockwork and intrusive alkaline-type U deposits in the *Liaoning U* region;
- the intermediate positioned Paleozoic *Ergun-Da Hinggan-Yanshan subdomain* (eastern part of the Paleozoic Altai-Hinggan fold system) affected by Mesozoic magmatism with volcanic-type U deposits and a few basal channel sandstone-type deposits in the *Daxing-anling-Yanshan* and *Guyuan-Duolun* volcanic belts in N Hebei-SE Inner Mongolia; and
- the *Eren-Hailar subdomain* within the relatively stable Upper Proterozoic Inner Mongolian Uplift with sandstone-type U deposits in the *Eren Basin* of central-northern Inner Mongolia A.R.

Sandstone-type U occurrences are also reported from the *Hailar* and *Song-Liao* Mesozoic-Cenozoic basins located in the Eren-Hailar and in the northern parts of the Erguna-Da Hinggan-Yanshan subdomains, respectively. In addition, the discovery (in 1999) of U mineralization in the Dongsheng area at the northern margin of the *Ordos* Basin might enlarge the U province southwestwards.

Minable U deposits are reported from the Liaoning region and Eren Basin. A mill exists at Lianshanguan.

The subsequent description is largely based on Liu Xingzhong and Zhou Weixun (1990), NUKEM (1999), Zhou Weixun (1997b, 2000), Zhou Weixun et al. (2002), and Zhou Weixun pers. commun. amended by data from other sources mentioned in the various sections.

1.2.1 Liaoning U Region (Liadong Block), Liaoning

This region is located to the south and east of Shenyang in eastern Liaoning Province (► Fig. 1.11). Uranium deposits and occurrences are reported from the *Lianshanguan Dome*, the *Saima Complex*, and the *East Liaoning Basin*. U mineralization in crystalline rocks is attributed to metasomatite (e.g. Lianshanguan deposit), intrusive alkaline syenite (Saima), and

(modified) synmetamorphic types. *Lianshanguan* (Benxi Mine) is the only deposit mined to date.

Sources of information. Guo Zhitian et al. 1996; OECD-NEA/IAEA 1997; Qin Fei and Hu Shaokang 1980; Zhong Jiarong and Guo Zhitian 1984; Zhou Weixun 2000; Zhou Weixun, pers. commun.

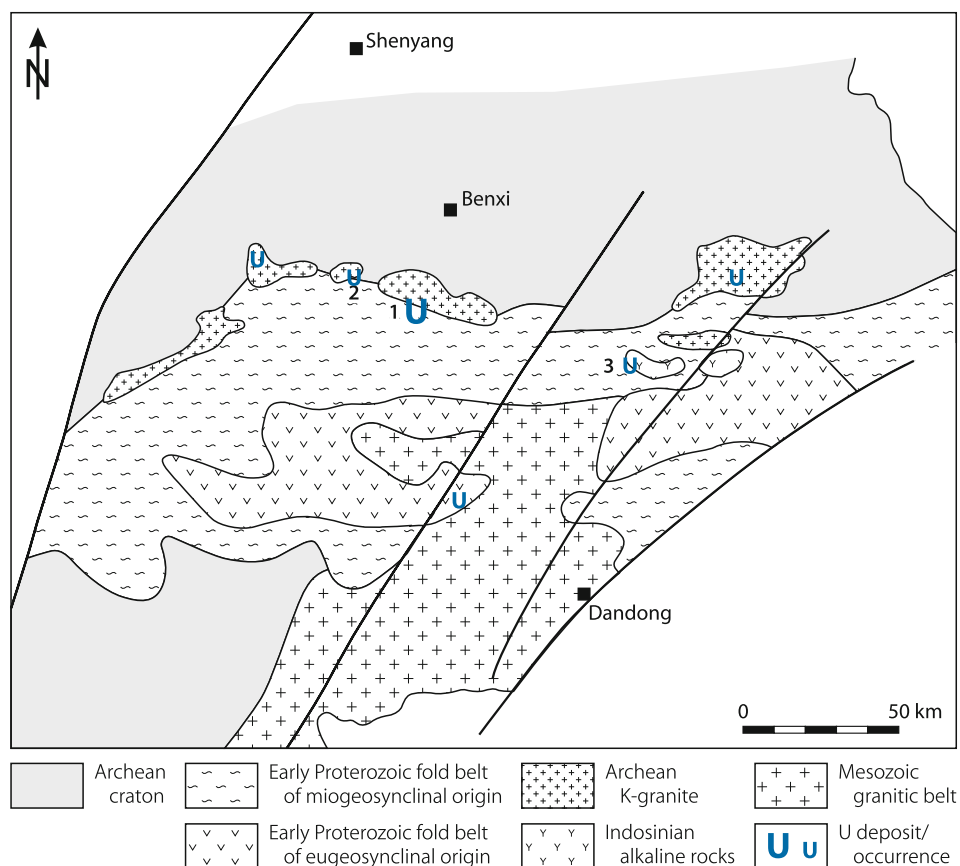
Regional Geological Setting of Mineralization

The Liaoning (or East Liaoning) uranium region occupies a northeastern segment of the North China Massif (or Platform), which evolved by multiple tectonic, metamorphic and magmatic events since the Archean. As summarized from Guo Zhitian et al. (1996), the Liaoning region comprises Archean craton segments, Paleoproterozoic fold belts, and Mesozoic tectono-magmatic mobile belts. Slightly metamorphosed Neoproterozoic and unmetamorphosed Phanerozoic platform cover sediments rest unconformably upon the Archean-Early Proterozoic crystalline basement including Mesozoic-Cenozoic sediments in a few downfaulted basins.

Archean rocks are often exposed in oval dome structures as in the Lianshanguan Dome and consist predominantly of granite with minor greenstone inliers. Granites include a sodic facies,

■ Fig. 1.11.

Liaoning U region, generalized map of principal geotectonic units and location of U deposits/occurrences (1 Lianshanguan, 2 Gongchanling, 3 Saima) (after Guo Zhitian et al. 1990)



2 750 Ma old, with a low U background (1–2 ppm); and a potassic facies, 2 530 Ma old, with increased U tenors (see further below). Greenstones/crystalline schists (referred to as *Anshan Group* by Qin Fei and Hu Shaokang 1980) occur as variably sized enclaves within granite massifs. Lithologies include amphibolite, leptynite, gneiss, schist, and banded, ferruginous quartzite that originated from mafic to intermediate-felsic volcanics with pelitic-arenaceous and siliceous-ferruginous sediments in the upper sequence by amphibolite facies grade metamorphism 3 000–2 900 Ma ago.

An E-W-trending *Lower Proterozoic fold belt* composed of metamorphosed eu- and miogeosynclinal facies of littoral-neritic origin (*Liaohu Group*, Qin Fei and Hu Shaokang 1980) and magmatic intrusions transgresses the Archean terrane in the East Liaoning region. Medium to low grade regional metamorphism transformed the geosynclinal lithologies into greenschist to epidote-amphibolite facies rocks.

The central zone of this former aulacogen exhibits a tripartitioned *eugeosynclinal* sequence. Its upper section consists of intercalated metamorphosed turbidite, thin-laminated feldspar-quartz sandstone, volcanic rocks, shale, and carbonate.

The middle section is dominated by tourmaline- and magnetite-bearing albite leptynite and granulite intercalated with minor plagioclase amphibolite and boron-bearing serpentized marble that derived from stratiform felsic volcanics rich in sodium, boron, and iron.

The basal section is made up of granite diapiric domes and batholiths emplaced in the core of anticlinal structures. These granites were intruded into centers of volcanic activity and locally into the overlying turbidite sequence during the initial stage of aulacogen development.

Miogeosynclinal facies are restricted to the margin of the Lower Proterozoic aulacogen and rest unconformably upon paleoweathered Archean rocks. Lithologies include metamorphosed pelitic sediments in the upper section, thick-bedded carbonate in the middle, and continental clastic rocks intercalated with intermediate to felsic volcanics at the base.

The *Luliangian Orogeny*, 1 900–1 700 Ma ago, finally consolidated the Archean-Lower Proterozoic complex to the crystalline basement of the North China Massif. The geosynclinal lithologies were transformed by medium- to low-grade regional metamorphism of epidote-amphibolite to greenschist facies and folded into a fold belt that connects the paleocontinental Archean segments. Both Archean and Lower Proterozoic rocks underwent strong migmatitization; orogenic movements generated approximately E-W-trending anticlinoria and synclinoria, and Archean granite was pierced into the overlying Lower Proterozoic strata in the form of diapiric domes along the northern contact of the fold belt to the craton. Coeval faulting produced about E-W-trending, deep faults, most of which were filled with gabbro or plagiogranite. Additionally, an irregular, E-W-trending alkali-metasomatic zone evolved in response to locally intense potassic and/or sodic metasomatism along ductile shear zones and interstratified faults at the contact between consolidated Archean blocks and Lower Proterozoic strata.

The Archean-Lower Proterozoic terrane was reactivated during the *Indosinian* and *Yanshanian* orogenies and NE to

NNE-trending tectono-magmatic mobile belts were formed. In the East Liaoning region, *Indosinian* (Triassic to Early Jurassic) magmatic activity was essentially restricted to the emplacement of the Fengcheng alkaline complexes including the U-Th-REE-bearing Saima alkaline massif; whereas intense tectono-magmatic activity characterized the *Yanshanian* (Jurassic) reflected by the intrusion of numerous large granite batholiths associated with regional upwarping and downfaulting of intracratonic basins.

Principal Characteristics of Mineralization, Geochronology, and Stable Isotopes

U deposits and occurrences are essentially restricted to sublatitudinal deep faults that trend within the transitional zone between the Early Proterozoic fold belt and northerly adjacent Archean segments. Four major varieties of uranium mineralization are identified in the East Liaoning region. They are classified and characterized by Guo Zhitian et al. (1996) as follows:

1. *Iron-uranium mineralization in Archean Si-Fe formations.*

Example: Gongchangling occurrence, about 30 km W of the Lianshanguan deposit. This kind of mineralization occurs at the margin of the Archean craton in metamorphic rocks near the contact to Archean potassic granites. Preferential host rocks are magnetitic quartzite, biotite-plagioclase gneiss, chlorite schist, and mica-quartz schist that are altered by chloritization, carbonatization, and others near U mineralization.

Mineralization consists of lenses, veinlets, and veins with pitchblende and minor uraninite. Associated metallic minerals are mainly specularite with minor pyrite, galena, and chalcocopyrite. Gangue minerals include quartz, calcite, and chlorite. Fluid inclusions in quartz associated with pitchblende indicate a formational temperature of 160–220°C. Sulfur isotope composition in pyrite shows a wide range of $\delta^{34}\text{S}$ values from +6.3‰ to –9.3‰. U-Pb dating of pitchblende yields 1 832 Ma. Metallogenetic considerations favor a metamorphic hydrothermal origin for this Fe-U mineralization.

2. *Monometallic uranium mineralization in Lower Proterozoic metamorphosed and migmatized terrigenous clastic rocks.*

Example: Lianshanguan-Gongchangling area. Major U occurrences including the Lianshanguan deposit are found near the southern edge of the Archean Lianshanguan granitic dome where they occur along a fault zone within a migmatized transition zone between Lower Proterozoic and Archean lithologies. Migmatized quartzite, quartz-mica schist, and Na-metasomatized granite provide the principal host rocks. The metasediments are of littoral-neritic origin and belong to the basal Liaohu Group of Lower Proterozoic age.

Principal wall rock alterations include albitization, sericitization, silicification, and minor chloritization, carbonatization, and fluoritization. Mineralization consists predominantly of pitchblende, minor coffinite, and locally uraninite, associated with Fe-, Pb-, Zn-, and Cu-sulfides, and some quartz.

Guo Zhitian et al. (1996) document three genetic types of U mineralization that may occur separately or combined in

a single deposit (see Sect. *Metallogenetic Aspects* for a synopsis of the metallogenetic evolution of these monometallic U mineralization regimes).

- a. Synmetamorphic (-sedimentary), low-grade mineralization consists of microgranular uraninite contained in the rock matrix or intergrown with metamorphic minerals such as garnet, biotite, and chlorite; it typically occurs in stratiform concentrations in quartzite and quartz-mica schist. Stable isotope analyses give an average $\delta^{34}\text{S}$ value of +6.1‰ for pyrite associated with uraninite, and $\delta^{18}\text{O}$ values of 10.64‰ for associated quartz. U-Pb datings yield an age of 2 114 Ma for uraninite.
 - b. Meso- to hypothermal alkali-metasomatic U mineralization (the most significant ore type in the Liaoning region) consists of pitchblende associated with alkali feldspar, sericite, and quartz. Ore bodies are of lenticular shape with an internal vein-stockwork structure controlled by interformational faults and saddle structures within the alkali-metasomatized zone. Mineralization temperature is 280–350°C. Pyrite associated with pitchblende has an average $\delta^{34}\text{S}$ value of +11.6‰ and the $\delta^{18}\text{O}$ of associated quartz averages 9.47‰. Pitchblende yields a U-Pb isotope age of 1 894 Ma.
 - c. Meso- to epithermal fissure filling mineralization composed of pitchblende with calcite and fluorite occurs as veins and veinlets mainly in altered granite at the margin of the alkali-metasomatic zone. This mineralization formed at a temperature of 160–230°C, averages a $\delta^{34}\text{S}$ value of +6.3‰ for pyrite associated with uranium, and gives a U-Pb age of 1 829 Ma.
3. *Boron-uranium mineralization in Lower Proterozoic volcanic-sedimentary strata*: U-B mineralization of synmetamorphic (sedimentary) origin occurs strata-bound in metamorphosed Lower Proterozoic boron-bearing, eugeosynclinal volcanic-sedimentary strata. It consists of microgranular uraninite intergrown with magnetite, ludwigite, and pyrite scattered in ludwigite layers. Uraninite yields a U-Pb age of 1 810 Ma. Veinlets with pitchblende also occur and are attributed to metamorphic hydrothermal reworking.
 4. *Uranium-thorium-REE mineralization in Indosinian alkaline intrusions*: Occurrences of this assemblage are reported from the Fengcheng Triassic alkaline complexes that were emplaced during the Indosinian Orogeny and include the Saima deposit. Mineralization includes three modes: Uraniferous rinkite containing 0.28–0.31% U in grass-green aegirine-nepheline syenite (the main mode of U mineralization in Saima); uraniumiferous pyrochlore-betafite in skarn; and veined pitchblende in alkaline volcanics and episyenite (as used in French terminology). The alkaline complexes were intruded 240–210 Ma ago; residual pneumatolitic-hydrothermal activity and associated metasomatism that formed rinkite and pyrochlore took place 220–210 Ma ago; and an age of 207–183 Ma was obtained for the magmatic hydrothermal process that generated veined pitchblende and thorite (for more details see Sect. 1.2.1.2: *Saima Alkaline Massif, East Liaoning*).

Potential Sources of Uranium

Precambrian rocks: Archean potassic granite of the Lian-shanguan and Gongchangling Massifs averages 5–8 ppm U but a recalculation based on the abundance of radiogenic lead indicates an original U endowment of 12–21 ppm U. Lower Proterozoic basal argillic-arenaceous miogeosynclinal rocks average 4–12 ppm U with local concentrations of syngenetic uranium. Coeval eugeosynclinal rocks average 1–2 ppm except for pyritic or magnetitic leptynite with contents of 4 ppm U. Some of the boron-rich (ludwigite) lithologies contain up to 50 ppm U.

Mesozoic rocks: Alkaline eruptive and intrusive facies of the Indosinian Saima Massif contain, in general, up to 20 ppm U and late differentiates as much as 122 ppm U (Guo Zhitian et al. 1996).

Metallogenetic Concepts

Guo Zhitian et al. (1996) elaborate on the metallogenesis in the East Liaoning region as summarized in the following. Favorable conditions for tectonic, magmatic, and hydrothermal activities were primarily provided by conjunction zones between different regional geotectonic units. Deep faults generated at these boundaries and acted as critical loci for metallogenetic processes. In East Liaoning, this is particularly true for an ancient and repeatedly reactivated lineament that trends E-W between a Lower Proterozoic fold belt to the south and Archean craton segments to the north. This structure controlled in an early stage the downwarp of the Early Proterozoic miogeosynclinal aulacogen that now forms the mentioned fold belt, while Archean terrane was uplifted. Weathering and related leaching liberated uranium and other mobile elements from Archean rocks (e.g. potassic granite). Uranium was transported into the sedimentary basin where it was preferentially precipitated in basal clastic sediments of the quartzite unit, Liaohe Group, to a large extent by adsorption on argillaceous, ferruginous, and carbonaceous matter.

During the *Luliangian Orogeny*, medium- to low-grade regional metamorphism transformed the Early Proterozoic sedimentary U accumulations into synmetamorphic, low-grade mineralization as reflected by recrystallized, microgranular uraninite in the matrix of metasediments or enclosed in rock constituents such as garnet, biotite, chlorite etc. U-Pb dating yields 2 114 Ma for uraninite.

In addition, multiple tectono-magmatic activities occurred along the above mentioned E-W-trending fault zone during the thermodynamic event at the end of the Paleoproterozoic. Plagioclase granite and intermediate to mafic dikes were intruded, and Archean granitic masses were remelted and reemplaced into the overlying Paleoproterozoic metasediments. Alkaline metasomatism associated with hydrothermal processes remobilized leachable elements including potassium, sodium, and uranium. U sources were provided by Lower Proterozoic uraniumiferous metasediments and Archean granite, metasediments,

and felsic volcanics (see Sect. *Potential Sources of Uranium* for U values). The resulting pregnant fluids migrated along fault zones and transformed the wall rocks into a WNW-ESE-trending metasomatite zone characterized by intense albitization and sericitization (muscovitization). This zone emerged with the reallocation of Archean granite blocks, a process that overprinted the regional Archean unconformity. Ductile shearing characterized this fault zone in an early stage; it was welded by alkali metasomatism, and again deformed by brittle structures at a later stage.

Since U mineralization is spatially closely associated with alkali metasomatized rocks in this zone, metasomatism-related meso- to hypothermal solutions are thought to be a salient

Liaoning region. This assumption is supported by U contents of as much as 0.4% U in fluid inclusions in quartz associated with U mineralization in the Lianshanguan deposit.

Uranium was selectively redeposited along the earlier mentioned E-W fault and its subsidiary structures at sites that provided the required space for U accumulation. But while sub-economic U occurrences are discontinuously found all along this fault zone at the northern margin of the Lower Proterozoic fold belt, commercial deposits such as the Lianshanguan deposit, are restricted to the earlier mentioned WNW-ESE-trending metasomatized structure at the margin of a reallocated Archean granite dome.

Early-stage U mineralization consists of micro-granular uraninite enclosed in or associated with garnet, biotite, and other metamorphic minerals and occurs as stratiform concentrations in quartzite and mica-quartz schist. However, most economic ore bodies were predominantly generated as pitchblende mineralized lenticular vein-stockworks 1 894 Ma ago (U-Pb age of pitchblende) from meso- to hypothermal solutions at mineralization temperatures of 280–350°C. Preferential sites of ore deposition were intersections of anastomosing and bifurcating fault-fracture systems and associated breccia intervals with ENE-WSW-trending, westerly plunging undulations. These undulations were superimposed on the limbs of a dome-shaped anticline with a reallocated Archean potassic granitic core that exhibits alkali metasomatism as reflected by albite veinlets. Saddle structures and ENE-WSW-trending axial faults and their subsidiary fractures that cut alkali metasomatites proved to be the most favored sites for the accumulation of ore. High-grade ore bodies are typically controlled by structural irregularities such as fault bends or fault clusters with increased fracturing and brecciation.

A slightly younger mineralizing episode that produced fissure filling pitchblende (dated at 1 829 Ma) derived from meso- to epithermal solutions at a temperature of 160–230°C. This and the earlier pitchblende forming process are considered to belong to the same mineralizing event as deduced from the close formation ages and similar mineralization characteristics.

A different kind of mineralization with U-Th-REE mineral phases was finally formed during *Indosinian-Yanshanian* tectono-magmatic mobilization as reflected by volcanic activity and magmatic intrusions. Rocks of the basement including uraniferous facies are thought to have suffered anatexis. This

material was intruded into the Early Proterozoic fold belt and formed alkaline massifs such as the Saima alkaline complex 240–210 Ma ago with U, Th, and REE mineralization dated at 220–183 Ma (Guo Zhitian et al. 1996). A late event generated some minor pitchblende veinlets (Zhaoshan pitchblende) 130 Ma ago (Zhou Weixun, pers. commun.).

1.2.1.1 Lianshanguan Dome, Liaoning

The Lianshanguan Dome is located to the south of Benxi City in central SE Liaoning Province, some 100 km SSE of Shenyang. A number of structurally controlled metasomatite-type U deposits and occurrences, including Lianshanguan were discovered in the 1970s, most of which are scattered in a zone about 40 km long along the southern margin of the oval shaped dome (► Fig. 1.12).

The subsequent description is largely based on Qin Fei and Hu Shaokang (1980) amended by data from Guo Zhitian et al. (1996) and Zhou Weixun (2000).

Regional Geology and Principal Characteristics of Mineralization

The Lianshanguan Dome is situated in the E-W-trending Fengcheng Uplift. This uplift is located to the south of the Neoproterozoic-Paleozoic Taizihe Depression that separates the Fengcheng Uplift from the likewise trending Qingyuan Uplift to the north. The latter is characterized by Archean grey gneiss that was later weakly reworked.

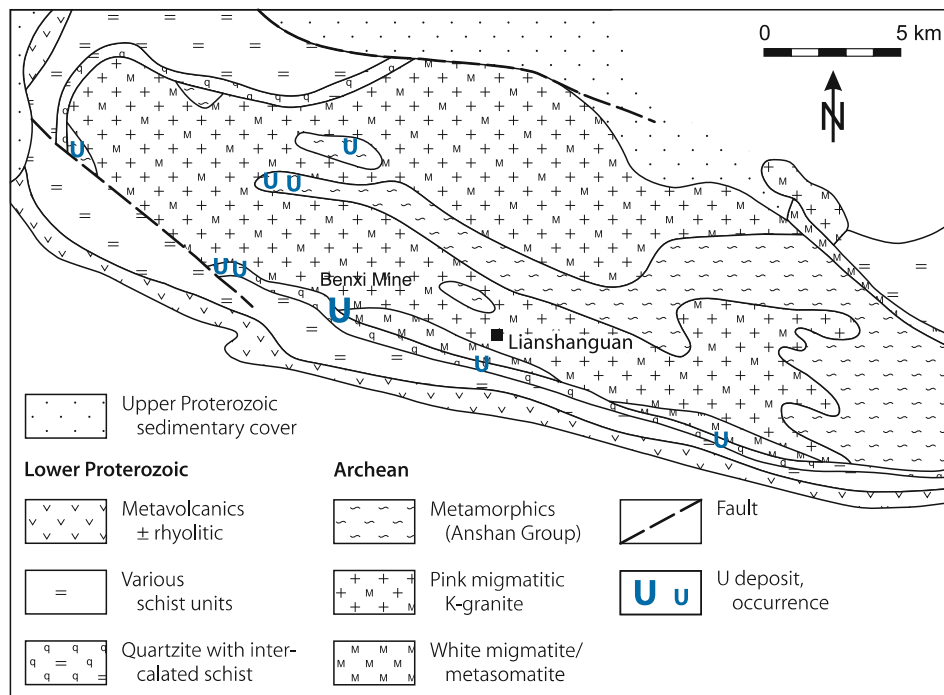
The Fengcheng Uplift consists of an E-W-trending zone of migmatized rocks that evolved from Neo-Archean granite-greenstone terrane during the Lulian Orogeny. These rocks form three domes within a 10–15 km wide and 200 km long zone; the Lianshanguan Dome is situated between the Gongchangling and Bahechuan domes.

The Lianshanguan Dome is an E-W-oriented brachyaxial anticline approximately 40 km long and 10 km wide composed of a core of Archean migmatitic granite and metamorphics of the Anshan Group enveloped by metamorphics of the Lower Proterozoic Liaohe Group. Both groups are separated by an unconformity but in the Lianshanguan area this contact is overprinted by metasomatism and partly by migmatite-metasomatic processes. Slightly metamorphosed Upper Proterozoic quartz sandstone, shale and limestone of neritic origin cover unconformably the crystalline basement in the north and northwest part of the area (► Fig. 1.12).

Migmatite is well developed in both Archean and Lower Proterozoic rocks along the axis of the Lianshanguan anticline, and occupies the greater part of the anticline. Although the intensity of migmatitization is variable, there is a trend of decreasing intensity from Archean to Lower Proterozoic rocks and from the axial part to the margin of the anticline as reflected by a regional transition from an inner pink migmatitic granite zone through a white migmatitic granite zone to a peripheral zone of white, Na-rich migmatitic metasediments that originated

Fig. 1.12.

Lianshanguan Dome, schematic geological map with location of the Lianshanguan deposit/Benxi Mine and other U occurrences (small U letters) (after Zhong Jiarong and Guo Zhitian 1984 and Qin Fei and Hu Shaokang 1980)



from Liaohe Group rocks and extends along the southern flank of the anticline.

Pink migmatitic granite of the inner zone is enriched in K-feldspar, of homogeneous texture, and covers 80% of the dome. This pink facies grades in the marginal part of the dome into white migmatitic granite that is enriched in Na (albite) and Si and has a relatively uniform or a banded structure due to the injection of albite veins with a magmatic texture. Additionally, albite veins and veinlets (without magmatic texture) of Na metasomatic origin also occur; they are often associated with replacement of quartz by albite in alkaline (Na-)metasomatized granite.

Uranium occurrences are found on the southern and northern flanks of the Lianshanguan Dome along the contact between the basal quartzite unit and white migmatitic granite; and additionally, in the axial part of the dome in inliers of Anshan Group rocks adjacent to pink migmatitic granite. Alkali metasomatic, especially Na-metasomatic processes that produced the above mentioned facies are considered a significant factor in uranium mobilization, migration, and reconcentration in the Lianshanguan Dome.

1.2.1.1.1 Lianshanguan Deposit

Discovered in 1978, the structurally controlled metasomatic vein-type Lianshanguan deposit (#3075) is located near Lianshanguan town, Fengcheng County, SE Liaoning Province, about 100 km SSE of Shenyang. In situ resources are on the order

of 1 500–5 000 t U and have grades between 0.3 and 1% U. Lianshanguan is exploited by the Benxi Mine named after the town of Benxi, located about 40 km to the north of the mine. Mining grades average 0.34% U. Underground mining started in 1996. Uranium is extracted by heap leaching methods and further treated by a mill at Lianshanguan.

Sources of information. Finch et al. 1993; Qin Fei and Hu Shaokang 1980; Zhong Jiarong and Guo Zhitian 1984, 1988; Zhou Weixun 2000.

Geological Setting of Mineralization

The Lianshanguan deposit is located at the southwestern rim of the Lianshanguan Dome. This terrane is underlain by pink and white migmatized Archean granites and Lower Proterozoic metamorphites that include the lithologies listed in the lithostratigraphic section below (Qin Fei and Hu Shaokang 1980).

- Quaternary overburden, 0.5–10 m thick: Alluvium, slope and residual gravel, sand, clay
- >Unconformity<
- Lower Proterozoic Liaohe Group (<500 m thick)
 - metamorphosed volcanic unit, >25 m thick: Submarine volcanic eruptives, mainly metamorphosed rhyolite-tuff and tuff-breccia locally
 - tremolite-marble unit, 95 m thick: Predominantly tremolite-marble interbedded with graphite-mica schist

- schist units, 180–290 m thick: Mainly garnet-quartz-mica schist with or without feldspar, graphite or staurolite, containing interstratified silica lenses in the middle and lower intervals and garnet-hornblende schist at the base. (This schist is a persistent unit throughout the mineralized area and serves as a marker horizon to define the U-bearing quartzite.)
- quartzite unit, 0–80 m thick (U ore host) (U background <17 ppm): quartzite interbedded with leucogranulite, quartz-mica schist, and quartzose metaconglomerate. Quartzite constituents include quartz, muscovite (sericite), argillaceous bands, and relatively abundant magnetite and impurities, such as clay, boron, and sulfur
- *Migmatitic transition unit* (main U host) (background <35 ppm U) subdivided into:
 - migmatitic metasediments (schist, quartzite)
 - taxitic migmatitic metasediments
 - homogeneous migmatite
 - transitional white migmatite granite
- >Unconformity<
- *Archean*: Ar₃ pink K-rich migmatitic granitoid and Ar₂ grey foliated Na-rich migmatitic granitoid (trondjemite?)

Although the preexistence and original nature of Archean granitoid in the Lianshanguan Dome is hard to identify due to intense reworking (migmatitization) during the Lulian Orogeny, its presence is indicated by U–Pb ages of 2 750 Ma for Ar₂ and 2 530 Ma for Ar₃ granitoids, and furthermore by outcrops of Archean granitoid in the Qingyuan Uplift. Some authors, as Guo Zhitian et al. (1996), note that Ar₂ granitoid is of sodic and Ar₃ granitoid of potassic nature; while others, as Huang and Zhou Weixun (pers. commun. 2003), consider a trondjemite composition for the original Archean granitoid.

Host Rock Alterations

Country rocks have been widely and intensely affected by K and Na migmatitization as mentioned earlier whereas host rock alteration is commonly only weakly developed. The latter includes pre-ore albitization and chloritization; pre-ore and particularly syn-ore sericitization and silicification, and syn- to post ore, weakly developed carbonatization, sulfidization with pyrite, galena and sphalerite, and rare fluoritization.

The U-mineralized basal quartzite unit has been converted into migmatitic rocks along the interface between mineralized quartzite and Archean pink migmatized granite. Relict fabrics preserved in metasediments adjacent to white migmatite suggest the white migmatite to be derived from quartzite.

Mineralization

Pitchblende is the principal ore mineral; other U minerals include uraninite, minor coffinite, and scarce U⁶⁺ minerals (gummite, uranophane, β -lambertite (uranophane), kasolite, billietite, autunite, and torbernite. Associated metallic minerals include

minor amounts of pyrite, pyrrhotite, chalcopyrite, galena, sphalerite, and molybdenite. Pyrite is the most common phase. Some native gold exists in small amounts of as much as 0.3 ppm. U correlates positively with Mo and Pb. Gangue minerals include minor chlorite, sericite, quartz, and carbonates. Chlorite veinlets cut or coat massive pitchblende; sericite and secondary quartz are closely associated with pitchblende and often occupy the center and/or the wall of pitchblende-bearing veins and veinlets. Concentrations of fine-grained to cryptocrystalline carbonates occur in high-grade ore shoots.

Pitchblende contains 71.9% U, 3.0% Pb, 1.8% Si, and 0.5% Ca. Pitchblende occurs in disseminated distribution in rock matrix and along schistosity planes, and as massive pitchblende with colloform habit in veins, veinlets, and breccia matrix.

U is hosted in metasediments of the basal Liaohe Group that are migmatized to a certain extent and usually albitized and chloritized, and exhibit interstratified brecciation, schistosity, and taxitic textures. Cataclastic, impure, grey to black-grey quartzite, mica-quartz schist, gneissic biotite migmatite, and taxitic migmatite (heterogeneous in both mineral composition and texture) and breccias are the prevailing host lithologies. These horizons are folded into a monocline and dip at 25–50° to the southwest (► Fig. 1.13). Uranium background tenors of the ore-bearing horizons average 25 ppm U but can be as high as 35 ppm U.

Shape and Dimensions of Deposits

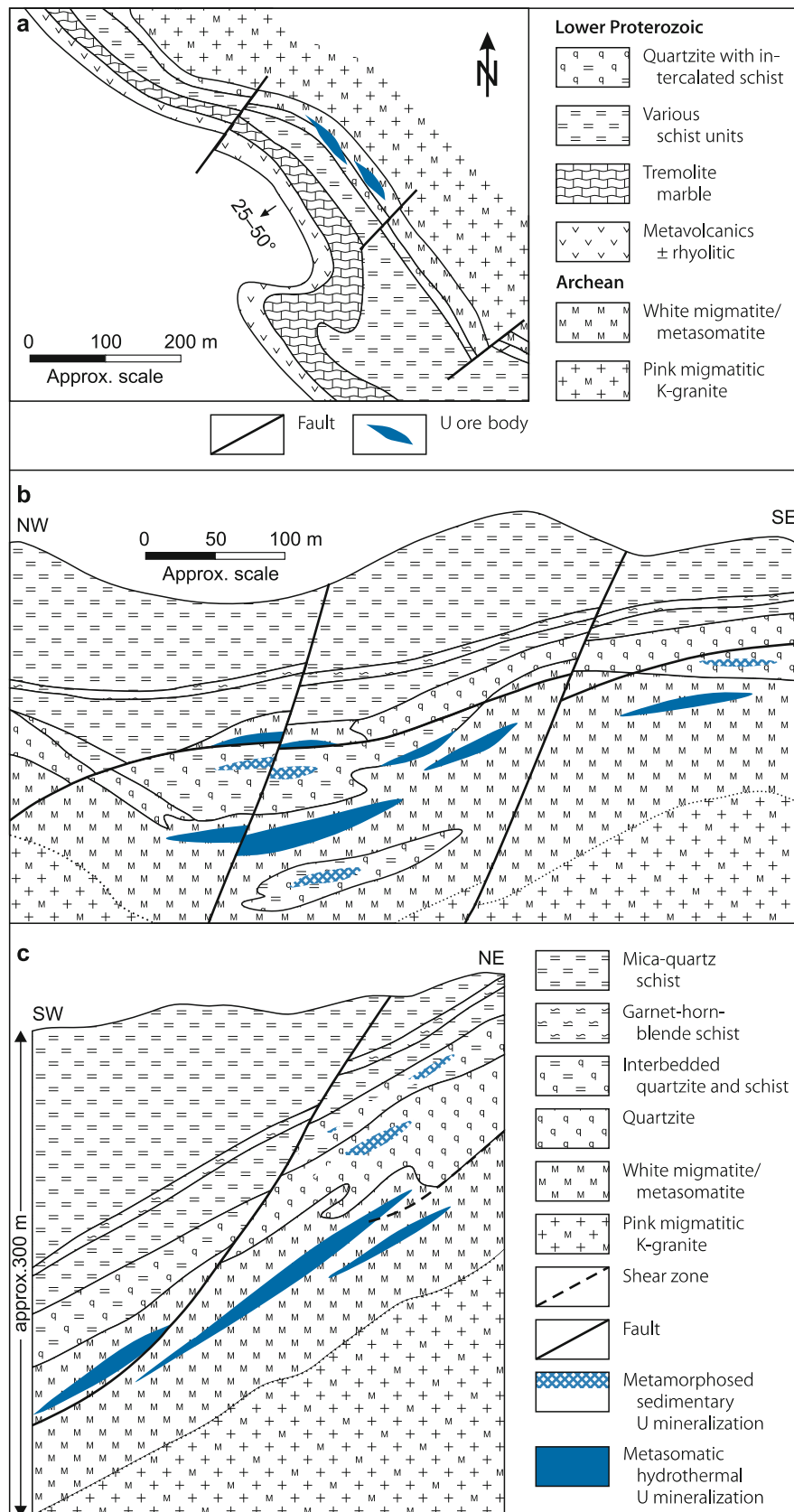
Lianshanguan is a structurally controlled metasomatite-type deposit of irregular shape composed of a number of ore bodies of complex configuration (Zhang Rong 2001). Ore lodes are of lenticular, veinlike, and nested shape and occur discontinuously at depths from 38 m to 250 m controlled by interformational faults, saddle structures, and fractured intervals (► Figs. 1.13b–d).

Lenticular lodes include the main ore body at Lianshanguan. This ore body has dimensions of up to 5.6 m in average thickness, 90 m in length, and 40 m downdip; it accounts for 75% of the total reserve of the deposit at grades averaging 0.5% U. It is emplaced in interstratified breccia zones within migmatitic and taxitic metasediments and has an internal structure of vein lodes and veinlets. Ore is composed of pitchblende and sulfides with rock debris cemented by clay minerals. The position and size of this ore body and similar ore lodes as well are a function of the morphology of the contact between Lower Proterozoic and Archean rocks. A higher intensity of tectonic fracturing at the convex part of the migmatite-metasomatic contact is accompanied by more extensive mineralization.

Layered lenses are up to 200 m long, from 15 to 40 m wide, and from 0.6 to 8.5 m thick, and occur on the upper levels of the deposit. The grade is lower than that of the above-mentioned lens-vein-type mineralization, but is relatively uniform. Mineralization consists of uraninite distributed along schistosity and gneissose foliation in quartz-mica schist interbedded with quartzite of the quartzite unit and in the migmatitic transition unit.

Fig. 1.13.

Lianshanguan deposit, schematic **a** geological map, **b** longitudinal NW-SE section, **c** SW-NE cross-section (after Zhong Jiarong and Guo Zhitian 1984)



Irregular uranium-bearing veinlets consist of pitchblende filling fracture systems in the homogeneous migmatite unit. Individual veinlets range in length from 10 cm to more than 10 m, and from millimeters to several centimeters in thickness. The intensity of mineralization depends upon the size and density of the fracture system. This veinlet-type mineralization is of subeconomic quality.

Ore Control and Recognition Criteria

Ore lodes in the Lianshanguan deposit are primarily controlled by structure, litho-stratigraphy, and metasomatic lithology including the following characteristics according to Qin Fei and Hu Shaokang (1980) (see Sect. *Metallogenetic Concepts* for genetic considerations):

Host Environment

- Marginal zone of Archean-Lower Proterozoic massif
- Archean craton segments with intervening Lower Proterozoic fold belt
- U ore is essentially restricted to a metamorphosed detrital sequence at the base of the Lower Proterozoic Liaohu Group and its migmatized lower part
- Main host rock is impure, grey and black-grey quartzite enriched in clay, iron, carbon, sulfur and other impurities
- U background averages 25 ppm (<35 ppm U) in ore-bearing horizons

Alteration

- Intense and widespread alkali metasomatism/albitization and silicification
- Weak wall rock alteration by chloritization, sericitization, carbonatization, pyritization, and rare fluoritization

Mineralization

- Three modes of U mineralization of different origin and age are identified:
 - lenticular stockworks (the only ore-forming mode) with simple ore composition; pitchblende (dated at 1 894 Ma) is the principal U mineral associated with sulfides and minor gangue minerals. Ore lodes are restricted to breccias and faults within the alkaline feldspar-metasomatized zone
 - veins and veinlets with pitchblende (1 829 Ma) associated with calcite and fluorite in altered granite
 - stratiform, syn-metamorphic(-sedimentary)-type mineralization represented by micro-granular uraninite (2 114 Ma) enclosed in metamorphic rock constituents mainly of quartzite and mica-quartz schist
- Pitchblende forms veins and veinlets in interstratified breccia, and forms rich ore-shoots where migmatite is in irregular contact with metamorphic rocks
- Micro-granular uraninite occurs in, or associates with metamorphic minerals (garnet, tourmaline, biotite, chlorite)
- Ore bodies occur in the transitional zone between metamorphic and migmatitic sequences and are tectonically controlled in fracture zones

- Ore bodies are commonly emplaced in albitized-chloritized rocks and hence albitization and chloritization are thought to have caused U mobilization, migration, and pre-concentration

1.2.1.2 Saima Alkaline Massif, East Liaoning

The Saima deposit was discovered in 1958, about 125 km SE of Shenyang and 50 km E of the Lianshanguan deposit in the alkaline Saima Complex in eastern Liaoning. An initial drilling program followed in 1965–1968. U mineralization is of intrusive (rinkite) and partly of skarn types (U-rich pyrochlore), with rare veinlike mineralization. Resources are estimated on the order of 5 000 t U, at grades of about 0.05–0.1% U. The deposit was not mined because of the refractory nature of the ore minerals.

Sources of information. Saima Deposit Research Group 1976; Saima Scientia Sinica 1977; Zhou Weixun 2000; Zhou Weixun pers. commun. 2003.

Geological Setting of Mineralization

The Triassic Saima alkaline massif is within an E-W-trending alkaline magmatic complex, some 200 km² in size, that includes four larger alkaline intrusive bodies and a great number of alkaline volcanic and subvolcanic rocks. The Saima Massif is the westernmost intrusion; it measures about 20 km² on surface, persists to depths exceeding 1 000 m, and occupies the core of an E-W-oriented brachyanticline composed of Proterozoic and Lower Paleozoic strata. Dolomitic marble of the Proterozoic Liaohu Group occurs to the north, west, and south of the massif; phyllite of the Liaohu Group to the southwest; and Sinian quartzite and Cambrian limestone to the northeast. Jurassic conglomerate, sandstone, and coal beds cover the eastern part of the massif.

The Saima Massif is composed of alkaline volcanic eruptive, intrusive, and dike rocks derived from a cognate alkaline magma. Potassium-rich *eruptive* rocks prevail at the top and margin of the massif and include leucitic porphyry, phonolite, trachyte, and pyroclastics. A *first intrusive phase* that intersects the eruptive suite consists of mica aegirine nepheline syenite that occupies the center of the massif and grades laterally into black-aegirine nepheline syenite. A *second intrusive phase* produced a suite of sodium-rich aegirine nepheline syenite mainly in the northwestern massif. These rocks are generally a few score and locally over 200 m thick and contain a large number of xenoliths of the earlier intrusive rocks. Three petrographic varieties are distinguished by the color of aegirine. Grass-green-aegirine syenite that grades laterally into green-aegirine nepheline syenite, while both varieties change into eudialyte grass-green-aegirine nepheline syenite with depth. These lithologies are enriched in a number of trace elements as documented in ▶ Table 1.5. Dikes and pockets of consanguineous pegmatite, aplite, and lamprophyre as well as veins of dark-green-aegirine

Table 1.5.

Saima Massif, average background values of trace elements (in ppm) in various rocks (Saima Deposit Research Group 1976)

Lithology	U	Th	Nb	Ta	Zr	Hf	Ce	La
Eruptive phonolite	21.9	58.2	123	3.0	993	54.9	355	140
1 st intrusive phase nepheline syenites	9.5–20.2	38.5–67.4	59–90	2.4–2.6	802–1602	45.9–81.2	294–424	103–210
2 nd intrusive phase nepheline syenites with								
• green aegirine	37.5	68.5	367	9.5	7 889	482.9	597	352
• eudialyte grass-green aegirine	47.5	33.7	370	7.7	8 101	513.9	586	274
• grass-green-aegirine	122.1	129.6	374	6.3	7 690	399	1005	469
Metasomatites	14.0–110.5	2.3–240	133–374	6.4	96–6 490	0.5–393.3	12–700	9–873

nepheline syenite cut these rocks. Alkaline skarn and fenite occur at the contact of alkaline intrusions with country rock.

The grass-green-aegirine nepheline syenite is the latest apgaitic product of magmatic differentiation and the essential ore-bearing rock in the Saima Massif; it contains up to 122 ppm U (at a Th/U ratio of about 1), substantial amounts of Th, Nb, CeRE, Zr, and abundant volatile components (F, Cl, S, H₂O). Rock constituents range in grain size from fine-grained to pegmatitic and include grass-green aegirine in the form of small needles (<0.005 mm wide) and blanket-like, radiate-fibrous, and irregular massive aggregates. This rock exhibits a gentle stratification due to magmatic differentiation as reflected by melanocratic layers rich in grass-green aegirine that alternate with leucocratic layers rich in feldspar and nepheline. Abundant xenoliths and remnants of rocks of the first intrusive phase are peneconcordantly arranged in these layers.

Host Rock Alteration

Contact metasomatism is extensively developed. Alkaline rocks in contact with phyllite and quartzite exhibit intense fenitization while country rocks are remodified to various fenites composed of alkaline minerals. When in contact with dolomitic marble and limestone, alkaline rocks are markedly skarnized. Early skarn is characterized by magnesian and calcareous-magnesian facies (humite-spinel-forsterite skarn, phlogopite-tremolite skarn, etc.) and later skarns by arfvedsonite and Mg-arfvedsonite, and commonly also by microcline and nepheline. These later skarns are termed “alkaline skarn” and constitute one of the important ore-bearing rocks in the Saima deposit.

Subsequent alteration processes ranged from metasomatic/pneumatolytic-hypothermal microclinization and nephelinization to meso-epithermal albitization, natrolitization, cancrinitization, analcimization, hydromicazation, chloritization, silicification, carbonatization, fluoritization, and hydrogoethitization. Hydrothermal alteration developed predominantly along late stage fractures in both endomorphic and exomorphic zones of the massif and is particularly pronounced in the western massif.

As a result of meso-epithermal alteration, various primary nepheline syenites are transformed into rocks resembling

alkali syenite in both appearance and composition; nepheline has vanished and dark minerals have disappeared partially or completely, whereas a number of authigenic minerals have been recrystallized. In order to discriminate this rock from primary syenite of magmatic origin it is locally termed “episyenite” (similar to the French definition of episyenite). Episyenite is also one of the ore-bearing rocks in the Saima deposit.

Mineralization

Mineralization at Saima includes three principal varieties: (1) Uraniferous rinkite in grass-green-aegirine nepheline syenite; (2) uraniferous pyrochlore and betafite in skarn; and (3) pitchblende in episyenite. Rinkite ore accounts for more than 90% of the total U reserves, pyrochlore ore for about 5%, while pitchblende ore occurs in a very small amount.

Elsewhere in the Saima Massif, there are small occurrences of uranothorite in fenite, uranthorianite in magnesian skarn, caryocerite in nepheline-acmite-augite skarn, pitchblende in altered phonolite, and shachialite (Sr-CeRE-Ti silicate with Zr, Th and U; similar to chevkinite) in green-aegirine nepheline syenite.

The *rinkite type*, the largest in size and main mode, of U mineralization consists of ore bodies that are strictly controlled by grass-green-aegirine nepheline syenite. This rock facies is prominent in the northwestern marginal segment of a syenitic intrusion where almost all rinkite ore bodies occur (Fig. 1.14).

Ores consist of a complex assemblage of rinkite and minor amounts of other radioactive minerals including lovchorrite, uranthorianite, uranothorite, and nenadkevite, as well as feldspar, nepheline and aegirine, and minor eudialyte, catapleite, lamprophyllite, loparite, pektolite, and sulfides and arsenides of Cu, Pb, Zn, Fe, Co.

Rinkite and alteration products thereof are the main carriers of U, Th, CeRE, and Nb and provide the principal ore minerals (Table 1.6). They may constitute as much as 40% of the ore. Rinkite occurs as slaty, columnar, and fibrous crystals, 0.2–2 cm with a maximum of 10 cm in length, that frequently form fan-like, radiate-fibrous as well as massive and vein-like

■ Fig. 1.14.

Saima alkaline massif, **a** generalized geological map, **b** NW-SE profile, and **c** nearly W-E section across a mineralized zone showing the affinity of U-Th mineralization to grass-green aegirine nepheline syenite (after Saima Deposit Research Group 1976)

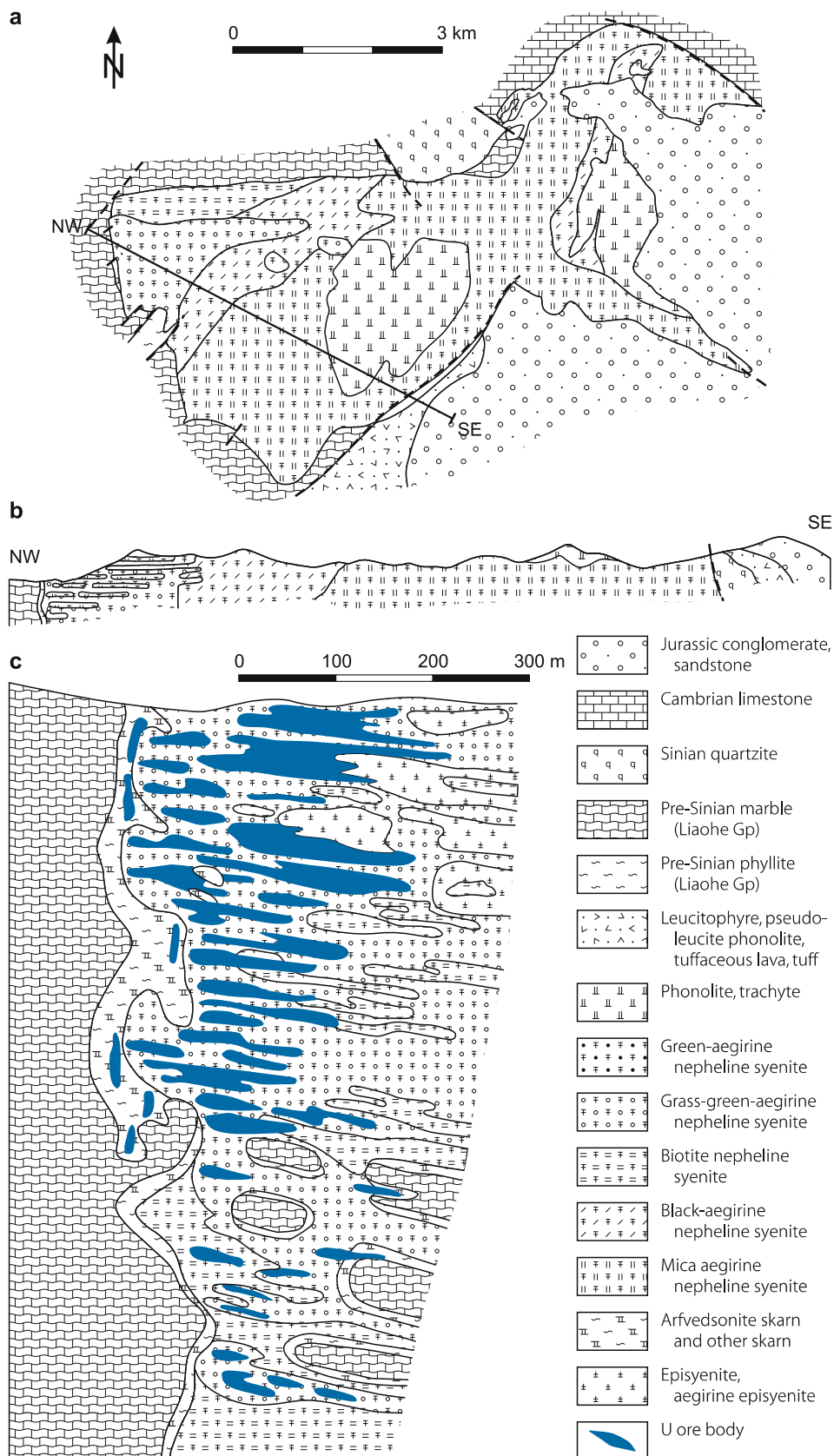


Table 1.6.

Saima deposit, content of selected trace elements (in %) in rinkite and its alteration products (Saima Deposit Research Group 1976)

Element	Rinkite			Altered rinkite	Wudjavrite
U ₃ O ₈	0.33	0.33	0.37	0.38	0.49
Th O ₂	1.90	1.18	2.39	3.86	4.15
REE ₂ O ₃	16.68	117.04	14.87	21.80	36.79
(Nb + Ta) ₂ O ₅	0.80	0.45	0.41	0.96	0.74
TiO ₂	9.13	11.25	10.33	10.31	10.15
ZrO ₂	0.05	0.10	0.06	0.08	0.03

aggregates; rinkite replaces and intersects feldspar, nepheline, and aegirine.

Most of the ore had been modified by late hydrothermal processes during which rinkite had been variably altered with an ultimate decomposition to mixtures of REE-carbonates, fluorite, and wudjavrite, and a redistribution of U and Th into minute U-Th minerals and new phases with absorbed uranium. Additional minerals in hydrothermally altered ore include a large amount of natrolite, chlorite, carbonate, illite, strontianite, brookite, anatase, zircon, and hydrogoethite.

Individual ore bodies are of tabular or lenticular shape with thicknesses of as much as 40 m and grades of 0.28–0.31% U. They occur en echelon arranged and concordantly within grass-green-aegirine nepheline syenite layers that dip 5–25°ENE. Ore bodies occur, although only sporadically, to depths of 800 m.

Uraniferous pyrochlore-betafite-type mineralization is controlled by relatively steep dipping skarn zones in the western part of the Saima deposit. Arfvedsonitite and phlogopitite are the main host rocks; and subordinately tremolite, carbonatized skarn, and episyenite in the endomorphic zone. Ore bodies occur as lenses composed of uraniferous pyrochlore and betafite that are irregularly disseminated, locally banded, or veinlets. Pyrochlore and betafite (in brackets) average 16.3 (24.5)% U₃O₈, 2.9 (1.4)% ThO₂, 1.9 (1.6)% RE₂O₃, 41.3 (29.9)% Nb₂O₅, among other chemical components. Additionally to these and skarn minerals, ore lithologies include feldspar, nepheline, apatite, sulfides, fluorite, zeolite, REE-carbonate and uranothorite.

Pitchblende-type mineralization is scarce and occurs as veinlets preferentially in the upper part of the deposit. It is controlled by fractured episyenite and aegirine episyenite in which it extends intermittently for great length, but with only a small thickness, along a set of NE-SW-trending and steeply dipping fractures. Pitchblende exhibits colloidal, commonly kidney-like and spherulitic, textures and contraction cracks. Associated minerals include pyrite, sphalerite, galena, chalcopyrite, hydrogoethite, quartz, chalcedony, calcite, and chlorite. Grades of pitchblende ore reportedly vary between 0.05 and 0.15% U.

Geochronology

Isotope ages obtained by K-Ar and U-Th-Pb methods give for primary rock constituents (biotite) and accessory minerals (rinkite and eudialyte) a time span from 240 to 220 Ma; 210–190 Ma for phlogopite in altered skarn; (that is thought to correlate with the age of U-rich pyrochlore mineralization); 190–170 Ma for thorite and zircon of hydrothermal origin (thought to correlate with the age of pitchblende-thorite mineralization); and 130 Ma for pitchblende, the latest product of the hydrothermal process (Saima Deposit Research Group 1976).

Zhou Weixun (2000 and pers. commun. 2003) provides the following ages: 240–210 Ma for the alkaline complex, 220–210 Ma for uraniferous pyrochlore and betafite in skarns, and 207–183 Ma for thorite, which is accepted as the mineralization age of veined pitchblende-thorite. He notes that 130 Ma old pitchblende is very rare and was only found in outcrops at Zhaoshan.

Ore Controls and Recognition Criteria

According to Saima Deposit Research Group (1976), favorable recognition criteria for the identification of this type of polymetallic, alkaline intrusive U deposits are as follows:

- Alkaline intrusion evolved by magmatic differentiation with development of late stage agpaite and ultraagpaite facies.
- Lithologies of the Saima Complex are characterized
 - mineralogically by a high content of aegirine and complex Na-Zr-Ti silicates (eudialyte, lamprophyllite, loparite, catapleite, rinkite, etc.),
 - petrochemically by a distinct oversaturation of alkali metals, high agpaite coefficient, high oxidation coefficient of iron, and low K/Na ratios, and
 - geochemically by a high abundance of U, Th, Nb, Ce, RE, Zr, Ti, Sr, lower Th/U ratios, and higher Nb/Ta ratios.
- Marginal and upper parts of the massif provide the most favorable sites for late magmatic differentiation products, concentration of volatile components, and uranium, thorium, and rare elements.
- Metasomatic/contact-metasomatic overprinting produced a variety of metasomatic facies including arfvedsonitite, tremolite-arfvedsonite, tremolite, phlogopitite, episyenite, aegirine episyenite, fenite, and skarn.
- Post-intrusive hydrothermal alteration includes intense albitization, natrolitization, carbonatization, silicification, and fluoritization along cataclastic zones.
- Intrusive-type mineralization occurs preferentially in contact zones of late stage agpaite rocks with metasomatites, particularly with Na-rich alkaline skarn and fenite.
- Calcareous country rocks tend to provide more favorable conditions for ore accumulation than siliceous rocks, particularly when in contact with rocks of late magmatic differentiation.

- Veined U mineralization is restricted to fractures and fissures in zones of intense hydrothermal alteration, particularly “episyenite”.

Metallogenetic Aspects

Following Saima Deposit Research Group (1976), geochronological data indicate that the development of the Saima Massif and related U, Th, REE mineralization lasted over a long time span from 240 to 183 Ma i.e. until the early Yanshanian Movement. The authors conclude that the long and thorough differentiation of alkaline magma is the fundamental prerequisite for the formation of the Saima deposit. Petrochemical and geochemical properties of the residual magma are critical factors for the formation of rinkite ore from residual magmatic-pneumatolytic processes, and the long-term evolution of the post-intrusive solutions is the main cause of the formation of uraniferous pyrochlore-betafite and pitchblende ore.

In more detail, the Saima Massif evolved by thorough differentiation of an alkaline magma that gradually changed from highly potassic to highly sodic and produced a suite of eruptive and intrusive rocks terminating with late magmatic agpaitic and ultraagpaitic rocks. Where these lithologies, particularly the late agpaitic facies, encountered calcareous or siliceous country rocks, extensive contact metasomatism took place and prepared the ground for emplacement of uraniferous pyrochlore-betafite ore.

Grass-green-aegirine nepheline syenite, the latest product of the magmatic differentiation, is characteristic of a residual magma; it contains up to 122 ppm U with a Th/U ratio of about 1 and substantial amounts of Th, Nb, CeRE, Zr, and abundant volatile components (F, Cl, H₂O, S). This agpaitic residual magma is the basic precondition for the formation of rinkite ore type.

During crystallization of grass-green-aegirine nepheline syenite, differentiation continued uninterrupted, forming early leucocratic layers, late melanocratic layers, and led to segregation and concentration of residual fluids with ore forming elements including uranium.

The minerogenesis of rinkite is a final result of crystallization-differentiation of residual magma. While the bulk of rock-forming minerals had crystallized during the main intrusive stage, volatile and ore-forming components (U, Th, REE, Ti, Nb) had been further concentrated and migrated in the form of complex compounds along layers of differential magmatic stratification within the grass-green-aegirine nepheline syenite body that had not been completely consolidated towards the marginal and upper parts of the massif. Pressure and temperature were lower in these sections and their drop caused the precipitation of the bulk of rinkite, which markedly replaced the preexisting rock-forming minerals. As a result, stratiform ore bodies were formed conformable to the differentiation stratification. Only a small amount of mineralizing fluid escaped to surrounding rocks (melanite mica nepheline syenite, arfvedsonite), and gave rise to small rinkite ore bodies.

Subsequent to the crystallization of grass-green-aegirine nepheline syenite and the formation of rinkite ore bodies, a

long lasting, but presumably discontinuous hydrothermal episode of pneumatolytic to epithermal activity affected the Saima deposit. These processes occurred over a time span as long as several tens of million years as suggested by the isotopic ages mentioned earlier. Residual fluids and post-intrusive solutions supplemented from the deep magmatic source rose along lithological contacts and fractures and caused the various metasomatic and hydrothermal alteration processes and originated uraniferous pyrochlore-betafite and pitchblende mineralization regimes.

Uranium was obviously further concentrated during the late to post-intrusive evolution while the content of Th and REE decreased. This assumption is supported by U background values in various lithologies and Th/U ratios. As shown in [Table 1.5](#), uranium contents in most metasomatites and altered rocks are universally high, in general higher than the average U content of most of the alkaline rocks and that of the massif itself as a total. Rinkite ore has a Th/U ratio of about 3, and contains considerable amounts of REE, whereas uraniferous pyrochlore-betafite ore has a Th/U ratio of only 0.3 and contains little REE, but pitchblende of the epithermal stage as a pure uranium ore.

Uraniferous pyrochlore-betafite mineralization is controlled by cataclastic skarn. This spatial relationship is explained by the reaction of the more acidic hypo-mesothermal, mineralizing solutions with skarn; the fluids were neutralized causing the precipitation of this U and Nb mineralization.

Pitchblende associated with thorite in veinlets and dated at 207–183 Ma occurs primarily in “episyenite”, a product of extensive and intense hydrothermal alteration of alkaline rocks including rinkite ore. It is postulated that at least a part of the pitchblende forming uranium originated by alteration of these rocks and ore bodies of the Saima deposit. This conclusion is based on the fact that rare element minerals of the late-magmatic and pneumatolytic-hypothermal stages (rinkite, eudialyte, lamprophyllite, etc.) were decomposed to minerals of simple composition (brookite, anatase, REE-carbonate, zircon, thorite, strontianite, etc.) by these meso-epithermal solutions, which permitted the liberation of U. Although this assumption may be correct, it does not exclude a derivation of U from other sources during a later event as suggested by isotope ages of 130 Ma for late pitchblende as found at Zhaoshan.

Repeated tectonic activity was a critical ingredient in the formation of the various types of mineralization. It promoted transport as well as local concentration of ore-bearing fluids that segregated in the late crystallization stage of the residual magma; and it also generated channel ways and space for ore deposition for the post-intrusive hydrothermal mineralization by post-consolidation fracturing.

In the first instance, the differential magmatic stratification of grass-green-aegirine nepheline syenite layers and associated rinkite ore bodies exhibit a rather gentle inclination that corresponds to a system of gently dipping primary joints in adjacent rocks of the first intrusive phase. This situation is thought to indicate only moderate tectonic activity during the emplacement of grass-green-aegirine nepheline syenite and, consequently, provided only restricted space but favorable conditions for ore

accumulation since it largely prevented the escape of mineralizing fluids and volatile components.

In contrast, tectonic activity was very pronounced during the formation of uraniferous pyrochlore-betafite and pitchblende mineralization as reflected by abundant fractures and steeply dipping veined ore bodies, as well as structurally controlled, large-scale host rock alteration.

The presence of calcareous country rocks is not only a prerequisite for the generation of skarn and, consequently, the herein contained uraniferous pyrochlore-betafite mineralization; it is also considered a critical factor for the formation of the Ca-rich rinkite ore due to provision of CaO to the magma.

1.2.2 Da Hinggan-Yanshan U Region, NE Inner Mongolia A.R. – N Hebei – W Liaoning

This region extends from the Da (Greater) Hinggan (also referred to as Daxing-anling) Range in NE Inner Mongolia to the Yanshan Range in N Hebei and forms part of the Yinshan-Liaoning metallogenetic zone (Fig. 1.10). While most U occurrences are of volcanic type, as found, for example in the *Guyuan-Duolun area*, there are some deposits/occurrences of basal channel sandstone type, but these are also closely related to volcanism, e.g. the *Qinglong ore field* (see below) in the southwestern and western Gangou Basin, respectively. The latter is located in Jianchang County, W Liaoning.

Source of information. Zhou Weixun 2000.

Regional Geology and Principal Characteristics of Mineralization

The Da Hinggan-Yanshan U region covers parts of the Altai-Hinggan Paleozoic fold system, which was affected by Mesozoic volcanism.

Structurally controlled U-Mo occurrences are associated with felsic volcanics within Jurassic depressions downwarped into Late Archean rocks; both units were overprinted by potassic metasomatism. Volcanic lithologies include trachyte and rhyolite lavas; subvolcanic bodies mainly of sub-rhyolitic porphyry, sub-granitic porphyry and related crypto-explosive breccia; and pyroclastic rocks including tuff and tuffaceous sandstone. Some U occurrences are also hosted by metasomatized granite, slate, and quartzite.

Two stages of mineralization and related alteration are identified. Most *ore bodies in trachyte and rhyolite lavas* were mainly formed by an early, main U stage, dated at 139–111 Ma, associated with albitization and pink coloration of wall rocks. A subsequent stage, dated at 110–90 Ma, was associated with pyritization and molybdenitization, and produced ore veinlets that overprinted the earlier mineralization. Deposits consist of several ore bodies of stratiform and lenticular shape that are from 30 to 50 m, rarely to 200 m long, and from 2 to 5 m, seldom to 10 m thick.

Ore lodes in subvolcanic porphyry bodies consist of early stage, mainly black and dark blue colored, disseminated mineralization

with a large amount of molybdenite; and late stage, pink colored vein-like mineralization at depth. Alteration is well developed and includes hydromicization associated with hematitization mainly at depth, whereas silicification and montmorillonitization prevail near surface.

1.2.2.1 Qinglong Ore Field, Gangou Basin, NE Hebei

The Qinglong ore field (Fig. 1.15) is in the Gangou Basin, which extends from Qinglong County, NE Hebei Province, into Jianchang County, western Liaoning Province. It contains basal channel sandstone-type U occurrences including three adjacent deposits, *Lingtou*, *Gangou* (also referred to as Jianchang), and *Shigaizi* in the Gangou Basin, and also structurally controlled volcanic-type U-Mo occurrences. OECD-NEA/IAEA (1997) reports resources of 8 000 t U for Qinglong at grades ranging from 0.03 to 0.1% U.

Sources of information. Zhou Weixun 2000, pers. commun. 2006; Yin Di 1990.

Regional Geological Setting of Mineralization

The Qinglong ore field is situated at the southwestern edge of the Gangou Basin (Fig. 1.15), a Mesozoic continental volcanic-sedimentary graben down-faulted along E-W-trending faults into a basement of Archean gneiss, migmatite and migmatitic granite, Proterozoic quartzite, schist and carbonatic rocks, and minor Early Yanshanian granite.

The basin is filled with fluvial and pyroclastic sediments that grade in age – from west to east – from Lower to Upper Jurassic. Respective lithologies include Upper Jurassic clastic sediments and andesite; Middle Jurassic uraniferous variegated, coarse- to fine-grained sediments, pyroclastic sediments and intermediate volcanics; and Lower Jurassic andesite and tuff. NW-SE-striking quartz syenite dikes are abundant and intersect the Jurassic strata.

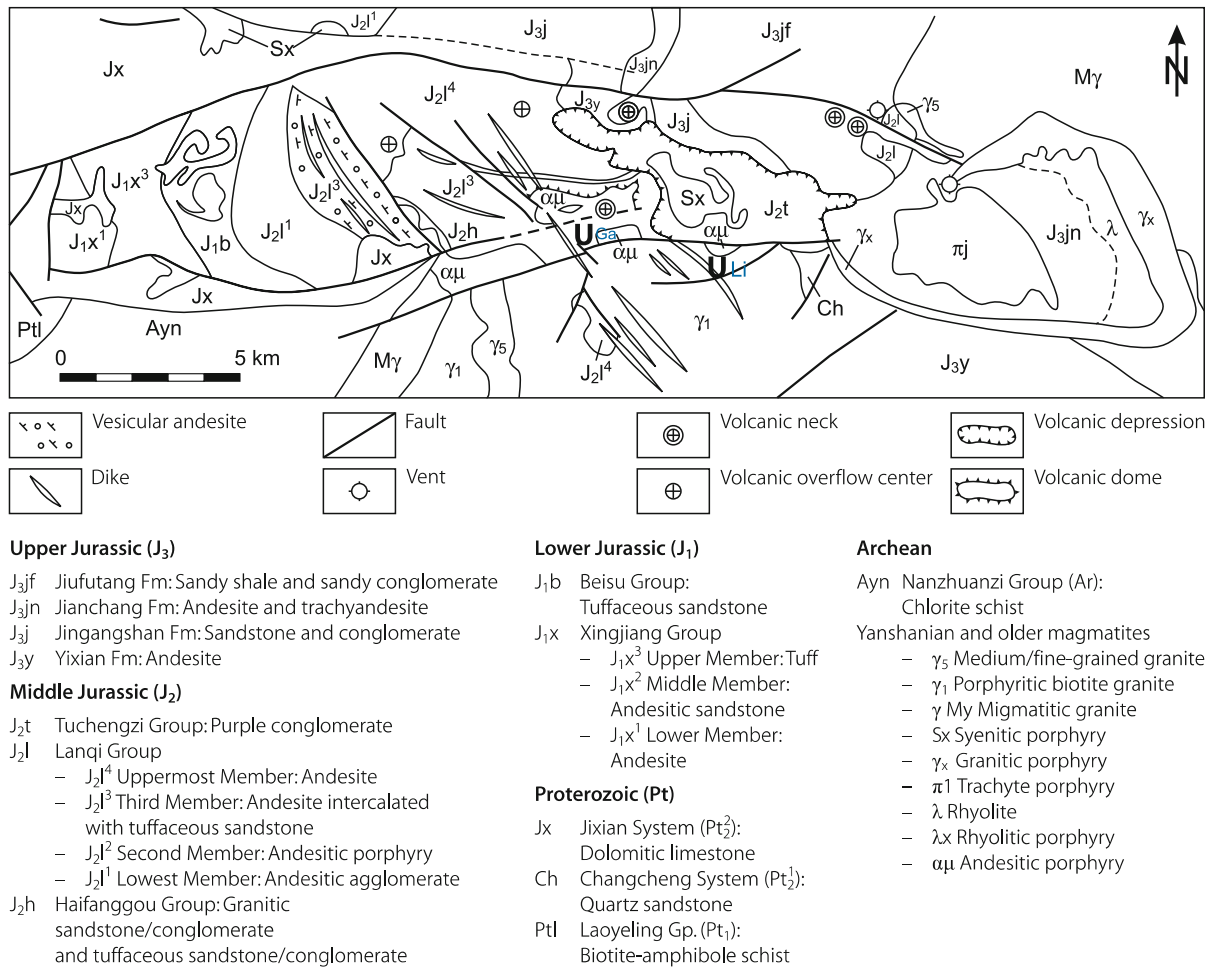
Uranium occurs in the tripartite Middle Jurassic Haifanggou Group:

- The Upper or Tuffaceous Member comprises tuff, tuffaceous siltstone and tuffaceous breccias; U mineralization occurs only locally.
- The Middle or Tuffaceous Conglomerate Member is composed of channel-filling polymictic conglomerate, carbonaceous tuffaceous conglomerate, and sandstone with intercalations of fine-grained sandstone and siltstone. This member hosts the Lingtou U deposit.
- The Lower or Granitic Conglomerate Member consists of granitic conglomerate with intercalated sandstone lenses of deluvial, alluvial fan and fluvial facies. Some U occurrences are hosted in this environment.

Thick-bedded andesite and associated clastic sediments of the Middle Jurassic Lanqi Group cover the Haifanggou Group.

■ Fig. 1.15.

Gangou Basin, Qinglong ore field, simplified geological map with locations of the two principal U deposits Gangou (Ga) and Lingtou (Li) (courtesy of Zhou Weixun 2006, based on Geological team no. 242, 1985)



1.2.2.1.1 Lingtou Deposit

Lingtou is the largest U deposit in the Gangou Basin. It occurs in a triangle-shaped fault block confined by basin-controlling E-W faults and NE-SW-oriented branch faults at the southern edge of the basin (Fig. 1.15).

U mineralization is preferentially hosted in fluvial channel facies of the Middle Member of the Haifanggou Group that directly overlie granite basement. *Host rocks* comprise granite-derived conglomerate and sandstone with abundant carbonaceous matter, tuffaceous components and pyrite; and, to a minor degree, tuffaceous lithologies. Andesite and andesitic agglomerate of the Lanqi Group, 150–300 m thick, rest on and interfinger with the mineralized sequence (Fig. 1.16).

Alteration phenomena include strata oxidation as well as carbonatization, chloritization, and argillization. Kaolinitization, montmorillonitization, dickitization, illitization, and damouritization are particularly well developed in wall rocks adjacent to veinlet and disseminated ores.

Mineralization consists predominantly of uranium adsorbed on clay minerals and organic debris that occurs together with

pyrite, and locally of pitchblende in the form of dissemination or mini-stringers associated with pyrite, chalcocopyrite, galena, sphalerite, hematite, fluorite, chalcedony, and calcite.

Ore bodies are of roll and tabular to lenticular shape with dimensions ranging from 30 to 70 m long and 1–9 m thick. Most ore bodies are located immediately above or close to the basement unconformity (Fig. 1.16).

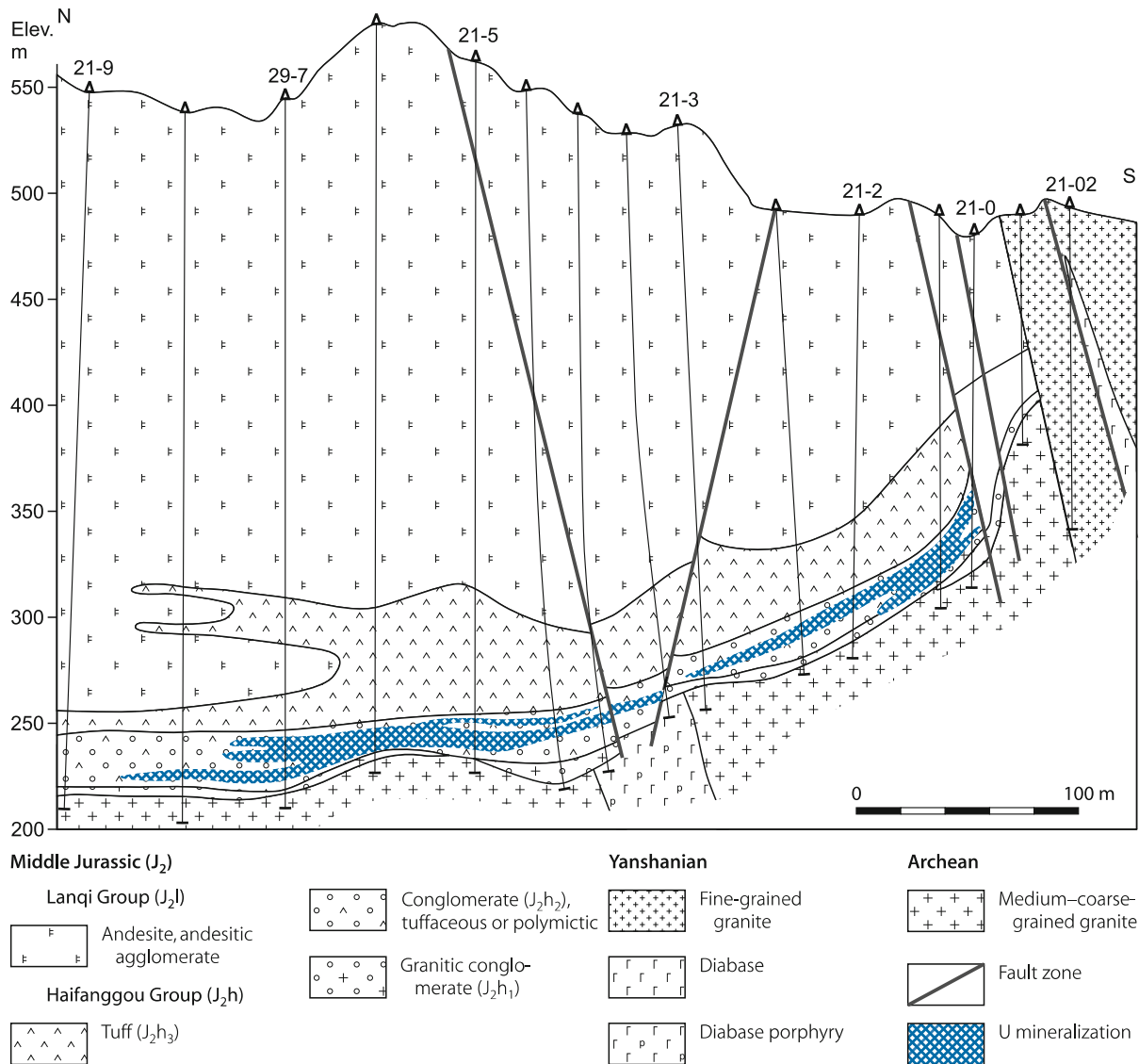
Metallogenetic hypotheses favor a redistributed (thermo-regenerated) origin of the ore (Yin Di 1990). U-Pb isotope systematics yield 160–150 Ma for low-grade ore, 140–110 Ma for high-grade ore, and 80–70 Ma for pitchblende in veinlets. The former age is thought to reflect the time of original basal-channel mineralization and the latter the age of quartz syenite dike-related hydrothermal processes that overprinted the former.

1.2.2.2 Guyuan-Duolun U Area, N Hebei – SE Inner Mongolia A.R.

The Guyuan-Duolun area occurs within the SW segment of the eastern branch of the Da Hinggan Mesozoic volcanic zone.

Fig. 1.16.

Gangou Basin, Qinglong ore field, Lingtou deposit, N-S section exhibiting the position of U mineralization in the basal part of the sedimentary-volcanoclastic succession of the Middle Jurassic Haifanggou Group (courtesy of Zhou Weixun for selection and translation from Chinese literature)



Volcanic-type U deposits/occurrences are found on both sides of the Inner Mongolia-Hebei border line. Reported occurrences in the Guyuan area include #16, 21, 22, 34, 160, 312, 335, 460, 531, 534, 571, 573, 715, 721, 767, and 781 (Luo Yi et al. 1996); none of these were mined.

1.2.2.2.1 Guyuan Deposit

The volcanic-type U-Mo Guyuan (#460) deposit is located in Guyuan County, Hebei Province. Explored in situ resources are between 1 500 and 5 000 t U at a grade averaging 0.1–0.3% U.

Sources of information. Luo Yi et al. 1996; Zhou Weixun 1997, 2000.

Geological Setting of Mineralization

Guyuan is situated at the northwestern edge of a down-faulted, Upper Jurassic volcanic basin that unconformably rests on the Late Archean Hongqiyingsi Group. This group originated from carbonaceous argillo-arenaceous rocks, intermediate-felsic volcanics, and minor carbonates, which were metamorphosed to granulite, gneiss, and marble, and which experienced intense potassium migmatization during the Luliang Orogeny.

Two large-scale volcanic episodes affected the area. During the Upper Jurassic/Late Yanshanian intermediate-mafic, intermediate-felsic and felsic volcanics, from the bottom to the top, were extruded, while basaltic material was extruded during the Himalayan taphrogenic event.

After the effusion of felsic volcanics (rhyolite, ignimbrite, breccia tuff and breccia-agglomerate lava) of the 3rd Member of the Zhangjiakou Group (K-Ar age: 143.2 Ma) during the Late Yanshanian event, regional collapse of the volcanic basin and intrusion of subrhyolitic porphyry bodies (U-Pb age for zircon: 121.9 Ma) occurred.

Four fault systems trending ENE-WSW (F45), NW-SE (F3), NNW-SSE (F7) and NNE-SSW (F2, F4, F5, F6) are noticed. The ENE trending fault (F45) is a repeatedly reactivated regional structure of Early Yanshanian age that, in combination with subsidiary NW-SE faults (F3), controls the position of the deposit.

The U-hosting subrhyolitic porphyry body occurs as an arc-shaped body oriented NW-SE and dipping NE along the F3 fault. Crypto-explosive breccia and breccia-agglomerate lava form the top of the subvolcanic body (Fig. 1.17).

Host Rock Alteration

Alteration phenomena include large-scale pre-ore hydromicazation and zeolitization, followed by syn-ore and post-ore hydrothermal products as listed below (Fig. 1.18).

Hydromicazation includes three varieties: pre-ore tabular hydromica, syn-ore fragment-like hydromica, and post-ore stringers of hydromica. While pre-ore hydromicazation is ubiquitous, alteration features restricted to wall rocks are expressed by vertically zoned silicification-limonitization in the upper, montmorillonitization in the upper to intermediate, and hematitization in the lower section of the deposit.

Silicification-limonitization is typical for the top of the subrhyolitic porphyry body and comprises a siliceous cap and gossan. It persists from surface to a depth of some 30 m (elevation of 1527 m). The silicified rocks are solid, massive, and light red, grey-black, and grey-white. The contents of K₂O and Na₂O in silicified subrhyolitic porphyry are reduced to 1.77% and 0.09%, respectively, while SiO₂ accounts for more than 85% as compared to values as high as 7.55% K₂O, 0.88% Na₂O, and 74.32% SiO₂ in unsilicified subrhyolitic porphyry. Light-colored fluoritization and limonitization overprinted, sometimes significantly, silicified rocks, mainly along fissures.

Montmorillonitization prevails in an elevation interval from 1527 to 1467 m. Montmorillonite replaces hydromica and commonly occurs in miarolitic cavities and along vein walls. Montmorillonitization is accompanied by purple-black fluoritization, hydromicazation, zeolitization, and kaolinitization. These alteration processes increased the porosity of subrhyolitic porphyry to 8–17% as compared to 2–4% in unaltered subrhyolitic porphyry. The resulting spongy texture provided favorable spaces for disseminated U and Mo mineralization in this section of the deposit.

Hematitization is mainly confined to the middle to lower section of the deposit and is most obvious near veins with pitchblende

and polymetallic sulfides. Hematitization is accompanied by K-feldspar alteration, purple-black fluoritization, hydromicazation, pyritization, and chloritization.

Mineralization

Guyuan encompasses a number of U-Mo ore bodies most of which occur within an area of 0.1 km² in the western half of a subrhyolitic porphyry body, and a few in rhyolite and breccia-tuff immediately adjacent to the porphyry body (Fig. 1.17b). Mineralization persists almost from the surface, which is at an elevation of 1560–1520 m, to depths of some 500 m.

Three kinds of mineralization have been identified. They occur vertically zoned in the following order downwards (Fig. 1.18):

- a **Blue-black mineralization** consists of hydrous uranomolybdate, ilsemannite, wulfenite, betpakdalite, dauberite/zippeite, pyrite, limonite, and light purple fluorite, which occur in sandy material on top of the porphyry body near the surface. This mineralization is mainly associated with rocks altered by red and grey-black silicification. Supergene infiltration processes in Neogene-Pleistocene and recent times are thought to have formed this ore from black ore.
- b **Black, disseminated mineralization** with low U (0.05–0.2%) but relatively high Mo grades (averaging 0.55% Mo); it is dated at 90 Ma and associated with widespread argillization. Ore constituents include pitchblende, jordisite, As-bearing colloidal pyrite, and minor sphalerite, marcasite, purple-black fluorite and grey-black chalcedony. Ore bodies are of irregular lenticular shape and occur mainly in the upper-middle part of the subvolcanic body at an elevation of 1527–1349 m.
- c **Red vein-breccia mineralization** consists of veins, stockworks of veinlets, and breccias with pitchblende, molybdenite, galena, sphalerite, studerite, marcasite, hematite, purple-black fluorite, and grey-black chalcedony. This assemblage is superimposed on earlier formed disseminated ore. Pitchblende yields an age of 24 Ma. U and Mo grades are relatively high (U about 0.3%, locally up to 2%). This ore is typical of lower levels at an elevation of 1476–1067 m and is contained in rocks altered by potash-feldspathization and hematitization. The origin of this ore is attributed to hydrothermal activity in the Himalayan and Yanshanian periods superimposed upon black disseminated mineralization.

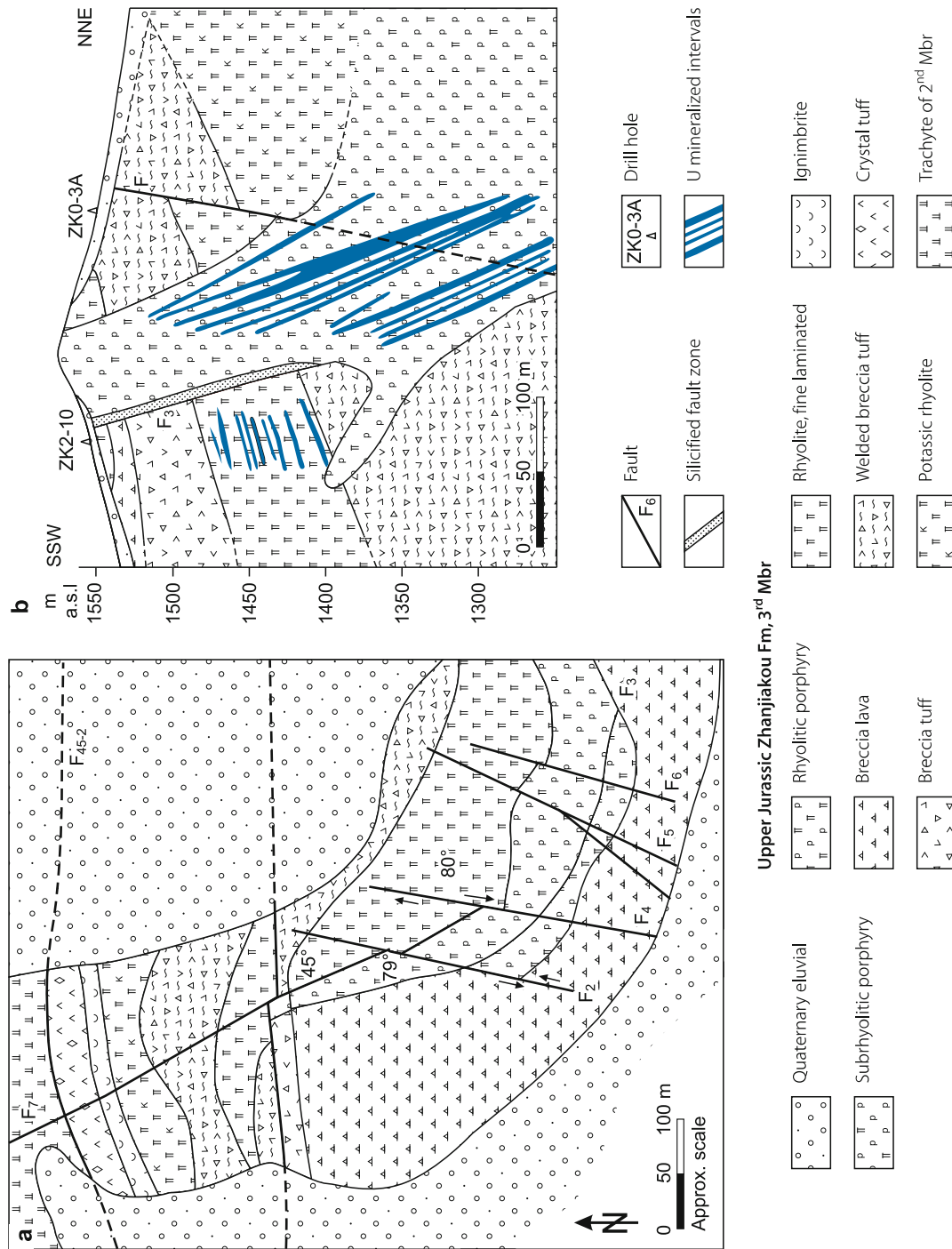
Mo mineralization also shows a vertical zoning reflected by disseminated jordisite in the upper to middle section and by molybdenite in the middle to lower section of the deposit. A near surface gossan and siliceous cap with limonite tops the deposit.

Shape and Dimensions of Deposits

The Guyuan deposit covers an area of slightly more than 0.1 km² in which mineralization persists almost from the surface to depths of some 500 m. Three depth-related zones in which

Fig. 1.17.

Guyuan deposit, Guyuan area, GUYUAN profile showing U association with a subvolcanic rhyolitic porphyry stock employed in Upper Jurassic felsic volcanics (after Luo Yi et al. 1996; b You Yunfei et al. 1996)



■ Fig. 1.18.

Guyuan area, Guyuan deposit, cross-section illustrating the framework of U mineralized structures and vertical zoning of alteration and U mineralization features (after Luo Yi et al. 1996)

Elev. m	Vertical zoning of veins	Fissure modes	Mode of U ore bodies	Host rocks	Alteration	Mineralization	Metallogenic periods
1500		Micro-veinlets, disseminated		Crypto-explosive breccia	Silicification, limonitization, montmorillonitization	Blue-black, sandy	Late Yanshanian
1400			Stockwork of intermittent veinlets	Subrhyolitic porphyry	Intense hydromicazation	Black, disseminated	
1300	Fine stockwork	Stockwork of continuous veinlets	Hydromicazation, hematitization		Red vein	Late Himalayan	
1200	Larger veins	Sparse veins, flat-lying, straight					Thick veins, flat, straight and brecciated
1100		Veins intermittent, pinching out	Hydromicazation				
1000							

ore-hosting structures differ in width, depth extension, spatial density, and strike direction are noted by Luo Yi et al. (1996). Characteristics of these zones are from top to bottom (Fig. 1.18):

- *Micro-vein-disseminated zone*: Shear fractures, NNE and NNW oriented, and arranged at limited density and scale of distribution dominate this zone.
- *Stockwork zone*: Main components are steeply dipping, NW- and ENE-oriented fractures as well as NNE and NNW-trending shear fractures. NW-SE fractures persist over a depth interval from 300 to 400 m. The width and extension of individual fractures are limited, but fracture density is high.
- *Large vein zone*: NNW and NNE striking and steeply dipping shear fractures of relatively large width and extension but minor fracture density prevail in this zone and control vein-type mineralization. These fractures/veins can persist to a depth of 500 m. Breccia-type mineralization occurs locally at the intersection of two fracture systems.

The scale and width of individual ore-hosting fractures gradually increase from the upper to the lower levels as reflected by widths of generally 1 mm in the upper, 1–2 mm in the intermediate, and over 2 cm in the lower part.

The deposit includes two rich ore intervals with grades up to 2% U. The upper interval is at 1 508–1 530 m and the lower interval at 1 300–1 400 m. These intervals consist of red vein-type ore that was superimposed upon black disseminated mineralization and which is mainly controlled by NW (F3) and NNW-trending (F7) faults.

According to Zhou Weixun (2000), individual ore bodies in both the upper and lower parts of the deposit are of lens or vein shape with lengths of 30–50 m, rarely up to 200 m, and thicknesses of 2–5 m, rarely 10 m.

Potential Sources of Uranium

Felsic volcanics of the Upper Jurassic 3rd Member of the Zhangjiakou Group contain 8–13 ppm U and subrhyolitic porphyry contains up to 15 ppm U; therefore, these rocks are considered the most favorable source of uranium.

Metallogenic Aspects

Luo Yi et al. (1996) postulate a polygenic evolution for the U-Mo Guyuan deposit. Their model involves a pre-ore and three subsequent hydrothermal stages as follows:

Pre-ore stage: Subsequent to intrusion of the (ore-hosting) subrhyolite-porphyry body, thermal fluids related to waning magmatic activity migrated upwards along structural zones and mixed with deep circulating groundwater. Heated to 300°C, according to fluid inclusion data, this solution caused large-scale hydromicazation and zeolitization and a related increment in rock porosity, as well as liberation of uranium from affected rocks. As such, these fluids prepared the ground and provided favorable conditions for the subsequent uranium metallogenesis.

Mineral stage 1 was generated due to reactivation of ancient faults (F45 and F3) in the course of late Yanshanian orogenic events that permitted ascension of deep seated, K-rich and weakly(?) uraniferous hydrothermal solution along permeable zones and their mixing with deep circulating groundwater. On its way upwards, this solution caused K-metasomatism and desilicification (at depth?) and formed alteration zoning of K-alteration-argillization, fluoritization, and silicification. During this process, the solution leached additional elements and became pregnant in elements collected at depth, as well as those extracted on its pathway such as U, Mo, Zn, Pb, Fe, S, and K to form the ore-forming solution.

As ore-forming solution entered the pre-ore hydromica-zeolite altered zone in the upper part of the subvolcanic porphyry body, uranium was precipitated and formed early-stage disseminated low-grade U mineralization. Associated with a further drop in temperature, H₂S in solution was disintegrated and sulfides were precipitated, jordisite in the first instance. Superimposition of these two mineralization phases produced black disseminated U-Mo mineralization in the upper section of the deposit at 90 Ma and a formation temperature of 300–250°C.

Mineral stage 2 resulted from hydrothermal reactivation in the course of taphrogenesis and related basalt extrusion during late Himalayan activity. Ore-controlling faults (F45 and F3) were reactivated and opened permitting deep-seated hydrothermal fluids to migrate and mix with descending groundwater. During upward migration, these fluids continuously extracted ore-forming elements from surrounding rocks, forming a solution enriched in U and Mo and other ore-forming elements. As these fluids migrated along faults and fractures at the hanging and footwalls of the subvolcanic body, reaction between uranium in solution and pyrite and other reductants in country rocks as well as a change in physical-chemical conditions occurred; the pH value decreased and the Eh value increased, causing silica in solution to precipitate in gel form (that may later recrystallize as quartz), and uranium to precipitate as pitchblende (dated at 23.7±2 Ma) in association with molybdenite, other sulfides and chalcedony as well as fluorite to form vein-type mineralization at a temperature 150–250°C. This mode of mineralization was commonly superimposed on earlier disseminated U-Mo mineralization and formed high-grade uranium ore.

Mineral/remobilization stage 3 evolved from the waning Himalayan Orogeny to Recent by an influx of groundwater and related supergene processes that reworked precursor mineralization. During this period of block faulting with small amplitudes, the deposit was slowly uplifted and its upper part exposed to oxygenated groundwater. Uranium and other ore constituents were leached, removed downwards, and reprecipitated at a redox interface at some depth, where they were superimposed onto black disseminated mineralization. As a result, high grade U and Mo, blue-black sandy mineralization was generated. The siliceous cap on top of the deposit provided an effective protection against renewed destruction of this near-surface ore interval.

1.2.3 Eren (Erlian) Basin, Central-North Inner Mongolia A.R.

The Mesozoic Eren (also spelled Erlian) Basin straddles the Chinese-Mongolian borderline to the south (► Figs. 1.1, 1.10). Several sandstone-type U deposits have been discovered to the north and east of the Lang Shan and Yinshan Ranges in the southern Gobi Desert since the beginning of exploration in 1980. *Nuheting* is the largest deposit discovered so far. Other deposits include *Subeng* (#861) and deposits #110 or *Naomugen*, #505, 2022, and 9131.

Huhe, *Mangheite*, and *Bayantala* are small sandstone-type deposits in the Bayantala Sag of the Tenggeer Depression. The small *Chelaomia* Basin, separated from, and located 20–30 km to the west of W edge of the Eren Basin contains the *Chelaomia* deposit.

Sources of information. Liu Xingzhong and Zhou Weixun 1990; Shen Feng 1995; Yu Dagan et al. 2002; Zhang Ruliang and Ding Wanlie 1996; Zhou Weixun 2000; Zhu Minqiang et al. 2002.

Regional Geology and Principal Characteristics of Mineralization

The Eren Basin is 1 000 km long in NE-SW direction, 50–200 km wide, and covers an area of about 130 000 km². This intermontane basin is located at the southern margin of the Hercynian Xingmong fold system. Proterozoic and Paleozoic slightly metamorphosed terrigenous lithologies, marine carbonate facies, mafic to felsic volcanics, as well as Variscan and Yanshanian intermediate and felsic intrusive rocks constitute the basement. These rocks form three, about E-W-oriented uplifts: The Wengduermiao Uplift borders the Eren Basin to the south and the Bayingbaolige Uplift to the north, while the Sunite Uplift divides the basin into the northern *Erennoer Depression* and southern *Tenggeer Depression*. In addition, a number of subbasins exist due to the irregular basement morphology.

Development of the Eren Basin began in response to prominent down faulting during the Jurassic and lasted through the Cretaceous. Uplift of the region terminated sedimentation at the end of the Upper Cretaceous until Tertiary time.

Jurassic and Cretaceous continental sediments of fluvial and alluvial-deluvial provenance fill the basin. They were deposited during an arid to semi-arid climate. Mostly thin Tertiary to Quaternary sediments rest upon the Mesozoic strata. Lithostratigraphic units include:

- Upper Cretaceous *Erendabusu* (*Erliandabusu*) Formation (K_{2c}): Variegated continental clastic sediments, bi-partitioned into two members. The upper Mudstone Member (K_{2c}²) consists of mud- and siltstone of lacustrine provenance, while the lower Sandstone Member (K_{2c}¹) is dominated by sand- and siltstone with intercalated dolomite and mudstone derived from a meandering fluvial system (details see at *Nuheting* deposit).

- Lower Cretaceous *Bayanhua Group* (K_{1b}) (from which oil is produced): Dominantly fresh to brackish lacustrine deposits with abundant organic material. Subunits include
 - *Saihan* (or *S*) *Formation* in which dark mudstone accounts for 0–45% of the sediments,
 - *Tenggeer* (or *T*) *Formation* with 60–90% dark mudstone,
 - *Aershan* (or *A*) *Formation* with 14–60% dark mudstone.
- Upper Jurassic *Xinganling Group* (J_3): Tuff, tuffaceous sandy conglomerate.
- Lower to Middle Jurassic *Alatanheli Group* (J_{1-2}): Coal-bearing sandy conglomerate of lacustrine, swamp facies.

Uranium mineralization is hosted by carbonaceous pelitic-psammitic sediments and occurs predominantly along the contact between the two members of the Erendabusu Formation but a few small roll- and basal channel-subtype deposits have also been found in Lower Cretaceous strata, such as *Huhe*, *Mangheite*, and *Bayantala*. Host rocks are locally altered by silicification, hematitization, and argillization.

The Upper Cretaceous contains tabular and lenticular U ore bodies preferentially in siltstone and mudstone, and occasionally in fine-grained sandstone. These ore bodies are less than 2 m thick and highly variable in lateral extension. Uranium occurs mainly adsorbed on clay minerals and rarely as pitchblende, coffinite, and uraniferous pyrite. Associated elements include Mo, V, and others.

1.2.3.1 Nuheting Deposit

Nuheting was discovered in the territory of Erenhot City, Inner Mongolia A.R., in 1990. The deposit is of tabular sandstone type and occurs in the Erennaoer Depression in the northeastern part of the Eren Basin. Explored resources are estimated in excess of 10 000 t U (Shen Feng 1995) at a grade ranging from 0.03 to 0.1% U.

Sources of information. Zhang Ruliang and Ding Wanlie 1996; Zhou Weixun 2000; Zhou Weixun et al. 2002.

Geological Setting of Mineralization

The U-hosting Upper Cretaceous *Erendabusu Formation* (K_{2e}) is flat-lying (▶ Fig. 1.19a) and reaches 230 m in maximum thickness in the Erennaoer Depression but is reduced to 65 m at Nuheting (▶ Figs. 1.19b,c). This formation includes an *upper Mudstone Member* (K_{2e}^2) composed of silty mudstone with intercalations of argillaceous siltstone of lacustrine provenance and a *lower Sandstone Member* (K_{2e}^1) of medium- to coarse-grained sandstone, fine-grained sandstone, and siltstone with intercalations of silty mudstone, sandy dolomite, and mudstone. Clastic sand-siltstone components are quartz and feldspar with Ostracoda and plant debris as well as minor dolomite, gypsum, and carbonate. Clasts in sandstone are poorly sorted and the maturity of the sandstone is low. Cement consists of hydromica, illite etc., with sporadic calcite or microcrystalline dolomite.

The Sandstone Member derived from a meandering fluvial system in a piedmont-alluvial environment and the Nuheting deposit is situated in middle-fan and fore-fan facies.

As mentioned earlier, the Erendabusu Formation rests on a Lower Cretaceous sequence that is subdivided into the S, T, and A Formations, from top to bottom. The intermediate T Formation consists 60–90% of dark mudstone and is an oil-source bed, while the remainder of sandstone acts as an oil reservoir and contains the JGS oil field. The Nuheting deposit is situated atop and at the margin of this oil field in overlying beds of the lower Erendabusu Formation.

Three major NE-SW-striking faults separate the Erennaoer Depression into three blocks (▶ Fig. 1.19a): the Naodong (Zhuodong) Depression, central fault zone, and Naoxi (Zhuoxi) down-faulted block. NNE and NW secondary faults are prominent in all blocks. These faults are mainly developed in the Bayanhua Group and resulted in a slight deformation of strata except for the Saiwusu fault at the southern margin of the depression, which is a growth fault and extends to the surface.

Mineralization/Shape and Dimensions of Deposits

Uranium is largely adsorbed on clay minerals. A minor amount occurs as pitchblende, coffinite, or is incorporated in pyrite and dolomite. Associated elements include molybdenum, gallium, indium, and vanadium.

Ore is grey to grey black in color, contains abundant pyrite, limonite, gypsum, carbonate (mainly dolomite and minor calcite), and carbonized plant debris, and is hosted some 80% in grey to blackish mudstone and siltstone and 20% in fine-grained sandstone. Pyrite is mostly fine dispersed and minor in the form of veinlets. Limonite is distributed along bedding planes and joints.

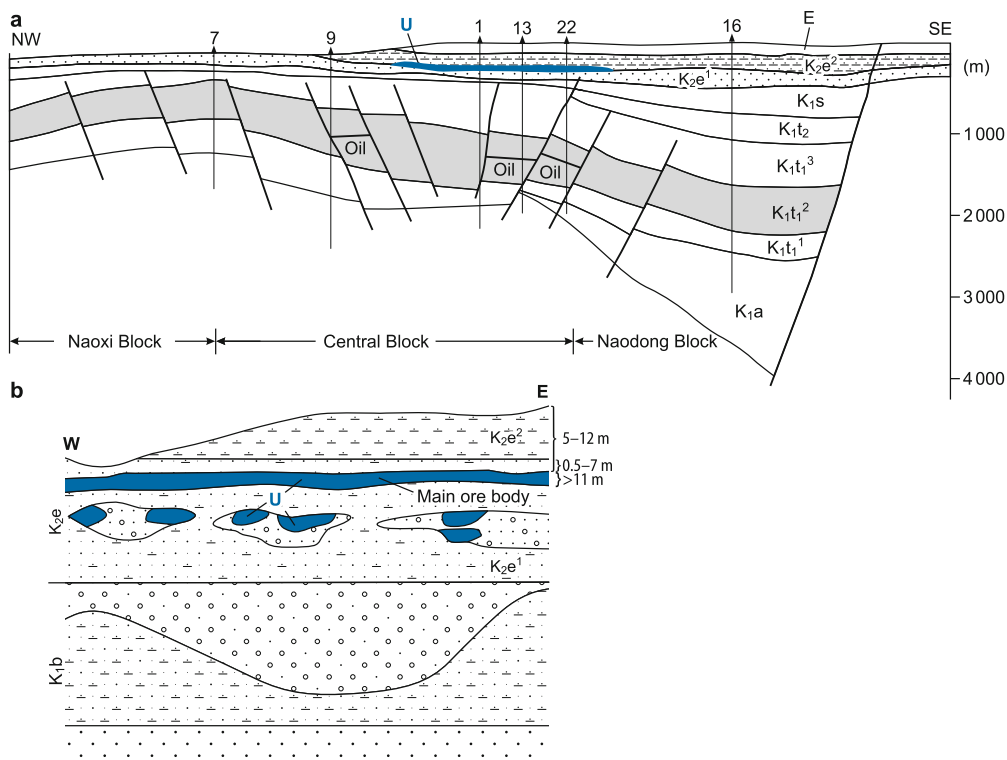
Nuheting consists of an upper main ore body and 13 lower, sporadically distributed small ore bodies (▶ Fig. 1.19b). U ore bodies consist of lenses and blankets with grades from 0.03% to 0.1% U. The main ore body is blanket shaped and located at the topmost position of the mineralized sequence, 5–12 m below surface and 0.5–7 m below the footwall of the Mudstone Member of the Erendabusu Formation. This ore body varies in thickness between 0.7 and 1.3 m, covers some 5 km² and accounts for more than 90% of the total resources. The main ore body is embedded in a mineralized zone seven times larger with 0.01% U or more over a thickness of 11 m.

Metallogenic Aspects

According to Zhang Ruliang and Ding Wanlie (1996), uranium mineralization at Nuheting, as well as at some other deposits in the Erennaoer Depression such as Subeng, is spatially and genetically related to oil-gas fields in the Bayanhua Group and was formed through time as reflected by isotope ages of U mineralizing events at 41±4 Ma, 18±1 Ma, and 6±1.8 Ma. Potential U sources are provided by basement as well as sedimentary rocks with elevated U contents, in particular Upper Proterozoic,

Fig. 1.19.

Eren Basin, Nuheting deposit. **a** Generalized NW-SE section of the Erenaoer Depression illustrating the stratigraphic position of oil fields in the Lower Cretaceous K_1t_2 horizon and U mineralization in the Upper Cretaceous K_2e^1 horizon, Erendabusu Formation, and their interconnection by faults. **b** Schematic W-E profile showing continuous tabular U mineralization below the mudstone member (K_2e^2) and discontinuous U mineralization further below. All U mineralization is hosted by the sandstone member (K_2e^1) of the Erendabusu Formation. **c** Litho-stratigraphic diagram of the U-hosting Erendabusu Formation (**a**, **c** after Zhang Ruliang and Ding Wanlie 1996; **b** after Zhou Weixun et al. 2002)



Subera	Epoch	Formation	Unit	Lithology	Thickn. (m)		
Q				Clay	1.40		
T	Eocene		Pg ₂ b	Mottled and pink sandstone	6.60		
	Paleocene		Pg ₁ n	Tan mudstone, siltstone	17.24		
K	Upper Cretaceous	Erendabusu FM (K ₂ e)	Mudstone Mbr K ₂ e ²	Grey mudstone, calcareous mudstone	23.32		
			Sandst. Mbr K ₂ e ¹	5	Grey-black fine-grained sandstone, siltstone	U	7.75
				4	Grey-black mudstone		4.79
				3	Grey fine-grained sandstone with interbedded siltstone	U	22.56
			2	Grey-yellow gravelly coarse- and medium-grained sandstone		25.46	
1	Variegated sandy conglomerate		4.59				
	Lower Cretaceous	Bayanhua Gp	K ₁ b	Brick-red sandy and silty mudst., variegated sandy congl.	16.67		

Paleozoic and Variscan and Yanshanian granitoid rocks with common contents of 4–13 ppm U; but also by grey and blackish argillaceous siltstone and pyritic siltstone of the Erliandabusu Formation with 12–38 ppm U, some 76–96% of which is in leachable form. Consequently, these authors postulate an epigenetic, multiphase origin for these deposits, which is related to interaction of upwelling oil and gas with oxygenated uraniumiferous groundwater and which they present in the following model.

Subsequent to deposition of the oil and gas-bearing Bayanhua Group, the region was slowly uplifted over a period of 115 Ma from Late Cretaceous onwards. During this period, the Bayanhua Group was covered under arid to semiarid conditions by a sedimentary suite less than 200 m in thickness including the Erliandabusu Formation. These conditions were favorable for a long-term influx of oxygenated, uraniumiferous solutions from the provenance area into permeable strata of the U host environment. A horizon of highly permeable, yellow sandstone underlying the main Nuheting ore body attests to the invasion of oxygenated groundwater.

Uplift of the region promoted migration of deep-seated oil- and gas-bearing water into permeable beds of the Erliandabusu Formation while impermeable beds prevented further upward movement of these solutions. Pathways for gas-oil migration were provided by prominent faults like the repeatedly, until Quaternary, reactivated Saiwusu growth fault at the southern margin of the Erennaoer Depression as well as major intraformational faults.

Introduction of oil and gas is documented by (a) oil-impregnated sandstone in U mineralized beds at Nuheting as indicated by a drill hole intercept at depths of 62–67 m where the thickness of U mineralization is 4.13 m and the grade is as much as 1.13% U; and (b) anomalous contents of hydrocarbons (mainly methane), H₂S and CO₂ also above the Nuheting and Subeng deposits. The hydrocarbons are similar in composition to gases associated with deep-seated oil although it cannot be excluded that H₂S and some CO₂ may also have resulted from the reaction of migrating gases with organic matter in wall rocks.

Oxygenated U-containing water was of Na-Ca-HCO₃ nature, and was capable of transporting uranium as a uranyl-carbonate complex. Where this fertile water encountered oil- and gas-bearing water, a redox zone was formed where U was reduced and deposited along with pyrite, dolomite, and calcite whereas hydrocarbons were oxidized, and silicates altered to clay minerals. Due to the capability of clay minerals and Fe-hydroxides to adsorb uranyl cations in solution, much of the uranium became bound in these minerals and formed ore bodies.

1.2.3.2 Other Deposits in the Eren Basin

Subeng (~1 700 t U, 0.03–0.756% U, av. 0.133% U) is located in the territory of Erenhot City and some 15 km NW of Nuheting. It was discovered in 1986 in exploration area #861. U occurs in tabular ore bodies in Cretaceous argillaceous sandstone of littoral-deltaic origin; plant debris and pyrite are abundant. Ore bodies range in thickness from 0.29 to 2.17 m and occur at depths from 5 to 37 m. Ore body 1 contains 87% of the total reserves of Subeng (Shen Feng 1995).

Mineralization is evidently related to invasion of oil-gas as reflected by brown-grey/black and grey-black, oil-soaked silty mudstone and oil-impregnated siltstone that was drill intersected at depth of 15.94–16.04 m where the mineralized body is thick, the uranium grade is high, and the radioactive equilibrium deviated to uranium. Anomalous contents of hydrocarbons (mainly methane), H₂S and CO₂ also occur above the deposit. The metallogenesis of Subeng is thought to be identical to that of Nuheting described above (Zhang Ruliang and Ding Wanlie 1996).

Naomugen/deposit #110 (several 100 t U) is situated some 40 km SSW of the town of Erenhot. Discovered in 1984, it was the first deposit found in the Eren Basin. U ore bodies occur in Tertiary carbonaceous, pyritic mudstone and argillaceous sandstone. Mineralization is in radiogenic disequilibrium in favor of uranium (Shen Feng 1995).

1.2.3.3 Bayantala Sag, Tenggeer Depression

The Bayantala Sag is part of the Tenggeer Depression and is located at the southeastern margin of the Eren Basin (► Fig. 1.20). It contains small basal channel and rollfront sandstone-type deposits with grades of 0.02–0.04% U at *Huhe* and *Mangheite* in Xianghuangqi County.

Sources of information. Yu Dagan et al. 2002; Zhou Weixun et al. 2002; Zhu Minqiang et al. 2002; unless otherwise cited.

Geology and Alteration

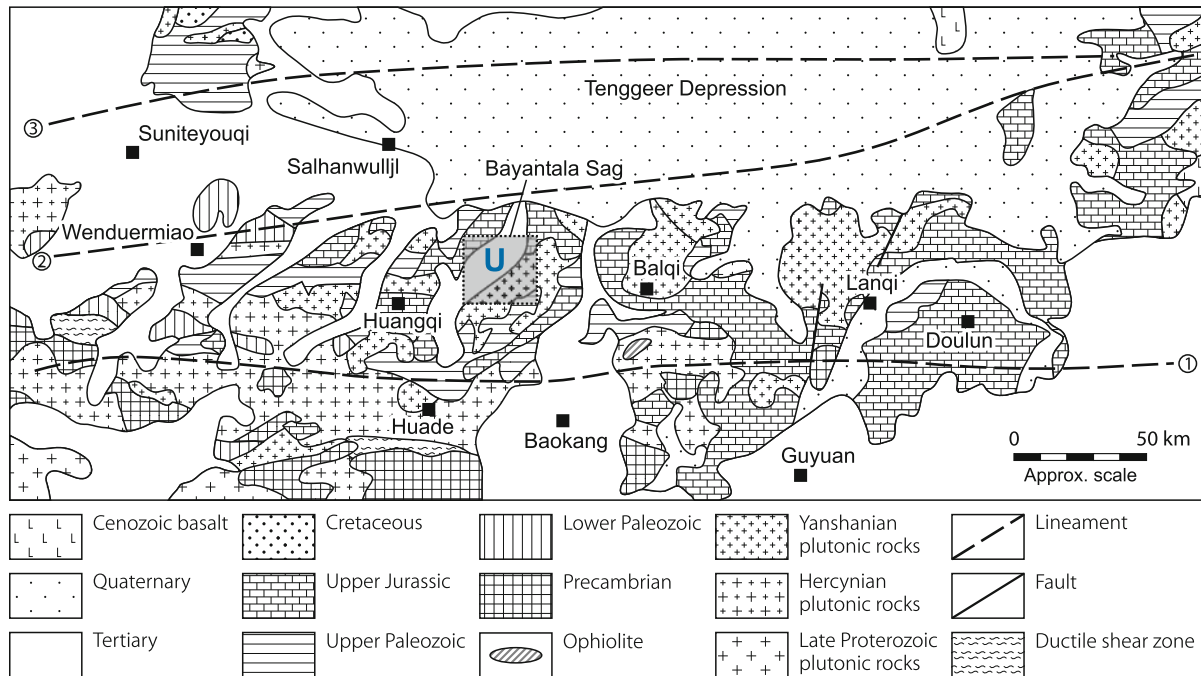
The Bayantala Sag is a fault-controlled depression, 64 km long in NNE-SSW direction, and 7–15 km wide. Rocks of a Hercynian fold belt, Early Permian intermediate-felsic volcanics, and Early Yanshanian granite constitute the basement (► Fig. 1.21).

The Lower Cretaceous *Bayanhua Group* is a prominent unit in the Bayantala Sag; it includes, in descending order, the *Saihantala* (*Saihan*) Formation of fluvial provenance, the *Tenggeer Formation* of a fan delta system, and the *Aershan Formation* of an alluvial fan system. Pliocene floodplain mudstone facies of the *Baogedewula Formation* and, locally, Pleistocene sediments rest upon the *Bayanhua Group*. The *Baogedewula Formation*, >165 m in thickness, comprises pink and yellow massive mudstone-siltstone rich in calcareous/manganese concretions, and locally intercalated thin-bedded sandstone and muddy conglomerate. U mineralization is restricted to the *Saihantala* and *Tenggeer Formations*.

The *Saihantala Formation* is subdivided into two members. The *Upper Member*, 40–50 m thick, is characterized by frequent alternation of sand and mud from meandering rivers. Light grey and yellow conglomerate and cross-bedded, medium-to coarse-grained sandstone form channel deposits and yellowish green, and variably pink, massive sandy mudstones form floodplain facies. The mineralized *Lower Member* is as much as 30 m thick and originated from a braided fluvial channel system (see further details below).

Fig. 1.20.

Southern Eren Basin, Tenggeer Depression with the southwesterly extending, U-hosting Bayantala Sag in the Wenduermiao Uplift (after Zhu Minqiang et al. 2002)



Braided channel deposits of the Lower Saihantala Formation have undergone paleophreatic oxidation. Later strata oxidation and secondary reduction affected this unit as well as the Tenggeer Formation.

Paleophreatic oxidation lasted from Late Cretaceous to the end of Paleogene. Sandstones and siltstones above the paleo-water table, which is near the bottom of incised valleys (Fig. 1.22a), are commonly yellow, yellowish green, or white, exhibit intense hydration of matrix material, and weak diagenesis. A bright yellowish oxidized bed (1–2 m thick) is commonly present above the paleo-water table.

Secondary reduction resulted from an influx of hydrocarbons, H_2S , and CO_2 along faults after deposition of red mudstone of the Baogedewula Formation. This alteration caused intense smectitization and kaolinitization of feldspars in the sandstones and turned their color into bluish or greenish shades in mineralized and adjacent areas.

Strata oxidation occurs near the fault-controlled outcrop of the Bayanhua Group and imposed a light yellow hue on sands in the fan delta front of the Upper Tenggeer Formation at Mangheite.

Mineralization in the Lower Member of the Saihantala Formation at Huhe

Basal-channel U mineralization occurs in 3–5 interconnected sand bodies of upward-fining arenite with a cumulative thickness

of 7–30 m (commonly 20–25 m). Highly carbonaceous lacustrine mudstone of the Upper Tenggeer Formation underlies, and mudstone of the Baogedewula Formation, 50–70 m thick, overlies the Saihantala Formation.

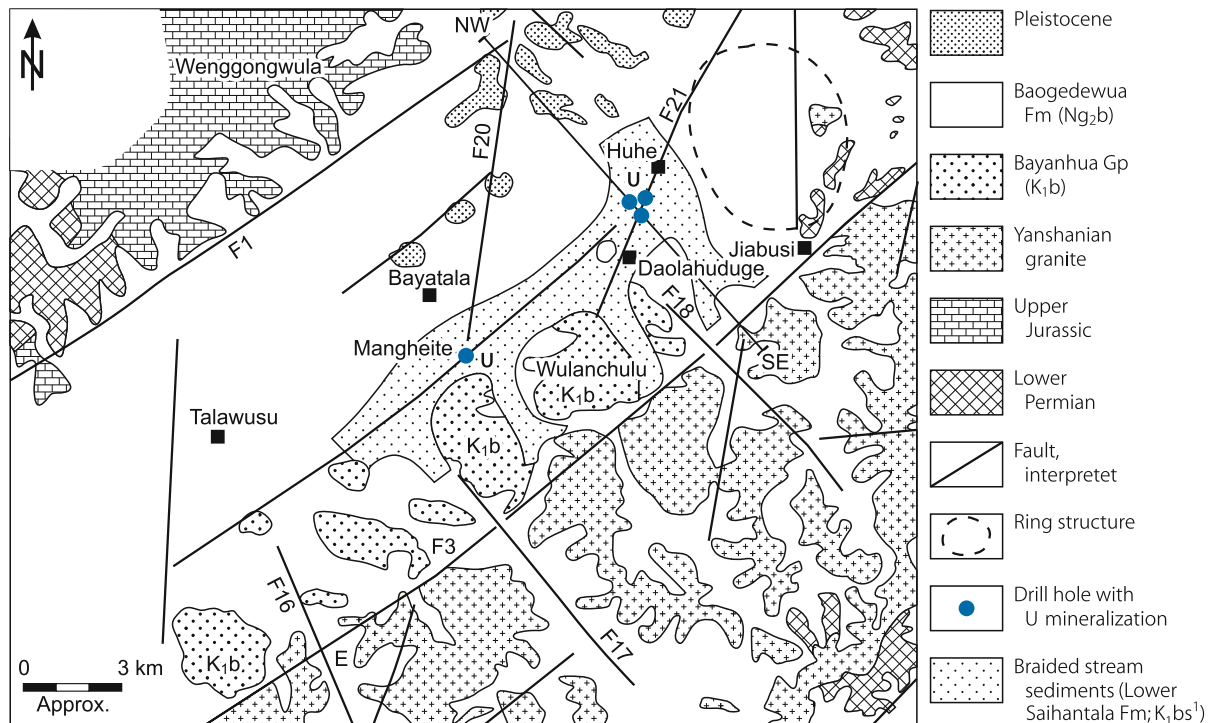
Ore bodies are tabular to lenticular in shape and located immediately above the unconformity in the center of a channel that is incised into muddy-sandy Tenggeer sediments (Fig. 1.22a). The slope gradient along this channel is $10\text{--}20\text{ m km}^{-1}$ increasing to 55 m km^{-1} at the SE margin.

Host rocks are mainly bluish grey, medium- to coarse-grained conglomeratic, and minor dark grey, thin-bedded, fine-grained quartz-feldspar sandstones. Dark grey siltstone and carbonaceous mudstone are locally mineralized. Sandstones are moderately sorted, unconsolidated, and permeable. Organic debris and remnants of laminated, carbonaceous mudstone are abundant. Feldspars are variably argillized. Mineralized sandstones have elevated background values of Re, Se, Mo, Sc and V, which correlate positively with U.

U mineralization is thought to be of either a one- or two-stage origin. Xia Yuliang et al. (2002) obtained a U-Pb isochronal age of 7 Ma for U mineralization in the Bayantala Subbasin and interpret this age to suggest that ore formation in the Saihantala Formation took place by paleophreatic processes prior to deposition of the impermeable Pliocene mudstone cover. The two-stage model forwarded by Zhu Minqiang et al. (2002) envisages an early mineralization stage related to phreatic oxidization and a later stage caused by interaction of U-bearing groundwater migrating down dip in permeable strata with hydrocarbons and H_2S migrating upwards along faults.

Fig. 1.21.

Southern Eren Basin, Bayantala Sag, geological map exhibiting the distribution of braided channel facies (Lower Saihantala Fm) and location of basal channel U mineralization (after Zhu Minqiang et al. 2002)



Mineralization in the Upper Tenggeer Formation at Mangheite

In the Mangheite area (Fig. 1.21, 1.22b), the Upper Tenggeer Formation consists of a fan delta system with delta plain, delta front, and pro-delta sediments. Distributary channels and mouth bar sand bodies are 4–30 m thick. These sand bodies are over- and underlain by lacustrine mudstones and inter-finger with lacustrine mudstone toward the center and grade into coarse-grained sandy conglomerates toward the margin of the sag.

Uranium is hosted by bluish grey, medium- to coarse-grained conglomeratic sandstones, which are intercalated with dark grey muddy siltstone, mudstone, and laminated fine-grained sandstone. Feldspar and quartz are the principal sand constituents with some volcanic clasts and lithic fragments of siliceous rocks. Kaolinitization is intense. Organic matter is abundant and amounts, in grey primary sediments, to 0.09–1.85% (av. 0.5%), in mineralized dark grey mudstone and siltstone, to 0.34–12.86%, and, in mineralized bluish grey sandstone, to 0.04–0.48% (av. 0.3%); the latter is almost as much as in oxidized zones. Fine-grained colloidal pyrite and marcasite occur as accessories. Sulfur contents in bluish grey sands are commonly 0.01–0.12%, and 0.06–0.69% with a maximum of 7.73% in mineralized intervals, suggesting an input of allogenic sulfur associated with hydrocarbons along faults.

Ore formation is attributed to block-faulting and related hydrodynamic processes in pre-Pliocene time. Due to uplift of

the SE segment of the Bayantala Sag, most of the Saihantala Formation was eroded or remained only as relics (several meters to tens of meters thick). In consequence, the delta plain was exposed and became a recharge area for U-mineralizing groundwater. At the same time, groundwater and hydrocarbons migrated upward along the F2 fault and generated a system of recharge-runoff-discharge, favorable for formation of roll-type U mineralization in channel sands of the frontal part of the fan delta.

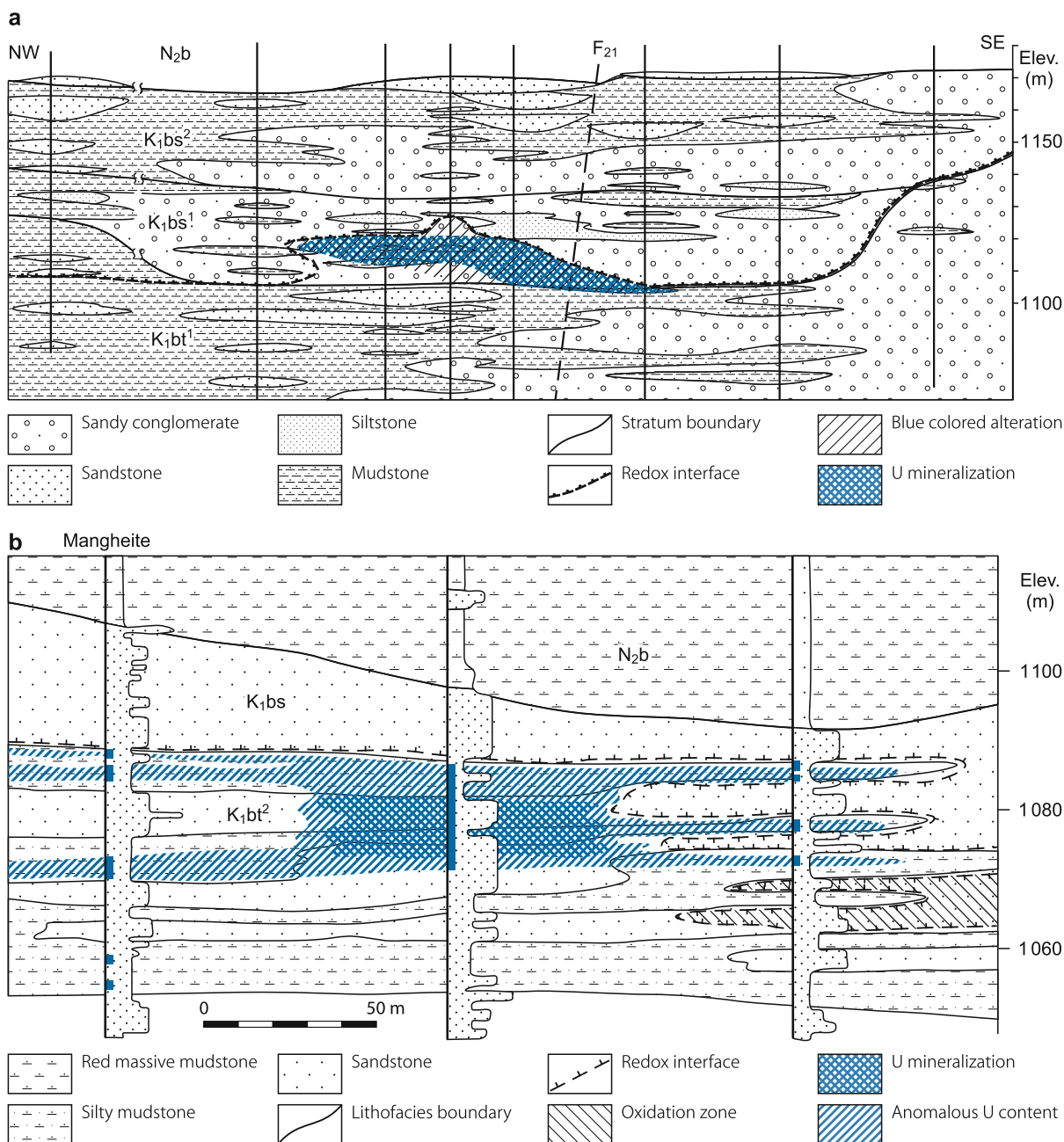
Shape and Dimensions of Deposits

Huhu site: Ore bodies are tabular or lenticular in shape and 2.4–14 m in thickness. The ore body shown in Fig. 1.22a is 200–300 m wide, 1 600 m long, and located at depths of 115–127 m. The grade is 0.01–0.039% equiv. U and 0.01–0.074% chem. U, respectively, with a maximum of 0.109% U; and the productivity factor is 1.27–3.2 kg U m⁻². The equilibrium coefficient ($K_p = Ra/U$) in the center of the ore body is almost 1 and at the margins about 1.5 indicating inflow of oxygenated water from both margins.

Mangheite site (Fig. 1.22b): An ore body as described by Zhu Minqiang et al. (2002) is of roll shape, 8.12 m in thickness, 100 m in width, occurs at depths of 90–105 m, averages 0.014% U and exhibits a productivity of 2.22 kg m⁻². K_p is 0.84. The maximum permeability coefficient of mineralized sandstone is 0.44 m/day.

Fig. 1.22.

Bayantala Sag, **a** Huhe site, **b** Mangheite site, schematic NW-SE cross-sections illustrating the distribution of U (*a*) as basal channel-type mineralization in braided channels of the Lower Member of the Cretaceous Saihantala Formation (K_1bs^1) and (*b*) as roll-type mineralization in fluvial-deltaic sands of the Cretaceous Upper Tenggeer Formation (K_1bt^2) (K_1bs^2 Saihantala Fm Upper Member, N_2b Pliocene Baogedewula Fm) (after Zhu Minqiang et al. 2002)



1.2.4 Yingshan Basins, Inner Mongolia A.R.

The Yingshan Basins are a group of small intermontane Mesozoic-Cenozoic basins located between the Eren Basin to the north and the Ordos Basin to the south in north-central China. These basins contain Jurassic to Lower Cretaceous strata similar to the Eren Basin but predominantly Tertiary fluvial sediments. Uranium occurrences and showings are present preferentially in Tertiary fluvial channel sandstones (Zhou Weixun et al. 2002).

1.2.5 Ordos Basin, Central-North China

The Ordos Basin and a number of peripheral small satellite basins are located in Shanxi and Shaanxi Provinces and Inner Mongolia A.R., central-north China (Fig. 1.1). The Ordos Basin is a major coal and oil producer, and contains significant gas resources. Systematic uranium exploration began in the late 1990s and resulted in the discovery of U mineralization in the Dongsheng area at the northern margin; and radioactive anomalies in the NW part of the Ordos Basin.

Sources of information. Chen Anping et al. 2002; Li Ziyang et al. 2005; Yu Dagan et al. 2002; Zhou Weixun et al. 2002.

Regional Geological Setting of Mineralization

The Ordos Basin is an intracratonic basin of about 250 000 km² filled with Late Permian to Cretaceous continental sediments that rest upon a Paleozoic platform. From Late Triassic to Middle Jurassic incised valleys were formed during successive subsidence. A large-scale uplift during the Early Yanshanian Orogeny by the end of Middle Jurassic caused a hiatus but sedimentation was resumed with deposition of widespread alluvial fan, fluvial and lacustrine, and locally eolian sediments in the Early Cretaceous. The basin was completely uplifted as a plateau by the Late Cretaceous, and subsequently several grabens were down faulted along its periphery in Miocene time.

As a result of this evolution, the Mesozoic litho-stratigraphic sequence in the Ordos Basin includes dominantly fluvial and partly eolian sediments of the Lower Cretaceous Zhidan/Liupanshan Group in the Tianhuan area and Yijinhuoluo and Dongsheng Formations in the Dongsheng area. The Mid-Jurassic Anding, Zhiluo and Yan'an Formations, Lower Jurassic Fuxian Formation, and Late Triassic Yanchang Formation underlie these formations. Sediments of the Late Triassic-Jurassic sequence are of fluvial-lacustrine origin and consist predominantly of greyish, medium-grained clastics in the lower section and pink argillaceous sediments in the upper section.

Basin sediments dip gently 10–30° SW without intense deformation. Regional faults produced mainly block-faulting. Two major E-W-trending structural zones occur in the north and south of the basin. The northern zone transects the Dongsheng area as a crest of uplift, while the southern fault cuts through the Zhaohuohao and Sunjialiang sites. Second-order faults trend N-S, NE-SW, and NW-SE.

A few U productive strata were identified in Lower Cretaceous, Middle Jurassic, and Triassic (Tr₁ and Tr₃), formations. The Middle Jurassic Zhiluo Formation contains U occurrences in the Dongsheng area described below, while radioactive anomalies are recorded from Lower Cretaceous alternating sandstone-mudstone beds in the northwestern Ordos Basin.

1.2.5.1 Dongsheng Area

This uranium area covers over 200 km² at the northern margin of the Ordos Basin in the territory of Ordos City, 130 km S of the town of Baotou, Inner Mongolian A.R. (Fig. 1.23a). First indications of sandstone type U mineralization were drill-intercepted in 1999. Three U mineralized sections have been identified so far in the Zhaohuohao area and exploration is still ongoing. Resources are estimated to amount to several thousand t U at a grade averaging 0.033% U (status 2002) [OECD/NEA-IAEA (2005) refers to this area as Zhaohuohao deposit in Erdos Basin and reports resources of 5 000 t U at an average grade of 0.2% U].

Sources of information. Cai C. et al. 2007; Chen Anping et al. 2002; Yu Dagan et al. 2002; Zhou Weixun et al. 2002.

Geological Setting of Mineralization

The Dongsheng U area is underlain by the Lower Cretaceous Dongsheng, Middle Jurassic Zhiluo and Yan'an, Lower Jurassic Fuxian, and Upper Triassic Yanchang Formations. Pleistocene and Quaternary sediments rest upon the Mesozoic strata.

The U-hosting *Zhiluo Formation* is tripartitioned into an

- *Upper Member*, 60–100 m thick, composed of purple red sediments of a highly sinuous meandering fluvial system. A weathered crust on top attests to deposition under arid climate and uplift;
- *Intermediate Member*, 20–40 m thick, of a slightly sinuous meandering fluvial system, composed of grey point bar sandstones interfingering with flood plain mudstone with interbedded coal seams; and
- *Lower Member*, 20–40 m thick, of channel, swamp, and inter-channel facies, which are part of a NNW-SSE-oriented proximal braided fluvial zone that was presumably laid down within a large scale humid alluvial fan when the northern part of the basin underwent regional uplift. Due to subsequent compression from the SE, the originally NNW-SSE oriented valleys were turned to a NE-SW direction. Uranium-hosting channels occur within a belt, 2–3 km in N-S width and 20–30 km in E-W length. These channels are incised into sediments of Unit V or IV of the Yan'an Formation (see below) and contain interconnected bodies, 20–40 m in total thickness, of dark-grey, coarse- to medium-grained and fine-grained sandstones with abundant organic matter and sulfides.

The underlying *Yan'an Formation* is some 170 m thick and composed of sediments of fluvial-lacustrine origin and includes five stratigraphic units, from top to bottom:

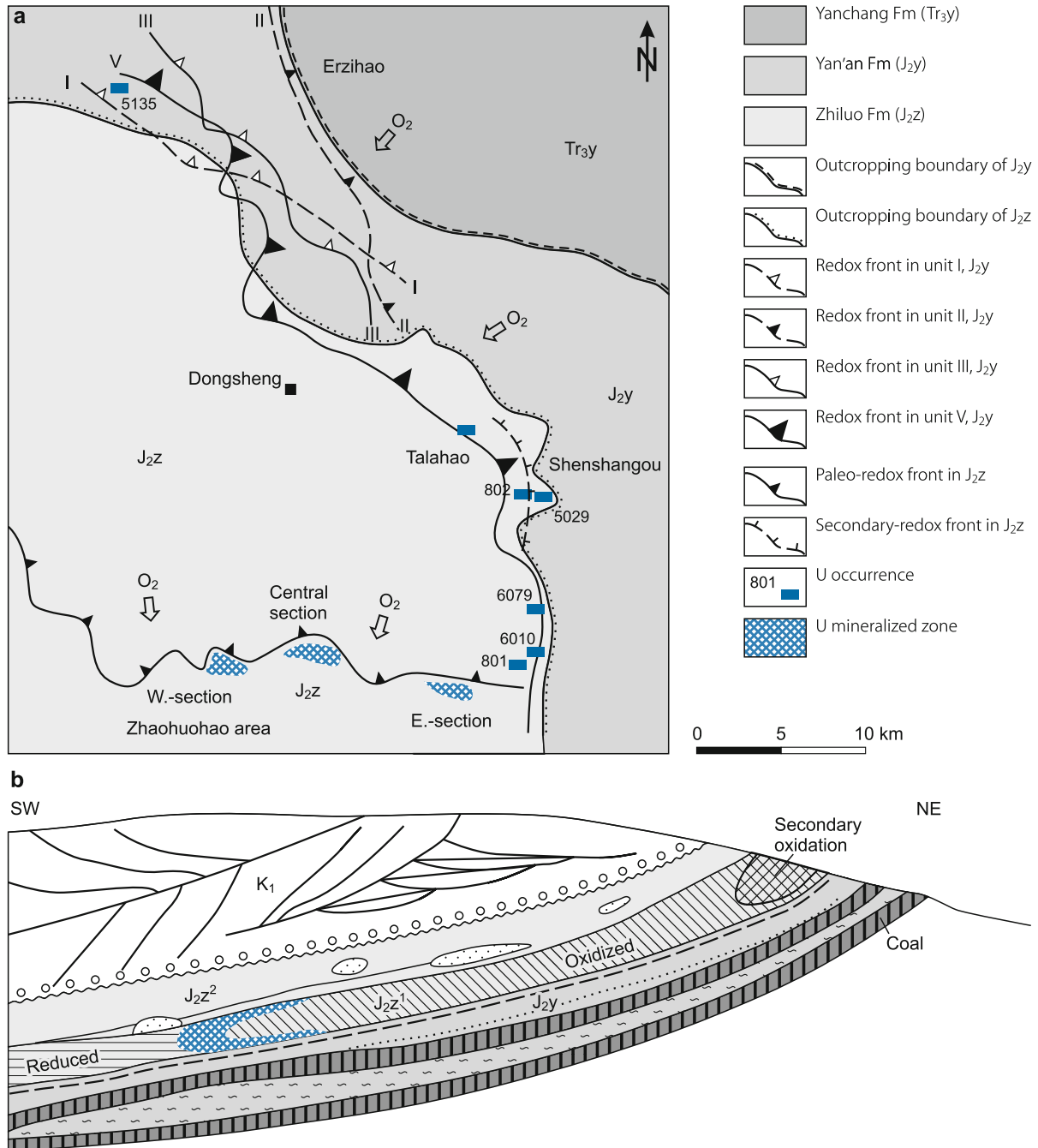
- *Unit V* is of fluvial origin. Its lower part is dominated by greyish, medium- and fine-grained sandstone intercalated with grey or black mudstone, whereas the upper section is mainly composed of greyish white, medium- or fine-grained sandstone with a weathering crust on top.
- *Units IV, III and II* comprise dark grey or black mudstone and siltstone with intercalations of greyish sandstone and black shale of a lacustrine delta system with a thickness of about 40–76 m of each unit.
- *Unit I* consists of fluvial, grey, coarse- to medium-grained sandstone or gravelly coarse-grained sandstone intercalated with siltstone and mudstone.

Host Rock Alteration

Chen Anping et al. (2002) describe alteration features in the two U-hosting formations in the Dongsheng area as follows.

Fig. 1.23.

Ordos Basin, Dongsheng area, **a** generalized geological map of the northeastern boundary zone of the basin showing redox fronts in Jurassic Yan'an and Zhiluo Formations and related locations of U occurrences; **b** schematic SW-NE section illustrating the position of a U ore body at the head of an oxidation front. (K_1 Lower Cretaceous Dongsheng Fm; J_{2z} Middle Jurassic Zhiluo Fm: J_{2z}^2 Upper Member, J_{2z}^1 Lower Member; J_{2y} Middle Jurassic Yan'an Fm; O_2 with arrow indicates flow direction of oxygenated groundwater) (after Chen Anping et al. 2002)



Zhiluo Formation: Two spatially separated interlayer oxidation zones are documented in the Lower Member (► Figs. 1.23a,b). In the southern Zhaohuohao area, inflow of oxygenated ground-water from the north generated an oxidation zone with a redox front some 40 km long in E-W direction. Later-stage reduction overprinted this early oxidation zone near the frontal interface of oxidized rocks and imprinted a light blue and greenish taint on the rocks in the north that gradually changes southwards into greyish black. The green zone ranges in width from several km to more than 20 km.

A second interlayer oxidation zone of yellow color with a redox front trending NW-SE for about 20 km occurs near surface along the E-NE limit of the Zhiluo Formation.

Green-altered sediments are characterized by: (1) an $\text{Fe}^{3+}/\text{Fe}^{2+}$ ratio of 1.29, as compared to a ratio of 1.84 in oxidized red and 0.972 in unaltered grey sandstone, indicating that part of the ferric iron has been reduced to ferrous iron in the alteration process from red stone to green stone; (2) relics of red and yellow sandstone or mudstone in green coarse-grained sandstone attesting to a precursor oxidation stage; (3) high concentration of hydrocarbons; and (4) presence of nickel-bearing chlorite and clinocllore, which cause the green color and form under reducing conditions.

Yan'an Formation: Redox fronts occur in sandstone horizons, from 10 to 20 m thick, sandwiched between mudstone beds in units I, II, III, and V as illustrated in ► Fig. 1.23a. The four redox fronts trend curvilinear NW-SE, the longest of which is in Unit V and extends for 50–60 km. Inflow of oxygenated water was from the E and NE. Fronts derived by an early and late oxidation stage, which imposed a purplish red and yellowish color, respectively, on the sediments. A reduction stage intervened between the two oxidation events. It is evidenced by a green and bluish sandstone that contrasts with primary reduced, dark greyish, pyritic rocks.

Mineralization

Zhiluo Formation, Lower Member: Uranium occurs adsorbed on clay minerals and as pitchblende. Uranium in an adsorbed state correlates positively with clay, disseminated pyrite, and detrital carbon contents. Pitchblende is closely associated with pyrite and occurs occasionally in calcite cement, or as an inclusion in biotite and chlorite.

U mineralization is preferentially located in the green to greyish altered transition zone where it is hosted in coarse- to medium-grained and to a minor degree in fine-grained sandstone with occasional intercalation of calcareous sandstone. Mudstone overlying and underlying mineralized sandstone contains sporadic mineralization. Mineralized sandstone is loosely consolidated and consists predominantly of moderately sorted and rounded quartz and feldspar with a matrix of hydromica and calcite.

The U-Ra coefficient in roll-shaped ore bodies inside the oxidation zone is in equilibrium ($K_p=0.9-1.02$), which indicates that mineralization at the head of the redox front was formed at the time of oxidation and has not been affected by later processes. In contrast, mineralization outside this oxidation zone is in disequilibrium ($K_p=0.7-0.8$), and is therefore thought to have

experienced secondary oxidation with U redistribution and re-enrichment in the pre-existing ore (Chen Anping et al. 2002).

Shape and Dimensions of Deposits

Zhiluo Formation, Lower Member: U occurs in roll and tabular shaped ore bodies in three discontinuous sections over a distance of 15 km along an E-W-trending redox front (status 2002). Established ore bodies are from several tens to one hundred meters long, 1–20 m thick, and average 0.02–0.05% U with a maximum of 0.235% U. Ore bodies in the

- eastern section are roll-shaped, occur at depth of 77 m, av. 11.4 m in thickness, and have a productivity factor of 5.56 kg U m⁻² with a maximum of 10.67 kg U m⁻²,
- central section are of tabular shape, occur at depth of about 100 m, av. 4.76 m in thickness, and have a productivity factor of 1.72 kg U m⁻², and
- western section are roll-shaped, occur at depth of 185 m, are 3–7.4 m in thickness, and have a productivity factor of 3.56 kg U m⁻².

Yan'an Formation: Only Unit V contains an ore body. The ore body is of tabular shape, has a grade of 0.01–0.02% U, and transgresses through several lithological beds; each of which has a maximum thickness of 3.3 m. Mineralization is preferentially hosted in dark grey, fine-grained sandstone with abundant detrital organic matter and sulfides, and partly in siltstone and mudstone. Oxidation and reduction phenomena are typical features in the host sands.

Mineralization in outcrops: A number of U occurrences, such as #801, 6010, 6079, 5029, 802, and 5135, have been found at the surface (► Fig. 1.23a). These occurrences are considered to be remnants of the secondary oxidation process, and are characterized by: (1) zonal distribution in feldspathic quartz sandstone of yellow color in the Zhiluo Formation; (2) relatively high grades ranging from 0.05% to 0.1% U, with a maximum of 0.843% U (with some visible U⁶⁺ minerals such as autunite and torbernite); (3) ore bodies are dozens of meters to 500 m in length, and commonly 0.5–3 m in thickness with extremes of 0.2 m and 11.57 m (Chen Anping et al. 2002).

Metallogenetic Aspects

Zhou Weixun et al. (2002) summarize the metallogenetic evolution of U mineralization in the Dongsheng area as follows. Sediments of the Zhiluo Formation are yellow in outcrop but are altered to blue to dark green on the up gradient side of U mineralized sandstone; Ni-bearing chlorite and/or clinocllore are thought to be the reason for the green coloration. This blue/dark green sandstone contains relics of pink altered sandstone that indicates an earlier stage of oxidation. Consequently it is assumed that the blue/dark green altered sandstone may reflect a secondary reduction of earlier oxidized sandstone due to the introduction of hydrocarbons from an underlying reservoir;

whereas the oxidized pink sandstone, located up dip of regional redox fronts, may have resulted from oxygenated waters that formed the roll-type ore bodies.

This situation may permit the following synthesis on metallogenetic evolution of U mineralization in the Dongsheng area: Waters in sands of the Lower Member of the Zhiluo Formation remained in hydrological connection with surface waters after they were covered by younger members of this formation because interbedded impermeable mudstone layers are discontinuous and as such water-flows were permitted to communicate vertically through the litho-stratigraphic section. As a result, waters in Lower Member sand bodies were locally of oxidizing and locally of reducing nature depending upon the distribution and influence of indigenous organic debris and the exchange with phreatic water. In such an environment, first-stage uranium mineralization produced widespread tabular ore bodies in basal sand horizons.

During the Early Cretaceous, the area was again uplifted and the Lower Member J_2z^1 sand bodies were exposed on surface and partly denudated; but at the same time, an E-W-striking redox front originated with a length of 40 km. Down-slope migrating oxygenated waters reworked locally pre-existing tabular ore bodies into roll-shaped ore bodies. The ore-forming process ceased with deposition of the Dongsheng Formation in late Early Cretaceous time, which disrupted the hydrological connection between the Lower Member of the Zhiluo Formation and surface waters. This inference is supported by an age of 107 ± 16 Ma (Xia Yuliang et al. 2002) for U mineralization.

1.3 Qilian-Qinling U Province, Central China

The Qilian-Qinling uranium province has a width of 100–150 km and extends for 1 300 km in a N-S direction from the Qilian Range in NW Gansu Province to the Lujing-Zongyang region in Anhui Province (Fig. 1.1). This region includes the Longshou Shan Range in Gansu, the Lenglongling Range at the Gansu and Qinghai boundary to the west, and the Qinling and Funiu Ranges in Shaanxi and Henan Provinces to the southeast.

Geotectonically, the Qilian-Qinling U province encompasses the edge of the North China Massif (or Platform) and peripheral fold belts to the south, and the Lower Yangtze rift zone between the North China and Yangtze Massifs.

U deposits and occurrences are mainly of intrusive and vein type and occur primarily in three areas: *Longshoushan* in the western, *North Qinling* in the medial, and *Lu-Zong* in the south-eastern part of the U province. Sandstone-type uranium mineralization is indicated in the *Qaidam Basin* where exploration was undertaken during the 1990s. A few U and polymetallic C-Si-pelite deposits are reported from the *South Qinling Fold Belt* in the western part of the U province.

1.3.1 Longshoushan Uranium Zone, Gansu

The Longshoushan U zone, some 180 km in length and averaging 20 km in width, is situated at the northeastern margin of the

Qilian-Qinling U province. Deposits herein are primarily of intrusive and vein type, as exemplified by the *Hongshiquan* and *Jiling* deposits, respectively. The former type prevails in the western and the latter in the eastern part of the U zone. Deposits are small with resources between 500 and 1 500 t U at grades between 0.03–0.1% U.

Sources of information. Liu Xingzhong and Zhou Weixun 1990; Shi Wenjin and Hu Junzhen 1996; Zhou Weixun 1997, 2000.

Regional Geological Setting of Mineralization

The Longshoushan U zone coincides more or less with the NW-SE-trending Longshoushan fold belt at the southwestern margin of the Precambrian Alashan (or Alxa) Block (or Massif) that was amalgamated with the North China Massif during the Zhongtiaon Orogeny (about 1700 Ma ago). Early Proterozoic metasediments of the Longshoushan Supergroup (gneiss, granulite, migmatite, marble) are the prominent lithologies in the Longshoushan fold belt. These rocks derived from Lower Proterozoic sediments by medium to high-grade regional metamorphism and migmatization and were intruded by alaskite during the Zhongtiaon Orogeny. Meso- and Neoproterozoic marginal marine sediments rest upon the Lower Proterozoic suites. Large-scale magmatic activity reflected by granitic batholiths occurred again during the Caledonian Orogeny. Some of the Zhongtiaon alaskite and Caledonian granite facies are uraniumiferous. Devonian molasse as well as Carboniferous-Permian coal-bearing sediments occur in some depressions.

Principal Characteristics of Mineralization

Intrusive-type U mineralization is typical for the western part of the Longshoushan U zone in which it is associated with Zhongtiaon pegmatoidal alaskite that was intruded into a Lower Proterozoic gneiss-schist assemblage. The alaskite averages 14 ppm U while higher contents of U accumulated in biotite-enriched hybrid facies along the alaskite contact with metasedimentary wall rocks. Part of this U occurs in the form of uraninite. Age dating yields 1 760 Ma for this primary uraninite. In a later stage, medium to low temperature hydrothermal processes intensely reworked the alaskite resulting in a superimposition of pitchblende-sulfide and pitchblende-hematite veins on the earlier-formed uraninite mineralization. Liu Xingzhong and Zhou Weixun (1990) give an age of 700–600 Ma for remobilized pitchblende while Shi Wenjin and Hu Junzhen (1996) attribute this hydrothermal activity to a Late Caledonian to Early Hercynian event. Supergene U enrichments in the form of black U products in fissures and uranium adsorbed on clay minerals occur locally on upper levels.

Vein-type U mineralization occurs typically in the eastern Longshoushan U zone within Caledonian granites with a high U background averaging 8–12 ppm U, and adjacent to these granite domes in a halo several hundreds of meters wide. Ubiquitous K and Na metasomatism characterize both U-productive granites

as well as surrounding metasediments. Structurally controlled hydrothermal processes of sodium and, finally, silicic nature overprinted these and formed two varieties of veins: *Uraniferous albite veins* transect intensely alkali-metasomatized precursor lithologies with slightly elevated U tenors that had originated by albitization associated with chloritization, hematitization, and carbonatization. These veins consist of sugar-granular albite with thuringite, hematite, carbonates, and pitchblende. *Silicic U veins* occur in granite and are enveloped by wall rocks that are strongly altered by silicification, kaolinitization, sericitization, penninization, and pyritization. Ore lodes comprise pitchblende and colloidal pyrite in red and black microcrystalline quartz.

1.3.1.1 Hongshiquan Deposit, West Longshouhan

This alaskite-related intrusive-type deposit is located in Shandan County, central-eastern Gansu Province. Resources are in the 500–1 500 t U category with grades between 0.03–0.1% U.

Uranium is hosted by pegmatoidal alaskite apophyses composed of microcline and quartz with minor perthite, plagioclase, and muscovite that enclose abundant xenoliths of metamorphosed rocks. These apophyses are up to 2 km long and 50–300 m wide. They occur within a hybrid zone 2–3 km wide that is characterized by alaskite with more or less assimilated Lower Proterozoic metamorphic rock remnants. Uraninite is the principal U mineral with minor black U products and pitchblende. Uranium is also contained in zircon, monazite, and xenotime, and is adsorbed on hematite and chlorite.

Two ore types are identified: *Grey-black ore* composed of the various U-bearing minerals associated with molybdenite, pyrite, and minor chalcopyrite and galena hosted by chloritized biotite pegmatoidal alaskite; and *red ore*, characterized by hematite-pitchblende veins superimposed on the grey-black ore.

These ore types are concentrated in elongated, narrow ore bodies several tens of meters in length with a maximum of 250 m, and 2 m thick on average with a maximum of 5–6 m. Ore bodies are concentrated in three belts in which they persist to depths of 110 m (Zhou Weixun 2000).

1.3.1.2 Jiling Deposit, East Longshouhan

Located in the vicinity of Jinchang city, central-eastern Gansu Province, this granite-related albitite vein deposit occurs at the southern edge of the Jiling diorite-granite massif of Early Paleozoic age (450 Ma) adjacent to Lower Proterozoic marble and biotite-quartz schist. Resources are in the 500–1 500 t U category with grades between 0.03–0.1% U.

Uranium lodes are confined to albitite veins that originated from diorite and granite by metasomatism and consist of 73–86% albite, 10–20% remnant minerals (biotite, hornblende, etc.), and 15–20% authigenic minerals (chlorite, hematite, calcite, and others).

Mineralized albitite veins are always altered and cataclased; fissures are filled with pitchblende-sulfide-calcite veinlets. Pitchblende, black U products, and other U minerals account for

60–70% of the uranium present in ore while U contained in sphene and baryte accounts for 15–20%, and U adsorbed on chlorite and hematite for the remaining 20–25%.

U fissures form ore bodies of lens, nest, or stockwork configuration. Three main ore bodies, 60–150 m long and 10–45 m thick, and tens of small ore bodies are delineated within two mineralized zones each 1 300 m long and 60–100 m wide. Albitite is dated at 430–400 Ma and pitchblende at 383–357 Ma (Zhou Weixun (2000)).

1.3.2 North Qinling Uranium Zone, S Shaanxi-SW Henan

The North Qinling U zone, 300 km long and 30–40 km wide, trends in NW-SE direction from southern Shaanxi into southwestern Henan. It includes the *Xi'an* and *Danfeng-Zhuyangguan-Shangnan* U areas with vein and intrusive pegmatite deposits, respectively.

Sources of information. Feng Mingyue et al. 1996; Liu Xingzhong and Zhou Weixun 1990; Zhou Weixun 2000.

Regional Geological Setting of Mineralization

The North Qinling U zone coincides spatially with the eastern extension of the North Qinling Caledonian fold belt that borders the SW margin of the North China Massif. Various gneisses, schists, graphitic marble, granulite, and amphibolite of the Lower Proterozoic Qinling Group underlie large parts of the North Qinling zone. Some Mesozoic (Yanshanian) uranium monzonitic granites occur in the western part of this zone (*Xi'an U area*) while Caledonian granite and associated pegmatites were intruded in its eastern segment (*Danfeng-Zhuyangguan-Shangnan U area* also referred to as *Eastern Qinling*). These Caledonian pegmatites include three petrographic facies that are concentrically arranged around a related granite massif: (a) an inner zone of biotite-plagioclase and two-mica-microcline pegmatite with REE and/or U mineralization; (b) an intermediate zone of muscovite-microcline-albite pegmatite with Nb, Ta, Be, Li, and muscovite mineralization; and (c) an outer zone of lepidolite-microcline-albite pegmatite with Li, Ta, Rb, Cs, and Nb mineralization.

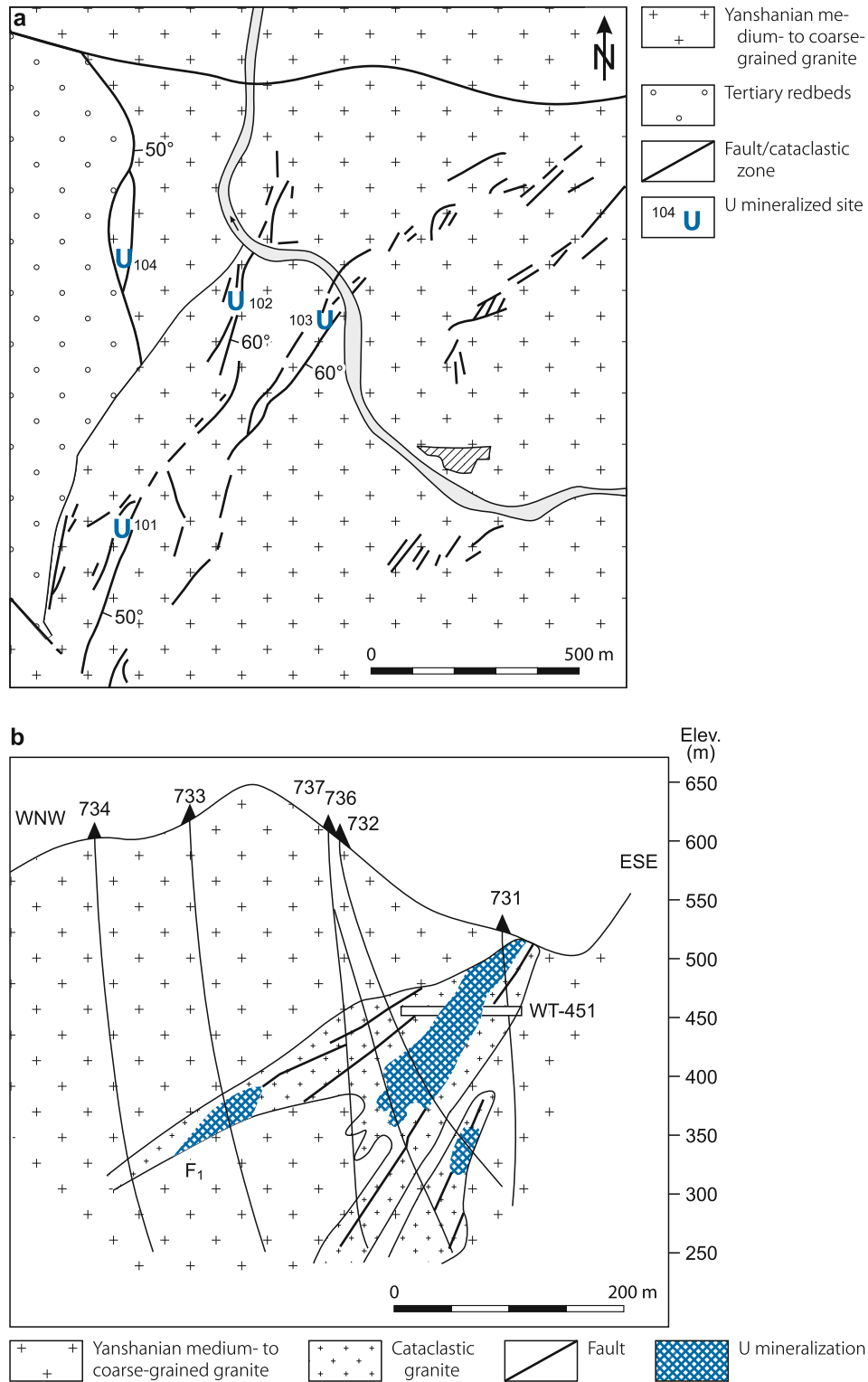
Principal Characteristics of Mineralization

The North Qinling U zone includes vein-type U deposits (e.g. *Lantian*) in the western, and pegmatite-type U deposits in its eastern segment.

Vein-type mineralization is defined as “clay-altered cataclastic” type and emplaced in Early-Middle Jurassic granitic bodies that occur within an area of 250–300 km². Mineralization comprises pitchblende, pyrite, hematite, and other metallic minerals. Gangue minerals include kaolinite, montmorillonite, hydromica,

Fig. 1.24.

Xi'an area, Lantian deposit, **a** schematic geological map with location of U concentrations; **b** sketch section along profile no. 73 at #102 site demonstrating the distribution of vein-type U mineralization controlled by cataclastic granite (after Zhou Weixun pers. information 2006, selected and translated from Chinese literature)



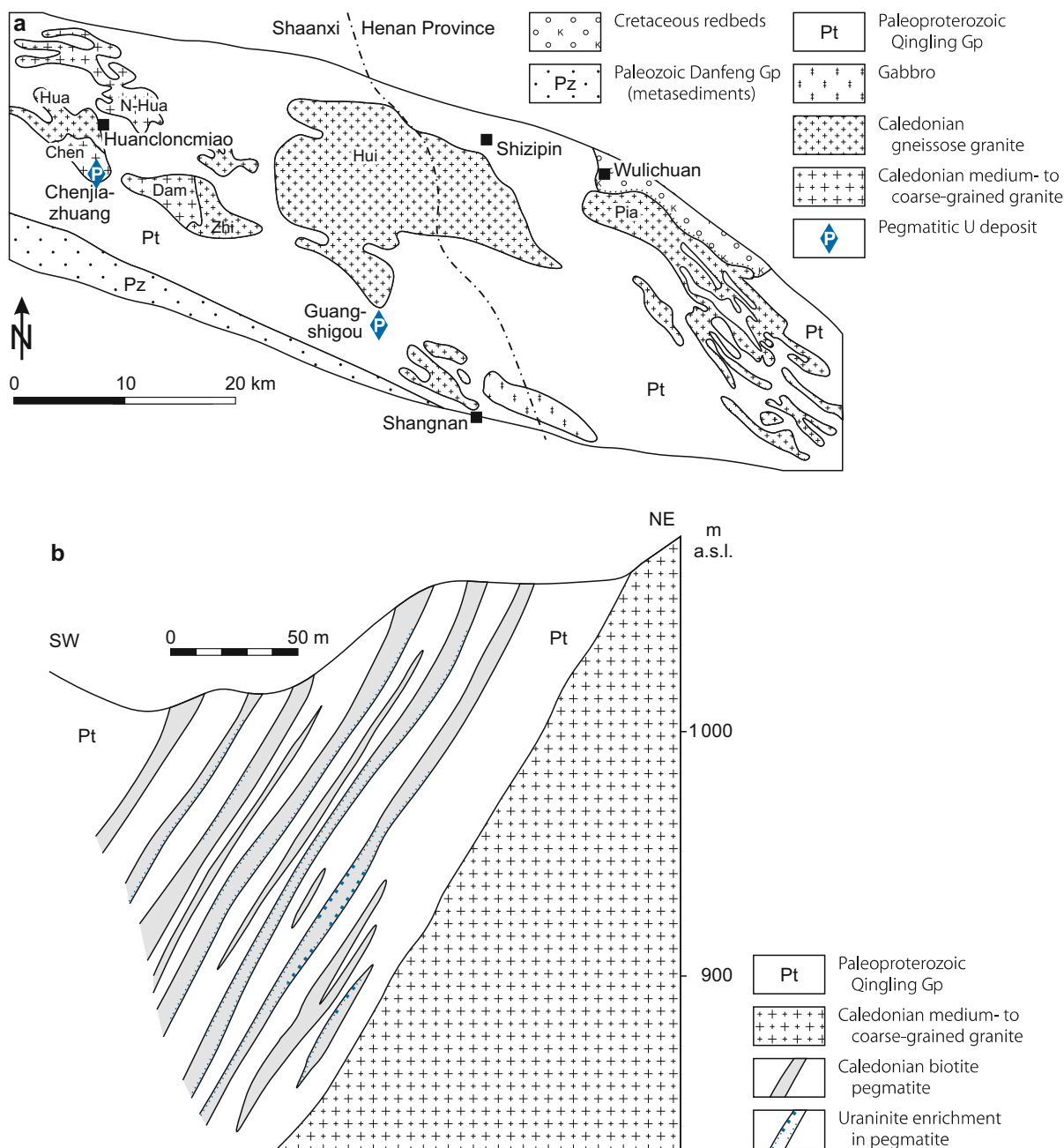
calcite, quartz, and fluorite. Ore lodes are of small lens, columnar, nest, and/or vein shape, and group to mineralized zones.

Intrusive-type mineralization (e.g. at *Chenjiazhuang*) is contained in biotite pegmatite dikes of a dike swarm that cuts Lower Proterozoic metamorphic rocks adjacent to Caledonian granitic massifs. Uraninite is the principal U mineral and accounts for 90% of the total uranium in ore. Uraninite occurs as tiny crystals

disseminated in pegmatite or enclosed in major rock-forming and accessory minerals; it is particularly concentrated in pegmatite intervals enriched in biotite and plagioclase, at the margin of dikes, at sites of marked thickening of dikes, and where the spatial accumulation of dikes is greatly changed. Individual uraniferous pegmatite dikes range in length from several tens to several hundreds of meters and in width from several to several tens of meters. Grades exceed 0.01% U and reportedly average 0.03% U.

Fig. 1.25.

Danfeng-Shangnan area, **a** generalized geological map showing Caledonian granite massifs and the two principal pegmatite-type U deposits *Chenjiazhuang* and *Guangshigou*; **b** *Guangshigou* deposit, SW-NE section along profile no. 8 indicating sites of uraninite concentration (dotted) in pegmatite dikes that cut Proterozoic metasediments (after Zhou Weixun pers. information 2006, selected and translated from Chinese literature) (*Granite massifs: Chen Chenjiazhuang, Dam Damaogou, Hui Huichi, Hua Huanglongmiao, N-Hua North Huanglongmiao, Pia Piaochi, Zhi Zhifangou*)



1.3.2.1 Lantian Deposit, Xi'an Area, Central-South Shaanxi

The Xi'an area lies in the northwestern part of the North Qinling U zone and contains endo- and perigranitic vein-type U deposits associated with Yanshanian granite. *Lantian*, located about 60 km SE of the provincial capital Xi'an, is a typical deposit in this area (Fig. 1.24). It comprises several ore bodies along fault zones in argillized granite. Uranium mineralization is 96 Ma old. The deposit is mined by open pit and underground methods including in-place leaching after blasting since 1993. Grades vary between 0.1 and 0.2% U. OECD-NEA/IAEA (1997) reports resources of 2 000 t U. In some contrast, OECD-NEA/IAEA (1995) reports that in-place block leaching after blasting was put into production at the Lantian Mine in 1990; and that ore body #30 had a geological reserve of 7 160 t U at an average grade of 0.171% U. Ore occurred in a zone of fractured granite averaging a width of 6.6 m.

1.3.2.2 Chenjiazhuang Deposit, Danfeng Area, SE Shaanxi

The northern Danfeng-Zhuyangguan-Shangnan U area is a segment of the southeastern North Qinling U zone in the Qinling Medium Massif. It contains intrusive-type U mineralization in pegmatite or pegmatitic granite as exemplified by the first discovered, small *Chenjiazhuang* (also referred to as *Danfeng*) and larger *Guangshigou* deposit in the Danfeng area (Fig. 1.25a). Uraniferous silicified veins in Early Paleozoic pyroclastics occur in the southern Danfeng-Zhuyangguan-Shangnan zone (Liu Xingzhong and Zhou Weixun 1990).

Chenjiazhuang (Fig. 1.25b) is an explored pegmatite-type U deposit in Danfeng County, SE Shaanxi Province. Resources are in the 500–1 500 t U category with grades of 0.1–0.3% U. The deposit comprises several en echelon-arranged, uraniumiferous biotite pegmatite dikes adjacent to a small granitic stock. Margins of the dikes are contaminated with metamorphic rock relics from several centimeters to several tens of centimeters in width. Individual dikes are more than 500 m long and reach a maximum of 4 000 m, they are commonly from 2 to 5 m thick, and persist mostly to depths of 100 m, locally to over 400 m. Ore bodies have elevated contents of uraninite, 100 g t⁻¹ on average with a maximum of 1 379 g t⁻¹ uraninite. Ore bodies are of tabular or lenticular shape, and range in length from 160 m to 480 m, locally to 805 m, and in thickness from 2 m to 4 m with a maximum of 7 m. U-Pb dating of uraninite yields an age of 457–466 Ma which correlates with that of the pegmatite host (Zhou Weixun 2000).

1.3.3 Lu-Zong Volcanic Basin, Anhui Province

The volcanic Lu-Zong Basin (Lu for Lujiang County, Zong for Zongyang County in S Anhui Province), also referred to as Lower Yangtze granite belt, forms the southeastern part of the Qilian-Qinling U province. The basin extends NE-wards from the town of Huashan to Lujiang in southern Anhui Province and

is bounded by the Yangtze (=Chang Jiang) River on the SE and by the NE-SW-oriented Dabie marginal fault along the NE edge of the Dabie Precambrian Block on the NW.

The Lu-Zong Basin is a significant mineral region within a polymetallic belt with Au, Co, Cu, Fe, Mo, Pb, V, U, and Zn mineralization that stretches along the middle course and down stream along the Yangtze River.

Chen Yifeng (1996) notes three sandstone hosted veinlike U deposits, none of which were mined, and some forty U occurrences in four areas within a belt 75 km long and several kilometers wide in the SE half of the Lu-Zong Basin. These four areas occur peripheral to quartz syenite massifs: (1) the *Kunshan* area at the north edge of the *Huangmeijian (HM) Massif* with U deposits #8411 (=Kunshan) and #8413; (2) the *Chengshan (CS)* area at the NE edge of the *Zongyang Massif*; (3) the *Qiaozhuang* area on the E side of the *Zongyang Massif*; and (4) the *Dalongshan* area with the homonymous deposit at the SW edge of the *Zongyang-Dalongshan Massif*. The *Dalongshan (DL)* and *Zongyang Massifs* are separated on the surface but connected at depth. A few U occurrences are associated with other massifs such as the *Chengshan (CS) Massif*, which has one U occurrence.

Sources of information. Chen Yifeng 1996; Zhang Bangdong 1990; Zhu Jiechen et al. 1996; amended by data from Zhou Weixun pers. commun. 2004.

Regional Geological Setting of Mineralization

A number of Mesozoic volcanic basins and Cretaceous-Cenozoic sedimentary graben basins occupy the Lower Yangtze depression including the volcanic Lu-Zong Basin. The Lower Yangtze depression was formerly a part of the Yangtze Craton but became a fault controlled depression along the Tan-Lu strike-slip fault during the Triassic.

The Lu-Zong Basin contains lacustrine sediments overlain by volcanic rocks of the Jurassic Xiangshan Group and Cretaceous redbeds. A litho-stratigraphic column of this sequence reads – from top to bottom – as follows:

- Cretaceous (K_{1f}) Fushan Fm: redbeds
- Jurassic:
 - (J_{3s}) Shuangmiao Fm: pyroclastic and volcanic rocks of alkali-rich, intermediate-basic composition
 - (J_{3z}) Zhuanqiao Fm: volcanic and pyroclastic rocks of alkali-rich intermediate composition
 - (J_{3l}) Longmenyuan Fm: volcanic and pyroclastic rocks of alkali-rich basic composition
 - (J₂) Luoling Fm: quartz-feldspar sandstone, siltstone, mudstone with thin coal seams and limestone lenses
 - (J₁) Moshan Fm: coal-bearing clastic sediments
- Triassic (Tr₃) Lalijian Fm: coal-bearing clastic sediments

A number of small syenitic-granitic massifs of Late Jurassic (Yanshanian) age have been intruded into the sedimentary suite; some of which such as the Chengshan (CS), Zongyang-Dalongshan (DL), Huangmeijian (HM), Yongchen (YC) domes in the Lower Yangtze granite belt have associated perigranitic

vein-type U deposits as mentioned earlier. Zhang Bangdong (1990) defines these intrusions as I-type (also referred to as syntexis-type) granite that includes a variety of rocks ranging from biotite-quartz syenite to alkali feldspar granite. The main facies have a medium- to coarse-grained texture. SiO_2 ranges from 60.5% in early to 73.6% in late stage facies. $\text{Na}_2\text{O} + \text{K}_2\text{O}$ are 10% or more. The rocks are oversaturated in alumina. Biotite is Mg-rich. Initial Sr ratios are <0.710 . REE content is high (>250 ppm). CE/Yb and La/Sm ratios vary in narrow ranges suggesting a non-crustal origin. U background is 7–17 ppm and the Th/U ratio is generally >3 . Uraninite is less abundant than in S-type granite. Comagmatic volcanics are commonly present. Zhang Bangdong (1990) interprets these and additional research data to suggest a mixed upper continental crust-depleted mantle origin with a fraction of about 55% mantle material for this I-type granite.

Chen Yifeng (1996) and Zhu Jiechen et al. (1996) define intrusions in the Lu-Zong District as syenite and quartz syenite and state that the three largest quartz syenite massifs, Huangmeijian, Chengshan, and Dalongshan, outcrop successively from north to south. These massifs have diameters of 15–20 km and an exposed area of some 280 km². Regional structures are oriented NE-SW and NNE-SSW. Subsidiary structures trend in various directions.

Principal Characteristics of Alteration

Host sandstones are markedly modified adjacent to igneous intrusions. Contact metamorphism generated locally hornfelsic sandstone and skarn. Metasomatic and hydrothermal alteration phenomena in sandstone are reflected by a variety of pre- and syn-ore authigenic phases. Brittle structures control the distribution of these alteration features.

Pre-ore alteration includes albitization, silicification, hydromicazation, and kaolinization. Hydromicazation prevails close to ore bodies. Albitization is related to autometamorphic, alkaline metasomatism. It is strongest developed near the intrusive contact from where it penetrates the host sandstone for 300–400 m with decreasing intensity. Sodium is thought to have been introduced from the intrusion during the evolution of the ascending alkali-enriched magma.

Major U ore bodies typically occur in zones of bleached sandstone that are often surrounded by a silica rim and originated from pre-ore albitization, silicification, and carbonatization. The albitization effect is reflected by the change in tenor of alkalis. While normal sandstone has K_2O and Na_2O contents of 2.72% and 0.07%, respectively, respective values in albitized sandstone amount to 1.23–2.36% K_2O and 1.76–3.49% Na_2O , and a $\text{Na}_2\text{O}/\text{K}_2\text{O}$ ratio of 1.43–2.14 (Chen Yifeng 1996).

Oré-stage alteration is reflected by pyritization, silicification, carbonatization, and hematitization products that occur as rock replacement and, particularly at rich ore lodes, in the form of veins and veinlets of black or red microcrystalline quartz, pyrite, carbonate and ankerite, and/or chlorite. In contrast, lean ore

bodies are associated with simple alteration effects, and hydrothermal veins are less abundant.

Ore-stage alteration is restricted to wall rocks of U mineralized faults and fissures. The intensity and dimensions of these aureoles correlate with the magnitude of the enveloped deposit. Large deposits are surrounded by halos several hundreds of meters wide while the halo at small deposits is on the order of meters to a few tens of meters (for details see Kunshan and Dalongshan deposits, respectively).

Principal Characteristics of Mineralization

The Lu-Zong Basin is within a polymetallic belt in which deposits of various elements or combinations thereof occur in discrete spatial and temporal distribution. Three regional metallogenetic stages are established for the Lu-Zong region (Chen Yifeng 1996):

Stage 1/Early Yanshanian: Au, Cu, Fe, Mo, Pb, Zn etc. (with dominance of copper) deposits of skarn, porphyry, and hydrothermal-metasomatic type. These deposits are associated with alkaline, high sodium quartz diorite and quartz diorite porphyrite that were intruded 176–167 Ma ago into Triassic carbonate and Silurian carbonaceous and siliceous shale in terrane uplifted during the Indosinian Orogeny. This first metallogenetic event is dated at 167–152 Ma.

Stage 2/Middle Yanshanian: Au, Ca, Co, Fe, alunite, and gypsum deposits with predominance of iron sulfides. These deposits are related to extensive, intermediate to basic, alkali-rich volcanism and subvolcanism in the Lu-Zong Basin. An age of 155–143 Ma is obtained for lithogenesis and 132–125 Ma for metallogenesis.

Stage 3/Late Yanshanian: Au, Cu, Fe, and U deposits with predominance of U. These deposits occur in endo- and exocontact zones of quartz syenite and moyite domes in the uplifted margin of volcanic basins.

U mineralization is of complex composition. Pitchblende and coffinite are the principal U minerals but U also occurs in adsorbed form. Pitchblende is dominant. Pitchblende in high grade ore has a unit cell parameter a_0 of 5.387–5.418 Å, contains 77–85% U, and has high tenors of REE, Sm, Nd, As, Hg, F, etc.; REE amount to 4400–33900 ppm, and include 103.5 ppm Sm, 219.2 ppm Nd, 500–800 ppm As, 500–570 ppm F, 2067–17760 ppb Hg. Ba, V, and Ca contents are also high in pitchblende.

Associated sulfides and arsenides include chalcopyrite, cobaltite, galena, molybdenite, niccolite, pyrite, sphalerite, and others. Gangue minerals consist of calcite, chlorite, dolomite, fluorite, sericite and quartz.

Zhu Jiechen et al. (1996) note two mineral stages in the Kunshan and Dalongshan deposits, which are represented by an earlier microcrystalline quartz-hematite-pitchblende and a later hydromica-hematite-carbonate-pitchblende assemblage; whereas Chen Yifeng (1996) recognizes an early uranium-bearing

hematite-microcrystalline quartz stage, and, typical for rich ore, three later U stages composed of pitchblende-black microcrystalline quartz, pitchblende-sulfide, and pitchblende-carbonate. Microcrystalline quartz and carbonates of these stages contain abundant ferrous iron and impurities such as clay/mud.

U mineralization is structurally and lithologically controlled. Four structural positions of U deposits are noticed: (1) Intersections of a fault with a contact zone; (2) segments sandwiched between exocontact faults and contact faults; (3) sandstone or marble/skarn xenoliths in quartz syenite; and (4) contact zones peripheral to quartz syenitic apophyses (see also Kunshan area, deposits #8411, #8413; and Dalongshan deposit). Within these structural settings, U mineralization occurs in breccias and veins/veinlets, the distribution of which is restricted to contact-metamorphosed arenite of the Middle Jurassic Luoling Formation at the exocontact of quartz syenite massifs. No mineralization occurs distant to any massif.

Contact-metamorphosed, pebble-bearing, medium- to coarse-grained, feldspar-quartz sandstone with high contents of pyrite and carbonaceous matter is the principal host rock accounting for 85% of the established U reserves. The remaining 15% of U reserves are contained in sandstones far away from the contact.

Mineralized sandstone intervals are characterized by a pronounced porosity and fracture density due to well developed interbedded and intrastrata structures. These fracture zones are controlled by laterally extensive (several km long) and deep faults that trend along the igneous massifs.

Two modes of ore quality, poor and rich, are noticed. *Poor ore* consists of an early uraniumiferous hematite-quartz assemblage. *Rich ore* occurs in complex veins of variable gangue mineralogical composition (see Sect. *Principal Characteristics of Alteration*) along with pitchblende. Rich ore is the product of a superimposed enrichment of poor ore by the earlier mentioned younger ore assemblages by which grade and scale of mineralization were greatly enhanced. High-grade ore lodes, as known from the Dalongshan and Kunshan deposits, are controlled by the intersection of major faults and associated subsidiary faults and occur within 150 m of the exocontact of the igneous massif. The shorter the distance between ore body and intrusive contact, the higher the grade (Chen Yifeng 1996).

General Shape and Dimensions of Deposits

Fe, Cu, and S form medium to large deposits while Co, Au, Mo, Pb, Zn, and U form medium to small deposits. Gold mainly occurs as an associated element. Nonmetallic minerals such as alunite and gypsum form large deposits.

Deposits independent of rich or poor ore consist of lenticular or columnar lodes, up to 10 m in length and 1–20 m in thickness, which persist to depths of 100–200 m. The lodes have an internal breccia, network, or stockwork structure in which pitchblende occurs in breccia matrix and interlacing small veins and veinlets.

Ore body grades are commonly on the order of several hundredths to a few tenths of one percent U; but some deposits also

include high grade ore shoots with U grades of several tenths of one percent and higher with maxima of 6% U (see Sect. 1.3.3.1 and 1.3.3.2: *Kunshan Area, Huangmeijian Massif and Dalongshan Area, Zongyang Massif*). Rich ore shoots are separated from wall rocks by a distinct, sharp boundary.

The thicknesses of high grade and poor ore bodies are similar since rich ore bodies were formed from poor ore bodies by superimposition of late ore-forming processes.

Stable Isotopes and Fluid Inclusions

Studies of fluid inclusions in microcrystalline quartz, calcite, dolomite, and baryte of the Kunshan and Dalongshan deposits indicate a dominance of K^+ , Na^+ , and Ca^{2+} among cations and HCO_3^- as the predominant anion in ore-forming solutions. CO_2 prevails in gas phases. No regular difference exists in the composition of solutions of different mineral stages. U concentrations in fluid inclusions range from 6.63×10^{-4} to 2.744×10^{-2} mol kg⁻¹ H₂O. Homogenization temperatures of early stage minerals vary between 300 and 350°C and in later stage minerals between 200 and 250°C. Eh values of 0.822 V and 0.555 V, and pH values of 8.22 and 7.33 were obtained for early and later ore-forming solutions, respectively. Formation pressures for early and later stage minerals are 270×10^5 Pa and $150\text{--}240 \times 10^5$ Pa (Zhu Jiechen et al. 1996).

Measurements of hydrogen and oxygen isotope compositions in solutions in equilibrium with various gangue minerals of different mineralizing stages show a wide range of ratios that exceed by far the $\delta^{18}O$ and δD range of normal magmatic fluids. These solutions are therefore interpreted to be of polygenetic heritage derived to various degrees from deep-seated sources, dewatering of country rocks, phreatic, and meteoric waters.

Based on $\delta^{34}S$ data of pyrite and chalcopyrite associated with pitchblende and that of later sulfides in the Dalongshan and Kunshan U deposits, the total S isotope composition of ore- and post-ore stage hydrothermal solutions at the crystallization point was calculated at 16‰ and 14.5‰, respectively, suggesting that the sulfur originated from sulfur enriched rocks in the crust (e.g. carbonatic rocks) Zhu Jiechen et al. (1996).

Regional Geochronology

Xiangshan Group sandstone and limestone with manganese concretions yield whole rock Rb-Sr isochronal ages of 177 ± 35 Ma and volcanics of the Fushan Formation yield 137 ± 9 Ma (Zhu Jiechen et al. 1996). Zircon (U-Pb) and whole rock (Rb-Sr) dating of syenite (Huangmeijian, Dalongshan, Chengshan plutons) yield two age intervals: 135–133 (137–130) Ma for biotite-quartz syenite and quartz syenite, and 119–115 (120–115) Ma for massive to fine-grained quartz syenite and moyite (Chen Yifeng 1996; in brackets data from Zhu Jiechen et al. 1996).

Four ore forming epochs are indicated by U-Pb analyses of pitchblende in the Lu-Zong region. Chen Yifeng (1996) reports stages at 152 Ma (Liujiaao occurrence), 130 Ma and 110 Ma (Dalongshan deposit), and 110 Ma and 60 Ma (Kunshan deposit).

The dominant epoch of mineralization is 110 Ma. Zhu Jiechen et al. (1996) provide the following ages of mineralizing events: 174 Ma, 137 Ma, 111.7 Ma, and 66.6 Ma. The 174 Ma age corresponds to the age of Xiangshan Group sandstone and synsedimentary U mineralization. The second stage is coeval with volcanic eruptions and the first magma intrusion. The third stage is close to the second magmatic event; and the last event is of local nature.

Potential Sources of Uranium

Country and igneous rocks as well as magmatic fluids are forwarded as potential U sources. Rocks in the Lu-Zong region have U background tenors as follows: Sandstone (Luoling Fm) 6–12 ppm with (diagenetic) local enrichments of 150–2 400 ppm; contact-metamorphic (hornfelsic) sandstone 3–29 ppm; volcanics 6.8 ppm; medium-grained (biotite-)quartz syenite 5.3–9.6 ppm, fine-grained quartz syenite and moyite 18–32 ppm. Most U in igneous rocks is bound in accessory minerals and these lithologies show only a little, if any, loss of U. U values in altered rocks are increased by as much as 10 times compared to those in progenitor lithologies (for more see next chapter).

Principal Ore Controls and Metallogenetic Concepts

As may be deduced from descriptions by Chen Yifeng (1996) and Zhu Jiechen et al. (1996) the following model may adequately illustrate the metallogenesis of U deposits in the Lu-Zong Basin.

U deposits occur structurally controlled in relatively narrow zones along the exocontact of or in xenoliths within intrusive massifs. Modified arenite is the principal ore host. Repeated magmatism, faulting, contact metamorphism, and metasomatic and hydrothermal processes have modified the country rocks in these zones.

Besides single stage U mineralization, high-grade pitchblende ore, as known from the Dalongshan and Kunshan deposits, occurs in the contact zones. Mineral parageneses and mineralization stages at 174, 137, 111.7, and 66.6 Ma document a multistage evolution of this rich ore. Mineralochemical, geochemical, and isotope data of ore and altered host rocks attest to a polygenetic provenance of constituents in high grade ore from magmatic as well as nonmagmatic sources.

The principal source of uranium is still open to debate. Chen Yifeng (1996) states that trace elements in pitchblende (see Sect. *Principal Characteristics of Mineralization*) as well as Pb, Sr, and S isotopes ratios suggest a provenance of ore constituents mainly from the quartz syenite-related magmatic chamber and quartz syenite itself with some contributions of U from sandstone. Since biotite-quartz syenite at the northern margin of the Huangmeijian Massif shows some loss of U (from original 10.5 to 8.6 ppm U) the author considers this facies to represent a viable U source for U mineralization. Ba, V, and Ca contents in pitchblende and a U loss from 6.57 to 4.4 ppm U as analyzed at the Kunshan deposit indicate contributions of U from sandstone.

Zhu Jiechen et al. (1996) reject quartz syenite as a noteworthy U source instead they favor arenite of the Jurassic Xiangshan Group. They point out that quartz syenite is relatively poor in U and that their geochemical surveys do not reveal a U loss in this facies; additionally, they argue that the igneous massifs are small in volume and only a limited quantity of hydrothermal fluids could have resulted from magmatic differentiation. Criteria forwarded by these authors in support of a U provenance from sandstone are as follows: Sandstone and contact-metamorphosed (hornfelsic) sandstone contain 3–22 ppm U but originally had a calculated tenor of 3.3–47 ppm U. In addition, sandstone beds contain diagenetically enriched U locally of as much as 1 500 ppm U. The computed U loss is 25–86% with the biggest decreases in hornfelsic sandstone. The contact-metamorphosed hornfelsic zone is up to 800 m in width and, consequently, the original U endowment must have been substantial, sufficient to constitute an adequate U source for the Lu-Zong U deposits.

Whatever the sources of uranium and other ore-forming elements might be, the integral components and temporal sequence of metallogenesis-related geological events are as follows. The Lu-Zong U district is located in a long active mobile zone at the margin of an old continent. Deep faulting or rift movements that controlled sedimentation, magmatic activity, and related metallogenesis characterize this zone. Magma evolved adjacent to the Tan-Lu deep fault zone by remelting of the lower crust admixed with material from the upper crust.

During the Early Jurassic, the Lu-Zong Basin was downfaulted and sediments dominated by lacustrine facies were deposited. Sedimentary and diagenetic processes preconcentrated uranium locally to protore in arenite of the Xiangshan Group. Subsequently, recurrent magmatic and structural events generated or reactivated hydrothermal systems, which introduced and/or redistributed uranium. Geochemical including isotope data of gangue and alteration minerals imply that hybrid solutions of multiple provenances were instrumental in the mineralizing process.

The first thermal and U concentrating event was related to main intrusions of alkaline plutons (Huangmeijian, Dalongshan, Chengshan etc.) in Late Jurassic time and eruptions of consanguineous volcanics (137 Ma). Magma emplacement presumably caused microfissuring and fracturing in surrounding rocks, and also mobilized various kinds of water (free water, adsorptive water, water in crystalline structures) in the rocks. At the same time, minor amounts of magmatic alkaline fluids may have entered the hydrothermal system. As this thermal solution migrated upwards, it constantly extracted various elements including U from the invaded rocks to form a U-fertile solution. Precipitation of U in favorable open structures established the first pitchblende generation.

The second thermal event, at 117 Ma, occurred in response to the second intrusion of massive to fine-grained quartz syenite and moyite. Associated structural and hydrothermal resurrection had the most significant impact on the accumulation of U ore.

The final U mineralization stage, at 66 Ma, is locally restricted. This stage includes descending meteoric water in the ore-forming process. Admission of the meteoric water to the preexisting

solution caused a drop in $\delta^{18}\text{O}$ values and temperature of the mineralizing solution.

Repeated reworking of precursor U mineralization in response to recurrent tectonic and magmatic activities resulted in a constantly increasing U concentration in the ore-forming solution that finally led to richer U ore in favorably prepared structures associated with marked wall rock alteration and veining. Zhu Jiechen et al. (1996) postulate that water and uranium in ore-forming solutions were basically derived from sediments, as outlined earlier, U essentially from hornfelsic sandstone, rather than magma. When magma ascended, the hydrothermal system became repeatedly reactivated, remobilized uranium, and circulated along permeable structures. With magma consolidation, the solution regressively flowed to the heat source and U was precipitated in an environment of adequate physico-chemical conditions to form rich U ore bodies close to intrusive bodies, particularly in xenoliths. In contrast, at some distance from intrusive bodies, U became disseminated in country rocks and only formed ore of ordinary grade. U and associated minerals apparently precipitated rapidly as inferred from distinct boundaries between rich ore lodes and wall rocks, abundant ferrous iron and clay/mud in microcrystalline quartz and carbonate associated with pitchblende, and diverse impurities in pitchblende.

According to Chen Yifeng (1996), physico-chemical criteria that conditioned U transport and ultimate enrichment to form the high-grade Lu-Zong ore lodes are as follows:

1. U was transported by an alkaline medium; the postulated mineralizing solution had a dominance of K^+ , Na^+ and Ca^{2+} cations, HCO_3^- as dominant anion, and pH values of 7.33–8.43. Uranium in solution may have existed in the form of uranyl-carbonate ions.
2. Adequate pathways for ascending and migration of hydrothermal solutions as well as favorable spaces for ore accumulation were generated by repeated faulting that imposed a multitude of brittle structures onto the contact-metamorphic zone and distinctly increased the fracture density and porosity of the host sandstone (see Kunshan deposit).
3. A reducing environment required for U reduction was provided by abundant pyrite and organic material in Xiangshan Group sandstone. Related redox interfaces tend to exist in the immediate vicinity of or at the intrusive exocontact as indicated by profile measurements of redox potential at the Dalongshan deposit. A change in δEh values is demonstrated on a profile from 32 mV within the massif to 13 mV in the contact zone to 50 mV in hornfelsic sandstone, indicating a transitional redox zone at the contact zone.
4. U deposition took place at low pressure conditions in an open or semi-open fault system as can be inferred from the fault systems hosting rich U ore bodies; and from experiments, which show that pitchblende co-precipitated with pyrite and carbonate under pressures of $50\text{--}150 \times 10^5$ Pa.
5. Low to moderate temperatures of the metallogenetic event are indicated by thermometry of pitchblende and associated pyrite and ankerite suggesting an ore-forming temperature of about 250°C for rich uranium ore.

In conclusion, the grade of an ore body is a function of the frequency of hydrothermal events, development degree of the structural host edifice, and the nature of solutions as reflected by modes and style of alteration phenomena. Poor ore bodies evolved by a simple process as reflected by simple alteration effects and only minor development of hydrothermal veins; whereas high grade U ore occurs in complex ore veins as a result of superimposition of multiple tectonic-hydrothermal processes and material derived from variable sources.

Since economic U ore bodies occur in zones of bleached sandstone that originated from pre-ore albitization, silicification, and carbonatization, Chen Yifeng (1996) postulates pre-ore albitization to be an essential precondition for metallogenesis. The role of hydromicazation, a typical wall rock alteration adjacent to ore bodies, is seen in its capacity to enhance the enrichment of uranium by changing the geochemical environment. The formation of abundant hydromica has consumed substantial H^+ in solution, turning an acid into an alkaline solution. The concomitant gradual rise in pH and drop in Eh values accelerated the disintegration of H_2S and increased the content of S^{2-} ions. All these changes promoted the precipitation and enrichment of uranium.

1.3.3.1 Kunshan Area, Huangmeijian Massif

The Kunshan (Kuanshan) area is located at the northern margin of the Huangmeijian Massif and includes deposits #8411 (or *Kunshan*) and #8413, each with resources between 100 and about 500t U and grades ranging from 0.05 to 0.3% U. Additionally, there are nine U occurrences in the Kunshan area including #8412, and #4360 besides numerous U showings. Occurrence #4360 with a grade averaging 0.394% U is located in the western section of the Kunshan area.

Sources of information. Chen Yifeng 1996; Zhu Jiechen et al. 1996.

Geology and Mineralization

U ore bodies occur externally adjacent to and partly within the northern margin of the E-W-elongated Huangmeijian Massif, controlled by the E-W-oriented Fushan-Huangmeijian basement fault zone of Indosinian age. This fault has a length of 50 km and a width of several kilometers; it controls the distribution of Lower-Middle Jurassic clastic sediments, as well as Yanshanian intrusive rocks and volcanic apparatus. Three E-W-oriented faults (F1, F5, F86) close to the exocontact of the massif are part of this fault.

Chen Yifeng (1996) notes the following tectonic settings of ore bodies: (1) Fault intersections of the contact zone of the Huangmeijian Massif control the position of ore zones # I–IV and deposit #8411; (2) sandwiched segments between the contact and the E-W faults F1 and F5 contain a part of deposit #8411, and deposit #8413 occurs between fault F86 and the contact zone; and (3) high grade lodes of deposit #8411 are located at depth on both sides of a quartz syenitic apophysis.

Sandstone in the exocontact zone of the massif exhibits a distinctly increased fracture density and porosity the origin of which is attributed to ascending magma. The porosity of coarse-grained sandstone was increased from 3.7% to 5%, that of medium-grained sandstone from 1.9% to 4.8%, and that of fine grained sandstone from 1.7% to 3.5%.

Syn-ore alteration at Kunshan persists in sandstone for 300–600 m in width from the intrusive exocontact and for up to 100 m in width from the endocontact.

Mineralization in deposits #8411 and 8413 is composed of U, Cu, Au, and Fe; U is the dominant element. Three major mineral parageneses/stages are identified: pitchblende-black microcrystalline quartz, pitchblende-sulfide, and pitchblende-carbonate.

Deposit #8411 contains high grade U ore bodies with grades in excess of 0.3% and some intervals with grades higher than 0.563% and a maximum of 5.97% U. These lodes occur within a zone up to 150 m wide bounded to the north by two E-W-oriented faults (F1 and F5) and to the south by the sublatitudinal trending northern margin of the Huangmeijian Massif. Subsidiary faults trending NW-SE and ENE-WSW cut the terrane between these faults and form an “X”-shaped fault system that controls the position of the rich ore bodies. The shorter the distance to the contact zone, the richer are the ore bodies. Medium to coarse sandstone of the 8th rhythm of the Luoling Formation is the host rock (Chen Yifeng 1996).

1.3.3.2 Dalongshan Area, Zongyang Massif

This area hosts the small but high grade *Dalongshan* deposit and 10 U occurrences, such as # 36 and # 80 in the southwestern Dalongshan Massif, which is a part of the Zongyang Massif as mentioned earlier.

Source of information. Chen Yifeng 1996.

Geology and Mineralization

In its southwestern segment, the Zongyang quartz syenitic massif encloses a number of roof pendants of Xiangshan Group sediments. Some of these pendants contain U showings controlled by the N-S-oriented Dalongling-Xueidian fault. Mineralized xenoliths consist of altered and bleached sandstone enclosed by a silicified crust. Alteration features include silicification, hydromicazation, hematitization, chloritization, and carbonatization.

The *Dalongshan deposit* consists of lithologically and structurally controlled ore bodies at shallow depths in a large xenolith. Major ore bodies occur in contact-metamorphosed, altered and bleached feldspar-quartz sandstone of the Xiangshan Group; while minor mineralization occurs in quartz syenite. Ore lodes are situated at the intersection of, and hosted by the above-mentioned submeridional fault and crosscutting subsidiary faults trending NW-SE. These structures carry high-grade ore within a range of several meters to 50 m from the quartz syenite contact.

As an ore hosting structure enters the quartz syenite body it becomes smaller and both alteration and U mineralization weaken or even disappear. The principal ore hosting structures were subjected to multiple structural-hydrothermal activities. Early deformation resulted in the development of schistosity, and later tectonic deformation led to the extension of altered rocks and deposition of pitchblende in cement of breccias and fragmented rocks to form rich U ore bodies.

Elemental and mineralogical composition of the ore equals that of the #8411 deposit. The average grade at Dalongshan is 0.805% U and the highest is 34.22% U.

1.3.3.3 Chengshan Area, Zongyang Massif

Five U occurrences including *Chengshan* and *Dashuzhuang* are located in the NE part of the *Zongyang Massif*. They are controlled by subsidiary faults of the ENE-WSW oriented Guangqiao-Chenghuanmiao fault (Chen Yifeng 1996).

1.3.3.4 Qiaozhuang Area, Zongyang Massif

This area contains five U showings including *Qiaozhuang* and *Taohuashan* on the eastern side of the *Zongyang Massif*, controlled by the N-S-oriented Dongyuemiao-Zhoujiashan basement fault and the NE-SW Toupao fault (Chen Yifeng 1996).

1.3.3.5 Yongchen Massif

The Yongchen Massif (YC) occurs south of the Yangtze River as the Lu-Zong Zone is north of the Yangtze River. The massif covers an area of some 130 km², and contains a single uranium occurrence. The Yongchen Massif is attributed to syntectonic type or type I by Zhang Bangdong (1990) and consists of 1st-stage biotite granite/K-feldspar granite, 2nd-stage hornblende granite and 3rd-stage fine-grained granite with dykes of aplite, granite porphyry and quartz porphyry.

1.3.4 North Qilian Caledonian Fold Belt, Gansu-Ningxia Huizo A.R.

The Caledonian North Qilian fold belt contains several uranium prospects with disseminated uranium mineralization (dated at 300–260 Ma) and uraniumiferous silicified veins within strongly albitized and hematitized zones in Na-metasomatized (albitized) Silurian-Devonian sandstone and conglomerate, and Early Ordovician andesitic breccias (Liu Xingzhong and Zhou Weixun 1990).

1.3.5 SW Qinling Metallogenic Zone/South Qinling Hercynian-Indosinian Fold Belt

Situated in E Qinghai-S Shaanxi-N Sichuan, the SW Qinling metallogenic zone lies within the NW-SE-oriented South Qinling

Hercynian-Indosinian fold belt. This fold belt stretches along the southwest side of the Qilian-Qinling U province, and is sandwiched between the North Qinling Caledonian fold belt to the northeast and the Yangtze Massif to the south.

The SW Qinling metallogenetic zone is known not only for C-Si-pelite-type U deposits such as found in the *Ruoergai District* (# 512) (Fig. 1.1) with deposit # 512/Luojungou, but also for gold, e.g. deposit # 510/*Larma* (Au with weak U contents) located to the west of Luojungou, and Hg-Sb-As deposits.

Sources of information. Liu Xingzhong and Zhou Weixun 1990; Shen Feng 1995; Tu Guangzhi 1990; Zhou Weixun 1997, pers. commun. 2006.

Regional Geological Setting of Mineralization

The SW Qinling metallogenetic zone, about 320 km long and on average 50 km wide, roughly coincides with the E-W-trending Beilungjiang (Beilungjiang) anticlinorium in the W Qinling marginal taphrogenic trough. U and Au deposits, the two types are separated from each other, are situated in the axial segment while some Hg and Sb occurrences with traces of Au occur in Devonian carbonates on the northern flank of the Beilungjiang anticlinorium.

The U and Au hosting sequence comprises slightly metamorphosed and folded sandstone, mudstone, and siltstone with interbedded lenses of chert and siliceous limestone of Cambro-Silurian age. Axial parts of domes or anticlines provide the most favorable sites for ore location.

Mineralization is strata-structure bound and of disseminated replacement nature confined to altered, strata-peneconcordant and -discordant fracture zones in thick, pyrite and carbonaceous matter enriched chert or siliceous limestone lenses and their transitional aureoles into other facies. The carbon content of mineralized sections ranges from some tenths of a percent to several percent. Alteration at mineralized intervals includes pronounced silicification, and variably intense argillization, pyritization, sericitization, and carbonatization. Quartz and carbonate veining is typical for cataclastic intervals.

U ore bodies are of irregular configuration and made up of pitchblende and black U products associated with diverse gangue and sulfide minerals of a variety of elements (see below *Ruoergai District*).

Tu Guangzhi (1990) postulates a provenance of As, Au, Hg, Sb, Tl, U and other elements from Paleozoic and Triassic carbonates, chert, siltstone, and mudstone beds that are enriched in carbonaceous matter and pyrite and contain anomalous amounts of these elements. Ore formation took place in the waning stage of the Yanshanian Orogeny as a result of reactivation of these elements by solutions. Oxygen and hydrogen isotope compositions attest to a meteoric origin of these ore forming solutions and sulfur isotopes of sulfides reflect a seawater origin for sulfur. Fluid inclusion thermometry suggests a formation temperature of 120–160°C as found in the *Ruoergai* deposit.

Liu Xingzhong and Zhou Weixun (1990) report isotope ages for U mineralization between 130 and 45 Ma whereas Tu

Guangzhi (1990) gives ages of 60–20 Ma, which would indicate an impact of post-Yanshanian events on the original U mineralization.

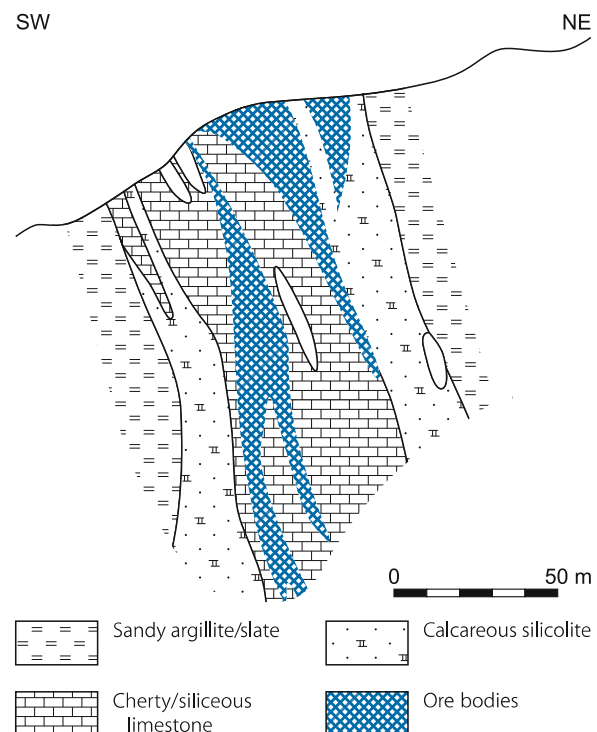
1.3.5.1 Ruoergai District, N Sichuan

This district (also named *Norgai* in some publications) is located on the northern wing at the western end of the Bailongjiang anticlinorium in northern Sichuan (Fig. 1.1). Several deposits are identified. They are hosted by chert-siliceous limestone lenses within sandy argillite/slate of Silurian age and include U deposit # 512/*Luojungou* and # 512/*Larma*, a gold deposit with weak U contents (Fig. 1.26).

Luojungou deposit (512): This deposit comprises several ore bodies of irregular shape and diffuse boundaries controlled by intra-formational fault zones in cherty/siliceous limestone or calcareous silicolite. Pitchblende and black U products (sooty pitchblende) are the principal U minerals. U ore bodies may contain anomalous amounts of As, Hg, Mo, Sb, Tl, and, commonly in lesser quantities, Ni, Cu, Pb, and Zn, but in some ore lodes Zn can be up to 0.5%. Base metals occur mainly in the form of chalcopyrite, galena, sphalerite (poor in Fe), Ni-sulfides and sulfo-salts; Mo is present as amorphous MoS_2 . Gangue minerals include quartz, calcite, dolomite, siderite, sericite, baryte, fluorite, and clay minerals. Alteration includes marked silicification, and, in variable intensity, argillization, pyritization,

Fig. 1.26.

Ruoergai district N Sichuan, simplified SW-NE section across a district C-Si-pelite deposit hosted in Middle Silurian weakly metamorphosed sediments (after Zhou Weixun 1997)



sericitization, and carbonatization (calcite, dolomite, ankerite and siderite) (Zhou Weixun 1997).

Larma deposit (# 510): Discovered in the late 1960s, this polymetallic deposit is located near the homonymous village to the west of Luo Jungou. Gold is the dominant metal of interest. U occurs as an associated element as well as Cu, Hg, Mo, Ni, V, and Zn. Most ore bodies occur at depth between 10–200 m and more controlled by intra-formational fault zones in Silurian siliceous limestone (You Yunfei et al. 1996).

1.4 South China Uranium Province

The South China Uranium Province accounts for the largest amount of explored uranium deposits and resources in China and was the most important uranium-mining region in the past. This U province spreads over an area up to 500 km wide and almost 1 200 km long covering some 600 000 km² in southeast China. It extends from Zhejiang Province in the northeast through parts of Hunan, Jiangxi, Fujian and Guangdong into Guizhou and Guangxi Zhuangzu A.R. in the southwest (Figs. 1.1, 1.27).

Several types of U deposits are identified; economically, *granite-related* vein deposits rank first, *volcanic-type* deposits second; and *black shale-related stockwork* U deposits third [the latter are in China referred to as carbonate-siliceous-pelite (C-Si-pelite) type as defined earlier; Zhou Weixun et al. (2003) use the term vein type in sedimentary rocks]. Some small *sandstone-type* U deposits are known from several Mesozoic-Tertiary basins. Individual deposits are commonly of small size, a few hundreds to some thousands of tonnes of uranium, and of low, rarely of medium grade (0.05–0.2% U). Besides uranium, S China is also renowned for W, Sn, Mo, Bi, Cu, Pb, Zn, and REE deposits.

Based on the preferential distribution and related geological setting of the first three deposit types, the South China U province is divided – as outlined further down – into an Eastern and Western metallogenetic domain, and an arbitrarily denominated granite-dominated domain that overlaps parts of the two former domains. Although these domains are characterized by the prevalence of a distinct deposit type, other types of U deposits may also occur.

- *Granite-related deposits* are scattered over most of the U province but prevail in the Nanling magmatic zone as discussed further down in Sect. 1.4.1: *Granite-Dominated Domain/Granitic Complexes and Related U Deposits*.
- *Volcanic-related deposits* are prominent in the *Eastern Domain* where they occur predominantly in the Gan-Hang volcanic belt (or Jiangxi-Hangzhou Belt, Gan is the abbreviation for Jiangxi and Hang for Hangzhou) and some in the Wuyishan (or Zhejiang-Fujian-Guangdong) magmatic zone to the E and SE of the Gan-Hang Belt.
- *C-Si-pelite/black shale-related stockwork U deposits* are typical for the *Western Domain* that encompasses the Precambrian Jiangnan Uplift (also referred to as Jiangnan Old Land) with the Xuefeng-Jiuling U zone and, located further to the south-east, the Late Paleozoic Xianggui Depression (also termed

Guangxi-Hunan-Jiangxi carbonate zone). A few granite-related deposits also occur in this domain.

The subsequent synopsis is largely based on Chen Zhaobo et al. (1982), Chen Yuqi et al. (1996), Liu Xingzhong and Zhou Weixun (1990), Zhang Zuhuan (1990), Zhenkai Yao et al. (1989), and Zhou Weixun (1997, 2000, 2003, and pers. commun.) if not otherwise stated.

Regional Geological Features of the South China U Province

Zhou Weixun (person. commun. 2003) delineates the South China U province as follows: The northern and southern boundaries coincide with the northern marginal fault zone of the Jiangnan Uplift and the southern edge of the Nanling tectonomagmatic zone (or perhaps with the Qingyuan-Zijing tectonic belt), respectively. The western limit is provided – from Ziyun in central-south Guizhou Province SSE-wards to Nandan in N Guangxi A.R. – by the NNW-SSE-trending Ziyun-Nandan fault zone while the eastern boundary correlates with the NNE-SSW-oriented Lishuai-Lianhuashan fault zone that can be traced from Lishuai in S Zhejiang through Fujian to Lianhuashan in SE Guangdong Province.

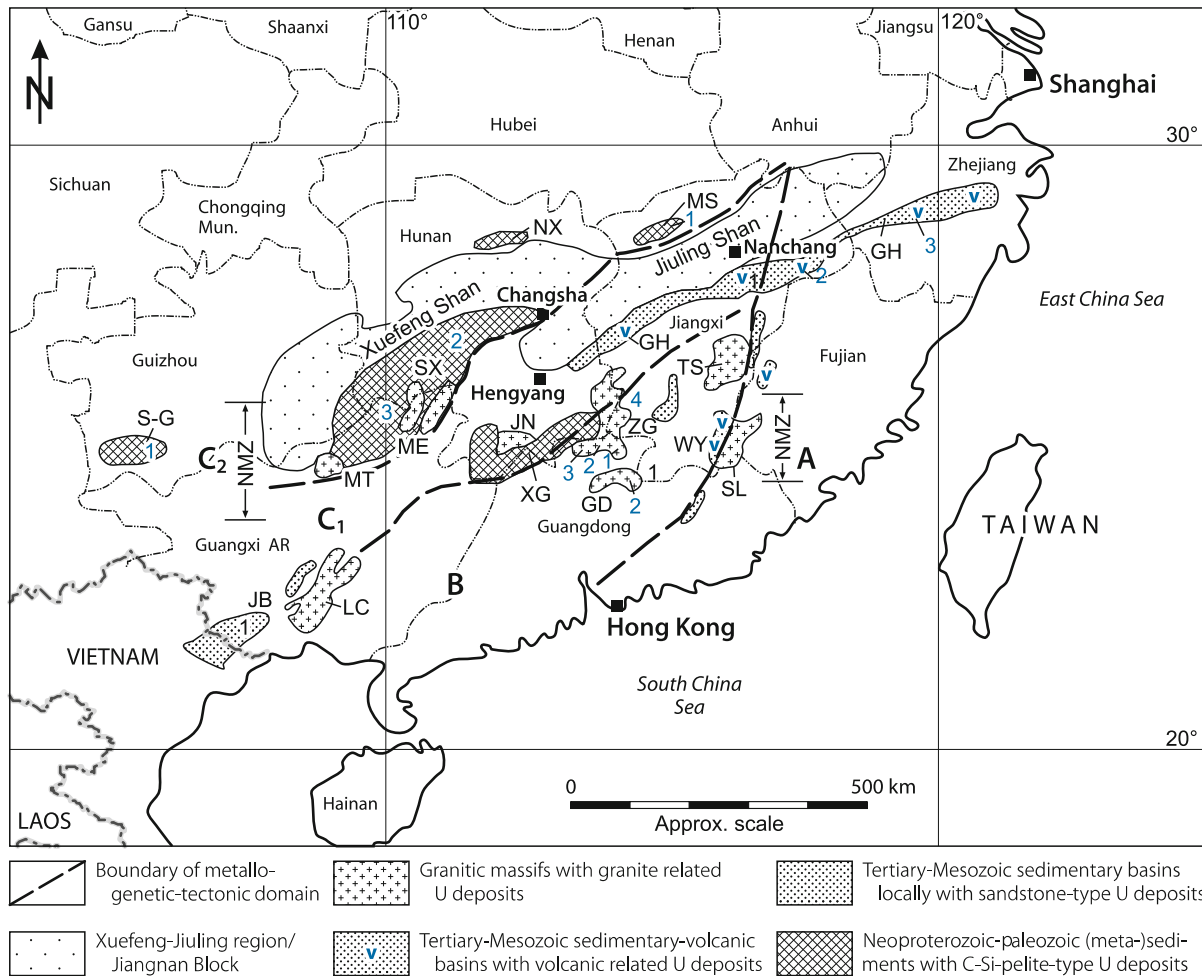
According to Chen Yuqi et al. (1996), the South China U province overlaps two major geotectonic units: the southeastern margin of the *Yangtze Massif* (or Platform) and the easterly adjacent *Nanhua Mobile Zone* (or South China Caledonian fold belt).

The SE margin of the *Yangtze Massif* encompasses the Jiangnan Uplift where the crust was consolidated between Middle and Upper Proterozoic and covered by Sinian to Lower Paleozoic sediments. Rocks in the *Jiangnan Uplift* range from Middle Proterozoic to Paleozoic. The Middle Proterozoic Jiuling and equivalent groups (1 800–1 000 Ma old) consist of a more than ten thousand meters thick sequence of shallow marine flysch-type sediments, mainly greywacke, sandstone, and mudstone/shale with intercalations of ultramafic, mafic, and intermediate submarine volcanic rocks including spilitic keratophyre. During the Sibao Orogeny (about 1 000 Ma ago) these rocks were intensely folded and regionally metamorphosed to greenschist facies grade to form phyllite, slate, quartzite, locally schist, and phyllitic schist. Some granitic and granodioritic batholiths mainly of tonalite and quartz-monzonite composition were intruded contemporaneously in what is now the western Jiangnan Uplift.

The Upper Proterozoic Banxi and equivalent groups (1 000–800 Ma old) rest unconformably on the Jiuling Group and consist of a thick sequence of slate, silty slate interbedded with meta-siltstone and -greywacke, and locally intermediate to mafic volcanics. This suite was folded and intruded by granites during the Xuefeng (Jinning) Orogeny, about 800 Ma ago, and subsequently uplifted to form the “Jiangnan Old Land”. The Xuefeng granites (850–700 Ma) are plagioclase or biotite granites and occur discontinuously along the Jiangnan Uplift; some of these plutons are uraniumiferous, such as the Motianling also known as Sanfang polyphase granite at the SW margin of the Jiangnan

Fig. 1.27.

South China, location of uranium domains, belts, and districts/ore fields (deposits). (Note: Sites of U districts/deposits and boundaries of domains, regions, belts, and massifs are approximate) (after Zhang Bangtong 1990; domains after Yao Zhenkai et al. 1989; U belts after Zhang Zuhuan 1990) **Metallogenic-tectonic domains:** A Eastern or Zhejiang-Fujian-Guangdong volcanic-dominated U metallogenetic domain, B Central or Nanling granite-dominated U metallogenetic domain, C Western (meta-)sedimentary (C-Si-pelite) U metallogenetic domain, C₁ Guangxi-Hunan-Jiangxi carbonate subdomain, C₂ Xuefeng-Jiuling pelite subdomain, NMZ Nanling metallogenetic zone. **Orogenies:** Cal Caledonian, Ind Indosinian, Yan Yanshanian. **Ore fields (OF)** and selected deposits in brackets



Granite Massifs (GM) with granite related U veins

GD Guidong GM (Ind-Yan) (OFs: 1 Xiazhuang, 2 Xiwang)
 JN Jiuyishan/Jinjiling GM (Yan)
 LC Liuchen GM (Ind-Yan) (Ma'andu)
 ME Mao'ershan and Yuechengling GMs (Cal) (Ziyuan OF)
 MT Motianling GM (Neo-Prot) (Sanfang OF)
 SL SL GM (Ind) (SL)
 TS Taoshan GM (Ind-Yan), (Dabu)
 ZG Zhuguang GM (Ind-Yan) (OFs: 1 Baishun, 2 Changjiang, 3 Chengkou, 4 Lujing)

Volcanic belts with volcanic-type U deposits

GH Gan-Hang (OFs: 1 Xiangshan, 2 Yingtan/Shengyuan, 3 Xiaoqiuvuran)
 WY Wuyishan Volcanic U Belt

Areas with C-Si-pelite-type U deposits

Xuefeng-Jiuling U Region
 – MS Mufu Shan area (1 Xiushi OF)
 – NX Northern Xuefeng Shan area
 – SX Southern Xuefeng Shan area
 (2 Central Hunan OF: Huangcai, Laowulong, Pukuitang; 3 Ziyuan OF: Chanziping etc.)
 XG Xianggui Paleozoic Basin
 (1 Jinyinzhai/Chenxian, Bentou)
 S-G Southwest Guizhou U Region
 (1 Chienxinan)

Mesozoic basins with sandstone-type U deposits

B Jingan Basin (1 Tunling)
 HB Hengyang Basin

Uplift as discussed later (Sect. 1.4.1.2.1: *Motianling Granite Massif, Motianling/Sanfang OF, Guangxi A.R.*).

During Sinian time, this region became a shallow marine basin and Sinian to Silurian sediments, more than 10 000 m thick,

were deposited without a major break but with some variations in different geotectonic terrane. In the Jiangnan Uplift and adjacent terrane, Sinian sediments include practically unmetamorphosed sandstone, mudstone/shale, tillite, and dolomitic

facies. They are overlain by Cambrian basal black shale about 100 m thick upon which carbonaceous-argillaceous limestone and calcareous shale rest. Ordovician and Silurian sequences consist of graptolite-bearing, fine-grained clastic sediments.

The *Nanhua Mobile Zone* includes the Xianggui and – to the E and SE thereof – the Cathaysian fold system; both evolved by the Caledonian Orogeny but were reactivated by Indosinian and Yanshanian intense tectono-magmatic activity. The *Xianggui* (also termed Hunan-Guangxi) fold system is characterized by a well developed Late Paleozoic cover resting upon the Caledonian basement, while the *Cathaysian* fold system (also termed SE China Caledonian orogenic belt or Post-Caledonian Uplift) lacks or has only poorly developed Late Paleozoic cover sediments. The Nanhua Mobile Zone is bounded to the south by the E-W-trending Mesozoic Nanpanjiang-Nanling fold belt.

The *Xianggui Depression* to the south of the Jiangnan Uplift in Hunan-Guangxi Provinces was a marginal marine basin during the Upper Proterozoic and Early Paleozoic; sediments deposited during this period were dominated by paraflysch facies with local intercalations of intermediate to felsic volcanics. These series were weakly metamorphosed and folded into the Xianggui fold belt of the Nanhua Mobile Zone by the *Caledonian Orogeny* (ca. 470–400 Ma ago) and intruded by granites. Most of these Caledonian intrusions consist of biotite-, two mica-, or monzonitic granite and gneissic granite while a minority consists of quartz diorite, granitic diorite, and plagioclase granite.

Renewed subsidence occurred in Late Paleozoic time, and Devonian-Carboniferous to Triassic sediments were unconformably deposited upon the Early Paleozoic metamorphics to form the Late Paleozoic Xianggui Depression. These Paleozoic strata include basal psammitic-psammitic facies that rest unconformably on the Caledonian paleosurface and grade upwards into psammitic-pelitic facies. A thick impure carbonatic unit with minor intercalations of clastic and coaly beds, and Lower Permian siliceous rocks derived from submarine exhalations lie upon the clastic sequence. These strata were folded and intensely faulted by the *Indosinian Orogeny* during the Middle to Late Triassic. Subsequently the whole region turned into a continental tectonic regime. It should be noted that Hercynian granites are absent in South China.

In the *Cathaysian fold system*, Sinian to Ordovician miogeosynclinal flysch-type sediments, mainly psammitic-pelitic sequences constitute most of the basement. These strata are time-equivalent and similar to basement lithologies in the Xianggui Caledonian fold belt, and were likewise weakly metamorphosed and folded into several NNE-SSW-oriented fold belts including – from west to east – the Zhuguang and Wuyi fold belts, and the Minzhe structural zone, and intruded by granites comparable to those mentioned earlier during the Caledonian Orogeny. Due to post-Caledonian uplift, Late Paleozoic sediments are largely absent, however.

Tectonic-magmatic reactivation of the Nanhua Mobile Zone during the Indosinian and Yanshanian orogenies resulted in rifting, emplacement of granitic batholiths, and volcanic activity. Indosinian (Tr₃) and Yanshanian (J-K) intrusions, the latter are commonly separated into an Early (J) and a Late Yanshanian stage (K), comprise predominantly biotite, two mica, and

monzonitic granites, and less abundant quartz diorite, granitic diorite, plagioclase granite, and alkali-miarolitic granite. The alkali-miarolitic granite (about 100 Ma old) is confined to the Zhejiang-Fujian-Guangdong coastal zone.

Most fertile U granites with associated U deposits were intruded during the Late Yanshanian Orogeny and evolved by polyphase intrusions. The E-W-oriented Nanling tectonic-magmatic belt with granitic batholiths and minor volcanic intrusions and extrusions is a marked product of this development.

Rifting and extensive faulting continued during the course of the Yanshanian Orogeny from the Jurassic onwards and generated NE-SW- and NNE-SSW-oriented regional faults and associated grabens or basins.

Intermediate to felsic volcanism was relatively widespread from Middle Jurassic, and more intense from Late Jurassic to Early Cretaceous; it was particularly pronounced in the eastern segment of the U province. High-seated granitic stocks were intruded simultaneously. The Gan-Hang and Wuyi U zones correspond to volcanic belts related to this event. Volcanics and small intrusions of this episode also occur in the Nanling zone.

Late Cretaceous and Paleogene downfaulted basins are filled with arenaceous redbed sediments and basaltic as well as alkali-basaltic lavas. Impressive giant quartz veins and silicified zones dipping at shallow angles cut through the boundaries of the basins and adjacent granites. A considerable number of U deposits occur close to these basins.

Geotectonic Distribution of U Deposits

As mentioned earlier, the South China U province is divided into an eastern and western metallogenetic domain, and an arbitrarily defined granite-dominated domain that overlaps parts of the two former domains (Fig. 1.27). The three principal U deposit types mentioned below show a preferential affinity to the one or the other domain in which they are often clustered in mineral belts and/or districts that are situated adjacent to Cretaceous-Tertiary redbed basins.

The dividing line between the eastern and western domains trends roughly along the *Chenzhou-Huaiji fault* (also referred to as Chenzhou-Beihai fault as abbreviated from Yichun-Chenzhou and Tengxian-Beihai fault systems). This fault can be traced from Yichun in Jiangxi Province SSW-wards through Chenzhou in Hunan, Huaiji in Guangdong to Teng Xian and further to Beihai at the coast in Guangxi A.R. (Chen Yuqi et al. 1996).

The *West Domain* includes the Jiangnan Uplift and the Xianggui Depression (or Xianggui fold system). U deposits are mainly of the C-Si-pelite type and most of them occur in the *Xuefeng-Jiuling U zone* located at the SW margin of the Jiangnan Uplift. This domain also contains vein U deposits in the Sanfang ore field associated with the Xuefeng/Upper Proterozoic Motianling (=Sanfang) granitic batholith at the south edge of the Jiangnan Uplift.

The *East Domain* is underlain by the Cathaysian landmass (or South China Caledonian fold belt) and contains predominantly volcanic-type U deposits related to large-scale Late Jurassic felsic volcanism. Most of the known volcanic-type

U deposits occur in the Gan-Hang volcanic belt while some occur in the Wuyishan magmatic belt located E to SE of Gan-Hang, and in the eastern extremity of the Nanling magmatic belt.

Although granite-related U deposits are scattered over most of the U province to the west of the Heyuan-Shaowu fault, they prevail in a region that is arbitrarily defined as *Granite-Dominated Domain* (also termed Central Domain by some authors) and includes the Nanling magmatic zone and granite massifs in central Jiangxi that are located within the eastern as well as in the western domain.

Sandstone-type U mineralization is not limited to any single domain but is found in Cretaceous-Tertiary basins adjacent to or within granitic massifs.

Uranium mineralization in all domains formed largely during Cretaceous and Tertiary time independent of host rock age and type of deposit. U mineralization occurs in several generations that yield U/Pb isotope ages between about 140 and 40 Ma (Du Letian et al. 1990; Zhenkai Yao et al. 1989; Zhang Zuhuan 1990; Zhou Weixun 2003).

1.4.1 Granite-Dominated Domain/Granitic Complexes and Related U Deposits

Granite-related U deposits are predominantly associated with Mesozoic granites but a few are associated with Caledonian and Upper Proterozoic granites. Mesozoic granite intrusions are widespread in the *Nanhua Mobile Zone* (or South China Caledonian fold belt) but are particularly abundant in the central and south portion of the South China U province. This granite-dominated terrane overlaps parts of the East and West domains in Hunan, Jiangxi, Guangdong Provinces, and Guangxi A.R. and is, in this treatise, arbitrarily defined as “Granite-Dominated Domain” (Fig. 1.27) (Du Letian et al. 1990 define it as “Central Domain”).

The domain in question is roughly bounded by the Jiangxi-Hangzhou (=Gan-Hang) volcanic belt to the north, the Qingyuan-Zijing tectonic belt to the south, the Heyuan-Shaowu fault to the east, and the Ziyun-Nandan fault to the west.

U mineralization mainly occurs in structurally controlled endo- and perigranitic deposits associated with “S-type granites”

(see below) in differentiated, large batholiths of predominantly Indosinian and Yanshanian (Late Triassic to Upper Jurassic) age (Figs. 1.28, 1.29).

The *Nanling Tectono-Magmatic Zone* is the most prominent U zone; it consists of several granitic complexes with related U districts. Some other uraniferous granites are separately distributed in central Jiangxi (e.g. *Taoshan*) and SW Guangxi A.R. (*Liuchen*) (Fig. 1.27). A few volcanic-type (e.g. in the eastern Nanling U zone) and sandstone-type deposits (e.g. *Wangjiachong* in S Hunan, *Puquitang* in central Hunan, *Tunlin* in SW Guangxi) are also known in this terrane.

Comprehensive geological coverage and generalized descriptions of granite-related U deposits in South China have been published (mostly in Chinese) by a great number of authors. Papers by Du Letian (1986), Du Letian et al. (1990), Yao Zhenkai et al. (1989), Zhang Bangdong (1990), Zhou Weixun (1997, 2002, pers. commun. 2003), Zhou Weixun et al. (2003) have been used for the following synopsis unless otherwise referenced.

Regional Geological Features of the Granite-Dominated Domain

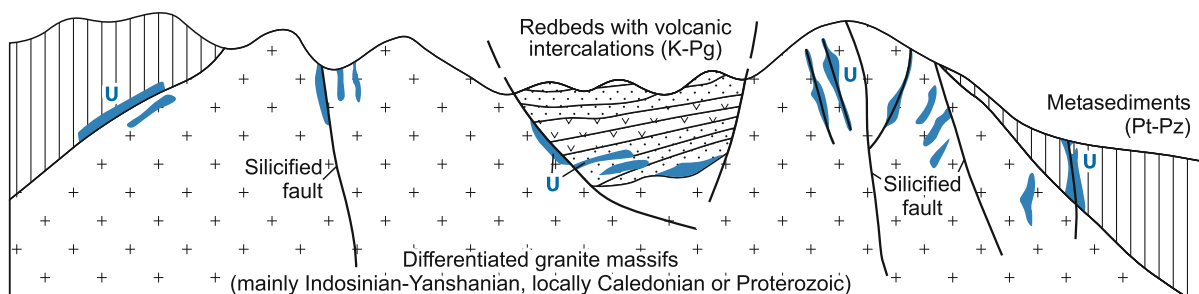
Most granite-related U deposits occur in the *Caledonian Nanhua Mobile Zone*. Sinian to Ordovician miogeosynclinal flysch-type sediments, mainly psammitic-pelitic sequences form the basement of the Nanhua zone. These rocks were folded, weakly metamorphosed, and intruded by granite during the *Caledonian Orogeny*. *Indosinian and Yanshanian* granites were subsequently repeatedly intruded (Table 1.7), commonly arranged in the form of discontinuous chains.

Granites occupy 34% of the province of Guangdong, 19% of Jiangxi, and 10% of Hunan (Du Letian et al. 1990) but only a fraction of these granites are regarded as U fertile (see Sect. *Regional Geochronology* for details on intrusions). A number of down faulted basins filled with Cretaceous-Eocene redbeds and/or Al-rich basalt or tholeiite are often located within or adjacent to U-hosting granitic massifs (Fig. 1.28).

Precambrian granite with related U deposits is confined to the SW margin of the Jiangnan Uplift where the *Proterozoic Motianling* (or *Sanfang*) granitic massif (845 Ma) hosts the

Fig. 1.28.

South China, scheme of geological setting of granite-related, endo- and exocontact U deposits (after Du Letian 1986)



■ Fig. 1.29.

South China, sketches of granite-related U deposits illustrating the unpredictable distribution of intra- and perigranitic U mineralized veins in selected granitic massifs (GM) (after Zhou Weixun 1997). *Lanhe* is an intragranitic deposit controlled by N-S-trending subsidiary structures. Ore bodies of *Dongkeng* are hosted by broken, metasomatized porphyritic granite in the footwall of a mylonite zone. The section of the intragranitic *Dabu* deposit illustrates the highly differentiated nature of the Taoshan granitic massif and the position of U ore bodies in strongly altered, fractured and brecciated intervals in Lower Jurassic, medium- to coarse-grained granite and Cretaceous granophyre. The perigranitic *Dawan* deposit in the Jiuyishan-Jinjiling granitic massif is in hornfels contact-metamorphosed Cambrian strata cut by granophyre dikes and several generations of calcite veins adjacent to Middle-Upper Jurassic, medium- to fine-grained biotite granite (Zhou Weixun 1997)

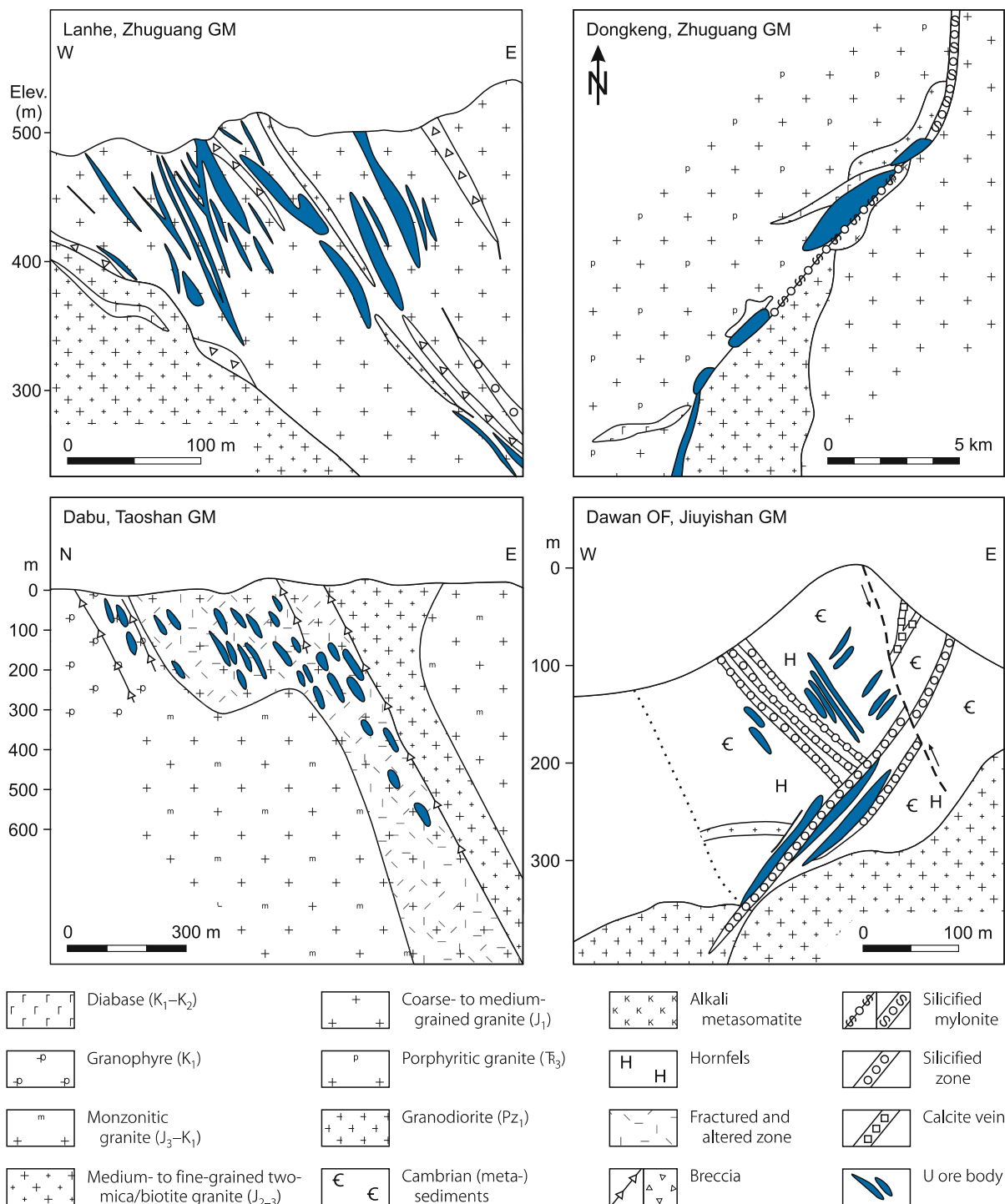


Table 1.7.

South China, magmatic, alteration, and mineralization stages in granite areas (after Du Letian et al. 1990)

Quartz (fluorite) generation	Wall rock alteration	Mineralization	Age(Ma)
$Q_{6'} F_{Y2}$ $Q_{5-2'} F_{Y2}$	White-green	2 nd U generation	
$Q_{5-1'} F_{Y2}$ Q_{4-2} Q_{4-1}	Yellow-green	1 st U generation,	±85 or later
Q_3 Q_2 Q_1	Grey-green		Ca. 90–10
Magmatic activity	Metasomatism	Mineralization/age	
Intermediate-mafic dykes λ_2	Alkaline metasomatism?	Pb-Zn?	
Downfaulting of Cretaceous redbed basins K_1, K_2			
$\lambda_1, C\pi$	Alkaline metasomatism	Pb-Zn	
$\gamma\pi$ Granite porphyry			
γ_5^3 Yanshanian granite	Greisenization, alkaline metasomatism	Nb, Ta, W, Sn	107, 102
γ_5^2 Yanshanian granite		W, Sn	162–141
γ_5^{2-2} Yanshanian granite			
γ_5^{2-1} Yanshanian granite		Skarn W, Sn	188–160 Ma
γ_5^{1-3} Indosinian granite			
γ_5^{1-2} Indosinian granite			
γ_5^{1-1} Indosinian granite			
VC_4 Hercynian granite and highwoodite			
$\eta\gamma_3$ Caledonian adamellite			
$\delta\gamma_3$ Caledonian granodiorite			
$M\gamma_3$ Caledonian migmatitic granite			

homonymous U ore field. This granite is emplaced in Middle Proterozoic (Pt_2^2) volcano-psammitic-pelitic metasediments upon which basically unmetamorphosed clastic sediments (Pt_3^1) locally with tuffaceous intercalations rest. Sinian-Silurian strata cover these units (for details see Sect. *Regional Geological Features of the South China U province*).

Principal Characteristics of U-Fertile Granites

Zhang Bangtong (1990) notes two varieties of U-fertile granites: S-(or transformation-)type and I-(or syntexis-)type granites. All economically significant U deposits in South China affiliate with S-type granites whereas I-type granites contain only small U deposits. The following description focuses on S-type granites and related U deposits.

Fertile U granite facies are of distinct petrographic-petrochemical nature referred to as “uranium ore-related (UOR) granites” by Zhou Weixun et al. (2003). Other granite facies produced W-Sn-Nb-Ta, Mo-Cu, or fluorine deposits. Although fertile U granites and W-Sn-Nb-Ta granites occur spatially close together, no economic W-Sn-Nb-Ta deposit is found in U granites and vice versa.

Most fertile U granites in SE China are of Mesozoic age and are known, e.g., from the *Guidong* (GD), *Zhuguang* (ZG), *Jiuyishan/Jinjiling* (JN), *Taoshan* (TS), and *Liuchen* (LC) batholiths (the LC granite is not necessarily considered a fertile granite

but rather to have played a role in the formation of close-by C-Si-pelite U deposits). Fertile U granites of Caledonian or Proterozoic age are scarce; the only ones known with U deposits are the Caledonian *Maoershan* (ME) and Xuefeng *Motianling* (MT) (also named *Sanfang*) polyphase granitic batholith at the SW edge of the Jiangnan Uplift (Fig. 1.27).

Du Letian et al. (1990), Zhang Bangtong (1990), and Zhou Weixun et al. (2003) note the following characteristics of Mesozoic U granites: They commonly occur in the form of multistage, highly differentiated batholiths with an exposed area in excess of 200 km², mostly of about 1 000 km² or more. Batholiths generally consist of main granitic bodies of Indosinian (Tr_3) and Early Yanshanian (J_{1-2}) age that contain xenoliths of Early Proterozoic intensely metamorphosed rocks and were mostly intruded into Sinian-Lower Paleozoic, weakly metamorphosed strata in long-term uplifted terrane. After an interlude of felsic volcanism during the Late Jurassic-Early Cretaceous, these batholiths were intruded by highly emplaced, small granite bodies during Late Yanshanian (J_3 -K) time, and felsic to mafic dikes. Contact-metamorphic aureoles, 1–2 km or more wide, surround the granitic bodies.

The *main intrusion* is formed by coarse-grained to porphyritic biotite or two-mica granite, rarely by K-feldspar granite or adamellite. Mineralogically, these facies are characterized by 35% or more, locally as much as 90% K-feldspar (mainly microcline); 0.8% to 8.5% biotite (Fe-rich biotite and siderophyllite), and zero to 5.6% muscovite. Muscovite tends to be of magmatic and

autometamorphic origin as well. Accessory minerals usually total less than 0.1% among which uraninite often exceeds 5 ppm and zircon up to 150 ppm; the latter often contains more than 0.2% U. Petrochemically, these granites are of peraluminous (12.5–14% Al_2O_3), high silica (68–75% SiO_2), and alkaline (7–9% $\text{K}_2\text{O}+\text{Na}_2\text{O}$, $\text{K} > \text{Na}$) nature. REE tenors are relatively low (>250 ppm); Ce/Yb ratios vary over a large range (5.9–87.0). Initial $^{87}\text{Sr}/^{86}\text{Sr}$ ratios are >0.710 suggesting an anatectic crustal origin.

U background figures range from 10 to 30 ppm and average 11.6 ppm in large massifs but are as low as 4 ppm in small granitic intrusions while Th/U ratios are about 3.49 and are almost the same everywhere independent of massif size. Th/U ratios decrease in polyphase granitic batholiths from early granitic intrusions to less than 2.0 in the latest stages indicating a relative increase of U in late granites. Leach tests attest that commonly over 30% of the background U occurs in leachable form whereas that in non-UOR granites is less than 20%. These background figures and leaching properties of U testify that these S-type granites are fertile U granites.

Subsequent intrusions are mainly composed of medium- to fine-grained and fine-grained inequigranular biotite granites with initial $^{87}\text{Sr}/^{86}\text{Sr}$ values greater than 0.710 and uranium contents of up to 20 ppm. In a final (post-volcanic) stage, garnet- and/or tourmaline-enriched, fine-grained muscovite or two-mica granitic stocks were emplaced; all these facies have low uranium (4 ppm), low thorium (6 ppm) and low REE (30–42 ppm) tenors.

Airborne spectrometric data yield Th/U and U/K ratios between 2.28 and 3.70 and between 1.91×10^{-4} and 3.18×10^{-4} , respectively, for UOR granites, and distinctly different values for non-UOR granites (Th/U ~ 5.14, U/K ~ 1.03×10^{-4}).

Mylonite and fracture zones and abundant felsic to mafic dikes of several generations dissect the batholiths in variable directions. Felsic dikes include fine-grained granite, aplite, pegmatite, granoporphyry, and quartz porphyry, while mafic dikes include lamprophyre, diabase, dioritic porphyry, and syenite.

Impressive giant quartz dikes and silicified zones, tens to hundreds of meters wide and several kilometers to tens of kilometers long, accompanied by numerous subordinate quartz veins and silicification zones transect the U-fertile granites.

Principal Host Rock Alterations

U-hosting granites and surrounding country rocks exhibit a variety of pre-, syn-, and post-ore alteration phenomena. Mantle rocks of plutons are overprinted by contact-metamorphism in a halo 1–2 km and locally more in width.

Pre-ore alteration is marked by widespread autometamorphism, most notably alkaline metasomatism, reflected by authigenic K-feldspar and albite, damourite, chlorite (predominantly pennine), as well as silicification, and locally uralitization of diabase dikes. K-feldspathization is a dominant feature for granite with endogranitic U deposits. K-feldspar, mainly microcline, replaces plagioclase and quartz; associated desilicification resulted in porous granite. Albitization occurs concomitant with

K-feldspathization but also alone at perigranitic U deposits. Damouritization (hydromicazation) of K-feldspar produced minute, broken flakes of green-tinted sericite and illite. This transformation was accompanied by dissolution of magnetite and ilmenite and the appearance of dispersed pyrite.

Ore-related wall rock alteration adjacent to uraniferous veins includes silicification, chloritization, hydromicazation/sericitization, montmorillonitization, fluoritization, carbonatization, pyritization, and/or hematitization. Du Letian et al. (1990) note three stages of alteration: hydromicazation-pyritization, inter-layered montmorillonite-hydromicazation, and montmorillonitization. The alteration aureole is generally 2–3 m wide but can be wider in bulging cataclastic zones. According to Zhou Weixun et al. (2003), hematitization persists for several mm to several cm from uraniferous veins into wall rocks but may also occur, although rarely, in fractured granite. Although referred to as hematite, the Fe-oxide phase in most granitic-related U deposits tends to be hydrogoethite. It appears under the microscope as hair-like, flaky and colloidal hydrogoethite that discontinuously fills micro-fissures in rocks or individual minerals and coats or sprinkles surfaces of feldspar, particularly perthite, and other minerals as well. Damourite in wall rocks is idiomorphic lath-shaped and as such differs in habit from the broken flakes of pre-ore stage sericite in altered granite. Syn-ore chlorite is of chamosite composition as compared to pre-ore pennine. At some deposits, wall rock alteration exhibits zoning reflected, from an ore lode outwards, by a transition from hematitization to chloritization, pyritization, silicification, and to peripheral damouritization/sericitization.

Post-ore alteration includes silicification, fluoritization, and weak carbonatization.

Silicification of the various stages is reflected by eight phases of siliceous veins/veinlets (Table 1.7, 1.8), composed of

- *pre-ore*: white quartz vein/silicified rock
- *syn-ore*: reddish hematite-bearing microcrystalline quartz; white comb quartz with some pyrite; black microcrystalline quartz with powdery/colloidal pyrite; purplish black fluorite/black microcrystalline quartz; and red calcite/microcrystalline quartz
- *post-ore*: white banded chalcedony, and white comb-quartz with white fluorite and calcite

► Figure 1.30 provides characteristic geological, mineralogical, and geochemical features associated with U mineralized veins.

Principal Characteristics of U Mineralization Associated with S-Type Granite

Primary mineralization consists of pitchblende and minor coffinite associated with mainly Cu, Fe, Pb, and Zn sulfides. Sulfides constitute up to 10% of the total ore mineral quantity and include, in *intragranitic* deposits, pyrite, sphalerite, galena,

chalcopyrite, marcasite, nickeline, molybdenite, and pyrrhotite; this suite is complemented in *perigranitic* deposits by tennantite, bornite, chalcocite, millerite, linneite, cobaltite, and argentite. Gangue minerals make up about 90% of the ore and include quartz, fluorite, microcrystalline quartz, calcite, and dolomite.

Supergene mineralization is marked by uranophane, β -uranophane, autunite, meta-autunite, tyuyamunite, torbernite, metatorbernite, uranocircite, and black U products as well as azurite, chalcocite, covellite, goethite, malachite, opal, kaolinite, and illite.

Pitchblende exhibits colloidal habits. Red and black quartz, and purple/purplish black fluorite are fine- to microcrystalline; pyrite, galena, and sphalerite are colloidal or fine crystalline.

Admixtures of alteration minerals (K-feldspar, albite, chlorite, illite, hematite, etc.) and a few fragments or minerals of host rocks (feldspar, quartz, mica, calcite, dolomite, clay) complete the ore assemblage (Zhou Weixun et al. 2003).

Ore and gangue minerals are present in several generations (Table 1.8), e.g. quartz in six main generations Q1 to Q6 and two substages. The two quartz substages Q4-2 and Q5-1 also contain fluorite and form the two principal U mineralization stages. The size of quartz grains decreases gradually from the pre-ore stage Q1 (>3 mm) through the first post-ore stage Q5-2 (<0.01 mm) at a synchronous increase of U until stage Q5-1 (Du Letian et al. 1990).

Du Letian (1986) and Du Letian et al. (1990) discern three types of U mineralization (in successive order) associated with microcrystalline quartz, fluorite, and argillization or altered cataclastic type.

Microcrystalline quartz-type U mineralization consists of grey-black to pink veins composed of up to 95% microcrystalline quartz (0.01–0.1 mm) interspersed with altered granite fragments, disseminated colloidal pyrite, goethite, and pitchblende. U content is direct proportional to pyrite content and reciprocal to the grain size of quartz; the smaller the grains, the higher the U content. Uranium enrichments typically occur

at intersections of veins with lamprophyre or diabase dikes. Veins of this ore type are mostly located within Na- and K-metasomatized granite. Some veins of similar composition also occur in silicified shale, siliceous limestone, and dolomite distant from any granite.

Fluorite-type U mineralization occurs as veins or stockworks composed predominantly of compact, dark purple fluorite (0.05–1 mm), and finely disseminated metacolloidal pitchblende associated with pyrite and/or marcasite. The fluorite type is superimposed on the quartz type and tends to result in an enrichment of uranium. Fluorite-type deposits are particularly well developed in and adjacent to two-mica granites and volcanics, which are intensely altered by hydromicazation.

Argillization-type U mineralization is restricted to cataclastic zones strongly altered by hydromicazation and argillization. It consists of 0.01–0.5 mm wide quartz and/or fluorite veinlets with disseminated pitchblende and pyrite. U is also concentrated along cracks in feldspars, cleavage planes of biotite, around fine-grained sulfides such as pyrite and sphalerite, and adsorbed on clay minerals.

The argillization type is further partitioned into a red and a green variety based on the abundance of hematite. The *red variety* is located at shallower depth above an alteration boundary (presumably due to phreatic alteration/weathering) in biotite-poor rocks such as alkaline metasomatized granite whereas the *green variety* occurs typically below the alteration boundary in biotite- and chlorite-rich lithologies.

Li Tiangan et al. (1996) provide information on the mineralogy of “rich and poor ores” based upon investigations of deposits in several granitic massifs. Mineral assemblages of rich vein ore comprise: (1) comb-like quartz-pitchblende; (2) purple-black fluorite-grey-black microcrystalline quartz-pitchblende; (3) grey black microcrystalline quartz-pitchblende; (4) carbonate-pitchblende; (5) chlorite-pitchblende; (6) uranophane-uranium mica. Mineral assemblages/types of poor ore include red microcrystalline quartz-pitchblende, argillaceous, and alkali-metasomatite types.

Table 1.8.

South China, typification of quartz veins associated with granitic massifs (after Du Letian et al. 1990)

Mineralization stage	Quartz stage	Quartz habit	Size (mm)	Composition	Formation T (C°)	U (ppm)	Th/U
Post-ore	Q ₆	Comb.	Variable	SiO ₂ containing calcite, zeolite	<210	20	0.3
	Q ₅₋₂	Light, aphanitic	<0.01	SiO ₂ with kaolinite	<210	19	1.2
Syn-ore	Q ₅₋₁	Dark, aphanitic	<0.01	SiO ₂ with some light fluorite, kaolinite	160–300	146–8 190	0.07
	Q ₄₋₂	Dark, microcryst.	0.01–0.1	SiO ₂ with pyrite, black purple fluorite, hydrogoethite	160–300	52–5 110	0.05
Pre-ore	Q ₄₋₁	Light, microcryst.	<0.01–0.1	Pure SiO ₂	220–280	1–90	0.05
	Q ₃	Fine crystal.	0.1–1	Pure SiO ₂	220–280	4	0.3–0.8
	Q ₂	Medium	1–3	Pure SiO ₂	320–340	4	0.3–0.8
	Q ₁	Coarse cryst.	>3	Pure SiO ₂	320–340	4	0.3–0.8

In addition to U deposits, various granitic complexes in South China host W, Sn, Mo, Bi, Pb, Zn, Cu, Fe, and REE deposits.

Structural Setting and Granite-relationship of U Deposits

Based on the prevailing granite-related setting of U deposits, Zhou Weixun et al. (2003) differentiate two modes of granites (► Figs. 1.28, 1.29, 1.30):

1. Granites at which nearly all U deposits occur peripheral in (contact-meta-)sedimentary rocks without any major deposit located within the batholith (perigranitic subtype).
 2. Granites in which almost all U deposits occur endogranitic and only a few exogranitic controlled by faults that persist from the batholith into surrounding strata (intragranitic sub-type); mineral assemblages are of similar composition in both settings.
- *Perigranitic U deposits* commonly occur within the contact-metamorphic aureole of a batholith mostly of Yanshanian and possibly of Caledonian age. Deposits in the contact-metamorphic aureole of Yanshanian granites are exemplified by the *Ma'andu* deposit at the Liuchen granite, *Xiangcao* at the Jinjiling granite, and *Shabazi* at the Central Zhuguang granite. Examples of deposits related to Caledonian granite may be seen in the *Chanziping* and *Kuangshanjiao* deposits. Both are located between the Mao'ershan and Yuechengling Caledonian batholiths; the type attribution of these two deposits is not unanimous, however; although attributed by some geoscientists to the perigranitic type, others attribute them to the C-Si-pelite type (see Sect. 1.4.3: *Proterozoic-Paleozoic Terrane and Related C-Si-Pelite U deposits/Western U Metallogenic Domain*).

The related Yanshanian and also the Caledonian batholiths occupy the core of uplifted, weakly metamorphosed domes. Yanshanian igneous facies comprise granodiorite, quartz-monzonite, and monzonitic granite, or two-mica granite and tourmaline-biotite granite; the latter two evolved by metasomatism. Caledonian batholiths are dominated by Caledonian hornblende-monzonitic granite with small Indosinian biotite granite and Yanshanian two-mica granite intrusions.

Mineralization forms strata-discordant as well as -peneconcordant lodes controlled by faults and, locally, breccias within organic carbon- and/or pyrite-enriched "hard sandstone or dolomite" intercalated with "soft slate".

- *Intragranitic U deposits* are preferentially located within large, multi-stage batholiths that contain xenoliths of intensely metamorphosed Proterozoic basement and other rocks; and, characteristically, many intragranitic deposits occur in these granites in the vicinity of down faulted redbed basins of Cretaceous-Eocene age. Occasionally, U veins persist from the granite into adjacent redbeds as, e.g. at the eastern edge of the Xinfengjiang Massif where veins extend from granite into Mesozoic redbeds of the Heyuan Basin. These

intragranitic U deposits consist either of macroscopic veins or disseminated mineralization in fracture zones in which ore is preferentially accumulated at the intersection of these structures with the contact of late, small granitic bodies or mafic dikes.

Vein mineralization consists of veinlets or stringers, from 1 mm to 10 cm in thickness that commonly cluster within reconsolidated fracture zones composed of silicified granite and fissures filled with pre-ore, coarse- or medium-grained quartz. Pitchblende, sulfides, microcrystalline quartz, fluorite, and calcite are essential ore components in veins but occur with variable dominance of one or the other mineral to form any aggregation between almost monomineralic and polymineralic assemblages. Some narrow veins constitute relatively high-grade pitchblende lodes due to a limited proportion of associated minerals.

Disseminated mineralization consists of minute particles and hair-fine stringers of pitchblende and metallic minerals (mainly pyrite) that occur within gangue minerals scattered over a relative wide range of broken rock. Pitchblende ranges in grain-size from 0.05 to 0.5 mm. Disseminated mineralization is controlled by sets of parallel orientated fractures or breccias which are enveloped by a halo of intense metasomatic and hydrothermal alteration, (K-feldspathization, albitization, muscovitization, greisenization, silicification, chloritization, illitization, and hematitization). Disseminated ore is generally of low grade. It occasionally constitutes independent ore lodes but more often borders uraniferous veins (Zhou Weixun et al. 2003).

General Shape and Dimensions of Deposits

Veins are commonly few centimeters to about 1 m and locally more thick, extend laterally and vertically from several meters to some hundreds of meters, dip mostly medium steep to vertical, and persist over depth intervals between 300 and 700 m. U distribution in veins is unpredictable as reflected by grades ranging from about 50 ppm to a few percent U with an average between 0.1 and 0.2% U. Veins often group to swarms or en echelon arranged zones and as such form sizable deposits with resources between some hundreds and 2 000 t U, rarely more.

Stable Isotopes and Fluid Inclusions

As estimated from oxygen isotope composition and crystallization temperatures of quartz, calcite, chlorite, and other gangue minerals, values of $\delta^{18}\text{O}$ (H_2O) vary between +13.9 and -10.6‰; values decrease gradually from early to late stage minerals. Fluid inclusions in quartz and fluorite from deposits #322 and 6 217, central-south Jiangxi granite belt, yield δD (H_2O) values from -50.4 to -66.5‰, and as such fall into the range of δD values of meteoric water of Mesozoic age (-50 to -70‰). $\delta^{34}\text{S}$ values from pyrite range over a broad span from -39.8 to +19.7‰, and the average $\delta^{34}\text{S}$ values from pyrite in ore and host rocks are similar indicating an in situ derivation of sulfur

for ore-associated pyrite. U and Pb isotope studies of samples from deposits #376, 380, and 6217 show very high initial $^{206}\text{Pb}/^{204}\text{Pb}$ ratios (19.56–34.85) documenting an enrichment of radiogenic Pb. Hence it is assumed that ore-forming substances including uranium originated from pre-existing uraniferous mineralization.

Homogenization temperatures of *fluid inclusions* in, and decrepitation tests on microcrystalline quartz, fluorite, and calcite yield pre-ore stage temperatures from 343 to 186°C with an average of 280°C; ore stage temperatures from 242 to 130°C, averaging 180°C; and post-ore stage temperatures from 200 to 50°C, averaging 130°C.

Ore-stage fluid inclusions from 8 deposits have salinities of 2.94–8.67 wt.-% while post-ore stage inclusions have lower salinities of zero to 3.05 wt.-%. Salinities of fluid inclusions in samples from the higher grade Dongken (#361) and Lanhe (#201) deposits, southern Zhuguang batholith, amount to 6.24 wt.-% and 8.67 wt.-%, respectively (Zhang Bangdong 1990).

In some contrast, Li Tiangang and Huang Zhizhang (1986) report for vein U deposits in the Xiazhuang ore field, Guidong granitic massif, that the salinity of ore solutions has been determined at 16–19 wt.-% and that inclusions with daughter minerals have a salinity of up to 23–30 wt.-%.

Based on the above given data, the pressure during ore formation was calculated at between 25 MPa and 66 MPa (250–660 bar) and during the post-ore stage at less than 30 MPa (300 bar). The first range may indicate a static pressure at depths of 1–2.5 km. The relatively low post-ore pressure is evidenced by comb textures of well-crystallized minerals in post-ore veins.

Gas phases of fluid inclusions consist mainly of CO_2 , CH_4 , CO, and H_2 ; CO_2 predominates, particularly in ore-stage inclusions. The liquid phase of ore-stage inclusions have higher Ca and Na and lower Mg and K contents; among anions concentrations, HCO_3^- is highest followed by F^- . U concentration is rather high, ranging from 8.7×10^{-4} to 4.6×10^{-3} mol kg^{-1} H_2O (Zhou Weixun et al. 2003).

Regional Geochronology

Although some uraniferous granitic plutons in the western part of the South China U province are of Proterozoic/Xuefeng (Sanfang/Motianling 845–688 Ma.) and Caledonian age (Maoershan), most granites with associated U deposits yield ages between 176 and 140 Ma i.e. they were intruded during the Yanshanian Orogeny and evolved by multiple intrusive stages as exemplified by Zhou Weixun et al. (2003) for the composite *Jiuyishan batholith*. This batholith comprises three major felsic magmatic stages: an early monzogranitic intrusion dated at 170 Ma/Middle Jurassic; an interim 156 Ma old volcanic dacite stage (Upper Jurassic); and a post-volcanic stage comprising 153 Ma old biotite granite, 150 Ma old subquartz porphyry, subgranitic porphyry, seriate-grained granite, and 140 Ma old granite porphyry (for details see Sect. 1.4.1.1.3: *Jiuyishan Granite Massif, S Hunan*).

Major intrusive bodies in the *Guidong Massif* yield ages of 196 Ma for two-mica granite in the eastern, 185 Ma for biotite granite in the southern, and 157 Ma for hornblende-biotite granite in the western part of the massif. In the eastern part of the massif (Xiazhuang OF), medium- to fine-grained granite with an age of 151 Ma is a last granitic phase of the pre-volcanic Jurassic intrusions (for details see Sect. 1.4.1.1.1: *Guidong Granite Massif, Xiazhuang Ore Field, N Guangdong*).

After an interlude of large-scale uplift and erosion, felsic volcanism (porphyroclastic lava and pyroclastic sediments) affected the region 143 Ma (K-Ar) ago.

Subsequent to this volcanic event, fine-grained granite and abundant intermediate to mafic dikes were intruded; they include in sequential order: Maofeng-type fine- or seriate-grained, phenocryst-bearing muscovitized biotite granite (143–138 Ma, K-Ar, Rb-Sr, U-Pb); WNW-ESE-striking diabase (140 Ma); Zhutongjian-type fine-grained, phenocryst-bearing muscovitized biotite granite, enriched in tourmaline and garnet (128–125 Ma); layered basalt (128.49 Ma); Zhushanxia-type bleached, fine-grained and isogranular two-mica granite; WNW-ESE-striking diabase (110–103 Ma); aplite and granite porphyry (90–88 Ma); and, finally, NNE-SSW-striking diabase porphyry and WNW-ESE andesitic porphyry dikes (90 Ma). Basalt and alkali basalt intercalated with continental redbeds in Cretaceous-Eocene basins yield an age range of 104–72 Ma (Zhou Weixun, pers. commun. 2003).

Five episodes of *U mineralization* are documented for deposits in the *Guidong* and *Zhuguang Massifs*: 138–130 Ma, 125–122 Ma, 104–95 Ma, 90–70 Ma, and 65–47 Ma, i.e. they correspond to Middle Yanshanian and Early Himalayan tectonic events (Zhou Weixun et al. 2003).

Principal Ore Controls and Recognition Criteria

Granite-related U deposits are structurally and lithologically controlled. The following parameters tend to be essential ore controlling or recognition criteria.

Host environment

- Peraluminous, highly differentiated, autometamorphosed leucogranite complexes containing xenoliths of Early Proterozoic metamorphics
- Granites with anomalous U tenor (>7 ppm), about 30% of the uranium is in leachable form
- Almost all granites with associated U deposits contain more than 5 g t^{-1} uraninite
- Exposed surface of granite massifs hosting U deposits is over 200 km^2 , and often about 1 000 km^2 or more
- U-hosting batholiths are marked by fault/fracture zones, abundant felsic to mafic dikes, major silicified zones, and giant quartz veins
- Quartz veins and silicified zones grade downward from continuous, solid silica masses into discontinuously silicified sections and then into altered fracture zones

- Younger veins are sometimes positioned at a lower level than older veins suggesting uplift of the region during the time of hydrothermal activity
- Elongated or irregularly shaped granite bodies tend to be more favorable hosts for intragranitic U veins
- Dome-shaped plutons are apparently less favorable for intragranitic veins supposedly due to almost absence of major faults, while perigranitic U veins may be present
- Preferential country rocks are uraniumiferous arenaceous and argillaceous sediments independent of age whereas carbonates and sequences interbedded with abundant mafic volcanics are unfavorable
- Sediments are only slightly metamorphosed (less than greenschist facies) and have high H₂O contents (>3%)
- Down faulted post-granitic basins or grabens filled with Cretaceous to Eocene redbeds and/or pyroclastic sediments commonly occur within or adjacent to U-hosting massifs

Alteration

- A multitude of variably intense alteration phenomena characterize U-hosting granites
- Pre-ore alteration features comprise widespread alkaline metasomatism (K-feldspathization, albitization), muscovitization of feldspars, and others
- Ore-related alteration includes silicification, fluoritization, sericitization, chloritization, argillization, pyritization, hematization
- Post-ore alteration includes fluoritization and carbonatization in addition to silicification

Mineralization

- Structural control is reflected by mineralization contained in veins and cataclastic argillaceous zones
- Simple mineralogy; principal ore components are essentially restricted to pitchblende, pyrite, and gangue minerals
- Several generations of ore and gangue minerals
- Metallic trace elements are similar in wall rocks and ore
- Three varieties of ore exist each is dominated by either microcrystalline quartz, fluorite, or argillaceous material
- Intragranitic veins are positioned
 - predominantly over a vertical interval from 300 to 1 000 m below surface
 - in blocks sandwiched between steeply dipping parallel faults
 - at the contact of varied granitic bodies, particularly of coarse-grained granite with fine-grained granite
 - at curvilinear faults
- Perigranitic veins are located
 - preferentially in the contact-metamorphic aureole, only locally beyond this aureole
 - occasionally in redbed sediments adjacent to granite
- U enrichments at intersections of veins with mafic dikes
- Later stage mineralization is positioned deeper than earlier stage mineralization in some deposits
- U deposits distribution tends to be restricted to granite in the vicinity of Cretaceous redbed basins

Metallogenetic Concepts

Various metallogenetic concepts have been forwarded for the evolution of vein-type U deposits associated with S-type granites. They range from supergene considerations, based on the coincidence of mineralization ages with the time of redbed sedimentation, to (residual) magmatic hydrothermal models, or a combination of both (see also chapters on metallogenetic aspects in description of ore fields and deposits).

Du Letian et al. (1990) present a model that involves the following string of uranium enrichment stages from natal sedimentation to the final concretion of deposits:

1. Syn- or post-sedimentary accumulation of U in clastic strata
2. Subduction of these sediments into the sphere of anatexis to form a granitic magma with pre-concentrated U [Zhang Bangdong (1990) concludes from petrochemical data, metasediments of the Proterozoic Sibao and Banxi groups to be the protoliths for S-type granite]
3. Intrusion and metasomatism/autometamorphism of granite with enrichment of U in metasomatized zones, and
4. Postmagmatic hydrothermal processes involving meteoric waters to form ore-bearing veins

In such a system, uraniumiferous granites and surrounding (meta-)sediments serve as sources of uranium. Deep reaching fault zones provided pathways for fluid migration. Dispersed uranium was leached from these source rocks as was silica and fluorine and transported by solutions of mainly meteoric origin as indicated by stable isotope values (Zhang Bangdong 1990). Solutions were generally Si-rich, as documented by the presence of six main stages (Q₁ to Q₆) and two substages of quartz, but the actual U ore forming solutions (Q₄₋₂ and Q₅₋₁) also contained fluorine as reflected by quartz-fluorite-pitchblende paragenesis. These acidic solutions also caused wall rock alteration by hydro-micazation, montmorillonitization, and pyritization.

Ore-forming fluids were epithermal with temperatures decreasing from 280° to 150°C and a pressure of less than 1 000 bar suggesting ore deposition at a depth of several hundred to 2 000 m (Du Letian et al. 1990). Zhang Bangdong (1990) arrives at somewhat lower temperatures of 200 to 100°C, and favors radiogenic heat sources to have mobilized the hydrogenic system.

In summary, Du Letian et al. (1990) suggest that in a first stage, quartz veins containing W, Sn, Mo, Bi, Cu, Pb and/or Zn mineralization were generated by alkaline metasomatic hydrothermal systems derived from mantle ichor ascending through the magma (the authors note 188–160 Ma for W-Sn skarn mineralization, 162–141 Ma for W-Sn, and 107 Ma and 102 Ma for Nb, Ta, W, Sn mineralization). Subsequently, U quartz veins were formed by mantle ichor that ascended along deep reaching faults and leached U and Si on their way through the granite. The formation time for most of the vein U deposits was during a taphrogenic event and coeval in time and space with Late Cretaceous deposition of continental redbed facies. A final supergene overprint appears to have caused some U redistribution and perhaps a further U enrichment in some deposits.

Based on geochronological data particularly from granite-related U deposits in the Guidong and Zhuguang Massifs, Zhou Weixun et al. (2003) postulate tentatively two time spans of U formation both posterior to the regional erosional and volcanic interlude; the earlier metallogenetic interval took place 138–95 Ma ago during the time of later stage granitic intrusions and the later interval occurred after this intrusive activity had terminated 100–90 Ma ago.

The *earlier interval* is evidenced by three episodes of U concentration each of which emanated subsequently to a magmatic event (see Sect. *Regional Geochronology* for details of intrusions). The *first* U episode at 138–130 Ma followed the intrusion of Maofeng-type granite (143–138 Ma) and WNW-ESE-oriented diabase dikes (140 Ma); the *second* U episode at 125–122 Ma succeeded the Zhutongjian-type granite (128–125 Ma) and extrusion of sheet-basalt (128.49 Ma); and the *third* U episode at 104–95 Ma occurred after emplacement of Zhushanxia-type granite and WNW-ESE-striking diabase dikes (110–103 Ma). These earlier U mineralization stages were closely controlled by ductile shear zones and associated with alkali feldspathization, hematitization, chloritization, and locally carbonatization. In essence, these metallogenetic processes are thought to be related to the mentioned granitic intrusive activities.

U mineralization of the *later interval* is spatially related to down faulted basins; it includes two, 90–70 Ma and 65–47 Ma old, generations that correspond approximately to the 5th and 6th phases of uraniferous siliceous veins. These veins are controlled by brittle fractures in silicified and damouritized rocks.

Zhou Weixun (1996) postulates a model that involves at least two ore-forming fundamentals for the generation of intragranitic U deposits:

- a Late magmatic hydrothermal processes for the earlier ore forming time span mentioned above. This concept involves residual, uraniferous fluids from a transitional magma chamber for each episode of granite intrusions after the felsic volcanic interlude; the uranium in fluids is of magmatic origin.
- b Supergene processes by meteoric waters for the later stage U mineralization. Meteoric waters extracted U from uraniferous granites and country rocks and then migrated downwards into depths where they mixed with hypogene fluids.

In earlier publications, Zhou Weixun has elaborated on the conditions that have presumably governed the younger metallogenetic episode. Critical components include: (1) U extraction from outcropping uraniferous granite by meteoric waters during favorable climatic conditions, i.e. during a (semi) arid climate as indicated by the Cretaceous-Eocene redbed sedimentation; (2) Migration of oxygenated uraniferous solutions from the granitic provenance area downward into the groundwater system; (3) Extensional tectonism concomitant with down-faulting of Cretaceous-Eocene basins created intense faulting, a high heat flow, and access to some deep-derived mineralizing and reducing components/agents. This system permitted a deep convective circulation of uraniferous meteoric waters that were heated and finally became uraniferous hydrothermal solutions; (4) Precipitation of uranium resulted from boiling of fluids triggered by pressure drop, and/or interaction with mafic dikes.

Selected Districts with Granite-Related U Deposits in South China

Significant U deposits associated with Mesozoic granites occur in the central to southeastern section of the South China U province in which they are essentially confined to granite massifs in the Nanling Magmatic Zone and in central Jiangxi (such as Taoshan GM) but a few deposits are also associated with Caledonian and Precambrian granites in the western South China U province (► Fig. 1.27).

1.4.1.1 Nanling Magmatic Belt, NE Guangxi to SW Fujiang

The Nanling Tectonic-Magmatic Belt/Nanling U zone extends sublatitudinally for some 600 km in E-W length and 50–150 km in width from NE Guangxi in the west through S Hunan, N Guangdong, and S Jiangxi to SW Fujiang in the east. The Nanling U zone may be subdivided into two subzones separated by the Yichun-Chenzhou fault (see Sect. *Regional Geological Features of the South China U province*): The *eastern subzone* is in the East Domain; it contains granitic massifs with related U deposits of only the intragranitic type; these granites were emplaced along regional faults. A few volcanic-related U deposits also occur in this subzone. The *western subzone* is in the West Domain and characterized by dome-shaped granitic plutons with both intragranitic and perigranitic U deposits.

Most granite-related U deposits in the Nanling Belt are associated with Mesozoic granites in the *Guidong* (GD), *Zhuguang* (ZG), *Jiuyishan/Jinjiling* (JN), and *Mao'ershan* (ME) batholiths (► Fig. 1.27). These batholiths also contain Caledonian granites, but Mesozoic granites predominate in the first three massifs whereas the main body of the *Mao'ershan* (ME) batholith consists of Caledonian granite with intrusions of small Mesozoic granitic bodies that host U deposits.

Additionally, a few vein-type U deposits are associated with the Precambrian *Motianling* (or *Sanfang*) granitic massif in the western extremity of the Nanling Belt; and a few small sandstone-type U deposits (as in the *Beimianshi* ore field, SE Jiangxi) occur in intermontane Mesozoic basins in the Nanling zone.

Zhou Weixun (2000) provides the following characteristics of the Nanling uranium zone.

Regional Geological Features of the Nanling Uranium Zone

The E-W-oriented Nanling Belt evolved in an intracontinental tectonic regime with widespread Caledonian granites. Xuefeng/Upper Proterozoic granites are confined to the westernmost extremity of the Nanling Belt. Tectonic-magmatic reactivation had affected the aforementioned eastern as well as western subzones during the Indosinian (Tr₃) and Yanshanian (J-K) orogenies. Caledonian granites were intensely denudated during the Indosinian Orogeny. Yanshanian felsic magmatism produced a series of composite granitic massifs including the Zhuguang,

Guidong, and Jiuyishan/Jinjiling batholiths located in the eastern and central part of the Nanling Belt along the borderlines of Hunan, Jiangxi, and Guangdong Provinces. These granitic massifs constitute the most prominent loci with intragranitic vein-type U deposits in China.

After uplift and exposure to the surface, these massifs experienced – in sequential order – an intrusion of diabase dike swarms, local eruption of felsic volcanics, and intrusion of high-seated granitic stocks during the Late Jurassic-Early Cretaceous. Subsequently, i.e. during the Late Cretaceous-Paleogene, basins were down dropped accompanied by the eruption of rhyolite and the effusion of basalt as basin-fill; while comagmatic dikes of granitic porphyrite, quartz porphyry-felsite, diabase porphyrite, and lamprophyre contemporaneously invaded the batholiths. (For geochronological data see Sect. *Regional Geochronology*.)

Intragranitic U deposits are preferentially hosted by Jurassic coarse- and/or medium-coarse grained biotite and two-mica granites. Alteration phenomena of these rocks include alkali feldspar metasomatism, silicification, sericitization, illitization, penninization, and montmorillonitization.

Intragranitic U deposits are commonly situated near Late Jurassic-Early Cretaceous high-seated small granitic bodies and/or Late Cretaceous-Paleogene basins and consist either of altered cataclastic zones or silicified fracture zones in which U is particularly concentrated at the intersection with mafic dikes.

Silicified fracture zone mineralization consists of veins and/or veinlets composed of reddish, hematite and hydrogoethite-bearing microcrystalline quartz, greyish-black microcrystalline quartz, black-purplish fluorite, calcite, pyrite, various sulfides, and pitchblende. There exists also a vein deposit in which uranium occurs only in the form of uranophane and autunite.

Altered cataclastic zones can be clay or alkali-feldspar altered; both varieties are transected by abundant micro-veinlets of and/or impregnated with pitchblende and/or coffinite, and locally uranium adsorbed on clay particles. Clay-altered cataclastic zones usually occur close to Late Cretaceous-Eocene down faulted red-bed basins. Alteration products include damourite (hydromica), chlorite, kaolinite, montmorillonite, and hematite; microcrystalline quartz, fine-grained fluorite, and pyrite are interspersed with micrograins of pitchblende and/or coffinite with some adsorbed uranium. Alkali-feldspar altered cataclastic zones typically occur in granite that is modified by K-feldspathization, hematitization, pyritization, chloritization, carbonatization, and clay alteration.

Ore bodies in intragranitic deposits can be of vein, lens, column, or nest configuration with dimensions ranging from 10 to 300 m in length, from 1 to 30 m in width, and depths between surface and 750 m. Mineralized depth intervals can range from 300 to 600 m.

Perigranitic vein-type U deposits occur mainly in the western Nanling zone. In this western area, granitic intrusions are often dome shaped and surrounded by a contact-metamorphic aureole, as much as 2 km wide, that has overprinted Lower Cambrian (meta-)sediments. Host rocks include carbonaceous biotite

sandstone, muscovite hornfels, and cordierite hornfels that are altered by silicification, chloritization, hematitization, hydromicazation, and carbonatization. Ore bodies are of stratiform lens or vein shape controlled by strata-peneconcordant intraformational and discordant fracture zones. Peneconcordant ore bodies have a length of 400–600 m and a thickness of 1.0–1.2 m. Strata-discordant lodes are several tens of meters long and locally as much as 8 m thick. Uranium exists mostly in the form of pitchblende, minor coffinite, and U⁶⁺ minerals contained in veins or veinlets of microcrystalline quartz, pyrite, and other sulfides. Mineralization is dated at 90–80 Ma and 50 Ma.

1.4.1.1.1 Guidong Granite Massif, Xiazhuang Ore Field, N Guangdong

The Guidong Massif is located in the SE Nanling Belt and the Xiazhuang (occasionally also referred to as Xiwang) ore field is situated in its eastern portion, in Wengyuan County, N Guangdong Province. The ore field, 320 km² in size, covers largely granitic terrane with some intermontane Mesozoic red-bed basins as well as peripheral Paleozoic metasedimentary terrane (Fig. 1.31). Original in situ resources were reported to be 12 000 t U (OECD-NEA/IAEA 1991, 2005).

About fifteen intragranitic U deposits are identified within the ore field including *Xiwang* (=Hope, #330), *Damaofeng* (331), *West Xinqiao* (*Xinjiao*) (332), *Zhushanxia* (333), *Zhaixia* (335), *Xiazhuang* (336), *Shituling* (337), *Xianrenzhang* (338), *Shijiaowei* (339) and *Zhutongjian*. Additional to these intragranitic deposits, the ore field also includes perigranitic deposits in metasediments including *East Xinqiao* (332).

First discoveries in the area date back to 1956 when two U occurrences were found in metasediments adjacent to the granite massif. One of the early occurrences (*Xiazhuang*) was associated with diabase dikes and proved to be a medium-size deposit. The first intragranitic deposit, *Xiwang*, was discovered in early 1958; it contained U in silicified fracture zones. With mining operations beginning in 1960, *Xiwang* became one of the first uranium mines in China.

Sources of information. Li Tiangang and Huang Zhizhang 1986; Shen Feng et al. 1992; Zhou Weixun pers. commun. 2003; unless otherwise cited.

Geological Setting of Mineralization

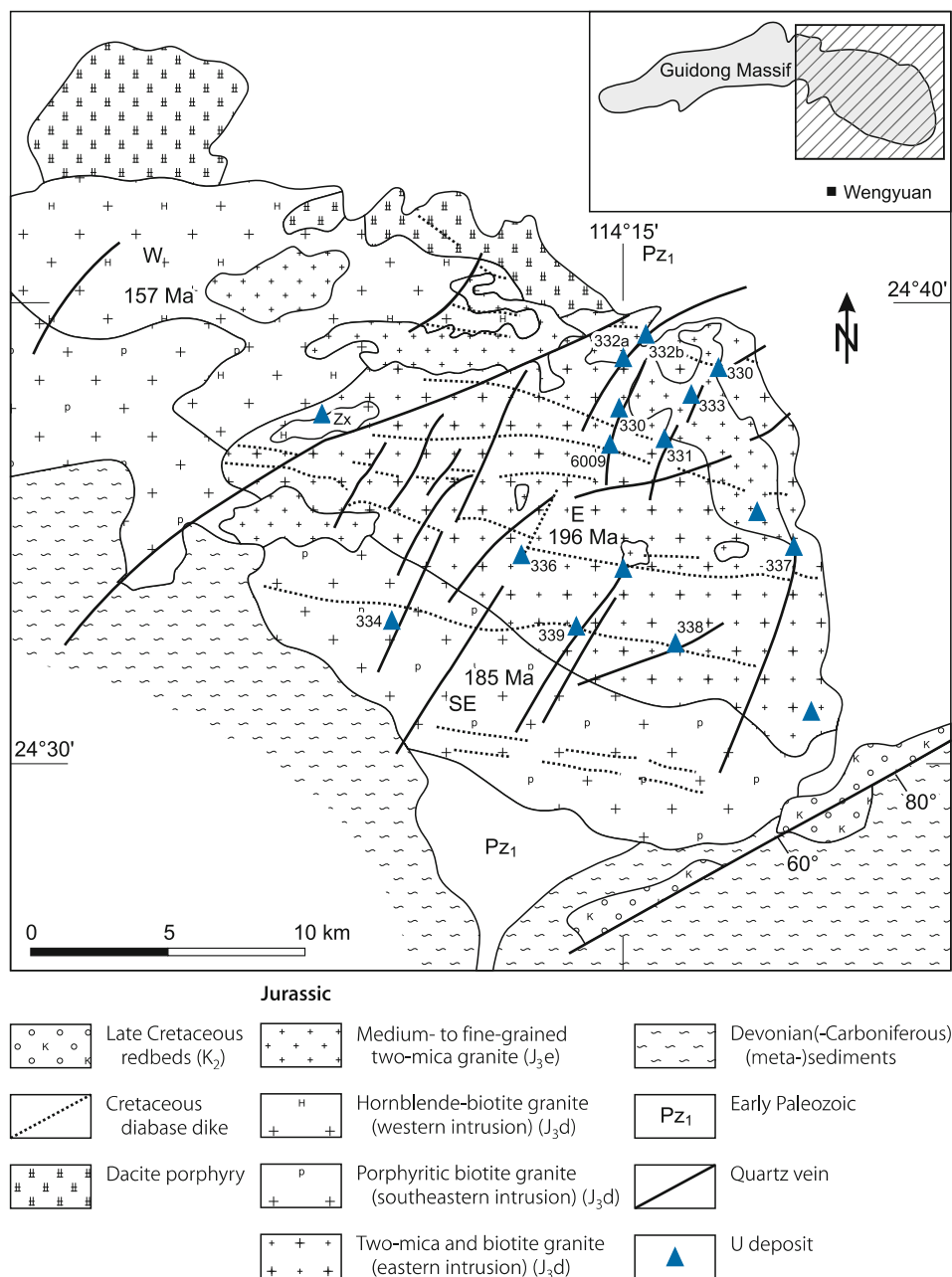
The polyphase granitic Guidong Massif is 68 km long, 12–18 km wide, and covers 1 000 km² at the intersection of the Cathaysian fold system with the Hunan-Guangxi fold system (or depression).

Cambrian and Ordovician strata prevail to the east and north of the massif while Devonian-Carboniferous strata prevail to the south and southwest. U tenors average 8–9 ppm U in Cambrian and Ordovician rocks and 5–13 ppm in Devonian and Carboniferous strata.

Several large Early Yanshanian granitic intrusions dominate the eastern Guidong Massif: *Xiazhuang*, an Early Jurassic

■ Fig. 1.31.

Guidong granitic massif, generalized geological map showing the various granite intrusions and location of U deposits (after Shen Feng et al. 1992 and Li Tiangang and Huang Zhizhang 1986). **Intragranitic U deposits:** *Xiwang* (= Hope, #330), *Damaofeng* (331), *West Xinqiao* (*Xinjiao*) (332a), *Zhushanxia* (333), *Zhaixia* (335), *Xiazhuang* (336), *Shituling* (337), *Xianrenzhang* (338), *Shijiaowei* (339) and *Zhutongjian* (Zx); **perigranitic deposits in metasediments** *East Xinqiao* (332b)



medium-grained two-mica granite (196 Ma) in the eastern section; Luxi, a Middle Jurassic coarse-grained porphyritic biotite granite (185 Ma) in the southeastern section; and Aizi, a Late Jurassic medium-coarse-grained hornblende-biotite granite body (157 Ma) in the western section. The relatively large Siqian pluton with medium- to fine-grained granite (151 Ma) is the last of the pre-volcanic Jurassic intrusions. A subvolcanic dacite porphyry belt (143–119 Ma) straddles the northern margin of the massif.

The first eruptions of felsic volcanism occurred in the Guidong Massif in Late Jurassic-Early Cretaceous (143 Ma); they produced granular porphyroclastic lava, felsic porphyroclastic lava, and pyroclastic sediments in the Xiazhuang ore field (Liu Ruzhou et al. 1995 in Zhou Weixun et al. 2003).

Later felsic intrusions include small stocks of fine-grained two-mica or muscovite granites (143–125 Ma) and pegmatite and aplite dikes. The latter two are ubiquitous but concentrate near the late granite stocks. Several generations of mafic and

intermediate dikes (140–90 Ma) consist predominantly of diabase with minor lamprophyre/spessartite and microdiorite (for more data see previous Sect. *Regional Geochronology ...*). These dikes as well as subsequently formed quartz veins, silicified structures, and faults are almost exclusively confined to the Xiazhuang and Luxi plutons.

In response to *block faulting* during the Late Cretaceous, the easterly granite segment was uplifted and exposed to erosion, before it subsided again accompanied locally by down faulting of some redbed basins.

Two major, more or less silicified fault zones, F1 and F2, some 20 km apart, limit the subsided block to the north and south. These two faults are ENE-WSW-oriented, steeply SE inclined, more than 50 km long, and several tens of meters wide. The southern fault controls Cretaceous-Tertiary basins on its footwall side.

The internal structural pattern of the subsided block is marked by three fault and fracture systems, oriented NNE-SSW, ENE-WSW, and ESE-WNW. Structures are several hundreds of meters to several kilometers in length and composed of brittle fault and breccia zones, silicified mylonite, silicified cataclastite with hydromicas, coarse- to fine-grained white quartz, variably colored microquartz, and fluorite.

The *Xiazhuang ore field* is located within this subsided block in which U deposits show a preference for the Xiazhuang granite. Prominent litho-structural elements in the ore field include: (a) five WNW-ESE-trending diabase dike swarms that are roughly equidistant from each other, some 3.5 km apart; individual dikes range in width from 2 to 10 m, locally to 100 m, and persist downdip in excess of 500 m; (b) five swarms of NNE-SSW oriented, silicified fracture zones composed of microquartz; (c) ESE-WNW and ENE-WSW-striking silicified fracture zones; and (d) two regional ENE-WSW-trending giant quartz veins.

Host rocks include various granites and intermediate to mafic dikes among which medium-grained, porphyritic two-mica granite of the Xiazhuang intrusion and lamprophyre/spessartite dikes belong to the most favored host facies according to Li Tiangang and Huang Zhizhang (1986). These authors describe the *two-mica granite* as a silica-, potassium-rich, and aluminum oversaturated acidic rock, mineralogically composed of 25.3% felsic plagioclase, 32.9% microcline, 33.5% quartz, 4.8% biotite, and 3.5% muscovite. Accessory minerals include apatite, zircon, pyrite, tourmaline, ilmenite, and uraninite. Uraninite occurs as intergranular grains between, and within the rock-forming minerals. Li Tiangang and Huang Zhizhang (1986) report a uraninite content in the granite of 6.3 g t^{-1} whereas Shen Feng et al. (1992) give a figure of 10 g t^{-1} .

Lamprophyre/spessartite is dark green, has an equigranular or porphyritic texture, and consists of 52.6% hornblende, 33.1% intermediate plagioclase, and 2.8% quartz. Accessories include apatite, ilmenite, epidote, and pyrite.

Host Rock Alterations

Large-scale metasomatism described as autometamorphism and, more restricted, allometamorphism affected the Xiazhuang two-mica granite and to some extent the Luxi porphyritic biotite

granite complexes. [Allometamorphism is defined by Li Tiangang and Huang Zhizhang (1986) as the recrystallization of minerals caused by younger intrusions within older igneous rocks; it is often associated with pegmatitization.] These metasomatized facies were later overprinted in the Xiazhuang ore field by syn-ore hydrothermal processes. Characteristic features of these rock modifications are addressed by Li Tiangang and Huang Zhizhang (1986) as follows.

- *Autometamorphism/metasomatism* is primarily reflected by K-feldspathization, albitization, and muscovitization; but tourmalinization and chloritization of biotite are also common features.
- *K-feldspathization* is an intense and widespread phenomenon documented by an increase of pink K-feldspar associated with chloritization of biotite, and a reduction of quartz, locally to zero.
- *Albitization* is reflected by fine-grained albite that crystallized later and is less widely distributed than K-feldspar. Locally, albitization forms relatively large metasomatic albite bodies, e.g. at the Zhushanxia U deposit.
- *Muscovitization* is a feature in the main granite body as well as in later, small intrusive bodies. Muscovite can be of autometamorphic, allometamorphic, or hydrothermal origin; and all three derivatives can be superimposed on each other. Autometamorphic muscovite replaces mainly biotite and, to a lesser degree, plagioclase on a regional scale. Allometamorphic muscovite occurs sporadically in larger flakes; the size of which decrease with distance from the intrusive body. Muscovitization caused by hydrothermal activity occurs together with silicification along faults and veins.

Autometamorphism and allometamorphism not only recrystallized the main rock constituents of the granites but also affected and decreased the quantity of uraniferous accessory minerals such as zircon, allanite, apatite, and xenotime.

Syn-ore hydrothermal alteration of wall rocks adjacent to a vein (vein is defined as a silicified zone of microquartz) is superimposed on autometamorphosed and allometamorphosed facies; the composition of these precursor facies had an impact on the intensity of alteration, mineral assemblage, and localization of U mineralization.

Veins in medium-grained porphyritic *two-mica granite* are fringed by wall rocks altered by silicification-hematitization and more extensively by argillization-pyritization. Argillization is reflected by the formation of hydromica and finally montmorillonite as a result of decomposition of plagioclase.

These alteration assemblages exhibit a lateral zoning that extends with decreasing intensity for a few meters from a central, ore hosting breccia zone cemented by fine- and microcrystalline, dark and pink quartz, into silicified, hematitized, hydromicatized, and pyritized cataclastic wall rocks. Silicification and hematitization are commonly most prominent close to ore bodies. The amount of hydromica and associated pyrite decreases with distance from the ore veins; hydromica changes from a long platy into a fragmental habit and turns in color from dark green to yellow-green. Weakly altered granite at the periphery of the alteration halo turns bright grey.

Wall rocks of veins in *lamprophyre/spessartite* may be altered by a quartz-hematite-hydromica, quartz-hydromica, and/or a chlorite-carbonate association. The quartz-hematite-hydromica association shows a pronounced zoning pattern particularly at the intersection of silicified zones, reflected by (a) an inner, partly ore-bearing zone, 0.1–0.2 m wide, of cataclastic, strongly altered and hematite stained rock, in which the original rock texture is destroyed and constituents are completely replaced by quartz, hydromica, and minor daphnite; (b) an intermediate zone, about 2 m wide, of weak silicification, hematitization, hydromicization but increased daphnitization; and (c) an outer, green or grey-green zone of chloritization and uralitization (Li Tiangang and Huang Zhizhang 1986).

Mineralization

Li Tiangang and Huang Zhizhang (1986) note three principal hydrothermal mineral stages:

Pre-ore stage: white, fine-grained quartz, from 0.1 to 1 mm in grain size, contains 1–10 ppm U; it commonly occurs in the form of breccia and fragmented relics in silicified zones.

Syn-ore stage: red or black microcrystalline quartz-pitchblende constitutes the main ore stage. The quartz, 0.01–0.1 mm in grain size, encloses clay minerals, sulfides, and hematite. The uranium content is highly variable ranging from several tens to thousands of ppm. Three mineral assemblages are identified in this stage:

- Red microcrystalline quartz, pitchblende, and coffinite form a widely distributed assemblage and represent the principal generation of mineralization;
- black microcrystalline quartz, pitchblende, coffinite, and sulfides also form a common but, compared with the previous one, a less well developed assemblage that evolved by thorough reworking and concentration of U; and a
- late, dark purple fluorite, pitchblende (locally with minor calcite) assemblage of more limited distribution and lower intensity than the previous two.

Pitchblende occurs disseminated or as massive, warty aggregates. Colloidal textures are common. Massive pitchblende is usually broken, veined and warty; disseminated pitchblende exhibits spheroidal habits and groups together in bands or cloudy accumulations. Coffinite is widespread but in minor quantities. It is younger than pitchblende and associates with marcasite. Coffinite commonly rims pitchblende and pyrite but also replaces and fills fine cracks in pitchblende. Platy and rhombic coffinite (about 0.01 mm in size) occurs locally within microcrystalline quartz.

Post-ore quartz-carbonate-fluorite stage: white comb quartz, banded microquartz, white calcite, and varicolored, but often dark purple fluorite. This stage may contain minor, low-grade uranium.

Mineralization is preferentially hosted in granite except for a few veins that extend from granite into Paleozoic metasediments as in the Xinqiao deposit.

Shape and Dimensions of Deposits – Ore Controls and Recognition Criteria

Ore bodies are of veinlike, lenticular, or columnar shape with stockwork structure. Ore bodies vary considerably in size, persist commonly over vertical intervals from 300 to 500 m, and have average grades between 0.1 and 0.5% U. Some deposits have surface exposures but most ore bodies are blind.

Position, configuration, and magnitude of intragranitic deposits and ore lodes are controlled by the following parameters or a combination thereof:

- primary control is by silicified fracture zones (▶ Fig. 1.32) that cut silicified granite, episyenite, diabase, and Lower Paleozoic carbonaceous sandstone
- segments of intense muscovitization and K-feldspathization within the main two-mica granite
- contacts between medium- to fine-grained two mica granite and late muscovite granite
- attitude of structures along the intrusive contact
- intersections of microquartz veins with intermediate to mafic dikes that cut alkali metasomatic rocks. (e.g. Shijiaowei deposit, ▶ Fig. 1.32a)
- en echelon arranged silicified zones; changes in strike and dip of silicified zones; and intersections of two or more silicified zones

In essence, the magnitude of any ore body and deposit is a function of the number of structural intersections; the size, attitude, and type of silicified and contact zones, and the size of dikes.

Shen Feng et al. (1992) provide additional details on unnamed U deposits of the following two structural settings:

- a Deposits located at the superimposition of WNW-ESE-trending silicified fracture zones and equally trending compressive structural zones (as thrusts) or blocks, which are sandwiched between diabase dikes and shear/mylonite zones, consist of ore bodies with an attitude similar to the WNW-ESE-trending compressive structural zones. The width of individual ore bodies ranges from 1 m to more than 10 m and the length can be up to 240 m. Ore grades vary depending on the nature of host rocks, ranging from 0.07 to 0.1% U in episyenite, from 0.1 to 0.17% U in silicified granite, and from 0.155 to 0.205% U in silicified diabase.
- b Deposits situated at the intersection of NNE-SSW-trending silicified fracture zones and WNW-ESE-oriented diabase dikes exhibit tabular or columnar shapes and often occur in swarms. Individual ore bodies are 1–3 m wide and 40–50 m long.

Metallogenetic Aspects

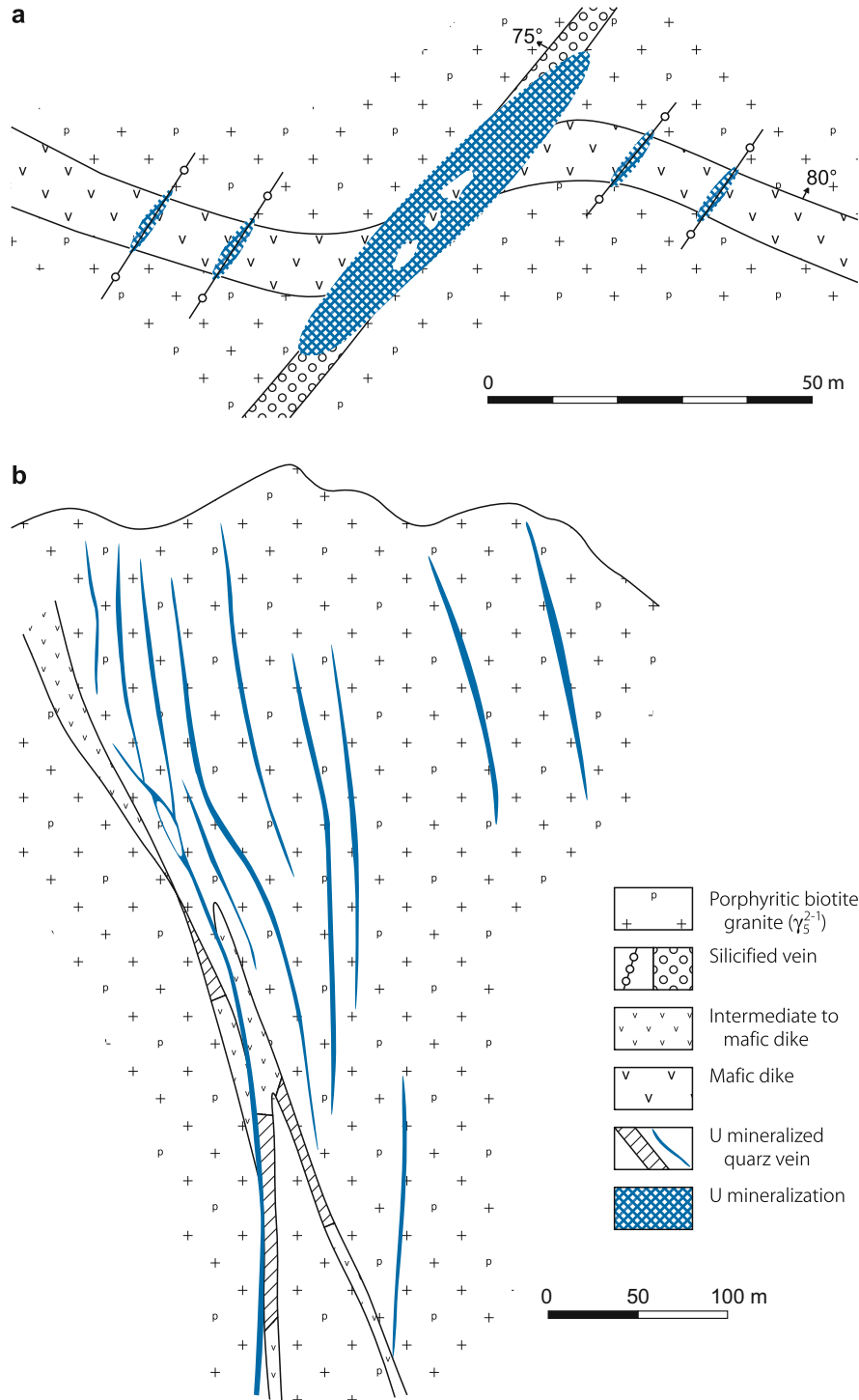
Li Tiangang and Huang Zhizhang (1986) address the metallogenesis of the Xiazhuang ore field and forward the following basic criteria in support of their model:

1. The period of major granite intrusions lasted from 185 to 135 Ma whereas U ore formation took place from 85 to 70 Ma,

Fig. 1.32.

Guidong granitic massif, **a** sketch map of the Shijiaowei deposit illustrating the affinity of U mineralised intervals in quartz veins to a mafic dike. The size of the deposit is a function of dike intersections, size and mode of silicified veins, and thickness of the dike.

b Cross-section of the Zhushanxia deposit showing the position of U quartz veins within and in the hanging wall of intermediate-mafic dikes (after Li Tiangang and Huang Zhizhang 1986)



- i.e. after a time gap of at least 50 Ma. This hiatus distinctly exceeds the time required for consolidation of the granite massif. Consequently, uranium and hydrothermal solutions could not have derived directly by magmatic differentiation; instead consolidated, anatectic granite with 10–27 ppm U (and a uraninite content of up to several g t^{-1}) have to be considered the actual U source.
- U deposits occur adjacent to small leucocratic stocks and intermediate to mafic dikes within a down faulted zone that resulted from tension stress within the continental crust. These late tectonic-magmatic activities initiated hydrothermal systems by generation of pathways for meteoric water to descend into depths where it was heated and became a critical ingredient for the metallogenesis.
 - Fluid inclusion data indicate mineralizing processes under decreasing temperature and pressure conditions, boiling of mineralizing solutions, and a significant escape of gas from such solutions as deduced from the following research results:
 - Fluid inclusions in pre-ore quartz contains 40–70 vol.-% CO_2 . The gas phase is dominant but liquid CO_2 inclusions also exist. Other fluid inclusions contain complex hydrocarbons. Fluid inclusions with variable gas-liquid ratios coexist. Daughter minerals of KCl, NaCl, CaCO_3 , or NaCl and CaCO_3 are common in three-phase inclusions. Boiling homogenization temperatures show a high degree of variation. Fluid inclusions in post-ore minerals have a greater liquid fraction, some of which are also characteristic for boiling.
 - Homogenization temperatures are calculated at 320°C for pre-ore, 280–150°C for ore, and 80°C for post-ore stage inclusions. A gasification temperature of 320–260°C has been determined for both ore and post-ore stages. Mineral inclusions formed at this temperature interval can be homogenized to the gas phase.
 - Pressure calculations give values of 220–510 bar with an average of 400 bar for the pre-ore stage and 10–60 bar for the ore and post-ore stage.
 - Salinities of ore stage solutions amount to 16–19 wt.-%. Inclusions with daughter minerals have a salinity of up to 23–30 wt.-%, i.e. 300–1 000 times higher than that of ordinary ground water and young hot springs.
 - Ca^{2+} is the main cation with minor K^+ and Na^+ in fluid inclusions in samples from two U deposits. HCO_3^- forms the largest anion fraction, followed by F^- , SO_4^{2-} and Cl^- . U contents in ore correlate with the CO_2 concentration in ore-stage fluid inclusions (correlation coefficient 0.824). These data are considered to provide circumstantial evidence, that carbonate-uranyl or fluorine-carbonate-uranyl complexes were probably the major transport medium for uranium in mineralizing solutions; and that these solutions were intermediate to weakly alkaline, became slightly acid during the ore stage, and turned alkaline in the post-ore stage. Ore formation proceeded in a transitional redox environment in which U was deposited at a slightly higher oxygen fugacity as attested by extensive hematitization in the vicinity of ore bodies.
 - All microcrystalline quartz veins contain Au and sulfides. Gold content correlates closely with U and S (correlation coefficient is 0.970 and 0.982, respectively). Gold in grey-black microcrystalline quartz can be as high as 295 ppb and exceeds that in medium-grained two mica granite (0.32 ppb) by more than 900 times; a fact that is explained by the authors to attest to hydrothermal solutions from a deep-seated source.
 - Stable isotope values of $\delta^{13}\text{C}$ vary between –6.99 and –7.89‰, i.e. they are close to the initial $\delta^{13}\text{C}$ values of –5 to –8‰ and reflect a deep source for the carbon. Pyrite in veins of various stages yields $\delta^{34}\text{S}$ values from –4.92 to –15.32‰. Since all these values are negative and tend to increase from older to younger veins, they are thought to evidence an evolution of hydrothermal solutions by deep circulation.

Pre-ore quartz yields $\delta^{18}\text{O}$ values between +1.52 and +8.5‰ with an average value of +7.2‰ ($n = 7$) while ore-stage red/gray/dark quartz yields an average value of +11.99‰ ($n = 7$).

The average δD (H_2O) values in the liquid phase of inclusions in pre-ore quartz ($n = 4$), ore-stage fluorite ($n = 4$) and post-ore light fluorite ($n = 2$) are –82‰, –65.5‰, and –74.5‰, respectively. The projection points fall into a transitional range between meteoric and magmatic waters in a $\delta^{18}\text{O}/\delta\text{D}$ diagram, and hence they suggest a mixed solution with predominance of meteoric water.

As a conclusion from the above listed parameters, Li Tiangang and Huang Zhizhang (1986) postulate, in synopsis, the following tectonic-hydrothermal model for U mineralization in the Xiazhuang ore field:

Specific granites with a significant background of U in the form of uraninite underwent autometamorphic modification prior to a large-scale subsidence under regional tensional stress. This tectonic regime generated deep reaching faults with a deep circulating hydrothermal system in which groundwater percolated downwards and then ascended after heating. Thermal solutions leached uranium and other components from granite during migration. Uranium was transported mainly as uranyl-carbonate and uranyl-fluorine-carbonate complexes, and possibly also as sulfate-uranyl complexes. A second fluid, derived from connate granite water and gases, was highly saline by accrued components leached from the granite on its migration path along faults. On its way upwards, this fluid entered into and intermingled with solutions of the groundwater-derived convection system. Gases and liquids from intermediate to basic magma chambers may have likewise become incorporated, however, in the hydrothermal system.

In response to intense brittle deformation at the ore stage, the hydrostatic pressure of the hydrothermal system decreased abruptly which caused boiling of the mineralizing solutions associated with release of a great amount of CO_2 and dissociation of uranyl-carbonate complexes. Silica began to precipitate and uranium was reduced by various reductants and crystallized as pitchblende together with SiO_2 .

Li Tiangang and Huang Zhizhang (1986) claim the drop in pressure to have played the dominant role in uranium precipitation, and they attribute only minor significance to temperature, pH, and Eh conditions since these parameters show only very small

changes during the ore-forming process. The authors also state, that intermediate-mafic dikes have played only a subordinate role in the location of U deposits, but may have caused an increase in mineralization grade.

Shen Feng et al. (1992) also point to the wide time gap between granitic intrusion and ore formation (the authors note an age of 135 Ma for muscovite granite as the latest product of felsic intrusions, 110–100 Ma for diabase dikes, and 86–60 Ma for ore formation in the Xiazhuang OF). Consequently, these authors also assume a provenance of the ore-forming uranium from consolidated uraniumiferous granite and not from magmatic differentiation. They provide evidence for this assumption by the high average U content of 20.2 ppm U at a Th/U ratio of about 1 in the Xiazhuang two-mica granite and by the fact that a large part of this U is bound in uraninite as reflected by an amount of 10 ppm uraninite in this facies. This uraninite has suffered dissolution; the U leaching rate is close to 60% of total U background in rocks. Lead-isotope analyses show a loss between 20 and 80% of uranium in the Xiazhuang granite compared with the calculated primary U content, consequently, the Xiazhuang granite body is considered a viable U source by the authors.

In some contrast to Li Tiangang and Huang Zhizhang (1986), Shen Feng et al. (1992) take also into consideration the intrusion of diabase dikes as a thermal source for heating deeply circulating solutions that are thought to have extracted uranium from granite and precipitated it at upper levels.

1.4.1.1.1.1 Xiwang Deposit, Guangdong

The Xiwang deposit (or Hope, #330) is located in Wengyuan County, Guangdong Province. It is an intragranitic deposit in the northeastern Guidong granitic massif. Original in situ resources were between 1 500–5 000 t U at grades of 0.1–0.3% U. The deposit was mined by underground methods.

Source of information. Zhou Weixun 2000.

Geology and Mineralization

Country rocks are dominated by Early Jurassic porphyritic, medium-grained biotite granite and Late Jurassic fine-grained muscovite granite that are cut by a swarm of WNW-ESE-trending diabase dikes. The deposit is associated with two NE-SW-trending and 60–80°NW-dipping silicified fracture zones, 280 m apart. Most ore lodes occur in the southeastern silicified zone, but some also occur in between the two zones at intersections with diabase dikes. Uraniferous veins are primarily composed of pink, microcrystalline quartz, colloidal pyrite, pitchblende, hydrogoethite, and hematite, and, to a minor degree, of greyish-black, microcrystalline quartz, fluorite, pyrite, marcasite, pitchblende, coffinite, and traces of Cu-, Pb-, and Zn-sulfides. Wall rocks are altered by silicification, hydromicazation, chloritization, and hematitization. Ore lodes exhibit vein, lens, and nest shapes of variable dimensions; a large lode measures more

than 200 m in length, over 20 m in thickness, and persists from surface for 300 m down dip.

1.4.1.1.2 Zhuguang Granite Massif, SE Hunan – SW Jiangxi – N Guangdong

The Zhuguang (or Zhuguanshan) polygranitic massif (6 140 km²) straddles in E-W direction the northern border of Guangdong Province with northward extensions into SW Jiangxi and SE Hunan. It includes several composite granitic batholiths including the Lujing, South Zhuguang, Central Zhuguang, and Longhuashan batholiths. Situated in the northeastern Nanling tectono-magmatic belt, the Zhuguang Massif is – besides the Guidong granite massif – the most prominent granitic complex in this belt with respect to granite-related U deposits.

Most deposits are grouped in four ore fields: three in the E-W-elongated Southeastern Zhuguang GM in N Guangdong, namely – from east to west – *Baishun*, *Changjiang*, and *Chengkou*, and the *Lujing OF* (termed Sanerer District by Min MZ et al. 1999) in the N-S-elongated Central Zhuguang GM in SW Jiangxi-SE Hunan.

There is also a *central-south Jiangxi granitic belt* postulated to cut across the Zhuguang GM but the position and extension of this belt are ill defined. Some geologists also include the Taoshan GM in central Jiangxi in this belt. Commonly, this belt is thought to be controlled by the NE extension of the Wuchuan-Sihui deep-seated fault, but it is still a question whether this fault strikes to N Guangdong and further into central-south Jiangxi. It also remains unclear as to where this belt intersects the Zhuguang GM, at the dumbbell-shaped central Zhuguang GM or at the Longhuashan batholith.

Sources of information. Pan Yongzheng and Zhang Jianxin 1996; Zhang Bangdong 1990; and Zhou Weixun 1997, pers. commun. 2003, 2006.

1.4.1.1.2.1 SE Zhuguang Granite Massif, N Guangdong

Deposits in the SE Zhuguang granite massif are concentrated between the towns of Nanxiong to the SE, and Tangdong and Changjiang to the NW in N Guangdong Province. U deposits are predominantly of intragranitic vein type while some deposits are hosted in adjacent redbed basins.

Three prominent ore fields with vein-type mineralization are delineated:

- *Baishun* in the Longhuashan area is the most significant ore field. It includes 5 intragranitic U deposits, of which *Dongkeng* (361) and *Lanhe* (201) are the most prominent in both grade and tonnage. These two were mined and are apparently depleted.
- The *Changjiang OF* consists of 5 U deposits and 2 occurrences including *Mianhuakeng* (305), which had a large tonnage but is now mined out.

■ Fig. 1.33a.

Southern Zhuguang granitic massif, simplified geological map with approximate distribution of Yanshanian to Caledonian intrusions and location of U ore fields and deposits (After Zhou Weixun pers. information 2006, selected and translated from Chinese literature; metamorphic core complexes according to Pan Yongzheng & Zhang Jianxin 1996)

[Metamorphic core complexes: FX Fuxi, LH Longhuashan, WG Waliogang

Ore fields (principal U deposits): I Chengtou (Tw Tangwan), II Changjiang (305 Mianhukuang), III Baishun (#201 Lanhe, 238 Zhongchun, 361 Dongkeng)]

Legend

Pg Paleogene, K₂ Upper Cretaceous, D Devonian, € Cambrian, Z Sinian

$\alpha\gamma_5^3$. Yanshanian fine-grained two-mica granite;

γ_5^{2-3} . Yanshanian fine-grained biotite granite;

γ_5^{2-2} . Yanshanian medium-grained two-mica granite;

γ_5^{2-1} . Yanshanian medium-/coarse-grained porphyritic biotite granite;

γ_5^{1-3} . Indosinian medium-grained two-mica granite;

$\eta\gamma_5^{1-2}$. Indosinian medium-coarse-grained porphyritic biotite monzonitic granite;

γ_5^{1-1} . Indosinian coarse-grained biotite granite;

γ_4^3 . Hercynian fine-grained biotite granite;

γ_4^2 . Hercynian medium-grained porphyritic granodiorite;

υE_4^1 . Hercynian mica-augite monzonite;

My_3^1 . Caledonian gneissoid/orbicular granite;

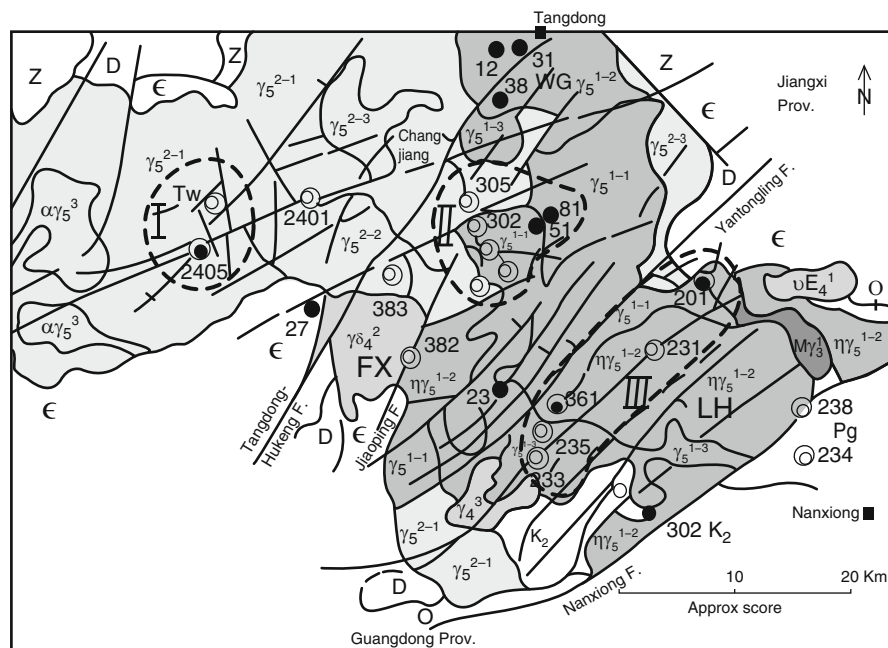
Fault/ fracture zone \pm silicified

⊙ Ore field

△ Uranium deposit;

▲ High-grade uranium deposit

▲ High-grade uranium occurrence



- The Chengtou (Chengke) OF, which includes the Tanwang deposit, is less important than the former two.

Additional U deposits and occurrences in the Southern Zhuguang GM include the Jiaoping (362) deposit with relatively high U grades.

In some contrast to the above delineation of the Baishun ore field, Pan Yongzheng and Zhang Jianxin (1996) define a Longhuashan ore field or area (named after the Longhuashan metamorphic-igneous complex in the eastern part of the southern Zhuguang GM) that encompasses the main (northern) part

of the Baishun OF with Dongkeng and Lanhe (see above) and the easterly adjacent Anquan-Shuiniukeng U mineralized area with Zhongchun (#238) and some other U deposits/occurrences.

Regional Geological Features of the SE Zhuguang GM

This southeastern segment of the Zhuguang granite massif is largely composed of Indosinian and Yanshanian granites but also of Hercynian and Caledonian adamellite, granodiorite,

migmatitic granite, with minor granite and highwoodite that were intruded into Early Paleozoic metamorphic rocks (► Fig. 1.33a).

The Tangdong-Hukeng and Nanxiong faults confine the SE part of the Zhuguang Massif to the NW and SE, respectively, where the principal U deposits occur. The *Tangdong-Hukeng fault* cuts through the Zhuguang granite massif with a length of 110 km and a width of 20–60 m, locally up to 160 m. It strikes NE-SW and dips 65–80° NW. Other NE-SW-trending mylonite or shear zones include the Gaodong, Nouweiling, Jiaoping, and Yantongling structures.

The *Nanxiong fault* strikes NE-SW for 140 km, dips 35–60° SE, and is composed of a silicified, quartz veined, mylonitized and/or fractured zone, from some tens of meters to more than 500 m wide. The Nanxiong fault separates the crystalline massif from the *Nanxiong Basin* to the SE. This basin extends for 120 km in a NE-SW direction and is filled with redbed sediments of the Middle-Upper Cretaceous Songshan and Nanxiong, and Paleogene Luofuzhai Formations, with a cumulative thickness of several 1 000 m. The strata dip gently NW in an imbricated pattern.

The southern Zhuguang Massif encompasses several heterogeneous complexes (referred to as “metamorphic core complexes” composed of Early Paleozoic metamorphics intruded by pre-Yanshanian, mainly Hercynian and Caledonian, igneous rocks that were or were not affected by Yanshanian intrusions.

The *Longhuashan heterogeneous complex*, 18 km long in a WNW direction, over 10 km wide, and covering an area of 200 km²; is the largest of these old complexes. Its northern margin is formed by the Lanhe-Fuzhu migmatite zone and the SE and NW boundaries by the Nanxiong and Yantongling faults, respectively. The

larger part of this complex is occupied by the Longhuashan igneous body with an outcrop of 147 km², oblong in a WNW direction and composed of greyish-white, medium-coarse-grained porphyritic biotite adamellite that contains large and abundant K-feldspar phenocrysts and shows some metasomatic effects. Isotope datings yield a Rb-Sr age of 371 Ma, a U-Pb age of 205 Ma, and a K-Ar age of 182 Ma for this intrusion, (i.e. it was probably intruded during the Caledonian Orogeny and was affected by Indosinian events; assuming that the ages can be verified).

The *Lanhe-Fuzhu migmatite zone*, 13 km in length and 1.5–3 km in width, extends in a NW to WNW direction from the Nanxiong to the Yantongling fault. Lithologies include biotite-migmatite gneiss and banded migmatite, at the marginal parts migmatitic quartz schist and slate with ferruginous quartzite; locally, migmatitic granite and gneissic granite (365–377 Ma). Diabase dikes, 108 Ma old, cut the massif.

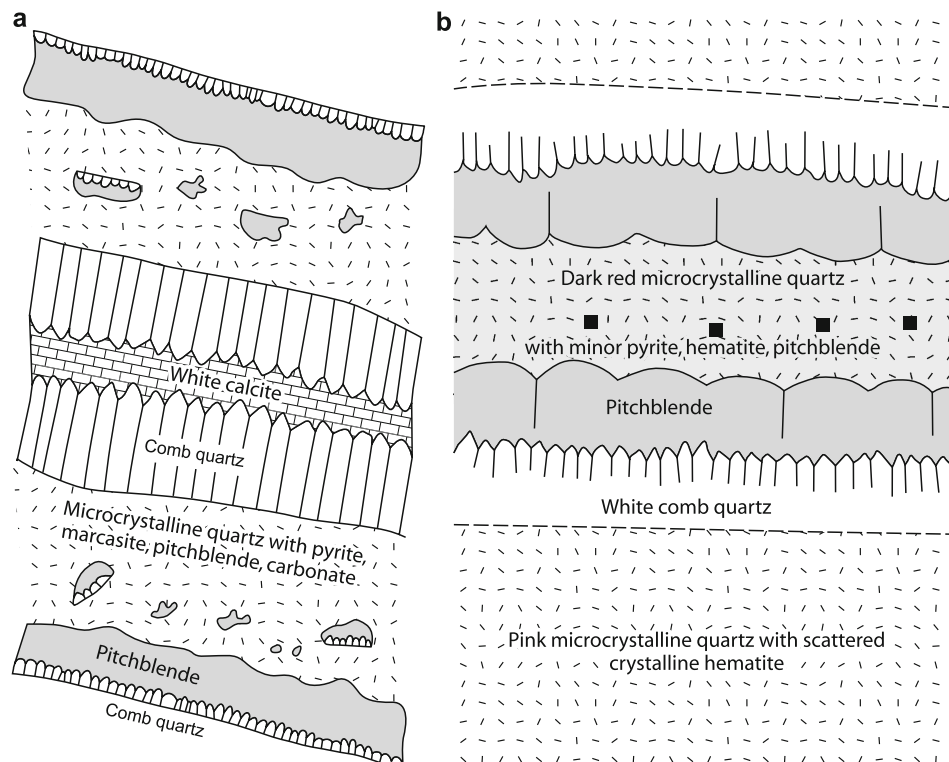
Other heterogeneous complexes to the east of the Tangdong fault include the *Waliaogang Complex* between the Tangdong, Gaodong, and Nouweiling faults; and the *Fuxi Complex* with the Hercynian Fuxi granodiorite body between the Hukeng and Jiaoping faults. The *Waliaogang Complex* is composed of Caledonian medium-coarse-grained adamellite intruded by the Yanshanian *Waliaogang granite*.

Geological Setting and Mineralization of U Deposits

Two types of mineralization locally termed red and black ore (► Fig. 1.33b) are noted in the Zhuguang Massif. Most U

■ Fig. 1.33.b.

Zhuguang granitic massif, mineral parageneses of quartz-pitchblende veins (approximate thickness from a few cm to 1 m) with **a** black (Lanhe/Baishun OF) and **b** red ore (Jiaoping/Changjiang OF) (after Li Tiangang et al. 1996)



deposits consist of “red ore”, and are exemplified by deposits in the *Changjiang* and *Chengkou* ore fields. Red ore occurs in simple veins controlled by silicified, high-angle, normal faults and consists largely of red microcrystalline quartz with U minerals (pitchblende), hematite, and locally pyrite. This ore type accounts for the bulk of proven resources but is of low/ordinary grade.

“Black ore” characteristically comprises greyish-black microcrystalline quartz, purplish-black fluorite, and pyrite with pronounced pitchblende concentrations. Some vein lodes are completely composed of comb-quartz-pitchblende ore with grades of 0.3–0.5% U. Typically major ore bodies have a breccia or stockwork structure with a relatively high-grade core enveloped in lower grade mineralization. This type is only known from a few but relatively large and high-grade deposits including *Lanhe*, *Dongkeng*, and the western part of *Zhongchun*. These three “black ore” deposits are located in the vicinity of intensely deformed, highly strained or plastic flow structures such as ductile shear, mylonite, and schistose/gneissic migmatite zones at the margin of the Longhuashan Complex.

Lanhe (201) occurs to the north of the Longhuashan Complex; 400 m off the Lanhe-Fuzhu gneissic migmatite zone, which is thought to be possibly an old ductile shear zone. Ore lodes consist of a system of comb quartz-pitchblende veins controlled by about N-S-oriented subsidiary structures that branch off to the N from a NW-SE fault (Fig. 1.29). Ore is hosted by adamellite adjacent to Yanshanian fine-grained biotite granite.

Dongkeng (351) is located to the SW of the Longhuashan Complex. U mineralization occurs in the footwall of a mylonite zone of the NE-SW-trending Yantongling fault and is hosted by cataclastic and brecciated, alkali metasomatized, medium-coarse-grained porphyritic biotite granite of Indosinian age. The

main ore body has the form of a large lens enveloped in a lower grade halo paralleling the mylonite structure (Fig. 1.29).

The *Zhongchun deposit* (238) is controlled by the Nanxiong silicified fault to the SE of the Longhuashan Complex. Ore lodes exist on both sides of this fault; they occur in brecciated and mylonitized alkali metasomatite in the western footwall of the Nanxiong fault, and in the form of low-grade mineralization in bleached Tertiary sandy conglomerate to the east of the fault (Fig. 1.33c).

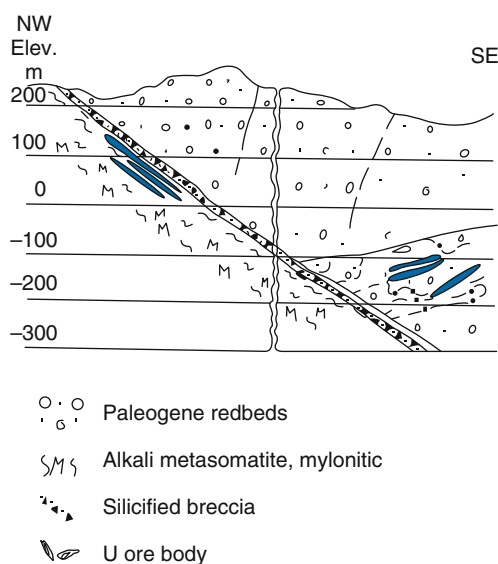
In summary, Pan Yongzheng and Zhang Jianxin (1996) propose that the Longhuashan heterogeneous complex and silicified border structures were formed by superimposition of brittle and plastic flow deformation, which was the main factors that controlled the distribution of large and high grade U deposits. U metallogenesis took place during down faulting of Mesozoic-Cenozoic basins.

Shallow brittle faults provided pathways for percolation of groundwater to form a circulation system of meteoric water with an oxidizing potential while plastic flow structures at depths offered conduits for ascending hydrothermal fluids with a reducing capacity. Interaction of these two solution systems formed a transitional redox zone. A high geothermal flux and high thermal gradient generated by Mesozoic-Cenozoic extensional tectonism heated descending meteoric water. This water extracted silica and uranium from granite on its way and precipitated the “red ores” in brittle, high-angle faults at the redox interface. Deep hydrothermal fluids extracted U and other elements from country rocks as they ascended, and “black ores” were formed where they contacted the redox front.

Horizontal zoning of black and red ores as seen by differential distribution in the southern Zhuguang Massif and particularly around the Longhuashan Complex would be compatible with such a model.

Fig. 1.33c.

Zhuguang granitic massif, Baishun/Longhuashan ore field, *Zhongchun deposit* (238), generalized NW-SE section. Ore bodies are controlled by a major mylonitic fault zone and occur in alkali metasomatite and structurally adjacent Paleogene redbeds. (After Pan Yongzheng & Zhang Jianxin 1996)



1.4.1.1.2.2 Lujing Ore Field, Huanfengling and Gaoxi Deposits, Jiangxi

The Lujing ore field is located in the N-S-elongated central Zhuguang granitic massif in southern Jiangxi Province and accounts for several granite-related vein U deposits (Fig. 1.34a): Lujing (#322; Lujing is Chinese for 322) with an intragranitic, major western part and a perigranitic, minor eastern section; intragranitic deposits include Huanfengling (325), Gaoxi (326), and Niuweiling (324); and the Shabazi (Shabon) deposit, which is largely hosted perigranitic in Lower Cambrian metasediments and partly in Indosinian and Yanshanian granites. Lujing is the largest deposit in the Lujing ore field.

Min MZ et al. (1999) refer to the Lujing ore field as *Sanerer U district* and provide a thorough presentation of a deposit what they call “Huangao” that was used for the following synopsis unless otherwise noted. (Note: “Huangao” is obviously an artificial name abbreviated from and referring to the two neighboring Huanfengling and Gaoxi deposits since there is no Huangao deposit in the Lujing OF. Occasionally, the term “Huangao District” is arbitrarily used for these two deposits because they occur close together, separated by a river. “Huangao” was discovered in the early 1960s and mined from the 1960s to 1970s.)

Regional Geology of the Lujing U Ore Field

The Lujing U ore field is largely underlain by the Mesozoic Lujing composite batholith (termed *Sanerer pluton* by Min MZ et al. 1999), about 120 km² in areal outcrop (see below), which is one of the plutons that form the central-southern Jiangxi granite/metallogenic belt within the dumbbell-shaped central Zhuguang granitic complex. This granite belt is controlled by the central Jiangxi lineament, which extends for about 240 km in NE-SW direction.

The polygranitic batholith was intruded into folded and weakly metamorphosed Precambrian and Cambrian carbonaceous shale, sandstone, and limestone (carbonaceous-siliceous pelites unit) of the Caledonian Cathaysian fold system. These strata were intensely contact-metamorphosed to hornfels, skarn, and marble by the granite intrusions. Cretaceous-Tertiary redbed sandstones and conglomerates, 400 m thick, fill a down-faulted basin 14 km² in areal extent in the center of the Lujing District.

Several NE-SW and NW-SE-oriented high angle fault and fracture zones composed of multiple individual faults transect the Lujing ore field. Fault zones are in excess of 10 km long, from 5 to 50 m wide, and consist of breccias cemented by medium- to coarse-grained quartz and fluorite.

The Lujing batholith comprises Indosinian granite intruded by two generations of Yanshanian granites:

1. Early Jurassic *Indosinian biotite granite* (for ages see Sect. *Regional Geochronology*) occupies most of the Lujing area and constitutes the main host of the Huangao deposit. Xenoliths of hornblende-plagioclase amphibolite and biotite-quartz schists are abundant in the granite. This granite is light to pinkish grey, exhibits a medium- to coarse-grained porphyritic fabric, and has an average modal composition of 30.6% quartz, 34.5% K-feldspar (perthitic microcline), 28.6%

plagioclase (oligoclase with minor interstitial albite), and 5.6% partially chloritized biotite. Accessory minerals include uraninite, uraniferous zircon and allanite, apatite, monazite, sphene, fluorite, magnetite, and ilmenite. Phenocrysts of microcline, perthite, and rare plagioclase make up 10–30% of the rock.

2. Middle Jurassic stocks of *Indosinian(-Yanshanian) medium-grained two-mica granite* occur in Indosinian biotite granite in the northern and southern district.
3. Late Jurassic *Yanshanian fine-grained porphyritic biotite granite* is present as small bodies in Indosinian biotite granite and is lithologically similar to this older granite.

Numerous dikes of diabase, lamprophyre, quartz porphyry, granophyric pegmatite, and porphyritic microgranite traverse the district.

Geology and Host Rock Alteration at Huangao

The “Huangao” deposit is situated in the eastern Lujing District near the SE margin of a Cretaceous-Tertiary redbed basin. Indosinian medium- to coarse-grained porphyritic biotite granite and, to a lesser extent, stocks of Yanshanian fine-grained porphyritic biotite granite provide the predominant host rocks. Major faults trend NE-SW and NNE-SSW. They control equally oriented, pre-ore alkali-metasomatized zones in granite, the position of the deposit as well as syn- to post-ore alteration phenomena.

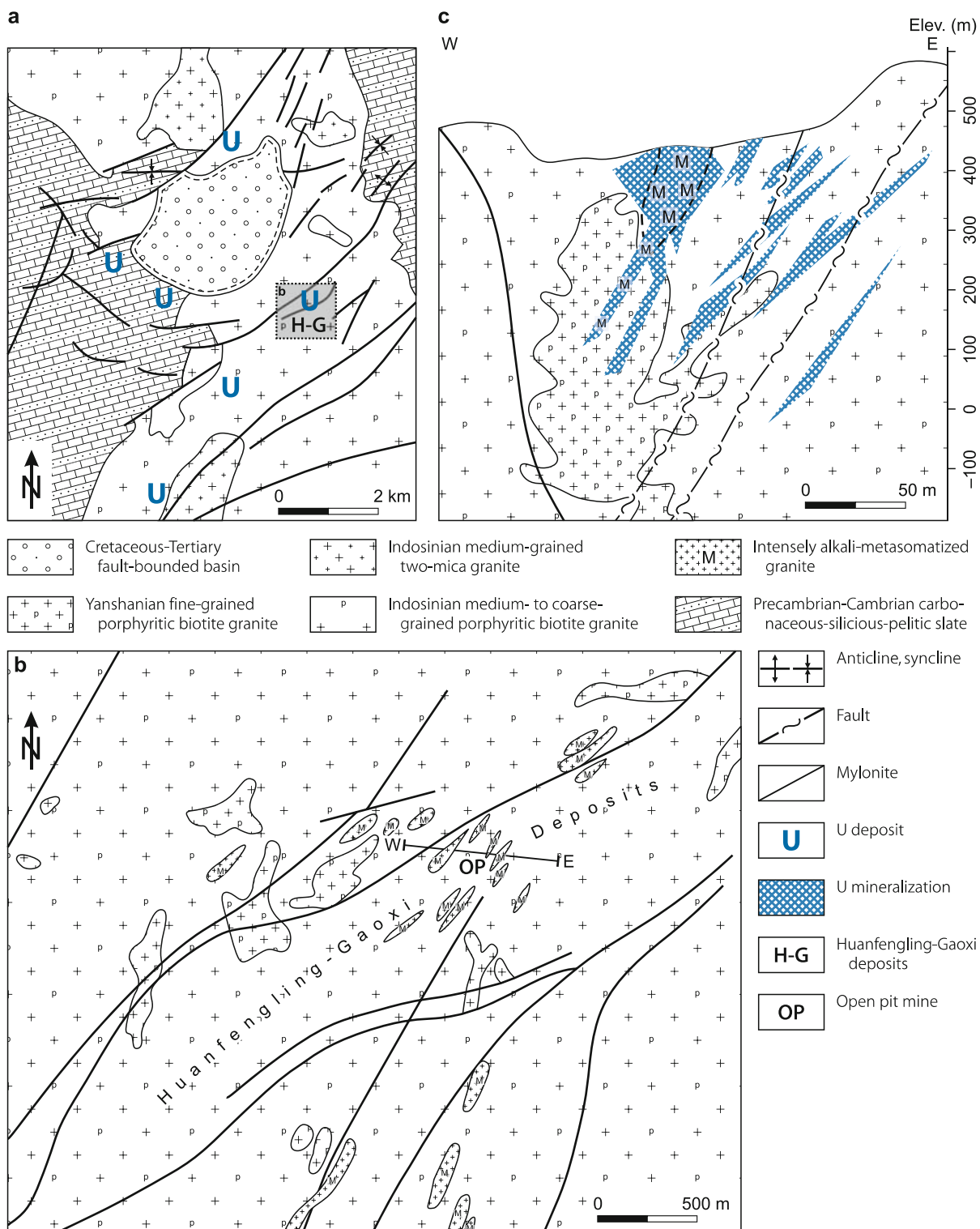
Alkali metasomatism is reflected by variably intense K-feldspathization, mainly microcline, and albitization that have modified narrow, irregular to linear zones from 0.5 to 10 m wide and up to 100 m long, that persist for a depth of at least 400 m. These metasomatized zones crosscut all granite varieties in terrane intruded by Yanshanian fine-grained granite and are commonly made up of an albite-rich core flanked by white or pink, albitized and K-feldspathized granite. Dissolution of quartz in metasomatized granite resulted in enhanced porosities (note: this dissolution tends to be related to metasomatism but the authors do not point out whether it really resulted from metasomatism or from hydrothermal activity).

Min MZ et al. (1999) report an age of 132 Ma for albitite and potassium-sodium-metasomatic granite and consider this age to reflect a time of alkali metasomatism closely following the intrusion of the Yanshanian biotite granite.

Ore-related alteration phenomena include hematite, pyrite, chlorite, silica, damourite, and carbonate that occur in narrow aureoles, 0.1–1.0 cm wide, along U mineralized veinlets but also disseminated in the host granites. Hematitization is most pronounced; it ranges from an early, slight reddening of feldspar in result of chloritization of biotite, to a distinct red color of the feldspar, particularly along microfractures. High-grade ore exhibits an increased degree of hematitization. Damourite replaces from 5 to 50% of feldspar crystals, particularly plagioclase. Chlorite replaces biotite and forms veinlets within fractures and breccias. Chloritization is accompanied by pyritization, silicification, and carbonatization throughout the deposit. Calcite occurs disseminated and as veins in the altered host rock; it was formed during pre-, syn-, and post-ore stages.

■ Fig. 1.34.

Zhuguang granitic massif, Lujing (Sanerer) ore field, **a** regional geological map with location of endo- and exogranitic U deposits; **b**, **c** Huanfengling-Gaoxi deposits, **b** geological map and **c** W-E section across a mineralized interval showing the intragranitic setting and configuration of ore bodies of this deposit (after Min M et al. 1999)



in width. Pitchblende garlands are frequent in microcrystalline quartz or coat sulfides. Galena grains occur in pitchblende or as isolated crystals in microcrystalline quartz.

- *Substage IV* is characterized by green and purple to black-purple fluorite veins, from 1 to 30 cm in width, with disseminated pitchblende, pyrite and minor galena, marcasite, hematite, sphalerite, calcite, and microcrystalline quartz.

Post-ore stage

- *Substage V* is dominated by comb quartz and calcite in veins and vugs with marcasite, hematite, and fluorite.
- *Substage VI* comprises U^{6+} minerals, essentially autunite, torbernite, and uranophane that coat joints of earlier minerals or impregnate pulverulent granite. Additional components include marcasite, hematite, goethite, and chlorite.

Shape and Dimensions of Deposits

The “Huangao” deposit consists of a number of ore lodes within a major, NE-SW-trending fault zone, up to about 1 000 m wide and several kilometers long, that is intersected by a NNE-SSW-oriented fault system. Ore lodes are preferentially controlled by intermediate to steeply NW-dipping splays or branches of the main faults along which they are confined to fractured and brecciated intervals within K-feldspathized and albitized granite on both sides of the interface between Indosinian biotite granite and Yanshanian granite stocks (► Figs. 1.34b,c). Veinlets of microcrystalline quartz, fluorite, pitchblende, pyrite, galena, and chlorite frequently crosscut the alkali-metasomatized granite.

Ore lodes are of lenticular, tabular, pod, or irregular shape in which pitchblende occurs disseminated or in veinlets along fractures, interstitially in granular minerals, and in the cement of breccias that mainly consist of finely crushed, metasomatized granite. Pitchblende veinlets range in width from 0.1 to 5.0 mm, rarely up to 2 cm, and disseminated pitchblende grains range from 0.01 to 1.0 mm in diameter.

Stable Isotopes and Fluid Inclusions

Initial $^{87}\text{Sr}/^{86}\text{Sr}$ ratios are 0.7229 in Indosinian biotite granite (Shen J 1991 in Min MZ et al. 1999), 0.7233 in Yanshanian fine-grained porphyritic biotite granite, and 0.7233 in K-Na-metasomatized granite including albitite. These values indicate a crustal origin of the granites and as such a definition as S-type granite.

Lead isotopic ratios of galena and pyrite separated from ore range from 19.2 to 25.0 for $^{206}\text{Pb}/^{204}\text{Pb}$ and 15.8–16.2 for $^{207}\text{Pb}/^{204}\text{Pb}$, and are clearly higher than respective values of 18.4–19.9 for $^{206}\text{Pb}/^{204}\text{Pb}$ and 15.7–15.9 for $^{207}\text{Pb}/^{204}\text{Pb}$ in K-feldspars (microcline, perthite) from the Indosinian and Yanshanian biotite granites. This relationship obviously excludes the granites as a Pb source for ore sulfides, i.e., the lead source for these sulfides must be much older than the granites. Additional support for this assumption is given by U-Pb isotope analyses; some pitchblende samples contain radiogenic lead that is apparently much older than the host granites, and hence this material must have derived from older basement rocks. Min MZ et al. (1999)

surmise the Precambrian-Cambrian carbonaceous-pelitic slates to be the most likely Pb source.

Sulfur isotope data of pre-ore pyrite yield a range of $\delta^{34}\text{S}$ values from -6.7 to 0.4‰ , with a mean of -1.3‰ . These values fall within the range of sulfur isotope values for the host granite [$\delta^{34}\text{S} = -12.4$ to 4.3‰ , mean -2.0‰ (Shen J 1991 in Min MZ et al. 1999)], which hints to the granite as the potential source for pyrite sulfur.

Pre-, syn-, and post-ore vein calcite have $\delta^{13}\text{C}$ values ranging from -8.3 to -6.3‰ (mean -7.1‰) and $\delta^{18}\text{O}$ values from -14.6 to -8.4‰ (mean -11.8‰). These low values are thought to result from isotopic exchange between the mineralizing solutions and granite ($\delta^{13}\text{C} = -18.2$ to 2.9‰), an interpretation also supported by -10.1 to -9.4‰ $\delta^{13}\text{C}$ values of fluid inclusions in syn- and post-ore vein quartz, i.e., similar to those of the host granite.

Oxygen and hydrogen isotope analyses from fluid inclusions in syn- and post-ore vein quartz give $\delta^{18}\text{O}$ values of 11.3 – 15.6‰ . Based on homogenization temperatures of 130 – 255°C for primary inclusions in syn- and post-ore quartz, calculated $\delta^{18}\text{O}_{(\text{H}_2\text{O})}$ values would be -4.0 to 3.6‰ for mineralizing solutions.

The $\delta^{18}\text{O}_{(\text{H}_2\text{O})}$ variation in these solutions is attributed to isotopes exchange between local meteoric water and the host granite ($\delta^{18}\text{O}_{\text{miner}} = 7.0$ – 9.3‰) [$\delta^{18}\text{O} = -8.0$ to -9.0‰ ; for meteoric water in Jiangxi Province during the time of ore formation (Zhang LG 1985, in Min MZ et al. 1999)]. ΔD values of fluid inclusions in syn- and post-ore vein quartz range from -81.3 to -56.6‰ and compare with δD values of local meteoric water during the time of ore formation. By plotting $\delta^{18}\text{O}$ versus δD values, the data points also fall into the meteoric water field, and consequently, Min MZ et al. (1999) assume that a meteoric provenance is most likely for mineralizing solutions.

Homogenization temperatures (T_h) of primary fluid inclusions vary between 200 and 260°C in pre-ore quartz, 120 and 247°C in syn-ore fluorite, and 100 and 140°C in post-ore calcite.

Salinity values in fluid inclusions range from 11.7 to 21.6 wt.-% NaCl equiv. (mean 15.2 wt.-%) in ore-stage fluorite, and from 0.7 to 5.8 wt.-% NaCl equiv. (mean 1.4 wt.-%) in post-ore calcite. The variation in salinity of fluid inclusions of similar T_h is interpreted by Min MZ et al. (1999) to result from mixing of ascending thermal solutions with descending meteoric waters.

Geochronology

Whole-rock Rb-Sr isochronal dating yields an age of 215 ± 6 Ma for Indosinian medium- to coarse-grained porphyritic biotite granite, 155.7 ± 4 Ma for Yanshanian fine-grained porphyritic biotite granite, and 132.1 ± 5.8 Ma for K-Na-metasomatized granite including albitite. A K-Ar age of 179 Ma was obtained from muscovite in Indosinian(-Yanshanian) medium-grained two-mica granite; and whole-rock K-Ar ages of 110.6 ± 4.0 and 105.1 ± 3.8 Ma for lamprophyre dikes (Du GS 1993, in Min MZ et al. 1999).

Pitchblende (4 samples) yields discordant U-Pb isotope ages of 103 Ma for one sample and 48 Ma for the other samples. The older sample has a low U content and contains many impurities

(fluorite, pyrite, quartz). Min MZ et al. (1999) consider the 103 Ma age as an approximate time of the earliest uranium generation. This assumption is supported by slightly older K-Ar ages of 123.5 ± 3.1 and 109.9 ± 3.3 Ma for two illite samples from hydrothermally altered Indosinian biotite granite at Huangao, which is in agreement with the slightly older to almost coeval textural relationship of vein illite in altered wall rocks with U mineralization.

The U-Pb isochronal age of 48 Ma is thought to reflect the most likely time for the main U mineralizing event. This age is in the time range with Early Himalayan (Early Tertiary) taphrogenesis that affected South China.

Metallogenetic Aspects

Min MZ et al. (1999) forward a model for the “Huangao” deposit that involves the following five metallogenetic stages:

1. *Preconcentration of uranium*: Isotope data suggest that granites in the Lujing District have evolved by anatexis of crustal protoliths, presumably from Precambrian-Cambrian carbonate-siliceous-pelitic slates. Such metasediments that outcrop in the district contain 11–30 ppm, locally in excess of 100 ppm U and represent a viable U source for the relatively high U background, in average 9 ppm U, in the granites.
2. *Deuteric U remobilization*: Extensive deuteric metasomatism affected the host granites after their consolidation and was caused by fluids expelled from oversaturated magma as indicated by oxygen isotope data. This process, denominated “green alteration” in China, includes chloritization of biotite, argillization of orthoclase and microcline, damouritization of oligoclase, and crystallization of albite. Most accessory mineral species (allanite, apatite, monazite, sphene, xenotime, zircon, etc.) were decomposed, and U and other metals liberated. Uranium recrystallized as micro-grained uraninite or pitchblende associated with some pyrite in cracks of rock-forming minerals in the altered granite.
3. *Supergene U remobilization*: In response to Early Tertiary (Himalayan) tectonism, the granitic complex was uplifted and exposed to erosion while the Lujing Basin was down faulted and filled with redbed sediments. The nature of these sediments suggests an arid climate at the time of deposition that facilitated remobilization of uranium and other elements by meteoric waters from weathered granites and metasediments including earlier formed micro-grained uraninite and pitchblende in metasomatized granites. These oxygenated waters carried uranium and other metallic elements, percolated down faults and became instrumental in ore formation some 48 Ma ago, i.e., during the Early Tertiary.
4. *Hydrothermal transport and enrichment of uranium*: Fertile meteoric waters circulated at depth, and were heated by regional tectonism and an elevated geothermal gradient due to radiogenic decay. The existence of an elevated geothermal gradient is supported by modern hot springs with temperature up to 98°C along the NE-SW-trending fault zones in the district.

Circumstantial evidence by fluid inclusion, oxygen and hydrogen isotopic data mentioned earlier (see Sect. *Stable Isotopes and Fluid Inclusions*) attest to a mesothermal to epithermal nature and a meteoric provenance of these solutions. These solutions driven by regional tectonism migrated along fault zones and may have further collected uranium and other elements on their way through granites and metasediments, until they finally became pregnant mineralizing fluids.

5. *Ore formation*: Uranium and associated metallic elements were deposited in NE-SW-oriented fracture and breccia zones as well as in porous sections in alkali-metasomatized granite that derived from dissolution of quartz.

Temperatures of mineralizing fluids dropped from 260°C in the pre-ore through 247–120°C in the syn-ore to 110°C in the post-ore stage as can be deduced from homogenization temperatures of primary fluid inclusions. The fluids were carbonate-rich suggesting a U transport in a uranyl carbonate complex together with significant amounts of hydrogen sulfide. In response to pressure release that resulted in CO₂ effervescence and consequently in dissociation of the uranyl carbonate complex, carbonate and pitchblende were concomitantly deposited.

Other factors that may have played a role in deposition of pitchblende and associated minerals include a change in temperature with distance from the heat source, fluid/rock interaction, and mixing of hydrothermal fluids with shallow meteoric water. Fluid/rock interaction is evidenced by oxygen and hydrogen isotope data that indicate not only a meteoric origin of the hydrothermal fluids but also an isotopic exchange of water with the host rocks. Early fluid was highly evolved whereas later solutions were less evolved, a circumstance, which is thought to have resulted from the mixing of hydrothermal solutions with shallow groundwater.

Hydrothermal self-sealing, repeated brecciation and supergene processes followed original ore deposition.

In summary, Min MZ et al. (1999) postulate as the most appropriate model for the origin of the “Huangao” deposit, and presumably also for the other deposits in the Lujing District, a hydrothermal system of mesothermal to epithermal solutions that operated in response to Himalayan regional tectonism during the Early to Middle Tertiary. Uranium and associated ore components were leached predominantly from granites and partially from the metasedimentary basement.

The episodic nature of mineralization, reflected by three syn-ore substages of mineralization and three more pre- and post-ore substages, is attributed to repeated tectonic events that caused renewed brecciation associated with remodification and sequential deposition of the various mineral substages.

According to Zhou Weixun (pers. commun. 2003) there are four U mineralization stages dated at about 107, 87, 67, and 47 Ma. The 87 Ma and 67 Ma old stages correspond to block tectonism and related hydrothermal activity during the Middle Cretaceous and Early Tertiary and are thought to be the more significant ore-forming events. The 107 Ma old stage may reflect post-magmatic hydrothermal leaching and the 47 Ma stage may reflect redistribution of uranium during Himalayan tectonism.

1.4.1.1.3 Jiuyishan Granite Massif, S Hunan

The composite Jiuyishan granite massif is located in southern Hunan Province and lies at the northern margin of the Nanling tectonic-magmatic zone. The massif is built up of four Yanshanian granitic/felsic volcanic complexes lined up in an E-W direction. Significant U deposits are of exogranitic type and occur at the periphery of the *Jinjiling* (JN) biotite granite batholith, which is exposed over an area of about 300 km². Two large, low grade deposits and several high grade, low tonnage deposits are recorded. They include *Xiangcao* (Xiangca) described below, and *Dawan* (382).

Sources of information. Zhou Weixun 1997; Zhou Weixun et al. 2003.

Regional Geological Features of the Jiuyishan Massif

The composite Jiuyishan batholith was intruded into Upper Sinian and Lower Cambrian metasediments and evolved by four Yanshanian felsic magmatic stages: (1) The Middle Jurassic Shaziling monzogranitic pluton (170 Ma) formed under a compressive regime. It was followed, after uplift and exposure of this pluton, by (2) an Upper Jurassic volcanic dacite stage (156 Ma) (now represented by only subvolcanic bodies while the other volcanic rocks are thought to have been eroded); by (3) the Upper Jurassic Jinjiling (and Xuehuading?) biotite granite (153.7 Ma); and subsequently by (4) the Tian'erzai intrusions (150.4 Ma) composed of subquartz porphyry, subgranitic porphyry, and seriate-grained granite; and granite porphyry (140 Ma).

Cretaceous-Tertiary grabens filled with tholeiite intercalated with redbed continental sediments occur at the periphery of the Jiuyishan Massif.

1.4.1.1.3.1 Xiangcao Deposit, Hunan

This U deposit is located in Lanshan County, Hunan Province. Resources are in the category of 1 500–5 000 t U at a grade of 0.1–0.3% U. Most geologists attribute *Xiangcao* (*Xiangca*) to the perigranitic vein type but some authors choose the C-Si-pelite type.

Xiangcao is situated between two granitic massifs, *Xuehuading* to the west and *Jinjiling* to the east; the two are separated by Upper Sinian and Lower Cambrian metasediments. Mineralization occurs along three prominent silicified fracture zones that traverse in a NNW-SSE, sub-meridional, and sub-latitudinal direction Lower Cambrian shale and sandstone contact-metamorphosed to muscovite hornfels, cordierite hornfels, and hornfelsic, carbonaceous biotite sandstone. These zones are filled with pre-ore white quartz locally with superimposed uraniferous veinlets. Brittle overprinting has generated secondary cataclastic and brecciated intervals that are filled with uraniferous veinlets composed of reddish microcrystalline quartz, pyrite, hematite, galena, fluorite, calcite, pitchblende, and U⁶⁺ minerals. Wall rocks are altered by silicification, hematitization, and carbonatization. Ore bodies are lens- or column-shaped and range

from 10 m to 100 m in length, 1–10 m in thickness, and dip to depths of more than 200 m (Zhou Weixun 2000).

1.4.1.1.4 Mao'ershan-Yuechengling Granite Massifs, Ziyuan Ore Field, Hunan-Guangxi

The polyphase Mao'ershan and easterly adjacent Yuechengling Caledonian granitic massifs occur at the western end of the Nanling tectono-magmatic zone where it overlaps with the southeastern Xuefeng-Jiuling U belt. The two massifs are both elongated in about a NNE-SSW direction and trend a few kilometers apart across the borderline between Guangxi and Hunan. Intragranitic U deposits in the *Ziyuan ore field* are associated with the Mao'ershan Complex. Other deposits of C-Si-pelite type such as *Chanziping* occur in Sinian-Cambrian metasediments between the two granitic massifs as well as to the east of the Yuechengling Massif e.g. *Kuangshanjiao* (*Kungji*) and *Guangzitian*. The latter two are hosted by Devonian sediments and commonly attributed to the C-Si-pelite type but a few geologists prefer to class them as a perigranitic U type (see Sect. 1.4.3.1.1: *Chanziping, Ziyuan Ore Field, NW Guangxi A.R.*).

1.4.1.1.4.1 Ziyuan Ore Field, Hunan-Guangxi A.R.

The Ziyuan ore field, SW Hunan-N Guangxi A.R., is commonly attributed to the Nanling U belt. It includes U deposits within the Mao'ershan Massif and in Sinian and Lower Cambrian (meta)sediments between the Mao'ershan and Yuechengling granitic massifs.

The Mao'ershan granite massif covers about 1 000 km². It consists predominantly of Caledonian hornblende-monzonitic granite (412 Ma) into which a number of small Indosinian (ca. 195 Ma) biotite granite and Yanshanian (ca. 150 Ma) two-mica granite bodies were intruded. The latter host U deposits. The Yuechengling Massif is of similar Caledonian age and lithology as the Mao'ershan Massif but lacks Indosinian and Yanshanian intrusions.

Deposits within the Mao'ershan Massif are hosted by bodies of Yanshanian two-mica granite and clearly defined as endogranitic type; these deposits are comparable to deposits in the Zhuguang Massif. In contrast, the type attribution of the deposits in metasediments is not unanimous. Although attributed to the perigranitic type by some geoscientists, others consider them to be of the C-Si-pelite type and part of the Xuefeng-Jiuling U belt such as *Chanziping*.

1.4.1.2 Other Granite Massifs with Related U Deposits in SE China

1.4.1.2.1 Motianling Granite Massif, Motianling/Sanfang OF, Guangxi A.R.

The Motianling (or Sanfang) granitic batholith in N Guangxi A.R. is located at the south end of the Xuefeng-Jiuling U belt that extends along the SW edge of the Jiangnan Uplift. This batholith

is the only U-hosting granitic massif of Precambrian age in South China. Several perigranitic U deposits occur in the *Motianling*, which is also referred to as *Sanfang* ore field including the *Xincun* and *Daliang* deposits.

As outlined earlier, the Jiangnan Uplift is a Precambrian orogenic belt formed by the Sibao and Xuefeng orogenies during the Meso- and Neo-Proterozoic-Sinian. The basement is composed of Middle Proterozoic volcano-psammitic-pelitic metasediments. The polyphase *Motianling* batholith with an outcrop of about 1 000 km² was intruded into this basement at the SW edge of the Jiangnan Uplift by repeated igneous activity during the Sibao and Xuefeng orogenies. The main igneous body consists of coarse- to medium-grained biotite granite that yields a Rb-Sr isochron age of 845 Ma. Small intrusions of medium- to fine-grained biotite granite, dated at 688 Ma (Rb-Sr), are placed within the older granite body.

Pitchblende yields an age of about 45 Ma that matches mineralization stages elsewhere in the South China U province but shows a hiatus of as long as 800 Ma with respect to the U-hosting main granite (845 Ma) (Zhou Weixun, pers. commun. 2003).

1.4.1.2.2 Liuchen Granite Massif, Ma'andu Deposit, Guangxi

The Liuchen granitic massif in SE Guangxi A.R. is of Yanshanian age and was intruded into Devonian sediments. A few U occurrences and the small *Ma'andu* (*Mada*) deposit occur in the contact-metamorphosed Devonian sediments aureole of this granite. *Ma'andu* is commonly attributed to the *exocontact subtype* of granite-related U deposits but some geologists also define it as a *hydrothermal-reworked C-Si-pelite* type deposit, and they consider the Liuchen granite not necessarily as a fertile granite but rather to have mainly played a role in the formation of close-by C-Si-pelite U mineralization.

1.4.1.2.3 Taoshan Granite Massif, Dabu Deposit, Jiangxi

The Taoshan GM in central-E Jiangxi has an outcrop size of 300 km². It hosts several deposits including Dabu, which are attributed to the clay-altered subtype of intragranitic deposits. Due to low grades of 0.05% U ore less, these deposits tend to be of no economic significance. Dabu (Fig. 1.29) is hosted in altered, fractured and brecciated medium- to coarse-grained granite (J_1) into which fine-grained two-mica granite and biotite granite (J_{2-3}) as well as monzonitic granite (J_3 - K_1) were intruded.

1.4.1.2.4 SL Deposit, Jiangxi

The small SL deposit is located in Ruijin County, SE Jiangxi, close to the border with Fujian Province, and associated with a granitic massif in the Wuyishan magmatic belt. Mineralization consists of disseminated pitchblende in hydrothermally altered granite at the fault-bounded NW margin of an Indosinian

granite. Ore lodges are controlled by NE-SW faults that were generated during the extensive graben-forming events of Yanshanian age in the region. This fault system is locally associated with andesitic volcanism, fluorite mineralization, and presently active hot springs (Simpson and Yu 1989; Han Zheaong et al. 1985).

1.4.2 Volcanic Belts and Related U Deposits/ Eastern Metallogenic Domain

The eastern metallogenic domain extends from Zhejiang through Fujian and Jiangxi into northeastern Guangdong Province in SE China (Fig. 1.27). Prominent U deposits in this domain are of volcanic-related type and account for most of the U deposits of this type in China. The *Gan-Hang* volcanic belt is the dominant host to volcanic U deposits. Some volcanic U deposits are also known from the *Wuyishan* magmatic belt and the eastern *Nanling* magmatic belt. In excess of sixty deposits have been identified in these belts (Chen Ranzhi and He Caiyi 1996).

The eastern *Nanling* magmatic belt also contains a few sandstone-type U deposits/occurrences in downfaulted redbed basins and mostly close to granite-hosted U deposits.

Source of information. The following synopsis is largely based on publications by Chen Ranzhi and He Caiyi (1996), Chen Yuehui (1995), Chen Zhaobo (1981), Chen Zhaobo et al. (1982), Chen Zhaobo and Fang Xiheng (1985), Li Wenxing (1990), Liu Yifa et al. (1990), Malan (1980), Wang Yusheng and Li Wenjun (1996), Yao Zhenkai et al. (1989), Zhou Weixun (1988, 2000, 2006b), and Zhou Weixun pers. commun. (2004, 2006) unless otherwise cited.

Regional Geological Features of the Eastern Metallogenic Domain

The eastern metallogenic domain is within the Cathaysian fold system. The domain is bounded to the east by the NNE-SSW trending Lishuai-Lianhuashan fault that can be traced from Lishuai, Zhejiang Province, through Fujian Province to Lianhuashan, Guangdong Province, and to the west by the Chenzhou-Huaiji deep fault zone. The latter is the boundary between the western and eastern metallogenic domain of the South China U province.

The Cathaysian fold system is part of the Nanhua or South China mobile zone. The Nanhua zone was stabilized during the Caledonian Orogeny and then uplifted to form the Post-Caledonian Uplift, which is characterized, by a lack of, or only minor Late Paleozoic cover sediments. Intense tectonic-magmatic activity reactivated the region during the Indosinian and Yanshanian orogenies. Regional deep faults trending NE to ENE and NW developed or were reactivated and their intersections govern the distribution and nature of volcanic complexes.

Mesozoic volcanism developed in SE China under continental conditions during a stage of crustal extension predominantly in Late Jurassic and Early Cretaceous time and produced

collapsed (caldera), downwarped, and downfaulted volcanic-sedimentary basins; subvolcanic bodies, volcanic vents, and diatremes.

Large-scale volcanism commenced 175 Ma ago and ended 75 Ma ago. Volcanic activities began at first in the western part of the domain and progressed gradually eastwards toward the coast. As a result of this chronological shift of Mesozoic volcanic activity, the stratigraphic position of U deposits changes from older to younger volcanic facies also from west to east.

The Mesozoic volcanic period is separated into an earlier stage from 175 to 120 (110) Ma and a later stage from 120 (110) to 75 Ma old. Felsic lithofacies with a high potassium calc-alkalic component are typical for the earlier stage volcanics whereas later stage volcanism is characterized by bi-modal volcanics of basalt-rhyolite with an alkalic tendency (Chen Ranzhi and He Caiyi 1996). Due to this evolution, felsic to intermediate volcanics with associated tuffs and ignimbrites prevail in the Gan-Hang Belt while the Wuyishan Belt is dominated by intermediate to mafic volcanics.

Principal Characteristics of Mineralization and Alteration

Colloidal pitchblende is present in many deposits and brannerite, coffinite, and uranothorite in some. Associated minerals include colloidal pyrite, jordisite, purple-black fluorite, collophane, chalcedony, and/or microquartz. Mo and P contents are generally high. Ore and gangue minerals are poorly crystallized.

Malan (1980, based on papers by Chen Zhaobo and co-workers) notes that mineralization 120 Ma old is characterized by pitchblende with large amounts of sulfide, fluorite, or alunite gangue, and strong albite alteration of wall rocks.

Illite alteration is dominant in 100 Ma old mineralization, which is composed of pitchblende with abundant apatite, chlorite, or carbonate gangue. Dickite is the dominant alteration product in mineralization 80–90 Ma old with deposit subtypes characterized by fluorite, sulfide, or carbonate gangue. Deposits with a dominant albite and illite alteration are more directly controlled by volcanic structures than are the younger deposits with a dickite-type alteration.

The majority of U deposits in the Gan-Hang and Wuyishan Belts are in silicic volcanic complexes that occur spatially related to tensional taphrogenetic zones, particularly in the vicinity of Cretaceous redbed basins. These volcanic complexes are dominated by rocks of rhyolitic and dacitic composition with subordinate andesite, trachyte, and basalt. Ignimbrite is the most important host rock, other hosts include subvolcanic bodies, and, locally, basement rocks underlying mineralized volcanic rocks (Malan 1980; Chen Zhaobo 1981).

U deposits in the Gan-Hang metallogenetic belt occur predominantly in fairly large volcanic basins that have been formed during the main stage of intense eruption (Ehuling cycle, see *Gan-Hang Belt*, further below); in contrast, U deposits and occurrences in the Wuyishan metallogenetic belt are preferentially related to small volcanic apparatus, including cryptoexplosive breccia pipes, of late volcanic activity.

While U deposits in the Gan-Hang Belt occur in volcanics that largely overlie Proterozoic-Lower Paleozoic metasediments, deposits in the Wuyishan Belt are in volcanics underlain by a granitic basement. Both, the Mesozoic volcanics and the basement lithologies in the two belts include U enriched facies (see Sect. *Potential Sources of Uranium*) that are considered favorable U source rocks. High Mo and P contents in ancient U-rich strata may also indicate that these rocks provided potential sources for these elements.

U ore bodies are preferentially located at structurally deformed margins of volcanic depressions or small volcanic apparatus in which faults and overthrusts as well as interlayered fault and fissure zones within and along the interfaces of volcanic beds are markedly developed. Moreover, ring and arcuate structures associated with subvolcanic rocks are also common at the margin of calderas where their contact zones with country rocks, e.g. metamorphic rocks, sandstone etc., apparently provided preferred sites for ore deposition.

General Shape and Dimensions of Volcanic-Related U Deposits

U deposits are controlled by lithology as well as structure and consequently exhibit an irregular structural attitude with variable configurations of ore bodies in an ore field and even in a single deposit.

Deposits consist of vein, stockwork, or stratiform ore lodes. Veins and stockworks are controlled by caldera-related structures such as ring fractures, radiating fractures, various collapse structures, and also by cryptoexplosive breccia pipes, subvolcanic bodies, or intrusive cupolas. Stratiform/tabular to lenticular ore bodies are typical for volcanic basins in which they are governed by gently inclined zones of interstratified fractures, contraction fractures in upper and lower portions of cooling units, and steeply dipping fractures. Dimensions of ore lodes are highly variable and are discussed in more detail in the subsequent chapters on the Gan-Hang and Wuyishan Belts.

Stable Isotopes and Fluid Inclusions

Fluid inclusions data of quartz from rhyolite indicate a temperature for rhyolite extrusions of 1150–1200°C. Pb isotopes obtained from Upper Proterozoic mica schist and granite gneiss (P), and Upper Jurassic rhyolite porphyry and ignimbrite (J) yield ratios of: $^{206}\text{Pb}/^{204}\text{Pb}$ (P) 18.258, (J) 18.184; $^{207}\text{Pb}/^{204}\text{Pb}$ (P) 15.547, (J) 15.618; $^{208}\text{Pb}/^{204}\text{Pb}$ (P) 38.803, (J) 38.455 which, by their similarity, indicate an anatectic origin of the volcanics from the Proterozoic basement. This is further supported by almost identical LREE patterns (showing distinct Eu depletion) in U mineralized volcanics and metamorphic basement rocks, and also by Sr isotope ratios of 0.709–0.719 in volcanic host rocks.

Stable isotope studies from fluid inclusions of structurally controlled U mineralization from the Xiangshan U district yield δD (fluid) values of about –80 to –50‰, and $\delta^{18}\text{O}$ values of –12

to +5‰, suggesting a mixed magmatic-meteoritic origin of the ore-forming solution (Liu Yifa et al. 1990).

Regional Geochronology

Volcanic rocks yield isotope ages ranging from 175 to 75 Ma that are separated into an earlier stage from 175 to 120 (110) Ma and a later stage from 120 (110) to 75 Ma.

Uranium mineralization in the *Gan-Hang* Belt is dated at 141 ± 7 , 119 ± 2 , and 90 ± 2 to 70 Ma. Age datings of various metallic deposits in the *Wuyishan* Belt yield ages of 103–99 Ma (Zijinshan Cu-U deposit, SW Fujian), 101.8–86.8 Ma (Maoyantou U deposit, N Fujian), and 55–52 Ma (Caotaobei U deposit, central-southern Jiangxi) (Chen Ranzhi and He Caiyi 1996; Liu Yifa et al. 1990).

Potential Sources of Uranium

Mesozoic volcanics and basement lithologies include U-enriched facies that are considered potential U sources. Respective U and Th background values of these facies in the *Gan-Hang* Belt are as follows:

- Regional U and Th background (Th and Th/U ratios in brackets) values of Jurassic felsic volcanics in
 - NE Jiangxi: 3.2–5.0 ppm U (19.6–31.8 ppm Th; 3.92–7.94 Th/U), av. 4.8 ppm U (21.7; 4.52);
 - SW Zhejiang of 3.2–4.9 ppm U (15.4–21.7; 17.8), av. 4.1 ppm U (17.8; 4.34).
- U and Th background values of ore hosting volcanics in
 - NE Jiangxi: 12.6–26.8 ppm U (22.1–30.9 ppm Th; 1.15–2.93 Th/U), av. 19.7 ppm U (25.9; 1.31);
 - SW Zhejiang: 12.8–14.8 ppm U (24.2–30.9; 1.64–2.45), av. 14.6 ppm U (24.7; 1.69).

Unmineralized and mineralized subvolcanic granite porphyry, quartz porphyry and felsite average 3.4 ppm U (12.5 ppm Th; 3.68 Th/U) and 22.8 ppm U (33.1 ppm Th; 1.45 Th/U), respectively.

U abundance in basement metamorphic rocks of the South China fold system averages up to 5 ppm U in Proterozoic rocks, and up to 30 ppm U in Early Paleozoic carbonaceous slate (Liu Yifa et al. 1990). For U background values of granites see *Wuyishan Belt*.

Principal Ore Control or Recognition Criteria

Volcanic-related U deposits are structurally and lithologically controlled; relevant criteria are as follows:

Host environment

- Tectonic-magmatic belts of Jurassic-Cretaceous age in SE China
- Silicic volcanic complexes dominated by rocks of rhyolitic and dacitic composition with subordinate andesite, trachyte, and basalt

- Volcanic complexes including collapsed (caldera), downwarped, and downfaulted volcanic-sedimentary basins; subvolcanic bodies, volcanic vents, and cryptoexplosive breccia pipes/diatremes
- U mineralized depressions are characterized by
 - calderas with large scale collapse
 - downwarped or downfaulted basins/grabens filled with alternating pyroclastic and sedimentary rocks
 - a size commonly larger than 100 km²
 - a basin fill 1 000 m or more thick
 - alternating permeable and impermeable volcanic-sedimentary layers
 - intraformational fractures and shrinkage cracks
 - very limited erosion
- Vicinity of mineralized volcanic complexes to Cretaceous basins filled with redbeds
- Uraniferous (source) rocks in basement
- Regional deep faults or lineaments accompanied by subsidiary faults and/or secondary fracture systems

Alteration

- Pre-ore alteration is primarily reflected by albitization, argillization, muscovitization, hydromicazation
- Ore-related alteration is expressed by
 - hydromicazation, chloritization, fluoritization, pyritization, and hematitization
 - marked alteration intensity at structure controlled deposits
 - less pronounced alteration intensity at stratiform deposits

Mineralization

- Simple ore mineralogy composed of pitchblende, brannerite, coffinite, and adsorbed uranium
- Associated minerals include sulfides, mainly pyrite, and a gangue of fluorite, apatite, and collophane
- Large type-variety, multiple litho-stratigraphic and structural positions of U ore bodies
- Concentration of U lodes at intersections of regional faults particularly at sites of superimposition of a multitude of structures of different age and quality
- Caldera hosted U mineralization is preferentially in peripheral ring and arcuate faults
- Caldera hosted ore bodies are rich and large, and persist into great depth
- Downwarped or downfaulted basins host mainly stratiform U mineralization in one or more layers
- Stratiform mineralization occurs in layers sandwiched between impermeable beds
- Stratiform mineralization occupies strata internal fractures and shrinkage cracks
- U deposits in cryptoexplosive breccia pipes are typical for *Wuyishan Belt*

Principal Aspects of Metallogenesis

A genetic model proposed by Chen Zhaobo (1981) for volcanogenic uranium deposits in SE China is designated as the

“double-mixing model”. The model postulates a dual origin for the mineralizing solution and the contained uranium. In this model, water in the mineralizing solution was primarily of meteoric provenance and circulated in a hydrothermal system activated by magmatism. On the other hand, the geochemical character and mineralizing agents derived from primary fluids of an anatectic zone at active continental margins. Uranium in the deposits originated from uranium-rich metasedimentary rocks that underwent anatectic melting. As the magma and related fluids ascended they were further enriched with U dissolved from other uraniferous strata and perhaps older U deposits on higher stratigraphic levels of the crust.

Fluid inclusion microthermometry and mineral parageneses indicate precipitation of uranium at low to moderate temperatures between 150 and 250°C, and later precipitation of fluorite, jordanite, and carbonate gangue at 80–100°C. Deposits are believed to have formed at depths from 700 to 2 500 m.

Liu Yifa et al. (1990) consider the following parameters as the principal ingredients of U-concentrating processes: About 95% of U-mineralized volcanics overlie uraniferous Proterozoic (av. 3–5 ppm U) and Lower Cambrian (<30 ppm U) rocks. Trace element associations (U-Rb-Th, U-Rb-F, and U-Th-Rb-K) in mineralization are identical with those in the basement. The authors propose that circulation of mixed magmatic and meteoric solutions partially dissolved this basement-contained uranium to form stratiform U mineralization during an early diagenetic stage. Carbon and phosphorous are abundant in pyroclastic-sedimentary layers and acted as reductants and absorbents for the formation of U-P-type mineralization in the course of epigenetic remobilization.

Further U concentration processes occurred during the Late Yanshanian tectonic event contemporaneously with downfaulting of basins and deposition of redbed sediments. Pneumatolytic-hydrothermal solutions are thought to have mobilized and transported U and alkalis to favorable fracture zones located close to redbed basins for ore deposition and concentration. Based on oxygen and hydrogen stable isotope studies, it is postulated that these (or later?) solutions derived from meteoric, oxygenated waters-which migrated from the redbeds into uraniferous country rocks, leached the uranium, and, after mixing with magmatic fluids, formed vein-type U deposits.

Chen Ranzhi and He Caiyi (1996) address the metallogenesis of volcanic U deposits in SE China with specific reference to the Gan-Hang metallogenetic belt as follows. Post-magmatic ore-forming hydrothermal systems evolved with the onset of Late Yanshanian tensional taphrogenesis, at first in the western Gan-Hang Belt after volcanic activity had terminated here but was still active in the east. The taphrogenetic event produced intense block faulting along hinge zones of geotectonic units and deep fault zones. During this event, major faults, as well as fracture zones in both sidewalls of these faults, were generated or reactivated. These structural systems of repeated brittle deformation produced the spatial prerequisites for evolution of geothermal systems, migration of fluids and, contemporaneously, sizable reservoirs for ore precipitation and accumulation by superimposition of a multitude of structures of different age and quality.

Basins were downfaulted and filled with Cretaceous redbeds during the final period of taphrogenesis; and U deposits were formed synchronously with these redbed basins.

Three prominent U ore-forming stages (see Sect. *Regional Geochronology*) have been identified in the Gan-Hang Belt. These episodes roughly coincide with three hiatus periods during the Upper Jurassic-Lower Cretaceous, Lower to Middle Cretaceous, and Middle to Upper Cretaceous (Liu Yifa et al. 1990). Chen Ranzhi and He Caiyi (1996) relate the first stage to initiation of Early Cretaceous basin formation; the second stage to development of these basins; and the third stage to Late Cretaceous redbed sedimentation.

According to Zhou Weixun (2000), the first and second stage correspond to the intrusion of porphyries after extrusive volcanism by rhyolite; and the third stage to down faulting of Cretaceous basins.

Zhou Weixun et al. (2006 in print) forward a bimodel approach for the metallogenesis of U deposits in the Xiangshan Caldera, Gan-Han Belt: a “*porphyry model*” and a “*downfaulted redbed basin model*”. The porphyry model postulates a uranium origin from a fractionated fluid related to “secondary boiling” in a magmatic chamber after crystallization of porphyries. In the down-faulted redbed basin model subsequent processes mobilized U from consolidated volcanic rocks in the course of pre-ore alteration that formed planar arranged hydromicization, to generate late stage U mineralization.

Critical ingredients for evolution of an ore-forming hydrothermal system are postulated to be the collapse of a magmatic chamber and subsequent swell by extrusion of volcanic rocks, intrusion of felsic dikes and related shattering of superjacent rocks, regional faulting, Late Cretaceous-Paleogene down-faulting of basins, and pre-ore alteration processes.

Two ore stages are identified by U-Pb dating of pitchblende, an early stage at 115 ± 0.5 Ma for ore deposits enveloped by pre-ore albitization and a later stage at 98 ± 0.8 Ma for deposits surrounded by pre-ore, planar arranged hydromicization.

The “*porphyry model*” is suggested for deposits with Th-free or Th-poor uranium mineralization at which porphyric stocks and/or dykes occur nearby or at depths. The model emphasizes that secondary boiling occurred in a transitional magmatic chamber after mineral crystallization to form various porphyries. Due to this boiling, an independent critical-supercritical fluid enriched in alkali, volatile components, uranium and associated elements was fractionated. While internal energy increased to a somewhat critical state, the closed system changed into an open system associated with fracturing, and formation of shattered zones or cryptoexplosive pipes above porphyry bodies and in adjacent country rocks. Albitization took place as a characteristic pre-ore alteration. Coeval, or immediately thereafter, a uraniferous hydrothermal cyclic-convection cell was formed by magmatic fluids and meteoric water, followed by ore-stage alteration (hematitization, carbonatization, chloritization) and uranium precipitation.

The “*downfaulted redbed basin model*” is applied for formation of deposits with a U-Th mineral assemblage that occur in well-developed planar distributed hydromica alteration zones and occasionally close to red bed basins. This model postulates a hydrothermal cyclic-convective system that was produced

contemporaneously with and in response to the down faulting of redbed basins and fracturing and intrusion of melanitic/trachytic dikes; the dikes provided heat and reducing gas components. The planar hydromica alteration process is thought to have mobilized uranium and alkalis in the volcanic-intrusive complex, particularly in porphyric rhyolite. The mineralizing solution transported the elements to fracture zones favorable for ore deposition and concentration.

1.4.2.1 Gan-Hang Volcanic Belt, SW Zhejiang-Central Jiangxi

The Gan-Hang (= Jiangxi-Hangzhou) volcanic belt (Gan is abbreviation for Jiangxi and Hang for Hangzhou) is the largest and most prominent metallogenetic belt with respect to volcanic-related U deposits in China. The belt is 50 to 80 km wide and extends for about 600 km from the town of Yuhuashan, Le'an County, central Jiangxi, in the southwest to Shaoxing, SW Zhejiang, in the northeast.

Original resources of the Gan-Hang Belt amounted at least to 30 000 t U that were largely contained in three U districts/ore fields, from SW to NE: *Xiangshan*, *Shengyuan* (also named *Shunyan* or *Yingtian*) in NE Jiangxi, and *Xiaoqiuyuan* (or *Dazhou*) in Zhejiang Province (Fig. 1.36). *Xiangshan* is the

most significant district while the other two have only small deposits. Additional deposits mentioned by Chen Ranzhi and He Caiyi (1996) occur in the *Longquan* (deposit #79) and *Suichang* areas, both in western Zhejiang, in which deposits are located in volcanic basins that border uplifted blocks composed of the Proterozoic Chencai and Badu groups.

[Note: In contrast to this denomination of U districts, Li Wenxing (1990) notes three discontinuous metallogenetic subzones in the Gan-Hang Belt, namely Lean-Dongxiang, Yujiang-Qianshan and Dazhou-Furongshan, and several mineral districts including Yuhuashan, Hengfeng, Tianhuashan, and Henxi. These subdivisions are apparently based on hydrochemical surveys and are hard to correlate with the commonly used mining-geological site denominations.]

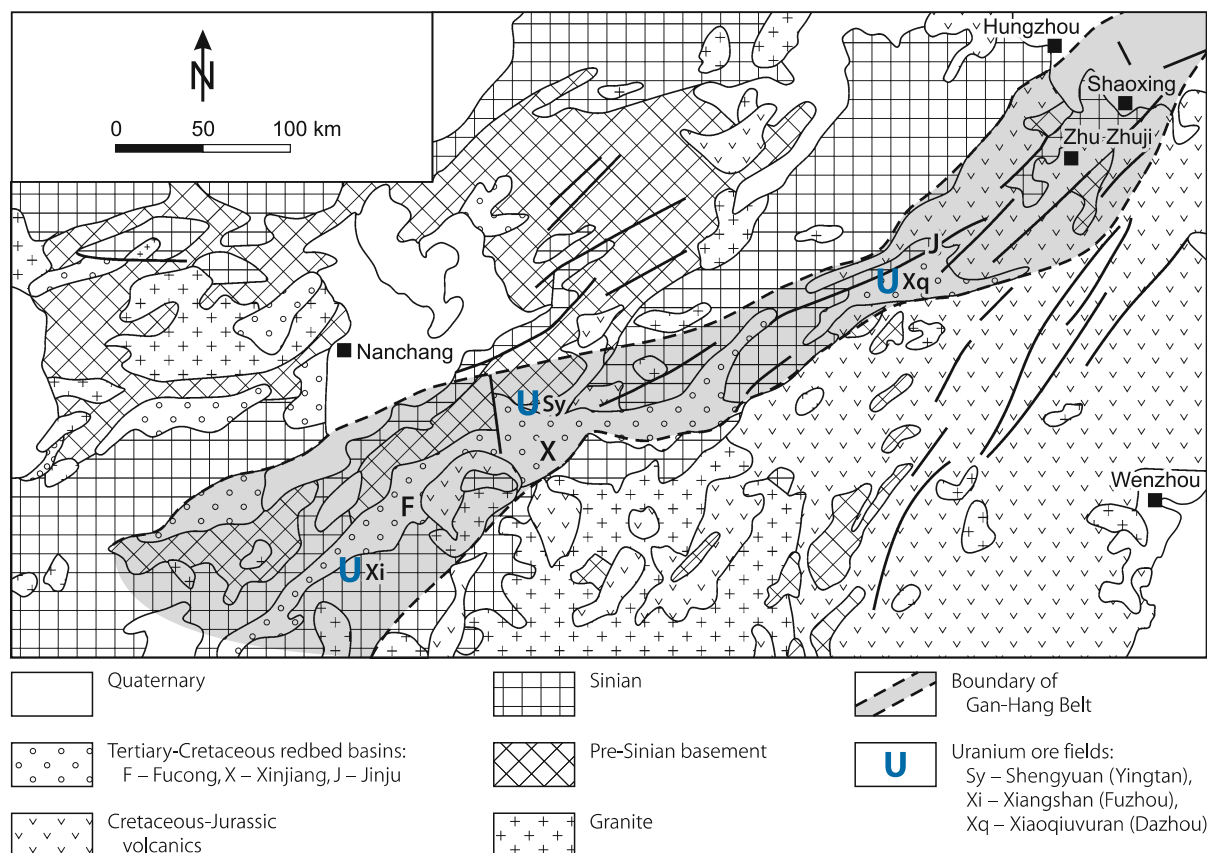
Sources of information. Chen Ranzhi and He Caiyi 1996; Li Wenxing 1990; Liu Yifa et al. 1990; Malan 1980; Wang Yusheng and Li Wenjun 1996; Yao Zhenkai et al. 1989; Zhou Weixun 1988, 2000, pers. commun. 2004; unless otherwise cited.

Regional Geological Setting of Mineralization

The Gan-Hang volcanic belt traces the Qingjiang-Shaoxing lineament (or Gan-Hang tectonic zone), a longtime repeatedly

Fig. 1.36.

Gan-Hang uraniumiferous volcanic belt, schematic geological map outlining the range of the belt and location of major U ore fields. (courtesy of Zhou Weixun 2006 based on selected Chinese literature)



reactivated suture that trends from Qingjiang, Jiangxi to Shaoxing, Zhejiang, roughly along the conjunction of the south-east margin of the Yangtze Massif and the Cathaysian (or Huanan) fold belt. The Gan-Hang fault is a major displacement structure slightly offset to the south of this lineament.

The region along this belt is underlain by a pre-Jinning basement comprising mainly Middle to Upper Proterozoic metamorphic rocks, and Sinian to Lower Cambrian uraniumiferous carbonate-silicic-pelite formations, which prevail to the west and grade into U-bearing carbonaceous sandy pelite facies to the east.

From Hercynian to Indosinian, the Gan-Hang Belt was a downwarped zone affected by repeated tectonic events that caused uplifting and downfaulting prior to volcanism, and subjected uplifted segments to denudation. As a result, Precambrian metamorphic rocks are exposed in uplifted blocks while Carboniferous, Permian, and Late Triassic-Early Jurassic continental and marine, partly coal-bearing sediments are preserved in depressions. The physiography of this terrane was marked by a paleosurface with a pronounced relief prior to Mesozoic volcanism.

Liu Yifa et al. (1990) identified five cycles of volcanism, three in Late Jurassic and two in Cretaceous time. Intense polycyclic and multiphase volcanism, as reflected by large and deep volcanic depressions and subvolcanic intrusions, occurred particularly during the Middle Yanshanian (Late Jurassic) tectonic event and ended in Late Yanshanian time (Cretaceous) coeval with the beginning of taphrogenesis.

As outlined earlier, Mesozoic volcanic activity progressed in the Gan-Hang Belt gradually from west to east; it lasted from 175 to 137 Ma in the western and from 150 to 95 Ma in the eastern part of the Gan-Hang Belt, i.e. volcanic activity lasted distinctly longer in the east than in the west. As a result of this shift, U deposits in early volcanics (Late Jurassic Daguding Fm) are confined to the western portion of the belt (Chen Ranzhi and He Caiyi 1996).

Regional deep reaching faults trend preferentially around NE to ENE and subordinately NW-SE. Second order fault systems complement the tectonic framework. Intersections of regional faults govern the position of volcanic centers and the nature of volcanic depressions. Repeated syn- and post-volcanic faulting resulted in generation of a horst and graben/basin pattern with a thick basin-fill of volcanic rocks, and thrust basement slabs over volcanic rocks.

Large volcanic depressions are typical for the Gan-Hang Belt; they include collapsed (caldera), downwarped, and downfaulted basins. Calderas are characterized by large-scale collapse depressions filled with lavas and pyroclastics, and post-collapse intrusions of subvolcanic rocks particularly along peripheral ring or arcuate fractures. Downwarped and downfaulted basins or grabens contain alternating pyroclastic and sedimentary rocks. Younger depressions are occupied by Tertiary-Cretaceous redbeds (► Fig. 1.37).

The volcanics are predominantly of calc-alkaline, felsic and subordinate intermediate composition. Favorable host facies are silica-rich (67–75% SiO₂), have a potassium tendency (K₂O/Na₂O ratio: 1–5), elevated U tenors (often >10 ppm U), and low Th/U ratios (1.3–1.7) (for more details see Sect. *Potential Sources of Uranium*).

Principal Host Rock Alteration

Pre-ore alteration features in mineralized volcanics include widespread albitization mainly at depth, but muscovitization, hydromicazation, argillization, and silicification prevail at higher levels.

Ore-related alteration: Structure-controlled U mineralization is associated with marked wall rock alteration phenomena reflected by albitization, hydromicazation, chloritization, fluoritization, pyritization, and hematitization. Alteration associated with stratiform U mineralization is less pronounced and includes hydromicazation or dickitization, and hematitization. Carbonatization is present locally.

Principal Characteristics of Mineralization

Ore is of simple mineralogy and mostly of disseminated texture. Pitchblende is the principal U mineral locally accompanied by brannerite and/or coffinite. Some deposits also contain uraniumiferous thorite and thorianite. Associated minerals are sulfides, mainly pyrite with minor Mo, Pb, and Cu species. Gangue minerals include fluorite, apatite, colophonite, and carbonates.

U mineralization is hosted by Upper Jurassic-Lower Cretaceous felsic lava, volcanic breccia, and pyroclastic sediments filling relatively large calderas and basins or grabens. Some ore lodes occur in subvolcanic intrusive bodies and basement rocks.

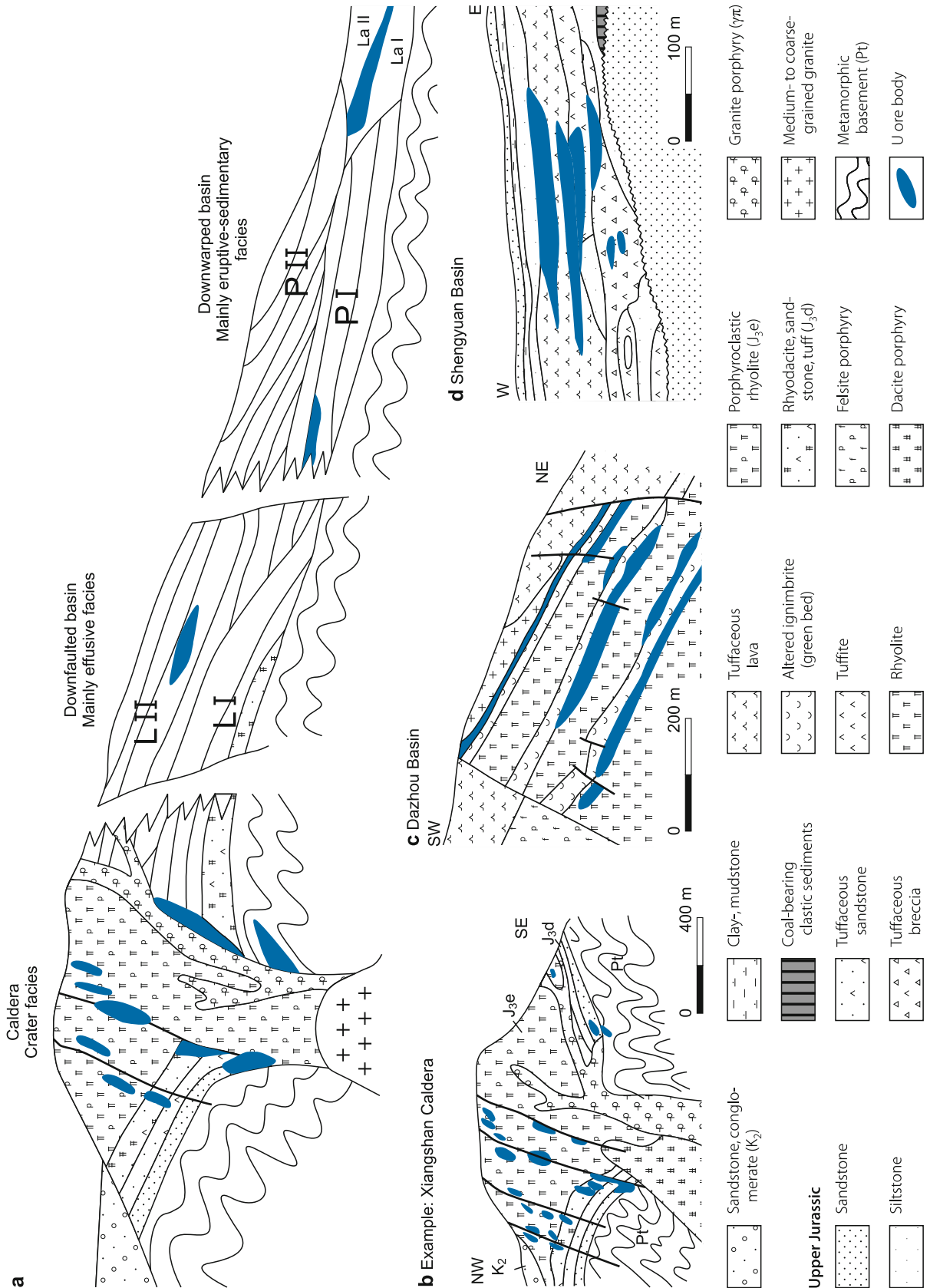
Several U mineralized formations and horizons are noted. In Jiangxi Province, two U mineralized formations occur in the Late Jurassic pyroclastic sequence: the *Daguding Formation* hosts stratiform U ore lodes in the 2nd layer (tuff), while the host in the *Ehuling Formation* is both the 2nd layer (porphyroclastic lava and stratified rhyolite) and 3rd layer (tuffaceous sandstone). Since the earlier Daguding volcanic cycle was active only in the western Gan-Hang Belt, U mineralization in the Daguding Formation is confined to the western part of the belt. The later Ehuling volcanic cycle, which was the most intense eruption phase, and was succeeded by multiple subvolcanic intrusions, affected the entire Gan-Hang Belt. Hence U deposits in Ehuling volcanics and slightly younger subvolcanics are distributed throughout the belt; they account for 56% of the total number of deposits in the belt.

In Zhejiang Province, U mineralization is contained in rhyolite and ignimbrite of the 2nd and 4th layer of the *Moshishan Formation*, the equivalent to the Ehuling Formation (Chen Ranzhi and He Caiyi 1996).

U deposits exhibit a striking affinity to volcanics that immediately overlie Proterozoic metamorphic basement; 40 deposits accounting for 97% of the total U reserves of the Gan-Hang Belt occur in this geotectonic position. This spatial affinity of volcanic U deposits to the metamorphic basement is more specifically illuminated by the Xiangshan and Yingtan ore fields in Jiangxi, and the Dazhou ore field in Zhejiang. Although Carboniferous, Permian, and/or Late Triassic-Early Jurassic strata locally occur peripheral to these ore fields, ore lodes are essentially confined to volcanics resting directly upon metamorphic basement.

Fig. 1.37.

Gan-Hang Belt. **a** Scheme of principal settings of volcanic-type U deposits in Upper Jurassic endo- and exocaldera environments (L-I lava cycle I; L-II lava cycle II; P-I pyroclastic-sedimentary cycle I (alternating ignimbrite and clastic sediments); P-II pyroclastic-sedimentary cycle II (sandstone interbedded with vitric tuff, tuffite); La lacustrine facies; after Chen Rhanzhi and He Caiyi 1996). **b–d** Examples of caldera-related settings of U ore fields; **b** caldera, **c** downfaulted basin, **d** downwarped basin (after Zhou Weixun 1997)



In western Zhejiang, between the counties of Juxian and Longquan, U occurrences in the Xiaoqiuvuran/Dazhou ore field, in the Suichang area, and deposit #79 in Longquan County, are confined to volcanic basins that border uplifted blocks of Proterozoic rocks of the Chencai and Badu groups.

General Shape and Dimensions of Deposits

Ore fields are typically located in large volcanic depressions such as calderas and downwarped or downfaulted basins/grabens in excess of 200 km² in areal size (Fig. 1.37). Both volcanic basins and sites of deposits and ore fields are controlled by intersections of the same major fault systems trending NE to NNE and NW.

Two principal kinds of deposits exist, structure-bound (veins and stockworks) and strata-bound (stratiform); but within this framework, ore lodes exhibit a large variety of types as well as multiple litho-stratigraphic and structural positions. The mode, configuration, and magnitude of deposits and ore bodies are controlled by the nature and pattern of brittle structures, volcanic host structures, and lithologies.

Structure-controlled U mineralization associated with a caldera constitutes the most significant U deposits. As exemplified by the Xiangshan District, the only example of this setting, deposits are composed of abundant, rich and large ore bodies persisting to great depth (920 m). These ore bodies are largely composed of disseminated U minerals concentrated within steeply dipping veins and stockworks. Ore is particularly concentrated at the intersection of fracture zones with volcanic structures such as ring-, collapse-, crater-structures, but also in breccia pipes/diatremes. Host rocks are predominantly microgranite-, quartz-, and felsite-porphyrries, rhyolitic mortar lava, and rhyodacite.

Veins are distributed over vertical intervals in excess of 300 m. Veins are from a few centimeters to few meters wide, persist laterally and vertically from a few meters to rarely a hundred meters, and contain from a few tonnes to some hundred tonnes U. Although individual veins are of relatively small size, the veins often group in clusters to form sizable deposits. For example, a large part of the resources of the Xiangshan ore field (total about 25 000 t U) is contained in vein U deposits.

Strata-bound/stratiform U mineralization occurs within downfaulted (e.g. Xiaoqiuvuran/Dazhou OF) and downwarped (e.g. Shengyuan/Yingtang OF) volcanic basins. Although of stratiform configuration and confined to favorable host horizons, U is essentially concentrated in intraformational fracture zones and intervals of shrinking cracks at lithological contacts and unconformities.

Host rocks include tuff, ignimbrite, tuffaceous sandstone beds, and rhyo-porphyrific and rhyolitic lava flows. Mineralized horizons are over- and underlain by more or less impermeable layers. U mineralization consists of disseminated U minerals and adsorbed U.

Deposits consist of discontinuous lenses from less than 1 m to several meters thick, up to several tens rarely hundreds of

meters long, and from several meters to as much as 50 m wide. Ore lodes occur from the surface to 300 m deep.

Selected U Districts and Deposits in the Gan-Hang Volcanic Belt

As mentioned earlier, the Gan-Hang volcanic belt encompasses several volcanic complexes/depressions and related U districts or ore fields including, from SW to NE, the Xiangshan and Shengyuan/Yingtang ore fields in Jiangxi Province, and the Xiaoqiuvuran/Dazhou ore field in Zhejiang Province.

1.4.2.1.1 Xiangshan Caldera, Xiangshan (Fuzhou) Ore Field, Jiangxi

The Xiangshan ore field is located in the synonymous caldera in Lean and Chongyi counties, about 70 km SE of the town of Qingjiang. The Xiangshan ore field was formerly listed as ore field #660 but miners commonly called it the *Fuzhou ore field* after Fuzhou, the nearest bigger city.

The Xiangshan Caldera, about 300 km² in areal extent, contains almost twenty U deposits and major occurrences situated at the northern, western, and eastern margin of the caldera (Fig. 1.38a). Typical deposits include *Hengjian* (#611), *Zoujiashan* (612), *Baquan* (617), *Yunji* (628), as well as deposits #670, and #681. Original in situ resources reportedly totaled some 26 000 t U, a large part of which was contained in vein U deposits. Average ore grades are on the order of 0.1–0.3% U.

Discovered in 1957, Hengjian was the first deposit identified in this district. Mining was and is by open pit and underground methods and started in 1963 at Hengjian. Ore is preconcentrated in the Hengjian plant and the concentrate is transported to the Hengyang mill for refining, drying, and packaging.

The subsequent summary including the description of selected deposits is largely based on Zhou Weixun et al. (2006b) amended by data from Zhou Weixun (2002 and pers. commun. 2004).

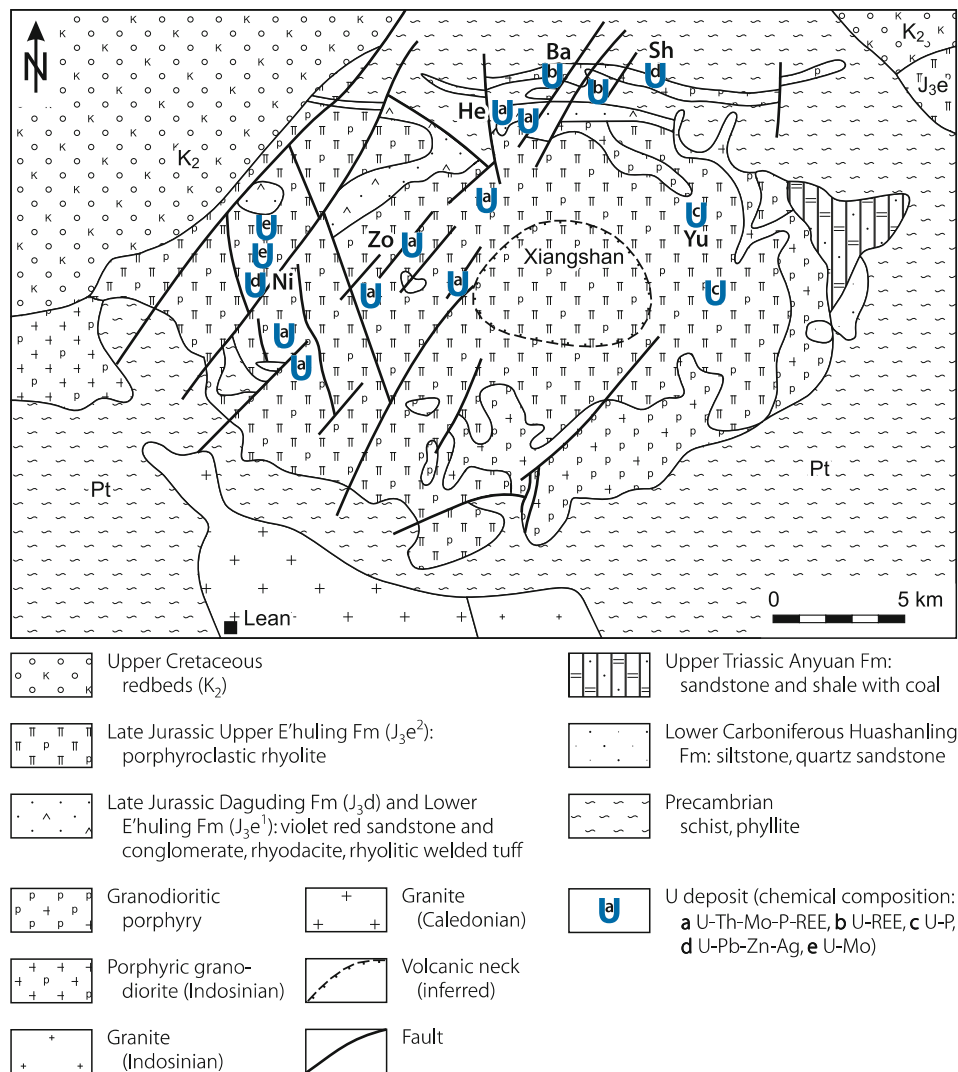
Geological Features of the Xiangshan Caldera

Morphologically, the Xiangshan complex forms a dome as a result of volcanic eruptions, effusions and large-scale, late extrusions. A litho-stratigraphic profile of the Xiangshan area includes the following units:

- *Upper Cretaceous* redbed sandstone, conglomerate
- *Upper Jurassic* Upper E'huling Fm (F₃e²) (*volcanic cycle 2*) and Lower E'huling Fm (F₃e¹) and Daguding Fm (F₃d) (*volcanic cycle 1*) (see below)
- *Upper Triassic* Anyuan Fm: feldspar-quartz sandstone, shale with coal
- *Lower Carboniferous* Huashanling Fm: siltstone and quartz sandstone
- *Indosinian* granodiorite
- *Caledonian* porphyric granitoid, gneissic granite
- *Precambrian* schist and phyllite

Fig. 1.38a.

Gan-Hang Belt, Xiangshan Caldera, generalized geological map with location of uraniumiferous deposits. U deposits mentioned in text are pinpointed: Ba Baquan, He Hengjian, Ni Niutoushan, Sh Shazhou, Yu Yunji, Zo Zoujiashan (after Zhou Weixun et al. 2006b)



Lithologies of the *first volcanic cycle* comprise rhyolitic tuff, vitric tuff, ignimbrite, and late rhyodacite lava (169–158 Ma), as well as tuffaceous sandstone, and sandstone.

After collapse and caldera development, the *second volcanic cycle* followed with eruption of dominantly rhyolitic ignimbrite associated with rhyolitic crystal tuff and deposition of sediments, and, finally, large-scale extrusion of porphyroclastic rhyolite (rhyolite with cataclastic, more or less idiomorphic quartz-phenocrysts) (150–140 Ma). The latter is prominent in the center of the caldera and forms the main part of the dome shaped edifice in the center of the volcanic complex. (For geochemistry of various volcanic facies see Chemillac et al. 2005a.)

Latest magmatic activity (135–114 Ma) is of subvolcanic nature and reflected by stocks, veins, or dikes along peripheral faults of granite porphyry, biotite monzonitic granite porphyry, biotite-quartz-monzonite porphyry, rhyodacite porphyry, and granodiorite porphyry.

Major faults primarily trend NE-SW, NNE-SSW, and N-S.

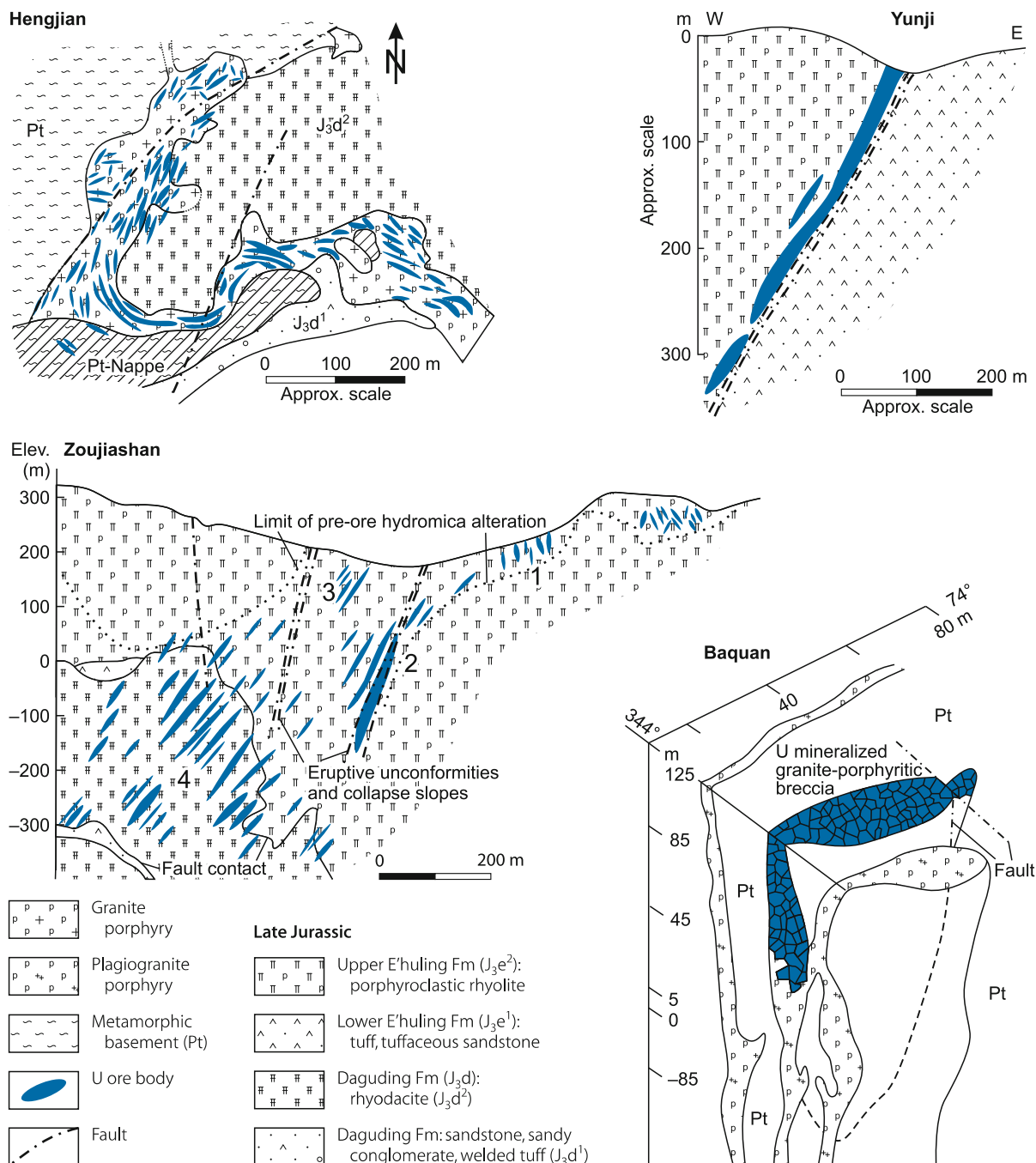
Principal Host Rock Alterations

Mineralized areas exhibit a variety of alteration phenomena. Pre-ore alteration is widespread and includes albitization, hydromicazation, kaolinitization, dickitization, montmorillonitization, and silicification. Albitization and planar distributed hydromicazation prevail. Both predate U mineralization but only slightly. Albitization is primarily found near the surface at the northern and eastern margins of the caldera where it surrounds lodes with Th-free or -poor uranium mineral assemblages. Syn-ore alteration grades from hematitization at ore lodes outwards to carbonatization and chloritization, and overprinted these albitized zones.

Planar distributed hydromicazation envelops lodes with U-Th ore near the surface in the western part of the caldera. Syn-ore alteration at this locality consists of fluoritization and linear arranged hydromicazation at the center and hematitization at the flanks. A vertical alteration zoning is identified at the western

■ Fig. 1.38b.

Gan-Hang Belt, Xiangshan Caldera, schematic geological maps and sections of typical deposits illustrating the variability of lithological settings, style and approximate dimensions of these deposits (after Zhou Weixun et al. 2006b)



margin of the caldera as reflected by replacement of planar hydromica by albitization at depths. (For alteration features associated with the various ore mineral assemblages see next chapter and description of deposits further below.)

Principal Characteristics and Distribution of Mineralization

Zhou Weixun et al. (2006b) separate various ore mineral/elemental assemblages of U mineralization in the Xiangshan OF

into two groups based on thorium presence: an early, Th-free or -poor group with U-REE, U-Mo, U/Pb-Zn-Ag, and U-P mineral assemblages; and a later thoriferous U group with a U-Th-Mo-P-REE mineral assemblage. The latter forms the most significant ore lodes in the Xiangshan ore field. An age of 115 ± 0.5 Ma was obtained by U-Pb dating of pitchblende for the Th-free/poor U group hosted in rocks altered by pre-ore albitization in contrast to 98 ± 0.8 Ma for the U-Th group hosted in rocks altered by planar hydromicization. For metallogenic considerations see previous Sect. *Principal Aspects of Metallogenesis*.

U-Th-Mo-P-REE assemblage (deposit examples: Zoujiashan, Hengjian). In addition to the afore listed elements, mineralization contains small amounts of Be, Cd, Ni, Pb, Sn, Sr, and Zn. The total REE content ranges from 323 to 9 050 ppm; HREE predominate. Pitchblende, Th-bearing pitchblende with up to 12% ThO₂, and brannerite are the principal U minerals. Other radioactive minerals include coffinite, Th-bearing brannerite, uraniferous titanate, wisaksonite, uraniferous thorite, uraniferous auelite, auelite, uraniferous apatite, thorite, and thorianite. Sulfide minerals are common and include pyrite, marcasite, molybdenite, and ilsemannite. Host rocks are altered by hydromicazation and fluoritization, which were often overprinted by collophanization.

Deposits with the U-Th-Mo-P-REE assemblage occur preferentially in the western and northern sections of the Xiangshan complex and are controlled by NE-SW-striking basement faults that intersect annular structures of the caldera.

U-REE assemblage (example: Baquan). Mineralization consists of pitchblende and traces of brannerite associated with pyrite and minor Pb-, Zn-, and Cu-sulfides. Ore averages about 815 ppm REE with a dominance of LREE. This assemblage occurs mainly at the northern margin of the ore field, in a part overthrust by a Precambrian nappe. Deposits are located at the intersection of NE-SW-trending faults with annular faults. Ore bodies are hosted in explosive breccia pipes or at the exocontact of granodioritic porphyry. Host rock alteration includes albitization and chloritization.

U/Pb-Zn-Ag assemblage (examples: Shazhou, Niutoushan). U mineralization is spatially associated with Pb-Zn-Ag mineralization. Pitchblende is the predominant U mineral. Pb and Zn ore bodies consist of galena and sphalerite; Ag is present in galena in the form of globules of native silver and cerargyrite. REE content is about 0.1% with HREE higher than LREE. Host rocks are altered by albitization and carbonatization. Deposits with the U/Pb-Zn-Ag assemblage occur at the NE (*Shazhou*) and SW margin (*Niutoushan*) of the caldera.

U-Mo assemblage. Mineralization includes almost Th-free pitchblende associated with pyrite, molybdenite, and rare Pb- and Zn-sulfides. Mo content can be as much as 0.2–0.3%. REE tenor averages about 550 ppm. Ore lodes occur in N-S-trending fracture zones within albitized and hydromica-fluorite altered rocks. Deposits with this assemblage are found to the north of the Niutoushan deposit at the western edge of the caldera where they occur within a rhombic block framed by NE-SW- and NW-SE-trending faults.

U-P assemblage (example: Yunji). Uranium is present as almost Th-free pitchblende. Associated metallic minerals include pyrite and minor galena, sphalerite, and molybdenite. Phosphorous content is relatively high with 3–8% P₂O₅ and reflected by authigenic small crystalline apatite. REE average 260 ppm. N-S-oriented fracture zones in albitized rocks that exhibit increased contents of chlorite, apatite, and carbonate minerals control ore lodes. Deposits of U-P assemblage occur in the eastern caldera.

Deposits of the various mineral assemblages are controlled by fault/fracture zones and often by intersections of major faults. Host rocks include porphyroclastic rhyolite lava, rhyodacite, subvolcanic porphyry bodies, crypto-explosive breccia, and to a minor degree metasediments and sediments adjacent to subvolcanic porphyry bodies.

Deposits consist predominantly of steeply dipping veins and lenses, and locally of pods. The former range from a few 10s to a few 100s of meters in length, 1–8 m in thickness, extend over vertical intervals of 300–400 m and occur locally to depths of 920 m.

Potential Sources of Uranium

Volcanic and some basement lithologies are thought to have provided potential sources of uranium during ore-forming processes. Volcanic rocks have background U values ranging from 3.14 to 8.8 ppm, averaging 4.82 ppm. U values tend to increase from first stage rhyodacite (3.92–4.35 ppm U, 21.68–21.50 ppm Th) to second stage porphyroclastic rhyolite (6.46 ppm U, 23.6 ppm Th), which forms the major part of the Xiangshan complex, and to late rhyodacitic porphyry (6.07 ppm U, 22.27 ppm Th). Basement lithologies with relatively high U tenors include Caledonian gneissic granite and metasomatic schist with 9.74 and 7.03 ppm U, respectively (Zhou Weixun et al. 2006b).

1.4.2.1.1.1 Hengjian (#611)

Hengjian (📍 Figs. 1.38a,b) occurs at the west end of the same nappe as the Baquan deposit (see below) (📍 Fig. 1.38a). The deposit consists of a group of lenticular ore bodies that are mainly controlled by fissure zones in granite porphyry, and less in adjacent Upper Jurassic sandstone and conglomerate, and Sinian mica-quartz schist. Mineralized fissure zones stretch in an arc along the NE, SE, and SW contact of the porphyry body. Mineralized zones strike parallel to the porphyry contact but dip with 60–70° in the opposite direction. These zones extend 1000 m along strike and 150 m down dip. Alteration includes early stage albitization with secondary hematite mainly in exocontact and late stage hydromicazation prevailing in intracontact fissure zones. Uranium is present as pitchblende and brannerite. Associated metallic minerals include pyrite, hematite, molybdenite, galena, sphalerite, and siderite. Gangue minerals are hydromica, quartz, fluorite, albite, calcite, and baryte.

Individual lenses are a few meters to several tens of meters long and 0.3 to a few meters in thickness. The largest are 260 m to about 350 m long, 1–10 m thick, and persist for 100 m down-dip. Grades range between 0.1 and 0.5% U.

1.4.2.1.1.2 Zoujiashan Deposit (#612)

This deposit (📍 Figs. 1.38a,b) lies in Lean County, Jiangxi Province. It is situated in the mid-western part of the Xiangshan

Caldera. Explored resources are in excess of 10 000 t U at grades of 0.1–0.3% U. Mining is by underground methods (status 2003).

The ore-hosting Upper Jurassic volcanic suite is divided into the Ehuling Formation, which outcrops at the deposit, and the subjacent Daguding Formation. The Ehuling Formation comprises an Upper Member of rhyolitic porphyroclastic lava and a Lower Member of rhyolitic ignimbrite and tuffaceous sandstone. The Daguding Formation includes an Upper Member of rhyodacite and a Lower Member of ignimbrite and purplish sandy conglomerate.

The deposit is located at the conjunction of two prominent fault zones trending NE-SW and NW-SE. Mineralization is hosted in rhyolitic porphyroclastic lava and rhyodacite along the NE-SW fault and off-branching, sub-meridional subsidiary fractures.

Among the earlier mentioned alteration phenomena, hydromica is a ubiquitous alteration product formed during three stages. Pre-ore hydromica has a greyish green color, replaces felsic matrix and phenocrysts of the volcanic parent rock, and occurs along the NE-SW-trending fault zone and its subsidiary faults. Ore-stage hydromica is dark grey, fills the ore-hosting faults and fissures, and replaces the wall rocks in association with pitchblende, fluorite, and sulfides. Post-ore hydromica is light green and occupies post-ore fractures.

Radioactive minerals comprise pitchblende, Th-bearing pitchblende, thorianite, and U-bearing thorite. Associated metallic minerals include jordisite, molybdenite, pyrite, galena, and chalcopryrite, and a gangue of hydromica, fluorite, and minor apatite. Mineralization is dated at 100 Ma.

The deposit comprises four major ore zones; OZ-4 is the largest one. Ore zones consist mainly of veins of variable dimensions and some stratiform ore lodes. Veins are bifurcating and coalescing along both strike and dip, and occur in clusters. Veins persist to depths of 920 m in OZ-4. Small ore bodies are tens of meters to about 100 m in length and 1–3 m in thickness while large ore bodies are 100–130 m in length and 5–8 m in thickness.

1.4.2.1.1.3 Baquan (#617)

Baquan (Fig. 1.38a,b) is located at the northern edge of the Xiangshan Caldera where a nappe of Precambrian basement is thrust over Jurassic volcanics of the Daguding Formation. Ore bodies occur in the western section of the nappe, mainly within a granite-porphyrific breccia pipe and less in intruded Sinian metasediments. This pipe and others occur at the intersection of a NE-SW-oriented fault with an annular fault system. Granite porphyry was intruded into these annular faults, followed by plagiogranite porphyry. The intrusion of the latter generated explosive pipes composed of granite-porphyrific breccia.

The mineralized pipe has an E-W-elongated diameter, 80 m long, is 40 m wide in maximum, and extends to a depth of about 190 m. The pipe consists of granite porphyry fragments, cemented with rock powder. Alteration is mainly reflected by albitization that has increased the Na₂O content of altered rock up to 6–8%. Uranium occurs in the powdery matrix in the form of pitchblende and brannerite. Associated minerals include

hematite, pyrite, molybdenite, galena, sphalerite, chalcopryrite, as well as albite, chlorite, and calcite. Ore grades average about 0.16% U at upper levels and 0.063% U at depth.

1.4.2.1.1.4 Yunji (#628)

This deposit (Fig. 1.38a,b) is located along the arc-shaped eastern fault zone (F1) that surrounds the collapsed center of the Xiangshan volcano. Uranium mineralization is hosted in albitized porphyroclastic rhyolite along a fissure zone in the hanging wall of fault F1. Albitization is most intense in the core of this zone from where it decreases outwards. Rocks in the core are transformed into albitite without any texture of the parent rock. Uranium is present as pitchblende, brannerite, and coffinite. Associated minerals include hematite, albite, apatite, and calcite with minor pyrite, galena, and sphalerite.

The above mentioned fissure zone is discontinuously mineralized over a N-S length of 4 km and a width of 10–40 m, locally with maxima of 100 m. Major ore bodies have the same attitude as the F1 fault. Most ore bodies are from several tens of meters to slightly more than 100 m long and 1–10 m thick. The largest ore body is 627 m long, 1–24 m thick, and persists for 350 m downdip. Grades range from 0.05% to 0.32% U and average 0.115% U.

1.4.2.1.1.5 Shazhou (#615) and Niutoushan

These two deposits (Fig. 1.38a) are attributed by Zhou Weixun et al. (2006b) to the U-Pb-Zn-Ag assemblage and consist of U mineralization spatially associated with Pb-Zn-Ag mineralization. U is mainly present as pitchblende; Pb-Zn lodes consist of sphalerite and argentiferous galena (see Sect. *Principal Characteristics of Mineralization*). Host rocks are altered by albitization and carbonatization.

Shazhou (615) is located at the NE margin of the Xiangshan Caldera (Fig. 1.38a). An E-W-oriented subsidiary fracture zone within E-W-trending granite porphyry hosts ore lodes. U ore bodies roughly coincide with Pb-Zn-Ag ore bodies.

Niutoushan is situated at the SW margin of the caldera. NE-SW-oriented fracture zones in porphyroclastic rhyolite that is cut by NE-SW faults control ore lodes. U lodes occur separated from Pb-Zn-Ag ore bodies.

1.4.2.1.2 Shengyuan/Yingtang Ore Field, Jiangxi

The volcanic Shengyuan or Yingtang ore field is in the Shengyuan (also referred to as Shunyuan) Basin in Guixi County, NE Jiangxi Province, near the town of Yingtang (and therefore also named Yingtang OF by miners). The downwarped basin covers in excess of 300 km² and hosts three U deposits, *Guixi (65)*, #60, and #70 (Fig. 1.39a). The first deposit, Guixi, was discovered in 1956. Mining began in the 1970s by open pit methods.

Sources of information. Chen Zhaobo 1980; Chen Zhaobo et al. 1979; Malan 1980; Wang Chuanwen et al. 1980; Zhou Weixun 2000.

General Geology and Mineralization

Upper Jurassic rhyolite ignimbrite and tuff layers alternating with fluvial sandstone are exposed at the margins of the Shengyuan Basin. These rocks overlie a pre-Devonian metamorphic basement. Cretaceous redbed sandstones and conglomerates cover much of the central part of the volcanic complex. Granitic stocks of Caledonian age outcrop near the southern margin of the basin.

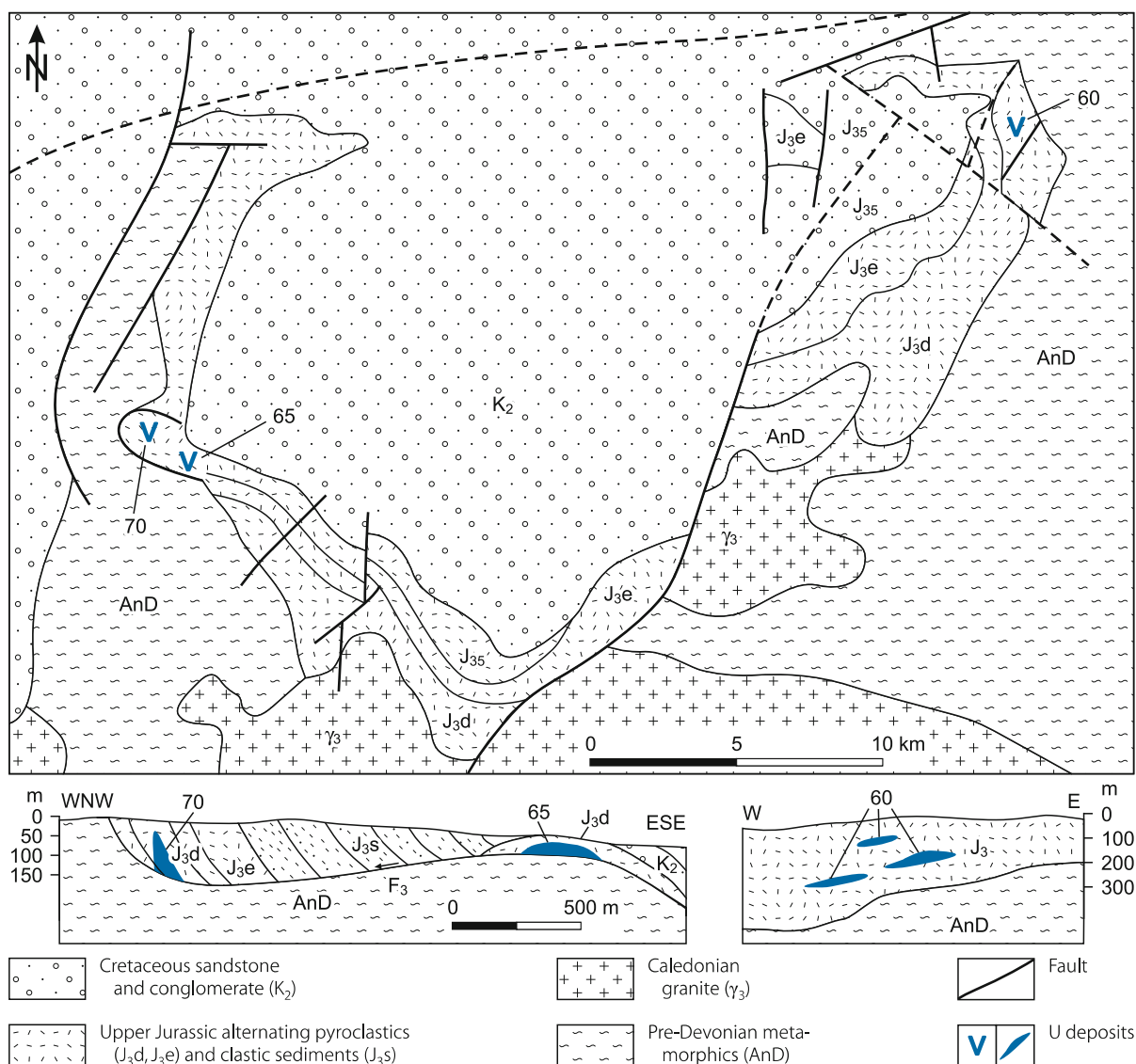
Deposits consist of tabular to lenticular ore bodies in Upper Jurassic alternating volcano-sedimentary rocks, such as

ignimbrite and tuffaceous sandstone. Ore bodies are 20–300 m long and 1–7 m thick and are enveloped by well-developed dickitization of wall rocks.

Deposits #65 (see below) and #70 are located at the western margin of the basin in a tectonic nappe, 2 km² in size that has been displaced along a low angle thrust fault. #70 (Figs. 1.39a,c) is some 1 500 m west of the #65 deposit and has similar features to #65 but has less resources and U mineralization occurs at greater depths of 50–150 m. Ore is composed of pitchblende and subordinate coffinite and brannerite, associated with abundant fluorite and moderate amounts of jordisite. Wall rocks are extensively altered by silicification, dickitization, and illitization. Early stage alteration products also include typical hypothermal minerals such as topaz and prosopite.

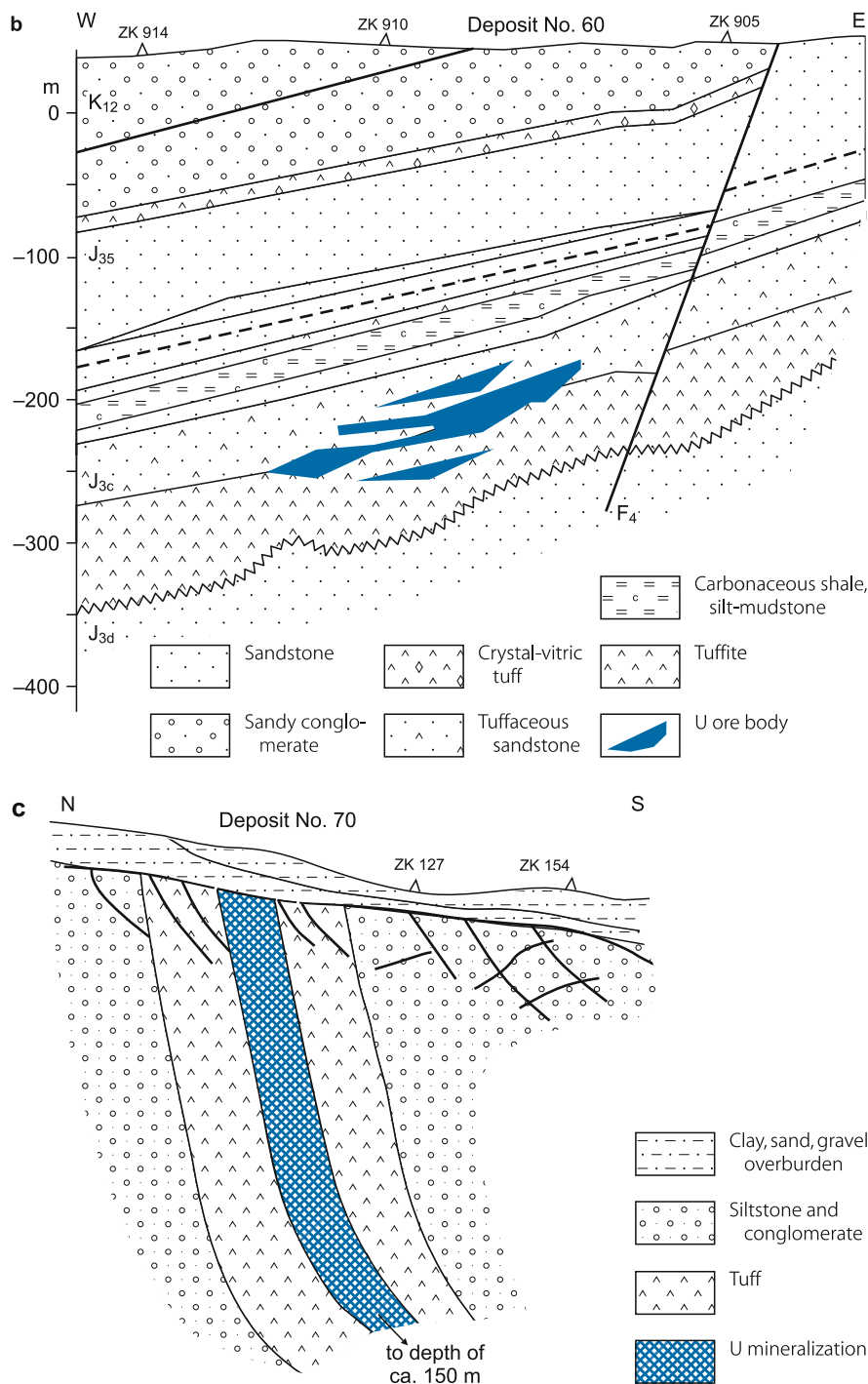
Fig. 1.39a.

Gan-Hang Belt, Shengyuan Basin, Shengyuan/Yingtian OF, generalized geological map and sections with location of U deposits. (Note: all scales are approximate) (after Malan 1980; Wang Chuanwen et al. 1980)



■ Fig. 1.39b,c.

Gan-Hang Belt, Shengyuan/Yingtian OF, sections of deposits **b** #60 and **c** #70 with position of U ore bodies (after **b** Chen Rhanzi and He Caiyi 1996 based on Geological Party no. 265, **c** Li Wenxing 1990)



Deposit #60 (► Figs. 1.39a,b) is situated at the eastern margin of the basin. Uraniferous colophane is the principal ore mineral. It was formed on a large scale at an early stage and was overprinted by smaller scale U-Mo mineralization. This deposit contains several superjacent U ore lenses in tuffaceous sandstone and tuffite at depths of about 230–300 m. These

units occur in the basal section of a Jurassic sequence of carbonaceous shale, silt-mudstone; sandstone; sandy conglomerate; tuffaceous sandstone; tuffite; crystal-vitric tuff; and pebble-bearing tuffaceous sandstone (Section #9 of deposit #60, Geol. Party #265 cited by Chen Rhanzi and He Caiyi 1996).

1.4.2.1.2.1 Guixi Deposit (#65), Jiangxi

The stratiform volcanic-type Guixi deposit (►Fig. 1.39a) lies in Guixi County, Jiangxi Province. It is situated in the western part of the Shengyuan Basin. Original resources were in the 500–1 500 t U category at grades of 0.1–0.3% U. The deposit was mined by an open pit operation and is depleted.

Source of information. Zhou Weixun 2000.

Geology and Mineralization

Locally outcropping basement rocks comprise Precambrian metamorphosed schist, Cambrian carbonaceous slate, Early Paleozoic/Caledonian granite, and Upper Triassic clastic sediments. Cover lithologies include Upper Jurassic volcanic and sedimentary rocks and Cretaceous clastic sediments.

The Daguding Formation forms the upper part of the Upper Jurassic. This formation is four-partitioned into an Uppermost Member of purplish red basaltic andesite; an Upper Member of purplish red siltstone, sandy conglomerate, and intercalated tuff; a Middle Member of greyish white ignimbrite; and a Lower Member of purplish red sandy conglomerate and siltstone.

A nappe of Upper Jurassic and Lower Cretaceous rocks had been thrust at the end of Early Cretaceous upon the Precambrian basement at the western edge of the basin along a NE-SW-striking, 23–32° NW inclined thrust fault (F_3). A N-S normal fault (F_1) trends along the eastern end of the nappe. Upper Cretaceous redbeds were deposited subsequently. U mineralization is restricted to a fractured and jointed ignimbrite horizon of the Middle Member in the basal, southern part of the nappe westerly adjacent to the F_1 fault.

Host rock alteration is dominated by two stages of dickite. Pre-ore dickite replaces feldspar phenocrysts and felsic matrix of ignimbrite; while ore-stage dickite cements fragmented ignimbrite or fills fissures to form ore-bearing veins/veinlets.

Mineralization consists of pitchblende, coffinite, and brannerite, associated with sulfides, hematite, dickite, fluorite, hydralite, apatite, and bituminous matter. A U/Pb age of 90 Ma that is thought to reflect the time of ore formation has been obtained for pitchblende.

Two ore bodies are delineated at depths between 20 and 50 m; the eastern ore body is lens-shaped, more than 20 m long, 2–3 m wide, and 3 m thick; the west one is blanket-shaped, 300 m long, 50 m wide, and 5.5 m thick on average.

1.4.2.1.3 Xiaoqiuvuran Ore Field, Dazhou Basin, Zhejiang

The Xiaoqiuvuran (Xiaoqiuyuan?) ore field is located in the Dazhou Basin in western Zhejiang Province and contains several deposits such as *Dachayuan* (661), *Leigongdian* (663), and #665. All deposits are hosted in the same strata and have the same features. The largest deposit is *Dachayuan*. None of these deposits in the Dazhou Basin has been mined.

The downfaulted Dazhou Basin is located in the Gan-Hang volcanic belt close to the intersection with the northern end of the Wuyi volcanic belt. The Xiaoqiuvuran ore field is situated in the north part of the basin where the basin-controlling NE-SW fault produced several NW-SE derivative faults, the latter of which control the distribution of U deposits.

U mineralization occurs in six Upper Jurassic rhyolite layers of near-crater eruption overflow facies. Thin tuffaceous clastic sediments separate the rhyolite layers. This sequence rests upon metamorphic basement. Ore bodies are confined to fractured intervals at the roof and bottom of the rhyolite layers (Chen Ranzhi and He Caiyi 1996).

Wall rock alteration is widespread and occurs mainly in form of hydromicazation. Most ore bodies are of lenticular shape, 500–800 m long, 1–35 m thick, and persist to depths of 450 m (Zhou Weixun 2000).

1.4.2.1.3.1 Dachayuan Deposit (661), Zhejiang

This deposit lies in the northern Dazhou Basin, within a block limited to the north by an E-W-trending fault (F_1) and to the south by the WNW-ESE-oriented *Dachayuan* fault.

Ore bodies are stratiform and are primarily hosted in fissure zones at the roof and bottom of the (from bottom to top): 1st, 2nd, and 3rd rhyolite horizons (for details see previous chapter).

Hydromicazation is the major alteration phenomena and formed at 3 stages. Pre-ore hydromicazation is mainly developed in pyroclastic interbeds and at the top and bottom of the rhyolite horizons, forming so-called green-altered zones. These zones are thought to have exerted a sealing effect on the ascending mineralizing fluid. Ore-stage hydromicazation resulted from hydrothermal activity within the fissure zones beneath the aforementioned green-altered zones. Post-ore hydromicazation produced jade green or yellowish green hydromica in post-ore fissures.

Ore bodies are hosted in zones altered by ore-stage hydromicazation and hematitization. The latter imprinted a reddish hue on the rock. The redder the ore, the higher the U grade.

Mineralization consists of pitchblende and brannerite, associated with hematite, pyrite, sphalerite, molybdenite, hydromica, fluorite, and microcrystalline quartz.

Ore bodies are commonly 500–700 m long, 1–33 m thick, and occur over a vertical interval of about 440 m (from 100 m to 540 m deep). Grades vary between 0.08 and 0.15% U (Zhou Weixun pers. commun. 2004).

1.4.2.2 Wuyishan Volcanic-Granitic Belt, S Jiangxi-W Fujian

The Wuyishan (or Wuyi) magmatic belt trends in NNE-SSW direction roughly along the boundary between Jiangxi and Fujian Provinces. It connects with the Gan-Hang Belt at its northern end and intersects the Nanling magmatic-tectonic belt at its southern extremity. The Wuyi Belt contains a number of U occurrences predominantly of vein/stockwork nature associated

with diatremes; and some strata-structure controlled U occurrences in pyroclastic and effusive layers including *Chaigan*, Guangdong Province, and *Shiyuanlong*, Fujian Province. Only two U deposits were reportedly mined, *Maoyantou* in N Fujian and *Caotaobei* in central-south Jiangxi.

Other ore fields with U occurrences mentioned in the literature include *Baimianshi* and *Hecaokeng*. *Baimianshi* (also reported as *Baimeishi*) is attributed by some geologists to the basal-channel sandstone type and by others to the volcanic type since some U showings occur in rhyolite.

Additionally, there are other metallic deposits that have some associated uranium such as the Zijinshan Cu deposit, SW Fujian, with some U mineralization related to rhyolite, and polymetallic deposits in the Wuyishan ring structure, Jiangxi-Guangdong-Fujian.

Most of the U deposits/occurrences in the Wuyishan magmatic belt have apparently only small U resources in the tens to hundreds of tonnes U range at grades ranging from 0.03 to several tenths of a percent.

Sources of information. Chen Ranzhi and He Caiyi 1996; Wang Yusheng and Li Wenjun 1996; Zhang Zuhuan 1990; Zhou Weixun, pers. commun. 2004; unless otherwise cited.

Regional Geology and Mineralization

The Wuyishan metallogenetic belt differs from the Gan-Hang Belt by its geotectonic position, basement lithologies, lithochemistry and younger age of volcanics, deposits typology, and less favorable U ore-forming conditions, except for U deposits hosted by cryptoexplosive breccia pipes/diatremes. In essence, the Wuyishan Belt does not constitute so much a volcanic-related U terrane but rather a granite one (Chen Ranzhi and He Caiyi 1996).

The Wuyishan metallogenetic belt correlates with the Middle Yanshanian (Late Jurassic-Early Cretaceous) Wuyishan granitic-volcanic zone within the South China Caledonian fold system. Autochthonous-subautochthonous migmatitic metasomatic granites, metasomatic-intrusive granites, and intrusive granites of Caledonian, Hercynian, and Indosinian origin constitute large parts of the basement.

The Wuyishan zone originated during Middle Yanshanian, Circum-Pacific orogenic movements that intensely reactivated regional deep faults trending NE to NNE. Movements along these regional faults accompanied by contemporaneous magmatic activity produced a belt of widespread hypabyssal intrusive granitic, subvolcanic, and effusive rocks. Volcanism postdated the emplacement of these Yanshanian granites.

The Paleozoic and Mesozoic granites include widespread exposed U-rich facies that are thought to be a significant U source. Chen Ranzhi and He Caiyi (1996) demonstrate the U fertility of these granites by examples from the *Hecaokeng* ore field where discrete granite facies average 14.6 ppm U, and the *Baimianshi* ore field where granites contain up to 18.6 ppm U. The authors also document a gradual increase of the mean U tenor from earlier to later stage granites in southern Jiangxi: Unaltered Caledonian granite contains 8.94 ppm U, Indosinian

10.2 ppm U, and Yanshanian granite 14.64 ppm U. Much of this uranium occurs in the form of uraninite.

Volcanic terrane is relatively sporadic in the Wuyishan Belt. As discussed earlier, volcanic activities began later in this belt than in the western part of the Gan-Hang Belt and were mostly of bimodal nature. Volcanic facies are dominated by intermediate to mafic litho-chemistry consisting mainly of andesite and andesitic basalt with minor rhyolitic facies. Small volcanic bodies such as subvolcanic stocks and volcanic vents with associated cryptoexplosive breccias are a typical feature in the Wuyishan Belt; they have been formed during late stage volcanic activity along NE- and NNE-trending deep faults at the intersection with other faults. In excess of 10 pipes have been identified so far (Chen Ranzhi and He Caiyi 1996).

Taphrogenetic zones controlled by the earlier mentioned regional faults evolved during Late Yanshanian tectogenesis. Repeated reactivation of this tectonic regime ultimately resulted in an uplifted block of a general NNE-SSW direction, bordered by the Yingtan-Auyuan and Ninghua-Wuping faults to the northwest and southeast, respectively, that correlates with the Wuyishan Belt. The Shaowu-Ruijin-Xunwu deep fault transects this block obliquely and formed a number of subsidiary uplifts and depressions.

Principal Characteristics of Mineralization

Volcanic U deposits are mainly controlled by small subvolcanic intrusions and are closely related to taphrogenetic zones that are controlled by the earlier mentioned regional faults and had evolved during Late Yanshanian tectogenesis.

Although a few U deposits such as *Chaigan* in Guangdong Province, and *Shiyuanlong* in Fujian Province, consist of lenticular to tabular ore bodies hosted in specific volcanic horizons, deposits of uranium e.g. *Caotaobei* as well as nonferrous, rare and precious metals in the Wuyishan metallogenetic belt are primarily related to small subvolcanic stocks and cryptoexplosive breccia pipes. Breccias and fractures generated by cryptical explosions not only provided migration pathways for ore forming fluids but also favorable spaces for ore deposition.

Deposits consist of discontinuous, complex pipe-, lump-, or arborescent-shaped ore bodies with an internal stockwork structure. Ore bodies are commonly steeply dipping, and are highly variable in lateral and vertical extension. Persistence along dip is longer than along strike. An irregular alteration halo surrounds the ore bodies.

Wang Yusheng and Li Wenjun (1996) postulate that volcanic events with cryptoexplosive breccia and associated mineralization are related to subvolcanism and pneumatolytic-hydrothermal activity. These diatremes occur in areas with a relatively uplifted, U-rich granitic basement, subvolcanic complexes, deep basement faults and their intersections with large volcanic complexes.

According to Zhang Zuhuan (1990), the time of ore formation is close to that of the volcanic extrusion. The uranium source seems to be granitic complexes. The volcanics provided only the site of U deposition. U transport was by meteoric waters.

Selected Districts and Deposits in the Wuyishan Belt

In addition to the below described U deposits, there are several other small deposits/occurrences mentioned in literature including *Shiyuanlong* (SYL), which is an explored small deposit in Fujian Province consisting of tabular ore bodies controlled by fracture zones at the interface between volcanic ash-flow and turbidite lithologies (Wang Yusheng and Li Wenjun 1996).

1.4.2.2.1 Maoyangtuo Deposit (#570), Fujian

This deposit (Fig. 1.40) is associated with the *Maoyangtuo diatreme* at the western edge of the *Fuluoshan Caldera*, near Pucheng City, N Fujian. The caldera is collapsed into Yanshanian U rich granite and filled with Upper Jurassic-Lower Cretaceous intermediate-felsic volcanic rocks. The collapse took place after a J_3 intermediate-felsic magma explosion and was followed by K_1 volcanism along an arc-shaped fracture zone (F_1) at the NW edge of the caldera that formed several diatremes. Maoyangtuo, which is one of the larger diatremes, is of lenticular configuration in planview. It is confined by a NE-SW-trending, arc-shaped fault (F_1) on the NW side that is filled with subgranitic porphyry in the form of an arc-shaped dike. Granite is widely exposed to the NW of the diatreme. A series of E-W-, NW-SE- and NE-SW-trending melanitic dykes occur close to the diatreme.

The diatreme comprises rhyolite, fragment-bearing rhyolite, and minor subgranitic porphyry in which mineralization is related to NE-SW-, NW-SE-, and E-W-striking faults.

Pre-ore hydromicazation covers the entire diatreme complex. Ore-related hydromicazation includes two stages: early ore-stage hydromicazation is associated with hematitization and is distributed in the hanging and footwall blocks of fracture zones, whereas late ore-stage hydromica occupies fracture-fissure zones in the form of black veins of pitchblende, sulfide, and hydromica.

Mineralization consists of pitchblende, coffinite, and uraniferous jordisite and uraniferous anatase, associated with colloidal pyrite, molybdenite, galena, chalcopyrite and sphalerite. Gangue minerals include quartz, fluorite, hydromica with minor chlorite, and calcite.

Ore bodies are mostly small and often of complexly structured veins, stockworks, lenses, pods, and arborescent-shaped lodes; veins and lenses predominate. Dimensions can range from 10 m to an exceptional 231 m in length, from 10 m to 252 m downdip, and 1–8 m in thickness. Grades are on the order of 0.3–0.4% U (Zhou Weixun, pers. commun. 2004).

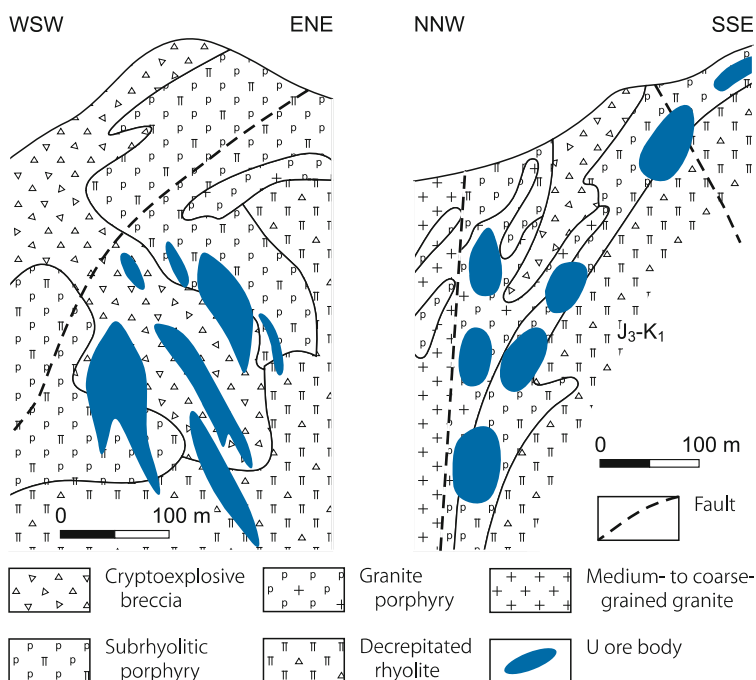
1.4.2.2.2 Wuyishan Ring Structure, Jiangxi-Guangdong-Fujian

The Wuyishan ring structure is a striking ring-shaped feature situated at the three corners junction of Jiangxi, Guangdong and Fujian Provinces. A group of cryptoexplosive breccia pipes containing U, W, Nb-Ta, Cu, Pb-Zn, Au, Ag, and/or fluorite mineralization occur at this ring structure.

The NW-SE-trending Shanghang-Yunxiao regional fault zone intersects the ring structure. The *Caotaobei* (#6722) U deposit is located at the NW intersection and Au-Cu-Ag, Cu-Au deposits that contain some U mineralization are located at the

Fig. 1.40.

Wuyishan Belt, Maoyangtuo (deposit 570), schematic sections showing distribution of U mineralization across the cryptoexplosive breccia pipe (after Zhou Weixun 1997)



SE intersection. The latter include the *Zijinshan* and *Bitian* Cu-Au deposits in Shanghang County, W Fujian Province, and the #430U showing close to the *Bitian* deposit. These deposits are all associated with diatremes cutting granitic basement (Wang Yusheng and Li Wenjun 1996).

1.4.2.2.2.1 Caotaobei Deposit (#6722), Jiangxi

This deposit is located in Huichang County, Jiangxi Province and hosted in the *Caotaobei diatreme* at the eastern margin of the Cretaceous downfaulted redbed *Huichang Basin*. The diatreme is elliptic in planview with a size of 450×350 m², irregular funnel-like in profile, and cuts Early Yanshanian uraniumiferous granite (10–20 ppm U).

The diatreme is filled with amphibole trachytic andesite and surrounded by a breccia zone. The breccia zone is 10–200 m wide and consists of cataclastic granitic breccia in the upper section that grades outwards and downwards into shattered granite; the latter persists to depths of 300–500 m. A series of later faults trending NE-SW and NNE-SSW as well as E-W-striking fissure zones cut the complex.

U mineralization occurs in cataclastic granitic breccia, shattered granite, and fractured trachytic andesite in the cone and volcanic neck of the volcanic apparatus within which it is controlled by NE-SW-striking major fault zones.

Granite, andesite, and Cretaceous red sandstone are mainly altered by pre-ore silicification. Ore-stage alteration is dominated by hydromicization in association with hematite, fluorite, and sulfides. Epigenetic alteration is quite intense, forming a violet colored oxidation zone that grades downwards into a green colored reduction zone; secondary enriched ore lodes occur along the interface of these two alteration facies.

U minerals include pitchblende and coffinite, associated with hematite, pyrite, minor marcasite, chalcopyrite, galena, hydromica, fluorite, chlorite, calcite, and quartz. Ore bodies are of lens, pod, nest, and arborescent shape, extend for 20–100 m in length, 2–10 m in thickness (maximum 20 m), and 20–120 m downdip at an angle of 15–20°. Grades vary within a range of 0.1–0.3% U (Zhou Weixun, pers. commun. 2004).

1.4.2.2.3 Renchai Basin, E Guangdong Province

Situated near the town of Pingyuan in eastern Guangdong Province, the volcanic Renchai (Rencha) Basin is at the intersection of the south end of the Wuyishan Belt with the Nanling zone (see Sect. 1.4.1: *Granite-Dominated Domain/Granitic Complexes and Related U Deposits*). The Renchai Basin is a downfaulted basin containing several U occurrences including deposits #278 and 279. *Deposit #278* is located in the southern Renchai Basin. Ore bodies occur in veins at the intersection of a WNW-ESE fault and a subrhyolite porphyry body.

Sources of information. Wang Yusheng and Li Wenjun 1996; Zhou Weixun, pers. commun. 2004.

1.4.2.2.3.1 Chaigan Deposit (#279), Guangdong

This deposit is located in the northern Renchai Basin, eastern Guangdong Province, in the eastern Nanling magmatic belt. Explored resources are presumably several hundreds of tonnes U at grades of 0.05–0.12% U.

Uranium occurs in an Upper Jurassic-Lower Cretaceous volcanic suite (J₃-K₁) that rests unconformably upon a basement of uranium-rich granite. The volcanic suite includes three units formed by three volcanic cycles. The oldest unit comprises basalt, andesite, rhyolite, and pyroclastic rocks. The intermediate main unit includes four members – from bottom to top: (1) a grey-reddish rhyolite tongue, (2) green gravel-bearing tuff, (3) violet welded tuff, and (4) grey crystallinoclastic tuff. Uranium mineralization is mainly hosted in green gravel-bearing tuff and the roof of the rhyolite tongue, less in grey crystallinoclastic tuff, while strongly welded violet tuff is barren. The youngest unit/cycle consists of felsic and mafic volcanic dikes. Redbeds (K₂) cover the volcanic rocks.

U mineralization occurs at the intersection of a NNE-SSW-trending main fault with a NW-SE-trending silicified zone and diabase dikes. Ore lodes consist of short veins and stockworks controlled by fractured intervals within the aforementioned layers, which are altered by strata-bound hydromicization. Ore bodies are lens-shaped, 30–200 m in length, 1–17 m in thickness, and persist from 5 m to 400 m below the surface.

1.4.3 Proterozoic-Paleozoic Terrane and Related C-Si-Pelite U deposits/Western U Metallogenic Domain

The Western Domain (Fig. 1.27) is known for *black shale-related stockwork* U deposits [in China referred to as carbonate-siliceous-pelite (C-Si-pelite) type with several subtypes as outlined further below] that occur in several Sinian-Early Cambrian basins predominantly in the *Xuefeng-Jiuling* U zone in the western Jiangnan Uplift; and scattered in the Late Paleozoic *Xianggui* Depression, in central-southern Hunan-northern Guangdong-southern Guangxi A.R. Significant deposits include *Chanziping*, *Jinyinsha*, *Bentou*, and *Daxin*, and some deposits in the *Xiushui (XS) ore field*. A similar deposit, *Baimadong*, has been discovered in a separate basin in SW Guizhou. (Note: names in brackets given in text were used as synonyms in former publications.)

Sources of information. Ju Yejun et al. 1990; Min MZ 1995; Zhang Zuhuan 1990; Zhou Weixun 1988, 1996, 2000, pers. commun. 2003; Yao et al. 1989; unless otherwise cited.

Principal Modes of C-Si-pelite-type Mineralization

C-Si-pelite-type U mineralization occurs in Sinian and Paleozoic sediments. Based on host rock facies, Yao et al. (1989) differentiate three lithological settings of C-Si-pelite-type U mineralization:

pelite, carbonate, and silicolite (also referred to as silicic breccia type). Deposits of these types occur strata-bound and structure controlled primarily in carbonaceous pelitic (more or less black shale) or siliceous carbonatic strata.

Three principal genetic modes of mineralization are defined: sedimentary-diagenetic (only small occurrences), phreatic infiltration (or leaching-accumulative), and, as economically the most important, hydrothermal-reworked C-Si-pelite U mineralization. The basic characteristics of these modes in South China are summarized below.

Regional Geological Setting of C-Si-pelite U Deposits

C-Si-pelite-type U deposits occur in weakly to unmetamorphosed argillaceous limestone, dolomite, and siliceous and carbonaceous mudstones. These strata were deposited during the Neoproterozoic and Cambrian along the margin of the *Jiangnan Uplift*, and during Devonian, Early to Middle Carboniferous, and Early Permian in the Late Paleozoic *Xianggui Depression*. At the Jiangnan Uplift, the U-hosting rocks rest upon volcanosammitic-pelitic metasediments of the Middle Proterozoic Jiuling and Upper Proterozoic Banxi or equivalent groups; and in the Xianggui Depression they overlie a Caledonian basement as outlined earlier.

Granite was intruded into the Paleozoic sediments during the Caledonian, Indosinian, and Yanshanian orogenies, and intermontane basins were downfaulted in various parts of the western domain during the Cretaceous-Tertiary.

Uranium is primarily hosted by two litho-stratigraphic series: *Firstly* by Late Sinian and Early Cambrian clastic and volcanogenic sediments deposited in shallow seas adjacent to the Jiangnan Uplift. These strata are enriched in silica, clay, organic carbon, and have U Clarke values ranging from 6 to 70, and locally to more than 100 ppm U; they constitute the most significant uraniferous rocks in S China. A *second* uraniferous lithologic sequence consists of Late Paleozoic shallow marine and lagoonal clastic sediments with background tenors of 3–30 ppm U; it occurs in the Xianggui Depression to the SE of the Jiangnan Uplift.

Principal Characteristics of Mineralization and Alteration of C-Si-pelite U Deposits

The three principal genetic modes of U mineralization mentioned earlier exhibit characteristics as described below (stratigraphy and host rock facies modified after Zhang D 1982 in Min MZ 1995). Economic U deposits are controlled by structures and lithologies (strata-bound, structure controlled type), and occur commonly near the margins of granite intrusions and/or near the interface of intermontane Cretaceous-Tertiary downfaulted basins with redbed sediments.

a *Sedimentary-diagenetic (with infiltration) C-Si-pelite U mineralization* consists of syngenic U accumulations in Late Sinian siliceous pelite overprinted by diagenetic and infiltration/redistribution processes; hence mineralization in

ore and host rocks is practically identical and consists mainly of U adsorbed onto clay minerals, with rare pitchblende micro-grains along the sedimentary bedding, and pitchblende micro-veinlets that fill fractures or cut mineral grain boundaries and sedimentary bedding planes of host rocks. Associated phases include pyrite, calcite, quartz, dolomite, and clay minerals. Occurrences of this type include (stratigraphic age of host rocks in brackets): *Machizai* (Sinian).

b *Phreatic infiltration (leaching-accumulative) C-Si-pelite U mineralization* is hosted by Late Sinian siliceous-pelitic slate, dolomitic-pelitic slate, and pelitic dolomite; and Late Sinian to Early Cambrian carbonaceous-pelitic slate, carbonaceous-pelitic limestone, and carbonaceous limestone. This mineralization was formed 33–25 Ma ago, i.e. equivalent to the Himalayan Orogeny, by U redistribution as a result of supergene phreatic infiltration without obvious alteration except for oxidation (hematitization, limonitization).

U minerals comprise pitchblende, coffinite, uranospathe, autunite, torbernite, uranophane, zeunerite, uranocircite, bassetite, and tyuyamunite. Associated minerals include minor azurite, malachite, pyrite, sphalerite, and Fe oxides, as well as calcite, clay minerals, and opal. Uranium is overwhelmingly adsorbed by clay and organic matter except for some pitchblende and coffinite grains from <0.1 μm to 0.1 mm in size and the listed U⁶⁺ minerals. Mineralized veinlets are rare. Deposits/occurrences of this type include: *Huangcai* (Huangcu), and *Laowulong* (Yaxi) (both Upper Sinian-Lower Cambrian), as well as *Baitu* (Baiti) and *Baofengyuan* (Baoyan) (Cambrian) in the Xiushui (XS) ore field.

c *Hydrothermal-reworked C-Si-pelite U mineralization* is economically the most important type and occurs in Early Cambrian carbonaceous-siliceous-pelitic slate; Middle-Late Devonian dolomitic pelite, pelitic dolomite, and pelitic limestone; Early Carboniferous carbonaceous-pelitic limestone, dolomitic limestone, and dolomite; and Early Permian siliceous rock. Hydrothermal-reworked mineralization is controlled by structure and lithology and derived by convection of meteoric solutions that caused deep hydrothermal leaching and reworking of older uraniferous rocks and low grade mineralization during Yanshanian and Himalayan tectonic events as indicated by isotope ages of 140–74 Ma and 65–22 Ma, respectively. Deposits/occurrences of this type include: *Baimadong* (Cambrian), *Bentou* (Benti, Sanbaqi) (Carboniferous), *Chanziping* (Chanpi) (Upper Sinian-Lower Cambrian), *Daxing* (Daping) (Devonian), *Jinyinzha* (Permian), *Kuangshanjiao* (Kuangji) (Devonian), *Ma'andu* (Mada) (Devonian), *Shabazi* (Shabon) (Lower Cambrian), *Xiangcao* (Xiangca) (Cambrian), *Xiaojiang* (Xudou) (Permian), and *Dongkeng* (Dongka/Xiushui ore field) (Upper Sinian-Lower Cambrian).

Chanziping, Daxing, Xiangcao, Jinyinzha, and deposits in the Xiushui (XS) ore field are of more importance, followed by the Bentou, Shabazi, Kuangshanjiao, Baimadong, and Ma'andu deposits. Xiaojiang is actually a small iron deposit with U mineralization.

Note: The type attribution of several of these deposits is debated; most geologists attribute Xiangcao, Shabazi, and Ma'andu, and a few geologists also the Chanziping and

Kuangshanjiao deposits to the exocontact subtype of granite-related U deposits instead of the C-Si-pelite type. See also Sect. *Selected Districts with Granite-Related U Deposits in South China*.

Mineralization exhibits veined and micro-veined disseminated textures and is composed of pitchblende, locally coffinite, associated with commonly minor to traces of molybdenite, pyrrhotite, pyrite, marcasite, bravoite, niccolite, millerite, nickeliferous pyrite, tennantite, antimonite, sphalerite, galena, chalcocopyrite, bornite, scheelite, ullmannite, hematite, and native silver. Gangue minerals include quartz, calcite, fluorite, dolomite, and clay minerals. Silica and Fe are slightly enriched while Ca and Mg are depleted. At *Ma'andu* and *Bentou*, Ag, Mo, Pb, and Zn grades are of economic magnitude. REE are commonly enriched in ore compared to host rocks. Ores contain indigenous organic matter of sapropelic (kerogen type I) and sapropelic-humic (kerogen type II) origin as well as solid bitumens as pore fillings and in veins, and cryptocrystalline graphite. The organic carbon content in ore and host rocks ranges from 0 to 5.8 wt.-%.

Mineralization originated during several stages. An early phase is reflected by Cu, Fe, Mo, Ni, Pb, and Zn sulfides; the subsequent stage includes pitchblende and coffinite, associated with pyrite, chalcocopyrite, galena, sphalerite, calcite, fluorite, and quartz. Minor amounts of gangue minerals constitute the third stage.

Pitchblende and coffinite replace and coat preexisting sulfides. Pitchblende occurs as disseminated grains up to 1 mm in size but predominantly as veinlets 0.5–5 mm thick that occupy fissures or transect mineral boundaries. Pitchblende also rims and cements fragments of minerals and wall rocks. Unit cell dimensions a_0 of pitchblende range from 5.396 Å to 5.428 Å; and oxidation coefficients from 2.31 to 2.46.

Metallic elements group into four associations: (a) U-Ni-Pb-Zn-Cu, (b) U-Mo-Re-V, (c) U-Ag-Pb-Zn-V, and (d) U-V. Groups *a*, *b*, and *c* are typical for hydrothermal-reworked deposits, while group *d* is typical for leaching-accumulative and sedimentary-diagenetic mineralization.

Wall rock alteration is commonly weak and may include K-feldspathization and chloritization in limestone, as well as bleaching associated with formation of silicates and aluminosilicates, and oxidation of organic matter (Min MZ 1995).

Stable Isotopes and Fluid Inclusions

Ore-related pyrite has a large variance of $\delta^{14}\text{S}$ ratios in the three modes of mineralization ranging from 1.4 to -8.9‰ (mean -3.8‰) in sedimentary-diagenetic, from 5.3 to -31.2‰ (mean -10.5‰) in leaching-accumulative, and from 19.6 to -48.2‰ (mean -11.2‰) in hydrothermal-reworked mineralization. Most values are between -3.8 and -13.8‰ and hence they are on the order of $\delta^{14}\text{S}$ values from -5.4 to -17.0‰ obtained from pyrite in host rocks. This correlation implies that pyrite in both ore and host rocks has a common sulfur source, and that the sulfur in ore was essentially derived from diagenetic sulfur species in host rocks. While most of the analyzed pyrite from ore is

enriched in ^{12}S , pyrite samples from deposits situated near granite have increased ^{14}S values as found in the Shabon deposit that may indicate at least a partial derivation of sulfur from granite.

Calcite samples from the *Bentou*, *Daxing*, *Kuangshanjiao*, and *Ma'andu* hydrothermal-reworked deposits have $\delta^{13}\text{C}$ values from 1.78 to -7.04‰ with a mean of -2.52‰ , and vein calcite from *Bentou*, *Daxing*, and *Ma'andu* shows a narrow range from 1.78 to -3.19‰ similar to $\delta^{13}\text{C}$ values of 0‰ in marine carbonate. This accord is thought to reflect an exchange of carbon isotopes between mineralizing fluids and host rock carbonates.

Quartz and calcite from the above mentioned and some other hydrothermal-reworked deposits yield a wide range of $\delta^{18}\text{O}$ values for mineralizing fluids, from -7.55 to 13.92‰ and show a tendency towards lower values through time; decreasing from a range of 7.38 – 13.92‰ in early stage fluids to a range of 5.96 – 11.90‰ $\delta^{18}\text{O}$ in middle stage fluids, i.e. these values are compatible with the typical range from 5 to 25‰ $\delta^{18}\text{O}$ in connate/tectonic hypogene solutions. Calculated late stage $\delta^{18}\text{O}$ values range from -7.55 to 3.76‰ and fall within the range from -17 to 5‰ for meteoric waters. These variations of $\delta^{18}\text{O}$ values in mineralizing solutions through time are attributed to an oxygen isotope exchange between connate fluids that were activated by regional tectonic movements, and meteoric waters with an increasing contribution of the latter with time. Deposits located near granite plutons, such as *Ma'andu* and *Chanziping*, presumably also received minor hypogene-magmatic water as indicated by $\delta^{18}\text{O}$ values from 6 to 9.5‰ .

Fluid inclusions in vein quartz, fluorite, and calcite give homogenization temperatures from 90 to 310°C that are interpreted to represent the temperature of mineralizing fluids, with the deposition of primary U minerals bracketed between 100 and 180°C (Min MZ 1995).

Principal Ore Controls and Recognition Criteria

According to Min MZ (1995), C-Si-pelite U deposits in S China are lithologically and structurally controlled. Principal criteria include:

Host Environment

- Precambrian and Early Cambrian neritic clastic and volcanogenic sediments enriched in silica, uranium, clay and organic carbon
- Late Paleozoic neritic and lagoonal clastics, and volcanogenic sediments including uraniumiferous lithologies
- Granite intrusions during Caledonian and Yanshanian orogenies
- Repeated regional tectonism
- Cretaceous-Tertiary intracontinental basins downfaulted during Yanshanian-Himalayan tectonism

Mineralization

Three principal modes of C-Si-pelite U mineralization: syn-sedimentary, epigenetic hypogene-tectonic hydrothermal, and supergene referred to as sedimentary-diagenetic, hydrothermal-reworked, and leaching-accumulative types of U occurrences:

- Synsedimentary-diagenetic mineralization consists of strata-bound, adsorbed U with minor diagenetic modification
- Epigenetic U mineralization is structurally controlled-strata-bound, principally governed by
 - brittle structures/faults, breccias, intraformational fracture zones providing permeable pathways for fluid circulation and sites for ore deposition,
 - host rocks enriched in organic matter, silica, phosphate, clay and pyrite providing reductants and sorbents for U,
 - sources for U and associated elements provided by Sinian-Paleozoic rocks and interim U concentrations and
 - local U sources of granite for nearby deposits,
 - hot and arid paleoclimate conditions favorable for leaching and percolation of U solutions through rock.
- Leaching-accumulative mineralization consists of supergene redistributed U in form of adsorbed U and U⁶⁺ phases – Economic U mineralization is restricted to hydrothermal-reworked deposits characterized by
 - pitchblende, locally coffinite, with minor sulfides of a great variety of metals,
 - quartz, carbonates, fluorite, and clay minerals as gangue minerals,
 - significant organic carbon contents (0.1 to 5.8 wt.-%) in the form of indigenous organic matter, solid bitumens, and cryptocrystalline graphite,
 - comparable sulfur and carbon isotopes in mineralization and host rocks,
 - multistage mineralization with mineral assemblages typical for low to intermediate formational temperature,
 - veined and micro-veined disseminated texture of ore,
 - weak alteration of wall rocks,
 - regional tectonism and locally granite intrusions providing heat for fluid circulation,
 - oxygen isotopes indicate a mixture of meteoric and connate/hypogene waters, locally with minor contribution of granite-related magmatic-hypogene fluids to be instrumental in ore formation.

Metallogenetic Concepts

As may be deduced from geological-mineralogical parameters, tectonic events and age datings, the metallogenesis of the various modes of C-Si-pelite U mineralization in southern China involved polygenetic processes that include in sequential order (a) leaching of U from Precambrian rocks during several episodes, (b) syngenetic accumulation of U in shallow marine or lagoonal sediments, (c) overprinting by diagenetic processes with formation of cogenetic/sedimentary-diagenetic U concentrations; followed, after a hiatus and brittle tectonic interlude, by (d) generation of epigenetic, hydrothermal-reworked deposits in favorable structures by convection of deep circulating, hydrothermal solutions of mixed connate and meteoric origin that leached and reworked precursor U concentrations in at least two episodes. A final, supergene process that partially overlaps with a late episode of the hydrothermal-reworked mineralization

stage, reworked previously formed mineralization and produced epigenetic U concentrations by adsorption of U onto amenable ore or rock constituents and crystallization of U⁶⁺ minerals to form the leaching-accumulative U occurrences.

In more detail, Min MZ (1995) proposes the following model for C-Si-pelite U mineralization and deposits: During the Late Proterozoic and Cambrian, calcareous, siliceous, pelitic sediments with abundant organic matter were deposited in shallow seas surrounding the Jiangnan Uplift. Uranium and other elements leached from older Precambrian rocks were transported into these seas and incorporated in the sediments to background tenors ranging from 6 to 70, locally to over 100 ppm U. Similar sediments were later deposited in the Late Paleozoic Xianggui Depression further to the east and south of the Xuefeng-Jiuling region in which carbonaceous pelitic sediments (\pm black shale) contain 3–30 ppm U.

These Proterozoic-Paleozoic sediments are favored as the primary U sources for the C-Si-pelite U deposits; but granite may have provided an additional U source, at least for deposits adjacent to granite stocks, such as *Ma'andu*, *Shabazi*, and *Xiangcao*.

Late diagenetic processes presumably have locally modified and further enriched synsedimentary uranium as indicated by rare micro-grains and short micro-veinlets of pitchblende without any associated minerals. This mode of U occurrence, denominated sedimentary-diagenetic U mineralization, has low U grades (few hundreds of ppm U) and is mainly confined to neritic and lagoonal horizons with abundant clay and pyrite that could act as an adsorbent and a reductant of uranium, respectively.

A number of intermontane basins were downfaulted during Cretaceous-Tertiary times in response to Yanshanian and Himalayan tectonism and filled with arenaceous redbeds under hot arid to subtropical climatic conditions. Under these paleoclimatic conditions, oxygenated meteoric waters could easily mobilize and transport uranium, and could also rework low-grade precursor ores. Sinian-Paleozoic strata provided the principal U source as indicated by stable isotope data. Pregnant waters percolated along faults and intraformational fracture zones and where they entered cataclastic sediments with abundant carbonaceous debris, clay minerals and pyrite, U was precipitated mainly by adsorption onto clay and organic matter, but also as U⁶⁺ species together with other supergene ore minerals, and rare pitchblende and coffinite due to U⁶⁺ reduction by pyrite and organic matter. As a result of this supergene process, the *phreatic infiltration type of U mineralization* was formed.

The origin of *hydrothermal-reworked* mineralization is related to deep circulating uraniferous hydrothermal solutions that were heated and activated by regional tectonism and, locally, granite intrusions. As noted earlier, $\delta^{18}\text{O}$ values for these solutions document a mixture of meteoric and connate waters with increasing fractions of the former with time. Minor granite-related hypogene-magmatic fluids were apparently also incorporated locally as indicated by $\delta^{18}\text{O}$ values in gangue minerals of deposits near granite plutons. These solutions had received their U endowment mainly from Sinian-Paleozoic source rocks.

The hot, U-bearing, hypogene hydrothermal solutions migrated upward through fracture zones and, on their way, may have further taken up uranium and other elements from rocks

that they permeated. Uranium was transported in the form of uranyl carbonate complexes together with significant amounts of hydrogen sulfide. In breccia zones and intraformational fracture zones, the uranyl carbonate complexes disintegrated due to (1) a drop in temperature at some distance from the heat source and (2) fluid/rock interaction. Hexavalent uranium in the fluids was reduced by sulfur species and organic matter to form pitchblende and locally, coffinite. Fluid inclusion data and distinct mineral assemblages suggest a low to intermediate temperature ranging from 90 to 310°C for the mineralizing fluids and from 100 to 180°C for deposition of pitchblende and associated minerals.

These hydrothermal-reworked U deposits have many features in common with intermediate to low temperature hydrothermal vein-type deposits in other parts of S China. In particular, the earlier given unit cell dimensions, oxidation coefficients and ages of pitchblende are comparable to those of pitchblende in granite-related vein deposits. This parity is thought to document time equivalent and correlative hydrothermal processes at low to intermediate temperatures for the two types and geological settings of U deposits.

1.4.3.1 Xuefeng-Jiuling U Belt

This U belt, referred to as the Xuefeng-Jiuling carbonate subdomain by Yao et al. (1989), stretches as an arc, concave to the NW, for 600 km NE-wards from northeastern Guangxi Province through western to northeastern Hunan into northwestern Jiangxi. Zhang Zuhuan (1990) delineates two U zones within the belt: one at the northern and the other at the southern periphery, respectively, of the Xuefeng Shan-Jiuling Shan ranges in which C-Si-pelite-type U mineralization occurs widespread in Upper Sinian-Lower Cambrian rocks. Three main ore fields are delineated: *Xiushi* in the Mufu Shan area/northern U zone, and the *Central Hunan* and *Ziyuan* ore fields in the southern U zone (Fig. 1.27).

Regional Geology and Mineralization

Geotectonically, the Xuefeng-Jiuling U Belt covers the western part of the Jiangnan (post-Xuefeng/Jinning) uplifted block and its SE margin (Ziyuan-Ningxiang zone). The latter is sometimes also referred to as post-Caledonian Uplift.

The two U zones delineated by Zhang Zuhuan (1990) in the Xuefeng-Jiuling U belt exhibit the following features: The *northern U zone* consists of a discontinuous belt in which U areas are restricted to Sinian and Cambrian paleoembayments filled with carbonate-dominated, siliceous-pelitic sediments. U deposits/occurrences are restricted to the *Mufu Shan area* (Xiushui ore field: *Baitu*, *Baofengyuan*, and *Dongkeng* deposits in NE Hunan-NW Jiangxi, Fig. 1.41), and the *northern Xuefeng Shan area* (= Jiuwandaishan-Xuefeng area) in N Hunan. The *southern U zone* extends for about 300 km along the southeastern margin of the Xuefeng Shan through central and southwestern Hunan and into N Guangxi A.R.; it includes *Laowulong* and *Huangcai*

in central Hunan, (Fig. 1.42) and *Chanziping* with several granite-hosted U deposits in the *Ziyuan* ore field as well as some other C-Si-pelite deposits in SW Hunan-N Guangxi A.R., on the SE side of the Jiangnan Block.

A sequence of Sinian-Cambrian melanocratic, straticulate carbonaceous argillite, siliceous argillite, dolomitic argillite, and carbonaceous silicolite provide the host rocks in which C-Si-pelite-type U mineralization is essentially confined to uppermost Sinian and basal Cambrian strata. Mineralization of individual deposits can be restricted to a single but may also occur in various litho-stratigraphic units. There is commonly no essential difference between the composition of mineralized rocks and host rocks, either in a single deposit or in different deposits.

U is hosted by repetitious beds that are persistent along strike and consist of \pm carbonaceous grey to black, siliceous, dolomitic or calcareous pelites within a unit 100 m and more thick. Background U tenors are high ranging from 30 to 100 ppm, locally up to 200 ppm. U mineralized bodies are stratiform and lenticular in shape controlled by faults and well-developed intraformational fracture zones.

Epigenetic *stratiform mineralization*, as found for example at *Baitu* and *Baofengyuan* in the Xiushui ore field, occurs as elongated lenses, from a few meters to tens of meters long and one to several meters wide; and is distributed over a vertical amplitude of up to 250 m. Uranium occurs largely in adsorbed form and less as pitchblende. Pyrite is often the sole metallic mineral.

Stockwork deposits, such as *Chanziping* and *Xiangcao*, occur in brecciated and fractured rocks of the above-mentioned strata. Ore bodies are mainly of lens shape with an internal stockwork or network structure composed of fissures filled with pitchblende, pyrite, and other sulfides. Mineralization persists over vertical intervals of up to 300–500 m.

Isotope ages vary between 79 and 23 Ma for both stratiform and stockwork U mineralization, and 800 and 500 Ma for host rocks (Yao et al. 1989). (It may be noted that pitchblende in the vein-type *Xincun* deposit hosted by the 760 Ma old Motianling/Sanfang granite at the SW end of the Xuefeng-Jiuling U belt yields an age of 46 Ma that also falls within this range (Zhou Weixun 2000).

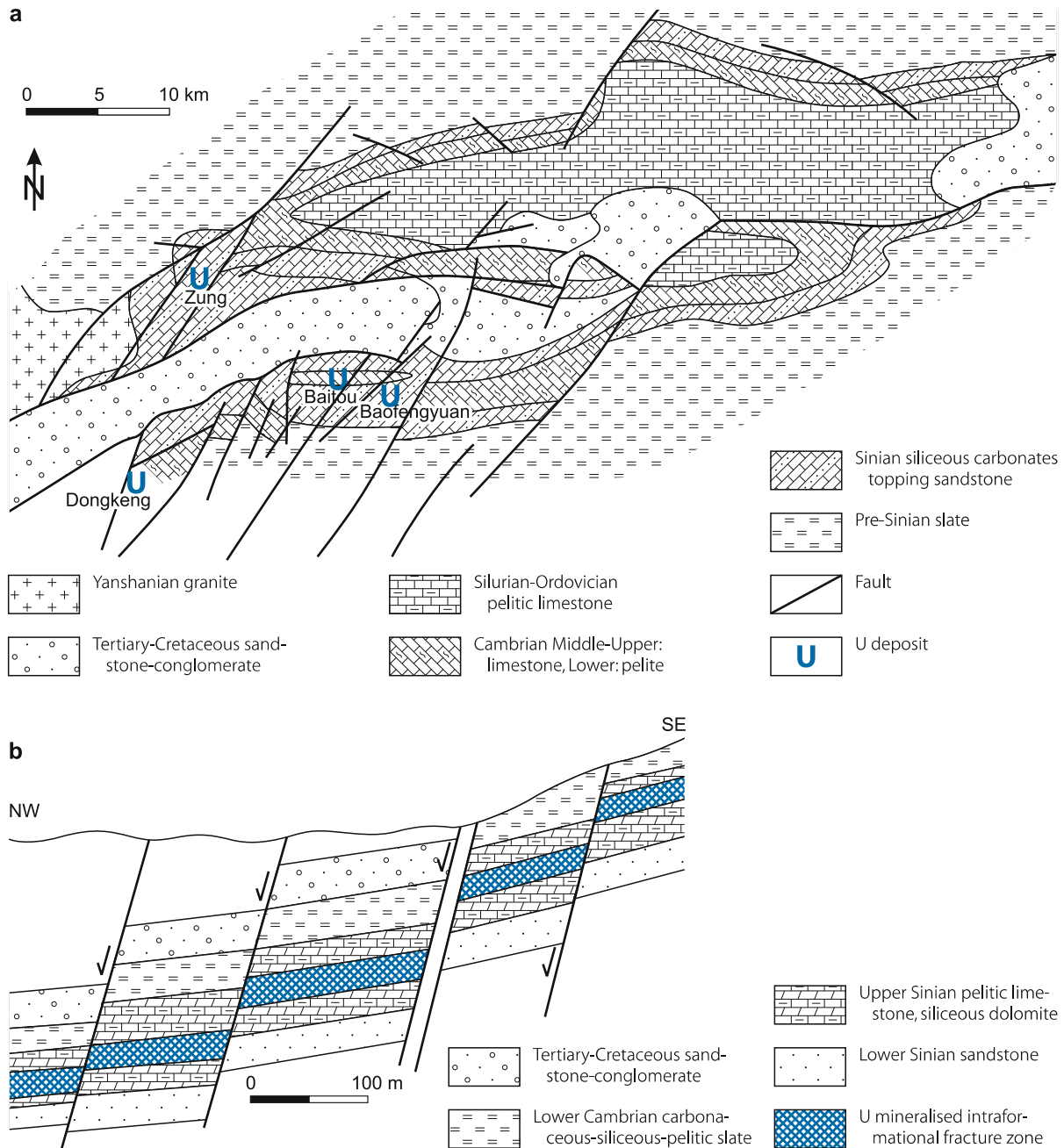
Most of this mineralization is thought to be of a modified black shale type that derived by supergene, phreatic infiltration without obvious alteration except hematitization and/or limonitization. Zhang Zuhuan (1990) interprets the U ore as derived by hydrothermal reworking or infiltration processes during the Tertiary.

1.4.3.1.1 Chanziping, Ziyuan Ore Field, NW Guangxi A.R.

Chanziping (also referred to as *Chanpi*) was discovered in 1956 in Ziyuan County, Guangxi A.R., and forms, together with several granite-hosted U deposits, the *Ziyuan ore field* in NW Guangxi A.R. on the SE side of the Jiangnan Block. Chanziping was explored in the 1960s–1970s but has not been mined. Resources are on the order of 2 500 t U at a grade of 0.2% U. Mineralization may be classified as vein-stockwork type in

Fig. 1.41.

Mufu Shan area, Xiushui ore field, **a** simplified map showing the geologic-tectonic location of C-Si-pelite-type U deposits and **b** NW-SE section of the Baitou deposit illustrating the spatial relationship of strata-bound, structure controlled U mineralization to a downfaulted Cretaceous-Tertiary basin (after Min M 1995)



sedimentary rocks or hydrothermal-reworked C-Si pelite type but some geologists attribute it also to the exocontact subtype of granite-related U deposits (see Sect. 1.4.1 and 1.4.1.1.4: *Granite-Dominated Domain/Granitic Complexes and Related U Deposits and Maoershan-Yuechengling Granite Massifs, Ziyuan Ore Field, Hunan-Guangxi*).

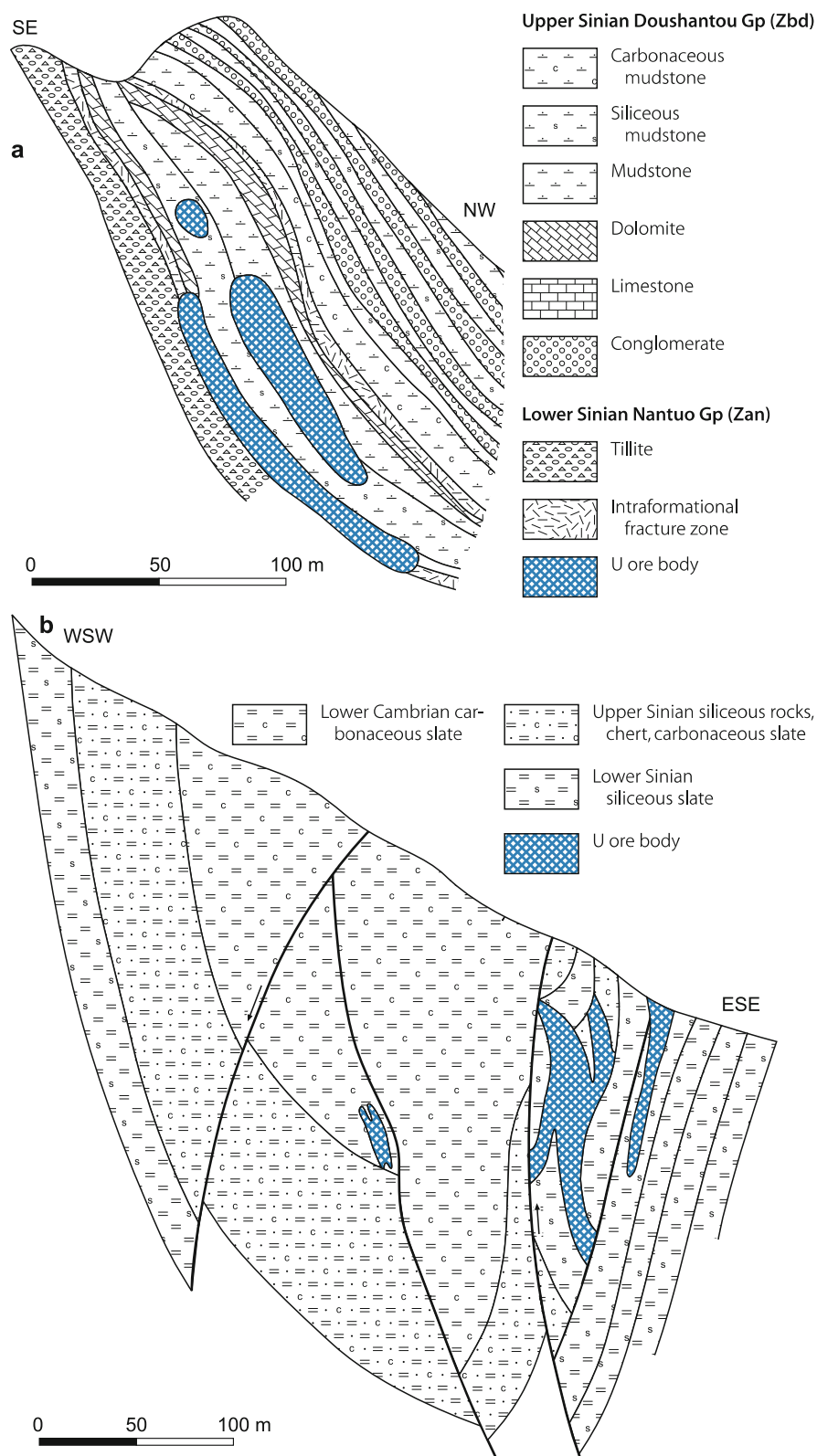
Sources of information. Simpson and Yu Shiqing 1989; Zhou Weixun 2000.

Geology and Mineralization

Country rocks include Sinian and Lower Cambrian carbonaceous-siliceous-pelitic sediments that form a syncline between, and were intruded by the Maoershan and Yuechengling Caledonian granitic massifs to the west and east, respectively. The Maoershan granite was later intruded by small stocks of Indosinian and Yanshanian granites. This complex is overlain by Devonian non-metamorphosed sediments.

■ Fig. 1.42.

Southern Xuefeng Shan area, **a** Laowulong and **b** Huangcai deposits, central Hunan, sketch profiles illustrating the confinement of U mineralization to intraformational fracture zones in folded Sinian sediments (after **a** Zhou Weixun 1997; **b** Min M 1995 based on Zhang D 1982)



Tertiary-Cretaceous continental redbeds cover the older lithologies (Fig. 1.43).

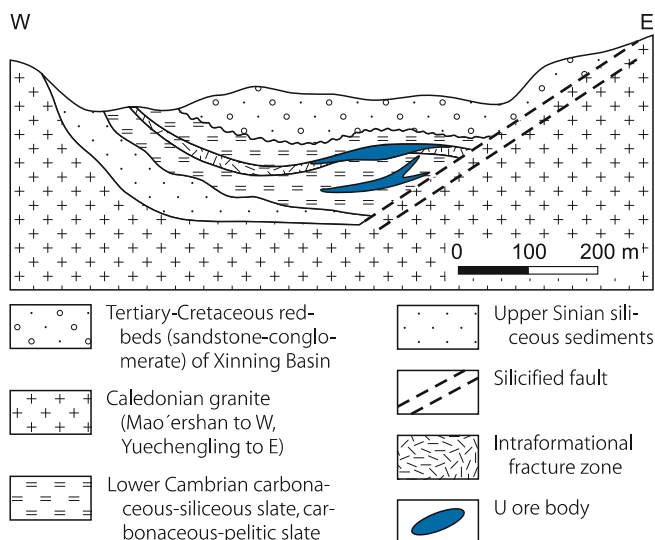
Host rocks comprise markedly cataclastic and brecciated siliceous shale, carbonaceous silicolite, carbonaceous slate, and carbonaceous sandstone of the lowermost Lower Sinian beds. Alteration includes pyritization, recrystallization of quartz, and pink coloration. Pitchblende is the only U ore mineral. Associated minerals include pyrite, sphalerite, galena, pyrrhotite, baryte, quartz, chlorite, fluorite, along with minor chalcocite, bornite, niccolite, hematite, and marcasite.

U-Pb ages obtained for the mineralization vary between 89 and 23 Ma with an isochronal age of 74 Ma that is thought to indicate hydrothermal mobilization of syngenetic U originally contained in Cambrian black shale. Fluid inclusion data indicate a mineralizing temperature of 310–140°C.

Mineralization occurs on both W and E flanks of the syncline bounded by the granites mentioned earlier, where it is controlled by a group of E-W-striking, intraformational fracture zones (F_2) located in the hanging wall of a major NNW to NW trending silicified fault zone (F_1). Ore bodies are of tabular and lenticular shape, range in length from several tens to 200 m, in thickness from several meters to 20 m, and occur at depths from about 50–100 m to 500–600 m (Zhou Weixun 2000).

Simpson and Yu Shiqing (1989) report six paired disseminated U ore bodies in an E-W-striking fault zone, that are lenticular in shape, dip at up to 36°, are up to 20 m in thickness, from 40 to 500 m long, and from 30 to 200 m wide. The grade ranges from 0.05 to 0.4% U.

Fig. 1.43. Southern Xuefeng Shan area, Ziyuan OF, Chanziping, longitudinal W-E section. C-Si-pelite-type U ore bodies are controlled by intraformational fracture zones in Cambrian sediments that form a syncline between two Caledonian granite massifs, Mao'ershan to the west and Yuechengling to the east (after Min M 1995)



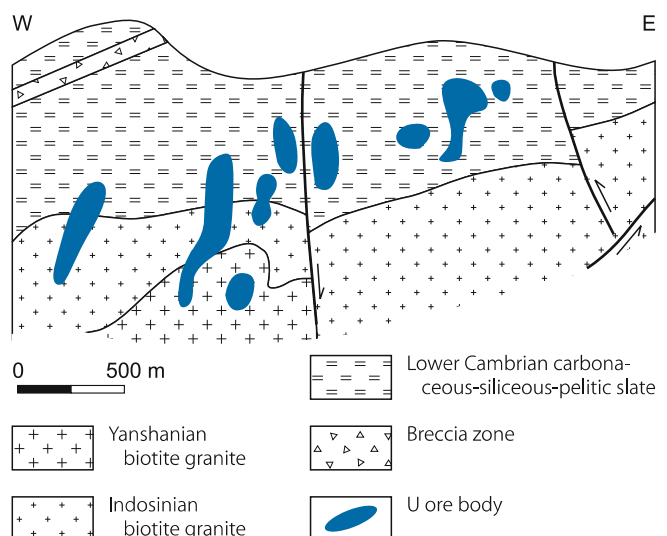
1.4.3.2 Xianggui Basin/Guangxi-Hunan-Jiangxi U Region

This uranium region covers over 120 000 km² in SE Hunan, NE Guangxi, and S Jiangxi. It correlates with the Late Paleozoic Xianggui Depression (including a series of basins) as referred to by Zhou Weixun (1997) (“Xiang” is the abbreviation for Hunan Province and “Gui” for Guangxi, hence, “Xianggui” is the abbreviation for Hunan Province-Guangxi A.R.) or Hercynian-Indosinian Depressions by Min MZ (1995), and lies within the Guangxi-Hunan-Jiangxi carbonate subdomain according to Yao et al. (1989) (Fig. 1.27). Deposits are of structurally controlled C-Si-pelite type, subtype silicolite pelite or collapse breccia, e.g. *Jinyinzhai*; or *Bentou*, respectively, but also of ambiguous nature as, for example, *Shabazi* (Fig. 1.44) in the Lujing ore field where ore is hosted in carbonaceous slate and in granite of the Zhuguang Massif (see Note in Sect. *Principal Characteristics of Mineralization and Alteration of C-Si-pelite U deposits*).

Regional Geology and Mineralization

U deposits occur irregularly scattered in various parts of the Xianggui Depression, hosted either by Devonian-Carboniferous non-metamorphosed impure carbonatic sediments (e.g. *Bentou*) or Lower Permian carbonaceous shale and siliceous rocks (e.g. *Jinyinzhai*). The former include impure, grey to black, carbonaceous and pyritic limestone and dolomite with pelitic intercalations, and high U background values ranging from 8 to 30 ppm

Fig. 1.44. Xianggui Basin/Zhuguang granite massif, Lujing ore field, Shabazi deposit, W-E sketch profile documenting the exo- and endogranitic setting of U mineralization in Cambrian carbonaceous pelite as well as in Indosinian and Yanshanian granites (after Min M 1995)



U. Individual uraniferous horizons are only a few meters thick at maximum but occur repetitiously in a sedimentary unit, as much as 100 m and more thick, at the base of a transgressive series that rests upon clastic rocks.

Mineralization is variable in composition and may consist of pitchblende associated with polymetallic constituents predominantly copper sulfides, while a few deposits contain tungsten. Yao et al. (1989) report ages ranging from 135 to 20 Ma for U mineralization and 380–320 Ma for host rocks.

Deposits consist of several ore bodies controlled by intraformational fracture zones or, more rarely, by paleokarst-related structures and caverns; they may therefore be classified as vein type in sedimentary rocks (Zhou Weixun 1997) and as collapse breccia type, respectively. Ore bodies are stratiform, tabular and lenticular, and are commonly several 10 m to 100 m long, and 1–5 m thick.

Silicolite pelite-type deposits are hosted by Lower Permian siliceous rocks that derived by submarine volcanic exhalations in deep trenches within the carbonate platform. Ore bodies are controlled by silicic breccia zones generated by brecciation and silicification of silicolite-siliceous shale (Zhou Weixun 2000).

1.4.3.2.1 Jinyinzhai/Chenxian Mine, SE Hunan

Jinyinzhai (also referred to as *Sanerlin* = deposit # 320 in Chinese) was discovered in 1955 near Chenzhou city (formerly named Chenxian), SE Hunan Province, and is classified as a structurally controlled C-Si-pelite (also referred to as veinlike or hydrothermally reworked silicolite or silicic breccia)-type deposit.

The deposit was exploited from 1962 into the 1980s by the Chenxian underground mine, which was served by several shafts and has produced reportedly some 10 000 t U, making it one of the largest deposits in China (Li Jian-Wei et al. 2002). Ore was transported to the central mill at Hengyang.

Li Jian-Wei et al. (2002) provide a comprehensive description of the Jinyinzhai deposit (to which they refer as *Sanerlin*), which is largely used for the following summary amended by information from Hou YQ et al. (1993), Li JW (1998), Li JW et al. (2001), Min MZ (1995), Min MZ et al. (1996), Simpson and Yu Shiqing (1989), Zhou Weixun (2000).

Geological Setting of Mineralization

The deposit is located in Upper Paleozoic sediments of the South China Block (or Yangtze Craton) near the SW margin of the Tertiary-Cretaceous Chaling-Yongxing Basin/Graben. Yanshan-ian granites (ca. 140 Ma) crop out 20–30 km to the south and north of Jinyinzhai (Figs. 1.45a,b) and underlie the deposit.

Litho-stratigraphic features of the deposit area including the Chaling-Yongxing Basin are shown in the following section (Li Jian-Wei et al. 2002; in brackets: U background values in ppm/No. of samples):

Tertiary

- Maoping Fm, 20 m thick: Fluvial deposits;
- Zaoshi Fm, 496 m thick: Clayey siltstone and sandy marl with thin gypsum lenses (2.6–4.9, av. 3.2 / 9).

Cretaceous

Conglomerate, coarse to fine sandstone, minor impure limestone, clayey siltstone, with 7 gypsum beds (referred to as redbeds), subdivided into the

- Daijia Fm, 1 500 m thick (2.1–4.1, av. 2.9/10),
- Sbenhuang Fm, 975 m thick (2.5–6.1, av. 3.4/17), and
- Dongjing Fm, 1 830 m thick (3.8–4.9, av. 4.1/14).

Upper Permian

- Douling Fm, 360 m thick: Sandstone with thin muddy siltstone and shale (2.2–6.5, av. 3.6/16)
- Dangchong Fm, 900 m thick: Carbonaceous, organic-rich black shale interstratified with quartz sandstone and thin coal beds. (8.7–180.0, av. 34/118)

Lower Permian

- Xixia Fm, 227 m thick: Limestone and dolostone with fine-grained sandstone at bottom and top (2.3–7.2, av. 4.5/11)

Carboniferous-Devonian

- 460 m thick: Sandstone, siltstone, muddy limestone, minor dolostone (3.9–10.2, av. 5.6/17)

During Early and Middle Jurassic (Yanshanian Orogeny), the Paleozoic sediments were folded into the regional South Hunan synclinorium with overprinted, secondary anticlines and synclines trending NNE-SSW. Granites were contemporaneously intruded.

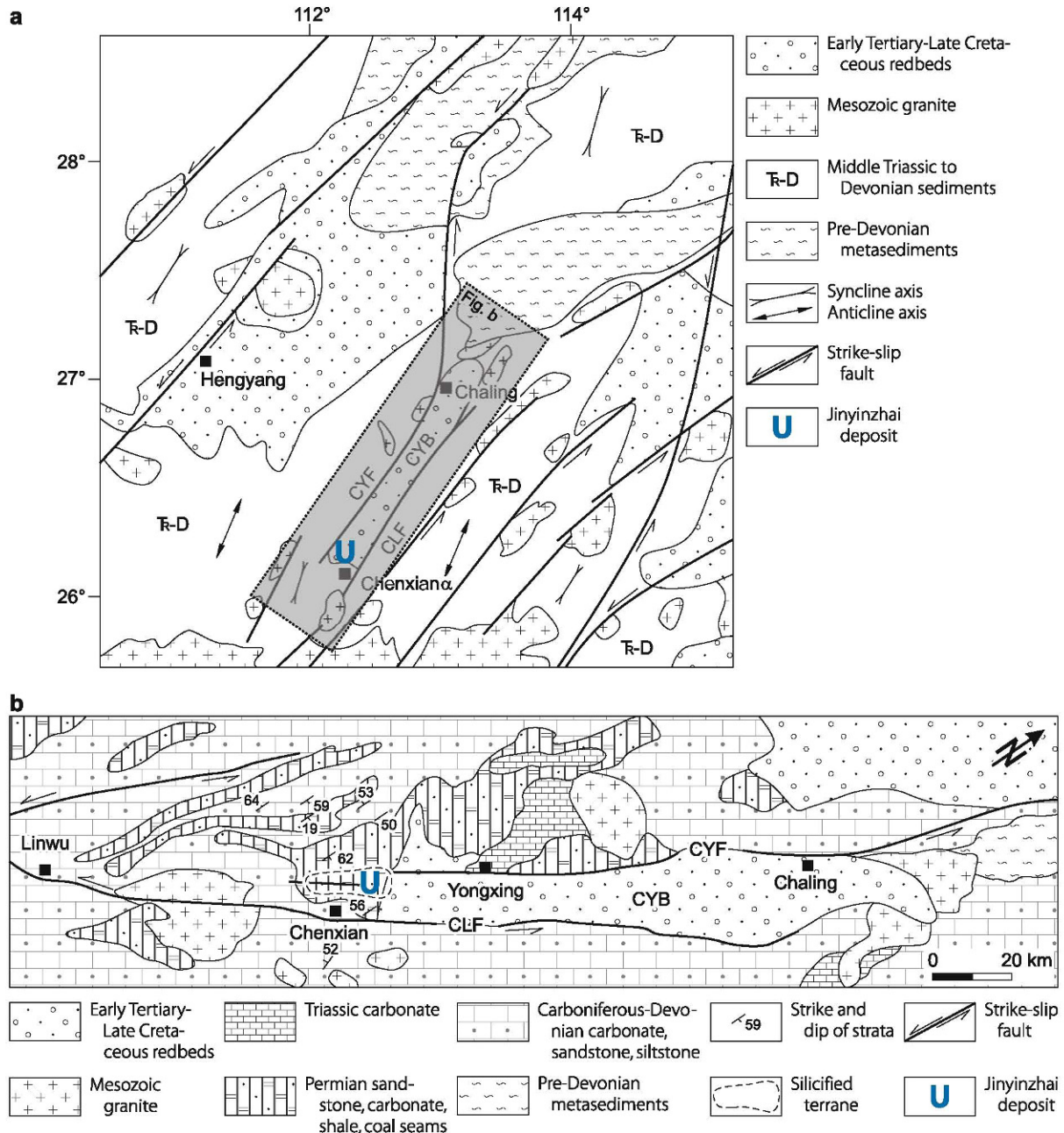
Repeated brittle tectonism from Early Jurassic to Early Tertiary generated a major NNE-SSW-oriented fault system with an estimated strike-slip of 1 km that can be traced for about 200 km (Li Jian-Wei 1998). The Jinyinzhai deposit occurs between the Chaling-Yongxing and Chenxian Linwu faults of this system. These two faults also control the narrow, NNE-SSW stretching Tertiary-Cretaceous Chaling-Yongxing Basin that is filled with redbed formations some 5 000 m in thickness; Jinyinzhai is located at the southern margin of this basin (Figs. 1.45a,b).

The Upper Permian Dangchong Formation is the main ore-hosting unit. It comprises very fine-grained quartz sandstone and black siliceous and carbonaceous shales that have been intensely silicified within the deposit area. Nine black shale beds are identified ranging from 15 to 42 m in thickness. These shales contain illite, chlorite, biotite, muscovite, pyrite, quartz, and abundant organic matter in the form of algae, lignite, and coal, and high U background tenors.

The Dangchong Formation exhibits locally intense brecciation; fifteen elongated breccia segments occur intermittently in the cores of three NNE-SSW trending secondary anticlines within the regional South Hunan synclinorium (Fig. 1.45c). Individual breccia segments are commonly 1 000–2 000 m long subparallel to the NNE-SSW anticline axes, 100–250 m wide, and persist to depths of some 700 m (Fig. 1.45d). The breccias are composed of angular fragments, from a few millimeters to several meters across, of grey-black silicified shale and sandstone

Fig. 1.45a,b.

Xianggui Basin, Jinyinzhai deposit area, simplified geological maps of **a** regional litho-stratigraphic and geotectonic features of the Chenxian-Hengyang region and **b** related setting of the C-Si-pelite(-breccia)-type Jinyinzhai deposit with respect to its spatial relationship to the Chaling-Yongxing (CYF) and Chenxian-Linwu (CLF) strike-slip faults, Tertiary-Cretaceous Chaling-Yongxing Basin (CYB), and fold structures (after Li Jian-Wei et al. 2002)



from the Dangchong Formation, and are cemented by quartz stringers and veins, and locally by calcite. The silica content of these rocks amounts to as much as 90% SiO_2 .

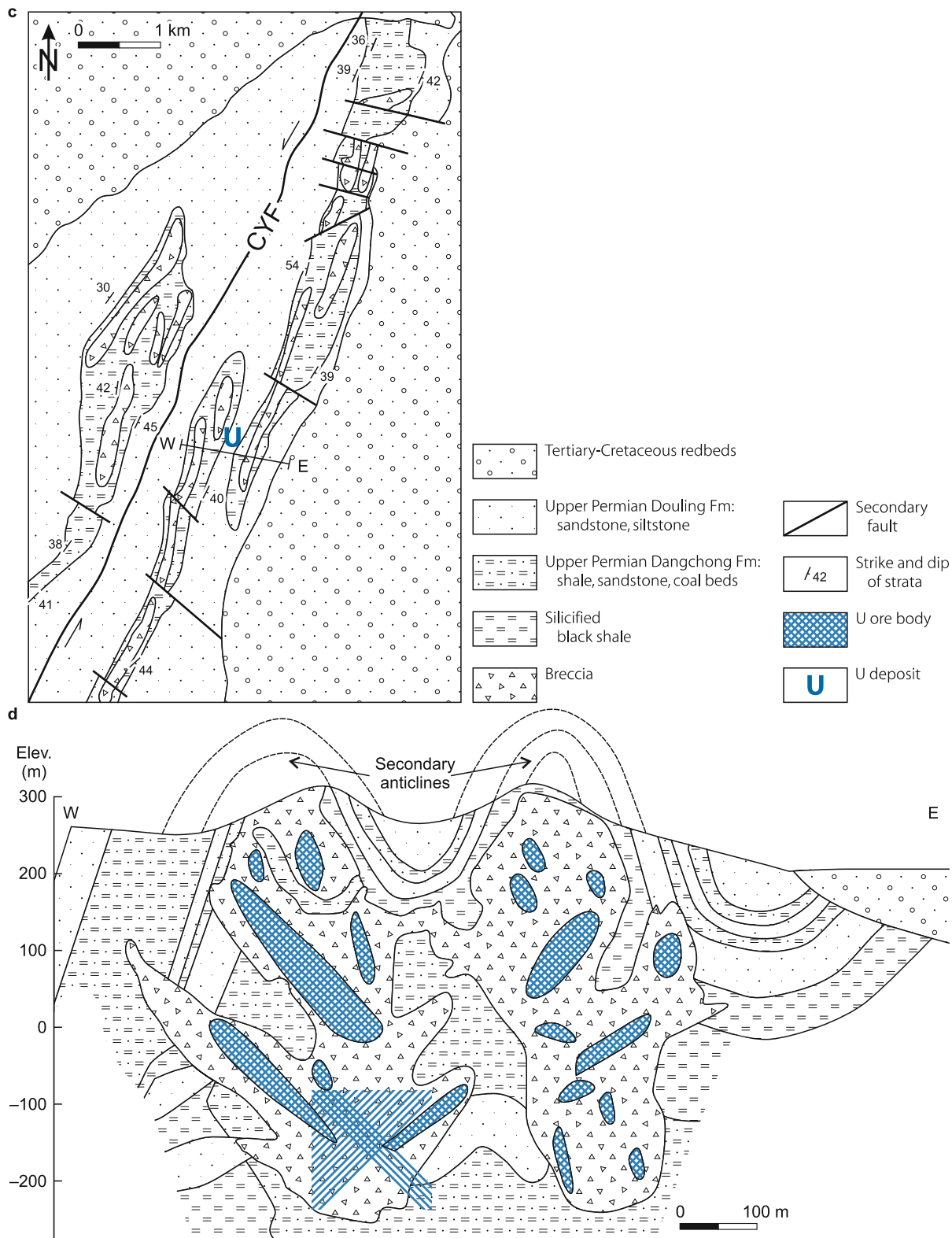
Alteration

As indicated above, pervasive and intense silicification is the most prominent alteration feature at Jinyinzhai; it pre-dates the

brecciation. Post-brecciation silicification has produced variably formed quartz veins ranging from millimeters to more than 30 m in length and from millimeters to 20 cm in width. The veins consist of early, very fine-grained silica intergrown with fine-grained pyrite and marcasite that cements wall rock fragments and coats vein walls. Relatively coarse-crystalline quartz with progressively increasing grain size towards the center of the veins was deposited next. Wall rock fragments up to 5 cm in diameter occur in many veins. Voids and cavities from 0.1 to 5 cm in diameter are

■ Fig. 1.45c,d.

Jinyinzhai deposit, **c** geological map and **d** W-E cross-section documenting the affinity of breccia zones to secondary anticlines of the Permian Dangchong Formation. The breccias typically occupy the cores of these anticlines and all ore bodies are confined to brecciated segments (after Li Jian-Wei et al. 2002)



common within both the fragments and hydrothermal cement of the breccia-vein bodies. Both barren and U mineralized veins are present. Barren veins predate the latter.

Wall rocks adjacent to uraniferous quartz veins exhibit abundant pyritization, carbonatization, sericitization, and hematitization. Alteration is more intense at deep levels, where detrital albite and microcline in rocks of the Dangchong Formation were altered to sericite that is intergrown with quartz and very fine-grained pyrite. At higher levels, alteration is far less pronounced, sericite is absent, alteration of the wall rocks is mainly represented by an envelope few millimeters wide of crystalline hematite; and the pyrite content in veins decreases.

Mineralization

Pitchblende and sooty pitchblende are the principal primary U minerals. Associated metallic minerals include arsenopyrite, galena, marcasite, molybdenite, pyrite, sphalerite, and minor chalcopyrite, greenockite, ilsemannite, vaesite, xianjiangite, and red microcrystalline hematite. Gangue minerals are dominated by quartz (chalcedony) and carbonate, with minor fluorite, kaolinite, gibbsite, illite, sericite, and hydromica. Uranophane, uranopilite, torbernite, zeunerite, and limonite prevail in oxidized zones within about 20 m of the surface.

Pitchblende (0.01–0.6 mm in diameter) exhibits botryoidal and colloform habits but also exists in sooty form. It occurs preferentially as disseminated grains in quartz veins or, locally, as a coating on rock fragments, and occasionally as veinlets, from 0.05 to 2 mm in width and from 0.5 cm to tens of centimeters in length. Molybdenite is ubiquitous and locally forms economic ore bodies. Mo grades increase with depth, while U grades decrease.

Li Jian-Wei et al. (2002) identified three stages of mineralization: *Stage 1* comprises quartz and sulfides including molybdenite, fine-grained pyrite, and chalcopyrite. *Stage 2* is reflected by pitchblende, associated with galena, sphalerite, relatively coarse pyrite, red microcrystalline hematite, quartz, fluorite, calcite, and hydromica. *Stage 3* is represented by minor amounts of gangue minerals and crystalline hematite.

Shape and Dimensions of Deposits

The Jinyinzhai deposit consists of irregularly distributed U ore bodies, which are exclusively hosted in fifteen breccia-vein bodies. These breccia bodies are separately located in the cores of three secondary anticlines of the Upper Permian Dangchong Formation (► Figs. 1.45c,d).

Ore bodies are of lenticular, nested, columnar, and ladder configuration and consist predominantly of uraniferous quartz veins and fragments of silicified rocks. Ore bodies range commonly from 10 m to some tens of meters in length and from 1 m to several meters in thickness. The largest ore body is over 200 m long, 50–60 m thick, and persists for 180 m downdip (Zhou Weixun 2000).

Simpson and Yu Shiqing (1989) describe a large, mined ore body that is presumably identical with the large ore body

mentioned by Zhou Weixun as follows. The ore body varies in shape from lenticular to columnar and dips at 70°SSE. It contains steeply dipping ore lodes predominantly composed of disseminated mineralization with some brecciated, uraniferous hematitic veinlets locally. Ore lodes are as much as 200–300 m long, 2–3 m wide, and 50 m deep. The boundary between the disseminated U ore body and wall rocks is commonly indistinct. Ore averages a grade of 0.1% U and also contains commercial quantities of Mo, Re, and Se. Geothermal waters with a temperature of 48°C enter into the underground mine workings.

Li Jian-Wei et al. (2002) (based on Liu SL 1980) provide the following assays results for U ore: 0.54 wt.-% U as an average of 186 samples, as much as 525 ppm Mo, 196 ppm Zn, 126 ppm As, 44 ppm Pb, and 253 ppm Cu. No V enrichment is recorded.

Fluid Inclusions, Stable Isotopes, and Geochronology

Fluid inclusions in vein quartz yield homogenization temperatures between 150 and 280°C, and have calculated salinity values between 5.6 and 13.4 wt.-% NaCl equivalent. Stable isotope values for $\delta^{18}\text{O}$ range from -2.2 to $+2.6\text{‰}$ and for $\delta\text{D}_{\text{H}_2\text{O}}$ from -134 to -110‰ suggesting that the mineralizing solutions predominantly derived from brines of the Chaling-Yongxing Basin. Fluid pressures estimated from fluid inclusions data are in excess of 360 bar and hence are sufficient to generate hydraulic fracturing. Sulfur isotope studies on pyrite from U mineralization yield $\delta^{34}\text{S}$ values of -48.2 to $+7.2\text{‰}$ and from Dangchong host rocks -30.6 to $+3.7\text{‰}$.

U-Pb dating of pitchblende gives concordant ages of 62.8–60.1 Ma according to Liu SL (1980; cited by Li Jian-Wei et al. 2002) while Simpson and Yu Shiqing (1989) report discordant U-Pb ages in the range of 106–61 Ma. This early Tertiary time of U mineralization coincides with the transtensional regime exerted by the regional strike-slip faults and the down faulting of the Chaling Yongxing Basin.

Potential Sources of Uranium

Sediments of the Dangchong Formation have an average content of 34 ppm U, with as much as 180 ppm U in the black carbonaceous shales (Liu SL 1980 in Li Jian-Wei et al. 2002). These black shales are considered the most significant uranium source. In addition, granites located to the south and north of Jinyinzhai contain up to 15 ppm U and may also have provided U to the deposit.

Metallogenetic Aspects

Li Jian-Wei et al. (2002) propose the following sequence of events in the formation of the Jinyinzhai U deposit:

1. Syngenetic pre-enrichment of uranium in sediments of the Dangchong Formation and particularly in black shale.

2. Folding along NNE-SSW axes and intrusion of (uraniferous) granite during the Early-Middle Jurassic.
3. Reactivation of regional NNE-SSW faults, down dropping of the Chaling-Yongxing Basin, and development of an abnormally high geothermal gradient during Late Jurassic to Early Tertiary.
4. Leaching of uranium from Dangchong sediments by oxygenated basinal formation waters and migration of the solutions into the cores of secondary anticlines where a fluid overpressure evolved caused by the impermeable Dangchong shales that acted as barriers to the hydrothermal fluids.
5. Hydraulic fracturing and brecciation in response to increased fluid pressure; and
6. P-T drop associated with a release of gaseous phases from the mineralizing fluids due to episodic hydraulic fracturing resulted in the precipitation of quartz, pitchblende, and other associated minerals.

The authors argue in favor of their metallogenetic model as follows: The Early Tertiary time of uranium mineralization coincides with a transtensional regime exerted by regional strike-slip faulting and the subsidence of the Chaling Yongxing Basin. The redbeds in this basin reflect an arid climate during the Cretaceous-Early Tertiary. The earlier mentioned hydrogen and oxygen isotope compositions in U ore minerals indicate a derivation of the mineralizing fluids largely from oxygenated basinal formation waters. This assumption is further supported by the fluid salinity, which is similar to that of formation waters of continental sedimentary basins.

These oxygenated waters are thought to have leached uranium and other metals from the Dangchong black shales as can be deduced from similar sulfur isotope compositions for pyrite from both U ore and Dangchong host sediments. In addition, supergene processes and ground waters may also have leached uranium from uraniumiferous granites located to the south and north of Jinyinzhai.

Fertile solutions migrated along the regional strike-slip fault system that intersects the Jinyinzhai area. Where these fluids entered fractured or brecciated ground, an abrupt P-T drop of the hydrothermal system occurred, which presumably caused fluid differentiation and thereby precipitation of quartz to form the vein network. Pitchblende and associated minerals were deposited almost simultaneously with quartz in response to an associated abrupt vapor loss from ore fluids.

Zones of brecciation are explained by some authors to have resulted from faulting or solution collapse whereas Li Jian-Wei et al. (2002) postulate a hydraulic fracturing mechanism. They argue that fluid pressure estimates along with geometry, texture, and structure of the breccia-vein system are most compatible with conditions that govern hydraulic fracturing. In their model, the required hydraulic pressure resulted from an accumulated invasion of hydrothermal solutions into the core of secondary anticlines where a fluid pressure built up due to the overlying impermeable seal. In combination with an abnormal geothermal gradient in the region, pressure was further increased to the critical level that exceeded the rock strength; fracturing and brecciation ensued. As a result of brittle rock deformation, temperature and pressure of the mineralizing solution abruptly

decreased, which caused an oversaturation of the fluid, and, consequently, precipitation of quartz, pitchblende, and associated minerals.

The presence of a major thermal anomaly is deduced from more than 100 hot springs with temperatures as high as 72°C including those in the Jinyinzhai area that are aligned along and controlled by the NNE-SSW-oriented strike-slip fault system.

1.4.3.2.2 Bentou, SE Hunan

Discovered in 1973; Bentou (Benti or Sanbaqi) is an explored U deposit located in Guiyang County, SE Hunan Province. It is classified as a structurally controlled C-Si-pelite-type deposit contained in collapse breccias. Resources are between 1 500 and 5 000 t U at a grade of 0.1–0.3% U.

Sources of information. Min et al. 1997, who use Sanbaqi for Bentou; Zhou Weixun 2000.

Geology and Mineralization

Bentou is situated in the central SW part of the South Hunan synclinorium formed by Upper Paleozoic mainly calcareous sediments, 2 500 m thick that are grouped into the litho-stratigraphic units shown in [Figs. 1.46a–c](#). The Paleozoic sediments were mildly folded along sublongitudinal axes by Indosinian tectonism but remained unmetamorphosed. Downfaulted Tertiary-Cretaceous basins occur in the vicinity of the deposit and are filled with continental sediments. Quaternary gravel, sand, and clay form a veneer on top of the older strata. Several NW-SE- and NE-SW-trending high angle faults and fracture zones transect the site of the deposit. There are no igneous intrusions or extrusions at or in the vicinity of the deposit.

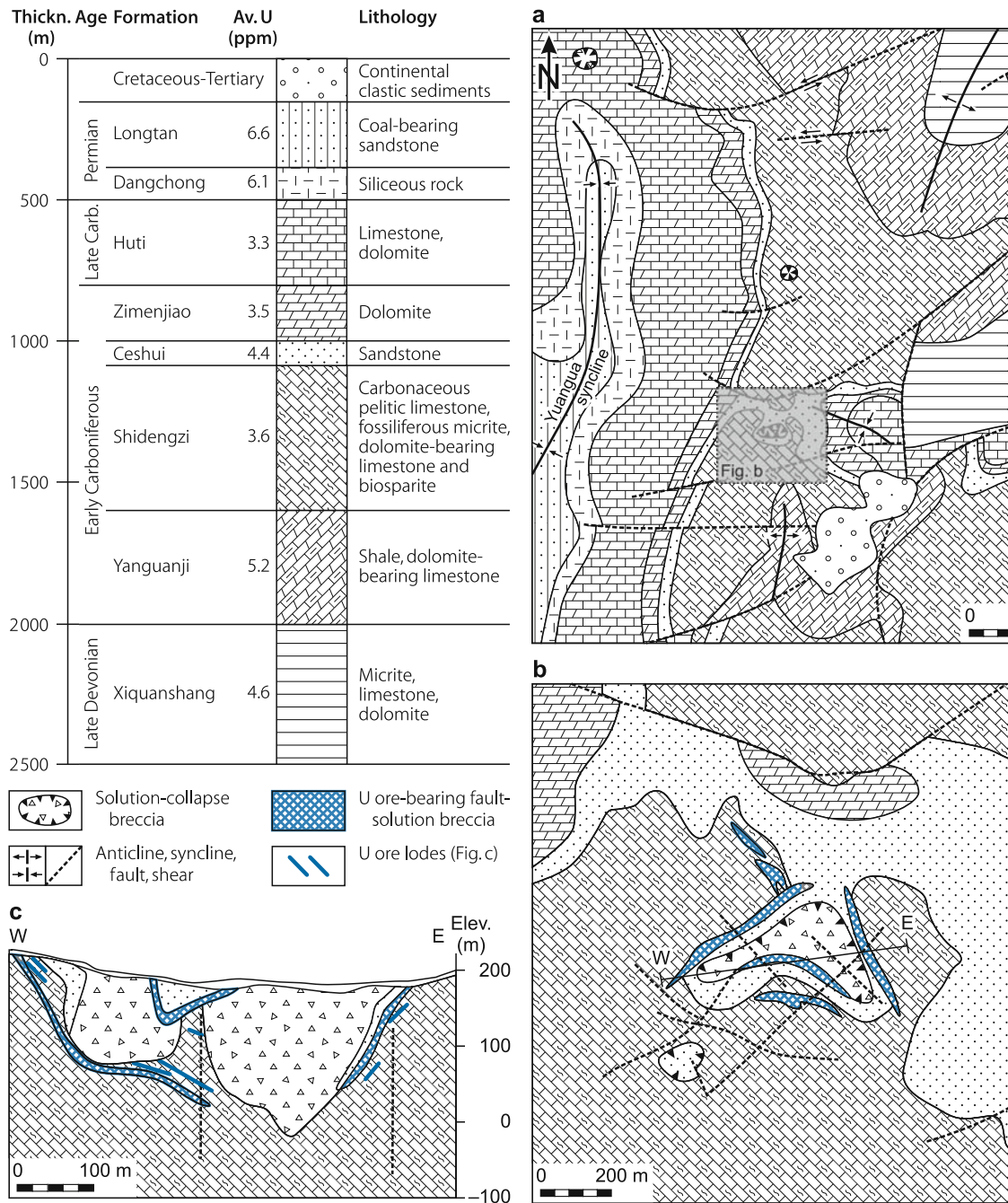
Karst-related solution collapse breccia cones or pipes occur in impure limestone with intercalations of marl and carbonaceous shale of the upper Shidengzi Formation, persist from the paleosurface to depths between 100 and 200 m, and are filled with fragments of dolomite and sandstone of the Zhimenjiao and Ceshui Formations, respectively, embedded in a fine-grained matrix. This collapse fill is barren of ore.

Ore bodies occur at shallow depth along annular faults that circumvent these collapse structures ([Figs. 1.46b,c](#)). U mineralization is preferentially concentrated at intersections of carbonaceous pelitic micrite and fossiliferous micrite with intercalated silty micrite and biosparite. The pelitic beds are dark grey to black, rich in pyrite and contain 7–16 ppm U and 1.5–2.1 wt.-% organic carbon.

Wall rock alteration penetrates in variable intensity for 0.1–1 cm vein walls along pitchblende lodes and related fractures. Alteration products include authigenic quartz, hydromuscovite, chlorite, carbonates, and pyrite as well as bleaching or yellow-green tinting due to dumortieritization. Alteration is chemically associated with a substantial addition of silica, iron and potash, and a slight decrease in organic carbon.

Fig. 1.46.

Xianggui Basin, Bentou (Benti, Sanbaqi) deposit, **a** and **b** geological maps exhibiting the litho-stratigraphic and geotectonic setting of the C-Si-pelite (silicic-breccia)-type deposit in Carboniferous sediments. **c** W-E section across fault-solution breccia bodies and related peripheral annular structures that control U mineralization (after Min M et al. 1997)



Mineralization consists chiefly of U adsorbed on carbonaceous matter, colloidal pyrite, and clay minerals, and only to a minor degree of pitchblende. Associated minerals include pre-U stage millerite, molybdenite, niccolite, pentlandite, ullmannite, dolomite, and chlorite; pre- to syn-U stage pyrite, goethite, hematite, chalcopryrite, galena, and sphalerite as well as dolomite, chlorite, quartz, clay minerals, and rare fluorite; and post-U stage antimonselite. Calcite is ubiquitous. U-Pb dating of pitchblende yields ages of 135–119 Ma.

Ore bodies vary in morphology from tabular, lenticular, cone-shaped, nested to irregular configuration with dimensions

from 10 m to several tens of meters in length and width, and several meters to tens of meters in thickness. Ore lodes are internally structured by networks of openings filled with fragments of wall rocks and fine-grained, carbonaceous pelitic matrix. Pitchblende occurs preferentially along fractures, and also in solution voids and cavities, interstitially in granular material, and as partial replacement of the argillaceous matrix.

Metallogenic aspects: Min et al. (1997) forward the following hypothesis on the evolution of the Bentou deposit (to which

they refer as Sanbaqi). A paleokarst-related solution network has controlled the location and formation of the ore lodes. At least four episodes of karst development are identified: Late Triassic-Early Jurassic, Late Jurassic-Early Cretaceous, Cretaceous-Tertiary, and Recent. The main U mineralizing phase tends to be related to the second karst episode. This is supported by isotopic ages of two pitchblende samples at 129 and 134 Ma. These ages correlate with Yanshanian movements in S China that are thought to have opened or reactivated the annular faults during Late Jurassic and Cretaceous time. The new fractures provided new pathways for solutions that generated irregular solution cavities throughout the brecciated limestone. These openings were filled with clastic material, carbonaceous clay, drip stones, pitchblende, and associated minerals. Mineralization in these reactivated fault-related breccias is also spatially related to the younger faults, referred to as “ore bearing tectonic belts”.

With respect to potential sources of U and associated metals, Min MZ et al. (1997) favor carbonaceous shales of the Lower Carboniferous Shidengzi and Yanguanji Formations with Clarke tenors of up to 16 ppm U.

Mineralogical, fluid inclusion, and isotopic data suggest that repeated pulses of hydrothermal activity generated the mineralization as we know it today. Ore-forming solutions had temperatures from 181 to 150°C as deduced from homogenization temperatures of fluid inclusions in ore-stage calcite ranging from 160 to 181°C and in post-ore calcite from 160 to 150°C. Based on formation temperatures of 150–181°C for ore stage calcite, $\delta^{18}\text{O}$ and δD values in this calcite were recalculated for mineralizing fluids and yield $\delta^{18}\text{O}$ and δD values ranging from 1.5 to 7.9‰ and from -30.4 to -54.8‰, respectively. These data indicate a mingling of meteoric and metamorphic solutions.

Salinities of fluid inclusions in ore-stage calcite range from 10.2 to 20.8 (mean 15.5) wt.-% NaCl equivalent that are distinctly different to inclusion salinities from 0.0 to <0.1 wt.-% NaCl equivalent in calcite from unmineralized brecciated limestone of the Shidengzi Formation.

Sulfur isotope compositions of vein pyrite in ore range from 1 to -15.30 (mean -7.1) $\delta^{34}\text{S}$ and of finely disseminated diagenetic pyrite in host rocks from 1 to -15.60 (mean -7.1) $\delta^{34}\text{S}$, which suggests that diagenetic pyrite of biogenetic origin was the likely sulfur source in mineralizing fluids.

Redistribution of earlier formed ore minerals in an open system added to the complexity of the paragenetic sequence. Isotopic data including U-Pb pitchblende datings suggest that younger episodes of mineralization were related to the later karst events during late Yanshanian tectonism in Cretaceous-Tertiary time and recently.

1.4.3.3 SW Guizhou Region, Baimadong Deposit/Chienxinan Mine, Guizhou Province

The SW Guizhou uranium region with the Baimadong deposit/Chienxinan Mine is located at the southwestern periphery of the Yangtze Massif. The region is also known for gold deposits discovered in the 1980s, as well as Hg, Sb, and As resources. Uranium occurs structurally controlled, strata-bound in a sequence of

siltstone, mudstone, carbonate, and chert of Paleozoic and particularly of Permian and Triassic age. Fractured siltstone tends to be the preferential host rock.

Baimadong, often referred to as *Chienxinan* (= Chinese term for SW Guizhou Province; Chien is the abbreviation for Guizhou), lies close to Xingyi city, SW Guizhou. Baimadong is actually an old mercury mine with hundreds of years of history in which U was discovered in 1956. Original resources amounted reportedly to some 6 000 t U. Uranium and molybdenum were mined as co-product of mercury by underground methods and are depleted.

Sources of information. Tu Guangzhi 1990; Zhou Weixun pers. commun. 2003.

Geology and Mineralization

Ore lodes at *Baimadong* are confined to altered fracture zones in Lower and Middle Cambrian dolomite and pelitic dolomite that typically exhibit quartz and carbonate veining. Alteration includes prominent silicification as well as argillization, pyritization, sericitization, and carbonatization. The latter is represented by calcite, dolomite, ankerite, and siderite. Ore lodes have irregular, diffuse boundaries and consist of disseminated replacements or stringers of pitchblende, and black U products (sooty pitchblende) associated with cinnabar, marcasite, pyrite, realgar, amorphous MoS_2 , with minor Cu, Ni, Pb, Zn sulfides, and anomalous amounts of As, Hg, Sb, and Tl. Gangue minerals include quartz, calcite, dolomite, siderite, sericite, baryte, fluorite, and clay minerals.

Ages of U mineralization are given at 60–20 Ma suggesting a post-Yanshanian mineralizing or redistribution event. Fluid inclusions in quartz and carbonate indicate a formation temperature of 120–160°C.

1.4.3.4 SW Guangxi Area, Daxin Deposit, Guangxi A.R.

The Daxin (Daxing) deposit is located near the town of Daxin, about 100 km W of Nanning city, SW Guangxi A.R. [Min MZ et al. (2002) refer to this deposit as Saquisan Mine = Chinese for Deposit 373]. This C-Si-pelite/carbonate sub-type deposit was discovered in 1960 and explored until the end of 1970.

Sources of information. Min et al. 2002; Zhou Weixun pers. commun. 2003.

Geology and Mineralization

Daxin occurs at the NE edge of a NE-SW-striking horst that is considered to be a structure of the ENE-WSW-trending southwestern Guangxi fold system. Slightly metamorphosed Cambrian clastic rocks occupy the center of the horst; they are unconformably overlain and surrounded by Devonian strata. The Lower Devonian includes three formations (D_{1p} , D_{1n} and D_{1y}) composed

of gravel-bearing, coarse-grained sandstone that grades upwards into sandstone, siltstone, argillite with marl, and limestone at the top. Middle Devonian (D_{2d}) sediments grade upwards from dolomitic limestone intercalated with dolomite, to dolomitized breccias, and to limestone. Thin-bedded limestone is the main Upper Devonian lithology.

An E-W-oriented normal fault (F_2) is the main structure in the region. It can be traced along the northern flank of the horst for 28 km, has a steep dip in the upper part that flattens at depth, and caused vertical displacements of some 400 m. At the Daxin deposit, Cambrian sediments occur in the footwall, and Lower and Middle Devonian strata in the hanging wall of the F_2 fault.

U ore bodies are hosted by clastic rocks and limestone with increased organic matter and pyrite contents of the D_{1y} and D_{2d} formations in which their position is controlled by the F_2 fault and second order interformational faults in its hanging wall (Fig. 1.47). Wall rocks are altered by silicification, pyritization, and dolomitization. Pitchblende is the only U phase. Associated minerals include pyrite, molybdenite, sphalerite with minor antimonite and arsenopyrite as well as dolomite, calcite, quartz, and clay minerals. These minerals impregnate pyritized mylonite, brecciated dolomitized limestone, and silicified rock to form ore.

Ore bodies are of lenticular and pod shape, from some tens of meters to 180 m in length, from a few meters to 40 m in thickness, and persist for as much as 280 m downdip.

1.4.4 Mesozoic-Tertiary Basins in South China/ Sandstone-Type U Deposits

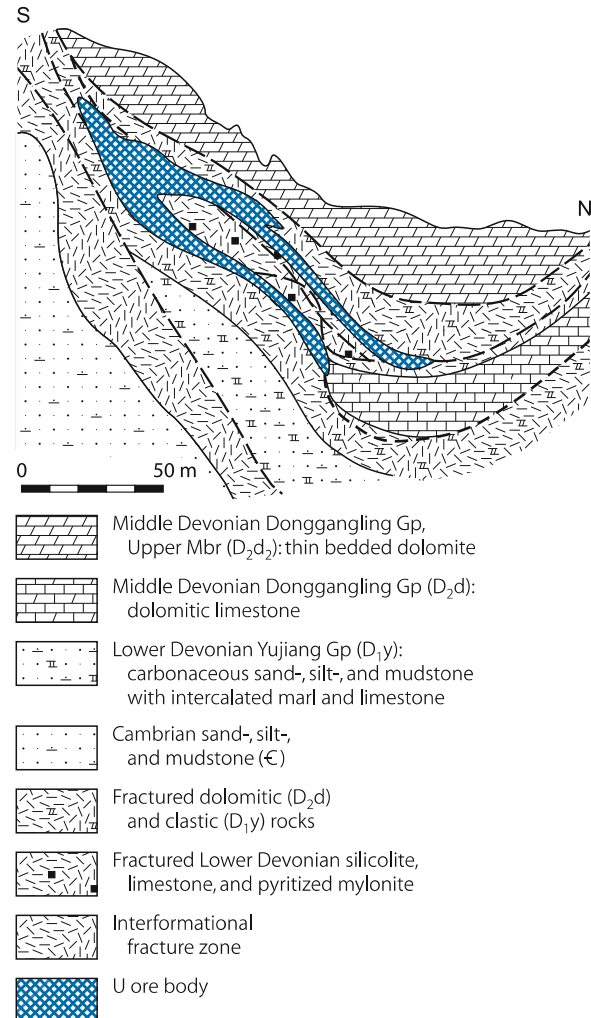
Sandstone-type U deposits of commonly small size and insignificant economic value have been found in several down-faulted Mesozoic-Tertiary basins, mainly in those of Late Cretaceous-Paleogene age. These basins are scattered throughout the South China U province and filled with continental redbed and/or pyroclastic sediments as well as effusive basalt and alkali-basaltic rocks. Most basins trend NE to NNE parallel to contemporaneous fault systems. U mineralization is of peneconcordant tabular habit but also of vein type discordant to the bedding. Deposits are preferentially situated adjacent to granitic or volcanic complexes that host related U deposits.

Deposits are reported from the *Hengyang Basin* in Hunan Province, *Xinwu Basin* in Jiangxi, and *Jingan Basin* in Guangxi, which will be briefly discussed below. Some minor deposits and occurrences are also known from the *Ganzhou* and *Ningdu Basins* in central-south Jiangxi, and from the *Heyuan*, *Nanxiong*, and *Mabugang Basins* in northern Guangdong. Most of these deposits are hosted in Late Cretaceous-Paleogene redbed strata and to a minor degree in dark-colored coal-bearing Neogene sediments as in the Mabugang Basin.

1.4.4.1 Hengyang Basin, Hunan

The Hengyang Basin hosts the *Wangjiachong* (also named Dapujie or Dabao) deposit, discovered in 1955, and three small

Fig. 1.47. Daxin deposit, SW Guangxi, S-N sketch profile showing C-Si-pelite-type U mineralization governed by an intraformational fracture zone at the contact between Devonian (D_{2d}) and Cambrian (ϵ) strata (Zhou Weixun 1997)



deposits, *Pukuitang* (Puquitang), *Sibbeichong*, and *Lulitang* in southern Hunan. These deposits occur over a NNE to SSW distance of about 50 km between the NE margin of Hengdong County and Hengyang City. Explored resources of Wangjiachong are in the 1 500–5 000 t U category at grades of 0.05–0.1% U and the other three deposits in the 500–1 000 t U category. Wangjiachong was mined in the 1960s by underground methods, and is dormant since early 1970 due to discontinuity of ore bodies, decrease in ore grade, and increase in carbonate content.

The *Hengyang Basin* occupies 3 900 km² and is filled with Cretaceous-Eocene redbed series. Host rock is light grey, fine- to medium-grained sandstone and siltstone of Middle Cretaceous age. The basin is controlled by NE-SW-trending faults and overlies a basement of Proterozoic to Early Paleozoic slightly metamorphosed rocks, Late Paleozoic-Early Mesozoic (D_2 - Tr_1) marine carbonate-clastic rocks, and Yanshanian granite.

The *Wangjiachong deposit* is controlled by E-W- and NE-SW-trending faults in the south flank of a brachyanticline. Host strata

dip 10–25° SE. The deposit consists of a number of ore bodies that are discontinuously distributed along strike and dip. Uranium occurs mostly adsorbed on organic matter and clay but also in the form of pitchblende and minor coffinite. Associated minerals are present in small amounts and consist mainly of pyrite with minor Cu-, Pb-, and Zn-sulfides. An isotope age of 68 Ma was obtained for pitchblende. Ore bodies are mostly of strata-concordant, tabular and lenticular shape, but some also cut the bedding, although rarely. Ore bodies range from 20 m to 200 m in length and width, mostly from 0.5 to 1 m in thickness, and occur at depths from surface to 150–200 m, exceptionally to 250 m.

1.4.4.2 Xinwu Basin, Beimianshi Ore Field, Jiangxi

The Xinwu Basin lies in Xinwu County, SE Jiangxi Province, and contains five adjacent basal-channel sandstone-type U deposits in the Beimianshi ore field. Total explored resources are in the 1 500–5 000 t U category at grades of 0.1–0.3% U. Small scale mining was discontinuously conducted by local people.

The Xinwu Basin consists of several small depressions, 22 km² in total area, in the eastern part of the Nanling magmatic belt. Middle Jurassic volcano-sedimentary rocks fill the depressions. This suite is divided into an *Upper Member* of alternating tuff and basalt, and a *Lower Member* with four units each of which consists in the lower half of sandstone and/or conglomerate and in the upper half of basalt. The lower half of the lowermost unit is composed of granitic conglomerate and sandstone and rests immediately upon the basement; it is covered by 20–60 m thick basalt. Quartz-porphry dikes cut the basin facies. The lowermost unit hosts U mineralization in carbonaceous sandstone in trough structures incised into the basement.

Host rocks are altered by hematitization, kaolinitization, chloritization, calcitization, and fluoritization. These alteration phenomena are particularly developed where quartz-porphry dikes intersect U-hosting sandstone beds.

Uranium is present in adsorbed form, pitchblende, black products (sooty pitchblende), and other U⁶⁺ minerals. Associated metallic minerals include pyrite, marcasite, galena, with minor sphalerite and chalcopyrite. Age dating gives ages of 153 Ma for pitchblende in paragenesis with amorphous organic gel and pyrite, 137–131 Ma for pitchblende in paragenesis with clay alteration minerals, and 102–86 Ma for pitchblende in paragenesis with hematite.

Ore bodies are largely of tabular to lenticular shape, except for rare veins. Stratiform ore bodies are 20–50 m in length with a maximum of 140 m, several meters to more than ten meters in width, 0.8–1.5 m in thickness with a maximum of 8.5 m, and occur at depths of 100–350 m (Zhou Weixun 2000).

1.4.4.3 Jingan (Shiwandashan?) Basin, Tunling Deposit, S Guangxi

The Mesozoic-Tertiary Jingan (Shiwandashan?) Basin is situated in southwestern Guangxi A.R. from where it extends into

Vietnam. The basin contains close to its NE rim the sandstone-type *Tunling* deposit, 65 km SE of Hengxian of. Explored resources are on the order of 100–500 t U. Average grade is about 0.05% U.

The Chinese part of the *Jingan Basin* is 240 km long in ENE-WSW direction, 40–60 km wide, and 11 800 km² in areal extent, and filled with continental Triassic-Jurassic arkosic sediments covered by Cretaceous and Tertiary strata.

The *Tunling deposit* is in the NE part of the basin not far to the SE of the Taima granitic batholith of Hercynian age. This batholith, also termed Dasi Massif, is part of the Darongshan-Shiwandashan Hercynian granitic zone. The Taima granite contains between 5 and 15 ppm U. Ore lodes are hosted by Middle Jurassic quartzo-feldspathic sandstone below the Cretaceous interface. U mineralization consists of pitchblende and coffinite associated with pyrite and some chalcopyrite, bornite, tetrahedrite, galena, sphalerite, and bournonite. Age datings yield 113 Ma for pitchblende only, 61 Ma and 51 Ma for pitchblende associated with coffinite and pyrite, and 38 Ma for pitchblende associated with coffinite and pyrite in calcite veins, cavity fillings, and as coatings of microfissures. Ore bodies dip steeply, are some 200–250 m in length, 1–2 m in thickness, and occur at depths of up to 270 m. Grades range from 0.05 to 0.93% U and rarely up to 2% (Simpson and Yu 1989).

1.5 West Yunnan U Province, Yunnan, SW China

The West Yunnan Uranium Province, also termed Dianxi (= Chinese term for western Yunnan) sandstone uranium belt, encompasses a number of Neogene intermontane basins between the Burma border and the Lancang Jiang (= river) in southwestern Yunnan Province (► Fig. 1.48). Two U regions are known: Gaoligong in the Gaoligong Uplift/Baoshan Medium Massif (► Fig. 1.49) and Lincang located to the west and north of the town of Lincang.

Gaoligong contains basal-channel sandstone-type U deposits in Pliocene-Pleistocene sediments whereas the *Lincang* region is known for lignite-related small U occurrences and large germanium deposits associated with uranium mineralization in Miocene continental sediments.

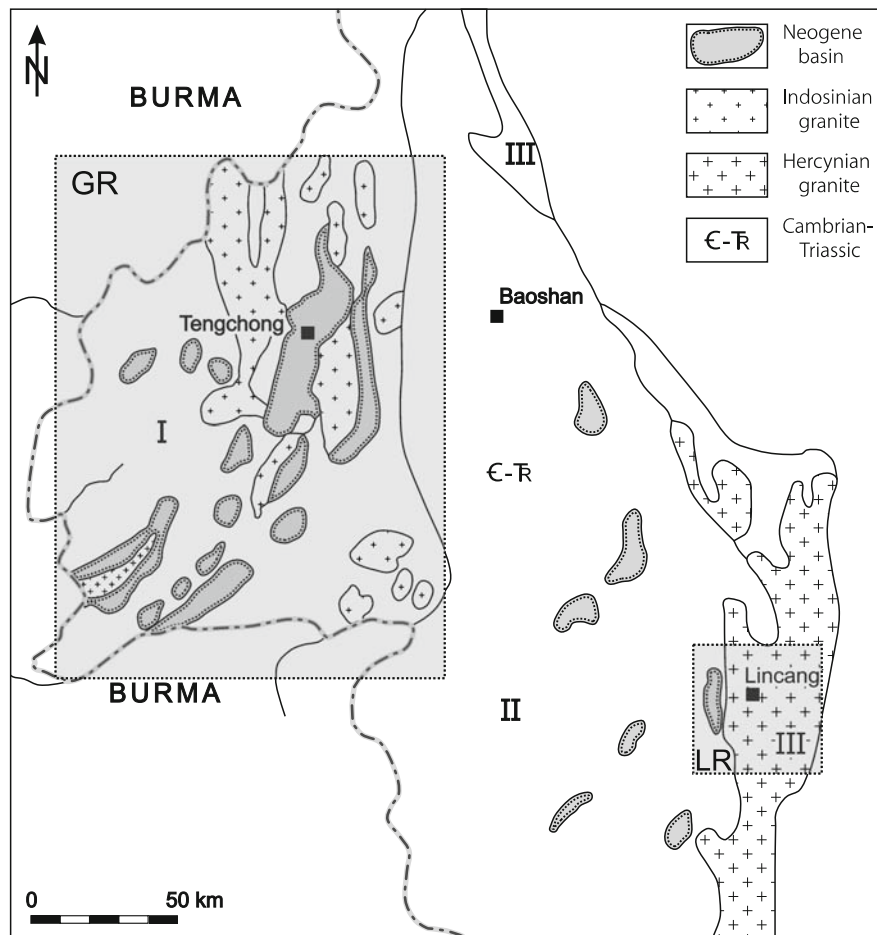
Sources of information The following description is largely based on Chen Youliang and Zu Xiyang (2002), Dai Jiemin (1990, 1996), Liu Xingzhong and Zhou Weixun (1990), Zhou Weixun (2000) and pers. commun., and Zhou Weixun et al. (2002), unless otherwise noted.

Regional Geology and Characteristics of Mineralization

The West Yunnan terrane occupies Precambrian terrane that originated from Gondwanaland and was amalgamated by Mesozoic-Cenozoic fold belts. A northern branch of the Neotethys, the Nujiang Basin, covered parts of the region until

Fig. 1.48.

West Yunnan U province, SW China, location map of Gaoligong (GR) and Lincang (LR) U regions (Dianxi sandstone U belt). (after Liu Xingzhong and Zhou Weixun 1990) I-III Baoshan Median Massif: I Gaoligong Uplift, II Baoyong Depression, III Lancang Uplift



the end of Jurassic. Syn- and post-tectonic granites were repeatedly intruded during the Caledonian (Yangtze/Guangxi), Hercynian, Indosinian, Yanshanian, and Himalayan orogenies. Block faulting related to the Late Himalayan Orogeny resulted in the down thrust of intermontane basins that were filled with Neogene and younger fluvial and lacustrine sediments. Pleistocene basalt covers portions of the region. Prominent, repeatedly reactivated structures trend N-S, E-W, NNE-SSW, and NNW-SSE.

The distribution of ore bodies tends to be controlled, at least partially, by these structures and their intersections. Ore bodies are commonly of tabular or lenticular configuration controlled by lithology-geochemistry but where host beds are cut by faults, the main ore bodies are of stack shape and are aligned, as are mineralized intervals, along the trend of main faults.

Ore bodies commonly occur in the reduced basal and intermediate section of the sedimentary sequence; and are positioned, without exception and age of the host sandstone, in horizons beneath infusorial earth (tripolite) or basalt layers (Fig. 1.50).

Ore lodes are enveloped in a hydrothermally altered halo reflected by silicification, carbonatization, argillization, hydromicazation, and pyritization of sediments. Basalt that overlies mineralized horizons exhibits bleaching, iddingsitization,

opalization, argillization, and carbonatization. Quartz grains are corroded in some deposits. In some surficial mineralization, a large quantity of sulfur and calc-sinter are found, and hydrogen sulfide is emanating from the surface.

Potential Sources of Uranium

Granites and Neogene sediments with elevated U background values are considered potential U sources for the West Yunnan U deposits. Indosinian, Yanshanian, and Himalayan granites average from 3.5 to 6.8 ppm U; part of which occurs as uraninite. The highest amounts of U (6.8 ppm) and uraninite are found in Early Himalayan granite. Neogene sediments contain commonly between 2 and 8 ppm U but feldspathic sandstone in the reduced basal section of the Neogene sedimentary sequence in Longchuanjiang Basin averages up to 18 ppm U (Dai Jiemin 1996).

Metallogenic Concepts

The formation of sandstone-type U deposits in western Yunnan seems to be a result of a combination of supergene,

■ Fig. 1.49.

Gaoligong U region, West Yunnan, generalized geological map with location of Neogene basins and sandstone-type U deposits (after Zhou Weixun 2002 based on Chen Youliang et al. 2002) [U deposit in Longchuanjiang Basin: 1 Wujiashai (384), 2 Yanzitou (50), 3 Chengzishan (#381)/Tengchong Mine, 4 Gejiazhai (382), and 5 Tuantian (506); Tengchong-Lianghe Basin: 6 Shuiyingsi (108) and 7 Shapo (602)]

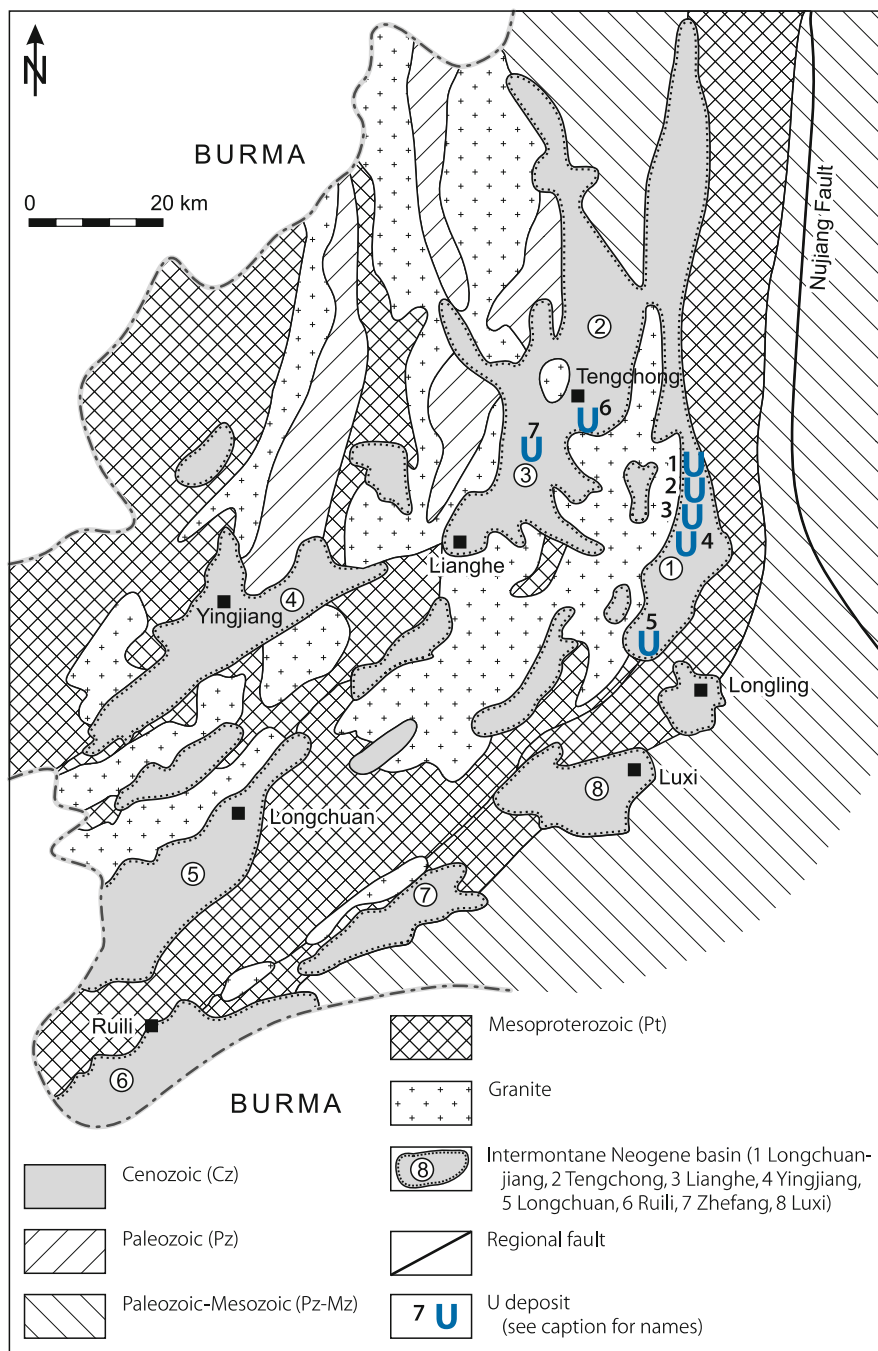
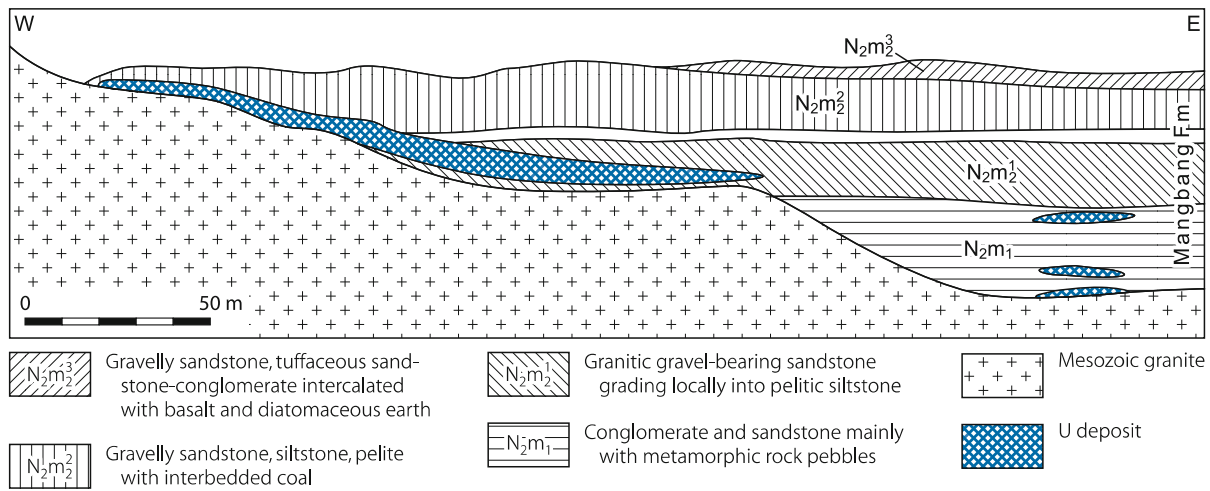


Fig. 1.50.

Longchuanjiang Basin, Chengzishan deposit (#381), schematic litho-stratigraphic section. with position of U ore bodies in the Pliocene Mangbang Formation (courtesy of Zhou Weixun based on Geological Team no. 209, 1985)



weathering- related, and hydrothermal, volcanism- and tectonism-related processes. Granite provided both the clastic material for Neogene and younger sediments and the uranium in the course of its weathering. Uranium was presumably transported in two modes into the basins; rock-inherent U in rock fragments and liberated uranium in solution. Where the former accumulated in clastic sediments, the sediments achieved elevated U background values and as such provided a potential U source. Dissolved uranium migrated downdip and was precipitated in the form of stratiform lenses where solutions encountered a reducing environment. This environment was provided by disseminated organic matter in some basins (e.g. in the Gaoligong Basins) and by lignite seams in others (e.g. in Lincang Basins). Hydrothermal activity remobilized the original U endowment along faults and formed veinlike or stacked ore bodies with tongue-like extensions into permeable horizons.

As deduced from Dai Jiamin (1996), hydrothermal activity and its effects are reflected by the following features. The U region of western Yunnan has been geothermally anomalous since the Neogene as documented by sedimentation of infusorial earth (tripolite) and effusion of intermediate-basic magma that suggest a universal increase of geothermal flux values. Repeated intense volcanic activity is recorded in the Gaoligong region from Neogene into Quaternary. Thermal springs are still active today within the Lincang and Gaoligong U regions and thermal groundwater is still abundant in some U deposits. Recent thermal groundwater has temperatures of as much as 30–70°C; and the geothermal gradient is 5–12°C per 100 m higher than the normal geothermal gradient.

The distribution of geothermal fluid activity is and presumably was controlled by fault systems as exemplified by the situation in deposit # 382/Gejiazhai, Longchuanjiang Basin (Fig. 1.51). The recent geothermal isograd pattern conforms to a set of NNE-SSW and partially of E-W-trending faults that were reactivated during the Late Himalayan Orogeny. A similar pattern is documented by U grade distribution in this deposit.

Uraniferous, siliceous solutions circulating in fissures are thought to be the medium for uranium transport within uranium deposit 602, Longchuanjiang Basin, as deduced from pyritic chalcedony vein fillings in the main fault that contain about 10.2 ppm U, and siliceous veinlets in wall rocks that contain 8.8–12.1 ppm U. In contrast, siliceous veinlets in sandstone-hosted uranium ore can be as high in U as 0.013–0.044%. Additional evidence is provided by veined mineralization composed of pitchblende-hematite, pitchblende-sphalerite-quartz, and/or pitchblende-pyrite as found in some deposits.

A proof for the involvement of hydrothermal solutions in U metallogenesis is also seen in the composition of associated minerals, particularly in the high content of trace elements in euhedral pyrite contained in uranium-bearing siliceous veins and main ore horizons. This pyrite contains 9–39 ppm and, rarely, up to 0.783% U, 0.03–0.08% As, 0.4–0.5% Ti, 0.05–0.10% Be, 0.02–0.05% Pb, 0.01% Co, and 0.02% Sb. The Co/Ni ratio is 1.5–5.0 with maxima of 10.0. Siderite in ores of deposit 381 can have up to 0.54% U.

Limited research by decrepitation tests on U-associated components in deposit 382 indicates a formation temperature of 197°C for pyrite associated with uranium. Fluid inclusions yield a homogenization temperature of 120–200°C and a composition enriched in SO_4^{2-} , Cl^- and F^- . Coffinite found in several deposits may indicate a silica component in, and an alkaline character of fluids. These parameters are compatible with a meso- and epithermal alkaline siliceous composition for the ore-forming solutions; a composition that is relatively close to that of recent thermal springs in the Gaoligong subregion.

U/Pb dating of pitchblende suggests that U mineralization took place during the final two episodes of the Himalayan Orogeny. An early, Late Miocene-Early Pliocene metallogenetic event at 6.2–5.4 Ma (9.3–7 Ma by Pb/Pb method) is indicated for U mineralization in the Lincang Basins; and a second, Late Pliocene, event at 4.4–2.2 Ma (4.0–3.5 Ma by Pb/Pb method) for U mineralization in the Gaoligong Basins. These ages correlate

■ Fig. 1.51.

Longchuanjiang Basin, Gejiazhai deposit (#382), **a** generalized geological section across the deposit; **b** isoline contour map of average U grades (Dai Jiamin 1990)

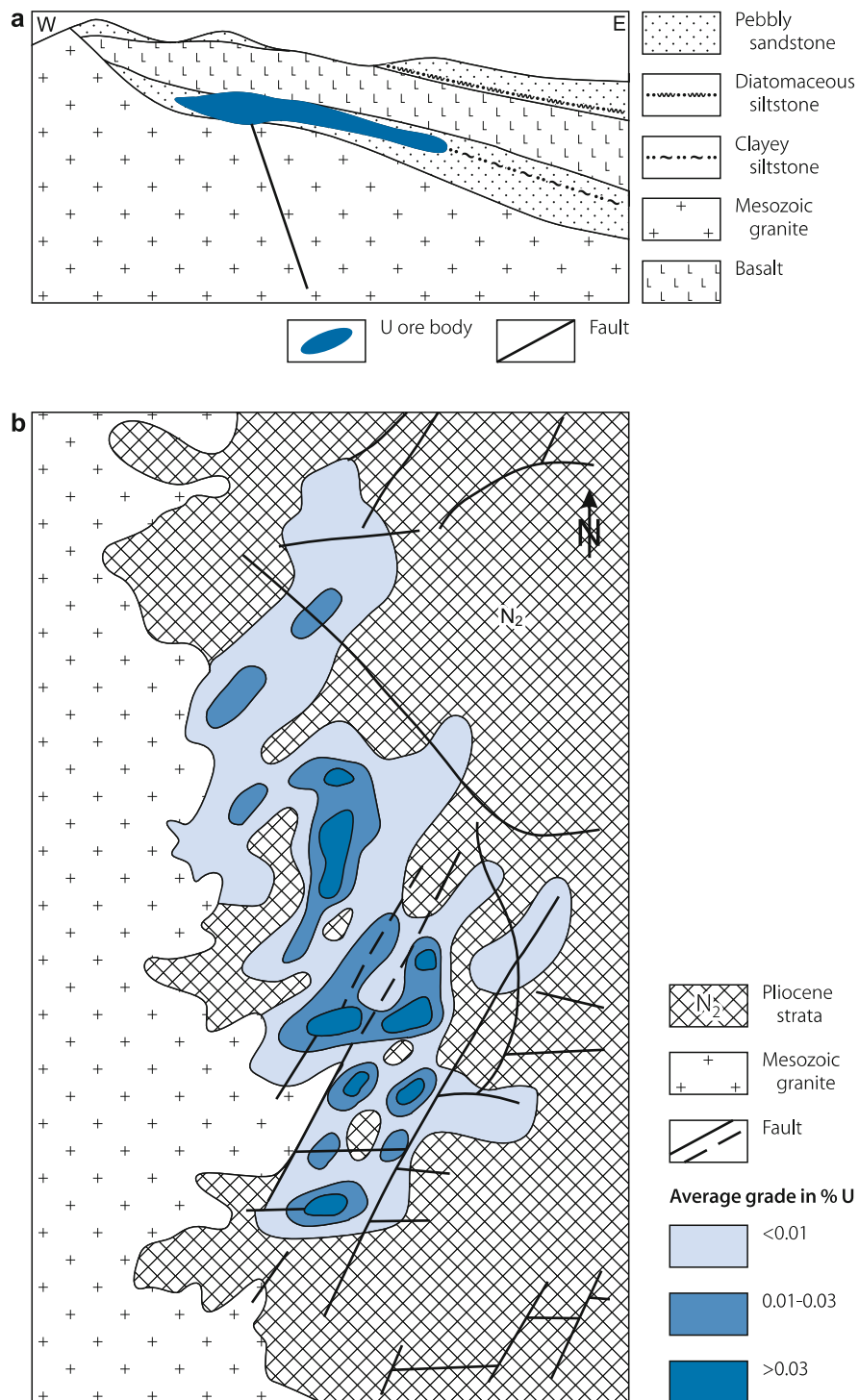
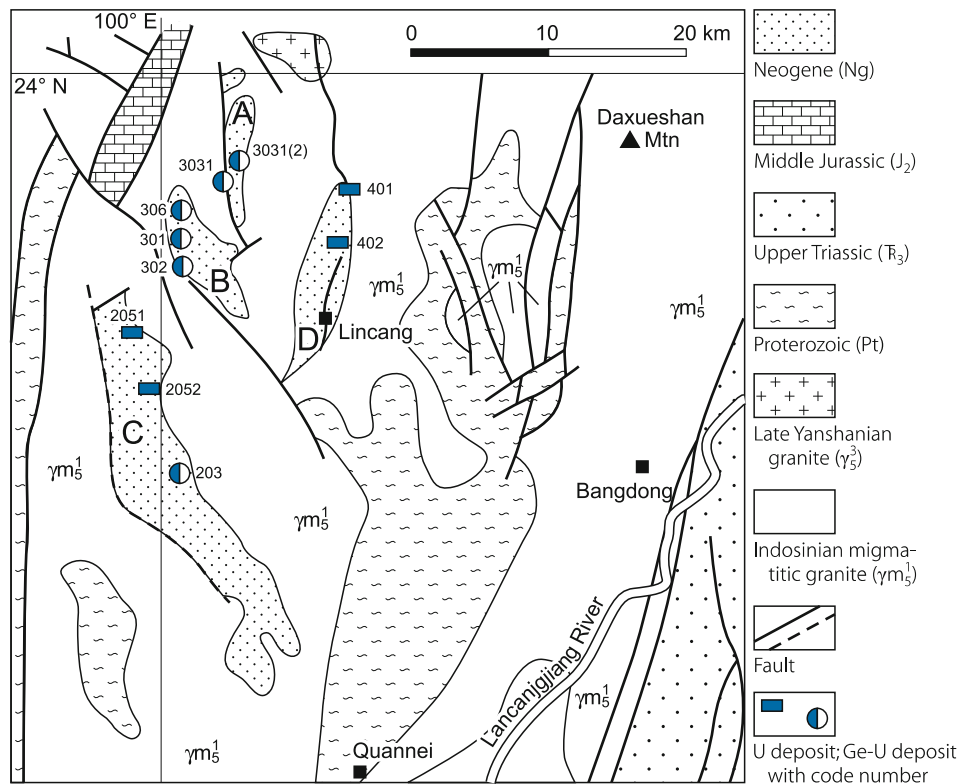


Fig. 1.52.

Lincang region, West Yunnan, sketch map showing the distribution of Neogene basins (A Mengwang, B Bangmai, C Mengtuo, D Lincang) and uranium deposits of ore field #303 (courtesy Zhou Weixun 2002 based on Chinese literature)



approximately with repeated volcanic events in the two regions; whole rock K-Ar ages for basalt yield 7.27–5.47 Ma for an early stage and 4.1–2.25 Ma for a later stage (Dai Jiemin 1996).

In summary, U deposits in the West Yunnan U belt may be classified as remodified basal-channel sandstone type that were formed by repeated metallogenetic processes, presumably of a different nature. Hydrothermal activity that occurred roughly coeval with volcanic episodes has played a significant role in the metallogenesis of these deposits. It remains an open question, however, as to what extent supergene or hydrothermal processes were responsible for formation of U accumulations in stratiform ore bodies.

1.5.1 Gaoligong Region

The Gaoligong region is located west of the Nu Jiang river and includes the town of Tengchong, a well-known spa with hot springs. Basal-channel sandstone-type U deposits in Pliocene-Pleistocene sediments are reported from the NNE-SSW-trending, valley-type Longchuanjiang and Tengchong-Lianghe Basins, separated by and situated to the west and east, respectively, of the Menglian granitic highland. The *Longchuanjiang Basin*, about 50 km² in size, is the principal uraniumiferous basin; it contains several U deposits including deposits *Chengzishan* (#381)/Tengchong Mine, *Gejiazhai* (382), *Tuantian* (506), *Wujiashai* (384), and *Yanzitou* (50). The *Tengchong-Lianghe*

Basin includes the *Shapo* (602) and *Shuiyingsi* (108) deposits (Fig. 1.49).

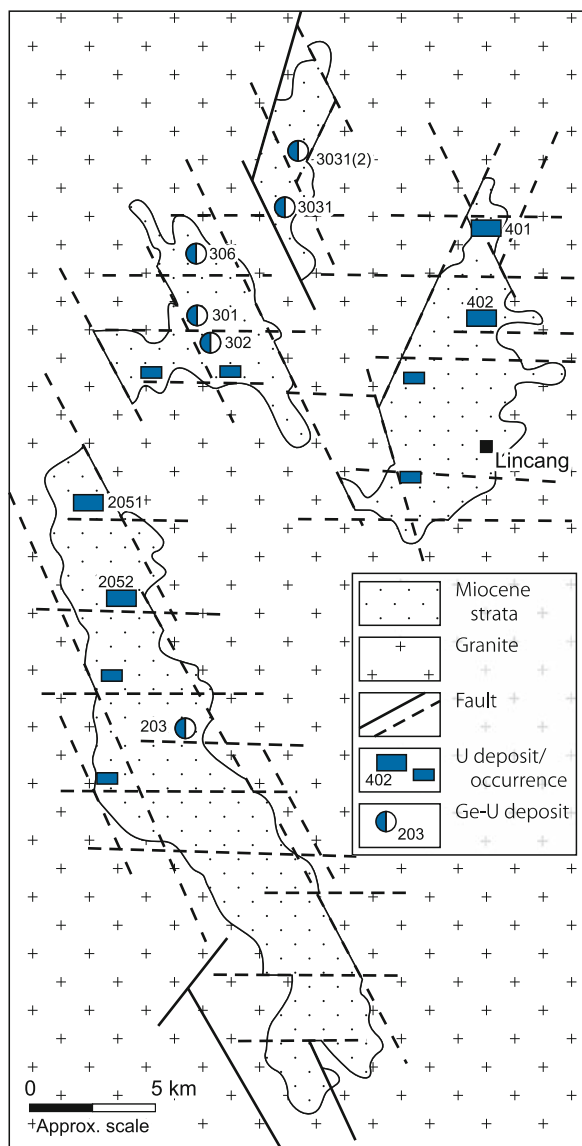
Sources of information. Dai Jiemin 1990, 1996; Zhou Weixun 2000; Zhou Weixun et al. 2002.

Regional Geology and Mineralization

Most of the Cenozoic basins in the Gaoligong region are unsymmetrical half-graben down-faulted basins that range from several tens to 700 km² in size. Each of these basins is related to a major fault zone. Basin fillings consist of Pliocene and partly Pleistocene continental sediments that rest upon a basement of Mesoproterozoic metamorphic rocks of the Tengchong and Baoshan fold belts, and Mesozoic granites. Pleistocene rocks consist essentially of basalt and andesite-basalt. Lignite-bearing clastic sediments with intercalations of basalt, tuff, and diatomaceous earth constitute the Upper-Middle Pliocene; while the Lower Pliocene is composed of grey, megaclastic molassoid deposits.

Uranium occurs in the form of tabular, lenticular, and locally fault-controlled, stacked ore bodies mainly in alluvial sediments of the basal Upper-Middle Pliocene sequence, and to a minor degree in the lower section of the Lower Pliocene molassoid unit. These sediments are attributed to the Mangbang (Mangbanzu) Formation. Most U deposits are hosted in basal fillings of

Fig. 1.53. Lincang region, U ore field #303, schematic structural map showing the relationship between the position of U deposits/occurrences and fault pattern in Neogene basins (after Dai Jiamin 1990)



tributary channels composed of sandstone, with minor siltstone and pelite. These channels are commonly 0.5–5 km long, 0.02–2 km wide, incised into the basement on the basin slopes, and trend perpendicular to the long axis of the main basin. Some mineralization occurs in bog deposits, and locally in eluvial matter upon regolithic granitic basement.

1.5.1.0.1 Chengzishan/Tengchong Deposit, Longchuanjiang Basin

This basal-channel U deposit lies in Tengchong County, Yunnan Province. Original resources were between 500–1500 t U at grades of less than 0.1% U. *Chengzishan* has been exploited by the *Tengchong* open pit mine and tested for ISL operation (Wang Jian and Dai Yuan Ning 1993).

Sources of information. Liu Xingzhong and Zhou Weixun 1990; Zhou Weixun 2000; Zhou Weixun et al. 2002.

Geology and Mineralization

The Chengzishan deposit (Fig. 1.50) is situated at the western edge of the Longchuanjiang Basin, close to the outcrop of granitic basement. Uranium occurs in the Middle Pliocene Mangbang Formation that is three-partitioned into an Upper, Middle, and Lower Member. Gravel-bearing sandstone, tuffaceous sandstone, conglomerate intercalated with basalt, and diatomaceous earth constitute the Upper Member. The Lower Member includes an Upper Submember mainly composed of siltstone and fine-grained sandstone; and a Lower Submember composed of (from top to base) grey megaconglomerate, conglomerate; greyish white gravel, conglomerate, and sandy conglomerate with intercalations of grey sandstone and carbonaceous sandstone; and basal grey megaconglomerate with intercalations of sandstone lenses. The uranium-hosting Middle Member consists of sediments of an alluvial fan and braided delta system that trends sublongitudinal and dips at 5–15° eastwards.

Ore bodies are of lens, tabular, and stacked shape and occur at depths from 10 to 200 m. Tabular and stacked lodes are from some 10 m to 160 m long, 1–8 m thick, grade 0.03–0.1% U, and occur at shallow depth in weakly cemented, seriate sands and sandy gravel with good permeability. Lenticular ore bodies are hosted by thin-bedded, silty argillaceous layers enriched in organic matter and pyrite in the deeper section of the deposit. Organic carbon contents range in sand from 0.13 to 0.27% and in silt-mud from 4 to 8%; CO₂ contents range from 0.8 to 1.7%.

Uranium occurs mainly adsorbed on organic matter, pyrite, and clay minerals, and less frequently in the form of pitchblende and secondary U minerals associated with pyrite, siderite, and anatase. Two pitchblende samples gave an isotopic age of 4.4 Ma and 2.2 Ma.

1.5.2 Lincang Region

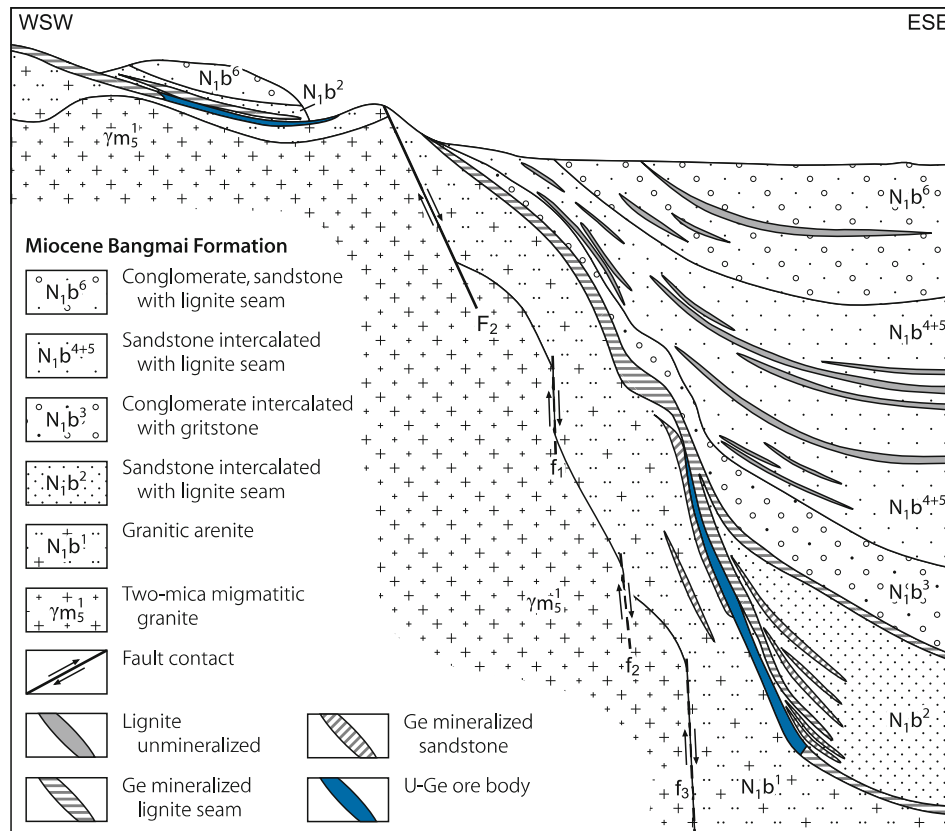
The Lincang region [referred to as South Lincang (Mekong) River metallogenic subbelt by Dai Jiemin 1990, 1996] includes a series of small Late Cenozoic basins. U and Ge-U deposits and occurrences are reported from the *Lincang*, *Mengwang*, *Bangmai*, and *Mengtuo* Basins in the area at and around the town of Lincang in southwestern Yunnan (Fig. 1.52).

Monometallic U mineralization forms only small occurrences such as #401 and 402 in the Lincang Basin whereas germanium deposits with associated U mineralization can be quite large. *Ore field #303* (with deposits 3031 and 3032) in the Mengwang Basin, and deposits 301/*Dazhai* (see below), 302, and 306 in the Bangmai Basin are examples of the latter type.

Sources of information. Dai Jiemin 1990, 1996; Zhou Weixun 2000, pers. commun.

Fig. 1.54.

Bangmai Basin, Dazhai deposit (#301), geological WSW-ESE profile along exploration line #0 illustrating the distribution of Ge and U-Ge mineralization in basal strata of the Miocene Bangmai Formation (courtesy of Zhou Weixun 2002 based on Chinese literature)



Regional Geology and Mineralization

The intermontane Lincang Basins occur in the South Lincang River fold belt and are filled with 120–2 000 m thick Miocene lignite-bearing continental sediments. Metamorphic rocks of the Mesoproterozoic Lincang Group, Hercynian and Indosinian granite, and minor Yanshanian granite form the basement. Fresh basement rocks have average background values of about 9 ppm U whereas the basement topping weathering crust, from 5 to 20 m, locally to 70 m thick, contains 30–70 ppm U.

Uranium is hosted by the Bangmai Formation composed of alternating sandstone, conglomerate, grit, siltstone, and interbedded lignite seams from 0.3 m to 14 m thick. Sediments in the lower section are reduced while sediments in the upper section are not.

Both *monometallic U ore* bodies as typically found in the Lincang Basin and *Ge(-U) ore* bodies in the Mengwang and Bangmai Basins (Fig. 1.53) are tabular and lenticular shaped. U mineralization occurs preferentially in poorly sorted, reduced feldspathic sandstone in the basal section. The sandstone contains 20–30%, locally up to 60%, subangular feldspar (predominantly potash feldspar), about 5% biotite, and often gravel and rock fragments that indicate a granitic source. The sandstone matrix includes 0.13–0.27% organic carbon, 4–18% clay, 0.3–1.5% pyrite, and 1.5–3.5% hematite. Monometallic U ore bodies and Ge(-U) ore bodies are also hosted in the 1st to 6th lignite seam

and interbedded sandstone of the Upper Member of the first cycle of the Bangmai Formation (N_{1b}^2) (Fig. 1.54). The first lignite seam, 6–12 m thick, is the major ore host. Conglomerate of the Lower Member (N_{1b}^1) is locally uraniferous.

The distribution of mineralization is controlled by structures as documented by the position of deposits and occurrences. They occur at the intersection of E-W- and NNW-SSE-trending faults and in isodistance distribution that correlates with the isodistance distribution of E-W-trending faults (Dai Jiemin 1996).

1.5.2.0.1 Dazhai Deposit, Bangmai Basin

Dazhai (#301) is a large germanium deposit with associated U mineralization, positioned in the steeply dipping western limb of a syncline near the western edge of the Bangmai Basin (Fig. 1.54). The deposit persists for some 200 m along strike and from tens of meters to 700 m downdip. It consists of a number of mineralized beds arranged in a broom-like configuration with a wide range of thickness. Monometallic Ge ore is mainly hosted in the 2nd to 6th lignite seam or in intercalated sandstone of the Bangmai Formation while U-Ge ore is only present in the 1st (basal) granitic arenite (Fig. 1.54).

Two varieties of Ge ore occur: (1) Ge-bearing lignite containing 0.045% Ge and accounting for 93% of the total Ge reserves with the bulk of these reserves (92%) contained in a

single seam; and (2) Ge-bearing carbonaceous sandstone with an average of 0.04% Ge accounting for 7% of the Ge reserves. The distribution and state of germanium are as follows: (1) High amounts of Ge occur evenly distributed in vitrinite (0.16–0.36% Ge) and geliform groundmass (0.05–0.21%). (2) 50–90% of the germanium is concentrated in the density fraction of 1.35–1.45 gmm⁻³, with highest concentrations in the 1.35 gmm⁻³ fraction. (3) Ge is mainly enriched in the coarse-grained fraction (1.6–3 mm) essentially composed of vitrinite. (4) The electro dialysis rate of Ge in ore samples is highest in a strong acid medium. (5) When humic acid and asphalt are extracted, most Ge in ore comes into solution, and Ge in dregs accounts for only 1.5–4.5%. (6) Most Ge is in the humic acid-connected state during progressive chemical extraction, accounting for 47–66% of the total Ge in ore, or 73–83% including other organic matter-connected forms (Zhou Weixun, pers. commun.).

References and Further Reading for Chapter 1 • China

For details of publications see Bibliography.

Cai C. et al. 2007; Chen Anping et al. 2002; Chen Ranzhi and He Caiyi 1996; Chen Yifeng 1996; Chen Youliang and Zu Xiyang 2002; Chen Yuehui 1995; Chen

Yuqi et al. 1996; Chen Zhaobo 1981; Chen Zhaobo and Fang Xiheng 1985; Chen Zhaobo et al. 1982, 1996, 2000; Chen Zuyi 2002; Chen Zuyi and Huang Shijie 1993; Dai Jiemin 1990, 1996; Deng Ping et al. 2002; Du Letian 1982, 1986; Du Letian et al. 1990; Fan Honghai et al. 2002, 2003; Feng Mingyue et al. 1996; Finch et al. 1993; Gu Kangheng and Wang Baoqun 1996; Guo Zhitian et al. 1996; Han Zheaong et al. 1985; Hou YQ et al. 1993; Huang Guangrong and Pang Yuhui 1987; Huang Shijie 1996; Huang Zhizhang et al. 2002; Jiarong Z and Zhitian G 1984; Ju Yejun et al. 1990; Li Jian-Wei 1998; Li Jian-Wei et al. 2001, 2002; Li Shengxiang et al. 2000, 2002, 2005; Li Tiangan et al. 1996; Li Tiangan and Huang Zhizhang 1986; Li Wenxing 1990; Li Ziyang et al. 2002, 2005; Lin Shuangxin et al. 2002; Liu Ruzhou et al. 1995; Liu Xiadong, Zhou Weixun 2005; Liu Xingzhong and Zhou Weixun 1990; Liu Yifa et al. 1990; Luo XZ et al. 1999; Luo Yi et al. 1996; Malan 1980; Min MZ 1991, 1995; Min MZ et al. 1996, 1997, 1999, 2002; NUKEM 1999; OECD-NEA/IAEA 1991–2005; Pan Yongzheng and Zhang Jianxin 1996; Peng Xinjian et al. 2002; Qin Fei and Hu Shaokang 1980; Raizhang Hu et al. 2008; Saima Deposit Research Group 1976; Saima Scientia Sinica 1977; Shen Feng 1991, 1995; Shen Feng et al. 1992; Shen J 1991; Shi Wenjin and Hu Junzhen 1996; Simpson and Yu Shiqing 1989; Tu Guangzhi 1990; Wang Chuanwen et al. 1980; Wang Jian and Dai Yuan Ning 1993; Wang Jinping et al. 2002; Wang Yusheng and Li Wenjun 1996; Xia Yuliang et al. 2002; Yao Zhenkai et al. 1989; Yin Di 1990; You Yunfei et al. 1996; Yu Dagan et al. 2002; Zhang Bangdong 1990; Zhang LG 1985; Zhang Rong 2001; Zhang Ruliang and Ding Wanlie 1996; Zhang Zuhuan 1990, 1991; Zhenkai Yao et al. 1989; Zhong Jiarong and Guo Zhitian 1984, 1988; Zhou Weixun 1988, 1996, 1997, 2000; Zhou Weixun and Chen Anping 2001; Zhou Weixun and Teng R 2003; Zhou Weixun et al. 2002, 2003, 2006a, 2006b; Zhou Wenbin et al. 2002; Zhu Jiechen et al. 1996; Zhu Minqiang et al. 2002.

Chapter 2

India

Uranium deposits/occurrences in India are of various types, commonly of small size and low grade. Deposits are confined to the *Singhbhum* region, Jharkhand (formerly Bihar) State; *West Khasi Hills/Meghalaya Plateau*, Meghalaya State; and *Cuddapah Basin*, Andhra Pradesh State. In addition, U occurrences are known from other regions including the *Bhima Basin*, Karnataka; *Chhattisgarh Basin/Sambalpur Granite Massif*, Madhya Pradesh-Orissa; *Aravalli* and *Delhi Basins*, Rajasthan; and other areas in India (► Fig. 2.1).

Byproduct U resources include (a) *uraniferous copper deposits* in the *Singhbhum* region, (b) *monazite placers* in Kerala, (which contain significant amounts of uranium at concentrations of up to 0.35% and associated thorium), and (c) *phosphates* used in the fertilizer industry.

According to OECD-NEA/IAEA (2005), India's in situ resources (RAR + EAR-I) are estimated at 84 600 t U and 64 800 t U of which as recoverable resources. 53.7% of these resources are hosted in vein type, 16.4% in sandstone, 7.7% in "unconformity-proximal", and 22.2% in other types of deposits.

India's production from 1967 through 2005 totaled an estimated 8 400 t U. Annual production was on the order of 200–250 t U. In 2004, about 230 t U were recovered. All ore came from vein deposits in the *Singhbhum* District and was treated in the Jaduguda and Turamdih mills. Additional production centers are planned in the *West Khasi Hills* (Domiasiat mill) on the Meghalaya Plateau, Meghalaya State, and at Lambapur-Peddagattu (Seripally mill) in the Cuddapah Basin, Andhra Pradesh State.

Uranium-related activities are restricted to the "Department of Atomic Energy" of the government of India, which conducts uranium exploration through the "Atomic Mineral Directorate for Exploration and Research" and mining through the "Uranium Corporation of India" (UCIL).

Sources of information. Awati and Grover 2005; Gupta and Sarangi 2006; Nagabhushana et al. 1976; OECD-NEA/IAEA 1997, 2005; Singh 2002; amended by data of other authors cited in the sections of the various uranium regions.

Historical Review

Systematic uranium exploration began in India in 1949, at first in the *Singhbhum* region, Bihar (now Jharkhand) State, where veinlike uranium mineralization has been known since 1937. As a result, the Jaduguda deposit was found as well as a number of other U(-Cu) deposits. Exploration activity was expanded to other regions in India in the 1970s and resulted in the discovery of mostly small and low-grade U deposits in the earlier mentioned regions (► Fig. 2.1) including the sandstone-type Domiasiat deposit in the West Khasi Hills, Meghalaya, NE India, in early 1980s.

During the early 1990s, a granite-hosted deposit was discovered proximal to the unconformity between basement granites and overlying quartzite at Lambapur in Nalgonda District, Andhra Pradesh; and by 1996, additional U occurrences in and at the margin of the Meso- to Neoproterozoic Cuddapah Basin, Andhra Pradesh, were found. Additional discoveries were made in the Proterozoic Aravalli-Delhi Basins, Rajasthan, and Neoproterozoic Bhima Basin, Karnataka.

The first Indian uranium mine, Jaduguda, commenced operation in 1968. Subsequently, the Bhatin (start-up 1987), Narwapahar (1995), and Turamdih (2003) mines, all in the *Singhbhum Thrust Belt*, went in production. The ore is treated in mills at Jaduguda (commissioned in 1967) and Turamdih (start-up 2003?).

2.1 Singhbhum Cu-U Belt, Jharkand

As listed by Sarkar (1986), the *Singhbhum Cu-U belt* in Jharkand (Bihar) State, eastern India, hosts deposits of veinlike nature in the following ore fields (from SE to NW and W): (1) *Khadandungri-Purandungri*, (2) *Bagjata-Moinajharia*, (3) *Bhalki-Kanyaluka*, (4) *Badia-Mosabani*, (5) *Surda-Rakha Mines*, (6) *Jaduguda-Bhatin*, (7) *Narwapahar*, and (8) *Turamdih-Keruadungri*.

Original U resources in the *Singhbhum Cu-U Belt* were estimated to be in excess of 215 million t containing 56 000 t U. Some 80% of the resources consist of low-grade ore at 0.012–0.041% U (Sarkar 1982). Jaduguda, with 0.057% U, has the highest grade but accounts for only 6% of total resources. Narwapahar is the largest U deposit.

Currently mined (2006) primary U deposits include *Jaduguda*, *Bhatin*, *Narwapahar*, and *Turamdih* (► Fig. 2.2), which are exploited by underground methods. Ore processing is in the Jaduguda mill (capacity 2100 td⁻¹ ore, 230 t U yr⁻¹). UCIL is the operator. Additional production is planned from deposits at *Bagjata* (UG), *Banduhurang* (OP), and *Mohuldih* (UG/OP). At Turamdih a new processing plant (3000 td⁻¹, 190 t U yr⁻¹) was commissioned in 2003 to serve these mines (OECD-NEA/IAEA 2005).

U is also recovered from copper concentrators as a byproduct from Cu(-U) deposits in three physical beneficiation plants at *Mosabani*, *Rakha*, and *Surda*. The plants began operation in the 1970s and 1980s and produce in total about 150 t d⁻¹ of concentrate with 800–1 500 ppm U.

Sources of information. Banerjee et al. 1972; Battacharyya 1992; Mahadevan 1988; OECD-NEA/IAEA 1997, 2005; Sarkar 1982, 1986; Singh 2002; amended by data of other authors cited.

Regional Geological Setting of Mineralization

The Cu-U belt coincides with the *Singhbhum Thrust Belt* (see below) that crosses Archean-Proterozoic terrane in arcuate, globally E-W-oriented fashion. Principal litho-stratigraphic units and geological-tectonic events in this terrane (► Table 2.1a) are as follows (Bhattacharyya 1992, for geochronological references see his paper):

■ Fig. 2.1.

India, location of uranium regions, active uranium mines, and planned production centers (after Awati and Grover 2005). **Federal states:** AP Andhra Pradesh, ARP Arunchal Pradesh, AS Assam, DE Dehli, GJ Guijara, HP Himachal Pradesh, JK Jharkand (formerly Bihar), J&K Jammu and Kashmir, KE Kerala, KT Karnataka, ME Meghalaya, MH Maharashtra, MP Madhya Pradesh, OR Orissa, RJ Rajasthan, TN Tamil Nadu, UP Uta Pradesh, WB West Bengal



Archean units: The *Older Metamorphic Group* (present as enclaves in Singhbhum Granite) is the oldest unit in the Singhbhum region. It is subdivided into the Older Metamorphic Gneiss (amphibolite, gneiss, schist) and the Older Metamorphic Tonalite Gneiss (intrusive in Older Metamorphic Gneiss). During the Older Metamorphic (or Iron Ore) Orogeny (3.15–3.0 Ga), the post-kinematic Singhbhum Granite was intruded and possibly the Chotanagpur Gneiss as well. Dolerite dikes transect the granitic complex.

Sarkar and Saha (1983) subdivide the *Singhbhum Granite* into three separate intrusive phases: (A) biotite granodiorite and tonalite; (B) granodiorite; and (C) biotite-muscovite adamellite. These authors postulate the deposition time of the Iron Ore Group to be posterior to phases A and B, but prior to phase C of the Singhbhum Granite whereas Bhattacharyya (1992) postulates a transgression of the Iron Ore Group upon the Singhbhum Granite (Table 2.1b).

The *Iron Ore Group* consists of metamorphosed shale, sandstone (arkose, orthoquartzite), conglomerate, mafic lavas and tuff, and iron formations (banded hematite quartzite), a major source of iron in India. This group occurs in two large basins at the eastern and western flanks, and in smaller measures along the northern margin of the Singhbhum batholith.

Paleoproterozoic units: The *Singhbhum Group* is made up of a monotonous flysch sequence of pelitic schists, intercalated with micaceous quartzites, and mafic to ultramafic volcanics. The *Dalma Volcanics*, a pile of submarine volcanic flows, are the largest occurrence of the latter. The *Singhbhum Group* was metamorphosed (M1 metamorphic event) with steepening of the thermal gradient from east to west (staurolite-kyanite in the eastern, staurolite-sillimanite in the central, and staurolite-andalusite in the western part). Partial melting of rocks gave rise

Fig. 2.2.

Jaduguda region, eastern Singhbhum Thrust Belt, simplified geological map with location of U deposits and Cu deposits with by-product U. Mine symbol indicates mines active in 2006 (after Bhattacharyya 1992; Nagabhushana et al. 1976; OECD-NEA/IAEA 2001; Sarkar 1986)

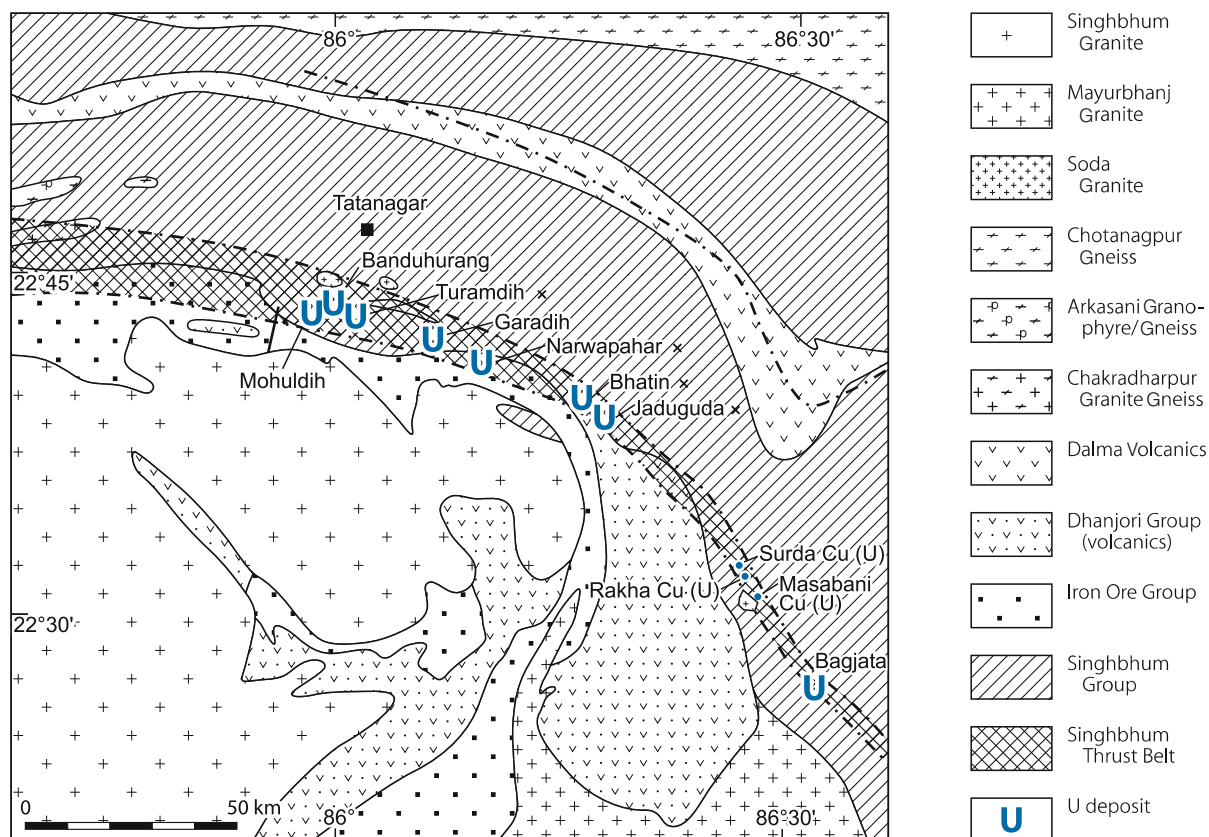


Table 2.1a.

Principal geological events in the Singhbhum region (Sarkar 1986)

Litho-stratigraphic unit/events	Age	Lithology/formation
Late mafic and ultramafic intrusives		
Younger granite rocks		Soda Granite, Arkasani Granophyre, Mayurbhanj Granite
<i>Singhbhum Orogeny</i>	1.6-0.9 Ga (metamorphic age)	(culminating in the development of the Singhbhum Thrust Zone)
Singhbhum Group		Chaibasa Fm: mainly pelitic sediments Dhanjori Fm: volcano-sedimentary pile (Dalma, Simlipal, Jagannathpur)
>Unconformity<		
Singhbhum Granite	~2.95 Ga	(Chakradharpur Gneiss Complex?)
<i>Iron Ore Orogeny</i>		
Iron Ore Group	(unclear, may be Proterozoic)	Pelitic sediments, banded iron formation; ± mafic volcanics
>Unconformity<		
Tonalitic gneiss	~3.8 Ga	
<i>Older Metamorphic Orogeny</i>		
Older Metamorphic Group		Metasediments

to the small bodies of syn- to post-F1-deformation granite and granodiorite (at Tebo in the west and Kuilapal in the east). This was followed by local prograde metamorphism (M2), syn- to post-kinematic with respect to F2 deformation, and later by a third, retrograde metamorphic event (M3).

The *Dhanjori Group*, situated in and immediately south of the thrust belt in the southeastern part of Singhbhum, consists of

amygdaloidal tholeiite, pyroclastics, and tuffaceous rocks interlayered with quartzite, arkose and ferruginous shale, and a discontinuous quartzite bed at the base that rests upon the Singhbhum Granite. The Dhanjori volcanics are correlated with the cryptovolcanic rocks of the *Simlipal Complex*, dated at 2.085 Ga.

Highly elongated granitoid bodies encircle the northern and eastern fringes of the Singhbhum Granite and coincide

■ Table 2.1b.

Comparison of stratigraphic units and geological events in the Singhbhum region (Bhattacharyya 1992)

Bhattacharyya (1992)	Sarkar and Saha (1983)
(4) 1.6 Ga: Hydrothermal-magmatic activity in the Singhbhum Shear Zone, U mineralization	
(3) 2.05-2.0 Ga: Singhbhum Orogeny, Soda Granite, Mayurbhanj Granite, mineralization	(6) 0.95 Ga: Singhbhum Orogeny, Soda Granite, Mayurbhanj Granite, mineralization
(2) Singhbhum Group, Cu-mineralization, Iron Ore Group	(5) Singhbhum Group, Cu-mineralization (4) 3.1 Ga: Iron Ore Orogeny, Singhbhum Granite (Phase C)
	(3) Iron Ore group (2) Singhbhum Granite (Phase A+B)
(1) 3.15-3.0 Ga: Older Metamorphic Orogeny with intrusion of Singhbhum Granite	(1) 3.4 Ga: Older Metamorphic Orogeny
Older Metamorphic group (present as enclaves in Singhbhum Granite) -Older Metamorphic Tonalite Gneiss (~3.8 Ga) -Older Metamorphic Gneiss	

with the Singhbhum Thrust Belt. The largest body is the *Chakradharpur Granite Gneiss* in the west, followed by the *Arkasani Granophyre/Gneiss* and the *Soda Granite* to the east (Fig. 2.2). Also associated with the thrust belt is the larger *Mayurbhanj Granite* body in the east.

The *Chakradharpur Granite Gneiss* is a composite batholith of banded trondhjemitic material intruded by tonalite, granodiorite, granite and alkali-feldspar granite, which was metamorphosed and deformed by the F3 event.

The *Arkasani Granophyre/Gneiss*, located in the western part of the belt in strike-continuation of the Soda Granite distribution, consists of granite and K-feldspar granite while the *Soda Granite* is an albitic rock without K-feldspar. The origin of both, Arkasani Gneiss and Soda Granite, is ambiguous; hypotheses include intrusions into the metasediments, or infolded or upthrust basement rocks, or a metasomatic derivation from mafic schists, which had originated from the Dhanjori volcanics.

The Paleoproterozoic or Archean *Chotanagpur Gneiss* comprises granitic, granodioritic, tonalitic, and other lithologies that occupy a vast terrane to the north of the Singhbhum Group. Many workers (e.g. Sarkar et al. 1988) consider this complex to be intrusive into the Singhbhum Group. In contrast, Bhattacharyya and Sanyal (1988) advocate that the Chotanagpur Gneiss constitutes the basement to the Singhbhum Group.

Rocks to the north of the thrust belt are usually metamorphosed to amphibolite grade whereas to the south of the belt rocks are generally of green schist grade, except for the Older Metamorphics.

Singhbhum Thrust Belt

The Singhbhum Cu-U Belt coincides with an intensely tectonized zone known as the *Singhbhum Thrust Belt* (STB), *Singhbhum Shear Zone* (SSZ) or *Copper Belt Thrust* (CBT). This thrust belt, 1–5 km in width, is an arcuate regional lineament, trending from SE to NW and then to W for more than 200 km that separates the Early Proterozoic Singhbhum Group to the north from the Archean Singhbhum Granite and Iron Ore Group to the south

(Fig. 2.2). The thrust belt evolved over a period from 2.05 to 1.6 Ga, exhibits signs of repeated reactivation, and affected a variety of stratigraphic units including the Singhbhum Group, Iron Ore Group, Singhbhum Granite, and smaller granitic bodies.

Thermo-tectonic to tectonic elements in this zone are reflected by compositional banding of rocks and schistosity subparallel or in acute angle with the dominant planar structures (mylonite, shear planes etc.) and almost down-dip folds and warps of variable size. The planar structures dip 45–70° N and NE. Prominent shear planes show down dip mineral lineation or striation. Several post-mineralization transverse faults with conspicuous displacements cut the belt.

Mafic schists, pelitic schists, quartzite, and quartz schists as well as albite-bearing gneisses and granitoids known as Soda Granite and Arkasani Granophyre are the dominant rock types. Soda Granite bodies prevail in the eastern part and the Arkasani Granophyre prevails in the western part of the belt as mentioned earlier.

Shear zone rocks show evidence of retrogressive metamorphism in the central part of the belt, where it is upper green-schist facies whilst it rises to lower amphibolite facies near both ends.

Although age data show a wide scatter in the Singhbhum Thrust Belt, two major events can be recognized, one at 2.05–2.0 Ga and another at 1.6 Ga. The latter event is obtained from apatite, uraninite, and Soda Granite samples. Evolution of the Singhbhum Thrust Belt, thus, spans a period from 2.05 to 1.6 Ga.

Principal Characteristics of Mineralization

Three different types of mineralization characterized by U, Cu, and apatite-magnetite ore are identified in the Singhbhum Thrust Belt. Locally, these types can spatially overlap but do not form consanguineous parageneses.

Uranium deposits: Uraninite is the principal U mineral; (sooty) pitchblende, autunite (meta-autunite), torbernite, schoepite (metaschoepite), and uranophane are present near

surface; minor ore components include clarkeite, davidite, and brannerite as well as allanite, apatite, monazite, and xenotime.

Uraninite occurs as discrete disseminated grains that may enclose microveinlets of chalcopyrite and/or galena (Sarkar 1984); thorium content is low ($UO_2/ThO_2 = 70-150$), lead is high ($PbO = 14-15\%$) (Rao 1977), and REE is moderate (Shankaran et al. 1970). Cell dimensions vary between 5.42 and 5.55 Å.

Chlorite, biotite, tourmaline, apatite, magnetite, and quartz in ore zones may contain uranium in crystal structures, in inhomogeneities, and/or in the form of uraninite inclusions.

Some U deposits (see description of individual deposits) contain minor Co, Cu, Ni, and/or Mo. Ni minerals include millerite, heazlewoodite, and rare melonite. Pyrite, chlorite, and biotite may also contain some nickel. Co is predominantly bound in sulfides, particularly pyrite, but also occurs as rare skutterudite (Sarkar 1984). Cu, if present, occurs chiefly as chalcopyrite. Molybdenite with magnetite occurs predominantly in late veins but is locally also found in disseminated mode. These metals do not occur in paragenesis with U but belong to separate mineralizing processes that spatially overlapped with U mineralization. Ore has a disseminated texture and is hosted in fractured quartz-biotite schist, autoclastic conglomerate, sericite-chlorite-albite schist, and apatite-magnetite rocks. Pb-isotope ratios indicate an age of U deposition between 1.6 and 1.5 Ga (Rao et al. 1979).

Copper mineralization is dominated by chalcopyrite, pyrite, and pyrrhotite. Minor and accessory ore minerals are magnetite, covellite, pentlandite, violarite, molybdenite, sphalerite, galena, marcasite, telluride species, native gold, silver, copper, and bismuth.

Apatite-magnetite mineralization consists of lenses of fluorapatite associated with variable proportions of magnetite. Three types of mineral assemblages are identified: apatite-magnetite-serpentine/chrysotile, apatite-magnetite-biotite-anthophyllite-xenotime, and quartz-kyanite-magnetite-apatite. This ore is hosted by biotite schist and chlorite-biotite schist and is associated with Soda Granite and Cu-U mineralized zones.

General Shape and Dimensions of Deposits

Ore bodies form lenses or sheets that are commonly elongated parallel to down dip mineral lineation and which parallel S_3 foliation, which, in turn, parallels lithological layering (S_0). Boundaries of ore bodies are both sharp and gradational. For more details of dimensions see description of selected deposits.

Principal Ore Control and Recognition Criteria

According to Sarkar (1986), Bhattacharyya (1992) and other authors, U mineralization in the Singhbhum Belt exhibits the following controls or recognition criteria:

- Mineralization is largely confined to Singhbhum Group metasediments and is spatially associated with Dhanjori volcanics

- host rocks are mainly biotite- and/or chlorite-rich (\pm apatite, magnetite) rocks, which originated from greywacke (Surda-Bhatin sector) or mafic volcanics
- deposits are spatially controlled by a mega-lineament, the Singhbhum Thrust Belt
- ore bodies are located along abyssal faults or regional shear zones within this belt
- Na metasomatism is typical along these zones (reflected, e.g. by Soda Granite)
- typical wall rock alteration is absent (hematitization noted in Jaduguda, Bhatin, and Narwapahar is neither intense nor correlatable with the intensity of U mineralization. Late fluorite veins and veinlets as at Narwapahar are also not correlatable with the uranium)
- three types of mineralization occur independently in the Singhbhum Thrust Belt: Cu, U, and apatite-magnetite
- any one of the three mineralization types may occur to the exclusion of the other, so that the three principal mineralization types could, but need not, have formed at different times
- uraninite with low Th and high Pb content is the principal U mineral
- Cu, Ni, and/or Mo minerals are locally associated with U mineralization but do not occur in paragenesis with U
- ore bodies are tabular and more or less concordant with secondary, intraformational planar structures
- ore shoots are subparallel to down-dip lineation and persist to considerable depth
- boundaries of ore bodies can be sharp or diffuse

Metallogenetic Aspects

The metallogenesis of U deposits in the Singhbhum Belt is still controversial. Although commonly referred to as vein deposits, U mineralization does not really fit the standard definition of an ore vein. Instead, U mineralization, as known today, tends to be modified, originally strata-bound mineralization, which experienced hydrothermal reworking with U redistribution into intraformational planar structures and, in consequence, exhibit a kind of veinlike configuration. The cause of this veinlike U concentration (from the progenitor strata-bound mineralization or other sources) is still enigmatic. The following models are proposed:

1. *Lateral secretion* processes during progressive or retrogressive metamorphism as suggested, e.g. by Rao (1977) and Rao NK and Rao GVU (1983). In their concept, uranium was an original constituent of basal metasediments of the Singhbhum Group (Chaibasa Formation) to the north of the thrust zone from which it was mobilized and reprecipitated during deformation and metamorphism and particularly during the tectono-thermal evolution of the Singhbhum Thrust Zone.
2. *Hydrothermal activity-related to deep-seated magmatism* as advocated by Bhola et al. (1966). These authors attribute ore formation to mineralizing hydrothermal solutions ascending from a cooling magma from which the Soda Granite derived.

In a somewhat similar concept, Bhattacharyya (1992) considers – as an alternative model to that given below – that magmatic-hydrothermal processes could have been generated by deep-seated felsic plutonic activity, syn- to post-kinematic in the Singhbhum Thrust Belt, as exemplified by the Mayurbhanj Granite that became instrumental in U ore formation.

3. *Metasomatism* as proposed by Banerjee et al. (1972), who suggest that uranium originated from migmatized rocks and was introduced from shear zones during migmatization. Sarkar (1982) assumes that uranium has migrated upwards from the middle-lower crust along deep reaching dislocation zones perhaps during the first major tectono-thermal event at the end of the Archean. Sarkar bases his conclusion on the fact that uranium is concentrated along abyssal faults or regional shear zones, the wall rocks of which are altered by Na metasomatism,

Bhattacharyya (1992) arrives at the following sequence of events leading to U and Cu mineralization in the Singhbhum Thrust Belt: The three principal types of mineralization – U, Cu, and apatite-magnetite – that are characteristic for the belt initially developed as synsedimentary, strata-bound Cu, U, etc. concentrations in Singhbhum Group sediments. Granite of the basement complex (mainly Singhbhum Granite) is thought to be the most likely source for U and Dhanjori volcanics for Cu for this strata-bound mineralization.

In a subsequent stage, these protore strata were affected by multiple deformation and metamorphism during the Singhbhum Orogeny (2.05–2.0 Ga). The Singhbhum Group was thrust towards south over the Archean Singhbhum Granite craton and the Singhbhum Thrust Belt developed as a prominent, repeatedly activated megalignement at the contact of these two complexes. In the course of this process, strata-bound Cu, U, and apatite-magnetite concentrations were deformed and metamorphosed within the thrust belt. Coeval or later hydrothermal activity-related to widespread felsic magmatic and/or metasomatic activity, as reflected by the emplacement of the Mayurbhanj

Granite and Soda Granite within the Singhbhum Thrust Belt, modified the deformed and metamorphosed strata-bound mineralization or could have redistributed ore-forming elements into a new ore generation.

A later period of hydrothermal activity at ca. 1.6 Ga obtained from uraninite and apatite samples imprinted further modification on rocks and deposits within the thrust belt.

With respect to the relationship of base metal (mainly Cu), uranium, and apatite-magnetite mineralization, Sarkar (1982) notes that the formation of these three types of mineralization took place in distinct but different metallogenic episodes as evidenced by discordant spatial disposition of major concentrations of these three ore types. In addition, there is also a difference in ore-forming processes. Sulfide mineralization, which is thought to be of volcanogenic hydrothermal origin, is possibly the earliest. Identification of any original genetic relationship of mineral parageneses is hampered, however, by later repeated deformation and metamorphism of the original stock.

Selected Deposits in the Singhbhum Cu-U Belt, Jharkand East District

Sources of information. Bholra 1972; OECD/NEA and IAEA 2001; Sarkar 1984, 1986; Bhasin 1997.

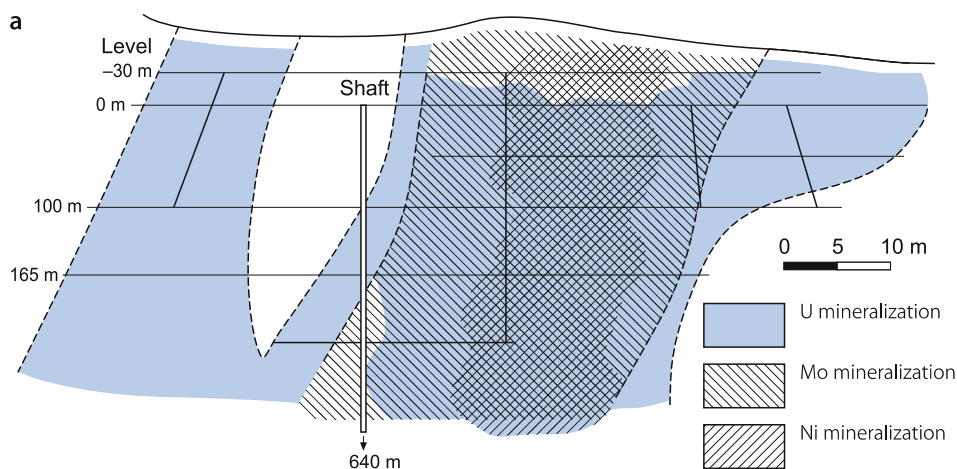
2.1.0.1 Jaduguda Mine

This polymetallic veinlike U deposit was and is the dominant U producer of India. Nickel and molybdenum are obtained as by-products. Jaduguda has been mined since 1967 to depths of 900 m. Access is by a main shaft (640 m deep), and, located 580 m to the north, by an auxiliary blind shaft between levels 555 and 900 m.

Ore consists of U minerals, mainly uraninite, locally with spatially associated Ni, Co, Mo, and/or Cu components. Ni sulfides

■ Fig. 2.3a.

Jaduguda deposit, longitudinal section illustrating the distribution of U, Mo, and Ni mineralization in the footwall lode (note: The mixed mineral assemblage continues into depth) (after Sarkar 1986)



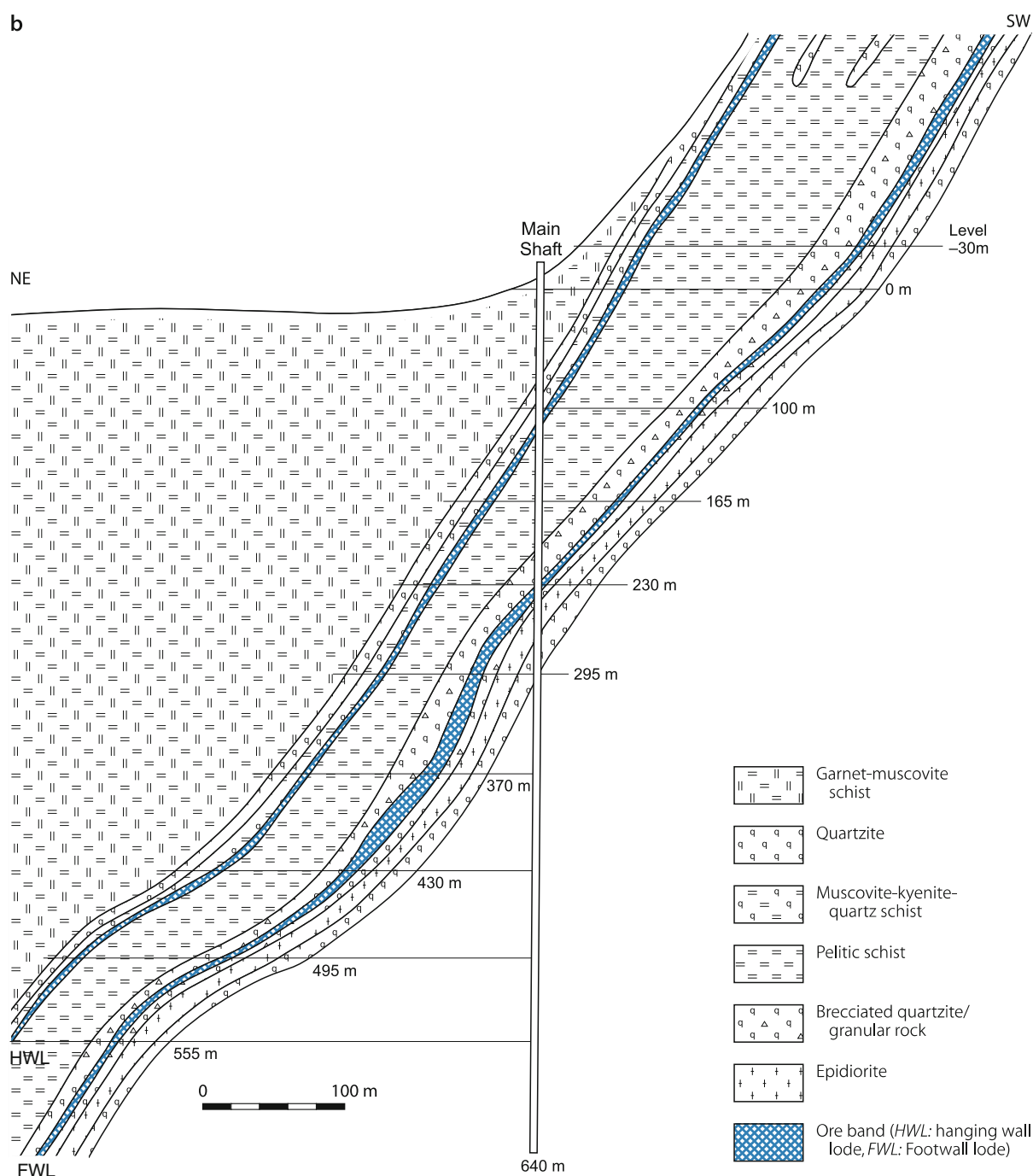
and sulfo-arsenides include millerite, ferruginous heazlewoodite, and rare melonite. Co is predominantly bound in sulfides, particularly pyrite, but also occurs as rare skutterudite. Mo is present as molybdenite and Cu as chalcopyrite (Fig. 2.3a).

Jaduguda contains two subparallel ore bodies, 60–100 m apart across strike, that lie conformable within the metasediments, which dip at an angle of 40–60° NE (Fig. 2.3b). Ore

shoots parallel the down-dip lineation. Host rocks are chlorite- and biotite quartz schist with apatite, magnetite, and tourmaline as accessories, biotite-chlorite muscovite-kyanite schist, brecciated quartzite, and autoclastic conglomerate. The smaller *hanging wall lode* (HWL), 200–300 m in NE-SW length and commonly 3–4 m in thickness, is confined to the eastern section of the deposit. The larger and better-mineralized *footwall lode*

Fig. 2.3b.

Jaduguda deposit, NE-SW cross-section showing the position of U mineralization in the hanging wall lode (HWL) and footwall lode (FWL) within a quartzite-mica schist sequence. Note that mineralization extends further than shown on this section to a depth of at least 900 m where it is accessed by a blind shaft (located 580 m N of the main shaft). (Note: granular rock is a local term and refers to chlorite and biotite-quartz schist with apatite, magnetite, and tourmaline as accessories) (after Bhasin 1997)



(FWL) is in excess of 1 km in NE-SW length with an intermediate barren zone of about 100 m that fades out down dip. Thickness ranges from about 6 m on upper levels to about 20 m at a depth of some 300 m and then starts thinning again. The footwall ore body persists for more than 1 000 m down dip. Below a vertical depth of 425 m the grade improves to an average of 0.057% U.

2.1.0.2 Bhatin Mine

This small deposit is located 3 km NW of Jaduguda and went into production in 1986. Exploitation is by adits and an incline to a depth of 500 m. The grade averages 0.045% U. Ni (millerite and heazlewoodite) and Mo (molybdenite) are obtained as by-products.

Bhatin tends to be an extension of Jaduguda from which it is separated by a major post-mineralization reverse fault that has uplifted the Jaduguda deposit. Geology at Bhatin is more or less similar to that at Jaduguda except that grade and resources are less. Chlorite-biotite schist is the principal host rock. The ore body has a thickness of 2–10 m and an average dip of 30–40° NE.

2.1.0.3 Narwapahar Mine

Located 12 km W of Jaduguda, Narwapahar is a low-grade but large tonnage deposit with a strike length in excess of 3 km. The deposit was commissioned in 1995. Access is by a 355 m deep vertical shaft and a decline.

Uraninite is the principal U mineral. Scheelite occurs locally. Ore is hosted in sericitic chlorite schist with abundant quartz and some feldspar or in chlorite-quartz schist with magnetite. Quartz and feldspar occasionally contain dusty hematite. The strata dip 30–40° NE.

Six mineralized zones are identified (Main Band I and II, Band # 3, Hanging wall lode west of fault, Khundungri I and II). These zones enclose lenticular to tabular ore bodies that lie conformable to dominant planar structures and follow down-dip lineation of the host rock. Ore bodies have a maximum strike length of 2 100 m, a thickness of 2.5–20 m, and extend to depths of 600 m. The average grade is 0.05% U.

2.1.0.4 Turamdih Ore Field

At *Turamdih*, 5 km S of Tatanagar and 24 km W of Jaduguda, a U zone in sericitized chlorite schist occurs 30 m above a copper zone. The ore averages 0.034% U. The deposit has been mined by underground exploitation since end of 2002. The *Banduhurang* deposit, a western extension of Turamdih, is amenable to open-cast mining. Turamdih and Banduhurang contain a total of almost 8 000 t U (Awati and Grover 2005).

The *Mohuldih* deposit, located 2.5 km W of Banduhurang, consists of a thin veinlike ore body that extends to a depth of 320 m. This deposit presents an underground mining situation. At *Keruadungri*, 1 km to the north of Turamdih, a leaner uranium zone of the same type has been identified.

2.1.0.5 Khadandungri-Purandungri, Bagjata-Moinajharia and Bhalki-Kanyaluka Areas

Ore bodies in these areas are of tabular shape, up to 800 m in strike length and 3 m in thickness. They lie conformable to the schistosity and are hosted in biotite schist, chlorite-biotite schist, and quartz-muscovite-biotite schist. At the first two locations, U ore is associated with apatite and magnetite while in the latter U and apatite-magnetite ore zones are separated by a barren interval of some 30 m. Patches of albitic schists or Soda Granite are present in the ore zone. Grades average 0.04% U. Wall rock alteration is absent. The planned *Bagjata* underground mine, located some 30 km SE of Jaduguda, consists of a thin veinlike ore body that persists to a depth of 600 m.

2.1.0.6 Mosaboni, Surda, and Rakha Cu (-U) Mines

Uraniferous tailings from copper ore beneficiation grading several 100 ppm U are collected near the copper concentrators in three U recovery plants at Mosaboni, Surda, and Rakha, and then shipped to the Jaduguda mill. Cumulatively, some 150 t of uranium concentrates with 800–1500 ppm U are produced per day.

Copper mineralization in the *Badia-Mosabani* region occurs mainly in Soda Granite, near its contact with Dhanjore metavolcanics. Bulk samples contained about 0.04% U and locally as much as 0.08% U (Bhola 1972).

In the *Surda-Rakha Mines* sector, copper ore lenses may contain as much as 0.07% U. Uranium occurs in close association with copper ore, but U and Cu are not necessarily coincident. The host rock is chloritic quartz schist with apatite, magnetite, biotite, and tourmaline.

2.2 Meghalaya Plateau, Meghalaya

The southern Meghalaya Plateau in Meghalaya State, NE India (► Fig. 2.1) hosts sandstone-type U mineralization in Cretaceous sediments spread over a W-E distance of some 100 km in the *West Khasi*, *East Khasi*, and *Jaintia Hills*. Similar U mineralization was found at Rongdinala near Balphakram in the *Garo Hills*, *Rongcheng Plateau*, which adjoins the West Khasi Hills to the west. The only deposits established so far occur in the *Domiasiat-Gomaghat* area in the West Khasi Hills (● Fig. 2.4).

2.2.1 West Khasi Hills Region, Meghalaya

The West Khasi Hills are located in the south-central part of the Meghalaya Plateau. U showings and occurrences are preferentially situated in the “Plateau Domain” (see below), in which sandstone-type U deposits occur in the vicinity of the town of *Domiasiat* and at *Wahkyn*, ca. 10 km SW of Domiasiat. Additional U occurrences are situated in the sectors of Nongmalang (ca. 5 km SW of Domiasiat), Gomaghat (15 km S of Domiasiat), Phlangdiloin (Sateek occurrence, 5 km SSE of Domiasiat), Rangjadong (15 km ESE of Domiasiat), and Mawkyrwat (Tyrnai

occurrence, 25 km E of Domiasiat). The *Domiasiat* deposit is in the planning stage for open cast mining.

Sources of information. Dhana Raju et al. 1989; Dwivedy 1995a; Gupta 2002; Kaul and Varma 1990; OECD-NEA/IAEA 2001, 2003, 2005; Saraswat et al. 1977; Sengupta et al. 1991; Singh 2002; Kumar et al. 1990.

Regional Geological Features of the Meghalaya Plateau

The Meghalaya Plateau is an uplifted horst bordered by the E-W-trending Dauki fault to the south and the Brahmaputra graben to the north. The plateau comprises Archean gneisses and schists and the Middle Proterozoic Shillong Group, mainly composed of phyllite-quartzite, into which Upper Proterozoic granitic plutons dated between 690 and 479 Ma and various dikes, were intruded. Plateau basalts and other volcanics of the Jurassic Sylhet Traps overlie this basement along the southern margin of the plateau. They had erupted through E-W-trending fissures of the Raibah fault. A thick sequence of Upper Cretaceous-Tertiary sediments was selectively laid down upon a pronounced unconformity of these traps, and upon Precambrian granite and gneiss to the north thereof.

Due to movements of the E-W-trending Raibah fault, that caused upheaval of a northern block and subsidence of a southern block, two geomorphic domains with distinct Upper Cretaceous-Tertiary sedimentary facies exist, the "Plateau Domain" with fluvial and the "Ghat Domain" with marginal-marine facies (► Fig. 2.5).

Continued uplift of the Meghalaya Plateau generated E-W and N-S to NE-SW block faulting; and after the deposition of the Tertiary strata, the segment with Sylhet Trap and Upper Cretaceous-Tertiary sediments to the south of the E-W-trending

Dauki fault were down dropped and covered with thick alluvium in the Bangladesh plains.

The various lithologies of the Meghalaya Plateau are documented in the following generalized litho-stratigraphic column (after Dwivedy 1995a based on Charaborthy and Bakshi 1972, and Geol. Surv. of India 1974).

Miocene-Oligocene Garo Group

- Chengapara Formation, 700 m thick: Sandstone, siltstone, clay and marl
- Baghmara Fm, 530 m thick: Feldspathic sandstone, conglomerate and clay
- Kopili-Rewak Fm, 500 m thick: Shale, sandstone and marl

Eocene-Paleocene Jaintia Group (lacustrine and marine facies)

- Eocene Shella Fm, 600 m thick: Alternating sandstone and limestone
- Paleocene Langpar Fm, 50–100 m thick: Calcareous shale, sandstone and impure limestone

Upper Cretaceous Khasi Group

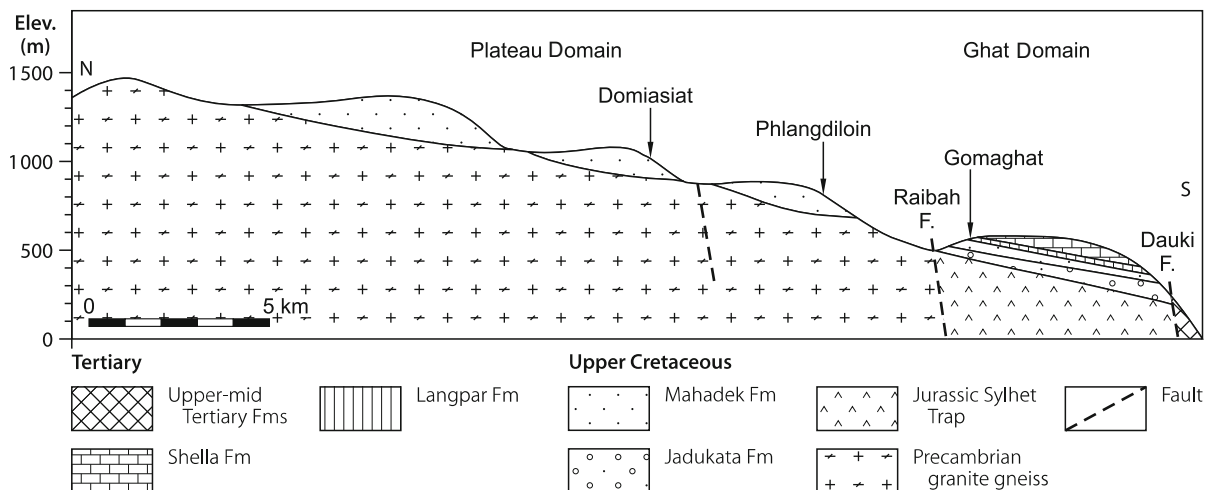
- Mahadek Fm, 215 m thick, separated into
 - Upper Member, ca.190 m thick: Littoral to marginal marine arkosic sandstone, oxidized, medium- to fine-grained, yellowish to purple brown
 - Lower Member, 25–60 m thick: Fluvial feldspathic sandstone, poorly sorted, medium-to-coarse grained, greyish-green, with abundant carbonaceous matter and framboidal pyrite, and intercalated, discontinuous clay bands
- Jadukata Fm, 235 m thick: Alternating sandstone-conglomerate of marine origin

>Unconformity<

Late Jurassic Sylhet Trap Basalt, alkali-basalt, andesite, rhyolite, felsic tuff, and carbonatite complexes

■ Fig. 2.5.

Southern Meghalaya Plateau, West Khasi Hills District, generalized N-S section showing: (1) the geological setting of the Plateau and Ghat domains separated by the Raibah fault and (2) the position of the U-hosting Upper Cretaceous Mahadek Formation (after Dwivedy 1995a)



Neoproterozoic Coarse, porphyritic granite, pegmatite, aplite, and quartz veins; epidiorite and dolerite

Mesoproterozoic Phyllite-quartzite sequence with basal conglomerate

>Unconformity<

Archean Biotite gneiss, granite gneiss, migmatite, mica schist, sillimanite-quartz schist, and granulite

2.2.1.1 Domiasiat Area/Deposit

The Domiasiat area is in the “Plateau Domain” and contains sandstone-type U occurrences in the Killung, Rangam, Umla, Pyrnotbri, Jimrey, and Tyrkhang blocks, which cover some 10 km² in and around Domiasiat and Phladiloin.

The Killung and Rangam blocks host the Domiasiat deposit with peneconcordant, tabular sandstone-type U mineralization and in situ resources on the order of 8 000 t at grades averaging 0.088% U (status 2005) making this U deposit so far the largest of its kind in India. With an average overburden of about 25 m and ore to overburden ratio of 1:6.7, this deposit is amenable to open cast mining (45 m deep). A small rivulet separates the deposit requiring two mining blocks.

Sources of information. See Sect. 2.2.1: *West Khasi Hills Region, Meghalaya*.

Geological Setting of Mineralization

U occurs in a depression generated by block faulting that contains weakly sorted lithic fragments and coarse mineral fragments of the Lower Mahadek Member (Fig. 2.6). Two facies are identified in this member: (1) channel-filling cross-bedded, unsorted, quartz arenite or feldspathic arenite with lithic fragments, flanked by (2) massive sandstone of flood plain facies. Different types of authigenic clays and cement reflect diagenetic changes. The channel arenite abounds in carbonaceous matter and pyrite, and provides the host for major uraniferous beds, while the flood plain sandstone is less enriched in carbonaceous debris and pyrite, and contains only minor mineralized lenses.

Mineralization, Shape and Dimensions of Deposits

Uranium is preferentially adsorbed by low rank bituminous coal and clay minerals, but also occurs as pitchblende and coffinite within organic substances. Goethite and leucoxene tend to contain minor uranium. Associated minerals include mainly framboidal and colloidal pyrite and melnicovite.

Quartz-arenite of the Lower Mahadek channel facies provides the principal host rock. It is composed of about 90% clasts and 10% matrix. Subangular to angular quartz constitutes 70–90% of the clasts; followed by 5–15% feldspar (microcline, ± albite-oligoclase, and perthite), and 2–3% rock fragments. Accessory minerals

include anatase, apatite, garnet, monazite, rutile, sphene, zircon, and opaque oxides. The matrix comprises chlorite and mica at *Domiasiat* (sericite at *Pdengshakap*, chlorite at *Gomaghat*) in addition to commonly present kaolinite, goethite, and carbonaceous matter. U mineralized arenite is friable to highly compact, medium- to coarse-grained, and locally pebbly. Its color is light to dark mainly caused by the kind and relative concentration of matrix material, such as carbonaceous matter, kaolinite, or Fe-hydroxides.

The *Domiasiat deposit* comprises several ore lodes in the Killung and the westerly adjacent Rangam block. Grades range from 0.01 to 0.35% U. Subsidiary mineralized lenses of limited extent are also present. Two principal ore lodes designated as hanging wall or main lodes, and a third lode, termed footwall lode, are identified. The latter occurs in the eastern part of the Killung block.

These ore lodes are essentially tabular-amoeba shaped and occur somewhat perched within the lower grey sandstone horizon, a few meters to some 10 m above granitic basement. Purple to red-brown or bleached yellowish brown, oxidized sandstone covers the grey sandstone.

The mineralized horizon ranges in thickness from 1 to 30 m (av. 3.70 m) both along and across the strike of the stratum. Thicker intervals have a core with relatively higher U grades. Overburden is from a few meters to over 25 m thick with an ore to overburden ratio of 1:6.7 (Fig. 2.7).

Ore Controls and Recognition Criteria

The *Domiasiat* and other deposits as well are characterized by the following ore controlling or recognition features:

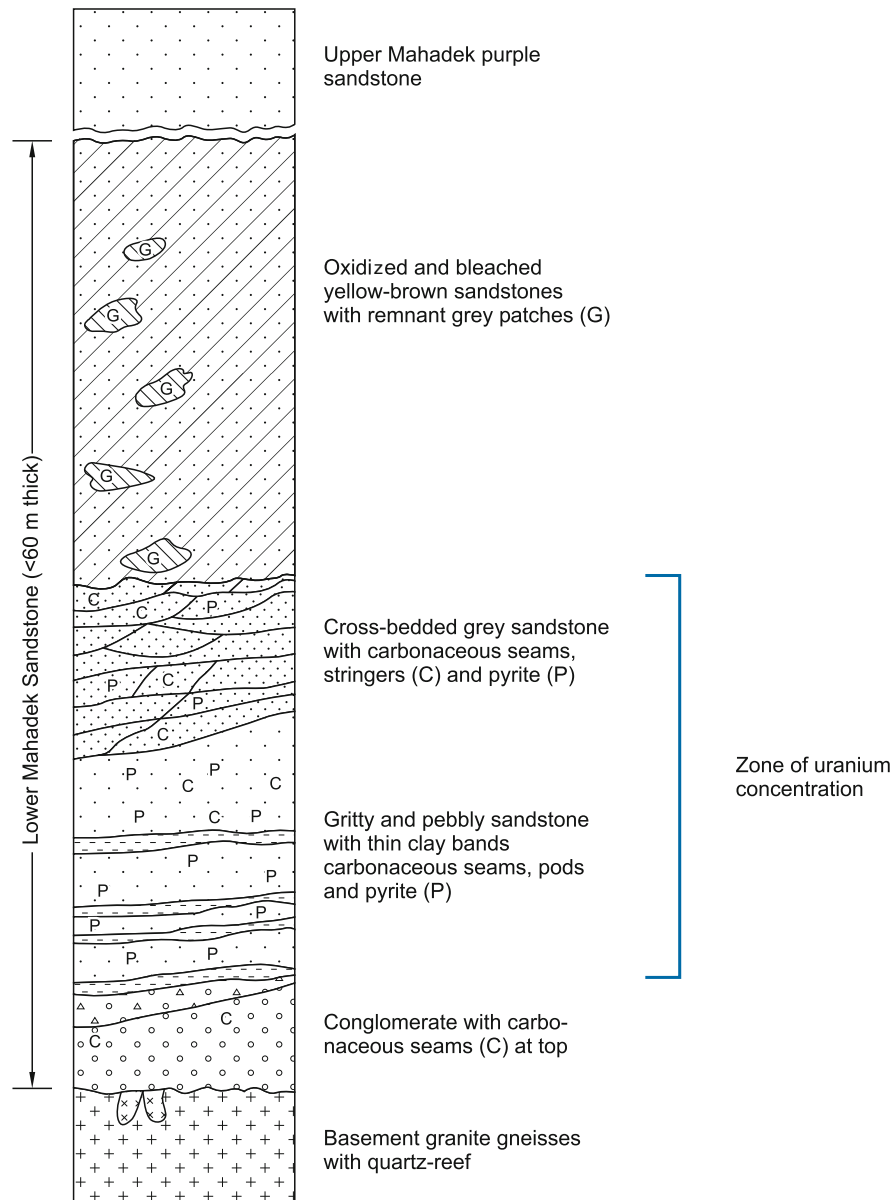
Host environment

- Mesozoic-Tertiary basins downfaulted into a Precambrian basement with uraniferous granites
- repeated reactivation of basement faults
- block faulting governs position, dimensions, and structure of basins
- basement faults and geomorphological features control the nature and distribution of basal basin infill
- basin fillings include basal continental fluvial facies of proximal, sandy-braided channel-type origin
- lacustrine and marginal marine facies rest upon the basal facies
- sediments have a low dip angle

Mineralization

- U occurs predominantly adsorbed on bituminous organic matter and clay minerals
- pitchblende and coffinite occur in subordinate quantity
- pyrite and melnicovite are the main associated minerals
- U ore forms peneconcordant, tabular lodes in basal arenites
- host rocks consist primarily of immature quartz (feldspathic) arenite and conglomerate with some clay bands
- host rocks abound in bitumen-type organic matter and biogenic Fe-sulfides indicating an anaerobic environment during deposition and diagenesis

■ Fig. 2.6. West Khasi Hills District, Domiasiat area, generalized litho-stratigraphic column illustrating the confinement of U mineralization to grey pyritic sandstone with intercalated carbonaceous seams (after Dwivedy 1995a)



- organic matter is particularly abundant at confluence of braided channels
- aquicludes are apparently lacking on top of the ore hosting basal arenites
- permeability barriers like clayey intercalations are discontinuous and only locally developed in host sandstones

Metallogenetic Aspects

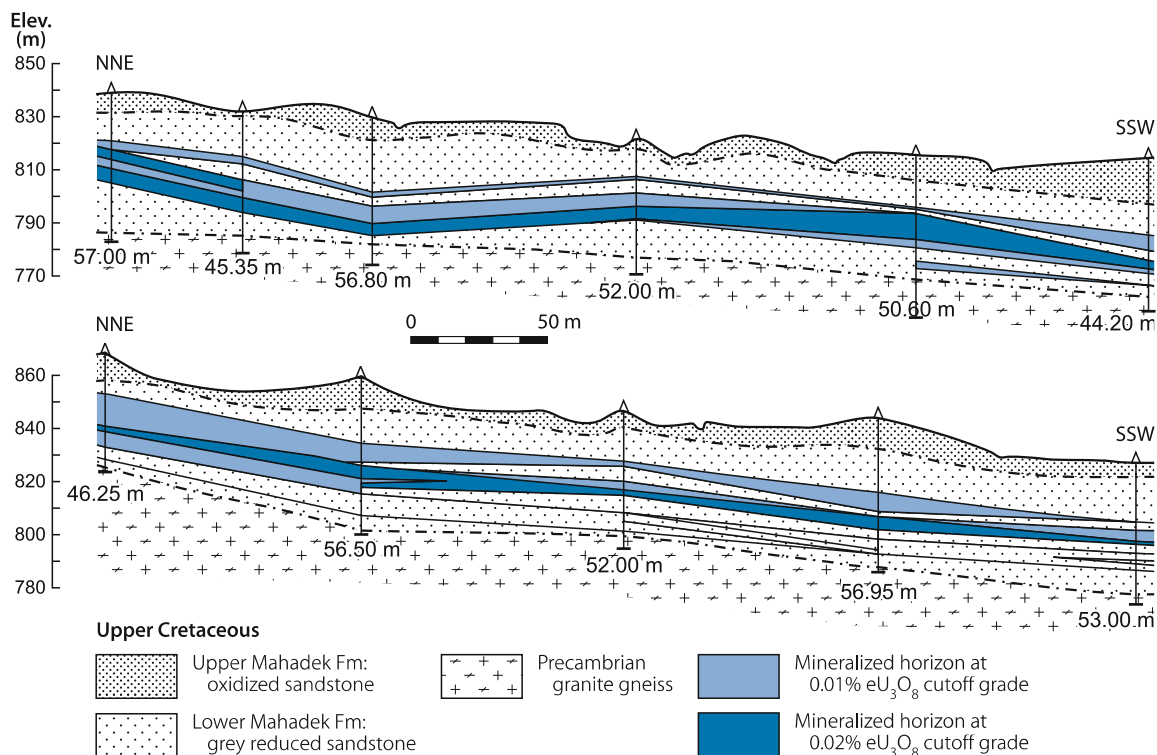
Dwivedy (1995a) summarizes metallogenetic considerations forwarded by a number of geoscientists. He points out that, in general, U mineralization appears to be intimately associated

with organic matter in the continental fluvial facies of the “Plateau Domain” whereas a redox interface tends to have controlled U accumulation in the fluvialite-marginal marine sediments of the “Ghat Domain” of the West Khasi Hills. Essential factors that are thought to have been instrumental in ore formation at *Domiasiat* include the following.

Weakly sorted lithic fragments and coarse minerals (Lower Mahadek Member) were deposited together with carbonaceous matter in basal portions of a depression formed by block faulting. This facies received also granite detritus including uraniferous clasts from the Khasi batholith and Myllem granite that have anomalous U contents (7–110 ppm U). Greater amounts of plant debris accumulated particularly at the confluence of

Fig. 2.7.

West Khasi Hills District, Domiasiat deposit, generalized sections illustrating the tabular configuration of U ore bodies in the Upper Cretaceous Lower Mahadek Formation (after Dwivedy 1995a)



braided system channels. Rapid deposition and burial of this basal facies precluded oxidation of carbonaceous matter and permitted development of Fe-disulfides, while upper parts of the Mahadek Formation were gradually oxidized as indicated by relict(?) mineralized intervals and grey sandstone patches in otherwise oxidized rocks above the reduced basal facies.

Uranium was most likely leached by oxygenated groundwater from these cap rocks and/or from granite or other basement rocks with anomalous U backgrounds that were exposed to oxidation at the basin rim and along faults that had reactivated the basement floor. Fertile solutions percolated down along the hydraulic gradient of permeable beds and/or along basement faults, which control the channels, and, where they encountered a reducing environment, U was precipitated as discussed below. Continued uplift of the Meghalaya Plateau may also have provided fresh pulses of U-bearing solutions to the depression.

Another scenario may also envisage U enrichment in connate water in response to diagenetic compaction and gradual removal of water from the host sediments. Where this U-fertile connate water interacted with decaying plant matter and H_2S that were abundant below the water table at the confluence of braided channels, pitchblende and urano-organic complexes precipitated. The close association of U-phases and pyrite in organic matter with negative δS^{34} values suggests that common biological processes were involved. A low temperature of ore formation is attested by framboidal

pyrite and melnicovite/colloidal pyrite as well as by low rank bitumens.

Sandstones with intercalated siltstones and clay-rich intercalations provided permeability barriers locally that are thought to have enabled a larger quantity of uraniferous solutions to interact with greater volumes of organic matter and pyrite-bearing horizons, with the result of thicker mineralized zones and higher grades.

2.2.2 Other Uranium Occurrences in the Meghalaya Plateau

Rongdinala near Balphakram in *Garo Hills*, Rongcheng Plateau, located to the west of the West Khasi Hills: Gupta (2002) reports U mineralization in three distinct medium- to coarse-grained sandstone horizons of the Lower Mahadek Formation situated between 2 and 30 m above the basement unconformity.

Dwivedy (1995) lists the following areas with U occurrences in the West Khasi, East Khasi, and Jaintia Hills in the southern Meghalaya Plateau (Fig. 2.4):

Nongmalang sector: Located 7 km SW of Domiasiat, U (<20×bg) is hosted in medium- to coarse-grained, crossbedded, feldspathic sandstone/Mahadek Fm with abundant carbonaceous matter and pyrite. Sandstone thickness increases in the south to 60–65 m.

Phlangdiloin sector: Located 5 km SSE of Domiasiat, U (0.008–0.21% U) is hosted in crossbedded, feldspathic sandstone/Mahadek Fm with abundant carbonized wood and disseminated carbonaceous matter. A small tonnage U deposit is delineated at *Sateek*.

Rangjadong sector: Located 12 km ESE of Domiasiat, U (<20×bg) occurs in feldspathic and argillaceous sandstone with appreciable amounts of carbonaceous matter and pyrite.

Mawkyrwat sector: Located some 25 km E of Domiasiat, tabular U mineralization (0.011–0.17% U) (coffinite, davidite) occurs in cross-bedded and massive feldspathic and argillaceous sandstones. Carbonaceous matter, pyrite, and honey-colored resin are very common. A small U deposit grading 0.09% U has been established at *Tyrnai*.

Mawsynram sector: U showings (0.009–0.11% U) are in calcareous sandstone of the Langpar and Jadukata Formations.

Cherrapunji sector: U (0.004–0.15% U) is contained in coarse-gritty arkosic sandstone/Mahadek Fm that grades into greenish grey massive sandstone. Sediments of the Langpar and Shella Formations overlie the Mahadek Fm.

Pdengshakap-Tarangblang sector: Pitchblende and coffinite associated with carbonaceous matter form lenses of very lean, uncorrelatable mineralization (0.008–0.025% U) confined to the top and bottom arkosic sandstone horizons in the Mahadek Formation. Mahadek sediments are fluvial in nature to the north and grade into marginal-marine (glauconite) sandstone southwards. They are covered by the Langpar and Shella Formations.

Bataw-Borghat sector: U (0.004% to 0.045% U) associated with carbonaceous matter occurs in spotty distribution in arkosic sandstone of the Mahadek Fm that is overlain by the Langpar and Shella Formations.

2.3 Meso-Neoproterozoic Cuddapah Basin, Andhra Pradesh, SE India

The Cuddapah Basin is located in Andhra Pradesh State in SE India (Fig. 2.1). U occurrences are widespread within and adjacent to the basin. They include a few deposits in the *Nalgonda* and *Guntur* Districts at the northern, and in the *Cuddapah* District at the south to southwestern margin of the basin. Three varieties of U deposits are identified: strata-bound, unconformity-proximal, and fracture-controlled types. Reported resources amount to at least 22 000 t U at grades of less than 0.1% U.

Sources of information. Banerjee 2005; Dhana et al. 1993; Dwivedy 1995b; Gupta 2002; Gupta and Sarangi 2006; Jeyagopal and Dhana Raju 1998; Rao et al. 2001; OECD-NEA/IAEA 2005; Roy and Dhana Raju 1997; Sharma et al. 1998b; Singh 2002; Sinha et al. 1995, 1996; Umamaheswar et al. 2001; Vasudeva et al. 1989; Zakaulla et al. 1998.

Regional Geological Features of the Cuddapah Basin

The crescent-shaped Cuddapah Basin covers 44 000 km² and encompasses the Chitravathi, Papaghi, Kurnool, Nallamalai, Srisaillam, and Palnad subbasins. A thick sequence of Meso- to Neoproterozoic sedimentary and pyroclastic rocks of the Cuddapah Supergroup and Kurnool Group fill the basin. Archean gneisses/Dharwar metasediments form the basement. Basement rocks are thrust over the Cuddapah Supergroup on the eastern margin of the basin. Fig. 2.8 outlines the various subbasins and shows the location of established U occurrences.

2.3.0.1 Nalgonda and Guntur Districts, N Margin of Cuddapah Basin

The *Nalgonda* District in the Srisaillam Subbasin at the northern margin of the Cuddapah Basin includes several uranium deposits at *Lambapur* and in the adjoining *Yellapur-Peddagattu* block (Fig. 2.8), which are planned for exploitation by one open pit to a depth of 15 m at an ore to overburden ratio of 1:4.2, and three underground mines about 70 m deep and accessed by declines. A uranium processing plant is planned at Seripally, 50 km distant from the mine sites.

These deposits (referred to as “unconformity proximal deposits” by Indian geologists) consist of flat ore lenses with varying thickness that occur at a depth from 15 m to 60 m along the unconformity that separates Archean basement granite from the Middle Proterozoic Srisaillam Formation. U mineralization is dominantly hosted in granite and only locally in gritty quartzite at the base of the overlying Srisaillam Formation. Mineralization at *Lambapur* is at shallow depth, several meters to some 50 m below surface (Fig. 2.9). Resources at *Lambapur* are estimated at 1 400 t U and at *Yellapur-Peddagattu* at 4 300 t U; grades average 0.08% U and 0.064% U, respectively.

The *Nalgonda* District also features extensive surface uranium showings around *Chitrial* to the west of, and in a similar geological setting as that of the *Yellapur-Peddagattu* block. U mineralization also occurs in basement granite, mafic dikes, and overlying quartzite of the *Banganapalle* Formation between *Rallavagu Tanda* and *Damarehela* in the northern Palnad Subbasin.

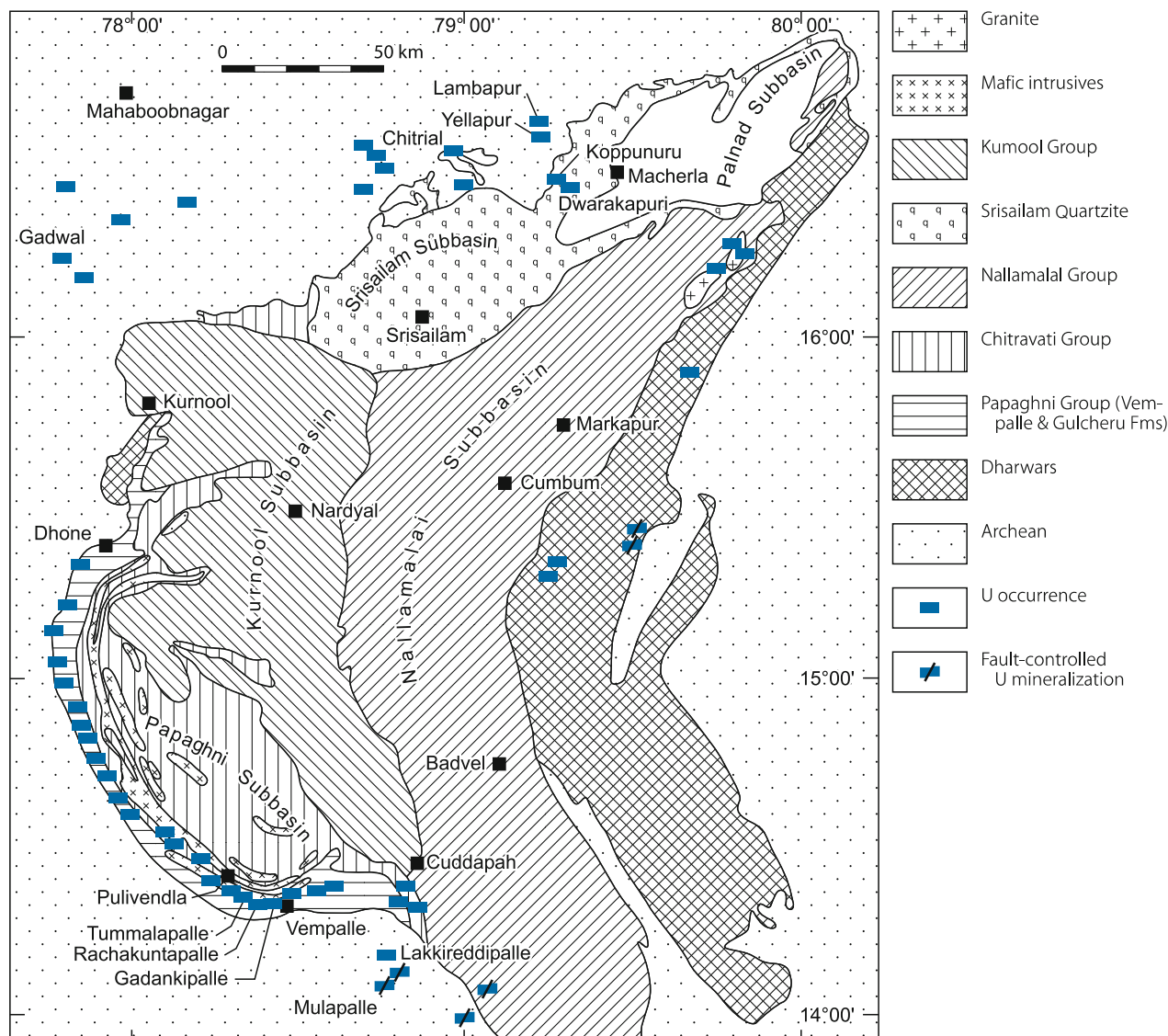
The *Guntur* District, located to the south of *Yellapur*, contains the small *Koppunuru* deposit (some 600 t U, 0.066% U) in basement granite and overlying quartzite of the *Banganapalle* Formation/Kurnool Group.

2.3.0.2 Cuddapah District, S-SW Rim of Cuddapah Basin

Located to the west and south of the town of Cuddapah, the Cuddapah District contains low-grade, strata-bound and fracture-controlled U occurrences. Strata-bound U occurrences (0.03–0.04% U) (*Tummalapalle*, *Rachakuntapalle*, *Gadankipalle*, *Chilavaripalle*, etc) are contained in impure dolostone of the

Fig. 2.8.

Cuddapah Basin, Andhra Pradesh, SE India, geological map with location of U occurrences (after Banerjee 2005)



Vempalle Formation/Papaghni Group (Lower Cuddapah Supergroup). Occurrences of this type group together in a belt that extends for over 140 km between the towns of Gadankipalle and Dhone along the W and SW margin of the Cuddapah Basin (Fig. 2.8).

Resources at *Tummalapalle* are estimated at 10 000 t U at an average grade of 0.036% U. Mineralization comprises ultra-fine pitchblende and coffinite associated with bornite, chalcopryrite, colophonane, covellite, digenite, molybdenite, and pyrite. Ore bodies are strata-bound and consist of thin veins with fairly uniform width and dip. They extend from surface to a delineated depth of 275 m.

Fracture controlled U mineralization occurs intermittently in the *Rachakuntapalle* area (*Madyalabodu-Gandi-Rachakuntapalle-Kannampalle* tract) and at *Idupulapaya*. Mineralization is hosted in quartz-chlorite breccia within fractured and faulted quartzite of the Gulcheru Formation/Papaghni Group. Mafic dikes intrude the

quartzite. An ore body at *Madyalabodu* is subhorizontal in nature and occurs about 3–8 m above the basement unconformity.

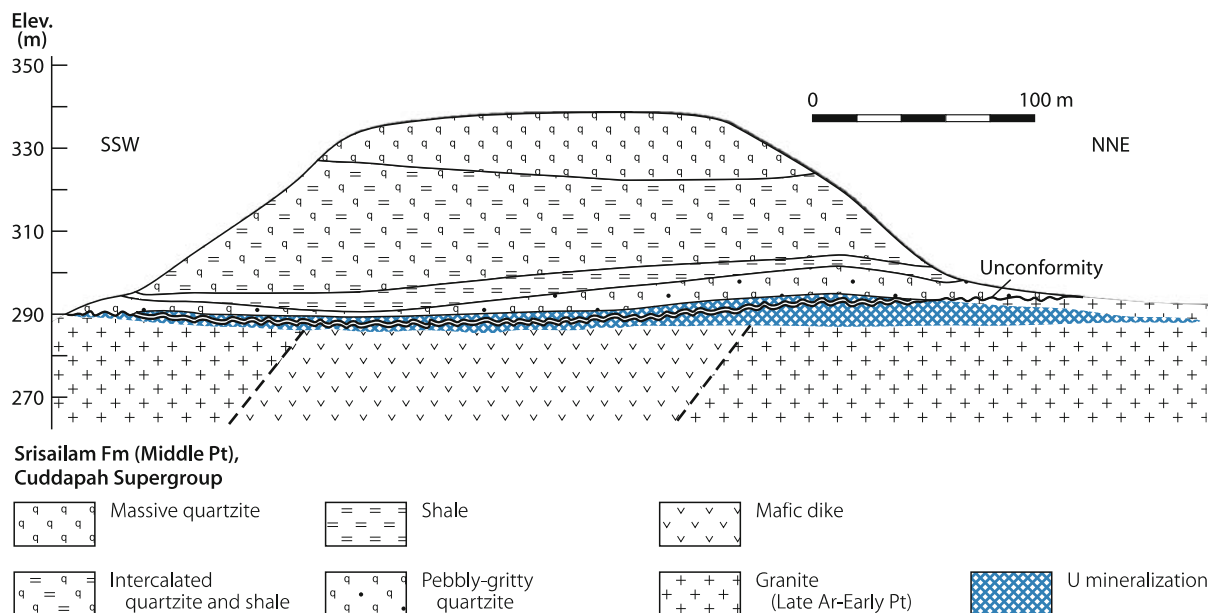
2.4 Bhima Basin, Karnataka

The Bhima Basin in Karnataka State spreads over 5 200 km² in NE-SW direction (Fig. 2.1). Basin fill consists of Proterozoic arenaceous, calcareous, and argillaceous sediments of the Bhima Group. The northwestern part is covered by Deccan Traps. A number of major faults trending E-W- and NW-SE transect the basin.

Between Gogi and Kurlagere in the *Gulbarga District*, an E-W-trending fault controls U mineralization in brecciated limestone, phosphatic limestone, and basement granite, close to the unconformity. Ore minerals include pitchblende and coffinite associated with chalcopryrite, galena, pyrite, and Co-Ni arsenides with appreciable amounts of silver.

■ Fig. 2.9.

Cuddapah Basin, Lambapur outlier, generalized geological SSW-NNE section documenting U concentration mainly in Late Archean-Early Mesoproterozoic granite at the unconformity with overlying sediments of the Mesoproterozoic Srisailam Formation, Cuddapah Supergroup (after Sinha et al. 1995)



A small U deposit has been delineated at the *Gogi* settlements. U associated with colophane occurs in phosphatic limestone and as veinlets of pitchblende and coffinite associated with carbonaceous matter and sulfides in brecciated dark grey limestone as well as in sheared granite. Resources are estimated at about 1 000 t U in limestone, and some 300 t U in granite; grades in both settings average on the order of 0.16% U. (Achar et al. 2001; Chaki et al. 2006; Gupta 2002; OECD-NEA/IAEA 2005; Sharma et al. 1998a).

2.5 E Margin of Chattisgarh Basin/ Sambalpur Granite Massif, Madhya Pradesh-Orissa

U showings with samples assaying up to 0.33% U were discovered near *Chitakhol*, *Renkhola*, *Bokarda*, and *Kumhamahar* in the *Korba District*, in the northeastern Chattisgarh Basin (► Fig. 2.1).

U (fine pitchblende, uranophane, autunite, brannerite, and U-Ti-Fe phases) is hosted in sheared and highly albitized basement granite and ferruginous mafic dikes close to the unconformity, and in overlying ferruginous, sublithic arenite of Chandrapur sandstone of the Chhattisgarh Supergroup (Gupta 2002; OECD-NEA/IAEA 2005).

2.6 Proterozoic Aravalli-Delhi Basins, Rajasthan

A zone of albitization, in excess of 320 km in length, referred to as “albitite line”, occurs along the contact of the Mesoproterozoic

Dehli Supergroup and Archean Banded Gneiss Complex (BGC) between Raghunathpura in Haryana and Ladera and Tal in Rajasthan. A number of uranium and uranium-thorium showings occur along this albitized zone including brannerite mineralization at *Ghateshwar* and, 5 km further to the south, uraninite mineralization at *Rohil*, Sikar District, Rajasthan, hosted in albitized rocks of the Delhi Supergroup.

The small *Rohil* (Rohili) deposit comprises uraninite veinlets with associated pyrite, pyrrhotite, molybdenite, chalcopyrite, and fluorite in albitized quartz-biotite schist and carbonaceous phyllite. Mineralization was traced over 1 050 m in strike length and a vertical depth of 300 m (defined as central block). Resources are estimated at 850 t U at an average grade of 0.07% U contained in two steeply dipping ore bodies, 25 m apart across strike, with a strike continuity of 500 m and 300 m. Drill-intercepts of U mineralization in albitite and pyroxenite within carbonaceous phyllite in the intervening segment between Rohil and Ghateswar and also to the south of Rohil may indicate a continuity of the central ore block (Gupta 2002; OECD-NEA/IAEA 2005).

References and Further Reading for Chapter 2 · India

For details of publications see Bibliography.

Achar et al. 2001; Awati and Grover 2005; Banerjee 1975; Banerjee et al. 1972; Banerjee 2005; Bhasin 1997; Bhattacharyya et al. 1992; Bhattacharyya and Sanyal 1988; Bhola 1965, 1972; Bhola et al. 1966; Chaki et al. 2006; Dhana et al. 1989, 1993, 2002; Dwivedy 1995a,b; Dwivedy and Sinha 1997; Gupta

2002; Gupta and Sarangi 2006; Gupta et al. 1989; Kaul and Varma 1990; Jeyagopal and Dhana Raju 1998; Kumar et al. 1990; Mahadevan 1988; Nagabhushana et al. 1976; OECD-NEA/IAEA 1997, 2001, 2003, 2005; Rao and Ramo 1975; Rao 1977; Rao et al. 1979; Rao and Rao 1983; Rao et al. 2001; Roy and Dhana Raju 1997; Sarkar 1982, 1984, 1986; Sarkar and Saha 1983;

Sarkar et al. 1988; Saraswat and Mahadevan 1989; Saraswat et al. 1977, 1988; Sengupta et al. 1991; Shankaran et al. 1970; Sharma et al. 1998a,b, 2001; Saxena et al. 2006; Sengupta 1972; Sharma et al. 1998; Singh et al. 1990; Singh 2002; Sinha et al. 1992; Sinha et al. 1995, 1996; Umamaheswar et al. 2001; Vasudeva et al. 1989; Viswanath and Mahadevan 1988; Zakaulla et al. 1998.



Chapter 3

Indonesia

Noteworthy U occurrences are reported from the Kalan region in western central Kalimantan. OECD-NEA/IAEA (2005) reports in situ resources of 6 797 t U RAR and 1 699 t U EAR-I including some 5 800 t U recoverable resources (RAR + EAR-I). CEA/COGEMA has explored the Kalan region in the early 1970s and estimated resources of 1 260 t U at a grade of 0.27% U for *Eko-Remaja*, some 500 t U for *Lemajung*, and around 100 t U for boulders (“Rirang boulders”) along the *Rirang* River. Exploration is conducted by BATAN, a state-owned institution. A pilot beneficiation plant has been installed 2 km N of the Remaja prospect.

Sources of information. CEA 1976–1977; Molinas and Dardel 1985; OECD-NEA/IAEA 2001, 2005; Sarbini and Wirakusumah 1988; Tjokrokardono and Sastratenaya 1988; Bruneton P pers. commun. 2007.

Regional Geology of the Kalan Basin, Western Central Kalimantan

The U-hosting Paleozoic Kalan Basin is located some 300 km ESE of Pontianak, the capital city of west Kalimantan. The basin fill consists largely of fine-grained, variably, epi- to mesozonally metamorphosed volcano-sedimentary strata, which are separated into two series.

- An *Upper Series*, about 3 000–4 000 m thick, comprises metamorphosed sedimentary, volcano-sedimentary, and volcanic rocks of relatively monotonous nature and fine grain size. Felsic metavolcanics reflected by ignimbritic tuff and lava flows of rhyolitic composition constitute a major component. Metamorphic grade is amphibolite facies with local crystallization of staurolite and kyanite.
- The *Lower Series* is dominated by metapelite and metasilstone of amphibolite grade facies with biotite, andalusite, cordierite, and sillimanite. Locally, these rocks are transformed into gneiss and migmatite with appearance of feldspar and occasional garnet. Other facies include quartzite and various metavolcanic rocks (dacite, rhyodacite, rhyolite, and ignimbritic tuff).

Tjokrokardono and Sastratenaya (1988) divide the basin fill into three units – from top to bottom: (a) mica schist-sericite schist, (b) quartzite-metasilstone with frequent intrusions of granitoids, and (c) tuffaceous metapelite-metapelite and argillite of volcano-sedimentary origin. Intrusive rocks include monzonite, quartz monzonite, monzonitic granite, and calc-alkaline and alkaline granites. Associated felsic diascist rocks include aplite, greisen, and pegmatite dikes; as well as volcanic dikes of andesite, dacite, lamprophyre, and dolerite. Diorite, tonalite, and granodiorite (“tonalitic complex”) cut by pegmatite and aplite dikes and greisens from the basement. Some migmatite facies

are associated with tonalite; they frequently grade from anatexite to migmatite. Greisenization is found in granodiorite, where microcline is altered to sericite or muscovite, plagioclase to muscovite and silica, and biotite to muscovite and chlorite.

Multiple NE-SW-oriented faults, of which the N-50°E-trending Kalan lineament is the most prominent, transect the Kalan Basin. Weathering is intense and affected the rocks to depths of some 50 m.

Larger U occurrences as known from the Remaja-Eko-Efka-Lemajun and Rirang River localities are hosted in the Upper Series whereas the Lower Series contains discontinuous minor vein-type U mineralization in the Jeronang River area.

3.1 Remaja-Eko-Efka-Lemajun Rivers Area, Kalan Region

Vein-stockwork U mineralization occurs at several sites in a zone some 5 km in length. Mineralization is hosted in metasilstone and adjacent schistose metapelite bands, which occur within a regional metapelitic unit referred to as Jeronang metapelites. The Jeronang metapelites are characterized by abundant brown biotite specks and by andalusite, oriented along the bedding. The transition to schistose metapelite is accompanied by progressive disappearance of andalusite and the development of distinct schistosity. The metasilstones are massive, fine to locally medium to coarse-grained rocks frequently showing well-defined bedding. Other sedimentary features correspond to slumps, slumps breccias, scattered soft pebbles, bioturbations, and load-casts. Episodic small intercalations of carbonaceous metashale are rich in organic matter, sulfides, and arsenosulfides (Bruneton, pers. commun).

The dimension of siltstone lenses and the degree of structural permeability of the schistose metapelite bands control ore bodies. Mineral parageneses consist of variable proportions of uraninite, brannerite, molybdenite, mispickel, pyrite, and pyrrhotite, associated with tourmaline, biotite, chlorite, quartz, and feldspar.

Eko occurrence: Sarbini and Wirakusumah (1988) provide the following characteristics of U mineralization encountered in an exploration tunnel 450 m long in N-50°E direction through the Eko Hills.

Six zones of almost parallel fault-breccia zones with mineralized bodies or veins 40–90 m apart were transected along the tunnel. These breccia zones are undulating and disrupt a metasilstone with adjacent schistose metapelite horizon. The metasediments strike NE-SW and dip 60°SE whereas the breccia zones trend generally WNW-ESE for 80–100 m and dip 60–70°N for ±400 m, i.e. they parallel the schistosity of the metasedimentary unit.

Mineralized breccia zones have two to three undulating planes that form a boudinage structure, 30–150 cm in thickness. Dendritic veinlets, 5–15 cm thick, locally accompany the breccia zones on both sides.

Mineralization comprises uraninite, autunite, and brannerite associated with sulfides and oxides. Gangue minerals include tourmaline, mica, quartz, and feldspar. Breccias of gypsum,

calcite, and chlorite intercept the ore bodies. These minerals occupy shear zones and associated breccias, folding-related openings between two beds and on crests of folds, and fractures, diachases, and schistosity planes.

Boudinage shape, structure, and lithology of the host rocks, whether metasilt or metapelite, as well as the frequency of gypsum, calcite, and chlorite breccias tend to control distribution and concentration of uranium. The more abundant these latter breccias are in an ore body, the lower the uranium content.

In *weathered, oxidized environment*, which persists to depths of about 50 m, ore distribution is highly irregular. Abundant breccias of gypsum, calcite, and chlorite characterize mineralized intervals. Grades range from 300 to 2 000 ppm averaging 600 ppm U, i.e. they are lower than in fresh rock and are an obvious indication that the weathering process has decreased the U content.

In *unweathered environment*, i.e. below the level of some 50 m, gypsum, calcite, and chlorite breccias are distinctly less than in the weathered interval. Lateral and vertical distribution of uranium is relative continuous and grades range from 750 to 3 000 ppm and average 2 000 ppm U. Lyaudet and Roche (1996) tested a bulk sample of 7 t ore from the Eko-Remaja area for beneficiation purposes. The crude ore contained 2 052 ppm U, 210 ppm Mo, and 0.42% S²⁻.

Efta occurrence: U mineralization is hosted in a 60–100 m thick layer of metasiltstone enveloped on both sides by schistose metapelite, 10–20 m in width. These rocks are embedded in the regional Jerong metapelite unit. The symmetrical arrangement of the metasiltstone-schistose metapelite assemblage corresponds to a simple monoclinical structure that dips steeply (70–75°) towards the south. An alternate thickening and narrowing is typical for this assemblage, suggesting the existence of channels in the preexisting sediments. U mineralization is confined to individual veins that crosscut the metasiltstone-schistose metapelite unit, but never the Jerong metapelites (Bruneton, pers. commun.).

3.2 Rirang River Area, Kalan Region

The Rirang River is a small tributary of the Kalan River. Mineralization in this area consists of a REE-U paragenesis and was found in boulders (“Rirang boulders”) and an outcrop along the riverbed (Tjokrokardono and Sastratenaya 1988). Two veins related to pegmatites are exposed in the outcrop. The veins are decimetric to metric in size, contain uraninite, molybdenite, tourmaline, and chlorite, and are controlled by ENE-WSW fractures (schistosity). Similar mineralization (uraninite, molybdenite, brannerite, tourmaline, and apatite) was also intersected by drill holes.

Mineralized boulders were found in irregular distribution along the Rirang Valley over a distance of almost 4 km up to the junction with the Kalan River. They are abundant at the upper and lower course but absent at the middle course of the Rirang River. These boulders contain between 0.6 and 6.67% U in addition to REE and other metals. Resources of these “Rirang boulders” are estimated at least at 100 t U at a grade of 2.5% U.

Most boulders are of centimetric to decimetric size, but can be as big as 2 m. Two boulder types are identified: banded or monazite-type boulders and tectonized boulders. They are thought to have most likely derived from pneumatolytic veins or cavity fillings.

Banded boulders are rounded and composed of a centimetric succession of grey-black and light tan-beige bands. The dark bands consist of fine-grained monazite, molybdenite, pyrite, rutile, and minor tourmaline, biotite and quartz. Uraninite is situated at the edges of the dark bands. The light bands are largely composed of beige monazite, few millimeters in size. These bands form geodic structures indicating a fissure filling by successive deposition of alternating layers of monazite, molybdenite, and uraninite. The dark bands are often cut and displaced by massive invasion of secondary monazite. The two monazite generations are both free of uranium and thorium; and uraninite also does not contain thorium. Some rare boulders consist only of a paragenesis of uraninite, molybdenite, and rare tourmaline whereas monazite is absent. These boulders contain some 30% U.

Tectonized boulders consist of metasiltstone in which stringers of uraninite, molybdenite, pyrite, and minor monazite and tourmaline occupy broken intervals.

Other Uranium Occurrences in the Kalan Region

Several occurrences consist of veins and veinlets ranging from a few mm (Dandang Arai) to 1–15 cm (Tanah Merah) and 1–100 cm (Jumbang I) in thickness. The veins contain uraninite associated with molybdenite, pyrite, pyrrhotite, magnetite, hematite, and ilmenite. Drill holes in Tanah Merah intersected 5 m of mineralization at depths of about 33 m, 40 m, and 50 m. Mineralization in the Mentawa sector occurs in multiple, horizontal to vertical lenticular zones.

References and Further Reading for Chapter 3 · Indonesia

For details of publications see Bibliography.
CEA 1976–1977; Lyaudet and Roche 1996; Molinas and Dardel 1985; OECD-NEA/IAEA 2001, 2005; Sarbini and Wirakusumah 1988; Tjokrokardono and Sastratenaya 1988; and pers. commun. by P. Bruneton.

Chapter 4

Iran, Islamic Republic

A few small U deposits/occurrences with total in situ resources of a little less than 2 000 t U (RAR + EAR-1) are known in Iran. The bulk of these resources (~1 400 t U) is contained in the Saghand ore field. Remaining resources are attributed to occurrences in the Gachin salt plug near Bandar Abbas (100 t U), Narigan 1 (60 t U), Khoshoumi 1 (300 t U), and Talmesi (100 t U as by product to Cu).

Two production centers with a combined capacity of 71 t U yr⁻¹ are under construction (status 2005). The plant at Arda-kan (50 t U yr⁻¹) will treat ore from the Saghand ore field and that at Bandar Abbas (21 t U yr⁻¹) will treat ore from the Gachin area. All uranium-related activities are in the hands of the Atomic Energy Organization of Iran (AEOI), a government institution of the Islamic Republic of Iran (OECD-NEA/IAEA 2005).

4.1 Bafq-Posht-e-Badam Zone

This metallogenic zone occupies Late Precambrian basement and Pan-African lithologies in which metasomatic and hydrothermal vein mineralization are associated with magmatic and metasomatic complexes. Three modes of uraniumiferous mineralization are identified and represented by the deposits mentioned (OECD-NEA/IAEA 2001–2005):

- Albite-amphibole metasomatic type with U-Th-REE mineralization [Saghand and Zarigan (U, Th, Ti, REE), both of Pan-African age];
- hydrothermal-metasomatic veins with U (Mo, Y) mineralization [Narigan (U, Mo, Co) of Pan-African age; and
- hydrothermal polymetallic U mineralization (Khoshoumi of Alpine age).

4.1.1 Saghand Ore Field, Bafq District

The Saghand area is located ca. 130 km NE of the town of Yazd, ca. 30 km E of the oasis of Saghand in the southern extremity of the Dasht-e-Kavir (Great Salt) Desert, central Iran. Distance to Teheran is some 550 km.

The Saghand ore field hosts, among others, structure-controlled metasomatite U deposits, which are the best in tonnage and average uranium grade discovered so far in Iran. OECD-NEA/IAEA (2005) reports total in situ resources of 1 367 t U recoverable at costs below U.S.\$130 per kg U for the Saghand 1 and Saghand 2 deposits. Of this total 491 t U are classified as RAR and 876 t U as EAR-I. Grades average 0.0553% U. Some 90% of the ore is planned to be extracted by underground and the remainder by open pit methods. Two shafts will be sunk to depth of 350 m each by the end of 2006.

Sources of information. OECD-NEA/IAEA 2001–2005; Ramezani and Tucker 2003; Samani 1988a,b, 1998; and other sources.

Geology and Alteration

Located within the Bafq-Posht-e-Badam metallogenic zone, the Saghand ore bodies occur in Vendian/Infracambrian metavolcanics and metasediments (pyroclastics, lavas, tuffs, carbonates, shales, and a clastic suite with interbedded iron formations) metamorphosed to greenschist facies. This sequence is in lateral fault contact with the uplifted Upper Proterozoic Tashk Formation, which is dominantly composed of schists and phyllites. Early Cambrian carbonates, evaporates, and intermediate lava flows unconformably overlie the older rocks.

Vendian/Infracambrian metavolcanics and metasediments have been subjected to several phases of partly intense Na, K, and locally carbonate metasomatism. Pervasive Na metasomatism as reflected by albitite and Na-amphiboles is the most common mode. These rocks underwent retrograde hydrothermal alteration along faults resulting in serpentinization, silicification, and minor carbonatization, pyritization, and locally phlogopitization. Later tectonic events were accompanied by talc development along structures. These metasomatized rocks occur in an E-W-oriented graben structure bounded by Precambrian metamorphics to the north, and Paleozoic (Cambrian) sediments and volcanics to the south.

Mineralization

Four stages of mineralization exist:

- Lithologically-controlled, early stage metasomatite mineralization with uranothorianite, complex U, Th, Ti, REE phases, and/or U, Th, Ti, Ta, Nb, Zr minerals
- mylonite(?) -controlled mineralization with U, Th, Ti, Nb, Zr, REE minerals
- structurally-controlled, late stage metasomatic-hydrothermal mineralization with uraninite, uranothorianite, and davidite(?), associated minerals may include magnetite, pyrite, and molybdenite
- structurally-controlled volcanic-hydrothermal(?) sulfide mineralization with some U in mafic volcanics

Stage a mineralization consists dominantly of disseminated grains and pockets (<5 cm in diameter) but also of veinlets up to 15 mm in thickness and few cm to >1 m long, which locally accumulated to patches up to a few meters in size interconnected by barren or weakly mineralized ground. Host rocks comprise a variety of more or less metasomatized rocks composed of variable quantities of amphibole, albite, and carbonate. Fine-grained albite-amphibole, and to lesser degree amphibole (-carbonate) metasomatites, are the best host rocks.

Stage c mineralization forms ore bodies in breccia zones within polyphase metasomatized and altered rocks. One of these ore bodies has a cone-shaped configuration and occurs in an

E-W-oriented breccia zone that dips variably 40–80° S. The cone is 50–70 m in diameter on surface and narrows to 0 at a depth of ca 160 m. Mineralization is confined to a 3–6 m wide shell surrounding a magnetite-rich core. The shell is composed of reconstituted fragments and matrix material of magnetite-martite and serpentinite with enclosed phenocrysts of Fe-sulfide (mainly pyrite, marcasite?). Some veinlets (1–2 mm wide) and vug fillings (<2 cm in diameter) of pink albite, occasionally associated with some carbonate occur in minor amounts. The mineralized shell is enveloped in a halo of talc-altered, pyritic serpentinite, 2–5 m in width.

Low-grade mineralization (up to few hundred ppm U) is ubiquitous throughout the shell, from surface to 160 m depth and over a width of 3–6 m. The low-grade material encloses several irregularly shaped and distributed intervals apparently arranged en echelon or in feather pattern, ca 10–50 cm wide, of slightly better grade. Some pinkish coloration and black minerals characterize this better grade material.

Another ore body with U-Mo mineralization is located to the E of the above described ore body, apparently on strike with the E-W-trending breccia zone but supposedly separated from that by a N-S fault. Ore occurs in an E-W-oriented, 60–80° N dipping breccia zone, ca. 5 m wide, and contains grades of 600 ppm U and 700 ppm Mo. Ore also occurs at and adjacent to the intersection of this breccia zone with a flat-lying magnetite-martite body at depths below 180–250 m.

The magnetite rock contains variable amounts of pyrite ranging in form from isolated phenocrysts (mm–cm in diameter) to almost massive sulfide bands a few cm to 30 cm thick, and irregularly distributed, fine-grained disseminations of uraninite(?) and molybdenite.

Low-grade U mineralization extends over a depth interval of ca 25 m in brecciated intervals of the magnetite body. It encloses better grades over intervals a few cm to 1 m in thickness. Lower grade mineralization is associated with pink speckled dark rocks containing pyrite. Better grade U mineralization occurs in slightly to strongly brecciated rocks composed of magnetite and sulfides often adjacent to highly sulfidic zones with >50% sulfide.

4.2 Gachin Salt Plug/Bandar Abbas Region

The Gachin salt plug is located in the southeastern Zagros Range about 45 km W of the harbor town Bandar Abbas, southern Iran, some 1 500 km from Tehran. U mineralization occurs in duricrusted surficial deposits associated with felsic volcanics. Individual U occurrences are small in size and resources (a few t to some 10s t U each) due to disruption of the surficial uraniferous layer by halokinetic uplift. Grades are variable and commonly range from 300 to 1 000 ppm U.

OECD-NEA/IAEA (2005) reports total resources of 100 t U (EAR-1) at grades averaging 0.2% U. Mining is by open pit methods and is carried out mainly in three blocks.

Sources of information. Espahbod 1985; OECD-NEA/IAEA 2005; Sulovsky 1994; and other sources.

Geological Setting of Mineralization

Basement rocks consist of the Upper Proterozoic Hormoz Formation, which includes felsic volcanics, evaporates (salt), and sediments. Prevailing rocks exposed are Miocene marine sediments of the Mishan Formation (ca. 700 m thick) that are folded and faulted along NW-SE- to WNW-ESE-oriented axes.

Salt diapirs originating from the Hormoz Formation were intruded during repeated halokinetic stages into the Miocene sediments, i.e. the intrusion of the Gachin salt plug must have occurred during or after the Lower to Middle Miocene. By this activity, the penetrated rocks including uraniferous volcanics were brought to the surface, and now occur as more or less distorted blocks and fragments of variable shape and dimensions (up to several 100 m across) suspended in salt.

At some episode of halokinetic inactivity, a surficial layer, up to 10 m thick, composed of alluvial, fluvial, and lacustrine deposits was formed. Its upper part was later indurated in variable intensity by duricrusting. Renewed halokinesis disrupted and distorted the duricrusted cap together with the underlying rocks. In consequence, the duricrusted layer lies partly flat on top of dissected small plateaus and partly in a tilted position.

Lithologic facies in the Gachin plug include evaporitic material (salt, gypsum, polyhalitic material); sedimentary and volcanic fragments (recycled debris of the Hormoz Formation such as rhyolite including uraniferous rhyolite/rhyolitic tuff and granophyre, diabase, sandstone, dolomite, metasediments, oligistehematite, and marl of the Miocene Mishan Formation).

Host Rock Alteration

Various kinds of alteration phenomena are recognized in the allogenic rocks in the salt plug. Rhyolitic rocks display locally intense hydrogenic alteration (bleaching, decomposition, argillization) associated with the formation of high-grade hematite/oligiste lenses and pockets. These features may have resulted from: (1) early volcanic hydrothermal processes, (2) later alteration by brines or meteoric waters, or (3) a combination of both. Surficial deposits show pervasive limonitization/hematitization (partly as ferricrete) and duricrust cementation mainly by gypsum and to a minor degree by calcrete or dolocrete.

Mineralization

Three principal varieties of U mineralization are noticed: (a) finely dispersed synmagmatic uranium in felsic volcanics and pyroclastics, (b) epigenetic, structure-controlled mineralization in altered felsic volcanics (very rare), and (c) redistributed uranium as surficial-type mineralization in duricrusted cover sediments.

Synmagmatic uranium in felsic volcanics and pyroclastics occurs as finely disseminated uranium and other metals (mainly Mo) in massive to banded rhyolite and bedded vitric rhyolitic tuffs as original rock constituents. The U content in these rocks commonly ranges from 5 to 25 ppm U but may increase locally to 100–150 ppm U, and exceptionally to a few hundred ppm U.

Dimensions of segments with better uranium contents (>100 ppm U) are small (few meters in diameter). Their distribution is irregular and spotty.

Epigenetic, structure controlled mineralization in felsic volcanics (rhyolite) or pyroclastics consists of small nodules and veinlets of pitchblende (coffinite?) (mm to 5 cm wide) in narrow and short fractures (10–20 cm wide, ca 0.5–1 m long and deep). Where pitchblende mineralization is well exposed, the host rocks display a halo of intense clay alteration and bleaching extending for 1–2 m from the mineralized structure into the wall rocks. (Analysis of a sample yielded 0.18% U, 0.11% Cu, 285 ppm Pb, 130 ppm Zn, 130 ppm As, 11 ppm Mo, and 47 ppm Th.).

Surficial-type mineralization occurs in a duricrusted red-brown surficial cover horizon 2–5 m thick composed of fluvial and/or alluvial pebbly-clayey material, which is locally underlain by or interbedded with laminated, calcareous tuffaceous layers. These surficial deposits were overprinted by supergene duricrust-type processes reflected by formation of ferruginous gypcrete and minor calcrete or dolocrete, or other duricrust material. Felsic volcanics (rhyolite), which are more or less clay-altered and bleached, form the base of the surficial horizon. Locally, stringers of mineralization extend into intensely altered rhyolitic rocks. This mineralization is more or less continuous but quantitatively highly irregular. Other metals (e.g. Mo) exhibit a similar distribution pattern. The thorium content is low.

Metallogenetic Aspects

A metallogenetic model for the evolution of the Gachin area and its uranium mineralization may include the following steps and processes.

After extrusion of rhyolite and pyroclastics with a high original stock of 5–25 ppm U in Late Proterozoic time, these rocks were affected by late to post-volcanic hydrothermal activity, which caused localized precipitation of colloidal pitchblende in fractures and clay alteration of the surrounding volcanic host rock.

Due to halokinesis during or after the deposition of the Miocene Mishan Formation, the area was intermittently uplifted associated with block faulting. During a subsequent period of tectonic quiescence, the older rocks were eroded and agglomeratic, fluvial, and lacustrine sediments were deposited in depressions upon an unconformity of minor relief. Circumstantial evidence suggests that this stage presumably occurred during Tertiary to subrecent times under semi-arid to arid conditions as suggested by partial consolidation of the loose sediments by duricrust processes.

During this episode of clastic sedimentation, the uraniumiferous rhyolite and associated pyroclastics were subjected to clay alteration and bleaching where exposed to meteoric agents. Uranium was leached and transported into the surficial deposits. Redeposition of the uranium took place in such surficial deposits overlying or adjacent to alteration-affected uraniumiferous volcanics. Fixing of the uranium occurred by adsorption or complexing in suitable minerals, most likely in clays and iron-hydroxides. It may also be postulated that uranium precipitated at the interface of uranium-transporting meteoric solutions and brines residing in the duricrusted cap rocks. In this case, however, it would be expected to see more distinct U minerals. A combination of both processes may likewise be considered.

Reactivated halokinesis generated limited uplifting of the area in subrecent times. Thereby, the surficial cover horizon was broken apart, displaced, and more or less tilted producing the present-day exposed geological configuration and morphology of the area.

References and Further Reading for Chapter 4 · Iran

For details of publications see Bibliography.
Espahbod 1985, 1986; OECD-NEA/IAEA 2005; Ramezani and Tucker 2003; Samani 1988a,b, 1998; Sulovsky 1994.



Chapter 5

Japan

Two ore fields with basal-channel sandstone-type U mineralization, *Tono* and *Ningyo-Toge* on Honshu island, and a number of minor U occurrences are known in Japan (Fig. 5.1). Japan's original U resources, all contained in sandstone U deposits, total 7 680 t U; of which these two ore fields account for 7 135 t (Kamiyama et al. 1976).

Some test mining was carried out at Ningyo-Toge from 1959 to 1987. A R&D mill with a capacity of 30 t U yr⁻¹ operated near Ningyo-Toge from 1964 to 1982 and a nearby heap leaching facility operated from 1978 through 1987; the former produced 58 t U and the latter 29 t U bringing Japan's U production to 87 t. Both facilities have been dismantled.

Power Reactor and Nuclear Fuel Development Corporation (PNC) is state-owned and is the owner and operator of all uranium-related activities in Japan. In 1967, it succeeded the Atomic Fuel Corporation (AFC), which had been established in 1956.

Sources of information. Hayashi 1970; Kamiyama et al. 1976; Katayama 1958; Katayama and Kamiyama 1977; Katayama et al. 1974; OECD-NEA/IAEA 1973, 1983, 1988; Okada et al. 1988; Sakamaki 1986.

Historical Review

Uranium was first reported in Japan in 1893, fergusonite had been discovered at *Nakatsugawa*, Gifu Prefecture. By around 1920, many radioactive minerals such as columbite, monazite, xenotime, and samarskite were found in the *Ishikawa*, *Naegi*, and *Tanokalli* areas. These three areas later became production centers for radioactive minerals.

Uraninite was found in 1936 at *Yanai*, Yallaguchi Prefecture, and subsequently U⁶⁺ minerals such as autunite, torbernite, and phosphuranylite were found in many areas. In 1954, zeunerite originating from coffinite was discovered in wolframite-cassiterite veins of the *Miyoshi* Mine, Okayama Prefecture. This was the first discovery of a U mineral in a pneumatolytic-hydrothermal metallic deposit. In 1957, uraninite was found along faults in hornfels near the *Nodatamagawa* manganese mine, Iwate Prefecture, and subsequently in some similar bedded manganese deposits of Paleozoic age. Around 1960, radioactive anomalies were discovered in some of the '*Kuroko*' deposits, which were producing copper, lead, zinc, and gypsum. Here, U occurs in argillaceous zones near ore bodies and is presumably adsorbed by clay minerals.

Systematic exploration for U deposits in Japan began in 1954 by the Geological Survey of Japan, and in 1955 a uranium deposit in Tertiary sandstone was found at Ningyo-Toge in southwestern Honshu. Subsequent discoveries of U occurrences similar to Ningyo-Toge include *Okutango*, Kyoto-fu, SW Honshu; *Oguni*, Yamagata Prefecture, NW Honshu; and *Sanin*, Shimane

Prefecture, SW Honshu, all in 1959; *Tarumizu*, Kagoshima Prefecture, Kyishu island, in 1960; and, in 1962, a U showing in the *Tono* area, Gifu Prefecture, that led to the discovery in 1964 of the *Tsukiyoshi* deposit, the largest in Japan.

In 1966, U occurrences were discovered in Cretaceous sandstone at *Yuya* and later at *Toyoda*, Yamaguchi Prefecture at the SW end of Honshu (Okada et al. 1988) (Fig. 5.1).

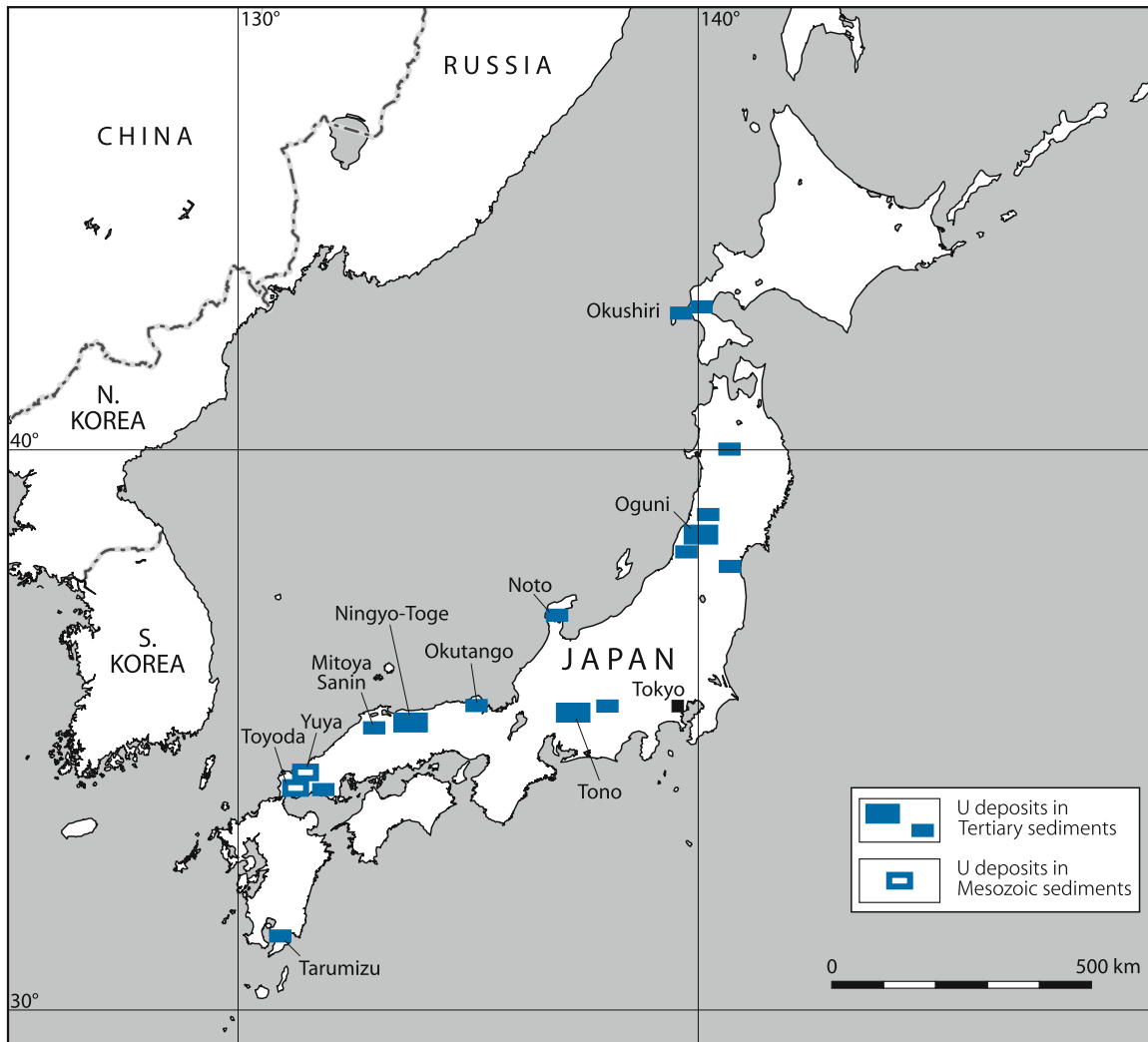
Principal Characteristics of Basal-Channel Sandstone-Type U Deposits in Japan

Noteworthy U deposits of basal-channel type are confined to Tertiary basins. Principal recognition criteria of these deposits include a granite mass in the basement, paleovalleys with tributary channels incised into the granitic paleosurface, permeable carbonaceous beds at the base of the Tertiary sequence, lithologic or tectonic traps for groundwater in the basal host sediments, and an aquiclude capping the host sediments.

As noted in the various papers by Kamiyama and Katayama (see References) and Okada et al. (1988), characteristic ingredients with respect to localization, size, and grade of uranium concentrations of basal-channel U deposits as they are known from the Ningyo-Toge and Tono ore fields, Honshu island, are primarily a function of host rock and basement lithologies, paleochannel morphology and position, and hydrodynamics/groundwater traps. Essential criteria of these parameters include:

- Intermontane basins filled with Neogene sediments
- carbonaceous, psephitic-psammitic sediments interbedded with pelitic and lignitic beds of fluvial-lacustrine origin occur at the base and finer grained marine facies including pyroclastics in the upper section of the Pliocene-Miocene sequence
- basement consists of Paleozoic sediments and Mesozoic granites
- basement paleosurface exhibits an irregular channel-basinal topography
- U mineralization occurs in basal parts of paleochannels and
- U deposits are almost exclusively confined to channel sections incised into granite
- narrow tributary paleochannels provide most favorable loci for ore bodies
- broad main channels contain U mineralization preferentially at the margin rather than at the center of a channel
- barriers causing changes in groundwater hydrodynamics in host beds tend to improve U accumulation; barriers include
 - abrupt thinning of host beds at the margin of channels and over basement highs
 - major displacement faults with gouge cutting the paleochannels
- carbonaceous feldspathic sandstone and conglomerate of fluvial provenance provide the principal host rocks
- mineralized horizons are commonly overlain by impermeable strata such as mudstone, shale, and tuff
- U is closely associated with finely dispersed vegetal-organic matter and authigenic pyrite

Fig. 5.1. Japan, location of sandstone-type U deposits/occurrences (after Okada et al. 1988; Katayama and Kamiyama 1977)



- U is partly present in the form of U minerals and partly in adsorbed state
- pitchblende and coffinite are the primary U minerals, and, additionally in the Ningyo-Toge deposits, ningyoite
- adsorbent phases include clay minerals, vegetal remains, and, in the Tono deposits, also zeolites
- ore bodies are commonly of blanket or lenticular shape, low grade and small size, and consist of disseminated mineralization

Katayama and Kamiyama (1977) elaborate on major ore controlling criteria and provide respective examples as follows.

Channel morphology and geological position: U deposits are almost exclusively confined to paleochannel sections incised into granitic basement while those channel parts overlying older sediments or (contact-) metamorphics only contain anomalies. Among channels, those with steeper slopes tend to be more

favorable than broad main channels; the latter are usually barren or weakly mineralized. This discriminative preference of U accumulation is thought to be the result of the balance between the migration rate of uraniferous solutions and the volume of the potential host sediments.

Aquifers: Ore bodies are commonly confined to permeable basal psephitic and psammitic channel facies in which their shapes and dimensions are predetermined by changes in hydrodynamics of groundwater and U precipitating agents. Katayama and Kamiyama (1977) postulate groundwater traps with stagnant groundwater that condition the form and quality of a deposit or ore body; or otherwise expressed, these properties of a deposit are a function of a forced change in hydrodynamics caused by a combination of spatial relationship and permissivity conditions of permeable host sediments and impermeable elements such as argillaceous layers or faults.

The influence of spatial aquifer-aquiclude relationships on setting and dimensions as found in many U deposits is illustrated by ore bodies in the *Asabatake channel* in the northeastern Ningyo-Toge OF. They occur in a thin aquifer at the bottom, in thickened arenite at the flank of the channel, and in intercalated thin permeable lenses overlain by and inserted within pelitic beds, respectively (Fig. 5.5a).

Accumulation of better grade ore can be exemplified by the *Nakatsugo-South ore body*, (Fig. 5.5b) in the southeastern Ningyo-Toge OF. This tabular, high grade (av. 0.5% U) deposit is located where the ore hosting conglomerate is locally distinctly reduced in thickness to a blanket sandwiched between a mudstone cap and a base of rather flat granite surface.

The *Tsukiyoshi* deposit in the Tono OF (Fig. 5.2) documents the impact of a structural control on U mineralization. Uranium occurs all along the base of the host channel but the main and best ore body is controlled by a fault that has placed impermeable sediments against the U-hosting bed (Figs. 5.3a,b). Highest ore grades are found at the fringes of the ore body whereas the fault is unmineralized. A redox front at the margin of this ground water trap at the wedge of the aquifer adjacent to the gouge-filled fault is thought to have generated the favorable conditions for increased U accumulation.

In contrast to those traps mentioned above, thick aquifers do not contain consistently stagnant groundwater but rather a geological-hydrodynamic regime that permits a dispersion of uraniumiferous groundwater and hence, thick aquifers tend to be unfavorable for the accumulation of uranium.

Reducing Environments: Uranium was very likely transported in the form of uranyl complexes in aqueous solution and precipitated in a reducing environment that was provided by organic matter and sulfate-reducing anaerobic bacteria. All U-hosting lithologies contain carbonaceous debris, in quantities, however, that fluctuate in a wide range and hence gave rise to a variety of U mineralization in quality and quantity.

Sporadic high U concentrations associated with wood fragments are not uncommon in tuff or tuff-breccias in basal Neogene sediments in Japan as, e.g., at *Sugawa*, Okutango District (Kyoto Pref.), where fragments of carbonized or silicified wood in tuffaceous sediments are selectively highly mineralized, as high as 18% U, in the form of coffinite, but the U tenor decreases sharply over a short distance from fossil wood remains.

Better reducing conditions for a larger precipitation of uranium, and hence for the formation of sizable ore bodies, are related to finely disseminated humus in sedimentary beds. Combined with other favorable criteria mentioned earlier, these environments also supported grade improvements. As can be seen in the afore-cited *Nakatsugo-South* deposit, fine particles of carbonaceous matter are disseminated in the matrix throughout the mineralized conglomerate bed. Organic carbon contents range from 0.3 to 0.6%, and sulfur isotope ratios of pyrites in the ore suggest a bacterial origin (Ando et al. 1969 and Sakai et al., respectively, in Katayama and Fukuoka 1970).

Adsorbent minerals: A substantial part of the uranium contained in the Japanese sandstone-type U deposits is adsorbed on clay minerals, chlorite, zeolite, and organic matter. Adsorbed U is not confined to the host aquifer, however, but also occurs in the fringes of adjoining fine-grained facies like mudstone, etc.

The twofold effectiveness of carbonaceous material can be demonstrated by ore bodies in the *Kannokura channel*, Ningyo-Toge OF, in which contents of uranium and humic acid correlate positively in spite of a wide fluctuation of the organic content. Organic matter was not only effective as an adsorbent but also as a reducing agent, for a part of the uranium has been incorporated into ningyosite or pitchblende.

Another example is given by the *Nakatsugo main ore body*, Ningyo-Toge OF, that contains two varieties of U ore related to organic matter. One consists of mineralized mudstone with U adsorbed on organic matter, in which the contents of U and sulfur do not correlate. The other is a sandstone or conglomerate with variable U grades where U is present in the form of ningyosite and sulfur is present in authigenic pyrite. In this case, U and sulfur contents show a positive correlation. Katayama and Kamiyama (1977) interpret these facts to mean that adsorption of uranium on organic matter is quite independent of the rate of production of hydrogen sulfide, while the formation of ningyosite relies on the activity of hydrogen sulfide producing bacteria.

In conclusion, the actual *ore forming process* involves groundwater that has circulated through, and leached uranium from basement granite and subsequently migrated into basal fluvial sediments. Where the oxygenated uraniumiferous groundwater encountered a reducing environment caused by carbonaceous material and anaerobic bacterial activity, a redox front was formed and U was deposited as U minerals or fixed by adsorbent minerals. A combination of required favorable conditions was apparently provided by narrow tributary paleochannels in particular.

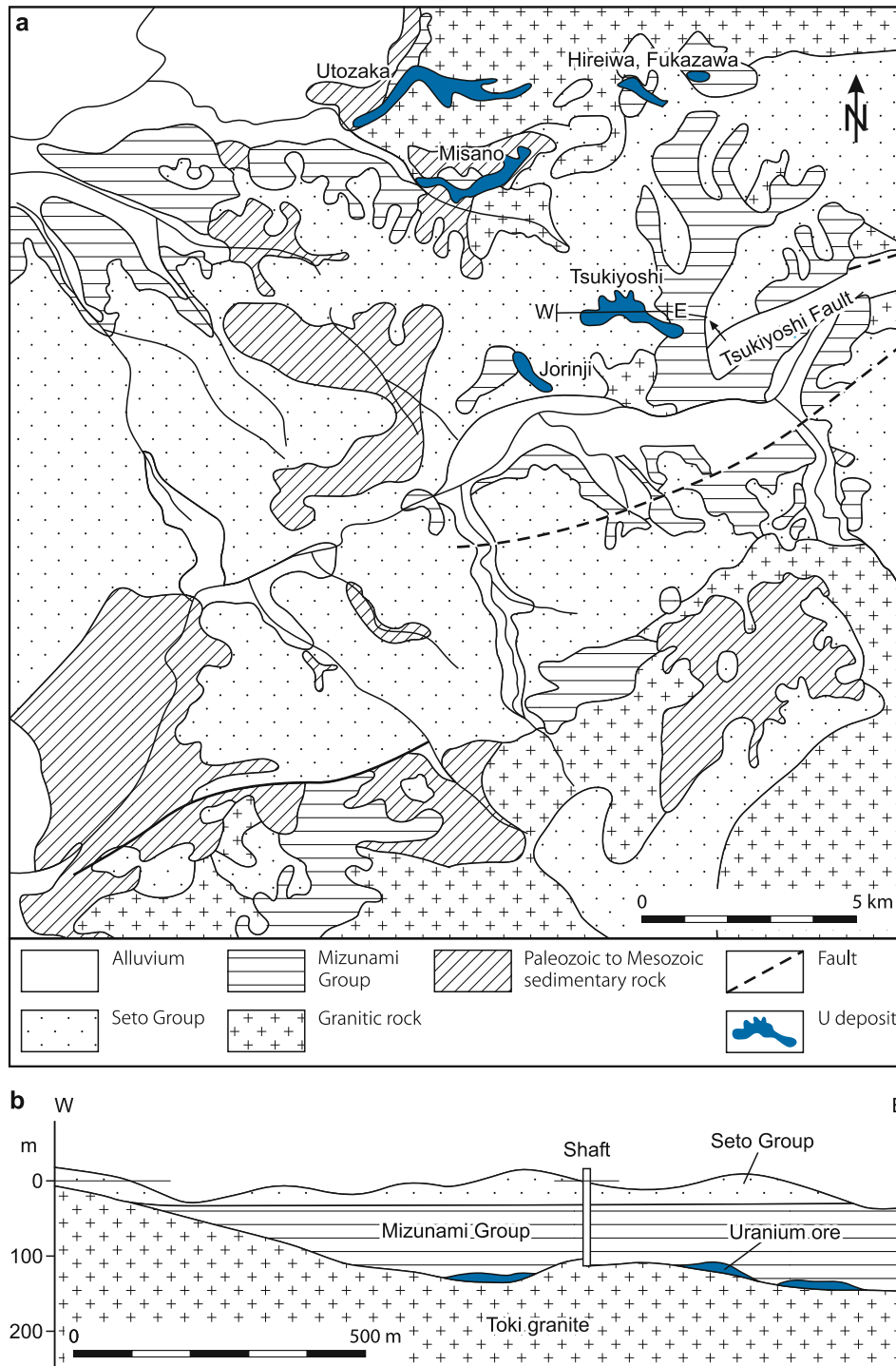
5.1 Tono Ore Field

This ore field is centered 30 km NE of Nagoya city in Gifu Prefecture, central-southern Honshu, and covers three adjacent Tertiary basins with an area of approximately 40 × 35 km. A number of basal-channel sandstone U deposits/occurrences have been identified including *Tsukiyoshi*, *Jorinji*, *Obara*, *Fukazawa*, and *Hireiwa* in the Mizunami or Toki Basin; *Misano* and *Utozaka* in the Kani Basin; and *Iwamura* in the Iwamura Basin. Resources total 5 040 t U at an average grade of 0.046% U (based on a cutoff grade of 0.02% U) (Kamiyama et al. 1976).

Tsukiyoshi also known as the *Tono Mine* (Fig. 5.2) is the largest deposit and accounts for the bulk of the resources. Exploitation was planned by underground methods for this deposit but has not materialized except for some test mining served by a 140 m deep shaft in the main ore body in the southern, hanging wall block of the Tsukiyoshi fault. The subsequent description focuses on the Tsukiyoshi deposit.

Sources of information. Katayama and Kamiyama (1977), Seo et al. (1989), Shikazono and Utada (1997), and Yamamoto et al. (1974).

Fig. 5.2. Mizunami Tertiary Basin, Tono area, **a** geological map with location of prominent U deposits/occurrences and **b** longitudinal W-E section of the Tsukiyoshi deposit/Tono Mine (after Shikazone and Utada 1997)



Geologic Setting of Mineralization

Pliocene-Miocene clastic and pyroclastic sediments with a maximum thickness of 600 m fill the Mizunami Basin. Lithologies consist of basal fluvial-lacustrine facies and overlying marine strata with volcanic components and variable

amounts of vegetal debris that rest upon a paleosurface with a marked relief of channel and trough morphology. Lithostratigraphic units in the Tono area, Mizunami Basin, include (Shikazone and Utada 1997):

Pliocene: Seto Group, >80 m thick: unconsolidated fluvial sediments unconformably overlying Miocene deposits

>Uplift/Unconformity<

Miocene: Mizunami Group, subdivided into Oidawara, Akeyo and Toki Formations

- Oidawara Fm, 100 m thick: marine tuffaceous sandstone, siltstone, and basal conglomerate
- Akeyo Fm, 200 m thick: marine arkosic tuffaceous sandstone, siltstone, tuff, and pumice
- Toki Fm, >170 m thick: sandstone-dominated fluvial-lacustrine sediments. Tuffaceous sandstone and pumice rest upon conglomerate and alternating (arkosic) sandstone and mudstone interbedded with lignite that overlie basal arkosic conglomerate composed mainly of granite and quartz porphyry pebbles, and abundant carbonaceous matter

>Unconformity<

Late Cretaceous: Medium- to coarse-grained biotite granite, porphyritic biotite granite, and medium-grained hornblende-biotite granodiorite porphyry intruded into Paleozoic sediments and volcanics that are contact metamorphosed peripheral to granite bodies.

A major overthrust, the curvilinear ENE-WSW-oriented and 60–70°S dipping Tsukiyoshi fault with displacements of some 20–30 m, dissects the western half of the Tsukiyoshi deposit and has pushed the southern over the northern wing of the deposit (▶ Figs. 5.3a,b).

Alteration

Diagenetic alteration products in lacustrine facies are dominated by abundant pyrite crystals, calcite, organic compounds, and small amounts of marcasite or pyrrhotite, whereas marine facies are characterized by sparse framboidal pyrite, calcite, and organic compounds, and a lack of marcasite or pyrrhotite. Other authigenic phases include clay species (smectite, montmorillonite, kaolinite), zeolites, siderite, and dolomite.

Pyrite is present in two habits. *Framboidal pyrite* occurs in small amounts in the Oidawara, Akeyo, and upper Toki Formations in which it occupies cleavages in pseudomorphous clay minerals after biotite (vermiculite/biotite mixed-layer minerals), encloses magnetite grains, and occurs in matrix volcanic glass that is partially replaced by smectite. *Euhedral-subhedral pyrite* is abundant in the lower Toki Formation and coexists with marcasite. Euhedral-subhedral pyrite coats framboidal pyrite and hence must be younger.

Calcite frequently replaces pyroxene, biotite, and amphibole in the lower horizon of the Toki Formation and underlying basement granite; it fills microvoids in smectite-rich horizons, and associates with quartz and pyrite. Calcite and gypsum veinlets are the latest alteration products. Small amounts of siderite and dolomite occur irregularly distributed in unmineralized horizons.

Smectite is thought to be an alteration product of volcanic glass, which is a major constituent in (tuffaceous) mudstone

overlying the U mineralized horizon. Smectite abundance decreases from the lower to upper Toki Formation but forms an almost pure smectite horizon between the U mineralized and overlying unmineralized section.

Zeolite group minerals are also considered to be alteration products of volcanic glass and include analcime, clinoptilolite, heulandite, and mordenite. These phases replace volcanic glass, form veinlets, and fill micro-cavities in smectite. Pyrrhotite, chalcocopyrite, and rutile occur as rare specimens in the Toki Formation. Pyrrhotite associates with biotite while chalcocopyrite and rutile associate with quartz that fills micro-cavities in smectite.

Oxidation processes are reflected by hematite enclosing some magnetite grains, and frequent dissolution of ilmenite lamellae in magnetite (Shikazono and Utada 1997).

Mineralization, Shape and Dimensions of Deposits

Mineralization in unoxidized zones consists of minute grains of pitchblende and coffinite and in an oxidized environment primarily of autunite and uranocircite. Pitchblende and coffinite occur preferentially adjacent to pyrite and ilmenite, and along cleavages in biotite. A large part of the U endowment, however, is adsorbed on clay (montmorillonite, kaolinite, etc.) and zeolite minerals (heulandite, clinoptilolite). Limonite and carbonaceous debris also contain adsorbed uranium. Calcite occurs sporadically in ore.

U mineralization is primarily hosted by arkosic sandstone and conglomerate of the basal horizon of the Toki Formation. Major detrital minerals in these sediments are quartz, plagioclase, K-feldspar, mica, amphibole with minor amounts of biotite and pyroxene. Accessorial magnetite is a common constituent in the lower part of the Toki Formation while ilmenite occurs in small amounts. Vegetal debris is abundant.

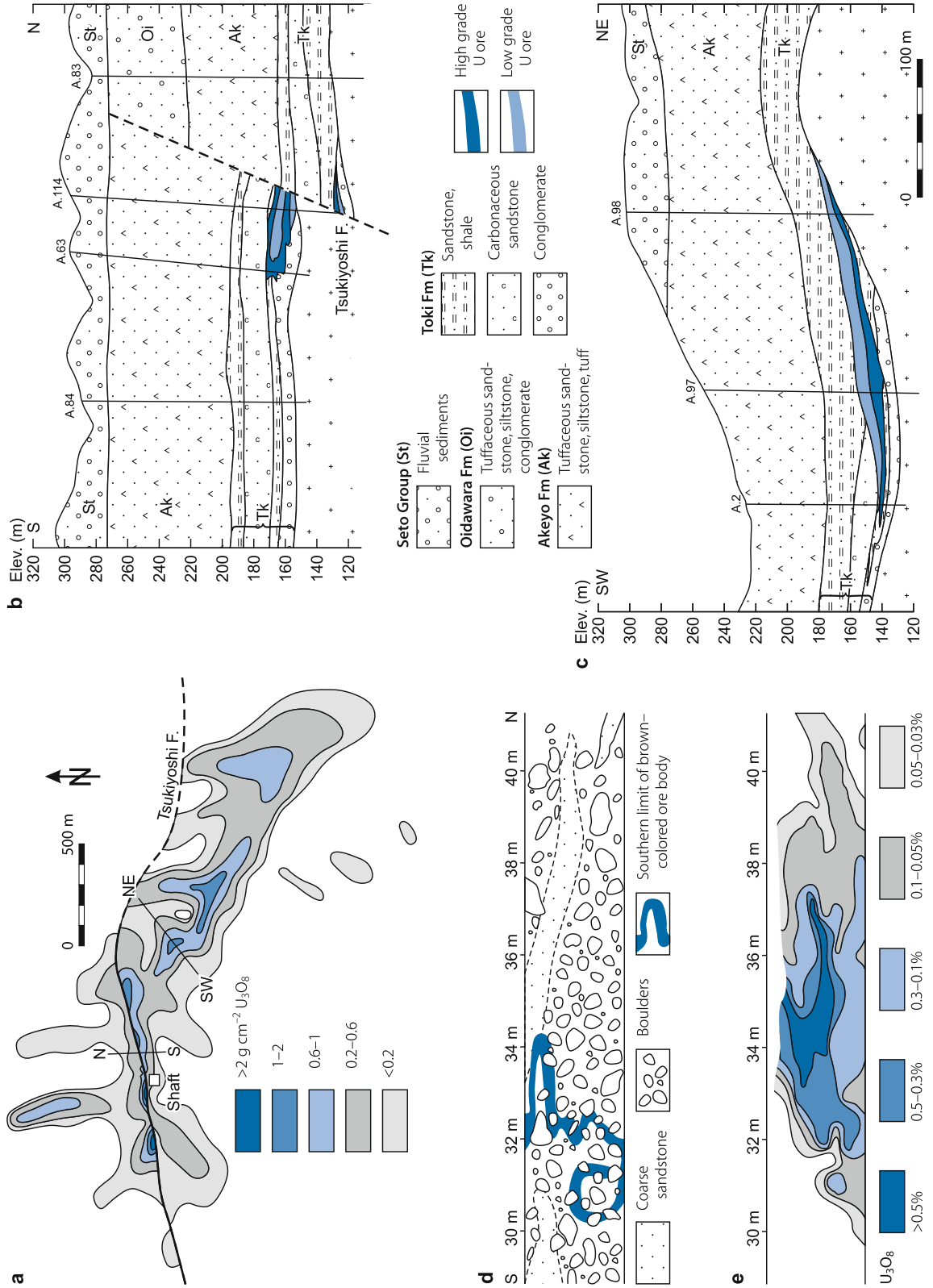
The Tsukiyoshi deposit extends for some 3 km in length along a paleochannel trending in a bend from W into SE. Widths are commonly 100–300 m but achieve up to 1 000 m where ore penetrates into tributary channels (▶ Fig. 5.3a).

Individual ore bodies are of lenticular to curvilinear shape, up to almost a kilometer in length, tens to a few hundreds of meters in width, and 1–3 m, locally over 10 m in thickness. Grades are variable and range from 0.02 (cutoff grade) to several tenths of a percent.

Ore bodies are confined to channel sections that rest immediately upon granite. In contrast, paleochannels are barren of U concentrations above Paleozoic sediments. Maximum U concentrations occur in the upper reaches of narrow paleochannels and at major faults with strong argillaceous gouge. The latter case is exemplified by the main ore body at Tsukiyoshi that occurs in the uplifted southern block adjacent to the Tsukiyoshi fault that is impermeable due to gouge (▶ Fig. 5.3b). Highest ore grades occur at the fringes of this ore body that abut against the fault whereas the fault is unmineralized. ▶ Figures 5.3a–e illustrate the principal setting and distribution of mineralization and related U concentrations. For ore controls and recognition

Fig. 5.3.

Tono OF Tsukiyoshi deposit, setting and qualitative distribution of U mineralization. **a** Planar outline of the deposit with vertical projection of U concentrations, **b** S-N cross-section across the main ore body at the Tsukiyoshi fault; **c** SW-NE section with U accumulation at a basement high, **d** and **e** lithology and grade distribution in a gallery wall (after Katayama et al. 1974; stratigraphy after Shikazone and Utada 1997) (legend for **b** and **c**: St: Seto Group; Mizunami Group: Oi Oidawara Fm, Ak Akeyo Fm, Tk Toki Fm; see text for lithologies of formations)



criteria see Sect. *Principal Characteristics of Basal-Channel Sandstone-Type U Deposits in Japan*.

Metallogenetic Aspects

Shikazone and Utada (1997) provide a metallogenetic model largely based on stable isotope studies for the Tsukiyoshi deposit/Tono Mine as follows:

U mineralization is hosted primarily by lignite-bearing fluvial-lacustrine sediments of the basal Miocene Toki Formation that originated from granitic basement in a low-temperature climate. The climate condition is deduced from fossil plants. A pelitic layer with abundant smectite, which is inferred to have been produced by the interaction of interstitial water with volcanic glass, separates the mineralized horizon from overlying unmineralized Upper Miocene marine beds.

The $\delta^{34}\text{S}$ values of framboidal pyrite in the Upper Miocene marine sediments are low (-14 to -8% CDT) and indicate only minor bacterial reduction of seawater sulfate; whereas euhedral-subhedral pyrite in the lower lignite-bearing fluvial-lacustrine arkose sandstone (Toki Formation) has variable and high $\delta^{34}\text{S}$ values ranging from $+10$ to $+43\%$, values which imply a closed system with substantial bacterial reduction of seawater sulfate.

Calcite in these fluvial-lacustrine sediments has low $\delta^{13}\text{C}$ values ranging from -19 to -6% PDB while those in marine facies are high (-11 to $+3\%$). This implies a larger proportion of marine carbonate in marine sediments than in the lower fluvial-lacustrine arenites, and that calcite in the latter derived by a significant contribution of carbon both from oxidative degradation of organic matter and dissolved marine inorganic carbon.

These $\delta^{13}\text{C}$ combined with $\delta^{18}\text{O}$ values of calcite are interpreted by the authors to reflect a mixing of two fluids: one is characterized by respective marine carbon and oxygen isotopes and the other by $\delta^{13}\text{C}$ and $\delta^{18}\text{O}$ values that almost correspond to those of modern groundwater in the Toki Formation.

As deduced from stable isotope data ($\delta^{13}\text{C}$, $\delta^{18}\text{O}$, $\delta^{34}\text{S}$) and the paragenesis of diagenetic alteration minerals, intense bacterial reduction of seawater sulfate resulted in the deposition of substantial amounts of euhedral-subhedral pyrite as well as calcite in microvoids in smectite during diagenesis of the lacustrine facies in the lower Toki Formation. This process was associated with concomitant oxidation of organic matter and hydrolysis reactions of organic matter that generated CH_4 and CO_2 . $\delta^{34}\text{S}$ and $\delta^{13}\text{C}$ data that deviate from a negative correlation line toward higher $\delta^{13}\text{C}$ values attest to a methanogenic CO_2 production.

While diagenetic alteration of the marine sediments was governed by a predominance of SO_4^{2-} among dissolved sulfur species, these research data indicate low Eh conditions during diagenesis within the lacustrine facies in which almost equal concentrations of CH_4 and HCO_3^- existed and reduced sulfur species (H_2S , HS^-) prevailed among aqueous sulfur species, i.e. an Eh-pH environment existed that was favorable for deposition of pyrite and calcite as well as for coffinite and pitchblende formation due to the reduction of U^{6+} to U^{4+} .

Low Eh values could be established for ancient interstitial waters as well as for modern groundwater (-335mV) in the lacustrine facies of the Toki Formation; and, consequently, it is assumed that a reducing environment in which U^{4+} is stable has been maintained since precipitation of U minerals and that almost no uranium has been removed from the site of ore deposition.

Katayama and Kamiyama (1977) explain the high-grade U concentrations in the main ore body at Tsukiyoshi that is situated in the hanging wall adjacent to the Tsukiyoshi fault, to have formed at a redox front at the margin of a groundwater trap in a permeable bed that abuts an impermeable fault.

5.2 Ningyo-Toge Ore Field

This ore field is centered some 30 km SW of Tottori, Okayama-Tottori Prefectures, in SW Honshu. It contains five larger and seven small basal-channel sandstone-type deposits (referred to as ore bodies) in several paleochannels in an area of 20 kilometers square within the Misasa Tertiary Basin. Original resources totaled 2 095 t U at a grade of 0.042% U, based on a cutoff grade of 0.02% U (Kamiyama et al. 1976).

Reported deposits include *Toge*, *Yotsugi*, *Takashimizu*, *Zyuni-gawa*, and *Kannokura* in the western part of the ore field, and *Nakatsugo* (main and south), *Onbara*, and *Tatsumitoge* in the eastern part (Fig. 5.4). The Nakatsugo-South ore body is unique among these deposits by its high average ore grade of 0.5% U.

Some mining was by underground methods at the Ningyo-Toge Mine/Toge deposit beginning in 1959 and by open pit methods at the Yotsugi deposit, about 1 km E of Toge, from 1978 to 1987. Ore was processed at the nearby test mill and a heap leaching facility producing cumulatively 87 t U.

Sources of information. Hayashi 1970; Kamiyama et al. 1976; OECD-NEA/IAEA 1973, 1983, 1988.

Geology and Mineralization

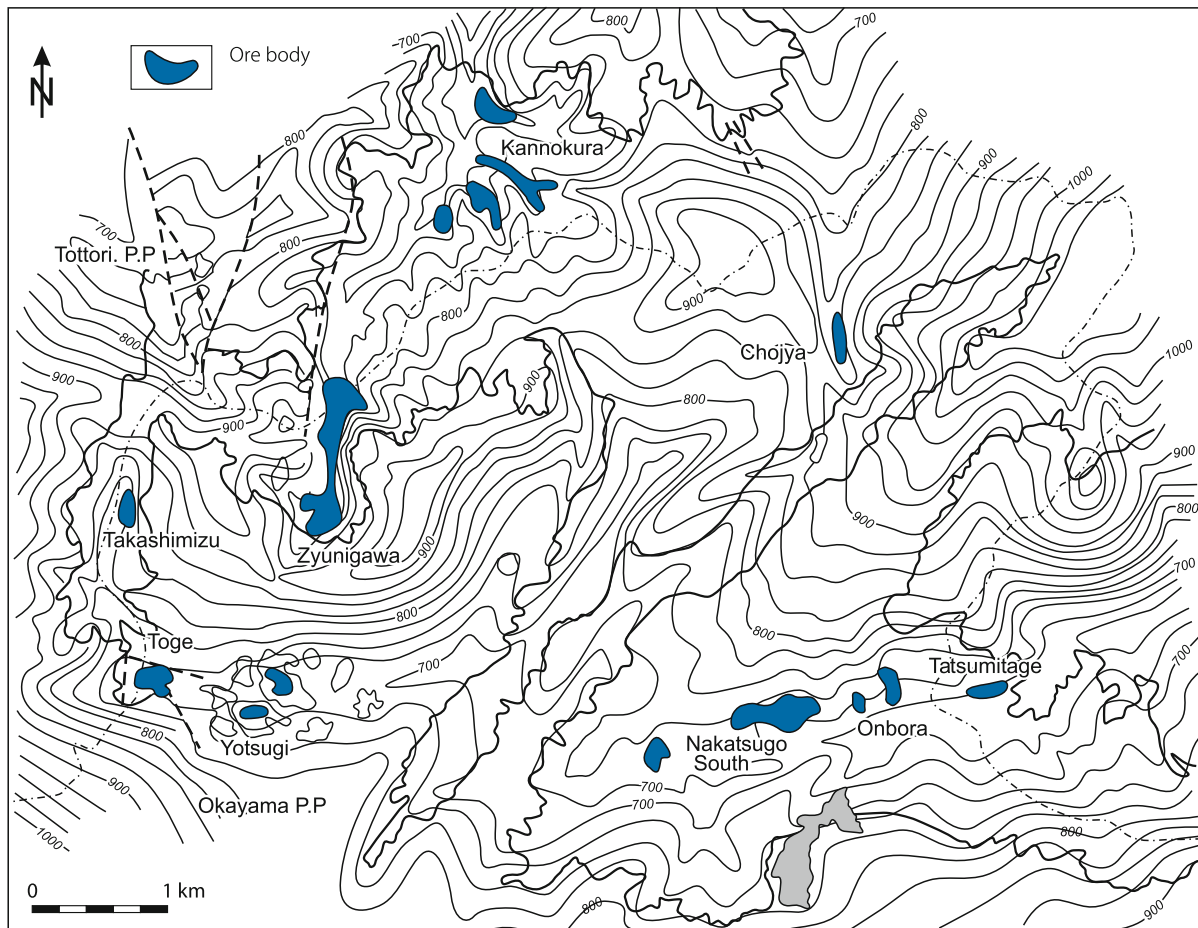
U mineralization occurs in basal parts of paleochannels that are incised into Cretaceous-Tertiary granite and Paleozoic sediments and contact-metamorphic rocks, and filled by the Late Miocene-Early Pliocene Misasa Group ranging from several tens of meters up to 500 m in thickness. This group is partitioned into the Ningyo-Toge Formation, a sequence of fluvial-lacustrine provenance and the superjacent Nakatsugo Formation of andesitic tuff, tuff breccias, and lava flows.

U mineralization is hosted by carbonaceous basal conglomerate and overlying arkose, sandstone, and mudstone in the lowest parts of paleochannels (Fig. 5.5). Ore bodies are restricted to channel sections incised into granite. Channel sections overlying Paleozoic sediments lack U concentrations.

Primary (unoxidized) mineralization is grey to black and consists of ningyoite, pitchblende, and coffinite associated with pyrite and gypsum (Muto 1961; Muto et al. 1959). Ningyoite is

■ Fig. 5.4.

Misasa Tertiary Basin, Ningyo-Toge ore field, topographic map of the pre-Tertiary unconformity with location of channel-type U deposits in the Miocene Ningyo-Toge Formation, Misasa Group (after Okada et al. 1988)



thought to be a reaction product of uraniferous solutions with apatite. Oxidized intervals are yellow to tan in color and dominated by autunite and minor amounts of other U^{6+} minerals. The ore is interspersed with clay minerals, Fe-oxides, and organic debris.

Ore bodies are of lenticular shape, up to 1 000 m in length, 100 m in width, and 1–2 m in thickness. Grades are highly variable ranging from 0.02% U to over 0.5% U locally as in the Nakatsugo-South ore body. Best grades commonly occur at the flanks of the paleochannels. For ore controls and recognition criteria see Sect. *Principal Characteristics of Basal-Channel Sandstone-Type U Deposits in Japan*.

5.3 Other U Occurrences in Japan

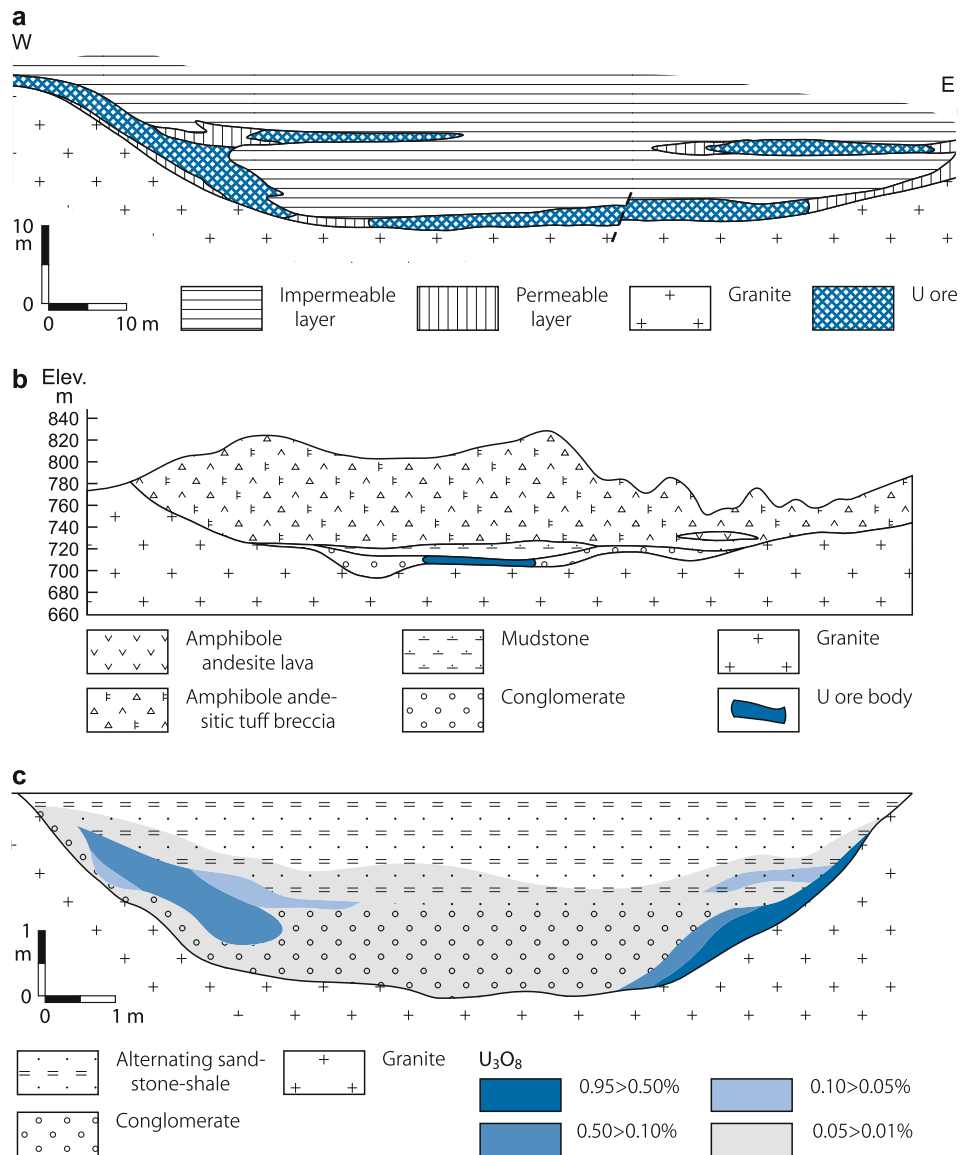
Sandstone-type U occurrences similar to those in the Ningyo-Toge ore field occur in several Tertiary and a few Cretaceous basins of Japan (► Fig. 5.1). Kamiyama et al. (1976) report the following occurrences with resources and grades. On Honshu island: *Mitoya*: 20 t U at 0.033% U; *Oguni*, Yamagata Prefecture:

75 t U at 0.025% U; *Okutango*, Kyoto-fu: 53 t U at 0.036% U; *Sanin*, Shimane Prefecture: 293 t U at 0.046% U; on Kyushu island: *Tarumizu*, Kagoshima Prefecture: 110 t U at 0.040% U; and *Okoshiri* (Okujiri) on Okoshiri island to the SW off Hokaido: 29 t U at 0.053% U. U prospects on the small Okoshiri island occur in Miocene-Pliocene, partly carbonaceous, tuffaceous sandstone and shale within an area 4×4 km.

At *Yuya* and *Toyoda*, Yamaguchi Prefecture, U mineralization occurs sporadically along a structural zone in a continental Cretaceous formation hosted by \pm carbonaceous sandstone and conglomerate, clayey zones, or along the cracks of andesite dikes or shears that cut the Cretaceous formation.

Minor U concentrations in metallic ore deposits are reported by Okada et al. (1988) as follows: *Ebisu* tungsten-bismuth mine: U in monazite, xenotime, and zircon within quartz veins and greisen associated with granitic rocks. *Miyoshi* tungsten-tin mine: Coffinite and zeunerite in quartz veins and greisen associated with granitic rocks. *Kurokawa* copper-lead-zinc mine: Coffinite, torbernite, and kasolite in clay veins adjoining the sulfide ore body in quartz-porphyry. *Kenzan* area: Very thin copper-chlorite-quartz veins with coffinite, cuprosklodowskite,

Fig. 5.5. Ningyo-Toge ore field, geological cross-sections illustrating typical settings of ore bodies in basal conglomerate and sandstone **a** in the Asabatake channel and **b** at the Nakatsugo-South ore body; **c** demonstrates the variable grade distribution in a narrow channel (after **a** and **b** Katayama and Kamiyama 1977; **c** Okada et al. 1988)



and kasolite in biotite granite. *Ogamo* gold mine: Coffinite and autunite associated with sulfides in clay veins in biotite.

Some Paleozoic bedded manganese ore deposits including the *Nodatamagawa* mine in Iwate Prefecture, contain pitchblende along faults or in hornfels near the ore bodies.

Uranium apparently adsorbed on clay minerals are noted in clayey zones near ore bodies of the '*Kuroko*' deposits producing copper, lead, zinc and gypsum.

References and Further Reading for Chapter 5 · Japan

For details of publications see Bibliography.

Doi et al. 1975; Hayashi 1970; Kamiyama et al. 1976; Katayama 1958; Katayama and Fukuoka 1970; Katayama and Kamiyama 1977; Katayama et al. 1974; Miyoda 2001; Muto 1961; Muto et al. 1959; OECD-NEA/IAEA 1973, 1983, 1988; Okada et al. 1988; Sakamaki 1986; Seo et al. 1989; Shikazono and Utada 1997; Yamamoto et al. 1974.



Chapter 6

Kazakhstan

Uranium deposits and major occurrences have been reported in nine regions and some isolated locations (Fig. 6.1). Deposits with resource estimates and mining potential are known from six regions: *Kokshetau* (Kokchetav), N Kazakhstan, *Pricaspian*, SW Kazakhstan, *Chu-Sarysu Basin*, south-central Kazakhstan, *Syr-Darya Basin*, S Kazakhstan, *Pribalkhash* or *Kendykta-Chuily-Betpak Dala* region, SE Kazakhstan, and *Ily Basin*, SE Kazakhstan. Deposits of limited economic interest are known from the *Turga-Priyrtish* region, N Kazakhstan, and the *Granitnoye* and *Zhalanshiksky* regions in central Kazakhstan.

Principal types of uranium deposits include sandstone, vein-stockwork, volcanic stockwork, lignite/coal and a special variety of organic phosphorite-type, viz. clay-hosted phosphatized fossil fish bone.

Remaining resources (RAR + EAR-I, status January 1, 2005) amount to 817 000 t U (OECD-NEA/IAEA 2005). More than 400 000 t U recoverable at less than \$130 per kg U are contained in sandstone-type deposits, about 120 000 t U in vein-stockwork, almost 100 000 t U in lignite/coal, in excess of 70 000 t U in volcanic and 64 000 t U in organic phosphorite deposits (OECD-NEA/IAEA 1999).

Cumulative production from 1953 to 2005 is estimated at about 100 000 t U. Conventional mining yielded until 1998 when it was interrupted 60 300 t U (38 700 t U of which by underground the remainder by open pit mines). ISL operations produced about 40 000 t U between 1969 and 2005. Uranium was produced from about 20 deposits in the first five regions mentioned above, and partly also during development work at other deposits.

In 2004 nine ISL sites in the Chu-Sarysu and Syr-Darya Basins with a capacity of 4 700 t U yr⁻¹ produced 3 412 t U and the Vostok underground mine, Kokshetau region, 317 t U. Operator of ISL operations is NAC Kazatomprom through its local subsidiaries except for three joint ventures with foreign companies. The Vostok deposit is mined by LLP Szepnogorski Mining and Chemical Corporation.

Two mills operated formerly in Kazakhstan, at *Stepnogorsk*, Kokshetau region, from 1958 to 1995 (nominal capacity 2 500 t U yr⁻¹) and *Aktau*, Pricaspian region, from 1959 to 1993 (2 000 t U yr⁻¹). Tselinny Mining and Chemical Combine was the operator of mining and milling facilities in the Kokshetau region while Pricaspiski Mining and Metallurgical Combine (PMMC, renamed to KASKOR Joint Stock Company) was the operator in the Pricaspian region. Ore from the Pribalkhash region was treated in the *Kara Balta* mill (nominal capacity 1.5 million tonnes of ore or 3 600 t U yr⁻¹) located 60 km W of Bishkek (formerly Frunze) in Kyrgyzstan. Mining and milling operator for this district was the Kyrgyz Combine, later renamed Yuzhpolymetal Production Company, headquartered in Bishkek, Kyrgyzstan.

Uranium exploration is in the responsibility of two subsidiary institutions of the Ministry of Geology of Kazakhstan, “Stepgeology” for northern and “Volkovgeology” for southern Kazakhstan.

Sources of information. Abakumov (1995), Boitsov AV pers. commun., Boitsov AV et al. (1995), Boitsov VE (1989, 1996), Fyodorov (2001, 2002, 2005), Fyodorov et al. (1997), IAEA (1995), Laverov et al. (1992a–c), OECD-NEA/IAEA (1993–2005), Petrov et al. (1995, 2000), Poluarshinov and Pigulski (1995), Yazikov (2002), Zhelnov (1994), amended by data of other authors cited in the sections of the various uranium regions.

The interested reader is in particular referred to the books of petrov et al. (1995 and 2000), which document in comprehensive and specific manner characteristic features of “exogenous” and “endogenous” uranium deposits, respectively, in Kazakhstan.

Historical Review

Exploration for uranium commenced in Kazakhstan in 1943 when the country was part of the former USSR. First discoveries were southwesterly of Lake Balkhash in volcanic rocks of the Caledonian *Kendykta* or *Pribalkhash* region where the Kurday deposit was found in 1951, followed by Botaburum in 1953 and Kyzylsay (or Kyzyltas) in 1957.

Exploration by the Stepnoi Expedition in the Caledonian *Kokshetau Massif*, northern Kazakhstan, resulted in the discovery of vein-stockwork-type deposits, Kubasadyrskoye, Balkashinskoye and Shatskoye in 1953, and Manybayskoye, Ishimskoye, Tastykol and Zaozernoje in 1954–1955. Later on more than fifty deposits were found including the large Vostok (1964) and Grachevskoye (1967) deposits.

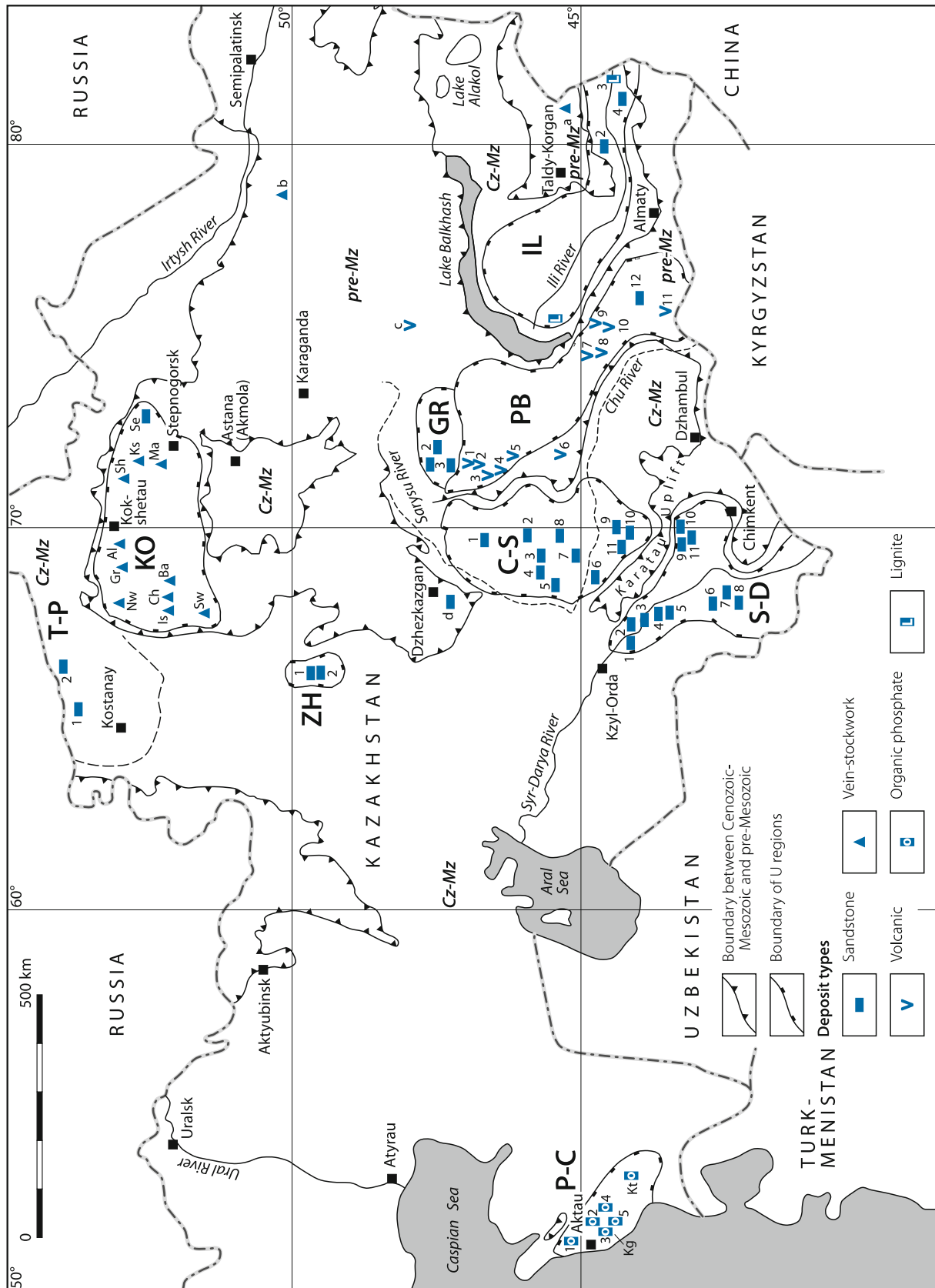
From 1954 to 1962, search by the Stepnoi Expedition for sandstone- and surficial-type deposits in Mesozoic-Cenozoic sediments at the southern margin of the Westsiberian Platform revealed a number of uranium occurrences such as Aurtav in Quaternary clays, Torfjanoye in Oligocene lignite, and Koitass and Pjatigorsk in Jurassic-Cretaceous clastic sediments in northern Kazakhstan but no minable deposits. Reassessment of data during the early 1970s and, in consequence, resumed exploration resulted in the discovery in 1973 of the sandstone-type Semizbay deposit at the inner margin of the Kokshetau Massif, and similar deposits in western Siberia such as Dalmatovskoye in the Transurals (see Russia).

The discovery of uraniferous fossil fish bones in Tertiary sediments near Shevchenko, now Aktau, on the northeastern shore of the Caspian Sea in 1954 (Melovoye deposit) established the *Pricaspian* uranium region.

During the period from 1957 to 1968 uraniferous coal deposits (Koldzhat 1957) were found in the *Ily Basin* but did not prove worthwhile mining. Also between 1957 and 1968, the sandstone-type deposits Uvanas and Zhalpak were discovered in the *Chu-Sarysu Basin*, and the volcanic-type Djidely in the *Pribalkhash* region.

Fig. 6.1.

Kazakhstan. Uranium regions and deposits (after Abakumov 1995; OECD-NEA/IAEA 1995, 1997; Petrov et al. 1995, 2000; Poluarshinov and Pigulski 1995; Yazikov 2002) (Type of deposit: lig lignite, org organic, phosp phosphate, ss sandstone (tab tabular/lenticular/stratiform,



b-ch basal channel, *roll* rollfront), *struc* structure bound, *stw* stockwork, *surf* surficial, *ve* vein, *volc* volcanic).

Region, ore field (OF),

KO Kokshetau Region (Proterozoic-Paleozoic, ve-stw)

(deposits/occurrences in brackets):

Is Ishimsky OF (Ishimskoye, Kamyshevoye, Shokhpak)

Ch Chistopolsky OF (Molodezhnoye, Dubrovskoye, Victorovskoye, Akkan-Burluk, Burlukskoye)

Ba Balkashinsky OF (Balkashinskoye, Vostok, Promeshutochnoye, Zvezdnoye, Tushinskoye, Olginskoye, Dergechevskoye)

Nw NW Kokshetau Area (Voskhed)

Gr Grachevsky OF (Grachevskoye, Sartubekskoye, Kosachinoye, Bolotnoye, Fevral'skoye, Dukonskoye)

Al Altybaysky OF (Slavyanskoye, Chaglinskoye, Abaiskoye, Kominsko-Krasnoyarskoye, Novogodnee)

Sh Shatsky OF (Glubbinnoye, Shatskoye 1+2, Agashkoye)

Ks Koksengirsky (or Zaozernoye) OF (Belagashkoye, Gvardaiskoye, Borovskoye, Koksorskoye, Koksorskoye South, Zaozernoye, Mezhozernoye, Tastykolskoye, Vostochno Tastykolskoye, Murzambetskoye)

Ma Manybaysky OF (Kerbayskoye, Manybayskoye, Yuzhno Manybayskoe, Bezymiannoye, Krugloye, Aksu)

Se Semizbay OF (Semizbay, Yuzhno Semizbay, Selentinsk, Kiziltuk)

Sw SW Kokshetau Area (Kubasadyr)

P-C Pricaspian/Mangyshlak Region (Oligocene)

Kg Karagiin OF

1 Tomak (org. phosph.)

2 Melovoye (org. phosph.)

3 Tasmurun (org. phosph.)

4 Taybagar (org. phosph.)

5 Sadyrnyn (org. phosph.)

Kt Karyntarskoye OF (org. phosph.)

C-S Chu-Sarysu Basin (Cretaceous-Tertiary)

1 Karakoyun (ss-roll)

2 Zhalpak (ss-roll)

3 Akdala (ss-roll)

4 Mynkuduk (ss-roll)

5 Inkay (ss-roll)

6 Budenovskoye (ss-roll)

7 Sholak Espe (ss-roll)

8 Uvanas (ss-roll)

9 Moynkum (ss-roll)

10 Kanzhugan-Tortkuduk (ss-roll)

11 Bars (surf?)

S-D Syr-Darya Basin (Cretaceous-Tertiary)

1 Irkol (ss-roll)

2 North Karamurun (ss-roll)

3 South Karamurun (ss-roll)

4 North Kharasan (ss-roll)

5 South Kharasan (ss-roll)

6 Zarechnoe (ss-roll)

7 Zhautkan (ss-roll)

8 Assarchik (ss-roll)

9 Kyzylkol (ss-roll)

10 Chayan (ss-roll)

11 Lunnoye (ss-roll)

P-B Pribalkhash Region (Silurian-Devonian)

1 Bezymiannoye (volc-struc)

2 Dzhideli (volc-struc),

3 Shorly (volc-struc)

4 Kostobe (volc-struc)

5 Daba (volc-struc)

6 Kurmanchite (volc-struc)

7 Kyzylsay (# 1 to VIII) (volc-struc)

8 Kyzyltas (volc-struc)

9 Botaburum (volc-struc)

10 Dzhusandalinskoye (volc-struc)

11 Kurday (volc-struc)

12 Kopalysayskoye (ss-tab)

GR Granitnoye Area (Cenozoic)

1 Talas (ss, b-ch)

2 Granitnoye (ss, b-ch)

IL Ily Basin (Jurassic-Tertiary)

1 Nizhne Ilyskoye (lig)

2 Suluchekinskoye (ss-roll)

3 Koldzhat (lig, ss-tab)

4 Kalkan + Aktau (ss-roll)

ZH Zhilanshiksky Region (Cenozoic)

1 Lazarevskoye (lig/ss, b-ch)

2 Lunnoye (Torgai) (lig/ss, b-ch)

T-P Turgai-Priyrtish Region

1 Tobolskoye (ss, b-ch, Up Jur.-L Cret)

2 Sensharskoye (ss, b-ch, Up Jur.-L Cret)

Koitass, Pjatigorsk (ss?, Up Jur.-L Cret)

Torfjanoye (lig/ss, b-ch, Olig)

Aurtav (surf?, Quat)

Isolated U Deposits/Occurrences

a Panfilovskoye, SE Kazakhstan (ve)

b Ulken Akzhal, E Kazakhstan (ve)

c Kyzyl, E Kazakhstan (volc-struc)

d Kuray, central Kazakhstan (ss, b-ch)

Successful testing of ISL uranium exploitation at Uvanas in 1969/1970 gave rise to intensified exploration for sandstone-type deposits, which was rewarded by the discovery of Kandjugan (1972), Moynkum (1976) and Mynkuduk (1976) in the *Chu-Sarysu Basin*; North and South Karamurun, and Irkol (1970–1975), and Zarechnoye (1977) in the southerly adjacent *Syr-Darya Basin*. More deposits were then detected in both basins in the late 1970s and 1980s.

Conventional uranium mining started in the *Pribalkhash* region in 1953. Underground operations produced uranium until 1990. Ore was shipped to the Kara Balta mill in Kyrgyzstan. In the *Kokshetau* region, exploitation commenced with the Manybayskoye open pit operation in 1957 followed by a number of underground mines, and lasted until 1995; it revived for a short while in 1997–1998 but was then again abandoned. A mill for the region operated at Stepnogorsk from 1958 to 1995. In the

Pricaspian region, mining (open pit) lasted from 1959 to 1993 and was served by the *Aktau* mill which started operation in 1959 and closed in 1993.

In situ leaching operations on a commercial basis began in the *Chu-Sarysu Basin* at Uvanas in 1977, followed at Kanzhugan and Mynkuduk in 1988 after several years of testing. Subsequently, ISL production was commissioned at Moynkum 1, and, in 2001, at Moynkum 2 and 3, Inkay, and Akdala. In the *Syr-Darya Basin*, ISL operations started at the North Karamurun deposit in 1985 followed by South Karamurun.

Annual production reached a peak of approximately 4 000 t U in the 1980s. In 1992, 2 802 t U were recovered from 14 deposits, decreasing to 1 090 t U in 1997. In that year, exploitation was confined to an underground operation in the *Kokshetau* region, one ISL operation in the *Syr-Darya Basin* and three ISL operations in the *Chu-Sarysu Basin*. In 2005 nine ISL sites in the two basins and the Vostok underground mine, *Kokshetau* region, were active.

6.1 Kokshetau Region, Northern Kazakhstan

The *Kokshetau* uranium region (Fig. 6.2) is situated in the *Akmola* region and coincides with the *Kokshetau* (*Kokchetav*) Median Massif at the southern margin of the West Siberian Plain, between the middle *Irtys*h river and its western tributary, the *Ishim* river. Major towns are *Kokshetau* in the northern and *Stepnogorsk* in the eastern part of the region.

Some forty uranium deposits have been delineated and a number of major occurrences have been identified. They are grouped in eight ore fields in crystalline rocks, and one ore field in sedimentary terrane. Some isolated deposits/occurrences are known in the northwestern and southwestern *Kokshetau* region. Table 6.1 provides the names and selected characteristics of significant deposits and occurrences.

Two types of U deposits are noticed in the *Kokshetau* region. Most deposits consist of structurally controlled mineralization classified as vein-stockwork-type deposits (in Russian literature referred to as vein-stockwork in folded complexes). Some deposits are hosted in paleovalleys incised into the pre-Upper Jurassic surface. They are classified as basal-channel, tabular sandstone-type deposits (stratiform – ground infiltration-type in Russian literature). The latter are restricted to the northeastern margin of the massif.

Vein-stockwork mineralization is partly monometallic and partly polymetallic. By-products include Mo, Sc, Y, REE, and phosphorous.

Remaining *in situ* resources in the up to \$130 per kg U cost category are about 200 000 t U, including 139 000 t U in the RAR + EAR-I category. 81 600 t U of these resources are attributed to the less than \$80 per kg U category. *In situ* ore grades average 0.1–0.2% U (OECD-NEA/IAEA 1993, 1995). These resources include at the Mine Management Unit # 1, 3, 4, and 5 of the *Tselinny* Combine measured and indicated resources (A, B, C1 categories) of 34 million t at an average grade of 0.129% U or 43 900 t U, 24 million t of inferred resources (C2) at an average grade of 0.114% U or 27 400 t U, and 17 million t of prognostic (P) resources at an average grade of 0.108% U or 18 400 t U. The

prognostic resources are generally based on an extrapolation of the ore-bearing structures beyond the measured, indicated, and inferred resource outlines. (Note: Discrepancies in resource figures are partly based on a change of the cutoff grade; calculations were based on a 0.03% U cutoff grade until 1991 and on 0.05% U thereafter.) (Pool T, pers. commun.).

The first deposits were discovered in the *Kokshetau* region in 1953. Mining started in 1957. Eleven vein-stockwork deposits have been exploited mainly by underground mines since, five of which are depleted and five operations are closed; one (*Vostok*) is again in operation. ISL methods were used at one sandstone-type deposit (Table 6.1).

A mill with a nominal capacity of 2 500 t U yr⁻¹ operated at *Stepnogorsk*. Total production through 1998 is speculated to be on the order of 30 000–35 000 t U. All mining and processing activities ceased in 1998 but the *Vostok* Mine was reopened again in 2003.

Sources of information. The subsequent description is largely based on Petrov et al. (2000), who provided a comprehensive documentation of U deposits in the *Kokshetau* region amended by data from Abakumov (1995), Birka et al. (2003), Boitsov AV et al. (1995), Boitsov VE (1989, 1996), Fyodorov et al. (1997), Laverov et al. (1992), Naumov et al. (1996), OECD (NEA)/IAEA (1993–2005), Omelyanenko et al. (1993), Petrov et al. (1995), Polyarshinov et al. (1994), Poluarshinov and Pigulski (1995), Yazikov et al. (1994), Zhelnov (1994), Boitsov AV, Pool TC, and staff of *Kazatomprom* pers. commun., unless otherwise noted.

Regional Geological Setting of Mineralization

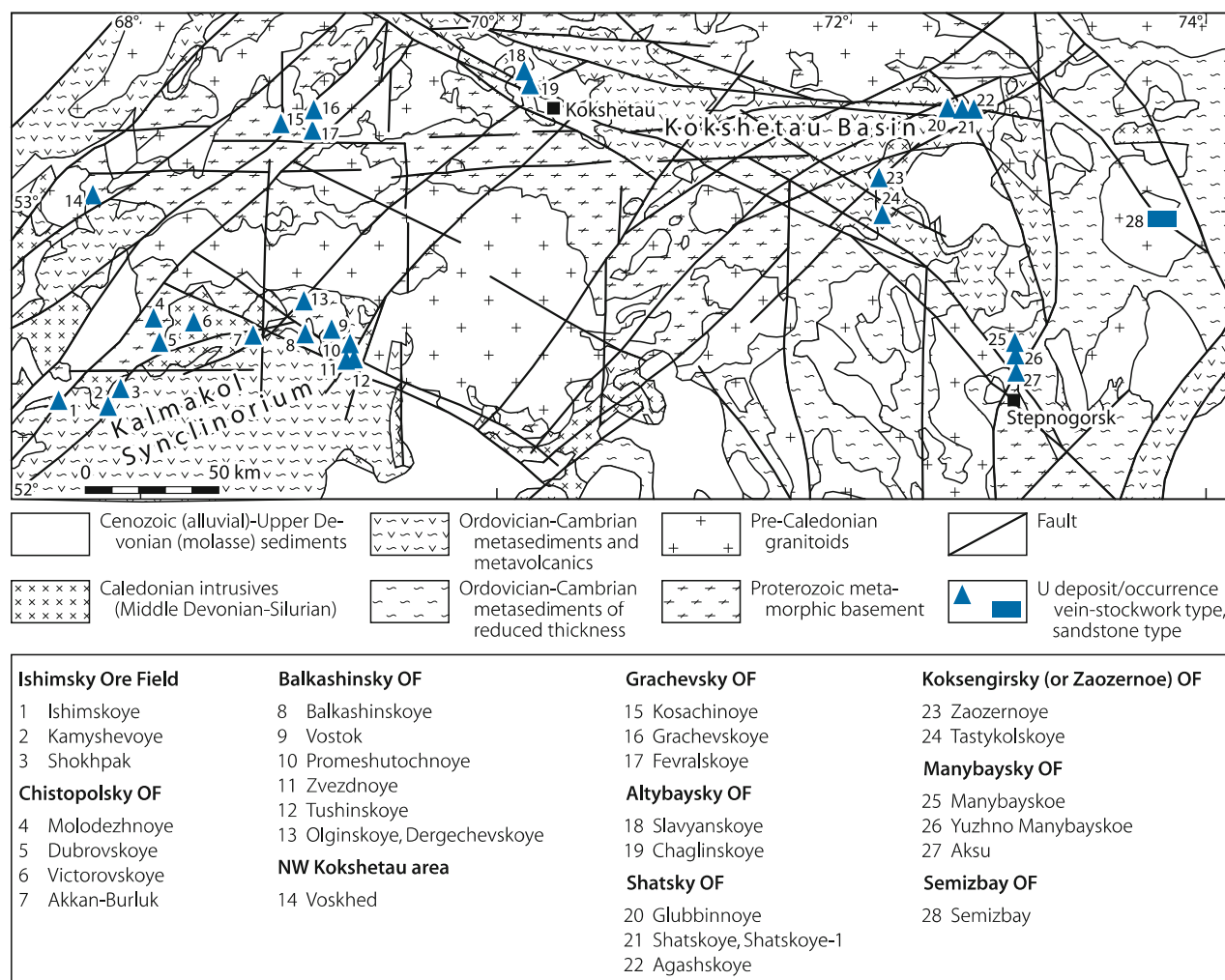
The *Kokshetau* uranium region is within the *Kokshetau* Massif, which is a segment of the Caledonian North Tien Shan Fold Belt of the Ural-Mongolian orogenic system. The massif is presumably a fragment of a Precambrian platform that was markedly reworked during the Caledonian geosynclinal and orogenic stages.

Proterozoic metamorphics (gneiss, amphibolite, schist, slate, quartzite, marble) constitute the oldest unit of the *Kokshetau* Massif. During the *Cambrian-Ordovician* most of the massif was a positive morphological feature but depressions within and marginal to the block, for example, the *Kalmakol* Synclinorium in the SW and the *East Kokshetau* Basin in the eastern part of the block, were filled with *Cambrian-Ordovician* volcanogenic and sedimentary deposits and *Middle to Upper Ordovician* flysch. These strata were tightly folded and weakly metamorphosed during the *Caledonian Orogeny*. The main folding phase was during the Silurian. Caledonian multi-phase intrusions ranging from early gabbro, diorite, granodiorite, and granite to late leucogranites invaded the older complex during the *Ordovician-Silurian* and *Early Devonian*. Mafic to felsic subvolcanic bodies and sheets as well as syn- and post-orogenic dikes are abundant. The latter often group in swarms.

Middle to Upper Devonian volcanics overlain by redbed molasse sediments occur in late orogenic volcanic-tectonic depressions where they rest with a distinct unconformity on the crystalline basement. Some depressions contain predominantly quartz porphyries while andesite porphyry, andesite-basalt, and

Fig 6.2.

Kokshetau region. Geological map of part of the Caledonian Kokshetau Massif with location of uranium deposits. #1–27 are vein-stockwork-type and #28 basal channel sandstone-type deposits (after Boitsov AV pers. commun., Laverov et al. 1992c, Petrov et al. 2000; Poluarshinov and Pigulski 1995)



related tuffs prevail in others as in the Olenty-Seletensk area in the eastern Kokshetau Massif.

Jurassic-Cretaceous alluvial-fluvial sediments occupy paleovalleys incised into the pre-Upper Jurassic peneplain. Valleys are up to few kilometers wide, up to 100 m and more deep and stretch for tens of kilometers from peripheral basins like the Pri-Irtish Syncline into the massif. Unconsolidated platform sediments of *Cretaceous* to *Cenozoic* age cover much of the Kokshetau Massif.

The following litho-stratigraphic profile provides, in more detail, the rock facies as found in the Central Kokshetau Anticlinorium (after Omelyanenko et al. 1993; based on Rozen et al. 1971 and Abdulkabirova 1987).

Cenozoic to Cretaceous: several 10s of meters and locally over 100 m thick, unconsolidated platform sediments.

Cretaceous-Jurassic: up to 100 m and more thick, alluvial-fluvial sediments in paleovalleys.

Devonian: grabens with redbed molasse (pink conglomerate, sandstone) topping volcanics (rhyolite to andesite-basalt sub-volcanic bodies, lavas, and related tuffs); dikes of quartz diorite porphyry, plagiogranite porphyry cutting Lower Devonian sediments.

Caledonian Orogeny: early orogenic (Silurian) diorite, granodiorite, granite; widespread skarnitization with Fe, Au, and polymetallic mineralization including propylitization with Fe and beresitization with Au mineralization; main orogenic (Silurian-Early Devonian) leucocratic granite intrusions associated with greisenization and Sn, W, and some Mo mineralization; syn- and post-orogenic mafic to felsic dikes.

Silurian-Ordovician: weakly metamorphosed flysch sediments in Ordovician geosynclinal troughs

Ordovician-Cambrian: weakly metamorphosed volcanogenic and sedimentary deposits in early geosynclinal Cambrian troughs with small intrusions of early gabbro, peridotite, pyroxenite

Table 6.1. (Continued)

Region/deposit	Type of deposit	Ore mode/alteration	Lithology/host rock	Stratigraphy	Length (m)	Width (m)	Depth (m b.s.)	Resource (t U)	Grade (% U)	Remarks/status
Kokshetau Region continued										
47 Aksu	ve-stw	U/alb	Pyrocl, sed	Mid Ord					0.102 ⁿ	Depl. ⁿ +0.05 Mo, 0.02% Zr, 0.085% Sr
(9) Semizbay OF										
48 Semizbay	ss, b-ch		ss, cgl, mds	Jur				17 000	0.057	Inactive, ISL
49 Semizbay South	ss, b-ch		ss, cgl, mds	Jur				Small	<0.1	Expl.
50 Selentinsk	ss, b-ch		ss, cgl, mds	Jur				Small	<0.1	
51 Kiziltuk	ss, b-ch		ss, cgl, mds	Jur				Small	<0.1	Expl.
NW Kokshetau area										
52 Voskhed	ve-stw		Amph, grd	L-Mid Camb						
SW Kokshetau area										
53 Kubasadyr	ve-stw?									

Type of deposit: *stw* stockwork, *ve vein*, *ss*, *b-ch* basal channel sandstone. **Ore mode/alteration:** principal U-ore constituents and associated type of alteration (*U-ox* pitchblende or uraninite, *U-Mo* U-oxides+Mo-sulfides, *U-Si* coffinite, *U-Ti* titanite and other U-Ti phases, *albit* albitization, *beres* beresitization).

Lithology: *amph* amphibolite, *cabs* carbonaceous, *cgl* conglomerate, *dio* diorite, *dolr* dolerite, diabase, *gab* gabbro, *grd* granodiorite, *grt* granite, *igs* igneous, *ls* limestone, *marb* marble, *mds* mudstone, argillite, *metased* metasediments, *metavolc* metavolcanics, *porph* porphyry, porphyrite, *pyrocl* pyroclastic, *sl* slate, *silt* silt, *spess* spessartite, *ss* sandstone.

Stratigraphy: L Lower, *Up* Upper, *Camb* Cambrian, *Dev* Devonian, *Jur* Jurassic, *Ord* Ordovician, *Pz* Paleozoic, *Pt* Proterozoic, *Sil* Silurian.

Dimensions: max. extensions of deposits but values are only approximate due to highly irregular shape of deposits. **Depths:** *m b.s.* meter below surface.

Resources of regions: original in situ RAR + EAR1 < \$130 per kg U. **Resources of deposits:** not specified, unclear whether original or remaining resources, may or may not include prognostic (P1) resources. **Grade:** in situ.

Status: *depl* depleted, *dev* developed prospect, *expl* explored, *ISL* in situ leaching, *OP* open pit, *UG* underground.

and related apatite, antophyllite-asbestos, Co, Ni, Cu, Au, Ag, Pt mineralization.

Proterozoic: Vendian Kokshetau Formation subdivided into: (thicknesses are approximate and refer to Grachevskoye area)

- *Andreevskaya Member* (V_{an}): 650 m thick psephitic-pelitic, weakly metamorphosed sediments (sandstones consist essentially of quartz with little sericitic cement, siltstone of poorly rounded quartz grains in hydromica-chlorite matrix, and mudstone with hydromica-chlorite and minute quartz grains). Three units are distinguished:
 - upper unit: 300 m thick, alternating 10–65 m thick medium- and fine-grained sandstone and mudstone-siltstone beds with local limestone lenses
 - middle unit: 200 m thick, medium-grained quartz-sandstone, overlying 100 m thick intercalated siltstone-mudstone, fine- and medium-grained sandstone
 - lower unit: 50 m thick, medium-grained, quartzose sandstone
- *Sharykaskaya Member* (V_{sh}): 1 000 m thick, pelitic-calcareous, weakly metamorphosed sediments divided into two units, at exocontact of granite transformed into skarn with Sn-W mineralization:
 - upper unit: carbonaceous and/or sericitic shale, dolomite, limestone often enriched with carbonaceous matter, mudstone, siltstone
 - lower unit: sericitic shale locally with <5 m thick intercalations of limestone that often contain organic substances

Riphean

- *Borovsk Formation*: porphyroids; actinolite, chlorite-actinolite and quartz-sericite-chlorite schists; and
- *Zerendin Formation*: eclogite, gneiss, amphibolite, mica schist, a.o.

Numerous faults cut the massif including deep rooted structures-which were repeatedly reactivated. Principal fault systems trend NW-SE, NE-SW, N-S and E-W (► Fig. 6.2). Deep-rooted faults divide the massif into uplifted blocks and downthrown grabens. The latter are filled with the afore mentioned Early-Middle Paleozoic geosynclinal lithologies or post-Caledonian continental rocks.

Principal Characteristics of Vein-Stockwork Deposits of the Kokshetau Region

(For description of characteristics of sandstone-type deposits of the Kokshetau region see Sect. 6.1.9: *Shokay Zone, Olenty-Seletinsk Area, Eastern Kokshetau Region.*)

Principal Host Rock Alterations

Principal alteration features in rocks surrounding uranium deposits include two *pre-uranium stages* one of alkali metasomatism essentially reflected by albitization with hematitization that

affected all lithologies, and another of beresitization (i.e. quartz-sericite-ankerite-pyrite alteration), which extends from mineralized structures for as much as 100 m into wall rocks. The pre-uranium beresitization process generated a marked porosity of the affected rocks that provided a favorable host environment for ore deposition. *Syn-uranium* beresitization associated with chloritization and hydromicazation is locally developed at some deposits. *Late- to post-uranium stage* carbonatization (mainly dolomitization) overprinted the former alteration facies for up to 100 m from mineralized structures.

Albitization and beresitization occur at most deposits, but in variable intensity. Both are typical for the Altybaysky and Chistopolsky ore fields whereas beresitization prevails at deposits of the Ishimsky and Balkashinsky ore fields; and albitization associated with chloritization and carbonatization in the other ore fields.

Principal Characteristics of Mineralization

Three marked minero-chemical varieties of mineralization are distinguished each dominated by either a uranium-apatite assemblage, e.g. in the *Tastykolskoye, Zaozernoye, and Vostok* deposits or a uranium-molybdenum mineral assemblage as found in the *Balkashinskoye, Grachevskoye, Ishimskoye, and Manybayskoye* deposits. The former predates the latter. The third variety consists of deposits with simple U mineralization (also referred to as uranium-albite mineralization) such as *Kosachinoye, Shokpak, and Kamyshevoye*. Overprinting of the various mineral assemblages often generated complex mineral associations.

Uranium-apatite mineralization may include uraniferous fluorine-apatite with minor pitchblende, coffinite, pyrite, marcasite, galena, chalcopyrite, arsenopyrite, zircon, thorite, and REE-bearing minerals. Gangue minerals are chlorite, hydromica, albite, and commonly large quantities of calcite and dolomite. Some deposits have high uranium contents bound in arshinovite. U-P mineralization occurs preferentially in highly broken intervals of Na-metasomatized Proterozoic and Lower Paleozoic rocks at and adjacent to Caledonian hypabyssal stocks and dike swarms.

U-Mo mineralization (0.02–0.5% Mo) consists of U oxide and U silicate (pitchblende, uraninite, coffinite) associated with sulfides of Mo (molybdenite, jordisite), Fe (mainly pyrite), Pb, Cu, and As. Gangue minerals are represented by carbonate (commonly ankerite, minor dolomite), sericite, chlorite, and some apatite. Zirconium (in arshinovite) occurs in significant amounts. Post-uranium carbonates (mainly calcite) can be present in large amounts and occur as veins and veinlets, and fill voids in ore. The carbonate fraction of U-Mo ore varies between 0.1 and 50% CO_3 . Ore minerals reflect a certain vertical zoning: Pitchblende with pyrite and galena prevail on upper levels, and pitchblende with molybdenite and coffinite at lower levels. U-Mo deposits typically occur in terrane of marked post-orogenic volcanism. Ore bodies are controlled by faults and highly cataclastic intervals within and at the exocontact of subvolcanic intrusions, volcanic structures, and complicated volcanic sheets of Paleozoic depressions. Wall rocks are commonly altered by beresitization.

Simple U mineralization may consist of U-oxide, U-Ti-, and/or late U-silicate phases (pitchblende, uraninite, brannerite, coffinite) associated mainly with carbonate and chlorite. Ore lodes occur in fracture zones on both sides of the Middle Paleozoic unconformity. Wall rocks may be altered by albitization, and/or carbonatization (mostly dolomite), silicification (quartz), chloritization, hematitization, goethitization, or pyritization. CO₃ content can exceed 10%.

Based on studies of deposits in the Ishimsky and Grachevsky ore fields, Boitsov et al. (1995) distinguish three principal *lithostratigraphic settings of U mineralization* and several lithology-related mineral assemblages. Although they are most typical for the Ishimsky and Grachevsky ore fields, they are partially or with variations also recognized in other ore fields:

- 1 Mineralization in Proterozoic crystalline basement rocks and intrusive Caledonian granites:
 - 1.1 Albitized granite and quartzite (type example: *Grachevskoye*): apatite-coffinite-REE paragenesis with yttrium and thorium; U grades are variable and can be up to >1%. Phosphorus ranges between 0.3 and 10% P₂O₅.
 - 1.2 Siliceous and argillic carbonaceous schist and diabase distant from granite (type example: *Kosachinoye*):
 - a coffinite-chlorite in albitized rocks,
 - b brannerite or brannerite-uraninite in carbonate-chlorite or quartz-goethite altered rocks, and
 - c late coffinite-pyrite in dolomitized rocks overprinting the former assemblages.

U grades of Type 1.2 ores are commonly low; carbonate content is in excess of 6% CO₃.
- 2 Mineralization in weakly metamorphosed *Lower Paleozoic* rocks cut by Caledonian igneous dikes and sills (type example: *Ishimskoye*): jordisite-coffinite and molybdenite-pitchblende in hydromica and carbonate altered rocks.
- 3 Mineralization in weakly metamorphosed *Lower Paleozoic* lithologies and unmetamorphosed Devonian redbeds at and immediately below and above the *Middle Paleozoic unconformity*. (type example: *Shokpak* in basement, *Kamyshvoye* in basement and redbeds):
 - a brannerite in quartz-goethite-carbonate altered albitized terrestrial rocks including conglomerate at upper levels of *Kamyshvoye*, (in excess of 10% CO₃)
 - b pitchblende-chlorite overprinting the brannerite phase resulting in a brannerite-pitchblende association at lower levels of *Kamyshvoye*

c uraninite-chlorite in hematitized, silicified quartzite unaffected by albitization (*Shokpak*)

Poluarshinov and Pigulski (1995) note that certain elemental ratios in uranium showings may be used for the determination of the erosional level of a deposit, i.e. for the potential of ore presence at depth. High As/U ratios may suggest limited erosion and as such a preserved blind ore body while high Mo/U and Pb/U ratios indicate most likely a deep erosion level with only the roots of an ore body preserved.

General Shape and Dimensions of Vein-Stockwork Deposits

Individual deposits range in size from few hundred tonnes to 95 000 t U and in grade from 0.05 to 0.18% U.

Deposits may consist of a number of ore bodies distributed over a depth interval from near surface to more than 1 000 m. Ore control is primarily by structure. Consequently, shapes and dimensions of deposits and ore bodies are highly variable and are governed by the local structural situation. U-P, U-Mo, and simple U mineralization occur in complexly-arranged and irregularly-mineralized stringers, veinlets, disseminations, and breccia matrix, which group to complex veins, linear, flattened lenticular or pipe-shaped or compact and almost isometric bodies with stockwork structure located often, but not necessarily, at the exocontact of or within hypabyssal intrusions of variable leucocratic to mafic composition. Linear ore bodies can persist for several kilometers along fault zones as at the *Kosachinoye* deposit. Ore distribution is irregular and discontinuous. This results in highly variable ore grades ranging from some 100s of ppm to several percent U. Details of dimensions, grades, and resources of individual deposits as far as known are provided in later chapters and summarized in [Table 6.1](#).

Regional Geochronology

Caledonian granites of the Orlinogorskii complex yield K-Ar ages between 420 and 360 Ma with a grouping of 390–380 Ma (Omelyanenko et al. 1993).

The main stage of uranium mineralization in vein-stockwork deposits of the Kokshetau region is dated at 380–360 Ma ([Table 6.2](#)), which corresponds to the Late Devonian. This is supported

Table 6.2. Northern Kazakhstan, Kokshetau region. Isotope ages of U mineralization and redistribution in endogenic deposits. (Petrov et al. 2000) (*italic: principal ages of ore formation*)

Mineralization type	Age (Ma)	Deposits example
Th-U in quartz-feldspar metasomatite	1 400–1 250, 600–510	East Dybrovskoye
P-U and U in Na metasomatite	490–460, 420–405, <i>380–360</i> , 330–310, 270–250	Grachevskoye, Kosachinoye, Fevral'skoye, Chaglinskoye, Zaozernoye, Tastykolskoye
Mo-U, U in Na metasomatite and beresite zones	470–450, 420–405, <i>380–360</i> , 330–310, 280–250	Agashskoye, Shatskoye, Glubinnoye, Manybai, Aksu, Shokpak, Kamyshovoye, Viktorovskoye
Mo-U, U in beresitization, argillization and feldspathization zones	480–450, 420–405, <i>380–360</i> , 330–310, 280–265	Ishimskoye, Centralnoye, Vostok, Zvezdnoye, Balkashinskoye, Dergachevskoye

by geological relationships; uranium mineralization occurs in Caledonian and pre-Caledonian rocks and in the overlying Middle to Late Devonian sediments but is absent in Carboniferous sediments. The ore forming event is attributed to a general uplift of the Kokshetau region during the waning episode of the Caledonian Orogeny.

Potential Sources of Uranium

Two principal lithologic units are considered as potential U sources, uraniferous crystalline rocks and black shale. Both may have contributed individually or in combination to ore formation in the Kokshetau region. The first group includes Precambrian and Lower Paleozoic lithologies with 3.2–7.2 ppm U, Middle to Upper Paleozoic leucogranites with 10–70 ppm U, and rhyolite with up to 10 ppm U. The igneous rocks are considered to be the product of granitization of crustal material, which may also have produced magmatic ore-forming solutions. The Paleozoic black shale contains 100–200 ppm U and formed in a geosynclinal regime at the margins of median massifs and geanticlinal uplifts composed of the afore mentioned rocks.

Principal Ore Controls and Recognition Criteria of Vein-Stockwork Deposits

Vein-stockwork-type deposits in the Kokshetau region are primarily controlled by structures and secondly by lithologies altered by Nametasomatism/albitization and/or beresitization. Typically, U-P ore is preferentially confined to Na-metasomatized, and U-Mo ore to beresitized, environments. Significant ore controlling parameters or recognition criteria of major deposits include:

Host Environment

Proterozoic crystalline basement overlain and surrounded by

- Lower Paleozoic, weakly metamorphosed, tightly folded geosynclinal facies of terrigenous and volcanic origin
 - Caledonian intrusions ranging from gabbro to leucocratic granite
 - orogenic and post-orogenic mafic to felsic dikes forming swarms
 - Devonian unmetamorphosed molasse redbeds and mafic to felsic effusives and pyroclastics filling grabens
 - Upper Jurassic to Lower Cretaceous alluvial sediments filling paleovalleys
 - Mesozoic to Cenozoic unconsolidated cover deposits including impermeable horizons
 - elevated U background values in Precambrian and Lower Paleozoic metamorphics, Caledonian leucogranite and rhyolite, and Paleozoic black shale
 - deep reaching lineaments and major fault systems trending NW-SE, NE-SW, E-W, and N-S, vertical displacements along which provoked horsts and grabens
 - intense fracturing and cataclasis along prominent faults and at faults intersections
- distinct unconformities between Lower Paleozoic and Middle Devonian, and Paleozoic and Upper Jurassic units
 - host rocks include
 - Devonian molasse-type redbed sandstone, conglomerate with intercalated effusive and pyroclastic volcanics,
 - Caledonian igneous rocks: granite, gabbro, quartz porphyry,
 - Lower Paleozoic weakly metamorphosed geosynclinal and flysch facies: shale/mudstone, sandstone, siltstone, and
 - Proterozoic high-grade metamorphics: gneiss, amphibolite, schist, slate, quartzite, marble

Alteration

- pre-uranium Nametasomatism (albitization associated with hematite, chlorite, carbonate alteration) of all Precambrian and Paleozoic rocks
- pre-uranium beresitization (sericite, carbonate [ankerite, minor dolomite], silica [quartz], pyrite alteration)
- minor syn-uranium beresitization with hydromica and chlorite alteration
- late to post-uranium carbonatization (dolomite, calcite)

Mineralization

General features:

- restriction of deposits to areas of Caledonian magmatism
- geotectonic position of deposits and ore bodies controlled by
 - deep reaching, long-lived and repeatedly reactivated prominent fault zones
 - intersections or junctions of such fault zones
 - highly fractured and/or cataclased intervals along faults or their intersections
 - dip- or strike-angle variation of faults
 - 2nd and 3rd order faults and their intersection sites with boundaries of Caledonian grabens
- restriction of ore lodes to rock facies of favorable physical-mechanical (brittle) and locally chemical (carbonaceous/graphitic) properties (heterogeneous lithologies with variable rockmechanical properties)
- restriction of mineralization to markedly altered rocks (albitization and/or beresitization etc.)
- several phases of mineralization reflected by two prominent polymetallic (U-P succeeded by U-Mo) parageneses, and simple U mineralization
- Mo/U, Pb/U, As/U ratios can be used for indication of erosion levels
- characteristics of *U-P mineralization* include
 - complex P-U-REE assemblage composed of uraniferous F-apatite and pitchblende associated with Cu-, Fe-, Pb-, As-sulfides, Th, Y, and REE-bearing minerals
 - prevailing associated gangue minerals are calcite, dolomite
 - deposits consist of intermittent ore bodies
 - ore bodies are commonly of columnar and lenticular shape with internal stockwork structure
 - geotectonic position of ore bodies at intersection, lacing and/or branching of faults, particularly at interformational deformation zones with a high degree of jointing/fracturing

- lithologic-tectonic position of ore bodies in albitized pre-Caledonian rocks at and adjacent to Caledonian hypabyssal intrusions (granite stocks, dike swarms)
- best U grades are in highly silicic rocks with low apatite contents
- U ore with high P contents are usually confined to carbonate rocks (marble, limestone)
- characteristics of *U-Mo mineralization* include
 - U-oxides and U-silicate (pitchblende, coffinite) associated with sulfides of Mo (molybdenite, jordisite), Fe, Pb, Cu
 - gangue minerals include carbonates, sericite, chlorite, some apatite
 - locally complex mineral assemblages due to overprinting of U-P by U-Mo parageneses
 - ore bodies consist of veins and flattened linear or lenticular bodies with internal stockwork structure composed of stringers, veinlets, disseminations, breccia fillings
 - ore bodies are related to faults and highly cataclastic intervals within and at exocontacts of subvolcanic intrusions, volcano-tectonic structures, and complicated volcanic sheets in Paleozoic depressions
 - spatial (and genetic) association with Caledonian andesite-diorite, granite, and rhyolite of late orogenic volcanism within folded Lower Paleozoic geosynclinal facies
 - restriction to host rocks altered by beresitization
- characteristics of simple *U mineralization* include
 - U-Ti, U-oxide, and U-silicate phases (brannerite, pitchblende, uraninite, coffinite) with sulfides of Cu, Fe, Pb
 - gangue minerals include carbonates, chlorite, sericite, some apatite
 - geotectonic position of ore in fracture zones at, above and below the Middle Paleozoic unconformity: U-silicate mineralization on upper levels in Devonian redbeds, replaced downward by U associated with carbonate in albitized metamorphic rocks of the Lower Paleozoic geosynclinal sequence
 - wall rocks may be altered by albitization, and/or carbonatization (mostly dolomite), silicification (quartz), chloritization, hematitization, goethitization, or pyritization

Metallogenetic Concepts

Several metallogenetic hypothesis are forwarded for the vein-stockwork uranium deposits of the Kokshetau region. Although U is hosted by Caledonian granite in some deposits, Laverov et al. (1992c) reject a genetic correlation of U mineralization with granite. Omelyanenko et al. (1993) also do not see a convincing relation of uranium deposits to the magmatic intrusions. They point out that the main uranium stage occurred during the Late Devonian as evidenced by the restriction of primary uranium mineralization to Devonian and older rocks and isotope ages of U minerals grouping at 370–350 Ma. The authors attribute the principal ore-forming event to a general uplift of the Kokshetau region during the waning episode of the Caledonian Orogeny in Late Devonian time.

A common model for the primary uranium event favors hypogene uraniferous fluids that evolved from late magmatic differentiation or uranium derived by leaching of uraniferous country rocks, or from both sources. All younger mineralization stages, as dated for the Upper Triassic-Jurassic, Paleogene and Neogene, are considered but redistribution processes. The Triassic-Jurassic ages are attributed to a major paleoweathering episode that resulted in an upgrading of the U content in deposits such as Kosachinoye and Grachevskoye (Skoros-pelkin 1981).

Boitsov et al. (1995) suggest a uniform hydrothermal system for ore formation. This system generated the various mineral parageneses during several phases, apparently in a series of pulsations, first the U-P phase (pitchblende, F-apatite), followed by the U-Mo phase, and finally, a U phase associated with carbonate, which derived by rejuvenation of earlier uranium mineralization.

Omelyanenko et al. (1993), based on their studies of the Grachevskoye deposit, conclude that the highly variable composition of altered rocks, and extent and intensity of alteration are a function of the chemistry of hydrothermal fluids, lithology of the parent rock, and the scope and grade of tectonic deformation preceding the various hydrothermal events (see also Sect. 6.1.4.1: *Grachevskoye*). The authors propose that alkaline, phosphorous-rich solutions have formed the ore-bearing metasomatites at Grachevskoye. As indicated by fluid inclusions and decrepitation tests, the alteration occurred at a temperature between 220 and 280°C. The metallogenetic and related precursor processes began with Nametasomatism (mainly albite), succeeded by apatitization that overlapped and postdated albitization, and were continued with coffinite crystallization, which was coeval with and after apatite. Pitchblende deposition postdated the former processes. Narrow veinlets of albite, and rare apatite, quartz, chlorite and sericite/hydromica, and pockets of carbonate formed last. The bulk of coffinite, apatite, chlorite, and other minerals precipitated during the terminal stage of the hydrothermal event and typically occur in zones of post-albite microfracturing. Repeated brittle deformation preceded the various alteration and mineralizing processes.

In contrast to Grachevskoye, at Kosachinoye and adjacent deposits situated some 20 km S of Grachevskoye, uraniferous albitized rocks, although containing a high calcium content, are not anomalous in phosphorous, which implies that two autonomous solutions were involved in the formation of these deposits.

The vein-stockwork deposits of the Kokshetau region are considered by the Russian authors to be fairly similar to the Beaverlodge veins in Canada but for the high apatite content in some deposits; hence, only deposits with simple U(-albite) may be considered comparable. In addition, the Kokshetau deposits have been compared with the vein U deposits hosted in albitites of the Ukrainian Shield, but the latter have formed at far higher temperatures of 300–450°C (Omelyanenko 1978).

6.1.1 Ishimsky Ore Field, Southwestern Kokshetau Region

This ore field is in the western part of the Ishimsk-Balkashinsk metallogenetic zone and includes the large *Ishimskoye* and

Kamyshevoye deposits, and the *Shokpak* deposit (► Fig. 6.2, Table 6.1).

Sources of information. Boitsov et al. 1995; Petrov et al. 2000; Poluarshinov and Pigulski 1995; amended by data from other sources.

General Geological Features of the Ishimsk-Balkashinsk Metallogenic Zone

According to Poluarshinov and Pigulski (1995), the Ishimsk-Balkashinsk metallogenic zone includes the Ishimsky and Balkashinsky ore fields. This zone is situated at the boundary of two structural units, the Kokshetau Block to the north and northeast and the Kalmakol Synclinorium to the south. Rocks of the Kokshetau Block include Precambrian gneiss, amphibolite and schists intruded by Caledonian granitoids, gabbro, and gabbro-diorite. The block was a positive element continuously during the Lower Paleozoic interval while the Kalmakol Synclinorium was a trough during the Caledonian geosynclinal stage. The synclinorium is filled with folded and weakly metamorphosed Cambrian to Ordovician volcanics and sediments and Middle-Upper Ordovician flysch. Late to post-orogenic grabens contain Middle to Upper Devonian pink molasse, which rests with a distinct unconformity on the crystalline basement. Some of the Devonian depressions contain mafic to felsic effusives and pyroclastics. The area is covered by a 40–60 m thick blanket of loose platform deposits, which increase in thickness to more than 100 m at some locations. Major structures trend mainly about NE-SW and E-W.

6.1.1.1 Ishimskoye

This deposit was discovered some 200 km SW of Kokshetau in 1957. Ore is of U-Mo vein type hosted in beresitized rocks. Original resources were in excess of 20 000 t U and averaged 0.204% U and 0.066% Mo. The deposit was mined underground and is depleted.

Ishimskoye ore bodies occur within the Ishim syncline composed of weakly metamorphosed Ordovician sandstone, siltstone, mudstone, which are overlain by Mid-Upper Devonian pink conglomerate and sandstone. Two groups of Silurian dikes cut the Ordovician sediments: shallow, 20–30°NW inclined lamprophyre and gabbro-syenite sills, and NNE-SSW-oriented, 60–70°SE dipping granodiorite-porphyry and diorite dikes.

The conformably to the Ordovician sediments NNE-SSW-trending, 35–40°NW dipping Carbonatny fault is the main structure at the deposit. It consists of 2–5 adjacent faults, 3–10 m thick each.

Pre-uranium beresitization (quartz, sericite, carbonate, pyrite alteration) is the principal alteration that altered all rocks along gently, strata-peneconcordant and steeply dipping structures but in a litho-differential mode. Carbonatization prevails in rocks of intermediate composition (spessartite and diorite dikes), whereas a combination of silicification and sericitization is typical for silicic facies, as well as for sandstone and shale.

Ore consists of the U-Mo paragenesis composed of pitchblende, coffinite and molybdenite/jordisite with sulfides of Cu, Fe, Pb, Zn, and As, and, locally, anthraxolite. Pitchblende constitutes 99% of the resources. Gangue is reflected by post-uranium stringers and veinlets of ankerite, and quartz-carbonate.

Ishimskoye consists of 15 ore bodies contained in a 2 km long and 1 km wide area. Three ore bodies occur in the Vesely sector and provided 66% of the resources, 7 in the Zmeiny and 5 in the Pryishimsky sector, which accounted for 27% and 7% of the resources, respectively.

Structural criteria exerted the principal ore control. Most favorable structural settings and high-grade ore are controlled by the intersection of steep faults with interformational, strata-peneconcordant, shallow-dipping, intensely-shattered fracture zones. High-grade ore also occurs in breccia zones, which developed at sites where steep faults cut dikes.

Ore bodies consist of veins but mainly of elongated, subhorizontal lens- or pipe-like shaped bodies with an internal stockwork structure. Ore bodies are 1–6 m, rarely up to 10 m thick, from 20 m to 1 000 m long, from 10 m to 500 m wide, and extend for 750 m down dip. Ore persists from depths of 50 m to 1 000 m below surface.

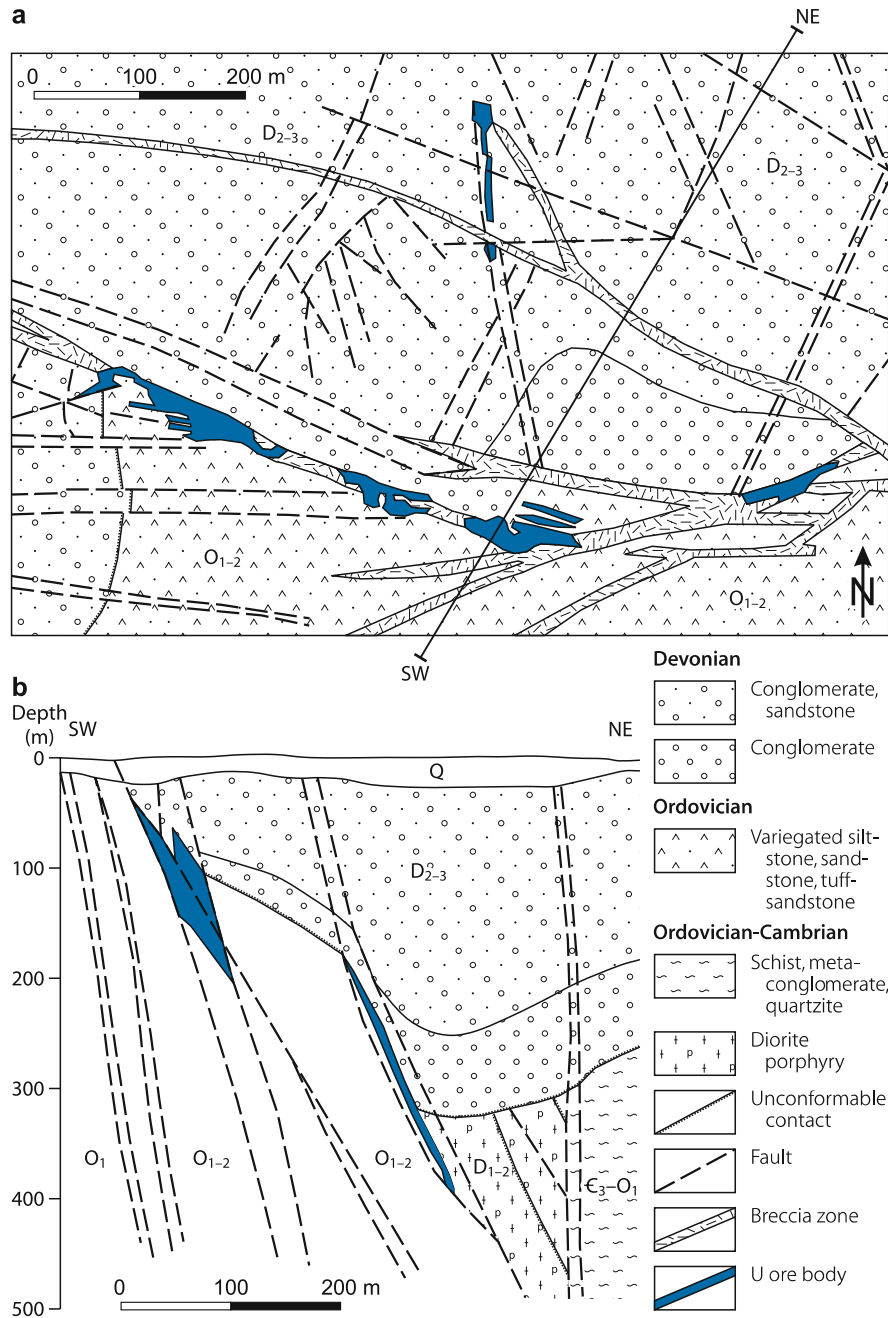
6.1.1.2 Kamyshevoye

This partly exploited deposit is located about 2 km SW of the Shokpak deposit and 170 km SW of Kokshetau. It was discovered in 1977 and explored by two shafts. Ore is of U-Ti and U-oxide vein-type and occurs in two ore zones. Original in situ resources totalled 20 700 t U at an average grade of 0.114% U (OECD-NEA/IAEA 1995); ore zone # 2 accounted for 87% of these resources. Remaining(?) inferred resources (C2 category) contained within ore zones # 1 and # 2 amount to 7 800 t U at an average grade of 0.12% U. The # 2 ore body contains additionally 5 000 t U prognostic resources (P) at an average grade of 0.082% U. (Basis for calculation: 0.03% cutoff grade and minimum thickness of 1 m.)

Kamyshevoye is situated at the SE edge of the Shokpak graben-syncline. Uranium occurs largely in a sequence of 80–300 m thick Devonian redbed molasse conglomerate and sandstone, which rests unconformably on a basement of slightly, metamorphosed Middle-Upper Ordovician terrigenous rocks (siliceous shale, siltstone, sandstone, and conglomerate) and andesite-basalt. These rocks are transected by N-S- and E-W-trending older faults which are cut by structures oriented about NW-SE (► Figs. 6.3a,b).

Two ore zones composed of discontinuous vein and stockwork ore bodies occur at depths from 70 to 1 000 m. Steeply-dipping, SE to ESE and N-S-trending fault-breccia zones control the ore zones and the setting of ore bodies. Ore bodies are of linear shape with lateral bulging at fault intersections. Ore bodies are from 50 m to 450 m long, and extend for as much as 700 m down dip (► Fig. 6.3b). At the upper levels, U mineralization consists of brannerite and is hosted in albitized silt- and sandstone affected by quartz-goethite-carbonate alteration similar to that on upper levels of the Kosachinoye deposit. This assemblage

Fig. 6.3. Kokshetau region, Kamyshevoe, **a** geological map and **b** SW-NE section showing the position of vein-stockwork ore bodies immediately at the Devonian/Ordovician unconformity (after Petrov et al. 2000)



was replaced immediately at and from the un-conformity downwards by a pitchblende-chlorite association. Where at depth brannerite ore in albitized lithologies were overprinted by the pitchblende paragenesis, a brannerite-pitchblende assemblage associated with carbonate has developed. Both the brannerite and pitchblende ores are considered to be of primary origin.

6.1.1.3 Shokpak

This deposit is located 165 km SW of Kokshetau and 2 km NE of Kamyshevoe. It was discovered in 1968 and is depleted. Original

resources averaged 0.135% U and amounted to 3 200t U contained in three ore zones: *Northern, Southern and Shirotnaya*; the Southern zone accounted for 62% of the resources.

The ore zones occur in an about 700 m long and up to 500 m wide strip along the curvilinear NE-SW-trending suboutcrop of the Lower/Middle Paleozoic unconformity, which separates Ordovician metasediments from Middle to Upper Devonian redbed molasse. Older faults trend about N-S and NW-SE. They are displaced by E-W- and NW-SE-oriented faults. Faults of all systems offset the unconformity.

Ore consists of U-oxide mineralization, essentially pitchblende associated with chlorite, that forms irregularly distributed

vein-stockwork ore bodies in beresitized rocks. Host rocks are Devonian hematitic, quartzose redbed sediments and mainly Ordovician weakly metamorphosed sand- and siltstone (silicified quartzite). Wall rock alteration includes beresitization (sericitization, carbonatization, pyritization, chloritization) and hematization. Albitization is absent.

Ore lodes occur discontinuously along about WNW, NE, and NW-trending faults at and immediately below the unconformity and are distributed from 50 m to 500 m below surface. Ore bodies are mainly of linear-isometric shape with dimensions from 60 m to 350 m long, from 6 m to 25 m thick, and persist over depth intervals from 90 to 200 m.

6.1.2 Chistopolsky Ore Field, Southwestern Kokshetau Region

The Chistopolsky ore field is some 140 km SW of Kokshetau and includes the small *Victorovskoye*, *Molodezhnoye*, *Dubrovskoye*, *Akkan-Burluiskoye*, and *Burluiskoye* vein-stockwork deposits. Host rocks are partly albitized and partly beresitized Precambrian and Paleozoic lithologies. Deposits range in size from a few 100 to a few 1 000 t U and exhibit average grades from 0.1 to 0.2% U (► Fig. 6.2, ► Table 6.1).

Sources of information. Petrov et al. 2000.

Most deposits occur in or adjacent to the western part of the Chistopol Basin, except Akkan-Burluiskoye that is in the eastern part. The basin is filled with Middle-Upper Devonian pink molasse (conglomerate, sandstone, siltstone). These sediments rest unconformably upon a basement composed of Precambrian metamorphites (amphibole-biotite gneiss, migmatite, amphibolite, schist), Lower Paleozoic effusive-sedimentary lithologies (conglomerate, tuff, gravel, sandstone, andesite porphyry), and Lower-Middle Ordovician siliceous-terrigenous sediments (siltstone, argillite, jasper, sandstone, conglomerate). Dikes occur in the western part and at the SW edge of the Chistopol Basin. Mineralization occurs in all rock types. The abyssal Ishim-Balkashin fault zone is a prominent regional structure, which trends adjacent to the Chistopol Basin.

6.1.2.1 Victorovskoye

This deposit is located within the SW margin of the Chistopol Basin. It was discovered in 1979 and explored by underground workings but not mined. In situ resources amount reportedly to 3 000 t U and average 0.107% U.

Ore bodies are hosted in Devonian sandstones with interbedded gravel and conglomerate, which were intruded by granite porphyry and dacite dikes. The dikes are up to 30 m thick and 1–1.5 km long, and occur in a belt, 300–400 m wide and 8 km long, situated 200–800 m from the S edge of the basin. Ordovician conglomerate, sandstone, and Cambrian spilite-diorite occur to the south of the Devonian sequence. Principal host rock alteration includes beresitization, albitization, and carbonatization.

Brannerite and uraninite are the principal U minerals. Brannerite mineralization is hosted in beresite altered, and uraninite mineralization in albite-carbonate altered pink Devonian sediments. Mineralization occurs in a 1.9 km long and 15 m wide zone controlled by the Northern fault zone, an up to 50 m wide structure with 2 steeply dipping faults. The ore zone includes 3 ore bodies with vein- and lens-like lodes, 25–250 m long, 0.7–40 m wide, and 50–250 m deep. 39% of the Victorovskoye resources occur in ore body # 1 and 53% in ore body # 3.

6.1.2.2 Molodezhnoye

This small deposit was discovered 1.5–2 km to the SW from the edge of the Chistopol Basin in 1963. The ore averages 0.113% U. Mineralization occurs to a depth of 250 m in NW-SE- and NE-SW-oriented fault zones that cut Lower–Middle Ordovician, slightly metamorphosed shale, conglomerate, and siltstone intruded by Devonian plagioclase porphyry and diorite. Five vein-type ore bodies are delineated, which are from 50 to 130 m long and persist over depths intervals from 50 to 110 m.

6.1.2.3 Dubrovskoye

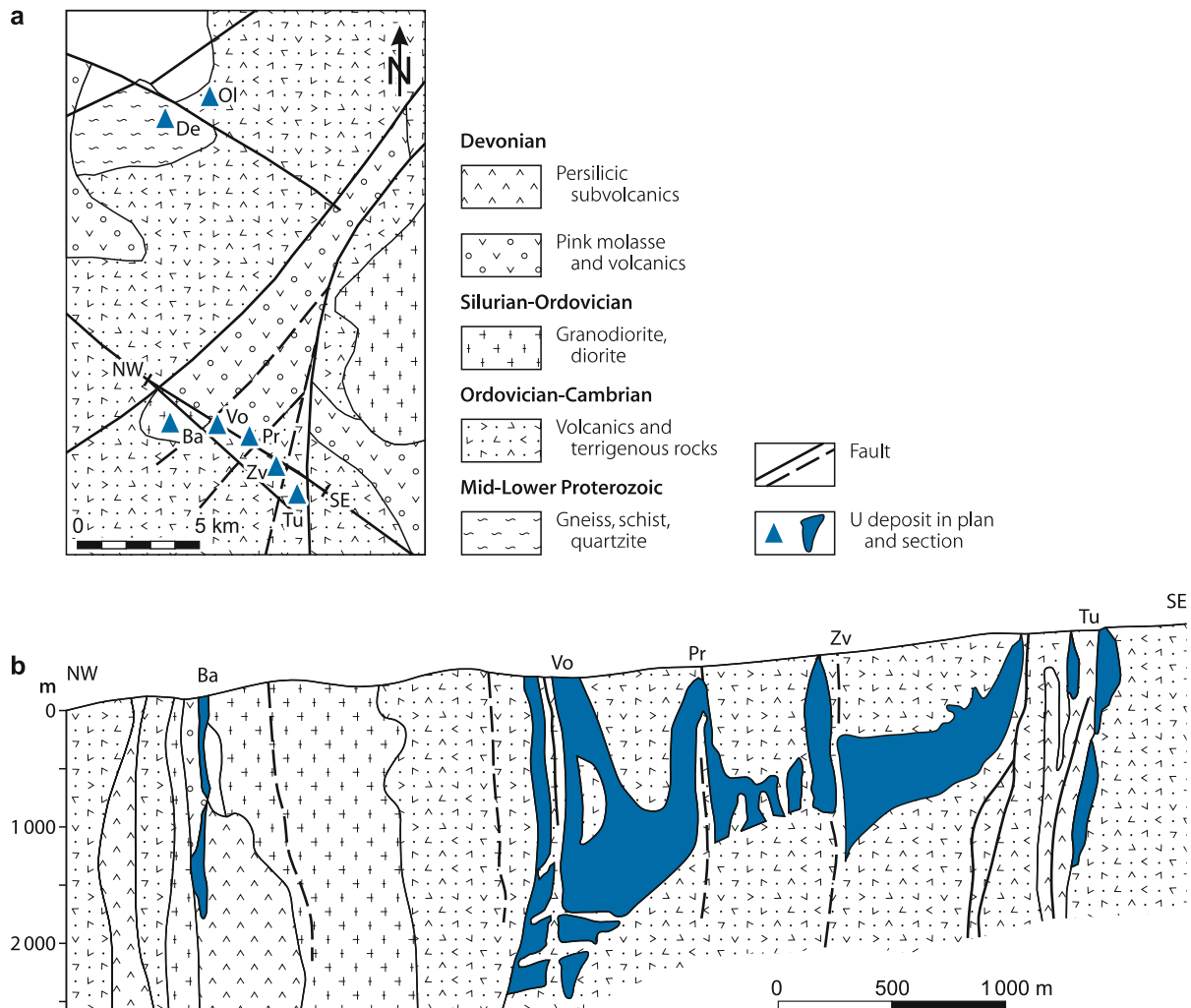
Discovered in 1969, Dubrovskoye is located in the northern Chistopolsky ore field, 1.5–5 km off the NW edge of the Chistopol Basin. Two ore sectors are recorded: the *Southeastern* with 8 ore bodies and 90% of the resources, and the *Northwestern* with 4 ore bodies. The ore averages 0.064% U, and 0.12% P₂O₅.

Mineralization occurs at the SW edge of a granite-gneiss dome within two Precambrian metamorphic units: Proterozoic gneiss of the Zerendin Series (amphibole, quartz and pyroxene paragneiss) and Vendian schist (coaly-siliceous phyllite, schist, quartzite) of the Sharyk Suite. Intrusions include spessartite, kersantite, and gabbro-diorite dikes, which occur predominantly in gneiss. Ore bodies consist of veins ranging from 100 to 730 m long, 3.5–4 m thick, and depths persistence from 90 to 300 m. Wall rocks are transformed by carbonate-albite alteration.

6.1.3 Balkashinsky Ore Field, Southwestern Kokshetau Region

This ore field (operated by Mine Management Unit # 1) is 40 km W of Balkashino and about 130 km SW of Kokshetau and contains the *Balkashinskoye*, *Zvezdnoye*, and the large *Vostok* deposits, which were mined prior to 1996. Additional deposits include *Promeshutochnoye* and *Tushinskoye*. Except for Balkashinskoye, the other four deposits may actually be regarded as a continuous single deposit controlled by a major NW-SE fault cut by N-S and NE-SW faults near the margin of the Kokshetau Uplift and the southwesterly adjacent Kalmykol Synclinorium. Ore is of U-Mo vein-stockwork type hosted in beresitized rocks of Ordovician terrestrial-pyroclastic provenance except for Balkashinskoye, which is in Devonian volcanics. Two additional deposits occur 15 km to the north of Balkashinskoye, *Dergachevskoye* in Lower Proterozoic gneiss and schist, and *Olginskoye* in Cambrian-Ordovician metamorphics (► Figs. 6.2, 6.4a,b, ► Table 6.1).

Fig. 6.4. Kokshetau region, Balkashinsky ore field, **a** geological map, **b** NW-SE longitudinal section (courtesy of Boitsov AV based on Russian literature). **U deposits:** *Ba* Balkashinskoye, *De* Dergechevskoye, *Ol* Olginskoye, *Pr* Promeshutochnoye, *Tu* Tushinskoye, *Vo* Vostok, *Zv* Zvezdnoye



Historical production of the Balkashinskoye ore field totals about 17 000 t U for the period from 1959 to 1995. The present geological inventory includes over 14 000 t U reserves (A, B, C1) and over 13 000 t U prognostic resources (P1) (based on a cutoff grade of 0.05% U).

Sources of information. Petrov et al. 2000; Poluarshinov and Pigulski 1995; unless otherwise cited.

6.1.3.1 Balkashinskoye

The Balkashinskoye U-Mo deposit is located 130 km SW of Kokshetau and was discovered in 1953. The deposit encompasses two sectors, *Central* and *Northern*. The bulk of the U resources are contained in the *Severnoye* (North) and *Glavnoye* (Main) ore bodies in the Central sector. Four small ore bodies are located in the Northern sector. Original resources totalled some 3 000 t U at a grade averaging 0.123% U. This figure includes 1 640 t U proven

resources contained in the Main and the North ore bodies. The depleted Main ore body was mined by open pit methods to a depth of 100 m from 1959 to 1966 and yielded 900 t U at a grade of 0.1% U. Remaining reserves of 740 t U at an average grade of 0.078% U (0.05% U cutoff grade) are contained in the North ore body. Prognostic resources (P1) of the two ore bodies total 4 300 t U and average between 0.06 and 0.08% U (Pool T, pers. commun.).

Mineralization occurs within a small depression, 2.5 × 1 km in size, filled with Middle-Upper Devonian sediments and volcanites (conglomerate, sandstone, tuff, with intercalated felsic and quartz porphyry layers). The basin is downfaulted into a basement of Ordovician gabbro and gabbro-diorite of the Shantobe Massif, which is cut by spessartite and diorite porphyry dikes. A regional, N-S-oriented and 60–85° inclined fault, 15–20 m wide, is the principal structure at the deposit; it trends along a conglomerate-quartz porphyry contact.

Ore occurs in ± vertically dipping vein-shaped bodies, controlled by the intersection of N-S and NE-SW faults. Pitchblende and associated Mo-sulfides are the essential ore minerals. Devonian

felsic subvolcanics (quartz porphyry), sandstone and conglomerate constitute the principal host rocks. Wall rock alteration is of beresitic nature, dominated by sericitization and silicification. Weathering persists to a depth of 30 m. Ore lodes are from 100 to 250 m long, and persist over depths intervals from 100 to 140 m. The bulk of the ore is distributed over a depth from 10 to 160 m below surface, but mineralization extends from subsurface to depths in excess of 1 500 m.

6.1.3.2 Vostok

Discovered in 1964, the Vostok deposit is some 130 km SW of Kokshetau. Ore is of the U-Mo vein-stockwork type and hosted in beresitized rocks. Original in situ resources were on the order of 20 000 t U at a grade averaging 0.17% U and 0.038% Mo contained in the *Severo-Zapadnoye* (Northwest) and *Glavnoye* (Main) ore bodies.

The deposit was mined from 1966 to 1995 and opened again in 2003. Production amounts to about 15 000 t U. The mined ore averaged 0.146% U. Mo was recovered as a by-product. The mine was serviced by three shafts as much as 780 m deep but working levels reach only 430 m below the surface. Remaining reserves total some 5 000 t U at grades that vary between 0.06 and 0.4% U and average 0.12% U at a cutoff grade of 0.03% U (Pool T, pers. commun.).

Vostok is situated in the central part of the Glavny (Main) fault, a NW-SE-oriented, about 7 km long and up to 2 km wide structural zone, which also contains the southeasterly adjacent interconnected *Promeshutochnoye*, *Zvezdnoye*, and *Tushinskoye* deposits. The zone follows a large, deep rooted, NW-SE fault, which is offset by NE and NNE faults and which widens to more than 4 km at its NW end where the *Balkashinskoye* deposit is located. Characteristically, numerous anomalies of uranium and indicator elements (Mo, Pb, As) are found in this zone.

Host rocks are Ordovician, slightly metamorphosed, continental argillaceous and arenaceous sediments, 1 100–1 400 m thick. The sediments were intruded by Ordovician granodiorite, diorite, and gabbro. Devonian sediments (largely conglomerate with intercalated sandstone beds) and volcanics (felsite, felsite porphyry, quartz porphyry, andesite porphyry), from 200 to 700 m thick, occur adjacent to the NE; they include a lower conglomerate and an upper tuff unit. Approximately 70 m thick unconsolidated overburden covers the Ordovician rocks.

Wall rock alteration is reflected by pre-ore beresitization (sericitization, silicification, chloritization, pyritization) and post-ore carbonatization.

Ore bodies occur from 50 m to more than 2 000 m below surface in highly fractured intervals of the Glavny fault zone. On upper levels of the deposit, ore bodies consist of multiple, steeply inclined, lenticular and columnar lodes composed of veined and disseminated U-Mo mineralization; these lodes converge at a depth of approximately 1 000 m to form a single, shallow dipping body. Dimensions of ore bodies are on the order from 10 m to over 500 m long, from 2 m to 10 m, rarely to 30 m, wide, and extend for over 1 500 m downdip. Prominent ore

accumulations are found at sites of strike and dip angle variations of the main fault plane (and not at fault intersections as in other deposits).

Two major ore bodies are identified: *Glavnoye* (Main) and *Cevero Zapadnoye* (Northwestern). The *Glavnoye* ore body has a lenticular shape, and is from 100 to 530 m long, and from 28 to 31 m thick. The *Northwestern* ore body has a columnar shape with a length from 150 to 200 m; its position is controlled by a flexure of the *Glavny* fault, where the strike turns from NW-SE to E-W (Fig. 6.5).

6.1.3.3 Zvezdnoye

This deposit is located about 2 km SE of the Vostok deposit. Original reserves at *Zvezdnoye* amounted to 8 630 t U contained in two major ore bodies, *Main* or *Glavnoye* (also referred to as *Zvezdnoye*), discovered in 1964, and *Eastern* or *Vostochnoye Zaleshi* (*Zaleh*), discovered some 700 m to the east in 1986. The *Glavnoye* ore body was mined from 1978 to 1992; it produced 995 t U at an average grade of 0.085% U and has remaining reserves of 1 600 t U at 0.124% U. The *Eastern* ore body accounts for 6 000 t U reserves (B, C category) at 0.21% U and prognostic resources (P1) of 3 350 t U at 0.19% U (Pool T, pers. commun.).

Zvezdnoye is controlled by the *Glavny* fault zone, and is of similar mineralization and geological setting as *Vostok*. The two ore bodies mentioned above have the following dimensions: The *Glavnoye* ore body is as much as 200 m long, up to 50 m thick, and extends for 660 m downdip at a 70–75°NW inclination. The *Eastern* ore body is from 60 m (at the depth of 60 m) to 650 m (at the depth of 850 m) long, and contains mineralization from 60 to 1 375 m below surface.

6.1.3.4 Tushinskoye

Discovered in 1973, *Tushinskoye* is situated in the SE part of the *Balkashinsky* ore field, about 2 km to the SW of *Zvezdnoye*. Three ore sectors are delineated: *North*, *Central* and *South*. Reserves of the *North* sector amount to almost 900 t U at 0.105% U and prognostic resources to 4 400 t U at 0.15% U (Pool T, pers. commun.).

Mineralization occurs at intersections of N-S, NW-SE and NE-SW faults. Mineralization in the *Central* and *Southern* sectors is controlled by these structures within a Devonian subvolcanic body. Host rocks are felsite, lava-breccia and tuffaceous lava. Mineralization occurs at the contact of felsite with explosive breccia and in fault zones. The host rocks are altered by beresitization. A vein-like and two columnar ore bodies are identified in the *Central* sector. The largest ore body measures from 20 × 25 m to 30 × 45 m in planview and persists to a depth of 230 m. The *Southern* sector consists of veins and ore nests, up to 20 m long and up to 3 m thick, which occur at depths from 230 to 290 m. The *Northern* sector contains ore in Ordovician argillite. Its main ore body is of complex shape and located at depths from 220 to 460 m.

6.1.3.5 Olginskoye

Olginskoye is located 10 km E of Dergachevskoye. It was discovered in 1962, exploited from 1968 to 1970, yielding 55 t U, and is depleted. The mining grade averaged 0.145% U as compared to an in situ grade of 0.182% U.

The deposit occurs in the eastern effusives of the Cambrian-Ordovician Yakshin volcanic structure composed of weakly metamorphosed rhyolite porphyry, quartz porphyry, felsite, and other rocks. The basement consists of chlorite schist. Mineralization is hosted in quartz porphyry altered by beresitization and forms a

complex lens-like ore body, 100 m long, 30–35 m thick, that persists over a depth interval of 30 m to the depth of 100 m. Uranium occurs as U^{6+} minerals, mainly autunite, torbernite, and other U micas.

6.1.3.6 Dergachevskoye

This depleted deposit is situated in the NW part of the Balkashinsky ore field, 15 km to the north of Balkashinskoye and to the east of the Yakshin volcanic structure. *Dergachevskoye* was discovered in 1962, mined (underground) from 1964 to 1969

Fig. 6.5. Kokshetau region, Vostok, **a** geological map, **b** NW-SE longitudinal section, **c** SW-NE cross-section through the NW part of the Cevero Zapadnoye ore body. As shown, U-Mo ore bodies occur structurally controlled along the Devonian-Ordovician contact (after a Petrov et al. 2000; b, c Pool T. pers. commun. 1996)

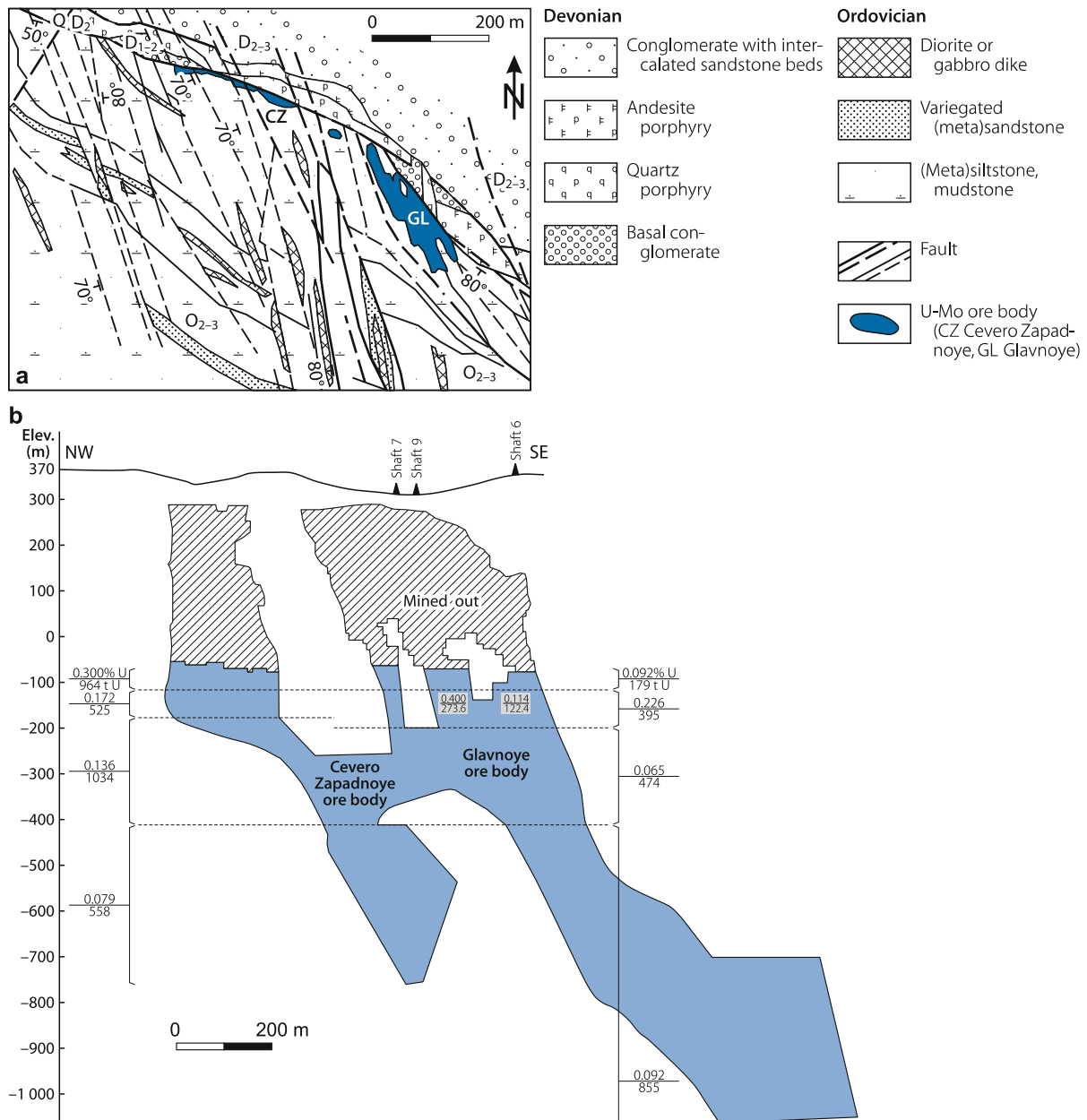
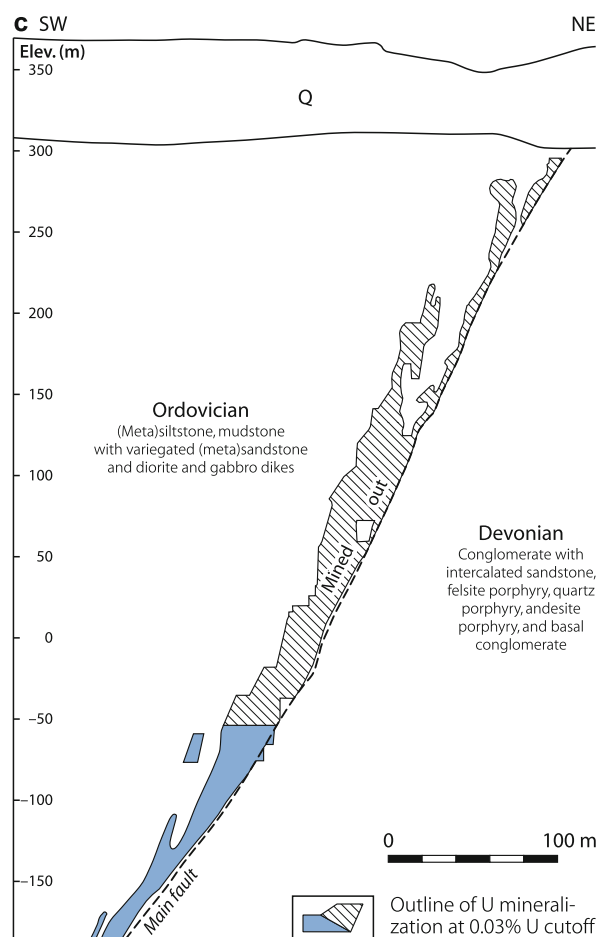


Fig. 6.5. (Continued)



and produced 320 t U at a mining grade of 0.21% U. The in situ grade averages 0.260% but 65% of the resources are in the grade class of 0.5–3.5% U. Two ore bodies are delineated: *Main* or *Glavnoye*, and # 2.

The host environment consists of Riphean crystalline schists and quartzite intruded by diabase dikes and cut by NW-SE-oriented and 40–80° NE dipping faults. The two ore bodies are confined to crystalline schists at a flexure of the NW-SE Savelevsky fault. Numerous, fault-controlled, small lenses form the *Glavnoye* ore body that is 170 m long, 25–30 m thick, and persists over depths intervals from 75 to 90 m. Ore body # 2 has an irregular shape, is 10–15 m wide in section, and 30 m long. Age datings yield 420±10 Ma and 380–330 Ma for the mineralization.

6.1.4 Grachevsky Ore Field, Northwestern Kokshetau Region

The Grachevsky ore field is, by resources, the largest in the Kokshetau region. It includes *Kosachinoye*, (>95 000 t U) the largest single deposit of the region. Another large deposit is the partly exploited *Grachevskoye* deposit. Additional deposits are *Fevralskoye*, *Sartubekskoye*, *Bolotnoye*, and *Dukonskoye* (Fig. 6.2, Table 6.1). Ore is of the vein-stockwork type with U-P and/or simple U mineralization hosted in albitized rocks.

Sources of information. Petrov et al. 2000; and others as cited.

6.1.4.1 Grachevskoye

Grachevskoye was discovered 100 km W of Kokshetau in 1967 and has been developed for underground mining to a depth of 700 m by two vertical shafts. At a 0.03% U cutoff grade, the original in situ resources amounted to almost 18 000 t U at an average grade of 0.128% U and 2.5% P₂O₅. Mining started in 1985 and produced 2 650 t U until the closure of the mine in 1995. Remaining resources (A, B, C categories) total about 14 000 t U at an average grade of 0.18% U and a 0.05% U cutoff grade.

Sources of information. The subsequent description is largely derived from Omelyanenko et al. (1993) amended by data from Boitsov AV et al. (1995).

Geological Setting of Mineralization

The Grachevskoye deposit occurs in Proterozoic-Cambrian metasediments at the southwestern intrusive contact of a Silurian-Devonian, medium- and coarse-grained leucogranite of the Legaevskii Massif (Fig. 6.6). Three granite facies of the Caledonian Orlinogorskii complex are distinguished in the Legaevskii Massif. The leucogranite is peraluminous (according to the chemical composition given by Omelyanenko et al. 1993) and is the earliest and most abundant facies; second is a porphyritic granite, and the latest is fine-grained aplitic granite and aplite, which occur within the previous granites and in rocks adjacent to the massif. The granites have elevated tenors of F, Li, Rb, Sn, Th, and U. Uranium background values of the first two facies both average 19 ppm U, while the aplitic granite averages 39 ppm U.

The granites were intruded into and imposed an up to 100 m wide contact-metamorphic aureole of hornfels upon folded sediments of the Upper Proterozoic (Vendian) Kokshetau Formation and overlying effusive-terrigenous Cambrian rocks, which fill a graben. Riphean porphyroids and schists form, with fault contact, the western boundary of the graben. The metasediments are cut by a stock (~200 m in diameter), and up to 15 m thick, NE-SW-trending dikes of Ordovician gabbro, retrograde metamorphosed to greenschist grade facies, and Silurian-Devonian porphyritic and aplitic granite dikes partly altered by greisenization. The quantity and thickness of the granite dikes increase markedly with depth. Quartz veins dissect both granites and metasediments. Unconsolidated, 10–120 m thick overburden covers the deposit.

The Kokshetau Formation consists of weakly metamorphosed sediments separated into two conformable members: the ore-hosting upper, arenaceous-pelitic Andreevskaya Member (650 m thick, sandstone, siltstone-mudstone), and the lower, pelitic-carbonatic Sharykskaya Member (limestone, dolomite, carbonaceous shale, and/or sericitic shale).

The deposit is positioned at the intersection of two deep rooted, repeatedly reactivated fault zones: the NE-SW-oriented, vertically dipping Volodarskaya and the 15–20 km wide, over

100 km long, E-W-trending Central Kokshetau fault zones. Both structures consist of a number of faults and related fractured, sheared and brecciated intervals.

Grachevskoye is confined to a 2 km long in E-W direction and up to 900 m wide tectonic wedge bordered to the N, SW, and SE by three major faults and internally deformed by numerous locally developed faults of various orientations. The western and southern segment of the wedge is occupied by highly distorted sediments of the Andreevskaya Member and the eastern segment is occupied by the earlier-mentioned gabbro stock and leucogranite. Adjacent to larger faults, strata are unpredictably folded into flexures associated with pronounced fracturing. The most prominent flexure is at the western flank of the deposit; it is bend along a 10 m wide zone of shearing and faulting along which displacement of sediments exceeds 100 m (► Fig. 6.6).

Host Rock Alteration

Pre-uranium metasomatism/alteration includes ubiquitous albitization succeeded and partially overlapped by apatitization. Subordinate alteration includes chloritization, carbonatization, sericitization/hydromicazation, and hematitization. The latter imposed, by finely dispersed hematite, a distinctive pink hue upon the altered rocks. Where late chloritization overprinted the earlier metasomatites, the rocks attained a dark green-grey color.

At upper levels of the Grachevskoye deposit, alteration overprinted predominantly sandstone and siltstone of the Andreevskaya Member whereas porphyritic and aplitic granite dikes were mainly affected at lower levels.

Alteration extent, intensity and nature are a function of the scope and grade of preceding tectonic deformation exerted by numerous strata-concordant and discordant faults, fractured and cataclastic zones, as well as the mineralogy of the parent rock. As a result, altered rocks are of highly variable composition. Extreme facies may be almost monomineralic albitite or they may consist predominantly of apatite, with gradual transitions between the two. The most-typical metasomatites consist of 60–80% albitite, 5–10% apatite, 5–10% relictic quartz, with the remainder of carbonate and hematite, and late stage chlorite, quartz, sericite, and carbonate. The amount of apatite varies between fractions of a percent and 60% as a function of the calcium content in the parent rock. Highest apatite contents are confined to limestone and gabbro (see also the following Sect. *Mineralization*).

Mineralization

The principal U mineral is coffinite associated and partly intergrown with chlorite and/or apatite, which form simple U(-albite)-type mineralization with transitions into a U-P type due to the intergrowth of coffinite with apatite. Some pitchblende occurs locally. Th and Zr are common but not everywhere are they constituents of the Grachevskoye ore. Inclusions and stringers of reddish-brown, amorphous material locally interspersed in high-grade U ore were identified by Omelyanenko et al. (1993)

as a mixture of zirtolite (zircon containing admixtures of Th, U and Hf) and ferrithorite.

The crystallisation sequence of principal ore constituents begins with albitite, succeeded by apatite, which overlaps and post-dates albitite, and continues with coffinite that crystallized coeval with and after apatite. Pitchblende postdates the former minerals. Narrow veinlets of albitite, and rare apatite, quartz, chlorite, and sericite/hydromica, and pockets of carbonate are the latest product. Most of the coffinite, apatite, chlorite, and other minerals precipitated during the terminal stage of the hydrothermal event and typically occur in zones of post-albitite microfracturing.

Ore is restricted to albitized and phosphatized rocks of the Andreevskaya Member and to porphyritic granite dikes where it is controlled by profoundly deformed sections along numerous strata-concordant and discordant faults, fractured and cataclastic intervals. Brittle rocks adjacent to the gabbro stock suffered the most intense fracturing due to the heterogenous physical properties of the various lithologies and the rigid behavior of the gabbro during tectonic deformation; consequently, ore-bearing metasomatites are markedly developed around the gabbro stock.

Ore hosted in metasomatite derived from interbedded sandstone-siltstone laminae has preferentially a disseminated or a banded to streaky, and that after granite dikes a brecciated-disseminated, texture. Disseminated ore prevails except for high-grade intersections where a streaky-disseminated texture is most typical due to coffinite accumulation in microcracks. Such rich ore is contained in dark-greenish-brown to reddish-brown, albitite-apatite rich, dense rocks cut by stringers of albitite, quartz, chlorite, and sericite. Regardless of the parent lithology, ore-bearing metasomatites are compact rocks with high strength due to intensive healing.

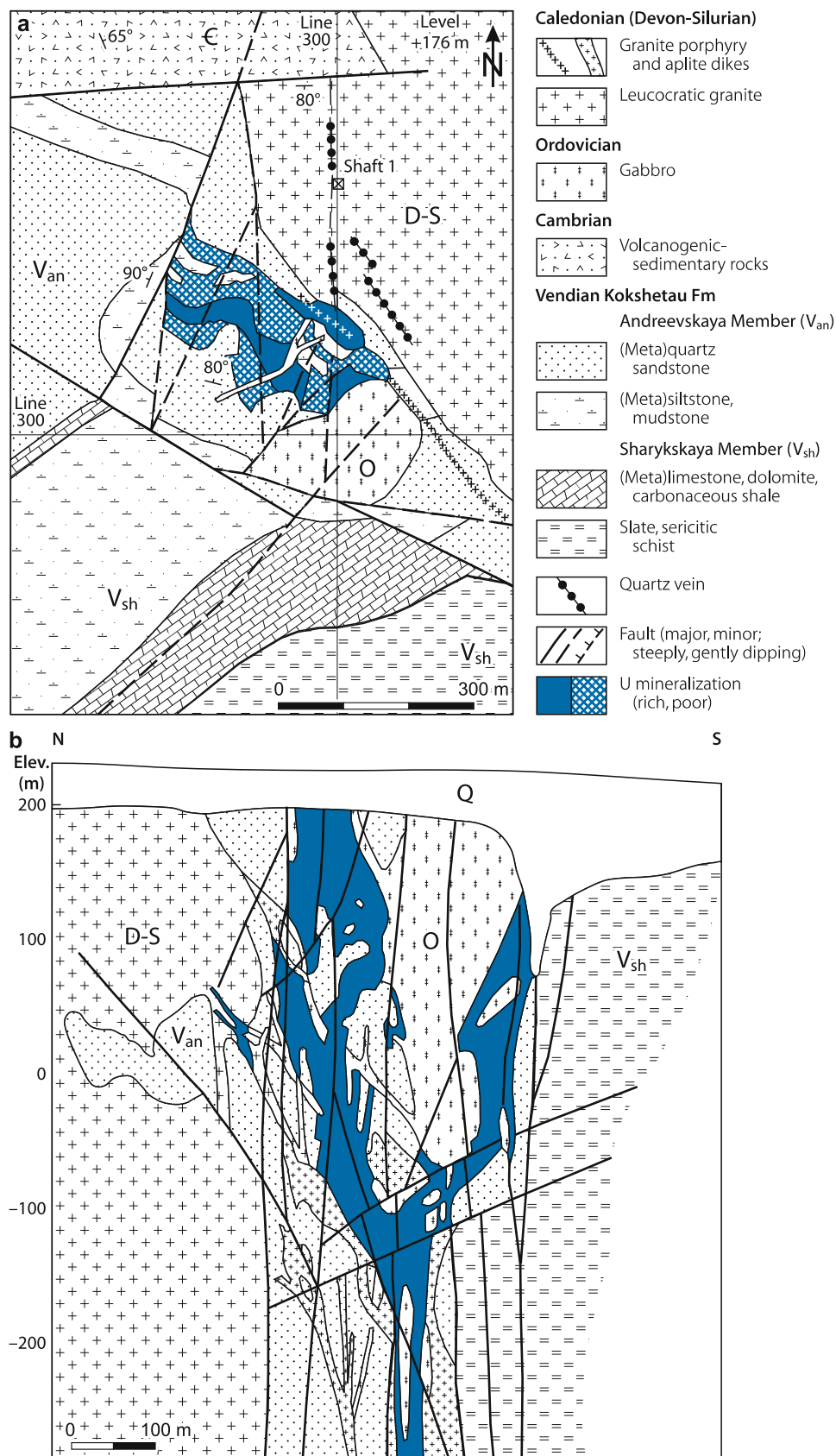
Most-essential structures, particularly for highly enriched ore as found e.g. to the N of the gabbro stock, correspond to narrow, rarely up to 2 m wide “zones of three-dimensional cataclasis”, i.e. lithologic intervals intensely broken by a dense and complex network of microcracks. Hydraulic fracturing in response to high pressure generated by ascending hydrotherms or, alternatively, tectonic movements along faults are thought to be reasons for their formation. This variety of brittle deformation is not found in unmineralized ground but is restricted to ore lodes; hence this type of cataclasis is considered a critical prerequisite for the localization of ore (and related alteration development), which is further supported by the fact that the morphology of ore bodies is not defined to any significant degree by prominent faults.

Shape and Dimensions of Deposits

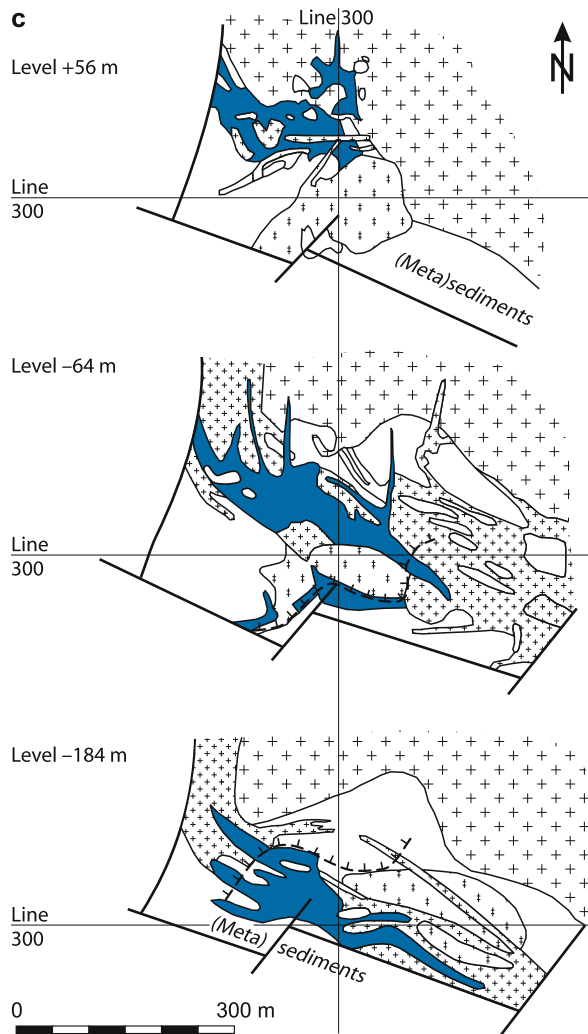
Grachevskoye covers a 400 m long and 200 m wide area in which U mineralization occurs in a more or less vertically plunging pipelike lode from 100 m to over 1 000 m below surface. The lode is of unpredictable morphology; it has a core with offbranching apophyses, and is partly split by gabbro into two branches. On upper levels, from a depth of some 350 m upwards, where ore is hosted by sediments of the Andreevskaya Member, the main branch is up to 300 m long and 150 m wide. At lower levels where ore is in steeply dipping porphyritic and aplitic granite dikes, the

Fig. 6.6.

Kokshetau region, Grachevskoye, **a** geological plan at level +176 m, **b** N-S section, and **c** planviews of selected levels. Planes and section illustrate the structural configuration of the vein-stockwork ore body at the contact of Proterozoic (meta)sediments and Caledonian leucogranite and intervening Ordovician gabbro. Host rocks are altered by early albitization and, locally, apatitization as well as various younger alteration products (after **a, c** Omelyanenko et al. 1993; **b** Laverov et al. 1992b)



■ Fig. 6.6. (Continued)



lode narrows to a width of some 50 m and becomes about 400 m long in a NW-SE direction. At higher levels, the dikes are as much as 10 m thick, but merge at a depth of 400 m into a 80–100 m thick single body. A steeply dipping NE-SW fault determines the NW limit of the lode, and the gabbro stock determines the SE border (► Figs. 6.6b,c).

The lode has a heterogenous internal structure reflected by an erratic U tenor of ore and intervening barren and weakly mineralized ground. U mineralization is ubiquitously distributed, although in a highly erratic manner, throughout the albite-apatite altered rocks. This is in contrast to most other deposits of the Kokshetau region where ore bodies are commonly confined to central sections of alteration zones.

U contents correlate with the intensity of cataclasis and degree of alteration of host rocks. The bulk of mineralization has grades ranging from hundredths to tenths weight percent U but small intervals can, exceptionally, be as high as 1% U or more (mining blocks are defined as ordinary ore with 0.05–0.1% U and rich ore with over 0.1% U) Phosphorus ranges between 0.3 and 20% and averages about 2.5% P_2O_5 . Most of the ore contains from hundredths to tenths weight percent thorium.

Ore consists overwhelmingly of disseminated, minute grains and to a lesser extent of irregularly shaped aggregates and tiny stringers of coffinite. Stringers are most commonly fractions of a mm thick and up to several cm long; only exceptionally do they attain a thickness of a few mm and a length of 1 m. Pitchblende occurs locally in small stringers within high-grade coffinite ore.

6.1.4.2 Kosachinoye

Discovered in 1973, Kosachinoye is located some 110 km W of Kokshetau (► Fig. 6.2) and encompasses several isolated sectors: *Central, Sartubek, Kutuzovsky, Bolotny, Dorozhny, Shakhtny, Vostochny (Eastern), Glukhariny, Lyubotinsky, and Zapadny (Western)*, which can be regarded as individual deposits. In situ resources total 95 700 t U (OECD-NEA/IAEA 1995). Ore grades average 0.109% U. About 70–80% of the resources occur in the Central, Sartubek, and Kutuzovsky sectors. Resources (outlined down to the 650 m level) are estimated to be 23 000 t U; they include 14 300 t U measured and indicated resources at an average grade of 0.106% U, and 9 000 t U inferred resources (based on a 0.05% cutoff grade) (Pool T, pers. commun.). The deposit is explored but not mined except for some parts in weathered rock that have been mined from an open pit.

Sources of information. Boitsov et al. 1995; Omelyanenko et al. 1993; Petrov et al. 2000.

The above mentioned individual sectors occur within an 8 km long and 4–5 km wide zone (► Fig. 6.7a), which is controlled by the interjunction of the large NE-SW-striking Volodarskaya and the E-W-oriented, steeply south dipping Central Kokshetau fault zone. Country rocks include predominantly

- *Lower Silurian-Upper Ordovician* andesite-dacite and basalt (diabase) porphyries, lava breccia, felsic tuff, conglomerate, limestone,
- *Middle-Lower Cambrian* (Lubotinskaya Suite) cherty and carbonaceous/graphitic argillite/slate, quartzite, metasiltstone, limestone/marble, diabase/basalt and other volcanic rocks, and
- *Proterozoic* (Vendian Andreevskaya and Lubotinskaya series) graphitic slate and quartzite, limestone/marble, quartzite, and gabbroic lava breccia.

Carbonaceous/graphitic slate and diabase are the favored host rocks. They are altered by ubiquitous albitization, which is overprinted along faults by deep-reaching (>1 400 m deep) carbonatization and chloritization, and, additionally, on upper levels by silicification (quartz) and hematitization to depths of as much as 600 m (► Fig. 6.7d).

Mineralization consists of pitchblende, coffinite, and U-Ti phases associated with a variety of gangue and Fe minerals, which occur in three ore parageneses: (a) brannerite or brannerite-pitchblende associated with carbonate-chlorite or quartz-goethite, (b) coffinite-chlorite, and (c) late coffinite-pyrite associated with dolomite. Carbonate content is in excess of 6%. Lower and intermediate levels of ore bodies are mineralized with coffinite-chlorite in

albitized rocks. Some brannerite and pitchblende both contained in carbonate-chlorite or quartz-hematite/goethite altered rocks are typical for upper levels. The zoning is camouflaged, however, by late dolomitization and pyrite-coffinite formation, which overprints the former two parageneses (Boitsov AV et al. 1995).

Uranium occurs in vein-stockwork ore bodies of variable shape and size. The main ore body is 800–1 000 m long, about 50 m thick, and persists to a depth of almost 1 500 m. It includes a better grade zone within a subvertical pipe-like body, which is confined to a brecciated and altered Cambrian carbonaceous limestone unit in contact with Lower Cambrian porphyritic diabase/basalt.

Ore bodies cumulate in the afore mentioned sectors. The two significant Central and Kutuzovsky sectors exhibit the following dimensions: The *Central* sector is 2,6 km long, from 100 to 400 m wide, from 350 to 400 m deep in the S and to 1 500 m deep in the N. Ore lodes occur along the Central fault, a N-S-oriented structure that trends along the contact of calcareous

schists of the Sharyk suite to the west and Cambrian subvolcanic basalts to the east. The *Kutuzovsky* sector extends over a length of several kilometers, a width of at least 1 500 m, and to a depth from about 100 m to about 1 000 m with sub-ore grade mineralization continuing in excess of 1 400 m deep.

6.1.4.3 Fevralskoye

This deposit is situated 5 km SE of Kosachinoye. It was discovered in 1971 and contains reportedly 4 600 t U at a grade of 0.097% U, and as high as 5% P_2O_5 . Mineralization occurs within the southern margin of the Sumalkol syncline and is hosted by Vendian carbonate/marble and schist, which were intruded by Silurian granite of the Zarendine Complex. The medium steeply dipping Rechnaya fault zone, 150–250 m wide, is the principal structure at the deposit. Three lenticular ore bodies are delineated controlled by steeply and shallowly dipping faults.

Fig. 6.7.

Kokshetau region, Kosachinoye, **a** generalized geological plan with position of ore sectors, **b** W-E cross-section and **c** longitudinal SW-NE section with ore grade distribution, **d** vertical projection of mineralization with allocation of uranium and alteration phases. Host rocks are albitized slate and diabase (after a–c Pool T. pers. commun. 1996; d Boitsov et al. 1995). **Ore sectors:** Bo Bolotny, Ce Central, Do Dorozhny, Gl Glukhariny, Ku Kutuzovsky, Ly Lyubotinsky, Sa Sartubek, Sh Shakhhtny, Vo Vostochny, Za Zapadny

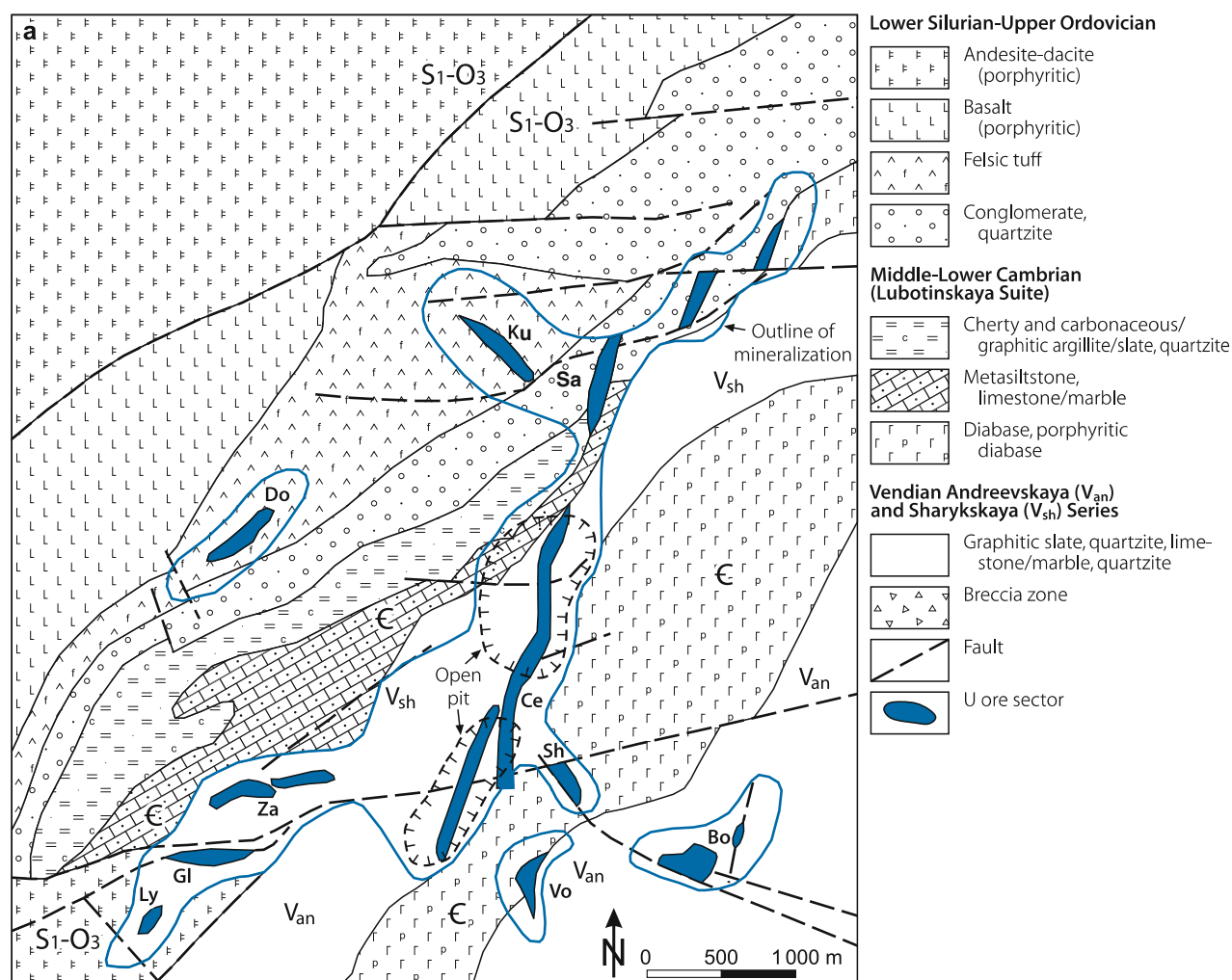
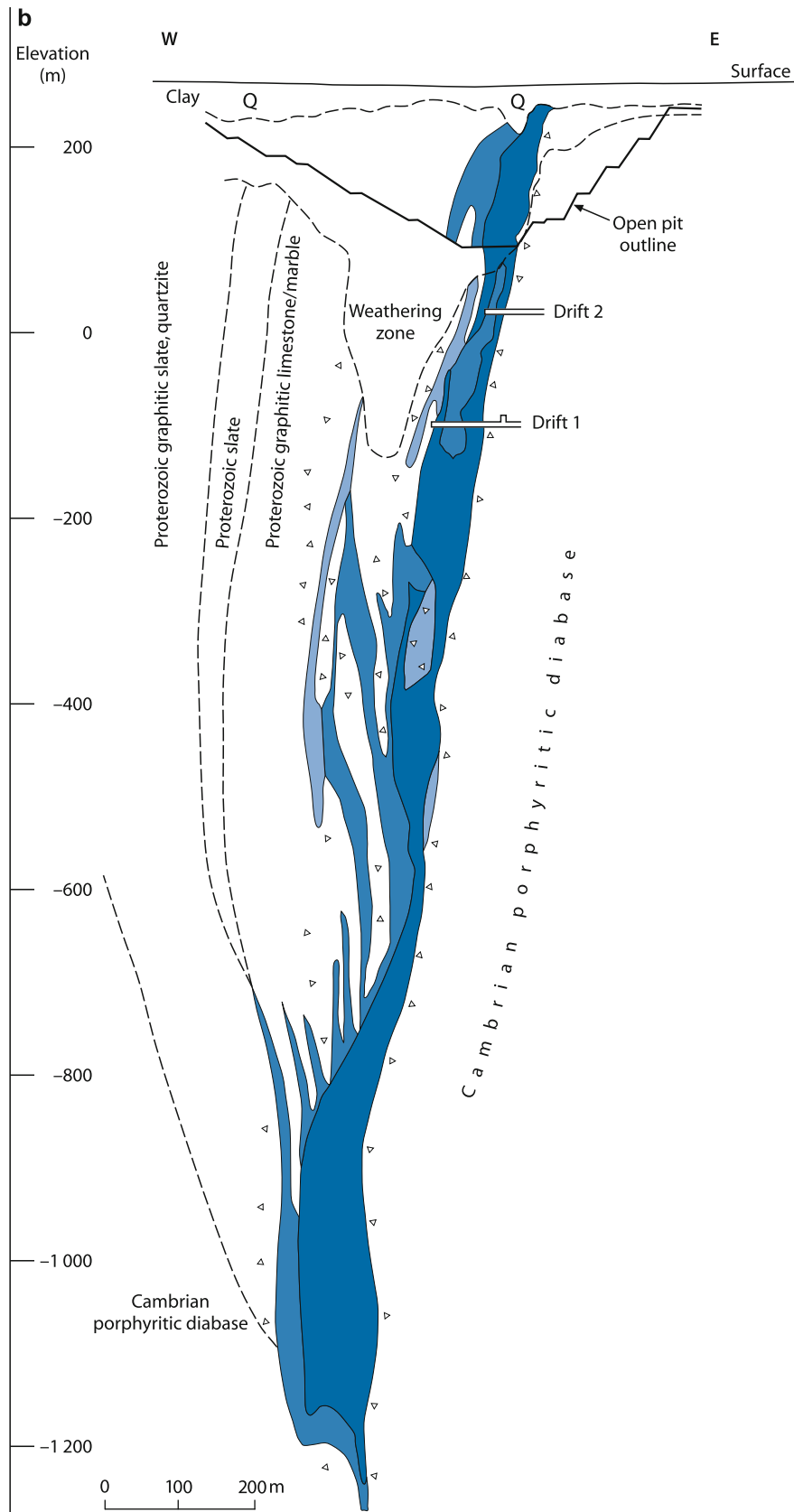
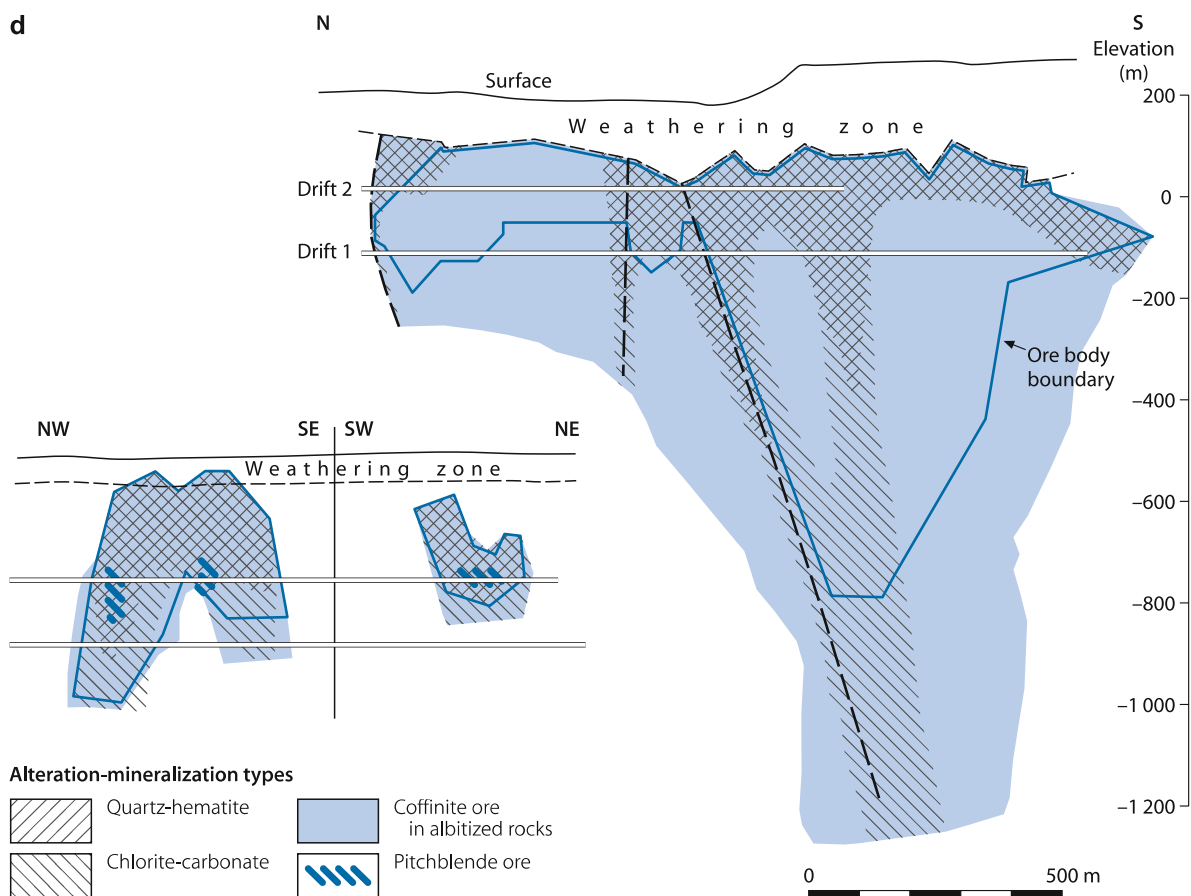
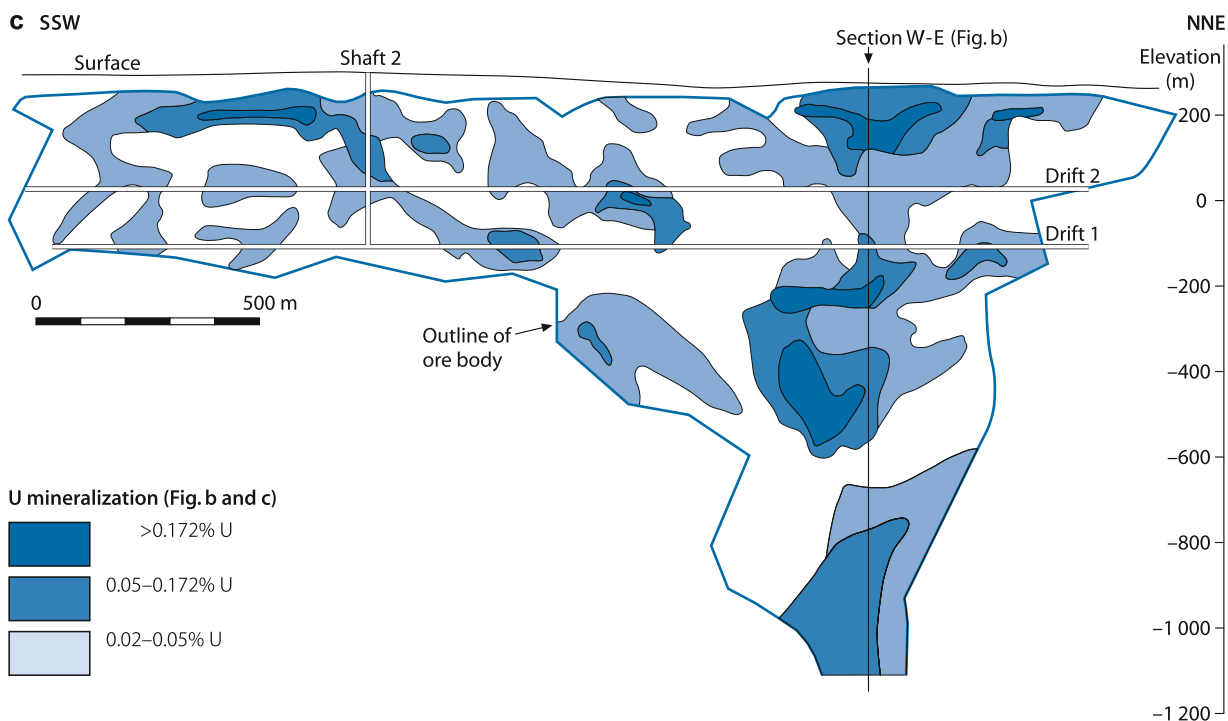


Fig. 6.7. (Continued)





The ore bodies are from 250 to 1 400 m long, from 0.2 to 20 m thick, and extend for 60–650 m down-dip. Brannerite and coffinite are the principal U minerals.

6.1.5 Altybaysky Ore Field

This ore field is situated in the Altybaysky block of the Kokshetau Massif and includes the *Slavyanskoye*, *Chaglinskoye*, and *Abayskoye* U deposits (and also the *Vasilkovskoye* gold deposit) (Fig. 6.2, Table 6.1). U deposits are of the vein-stockwork type, some hosted in albitized, and others in beresitized rocks. None of the deposits were mined due to low grades of less than 0.1% U.

Source of information. Petrov et al. 2000.

6.1.5.1 Slavyanskoye

Slavyanskoye is located 35 km NW of Kokshetau and 20 km NW of Chaglinskoye. It was discovered in 1973 and accounts for in situ resources of 5 300 t U at an average grade of 0.075% U contained in three ore zones, *Eastern*, *Central*, and *Western*. The deposit occurs in a granite-gneiss dome composed of granite, gneiss, amphibolite and schist of the Zarendine Complex, which was intruded by granite porphyry. Several large E-W faults and numerous N-S fractures control the mineralization at sites where they intersect granite-gneiss and schist. The three ore zones are 600–1 200 m long, 3–70 m wide, and extend to depths from 350 to 650 m. These ore zones contain small ore lenses from 50 to 650 m below surface composed of pitchblende, coffinite, molybdenite, and femolite. The ore grade averages 0.075% U but some intersections yield 0.3% U. Molybdenum averages 0.042%.

6.1.5.2 Chaglinskoye

This deposit was discovered 20 km SE of Slavyanskoye and 10 km W of Kokshetau in 1977. In situ resources amount to 14 000 t U with an average grade of 0.069% U contained in 5 vein-type ore bodies. Ore body # 1 contains 30% of the U resources. In addition to U, it contains an average of 0.024% Mo and 0.6–0.8 ppm Au. Ore body # 2 accounts for 60% of the resources of Chaglinskoye.

Chaglinskoye occurs in an area divided into two blocks by the regional, NW-SE-trending, about 70° dipping Dongulash fault. The NE block includes Precambrian diorite and granodiorite of the Zarendin Complex and Vendian metasediments; and the SW block Ordovician-Silurian effusive-sedimentary rocks. Host rocks are Vendian and Lower Paleozoic, weakly-metamorphosed, terrigenous and volcanic sediments altered by albitization and carbonatization. Ore controlling faults trend NW-SE and N-S. Three ore bodies are controlled by the NW-SE-trending contact fault and two ore bodies by N-S-oriented faults. The prevailing U minerals are coffinite and U-Ti phases (brannerite). Pitchblende and uraniumiferous F-apatite are rare. Ore bodies consist of veins and some small lenses; they have lengths from 500 to 4 000 m, widths from 1 to 24 m, and extend to 500–700 m deep.

6.1.5.3 Abayskoye

Abayskoye is located 2–3 km to the south of and may be considered an appendix of Chaglinskoye. The small deposit was discovered in 1979. The ore averages 0.058% U. Three ore zones are identified: *Northwest*, *Central*, and *South*; the latter contains the bulk of the resources.

The deposit is situated in Middle-Upper Devonian redbed molasse near the SE margin of the Kokshetau Graben. Host rocks are grey-green conglomerate and sandstone beds, 10–20 m thick, which are weakly altered by albitization and beresitization. Host sediments are folded into a brachy-fold. Beds trend NW-SE and dip steeply near NW-SE-oriented branches of the Kokshetau fault zone.

The ore zones are from 1.8 to 2.2 km long and from 100 to 800 m wide. Each zone contains as much as six tabular- to lens-shaped ore bodies that range from 700 m to 1 500 m long, 100 m to 600 m wide, and 1 m to 4 m, locally up to 15 m, thick. Pitchblende and sooty pitchblende are the principal U minerals, and locally coffinite. Associated minerals include sulfides and/or selenides of Fe, Cu, Pb, and Zn. Carbonate content of the ore is less than 5%.

6.1.6 Shatsky Ore Field, Northeastern Kokshetau Region

The Shatsky ore field is 140–170 km E of Kokshetau in the Lower Paleozoic East Kokshetau Basin at the boundary with the Precambrian Shatsky Uplift. Four small deposits, *Shatskoye-1*, *Shatskoye-2*, *Glubbinnoye*, and *Agashskoye* (from W to E), are delineated along the sublatitudinal Shatsky fault (Fig. 6.2, Table 6.1). Ore is of the U-Mo vein-stockwork type hosted in albite-carbonate altered rocks. The first three deposits occur in Upper Ordovician volcanics while Agashskoye is within Caledonian granite. All deposits are explored in detail but have not been mined.

Source of information. Petrov et al. 2000.

6.1.6.1 Shatskoye-1

Discovered in 1953, Shatskoye-1 is located some 145 km E of Kokshetau. It contains ore that averages 0.083% U and 0.127% Mo.

The deposit is controlled by the regional WNW-ESE-oriented Shatsky fault zone and consists of an ore zone that occupies intensely brecciated ground between the southern branch of the Shatsky fault and a NW-SE-trending fault. The southern branch separates the area into two blocks; the southern block is characterized by Ordovician andesite-basalt and porphyry, and the northern block by dacite and andesite intruded by Devonian granite.

The ore zone is 2.5 km long and encompasses seven stockwork ore bodies that range in lengths from 200 to 600 m, in thickness from 1 to 17 m, and persist for 100–600 m down-dip. Pitchblende and brannerite are the principal U minerals. Wall rocks are altered by albitization and carbonatization, essentially ankerite.

6.1.6.2 Shatskoye-2 and Glubbinoye

These two deposits are commonly considered as one deposit controlled by the WNW-ESE-oriented Shatsky fault zone as is Shatskoye-1. Glubbinoye is located adjacent to the east of Shatskoye-2. The latter is separated from Shatskoye-1 by a barren interval of ca. 3 km. Resources amount to 600 t U at an average grade of 0.056% U at Shatskoye-2 and to 6 600 t U at an average grade of 0.104% U at Glubbinoye. Shatskoye-2 also contains higher grade U mineralization at a depth of some 1 000 m. Associated Mo and Zr occurs in grades averaging 0.021% and 0.169%, respectively.

These two deposits occur in a tectonic-stratigraphically tripartitioned terrane: a northern block consists of Devonian volcanics, a southern block of Middle Ordovician porphyrite and tuff, and a central block of Ordovician(?) sediments and volcanics. Seven ore zones are identified, which occupy breccia zones, six of which occur in the Central block. These ore zones contain stockwork and lenticular ore lodes that range in lengths from 50 to 1 300 m, in widths from 2 to 40 m, and persist for 30–300 m down dip. Coffinite is the principal uranium mineral.

Glubbinoye occupies an approximately 1 000 m long and 50 m wide stretch elongated along the sublatitudinal Shatsky fault. Host rocks are Upper Ordovician tuffs altered by albitization and carbonatization. Ore occurs in linear stockwork bodies, about 3–5 m thick. Ore persists over a depth interval from 300 m to more than 1 000 m below surface.

6.1.6.3 Agashskoye

Agashskoye is located 2 km NE of Shatskoye-1 and about 170 km E of Kokshetau. The 1974 discovered deposit has in situ resources of 6 170 t U with an average grade of 0.146% U. Associated zirconium grades 0.038%.

Mineralization occurs intragranitic at the periphery of the Agashky granitic massif. The host rock is Caledonian (Silurian) leucogranite with xenoliths of porphyrite and some diabase dikes altered by albitization, carbonatization (ankerite, calcite), and chloritization. The deposit is as much as 970 m long and contains 23 steeply dipping vein- and lens-like ore lodes over a depths interval from 30 to 750 m below surface. The lodes are 0.2–20 m, in average 3 m, thick and 200–300 m long emplaced at the intersection of the E-W-trending Shatsky fault and the NE-SW-oriented Koksorsky fault. Ore bodies are controlled by fracture/breccia zones and faults at the contact of granite with porphyrite xenolith. Mineralization consists of coffinite with minor pitchblende and U-Ti phases (brannerite). Molybdenite is present in small amounts. Ore lode 1, 2, 6, and 14 contain 85% of the above mentioned resources.

6.1.7 Koksengirsky (or Zaozernoye) Ore Field, Central-Eastern Kokshetau Region

This ore field is 130–140 km ESE of Kokshetau, in the eastern segment of the Koksengirsky Trough and includes the

partly mined *Zaozernoye*, depleted *Tastykolskoye*, and the explored *East Tastykolskoye*, *Koksorskoye*, *South Koksorskoye*, and *Boroskoye*, and *Mezhozernoye* deposits, as well as a number of scattered U occurrences (Figs. 6.2, 6.8a, Table 6.1). All deposits have been discovered between 1954 and 1956.

Source of information. Petrov et al. 2000.

Mineralization is of the U-P vein-stockwork type and consists of uraniumiferous F-apatite, U-arshinovite, pitchblende, and U-Ti-phases (brannerite). Deposits are controlled by inter-sections of NW-SE with N to NE-oriented faults. Host rocks include Na-metasomatized rocks of the entire litho-stratigraphic section.

The area is underlain by weakly metamorphosed Middle Ordovician intermediate to mafic volcanics/pyroclastics (inter-layered tuff, andesite, basalt with minor limestone), Upper Ordovician siltstone, sandstone, and hematitic limestone, and unconformably overlying, unmetamorphosed Mid-Upper Devonian molasse redbeds. A number of small stocks (500 m by 1–2 km) of Ordovician granodiorite and monzonite porphyry are also present.

6.1.7.1 Zaozernoye

Zaozernoye is 130 km ESE of Kokshetau. With original reserves of about 20 000 t U, a large part thereof contained in ore body N-3, it is the largest deposit of the ore field. In situ grades average 0.1–0.3% U, up to over 20% P₂O₅, and up to 1 600 ppm REE including 5–10 ppm Sc. Zaozernoye is partly exploited. Mining commenced in 1961 and was suspended in 1992; it reached to a depth of 500 m. Remaining measured and indicated resources (between the –350 m and –1 010 m level) are reported to be 7 500 t U at an average grade of 0.123% U and 19.5% P₂O₅.

The deposit is positioned at the sinuous N to NE-trending Tastykolsky fault (Fig. 6.8a). Impure Upper Ordovician limestones with tuffaceous and argillaceous intercalations (Tastykol Horizon) are the predominant host rocks. Two intercalated intermediate tuff horizons, up to 50 m thick, serve as marker horizons. Beds strike NNE-SSW and dip at 80–85°E in the central part and at less than 45°E in the northern part of the deposit. These rocks underlie Upper Ordovician arkose, sand- and siltstone with intercalated diorite sills (Karamolin Horizon) and overlie Middle Ordovician intermediate to mafic volcanics. Some ore occurs in granite porphyry dikes. Silicate-bearing beds and igneous dikes are albitized.

Uraniferous F-apatite is the predominant ore mineral; coffinite and U oxides are subordinate. Associated minerals/elements include carbonate, chlorite, hydromica, albite, and P, Th, Zr, and F respectively. Two ages of U-P mineralization are recorded. A 420 Ma age is believed to represent syngenetic mineralization that formed along bedding planes in a reef environment at a temperature in the range of 180–220°C. The younger age of 320–280 Ma is thought to reflect secondary enrichment of uranium and phosphate minerals by lateral migration of solutions along

crosscutting fractures orthogonal to the bedding planes of the carbonate layers.

Main ore bodies are of a tabular, peneconcordant shape from which conjugate apophyses branch off (► Figs. 6.8b,c). The distribution and size of ore bodies are controlled by strata-peneconcordant and -discordant cataclastic intervals adjacent to prominent faults.

The deposit extends for 2 000 m in length and 1 000 m in width. The largest ore body, N-3, spreads over 2 000 m long and 50–400 m wide, and persists from 100 to 1 200 m in depth. Ore lodges are about 40 m thick.

6.1.7.2 Tastykolskoye and East Tastykolskoye

Discovered in 1954, these two deposits include three ore-bearing sectors in the southern Koksengirsky ore field: *Central*, *Northern*, and *Eastern*. The Central sector accounts for 80% of the resources with grades averaging 0.105% U, 18.3% P₂O₅, 0.8% Zr, and 0.23% Sr. Tastykolskoye (or Central sector?) was mined by open pit and underground methods until 1981; it produced on the order of 3 000 t U and is depleted.

Mineralization occurs in the eastern and western wings of the Tastykol horst-anticline. Ordovician volcanics constitute the core while limestone overlain by sandstone/siltstone forms the wings of the anticline. Plagiogranite and diorite porphyry dikes are abundant. The steep Tastykolsky fault intervenes between the effusive and the limestone horizons.

Mineralization consists of an P-Zr-U assemblage composed of two mineral associations: arshinovite-uraninite-apatite and apatite-arshinovite-ankerite. These assemblages form lenticular ore bodies that range in lengths from 20 to 500 m, in thickness from 0.5 to 30 m, and persist from 40 to 400 m in depth. The ore lodges occur stratabound in limestone and siltstone adjacent to the contact of these two lithologies.

6.1.7.3 Koksorskoye

Koksorskoye was discovered in the northern Koksengirsky ore field in 1954. Six ore bodies are delineated; ore body 1 contains 70% of the resources, which amount reportedly to 760 t U. Grades average 0.088% U, 4–5% P₂O₅, 0.2% Zr, and 0.18% Sr. U-oxides contain 70% of the U endowment; the remainder is incorporated in Ca-phosphate.

The deposit occurs in the Koksor anticline, composed of Proterozoic(?)–Ordovician volcanics and (meta-)sediments. Tuff and porphyry form the core, and siltstone, limestone, sandstone, conglomerate, and tuff the wings of the anticline. Intrusions include diorite and granosyenite dikes and stocks. The anticline is dissected by the NE-SW-oriented Koksor fault zone and NW-SE-trending, 60–90° dipping faults. The latter control the ore where they cut calcareous sandstone and siltstone of the Tastykol Horizon.

The Koksorskoye ore zone, 1 km long, 120–180 m wide and 250 m deep, includes vein- and/or lens-shaped ore bodies that range from 50 to 700 m long, and persist from 50 to 150 m down dip.

6.1.8 Manybaysky Ore Field, Southeastern Kokshetau Region

The Manybaysky ore field is 210–220 km SE of Kokshetau, at the southeastern margin of the Cambrian-Ordovician *East Kokshetau Basin* adjacent to the Eshkrolmessky block (► Fig. 6.2, ► Table 6.1). It includes the depleted *Manybayskoye* and *Aksu* deposits and the explored *Kerbayskoye*, *Yuzhno (south)-Manybayskoye*, *Bezymannoye*, and *Krugloye* deposits. Ore is hosted by albite-carbonate altered rocks. Three uraniferous

► Fig. 6.8. Kokshetau region, Koksengirsky ore field, **a** schematic geological map documenting the control of U-P deposits by major faults, **b** geological plan of the –190 m level and **c** NW-SE cross-section of the Zaozernoye deposit showing the structure-controlled position of ore bodies in impure Ordovician limestone (after a Boitsov VE 1989; **b, c** Petrov et al. 2000) **U-P deposits:** *Bo* Borovskoye, *Me* Mezhozernoye, *Ko* Koksorskoye, *Ko-S* Koksorskoye South, *Ta* Tastykolskoye, *Ta-E* Tastykolskoye East, *Za* Zaozernoye

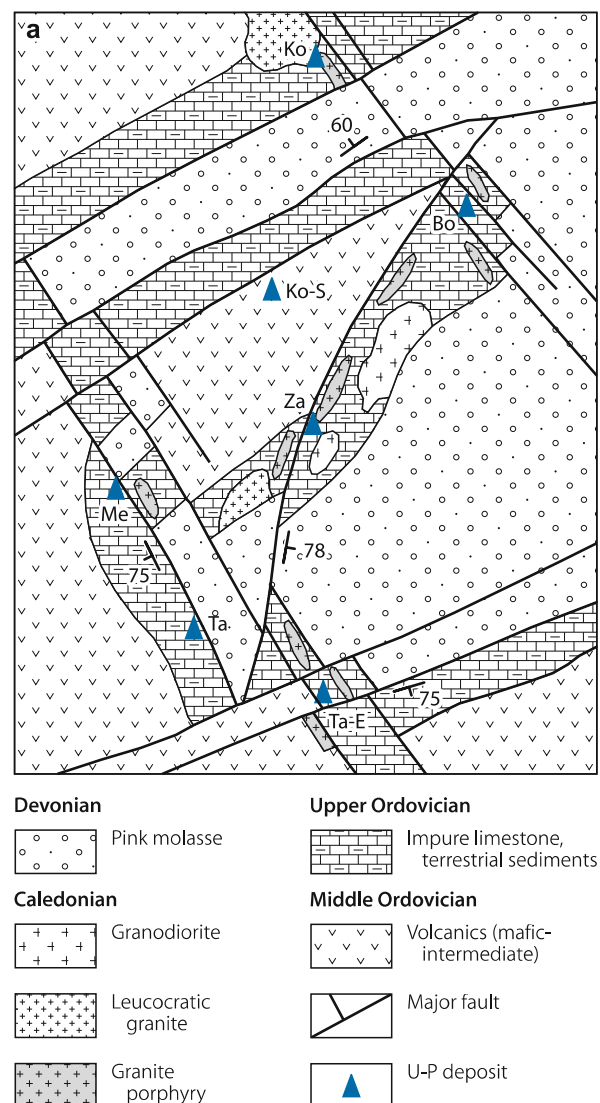
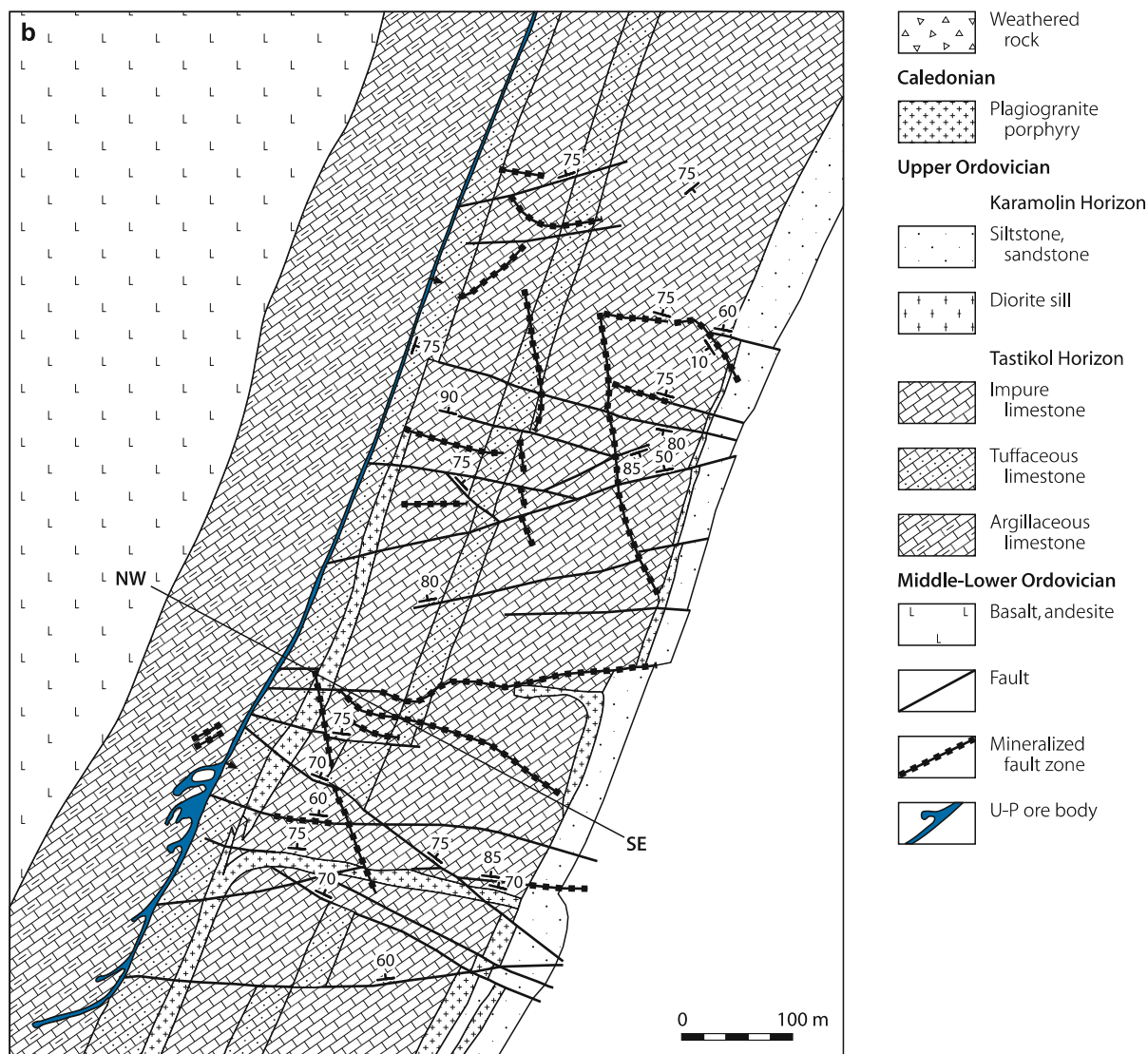


Fig. 6.8. (Continued)



mineral assemblages are differentiated: P-Zr-U (apatite-arshinovite with chlorite-brannerite-coffinite), Mo-U (molybdenite-coffinite-pitchblende), and simple U (pitchblende-coffinite). *Manybayskoye* is an example of the Mo-U type (see below) and *Aksu* of the latter type. Mineralization at *Aksu* consisted of pitchblende veinlets in albitized Ordovician pyroclastic and terrigenous sediments.

Source of information. Petrov et al. 2000.

6.1.8.1 Manybayskoye

This deposit is located 15 km N of Stepnogorsk. Original reserves amounted to some 20 000 t U. The ore grade was 0.086% U and 0.044 Mo. Mining by open pit methods commenced in 1957 and ceased with the depletion of the deposit in 1981.

Host rocks are Middle Ordovician pyroclastic and terrestrial sediments with strata-peneconcordant lamprophyre or diabase sills folded around a NE-SW-oriented axis. The deposit occurs

in the core of the fold where it is cut by intersecting NNE-SSW- and NE-SW-trending faults. Wall rock alteration includes albitization, carbonatization, chloritization, and hematitization.

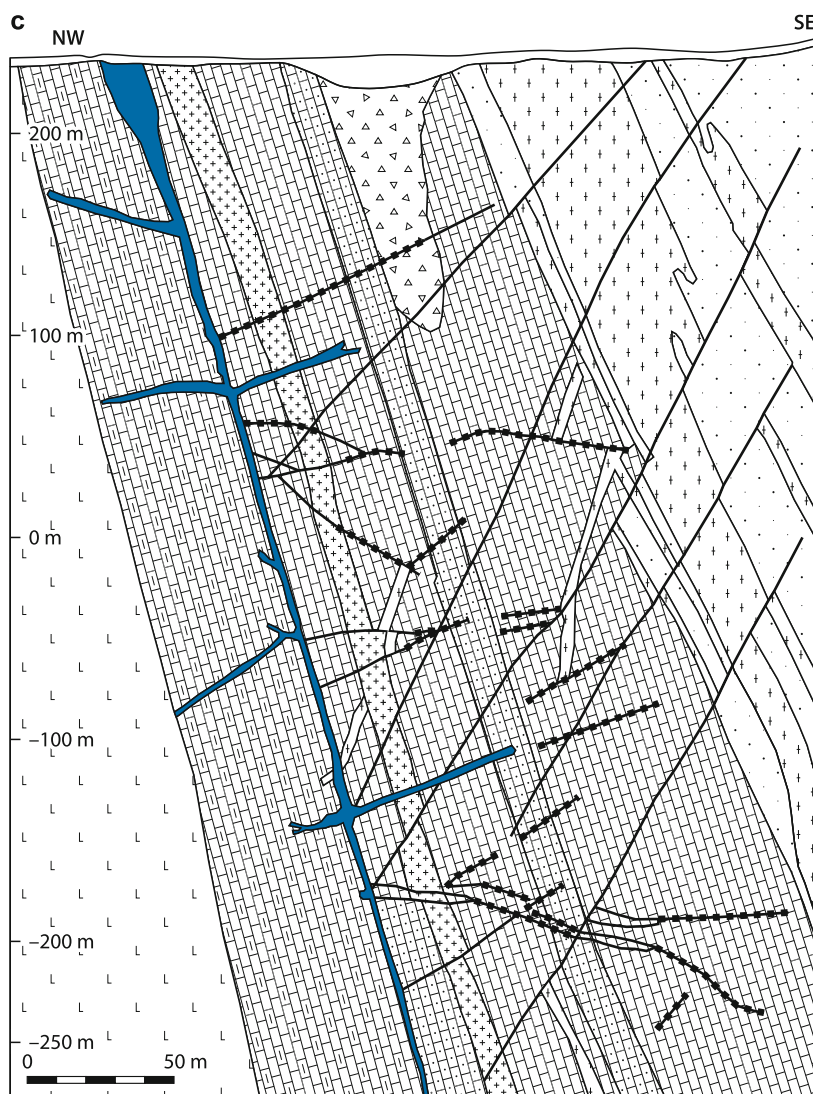
U-Mo minerals constitute the bulk of the ore. One ore body had a more refractory mineralization with uraniferous zircon. Associated minerals include sulfides of Cu, Fe, Pb, Zn, and As. Hydrocarbons occur locally.

Manybayskoye included seven ore lodes within a mineralized column-like body that persists to depths of 1000 m, and to a length of 500 m in the upper part and to 100 m at depths below 700 m. Ore lodes NW, Glavnoye, and SE occur to depths of 200 m, lodes # 1 and # 2 between 200 and 400 m, and lodes # 3 and # 4 below 400 m. The lodes are of stockwork or column-like shape. Siltstone and silt-sandstone are the preferential host rocks.

6.1.8.2 South Manybayskoye

This small deposit, discovered 2 km S of *Manybayskoye* in 1954, consists of four ore bodies with grades averaging 0.08% U and

■ Fig. 6.8. (Continued)



0.02% Mo. The deposit area is underlain by Middle Ordovician sandstone, siltstone, mudstone with interbedded tuff and limestone, which are folded into a syncline. Diorite was intruded into the west wing of the syncline. The country rocks are cut by a regional NE-SW fault and NW-SE as well as N-S faults. Ore bodies are of lenticular shape and occur in tuff and sediments along NW-SE, N-S, and interstratified faults to depths of 250 m. The lodes range in length from 50 to 300 m, in thickness from 0.2 to 3 m, and extend for 100–200 m downdip.

6.1.8.3 Aksu

This small, depleted deposit is located in the southern Manybayskoye ore field. It consisted of vein and lenticular ore bodies that ranged from 15 to 170 m long and from 7 to 9 m thick, extended from 10 to 350 m deep, and averaged 0.102% U, 0.05% Mo, 0.02% Zr, and 0.08% Sr. The NE-SW-trending Aksu fault controls the position of the lodes in folded Ordovician carbonaceous-siliceous sediments close to the contact with porphyry dikes.

6.1.9 Shokay Zone, Olenty-Seletinsk Area, Eastern Kokshetau Region

The Olenty-Seletinsk area is within the Shokay metallotectonic zone in the eastern Kokshetau Massif near the margin of the Pri-Irtysh Basin (► Fig. 6.2, ► Table 6.1). A number of basal-channel sandstone-type deposits are reported including *Semizbay*, *Seletinsk*, and *Kiziltuk*. Mineralization occurs in paleovalleys filled with Lower Cretaceous–Upper Jurassic alluvial-fluvial sediments and buried under as much as 100 m thick Cretaceous and younger sediments.

6.1.9.1 Semizbay

Semizbay is a basal-channel sandstone-type deposit located some 250 km ESE of Kokshetau and 60 km E of Stepnogorsk. Original resources are reported to total 17 000 t U at an average grade of 0.057% U (based on a minimum grade of 0.01% U and a minimum grade-thickness product of 0.04 m-%), almost two thirds of which are thought to be recoverable by in situ leaching

methods. The deposit was discovered in 1973 and partly exploited by ISL techniques from 1982 to 1990.

Sources of information. The following description is primarily based on Poluarshinov and Pigulski (1995).

Geological Setting of Mineralization

U deposits occur in a complexly branched paleochannel system, which was incised into the Proterozoic-Paleozoic basement of the eastern Kokshetau Massif and which dewatered eastwards to the Pri-Irtysh Basin (now the West Siberian Lowlands) during Late Jurassic and Early Cretaceous time. Channels extend for tens of kilometers from the basin into the massif. A regolith profile of the crystalline rocks attests to intense weathering prior to the deposition of the Late Jurassic and younger sediments.

Semizbay is in the upstream (apex) part of the Semizbay paleovalley, about 25 km inland from the eastern edge of the Kokshetau Massif. At the site of the deposit, the channel trends curvilinear E-W and is incised for up to 150 m into granites of the Zhaman-Kotass Massif (Figs. 6.9a–c).

Basement rocks at and around the deposit are dominated by Middle to Upper Devonian alaskitic granite and granite porphyry dike swarms, which were intruded into Silurian to Lower Devonian biotite granite and Upper Ordovician to Lower Silurian diorite and granodiorite. Andesite porphyry, andesite basalt and related tuffs, and some Lower Paleozoic metasediments occur locally.

Valley fill consists of the up to 100 m thick Lower Cretaceous–Upper Jurassic Semizbay Formation (Sm) of fluvial-alluvial origin. Five horizons are distinguished. They are, from top to bottom (Fig. 6.9c):

- mottled argillaceous conglomerate and sand with interbedded clay-sand lenses (“slope facies”, Sm₂),
- grey clay-silt flood plain facies with intercalated sand and mud-silt lenses (Sm₂),
- grey clay-silt flood plain facies with some sandy intercalations (Sm₃),
- grey sand with intercalated mud-silt lenses (Sm₃), and
- grey gravel beds with interbedded sand lenses (Sm₁).

A conterminous clayey layer of the Lower Cretaceous Kijalin Formation had originally covered the sediments of the Semizbay Formation but it is now, to a large extent, eroded. It provided a regional aquiclude additional to upper Campanian argillaceous beds.

Host Rock Alterations and Mineralization

Besides pre-Upper Jurassic weathering of the basement, the basal part of the Semizbay Formation exhibits early oxidation documented by Fe-hydroxides and bleaching associated with destruction of organic debris. Subsequent reduction is reflected

by Fe-sulfides (pyrite). Post-ore alteration features include carbonatization and chloritization. The temperature of carbonate formation is given as 150–200°C by Poluarshinov and Pigulski (1995).

The principal uranium minerals are coffinite, pitchblende, and sooty pitchblende. Associated elements include Se, Ge and substantial amounts of scandium. Carbonate and chlorite are the main gangue minerals. Ore texture is of a disseminated nature with U primarily contained in the matrix of sandy facies. Isotope dating of pitchblende yields ages of 120–110 Ma, which is considered the principal ore-forming period.

Shape and Dimensions of Deposits

Semizbay consists of a number of ore bodies distributed over a 15 km long and 500 m wide channel section. The ore bodies occur intermittently in two horizons (Sm₁² and Sm₂¹) separated by a 10–15 m thick argillaceous horizon (Sm₁³). The upper horizon is 30–35 m thick and carries ore in basal grey sand lenses. The lower horizon is 15–20 m thick and contains several superimposed ore bodies in grey sand beds (Figs. 6.9a,b).

Mineralization forms ore bodies of discontinuous, almost horizontal, stratiform ribbons, elongated lenses, or tabular and roll- or pocket-like bodies. Thicknesses of ore bodies range from tens of centimeters to 7.5 m and average 2.1 m. Ore bodies are from about 500 m to 5 km long, 20–80 m rarely up to 200 m wide and occur at depths from 50 to 150 m below surface. Grades are highly variable ranging from several tens of ppm to 0.5% and locally up to 8% U; the average is about 0.05–0.07% U.

Sources of Uranium

Alaskitic granite and granite porphyry contain background values of 3–10 ppm U and localized concentrations of syngenetic uranium. Other elements like Sc, Be, Sn, Mo, and Y are present in anomalous amounts. At least some of the uranium is present as uraninite, i.e. in leachable form. As such these rocks are thought to be a viable source of uranium for the formation of the deposit.

Ore Controls and Recognition Criteria

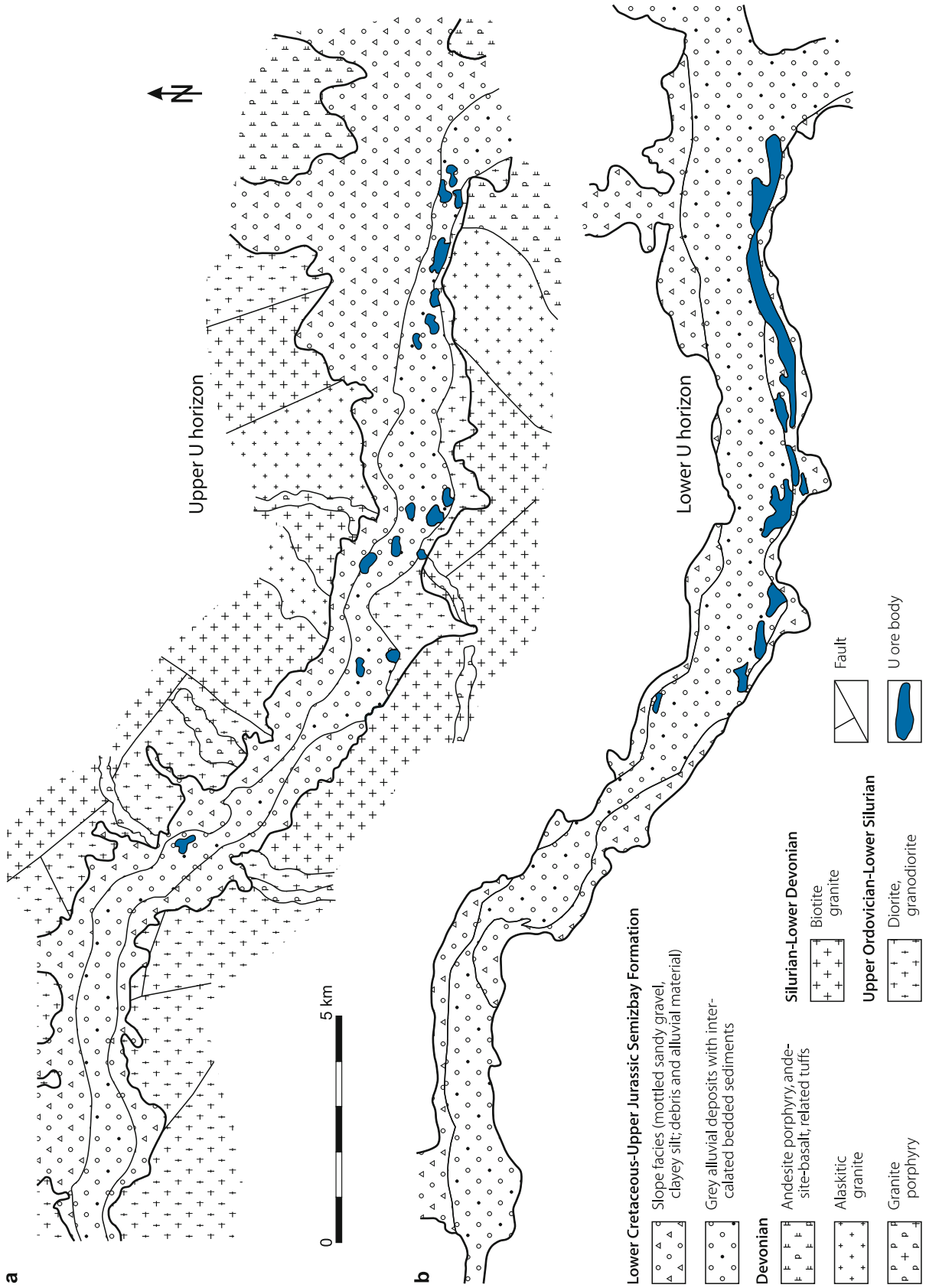
Significant ore controlling and recognition criteria of the basal sandstone-type Semizbay ore bodies are as follows:

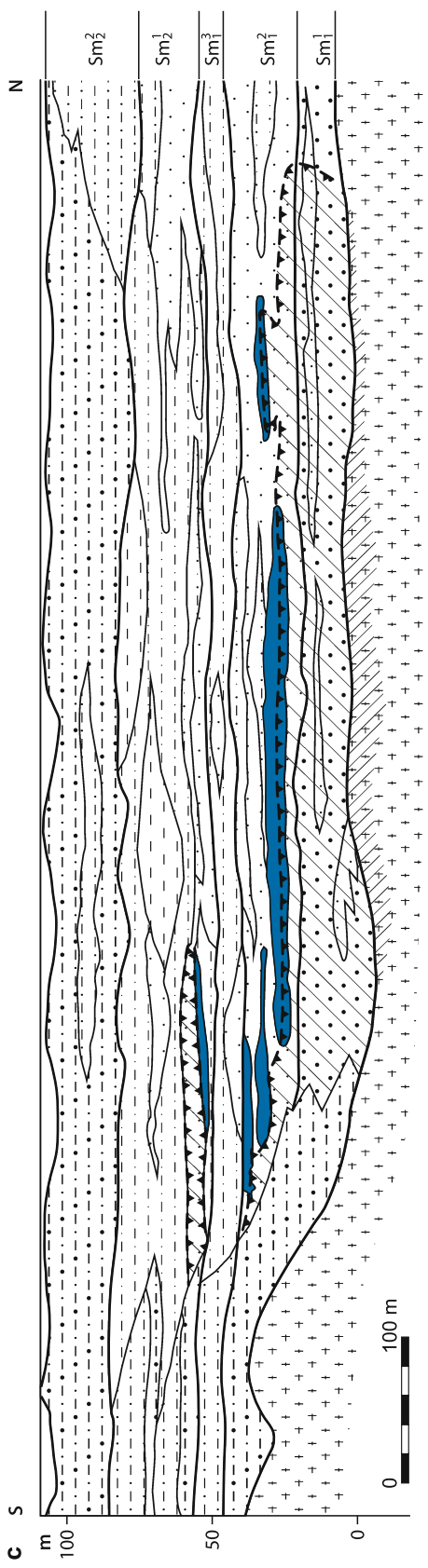
Host Environment

- paleovalleys predominantly incised into leucocratic granitic basement
- alternating permeable and more or less impermeable fluvial beds in paleovalleys
- intraformational hiatuses
- valley fill covered by impermeable clay blanket
- host rocks consist of carbonaceous, reduced sandy facies
- reductants in form of carbonaceous matter and sulfides

Fig. 6.9.

Kokshetau region, Semizbay, geological maps of two levels of the U mineralized Lower Cretaceous-Upper Jurassic paleovalley. The Semizbay Valley is incised into Lower Paleozoic slightly metamorphosed clastic sediments cut by Caledonian intrusions. U ore lenses are of basal-channel sandstone type and occur at two levels preferentially in the lateral basal part of the channel as documented in **a** (upper) and **b** (lower level), and along intraformational oxidation zones, as shown in section ϵ (after Poluarshinov and Pigulski 1995)





Upper Ordovician-Lower Silurian

- | | | | | | |
|--|--|--|------------------------------------|--|---------------------------------|
| | Overburden | | Alluvial facies | | Upper Ordovician-Lower Silurian |
| | Mixed clayey gravel, sand and assorted temporary facies | | Gravel | | Diorite, granodiorite |
| | Mixed sandy and clayey fan sediments | | Sand | | Paleoweathering zone |
| | Lumped clay of drying reservoirs (with shrinkage cracks) | | Sandy clay-silt of stagnant waters | | Oxidation zone |
| | | | Silt-clay of flood plains | | U ore body |

- arid climate episodes permitting liberation and transport of U into valley sediments

Alteration

- early oxidation of valley fill reflected by oxidation zones in basal channel facies
- subsequent reduction of alluvial sediments reflected by bleaching associated with destruction of organic matter
- ore-related sulfidation
- post-ore carbonatization (calcite)

Mineralization

- coffinite, pitchblende, sooty pitchblende
- associated elements include Se, Ge, Re, Sc and Y-bearing minerals
- gangue minerals are mainly carbonates and chlorite

Metallogenetic Aspects

As may be deduced from the works of Poluarshinov and Pigulski (1995) and others, the metallogenesis of the Semizbay and other basal-channel sandstone-type deposits in the Kokshetau Massif may have occurred as follows:

During periods of Mesozoic tectonic activation and arid climate, uranium was liberated from granitic basement rocks. Quiet interludes between tectonic activities permitted a steady infiltration of oxygenated, uranium-bearing waters into depressions. Favorable geologic-structural and paleohydrological conditions for ore formation existed in smaller artesian depressions, which contained: (1) permeable sandy horizons permitting the percolation of fertile solutions and (2) reducing agents in the sedimentary sequence such as organic material for uranium reduction and deposition. So-called “ancient” zones of stratiform oxidation as they are retained in the basal part of the Semizbay Formation were generated in pre-Cretaceous time. Uranium was deposited in form of coffinite (and black products?) at the geochemical interface of the “ancient” oxidation zones. Subsequently some uranium was redistributed by a high temperature carbonatization event of 150–200 °C.

An alternative model assumes a polygenetic origin of the Semizbay ore. Fluid inclusions/homogenization and decrepitation analyses indicate a high crystallization temperature of about 150 °C for post-uranium calcite, which is thought to suggest the involvement of hydrothermal fluids. Such solutions presumably migrated along faults and permeable beds and introduced the bulk of the uranium. A later exogenetic process generated stratiform oxidation and redistributed some of the preexisting uranium.

6.1.10 Other Uranium Occurrences in the Kokshetau Region

6.1.10.1 Voskhod, NW Kokshetau Region

This small deposit was discovered at the western margin of the Voladar metallogenetic zone in the NW Kokshetau Massif at

the end of the 1950s. The area is underlain by Lower-Middle Cambrian schist, gneiss, and amphibolite intruded by porphyry, lamprophyre, and granodiorite dikes of the Baksan Massif. Vein-stockwork ore bodies occur at the intersection of E-W with NW-SE faults. Amphibolite and granodiorite altered by beresitization (quartz-chlorite-sericite) are the preferential host rocks (Petrov et al. 2000).

6.2 Pricaspian (or Mangyshlak) Uranium Region, West Kazakhstan

The Pricaspian uranium region is located to the east of the town of Aktau (formerly Shevchenko) on the Mangyshlak Peninsula at the northeastern coast of the Caspian Sea, western Kazakhstan (Fig. 6.1). Within this region, two ore fields are established. The *Karagiin* ore field contains the partly mined deposits *Melovoye*, *Tasmurun-Ashisai*, *Taybagar*, *Tomak*, and *Sadyrnyn* (Fig. 6.10), and the *Karynzhyark* ore field with three subeconomic occurrences, located some 80 km to the southeast of the *Karagiin* field.

Ore deposits of the Pricaspian region consist of uraniferous mineralization associated with fossil fish bones hosted in pyritic clays. These deposits are classified as organic phosphorous type, a unique type of U deposits recorded only near the northern Caspian Sea in western Kazakhstan and in the Ergeninsky region, Kalmyk Autonomous Republic in Russia.

Remaining resources of the Pricaspian region (status 1995) are 64 400 t U in the \$80–130 per kg U RAR category, 43 800 t U of which are contained in *Melovoye*. Other deposits in the *Karagiin* ore field have resources varying between 4 000 and 9 000 t U.

Ore grade averages 0.04–0.06% U and although this grade is very low, the bone detritus is easily separated from the matrix and yields a concentrate with a U content 2–3 times higher and a phosphate content of about 30% P₂O₅. In addition to the uranium and phosphorus, rare earth elements and scandium were recovered from the detritus.

Uranium was discovered in 1954. Mining started in 1959 and lasted until 1993 when economic reasons forced the shut down of operations. Exploitation was by open pit methods with a total production of about 15 000 t U. Uranium recovery was by means of ion exchange in a mill near Aktau situated 20 km W of the *Melovoye* deposit. The “Pricaspiski Mining-Metallurgical Combinat” was the operator until the early 1990s when it was reorganized into the “Joint Stock Company KASKOR” (OECD-NEA/IAEA 1993, 1995).

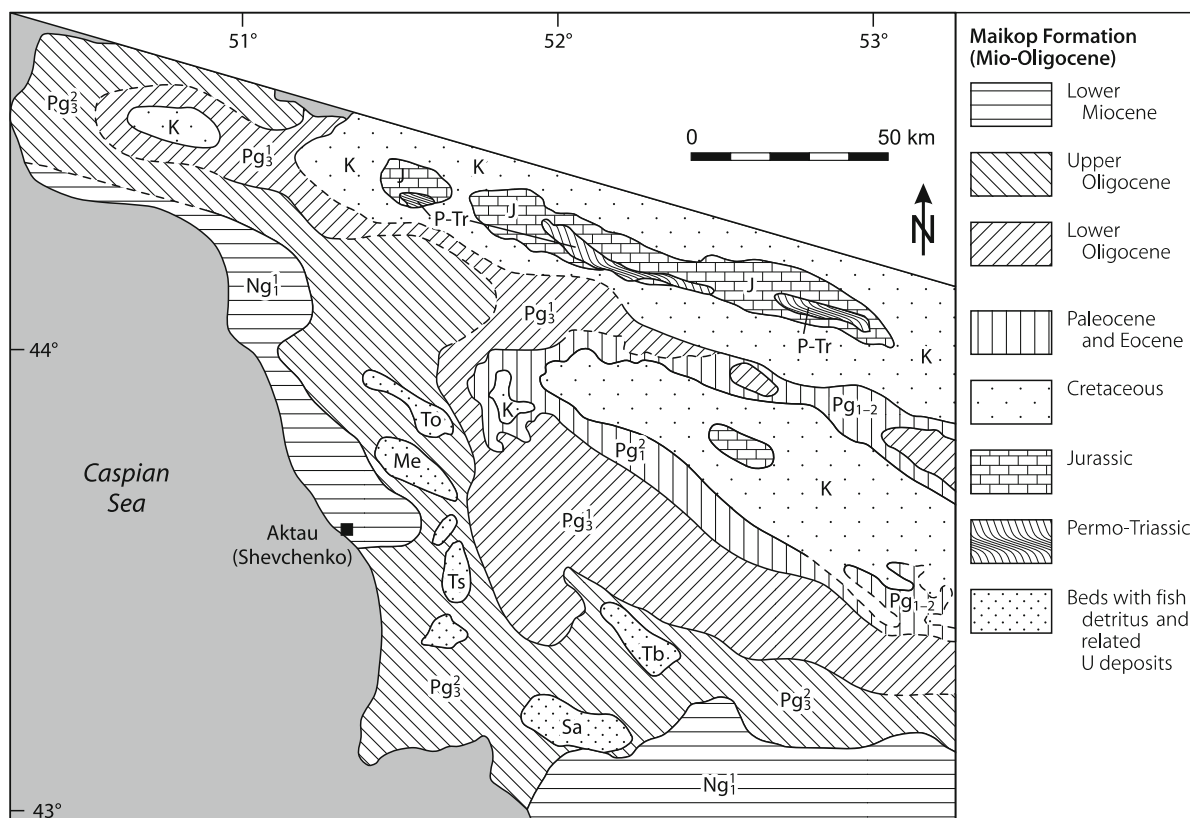
Sources of information. Abakumov (1995), Laverov et al. (1992b, c), OECD-NEA/IAEA (1993, 1995, 1997), Petrov et al. (1995), Stolyarov and Ivleva (1995).

Regional Geology and Mineralization

The litho-stratigraphic profile of the *Karagiin* ore field comprises Neogene to Cretaceous marine sediments resting upon a

Fig. 6.10.

Pricaspian region, Karagiin ore field. Geological map with location of U deposits (Neogene-Quaternary cover not shown). Mineralization consists of stratiform accumulations of uraniferous, phosphatized fish bone detritus in pyritic clay horizons of Oligocene age (after Stolyarov and Ivleva 1995) U deposits: Me Melovoye, Sa Sadyrnyn, Ta Taybagar, To Tomak, Ts Tasmurun



basement of folded Jurassic and Permo-Triassic sediments. The cover sequence includes, from top to bottom:

- Neogene-Quaternary, 10–90 m thick clay strata with interbedded marl
- Lower Miocene to Lower Oligocene Maikop Formation, over 800 m thick, divided into
 - Lower Miocene Kashkaratin Member, up to 100 m thick (mud, clay)
 - Upper Oligocene Karagiin Member, up to 400 m thick (U)
 - Middle Oligocene Kenjalın Member
 - Lower Oligocene Uzunbas and Kuyules Members
- Paleocene-Eocene and Cretaceous sediments

The mineralized Karagiin Member is subdivided into three units with the following characteristics:

- upper unit: up to 80 m thick, greenish-grey clay with disseminated pyrite concretions and intercalated mud beds
- middle (or fish) unit: 40–150 m thick, dark clay with beds enriched in pyrite and melnicovite concretions (0.01–0.05 mm in diameter), fish bones, and fish scales (mainly herring relics)
- lower unit: up to 90 m thick, greenish-grey, partly carbonatic clay with rare shell and “mud eater” fossils

Mineable U mineralization is restricted to the middle (fish) unit of the Karagiin Member. It contains between one and

four superjacenty-stacked, uraniferous, phosphatic fish bone horizons which, in some deposits, feather out into several beds to form a horse-tail pattern (Figs. 6.11a–c).

Uraniferous beds are from 0.1 m to 11 m thick and extend laterally for up to 18 km in length and several kilometers in width (details see at individual deposits). Mineralization is found from surface (Tasmurun, Sadyrnyn) to 240 m deep (Taybagar).

Individual fish beds contain from few percent to 75% fish detritus, 1–25% P_2O_5 , 10–60% sulfides (5–30% S_{py}), and concentrations of U, La, Sc, Y, lanthanides (except promethium), Co, Ni, and Mo. Total REE content varies between 0.5 and 2.1%. Scandium ranges from 13 to 77 ppm and uranium from 1 ppm to a few percent averaging 0.02–0.06% U. Average values for deposits are given in Table 6.3. Phosphate is present in fossil fish bones and as a rock constituent. Uranium, scandium, and REE are primarily incorporated in phosphatized fish bone detritus.

The uranium-bearing unit extends southeastward beyond the Pricaspian mining district, but occurs at greater depth. It is also found to the northwest of the Caspian Sea where U occurrences are reported from the Kalmyk Autonomous Republic.

Principal Ore Controls and Recognition Criteria

Significant ore-controlling parameters or recognition criteria of the major deposits in the region, include:

Table 6.3.

Pricaspian region, Karagiin ore field. Average mining grades of deposits (Stolyarov and Ivleva 1995)

Deposit	Average content												
	U (%)	RE ₂ O ₃ (%)	Mo (%)	Ni (%)	Co (%)	Sc (ppm)	Re (ppm)	P ₂ O ₅ (%)	S _{py} (%)	Al ₂ O ₃ (%)	U/P ₂ O ₅	RE ₂ O ₃ /P ₂ O ₅	RE ₂ O ₃ /U
Melovoye	0.042	0.18	0.022	0.060	0.015	27	1.0–2.0	4.32	11.1	12.5	0.010	0.042	4.28
Tomak	0.062	0.26	0.014	0.067	0.017	22	0.3–0.6	8.50	11.2	11.5	0.007	0.031	4.19
Taybagar	0.043	0.21	0.015	0.057	0.013	–	–	8.00	9.3	10.0	0.005	0.026	4.88
Tasmurun	0.040	0.15	0.042	0.075	0.026	15	–	5.16	15.3	7.0	0.007	0.026	3.75
Sadyrnyn	0.022	0.10	0.035	0.050	0.017	13	–	3.14	9.5	12.0	0.007	0.032	4.54

Host Environment/Host Rocks

- Argillaceous marine sediments of Tertiary age filling gentle basins
- Host formation of 20–60 m thick pyritic clay unit containing intercalated beds with abundant fish remains

Mineralization

- U associated with Sc and REE incorporated in phosphatized fossil fish bones and scales
- Low U ore grades (<0.06% U)
- Variable phosphate content ranging from 1 to 25% P₂O₅ averaging 3–8.5% P₂O₅
- High sulfide content ranging from 5 to 30% S_{py} averaging 9–15% S_{py} in various deposits
- REE, phosphate, and pyrite recoverable as byproducts to uranium
- Large lateral extension of mineralized beds, up to 70 km² in size
- 0.1–1.1 m thick argillaceous, uraniferous fish bone beds alternating with clay beds
- Feathering out of fish bone horizons in horse-tail pattern

Metallogenetic Concepts

A diagenetic concentration of uranium and other metals by sorption on phosphate or phosphatized fish bone detritus is generally accepted as the ore-forming mechanism. Sea water is thought to be the source of the ore-forming elements. The enormous accumulation of fish bone debris is attributed to a marked increase in hydrogen sulfide in seawater resulting in a catastrophic impact on the fish population.

6.2.1 Karagiin Ore Field

This ore field encompasses five U deposits: *Melovoye*, *Tomak*, *Taybagar*, *Tasmurun*, and *Sadyrnyn*. *Melovoye* differs from the other deposits by its large size and ore characteristics. Sediments were deposited in a deep sea environment, which was obviously more favorable for U, REE, and Sc accumulation in bone phosphate, and for Re incorporation in sulfides than in the *Tomak* and *Taybagar* deposits. Sedimentation forming the latter two deposits occurred coeval with that at *Melovoye* but under shallow marine conditions. This resulted in a doubling of the content of fish bone debris in ore beds as reflected by the phosphate

content, and locally in a higher carbonate component. But the U tenor did not rise in proportion as illustrated by the U/P₂O₅ ratio decreasing by 30–50%, from 0.01 at *Melovoye* to 0.007 at *Tomak* and to 0.005 at *Taybagar*. Horse-tail patterns of ore beds are typical for each of the three deposits.

Tasmurun and *Sadyrnyn* in the southeastern part of the ore field consist of the most recent fish bone-bearing sediments. The ore bed configuration in these deposits is commonly of a simple tabular or lenticular nature. Grades of ore-forming elements are lower than in the afore-mentioned deposits.

6.2.1.1 Melovoye

Melovoye is located some 10 km NE of Aktau. Mining was by open pit methods and lasted from 1959 to 1993. Remaining reserves are 43 800 t U (grades are given in Table 6.3). Fish bone concentrate contains 0.185% U.

Melovoye is 18.5 km long, up to 7 km wide, and covers an area of 88.6 km². Uranium occurs in four horizons with abundant fish bones within a 20–60 m thick pyritic clay unit of the middle Karagiin Member. The horizons join to the south and east and feather out in horse-tail fashion in opposite directions (Fig. 6.11). A 10–60 m thick clay horizon overlies, whereas clayey sediments with rare fish bones and other fossils underlie, the uranium bearing unit. The sequence rests on silty and carbonatic clays of the Middle Oligocene Kenjalın Member.

Dimensions of the ore beds are as follows:

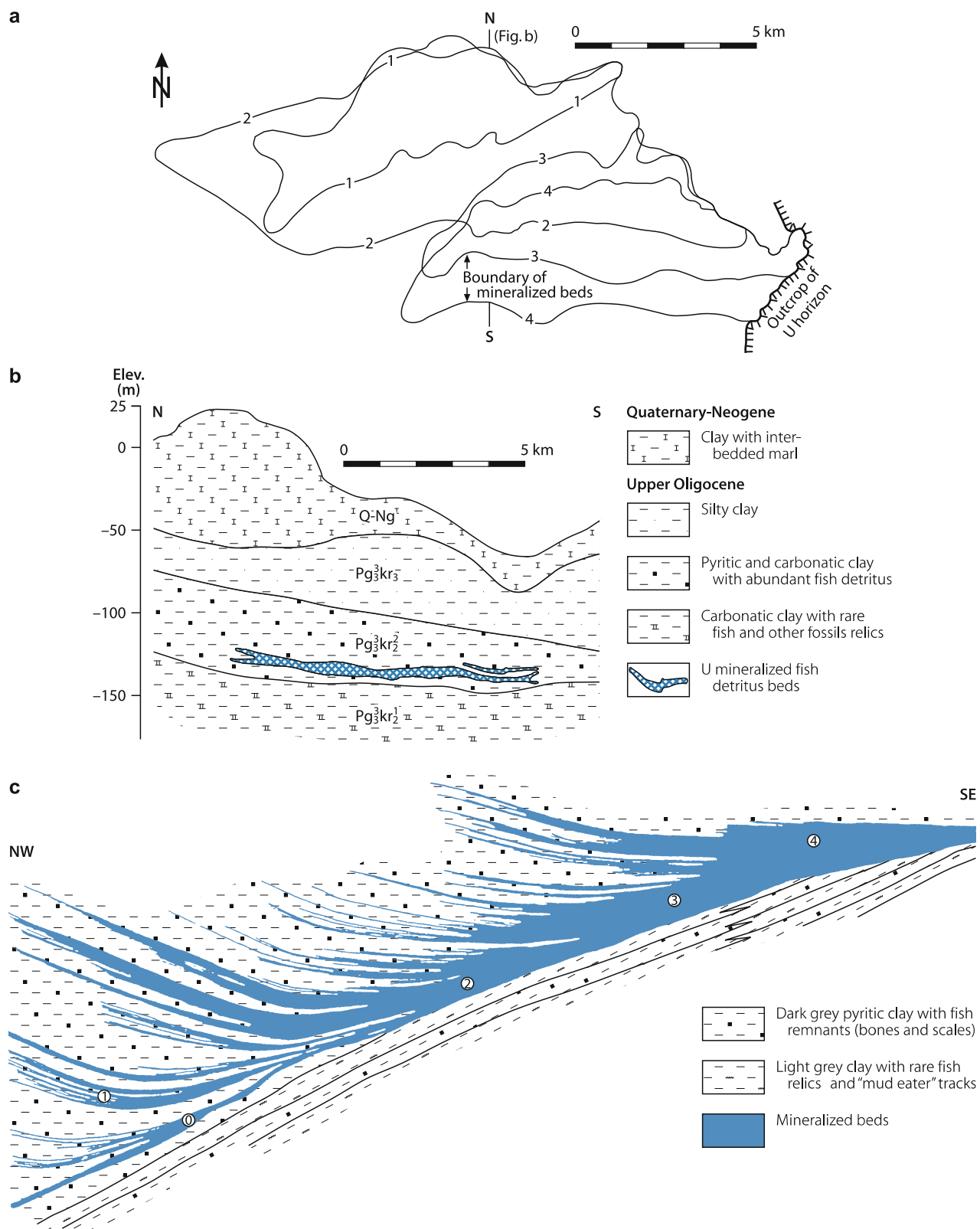
- *Ore bed 1*, situated in the NW part of the deposit, is 0.2–0.6 m (av. 0.5 m) thick, 11 km long, up to 3 km wide, and covers an area of about 20 km². Mineralization occurs in up to 10 cm thick laminae. Reserves are insignificant.
- *Ore bed 2* is from less than 1 m to several meters thick, 17 km long, up to 6 km wide, and covers 70 km². It contains the principal U and REE reserves.
- *Ore bed 3* (in SE part of the deposit) is 0.3–2.5 m thick, 11 km long, up to 4 km wide, and covers 25 km².
- *Ore bed 4* (in SE part of the deposit) is 0.5–1.5 m thick, 12 km long, up to 4 km wide, and covers 33 km².

6.2.1.2 Tomak

Tomak is situated some 20 km NE of Aktau and was mined by open pit methods until 1993. Remaining resources are less than

Fig. 6.11.

Pricaspian region, Melovoye deposit. **a** Distribution and size of the four U mineralized clay beds with fish detritus in the Upper Oligocene Karagiin Member, Maikop Formation; **b** litho-stratigraphic N-S section, and **c** schematic longitudinal NW-SE section documenting the horse-tail structure of mineralized beds (after Stolyarov and Ivleva 1995)



7 000 t U (grades are given in [Table 6.3](#)). Tomak covers an area about 20 km long and 1 km wide in which four ore horizons occur. The sediments were deposited in a more shallow marine environment than at Melovoye and a different ore composition resulted. U and REE contents of bone detritus are comparably higher, and clay beds are partly dolomitic.

6.2.1.3 Tasmurun

Tasmurun (also Tasmurun-Ashisai) is located about 13 km ESE of Aktau. Resources are less than 5 000 t U (grades are given in [Table 6.3](#)). The deposit consists of several ore bodies. The main ore body is 8 km long, 0.6–2.5 km wide and covers an area of 24.4 km². It is of tabular morphology, 0.7–1.5 m thick in the central part but thinning to 0.3–0.4 m in peripheral segments. Fish bones are evenly distributed. Ore composition differs from that of Melovoye by a 30% lower U/P₂O₅ ratio and a 40% higher sulfide content.

6.2.1.4 Taybagar

Taybagar is situated about 35 km ESE of Aktau. Resources are less than 7 000 t U (grades are given in [Table 6.3](#)). Fish bone concentrate contains 0.11% U.

Taybagar covers an almost 20 km long and 1–7 km wide area in which four ore horizons occur. They finger out in a SE direction associated with a thinning of mineralized beds from 7–8 m down to 0.25 m. Mineralized beds are always separated by a clay horizon a few meters thick. The carbonate content in lower beds is low but increases upward to between 16 and 39% CO₂ in the upper bed whereas the sulfide content is reduced to 3.7% S (in pyrite).

6.2.1.5 Sadyrnyn

Sadyrnyn is located about 35 km SE of Aktau. Resources are between 4 000 and 9 000 t U (grades are given in [Table 6.3](#)). Sadyrnyn contains several tabular or lenticular ore beds, which are spread over an area more than 20 km long in a NW-SE direction. Thicknesses of the ore beds average 0.8 m but vary between 0.2–0.3 m in the central part and 1.5–1.8 m in the SE sector where they feather out.

6.3 Chu-Sarysu Basin, South-Central Kazakhstan

The Chu-Sarysu Basin is located in south-central Kazakhstan ([Fig. 6.1](#)). It is as much as 250 km wide and extends for more than 600 km from the foothills of the Tien Shan mountains to the south and southeast, and merges into the flats of the Aral Sea depression to the northwest. The northern and western boundary coincides roughly with the course of the Sarysu River while the Chu river flows across the southern part of the basin. The basin is bounded to the SW by the NW-SE-trending

Karatau mountain range, which separates the Chu-Sarysu Basin from the southwesterly located Syr-Darya Basin (see next chapter). These two basins originally formed a single basin before they were separated by periodical uplifts of the Karatau Range. The separation took place after the formation of the U deposits.

Yazikov (2002) reports a total inventory of 973 000 t U for the basin. According to Abakumov (1995) (remaining?) resources amount to 221 000 t U in the RAR + EAR-I <\$80 per kg U cost category, 74 000 t U of EAR-II, and 20 000 t U of prognosticated resources. Ore grades average from 0.02 to 0.07% U.

Most deposits are grouped in two districts: the *Kenze-Budenovskaya District* in the central-western basin, and the *Uvanas-Kanzhugan District* in the central-southern basin. Isolated occurrences include *Karakoyn* in the northern, *Sholak Espe* in the central, and *Bars* in the southern basin ([Figs. 6.1, 6.12](#)).

U mineralization is controlled by dynamic redox fronts in arenite strata. Deposits are therefore classified as sandstone-rollfront type. Some ore bodies are of the tabular sandstone type.

Uranium was discovered in the Chu-Sarysu Basin in the 1960s, first at Uvanas and Zhalspak. When conventional mining proved unfeasible, ISL techniques were tested at the Uvanas deposit in 1969–1971. Positive results triggered more intensive exploration that led to additional discoveries: Kanzhugan in 1972, Mynkuduk in 1973, and, later in the 1980s, Inkay, Budenovskoye, Akdala, Sholak Espe, and Karakoyn (see Sect. *Historical Review*).

Exploitation has been only by ISL techniques to-date. In 2004, six deposits were in production. Uvanas was the first operation; it started in 1977 and was followed by Mynkuduk in 1978, Kanzhugan in 1982, Inkay, Moynkum, and Akdala in 2001. Total production was some 27 000 t U through 2005.

Operators of these production facilities are the Kazatomprom (formerly KATEP) subsidiaries: Mining Company Stepnoye (Uvanas and Mynkuduk-Vostochny/East) and Centralnoye (Kanzhugan and Moynkum south or site 1), and three joint ventures of Kazatomprom with Cogema (Katko Co.; Moynkum Central and North or sites 2 and 3), and Cameco (Inkay), and the Bepak Dala J.V. at Akdala. Nominal total production capacity is 4 100 t U yr⁻¹ (OECD-NEA/IAEA 2005).

Sources of information. The description presented hereafter is based largely on Abakumov (1995), Fyodorov (1997, 2002, 2005), IAEA (1995), Kislyakov and Shchetochkin (2000), OECD-NEA/IAEA (1995–2005), Petrov et al. (1995), Shakhverdov (2003), Shchetochkin and Kislyakov (1993), Shor and Kharlamov (2003), Yazikov (2002), Zinchenko and Stoliarenko (2002), as well as pers. commun. by Yazikov, Petrov, staff of Central Mining Co./Kazatomprom 2003, and Boitsov VA and Catchpole 2005, unless otherwise stated.

Regional Geological Setting of Mineralization

The Chu-Sarysu Basin is located at the eastern margin of the Turan Platform. The basin is bounded to the southwest by the NW-SE-trending Big Karatau Uplift, a mountain range composed of Proterozoic to Ordovician crystalline schists unconformably overlain by Carboniferous and Devonian limestone and

sandstone. The Chuily-Kendyktas Uplift forms the northeastern, the Kirgizian Range (a branch of the Tien Shan mountains) the southern, and the Ulatau Massif the northern limit. The basement and surroundings are part of the Caledonian Orogen.

The basin is filled with up to 2 000 m thick Quaternary to Cretaceous, mainly continental and minor shallow marine sediments, which are divided by a major unconformity into two stratigraphic-structural units. The *upper unit* consists of Quaternary-Neogene sediments up to several hundreds of meters thick. The uranium-bearing, up to 500 m thick *lower unit* includes Eocene to Upper Cretaceous, largely unconsolidated alluvial/fluvial, deltaic, and lacustrine sediments deposited on a large alluvial plain at the margin of the huge Turan Platform. During the waning period of the Eocene, the region was flooded and shallow marine, grey-green, argillaceous sediments as much as 150 m thick were laid down. Subsequent orogenic activity, which was

strongest during the Oligocene, caused uplift of basement blocks such as the Tien-Shan mountains located to the south of the basin. Associated erosion led to the deposition of pink-colored continental facies of the upper unit upon the Paleogene unconformity. It was during this period that the basin became artesian.

The following *litho-stratigraphic profile* provides a synopsis of the sedimentary facies in the central basin based on Petrov et al. (1995) (from surface downwards):

Upper Unit

- *Quaternary-Pliocene*: few meters to 200 m thick, sand and clay-silt
- *Pliocene-Miocene* Todusken Formation: 20–300 m thick, limy clay overlying sand beds with minor clay-silt lenses
- *Oligocene-Miocene* Betpak dala Fm: 10–50 m thick, sand and limy clay (pink series)

Fig. 6.12.

Chu-Sarysu and Syr Darya Basins, **a** generalized geological map and **b** SW-NE cross-section with location of redox fronts and related U deposits (after a Fyodorov 2002; b Petrov et al. 1995)

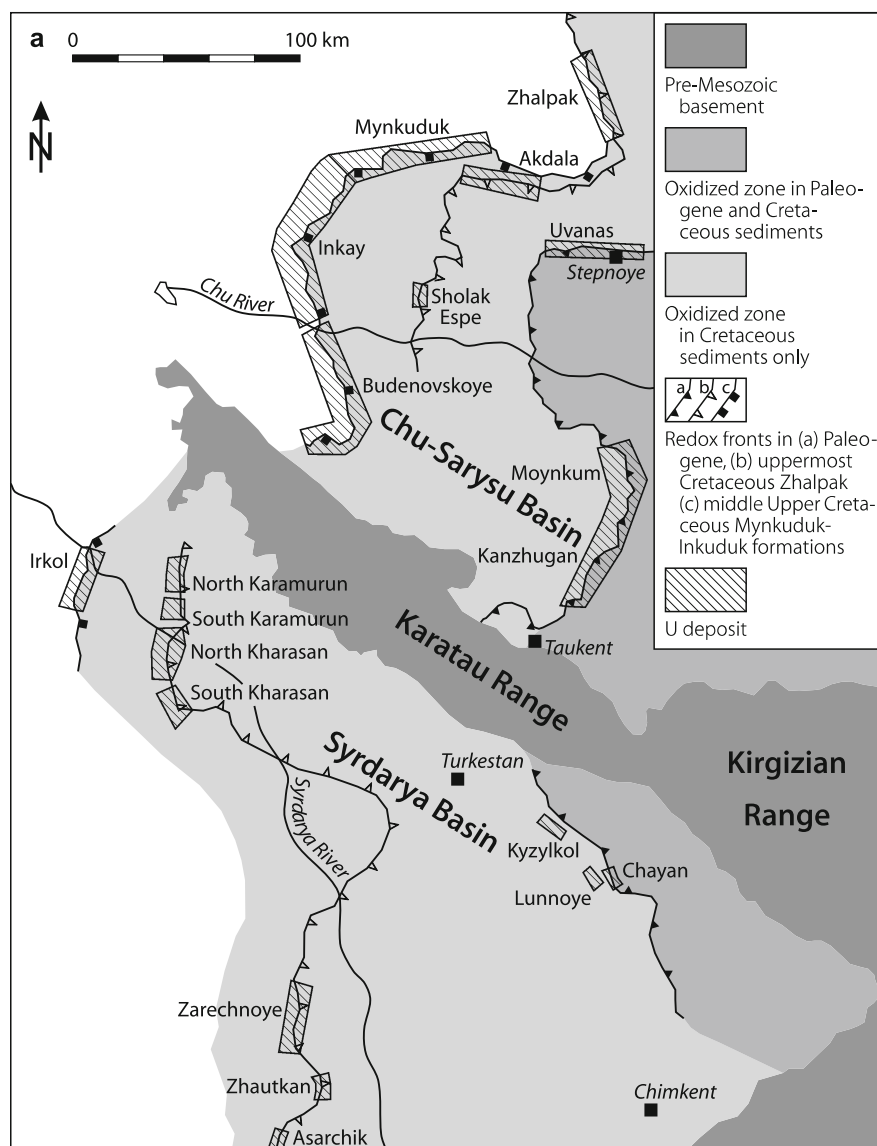
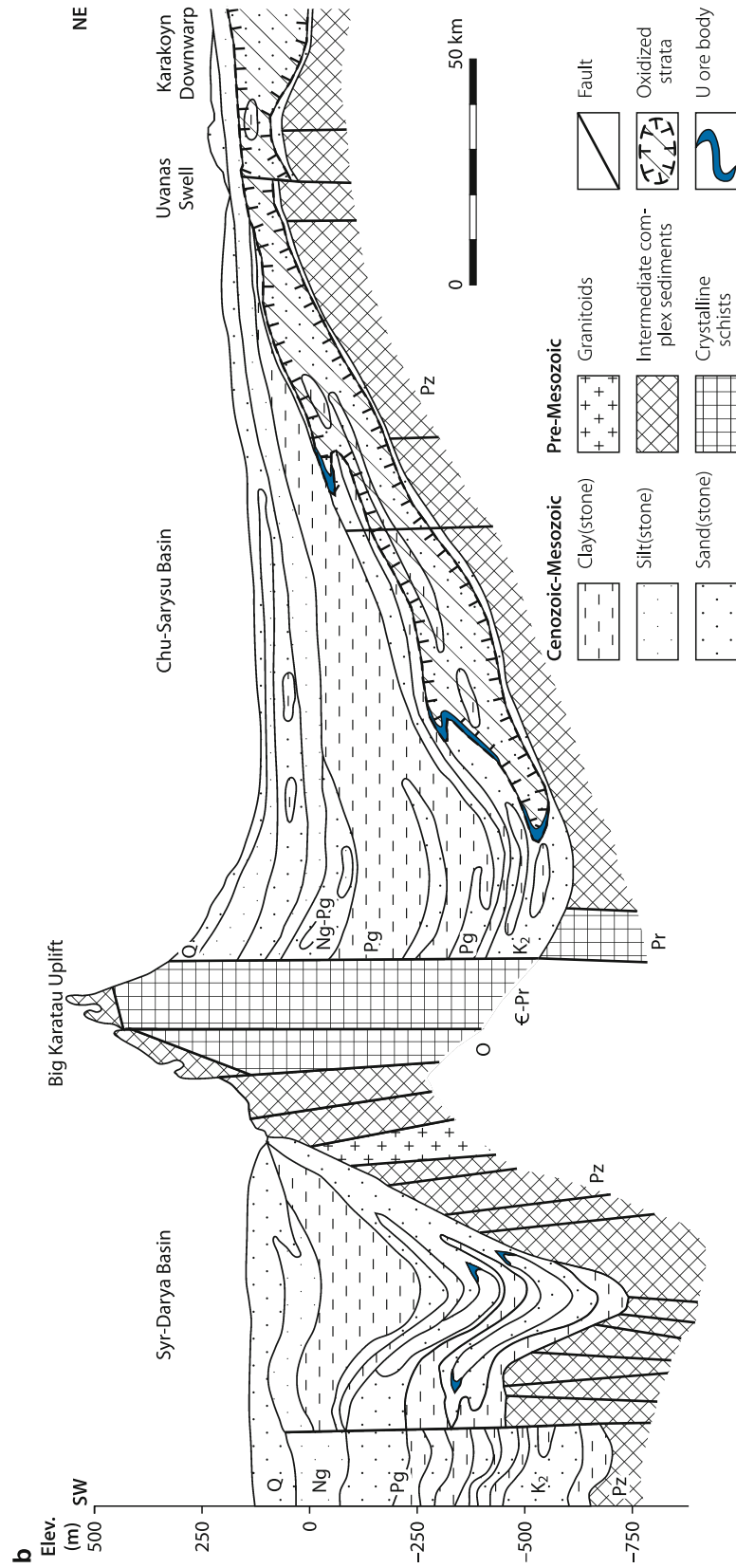


Fig. 6.12. (Continued)



>Major unconformity<

Lower Unit

- *Paleogene*: three U-bearing formations separated by unconformities
 - *Upper Eocene* Intymak Fm: regional, 20–150 m thick, grey-green clay-silt horizon with minor sandy lenses at base
 - *Middle Eocene* Ikan Fm: 5–60 m thick, clay and sand of deltaic origin, U-mineralized
 - *Lower Eocene* Uyük Fm: 5–65 m thick, clay and sand of deltaic origin, U-mineralized
 - *Paleocene* Uvanas/Kanzhugan Fm: 5–70 m thick, alternating sand, sandy gravel, and clay-silt of fluvial/alluvial and lacustrine provenance, U-mineralized
- *Upper Cretaceous*: three U-bearing formations separated by unconformities, cumulatively 250–300 m thick, of cyclic depositions of mainly gravel and sand with minor intercalated clay-silt lenses of fluvial and lacustrine origin
 - *Maastrichtian-Campanian* Zhalpak Fm: 30–90 m thick, contains more organic debris than Inkuduk and Mynkuduk Fms
 - *Santonian-Turonian* Inkuduk Fm: 40–120 m thick, separated into 3 horizons/cycles, U in lower and middle parts
 - *Lower Turonian* Mynkuduk Fm: 20–80 m thick, U mainly in lower part
- *Cenomanian*: 10–30 m thick, argillaceous sands
- *Lower Cretaceous/Albian* Tantei Fm: 0–140 m thick, sandstone overlain by sandy mudstone
- >Major unconformity<
- *Lower-Middle Jurassic*: 0–400 m thick, sandstone-mudstone
- *Permian-Carboniferous*: consolidated siltstone, sandstone, and limestone
- >Major unconformity<
- Proterozoic-Cambrian-Ordovician: crystalline schists

The marine Upper Eocene clays constitute the upper confinement and Paleozoic, locally Jurassic, rocks the basal regional confinement for hydraulic systems in the Cretaceous to Eocene stratigraphic-structural unit of the Chu-Sarysu Basin.

Uranium is hosted in six continental, 20–150 m thick, stratigraphic formations (termed “horizons” in Kazakh-Russian literature) of Paleogene (Uvanas-Kanzhugan zone) and Late Cretaceous age (Kenze-Budenovskaya zone). Deposition of these formations occurred in macrocycles which, in turn, are composed of a great number of microcycles with different permeabilities. As indicated in the litho-stratigraphic column above, the three *Paleogene* uraniumiferous formations are in Paleocene and Lower-Middle Eocene sediments of mainly medium- to fine-grained, weakly carbonaceous sands separated by continuous argillaceous beds. The three mineralized formations in *Turonian* to *Maastrichtian* strata consist of several, 10–40 m thick horizons each starting with an up to some 10 m thick basal gravel

bed grading upward into variably sized, mostly coarse-grained sands. 80–90% of these arenites are of permeable nature. Discontinuous argillaceous and silty lenses overly and intervene between the horizons (see Sect. *Principal Characteristics of Mineralization* for host rock composition).

The *structure* of the basin is dominated by a large monocline in the central-western segment while the eastern basin is more complex with a major basement rise of NW-SE orientation (Uvanas swell), local brachyantoclines, and subbasins like the Karakoyun trough. Sediments of the monocline dip gently southward from the Uvanas swell toward the Karatau Range in front of which they warp upward and transition into a medium steep NE inclination (Fig. 6.12b).

Regional faults trend predominantly NW-SE and to a minor degree N-S and E-W. Their manifestation decreases in the Mesozoic-Cenozoic cover from bottom to top. Synsedimentary, pre- to syn-Oligocene faulting caused major displacements in the lower unit of the basin. The Proterozoic-Paleozoic basement is block faulted.

Groundwater influx into the Chu-Sarysu Basin is from the northern Tien Shan. The groundwater migration is directed towards northwesterly discharge areas at the Aral Sea. Annual flow rates average 1–4 m depending on the permeabilities of the various sand horizons. Groundwater in Paleogene sediments has drinkwater quality whereas that in the Cretaceous sediments contains from 1 to 6 g l⁻¹ dissolved salts.

Principal Host Rock Alterations

A regional oxidation zone (referred to as “stratum oxidation zone” in Russian terminology) is the prominent alteration feature in the artesian lower stratigraphic-structural unit of the Chu-Sarysu Basin. A still active hydrodynamic system of oxygenated groundwater, which commenced in Late Oligocene time migrated northwestwards, down-dip the regional trend of aquifers, and multilevel redox fronts, up to 300 km long, were established within aquifers of six superjacent litho-stratigraphic units. Permeable grey arenitic horizons reduced by diagenetic processes became oxidized and mostly speckled-colored. Due to variable permeabilities of the aquifers, the redox fronts advanced differentially. Oxidation fronts in the Upper Cretaceous sediments of the Kenze-Budenovskaya zone progressed for a distance of as much as 500 km whereas those in the Paleogene sediments of the Uvanas-Kanzhugan zone migrated for some 350 km from the recharge area in the Tien Shan mountains. The Inkuduk Formation has the highest permeability and therefore contains the farthest advanced redox front, which is 10–18 km ahead of that in the Mynkuduk aquifers.

In response to the oxidation process, organic debris decayed associated with generation of hydrocarbons and hydrogen. The water-dissolved gases are concentrated in the redox zone at the head of the regional oxidation tongue where their concentration is 6–8 times higher than normal and, as such, provided the reducing agents required for uranium deposition.

Principal Characteristics of Mineralization

Uranium ore in the Chu Sarysu Basin is mostly monometallic but, locally, also polymetallic at sites where Re and/or Se are concentrated to recoverable grades. Pitchblende, coffinite, and black products (sooty pitchblende) are the principal *uranium minerals*. *Associated minerals/elements* include marcasite, pyrite, sphalerite, goethite, hydrogoethite, pyrolusite, calcite, siderite, and radiobaryte, which are present in limited quantities, and minor to trace amounts of As, Ge, Mo, Re, Se, V, Y, REE, and others. Se, V, and As typically occur in oxidized sands at the rear of a roll while Mo is present in the reduced front part. Re is distributed throughout an ore body and extends into non-uraniferous, grey facies. Table 6.4 provides a summary of selected trace elements.

Mineralization has a disseminated texture. Uranium phases occur finely dispersed in the clayey-silty matrix of arenites, fill voids and microfissures in rock fragments, coat sand grains, and pseudomorph plant remains.

U mineralization is contained in at least nine arenaceous horizons within six stratigraphic formations. Two prominent regional redox fronts control deposits of the Uvanas-Moynkum-Kanzhugan zone in the Paleogene Uvanas/Kanzhugan Formation, and deposits of the Kenze-Mynkuduk-Inkay-Budenovskaya zone in the Late Cretaceous Zhalpak, Inkuduk, and Mynkuduk Formations. A third redox front positioned between these two zones controls the Sholak Espe deposit in the Zhalpak Formation.

Some deposits (Inkay, Mynkuduk, Uvanas) occur in fluvial sediments of large rivers while others (Moynkum, Kanzhugan)

are hosted by delta sediments. Mineralized fluvial channel facies consist of grey sands and gravel, which are generally composed of 60–80% quartz, 10–15% feldspar, 2–15% clay particles, 1–5% heavy minerals, and 0.01–0.1% organic matter; in ore zones these channel facies also contain <0.1% pyrite and 0.01–0.2% calcite.

General Shape and Dimensions of Deposits

Uranium occurs in at least nine arenaceous horizons at depth intervals from 80 m to more than 500 m along highly extensive, up to several hundreds of kilometers long, almost continuous mineralized zones along sinuous redox fronts, individual sections of which are arbitrarily defined as deposits. Deposits consist of a number of individual ore bodies separated by barren or weakly mineralized ground. In situ ore has a wide range of grades, from <0.01 to 0.4% U and locally more, and exhibits average deposit grades between 0.02 and 0.07% U.

Ore bodies linked to redox fronts are predominantly of roll shape while lenticular or tabular ore bodies occur at variable distances behind the redox fronts. In planview, roll-type ore bodies appear as continuous, winding ribbons, a few kilometers to as much as 30 km long and from 20 to 1 000 m wide; in cross-section, they predominantly display an asymmetric crescent, 1–30 m thick, with tails of variable length. Multilevel ore zones contain superjacent stacked ore bodies with a cumulative thickness in excess of 30 m.

Ore body position, configuration, and dimension tend to be primarily a function of the simple nature of sedimentary cycles,

Table 6.4.

Chu Sarysu Basin. Selected trace elements in ore and sand horizons. Zone of U loss refers to strata intervals from which U was removed (Maksimova et al. 1995)

Deposit/ –Formation	Environment	Sc (ppm)		Y (ppm)		Yb (ppm)		La (ppm)		Ce (ppm)		Nd (ppm)	
		∅	Max	∅	Max	∅	Max	∅	Max	∅	Max	∅	Max
Kainar ^a –Kanzhugan Fm	High grade ore	2.6	6.4	–	150	6.6	16.0	–	–	–	–	–	–
	Zone of U loss	2.5	3.0	45	126	2.3	3.2	–	–	–	–	–	–
Budenovskoye –Zhalpak Fm	Oxidized sed.	2.7	2.7	36	77	3.0	4.5	–	–	–	–	–	–
	Unaltered sed.	2.2	2.6	–	–	1.9	1.4	–	–	–	–	–	–
	High grade ore	5.0	12.4	91	276	2.3	5.0	71	226	39	135	38	122
	Zone of U loss	3.3	4.1	15	17	1.6	3.0	17	25	11	15	13	15
Inkay –Inkuduk Fm	Oxidized sed.	3.2	13.0	15	28	1.9	3.7	19	21	<20	<20	13	16
	Unaltered sed.	3.2	6.0	13	26	–	–	–	–	–	–	–	–
	High grade ore	6.3	19.0	28	53	3.0	5.0	–	–	–	–	–	–
	Zone of U loss	6.0	15.0	16	31	2.4	3.0	–	–	–	–	–	–
–Mynkuduk Fm	Oxidized sed.	3.7	5.8	15	28	2.0	4.0	–	–	–	–	–	–
	Unaltered sed.	–	5.8	–	30	–	1.4	–	–	–	–	–	–
	High grade ore	10.0	23.0	67	1208	4.0	1.8	17	29	49	76	10	22
	Zone of U loss	–	3.3	11.8	11.8	–	1.4	–	12	–	49	–	10

^aKainar is at SW end of the Kanzhugan deposit.

degree of permeability, and confinement of mineralized strata by aquicludes as evidenced by ore transecting the host lithologies independent of their texture. Textural parameters of host beds such as grain size, crossbedding, or clay content in the matrix of arenites exerted, however, a certain although subordinate impact as reflected by a more complex internal structure of the ore bodies.

Regional Geochronology

U/Pb ages of U minerals vary within a wide range. Most reliable ages group in the time interval from 35 to 22 Ma and from 250 000 to 100 000 years ago. This indicates that ore formation commenced in Oligocene time contemporaneously with the uplift of the Tien Shan ranges. The younger ages indicate uranium redistribution processes, which are still active as documented by younger ages of mineralization at the front of ore rolls compared to ages obtained from the rear part of rolls (Fyodorov 2002).

Potential Sources of Uranium

Circumstantial evidence suggests that the Tien Shan mountains, which abut the Chu-Sarysu Basin to the S and SE not only furnished sediments to the basin, but also provided U and other ore-associated elements. Ordovician and Silurian granites, which intruded coeval with granodiorite into crystalline schists and slates of the Tien Shan are considered a viable source of these elements. Another potential source for uranium and other elements found in the uranium deposits may be seen in felsic volcanics exposed to the east of the basin in the Kendyktas-Chuily-Betpak Dala uranium region.

Principal Ore Controls and Recognition Criteria

Significant ore controlling parameters or recognition criteria of the major deposits in the Chu-Sarysu Basin include:

Host Environment

- Artesian basin situated at the margin of a large platform and partly fringed by mountain ranges
- Basin containment of two stratigraphic-structural units separated by a major unconformity
- Upper unit of Quaternary-Neogene marine and continental sediments
- Uranium-bearing lower unit is composed of Paleogene-Upper Cretaceous continental fluvial/alluvial and lacustrine facies deposited in megacycles, and minor shallow marine sediments
- Host rocks are mainly fluvial/alluvial, grey, slightly carbonaceous, partly arkosic sand and gravel beds mostly of the middle and basal parts of sedimentary cycles
- Host rocks have interbedded mottled or green argillaceous and/or silty beds continuous in Upper Cretaceous and discontinuous in Paleogene strata

- The uranium-hosting lower unit is vertically confined by a regional argillaceous horizon of Upper Oligocene age on top, and Paleozoic rocks at the base
- The western part of the basin is characterized by a large monocline whereas the eastern basin has a more complex structure caused by swells and brachyanticlines
- Major displacements are bound to synsedimentary, pre- and syn-Oligocene faults

Alteration

- Diagenesis-related reduction of lower unit reflected by grey arenites and green or mottled clay-silt
- Regional epigenetic oxidation zone documented by pink arenites terminating at front-end redox interfaces
- Decay of vegetal remains by thermo-oxidative, aerobic and anaerobic bacterial destruction associated with generation of hydrocarbons and hydrogen providing the principal reductants
- Abnormal concentration of water-dissolved hydrocarbons and hydrogen gases restricted to redox front

Mineralization

- Predominantly monometallic ore characterized by U-oxides and U-silicate
- Locally minor polymetallic Se, Re and/or Sc mineralization with or without U
- Accessory minerals represented by limited quantities of Fe- and Zn-sulfides, Fe-hydroxides, carbonates, radiobaryte
- Large number of accessory elements in minor to trace quantities
- Disseminated texture of mineralization
- Predominantly roll-type and minor tabular or lenticular ore bodies
- Strata transgressive distribution of mineralization and simple structural characteristics of ore bodies primarily due to relative uniform permeability of host lithologies in response to a simple nature of cyclic sedimentation and confinement of mineralized strata by aquicludes
- Limited complexity of internal structure of ore bodies caused by texture of host beds such as grain size, crossbedding, and/or clay content in the matrix of sands
- Deposits are of large size but composed of more or less interconnected ore bodies
- Low ore grades

Metallogenetic Concepts

As may be deduced from descriptions of the various geoscientists reporting on uranium deposits in the Chu-Sarysu Basin (see Bibliography), the metallogenetic evolution of the Chu Sarysu Basin may be summarized as follows.

Basic ingredients for ore formation include an initial diagenetic reduction of Upper Cretaceous and Paleogene sediments of the lower stratigraphic-structural unit of the artesian basin followed, from Oligocene-Miocene to date, by an oxidation overprint of the reduced sediments (strata oxidation) reflected by a regional oxidation tongue. The influx of oxygenated waters

was triggered by the uplift of the Tien Shan and continued subsidence of the axial segment of the Turan Plate. The oxidation front advanced differentially in the various aquifers from the Tien Shan downdip to the NW. Oxygenated waters transported uranium and other metals to the site of precipitation. Sufficiently reducing conditions were and are provided at the redox front at the downdip head of the oxidation zone by water-dissolved reductants which had evolved by thermo-oxidative and bacterial destruction of vegetal material. As documented for the Kanzhugan-Tortkuduk deposit, this kind of decay of carbonaceous matter resulted in an epigenetic zoning formed by six thermal groups that occupy distinct positions across the redox profile and correlate with the spatial distribution of distinct bacterial populations. Six bacteria species are distinguished (going from oxidized rock across the ore roll into reduced rock): (1) sulfate forming, (2) cellulose decomposing aerobic, (3) hydrogen forming, (4) sulfate reducing/hydrogen sulfide forming, (5) methane forming, and (6) cellulose forming anaerobic bacteria (Shchetochkin and Kislyakov 1993 based on data from Maksimova MF, Shugina GA, and Urmanova AM).

The confinement of aquifers by hanging and footwall aquicludes allowed the formation of roll-type ore bodies. Due to the regional nature of the oxidation front and the simplicity of the lithology of host rocks, laterally extensive ore bodies of a relatively simple crescent shape evolved.

Ore formation began during Oligocene time. Redistribution processes are still active as evidenced by younger ages of mineralization at the head of rolls as compared to rear parts of rolls, tails, and tabular ore.

6.3.1 Kenze-Budenovskaya District

The Kenze-Budenovskaya District correlates with a winding, S-forming redox front, some 400 km long, in the northern and central-western Chu-Sarysu Basin. The redox front constitutes the northwestern limit of a regional, NW to W migrating oxidation tongue in Upper Cretaceous sediments. Deposits of this zone include from north to south: *Zhalpak*, *Akdala*, *Mynkuduk*, *Inkay*, and *Budenovskoye*. The *Kenze* and *Karakoyun* occurrences are at the northern extension of the redox front zone. A small U deposit, *Sholok Espe*, occurs at a slower-moving redox front southeasterly behind the major deposits of the Kenze-Budenovskaya zone (Figs. 6.1, 6.12a).

6.3.1.1 Zhalpak

Zhalpak is located 50 km NE of Akdala and was discovered in 1964 as the first deposit of the Kenze-Budenovskaya zone. Three ore zones are identified, *North*, *Central*, and *South*. Resources are reportedly almost 15 000 t U at a grade averaging 0.035% U.

Sources of information. Fyodorov 2005; Petrov et al. 1995; Yazikov 2002.

The mineralized, alluvial, Upper Cretaceous *Zhalpak Formation* is 45–75 m thick and is subdivided into an upper

member, 25–35 m thick, composed of pale sands with clay and limy sandstone beds, and a lower member, 15–30 m thick, of grey, carbonaceous, hetero-granular quartz-feldspar sands and light green sands with intercalated clay laminae. The lower member is the principal ore host.

The Eocene Intymak Horizon, a 40–45 m thick sequence of – from top to bottom – grey-green sandstone, sand, silt, and clay, unconformably overlies the Zhalpak Formation except in the southern part of the deposit where up to 10 m thick relics of sand lenses of the Uvanas Horizon rest upon the Zhalpak Formation. Fluvial psephitic sediments, 40–60 m thick, of the Inkuduk and Mynkuduk Formations underlie the Zhalpak Formation and rest upon Paleozoic siltstone and mudstone of the Zhidelisai, and sandstone of the Kengir Formations.

Uranium mineralization is of a disseminated texture and is dominated by coffinite. (Sooty) pitchblende occurs subordinately. Associated minerals and elements include pyrite, marcasite, bravoite, up to 200 ppm Se (av. 12 ppm), up to 13 ppm Y, up to 62.5 ppm Re, 1.9–4.7 ppm Sc, and REE averaging 106 ppm.

Three modes of ore are distinguished: dark grey sandy ore with relatively high U and organic matter contents, pyrite enriched grey and greenish-grey sandy ore barren of organic material, and bleached, light grey sediments with low U grades.

The Zhalpak deposit extends over a N-S length of some 45 km. Eight ore bodies are delineated at a depth from 125 to 145 m in the northern and central segments, and as much as 200 m deep in the southern part. Four of the ore bodies account for 75% of the total resources, and 30% are contained in ore body # 2.

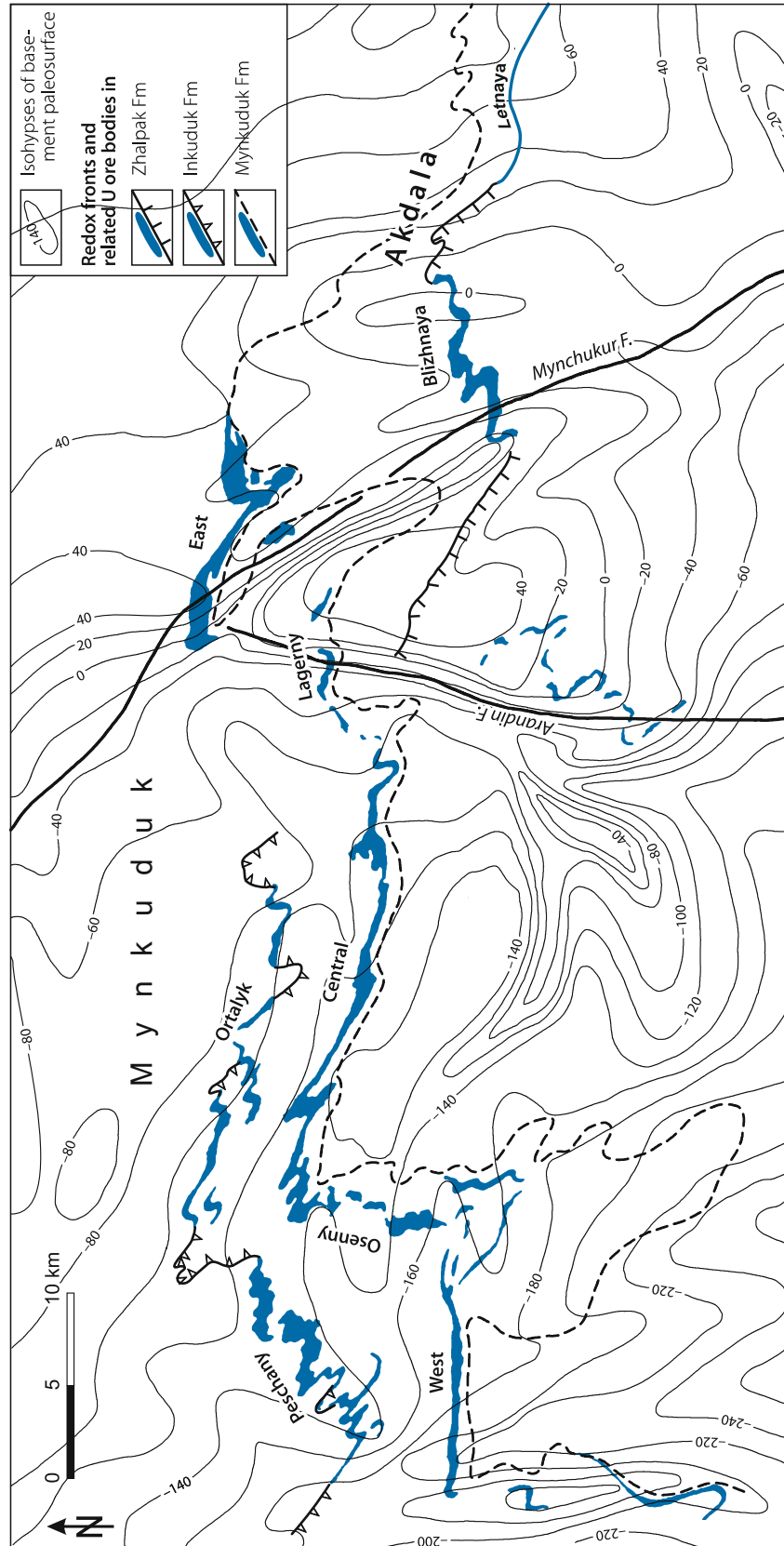
Ore bodies are of tabular to lenticular and semi-roll configuration. They are from 25 to 850 m wide, from 0.5 to 15 m thick, and extend from 3 to 7 km in length except for ore body # 2, which is 22 km long. Ore grades vary between 0.01 and 0.4% U with local peaks of 0.85% U.

6.3.1.2 Akdala

Akdala is located in the northwestern part of the Chu-Sarysu Basin, adjacent to the eastern portion of Mynkuduk. Akdala may be considered an eastern extension of the latter, but separated from the bulk of the Mynkuduk ore bodies by a major NNW-SSE-trending fault. Akdala has reserves of 14 250 t U at an average grade of 0.059% U (OECD-NEA/IAEA 2005); about 40% of these reserves are of higher grades. This deposit is exploited by ISL techniques since end of 2001.

The rollfront-type deposit includes two ore zones, *Blizhnaya* and *Letnaya*, within an E-W-trending, about 30 km long strip. These ore zones are controlled by a curvilinear, E-W-oriented redox front in the 50–70 m thick Upper Cretaceous *Zhalpak Formation*. Sediments are dominated by alluvial sandy facies with intercalated, 1–2 m thick, feldspar-quartz sands. Coffinite is the dominant U mineral. It constitutes 65%, and sooty pitchblende 35%, of the U minerals. Ore bodies occur at depths from 135 to 195 m, av. 6.6 m in thickness, 0.057% U, 0.5% Fe-sulfide, 0.1% carbonate, and 0.09% organic carbon (Fyodorov 2005). Ore bodies # 19 to # 21 contain increased amounts of rhenium (>0.2 ppm Re), which correlate with the uranium contents.

Fig. 6.13. Chu-Sarysu Basin, Mynkuduk-Akdala ore field, geological map exhibiting the course of redox fronts and related U ore bodies in the Upper Cretaceous Zhalpak, Inkuduk, and Mynkuduk Horizons (after Fyodorov 2005; Petrov et al. 1995)



Scandium amounts to 2.8 ppm in ore body # 19. REE averages 91 ppm, and Y 19.3%. Selenium occurs locally, and also outside U ore bodies, in concentrations of more than 0.01% Se (Petrov et al. 1995). The ore interval exploited first (since 2001) consists of an up to 14 m thick coarse- to medium-grained sandstone poor in clay and carbonate, higher in U grade than other portions of the deposit, and yields a productivity of 12–14 kg U m⁻¹.

6.3.1.3 Mynkuduk

Mynkuduk is located in the northwestern part of the Chu-Sarysu Basin. The deposit encompasses seven ore zones: *Peschany* (Sandy) and *Ortalyk* are in the Inkuduk Formation; *West*, *Osenni*, *Central*, *Lagerny*, and *East* are in the Mynkuduk Formation. Mynkuduk contains a total of 127 000 t U in situ resources. These resources include 48 000 t U at 0.047% U in the Central and 24 000 t U at 0.042% U in the East zone. (Other sources report original reserves for the Central zone as C1 = 42 528 t U, and C2 = 5 125 t U, at 0.047% U over a thickness of 7.23 m; and for the East zone as C1 = 23 245 t U, and C2 = 4 707 t U, at 0.025–0.040% U). Exploitation is by ISL techniques but only in the East zone. A pilot plant began operation in 1977 and full production was achieved in 1988.

Sources of information. Catchpole 1997; Fyodorov 2005; Petrov et al. 1995; Yazikov 2002.

Geology and Mineralization

U mineralization at Mynkuduk occurs in an Upper Cretaceous sequence, which is overlain by Late Oligocene to Quaternary sediments and underlain by Permian to Upper Devonian strata. The Late Paleozoic unconformity is at a depth of 220 m in the eastern and 450 m in the western section of the deposit. The lowermost basement complex consists of folded continental Cambrian and Ordovician formations the top of which is at a depth of 2–3 km.

Ore zones of the Mynkuduk deposit are controlled by regional redox fronts within three Upper Cretaceous formations (► Figs. 6.13, 6.14a,b).

The *Zhalpak Formation*, which rests conformably upon the Inkuduk Formation, is a common sedimentary cycle, 40–75 m thick, dominated by alluvial sandy facies with intercalated, 1–2 m thick, feldspar-quartz sands. Quartz and siliceous debris constitute some 81% of the *Zhalpak* facies; feldspar, muscovite, biotite, kaolinite, montmorillonite and limonite 18%; and calcite, siderite, pyrite and marcasite 1%. Increased values of organic matter occur in the lower section of the formation. Ore zones within the *Zhalpak* Horizon occur only to the east of Mynkuduk, in the adjacent *Akdala* deposit.

The *Inkuduk Formation* is 40–130 m thick and consists of three sedimentary cycles of greenish-white arenites, silts and clays. Hetero-grained sands with gravel prevail. Quartz and siliceous debris constitute 84.5% of the *Inkuduk* facies; feldspar, muscovite, biotite, kaolinite, montmorillonite and limonite 15%; and calcite, siderite, pyrite and marcasite 0.5%. Bleached sands are confined to the *Ortalyk* sector. Sand thickness increases from

50 m in the east to 100 m in the west. The *Inkuduk Formation* was unconformably laid down upon the *Mynkuduk Formation* after an erosional hiatus. *Inkuduk*-hosted ore bodies are confined to the *Peschany* (Sandy) and *Ortalyk* sectors in the western and central part of the deposit, respectively.

The *Mynkuduk Formation*, the main ore-hosting unit, is 30–90 m thick and is derived from SW- and almost S-flowing rivers, which deposited clastic sediments in two cycles. The lower cycle is 15–20 m thick at the eastern margin of the deposit and increases to 35–40 m in the central and western segments. Each cycle is characterized by a gradual transition from coarse- to medium- and to fine-grained sands and then to clays. Fine- and medium-grained sands predominate. Quartz and siliceous debris constitute 79% of the *Mynkuduk* facies; feldspar, muscovite, biotite, kaolinite, montmorillonite and limonite 20%; and calcite, siderite, pyrite and marcasite <1%. The *Mynkuduk Formation* is 30–40 m thick in the *East* and *Lagerny*, and up to 70 m in the *Central*, *Osenni*, and *West* ore zones.

Sand horizons in the three formations have high horizontal permeabilities. Filtration coefficients range from 9 m d⁻¹ in the *Zhalpak* to 12 and 13 m d⁻¹ in the *Mynkuduk* and *Inkuduk* aquifers, respectively.

Mineralization consists of coffinite and (sooty) pitchblende, and has a disseminated texture. Pitchblende occurs as micron-sized globules and spherical aggregates, and coffinite as tiny crystals. Coffinite prevails in ore of the *Inkuduk Formation* whereas pitchblende is dominant in that of the *Mynkuduk Formation*.

Sulfide and carbonate contents are low; ore in the *Inkuduk* and *Mynkuduk* Horizons contain an average of 0.26% and 0.73%, respectively, of combined pyrite and marcasite, 0.19% and 0.23% of calcite and siderite, and 0.04% and 0.07% of vegetal matter. Selenium contents commonly range from 0.01 to 0.06% but can be as high as 0.2%. Maximum Se grades are confined to the frontal segment of the ferruginous oxidation tongue. In the *West* and *Osenni* sectors, 75% of sampled intervals contain in excess of 0.01% Se. Selenium also occurs independent of uranium, in lenses as much as 200 m long and 10 cm thick. Scandium can be as high as 4.8 ppm as in ore body # 14 in the *Mynkuduk Formation* of the *Osenni* zone. Maximum Sc values of up to 21.1 ppm (av. 13.8 ppm) occur in impermeable clays. Yttrium amounts to 22.5 ppm and REE to 100 ppm in U ores of the *Mynkuduk Formation* (Petrov et al. 1995).

Shape and Dimensions of Deposits

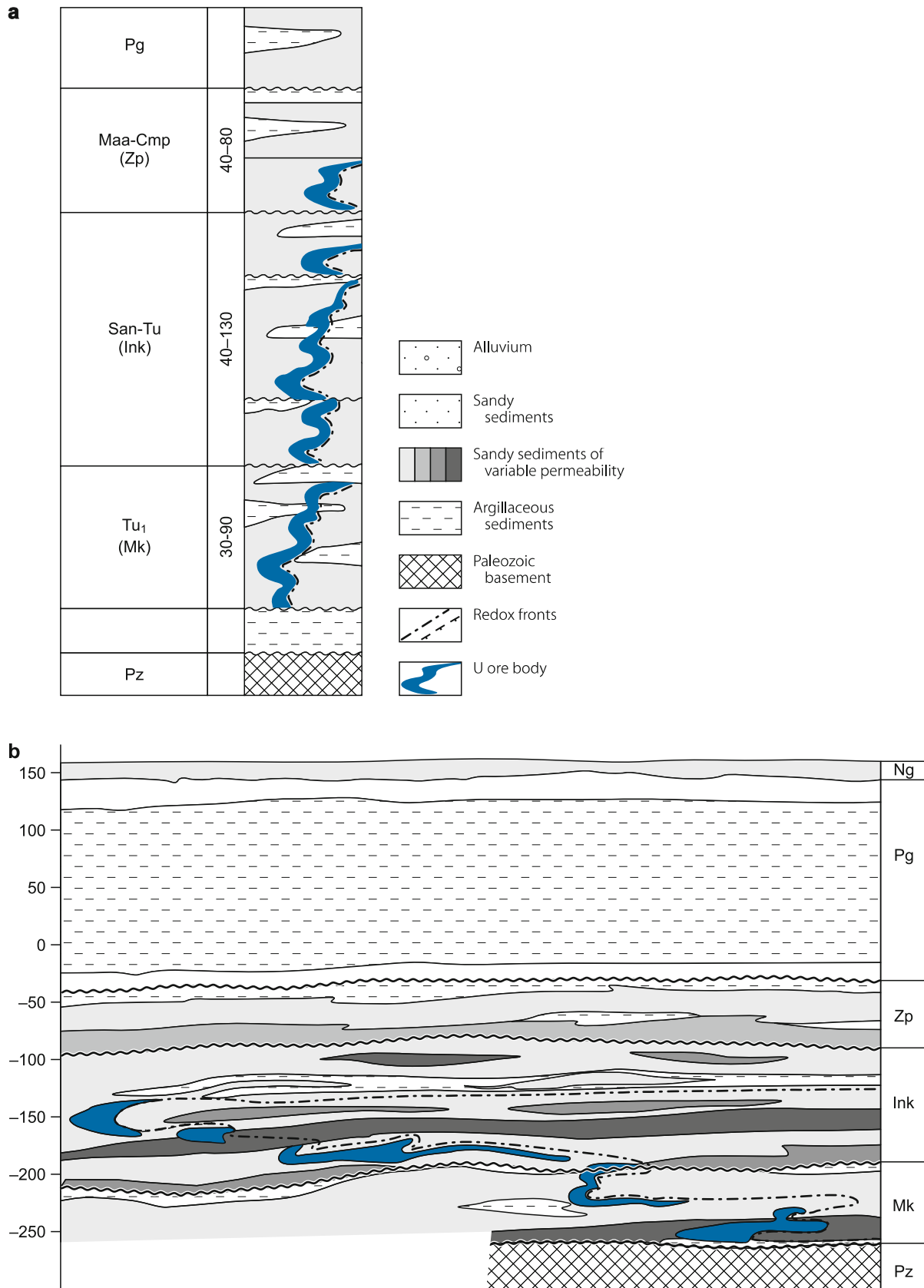
Ore zones of the *Mynkuduk* deposit occur within an E-W-trending, 65 km long and up to 10 km wide strip in which roll-shaped ore bodies are controlled by twisted, globally E-W-trending redox fronts (► Fig. 6.13).

The redox fronts have a cumulative strike length of 90 km along which some 30 ore bodies have been delineated, 16 of which are hosted by the *Mynkuduk Formation* at depths of 205–430 m and the remainder by the *Inkuduk Formation* at depths of 225–325 m.

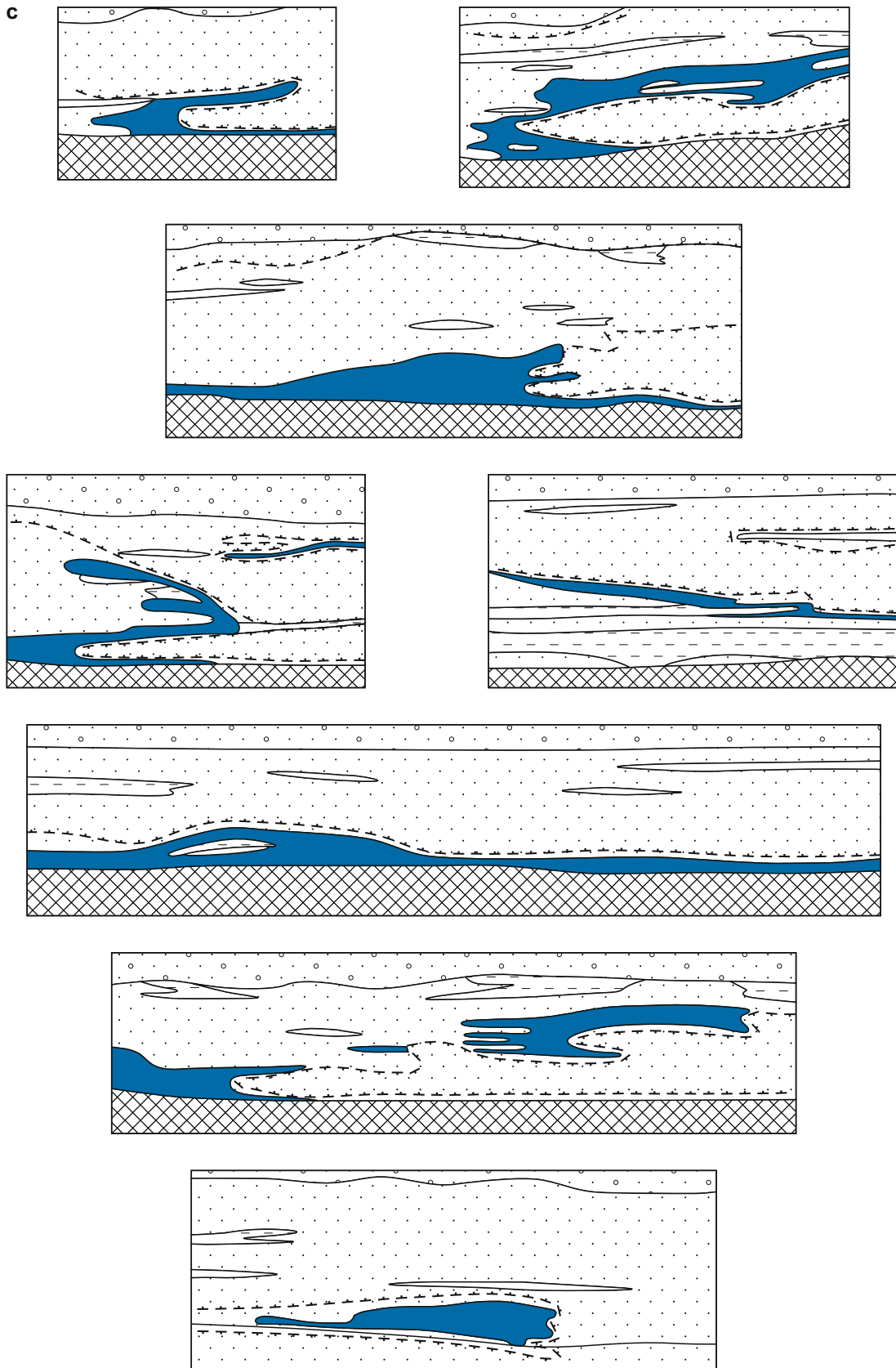
The *Ortalyk* and *Peschany* ore zones are hosted in the *Inkuduk Formation* and contain 11% of the total reserves of

Fig. 6.14.

Chu-Sarysu Basin, Mynkuduk and Inkay deposits, **a** litho-stratigraphic column and **b** schematic cross-section of the Paleogene-Cretaceous sequence indicating the position of U-bearing horizons, **c** examples of ore bodies morphology at Mynkuduk. (After **a**, **b** Fyodorov 2005; **c** Yazikov 2002)



■ Fig. 6.14. (Continued)



the Mynkuduk-Akdala ore field at an ore grade averaging 0.028% U. Respective figures for ore zones hosted in the Mynkuduk Formation are as follows (percent share of reserves/average U grade). West: 2.3%/0.038% U; Osenni: 7.5%/0.037% U; Central: 36.9%/0.047% U; Lagerny: 2.3%/0.025% U; and East: 21.8%/0.030% U.

Ore bodies appear in plan view as continuous, sinuous ribbons, up to 20 km long (without accounting for corrugation) and 50–500 m, locally up to 1 700 m wide as in ore body # 1. Barren intervals between individual ore bodies range laterally, i.e. on the same stratigraphic level, from few hundred meters to several kilometers. In cross-section, ore bodies commonly consist of one major, although variably shaped, up to 25 m thick roll in a given horizon. Ore rolls may have one or several, 2–10 m thick tails and isolated ore bodies some distance behind the major lode separated from it by barren ground (Figs. 6.14b,c). U grades vary in a wide range, from 0.015–0.15% U and may locally be in excess of 0.4% U.

6.3.1.4 Inkay

Inkay was discovered in 1976 in the western Chu-Sarysu Basin, 160 km ENE of the town of Kzyl-Orda. Inkay is one of the largest U deposits in the basin. The sandstone rollfront-type deposit includes three segments, *North*, *Central*, and *South*. Global resources are estimated at 330 000 t U including 55 000 t U RAR + EAR-I at an ore grade averaging 0.06% U (Catchpole 1997); OECD-NEA/IAEA (2005) reports reserves of 42 500 t U at 0.063% U for Inkay-sites 1 and 2 operated by the Inkay joint venture. An ISL pilot plant commenced operation in late 2001.

Sources of information. Abakumov and Zhelnov 1997; Catchpole 1997; Fyodorov 2005; Petrov et al. 1995; Yazikov 2002.

Geology and Mineralization

The general geology of the area corresponds to that of the northeasterly adjacent Mynkuduk deposit (see above). U mineralization is restricted to the Upper Cretaceous Inkuduk and Mynkuduk Formations. An intraformational unconformity separates the two horizons. The *Inkuduk Formation* consists predominantly of medium- to coarse-grained, weakly sorted sands. The subjacent *Mynkuduk Formation* is composed of several, one to several meters thick sedimentary cycles each starting with coarse-grained facies grading upward into fine-grained sediments. Medium- to fine-grained sands predominate. Impermeable pelite beds constitute 10% and 20% of the Inkuduk and Mynkuduk Formations, respectively. Unoxidized facies are grey or grey-green in color. The various sands have high horizontal permeabilities. Filtration coefficients range from 7 to 19 m d⁻¹ in the Mynkuduk and from 7 to 20 m d⁻¹ in the Inkuduk aquifers.

Multilevel oxidation tongues have developed in response to the multicycle structure of the sedimentary sequence. Sinuous, highly twisted redox interfaces at the head of the tongues are regionally NE-SW oriented in the northern part of the deposit;

they turn, in the central part, to a NNW-SSE direction. Due to the indented nature of the redox fronts, the cumulative length of all the fronts in subhorizons of the Inkuduk Formation is 726 km, while that in the Mynkuduk Formation is 427 km.

Uranium mineralization consists of (sooty) pitchblende and coffinite; the former constitutes about 80% of the uranium fraction. Associated minerals include marcasite, pyrite, calcite, and siderite. Several trace elements are present but in uneconomic amounts. Tenors of Re are less than 0.1 ppm, Sc 2.8–4.5 ppm, and REE 89–120 ppm (see also Table 6.4). U mineralization occurs in all lithologies, but preferentially in sands where it exhibits a finely-disseminated texture.

Shape and Dimensions of Deposits

The Inkay deposit covers a 55 km long and from 7 to 17 km wide stretch partitioned into a North zone of general NE-SW trend, a Central zone occupying the hinge joint, and a South zone of NNW-SSE orientation (Fig. 6.15). The Central zone is further divided into Section # 1 and # 2.

Uranium occurs in nine permeable beds in the Inkuduk and Mynkuduk Formations. Inkuduk sands contain 65% and Mynkuduk horizons 35% of the total RAR and EAR-I of Inkay. A breakdown of reserve percentage distribution and other ore-related parameters by the four zones are shown in Table 6.5.

Ore bodies are predominantly of a roll shape controlled by redox fronts, but lenticular and tabular lodges also occur. Eight major ore bodies are delineated, five in Inkuduk and three in Mynkuduk strata.

Ore bodies appear in planview as continuous, winding and highly twisted ribbons, from 9 to 31 km long and from 100 to 400 m wide, and are situated at a depth interval from 260 to 525 m. Barren intervals between individual ore bodies range from a few hundred meters to several kilometers. In cross-section, ore bodies commonly consist of a main, variably shaped roll, on average 4.2–7.4 m thick. Ore rolls may have one or several tails; some isolated ore bodies also occur some distance behind the principal ore lode and separated from it by barren ground (Figs. 6.14b,c).

Ore bodies have highly variable U grades, which average 0.045–0.063% U. Carbonate contents in ore average 0.1–0.2% CO₃ in the Inkuduk, and 0.2–0.3% CO₃ in the Mynkuduk horizons.

6.3.1.5 Budenovskoye

Budenovskoye was discovered in 1979 on the SSE extension of the redox front that controls the Inkay deposit. A barren or weakly mineralized interval, some 20 km long, separates the two deposits. Total in situ resources are speculated at 300 000 t U including 41 000 t U at an in situ grade of 0.09% U in the EAR-I category. Trace elements are given in Table 6.4. The redox front exceeds 90 km in length, including 50 km in the southern sector. Mineralization occurs in Zhalpak, 40–80 m thick, Inkuduk, 30–100 m thick, and Mynkuduk, up to 30 m thick horizons at depths between 550 and 700 m. Ore bodies average a thickness of 5 m.

■ Fig. 6.15. Chu-Sarysu Basin, Inkay, planview of redox fronts and related U ore bodies in the Mynkuduk Horizons (after Fyodorov 2005)

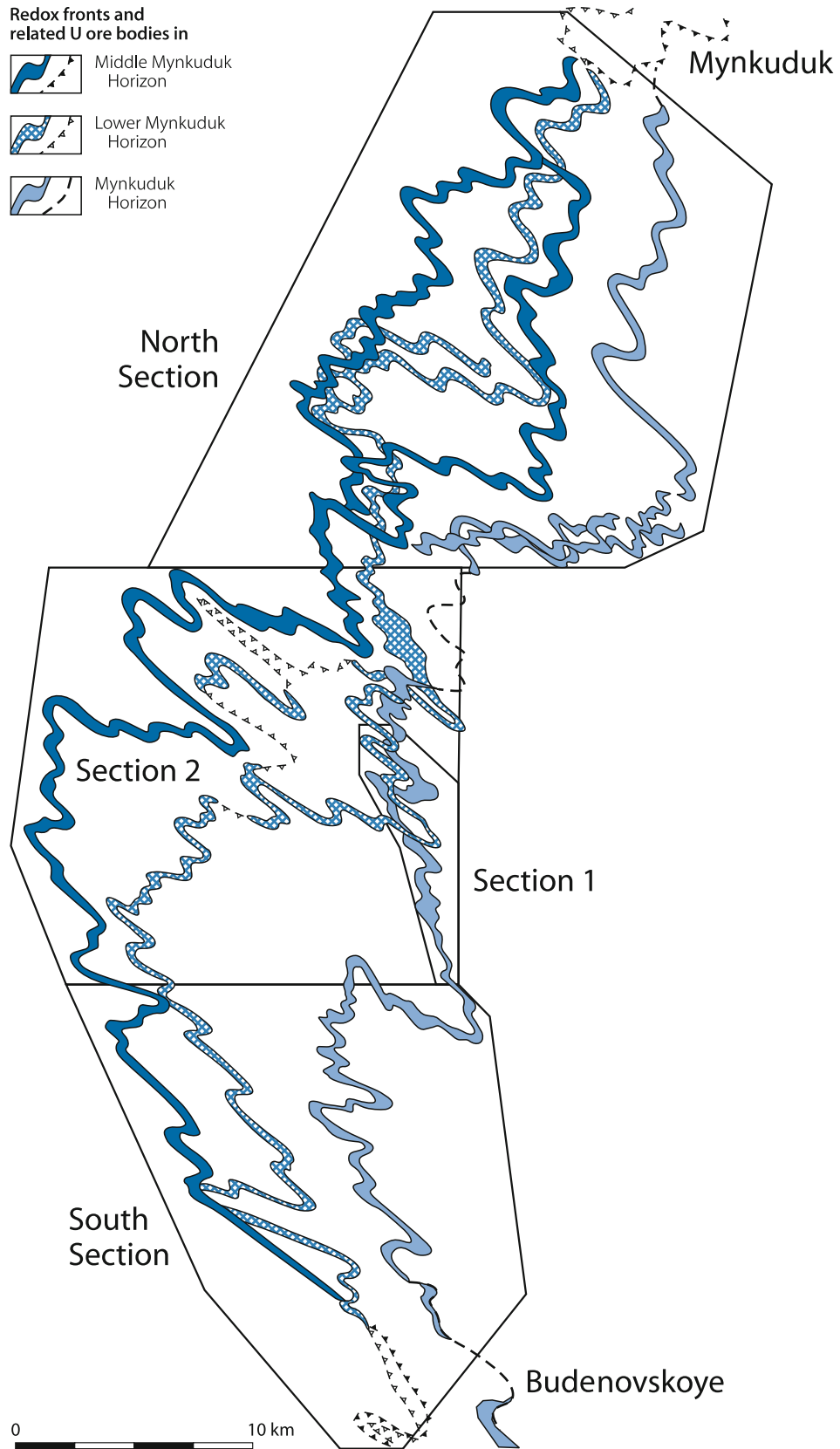


Table 6.5.

Inkay deposit. Selected characteristics of ore zones (Fyodorov 2005)

Parameter	Zone			
	North	Central #1	Central #2	South
Inkuduk Formation				
Reserves (% share) ^a	19.1	0.6	28.9	16.4
Average grade (%)	0.051	0.047	0.037	0.057
Average carbonate content (% CO ₃)	0.1	0.1	0.2	0.2
Average thickness of ore bodies (m)	5.2	4.9	7.4	4.2
Average width of ore bodies (m)	200	100	250	200
Depth of ore bodies (m)	290–370	430	330–380	350–420
Mynkuduk Formation				
Reserves (% share) ^a	7.6	12.3	3.6	11.5
Average grade (% U)	0.054	0.072	0.050	0.041
Average carbonate content (% CO ₃)	0.2	0.3	0.3	0.3
Average thickness of ore bodies (m)	3.50	6.08	5.83	6.28
Average width of ore bodies (m)	100	400	350	150
Depth of ore bodies (m)	430	515	480	510

^a Reserves refer to share of total RAR + EAR-I of the deposit.

6.3.1.6 Sholak Espe

This deposit is located some 50 km to the east and southeast of the Kenze-Budenovskaya zone. Roll-type U mineralization occurs in the Zhalpak Formation. The ore controlling redox front in this formation did not advance as far as those in the underlying Inkuduk and Mynkuduk horizons but stayed behind for approximately 40–60 km (Fig. 6.12). Resources are reportedly in excess of 5 000 t U. Ore grades vary between 0.01 and 0.04% U.

6.3.2 Uvanas-Kanzhugan District

The Uvanas-Kanzhugan District corresponds to an irregularly submeridional-trending redox front at the head of a regional oxidation tongue in Paleogene sediments in the south-central Chu-Sarysu Basin (Fig. 6.16). Rollfront-type deposits associated with this front include, from N to S: *Uvanas* (N of Chu River), and to the south of the Chu River *Moynkum* and *Kanzhugan(-Kainar)*. Moynkum is offset approximately 50 km to the ESE from Uvanas by a regional WNW-ESE fault whereas Moynkum and Kanzhugan are continuous and actually form a large ore zone. A small sandstone, basal-channel-type U deposit, *Bars*, is also found in this area.

6.3.2.1 Uvanas

Uvanas is located in the central part of the Chu-Sarysu Basin, 350 km N of the town of Chymkent. Original in situ resources amounted to 20 000 t U (Abakumov 1995) with an average ore grade of 0.02–0.04% U. This sandstone rollfront-type deposit was discovered in 1963 and has been exploited by ISL techniques since 1977. Steпноye Mining Company is the operator.

The deposit is partitioned into four sectors. The *East*, *Central* (with ore bodies # 2 and # 4) and *West* (with ore body # 1) sectors are controlled by a generally E-W-trending redox front whereas the *Koskuduk* sector is a NE-SW-trending ore zone situated to the SW of the main zone and offset for 2–3 km to the south by a NW-SE-striking fault. The East sector includes ore body # 5, *East Flank*, and *Kyzemchek East*. The latter is a NE-oriented, curved zone with subeconomic ore situated to the N of the East sector (Fig. 6.17a).

Source of information. Petrov et al. 1995; amended by information from staff of Central Mining Co./Kazatomprom pers. commun. 2003.

Geology and Mineralization

Uranium is hosted by the Paleocene Uvanas Formation (equivalent to Kanzhugan Formation at Moyinkum), which is overlain by more or less impermeable horizons of Eocene to Quaternary age and underlain by Upper Cretaceous and Paleozoic sediments (Fig. 6.17b). The Eocene section is reduced in the Uvanas area due to an erosional interval during the early-middle Oligocene. In more detail, the litho-stratigraphic profile of the Uvanas area may be summarized after Petrov et al. (1995) as follows:

- *Quaternary-Pliocene*: 20–50 m thick, pink and brown clay-silt, and sand
- *Upper Eocene Intymak Fm*: 40–60 m thick:
 - Upper bed, 2–5 m thick, dark grey clay with dispersed vegetal debris
 - Middle bed, 3–15 m thick, sand and blue-grey clay
 - Lower bed, 15–30 m thick (up to 47 m in Koskuduk sector), grey-green clay

- Basal bed, 1–4 m thick, green clay, mud, sand with phosphorite pebbles and detrital fish bones
- Lower Eocene Uyak Fm: 5–8 m thick, grey sand with clay and calcareous beds (only developed in Koskuduk sector)
- Paleocene Uvanas Fm: 1–8 m thick in E increasing to 20–30 m in the Central and to 45–50 m in the Koskuduk sector; main U-hosting formation separated into
 - Upper unit (cycle): <20 m thick, pink and green argillaceous sand and pelite with lignite seams,
 - Middle unit (cycle): <15 m thick, bleached sand with low silt-clay fraction,
 - Lower unit (cycle): <15 m thick, carbonaceous, sulfidic sand with lignite seams and 3–6 m thick clay-silt lenses
- Upper Cretaceous:
 - Maastrichtian-Santonian Zhalspak Fm: increasing from 25 m thick in E to 75 m in W sector, sand with minor gravel and mud lenses

■ Fig. 6.16.

Chu-Sarysu Basin, Uvanas-Kanzhugan District, geological map with course of redox fronts and related U deposits. U ore bodies occur preferentially in the Paleocene upper Kanzhugan Horizon and to a minor degree in the middle horizon of the Eocene Uyak Formation (after Petrov et al. 1995)

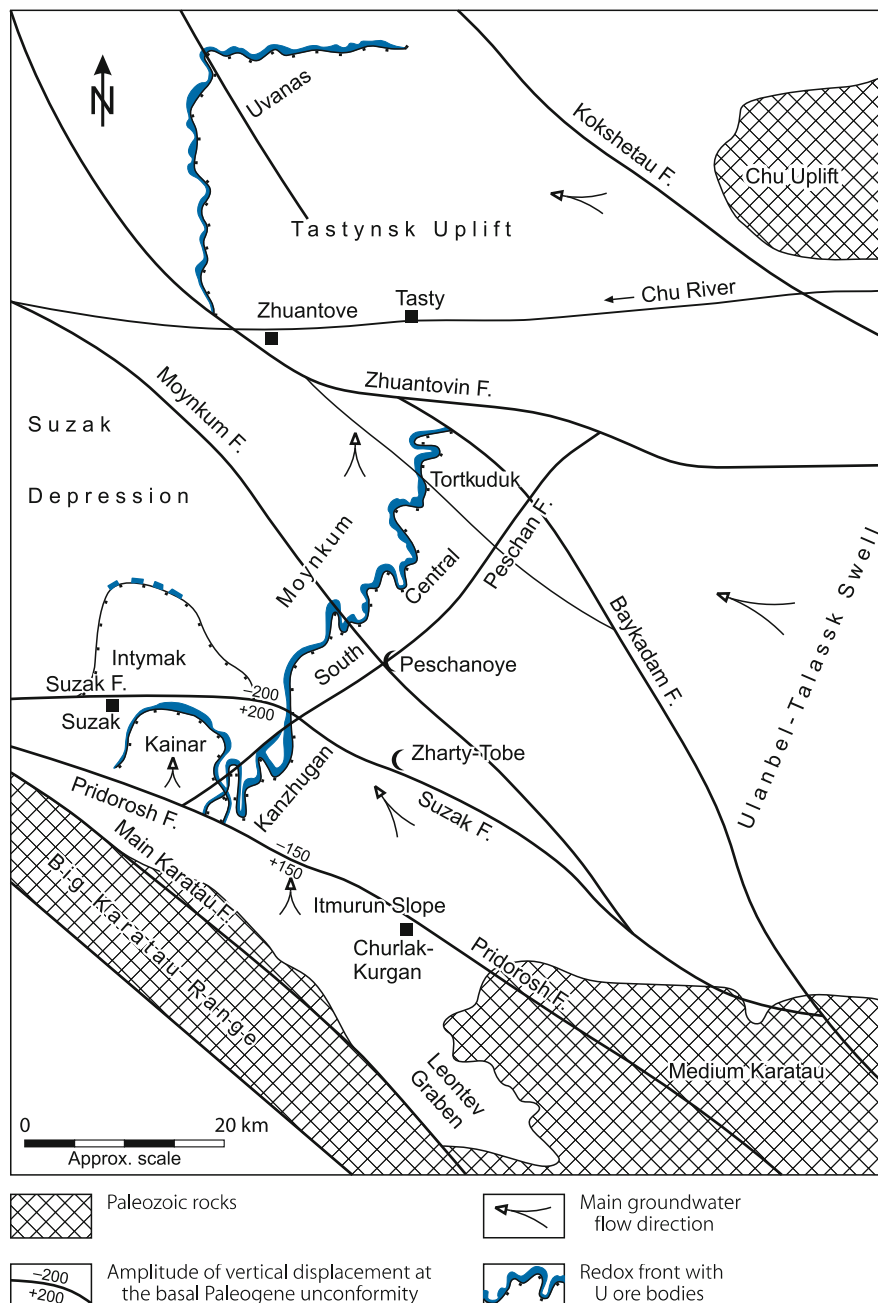
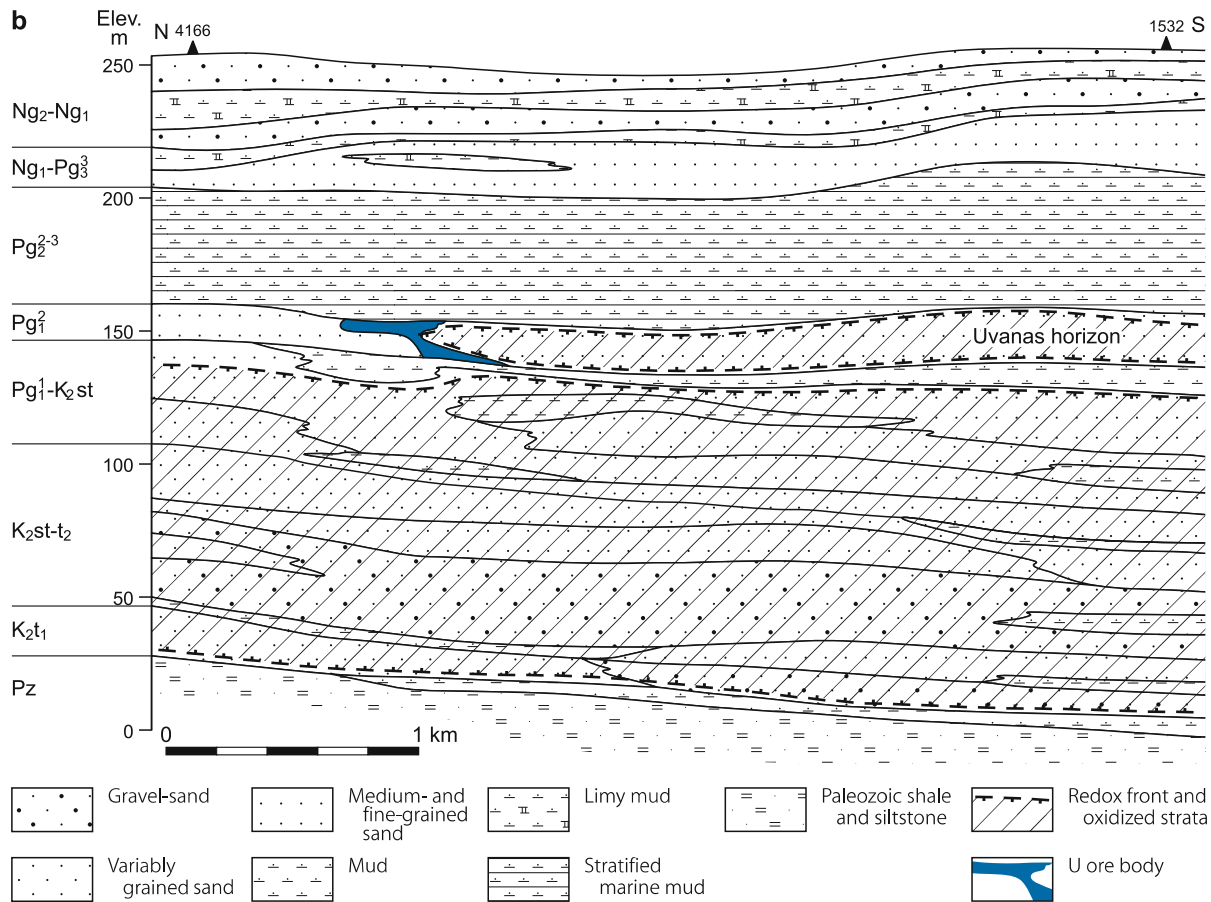


Fig. 6.17. (Continued)



Exploitation is by ISL techniques and started in 2001; the South sector by the Central Mining Company of Kazatomprom and the Central sector by KATCO, a joint venture of Cogema and Kazatomprom. Original in situ resources totalled 82 500 t U (Abakumov 1995) at a grade of 0.01–0.04% U. OECD-NEA/IAEA (2005) reports reserves of 67 360 t U at a grade of 0.064% U for the Central sector (Moynkum 2 and 3) operated by KATCO.

Sources of information. Petrov et al. (1995) amended by information from staff of Central Mining Co./Kazatomprom pers. commun. (2003).

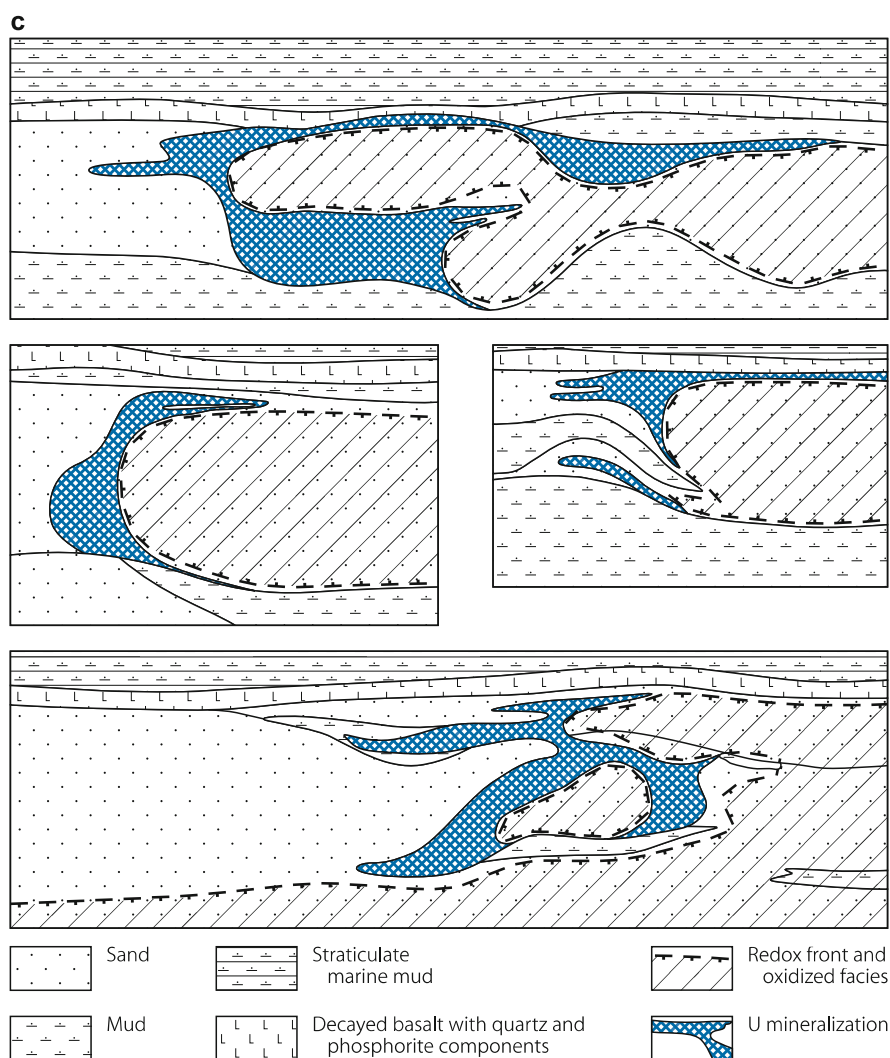
Geology and Mineralization

Moynkum is situated within the Suzak depression, the most submerged part of the Chu-Sarysu Basin. Moynkum is 30–40 km long and is conterminous with the southwesterly adjacent Kanzhugan deposit. As such, these two deposits actually form one large ore zone along a sinuous redox front in Paleogene aquifers. The boundary of the two deposits is given by the Suzak fault, a major WNW-ESE-trending fault zone that uplifted for up to 200 m the Kanzhugan side.

A synopsis of the litho-stratigraphic section of the Moynkum-Kanzhugan zone, drawn from Petrov et al. (1995), displays the following characteristics:

- *Pliocene-Miocene* Todusken Formation: 5–250 m thick, yellow-brown and red-brown limy clay and sand
- *Oligocene-Miocene* Betpak Dala Fm: 5–200 m thick, red-brown clay and sandy clay
- *Upper Eocene* Intymak Fm: 70–120 thick, occurs between surface and 480 m deep, grey-green and grey marine clay, mud and silt, resting upon basal clayey sand with gravel and remnants of gastropods and fish bones
- >Unconformity<
- *Middle Eocene* Ikan Fm: 5–60 m thick, roof in uplifted blocks at 70–260 m and in downfaulted blocks at 380–500 m below surface, sand constitutes 60% of the formation. Two horizons are recognized separated by a 0.5–5 m thick bed of black and grey clay:
 - Upper horizon: quartz sand with intercalated clay and mud lenses
 - Lower horizon: littoral to marine, fine- and medium-grained feldspar-quartz sands
- *Lower Eocene* Uyak Fm: 50–55 m thick, includes three horizons:
 - Upper impermeable horizon: 13–50 m thick, clay, mud, argillaceous sand, in lower section lignite and black clay beds, up to 1 m thick
 - Middle horizon (U-bearing): <50 m thick, medium- and fine-grained quartz sand with low clay component, about

Fig. 6.17. (Continued)



10% composed of interbedded mud and clay lenses, up to 10 m thick

– >Unconformity<

– Lower Kyzylchin horizon: <20 m thick, mainly clayey sediments

• >Unconformity<

• *Paleocene* Kanzhugan Fm (equivalent to Uvanas Fm): mainly delta and shallow marine sediments subdivided into two horizons

– Upper Kanzhugan horizon (main U horizon): 60–80 m thick, fluvial sediments including channel sand, argillaceous sand, mud, black clay (alternating variegated clay and sand), roof in uplifted block at 130–390 m and in downfaulted block at 440–550 m below surface

– Lower Kanzhugan horizon: 10–15 m thick, fine-grained quartz-feldspar sand, clay, mud, depth 520–550 m

• *Paleocene* Variegated Fm: 20–70 m thick, alluvial sediments, variegated marl, silt, quartz-feldspar sand, overlying unconformably Mesozoic or older rocks including:

• *Upper Cretaceous*: <100 m thick and locally more, yellow, bleached alluvial sands with pink clay laminae

• *Jurassic*: <400 m thick, lithified, coarse-grained arenites with lignite lenses

• *Paleozoic*: <2 000 m thick, consolidated terrestrial sediments and limestone

• *Precambrian*: gneiss, crystalline schists, metaconglomerate

Uranium ore bodies are controlled by a redox front at the head of a regional oxidation tongue in permeable arenite beds sandwiched between impermeable silt-clay layers, all of Eocene and Paleocene age. The redox front developed initially by waters derived from the Kirgizian range. At a later stage, infiltration from the Big Karatau range became more significant due to the uplift of this range. Present-day groundwaters percolate northwards in the Moynkum-Kanzhugan ore zone, at a sharp angle to the general strike of the zone.

Quartz sand with a 6–7% clay fraction is the preferential host rock. Sands on the rear side of the redox front are altered by limonitization. Micazation, reflected by a 4–5% fraction of muscovite/sericite in the host rock, is a typical alteration feature near ore.

Uranium is essentially represented by coffinite except for the Tortkuduk sector where coffinite and (sooty) pitchblende occur in a 65–35% ratio. U minerals fill interstices and coat sand grains

giving a finely disseminated texture to the ore. Associated minerals include pyrite, hematite, and goethite. Carbonate content is less than 0.5%. U is accompanied by a wide range of trace elements including Ge, Mo, Re, Se, Y, and REE as outlined further below.

Shape and Dimensions of Deposits

Moynkum and the adjacent Kanzhugan deposit consist of numerous U ore bodies that occur in highly erratic and discontinuous fashion associated with the redox fronts within aquifers of the Uyuk and Kanzhugan Formations at a depth interval of 50–500 m. Small relic ore bodies are found within oxidized ground at the rear of the redox fronts. U-hosting sand beds are highly variable in thickness ranging from 0.2 to 15 m.

Ore bodies are primarily of the roll-type but tabular- or lenticular-shaped lodes also occur. U grades are variable ranging from <0.04 to 0.2% U; and they are lower in the main part of rolls than in tails or in lenticular ore bodies. Large roll ore bodies are from 100 to 1 000 m wide and extend as ribbons for 3–30 km along redox fronts. Stratiform ore occurs in medium size lodes, which form elongated lenses, 1–3 km long and 50–200 m wide, or tabular blankets, 1.5–2.5 km wide. Small ore bodies are from 100 to 1 000 m long and 50–100 m wide. The South sector U ore body mined by Central Mining Co. is 10–15 m thick, 440–460 m deep, and has a productivity of 4–8 kg U m⁻².

Selenium commonly amounts to 240 ppm in the Kanzhugan, 60 ppm in the Uyuk, and 40 ppm in the Ikan Formation. In the South sector of Moynkum, the Se tenor increases to 0.447% in the Uyuk, and to 0.353% in the Kanzhugan Formation. Selenium mineralized lenses with more than 100 ppm Se also occur separated from U ore lodes. Such Se lenses are as much as 400 m long, up to 150 m wide, and 0.2–5 m thick. Rhenium tenors generally range from 0.08 to 0.38 ppm. Maximum values are 3.85 ppm Re in the Uyuk, and 4.8 ppm Re in the Kanzhugan Formation in the Tortkuduk sector and in the southern part of Kanzhugan. Re-bearing lenses containing in excess of 0.5 ppm Re are as much as 50 m wide and 0.1–10 m thick. Scandium averages 2.3–3.2 ppm in U ore. Markedly increased Sc values of 3–10 times that in sands are identified in clay where Sc can augment to 21 ppm.

Tortkuduk Sector of the Moynkum Deposit

The Tortkuduk sector is situated at the northern extremity of the Moynkum deposit. It is separated from the Central sector by a NW-SE-striking fault (► Fig. 6.16), and displays the following features (Shchetochkin and Kislyakov (1993): Tortkuduk is, in plan-view, a roughly N-S-elongated zone with converging, winding redox fronts. Roll-type U mineralization is contained in an arenite horizon, about 40 m thick, sandwiched between clay-silt horizons and intercalated with dark grey clay and silt lenses up to a few meters thick. An extensive clay lens splits the arenite horizon into two sub-units and results in the development of two superjacent oxidation tongues. Host rocks are irregular lenses of grey, carbonaceous, medium- and fine-grained sands deposited in a deltaic environment. Sands on the convex side of ore rolls are altered by limonitization. Filtration coefficients of the sands range from 5–10 m d⁻¹. Vegetal

debris has been decomposed by thermo-oxidation and bacterial activity as described earlier (Sect. *Metallogenetic Concepts*).

U mineralization persists for about 10 km along a winding redox front. Due to the litho-geochemical splitting, uranium occurs in a complexly-shaped double roll at the redox front. The forward section of the roll is almost 20 m thick; tails are up to several meters thick and more than 400 m long. A rhenium halo (>0.1 ppm Re) coincides with the uranium distribution and surrounds the frontal section of the roll where it persists for up to 60 m or more into the grey facies. A selenium zone with >50 ppm Se prevails in the rear part of the roll (► Fig. 6.18).

6.3.2.3 Kanzhugan

This deposit is located on the same redox front as, and immediately to the south of, Moynkum. The WNW-ESE-striking Suzak fault separates the two deposits. The production centers of Kanzhugan and the South sector of Moynkum are 18 km apart. Kanzhugan includes two sections, *Central* or *Kanzhugan* proper, and *Kainar*. A U occurrence, *Intymak*, occurs on a separate redox front to the north of Kainar (► Fig. 6.16). Original in situ resources of the roll-type deposit totalled 50 000 t U (Abakumov 1997). (Remaining proven resources in 2002 were reportedly 15 000 t at a grade of 0.033% U). Kanzhugan was discovered in 1972. ISL tests commenced in the Central section in 1982 and commercial production by ISL techniques started in 1988. Centralnoye Mining Company is the operator.

Sources of information. Petrov et al. 1995; Zinchenko and Stoliarenko 2002.

Mesozoic-Cenozoic sediments attain a thickness of 350 m. The upper 120–200 m thereof represent the upper stratigraphic-structural unit, which is composed of Neogene and Quaternary, mainly argillaceous and silty, sediments. Uranium is hosted in Eocene strata of the lower stratigraphic-structural unit. The Eocene sequence is 80–150 m thick and includes five sandy horizons separated by clay-silt layers 3.5–30 m thick. Two of the sandy horizons, Kanzhugan and Uyuk, host U ore bodies (► Figs. 6.19a,b). Medium- and fine-grained quartz (63–69%) and feldspar (10–15%) are the main host rock constituents. Ore-bearing horizons are up to 20 m thick. The lower horizon is at a depth of 220–290 m.

The Central or Kanzhugan sector occupies a generally NNE-SSW-trending, but highly sinuous, redox front some 20 km long, which switchbacks northward at a NW-SE fault at its south end to form the Kainar sector.

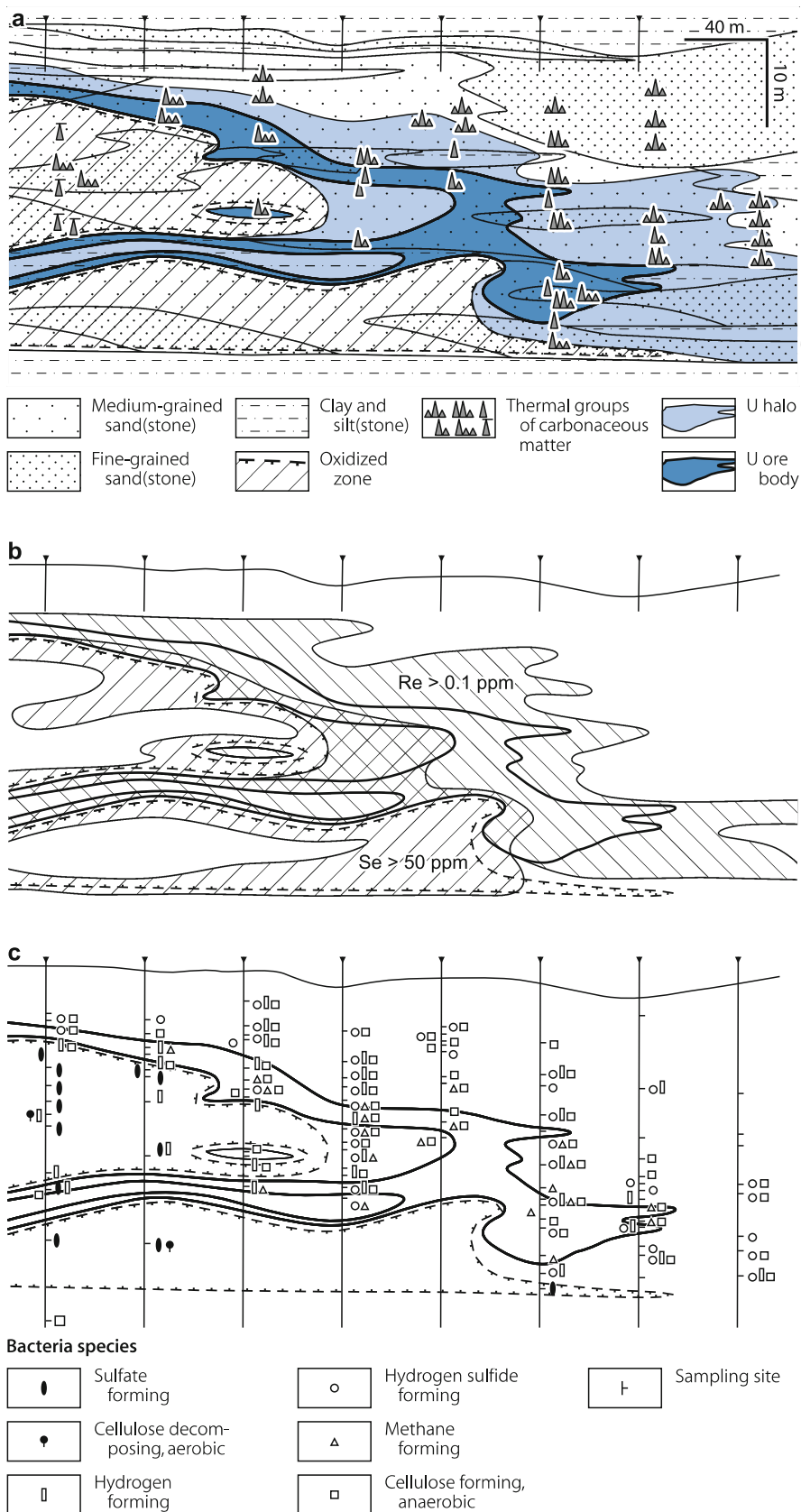
The Kanzhugan deposit exhibits a comparable ore body distribution as Moynkum (see above). Ore bodies are related to sinuous redox fronts that extend for a length of as much as about 10 km. Ore bodies have roll and tabular morphologies. Their width is 40–800 m. Thicknesses vary between 1 and 20 m and average 5.3 m. Ore grades range widely and average 0.038% U. Values of trace elements in the Kainar sector are provided in ► Table 6.4.

6.3.2.4 Bars

Bars is a small basal-channel-type sandstone U deposit situated between the Uvanas and Moynkum deposits. U lenses occur in

Fig. 6.18.

Chu-Sarysu Basin, Moynkum-Tortkuduk sector, litho-geochemical profile illustrating the distribution of **a** U, **b** Se and Re, and **c** bacteria species (after Shchetochkin and Kislyakov 1993 including data from Maksimova, Urmanova, and Shugina)



a Cenozoic channel filled with sand, mud, and lignite. Resources are reportedly a few 1 000 t U at an ore grade on the order of several 100 ppm U. Vanadium is an associated element (Petrov et al. 1995).

6.4 Syr-Darya Basin, S Kazakhstan

The Syr-Darya Basin is located in southern Kazakhstan. It is bounded to the NE by the NW-SE-trending Big Karatau range and to the south by the Chatkal-Kuramin range/Tien Shan mountains at the Uzbekistan and Kyrgyzstan border. The Karatau range separates the Syr-Darya from the Chu-Sarysu Basin with which it was originally united.

Uranium deposits in the Syr-Darya Basin are hosted in arenites controlled by dynamic redox fronts. They are therefore

classified as sandstone-rollfront type. Mineralization consists either of a U-Se or a U-V(-Se) paragenesis. Original in situ resources were 143 000 t U and included 77 300 t U proven reserves (RAR + EAR-I) in the <\$80 per kg U cost category, 10 700 t U estimated additional (EAR-II) and 55 000 t U prognostic resources (Abakumov 1995). Average grades range from 0.03 to 0.08% U.

Deposits are found in three districts; the *Karamurun District* in the northwestern, the *Karaktau District* in the central western, and the *Kyzylkol-Chayan District* in the eastern part of the basin (Fig. 6.12a). Uranium was discovered first at North Karamurun in 1972, at Irkol in 1976, and at Zarechnoye in 1977. More discoveries were made in the 1980s. Commercial exploitation by ISL methods started in 1985 at North Karamurun, followed by South Karamurun (see further below).

Fig. 6.19. Chu-Sarysu Basin, Kanzhugan, a simplified plan of the central part of the deposit (ore bodies 1k–4k in Kanzhugan and 2u–6u in Uyuk Horizon), b WNW-ESE section demonstrating the structural complex situation of ore lodes (after Petrov et al. 1995)

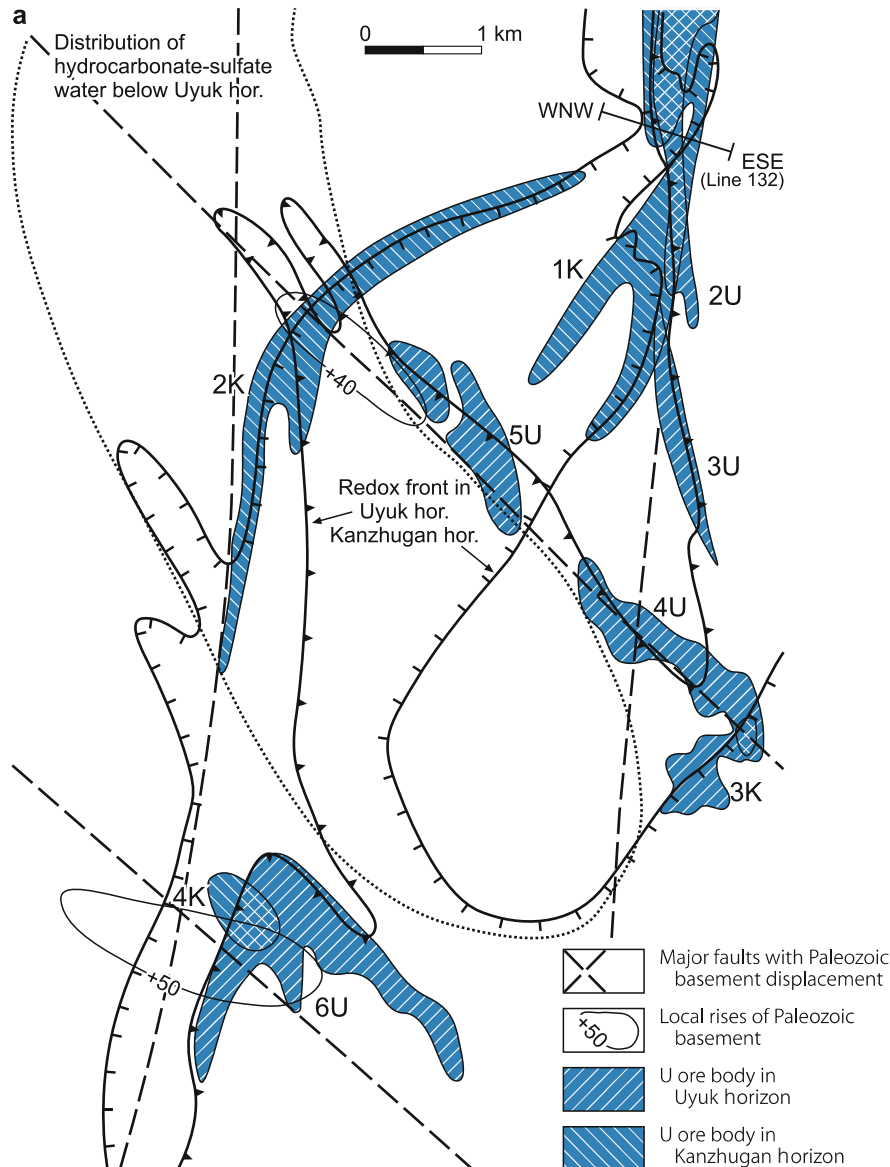
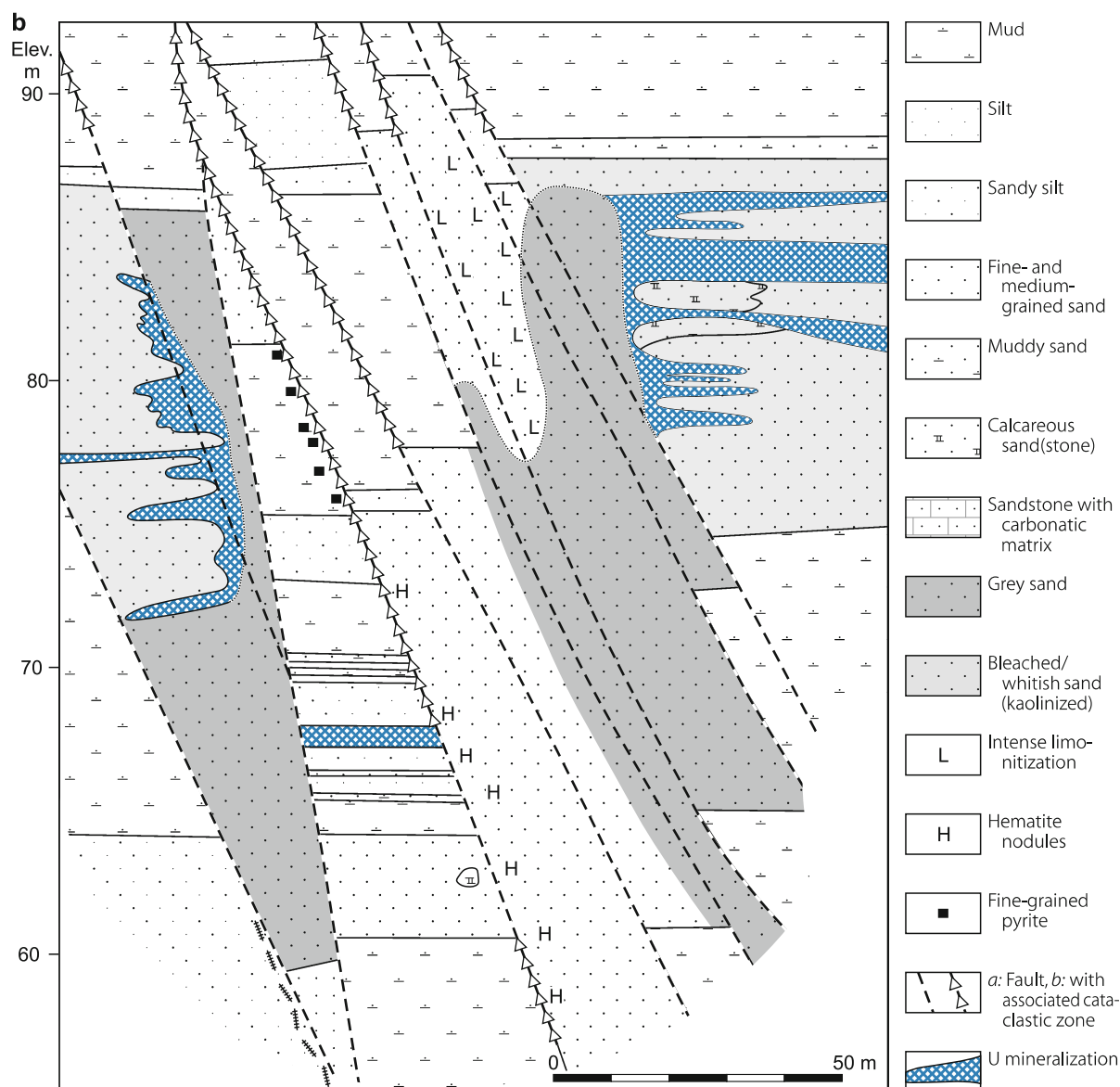


Fig. 6.19. (Continued)



Sources of information. Abakumov (1995), Fyodorov (1997), OECD-NEA/IAEA (1995–2005), Petrov et al. (1995), Yazikov (2002), Zabaznov (2002), and pers. commun. by Petrov and staff of Mining Co. # 6 (2003).

Regional Geological Features of the Syr-Darya Basin

The artesian Syr-Darya Basin is bounded to the NE by the NW-SE-trending Big Karatau Uplift, a mountain range composed of Proterozoic to Ordovician crystalline schists upon which Carboniferous and Devonian limestone and sandstone rest unconformably. The southern margin is the Chatkal-Kuramin Uplift, which is composed of Proterozoic and Paleozoic limestone, crystalline schists, granite, and mafic to felsic volcanics, and the southwestern limit by the Central Kyzylkum Uplift,

which separates the Syr-Darya Basin from the SW situated Kyzylkum U region and the Amu-Darya Basin in Uzbekistan (Fig. 7.1).

The Syr-Darya Basin is a complex depression filled mainly with continental (including pyroclastic) and minor marine sediments, as much as 3 000 m thick. An upper stratigraphic-structural unit of Quaternary-Neogene sediments rests unconformably upon a lower stratigraphic-structural unit of Paleogene-Upper Cretaceous sediments up to 500 m thick.

The Cenozoic-Mesozoic strata dip and increase in thickness from the Karatau Uplift in a SW direction for about 50–80 km. Further southwestwards, they warp upwards coupled with a decreasing thickness of the Neogene sediments. Pre-Neogene synsedimentary vertical faults caused displacements of up to 250 m or more associated with a thickening of the sedimentary sequence in the western part of the basin. Regional faults trend NW-SE and NE-SW.

The Mesozoic sequence rests unconformably upon a *basement* affected by the Hercynian Orogeny and composed of Carboniferous limestone and dolomite as well as Devonian continental sediments, which overly Proterozoic to Ordovician crystalline schists. Igneous rocks include Upper Paleozoic granitoids, felsic intrusives, and dacite-andesite sheets. The basement is block faulted with major displacements. Locally downthrust grabens are filled with Jurassic-Lower Cretaceous terrestrial sediments. Basement relief is in excess of 300 m (Fig. 6.12b).

Uranium deposits are restricted to the artesian lower stratigraphic-structural unit where they are contained in Eocene and Upper Cretaceous strata. Host rocks are sand and gravel-sand beds with high permeabilities (1–12 m d⁻¹ filtration coefficient). Contents of carbonaceous matter are generally low but can be as high as 5% in U deposits. Argillaceous aquicludes separate the arenitic horizons. An Upper Eocene clay horizon constitutes the upper regional confinement and Paleozoic and Early-Middle Mesozoic lithified rocks along the pre-Cretaceous unconformity are the lower limit for all hydraulic systems in the lower stratigraphic-structural unit.

The most characteristic *alteration* features are associated with multilevel regional oxidation tongues in Cenomanian to Eocene aquifers in the western and eastern half of the basin. Three redox fronts have been delineated. The westernmost redox front trends sinuously about N-S, is hosted by Upper Cretaceous sediments, and controls the Irkol deposit. Some 30–50 km to the east of this front, another curvilinear N-S-oriented redox interface also occurs in Upper Cretaceous strata. This front extends from the Tien Shan mountains for 350 km or more northwards and controls deposits of the Karamurun District in the north and those of the Karaktau District about 140 km to the south. The third redox front is located in the eastern Syr-Darya Basin, approximately 120 km to the east of the aforementioned redox front; it controls deposits of the Kyzylkol-Chayan District. Alteration features of the redox fronts compare to those of the Chu Sarysu Basin.

Uranium deposits in the Syr-Darya Basin are very similar to those in the Chu-Sarysu Basin. Ore grades for deposits average 0.05–0.08% U while those of individual ore bodies range from 0.01 to 0.6% U. Several deposits contain significant amounts of selenium and/or vanadium as well as other trace elements such as Ge and Re. Ore occurs at depths of 100–700 m. Deposits may consist of up to 9 stacked ore zones. The largest deposits occur in Upper Cretaceous strata.

Regional geochronology, potential U sources, ore controls, recognition criteria, and metallogenetic considerations are practically identical with those of the Chu-Sarysu Basin except that potential U sources may also be seen in the Chatkal-Kuramin uranium region at the border to Uzbekistan and Kyrgyzstan.

6.4.1 Karamurun District

The Karamurun District is spread over both sides of the Syr-Darya river near the mining town of Shieli (or Chiili) in the northwestern Syr-Darya Basin. The district includes the *Karamurun-Kharasan* and *Irkol ore fields*. Irkol occurs offset from the Karamurun-Kharasan deposits some 30 km to the W-NW

and is controlled by a further advanced redox interface. All deposits are hosted by Upper Cretaceous sediments (Figs. 6.12a, 6.20a,b). Original in situ resources of this district amount to about 80 000 t U RAR + EAR-I (including production of some 11 000 t U from 1973 through 2003) and an additional 50 000 t U of potential resources according to IAEA (2002b/Annex II).

Sources of information. Petrov et al. 1995; amended by data from IAEA 2002b/Annex II, and pers. commun. by staff of Mining Company # 6.

General Geology and Mineralization

Geology of the Karamurun District includes Quaternary to Oligocene suborogenic sediments deposited upon Paleogene and Cretaceous platform sediments. This sequence is as much as 3 000 m thick. Paleozoic rocks constitute the basement. A synopsis of the litho-stratigraphic section of the district, drawn from Petrov et al. (1995), includes the following units:

- *Quaternary-Oligocene*: suborogenic sediments
- *Upper Eocene*: <220 m thick, grey-green silt and clay
- *Middle Eocene*: ~50 m thick, marl and clay
- *Lower Eocene*: ~35 m thick, sand and grey clay
- *Paleocene*: 20–40 m thick, dolomitic sandstone, siltstone, dolomite, limestone
- >Unconformity<
- *Maastrichtian*: ~40 m thick, alluvial-deluvial sand, partly marine grey sand (principal U host at N and S Karamurun)
- *Campanian*: ~20 m thick, alluvial clay and sand (contains U at N and S Karamurun and Irkol)
- *Santonian*: ~80 m thick, pink clay and minor sand; U in grey alluvial facies
- *Coniacian*: ~60 m thick, alternating beds of grey gravel and fine-grained sand (principal U host at Irkol)
- *Turonian*: 40–50 m thick: including:
 - Upper Turonian: predominantly green-grey, fine-grained alluvial sand interbedded with grey lacustrine clay, silt, and sand (contains 10% of the resources of Irkol)
 - Lower Turonian: red-brown clay and silt
- *Cenomanian*: <50 m thick, gravel
- >Unconformity<
- *Pre-Mesozoic* basement: Middle Devonian terrestrial sediments and Lower Carboniferous limestone and dolomite, intruded by Upper Paleozoic granite

6.4.1.1 Karamurun-Kharasan Ore Field

This ore field is situated some 170 km SE of the town of Kyzyl-Orda and actually consists of a single large deposit that is arbitrarily subdivided, from N to S, into the *North Karamurun* Se-U deposit, the *South Karamurun* U deposit, and the *Kharasan* deposit [formerly separated into North and South Kharasan, and several isolated, small (some 100 t U) deposits]. The Karamurun deposits occur on the north and the Kharasan deposits on the south banks of the Syr-Darya river.

OECD-NEA/IAEA (2005) reports for the Karamurun North and South deposits combined remaining reserves of 33.860 t U at a grade of 0.086% U as per January 1, 2005. The nominal ISL production capacity of these two operations is 600 t U yr⁻¹. Total production through 2003 was approximately 7 000 t U. The operator was formerly Vostochny (Eastern) Mining and Chemical Combine and is now the # 6 Mining Company, a Kazatomprom (formerly KATEP) subsidiary.

Ore bodies occur at depths from some 400 m in the north to 800 m in the south controlled by a generally N-S-trending but sinuous redox front, approximately 60 km long, in Upper Cretaceous aquifers. The redox front migrates westwards from the Karatau Uplift.

Coffinite and (sooty) pitchblende are the principal U minerals. Associated minerals/elements include selenium in the form of native Se and ferriselite, vanadium (locally up to 4% V₂O₅) as tyuyamunite and h aggite, <0.3% Ge, <0.2% As, and <19 ppm Re.

Deposits consist principally of roll-shaped ore but there exist also lenticular ore bodies due to highly erratic interrelationships of arenaceous and pelitic facies. Ore bodies are from 750 to 5 500 m long, 25–450 m wide, 6–24 m thick, and average 0.07–0.08% U. Ore with grades in excess of 0.01% U are confined to grey facies. Footwall boundaries of deposits vary in depth between 300 and 700 m.

North Karamurun had reportedly original in situ resources of some 28 000 t U at a grade of 0.07–0.08% U and approximately 17 000 t Se. Ore bodies occur at depths from 400 to 550 m. Testing of ISL techniques at this deposit began in 1976 and commercial production in 1984.

South Karamurun continues southwards from the North Karamurun deposit for about 15 km to the Syr-Darya river. Original in situ resources totalled 12 000 t U at grades averaging 0.06–0.09% U. The deposit was tested by ISL techniques in the 1970s and is in production since 1979. The cutoff for recoverable

Fig. 6.20.

Syr-Darya Basin, Irkol and Karamurun-Kharasan ore fields, a generalized map indicating the distribution of U ore bodies in Upper Cretaceous strata below younger strata (Quaternary and Upper Pliocene cover not shown) and b the position of ore lodes in the Irkol (Ir) and Karamurun North (KN) and South (KS) deposits (after Petrov et al. 1995 based on VV Kazarinov)

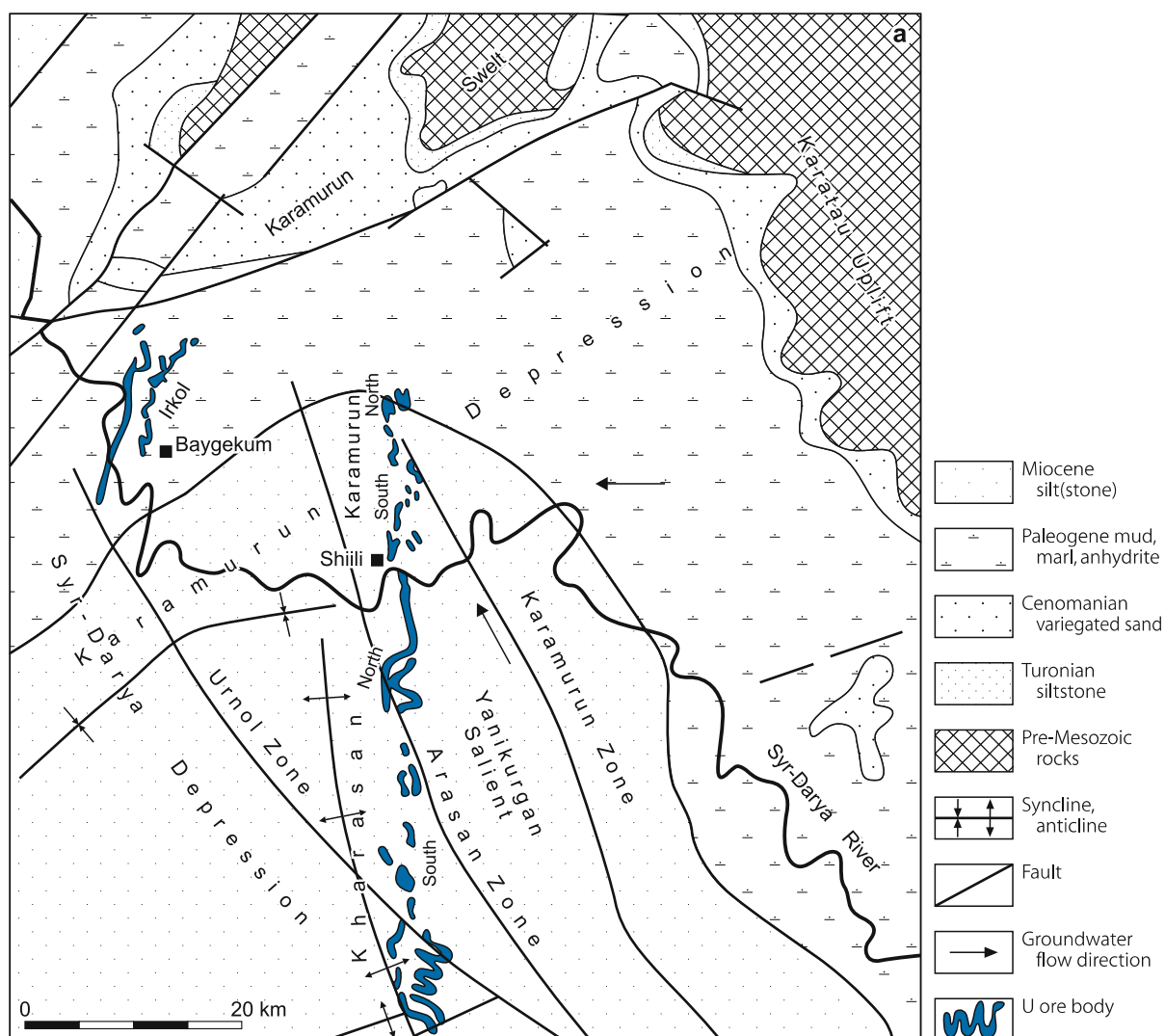
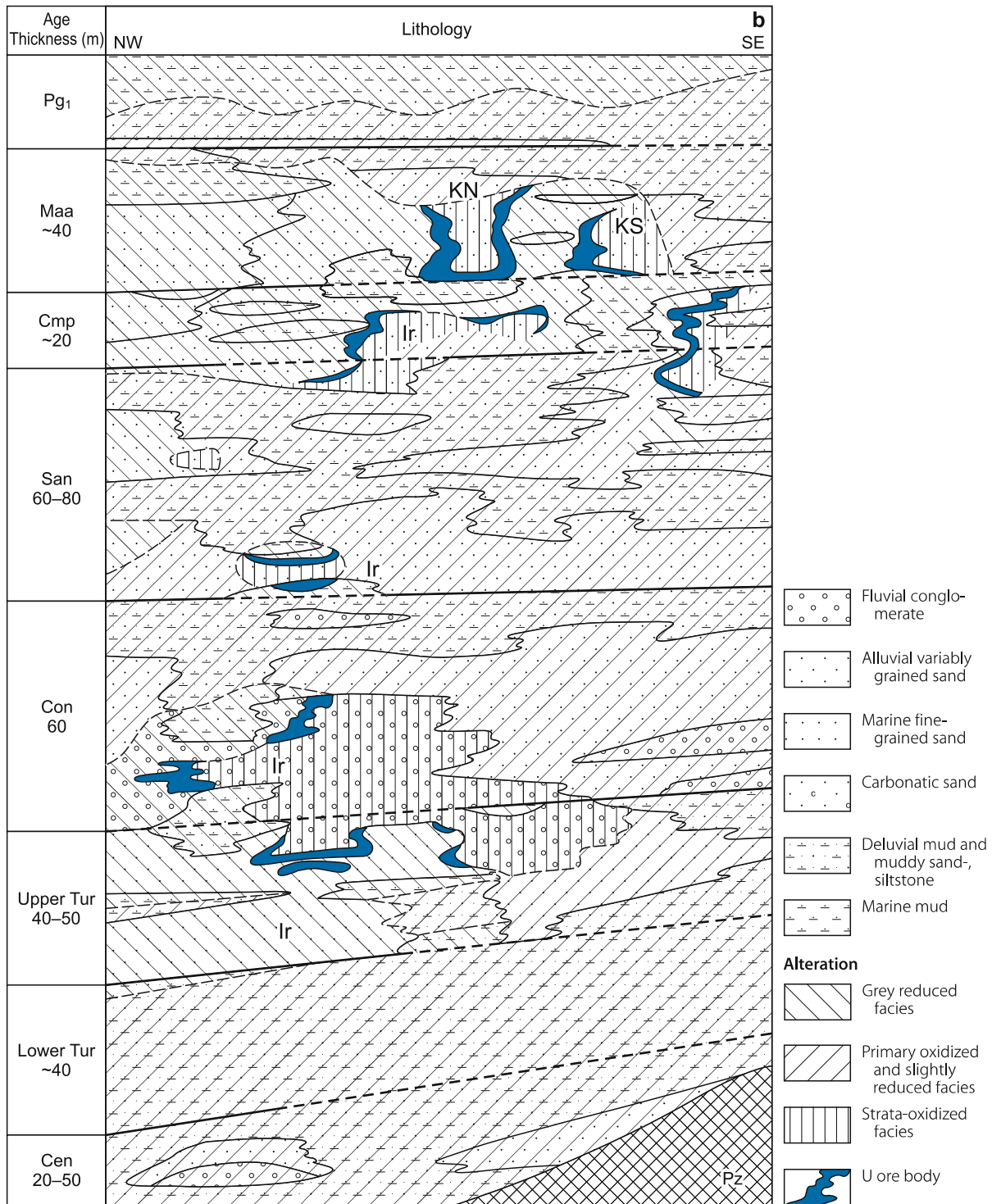


Fig. 6.20. (Continued)



reserves is 2 kg U m^{-2} while much of the ISL-mined ore bodies (status 1996) have reportedly grade coefficients from 5 to 15 kg U m^{-2} (IAEA 2002b/Annex II). Host rocks are Campanian and Maastrichtian fluvial, fine-grained, feldspathic quartz sands (80–90% quartz, ca. 10% feldspar) characterized by low contents of carbonate ($0.5\% \text{ CaCO}_3$) and carbonaceous debris, high permeability ($15\text{--}20 \text{ m d}^{-1}$ infiltration coefficient) and an increased temperature of $40\text{--}42 \text{ }^\circ\text{C}$. Three major ore bodies are outlined;

they are 25–450 m wide, 6–24 m thick, and spread over a length of about 5 km at depths of 450–670 m. The ISL-exploited ore-bearing aquifer occurs at depths from 550 to 670 m and is overlain by a 360 m thick aquiclude of massive clay upon which 100–120 m thick Pliocene and Quaternary sediments rest.

North Kharasan extends southwards from the Syr-Darya river for almost 15 km. It consists of several ore bodies at depths from 590 to 680 m. *South Kharasan* continues from North Kharasan

for almost 30 km further southwards and includes ore bodies as deep as 800 m. Resources of the two deposits combined are reportedly 42 000 t U at a grade of about 0.1% U.

6.4.1.2 Irkol Ore Field

Irkol is located on the NE banks of the Syr-Darya river in the northwestern Syr-Darya Basin, 140 km SE of the town of Kyzyl-Orda. Ore is controlled by a redox front some 30 km to the west of the redox front, which controls the Karamurun and Kharasan deposits (Figs. 6.12a, 6.20a). Reported in situ resources amount to 38 000 t U including 21 100 t U proven reserves at an average grade of 0.042% U. Carbonat content is 0.2%. Ore bodies occur at depths from 390 to 700 m with the bulk of the ore at depths between 400 and 450 m (Yazikov and Zabaznov 2002).

Ore bodies are of rollfront configuration, have a thickness between 1 and 20 m (av. 5 m) and range in grade from 0.01 to 0.07% U. Uranium is hosted by sand horizons, from 20 to 80 m thick, of Campanian to Turonian age. Compared with Karamurun, the ore-bearing sand horizons are thicker and the Se content lower. The deposit was tested by ISL techniques in 1985 but did not go in operation.

6.4.2 Karaktau District

The Karaktau District is located in the central western part of the Syr-Darya Basin, about 150 km to the west of the town of Chimkent. The district includes the Se-U deposits *Zarechnoye* and, some 50 km to the south, *Zhautkan* (<5 000 t U), and the U-V deposit *Assarchik* (>5 000 t U), located about 40 km to SE of *Zarechnoye* (Fig. 6.12a). All deposits are hosted in Upper Cretaceous sediments.

Source of information. Petrov et al. 1995.

General Geology and Mineralization

A litho-stratigraphic profile of the Karaktau District shows a sequence of Paleogene and Cretaceous platform sediments more than 1 300 m thick covered by Quaternary sediments. Deposits occur along bending, generally NNW-SSE-trending redox fronts in Upper Cretaceous aquifers. The Paleogene-Cretaceous sequence includes (from top to bottom) Paleogene sands; Maastrichtian, 40–120 m thick, sand-clay and limy clay; Campanian, 40–100 m thick, grey sands with interbedded silt-clay; and Lower Cretaceous, approximately 560 m thick, variegated siltstone with intercalated clay, marl, and limestone beds. This suite rests unconformably upon a basement of Paleozoic terrestrial sediments, which overlie Devonian-Silurian metamorphics.

6.4.2.1 Zarechnoye

Zarechnoye is an explored U-Se deposit that was discovered in 1977 and exhibits a geological setting and composition similar

to U deposits in the Karamurun ore field. In situ resources total an estimated 40 000 t U including almost 20 000 t U of proven reserves at a grade averaging 0.056% U.

Geology and Mineralization

Cenozoic-Mesozoic platform sediments in excess of 1 300 m thick rest unconformably upon Silurian-Devonian metasediments intruded by Late Paleozoic granite. The stratigraphic column includes (from top to bottom):

- *Quaternary*: up to 250 m thick, brown and reddish alluvial sand and clay
- Eocene-Paleocene sediments
- *Upper Cretaceous*: up to 800 m thick, marine and continental sandy and clayey sediments
- *Lower Cretaceous*: up to 560 m thick, variegated siltstone with clay, marl, and limestone beds

Campanian and Maastrichtian sediments host the U mineralization. The Campanian includes three rhythms, 15–30 m thick each, of fine-grained, grey sands with clay, sandstone, and siltstone beds; and the Maastrichtian includes 2 rhythms of 40–120 m thick deltaic and inshore marine sediments, the lower rhythm consists of sandy-clay and the upper of clay-carbonate. Within these units, 3 Campanian and 2 Maastrichtian permeable sand horizons contain mineralization at depths from 400 to 700 m. U is confined to grey, reduced facies while Se mineralization occurs in yellow, oxidized sandy intervals. Ore is controlled by redox fronts that are from 10 to 30 km long and spread over widths of as much as 5 km.

Ore consists of disseminated U and Se minerals. Coffinite constitutes 70–90% of the U endowment and pitchblende the rest. Native Se and minor ferroselite represent selenium. Carbonates comprise less than 1%.

U and Se commonly form individual ore bodies. Selenium ore bodies coincide to 70% with the contour of uranium mineralization but also occur between U ore lodes. U ore bodies are of roll shape and average a thickness of 5 m with a maximum of 12 m. Individual Se ore bodies exhibit the same dimensions. Combined U-Se lodes range in thickness from 2 to 20 m and average 8–12 m. Lodes contain from 0.01 to 0.6% U and from 0.04 to 0.055% Se.

6.4.3 Kyzylkol-Chayan District

This district is situated in the eastern part of the Syr-Darya Basin, near the Karatau range, about 100 km to the north of the town of Chimkent. Discovered in 1961–1963, this district includes the small *Kyzylkol*, *Lunnoye*, and *Chayan* deposits, as well as the *Dzedykuduk*, *Buyun*, and *Glinkovo* occurrences hosted in Eocene sediments of the Kyzylkol-Prytashkent zone (Fig. 6.12a).

Sources of information. Petrov et al. 1995; Petrov pers. commun. 2003.

Geology and Mineralization

A litho-stratigraphic profile of the Kyzylkol-Chayan District shows Oligocene to Quaternary suborogenic sediments resting on Paleogene and Cretaceous platform sediments. Paleozoic terrigenous clastic and carbonatic sediments constitute the basement. The Tertiary-Cretaceous suite includes the following lithologies:

- *Miocene-Oligocene*: <250 m thick, clay
- *Upper Eocene*: 200–250 m thick, green-grey clay
- *Middle Eocene* Ikan Formation: 30–40 m thick, quartz-feldspar sand with interbedded sandstone and dolomite beds, including an up to several meters thick ore-bearing horizon
- *Lower Eocene* Uyuk Formation: 50–60 m thick, with a U-bearing 15–25 m thick sand bed between two clay layers
- *Eocene-Paleocene*: 100–130 m thick sediments
- *Cenomanian-Albian*: variegated and pink continental sediments
- *Turonian*: marine grey clay

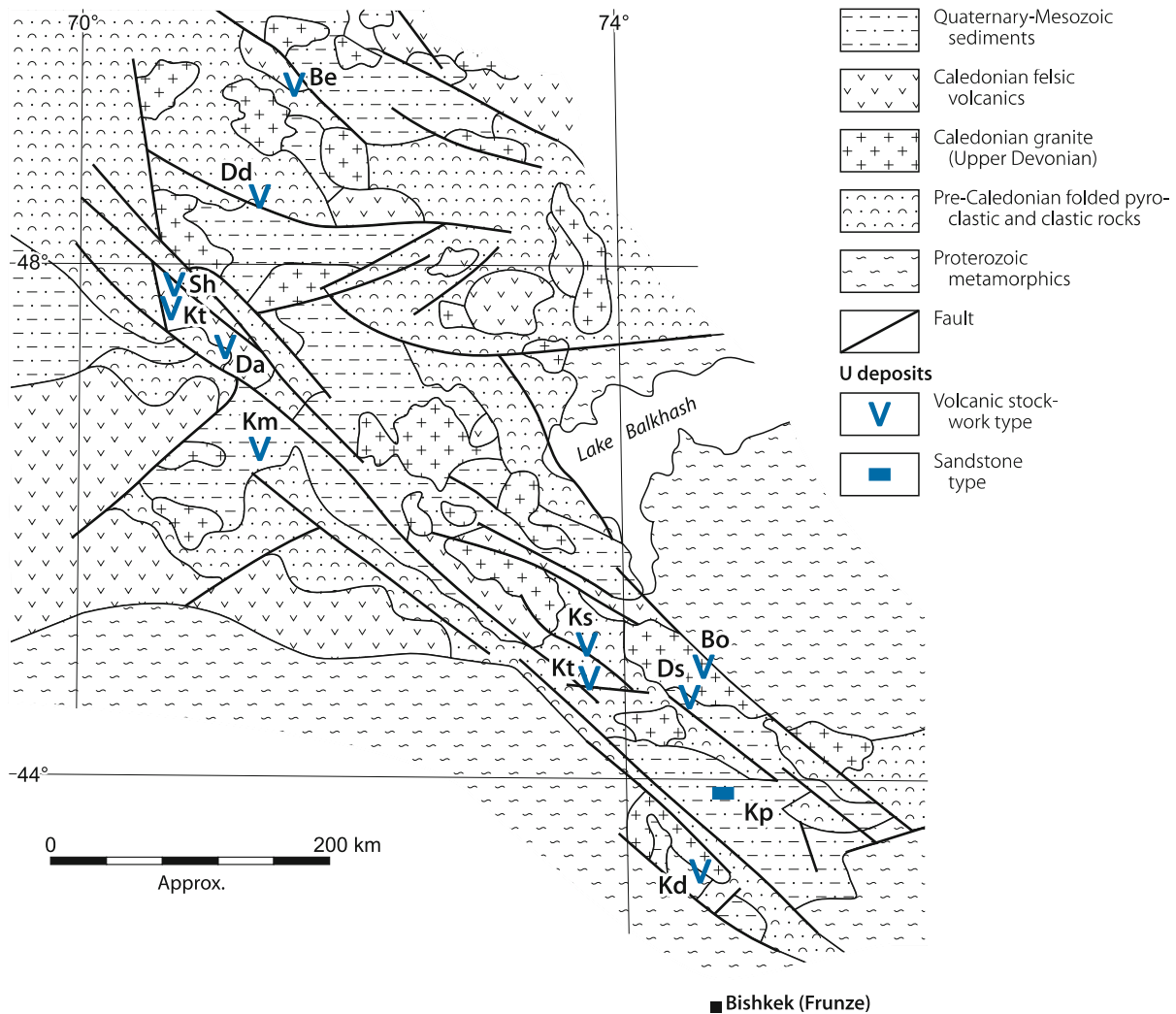
Deposits of the Kyzylkol-Chayan District occur along a NNW-SSE-trending redox front in Tertiary aquifers that contain carbonate lenses. Ore bodies are of roll shape and consist of finely dispersed coffinite and (sooty) pitchblende. Rolls are a few meters thick, range from 100 m to few kilometers long, and from 10 to 300 m wide. Ore at Kyzylkol occurs at depths from 130 to 200 m, and at Lunnoye from 310 to 530 m.

6.5 Pribalkhash (Lake Balkhash)/Kendyktas-Chuily-Betpak Dala Region, SE Kazakhstan

The Pribalkhash uranium region stretches from the Kyrgyzstan border in the Kirgizian range (north of the town of Bishkek in NW Kyrgyzstan) to the area west of Lake Balkhash and further north and northwestwards into the Betpak Dala (Hunger Steppe) in central-south Kazakhstan. Deposits group primarily in the

Fig. 6.21.

Pribalkhash uranium region, simplified geological map of the Caledonian Chuili-Kandyktas Uplift and associated volcanic- and sandstone-type U deposits (after Laverov et al. 1992c). **U deposits:** Be Bezymyannoye, Dd Dzhideli, Sh Shorly, Kt Kostobe, Da Daba, Km Kurmanchite, Ks Kyzylsay (# I to VIII), Kt Kyzyltas, Bo Botaburum, Ds Dzhusandalinskoye, Kd Kurday, Kp Kopalysay



northern *Betpak Dala* and the central *Chuily* (also spelled *Chully*) area. Additionally, some small deposits are known such as *Kurday* in the southern *Kendykta*s and *Karatal* in the *Shuisky* area (Figs. 6.1, 6.21). The northwestern part encloses the *Granitnoye ore field*, a small sedimentary basin with a few basal-channel sandstone-type deposits. Most other deposits, except *Kopalysay*, which is of the sandstone rollfront type, are associated with volcanics and consist of structurally controlled stockwork mineralization. They are therefore classified as volcanic stockwork type (in Russian literature referred to as vein-stockwork deposits in continental volcanic complexes or as hydrothermal Mo-U deposits associated with the rhyolite-granite association in subvolcanic massifs or in exploration pipes and necks, respectively).

Original(?) in situ resources of the Pribalkhash region amount to 71 900 t U RAR + EAR-I. They include 21 900 t U RAR (Abukumov 1995; OECD-NEA/IAEA 1993). Resources in volcanic-type deposits amount to more than 65 000 t U, and in sandstone-type to less than 7 000 t U. Ore grades range from ca. 0.1–0.3% U.

The first deposit, *Kurday*, was discovered in 1951. Mining started in 1953 and lasted until 1990. Exploration was performed by Stepgeology while the Kyrgyz Mining Combine, later renamed Yuzhpolymetal Production Enterprise, based in Bishkek, was the mining operator during these years. About 15–20 mostly small U deposits have been exploited. Total production is speculated to be on the order of 10 000 t U. Ore was treated in a mill at Kara Balta (Kyrgyzstan), ca. 60 km W of Bishkek, that had a nominal capacity of 1.5 million t ore yr⁻¹ and an estimated U production capacity on the order of 3 600 t U yr⁻¹.

Sources of information. Petrov et al. (1995, 2000) amended by data from Abukumov (1995), Laverov et al. (1992a–c), OECD-NEA/IAEA (1993, 1995).

Regional Geological Setting of Mineralization

The Pribalkhash uranium region is within the *Chuily-Kendykta*s Uplift, a fragment of the Ural-Mongolian fold belt of Caledonian age. Precambrian gneiss and schist and Late Silurian-Early Devonian continental felsic to mafic volcanics constitute the basement. Devonian granites and felsic volcanics were intruded and extruded, respectively, during the Caledonian Orogeny. Most of the uranium deposits are located within the margin of this Devonian igneous belt. Mesozoic-Cenozoic sediments rest on the crystalline rocks.

The Silurian-Devonian continental volcanic suite consists of folded alternating layers of rhyolite to andesite lavas intercalated with pyroclastic and clastic rocks. Caledonian subvolcanic stocks of rhyolitic composition and small hypabyssal batholiths of granite were intruded into this suite in a linear belt oriented NW-SE. The belt is a horst and graben structure up to several hundreds of kilometers wide controlled by NW-SE-trending, deep seated lineaments with NW-SE-oriented first order structures of large vertical and horizontal displacements in the pre-Caledonian basement. These structures are expressed by wide

zones of brecciation and/or intense fracturing and jointing, tens to hundreds of meters wide, and by subvolcanic intrusions and dike belts in the overlying volcanic suite. Younger fault systems of variable orientation imposed additional deformation on the magmatic belt.

Principal Host Rock Alterations

Principal alterations associated with structurally controlled U deposits include propylitization, beresitization, and argillization. *Propylitization* is reflected by calcite and chlorite after muscovite and biotite; *beresitization* by pyrite-sericite, hydro-mica-carbonate and chlorite-hematite associations; and *argillization* by kaolinite, quartz, and hydromica. The transformation process occurred during the Upper Devonian to Lower Carboniferous and typically affected the various deformed lithologies within U-hosting regional fault zones but also occur along the contacts of Devonian granitic massifs. The alteration facies are distributed in a centripetal zoning around U deposits grading from propylitization at the periphery to beresitization, and argillization. At some deposits, e.g. at *Dzhusandalinskoye*, the country rocks are Na metasomatized reflected by albitization.

Principal Characteristics of Mineralization/General Shape and Dimensions of Volcanic-Type Deposits

Volcanic-type mineralization is polymetallic composed of a uranium-molybdenum paragenesis. Pitchblende and locally coffinite are the principal uranium minerals. Associated minerals are jordanite, molybdenite, marcasite, pyrite, and other sulfides in minor amounts. Gangue minerals include quartz, sericite, carbonates, and fluorite.

Deposits consist of structurally controlled ore bodies of highly irregular configuration, size and grade with uranium tenors ranging from 0.03 to as much as 10% U or more as in some ore shoots at *Dzhideli*. Ore bodies are composed of a complex system of interlinked veins, lenses, and/or stockworks in which the ore occurs in disseminated, streaky and, more rarely, massive texture. Most deposits mined had original reserves between 1 000 and 2 000 t U except *Botaburum* which contained some 10 000 t U. Felsic effusive sheets, pyroclastics, and volcanic dikes and necks composed of felsite, quartz-porphyry, and rhyolitic lava, breccia, and tuff provide the prevailing host rocks except at *Kurday* where the ore is hosted by granodiorite porphyry but in immediate contact to a steeply dipping felsite body (Figs. 6.22a–c). Structural and lithologic elements, which control the position and configuration of ore bodies are listed further down.

Regional Geochronology

The main stage of structurally controlled uranium mineralization in the Pribalkhash region is dated at 370–350 Ma, which corresponds to the Late Devonian. Additional episodes of U introduction or redistribution yield 330–310 and 285–265 Ma

Fig. 6.22. Pribalkhash region, Shorly deposit, **a** map and **b** W-E cross-section, **c** Kurday deposit, SW-NE cross-section, illustrating the litho-structural setting of stockwork-type U mineralization (after **a**, **b** Petrov et al. 2000; **c** courtesy of Boitsov AV based on Russian literature)

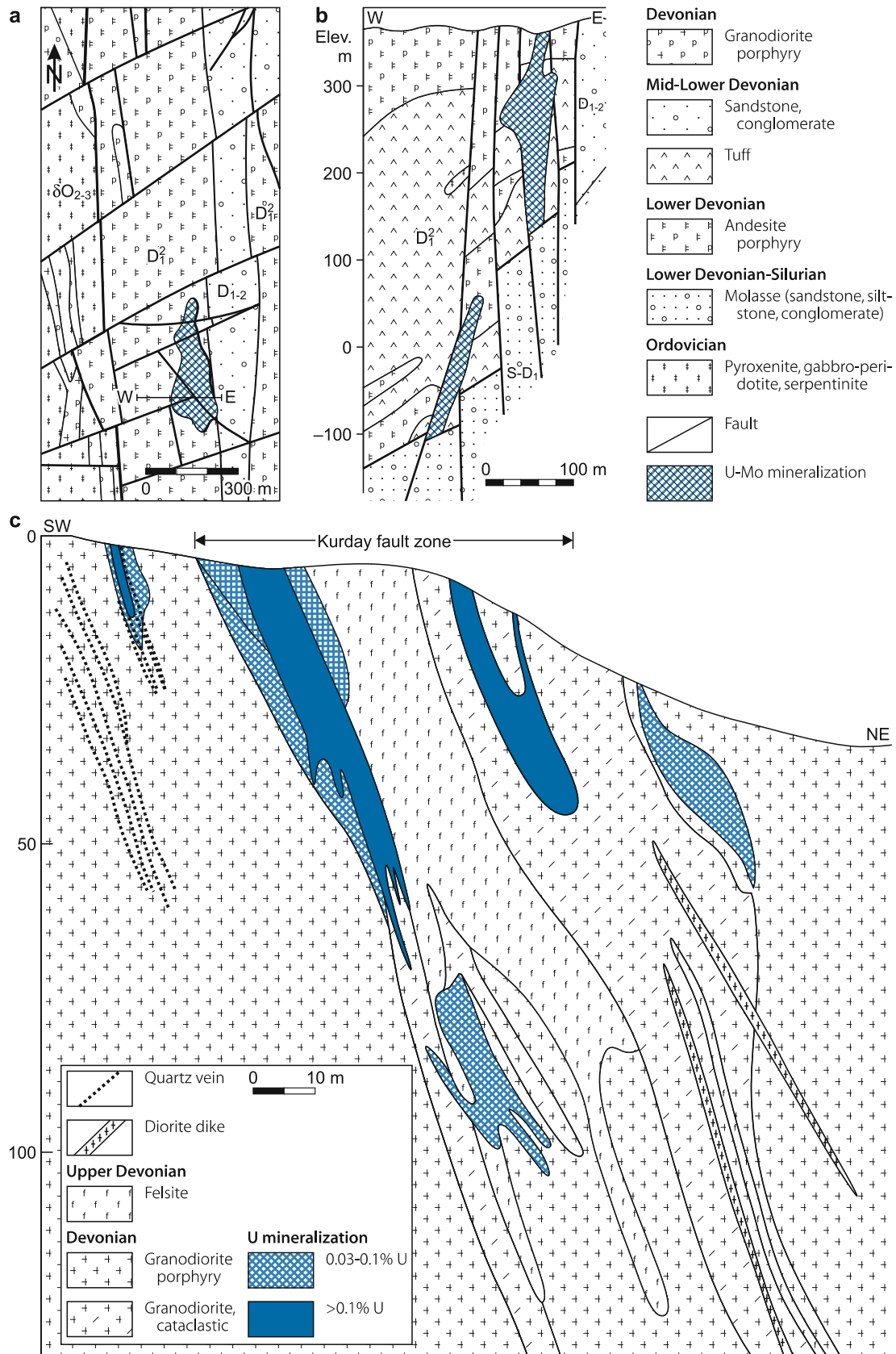


Table 6.6.

Chuilu-Betpak Dala region, Isotope ages of U mineralization and redistribution in endogenic deposits (Petrov et al. 2000). *In italic:* principal age of ore formation

Mineralization type	Age (Ma)	Deposits example
P-U, U in Na metasomatite and beresitization zones	486–450, <i>370–350</i> , 330–310, 285–265	Kostobe, Daba, Dzhusandalinskoye
Mo-U, U in beresitization, argillization, and feldspathization zones	<i>370–350</i> , 330–310, 285–265	Botaburum, Kyzylsai, Dzhideli, Shorly, Kurday

while an early P-U mineralization, dated at 486–450 Ma, is identified at some deposits (Petrov et al. 2000) (Table 6.6).

- low to high average grades (0.046–0.6% U)
- commonly small to medium tonnage (few tens to rarely a thousand t U)

Principal Ore Controls and Recognition Criteria of Volcanic-type Deposits

Significant ore controlling parameters or recognition criteria of the major volcanic-type deposits in the Pribalkhash region, include:

Host Environment

- Large volcanic belt dominated by felsic facies of Caledonian age controlled by deep reaching regional faults
- Association of U deposits essentially with felsic/rhyolitic volcanics
- Regional faults associated with extensive cataclastic zones along which the position of ore bodies is controlled by one or several of the following parameters:
 - intersections of faults along axial trend over basement highs
 - intersection of transverse fractures with dikes
 - axial faults following steeply-dipping contacts between extrusive volcanics and hypabyssal granite
 - sharp changes in dip of facies contacts cut by a fault
 - volcanic necks and granite porphyry dikes in annular fault zones
 - contacts of volcanic lithofacies

Alteration

- Predominantly propylitization, beresitization, and argillization
- Na metasomatism/albitization at some deposits

Mineralization

- Polymetallic U-Mo assemblages primarily composed of pitchblende, minor coffinite, molybdenite, jordisite
- Associated metallic minerals are dominated by sulfides (mainly Fe-sulfides)
- Gangue of quartz, sericite, carbonates, and/or fluorite
- Ore textures range from disseminated, to streaky and locally massive
- Deposits commonly consist of a number of ore bodies
- Ore bodies are characterized by
 - a complex system of interlinked veins, lenses, and stockworks

Metallogenetic Concepts of Volcanic-Type Deposits in the Pribalkhash Region

As far as known, the metallogenesis of the volcanic-type U deposits in the Pribalkhash region was only dealt with in a larger scope, together with this type of deposits particular in the Streltsovsk District, Russia, and the Karamazar region, Uzbekistan, from where more specific, substantiated descriptions are published. The reader is therefore advised to find information provided in the respective chapters on metallogenetic aspects of these two areas.

6.5.1 Northern Betpak Dala Area

The northern Betpak Dala area includes four uranium ore fields: *Dzhideli*, *Koskarin*, *Shorly-Kostobe*, and *Daba*. Exploration started in the 1950s. Mining began in the 1960s following the discovery of the *Dzhideli* deposit and lasted until the mid 1980s. The area is located in the western part of an intrusive-volcanic belt. Two geological structures dominate the terrane, the Buruntay anticlinorium, a linear, NW-SE-oriented structure, 300 km long and 60–180 km wide, and the westerly adjacent Zhalaïr-Naiman synclinorium, 250 km long and 20–90 km wide. Mesozoic-Cenozoic sediments of the Chu-Sarysu Basin cover the latter.

Source of information. Petrov et al. 2000.

6.5.1.1 Dzhideli Ore Field (Dzhideli and Sarytas Deposits)

This ore field is centered 110 km south of the town of Karashal in the Dzhezkazgan region of central Kazakhstan. It is located in the Sasyrlyk volcanic basin, a western fragment dominated by andesite-dacite and rhyolite facies of the Devonian intrusive-volcanic belt. The basin is 200 km long in NW-SE direction and 100 km wide, and bordered by the large Shabdar fault to the SW, the Akdala fault to the SE, and the Atasui fault to the NE. The ore field contains the medium size *Dzhideli* deposit, the small *Sarytas*

deposit, and the *Kostakyr*, *Proktasskoye*, *Gravitacionnoye*, and *Kuntau* occurrences. The ore lodes are classified as structurally controlled volcanic type, which relate in Russian classification to the molybdenum-uranium type in the zones of beresitization, argillization, and feldspathization.

The Dzhideli deposit was discovered in the southern part of the same named volcanic structure in 1961 and contained resources in the 1 500–5 000 t U resource category. Grades averaged about 0.4% U but some ore shoots had grades in excess of 10% U. Mining was by open pit and underground methods but has ceased in the mid 1970s.

Three suites of Middle to Upper Devonian volcanics contain U mineralization (from top to bottom): (a) plagioclase porphyry, tuff-sandstone, and volcanic breccia; (b) two horizons of welded felsite tuff, up to 170 m thick (principal host rocks); and (c) plagioclase-quartz porphyry, tuff, ignimbrite, and lava-breccia, up to 350 m thick. NW-SE- and W-E-striking diabase and diabase porphyry dikes dissect this volcanic suite. Principal structures are the NW-SE- and NE-SW-trending Northern, Southern, and Dzhideli faults. Host rock alteration phenomena include pre-ore chlorite-albite, ore-related pyrite-ankerite, and post ore quartz-calcite-sulfide.

Mineralization is of polymetallic nature dominated by uranium-molybdenum associated with As, Bi, Co, Ga, Pb, Sb, and Zn. Two ore types are distinguished: femolite-pitchblende and pitchblende-sooty pitchblende. Uranophane, beta-uranotile, autunite, etc are typical for the oxidation zone, which extends to a depth of 100 m. Primary mineralization is dated at 360 ± 8 Ma, and redistributed mineralization at 210–100 Ma.

Ore bodies # 1, 2, 5, 6, and 8 have a lenticular shape and occur in fault zones within welded felsite tuff at depths from 30 to 180 m. Ore bodies # 1, 2, and 5 contain 95% of the Dzhideli resources. Ore body # 1 is 400 m long, 0.5–35 m (av. 10 m) thick, persists from 30 to 80 m deep, and has a grade of 0.228% U. Ore body # 2 is 1 000 m long, from 2 to 18 m (in average 6 m) thick, occurs at depths from 70 to 140 m, and averages 0.213% U. Ore body # 5 contains high-grade ore with an average of 2.42% U. It is 160 m long, from 2 to 25 m (av. 7.5 m) thick, and occurs at a depth interval from 30 to 70 m.

Sarytas is a small deposit with an average grade of 0.077% U. It was discovered in 1965 almost 100 km to the SW of the town of Karazhal in the southern part of a volcanic dome. Country rocks are a Devonian andesite porphyry, up to 400 m thick; a volcanic-terrestrial horizon, 40–95 m thick; a felsite horizon, about 120 m thick; and a volcanic sandstone, 200 m thick. Lenticular ore bodies, 2.3–7 m thick, are restricted to the lower felsite horizon in which they are controlled by the intersection of the N-S Glavnaya with the NW-SE Anomalnaya fault zone. Wall rocks are altered by pyritization, chloritization, sericitization, and carbonatization. Pitchblende and sooty pitchblende are the principal U minerals. Associated minerals include molybdenite, arsenopyrite, and galena.

6.5.1.2 Koskarin Ore Field (Bezmyannoye Deposit)

This ore field includes the explored *Bezmyannoye* deposit located 70 km N of the Dzhideli deposit in the NW part of the Sasyrlyk

volcanic basin. Resources of *Bezmyannoye* are less than 1 500 t U and average 0.15% U. Country rocks include Devonian ignimbrite with sandstone intercalations that rest upon quartz porphyry tuff and lava. Mineralization is hosted by breccia zones in ignimbrite close to the contact with a subvolcanic felsite body. The wall rocks are altered by sericitization, silicification, and chloritization. Pitchblende and molybdenite are the principal ore minerals. Associated elements include Be, Sn, Zr, and F. Ore bodies are of vein and lenticular configuration. They are up to 300 m long and up to 20 m thick, and occur in a 300–500 m wide zone close to the N-S-trending *Bezmyannoye* fault.

6.5.1.3 Shorly-Kostobe Ore Field (Kostobe and Shorly Deposits)

Shorly is located 50 km SW of the Dzhideli deposit and forms with the about 10 km to the south situated Kostobe deposit the Shorly-Kostobe ore field.

Shorly was discovered in 1980. In situ resources amount to 1 300 t U at a grade of 0.125% U. The deposit occurs in a tectonic block, which is limited by N-S and NE-SW faults. Host rocks are Lower Devonian sedimentary and volcanic rocks, as much as 500 m thick, composed of lithoclastic tuff, breccia, tuff-sandstone, and andesite porphyry. Devonian granodiorite dikes cut this sequence. Silurian to Lower Devonian pink molasse underlies unconformably this unit. The steeply inclined, NNW-SSE-oriented Western Ulkensor fault exerts the principal ore control.

Mineralization is of polymetallic U-Mo composition. Coffinite is the prevailing uranium mineral, pitchblende is of minor abundance; molybdenum occurs as molybdenite and femolite. Ore consists of three mineral associations: femolite-anatase-pyrite-arsenopyrite, coffinite-pyrite, and femolite-pyrite. The ore contains elevated concentrations of up to 1% (in average 0.22%) Cu, up to 0.7%, (av. 0.28%) As, and up to 0.07% (av. 0.01%) Pb.

Two ore bodies are identified. The upper *ore body # 1* is of lenticular shape with an internal stockwork structure. It is 500 m long, up to 40 m thick, occurs at the depth interval from 25 to 260 m, and contains 70% of the resources at a grade of 0.131% U. The lower *ore body # 2* is a steep lens, 250 m long, up to 40 m (in average 10 m) thick, and persists from 250 to 500 m down dip (► Figs. 6.22a,b).

Kostobe was discovered in 1977 and mined by open pit methods. Original resources were less than 1 500 t U at a grade of 0.201% U. Country rocks consist of Lower to Middle Devonian volcanic-sedimentary rocks bi-partitioned into an upper unit, as much as 110 m thick, of andesite-porphyry, tuff, tuff-conglomerate, and porphyry; and a lower unit, 500–650 m thick, of volcanic conglomerate, sandstone, and gravel. NW-SE and E-W fault systems dissect the area. Shallow to intermediate steeply dipping faults, most of them occur interstratified in the upper horizons, control the uranium mineralization. Ore bodies are composed of veinlets and finely disseminated uranium minerals and are distributed at depths from 20 to 200 m. Two main

ore bodies are identified. Ore body # 1 consists of some lenses hosted by beresite-altered porphyry. It is 250 m long, from 1 to 23 m (av. 13 m) thick, persists at depths from 17 to 125 m, and contains 80% of the Kostobe resources at an average grade of 0.216% U. Ore body 2 occurs 80–100 m below ore body # 1 in tectonic breccia within gravel and sandstone of the lower unit. The lens-shaped lode is from 35 to 40 m long, up to 15 m (av. 9 m) thick, extends to depths from 140 to 200 m, and averages 0.2% U.

6.5.1.4 Daba

Daba is an explored U deposit situated ca. 50 km SE of the Kostobe deposit. It was discovered in 1979 and contains resources in excess of 5 000 t U in the two sectors # 1 and # 2.

Daba is located at the NE contact of the Ordovician Keepchakbai hyperbasite massif with Upper Ordovician continental rocks. The latter host the ore in a volcanic-sedimentary sequence, up to 700 m thick, composed of (from top to bottom) a flysch-type sedimentary-volcanic formation, 300 m thick, with conglomerate, gravel, sandstone, tuff, and andesite porphyry; massive aphanitic limestone 100–200 m thick; and black carbonaceous-silica siltstone with interbedded sandstone. Devonian tuff with sandstone layers and andesite porphyry lenses rest unconformably upon the Ordovician. The Devonian is overlain by Mesozoic-Cenozoic sediments, 1–25 m thick, composed of Triassic to Jurassic eluvial material, Paleogene conglomerate, and Quaternary clay-sand. Intrusions are represented by Ordovician ultrabasite (dunite, pyroxenite) and gabbro bodies to the W of the deposit and a complex of Middle Devonian diorite and diabase porphyry dikes. Some dikes are 200–700 m long and 10–20 m thick. The rocks are folded to a monocline of NW-SE strike and 20–40° to 60–80° NE dip. NW-SE faults offset by ENE-WSW faults are the predominant brittle structures. Host rock alteration is reflected by carbonatization, propylitization, and bleaching.

Ore lodes occur in two sectors, which contain mineralization of two different mineral associations and ages. An early Paleozoic metamorphic stage, dated at 500–430 Ma, is reflected by low-grade, stratiform pitchblende-apatite ores, whereas late Paleozoic orogenic tectonic-magmatic activity, dated at 350 Ma, generated vein pitchblende-sulfide ores.

Sector # 1 covers a 3.7 km long zone in the southern part of the deposit in which ore lodes occur at depths from 0 to 250 m, distributed over vertical intervals that average a thickness of 36 m. Host rocks are preferentially brecciated, carbonaceous sandstone but also carbonaceous siltstone, sandstone, gravel, and andesite. Mineralization consists of a pitchblende-apatite (frankolite) association. Apatite contains up to 0.3% U, 3% Zr, and 0.6% Sr. Ore lodes average 0.043% U and have elevated concentrations of up to 11% P₂O₅, 0.7% F, 0.33% Sr, and 0.22% Zr. Separate lenticular ore bodies occur strata-concordant within the litho-stratigraphic profile.

Sector # 2 is an 850 m long zone situated in the northern part of the deposit, at the contact of the Upper Ordovician volcanic-sedimentary sequence with hyperbasite. Mineralization consists of a pitchblende-sulfide (chalcopyrite, pyrite, sphalerite) association, which forms vein or stockwork ore bodies with a thickness from 12 to 15 m and an average grade of 0.064% U (max.

0.174% U). The ore lodes are controlled by intersections of ENE-WSW and NW-SE faults.

6.5.2 Central Chuily Area

This area is located in the Chuily Uplift to the south of the western end of Lake Balkhash and the Kyrgyzstan border. It includes three ore fields: *Kyzylsay*, *Botaburum*, and *Mynaral*. Principal deposits occur within the first two ore fields. A Devonian volcanic-intrusive belt and abyssal fault zones control these fields. Exploitation started in the late 1950s following the discovery of the Botaburum and Kyzylsay deposits. Some isolated deposits/ occurrences are also reported such as the stockwork-type *Kurmanchite* deposit that is located at the western margin of the Chuily area about 420 km NW of Almaty.

Source of information. Petrov et al. 2000.

6.5.2.1 Kyzylsay Ore Field

This ore field was discovered 340 km NW of Almaty in 1957 and coincides with the same named caldera. *Kyakhtinskoye*, *sector 2*, *Blishnee*, *sectors 4, 7, 8*, and *Zhamantas* are deposits within the Kyzylsay Caldera while the small *Kyzyltas* deposit occurs at the southern margin of the caldera. Original resources were reportedly in excess of 5 000 t U at a grade of about 0.1% U. Most deposits were mined underground and are depleted.

The Kyzylsay Caldera is a circular structure, 20–30 km in diameter, composed of Devonian volcanic (rhyolite, ignimbrite, dacite porphyry) and terrigenous rocks intruded by Late Devonian stocks and dikes. Ore lodes are controlled by E-W structures. Preferential host rocks are Devonian felsic porphyry and lava breccia affected by propylitic-beresitic and feldspar-argillic alteration. Ore mineral associations comprise uraninite-molybdenite-magnetite, pitchblende-molybdenite, and pitchblende-femolite-pyrite. The *Kyakhtinskoye* and *sector 2* deposits occur in the central block of the ore field. *Sector 2* mineralization consists of lenses and veinlets, which form several stockwork ore lodes within a fracture zone that cut rhyolite. Stockworks range from 30 to 150 m long, up to 20 m wide, and persist to 300 m deep. Grades average 0.12% U and 0.06% Mo.

6.5.2.2 Botaburum Ore Field

This ore field was discovered about 260 km NW of Almaty in 1953. Original resources were reportedly some 10 000 t U at an average grade of 0.157% U contained in several separate ore bodies. Mining was by underground methods and has ceased. Molybdenum was recovered as a by-product to uranium.

Botaburum is located within the homonymous volcanic caldera, which is characterized by rhyolite, eruptive breccia, and rhyolite porphyry tuff-breccia. Country rocks include rhyolitic and andesitic volcanics and clastic sediments of the Upper to Mid Devonian Karasay Formation (or suite) and the Lower Devonian Koktaus Formation. Upper Devonian leucogranite of

the Dzhusandaly Massif occurs as cupolas. Intrusive stocks, dikes, and/or sills consist of quartz-, granite-, diabase-, diorite-, and gabbro-porphry, and andesite-basalt. Wall rocks are altered mainly by beresitization.

Mineralization consists of coffinite, uraninite, and brannerite associated with Mo and other sulfides that form stockwork-type ore bodies. Most ore lodes occur in subvolcanic rhyolite bodies close to the contact with granite controlled by the intersection of steep, NE-SW-oriented fracture zones with the NNW-SSE-trending, 65° W dipping contact fault. Some ore bodies also locate in fracture zones at the contact of extrusive and intrusive volcanics. Ore bodies range from 50 to 220 m long and deep, from 3.5 to 40 m thick, and have grades from 0.08 to 0.5% U. Ore persists to depths of 1 200 m.

6.5.2.3 Dzhusandalinskoye

Dzhusandalinskoye is a developed prospect situated 12 km SW of Botaburum. It was discovered in 1981 and consists of the *Northern* and *Southern sectors*. Resources are in excess of 5 000 t U and average 0.239% U.

Host rocks consist of Upper Devonian leucogranite and microcline granite of the Dzhusandaly Massif, which are cut by diorite, diabase porphyry, and quartz porphyry dikes. Three structural elements dominate the deposit terrane: the NNE-SSW-trending Daike zone, 600 m wide, with 7 fracture and cataclastic zones, each 10–50 m wide; ENE-WNW fracture zones; and the N-S-oriented Dzhusandalin structure with eight, from 8 to 20 m wide faults. Mineralization consists of coffinite and pitchblende contained in stockwork or column-like ore bodies that are embedded in wall rocks altered by quartz-carbonate-albite and hydromica-calcite facies. Ore bodies group in the Northern and Southern sector in which they are controlled by the intersection of the Daike and Dzhusandalin zones with quartz porphyry dikes. Each sector consists of isolated ore bodies distributed to depths of 1 000 m. Ore bodies are from 300 to 400 m long, 12–120 m thick, persist for 140–160 m down dip, and grade from 0.03 to 1.4% U.

6.5.3 Southern Pribalkash Region

The southern Pribalkash region includes the *Kurday* and *Kopalysay* U deposits. The latter is a small sandstone rollfront-type U deposit in Lower Silurian sandstone with resources of less than 5 000 t U at a grade of <0.1% U.

6.5.3.1 Kurday, Kendyktas Area

Kurday is a volcanic stockwork deposit located in the Kendyktas area, about 200 km W of Almaty and 40 km E of Georgievka. It was discovered in 1951 and had original resources of about 3 500 t U at an average grade of 0.6% U. The deposit was mined by open pit and underground methods and is depleted.

Kurday is hosted in Devonian porphyritic granodiorite of the Kurday Complex, which was intruded into Upper Proterozoic-

Lower Cambrian metamorphites. Upper Devonian-Carboniferous dioritic dikes and stocks, felsite dikes, and quartz-sulfide veins dissect the country rocks. The regional Kurday fault zone is a major, NW-SE-trending, steeply NE-dipping structure in the area and exerts the primary control on the position of the Kurday ore lodes. Ore lodes occur within this fault zone at the intersection with other structures, but likewise along blastomylonite sutures, felsite dike contacts, and fracture zones (► Fig. 6.22c). The ore hosting lithologies are altered by albitization, beresitization, and carbonatization.

Mineralization occurs in discontinuous lenticular stockwork and vein lodes, which are from 1 to 300 m long, from 1 to 50 m thick, and persist over vertical intervals from 30 to 210 m. Grades range from 0.03 to 1.5% U. Major lodes occur on both sides of a steeply NE-dipping, up to 20 m wide felsite dike. Rocks are heavily brecciated and altered for up to 30 m wide on the NE side and for up to 10 m wide on the SW side of the felsite. Each of these two cataclastic zones contain a stockwork-type U-Mo ore body composed of an up to 8 m wide core with grades in excess of 0.1% U. The core in the NE zone extends to a depth of ca. 30 m and that in the SW zone to about 65 m. Both ore zones are surrounded by lower grade aureoles ranging from 0.03 to 0.1% U. The lower grade NE zone is up to 35 m wide and persists to a depth in excess of 130 m. The SW zone is about 15 m wide near surface, narrows down at depth and extends, with barren intervals, to about 100 m deep. Several narrow ore bodies with variable depths extensions occur discontinuously on both extremities but particularly on the NE side of the main ore zones to depths of 500 m.

6.5.4 Granitnoye Ore Field

The Granitnoye ore field is located in a Cenozoic depression at the northern margin of the Betpak Dala area (► Fig. 6.1). Two basal-channel sandstone-type U deposits, *Talas* and *Granitnoye*, each containing a few hundred tonnes of uranium at ore grades of less than 0.1% U, occur in Miocene paleochannels filled with carbonaceous, clayey, and gravelly sands overlain by mud and gravel sand.

At *Talas*, mineralization occurs as lenses in basal sediments of the Aral-Pavlodar complex. Lenses are some tens of meters wide, up to 1 m thick, and range in length from some tens to several hundreds of meters elongated along the channel axes. Uranium is preferentially concentrated in grey, carbonaceous, argillaceous sediments close to the contact with sands while sands tend to contain only minor mineralization. At *Granitnoye*, the ore setting is similar to *Talas* but U mineralization occurs additionally in the weathered crust of the underlying pre-Mesozoic granite basement (Petrov et al. 1995).

6.6 Ily Region, SE Kazakhstan

The Ily uranium region is situated in southeastern Kazakhstan. It stretches along the Ily River from Lake Balkhash to the Chinese border and into NW China. The Ily region occupies parts of two basins, to the north a western segment of the Balkhash Basin referred to as Nizhne-Ily Subbasin, and the southerly adjacent Ily Basin.

Resources of the Ily region are about 130 000 t U in the <\$130 per kg U cost category. They include 92 900 t U RAR + EAR-I and 37 000 t U EAR-II. 28 900 t U of the RAR are attributed to the <\$80 per kg U cost category (Abakumov 1995). The given uranium resources are contained in three major deposits, the lignite-type *Nishne-Ilyskoye* and *Koldzhat* and the sandstone-type *Suluchekinskoye* deposits, which were developed but never mined. In addition, a number of small sandstone-type U deposits also occur, such as *Kalkan* and *Aktau* (► Fig. 6.1).

6.6.1 Western Balkhash Basin/Nizhny-Ily Subbasin

The large Balkhash Basin extends from Lake Balkhash for hundreds of kilometers eastwards into the Xinjiang region in NW China and southwards to about Almaty. The basin includes in its northwestern section the Nizhne-Ily Subbasin, which hosts the Nizhne Ilyskoye lignite-uranium deposit.

Sources of information. Abakumov (1995), Kislyakov and Shchetochkin (2000), Petrov et al. (1995), and Shchetochkin and Kislyakov (1993) unless otherwise cited.

Regional Geological Features of the Nishny-Ily Subbasin

The Nizhny (Lower)-Ily Subbasin is characterized by and resulted from block faulting along NW-SE- and about N-S-oriented deep faults. Grabens are downfaulted into Paleozoic rocks and filled with Jurassic sediments including a 125–260 m thick unit of Lower to Middle Jurassic lignite-bearing facies. The lignite facies lies at a depth of 100–500 m. Upper Tertiary and Quaternary sediments up to several hundred meters thick cover the pre-Tertiary lithologies.

The grabens are relics of Mesozoic intermontane depressions within a large central Asian orogenic belt. Tectonic reactivation in pre-Oligocene time generated sublongitudinal faults, which now define the geometry of the grabens. Rocks of uplifted blocks were strongly eroded leaving only thin remnants of Jurassic strata.

6.6.1.1 Nizhne Ilyskoye

The Nizhne Ilyskoye lignite-U deposit was discovered approximately 300 km NW of Almaty near the western margin of the Nizhny-Ily Subbasin in 1973 and was explored from 1978 to 1980. In situ resources are 60 000 t U at a grade on the order of 0.1% U. The deposit is developed but mining has been postponed due to unfavorable economics.

Geological Setting of Mineralization

The Nizhne Ilyskoye deposit occurs in a buried NW-SE-oriented, 100 km long and 15–20 km wide graben. The graben is downfaulted into a basement composed predominantly of Devonian

porphyry (► Figs. 6.23a,b). A bauxite-bearing paleoregolith zone, as much as 40 m thick, is developed on the basement.

Jurassic continental sediments fill the graben. A single sequence of Lower to Middle Jurassic alternating alluvial, lacustrine, and paludal sediments up to 200 m thick forms the basal unit. Medium-grained, polymict sandstone is the prevalent lithology. It encloses discontinuous, partly carbonaceous gritstone and pelite beds from a few meters to 25 m thick, and in the upper section a lignite seam up to 56 m thick. On the NE side of the graben, the seam is of massive nature and abuts against the paleovalley slope. The seam splits up and pinches out to the southwest. Upper Jurassic arenite, 20–100 m thick, rests on the older Jurassic suite. A blanket of 100–120 m thick Neogene (Ng₂) mud-silt overlain by 80–100 m thick Quaternary sand buries the Jurassic rocks (► Figs. 6.23b,c).

The Jurassic sediments are almost horizontally bedded while the overlying Cenozoic sediments are distinctly inclined to the east attesting to a complex tectonic history of the region.

Host Rock Alteration

Prominent regional alteration features in Jurassic rocks include oxidation and reduction effects reflected by grey, pink, and yellow-colored facies. They derived by three prominent alteration stages (► Fig. 6.23c):

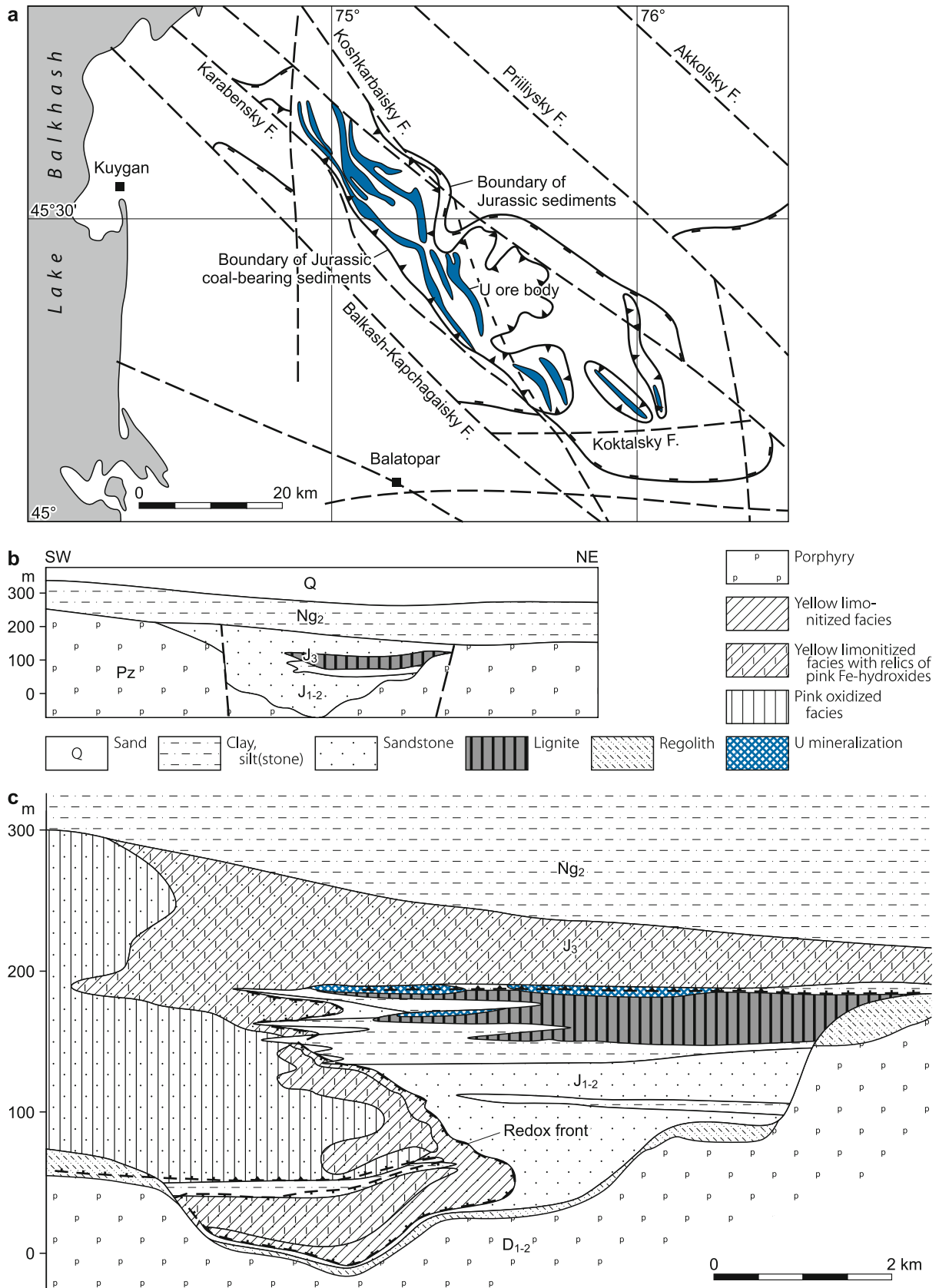
1. An early epigenetic oxidation stage has transformed originally grey facies into pink (hematitic) facies prior to their burial under an aquiclude of Neogene clay and gypsiferous sand. The process affected the whole of the Upper Jurassic sediments overlying the lignite seam and, in sections where the seam wedges out, the complete Jurassic sequence down to and into the basement. Remnants of this oxidation phase are also found in re-reduced facies. Circumstantial evidence deduced from other parts of central Asia suggests that the oxidation period occurred during Late Jurassic time.
2. Re-reduction followed the oxidation period and affected parts of the sedimentary accumulation. Reducing agents supposedly evolved by oxidation of organic matter that generated organic acids and associated reductants such as hydrogen sulfide, hydrogen, and methane, which migrated through and reduced parts of the formerly oxidized sediments.
3. Late oxidation reflected by yellow colored, limonitized rocks overprinted predominantly re-reduced facies. It extends only slightly into the zone of early oxidation.

Mineralization

Mineralization is polymetallic composed primarily of U-Mo accompanied by trace amounts of other elements. *Uranium minerals* include pitchblende and sooty pitchblende (black products), which constitute approximately 80% of the U minerals fraction while coffinite accounts for about 20%. Additional U minerals include rare ianthinite, mourite, fourmarierite, U-selenide, and studtite. A major fraction of the uranium is adsorbed by carbonaceous matter in limonitized lignite. The principal *Mo-minerals* are ilsemannite, jordisite, and less common molydenite and

Fig. 6.23.

Ily Regin, Balkhash Basin, Nizhne-Ilyskoye, **a** map of the northwestern Balkhash Basin showing the graben structure hosting uraniferous lignite seams. U is concentrated in the roof section of the seams. **b** Litho-stratigraphic SW-NE section, **c** litho-geochemical section illustrating the style and distribution of alteration features, (after **a** Petrov et al. 1995; **b, c** Shchetochkin and Kislyakov 1993)



molybdenite. *Associated minerals* include mainly ferroselite, marcasite, pyrite, and minor to rare, arsenolite, chloantite, galena, orpiment, radiobaryte, realgar, skutterudite, sphalerite, tennantite, and native lead and selenium.

A number of *trace elements* occur in the deposit. Two elemental groups are distinguished: Uranium ore zones contain Ag, Cd, Co, Ga, Ge, Mo, Ni, Re, Tl, and Zn, while limonitized lignite contains Be, Cu, Pb, Sc, Se, V, Y, Zr, and REE.

Shchetochkin and Kislyakov (1993) report an oxidation-related vertical zoning of ore grade. From top to bottom:

1. oxidized clastic sediments subdivided into a subzone of pink facies (due to pink Fe-hydroxides) and a subzone of yellow facies (due to yellow Fe-hydroxides);
2. strongly oxidized limonitized lignite with appreciable high residual concentrations of up to 0.03% U;
3. weakly altered mineralized lignite subdivided into disintegrating ore, high-grade ore (>0.1% U), average ore (>0.05% U), and marginal U concentrations; and
4. unaltered barren lignite.

Ore minerals occur in a finely dispersed distribution concentrated in lenses in the hanging wall part of the lignite seam. The position of ore lenses is controlled by the permeability of overlying clastic sediments. U grades are highest below fluvial gritstone and coarse-grained sandstone channels located at the base of the Upper Jurassic suite. The uranium content drops sharply where argillaceous beds, even of thin thickness, overlie the lignite seam.

The bulk of the uranium ore is confined to lignite. Carbonaceous clays have poor U tenors. No uranium is found at the boundary of oxidation zones with grey sandstone.

Shape and Dimensions of Deposits

The Nizhne Ilyskoye deposit consists of 48 ore bodies contained in a zone about 40 km long and 100–2 000 m wide positioned in a NW-SE-oriented graben structure. Ore occurs at depths from 100 to 500 m. Ore bodies are of lenticular configuration and are largely restricted to the upper two meters of the lignite seam. Lenses are from less than 1 m to 4 m thick, range in size from 0.1 to 3.2 km², and contain from less than 0.05 to 2% U averaging 0.1% U, 0.03% Mo, <30–60 ppm Ag, and <2–5 ppm Re. Barren or weakly mineralized ground interlinks the ore bodies.

Ore Controls and Recognition Criteria

Host Environment

- Intermontane, narrow but long graben structure
- Graben downfaulted along NW-SE-trending regional faults cut by younger N-S faults
- Basin fill of Jurassic continental, lignite-bearing sediments of various provenance
- Overburden of Neogene and Quaternary ± impermeable sediments
- Basement largely composed of porphyry
- A lignite seam is host for mineralization

Alteration

- Oxidation during two events, a late synsedimentary and a postsedimentary
- Re-reduction intervening between the two oxidation events

Mineralization

- Polymetallic U-Mo mineralization associated with a great number of trace elements
- Lenticular ore bodies composed of adsorbed U and dispersed ore minerals
- Highly variable U grades
- Discontinuous distribution of ore bodies
- Location of ore bodies almost exclusively within top part of a thick lignite seam

Geochemistry

- Reducing environment provided by organic material and gaseous reductants
- Gaseous reductants (H₂S, methane) generated by oxidative destruction of organic matter
- Presumable involvement of appreciable amounts of organic acids in metallogenesis
- Probably only low U tenors in mineralizing groundwater
- Mineralizing solutions presumably identical with waters that generated secondary oxidation
- Deposition of mineralization at a secondary oxidation front (yellow facies) within altered lignite

Metallogenetic Aspects

Following Shchetochkin and Kislyakov (1993), the Nizhny-Ily Subbasin evolved through and experienced a number of geological, climate-related geochemical and geohydrological processes, which finally led to the formation of the Nizhne Ilyskoye U-Mo deposit. The following sequence of events is recorded:

1. Downthrust of a deep graben in an area of rugged morphology with high relief.
2. Intense and deep weathering of the Paleozoic rocks not later than Early Jurassic.
3. Filling of the graben by various carbonaceous clastic sediments of continental provenance during Jurassic time.
4. Development of a hydrodynamic system by more or less vertically percolating, oxygenated waters (ground infiltration) during the waning episode of sedimentation and the structural completion of the graben. Contemporaneous change of climate to semiarid conditions of about savanna type during the Late Jurassic.
5. Mobilization and transport of uranium by oxygenated groundwater but uranium transport probably in very minor concentrations as may be deduced from the Late Jurassic climate and sites of uranium deposition. The climate was characterized by considerable annual rainfall, which supposedly controlled the irrigation regime of groundwater and prevented, due to its quantity, any appreciable concentration of uranium in the groundwater. A complete lack of U

concentration at redox boundaries between pink and grey sandstones is considered indicative for low U contents in groundwater.

6. Substantial amounts of U only accumulated only at interfaces with a distinct reduction-oxidation contrast, which only existed in highly carbonaceous sediments like lignite.

The development of an early, more or less vertically progressing oxidation process by unconfined oxygenated waters is the critical element in the formation of the U-Mo mineralization. This event oxidized parts of the grey Jurassic sediments and turned them into a pink facies. This early oxidation stage must have been active prior to the burial of the Jurassic sequence under a Neogene argillaceous aquiclude as indicated by the distribution of the pink facies. Circumstantial evidence from similar continental basins in central Asia suggest that the most likely time of this oxidation event was during the Late Jurassic.

A favorable, strongly reducing environment was presumably achieved by the decomposition of carbonaceous matter by oxidation, which generated organic acids and reductants such as hydrogen sulfide, hydrogen, and methane. Migration of the reductants re-reduced the earlier formed pink facies and also acted as reductants for the U⁶⁺ in solution.

The presence of a large variety of trace elements in mineralized lignite including those of low migration capacity in a supergene environment (Zr, Be, Y, REE, SC etc.) suggests the involvement of considerable amounts of organic acids in the metallogenesis. The formation of the acids in response to oxidative disintegration of organic substances is supported by the presence of carboxyl (COOH) compounds in limonitized lignite.

Precipitation of uranium (and other elements?) occurred preferentially in the upper part of the main lignite seam but substantial ore grade accumulation developed almost exclusively at sites where the seam was overlain by permeable channel facies. Mineralization starts about 0.2–0.4 m below the hanging wall contact. This interval coincides with the interface of unoxidized lignite and yellow colored, secondarily oxidized facies with remnants of the pink facies. These lithologic-geochemical relationships and the kind of ore distribution suggest that the ore-forming processes took place in late or post-Jurassic time and were associated with the yellow coloring oxidation event.

6.6.2 Ily Basin

The Ily Basin is an E-W-elongated depression extending from west of Almaty eastwards to the Chinese border and into Xinjiang in NW China where the basin has the largest expansion. A number of U deposits/occurrences of lignite type, such as *Koldzhat*, and of sandstone type are reported. The latter include the large *Suluchekinskoye* and several small deposits such as *Kalkan*, *Aktau*, and *Malai-Sary* (► Fig. 6.1).

Sources of information. Abukumov 1995; Kislyakov and Shchetochkin 2000; Petrov et al. 1995; Shchetochkin and Kislyakov 1993; Petrov and Yazikov pers. commun. 2003.

Regional Geological Setting of Mineralization

The Ily Basin is an E-W-oriented depression, up to 100 km wide, filled with Mesozoic-Cenozoic sediments. Paleozoic rocks constitute the basement. The litho-stratigraphy section consists of continental clastic sediments separated into a Tertiary-Cretaceous and a subjacent Middle to Lower Jurassic suite. Both units contain lignite seams. Lignite-bearing Jurassic sediments occur in the Kazakh part of the basin over a length of 30 km along regional strike and 30 km down-dip. The lignite-bearing sequence crops out in the southern part of the basin and dips at 5–7° N. It reaches a depth of 1 500 m or more in the axial zone of the basin.

6.6.2.1 Koldzhat

The Koldzhat deposit (also spelled Koldjat) is located approximately 300 km E of Almaty and extends from the Chinese border in the SE toward the NW. Koldzhat is considered a U-Mo-lignite deposit. Coal was discovered in 1957 and two years later (1959) two uraniumiferous coal seams were intersected by drilling. Underground exploration to a depth of 600 m took place from 1969 to 1978. In situ resources of Koldzhat amount to 37 000 t U. Grades average about 0.1% U. The subsequent synopsis is largely based on Petrov et al. (1995).

Geological Setting of Mineralization

Koldzhat is situated at the southwestern flank of the Ily coal basin. Basin fill consists of Cenozoic-Mesozoic continental sediments, up to 1 000 m thick, which rest unconformably upon Upper Paleozoic sediments and volcanics. The litho-stratigraphic sequence includes:

- *Quaternary*: up to 150 m thick, boulder-pebble sediments
- *Pliocene*: up to 140 m thick, yellow sandstone
- *Miocene-Oligocene*: 30–35 m thick, pink mudstone
- Late Cretaceous:
 - *upper unit*, 120–200 m thick, alluvial and lacustrine sandstone with pelite lenses
 - *lower unit*, 30–50 m thick, red-brown conglomerate, gravel, sand-, silt-, mudstone
- >Unconformity<
- *Middle-Lower Jurassic*: 50–220 m thick, grey, pink or yellow-brown oxidized lacustrine, alluvial, and peat sediments. This suite is 50–100 m thick in the southern, and thickens to 180–220 m in the northern part of the deposit; it occurs within a depth interval from 25 to 450 m in the S and from 550 to 700 m in the N part of the deposit. Five sedimentary cycles are recognized each consisting of conglomerate (partly with carbonate cement), gravel, sand-, silt-, mudstone beds with interbedded lignite seams. Cycle thicknesses are: cycle 1: 20–25 m, cycle 2: 15–17 m, cycle 3: 25–65 m, cycle 4: 25–35 m, and cycle 5: 40–120 m
- *Upper Triassic*: grey and yellow-brown mud-, silt-, sandstone, 180–210 m thick; and conglomerate, 65–85 m thick
- >Unconformity<

- *Middle-Upper Permian*: 200–250 m thick, tuff
- *Lower Permian*: andesite and diabase porphyrite and their tuffs

Host Rock Alteration

Prominent regional alteration features in Jurassic rocks include oxidation and reduction effects reflected by grey, pink (ground oxidation), and yellow-brown-colored (bed oxidation) facies.

Mineralization

Pitchblende, sooty pitchblende, and coffinite are the principal uranium minerals; they constitute 76%, 14%, and 10%, respectively, of the total U present. Molybdenum minerals include ilsemannite, jordisite, and molybdenite. Associated Fe-sulfides include pyrite and marcasite. Mineralization has a disseminated texture and occurs in variably shaped ore bodies within Jurassic lignite-bearing clastic sediments. Uranium is concentrated in lignite seams as well as in sand-conglomerate beds (see below) while molybdenum enrichment is restricted to U ore bodies in lignite.

Shape and Dimensions of Deposits

The Koldzhat deposit covers an arcuate, NW-SE-elongated area, some 16 km long and as much as 7 km wide, in which several lignite seams exist including two major seams: # IV and # V. *Seam # IV* is 11 km long, 7 km wide, covers 62.6 km² and occurs at depths from 120 to 190 m; it is 2.5–3 m, locally as much as 5.6 m thick and averages a thickness of 2.77 m. *Seam # V* is 20–23 m thick, 7 km long, 5 km wide, covers 32.5 km², and occurs within a depth interval of 300–600 m.

Uranium occurs in 7 horizons, 3 lignite and 4 sandstone, within two curved, NW-SE-trending belts (in planview). The *southern belt* is 12 km long, up to 1.5 km wide, with depths of 30–50 m in the eastern, 120–300 m in the central, and 1 000–2 000 m in the northwestern section; it contains uranium in the # III and # IV lignite horizons, and in the # IV sandstone horizon. The *northern belt* is 16 km long, 1–2 km wide, and 300–600 m deep; it contains uranium in lignite horizon # V, and sandstone horizons # II, # III and # V.

Lignite contains 58.5% and sandstone 41.5% of the uranium resources of Koldzhat. The resources are distributed in the various horizons as follows: lignite horizon # III contains 6%, # V 51%, and # VI 2%; sandstone horizon # II contains 6%, # III 26%, # IV 6%, and # V 3%.

Uranium ore bodies have roll, tabular, and lenticular shapes. Roll-type lodes are typical for sandstone hosted ore while tabular and lenticular ore occurs preferentially in lignite. Ore bodies are from 0.5 to 14.5 km long, 20–2 000 m wide, and as much as 2 m thick. The uranium content is irregular but ranges commonly from 0.05 to >0.1% U.

Ore Controls and Recognition Criteria

Host Environment

- Intermontane, narrow but long basin of graben structure
- NW-SE-trending regional faults control the graben
- Younger N-S faults cut the graben fill
- Basin is filled with Cretaceous and Jurassic continental, lignite-bearing sediments
- Overburden consists of Neogene and Quaternary sediments
- Basement is largely composed of mafic to intermediate volcanics
- Host rocks include lignite and sandstone-conglomerate

Alteration

- Oxidation during two events, a late synsedimentary and a postsedimentary
- Re-reduction intervened between the two oxidation events

Mineralization

- Polymetallic U-Mo mineralization in lignite, simple U mineralization in sandstone and conglomerate
- Disseminated texture of ore
- Lenticular and tabular ore bodies in lignite, roll-type ore bodies in sandstone beds
- Location of lignite-hosted ore almost exclusively within top part of lignite seams
- Variable U grades
- Discontinuous distribution of ore bodies

Metallogenetic Aspects

The evolution of the Ily Basin and the formation of the Koldzhat deposit are thought to be similar to that of the Nizhny-Ily Subbasin and of the Nizhne Ilyskoye U-Mo deposit, respectively, described in the previous chapter.

6.6.2.2 Suluchekinskoye

Suluchekinskoye is located 5 km N of the Ily river in the north-eastern Ily Basin, close to the Chinese border and some 200 km NE of Almaty. It was discovered in 1978 and contains 33 000 t U at grades ranging from 0.07–0.13% U. The rollfront-type sandstone deposit was developed for ISL operation but did not reach production.

Ore bodies of the Suluchekinskoye deposit occur at the East Kalkanskaya anticline, which is composed of Middle Cretaceous to Neogene sediments. Host rocks are fine- and middle-grained quartz-feldspar sandstones with some interbedded clay, silt, and gravel lenses of the 60–120 m thick Lower Paleogene-Middle Cretaceous Ily Formation. They are overlain by pink or mottled sandstone and green-grey clay of the Eocene Aktau Formation upon which limy and silty clays rest. Neogene sediments form the uppermost layer and include the 60–90 m thick Pavlodar Clay Suite and the 50–330 m thick Ily Suite. The latter is composed of silt, sand, and clay. Paleozoic

tuff and tuffaceous sandstone form the basement and outcrop to the northeast and west of the deposit.

Alteration includes epigenetic reducing processes with intense pyritization of the host rocks. Subsequently, an oxidation tongue penetrated the Ily Formation from the east. Rollfront-type ore bodies occur at the redox interface and display a zonal distribution of elements. Rhenium penetrates furthest into reduced ground followed by a U-Re zone. Selenium forms the rear of a roll in oxidized ground. Ore grades vary between 0.07 and 0.13% U, 1 and 24 ppm (av. 1–2 ppm) Re, and 10 and 30 ppm Se. Se can increase to more than 100 ppm in limonitized intervals. Uranium is present as pitchblende and coffinite. The former constitutes 82% of the ore. Selenium occurs as native selenium and ferriselite.

Ore bodies are spread over an area 24 km long in an E-W direction and 150–8 000 m wide. Depths range up to 700 m. Individual ore bodies are 2–6 km long, 150–2 000 m wide, and 2–3 m thick.

The metallogensis is attributed to strata-infiltrational processes that took place during the Late Oligocene-Miocene; but the ore formation was apparently hampered and complicated by the injection of abyssal reducing solutions, which entered the aquifers along deep faults.

6.6.2.3 Kalkan, Aktau, Malai Sary

Kalkan (or Kalkanskoye) and Aktau occur some 5 km W and 10 km SE of Suluchekinskoye, respectively, and Malai-Sary and other small deposits about 50 km NE of Almaty. These deposits belong to a group of small sandstone-type U deposits hosted by Tertiary-Cretaceous continental clastic sediments. Most of these deposits are controlled by small islands of relic grey, reduced facies in the basal part of Campanian and Maastrichtian strata that rest upon Permian, mostly volcanic strata.

6.7 Zhalsniksky Region, Central Kazakhstan

Two sandstone-type U occurrences are known in this region, *Lazarevskoye* and *Lunnoye* (in Torgae) (Fig. 6.1). U mineralization associated with disseminated vegetal debris occurs as lenses, as much as several hundred meters long, in Paleogene argillaceous sand- and siltstone. The mineralized strata are sandwiched between clay beds and contain up to 0.4% U. Organic carbon ranges from 10 to 27%. Pitchblende and coffinite are identified with organic matter in high-grade ore (Petrov et al. 1995).

6.8 Turgai-Priyrtish Region, Northern Kazakhstan

Several U occurrences are known in the Turgai-Priyrtish region in northern Kazakhstan in the southern extension of

the Transural region, Russia. They tend to belong to the same basal-channel sandstone-type deposits as those in the Transural region. Reported occurrences include *Tobolskoye*, *Sensharskoye*, *Koitass*, *Pjatigorsk*, *Torfjanoye*, and *Aurtav* (Fig. 6.1).

6.9 Isolated Uranium Deposits/Occurrences in Kazakhstan (Fig. 6.1)

6.9.0.1 Panfilovskoye, SE Kazakhstan

This deposit is located 270 km ENE of Almaty within the South Dzhungar Basin. Permian felsite-porphyry forms the core of a syncline, which is cut by steeply inclined tectonic zones intruded by diabase-porphyry dikes and stocks that control the mineralization. Seven steep ore zones, 800–1 500 m long and from 50 to 150 m apart, are identified; four zones are of simple configuration associated with one dike, and three are of complex configuration associated with several dikes. Simple zones are up to 2 m and complex zones up to 60 m thick. Wall rocks are altered by carbonatization, hematitization, and chloritization.

Mineralization occurs in veins with pitchblende and uraninite as the principal U minerals; in stockworks which typically contain uranophane, sooty pitchblende, and uranospinite; and in small lenses composed of thin carbonate-pitchblende veinlets as much as 5 cm thick. Four stockwork ore bodies occur in the central part of the deposit, they are from 22 to 70 m long, 2–17 m wide, and persist to depths of 400 m. Grades average 0.061–0.086% U (Petrov et al. 2000).

6.9.0.2 Ulken Akzhal, E Kazakhstan

Ulken Akzhal is situated in the central part of the Chingiz-Zaisan area, some 300 km W of Semipalatinsk in eastern Kazakhstan. Resources amount reportedly to about 2 000 t U and average 0.172% U. The deposit is explored but not yet mined (status 2004).

The area is underlain by Carboniferous to Permian granitoids and Permian volcanics. A caldera filled with felsic volcanics, 1 200–1 700 m thick, includes, from top to bottom, trachyrhyolite-porphyry, felsite, dacite, and andesite-porphyry, and contains U mineralization in the hanging and footwall of a brecciated dacite horizon, 400 m thick, which occurs in the intermediate part of the volcanic sequence. Several ore sectors are identified with principal resources contained in the Central sector. Mineralization occurs in steep NE-SW fault zones along the contact of lithified rhyolite-dacite and felsite breccia. Wall rocks are altered by argillization, beresitization, and hematitization. Oxidation penetrates from surface to depths of as much as 40 m and to 250 m along faults. Primary ore consists of pitchblende associated with sulfides that form lens, vein, stockwork, or column-like ore bodies with dimensions of up to 100 m long, up to 9 m thick, and up to 140 m deep (Petrov et al. 2000; Petrov pers. commun. 2003).

6.9.0.3 Kyzyl, E Kazakhstan

This deposit is located 115 km N of Lake Balkhash in central-eastern Kazakhstan. Resources are less than 5 000 t U. Country rocks consist of volcanics of the basal Upper Carboniferous Keregetas Formation composed of dacite porphyry and rhyolite, and the Upper Carboniferous–Lower Permian Arkharlin Formation. Intrusions include felsic subvolcanic stocks, sills, necks, and dikes. The deposit occurs at the intersection of the NW-SE-oriented Ulken-Karaobin and the NE-SW Keregeshal-Symbyl abyssal zones.

Five lenticular ore bodies with pitchblende as the principal U mineral occur to depths of 175 m in fracture zones in the hanging and footwall of the NW-SE Rudny fault. Host is rhyolite porphyry tuff altered by argillization, hematitization, and silicification. Ore bodies are 80–220 m long, 1–10 m thick, and persist from 30–50 m down dip. Ore grade is as much as 0.6% U and averages 0.226% U in the largest ore body # 4 (Petrov et al. 2000).

6.9.0.4 Kuray, Central Kazakhstan

Kuray is a basal-channel sandstone-type U deposit located S of the town of Dzhezkazgan in central Kazakhstan. Uranium

occurs in a 4–7 km wide channel incised into a pre-Mesozoic basement. The channel is filled with Senonian-Paleocene argillaceous sands, which are oxidized in the marginal zones and reduced in the axial part of the channel. Several elongated ore bodies, up to several kilometers long, are delineated in the reduced sediments. Mineralization consists of U associated with Mo and Se; the latter two range from 0.01 to 0.1% (Petrov et al. 2000).

References and Further Reading for Chapter 6 · Kazakhstan

For details of publications see Bibliography.

Abakumov 1995; Abakumov and Zhelnov 1997; Berzina et al. 1974; Birka et al. 1995, 2005; Boitsov AV pers. commun.; Boitsov et al. 1995; Boitsov 1989, 1996; Cameco Annual Report 2000; Catchpole 1997; Fyodorov 2001, 2002a,b, 2005; Fyodorov et al. 1997; IAEA 1995, 2002; Ischukova et al. 2002; Kazansky and Laverov 1977; Kislyakov and Shchetochkin 2000; Laverov et al. 1992a–c; Magnuson and Stover 2006; Maksimova et al. 1995; Naumov et al. 1996; OECD-NEA/IAEA 1993–2005; Omelyanenko 1978; Omelyanenko et al. 1993; Petrov et al. 1995, 2000; Poluarshinov and Pigulski 1995; Pool T, pers. commun.; Shakhverdov 2003; Shchetochkin and Kislyakov 1993; Shor and Kharlamov 2003; Stolyarov and Ivleva 1995; Yazikov 2000, 2002; Yazikov and Zabaznov 2002; Zabaznov 2002; Zinchenko and Stoliarenko 2002.



Chapter 7

Kyrgyzstan

Uranium deposits of three types occur in the *eastern Karamazar* and *northeastern Fergana region* in central-western Kyrgyzstan: bituminous carbonate-type hosted in Paleogene limestone, sandstone-type in Neogene sandstone, and vein-type. Surficial karst cavern-type deposits occur in the *Tyuya-Muyun District* to the south of the Fergana Valley, SW Kyrgyzstan. Uraniferous coal deposits are reported in the *Min-Kush* and *Naryn* Jurassic basins in central Kyrgyzstan, and the *Sogut-Issyk-Kul* Basin in east-central Kyrgyzstan, south of Lake Issyk-Kul (▶ Fig. 7.1). No minable resources are recorded for the country.

Deposits mined include *Tyuya-Muyun*, *Mailuu-Suu* (or *Mailisu*), *Mailisay*, *Shakaptar*, and uraniumiferous lignite deposits in the *Min-Kush* and *Sogut* coal basins. Cumulative production is estimated by some sources to be on the order of 11 000–13 000 t U while other sources estimate only some 2 000 t U.

A mill with a nominal annual capacity of 1.5 million t of ore or 3 600 t U was built at *Kara Balta*, some 60 km west of the capital Bishkek (formerly Frunze) to process ore from central Kyrgyzstan, southern Kazakhstan (Pribalkhash region), and Russia. Yuzhpolymetal Mining and Metallurgical Combine was the former operator of the mill. Its successor is the Kara Balta Ore Processing Combine. Uranium ore processing started in 1955 and lasted until 1989 when conventional mining in southeast Kazakhstan was abandoned. A total of 30 million t of mill tailings indicate an average annual throughput of about 0.9 million t of uranium ore. Subsequently, the mill has processed yellow cake slurries from ISL operations in southern Kazakhstan. Since 1994, the process rate has been 1 000 t yr⁻¹ of concentrate containing 40–45% U yielding a final product of approximately 400 t U. In recent years the circuit has been partly reconfigured to treat commodities other than uranium, including gold ore.

Ore from the west Kyrgyzstan mines was mainly processed at the Leninabad mill, near Khudzhand (formerly Leninabad) in NW Tajikistan (see Chap. 12: *Tajikistan*).

Sources of information. Boitsov 1999, pers. commun.; IAEA 1995; Kazansky 1970; Kazansky and Laverov 1977; Laverov et al. 1992a–c; OECD-NEA/IAEA 1993, 1995, 2001; Savchenko et al. 2003; Thoste 1999; unless otherwise cited.

Historical Review

Earliest uranium reports came from the Alai Range to the south of the Fergana Valley in the former Russian territory of Turkestan where, in 1902, U–V ores were detected near the Tyuya-Muyun pass. Extended prospecting found additional uranium occurrences in that region scattered over an area of 2 500 km². Later on, uranium was discovered in the eastern Karamazar region,

Mailuu-Suu in 1934, Shakaptar and Mailisay in 1946, and Charkasar in 1954–1955. Uraniferous lignite was discovered at Dzhilkoye in 1947.

First mining of uranium in the Russian Empire for recovery of radium was in or near the Fergana Valley and dates back to 1908. Famous mines were at Tyuya Muyun in the Alai Range where vanadium-uranium ore was recovered from karst caverns in Carboniferous limestone. Copper was mined from deposits in this area possibly as early as in the Bronze Age. Post World War II mining started in 1946 and lasted until the end of the 1960s. Deposits mined include those mentioned earlier.

7.1 Eastern Karamazar-Northeastern Fergana Region, Central-Western Kyrgyzstan

This uranium region is located in Osh Province at the northeastern margin of the Fergana Valley in the northwestern Tien Shan mountains. A larger town is Tash Kumyr on the Naryn river. The region is the eastern extension of the Karamazar uranium region, which covers parts of NW Kyrgyzstan and adjacent terrane in Tajikistan and Uzbekistan (see respective chapters and ▶ Figs. 7.1, 7.2).

Several deposits were exploited including the vein-type *Charkasar*, and the *Mayluu-Suu*, *Shakaptar*, and *Malisay* deposits (▶ Fig. 7.2) referred to as bituminous limestone-type with structure controlled uranium mineralization in hydrocarbon-bearing carbonates. These four deposits were mined by underground methods between 1946 and 1968 and are depleted. Their cumulative production is thought to be between 11 000 and 13 000 t U. Grades ranged from 0.03 to >0.1% U (IAEA 1995).

Sources of information. IAEA 1995; Laverov et al. 1992; Roslyi 1975; Thoste 1999; and other sources.

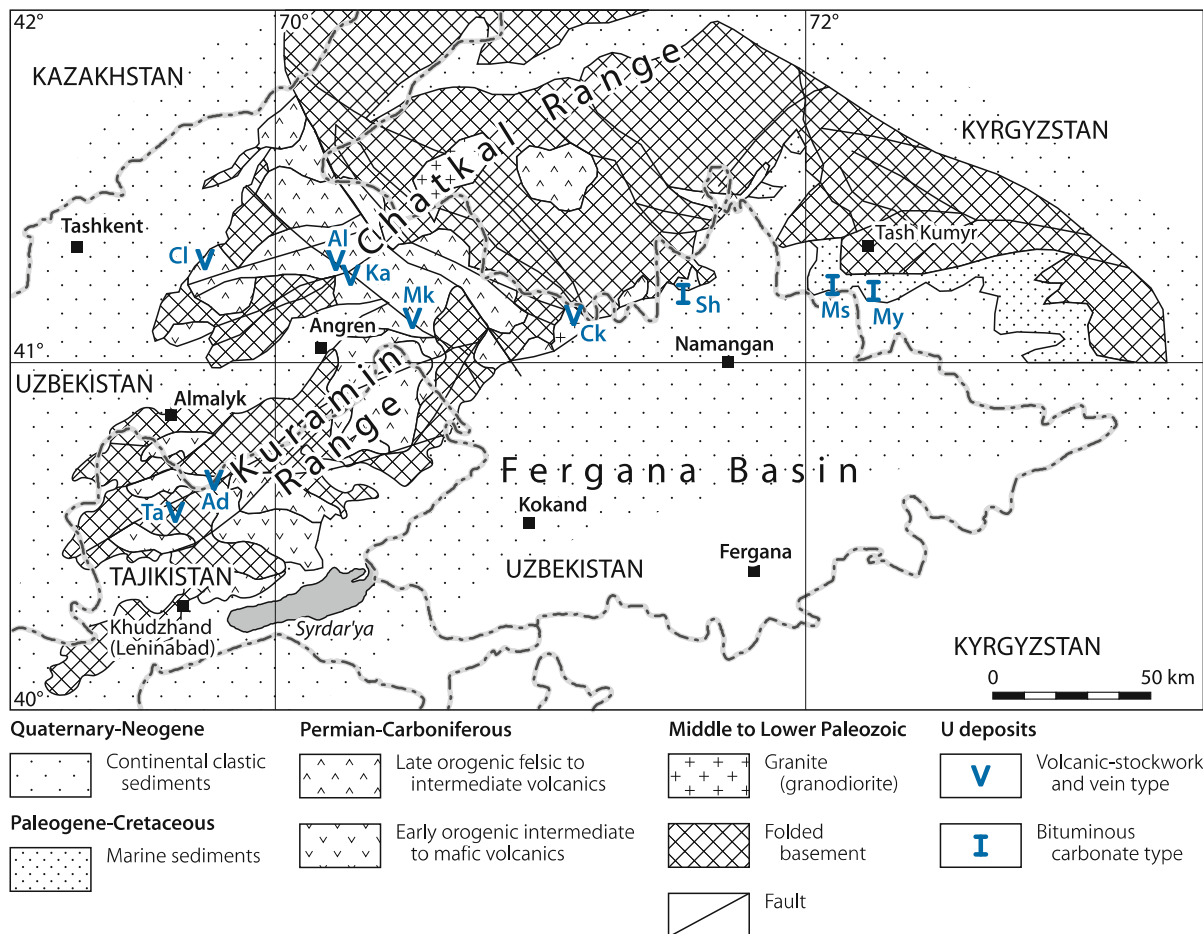
7.1.0.1 Mailuu-Suu

The depleted Mailuu-Suu (or Mailisu) deposit (▶ Fig. 7.3) was discovered at the Mailuu-Suu River in central-western Kyrgyzstan, to the NE margin of the Fergana Valley in 1934. The deposit is subdivided into several sectors covering a mining area of 36 km². Six underground mines recovered uranium between 1946 and 1968 and produced in total some 10 000 t U from 9.1 million t of ore. Ore grades ranged from 0.03% to over 0.5% U. Ore produced had the following distribution of ore grade: 45% of 0.03–0.1% U, 30% of 0.1–0.2% U, 20% of 0.2–0.5% U, and 5% in excess of 0.5% U (Thoste 1999).

Roslyi (1975) provides a description of uranium mineralization in petroliferous carbonatic sediments of the Bedre sector in the NW section of the Mailuu-Suu deposit. Roslyi does not name the deposit locality but meanwhile available information identifies the locality as the Bedre sector. Although Roslyi describes only this sector, his presentation tends to illustrate the principal properties of this type of deposits.

Fig. 7.2.

Karamazar region, generalized geological map with location of volcanic-stockwork-type U deposits in the Hercynian Chatkal-Kuramin uplift and bituminous carbonate-type U deposits in adjacent areas (after Laverov et al. 1992c). *Vein or volcanic-stockwork-type deposits in Tajikistan: Ta Taboshar, Ad Adrasman; in Uzbekistan: Cl Chauli, Al Alatanga, Ka Kattasay and Djekindek, Mk Maylikatan; in Kyrgyzstan: Ck Charkasar. Bituminous carbonate-type deposits in Kyrgyzstan: Sh Shakaptar, Ms Mayлуу-Suu, My Maylisay*



Bedre Sektor of Mailuu-Suu

The Bedre sector contributed approximately 20% of total Mailuu-Suu U production. Ore grades ranged from 0.03 to over 0.5% U. The Bedre sector (Fig. 7.4), as documented by Roslyi (1975), is characterized by the following features.

Geological Setting of Mineralization

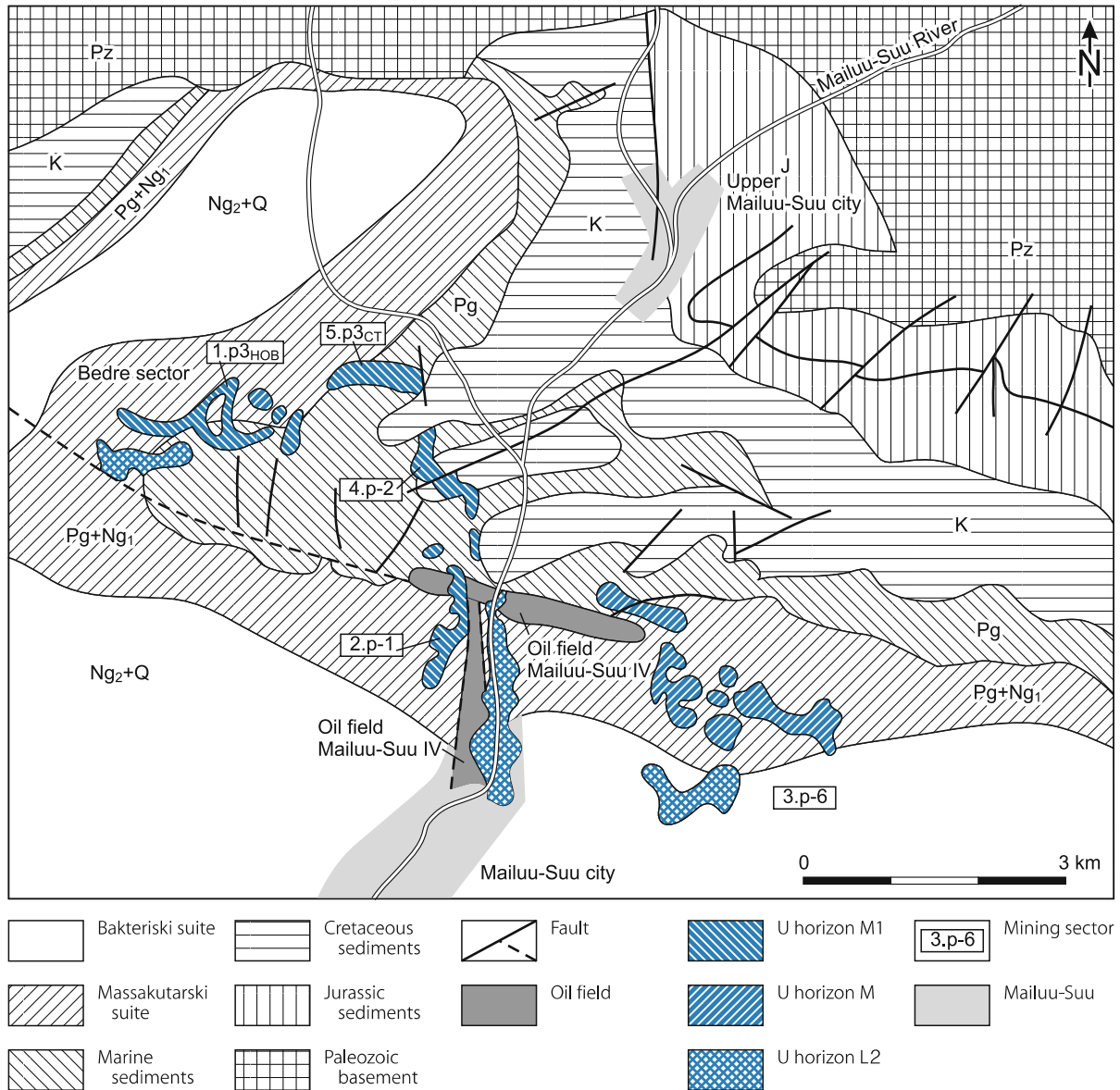
Carbonate-hosted uranium mineralization is restricted to Oligocene-Paleocene bituminous/petroliferous calcareous sediments. The sediments are folded and ore bodies are positioned on the wings of anticlines, the crests of which are eroded. Host rocks include oolitic and dolomitic limestone, dolomite, and marlstone intercalated with sandstone or gritstone. The Bedre zone is located on the NW flank of a domal uplift where strata dip in a northwesterly direction.

The ore-hosting sequence is about 4–5 m thick (Fig. 7.5) and composed of the following lithologies:

- *Hanging wall unit* (thickness 2.5 m): arenaceous-argillaceous continental sediments, pink in the upper part grading downward into greenish
- *Upper limestone unit*: oolitic, stylonitic and organic detrital limestones containing 1–3% insoluble residues and intercalated oyster beds
- *Lower limestone unit* (2 m thick): relatively dense argillaceous, dolomitic limestone with laminae of dolomitic marl
- *Footwall unit*: dolomitic marl and pink arenaceous-argillaceous continental sediments

Mineralized segments are characterized by intense structural disturbances including major faults, fractures/fissures, and shear zones. A prominent, curvilinear E-W-oriented, S dipping reverse fault with splay faults forms the southern boundary of the ore zone. Fracturing is particular abundant in the upper, purer limestone unit as reflected by a fracture density 4–5 times higher than in the lower argillaceous dolomitic limestone unit. Several fissure and shear-fracture systems are distinguished. NW-SE-oriented fracture zones extend in excess of 1 000 m and

Fig. 7.3. Eastern Karamazar region, Mailuu-Suu deposit, schematic geological map with distribution of U-mineralized horizons and sectors (after Thoste 1999)



change strike direction particularly along NE-SW-oriented planes, which correspond to flexures of the limestone beds.

Host Rock Alterations

Alteration of ore-bearing calcareous sediments resulted from several reduction and oxidation processes (Figs. 7.5, 7.6a,b).

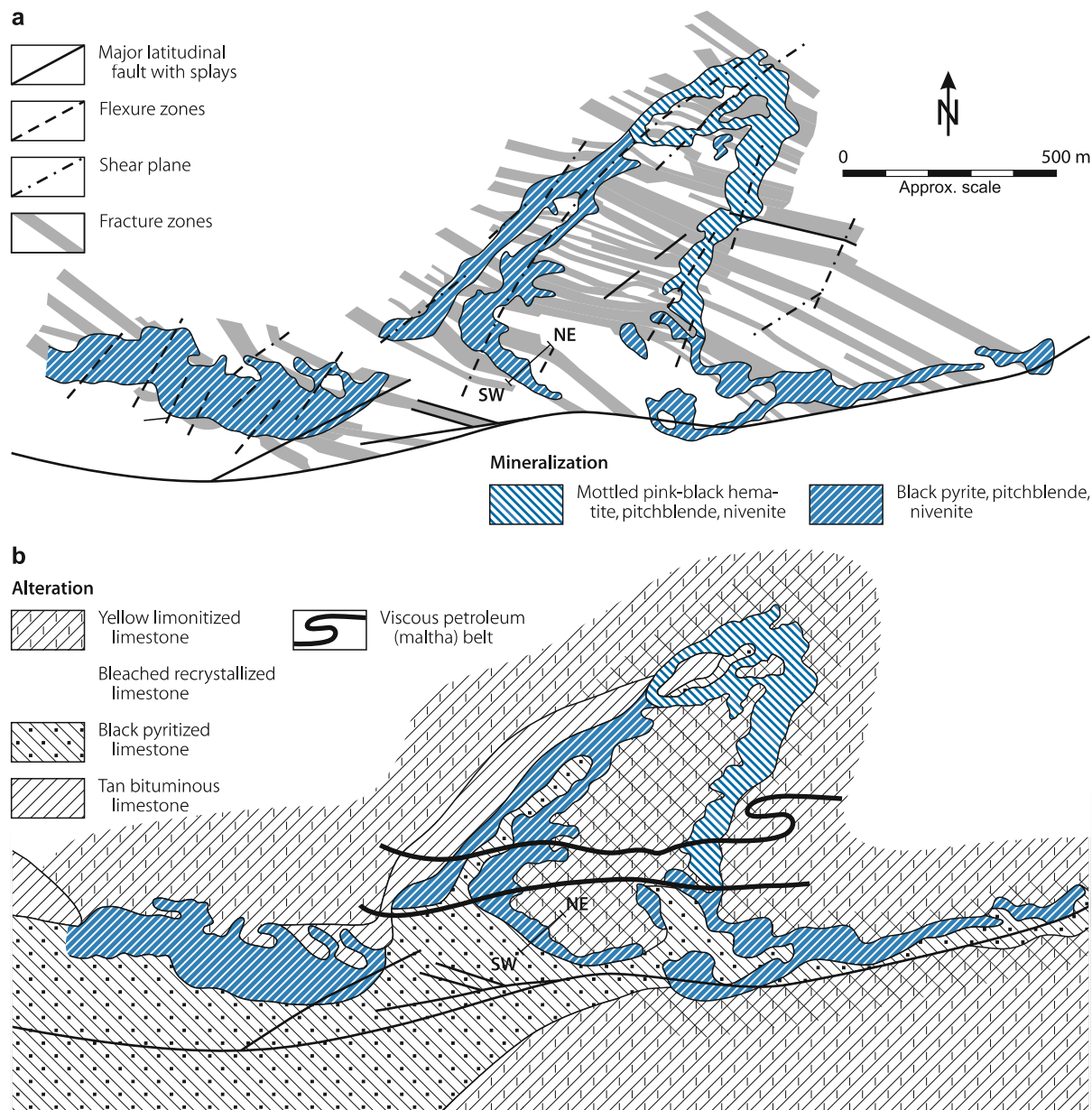
Pre-uranium stage alteration: The earliest alteration was by reduction of regional extent, which turned red beds over- and underlying the uranium bearing calcareous unit into green and light grey colors, respectively. It remains debatable whether this event also generated pyritization of limestone or not. Pyrite is present as finely dispersed inclusions in black limestone.

The earliest alteration in the carbonate unit is evidenced by limonitization; it imprinted a yellow hue on the rocks and locally on reduced super- and subjacent strata to a depth in excess of 500 m. Voids and fractures were filled with Fe-hydroxides during this process. Oxygenated waters considered responsible for the limonitization presumably entered the ore horizon from the north, the site of basement outcrops.

Subsequent alteration affecting permeable limestone of the upper and middle parts of the ore horizon includes first leaching, then argillization (*hydromicazation*) and bleaching associated with removal of iron. A subsequent lateral effect is indicated by hematitization due to redeposition of iron in form of lavender-pink hematite-hydrohematite rims at the margin of bleached, light beige-grey zones. Leaching took place in the most permeable, fractured, and stylonitic limestone. Two varieties are

Fig. 7.4.

Mayлуу-Suu, Bedre sector (1.p3_{HOB}), **a** Structural pattern and distribution of mineral assemblages in the upper U mineralized carbonatic horizon (L1), and **b** associated wall rock alterations (after Roslyi 1975)



distinguished, (a) limonitic limestone with leached-out stylolite cavities and dispersed minute leaching pores and (b) bleached, porous, chalky facies present as lenses along leached-out stylolites in the former variety. Stylolites, sutures, and microfractures in both varieties contain greenish hydromuscovite. Leaching also occurred in argillaceous limestone of the lower part of the carbonate unit in the southern part of the ore field.

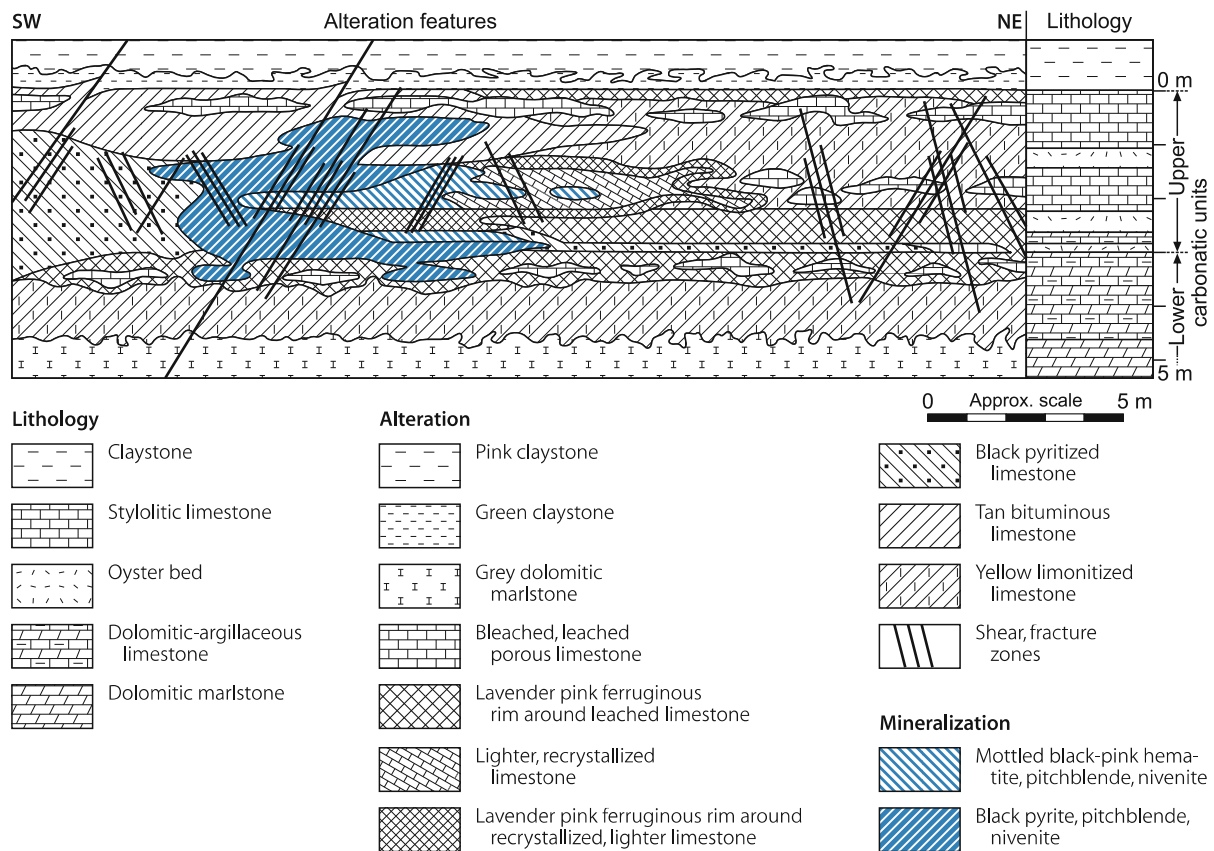
In a following stage both limonitized and bleached rocks were affected by *recrystallization* associated with *calcitization* and minor *pyritization*. Laminae of highly permeable, stylolitic, bleached limestone experienced a high degree of recrystallization. Porous, chalky facies of leached limestone turned into a white porcelain material. Limonitized facies lost their color as a result of loss of iron and acquired a lavender-pink ferruginous

rim similar to that mentioned previously. Scattered specks of yellowish Fe-hydroxides are still preserved in the ground-mass of the bleached recrystallized facies. Vugs and pores are filled or coated with coarse-crystalline calcite and minute crystals of pyrite. Stylolites, sutures, and microfractures contain hydromuscovite and minute crystals of pyrite. Pyrite is partly replaced by Fe-hydroxides suggesting a renewed oxidation period.

Syn-uranium stage alteration is reflected by hematitization followed by pyritization. Both are associated with deposition of pitchblende and nivenite. Intensive hematitization is manifested in front of pitchblende-nivenite mineralization and apparently preceded the U deposition (see also next paragraph).

Fig. 7.5.

Mayлуу-Suu, Bedre sector, SW-NE section across a mineralized lode illustrating the distribution of principal ore assemblages and related alteration features (left) combined with a lithologic column (to right) (see Fig. 7.4 for position of section) (after Roslyi 1975)



Post-uranium stage alteration of a reducing nature is evidenced by bitumenization (colored, less commonly black, insoluble solid bitumens) imposing a tan hue on the limestone in a narrow zone along the NW and W margin of the ore zone. This process was followed by an – to-day still active – influx of viscous petroleum (maltha) into the calcareous unit. The maltha forms a band parallel to the major fault on the south side of the ore zone. Its position tends to be controlled by the pressure of fault-water on the viscous petroleum.

Most recent alteration is expressed by near-surface limonitization associated with the formation of hexavalent U-V minerals spreading in a NW direction from the eroded crest of a domal uplift in the SE.

Mineralization

All mineralization of the Bedre sector is restricted to the foot-wall block of the large, E-W-oriented and southerly dipping reverse fault. The host unit is a 4–5 m thick, variably altered, water- and hydrocarbon-bearing carbonate sequence in which mineralization occurs structure bound controlled by faults and fractured intervals.

Pitchblende, nivenite, and sooty pitchblende are the principal uranium minerals. About 20% of the ore contained U is bound to post-uranium bitumen (kerite). Minor amounts of U-V minerals occur in surface near zones. Associated ore minerals are either hematite or pyrite. Associated elements include up to 0.8% Fe, 0.1% V, 0.06% Mo, 0.06% As, 0.03% Pb, 0.03% Ni, and 0.01% Co.

U minerals are developed in stylolites, sutures, microfissures, interstices between carbonate grains, and on walls of leached-out voids, pores, oolite grains, fragments of oyster shells, small pelecypods, gastropods, and foraminifera. Microfissures and stylolites also contain greenish hydromuscovite, and colored and black solid bitumens. The latter often cement minute fragments of pitchblende and nivenite.

Two mineralization varieties are distinguished, an older mottled black-pink hematite-pitchblende-nivenite, which is practically free of pyrite, and a massive, black pyrite-pitchblende-nivenite assemblage (Fig. 7.6).

Mottled black-pink mineralization is present as small lenses in which the ore minerals fill stylolites, penetrate limestone along joints and hair fractures above and below the stylolites, and form globular to irregular shaped inclusions. Black aggregates of U minerals are surrounded by vivid lavender-red halos, some 3 cm

wide, in the limonitic or pale rocks but a light colored, from a fraction of a millimeter to one centimeter wide fringe always separates both. Closely spaced, minute crystals of hematite and specks of pink Fe-oxides and hydroxides form the red aureoles. Mottled black-pink mineralization is restricted to fractured intervals in stylolitic, lighter colored, recrystallized limestones and denser, limonitic rocks adjacent to zones of recrystallization and bleaching of the about 2.5 m thick upper carbonate unit.

Massive black mineralization consists of pitchblende and nivenite intermixed with finely dispersed pyrite. The ore minerals occupy sutures, stylolites, microfissures, leached-out pores and coat oolites and shell fragments. Larger corroded stylolites are occasionally completely filled with lustrous black pitchblende,

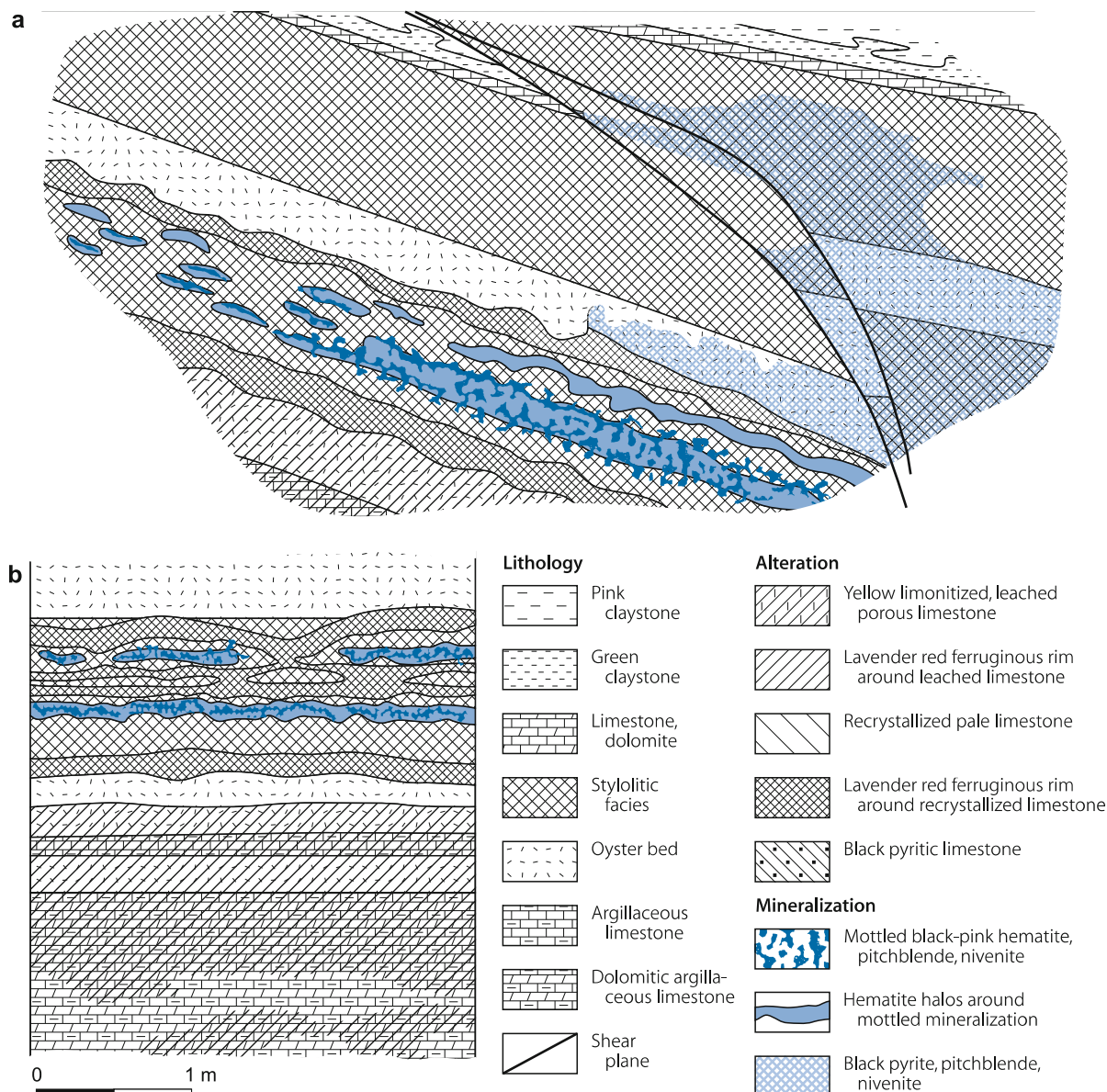
which penetrates and replaces the wall rock. Stringers of insoluble, solid bitumens cut pyrite-pitchblende-nivenite aggregates. Massive black mineralization occurs within and correlates to a large extent with the outer margin of black pyritized rocks of the upper carbonate unit and locally of the upper part of the lower carbonate unit (Fig. 7.6). Some isolated small lenticular ore bodies also occur in front of this zone within limonitic strata.

Shape and Dimensions of Deposits

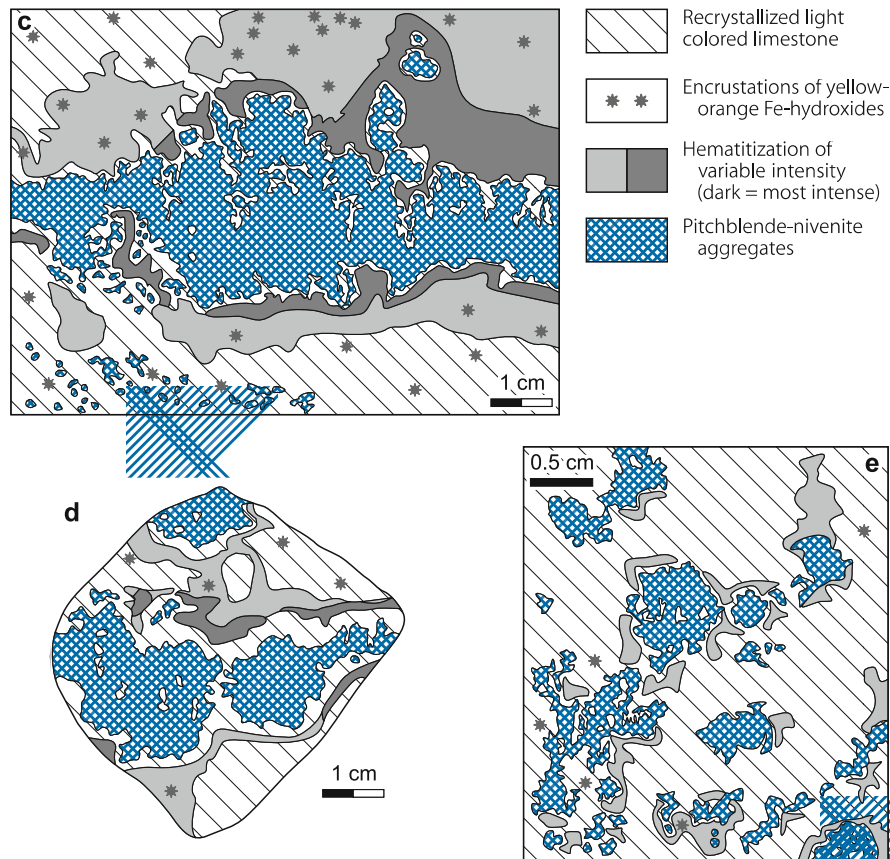
The Mailuu-Suu deposit consists of several discontinuous ore trends/sectors irregularly spread over a total extension of approximately 10 km in a NW-SE, and up to 5 km in a N-S

Fig. 7.6.

Mailuu-Suu, NE part of Bedre sector. **a** and **b** Detailed sketch sections illustrating distribution of ore and alteration phenomena in leached carbonate beds (**b** is perpendicular to lower U horizon in **a**). **c**, **d** and **e** Sketches of specimens of mottled black and pink hematite-pitchblende-nivenite mineralization (after Roslyi 1975)



■ Fig. 7.6. (Continued)



direction. Besides a number of smaller ore zones, some ten major ore trends have been identified including the Bedre sector in the NW part of Mailuu-Suu deposit (Fig. 7.3).

The Bedre sector is almost 2 000 m long in an E-W direction along the major latitudinal fault from where it bulges for about 900 m to the NE (Fig. 7.4). Bedre includes several ore zones composed of discontinuous, lenticular and roll shaped ore bodies contained in the upper 3–3.5 m of the up to about 5 m thick carbonate unit (Figs. 7.5, 7.6). Three varieties of geological setting and ore body configuration are distinguished, fault associated, layered fracture associated and roll shaped types (roll in sense of a morphological term rather than a genetic).

Mottled black-pink mineralization occurs in the Bedre sector in a curved, about 200 m long and up to 20 m wide ribbon-like ore zone, the orientation and configuration of which is controlled by flexures of the strata and changes in attitude of shear planes. This zone is composed of small isolated or interconnected ore lenses, which occur adjacent to shears along which they can be traced in form of bands. Lenses are mostly positioned in the footwall of shears. The lenses are from less than 1 m to about 10 m long, a few centimeters to 0.5 m thick and locally more, and extend from a shear for 1–5 m into the wall rock. In zones of closely spaced shears, the ore lenses thicken appreciably and merge to columnar lodes of better grade ores. Due to the fracture controlled setting, this kind of mineralization is defined as *layered, fracture-associated type*.

Black pyrite-pitchblende-nivenite mineralization occurs in discontinuous lenses similar to those of the mottled black-pink ore and in crescent-shaped bodies. The ore lodes group to an irregular winding band, about 500 m long and up to 50 m wide, the position and configuration of which tends to be controlled by the major south fault, flexures of strata, and changes of the attitude of shears.

Large lenticular bodies (in the eastern part of the Bedre sector) are directly associated with the latitudinal fault along which they persist over a distance of approximately 200 m. They are referred to as *fault associated type*. Isolated small lenticular ore bodies are also present outside the black ore band. These lenses are associated with laminae of permeable, limonitic limestone near the top of the calcareous unit where they are bound to intersections of stylolites and shears.

Roll-type ore bodies are (multi-)crescent shaped in cross-section and typically occur in oxidized zones. Rolls are few meters to about 10 m wide perpendicular to the strike of strata, up to 3 m thick at their thickest compact section while tails are from several centimeters to approximately 1 m thick (Fig. 7.5). Internal structure and mineral distribution is in rolls similar to that of layered, fracture associated mineralization. The extended upper segment of rolls is developed along continuous stylolites in beds near the top of the carbonate unit while the lower part is in less permeable dolomitic, argillaceous shell beds and is poorly developed if not missing. Rolls commonly split up down-dip, towards limonitic limestone. Enriched segments of black ore are

often related to closely spaced shears. Contacts between massive black ore and limonitic and lighter colored, recrystallized rocks are sharp.

Potential Sources of Uranium

Felsic volcanics and perhaps granites of the Chatkal and Fergana ranges to the northwest and north, respectively, of the ore zone are presumably the most likely source of uranium and other elements contained in the bituminous limestone deposits.

Ore Controls and Recognition Criteria

Significant ore controlling parameters or recognition criteria of the major deposits in the region, include:

Host Environment

- Folded calcareous marine sediments sandwiched between continental redbed facies of Tertiary age located adjacent to a crystalline basement containing felsic volcanics
- Intense deformation of ore-hosting strata by faults, fractures, shears
- Flexures of strata and shears tend to play a significant role in ore localization
- Host rocks consist of a 4–5 m thick sequence of an upper bituminous/petroliferous, stylolitic and organic limestone, and a lower dolomitic, argillaceous limestone horizon; the upper, more permeable horizon is the preferential ore host

Alteration

- Several stages of oxidation and reduction
- Pre-ore alteration is reflected by limonitization, recoloring (green, grey), leaching, argillization/hydromicazation, and bleaching associated with lateral hematitization, and pyritization
- Ore-related alteration includes early hematitization and later pyritization
- Post-ore alteration is reflected by bitumenization and late, supergene oxidation

Mineralization

- Two varieties of mineral assemblages: older mottled black-pink hematite-pitchblende-nivenite practically free of pyrite, and massive black pyrite-pitchblende-nivenite
- Irregular distribution of U minerals in stylolites, sutures, microfissures (which also contain greenish hydromuscovite, and colored and black solid bitumens), interstices between carbonate grains, on walls of leached-out voids, pores, oolite grains, and fragments of fossils
- Solid bitumens often cement minute fragments of pitchblende and nivenite

- Primary control of position and configuration of ore bodies and ore zones by faults, fractures, flexures of strata, and changes of the attitude of shears
- Geological setting and configuration of mineralization is of three types: lenticular fault associated, lenticular layered fracture associated, and roll shaped

Metallogenetic Concepts

Metallogenetic considerations favor an exogenic-epigenetic origin of the uraniumiferous bituminous limestone deposits. The principal ore-forming stage was during the Miocene. Potential uranium sources are presumably felsic volcanics, which are abundant in the adjacent Karamazar region.

Roslyi (1975) proposes the following processes and sequence of events for the formation of ore: Mineralization was preceded by several alteration events of alternating oxidation and reduction processes:

Pre-ore alteration stages include (1) an early oxidation stage with replacement of ferrous iron minerals by goethite and hydrogoethite forming the yellow limonitized limestone facies. This was followed by (2) a reducing stage reflected by leaching, hydromicazation and bleaching of limonitic limestone, which was succeeded by recrystallization. These alteration effects were accompanied by weak pyritization, removal of iron and its redeposition as hematite-hydrohematite at the margins of alteration zones. Subsequently, (3) a late oxidation stage evolved as indicated by replacement of newly formed pyrite by Fe-hydroxides. Oxygenated waters, which caused the alteration of stages (1) and (3) presumably entered the calcareous unit from the north, i.e. from the outcrop of the crystalline basement.

Mineralization stages include (4) the introduction of U, Fe, V, Pb, and Cr as a base for the deposition of a hematite-pitchblende-nivenite assemblage (mottled black-pink ore, practically free of pyrite). The assemblage was superimposed on the lighter colored recrystallized and limonitized limestone affected by late stage (3) oxidation. Invading solutions probably migrated from south to north and generated intensive hematitization in front of the developing pitchblende-nivenite mineralization. U minerals are surrounded by hematite halos but separated from them by reduction fringes and repulsion of iron, which suggests that hematitization preceded crystallization of the U minerals. A second, supposedly transitional mineralizing event generated (5) a pyrite-pitchblende-nivenite assemblage (black ore) by introduction of Fe, V, Mo, As, Ni, Co, Pb, Cr, and S. Deposition occurred in a band bordering pyritized limestone and overprinted all types of previously altered rocks as well as the mottled black-pink ore. Transitional varieties between stage (4) and (5) ore suggest a gradational evolution without a hiatus between the two ore stages.

Post-ore stages (associated with block faulting during Pliocene-Quaternary) include (6) bitumenization of limestone as a result of oil infiltration along faults as reflected by insoluble solid

bitumens that developed in a narrow zone separating black roll-shaped ore bodies from limonitic lithologies. Since these bitumens have the identical chemical and physical properties and the superimposed character as those found in mineralized, pyritized and oxidized zones, it is postulated that bitumenization postdates all epigenetic alteration and mineralization events. This is supported by the fact that no older inclusions of hydrocarbons have been observed. As such, oil infiltration and associated bitumenization is not considered essential in the ore-formation but probably caused the discontinuation of the ore forming process. At the same token, the bituminous facies may have acted as a geochemical barrier preventing the dissolution of the U mineralization. (7) A late ingress of viscous petroleum (maltha) formed a narrow maltha belt semi-parallel to a major fault. The position of this belt is considered to be a result of fault-water pressure. The migration of maltha is indicated to be recent by abundant maltha seepages from young fissures. (8) Current surface-related oxidation is documented by yellow Fe-hydroxides and U-V micas in near-surface fractures in limestone spreading northwestward from the eroded crest of a domal uplift in the southeast.

7.1.0.2 Other Deposits in the Northeastern Fergana Region of Kyrgyzstan

Maylisay (or Maili-Sai) is situated 20 km ESE of the town of Tash-Kumyr, W Kyrgyzstan. Uranium was known before World War II but it was only in 1945 that a minable deposit was established. Mining took place from 1955 to 1960 and produced a few hundred tonnes U. Mineralization was hosted in fractured, organic-oolitic sandstone, dolomite, dolomitic clay and marl of Oligocene-Paleocene age. Ore grades were less than 0.1% U (IAEA 1995).

Shakaptar (or Shakoptar) (Kassan-Varzykskoye ore field), a deposit of similar geological setting and size as Maylisay, is located near the settlement of Sumsar, about 40 km NW of the Uzbek town of Namangan in the Fergana Valley. It was discovered in 1946. Mining lasted from 1950 to 1958 and produced a few hundred tonnes U.

Charkasar was discovered in 1955/1956 at the southern margin of the Chatkal Range, some 50 km WNW of the Uzbek town of Namangan. This vein-stockwork-type deposit is related to Permian felsic volcanics. Charkasar was mined by underground methods in the late 1950s. Production was on the order of a few hundred tonnes U. Ore averaged <0.1% U.

7.2 Tyuya-Muyun District, Southwestern Kyrgyzstan

The Tyuya-Muyun uranium district is in Osh Province, about 2 km to the west of the 250 m deep Tange gorge of the north-flowing Aravan river in the semiarid northern Alai range of the

southern Tien Shan mountains. Osh is the nearest town. It is 25 km to the NE at the margin of the eastern Fergana Valley.

Uranium was discovered at Tyuya-Muyun (meaning two camel humps) in 1902. The site inherited its name from the nearby Tyuya-Muyun pass. Subsequent exploration identified a number of scattered, small U deposits.

Mining in the region dates back to ancient times with copper recovery possibly as early as the Bronze age. U mining began at Tyuya-Muyun by the Fergana Co. in 1908 when vanadium-uranium ore was recovered from karst caverns in Carboniferous limestone. By 1913 about 1 000 t of ore had been recovered. 750 t thereof with a grade of 0.97% U_3O_8 , 3.36% V_2O_5 , and 3.72% Cu were shipped for radium extraction to St. Petersburg and yielded 2.39 g Ra. Discontinuous mining went on over several decades. In 1926, a second mining period was started in order to provide ore for radium production (together with ore from Taboshar), the first radium produced by the Soviet Union, but water inflow at the mine disrupted the activities. Reportedly, 526 t of hand-sorted ore were shipped to a special plant in Leninabad (now Khodzent) for radium recovery. The final exploitation period lasted from 1947 for a short time. Exploration for additional U deposits continued until 1954 but without success. The final period included the opening of a tunnel almost two kilometers long from the Aravan river banks to the Tyuya-Muyun lode under the hypothesis forwarded by Fersman (1927) that additional mineralized solution pipes or karst caverns may occur in the given geological environment but none of either was intercepted.

By 1922, resources were estimated at about 5 000 t of ore but exploration during 1924 through 1934 had discovered additional deposits enlarging the resource base. Selectively mined ore contained up to 3% V_2O_5 and 1% U.

Sources of information. Bain 1950; Chervinsky 1925; Fersman 1927, 1930; Fersman and Shcherbakov 1925; Heinrich 1958; Kazansky 1970, pers. commun. 1998, 2002; Kirikov 1929; Nenadkevich 1917; Pavlenko 1933; Shcherbakov 1924, 1937, 1941; Shimkin 1949; Smirnov 1947.

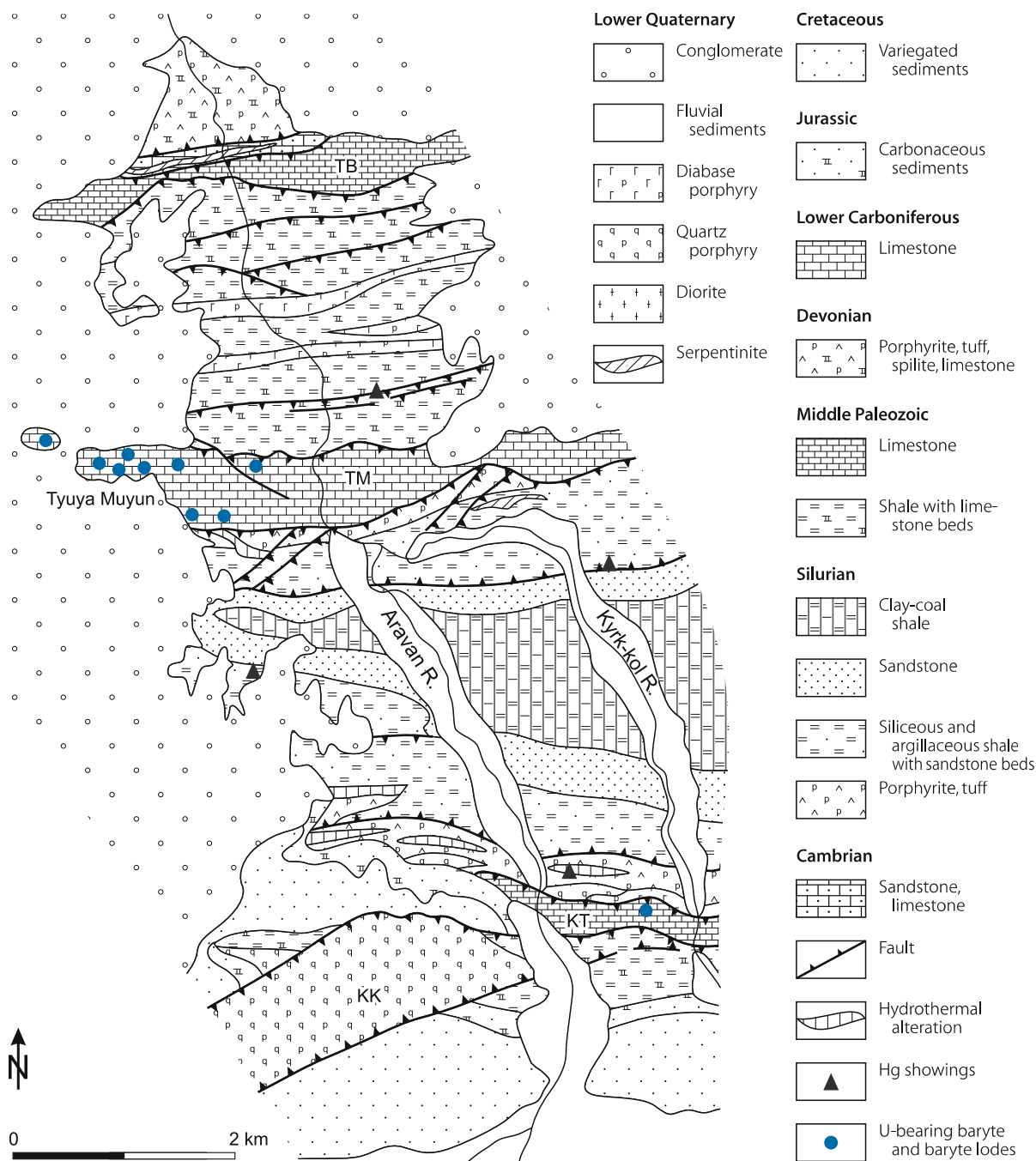
Regional Geology and Alteration

The sublatitudally trending Precambrian-Paleozoic Alai range of the western Tien Shan mountains marks the regional geology of the Tyuya-Muyun uranium district. This range forms the southern rim of the intermontane Fergana Valley, a downfaulted basin, 300 km long in an E-W direction and up to 150 km wide, filled with Mesozoic-Paleogene marine sediments and Neogene-Quaternary coarse-grained clastics.

The ore-hosting Aravan river area in the northern part of the Alai range is composed of folded Lower Carboniferous limestone and Silurian carbonaceous graptolite-bearing black shales and quartzose schists. Volcanic breccias and tuffs are interstratified. Fold axes trend sublatitudally (► Figs. 7.7, 7.8). Dikes of keratophyre, sills of diabase, and numerous baryte veins, up to 1.5 m thick, cut the sedimentary-volcanic suite. Baryte veins persist to a depth of at least 500 m. The black shales contain up to 500 ppm U and 1 000 ppm V (Fersman 1927).

Fig. 7.7.

Northern Alai range/Tien Shan mountains, generalized geological map of the Tyuya-Muyun mining district in the Aravan river area (after Kazansky 1970) (Lower Carboniferous Limestone ridges: TB Taylibeltash, TM Tyuya-Muyun; KK Kyzyl-Kungey, KT Karatash)



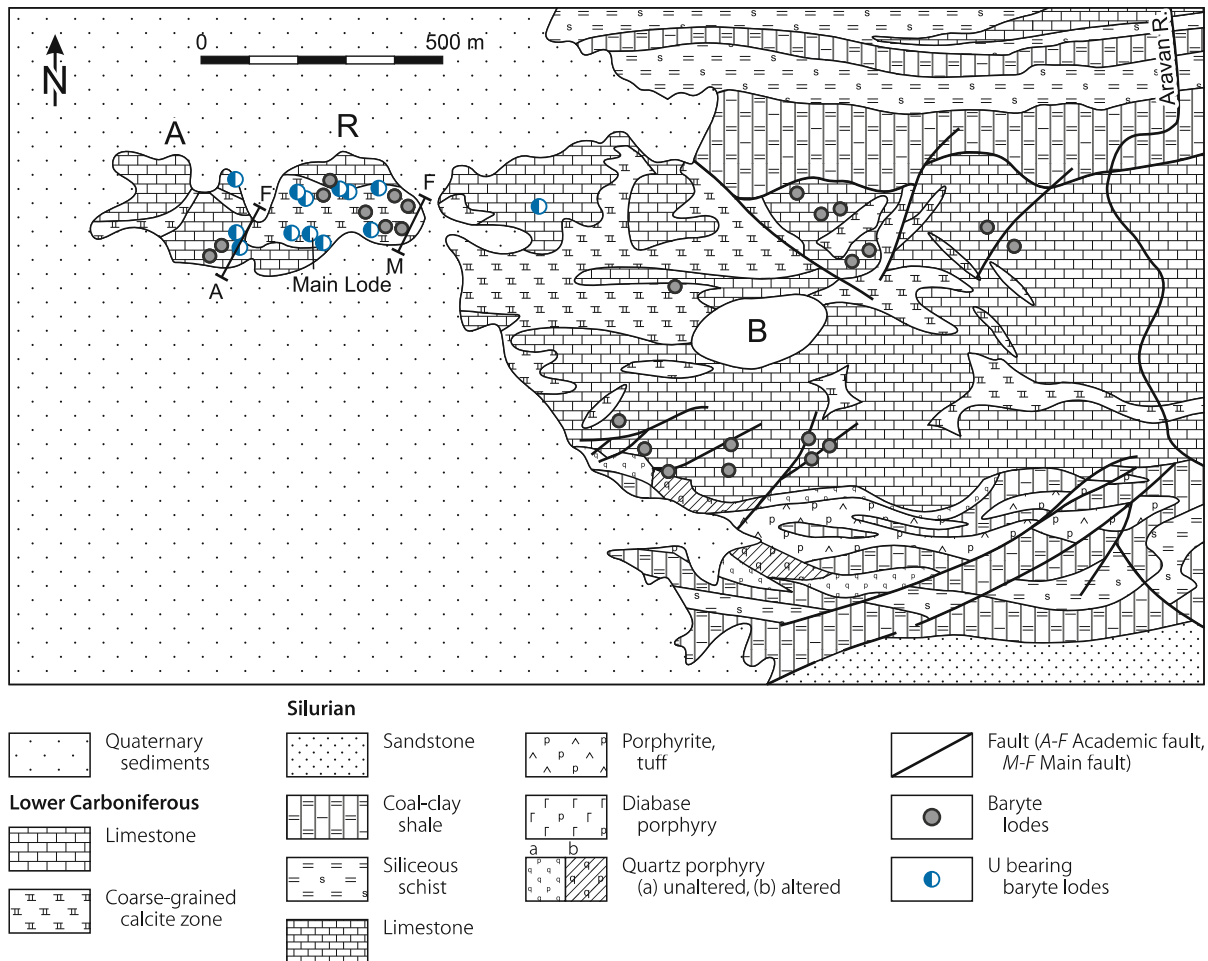
A fractured and locally brecciated, coarse-grained, pinkish or brownish violet limestone veined by calcite is the host rock. Limestone beds strike about E-W and dip from medium steep to near vertical. Extensive karst-related solution channels and pipelike caverns occur in the limestone (Fig. 7.9). Cavities are partly filled with radial aggregates, stalagmites, and crusts of calcite. Caverns contain stalagmitic onyx in form of pipes and wall coatings. The onyx is banded and is composed of laminae of calcite, baryte, and, locally, U minerals.

Mg metasomatism has dolomitized the limestone around mineralized structures.

Principal Characteristics of Mineralization

Tyuyamunite is the principal U mineral. Associated minerals include Cu- and Ca-vanadates (volborthite var. uzbekite, calcio-volborthite var. tangeite, turanite), vanadium-bearing clays,

Fig. 7.8. Tyuya-Muyun District, generalized geological map of the western Tyuya-Muyun ridge showing the distribution of baryte and uranium- baryte lodes. U lodes are essentially restricted to the Radium-Academic hills while baryte lodes occur beyond this center (after Kazansky 1970). A Academic Hill, B Baryte Hill, R Radium Hill



chrysocolla, malachite, goethite, baryte, calcite, and quartz. The baryte is radioactive. Some Ra-bearing carbonate is found. The ore texture is fine-grained and massive, banded, brecciated, or vuggy.

Ore occurs in karst caverns and fissure veins (to some extent in a similar geological setting and mode as the karst-type U-V deposits in the Pryor Mountains, Montana-Wyoming). Caverns contain ore minerals as crusts on the walls, and as concentric encrustations or geodes in a depth interval from near surface to the paleowater level and below. Mineralized geodes are up to several meters in diameter and consist commonly of a core of coarse-grained calcite that is overgrown first by yellow and then by pink baryte. A next layer consists of quartz with disseminated tyuyamunite containing 0.6–4% U_3O_8 plus 1–7% V_2O_5 . The outer shell consists of acicular calcite.

U mineralized fissures range in thickness and length from few centimeters to 1.5 m and more. They encompass 1–3 mm

thick bands and up to 5 mm thick lenses of fine-scaled tyuyamunite and/or disseminations of tyuyamunite with Cu-vanadates.

At least 13 uraniumiferous and about 30 U-barren baryte lodes or veins were found. The former, including the Tyuya Muyun deposit, are grouped in the western part of the district most of them in strips paralleling the E-W strike of the sediments. Baryte veins occur for up to 1 500 m beyond this center (Fig. 7.8).

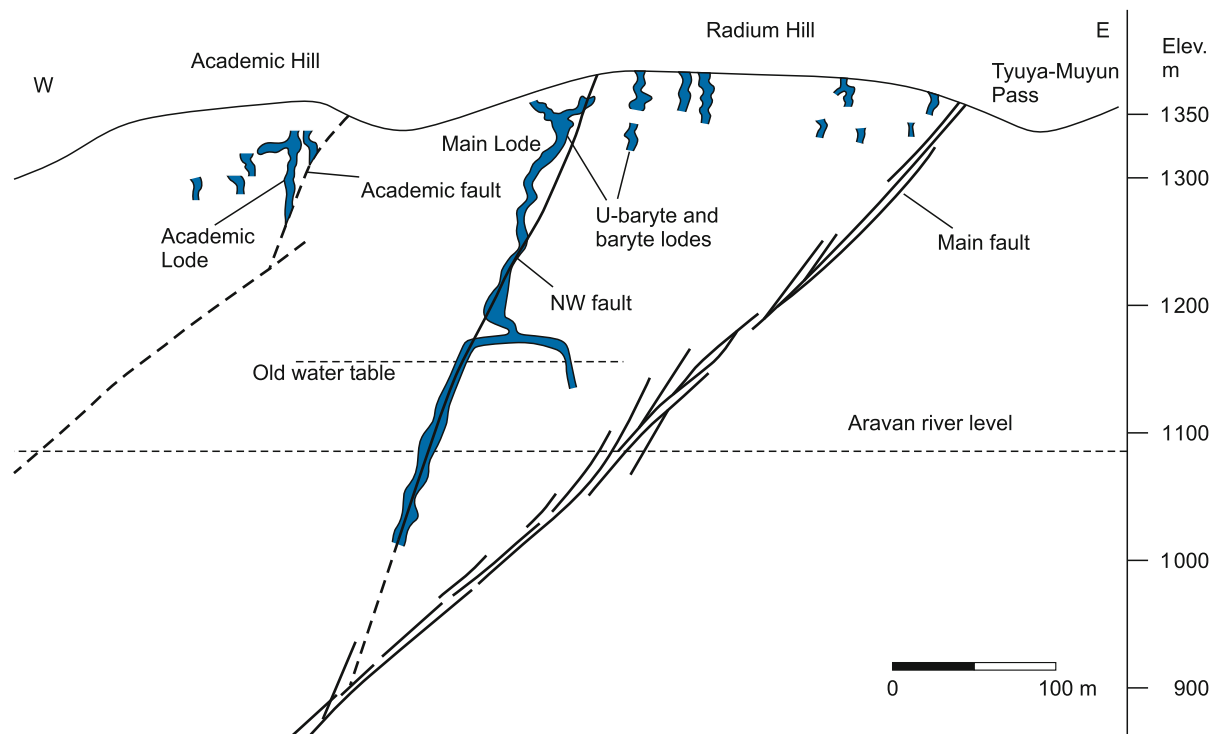
7.2.0.1 Tyuya-Muyun Deposit

The Tyuya Muyun deposit proper is located on the western flank of Radium Hill and consists of the *Main Lode*. A similar but smaller deposit, the *Academic Lode*, occurs 150 meters to the west of the Main Lode (Fig. 7.9).

Reserves remained unpublished. Aleksandrov (1922) reported for the then known Main Lode ore reserves of 5 000 t.

Fig. 7.9.

Tuya-Muyun deposit, schematic latitudinal projection of mineralized karst structures and faults (after Kazansky 1970)



Mining grades were variable ranging from 0.5 to 4% U averaging 1.4% U, 1.5–7% (av. 3.8%) V_2O_5 , 1.5–7 (av. 3.0%) CuO, 1.5–5% (av. 3.6%) (Al, Fe) $_2O_3$, 0–20% (av. 2.7%) $BaSO_4$, 0.5–5% SiO_2 , 37–49% (av. 46.6%) CaO, 28–39% (av. 35.7%) CO_2 (Heinrich 1958).

Kazansky (1970) provides a comprehensive account on the exploration history, geology, and mineralogy of the Tyuya Muyun deposit. A summary is given below.

Geology and Mineralization

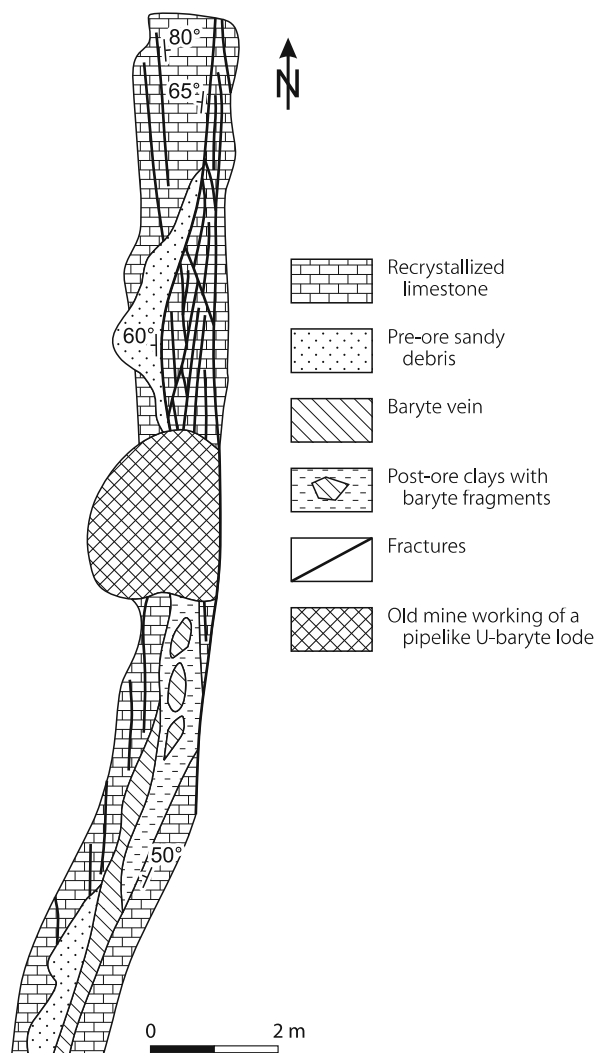
The Main Lode is a steep plunging mineralized solution pipe with some bifurcating subhorizontal channels hosted by Lower Carboniferous recrystallized limestone. A repeatedly reactivated, NW-SE-striking and 65–85° SW inclined fault/fracture system controls the pipe setting. The fault system coincides with a vein of coarse-grained calcite and defines the setting of pre-ore and post-ore karst structures (Figs. 7.9, 7.11a,b). At a depth of some 400 m, the Main Lode is intersected by the NNE-SSW-trending and medium steep westerly dipping Main Fault that is filled by pre-ore, karst-related pebble and sandstone debris, baryte veins, and post-ore clay. Similar characteristics are found in the mineralized Academic fault (Fig. 7.10).

The Main Lode has a diameter of few to over 10 m and persists to at least 280 m below surface. The groundwater table is at a depth of 180 m below surface from which the Main Lode continues for at least 100 m without any major change in orientation, size- and mineral filling. The Main Lode is largest at the lower levels except for the so-called “Academic Cave” at a higher level. At the lowest explored level, the Main Lode has a diameter of 6–10 m and plunges westerly at 70°. In centripetal direction, the lode is composed of seven concentric layers: starting with columnar calcite, followed by “ore marble”, pink foliaceous baryte, hematite with quartz and calcite, tan and honey colored baryte, tan plumose baryte, and finally columnar calcite. The interior is an open cavity. The peripheral band overgrows recrystallized limestone and thin laminae of karst-derived marl (Fig. 7.11c).

“Ore marble” (referred to as onyx by Fersman) consists, both above and below the groundwater table, of medium-grained calcite with finely dispersed colloform tyuyamunite, tangeite, alaite, hematite, and traces of malachite, chalcocite, chrysocolla, covellite, and pyrite. No U-oxides such as pitchblende have been encountered.

At higher levels up to the present-day surface, the Main Lode maintains the same concentric-zonal structure and mineral composition except that at depth the baryte and calcite layers are six to eight times thicker while the thickness of “ore marble” remains practically stable.

■ Fig. 7.10. Tyuya-Muyun District, planview of a fraction of the Academic fault (after Kazansky 1970)



Metallogenetic Aspects

A variety of metallogenetic hypotheses have been forwarded for the development of karst openings such as those forming the Tyuya Muyun solution pipe and therein-contained mineralization.

Karst forming processes must have occurred in pre-Jurassic time, perhaps starting as early as in the Paleozoic. Ore formation is thought to have evolved by a combination of weak hydrothermal and supergene solutions leaching uranium and other ore forming elements from the Silurian black shales, which are exposed in the Alai Range. These shales contain up to 500 ppm U and 1 000 ppm V (Fersman 1927).

Chervinsky (1925) considers an origin of the Tyuya-Muyun deposit by postvolcanic solutions and a secondary, presumably still active process for the formation of the uranyl minerals. He argues that the baryte veins with their

dolomitized wall rocks can only be hydrothermal and that the karst-hosted mineralization probably represents a supergene redistribution of material derived from the oxidized baryte veins. On-going mineralization up to Recent is supported by tyuyamunite found on human bones, which remained in the Tyuya-Muyun Mine for several years during the Bolshevik revolution.

Shimkin (1949) suggests an ore forming sequence starting with vein-type ore deposition from low temperature solutions related to the Hercynian Orogeny. Faulting occurred during the Alpine Orogeny. Karst developed in post-Eocene time and was associated with partial destruction of veins, reworking and reconcentration of the ores.

Kazansky (1970) presents the following concept at the end of final investigations of the Tyuya Muyun deposit. Pre-karst meridional faults offered and prepared the environment for karst development resulting in pipe and channel structures. Regional studies suggest two probable periods of pre-ore karst development: the Upper Carboniferous and the Upper Permian-Triassic.

Open cavities were subsequently and selectively occupied by baryte or U-V-bearing baryte phases as reflected by zonal distribution of ore bearing and ore-free baryte lodes within the Tyuya-Muyun limestone ridge. The presence of equal modes of karst structures and ore infillings continuing from far above to deep below the present-day groundwater table rules out a Quaternary age of ore formation as suggested by Chervinsky (1925). Chervinsky's observations rather suggest a redistribution of the ore forming elements in recent times.

Both, the ore bearing and barren baryte lodes were formed from ascending thermal solutions in ancient karst openings below the groundwater table. The origin of these solutions remains obscure, however.

7.3 Jurassic Coal Basins in Central and Eastern-Central Kyrgyzstan

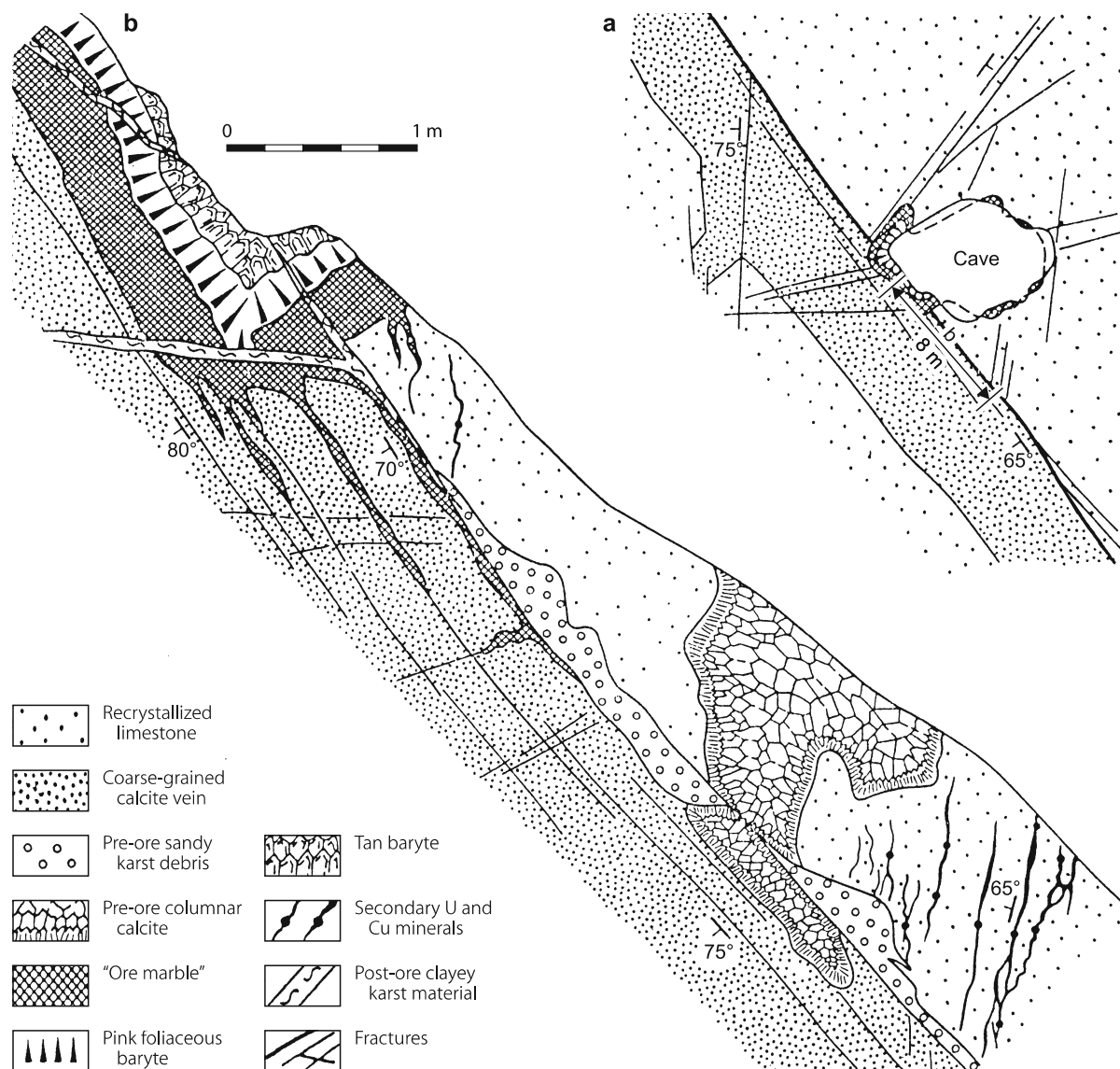
A number of small intermontane coal-bearing basins in the Tien Shan mountains of central and eastern Kyrgyzstan contain uraniumiferous lignite seams that were mined for uranium. Reported localities include the *Min-Kush*, *Sogut-Issyk-Kul*, and *Naryn Basins* (● Fig. 7.1).

Sources of information. Kislyakov and Shchetochkin 2000; and others.

The *Min-Kush Basin* is a narrow coal basin, 8–9 km long, in the central part of the northern Tien Shan mountains, central Kyrgyzstan. Uranium was discovered in lignite in a Jurassic coal-sandstone sequence near the town of Naryn during exploration for coal in the 1950s. Several uraniumiferous lignite deposits, referred to as Kavak group of U-coal deposits, are reported: *Agulak*, *Kashka-Suu*, *Sarykamysh*, *Sasyktash*, *Turakavak* (also known as *Min-Kush*), and *Tuyuk-Suu* (= *Dzhilskoye*). Each of them contained between 1 500 and 5 000 t U. Ore grade (in ash?)

Fig. 7.11a,b.

Tuya-Muyun deposit, **a** schematic and **b** detailed plan of the structure of the Main Lode at the Fersman cave level (after Kazansky 1970)



was 0.1–0.3% U (IAEA 1995). Uranium production was associated with the extraction of lignite by strip-mining and lasted from 1955 to 1960 (Turakavak). Tuyuk-Suu reportedly produced 2 626 t U. Mill concentrate was transported by truck to the processing plant at Kara Balta, 200 km to the north.

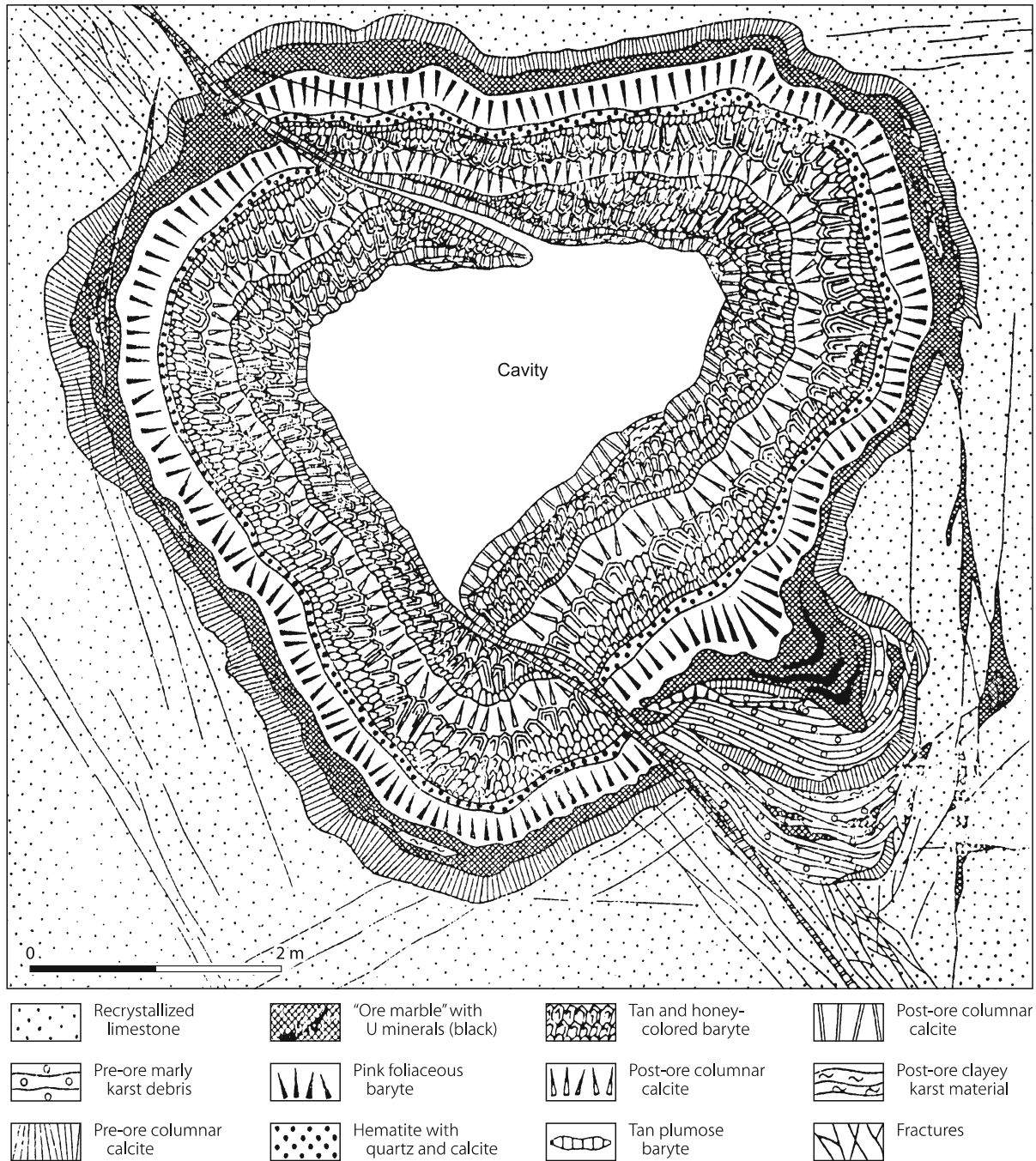
The *Sogut-Issyk-Kul Basin* in east-central Kyrgyzstan contains uraniferous lignite, which was mined by underground methods at *Dzhilskoye* (= *Tuyuk-Suu*) (discovered 1947) near Kadzhi-Say on the south shore of Lake Issyk-Kul from 1948 to 1966. *Dzhilskoye* was one of the earliest Soviet uranium mining sites. A special plant, N8, was locally built to process the uraniferous lignite; it was closed in 1956 for subeconomic reasons.

7.4 Other Uranium Occurrences in Kyrgyzstan

At *Almalyk* in the Fergana Valley region, Carboniferous limestone hosts veins with Cu, Fe, Mn, Ni, and radioactive minerals in a baryte-calcite gangue grading up to 3% U_3O_8 , and veins with galena, sphalerite, cerussite, wulfenite, chrocoite, turanite and usbekite in a baryte gangue (Komischau 1927).

Some U was said to have been produced from yttrium and REE ore mines at the eastern end of the *Chu* (or *Tshu*) valley, and from *Kyzyl-Dhzar* (U + Au) and *Sumsar*. Silurian uraniferous black shale containing about 100 ppm U is reported from the *Alai Range* in SW Kyrgyzstan (Bain 1950).

Fig. 7.11c. Tuya-Muyun deposit, horizontal section of the Main Lode below the groundwater table illustrating the sequential deposition and mineralogical composition of the pipe lode. The diameter of the lode varies between 6 and 10 m (after Kazansky 1970)



References and Further Reading for Chapter 7 · Kyrgyzstan

For details of publications see Bibliography.

Aleksandrov 1922; Bain 1950; Boitsov 1999, and pers. commun.; Chervinsky 1925; Fersman 1927, 1930; Fersman and Shcherbakov (1925); Häusser et al. 1997; Heinrich 1958; IAEA 1995; Karimov et al. 1996; Kazansky 1970, and

pers. commun. 1998, 2002; Kazansky and Laverov 1977; Kislyakov and Shchetochkin 2000; Kirikov 1929; Kohl 1954; Komischau 1927; Laverov et al. 1992a–c; Mashkovtzev and Naumov 1999; Melnikov et al. 1996; Minerals Yearbook 1946, 1949; Nenadkevich 1912; Pavlenko 1933; OECD-NEA/IAEA 1993, 1995, 2001; Roslyi 1975; Savchenko et al. 2003; Shcherbakov 1924, 1937, 1941; Shchetochkin and Kislyakov 1993; Shimkin 1949, 1953; Smirnov 1947; Thoste 1999; Venatovsky 1993.

Chapter 8

Mongolia

Although uranium occurrences are widespread in Mongolia, minable or potentially economic deposits are restricted to date to the *North Choibalsan* region (Mardai/Dornod District, referred to as Mardai in Mongolian and Dornod (or Dornot) in Russian papers) in NE Mongolia and to the *Gobi Desert* in S Mongolia (e.g. Choir, Khairkan, Undurshil, Sainshand Basins) (Note: data given for U deposits in Mongolia are based on 1995 status unless otherwise cited). Deposits in these two regions are of volcanic and sandstone type, respectively. Other types of U mineralization found in Mongolia include vein-, surficial-, metasomatite-, intrusive-, metamorphite-, lignite-, and phosphorite-types.  **Figure 8.1** shows the distribution of principal uranium regions and districts or areas.

Proven and probable in situ uranium resources (RAR + EAR-I) amount to 80 000 t U, 57 000 t U of which are contained in volcanic-type deposits and about 19 000 t U in sandstone-type deposits. Other types of deposits contain 4 000 t U (Mironov et al. 1993). OECD-NEA/IAEA (2005) reports recoverable resources of 46 200 t U RAR and 15 750 t U EAR-I.

The *Dornod*, *Gurvanbulag*, and *Mardaingol* deposits in the Mardai District, North Choibalsan region were developed for mining in the late 1980s. Mining lasted from 1989 to 1995 and produced 535 t U at grades ranging from 0.098% to 0.145% U. ERDES Mining Enterprise (a state-owned JV of Mongolia and USSR/Russian Federation) was the operator. Ore was shipped by rail (485 km) to the mill at Krasnokamensk in Transbaykalia, Russia.

Uran Company Ltd., a state-owned Mongolian enterprise, is in charge of uranium-related activities.

Sources of information. Batbold 2001; Filonenko et al. 1993; IAEA 1995, 2007; Mironov 2003; Mironov and Rogov 1992, 1993; Mironov et al. 1993, 1995; OECD-NEA/IAEA 1993, 1995, 1997, 2005; pers. commun. by Chuluun O and staff of Uran Company of Mongolia Ltd., and staff of ERDES Mining Enterprise.

After finishing the manuscript, some new publications became available and the interested reader is in particular referred to the books by Ischukova et al. (2002) and Mironov (2003). Mironov's (2003) book "Uranium of Mongolia" provides the most comprehensive and specific compilation on uranium deposits and resources of this country based on material that was obtained from the 1950s to the early 1990s by Soviet geologists working in the Mongolian People's Republic.

(Note: Due to discrepancies in the various sources of available information and errors in the English translation or transcript of Russian or Mongolian terms and names, some of the here presented descriptions and figures may be incorrect and names may be spelled differently.)

Historical Review

Limited uranium exploration from 1945 to 1960 resulted in the discovery of uraniumiferous lignite occurrences in eastern Mongolia. Systematic exploration for uranium and other metals was conducted from 1970 to 1990 by the former Soviet "Mongolian Geological Survey Expedition" (renamed "Eastern Complex Exploration Expedition" in 1990, a subsidiary of the "USSR Ministry of Geology") and "May Survey Expedition" (VSEGEL/Geological Institute in St. Petersburg). As a result, in excess of 1 600 uranium showings or radioactive anomalies, about 100 U occurrences, and 6 deposits were detected.

Dornogovi (Dorno Gobi) region: Uranium-related exploration was first conducted in 1955–1958 and resulted in the discovery of three lignite-type uranium occurrences. Subsequent exploration identified several volcanic-type occurrences, including Ulaan-nuur, in 1971–1973, and sandstone U mineralization including the Kharaat deposit and several occurrences in the Choir Basin in 1986–1988.

Exploration in the *northern Choibalsan region* was successful in the 1970s with the discovery of four uranium deposits, Dornod in 1973, Gurvanbulag in 1974, Mardaingol in 1979, and Nemer in 1987, and several occurrences, which became the Mardai/Dornod District. Since the 1990s, several foreign companies continued exploration in joint ventures with Russian and/or Mongolian institutions.

Regional Features of Uranium Distribution in Mongolia

Uranium Provinces and Associated Uranium Occurrences Four metallogenetic provinces are outlined in Mongolia (from N to S): Northern Mongolian, Khentei-Daur, Mongol-Priargun, and Gobi-Tamtsag ( **Fig. 8.1**). Each of these provinces differs by its geological setting, type of uranium mineralization, association of minerals, and mineralization age. Some forty areas with U mineralization occur in these provinces.

The Mongol-Priargun metallogenetic province spatially coincides with the homonymous continental Mesozoic volcanic belt in eastern Mongolia. This belt can be traced for 1 200 km in NE-SW direction and 70–250 km in width and includes several caldera structures with volcanic-type U deposits in North Choibalsan, Berkh, Eastern, and Middle Gobi regions as well as sandstone and lignite U mineralization in Cretaceous basins. Sandstone U deposits include Kharaat in the Choir Basin and some small deposits/occurrences in the Gurvansaikhan, Khairkan, Oshiin-nuur, Tavansuveet, Undurshil (Ongiingol) basins; uraniumiferous lignite is reported from the Choibalsan and Ulziit basins.

The Gobi-Tamtsag U province covers 1 400 km in NE-SW length and 60–180 km in width at the southeastern periphery of Mongolia. This province encompasses the Tamtsag, Sainshand,

Zuunbayan, and Undurshil Cretaceous basins with sandstone-type U occurrences including the Nars deposit in the Sainshand Basin.

The Khentei-Daur U province is 700 km long and 250 km wide and covers the Khangai and Khentei mountains in central and NE-central Mongolia. Vein U-Th-REE mineralization in fractured Mesozoic leucogranite as known, e.g. from the Janchivlan granitic massif, are typical for this U province. The Chuluut area, northern Khangai region, contains sandstone hosted U mineralization (basal channel type?) in Cenozoic sediments of the Suimin-gol Basin.

The North Mongolian U province covers a 1 500 km long and 450 km wide terrane in northern and northwestern Mongolia. Various types of complex U mineralization associated with a variety of rocks of mainly Late Proterozoic and Paleozoic age occur in this province.

Types of Uranium Deposits

Uranium in Mongolia may be attributed to volcanic, sandstone, lignite, metasomatite, intrusive, and phosphorite types as well as to vein and/or structure controlled surficial types in leucocratic granite and metamorphics. Deposits of economic interest are restricted to volcanic and sandstone types.

Volcanic-type deposits include structure-bound and strata-bound ore bodies (in Russian literature referred to as F-Mo-U deposits in volcanic-tectonic structures). Most deposits are associated with Upper Jurassic-Lower Cretaceous effusives and sediments of rhyolite and basalt-rhyolite composition within the intracontinental Mongol-Priargun volcanic belt. Significant deposits exist in the North Choibalsan region (Mardai/Dornod District); they are similar to the volcanic-type deposits in the Strel'tsovsk District in Transbaikalia, Russia. Small deposits/occurrences are known from the North Kherlen and Baiderin uplifts in the Central Mongolian fold belt, as well as from the South Mongolian, Mongol-Transbaykal, and North Mongolian fold belts/systems.

Sandstone-type deposits include tabular/peneconcordant (related to surface-bound oxidation and at depth to partially oxidized permeable strata), basal channel, and rarely roll-shaped subtypes (referred to as uranium in weakly lithified deposits associated with zones of ground and stratum oxidation and reduction). Sandstone-type mineralization is widespread in intermontane Cretaceous basins in the Dornogovi (Eastern Gobi) and Gobi-Tamtsag regions in southern and southeastern Mongolia. Some basal channel(?) U occurrences were discovered in Cenozoic sediments in the Chuluut area, Khentei-Daur U province.

Vein-type uranium occurrences consist mainly of disseminated U^{6+} minerals (of surficial/supergene origin?) within fractured, highly radioactive Mesozoic leucogranite massifs such as

in the Khangai and Khentei-Daur uplifts in the Mongol-Transbaykal fold belt.

Lignite-type U concentrations are reflected by syngenetic and redistributed U in lignite seams in Lower Cretaceous basins. Grades average up to 0.05% U. Uraniferous lignite is reported from the Sumiin-nur basins in the North Choibalsan region and several basins in the Dornogovi and Gobi-Tamtsag regions.

Metasomatite-type U occurrences and showings with U-Th-REE or U-Th mineralization are known from metasomatized (mainly albitized) zones in subalkaline and alkaline granite and syenite intrusions, and in pegmatite in the North Mongolian U province. Mineralization occurs in the form of discontinuous lenses, pods, or aggregates with impregnated uraninite, uraniferous titanate, zircon, monazite, thorite, and orthite.

Phosphorite-type U mineralization consists of small occurrences of uraniferous apatite in Cretaceous continental clastic sediments. Grades average a few hundred ppm U but can locally be up to 0.3% U with P_2O_5 contents of commonly a few percent with local maxima of 20%.

Many of the identified U occurrences and particularly those described as migmatite, metamorphite, phosphorite, and lignite type are mainly reflected by elevated U and/or Th background values. Some of the sites have minor uranium enrichments mostly due to locally restricted supergene concentrations in the form of fracture-bound, surficial-type mineralization.

8.1 North Choibalsan Region, Dornod Aimag

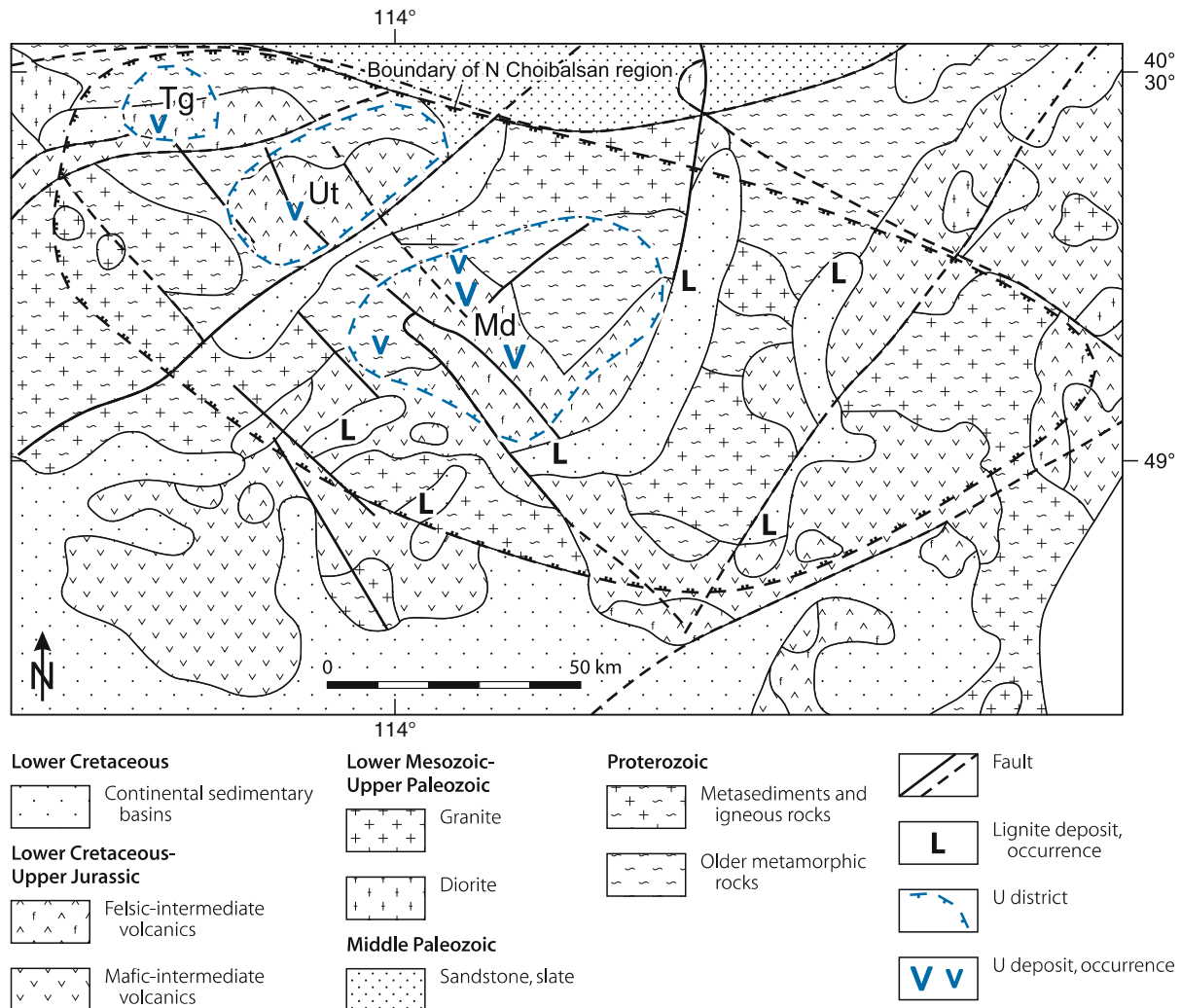
Four uranium districts have been established in the North Choibalsan volcanic region, Mardai (Dornod), Ugtam, Turgen, and Engershand (Fig. 8.2). All contain volcanic-type (fluorine-molybdenum-uranium-type in volcano-tectonic structures in Russian terminology) uranium deposits.

Uraniferous lignite occurs in the Cretaceous Sumiin-nuur Basin (Delger-nuur, Shinebulag, and Bagazos-nuur occurrences) located adjacent to the southwest of the North Choibalsan volcanic region, and further to the south in the Cretaceous Choibalsan Basin (e.g. Choibalsan, Bayan-bulag, and Khashaat occurrences).

8.1.1 Mardai (Dornod) District, Dornod Aimag

The Mardai District (in Russian literature referred to as Dornod or Dornot District) is located in Dornod aimag (= province) in northeastern Mongolia, some 600 km east of Ulaan Baatar. This district includes the uranium deposits *Dornod*, *Gurvanbulag*, *Mardaingol*, and *Nemer*, and a number of occurrences (Fig. 8.3) (although termed deposits in Mongolian and Russian papers, these are actually ore fields composed of ore zones with several deposits/ore bodies). Original resources (RAR + EAR-I) of the four deposits total about 50 000 t U at a grade of 0.16% U.

Fig. 8.2. North Choibalsan region, generalized geological map with location of U districts (*Md* Mardai, *Tg* Turgen, *Ut* Ugtam) (after Mironov and Rogov 1992)



The district also contains deposits of Pb-Zn-Ag with some U (Bayandun, Muhar, Tsav, Ulaan), fluorite (Baruun-su, Hubbulag, Khooley), gold (Urlinobin), molybdenum (Arbulag, Avdar-Tolgoy), and tungsten (Chuulun-Khuriete).

In 1989 the Dornod, Gurvanbulag, and Mardaingol deposits had been developed for underground mining and ore bodies # 2a-2b of the Dornod deposit had been developed for open pit mining. Production capacity was planned at 2 million t of ore annually. Underground mining ceased, however, in 1992, while open pit mining continued until 1995. Production amounted to 93.6 t U (at a grade of 0.117% U) in 1989, peaked at 105.2 t U (0.118% U) in 1992, and dropped to 20.2 t U (0.145% U) in 1995. A total of 535 t U were recovered during this period. All ore was transported 485 km by rail to the Krasnokamensk mill in Transbaykalia, Russia.

Sources of information. Batbold 2001; Filonenko et al. 1993; IAEA 1995, 2007; Mironov 2003; Mironov and Rogov 1992, 1993; Mironov et al. 1993, 1995; OECD-NEA/IAEA 1993, 1995, 1997; Petrov et al. 2002, 2003; and pers. commun. by Chuluun O and

staff of Uran Company Ltd. of Mongolia and ERDES Mining Enterprise. Additional information is available in the more recent publications by Ischukova et al. (2002) and Mironov (2003).

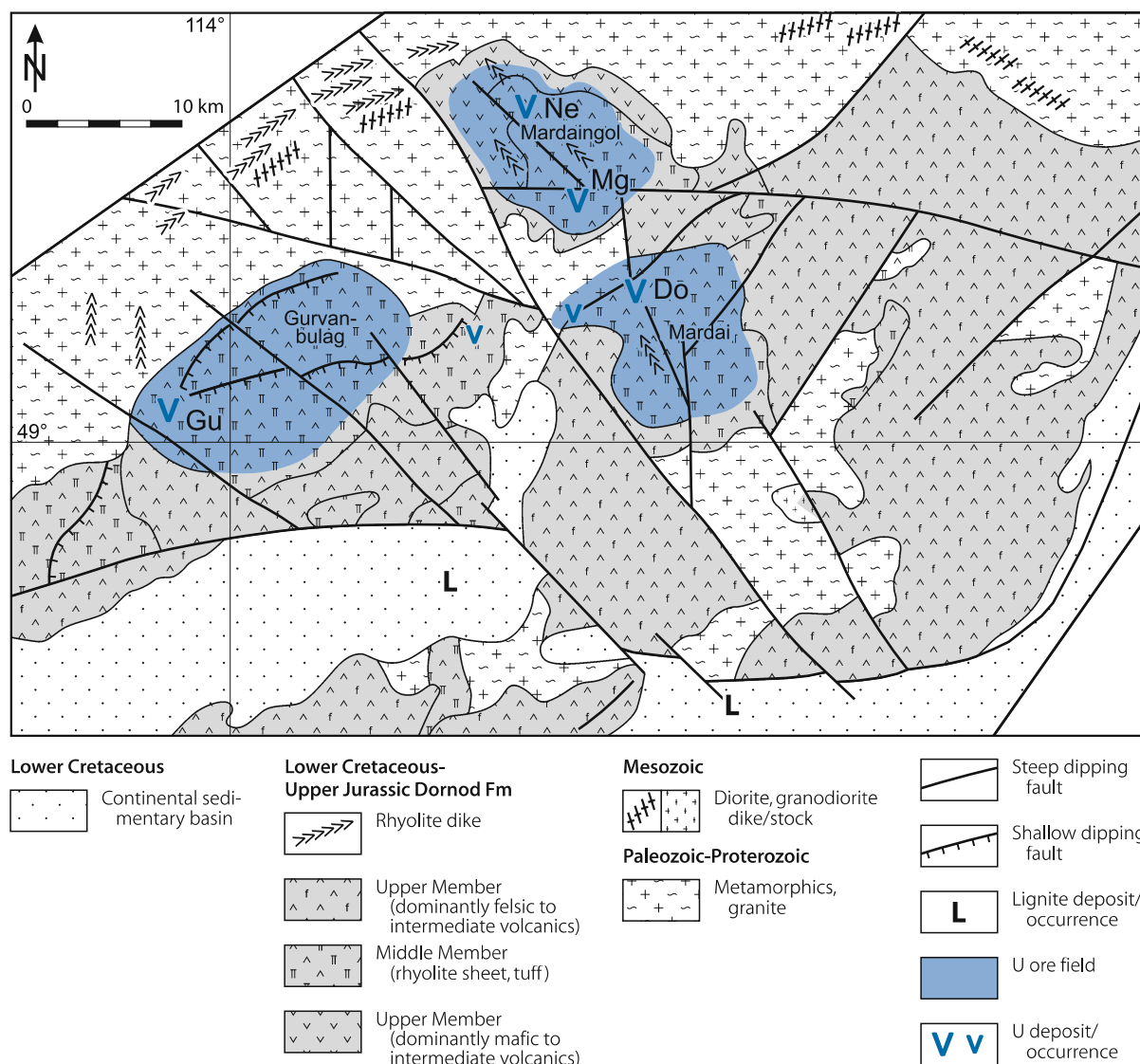
Regional Geological Setting of Mineralization

The Mardai District is at the northern margin of the *Dornod Volcano-Tectonic Structure*. This is one of the largest volcanic complexes within the Mongol-Argun intracontinental volcanic belt. It evolved during Late Mesozoic tectonic-magmatic activation that affected the Precambrian Manzhur-Chinese Platform. The belt extends for 1 200 km in SW-NE direction from the edge of the Mongolian Altai mountains in southern Mongolia to the Pri-Argun area in southeastern Transbaykal in Russia where volcanic-type U deposits are exploited in the Streltsovsk District.

The Mardai area is underlain by two geological units: a Late Mesozoic continental sedimentary-volcanic sequence that rests unconformably upon a crystalline basement of Proterozoic to early Mesozoic age.

Fig. 8.3.

North Choibalsan region, Mardai (Dornod) U District, generalized geological map with location of volcanic-type U ore fields and deposits (after Mironov and Rogov 1992). (U deposits: *Do* Dornod, *Gu* Gurvanbulag, *Mg* Mardaingol, *Ne* Nemer)



The *Late Mesozoic upper unit* consists of the Zuunbayan Formation composed of Early Cretaceous lignite-bearing continental sediments and the underlying Dornod Formation of Early Cretaceous-Late Jurassic continental, subalkalic, volcanogenic, and sedimentary facies, which fill graben structures. The *Dornod Formation*, 1 000–1 500 m thick, is subdivided into three members each characterized by volcanogenic suites derived by subsequent cycles of volcanism:

- an *Upper Member* (>1 000 m thick) of rhyolite-trachyrhyolite-trachyandesite
- a *Middle Member* of rhyolite, and
- a *Lower Member* (<400 m thick) of basalt-trachyandesite/dacite-rhyolite

About 75% of the Dornod lithologies consist of stratified pyroclastic and outflow volcanic rocks composed of rhyolite, quartz-feldspar porphyry, andesite-basalt, and weakly fluidal felsite. Intercalated continental clastic and lacustrine

sediments containing organic matter constitute the remainder. Conglomerates overlain by gritstone, sandstone, and siltstone beds occur at the base of the Dornod Formation in paleo-depressions.

The *crystalline basement* includes

- Jurassic granite-porphyry, granodiorite and diorite bodies, syenitic, dioritic, and diabase dikes, and subsequent subvolcanic bodies and dikes of felsic and andesitic porphyries
- large bodies of Late Paleozoic granite, diorite, and gabbrodiorite (Tsenkher-gol Complex)
- widely distributed Early Paleozoic K- and Na-metasomatized granodiorite and diorite (Modochudag Complex)
- Proterozoic granite-gneiss and porphyroblastic granite, and
- an older complex of Proterozoic to Early Paleozoic regionally metamorphosed (amphibolite facies) geosynclinal and continental sediments (schist, gneiss, marble) and volcanics

Structural elements of the region are characterized by arched uplifts and downfaulted grabens largely controlled by NE-SW- and NW-SE-trending regional faults.

Principal Host Rock Alteration

Ore-related host rock alteration is primarily argillization. Alteration products include hydromica, montmorillonite, kaolinite, chlorite, carbonate, fluorite, quartz, and hematite. Most intense is hydromica-montmorillonitization. Hematitization tends to be related to mineralized zones and its intensity seems to correlate with the uranium grade.

A distinct primary geochemical dispersion halo of U and associated elements such as Pb, As, Ag, and Mo envelopes ore bodies. The halo is controlled by, and commonly confined to the ore-hosting permeable cataclastic lithologies and/or faults. Fault-related halos are generally of elongated shape. Halo dimensions surpass those of ore bodies by one to three times. Uranium forms the most extensive aureole and may extend in excess of 500 m from ore bodies.

Weathering-related alteration is very limited and is essentially restricted to major fault zones along which it persists to depths up to 300 m.

Principal Characteristics of Mineralization

Coffinite and pitchblende are the principal U minerals. Brannerite, uraniferous leucoxene and titanite occur in minor or accessory amounts. Hexavalent U phases such as uranophane, beta-uranotile, curite, woelsendorfite, kasolite, or amorphous U-hydroxides replace primary uranium minerals in oxidized zones.

Associated ore minerals include arsenopyrite, chalcopyrite, galena, marcasite, molybdenite, pyrite, sphalerite, and hematite. Gangue minerals are dominated by quartz, biotite, hydromica, montmorillonite, and chlorite (chamosite); K-feldspar, fluorite, muscovite, ankerite, calcite, siderite, baryte, leucoxene occur in minor amounts; and sericite, tourmaline, zircon, titanomagnetite, and anatase occur in traces.

Uranium minerals occur mostly as fine- to coarse-grained aggregates, 0.001–0.5 mm in size, and more rarely as up to 2 mm thick veinlets. Ore textures exhibit impregnation, stringer, reticulate, rarely banded and earthy, and, in high grade mineralization (>0.3% U), breccia and cement modes.

Mineralization can be monometallic or polymetallic consisting of uranium and molybdenum as in the Mardaingol deposit. Both elements correlate geochemically and their spatial distribution is often identical. Similar to uranium, molybdenum distribution and tenor are commonly highly irregular.

The principal host is the Dornod Formation but some uranium veinlets also occur in the crystalline basement. In the Dornod Formation, U is distributed in almost all types of rocks. Sizable ore-grade accumulations, however, are restricted to permeable, mostly cataclastic horizons within certain sedimentary and volcanogenic horizons at the base and within the Lower and

Middle Member of the Dornod Formation, in which principal ore-hosting lithologies include

- brecciated andesitic-basaltic pillow lava (example: Dornod ore body 7),
- clastic sediments (sandstone/arkose, conglomerate) containing detrital plant remains (ex.: Dornod ore bodies 2, 3a, 3b; Gurvanbulag, and Nemer deposits),
- oligophytic rhyolite lava and related tuff (ex.: Dornod ore bodies 1, 4, 5, 6, 8, 10; and Mardaingol deposit), and
- vitroclastic felsic tuff and vitric felsite (ex.: Gurvanbulag deposit).

Most sites favorable for tabular mineralization are controlled primarily by strata-peneconcordant, flat to shallow dipping faults and, to a lesser degree, by steeply dipping faults. The latter also constitute the host for veinlike to stockwork-type mineralization particularly at their intersections with shallow structures.

General Shape and Dimensions of Deposits/ Characteristics of Individual Ore Bodies

Deposits consist of several ore zones containing one to several ore bodies enveloped in a geochemical dispersion halo. Ore bodies are composed of ore lenses or lodes defined by a minimum uranium content of 0.06% U. Sub-ore grade mineralization commonly intervenes between ore shoots. Distances between ore bodies within an ore zone vary from 50 m to 350 m. Ore bodies are distributed blindly over a vertical interval from 30 to 600 m below surface.

Ore bodies are of peneconcordant-tabular and veinlike to stockwork configuration and exhibit the following characteristics:

Tabular ore consists of heterogeneously distributed uranium forming strata-peneconcordant tabular to lenticular, in plan view elongated to trapezoid-shaped bodies controlled by cataclastic zones along flat to shallow dipping faults. Ore bodies may contain several, laterally adjacent and/or superjacent ore lenses enveloped by weak mineralization. Dimensions of tabular ore are given in [Table 8.1](#).

Veinlike to stockwork ore bodies are predominantly of irregular shape and may grade laterally into tabular ore. They consist of low-grade mineralization enveloping unpredictably distributed, variably structured lodes composed of ore pods, pockets, and/or lenses interconnected by joint fillings, stringers, and veinlets of ore-grade material. Subparallel, steeply dipping NW-SE- or N-S-oriented faults cutting (1) intraformational and (2) flat to shallow inclined fault and fracture zones positioned at strata contacts control the position of these lodes. Dimensions of vein-stockwork ore are of the order of magnitude shown in [Table 8.2](#).

Regional Geochronology

U-Pb systematics of U minerals yield ages from 153 to 136 Ma. Golubev et al. (1994) report an age of 138–136 Ma for U deposition in the Dornod volcano-tectonic structure. These Late

Table 8.1.

Mardai District, order of dimensions of ore zones with tabular uranium mineralization

Parameter	Ore zones	Ore bodies	Ore lenses
Length (m)	<100–3100	<100–1700	<10–>1000
Width (m)	<50–1600	<50–900	<10 to several 100
Area		Several 10 m ² to 0.5 km ²	
Thickness (m)		<1–40	0.3–9
– ore bearing interval	<1–40		
Resources (t U)	<10–14000	<10–5000	<1–>1000
Grade (% U)	0.09–0.6	0.06–0.7	0.06–>1

Table 8.2.

Mardei District, order of dimensions of ore zones with vein-stockwork uranium mineralization

Parameter	Ore zones	Ore bodies
Length (m)	40–1200	10–100
Width (m)	<1–500	0.3–25
Depth extension (m)	50–370	<10–60
Thickness of individual lodes (m)		0.3–20
Resources (t U)	Some 10s to 7000	Few 10s to 150
Grade (% U)	0.09–0.18	0.06–0.7

Jurassic to Early Cretaceous ages are practically time equivalent to deposits in the Streltsovsk Caldera in Russia (136–134 Ma).

Dating of sericite derived by propylitization associated with polymetallic mineralization give K-Ar ages of 161 ± 7 Ma while K-Ar ages of pre-uranium hydromicas yield 145–143 Ma. Rb-Sr ages of 170–140 Ma were obtained for rocks of the Lower Member of the Dornod Formation.

Potential Sources of Uranium

Felsic volcanics tend to constitute potential sources for uranium and other metals. These rocks contain from 6 to 21 ppm U or more with highest amounts in vitric rocks. Chemillac et al. (2005b) report 13.6–24.9 ppm U contained in melt inclusions in comanditic rhyolite.

Principal Ore Controls and Recognition Criteria

Ore bodies are predominantly of tabular and subordinately of vein-stockwork configuration controlled by lithology and structure as reflected by the following criteria:

Host environment

- Calderas composed of felsic to mafic effusives and pyroclastics, and terrigenous sediments (Dornod Formation)
- Preferential host rocks include cataclastic, permeable
 - tuffaceous horizons (vitroclastic felsic ash tuff, felsite/rhyolitic tuff,

- felsic and mafic volcanic lava sheets (oligophyric rhyolite lava, volcanic glass and vitric felsite horizons, andesitic-basaltic pillow lava),
- quartz-feldspar porphyry/felsic porphyry dikes,
- clastic sediments with abundant vegetal matter.
- Brittle deformation is associated with
 - major and regional faults of steep dip and oriented mainly NW-SE and NE-SW and their intersection, and
 - flat to shallow dipping fault-fracture zones positioned intraformational and at facies boundaries of favorable lithologies (andesitic-basaltic pillow lava, vitrophyric felsic ash tuff, felsite/oligophyric rhyolite).

Alteration

- Pre-ore hydromicazation-montmorillonitization
- Syn- or post-ore argillization, carbonatization, hematitization
- Direct relation of hematitization to U mineralization and grade of ore
- Limited weathering effects but extending to great depths along major faults

Mineralization

- U-oxide and U-silicate minerals with sulfides of Fe, Mo, Pb, Zn, Cu, and quartz, phyllosilicates, carbonates are the principal ore constituents
- Ore texture is largely of impregnation nature
- Ore bodies are enveloped in halos of low grade U, As, Mo, and Pb concentrations

- U mineralization is structure-bound and occurs in strata-peneconcordant tabular or vein-stockwork lodes of highly variable dimension and configuration
- Ore bodies are controlled by
 - steeply dipping major faults and their intersection,
 - flat to shallow inclined fault-fracture zones positioned intraformational and at facies boundaries,
 - intersections of steeply dipping with flat to shallow fault zones.
- Tabular mineralization is restricted to flat or shallow dipping fault, shear, and breccia zones, which occur particularly
 - at the contact of volcanic sheets with tuffaceous and sedimentary horizons and most intensely at the base of oligophyric rhyolite,
 - in tuffaceous-sedimentary beds, which separate the Lower and Middle Member, and
 - in andesitic-basaltic pillow lava of the Lower Member of the Dornod Formation.
- Some intraformational, flat lying faults form hanging or footwall boundaries of ore lodes in some deposits suggesting that these faults acted as impermeable barriers to ore-forming solutions
- High angle faults form lateral boundaries of, and partly govern the grade distribution of uranium in tabular ore bodies
- Vein and stockwork mineralization favor high angle faults trending NW-SE and, to a minor extent, N-S, and their intersections with favorable lithologies such as tuff, felsite, and/or quartz-feldspar porphyry
- Vein-stockwork ore lodes are generally small
- Potential sources of uranium and other metals are provided by U-bearing felsic volcanics
- Reducing potential is provided by
 - abundant detrital vegetal matter in terrigenous sediments, and possibly by
 - ferric iron or other elements of reducing capacity in mafic volcanics.

Principal Aspects of Metallogenesis

The metallogenesis of U deposits in the Mardai District is still enigmatic. U mineralization tends to be related to volcanics, particularly of felsic composition. These felsic volcanics constitute a potential source of uranium and other metals associated with uranium mineralization as documented by Chemillac et al. (2005b). These authors investigated hydrothermally altered and brecciated samples of alkali rhyolite of the second volcanic cycle, and, in addition, melt inclusions in quartz phenocrysts unaffected by alteration.

Relic primary minerals consist of quartz, rare K-feldspars (Or 91–94), plagioclase (An 20–32), biotite, and zircon embedded in an argillized matrix (mainly sericite). Late carbonate and fluorite occupy fractures and hematite occurs within sericite aggregates in extremely altered material. Devitrification features such as spherulites and perlitites are common. Mineralized samples with up to 0.1% U contain hydrothermal uraniferous zircon, brannerite, coffinite, and, as late phases, bastnaesite and strontianite. *Bulk*

rock chemistry of rhyolite and rhyolitic breccia show medium to high silica (72.87–78.85% SiO₂), high alkalis (3.8% Na₂O + 8.3% K₂O), medium Fe (1.0–2.2% Fe₂O₃), and extremely low Ca, Mg, Mn, Ti, and P contents. Trace elements amount to 205–288 ppm REE, 49–93 ppm Nb, 4.2–8.2 ppm Ta, 32–53 ppm Th, 63–157 ppm Y, 257–418 ppm Zr, 3–233 ppm Ba, and 24–141 ppm Sr, values, which are typical for fractionated peralkaline magmas. The chemistry of *melt inclusions* is also characterized by high silica (74%) and alkalis (8.1–11.4%), and low Ca, Ti, P, and Cl contents, but show high F (0.8–3.5%) contents, and elevated U (13.6–24.9 ppm), Th (21–49 ppm), REE (215–224 ppm), Zr (233–263 ppm), Y (53–76 ppm), and Nb (52–76 ppm) values whereas Ba (11–32 ppm) and Sr (1–10 ppm) are clearly depleted.

Chemillac et al. (2005b) deduce from these data that the initial rhyolitic magma preserved as melt inclusions in quartz had a highly evolved comenditic composition, was mildly peralkaline, and enriched in F, U, Th, REE, and Zr. Their U and Th contents match those in rhyolitic melts of the Streltsovsk Caldera, Russia (Chabiron et al. 2001). These comenditic rhyolites constitute substantial sources of uranium. The initial U content in the melt combined with the volume of erupted rhyolite are largely sufficient to explain the ore resources. Mobilization of the ore-forming elements was by hydrothermal activity, which is indicated by the largely aphyric nature of these rhyolites.

According to the various papers by Mironov and co-workers, the postulated hydrothermal solutions were either of late volcanic, intraformational, or meteoric origin, or a combination thereof. Late volcanic events may have provoked mobilization of such fluids. Reducing conditions required for reduction and arrest of uranium existed particularly at sites where sediments contained abundant plant remains. An additional reductant may have been ferric iron of mafic minerals as found in andesite and basalt. Physico-chemical conditions (effervescence, break up of fluid components etc.) may have otherwise contributed to uranium precipitation particularly in volcanic outflow facies.

Tectonic activity was an additional crucial prerequisite for ore formation. Large, high-angle and flat to shallow dipping, strata-peneconcordant faults and associated cataclastic zones in volcanic effusive and pyroclastic rocks, and permeable continental clastic sediments provided favorable pathways for migration of mineralizing fluids and open space for ore accumulation as reflected by the containment of the major portion of tabular mineralization in these zones. Cataclasis of felsic volcanics may also have been a prerequisite for uranium leaching in case, these facies are considered the source of ore-forming uranium and other metals.

Isotope dating of uranium minerals indicate a time interval for metallogenic event(s) between 153 and 136 Ma and a most likely time interval for U ore formation 138–136 Ma ago, i.e. during Late Jurassic and Early Cretaceous periods. This latter time bracket virtually corresponds to U ore formation in the Streltsovsk Caldera, located to the northeast in the same volcanic belt in Asian Russia. Hence it may be assumed that the formation of the volcanic-type U-Mo deposits in the Mardai District evolved by similar complex and perhaps multistage processes as deposits in the Streltsovsk Caldera (see Chap. 10: *Russian Federation, Asian Territory*).

8.1.1.1 Dornod Deposit

The Dornod deposit is located some 90 km north of Choibalsan. This volcanic-type deposit contains twelve ore zones composed of one or more ore bodies of monometallic, peneconcordant-tabular and/or veinlike to stockwork mineralization (► Fig. 8.4). Original resources totaled 33 000 t U, including 29 000 t U RAR + EAR-I at a grade of 0.17% U.

Ore bodies 2b and 2c were mined by open pit methods (130 m deep) from 1988 to 1995. The # 7 ore body was mined by underground techniques (520–580 m deep) from 1989 to 1992 when exploitation was stopped. Planned underground production (partly by underground leaching) was 1.5 million t ore per year.

Sources of information. IAEA 1995, 2007; Mironov 2003; Mironov and Rogov 1992, 1993; Mironov et al. 1995; pers. commun. by Chuluun O and staff of Uran Company Ltd. of Mongolia and ERDES Mining Enterprise.

Geological Setting of Mineralization

Situated in the central part of the Dornod Volcanic-Tectonic Structure, the Dornod deposit exhibits a geologic setting, which comprises a crystalline *basement* of predominantly palaeogenetic, K- and Na-metasomatized granodiorite of the Paleozoic Motochudag Complex, and which contains xenoliths of Proterozoic schist, gneiss, and marble. Separated by a distinct unconformity, Late Jurassic-Early Cretaceous sedimentary and volcanogenic facies of the Dornod Formation overly the basement. Dominant facies are stratified volcanics covering approximately 90% of the area.

The *Dornod Formation* consists of three members derived by subsequent cycles of volcanism. The *Upper Member* is weakly developed and consists of trachy-andesite sheets. The *Middle Member* includes 750 m thick stratified (from top to bottom) feldspathic rhyolite, lithic ignimbrite, oligophyric rhyolite, and a basal rhyolitic tuff horizon. The *Lower Member* is composed of, from top to bottom, lacustrine sediments, sheets of andesitic-basaltic pillow lava, which are dominant, an assemblage of interbedded carbonaceous lacustrine sandstone, mudstone and tuffite, and a basal conglomerate in paleo-depressions.

Fault systems are oriented NE-SW, N-S, and NW-SE. Horsts and grabens are primarily controlled by NE-SW-trending faults. Repeated reactivation of N-S and NW-SE structures generated high angle and shallow dipping faults, shear and breccia zones. Shallow dipping cataclastic zones with good permeability developed preferentially at or near the contact of volcanic sheets with tuffaceous and sedimentary beds. Their development is most intense in tuffaceous-sedimentary beds at the base of oligophyric rhyolite, which separate the Lower and Middle Member, and in andesitic-basaltic pillow lava of the Lower Member.

Host Rock Alteration

Most prominent is pre-ore hydromica-montmorillonitization. Ore-related alteration features include carbonatization, hydromicization, montmorillonitization, kaolinization, chloritization, and hematitization. Hematitization is directly

related to mineralized zones and its intensity tends to correlate with the grade of mineralization.

A distinct geochemical halo of U and associated elements such as Pb, As, and Mo is developed around ore bodies. Halos are commonly of elongated shape largely controlled by faults. The dimensions of halos surpass those of ore bodies by 2–3 times. Uranium forms the most extensive aureole extending in excess of 500 m from ore bodies.

Alteration by weathering is very limited and essentially restricted to major fault zones along which it locally extends to depths in excess of 400 m.

Mineralization

Coffinite and pitchblende are the principal U minerals. Uraniferous leucosene and titanate, minor brannerite and uranophane are ubiquitous in ore body # 7. Secondary U minerals include uranyl silicates (uranophane, beta-uranotile) and hydroxides (clarkeite, masuyite).

Associated ore minerals include chalcocopyrite, galena, marcasite, molybdenite, pyrite, sphalerite, hematite, and minor arsenopyrite. Quartz, biotite, hydromica, montmorillonite, chamosite, minor ankerite, calcite, siderite, fluorite, baryte, leucosene, K-feldspar, muscovite, and rare tourmaline and anatase occur as gangue or ore accompanying minerals.

Uranium minerals occur mostly as fine- to coarse-grained aggregates, 0.001–2 mm in size. Ore texture is of impregnation type reflected by finely disseminated, globular, stringer, rarely banded and earthy features. Rich uranium mineralization has breccia and cement textures.

Ore-grade uranium is restricted to the Dornod Formation but low-grade mineralization occurs as stringers also in the basement.

Although uranium is found in almost all types of Dornod rocks, sizable ore-grade accumulations are confined to sedimentary and volcanogenic horizons at the base of and within the Lower and Middle Member of the Dornod Formation, and to faults cutting volcanic horizons at shallow angles. The principal host lithologies are

- brecciated andesitic-basaltic pillow-lava (ore bodies in zone # 7),
- carbonaceous sandstone/arkose containing up to 4% detrital vegetal matter (ore bodies 2a–c, and 3a–c), and
- oligophyric rhyolite sheets and vitroclastic felsic tuff (ore bodies 1, 4, 5, 6, 8, 10).

Three varieties of uranium assemblages related to host rock settings are noted:

- pitchblende-coffinite with uraniferous titanate in brecciated andesitic-basaltic pillow-lava (ore bodies in zone 7),
- pitchblende-coffinite in clastic sediments containing detrital plant remains (ore bodies 2a–c, and 3a–c), and
- pitchblende-coffinite in felsic effusive and pyroclastic rocks (ore bodies 4 and 5).

U⁶⁺ minerals occur in vein-stockwork ore bodies to depths of 500 m. They constitute 35% of the entire U mineralization in ore body 5.

Fig. 8.4. Mardai/Dornod deposit, generalized **a** geological map with location of ore bodies, **b** E-W and **c** N-S section illustrating the litho-stratigraphic position of ore bodies in the Dornod Formation (after a, b Mironov et al. 1995; c Mironov and Rogov 1992)

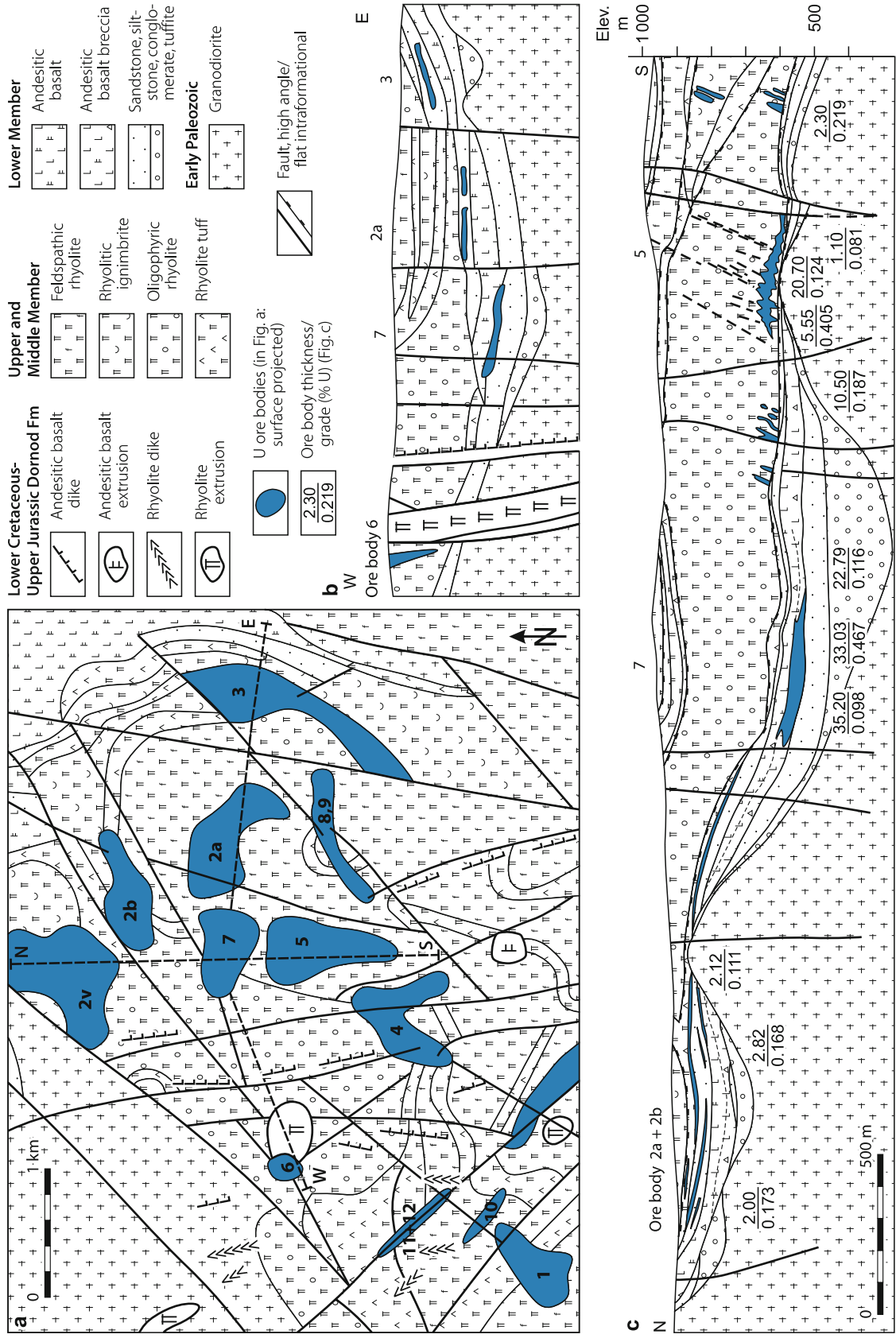
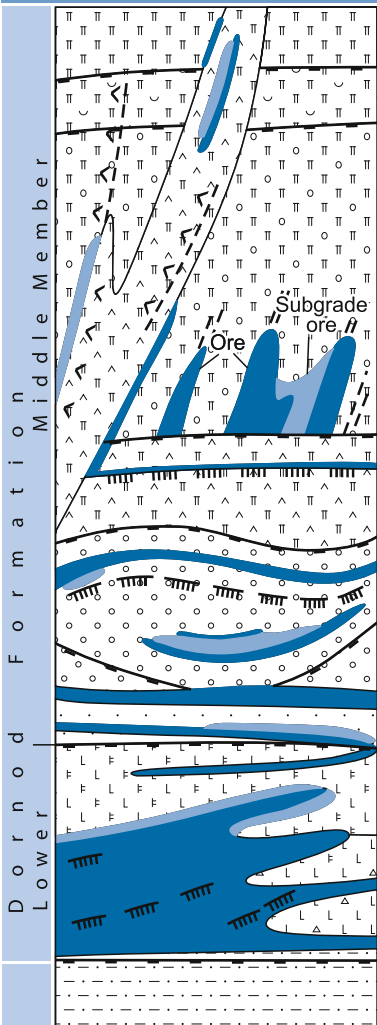


Fig. 8.5.

Mardai/Dornod deposit, scheme of geological setting, distribution, and configuration of ore bodies, and their percentage contribution to the reserves of the deposit (legend see Fig. 8.4) (after Mironov and Rogov 1993)

Litho-stratigraphic column	Lithologic-structural levels	Shape of ore bodies	Ore zone (number)	Ore body (number)	Percent of total reserves
	Contact of felsic extrusions and flow sheets	Small complex veinlike and stockwork	6		
			10		
			11		
			12		
	Steep fracture zone in basal oligophyric rhyolite sheet	Vein and stockwork	1		4
			4		13
			5		1
			8		
	Cataclastic zone in tuff, conglomerate, and fine clastic rocks enriched in organic matter located at contact of Lower and Middle members of Dornod Fm	Strata-bound tabular flat-lying	2	2a	4
				2b	10
				2c	12
		3	3a	3	
3b			1		
3c			2		
9		1			
Cataclastic zone of coarse-fragment breccia in basal basaltic andesite sheet	Lenticular and tabular bodies with irregular margins	7		49	

Shape and Dimensions of Deposits/Characteristics of Individual Ore Bodies

The Dornod deposit comprises twelve ore zones within an area of about 20 km². Individual zones contain one or more ore bodies (Fig. 8.4). The bulk of U resources is contained in ore zones 2, 3, 4, 5, 7, 8, and 9, which are grouped in an area 3 700 m long and 2 500 m wide. These zones account for 29 000 t U RAR + EAR-I at a grade of 0.175% U. Some 4 000 t U of subeconomic resources are delineated in ore zones 1, 6, 10, 11, and 12 in the Khavar sector in the W to SW part of the deposit. (Calculation of grades for (a) underground and (b) open pit mining is based on a cutoff grade of (a) 0.04% U, (b) 0.03% U, a minimum grade for ore sections in planview of (a) 0.06, (b) 0.05% U, and a minimum grade for mining blocks of (a) 0.10, (b) 0.08% U.)

Ore bodies are of peneconcordant-tabular and veinlike to stockwork configuration with characteristics as outlined below and shown in Fig. 8.5. All ore bodies are blind and occur over

a vertical interval from 30 to 600 m below surface. Distances between ore bodies are 50–350 m. Zones # 2, 3, and 7 contain the largest ore bodies.

Tabular Ore Bodies

Peneconcordant-tabular mineralization forms ore bodies in ore zones # 2, 3, 7, and 9 (Figs. 8.4a,c).

Ore zone # 7 is the largest ore zone of the Dornod deposit. It is located in the central part of the deposit at a depth of some 500 m and accounts for about 14 000 t U at a grade of 0.23% U contained in nine ore bodies (# 1–9). This peneconcordant, subhorizontally dipping zone has in planview a trapezoidal shape 800 m in length and 480 m in width. The upper edge of the zone dips from 540 m to 505 m a.s.l. Ore is hosted in a 20–40 m thick brecciated section within the ca. 40 m thick third

andesitic-basaltic pillow-lava sheet of the Lower Member of the Dornod Formation. The cumulative thickness of superjacent ore shoots averages 11 m. Ore shoots are separated by sterile intervals up to 3 m thick. The lava is interbedded with terrigenous, lacustrine sediments and fills a large paleovalley incised into the basement. Ore is restricted to the marginal part of the brecciated lava sheet where the sheet gradually pinches out. Uranium associates predominantly with matrix material. High-grade mineralization is confined to intervals of fine-grained fractions within the brecciated lava. Richest ore with a grade of 0.2–0.45% U is concentrated in the central part of zone # 7, which averages 30–33 m in thickness and contains the bulk of the ore. The grade gradually decreases laterally. A large low-grade uranium aureole surrounds this ore zone.

Ore zones # 2, 3, and 9 (ore bodies # 2a, 2b, 2c; 3a, 3b, 3c; and 9) are located in the northern and eastern part of the Dornod deposit and account for about almost 10 000 t U, some 8 000 t of which are contained in ore zone # 2 and some 1 700 t U in zone # 3. Grades vary between 0.06 and 0.6% U (2b + 2c: av. 0.1–0.175% U at 2 m thickness). The shallow dipping, tabular ore bodies occur immediately below a rhyolite sheet in sandstone, siltstone, and conglomerate, which fill a paleovalley. Mineralization occurs in several superjacent levels associated with jointed zones within lenses and interbeds of highly carbonaceous, fine- and coarse-grained sediments and tuffs at the contact between the Lower and Middle Member of the Dornod Formation. Distance between ore bodies is up to 40 m. A wide aureole of low-grade mineralization envelops the ore bodies.

Veinlike-Stockwork Ore Bodies

Ore zones 4, 5, and 8 are located in the central and *ore zones 1, 6, 10, 11, and 12* in the western and southwestern (Khavar) sector of the Dornod deposit (Fig. 8.4a). These zones contain about 7 000 t U, some 5 000 t U of which are considered of economic magnitude. Ore zones consist of one or several ore bodies at depths from 280 to 520 m. Grades of ore bodies average 0.1–0.2% U but ore grades are highly variable ranging from 0.05 to 1% U due to concentration of uranium in small, separated ore shoots. Thicknesses range from 0.5 to 20 m and vertical persistence is commonly less than 50 m but can be up to 80 m.

Ore zones and related ore bodies are controlled by the Central and Baga-Erchtyyn fault zones. The major part of the ore occurs as fault, fracture, and joint fillings in the form of stockworks controlled by shallow dipping, about N-S and NW-SE-oriented en echelon faults in the basal part of a sheet of oligophyric rhyolite and associated vitroclastic felsic tuff.

8.1.1.2 Gurvanbulag Deposit

This monometallic volcanic-type deposit is located some 90 km north of Choibalsan, and ca. 30 km west of the Dornod deposit (Fig. 8.3). It includes three sectors, Central, Intermediate, and

Southwest (Fig. 8.6). Each sector contains several ore zones with several ore bodies predominantly of peneconcordant-tabular and minor vein-stockwork configuration. Resources total some 17 000 t U, which include 9 000 t U at a grade of about 0.2% U RAR and about 7 000 t U at 0.12% U EAR-I. The Central sector was prepared for underground mining in the late 1980s (planned depth 526 m) but not mined.

Sources of information. IAEA 1995, 2007; Mironov 2003; Mironov and Rogov 1992, 1993; Mironov et al. 1993, 1995; pers. commun. by Chuluun O and staff of Uran Company Ltd. of Mongolia and ERDES Mining Enterprise.

Geological Setting of Mineralization

The deposit is situated in the western Dornod Volcanic-Tectonic Structure. Proterozoic amphibolite, schist, and gneiss intruded by gabbro-diorite, diorite, and granite of Paleozoic age constitute the *basement*. Late Jurassic-Early Cretaceous sedimentary and volcanogenic facies of the *Dornod Formation* overly unconformably the basement. The strata form a flat, 5–20° SE-dipping monocline.

The *Dornod Formation* consists of three members derived by successive cycles of volcanism. The *Upper Member* is restricted to the SE part of the deposit and consists of a trachyandesite sheet underlain by terrigenous sediments. The *Middle Member* consists of a 300–800 m thick sequence of felsic volcanic sheets, the thickness of which increases towards SE. Facies are, from top to bottom: fluidal felsic ignimbrite, massive felsic ignimbrite, rhyolitic tuff (vitroclastic felsic ash tuff, felsite tuff), oligophyric rhyolite (including volcanic glass and vitric felsite horizons), and trachydacite. Mudstone, sandstone, and conglomerate beds are intercalated with, and occur at the base of the volcanics. The *Lower Member* is composed of sheets, from top to bottom, of andesite-basalt, trachydacite and quartzfeldspar porphyry interbedded with clastic sediments and tuffs. A basal unit of conglomerate and sandstone fills paleodepressions.

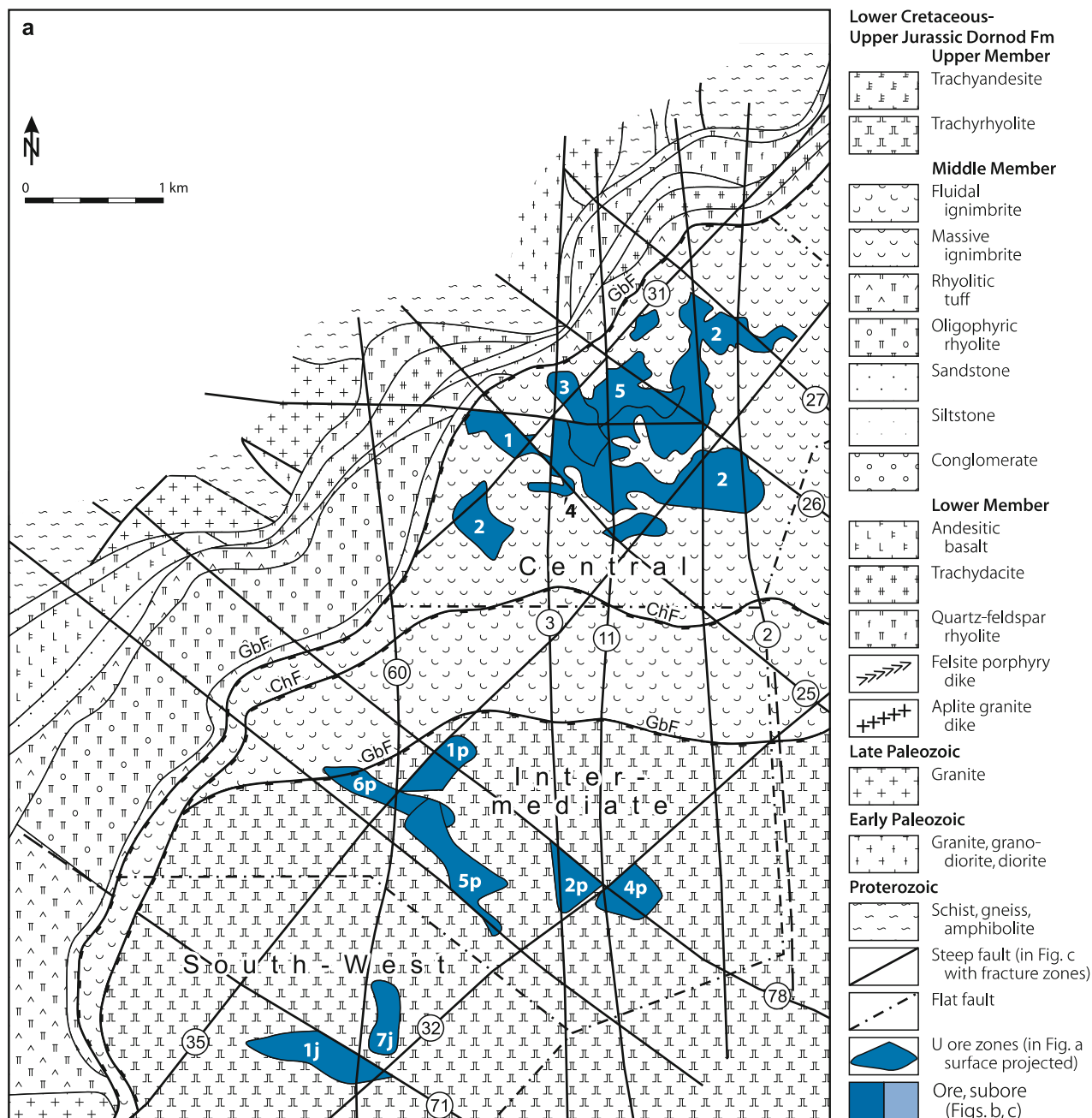
The *structural pattern* is dominated by steeply dipping, NE-SW-, N-S- and NW-SE-oriented fault systems, and large, flat to shallow dipping intraformational fault- and fracture zones. NW-SE-trending fault zones can be up to 300 m wide and several tens of kilometers long. NE-SW-oriented faults are commonly of small extension but are accompanied by highly fractured zones up to 30 m wide.

Flat to shallow, 5–10° SE dipping faults and cataclastic zones occur as peneconcordant structures particularly at the interface of volcanic and sedimentary horizons. Lateral extension and thickness of these zones vary considerably. Largest faults of this kind are the Gurvanbulag, Chayach, and Churtyynbulag faults, which could be traced for several kilometers.

The Gurvanbulag fault zone, up to 80 m thick, dipping 5–15° SE, is the most prominent ore host. This zone is confined to a vitric horizon of the Middle Member that is embedded between a coarse fluidal felsite sheet on top and felsic tuff on bottom. This zone has a complex inner structure of branching, shallow dipping faults associated with subparallel and diagonal fractures,

Fig. 8.6.

Gurvanbulag deposit, **a** simplified geological map showing the location of the Central, Intermediate, and South-West sections and related ore zones/bodies (with numbers); **b** geological plan of ore zones 1 and 2 at level +800 m in the central section, and **c** NW-SE section across ore body 2 (see **b** for location) (after Mironov and Rogov 1993). Major shallow inclined faults: *CbF* Churtinbolag; *ChF* Chayach, *GbF* Gurvanbulag



shears, and joints. Two distinct faults, which coincide with the upper and lower boundaries of the vitric horizon, form the hanging and footwall of the Gurvanbulag fault zone. The Chayach and Churtynbulag faults have a structural pattern similar to that of the Gurvanbulag fault. They also contain ore.

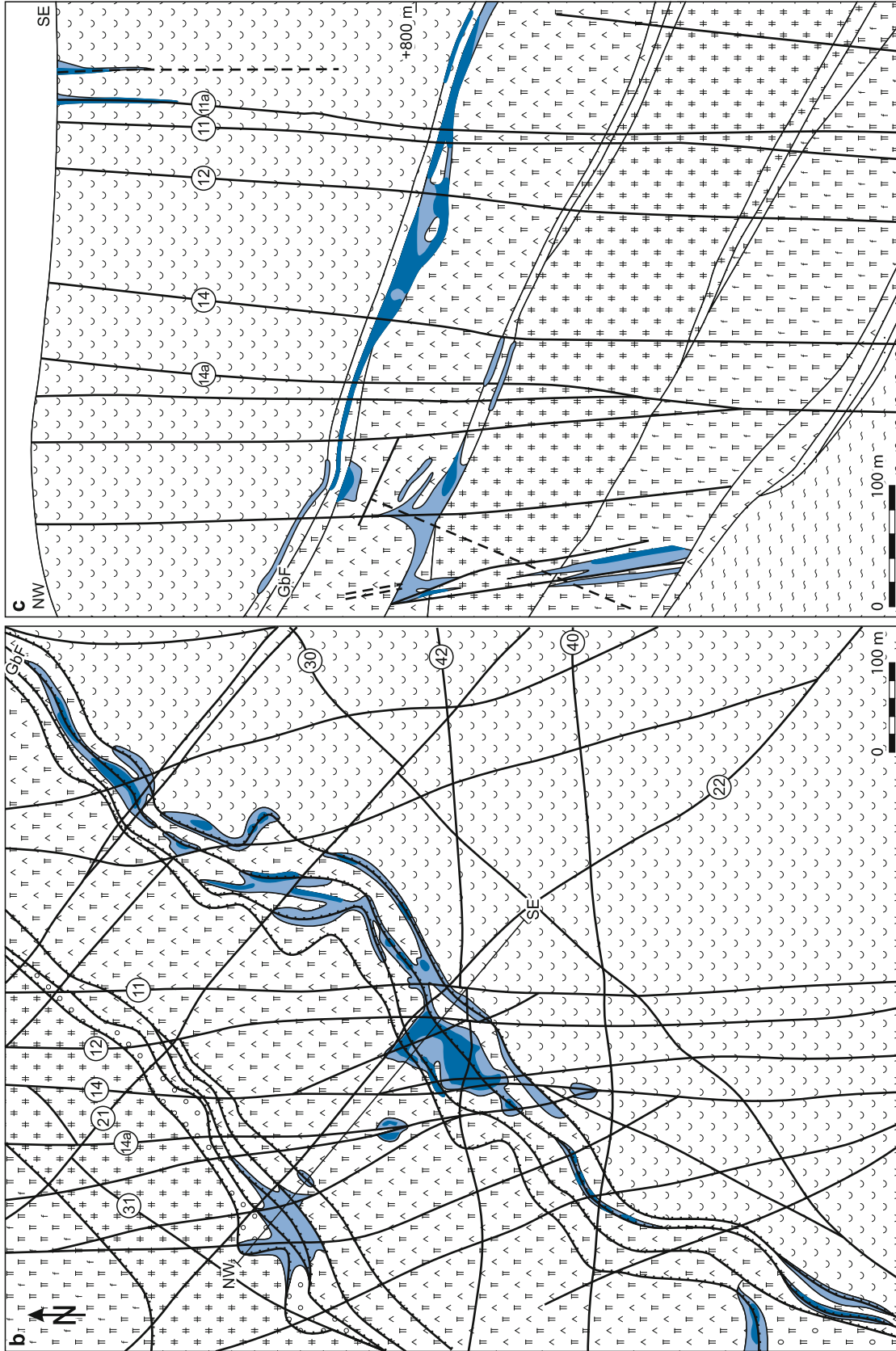
Host Rock Alteration

Regional alteration phenomena include feldspathization and silicification, and ore-related alteration features carbonatization,

hydromicazation, montmorillonitization, kaolinitization, chloritization, and hematitization. Hydromicazation and montmorillonitization are most intense. Hematitization is directly related to mineralized zones and its intensity tends to correlate with the grade of mineralization.

A distinct geochemical halo of U and associated elements such as Pb, As, and Mo surrounds ore bodies. The halo is commonly of elongated shape and largely controlled by faults. The dimensions of halos surpass those of ore bodies by 2–3 times. Uranium forms the most extensive aureole extending in excess of 500 m from ore bodies.

Fig. 8.6. (Continued)



Weathering-related oxidation persists to depths of 250–300 m and up to 400 m along high-angle faults in the central part of the deposit.

Mineralization

Coffinite, pitchblende, and uranophane are the dominant U minerals. Coffinite prevails in most ore bodies except in the central and NE part of ore body 2, where pitchblende and uranophane dominate over coffinite. U⁶⁺ minerals (uranophane, β -uranotile etc.) occur throughout the weathering zone and along high-angle faults in the central part of the deposit where they constitute 30–60% of the U mineralization.

Associated ore minerals include chalcopyrite, galena, marcasite, molybdenite, sphalerite, hematite, and minor arsenopyrite. Gangue or ore accompanying minerals include quartz, biotite, hydromica, montmorillonite, minor ankerite, fluorite, K-feldspar, muscovite, and rare anatase, leucocoxene, sericite, and tourmaline.

U minerals occur mostly as fine- to coarse-grained aggregates, 0.001–2 mm in size. Ore texture is of impregnation nature featuring disseminated, globular, stringer, rarely banded, and earthy varieties. High-grade mineralization with 0.3% U or more exhibits breccia and cement textures.

Uranium mineralization is stratigraphically restricted to the Dornod Formation. In its Middle Member, uranium occurs on six lithologic-structural levels associated with peneconcordant, flat to shallow dipping fault-fracture zones within vitroclastic felsic ash tuff, felsite tuff, volcanic glass, and vitric felsite horizons. Other host rocks are clastic sediments containing detrital vegetal matter; they separate the volcanics of the Middle and Lower Member, and quartz-feldspar porphyry of the Lower Member.

Tabular ore lodes are confined to the large Gurvanbulag, Chayach, and Churtybulag faults. High-angle faults bound these ore bodies and also control the grade distribution of uranium. Veinlike to stockwork mineralization, which is of only subordinate importance, is associated with steeply dipping, NW-SE and, to a minor extent, N-S faults in which ore is restricted to intersections with tuff, felsite, and quartz-feldspar porphyry.

Shape and Dimensions of Deposits/Characteristics of Individual Ore Bodies

The Gurvanbulag deposit covers an area ca. 9 km in NE-SW length and 1.5–4 km in width. Twelve ore zones contained in the Central, Intermediate, and Southwest sectors are delineated. Nine ore zones contain tabular and three contain vein-stockwork ore bodies.

Ore bodies are distributed over a depth interval from 15–40 m to 750 m below surface. Ore bodies consist of lenses or shoots with lateral dimensions ranging from several tens of square meters to 0.5 km². Thickness varies between 0.6 and 10 m and rarely 30 m. Low-grade mineralization or barren ground some tens to a few hundred meters wide in lateral and vertical direction separates individual ore shoots.

Tabular ore bodies can be large and constitute the bulk of the total resources of the deposit. Grades range from 0.06 (cutoff grade) to 0.6% U and average 0.11–0.2% U. Veinlike to stockwork

ore bodies are lower in grade and smaller in tonnage. Ore contains up to 0.6% carbonate and 2% fluorite.

The *Central sector* is 4.3 km long, 1.7–2.7 km wide, covers about 9 km², and accounts for 78% of total deposit resources. It includes three ore zones, # 1, 2, and 4, with tabular ore bodies located at depths from 40 to 500 m along and in the flat to shallow dipping Gurvanbulag fault, and two zones, # 3 and 5, with stockwork ore bodies extending to depths of 750 m controlled by high-angle faults.

60% of the deposit resources are contained in the large # 2 *Ore Zone*. This zone stretches for 3 100 m along NW-SE strike and 500–1 600 m down dip; inclination is 5–10° SE. Grades range from 0.06 (cutoff grade) to more than 0.3% U and average 0.17% U. 17 tabular ore bodies hosted by a tuff horizon are delineated over a vertical interval from 40 to 500 m below surface. Individual ore bodies are 0.8–5.3 m, locally to 13.5 m thick, and 4 000–500 000 m² in size. Grades of ore bodies average from 0.11 to 0.2% U. Low-grade mineralization up to 100 m wide ground intervenes between the ore bodies.

Located 2.5 km south of the Central sector, the *Intermediate sector* contains tabular, flat to shallow dipping ore bodies in four ore zones, and stockwork ore in one zone. Tabular ore zones are from 450 to 1 000 m long, 150–400 m wide down dip, 1–9 m thick, and have grades between 0.1 and 0.7% U. The stockwork ore zone is 1 200 m in NE-SW length, varies between 0.7 and 6.8 m in thickness, and persists from 40 to 120 m down dip at an inclination of 75–85° SE. Grades range from 0.06–0.3% U.

The *Southwest sector* is located 4.5 km SSW of the Central sector. It contains two ore zones with tabular ore bodies at grades from 0.1 to 0.16% U and dimensions similar to those of the Intermediate sector.

8.1.1.3 Mardaingol Deposit

Mardaingol is located some 95 km north of Choibalsan and ca. 5 km NNW of the Dornod deposit (Fig. 8.3). The volcanic-type deposit encompasses two sectors with seven mineralized zones composed of tabular and vein-stockwork ore bodies. Mineralization is monometallic. Ore bodies are of small size, low grade, and situated far apart.

Underground exploration had commenced in the late 1980s but was abandoned in 1992. One shaft, 180 m deep, was sunk and investigations conducted on two levels, 550 m and 700 m a.s.l. Resources amount to about 1 100 t U at 0.12% U.

Sources of information. IAEA 1995, 2007; Mironov 2003; Mironov and Rogov 1992, 1993; Mironov et al. 1993, 1995; pers. commun. by Chuluun O, staff of Uran Company Ltd. of Mongolia, and ERDES Mining Enterprise.

Geological Setting of Mineralization

Mardaingol is situated in the northern part of the Dornod Volcanic-Tectonic Structure. Early Paleozoic biotite granite-gneiss and granodiorite intruded by Late Paleozoic leucocratic biotite granite, aplite and microdiorite dikes constitute the *basement*. Separated by an unconformity, Late Jurassic-Early Cretaceous

sedimentary and volcanogenic facies of the *Dornod Formation* overly the basement. The strata dip 10–20° NE.

The *Dornod Formation* is represented by only the Middle and Lower members (700–800 m thick). The *Middle Member* is 300–450 m thick and consists of sheets of polyfacies felsic volcanic outflows and their tuffs.

The *Lower Member* is composed of a 100–300 m thick unit of sheets of andesite-basalt, trachydacite, and trachyrhyolite interbedded with clastic sediments and tuffs, and a basal unit of conglomerate, up to 200 m thick, in paleodepressions.

Subvolcanic bodies of felsic porphyry and a variety of dikes and sills, the youngest being trachydacite dikes, were intruded into the older rocks. A large felsite body separates the western and eastern mineralized sectors.

The *structural pattern* is dominated by steeply dipping NW-SE-, N-S-, E-W-, and NE-SW-oriented fault systems, and strata-peneconcordant, shallow, 5–30° dipping fracture zones at the contact of beds and within sedimentary and tuffaceous strata.

NW-SE faults dip 65–85° SW and NE. They include the prominent, 15 km long and ca. 1.5 km wide Dagai fault zone, which controls the uranium mineralization. The Dagai fault zone is composed of three main faults, numbered 1, 2, and 3, and branching and intersecting subsidiary faults with associated, up to 70 m wide cataclastic zones. About N-S-oriented major faults dip 60–85°, trend subparallel 200–400 m apart, and can be traced for up to 4 km.

Host Rock Alteration

Ore-related alteration is reflected by hydromica-montmorillonite, kaolinite, chlorite (chamosite), carbonate, quartz, fluorite, and hematite. Extension of the alteration aureole can be as much as double that of the related ore body.

A primary geochemical halo of U and associated elements such as Pb, As, Ag and Mo is developed around ore bodies. The halo is controlled by, and commonly confined to permeable cataclastic lithologies and/or faults, which also host the ore. Dimensions of uranium halos can be twice as much as that of related ore bodies.

Mineralization

Coffinite and pitchblende are the principal U minerals. U⁶⁺ minerals (uranophane, β -uranotile, and curite) occur in oxidized intervals. Associated ore minerals include arsenopyrite, galena, marcasite, pyrite, and rare molybdenite and chalcopyrite. Gangue is mainly composed of quartz, hydromica, and montmorillonite, with minor calcite, fluorite, K-feldspar, plagioclase, and rare anatase, titanomagnetite, and zircon. Ore minerals occur mostly as fine- to coarse-grained aggregates, 0.001–0.5 mm, rarely up to 2 mm in size. Ore exhibits impregnation, stringer, reticulate and, in high-grade sections (>0.3% U), breccia and cement textures.

Uranium mineralization is restricted to the *Dornod Formation* within which it occurs on the eastern and western flank of a large subvolcanic felsite body. Ore distribution is controlled by intersections of the Dagai fault zone with N-S

structures. Although uranium occurs at intersections with all rock facies, felsic porphyry dikes, oligophyric rhyolite lava and related tuffs are the most prominent host rocks.

Shape and Dimensions of Deposits/Characteristics of Individual Ore Bodies

The deposit covers approximately 1 km² in which two mineralized sectors occur, *Sector One* to the east and *Sector Two* to the west. The two sectors are in excess of 750 m apart in E-W direction. They contain seven ore zones composed of discontinuous ore bodies distributed over a vertical interval from 80 to 650 m below surface.

Ore bodies are predominantly of vein-stockwork and minor tabular configuration. Stockwork ore bodies are of unpredictable shape and consist of irregularly distributed veins, pockets, and lenses of ore grade material enveloped in weak mineralization. Subparallel, steeply dipping, about N-S- or NW-SE-oriented faults cutting structures of the Dagei fault zone control the position of the lodes.

Sector One is 700 m long in NW-SE direction, 80–180 wide, and contains 360 t U in two ore zones: “NW” and “SE”, which are about 140 m apart. Mineralization is discontinuously distributed over a depth interval from 80 to 280 m. Individual ore lodes are 0.8–5.3 m thick and have grades ranging from 0.06 to 0.6% U, averaging about 0.1% U. Mineralization is located along hanging and footwalls of felsic porphyry dikes where these are broken up by subparallel, steeply dipping N-S faults.

Sector Two is 800 m long in N-S direction, 140–450 m wide, and contains 740 t U in three ore zones with vein-stockwork and two zones with tabular mineralization. Mineralization is distributed over a depth interval from 80 m to 230 m bounded atop by flat-laying faults. High-angle N-S and NW-SE, and flat-laying faults control the ore lodes.

Stockwork ore bodies are up to 100 m long and 25 m thick, and have grades of up to 0.4% U. Lenticular mineralization is bound to flat-laying faults that peneconcordantly transect tuff beds within a tuff-sandstone horizon in the upper part of the stratigraphic sequence and at the bottom of basal clastic sediments. Ore lenses are 0.3–2.1 m in thickness and grade 0.06–0.3% U.

8.1.1.4 Nemer Deposit

Nemer is located some 100 km north of Choibalsan and ca. 10 km NNW of the *Dornod* deposit (Fig. 8.3). The deposit consists of three ore zones with tabular and minor stockwork ore bodies. Mineralization is of monometallic and polymetallic (U, Mo) volcanic type. Resources (EAR-1) amount to some 2 500 t U at 0.15% U and almost 500 t Mo. Potential resources are estimated at 1 500 t U. Polymetallic U-Mo mineralization constitutes some 20% of the total resources.

Sources of information. IAEA 1995, 2007; Mironov 2003; Mironov and Rogov 1992, 1993; Mironov et al. 1993, 1995; pers. commun. by Chuluun O and staff of Uran Company Ltd. of Mongolia, and ERDES Mining Enterprise.

Geological Setting of Mineralization

The Nemer deposit is in the northern part of the Dornod Volcanic-Tectonic Structure. Proterozoic metasediments intruded by Early Paleozoic granite and granodiorite of the Motochudag Complex, and Late Paleozoic K- and Na-metasomatized biotite leucogranite constitute the *basement*. The latter granite is the dominant facies in the deposit area. An uplifted basement block forms the NE flank of Ore Zone 3 and the NW part of Ore Zone 2.

Separated by an unconformity with distinct relief, an up to 800 m thick sequence of Late Jurassic-Early Cretaceous sedimentary and volcanogenic facies of the Middle and Lower members of the *Dornod Formation* overly the basement. The strata dip 10–20° NE. This sequence is reduced to a thickness of some 200 m in the NW part of the deposit. Numerous subvolcanic stocks, dikes, and sills of felsic porphyry were intruded into these older rocks.

The *Middle Dornod Member* is 150–320 m thick and consists of polyfacies felsic volcanic outflows and tuffs with intercalated clastic sediments. The *Lower Member*, 300–500 m thick, is composed, from top to bottom, of

- a unit, 5–10 m and in paleo-depressions up to 60 m thick, of interbedded and interfingering clastic sediments (sandstone, argillaceous sandstone, gravel, conglomerate) with abundant vegetal matter, and tuffaceous horizons
- a unit, 60–160 m thick, of andesite-dacite and rhyolite-dacite lava-breccia and related tuffs
- a volcanic sheet, 100–150 m thick, of andesite-basalt and
- a basal sedimentary unit, up to 90 m thick, composed of coarse fragmental conglomerate-breccia, conglomerate, and sandstone, which is particularly prominent in a NW-SE-trending graben structure

The structural pattern is dominated by steeply dipping, about NW-SE-, N-S-, and E-W-oriented fault systems, and strata peneconcordant, shallow, 5–30° dipping fault-fracture zones.

Most prominent is the Dagai fault zone. It trends NW-SE for 15 km, is 500 m wide, and consists of several major faults (# 8, 10, 10a, and 11), which dip 70–85° NE to SW, and numerous branching and intersecting subsidiary structures and associated cataclastic zones. Fault # 10 with displacements of up to 150 m is one of the main ore controlling structures. A 160–300 m wide cataclastic zone accompanies this complex fault.

Flat to shallow dipping faults occur intraformational and along the contact of beds of different physico-mechanical properties. They constitute important uranium hosts.

Host Rock Alteration

Ore-related alteration products include hydromica-montmorillonite, kaolinite, chlorite (chamosite), carbonate, and quartz. Extension of the alteration aureole is as much as double as that of related ore bodies.

A *primary geochemical halo* of U and associated elements (Pb, As, Mo), controlled by structural elements, surrounds ore bodies. A *secondary dispersion aureole* also exists and is

displaced from the primary halo. The uranium aureole is most extensive extending along strike of permeable zones in excess of 500 m from ore bodies. The halo of associated Pb, As, and Mo is smaller; their tenor is highest near high-grade uranium ore. Uranium and other elements correlate positively in the vicinity of ore bodies.

Alteration by weathering is very limited, essentially restricted to major faults along which it may locally extend to depths of 300 m.

Mineralization

Principal U minerals are coffinite and pitchblende. U⁶⁺ minerals (uranophane, β -uranotile, rare woelsendorfite, kasolite, amorphous U-hydroxides) occur in oxidized zones. Associated ore minerals include galena, molybdenite, pyrite, and rare arsenopyrite and chalcopyrite. Gangue or ore accompanying minerals are biotite, hydromica, montmorillonite, and quartz, with minor ankerite, siderite, baryte, fluorite, K-feldspar, muscovite, and rare anatase, sericite, and tourmaline.

Ore minerals occur mostly as fine- to coarse-grained aggregates, 0.001–0.5 mm, rarely up to 2 mm in size and show colloform, granular, grating, or spherulitic textures. Ore is of the impregnation type showing dispersion, maculose, globular, stringer, and rarely banded or earthy features. Rich ore (>0.3% U) has breccia textures.

Mineralization is found in almost all rock facies including basement rocks where minor, mostly low-grade mineralization occurs. Ore bodies are restricted, however, to the Lower and the Middle Member of the Dornod Formation in which they occur in carbonaceous, coarse clastic sediments at the base of the Dornod Formation, and in intraformational, carbonaceous sedimentary and tuffaceous horizons and cataclastic coarse-grained felsic tuff affected by peneconcordant, flat to shallow dipping faults.

Two varieties of host rock settings and uranium mineral assemblages are noticed: Pitchblende-coffinite-molybdenite in carbonaceous sediments; and pitchblende-coffinite in effusive and pyroclastic volcanics.

Shape and Dimensions of Deposits/Characteristics of Individual Ore Bodies

The Nemer deposit contains three ore zones with tabular and some stockwork ore bodies in a 2 500 m long and 500 m wide area, and at depths from 120 to 320 m. U-Mo mineralization with 0.15% U and 0.13% Mo on average constitutes some 20% of the total resources. This ore prevails at lower levels. Dimensions and characteristics of ore zones and ore bodies are as follows:

Ore Zone I contains two tabular, polymetallic (U, Mo) ore bodies in fractured, interbedded carbonaceous sandstone, mudstone, conglomerate, and tuffaceous sediments, which form the transition from the Lower to the Middle Member of the Dornod Formation. Ore lenses are positioned along margins of strata, which are intensely broken by flat-laying fracture zones and

intersecting, steeply dipping, subparallel NW-SE-oriented faults. Ore lenses are 0.3–3.5 m thick, subhorizontal, elongated, and superjacent stacked, 5–15 m apart. They consist of irregular mineralization with grades ranging from 0.07 to 0.9% U. Flat-laying faults constitute the hanging wall and undisturbed sediments the footwall boundaries of the ore lenses.

Ore Zone II consists of two tabular, monometallic ore bodies in highly fractured tuff of the Upper Dornod Member at depths from 130 to 230 m. Ore is restricted to intersections of a flat-laying fault with high-angle, NW-SE-oriented faults. Sub-ore grade mineralization occurs as small lenses and joint-fracture filling at contacts of various lithologies.

Ore Zone III is located adjacent to the NW of Ore Zone II and contains several tabular to stockwork U-Mo ore lodes immediately above the basement at depths of 200–300 m. Ore lodes are hosted in cataclastic sandstone, conglomerate, and coarse fragmental conglomerate-breccia that form the basal sedimentary unit in a NW-SE graben structure. Main ore-bearing structures within the basal conglomerate-breccia beds are intraformational, strata-peneconcordant, flat to shallow dipping faults and fracture zones located near a high-angle fault. Richest mineralization is in the SE part of Zone III where it occurs in the form of flattened stockworks composed of small, subhorizontal lenses interconnected by steeply dipping mineralized fissures. To the northwest, the shape becomes more and more tabular and mineralization gradually fades out.

Several small vein-like ore bodies, as much as 4 m thick, containing 0.08% U and up to 0.05% Mo were drill intercepted in leucocratic granite of the basement at a depth of 280 m.

8.1.1.5 Additional U Occurrences in the Mardai/Dornod District

In addition to the above-mentioned deposits, several uranium occurrences were identified in the Mardai/Dornod District, some of which are associated with Pb-Zn or fluorite deposits. U resources are commonly several hundred tonnes U at grades between 0.01 and 0.15% U.

The *Davaan*, *Dorozhnoye*, *Muhar*, and *Ulaan* occurrences exist in a geological setting similar to the Gurvanbulag deposit. Their position is controlled by the shallow to flat dipping Gurvanbulag fault. *Davaan* consists of eight ribbon-like uraniumiferous lenses with resources estimated at 500 t U, and a grade of 0.01% U. *Dorozhnoye* contains 420 t U at 0.14% U in a tabular ore body. *Muhar* is situated close to the Muhar Pb-Zn deposit. Small veins and lenses occur in the Gurvanbulag fault at the base of a rhyolite horizon. *Ulaan* coincides spatially with the same named Pb-Zn deposit. Resources amount to 270 t U at 0.11% U. Some 90% of these resources are monometallic and the rest polymetallic (U with Pb-Zn).

The *Ilreh* and *Tsever* occurrences are located in the Mardaingol block. Both the geological setting and mineralization are similar to Mardaingol. *Ilreh* has almost 300 t U at a grade of 0.13% U in a tabular ore body.

Tsagaan-nuur is located 1.5 km E of and occurs in a similar geological setting as the Dornod deposit. Tabular and vein mineralization occurs at depths from 200 to 650 m in zones altered by hematitization, silicification, fluoritization, and pyritization.

8.1.2 Other Uranium Occurrences/Areas in the North Choibalsan Region

Besides the Dornod Volcanic-Tectonic Structure, the North Choibalsan region encompasses the Ugtam, Turgen, and Engershand volcanic-tectonic complexes with uranium occurrences as well as gold, fluorite, tungsten (scheelite), polymetallic (Pb-Zn-Ag), and graphite deposits.

Sources of information. Mironov and Rogov 1992, 1993; Mironov et al. 1993, 1995; pers. commun. by Chuluun O and staff of Uran Company Ltd. of Mongolia, and ERDES Mining Enterprise.

8.1.2.1 Ugtam Area

Ugtam is situated about 50 km NW of the Mardai District. The area coincides with the Ugtam Volcano-Tectonic Structure, a volcano-sedimentary complex similar to the Dornod Volcano-Tectonic Structure. One U occurrence, *Ugtam*, has been investigated. It consists of 0.7–6.5 m wide veins contained in two zones within a 3 km long and 350–800 m wide area. Resources are estimated at 4 200 t U at a grade of 0.02% U. In addition, several deposits of gold (*Ugtam*, *Doos*), fluorite (*Zharaahai*, *Ugtam*), scheelite (*Tenger*), and polymetals/Pb-Zn-Ag (*Bolotinskii*, *Nairin*) occur in the structure.

8.1.2.2 Turgen Area

Turgen is situated about 80 km NW of the Mardai District at the northwestern extremity of the North Choibalsan region. The area coincides with the Turgen Volcano-Tectonic Structure, a 750 km² large volcano-sedimentary complex similar to the Ugtam and Dornod structures but of smaller size. Resources of the Turgen area are estimated at 5 000 t U, at a grade on the order of 0.05% U. In addition, this area has gold (*Hooloi*, *Tsagaan-Chuluut*) and fluorite (*Khalchin*, *Bat*, *Zhargalant*) deposits.

Two U occurrences, *Tsagaan-Chuluut* and *Baruun-Hooloi*, have been explored.

Tsagaan-Chuluut is hosted in the Upper Member (basalt-andesite, tuff, tuffaceous sandstone, and conglomerate) of the Dornod Formation. Mineralization occurs in three configurations, two are structure-bound and one is strata-bound. A 900 m long zone along a N-S fault contains gently dipping lenticular ore bodies within strata-internal cataclastic segments, and a series of contiguous, steeply dipping, 1–6 m wide veins with grades of 0.06–0.08% U. Strata-bound mineralization with

grades of 0.02–0.04% U bound in collophane, occurs in ten phosphatic silt- and mudstone layers, 0.2–10 m thick and up to a few hundred meters long.

Baruun-Hooloi is positioned in the Middle Member (felsite, rhyolite, rhyolitic tuff) of the Dornod Formation. Mineralization consists of uranophane and autunite contained in structurally controlled lenticular bodies along an about E-W-trending fault. The host rock is strongly fractured extrusive felsite porphyry. Ore sections are enveloped in an aureole of intense hydromineralization and fluoritization. Grades average 0.05% U.

8.1.2.3 Engershand Area

This area covers the Engershand Volcanic-Tectonic Structure in the SE part of the North Choibalsan region, some 100 km NE of Choibalsan (Fig. 8.1). A few uranium showings are recorded as well as some polymetallic deposits like the Pb-Zn-Ag deposit Tsav (15–16% Pb + Zn, 200–500 ppm Ag, 2 ppm Au; at depths from surface to more than 270 m).

8.2 Berkh Region, Khentei Aimag

The Berkh region is located some 400 km ENE of Ulaan Baatar in the NE part of Khentei aimag (Fig. 8.1). Four volcanic F-Mo-U type occurrences are reported from the *Batnorov* and *Ulziit-Saikhanuul* volcanic structures, in addition to a vein-type uranium occurrence (*Mizer*) in leucogranite of the basement. This region also includes five fluorite deposits (*Berkh*, *Kovalev*, *Chemindyn*, *Delger-Haan*, *Khavtgai*).

Sources of information. Mironov and Rogov 1992; pers. commun. by staff of Uran Company Ltd. of Mongolia.

Regional Geological Setting of Mineralization

The Berkh region is in the central part of the North Kerulen tectonic zone and within the intracontinental Mongol-Priargun Volcanic Belt. Metamorphic rocks are of Upper Proterozoic to Early Cambrian (schist, marble, amphibolite preserved as xenoliths in granite) and Permian age (Ulziin Formation: slate, quartz-sericite schist).

Depressions are filled with continental sediments and volcanogenic rocks of the Early Cretaceous Zuunbayan Formation. The formation consists, from top to bottom, of an Upper Series composed of sand- and mudstone, a Middle Series of andesite, and a Lower Series of conglomerate, sandstone, carbonaceous mudstone/siltstone, basalt, and trachyte.

Granitoid rocks were intruded during three periods: granite, granodiorite and diorite during Early Paleozoic, leucogranite and granodiorite during Middle Paleozoic, and leucocratic biotite granite, alkaline granite porphyry and granosyenitic porphyry during Middle and Late Jurassic. The latter facies form the Erdenedavaa Intrusive Complex.

Felsic volcanism occurred during Middle and Late Jurassic. It was followed by Late Jurassic to Early Cretaceous mafic volcanism.

Principal Characteristics of Mineralization

Uranium mineralization is of volcanic type, attributed in Russian literature to the U-Mo-F paragenesis. Ore settings are controlled by faults or cataclastic continental sedimentary or volcanic rocks. All uranium occurrences show an affinity to rhyolitic facies.

8.2.1 Batnorov Area

This area lies in the southwestern part of the Berkh region. Two larger volcanic-type uranium occurrences hosted by mafic to intermediate volcanics interbedded with continental sediments are established: *Ikh-bulag* and *Tanai*.

Ikh-bulag occurs in a depression filled with sandstone, conglomerate, quartz dacite tuff, andesite, quartz porphyry, and felsic lava. Felsic volcanics form two small necks. One of these necks contains uranium (uranophane, autunite, and metatorbernite) associated with Cu, Mo, Pb, and Zn in the form of low-grade mineralization that envelopes two parallel, 170 m long and 0.5–5 m thick lenses composed of stockwork and tabular mineralization with grades of 0.06 and 0.16% U, respectively. The tenor of Cu, Mo, Pb, and Zn is several hundredths of a percent, and that of As and F is several tenths of a percent. U resources are estimated at 2 000–3 000 t.

Tanai is hosted by an arkosic grus horizon that is covered by an andesite-basalt sheet of the Lower Series of the Zuunbayan Formation. Host rocks are enriched in carbonaceous detritus, kaolinite, hydromica, and fluorite. Autunite and black products (sooty pitchblende) are the principal U minerals. Associated elements include Ag, As, Ge, Mo, Pb, and Zn. Mineralization is of tabular shape and was traced over a length of 230 m. Ore bodies are about 2 m thick and grade 0.05–0.08% U.

8.2.2 Ulziit-Saikhan-Uul Area

This area corresponds to the Ulziit-Saikhan-Uul Volcano-Tectonic Complex in the NE Berkh region. This complex is a semi-ring structure, 2.4 km² in size, composed primarily of felsic effusives and subvolcanic stocks. Early to Middle Paleozoic granites form the basement. A volcanic-type uranium occurrence, *Tumen-Haan*, has been investigated. The geological setting of this occurrence is similar to deposits in the Dornod District. Mineralization is hosted by a quartz-feldspar porphyry sheet 250–600 m thick in which it is controlled by the intersection of E-W fracture zones with a NW-SE-trending fault zone. U minerals (coffinite, uranophane, and uranospinite) occur in irregular distribution in up to 2 m thick veins and lenses. Associated elements include As, Cu, Pb, and Zn. Grades range from few hundredths to 0.4% U.

8.3 Dornogovi (Eastern Gobi) Region

A number of uranium occurrences of sandstone, volcanic, lignite, phosphorite, vein?, and surficial? type are recorded from the Dornogovi region in SE Mongolia. They are grouped in several areas (► Fig. 8.1). One sandstone-type deposit is delineated, Kharaat in the Cretaceous Choir Basin.

Sources of information. IAEA 1995, 2007; Mironov 2003; Mironov and Rogov 1993; Mironov et al. 1995; pers. commun. by staff of Uran Company Ltd. of Mongolia.

Regional Geology of the Dornogovi Region

The Dornogovi region is within the Caledonian Central Mongolian fold belt and covers in part the western section of the Late Jurassic-Early Cretaceous Mongol-Argun volcanogenic metallogenic belt, which is part of the Mongol-Transbaykal metallogenic province. Precambrian and Paleozoic metasediments, Precambrian to Mesozoic granites, and Paleozoic to Mesozoic volcanic complexes of mafic to felsic composition constitute the basement. Regional faulting generated a basin and range geomorphology. Archlike uplifts of Precambrian to Late Mesozoic lithologies are separated by downfaulted, intermontane basins filled with Early Cretaceous terrestrial sediments with intercalated lignite seams. Alluvial sediments of Late Cretaceous-Paleogene age cover the older basin infill. Prominent faults and lineaments trend E-W, NW-SE, and NE-SW.

Basement rocks below Cretaceous basins and exposed in uplifts include

- *Early Cretaceous to Late Jurassic* continental rhyolite to trachybasalt
- *Late to Middle Jurassic* leucocratic, K-feldspar granite in the southwest and northeast part of the region
- *Triassic-Permian* felsic volcanics and subalkaline alaskite (with REE and polymetals enrichments e.g. in Bor-Undur Complex) prevailing in the NW and central part of the region
- *Permian-Carboniferous* biotite granite
- *Carboniferous* andesite-dacite
- *Early Paleozoic* gabbro-diorite-granite plutons present as cores in dome structures in the central part of the region
- *Early Cambrian* metasediments
- *Precambrian* gneiss, granite-gneiss, schist, amphibolite, quartzite, and marble, prominent in the SW part of the region

Regional Characteristics of Mineralization

A variety of mineralization is noticed in the Dornogovi region including

- *volcanic-type* F-Mo-U-bearing veins, stockworks, and tabular ore bodies controlled by hydrothermally altered fault-fracture zones within volcano-tectonic complexes. Two mineral assemblages are reported: pitchblende-coffinite-sulfide-quartz (examples: *Bor-Undur*, *Hongor*, *Zurkhin* occurrences), and

fluorite-pitchblende-coffinite-quartz-fluorine-apatite (examples: *Khara-Tolgoi*, *Ikh-Khet*, *Ulaan-Nuur-2* occurrences)

- *sandstone- and lignite-type* U-rare metals-REE mineralization in non or weakly lithified Late Mesozoic and Cenozoic sediments in intermontane basins. Two parageneses are distinguished: U-rare metals-minor REE associated with near-surface oxidation zones (example: *Kharaat* deposit and a number of occurrences), and rare metals-REE-minor U related to diagenetically altered zones (example: *Jargalant-Nuur* occurrence)

Other mineralization includes volcanic-related epithermal fluorite deposits. Differentiated granites and alkaline complexes contain Mo, Sn, W, and REE mineralization. Iron ore is present in metasediments, contact-metasomatic skarn, and veins.

8.3.1 Choir Cretaceous Basin, Dornogovi (East Gobi) Aimag

Located some 250 km SSE of Ulaan Bataar in central-southeastern Mongolia, the Choir Basin is a submeridional, 150 km long and 10–25 km wide, curvilinear depression (► Fig. 8.7). Uranium showings are found in a 110 km long and 2–8 km wide stretch. One sandstone U deposit, *Kharaat*, was delineated along with a number of sandstone- and lignite-type uranium occurrences.

Total uranium resources in the Choir Basin are estimated at 90 000 t U, some 10 000 t U (EAR-1) of which are estimated for the *Kharaat* deposit while the rest are speculative resources (references see above).

Regional Geological Setting of Mineralization

A sequence of continental, weakly to non-lithified sediments of Paleogene and Cretaceous age, up to 1 500 m thick, fill the Choir Basin. The sediments are subhorizontally bedded with a monoclinical dip increase to 10° at the flanks of the basin. Basin lithologies include, from top to bottom

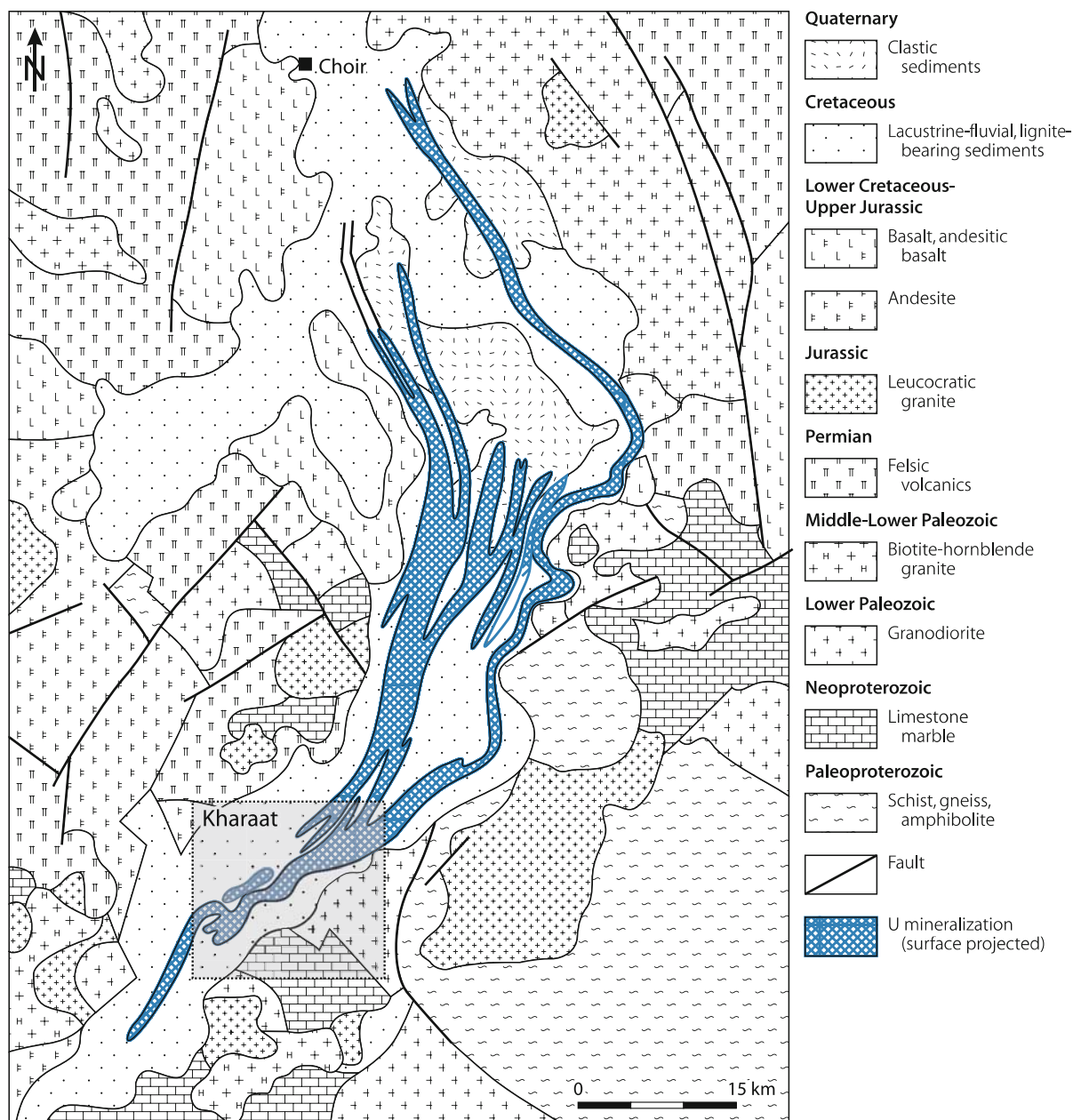
- *Quaternary*: Clastic sediments (only locally developed)
- *Upper Cretaceous* Sainshand Formation: Alternating, discontinuous beds of weakly cemented, variegated (red, green etc.) alluvial sand, gravel, and conglomerate
- >Unconformity<
- *Lower Cretaceous* Zuunbayan Formation: Fluvial, lacustrine, and paludal sediments composed of grey, unconsolidated, carbonaceous, and sulfidic clays, argillaceous, partly limy sands, silts, and sands, which contain abundant vegetal matter and iron sulfides and are intercalated with lignite seams

Basement

- *Lower Cretaceous-Upper Jurassic* mafic volcanics (basalt, andesite)
- *Jurassic* leucocratic granite
- *Permian* felsic volcanics (rhyolite)
- *Middle-Lower Paleozoic* biotite-hornblende granite
- *Lower Paleozoic* granodiorite and pegmatite

Fig. 8.7.

Choir Basin, schematic map of the geological setting of the intracratonic basin with distribution of U mineralization and location of the Kharaat deposit (after Mironov and Rogov 1993)



- Neoproterozoic marble
- Paleoproterozoic metamorphics (schist, gneiss, amphibolite)

Faults exposed in the basement trend about NE-SW, NW-SE, and E-W. Major structures include the Khar Airag-Choir fault system, which tends to control the position of paleovalleys in the Choir Basin.

Principal Host Rock Alteration

Common host rock alteration apparently includes weathering-related surface-bound oxidation as reflected by limonitization,

which persists to depths of 30 m, and, at depth, kaolinitization, hydromicazation, carbonatization, silicification, and sulfidization. Sulfides are restricted to zones containing organic carbon.

Principal Characteristics of Mineralization

Two principal types of U mineralization are reported, sandstone- and lignite-hosted uranium. Sandstone-type mineralization occurs in two settings: (a) along the footwall boundary of the surface-related oxidation interval and (b) at depth in grey,

reduced sediments in the vicinity of oxidized zones. Preferential host environments are carbonaceous and sulfide-bearing sand lenses and their contacts with argillaceous intercalations in paleochannels.

U oxide phases (pitchblende, black products) are the principal U minerals in reduced environments while U^{6+} minerals (mainly autunite) are prevalent in oxidized environments. Associated minerals/elements include Fe- and Mo-sulfides and a variety of rare and rare earth elements (details see Kharaat deposit).

General Shape and Dimensions of Deposits

Uranium mineralization is ubiquitous in the Choir Basin as indicated by the numerous occurrences and showings. Most of the occurrences have low grades, however, on the order of 100–300 ppm U while better grade bodies with grades in excess of 0.05% U tend to be limited in size and tonnage, at least as far as established to date.

Mineralized bodies exhibit pod and lenticular configurations and are arranged peneconcordant to strata. They occur individually or superjacent stacked. Common dimensions are on the order of up to a few hundred meters long, up to a few tens of meters wide and from less than a half to a few meters thick.

Principal Aspects of Metallogenesis

Two genetic modes of U concentration are noticed:

- *Diagenetic* U concentration is reflected by low-grade (few hundred ppm U) lenses and bands, up to a few meters thick along the contact of grey sands and mottled clastic sediments, or at the contact of grey clays with organic matter and lacustrine sands. This mode is known from several occurrences but is only of potential interest.
- *Epigenetic* U concentration is controlled by surface-bound oxidation zones in the Cretaceous sands. The Kharaat deposit and most occurrences belong to this mode. Isotope dating yields a time range from 20 to 30 Ma (Neogene) for this mode of mineralization in the Kharaat deposit.

Felsic volcanics and intrusives of the basement such as sub-alkaline alaskite of the Bor-Undur Complex are considered the source of uranium and associated elements. Fixing of uranium occurred by reducing substances such as carbonaceous matter and sulfides particularly along surface-bound oxidation boundaries and intraformational redox interfaces, and by adsorption on organic and inorganic material (plant remains, clay particles, Fe-oxides etc.).

8.3.1.1 Kharaat Deposit

The Kharaat deposit was discovered in 1988 in Dornogovi aimag, some 250 km SSE of Ulaan Bataar and about 70 km SSW of the railroad settlement Choir also referred to as Sumber. The deposit contains polymetallic sandstone-type uranium mineralization.

Resources amount to some 10 000 t U (RAR + EAR-I) at a grade of 0.03% U including almost 4 000 t U grading in excess of 0.07% U (status 1995). (Note: The calculation is based on a cutoff grade of 0.01% U, a minimum thickness of 0.5 m, and a maximum thickness of 2 m for barren rock.)

Sources of information. IAEA 1995, 2007; Mironov 2003; Mironov and Rogov 1993; Mironov et al. 1995; pers. commun. by staff of Uran Company Ltd. of Mongolia.

Geological Setting of Mineralization

Mineralization occurs along the southeastern flank of the Choir Basin in upper horizons of the Early Cretaceous Zuunbayan Formation (► Fig. 8.8). These horizons consist of alternating, discontinuous, 0.2–20 m thick lenses and beds of grey carbonaceous sandy gravel, sand, silt, argillaceous sand and silt, and mud that fill a paleovalley. Sands with high contents of vegetal remains and sulfides (pyrite, marcasite) provide the most favorable host rocks.

Host Rock Alteration

Host rock alteration is twofold. Weathering-related oxidation reflected by limonitization penetrates from surface to depths from 1 to 30 m. It is overprinted at depth by kaolinitization, hydromicazation, carbonatization, silicification, and sulfidization (mainly pyrite). Sulfide distribution is restricted to zones containing organic carbon.

Mineralization

U-oxide phases (pitchblende, black products) occur disseminated and as dispersed globular aggregates associated with carbonaceous matter in reduced environments. Autunite, torbernite, schroëckerite, and earthy aggregates of bergerite and phosphuranylite are typical for oxidized zones in which they fill cracks and occur as matrix constituent in sand.

Associated minerals/elements include marcasite, pyrite, colloidal MoS_2 , rare galena, and REE and rare metals (Ce, Ge, La, Re, Sc, Yb, Y). Tenors of molybdenum and selenium are up to 0.15% and 0.05%, respectively.

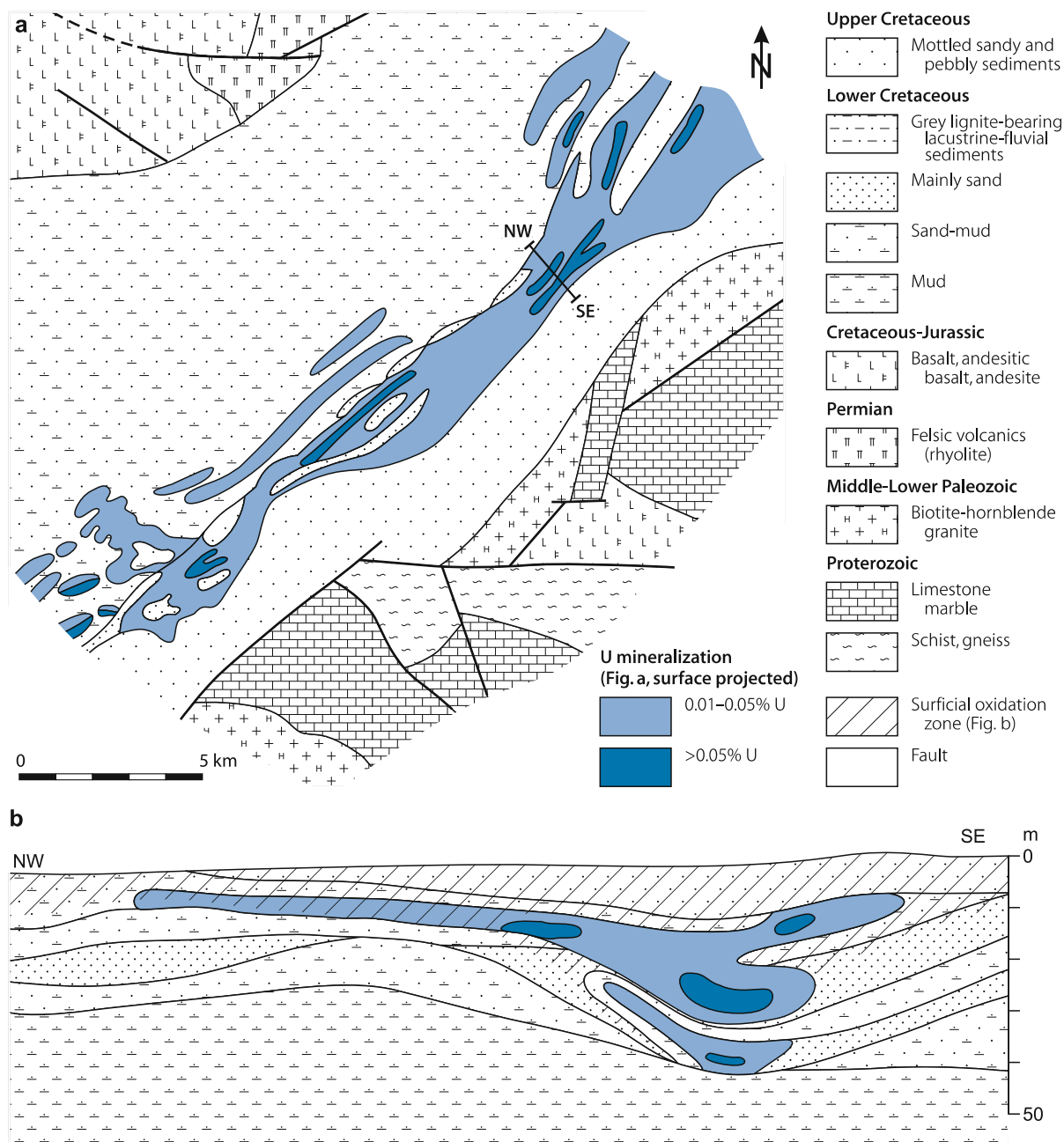
Mineralization occurs along the footwall boundary of the surface-related oxidation interval and further below in grey, reduced sediments in the vicinity of oxidized zones. Preferential host environments are paleochannels in which carbonaceous and sulfide-bearing sand lenses and the contacts of these sands with argillaceous intercalations are favored sites for uranium concentrations.

Shape and Dimensions of Deposits/Characteristics of Individual Ore Bodies

Mineralization of the Kharaat deposit is spread in the form of a ribbon some 20 km in NE-SW length and 0.5–2.5 km in width.

Fig. 8.8.

Choir Basin, Kharaat deposit, **a** schematic geological map and **b** NW-SE section illustrating the distribution of U mineralization in grey, lignite-bearing lacustrine-fluvial sediments and concentration of better grade mineralization associated with channels (after Mironov et al. 1995)



Mineralized material (0.02% U or more) is distributed in peneconcordant lenses and pods, which occur individually or stacked superjacently.

Five principal lens-shaped ore bodies are delineated. They have dimensions of 300–600 m long, 50–60 m wide, and 0.5–17 m thick. Ore bodies are enveloped in subhorizontal, irregularly shaped, ribbon-like zones of low-grade mineralization, which follow paleovalleys. These low grade zones are 400–2 500 m long, 50–300 m wide and 1–33 m thick, and occur at depths from 0.5 to 45 m. Ore grades range from 0.02 to 0.07% U or

more in small lenses and pods positioned in the bottoms of paleovalleys, but grades of as much as 5% U may be encountered locally.

The mode and distribution of ore bodies differs in the northern and southern portion of the Kharaat deposit.

Northern Part: Lenticular and ribbon-shaped ore bodies (<15 m in thickness, <0.1% U or more) occur predominately within the surface-bound oxidation zone hosted by sand and clay enriched in organic material. Dispersed U oxides represent

primary U mineralization whereas oxidation zones contain disseminated autunite, bergerite, and phosphuranylite. Two varieties of uranium-bearing clays are distinguished: (a) grey or light tan, 10–50 cm thick silty clay beds with autunite in fissures and U oxides in clay substrate; and (b) black, unoxidized uraniferous clay with high concentrations of organic material (<8%) and uranium (>0.1% U) in the form of U oxides.

Southern Part: Mineralization occurs on two levels. Tabular ore bodies on the upper level are 0.5–6 m thick and grade 0.02–0.05% U; they are hosted in oxidized clay and sand rich in organic matter. Neogene yellow gravel beds rest upon the mineralized unit. Ore lenses of the lower level are 2–12 m thick and grade 0.1% U or more. These lenses are positioned at the lower boundary of the surface-bound oxidation zone. Mineralization consists of dispersed pitchblende. High U concentrations associate with carbon detritus. Radioactive disequilibrium decreases from the upper levels to the lower levels, which is thought to reflect oxidative solution and redistribution of primary U mineralization.

Ore Control and Recognition Criteria

Ore bodies of the Kharaat deposit are predominantly lens-shaped and composed of polymetallic, low-grade mineralization controlled by lithology and redox interfaces as reflected by the following criteria:

Host environment

- Intermontane basin
- Paleovalleys
- Essentially unconsolidated, carbonaceous and sulfidic sand lenses and argillaceous beds

Alteration

- Weathering-related near-surface oxidation
- Oxidation zones at depth overprinted by reducing processes as reflected by sulfidization

Mineralization

- Polymetallic U-REE-rare metals assemblage
- Control of U, Mo, Se, Re by redox interfaces and of Sc, Y, REE by neutralization zones
- Ore minerals occur disseminated within ore lenses and pods
- Ore is concentrated at interfaces of sand lenses/beds with argillaceous intercalations, and
- At and below the footwall boundary of a surface-related oxidation zone

8.4 Gobi-Tamtsag Region, Dornogovi-Omnogovi-Suhbaatar-Dornod Aimags

The Gobi-Tamtsag region stretches as an ESE-WSW-oriented belt 100–400 km wide and 2 000 km long from the Tamtsag area in the east to the Gobi Altai mountains in the south of Mongolia.

The region covers part of the Caledonian South Mongolian and southerly adjacent South Gobian fold belts and accounts for a number of sandstone-, vein-, and volcanic-type uranium occurrences (Fig. 8.1) including the sandstone-type Nars deposit in the Sainshand Basin.

8.4.1 Sainshand Cretaceous Basin, Dornogovi (East Gobi) Aimag

This basin is some 500 km SSE of Ulaan Bataar in SE Mongolia. The railroad town Sainshand is in the center of the basin (Fig. 8.1). Systematic exploration for uranium begun in 1977 and resulted in the discovery of a number of sandstone- and lignite-type uranium occurrences including the sandstone-type Nars deposit and several noteworthy occurrences, such as *Durbulja*, *Nars 2*, and *Yant*.

Sources of information. IAEA 1993; Mironov 2003; Mironov and Rogov 1993; pers. commun. by staff of Uran Company Ltd. of Mongolia.

Regional Geological Setting of Mineralization

A basement of Proterozoic to Jurassic sediments and igneous rocks, predominantly granites, underlies the Sainshand region. The Caledonian Orogeny affected the older rocks. Basins were downfaulted during Cretaceous time. They are filled with Early to Late Cretaceous continental alluvial, fluvial, lacustrine, and limnic sediments, which are covered by Paleogene to Quaternary alluvium. Oil and gas deposits occur in the Sainshand Basin. Lithologies include, from top to bottom:

Basin fill (up to 1 500 m thick)

- *Quaternary-Paleogene* (<50 m thick, only locally developed): reddish-tan and variegated, lacustrine and alluvial sediments;
- *Santonian-Turonian* Bayanshiree Formation (350–400 m thick): pink-variegated clay, sand, and rare gravel

>Minor unconformity<

- *Cenomanian* Sainshand Formation (100–350 m thick): three cycles of variegated, lacustrine and alluvial sediments (conglomerate, sand, silt, mud/clay) grading downwards into
- *Albian-Hauterivian* Zuunbayan Formation (<1 500 m thick): grey clastic, lacustrine and limnic sediments (clay, shale, silt, sand, conglomerate, partly containing dispersed vegetal matter and minor lignite seams, and intercalated lenses of marl and limestone)

>Unconformity<

Basement

- *Lower Cretaceous-Upper Jurassic* Tsagaant Formation and volcanogenic Dornod Complex: limnic and continental volcanogenic sequence (basalt, andesite, rhyolite, sandstone, tuffaceous sandstone)

- *Upper Jurassic* Sharlin Formation: clastic sediments (variegated conglomerate, sandstone, siltstone)
- *Upper to Middle Permian*: felsic and intermediate volcanics (rhyolite, rhyodacite, clastic and tuffaceous sediments)
- *Upper to Middle Carboniferous* Dusinobin Formation: intermediate to felsic volcanics (andesite, andesite-dacite, rhyolite)
- *Lower Carboniferous* Gunbayan Formation: clastic sediments and mafic to felsic volcanics (sandstone, tuffaceous sandstone, siliceous tuffite, basalt)
- *Upper-Middle Devonian* Gurvansaihan Formation: clastic sediments, limestone, felsic to mafic volcanics and tuffs
- *Middle-Lower Devonian* Undurud Formation: clastic sediments and mafic volcanics
- *Silurian*: continental volcanogenic and carbonatic molasse sediments
- *Cambrian*: clastic sediments and limestone
- *Proterozoic*: geosynclinal sequence of spilite-diorite, quartzite, schist, gneiss, and marble

Magmatic intrusions

- *Lower Cretaceous-Upper Jurassic* subvolcanic intrusives of quartz porphyry and microgranite porphyry
- *Upper-Middle Jurassic, Triassic, and Permian* leucocratic and alkaline granites
- *Devonian* subalkaline and alkaline granites and grano-syenites
- *Upper-Middle Carboniferous* granite, granosyenite, granodiorite, and gabbro-diorite

Major faults are oriented about NE-SW and NW-SE. Block faulting along these structures resulted in horst and graben structures.

Principal Host Rock Alteration

Host sediments are altered by weathering-related, surface-bound limonitization, and, at depths, by kaolinitization, hydromicazation, sulfidization (pyrite, marcasite, galena), patchy and banded hematitization, and bitumen formation. Reduction is particularly prominent along faults.

Principal Characteristics of Mineralization

Coffinite, pitchblende, and black products/sooty pitchblende are the principal U minerals. They are partly intergrown with bitumen. Autunite, uranophane, and schroëckingerite are typical for oxidized environments. Associated minerals include galena, marcasite, pyrite, rare colloidal MoS₂, quartz, and minor carbonates. The ore contains minor amounts of lanthanum, scandium, selenium, and yttrium.

Uranium mineralization is hosted in carbonaceous clastic sediments of the Zuunbayan and Sainshand Formations. Three ore settings, which are often overlapping are noticed:

- stack-type mineralization related to reduction zones along faults (example: *Ingin sector* of Nars deposit)

- tabular mineralization associated with boundaries of strata-bound oxidation zones (example: *Durbulja* occurrence, *Mys (Miso) sector* of Nars deposit)
- tabular mineralization bound to basal contacts of surface-related oxidation zones (e.g.: *Nars-2* and *Yant*)

General Shape and Dimensions of Deposits/ Characteristics of Individual Ore Bodies

Ore bodies exhibit peneconcordant lens and blanket shapes as well as stack and roll morphologies. In more detail, the earlier mentioned three varieties of ore settings show the following characteristics:

Stack- and roll-type mineralization of the *first variety* is typical for the *Ingin sector of the Nars deposit* (for grades and tonnage see Nars deposit) and many other occurrences. Ore is distributed within a 30–120 m thick section of variegated green and grey colored, alternating clayey and sandy lithologies. This unit is overlain by 40–50 m thick pink colored and underlain by 40–60 m thick variegated argillaceous horizons of the Sainshand Formation. Mineralization is confined to intervals intersected by fault zones. Uranium is concentrated in lenses, blankets, rolls and fractures at the margins of sulfidized and hydromica altered, grey and light green sands in which U minerals fill interstices, joints, and microfractures.

Tabular mineralization of the *second variety*, as exemplified by the *Durbulja occurrence*, is confined to the contact of interbedded, reduced grey siltstone with oxidized yellow sandy gravel beds of the Zuunbayan Formation. The deposition site is controlled by edges of stratiform oxidation, which developed in highly permeable clastic sediments. Mineralization at *Durbulja* occurs at a depth of 350 m. Ore thickness is 0.4–1.9 m. Grades average 0.017–0.026% U. The highest drill intercept is 0.112% U.

Tabular mineralization of the *third variety* resembles that of the Kharaat deposit in the Choir Basin. Uranium is near surface concentrated in ribbon-like bodies in grey sandy-clayey layers rich in organic matter of the Zuunbayan Formation, immediately below oxidized, variegated, coarse-grained sediments of the Sainshand Formation. Apparent control of the mineralization is the lower boundary of the weathering-related oxidation zone. The type example is the *Nars-2* occurrence. Mineralization of *Nars-2* can be traced intermittently over a length of 11 km and is hosted by narrow, 50–250 m long and 0.2–1.5 m thick lenses of grey siltstone containing abundant vegetal matter. Ore grades vary between 0.01 and 0.34% U. Uranium minerals are autunite, uranophane, and schroëckingerite. Associated elements are selenium, yttrium, lanthanum, and scandium. The *Yant* occurrence has an identical geological setting as *Nars-2*.

Principal Ore Control and Recognition Criteria

Mineralization occurs in tabular and roll-shaped configurations controlled by lithology, structure and redox interfaces as reflected by the following criteria:

Host environment

- Intermontane basin
- Unconsolidated, carbonaceous and sulfide-bearing sand and gravel beds interbedded with argillaceous horizons
- Steeply dipping fault zones

Alteration

- Oxidation and reduction are reflected by hematitization, carbonatization, hydromicazation, and sulfidization
- Reducing processes have overprinted oxidized strata along faults as documented by sulfidization
- Sulfidization may have resulted from an influx of hydrocarbons

Mineralization

- U-REE-rare metals assemblage
- U associates with hydrocarbons (kerite)
- Ore minerals occur disseminated in lenses, blankets, stacks, and rolls, and as fracture filling
- Lenses and blankets occur at interfaces of permeable and impermeable beds, and
- Stacks and rolls at redox fronts associated with faults
- Radioactive disequilibrium is in favor of uranium

Principal Aspects of Metallogenesis

Mineralization is thought to have formed during Neogene to Quaternary time by epigenetic processes. Permeable sediment horizons as well as permeable fault zones apparently acted as important conduits for mineralizing solutions as indicated by the position of better grade ore bodies along major faults. These faults may also have been pathways for migrating hydrocarbons. Fixing of uranium occurred by reduction and adsorption of uranium and associated elements along fault-bound and intraformational redox interfaces, and at surface-bound oxidation boundaries. Potential reducing substances include carbonaceous matter, sulfides, and perhaps hydrocarbons derived from oil and gas reservoirs. Adsorbing agents include plant remains, clay particles, Fe-oxides, etc. Felsic volcanics and intrusives of the basement are considered to be the source of uranium and associated elements.

Fault-related mineralization, as found in the Ingin sector of the Nars deposit, exhibits to some extent similarities with uranium deposits in South Texas, USA, where hydrocarbons played a critical role in generating reducing conditions and as such provided a favorable environment for forming rollfront uranium ore bodies.

8.4.1.1 Nars Deposit

This sandstone-type deposit was discovered in 1978 in Dornogovi aimag, some 500 km SSE of Ulaan Bataar and about 65 km NE of the railroad town Sainshand. The deposit consists of two separated sectors, Mys (or Miso) and Ingin. Ingin contains approximately 1 000 t U (references see above).

Geological Setting of Mineralization

The Nars deposit is positioned at the NE margin of the Tugrikiin horst near the southern rim of the Sainshand Basin. The stratigraphic column of Tertiary and Cretaceous sediments at the deposit includes, from top to bottom:

- *Neogene-Paleogene* sediments of minor thickness
- *Santonian-Turonian Bayanshiree Formation* (350–400 m thick): pink silt, grey sand, resting upon variegated, grey, massive and horizontally bedded silt
- *>Minor unconformity<*
- *Cenomanian Sainshand Formation* (100–350 m thick): pink and variegated clay and silt overlying grey, fine- to medium-grained sand and gravel;
- *Albian-Hauterivian Zuunbayan Formation*: weakly to unconsolidated, grey, partly carbonaceous limnic sediments, in the upper section predominantly composed of rhythmically alternating grey silt, sand, and gravel beds underlain by black and greenish-grey, foliated clay, argillaceous and bituminous shale with intercalated lenses of marl and limestone. This suite rests unconformably upon the basement

Mineralization is hosted by a 30–110 m thick sequence of the Sainshand Formation, which is composed of weakly to non-lithified, variably grained sand and gravel beds interbedded with impermeable horizons of pink and mottled clay and argillaceous silt. Ore-bearing sands vary in length from 800 m to few kilometers and are from 100 to 400 m wide. Within this stratigraphic sequence, mineralization is restricted to segments intersected by the NW-SE-trending Sainshand fault, a 1–1.5 km wide zone of intense faulting, fracturing, shearing, dragging of strata, and interspersed carbonate veinlets.

Host Rock Alteration

Alteration features include oxidation of permeable strata as documented by patchy to banded hematitization associated with kaolinitization, and reduction along fault zones. The latter extends tongue-like into permeable horizons and is reflected by sulfidization (pyrite, marcasite, galena), hydromica, and bitumen formation.

Mineralization

Pitchblende, partly associated with bitumen, black products (sooty pitchblende), and coffinite are the principal U minerals. Associated minerals include pyrite, marcasite, galena, rare colloidal MoS₂, quartz, and minor carbonate. Additional elements include various enrichments of As, Ba, Cr, Cu, Ge, La, Sr, V, W, Y, and Zn.

Three mineral assemblages are distinguished: pitchblende-kerite, pitchblende-black U products, and pitchblende-coffinite. Pitchblende-kerite is the prevailing assemblage. It is characterized by a close intergrowth of pitchblende with the carbon phase.

Mineralization exhibits predominantly disseminated and rarely veined textures. U minerals fill interstices, joints, and microfractures, form pseudomorphs after vegetal detritus in sulfidized, grey and light green sands, and occur along interfaces of lithologies of different permeability.

Shape and Dimensions of Deposits/Characteristics of Individual Ore Bodies

Two mineralized sectors exist at the Nars deposit, Ingin and Mys.

Resources (EAR-II) of the Ingin sector are estimated at 1 000 t U at a grade averaging 0.04% U (calculated on an average thickness of 3 m, and a cutoff grade of 0.02% U. The Mys sector is considered to be of no economic potential.

Mineralization at Ingin occurs at depths from 180 to 480 m. It occupies a zone 100–400 m in width and 4.5 km in length along the Sainshand fault. The zone is composed of contiguous, en echelon arranged, subhorizontally dipping ore bodies positioned on several stratigraphic levels. Ore grades range from 0.016 to 0.7% U.

Ore bodies in the Ingin sector are predominantly of strata-discordant stack- or roll-type and occur along the contact of

grey, sulfidized and hydromica altered sands. Mineralization in the Mys sector occurs as peneconcordant, lenses and blankets in permeable strata.

Dimensions of individual ore bodies are as follows:

- Blanket ore bodies: 200–300 m long, 100–200 m wide, 0.5–3 m thick
- Lenticular ore bodies: 800–1 200 m long, 100–200 m wide, 0.3–3 m thick
- Stack- or roll-shaped ore bodies: 80–150 m long, 100–200 m wide, 3–7 m thick

References and Further Reading for Chapter 8 • Mongolia

For details of publications see Bibliography.

Batbold 2001; Budunov 2002; Chemillac et al. 2005b; Chuluun and Oyunbaatar 1994; Filonenko et al. 1993; Grushevoi and Pechenkin 2002; IAEA 1995, 2007; Ischukova et al. 2002; Kovalenko and Yarmolyak 1995; Mironov 2002, 2003; Mironov and Rogov 1992, 1993; Mironov et al. 1991, 1993, 1995; OECD-NEA/IAEA 1993, 1995, 1997, 2005; Petrov et al. 2002, 2003; and pers. commun. by Chuluun O, staff of Uran Company of Mongolia Ltd., and staff of ERDES Mining Enterprise.



Chapter 9

Pakistan

Uranium deposits and noteworthy occurrences are reported from the *Dera Ghazi Khan District*, Sulaiman Range, the *Bannu Basin*, and *Issa Khel*, Mianwali District, in central Pakistan, and from the Kirthar Range in south Pakistan (Fig. 9.1). Known deposits are of sandstone type, small in size, and of high cost uranium.

Pakistan's former U production was essentially concentrated in the Dera Ghazi Khan District; OECD-NEA/IAEA (2005) estimates a cumulative production of 970 t U from 1971 through 2004, and an annual production on the order of 40 t U in the early 2000s. Mining was by conventional and ISL techniques. The "Baghal Chur-I" (BC-I) mill at Dera Ghazi Khan served the Dera Ghazi Khan District. It started up in 1971 as a pilot plant. Issa Khel was mined by open pit and underground methods and the ore processed by heap leaching. In recent years, ISL operations in the Bannu Basin may also have provided some production.

A number of radioactive localities associated with alkaline igneous rocks, pegmatites, and schists have been discovered in the mountainous northern part of Pakistan.

All uranium exploration is in the responsibility of the state-owned Atomic Energy Minerals Centre (AEMC) based in Lahore. The following description is based on Baig (1990), Moghal (1974a,b), OECD-NEA/IAEA/IUREP (1978), OECD-NEA/IAEA (1997, 1999) amended by data from other authors cited in the sections of the various uranium districts.

Historical Review

First reports on the discovery of uranium mineralization date back to the year 1959. U was found in Siwalik sandstone near *Rakhi Munh* in the Sulaiman Range. Subsequent exploration led to the discovery of about a dozen small U deposits in the Dera Ghazi Khan District in the early 1970s. *Taunsa*, discovered in 2000/2001 in this district, was the latest success.

Exploration in other parts of Pakistan resulted in numerous U showings in Siwalik sediments and crystalline rocks but no deposits, except for the small *Qubul Khel* deposit in the Bannu Basin and *Kallar Kahar* in the Salt Range (OECD-NEA/IAEA 1999).

By 1976 uranium resources of Pakistan were calculated at 150 000 t of ore at a grade of 0.12% U, containing 181 t U based on a cutoff grade of 0.09% U (IUREP 1978). U mining began in Pakistan at Baghal Chur in 1971.

Regional Distribution and Characteristics of the U-hosting Siwalik Group

Continental sediments of the Tertiary Siwalik Group (or System), partitioned into three divisions (see below), provide the only productive uranium host in Pakistan as known so far. This group,

4 600–5 500 m thick, was almost continuously deposited from Middle Miocene to Lower Pleistocene. The Siwalik System or its equivalents in time, respectively, extend continuously along the Himalayan foothills from Assam in the east to southern Kashmir, and across the Indus Valley in Pakistan through the Potwar Plateau and Balillu Plains where they turn southwesterly into the Bannu Basin and then south into the Sulaiman Range. From this point, they continue as a more marine facies to the Arabian Sea.

Siwalik sediments have been denominated differently in different regions: Siwalik System along the outer Himalayas, Manchhar System in Sind, Mekran Series in Baluchistan, Dihing Series in Assam, and Irrawady System in Burma.

The Siwalik System is a typical sequence of flood-plain sediments of major rivers that was deposited in the foredeep between the Indian Shield and the rising Himalayas and other ranges to the west and south in Pakistan. These fluvial facies grade into shallow marine equivalents in southwestern Pakistan. Fluvial-lacustrine sediments comprise compacted sands, clays, and conglomerates that originated from a wide range of sedimentary, metamorphic, and igneous rocks. A notable feature is the common occurrence of plant and animal remains, locally in considerable profusion. Pyroclastic layers up to several meters thick occur at several levels within the Middle Siwalik System in various areas. During later phases of the Himalayan Orogeny, the Siwalik strata have been folded, faulted, and overthrust, and rest with marked unconformity upon older formations.

Intermittent U mineralization in Siwalik sandstones, mainly in the Middle Siwalik Dhok Pathan Formation, is known for at least 1 000 km along the sinuous outcrop of this group from 50 km south of Dera Ghazi Khan along the Sulaiman Range, to the Bannu Basin and other areas to the north in Pakistan, and further to the east within India.

9.1 Sulaiman Range, Dera Ghazi Khan District, Punjab

The Dera Ghazi Khan District lies in the Sulaiman Range, a prominent morphological element in the Sulaiman physiographic province in central Pakistan. Numerous radioactive anomalies, some with visible U minerals, are spread over an outcrop length of more than 160 km along the foothills of this range. They include about a dozen small blanket sandstone-type U deposits confined to a single horizon near the base of the Middle Siwalik Member in a N-S strip to the west of the town of Dera Ghazi Khan. Reported deposits include *Baghal Chur* (or *Baghal chor*), *Rakuchur*, *Rakhi Munh*, *Nangar Nai*, *Kaha Nalo*, *Rajanpur*; and, located to the north of the district, *Taunsa* (Fig. 9.2). *Taunsa* is a recent discovery from 2000/2001.

Most resources of the early discovered deposits are exhausted. Some early mining of these deposits was by conventional open pit and underground methods to depths of 150–200 m and later by ISL techniques and produced an estimated total of some 800 t U. At a cutoff grade of 0.03% U, the ore had grades of 0.1% U as maximum. ISL operations began at *Rakhi Munh* in 1995 and were tested at *Nangar Nai* in 1997.

■ Fig. 9.1.

Pakistan, distribution of Tertiary Siwalik Group sediments and location of the Baghal Chur and Qabul Khel U deposits (after Moghal 2001)



Sources of information. Basham 1980; Basham and Rice 1974; Moghal 1974a,b.

Regional Geological Setting of Mineralization

Rocks from Jurassic to Pleistocene age occur in the Sulaiman physiographic province, the central core of which is marked by mafic and ultramafic intrusions. The Middle Miocene to Lower Pleistocene Siwalik Group is exposed in the Sulaiman Range as a narrow north-south-trending belt, some 300 km long and dipping to the east. This group has been tripartitioned into an Upper, Middle, and Lower division (Moghal 1974, based on Wadia 1961):

Upper Siwalik Division, 1 800–2 400 m thick: Coarse boulder conglomerates, thick-bedded earthy clays and silts, whitish grey sands, and grit. The Upper Siwaliks are generally more argillaceous than the underlying strata, and, in the Dera Ghazi Khan District, a thick, extremely coarse, siliceous-boulder conglomerate caps them.

Middle Siwalik Division, 1 800–2 400 m thick: Thick, massive beds of grey arenites (sandstone, subarkose, subgreywacke)

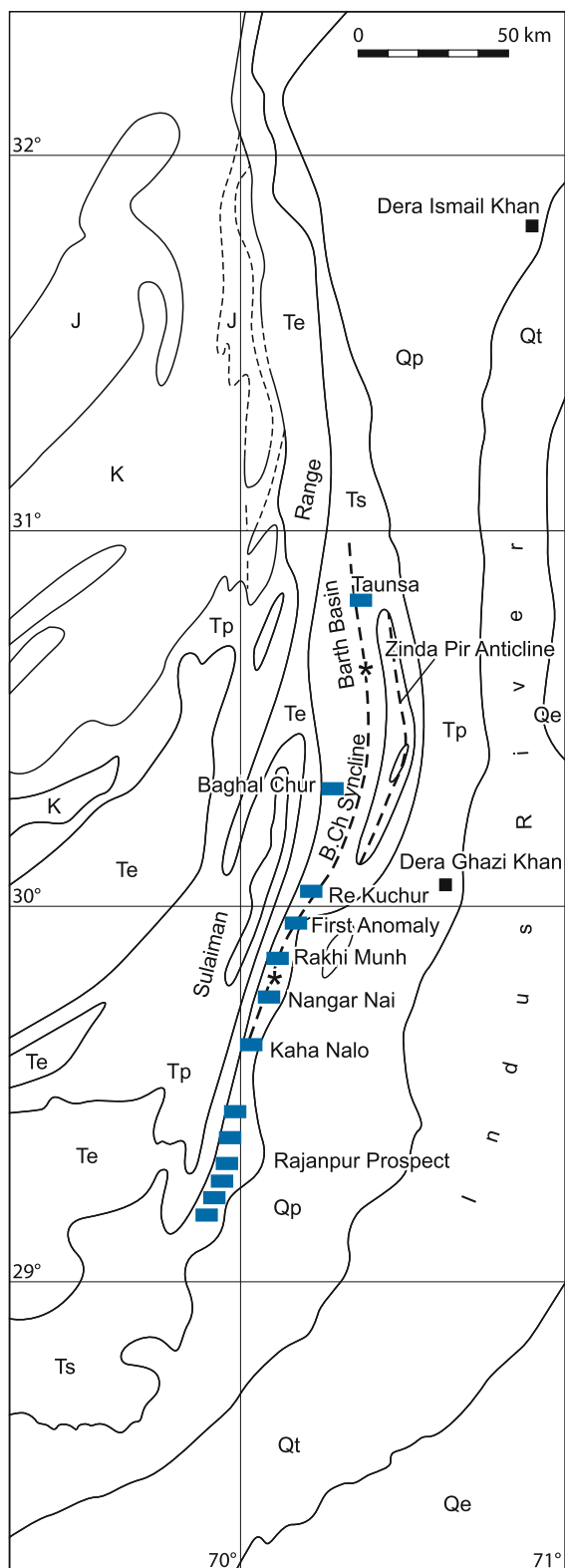
intercalated with minor drab and grey clays and shales as well as some thin conglomerate and hard sandstone lenses. The sands are soft, friable, poorly sorted, and cross-bedded; the matrix is highly variable, much of it consists of hard calcareous concretions but most of the rock is soft.

The Middle Division is subdivided into the Dhok Pathan Formation and the underlying Nagri Formation. Both consist mainly of subgreywacke and lithic arenite but are differentiated by their fine-grained facies that comprise mudstone and siltstone with rare clay in the *Dhok Pathan* Formation and clay/siltstone in the *Nagri* Formation. Pyroclastic constituents occur in both formations.

Lower Siwalik Division, 1 500 m thick: Fine-grained, more or less consolidated, micaceous sandstone interbedded with abundant bright red, brown, and purple shales and minor conglomerates.

Silicified wood debris and tree trunks are abundant throughout the Siwalik sandstones whereas leaf remnants occur preferentially in the shales. In the Baghal Chur area, the wood and logs are almost entirely limonitized to soft, earthy ochre.

Fig. 9.2. Sulaiman Range, Dera Ghazi Khan U district, generalized geological map with location of U deposits/occurrences (after Moghal 1974a, 2001). *Qt* Recent fluvial deposits; *Qp* Recent piedmont deposits; *Ce* Early Recent eolian deposits; *T* Siwalik Formation, *Ts* Lower Pleistocene-Middle Miocene, *Te* Eocene, *Tp* Paleocene; *K* Cretaceous; *J* Jurassic



Folding of the Siwalik sediments resulted in the formation of a series of asymmetrical anticlinal and synclinal structures of a general northerly trend. Baghal Chur and other U deposits are located in an asymmetrical syncline stretching for approximately 300 km along the eastern flank of the Sulaiman Range. Superimposed secondary folding extends across all structures and, at Baghal Chur, has resulted in a slight rise of the large syncline causing it to have a double plunge. The depression north of the bulge is denominated *Barthi Basin* and to the south *Baghal Chur syncline*. Strata are only gently tilted over most of the two synclines but they steepen abruptly with dips of 30–60° on the western (Sulaiman anticline) and eastern (Zinda Pir anticline) sides. The Upper Siwalik Member is absent within the crest of this bulge.

Although U anomalies are found in a basal Middle Siwalik sand horizon/Dhok Pathan Formation all along the major syncline, all U deposits referred to above occur south of the minor structural rise except for Taunsa, which is situated further to the north. Baghal Chur is in terrane of gentle dip while the Siwaliks have dips approaching 50–60° at the other U deposits/occurrences to the south.

9.1.0.1 Baghal Chur

The blanket sandstone-type Baghal Chur deposit lies about 40 km NNW of Dera Ghazi Khan. Original resources are not published but are assumed to have been on the order of a few hundreds tonnes U at grades of 0.05% U. The deposit was mined from 1971 to 1999 by conventional methods and is depleted.

Geological Setting of Mineralization

Baghal Chur is situated in the asymmetrical Baghal Chur syncline; its eastern (Zinda Pir) flank dips 30–50° W while the major portion of the western limb, that hosts all U lodes, shows gentle and uniform 5–10° easterly dips which, however, increase sharply near the western anticline.

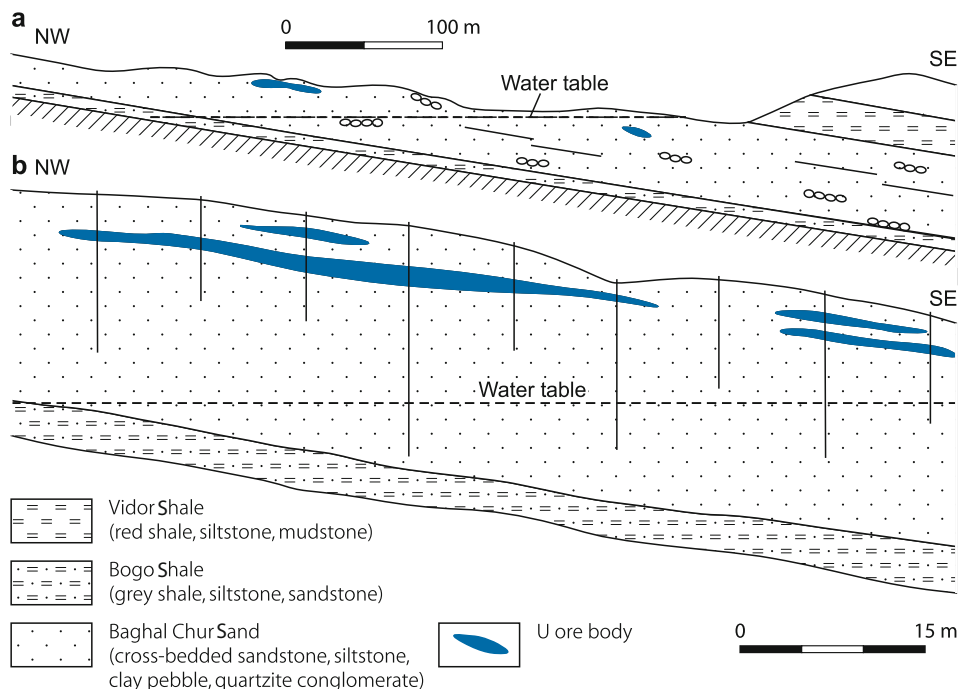
Host rocks are fluvial-lacustrine sediments of the Dhok Pathan Formation, Middle Siwalik Division in which U mineralization is confined to an NE-SW-striking and 5–10° SE dipping arenite horizon, about 60–75 m thick, termed Baghal Chur Sand. Shale beds occur below (Bogo Shale) and locally above (Vidor Shale) the sands (Fig. 9.3a).

The *Baghal Chur Sand* was deposited primarily as sheets by southerly flowing rivers. It is a light grey, poorly to well sorted, commonly medium- to fine-grained, soft, and friable subarkose or subgreywacke. Major constituents are quartz, feldspars (10–25% plagioclase, microcline, orthoclase), muscovite, and biotite. Lithic rock fragments of magmatic and metamorphic provenance are common and include chips of occasionally pyritiferous slate and carbonaceous schists. Some rock fragments may represent diagenetically altered volcanic tuff.

Accessory minerals occur in a large variety and are often dominated by magnetite. Based on frequency of feldspars or lithic fragments the sands may be defined as subarkose,

■ Fig. 9.3.

Dera Ghazi Khan U district, Baghal Chur area, NW-SE cross-sections illustrating **a** the general litho-stratigraphic position of the U-bearing Baghal Chur Sand, Dhok Pathan Formation, Middle Siwalik Division; and **b** the distribution of U lenses in the Baghal Chur Sand (after Moghal 1974a)



subgreywacke, or sandstone. The detrital components are cemented to variable extent by calcite with subordinate but fairly common heulandite; in some sections cement is absent while in others the sand is relatively well cemented. Erratic pebbles of quartzite, limestone, or calcareous clay pellets are sporadically distributed throughout the section.

Some interlayers consist of a friable, medium to coarse grained, siliceous sandstone without rock fragments. This facies is rich in biotite, and muscovite, disseminated pyrite partly as aggregates up to 1 cm in diameter, and plant debris are common. The organic debris is frequently pyritiferous.

The arenite horizon contains numerous intercalated, pinkish lenses, commonly 0.5–1 m, locally up to 3 m thick, composed of quartzite and limestone pebbles in a sandy, silty, and clayey matrix. These lenses persist in a N-S direction for several tens to over a hundred meters, but pinch out rapidly in perpendicular direction, and are thought to mark paleochannels.

The *Bogo Shale* is grey, locally silty shale, containing siltstone lenses about 1 m thick. It attains a thickness of 12 m at the deposit; but elsewhere it thins considerably. The *Vidor Shale*, about 25 m thick, is brown to dark brown, locally also silty, and more continuous than the Bogo Shale.

Host Rock Alterations

Surficial oxidation is the most prominent alteration feature above the present-day groundwater table (some 30 m deep). In this zone, plant remains including logs can be completely replaced by earthy iron (hydro)oxides, and magnetite is commonly martitized.

Other alteration phenomena are of highly variable but mostly minor degree and include argillization, sericitization, silicification, desilicification, calcitization, sulfidization, zeolitization, and barytization. To what extent these alterations are related to diagenetic, mineralizing, and/or other processes remains unclear since there is no color or mineral change noticed at the sites of mineralization.

Some typical alteration features are as follows: Feldspars, particularly plagioclase, are altered to sericite and/or calcite, and to a fine-grained unidentified material. Some schist fragments are extensively replaced by calcite and occasionally by heulandite. Calcitization with subordinate zeolitization (clinoptilolite, heulandite) cement variably the host sands. Quartz grains are corroded. Bones and rocks are partly silicified. Some montmorillonitized rock fragments may represent diagenetically altered volcanic tuffs. Sulfidization is reflected by pyritized plant debris and disseminated pyrite that occurs in part as aggregates up to 1 cm in diameter.

Mineralization

Uranium(-vanadium) mineralization occurs above and below the groundwater table, respectively, in oxidized and non-oxidized greywacke in which schist fragments, biotite and feldspar predominate. In both environments, mineralization is out of equilibrium.

Non-oxidized mineralization: Pitchblende and coffinite are the principal U minerals in the non-oxidized zone. In addition, uranium is adsorbed by goethite, hematite, martite, biotite, clay minerals, and plant remains. An appreciable uranium content is also bound in zeolite (clinoptilolite, heulandite) that occurs as

discrete diagenetic crystals in pore cavities. Associated minerals include anatase, calcite, haggite, and an expanding (vanadiferous?) clay mineral.

Uranium minerals commonly form a skin around and line cavities within partially or completely altered plagioclase. They typically occur also within quartz-mica schist fragments particularly in those with carbonaceous material. Most highly mineralized samples comprise carbonaceous rock fragments that are almost completely replaced by pitchblende. Interstices within the host rock are also frequently lined with pitchblende, and in both cases pitchblende exhibits a micro-spheroidal habit.

Haggite is the major vanadium mineral in the non-oxidized ore besides a possibly vanadiferous clay mineral. Both coat detrital grains while haggite typically also occurs as cavity infillings and as acicular crystals dispersed in a blue-grey clay coating.

Analyses of selected bulk samples of ore show a range from 760 to 6 200 ppm U, 570–9 800 ppm V, 10–40 ppm Cu, and 5–30 ppm Th (Basham and Rice 1974). Carbonate content is 5% and more and the mineralized horizon has a sand-to-shale ratio of 4:1.

Oxidized mineralization: Tyuyamunite is the principal U mineral but some carnotite occurs occasionally. These minerals, in the form of a greenish-yellow amorphous powder, coat grains, pebbles, and clay pellets, impregnate the interstices between clasts, and locally also associate with crossbeds of heavy minerals. In the latter case, bands of yellow U minerals about 1 cm thick follow above or below, or on both sides 5–10 mm thick black, primarily magnetite, heavy mineral bands and crossbeds.

An appreciable amount of U is adsorbed, however, by earthy iron oxides and or organic debris replaced by similar ferruginous phases. Completely limonitized plant remains, wood logs, or individual pieces of silicified bone often have the highest U concentrations. Samples from the oxidized zone contain amounts of U, V, Cu, and Th comparable to those from the unoxidized zone.

Intercalated coarse-grained sandstone barren of rock fragments is only insignificantly mineralized and the only uraniumiferous material tends to be pyritiferous plant debris. Vanadium values are much lower than in the mineralized zones but Th and Cu tenors are comparable.

Shape and Dimension of Deposits

The deposit consists of a group of overlapping ore bodies distributed from surface to depths of 150–200 m. Ore bodies are of strata peneconcordant, elongated to amoeba shape (► Fig. 9.3b); boundaries are indistinct or transitional. Ore bodies are from tens of meters to more than 100 m long, from 0.3 to more than 3 m thick, and have tenors ranging from 0.04 to over 0.5% U but presumably average on the order of 0.05% U.

Ore Controls and Recognition Criteria

U occurrences are distributed in a random nature and U mineralization shows a lack of preference for any sedimentary, textural or structural feature of the host rock except for the position near or at paleovalleys. In spite of this situation certain recognition criteria are noticed by Moghal (1974a):

Host environment

- Preferential host rock is grey to tan, fine- to medium-grained subgreywacke or subarkose with interbedded grey and red to brown shale of fluvial-lacustrine origin
- Lithic fragments indicate a provenance from igneous and metamorphic terrane
- Grain size is fine to coarse, sorting poor to medium, selective weak cementation by calcite and minor zeolites
- Sand-to-shale ratios are 4:1
- Strata dip with 5–10° at Baghal Chur; at other U deposits in the district dips approach 50–60°

Alteration

- Oxidation above the present-day groundwater table
- Silicification, desilicification, calcitization, sulfidation, zeolitization, and barytization
- No color or mineral change at the sites of mineralization

Mineralization

- Unoxidized environment: pitchblende, minor coffinite, and adsorbed U
- Oxidized environment: tyuyamunite, sparse carnotite, adsorbed U
- Associated elements: vanadium, possibly selenium (selenite?)
- Fairly high carbonate content particularly above the groundwater table
- Potential reducing agents: sparse, mostly very fine-grained, disseminated pyrite and rare vegetal remains
- Vegetal matter is almost always completely limonitized to soft and earthy ochre
- Blanket-type, strata peneconcordant elongated to amoeba-shaped ore bodies
- Superjacent arrangement of ore lenses
- Apparent relationship of U lenses to paleochannels

Metallogenetic Aspects

Following Basham (1980) and Basham and Rice (1974), replacement textures and the evidence of adsorption by earthy phases such as goethite and hematite, clays, and other phases in the unoxidized ore at Baghal Chur indicate an epigenetic precipitation of uranium from pore-water solution in the reducing microenvironment of rare, organic-rich lithic fragments. This is contradicted, however, by the lack of any significant U enrichment in the coarse-grained sand barren of lithic fragments, in spite of considerable amounts of plant debris; unless one assumes that these rocks may represent a position above the permanent water table from which uranium has been leached.

As may be deduced from the common calcite cement, mineralizing solutions were rich in carbonate. The high calcite content in the oxidized zone may be attributed in part to the present (and past?) aridity of the climate that promoted the loss of CO₂ from groundwater and as such would cause precipitation of U by reaction with vanadate ions to form tyuyamunite.

Another scenario may consider epigenetic processes caused by periodic upheaval and related fluctuation of the groundwater

table that led to reworking and concentration of U at a redox interface. Whatsoever the mechanism of U transport and deposition, the ultimate origin of the uranium and vanadium is enigmatic.

9.1.0.2 Other U Deposits/Occurrences in the Baghal Chur District and Barthi Basin

Baghal Chur District: Several other U deposits/occurrences are located to the south of Baghal Chur (► Fig. 9.2) in the same Middle Siwalik arenaceous horizon and exhibit, on surface, bright yellow mineralization in lenses mostly elongated along strike. Single lenses can persist for as much as 60 m. At two of these sites, mineralized lenses, both large and small, are scattered over a distance of 3–5 km along the strike, while at others mineralization is scattered over 1 km. The major part of the uranium outlined at these locations has been mined out except for ore bodies at Nangar Nai that, as of 1997, were being tested for exploitation by ISL methods.

The *Taunsa* deposit was discovered 70 km N of Dera Ghazi Khan city in 2000/2001. U mineralization occurs in a 13 km long stretch within sands of the Siwalik Group. Exploitation is planned by ISL techniques.

The Barthi Basin, located to the north of the Dera Ghazi Khan District, contains in its southern part three areas with wide-spread radioactive anomalies. The anomalies in each area are spread over a distance of more than 3 km. U mineralization is rare and, wherever noticed, is associated with limonitized wood logs. Conglomerate beds are common in these areas, and are thought to mark braided paleochannels (Moghal 1974a,b).

9.2 Bannu Basin-Surghar Range, NW Pakistan

The Bannu Basin is located in the North-West Frontier Province of Pakistan. It contains the small *Qabul Khel*, *Eagle Hill*, and *Shanawah* sandstone U deposits in the *Surghar Range*, an eastern marginal hill range of the basin. U showings hosted by Middle Siwalik molasse also occur intermittently over a strike length of 30 km between Kundal and Baggi Qammar in the *Khisor Range*, a continuation of the *Surghar Range*, south of the Kurram River. *Qabul Khel* is the only deposit explored in more detail and prepared for exploitation in the Bannu Basin.

9.2.0.1 Qabul Khel, Surghar Range

Qabul Khel (Kubul Khel), named after a small nearby village, is located in the southern *Surghar Range*. No resources are reported. Grades are about 0.05% U.

A number of small ore bodies were explored in the early 1980s. An experimental underground mining operation was carried out initially but ISL mining was finally adopted and a semi-commercial scale ISL operation began in mid-1995 on one ore body. Conventional and ISL mining, respectively, are

hampered by the shape of the ore body, high dip of strata, structural complications, poorly cemented rocks, poor solution confinement, influx of a high quantity of water, absence of bottom shale at places, high calcium content in water, and a water table cover of only 3 m (Mansoor et al. 2002).

Sources of information. Baig 1990; Mansoor et al. 2002; Moghal 1992, 2001; OECD-NEA/IAEA 1999.

Geological Setting of Mineralization

The *Qabul Khel* deposit is located in the plunging, southern part of the *Surghar* anticline at the eastern margin of the structural *Bannu Basin*. This basin consists of folded molasse of the *Siwalik Group*. Ore bodies are hosted by the *Dhok Pathan Formation* that forms the upper unit of the *Middle Siwalik Division*. The *Dhok Pathan Formation* is a cyclic alternating sand-shale sequence that is variably inclined, between 20 and 45° SW, in the *Qabul Khel* area.

At the deposit, the sandstone beds are 40–60 m and the intercalated shales 10–15 m thick. The sandstones are grey, soft and friable, and the shales dull brown and grey. The shales are silty and often contain variable amounts of volcanic material in the form of bentonite and bedded ash with glass shards.

Uranium is hosted near the top of the *Dhok Pathan Formation* in the locally termed *Qabul Khel Sandstone*, a commonly whitish grey, medium- to coarse-grained sublithic to subarkosic arenite with repeated intercalations of fine-grained sandstone, and interspersed calcified hard sandstone lenses, 10–50 cm in thickness and several meters in length. Major arenite constituents include quartz, mica, feldspars, amphiboles, and rock fragments; some carbonaceous matter, micro-fine humic material, and diagenetic pyrite occur locally. The calcite content is high as reflected by CaO values ranging from 2.8 to 5.9%. The arenite is poorly cemented, semi consolidated, friable, and bears good porosity and permeability (hydraulic conductivity is 2–4 md⁻¹ and effective porosity 30–40%).

The *Qabul Khel Sandstone* rests upon the *Qabul Khel Shale*, 5 m in average thickness and comprised of brownish grey to tan mudstone intercalated with silty mudstone, shale, and siltstone, which contain abundant volcanic ash and some organic matter. The sandstone is covered by the *Lakka Manja II Shale*, a 5 m thick on the average, finely bedded, grey shale.

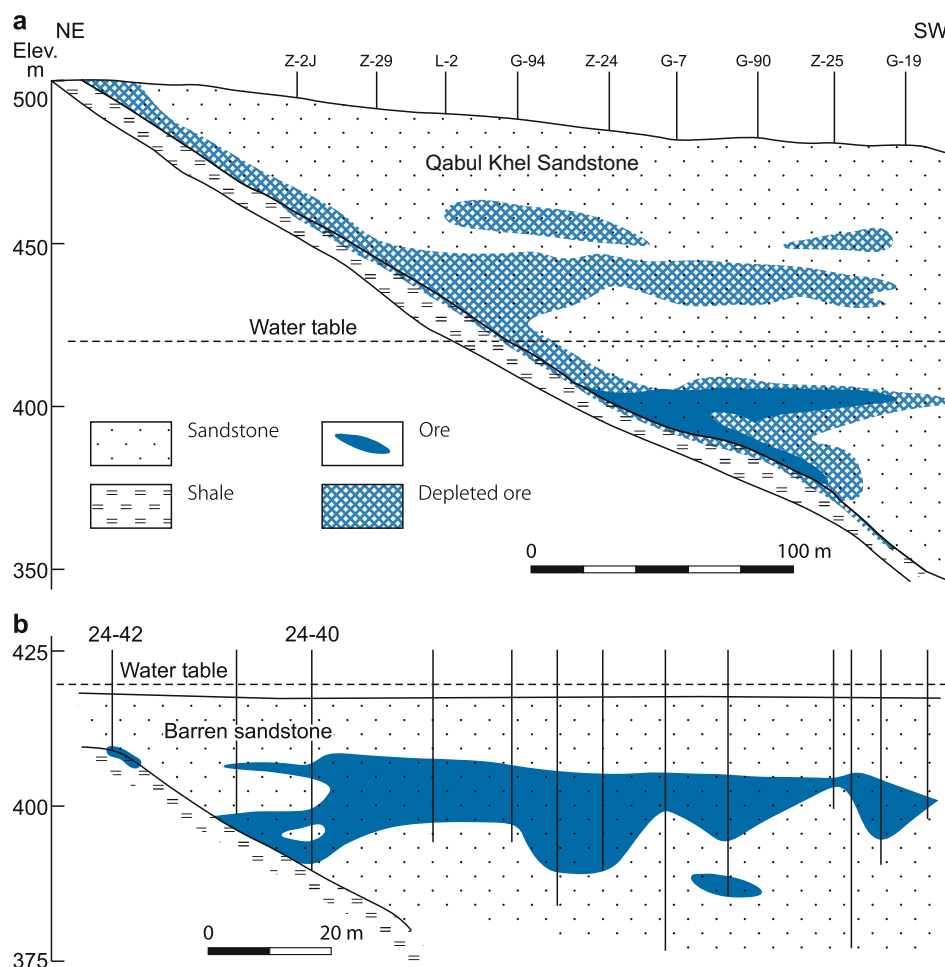
Brittle tectonism resulted in numerous strata discordant and some intraformational faults, fractures, and joints in the *Qabul Khel* area that are filled with sand and are partly calcified but only above the water table.

Mineralization

Coffinite and pitchblende are the principal U minerals in the unoxidized environment below the water table; they occur as pore fillings whereas pitchblende also occurs as micro-fine globules. Uranophane is typical for the oxidized zone. The ore minerals are contained in an assemblage of predominant amphibole, calcite, quartz, mica, and clay minerals. The ore is poorly cemented, largely unconsolidated, and fragile.

Fig. 9.4.

Bannu Basin, Qabul Khel deposit, NE-SW cross-sections along drill fences 0 (a) and 10 (b) showing the irregular shape of the main ore body in Qabul Khel Sandstone and its relationship to the Qabul Khel Shale horizon and the water table (after a Moghal 2001; b Mansoor et al. 2002)



Shape and Dimensions of Deposits

The Qabul Khel deposit consists of a number of ore bodies. Some information is published on one ore body that was tested for ISL mining (beginning in 1995).

Ore is hosted by Qabul Khel Sandstone at the contact with underlying shale; these beds strike NW-SE and dip about 27° SW. Ore is located below the groundwater table. The water table is 65 m below the surface and the ore-hosting sandstone is under unconfined conditions (Fig. 9.4).

The ore body is of irregular tape-like configuration; it has a NW-SE length of some 200 m, a thickness commonly from 2 to 15 m averaging 6.5 m, persists over a depth interval from 68 to 118 m below the surface, and averages 0.053% U.

The ore follows, in NW-SE direction, the trace of the water table at the contact of the Qabul Khel Sandstone with underlying shale. Most of the ore is concentrated along the interface of the sandstone with the underlying shale, but at places the ore forms another limb penetrating strata discordant into the sandstone for as much as 120 m, parallel to the present-day water table. The hinge portion of the two limbs is bulbous, attains a maximum

thickness of up to 24 m, and contains about 80% of the ore. (Fig. 9.4a).

Metallogenic Aspects

The Qabul Khel uranium deposit is thought to have evolved through multiple reworking by infiltration. Continual leaching and migration of uranium to its present position occurred during successive tectonic activity and related fluctuation of the water table in response to Himalayan tectonism. U precipitation was caused by permeability barriers combined with upward migrating hydrocarbons, which are considered to have provided the required reductants.

9.3 Other Uranium Occurrences in Pakistan

Minor U occurrences are reported from various parts of Pakistan including the following sites:

Kirthar Range, Sind Province, south Pakistan: U mineralization occurs discontinuously over a strike length of 25 km in sandstone of the Lower Manchar Formation in the Karunuk-Sehwan, Rehman Dhora (Aamri), and Wahi Pandi areas. Uraniferous lenses range from 200 to 1 000 m in length. Samples yield from 0.02 to 4% U. U minerals include carnotite, curite, phurcalite, and saleeite.

Shanawah near Karak, Northwest Frontier Province: U mineralization extends over a strike length of 2 km. The average thickness is as much as 17 m and averages 10 m. Grades average 0.04% U. Carnotite occurs in the oxidized zone above the water table whereas pitchblende prevails below the water table.

Kallar Kahar, Salt Range, central-north Pakistan: Uranium occurs in sandstone of the Middle-Late Miocene Kamli Formation near Kallar Kahar in the Salt Range, some 120 km SSW of Islamabad. The formation consists of purple-grey and brick red sandstones interbedded with purple shales. Partly calcified and non-calcified sandstones that contain abundant organic matter and more or less devitrified volcanic material host the U mineralization.

Maraghzar Area, north Pakistan: A vein system with U concentrations cutting across the Swat granitic gneiss complex occurs in the high mountains at Maraghzar area in the Swat region, but depths and strike continuity remain to be established.

Sallai Patti Carbonatite, north Pakistan: Several radioactive carbonatites have been found in northern Pakistan including one near Sallai Patti village in Malakand Agency. The Sallai Patti carbonatite is a sheet like body with moderate to vertical dip, from 2 to 30 m in width, and about 12 km in length. It was intruded along a NW-SE contact fault between granite and schist. Another elongated carbonatite body, 2–7 m thick and intruded in schists, parallels and joins the main carbonatite body in the eastern and western parts of the area. Uranium mineralization is structurally controlled and can be traced along both the strike and dip of the main carbonatite body. Pyrochlore is the main source of radioactivity. The Sallai Patti carbonatite contains 70% calcite (68% CaCO_3), 0.4% pyrochlore, (200 ppm U, 600–800 ppm rare metals), 7.1% apatite (3% P_2O_5 , 0.2% REE), and 5.0% magnetite (3.0% Fe). U resources are speculated at a few thousand tonnes uranium at an average grade of 0.02% U (Moghal 2001).

References and Further Reading for Chapter 9 • Pakistan

For details of publications see Bibliography.

Azhar et al. 2003; Baig 1990; Basham 1980; Basham and Rice 1974; Mansoor et al. 2002; Moghal 1974a,b; 1992, 2001; OECD-NEA/IAEA 1997, 1999; OECD-NEA/IAEA/IUREP 1978.

Chapter 10

Russian Federation, Asian Territory

Uranium deposits and significant occurrences are reported from ten regions of Asian Russia. They include all significant districts and present production centers in Russia (► Fig. 10.1).

OECD-NEA/IAEA (2005) reports a total of 172 400 t U as remaining resources recoverable at <\$80 per kg U, 131 750 t U of which are attributed to the RAR and 40 650 t U to the EAR-I category. Resources distribution by types of deposits amounts to 117 120 t U in volcanic-, 21 410 t U in sandstone-, and 33 870 t U in vein-type deposits.

The *Strel'tsovsk District* in Transbaykalia is the prominent uranium district in Russia. In 2005, it had remaining reserves (RAR) of 117 120 t U in the <\$80 per kg U category contained in volcanic-type deposits. Two other deposits with sandstone-type U mineralization in the *Transural* and *Vitim*/Transbaykalia Districts have cumulative resources of some 22 000 t U in the RAR + EAR-I, <\$40 per kg U cost category.

Other regions contain in excess of 450 000 t U that are defined as explored, non-balance sheet inferred resources. Deposits in these regions were discovered, explored and technically and economically evaluated in the 1950s to 1980s, and require an up-to-date calculation of their resource cost categories.

Russia's cumulative uranium production from 1951 to end of 2005 is 123 000 t U. In 2005, active mining was restricted to the *Strel'tsovsk* (conventional underground) and *Transural* (ISL) districts while ISL production was planned to begin in 2006 in the *Vitim* District.

A mill at *Krasnokamensk* with a nominal production capacity of 3 500 t U yr⁻¹ serves the *Strel'tsovsk* District. JSC "Priargunsky Mining and Chemical Production Association" (PPGHO) is the operator of this production center. JSC "Dalur" is the operator in the *Transural* (capacity 800 t U yr⁻¹) and JSC "Khiagda" in the *Vitim* (capacity 1 000 t U yr⁻¹) district. All mining enterprises belong to the state corporation "TVEL".

Since 2004, all uranium exploration is in the responsibility of the state-owned enterprise "Urangeorazvedka" (formerly "Central Geological Exploration Division" or "Geologorazvedka"), which is financed by the federal "Ministry (or Committee) of Natural Resources" and, since 2004, by the "Federal Subsoil Resources Management Agency". Mining is in the hands of regional subsidiaries under supervision of "Atomredmetzoloto", a section of the "Ministry of Atomic Energy" (Minatom). All federal institutions related to uranium exploration and mining are based in Moscow.

The following compilation is based on Boitsov AV (1999), Boitsov AV and Nikolsky (2001), Boitsov VE (1996), IAEA 1995; Laverov et al. (1992a–c, 1995, 2000), Naumov (1999), OECD-NEA/IAEA (1997, 1999, 2005), amended by data of other authors cited in the sections of the various uranium regions, and pers.

commun. by Boitsov AV, Boitsov VE, and Kazansky VI. [Note: After finalizing this manuscript a publication by Ischukova et al. (2002) became available addressing uranium deposits in volcano-tectonic structures and the reader is referred to this comprehensive volume for districts with volcanic-type U deposits in CIS countries and Mongolia.]

Historical Review

First reports on the discovery of uranium minerals of the present Asian territory of the Russian Federation date back to 1827 when C.F. Blondeau mentioned a "green uranite" (in later publications referred to as "chalcolith" (torbernite) from Siberia. The specimen was supposedly found near Yekaterinburg (formerly Sverdlovsk) on the eastern slopes of the central Ural mountains from where Leymerie (1859) reported "chalcolith" and Arzruni (1885) torbernite in talc schist from the Beresovsk gold mining district, located NE of Yekaterinburg.

Systematic exploration for uranium, however, did not get under way until 1944, efforts that began to meet with success in 1946. At that time deposits had been found in the Yenisey region, western Siberia. Next, uranium was discovered in the Aldan region in 1961, the *Strel'tsovsk District* in the Transbaykal region in 1963 (still the most important find), followed by discoveries in the *Vitim* and *Transural* districts in the late 1960s and 1970s. In total, twelve uranium regions or districts have been identified, four of which are in European Russia and eight in Asian Russia (► Fig. 10.1).

Despite the enormous scale of the exploration effort, vast areas remain virtually unexplored, notably the remote region bounded to the west by the Ural mountains, to the south by the 60th parallel, the northeast by the Chukotsky Peninsula and the southeast by Sakhalin Island. The reason for this apparent neglect was caused by major discoveries of ample uranium resources in the then-Soviet republics of Kazakhstan and Uzbekistan.

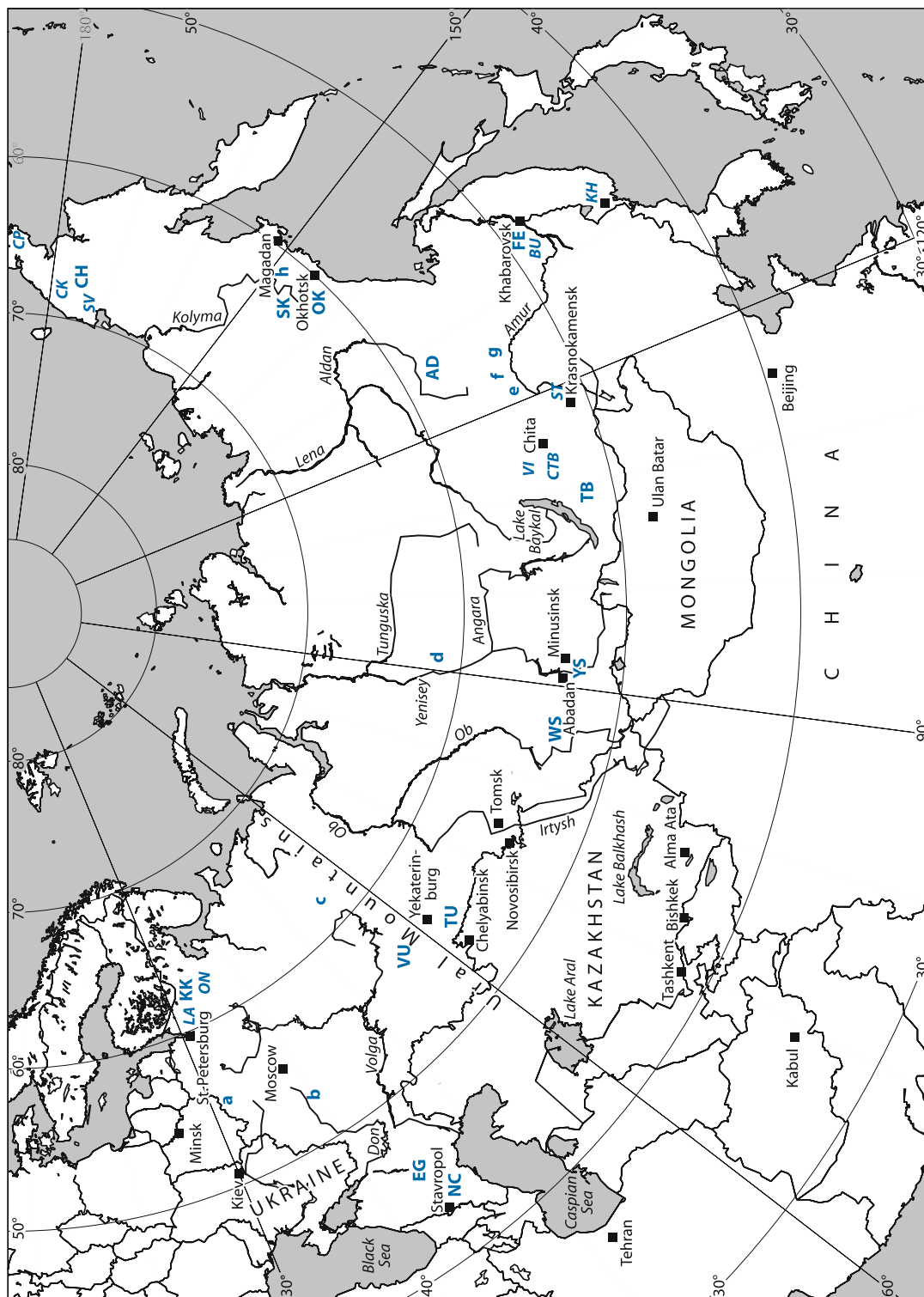
First *uranium mining* in the former imperial Russia took place in the central Asian regions of the country at the beginning of the 20th century. Famous mines were at Tyuya-Muyun in the Fergana Basin, now Kyrgyzstan (for details see there). From 1904 to 1914 about 700 t of uranium ore were mined and three quarters thereof were shipped to and beneficiated at St. Petersburg yielding 2.3 g radium (Chervinsky 1923/1925).

Uranium mining on present-day Russian territory started first in the *Stavropol* District, Caucasus region, in 1951 where it lasted until 1990 and produced 5 700 t U.

A small deposit, *Sanarskoye* in the western *Transural* region, was exploited by ISL methods and yielded 440 t U between 1968 and 1980. Two isolated small deposits, *Butugichag* and *Severnoye*, were mined in eastern and northeastern Siberia, respectively. At least a small quantity of uranium was presumably also produced during exploration work in the *Aldan* region in eastern Siberia. The presently (2006) active *Strel'tsovsk District* in Transbaykalia started up in 1968 and produced from ten deposits about 110 000 t U until 2005.

Fig. 10.1.

Russian Federation. Location of uranium regions, districts and areas (after Boitsov AV 1999; Laverov et al. 1992c, 1995). *Uranium regions and districts: NC N* Russian Federation./Stavropol Dist., *EG* Ergeninsky reg., *KK* Karelian-Kolsky (Baltic Shield) reg., *ON* Onezhsky (Lake Omega) Dist., *LA* Ladozhsky (Lake Ladoga) Dist., *VU* Volga-Ural reg., *TU* Transural reg., *WS* West Siberian reg., *YS* Yenisey reg., *TB* Transbaykal reg., *VI* Vitim Dist., *CTB* Central Transbaykal subreg., *AD* Aldan reg., *FE* Far East reg., *BU* Bureinsky Dist., *KH* Khankaisky Dist., *CH* Chukotsky reg., *SV* Severnoye, *CK* Chaika etc., *CP* Chaplinskoye, *OK* Okhotsk reg., *SK* South Kolima River reg. *Isolated U deposits/occurrences: a* Belskoye, *b* Briketno/Zheitunghinskoye, *c* Badieiskoye, *d* Kedrovoe, *e* Kremnistoye, *f* Kavly, *g* Dzhhigda, *h* Butugichag)



Annual uranium production in Russia is speculated at 300–400 t U until about 1970. It reached a peak of about 4 000 t U in the 1980s. In 1990, 3 776 t U were recovered, decreasing to 2 160 t U in 1995. A turn around in the downward trend was achieved with an increase to 2 605 t U in 1996 and to 3 280 t U in 2004.

10.1 Transural Region/Kurgan Area

The Transural region stretches for 600 km from the Sosva river southward to the Tobol river in southwestern Siberia but extends from Russia further south- and southeastward for several hundreds of kilometers into Kazakhstan. Major towns are Kurgan and Chelyabinsk (► Fig. 10.2, 10.3).

A number of deposits and occurrences of basal-channel sandstone-type are reported. The most significant ones occur in the southern part of the region, to the south of Kurgan. They include *Dolmatovskoye* (10 200 t U RAR), *Dobrovolnoye* (7 700 t U RAR + EAR-I) and *Khokhlovskoye* (speculated 10 000 t U). Two small deposits are *Vinogradovskoye* and *Cherepanoskoye* each containing less than 1 000 t U. Ore grades average 0.04–0.05% U. The total potential resources of the entire Transural region are thought to be on the order of 120 000 t U.

One deposit of surficial or sandstone type, *Sanarskoye*, located in the western extremity of the Transural region was mined by open pit and ISL methods from 1968 to 1980 yielding 440 t U. Ore grade was 0.08% U. The depleted deposit was hosted in a valley filled with Quaternary carbonaceous sandy sediments. Uranium was associated with organic matter.

The former operator was S.C. “Malyshevsk Mining Administration” based at Asbest, Sverdlovsk Province, established in 1967 originally for the supply of beryllium and tantalum to the nuclear industry recovered from pegmatites in the Ural mountains.

ISL mining began at *Dolmatovskoye* in 2002 with a nominal production capacity of 800 t U yr⁻¹ (production was about 250 t U in 2005). *Khokhlovskoye* is in the development stage for U extraction by ISL techniques. Operator is the recently formed joint-stock company JSC “Dalur”.

Source of information. Boitsov 1999; Laverov et al. 1992; and Loutchinin 1995a, 1995b unless otherwise stated.

Regional Geological Setting of Mineralization

The Transural uranium region is in the SW part of the West-Siberian Platform. The region is characterized by *Middle to Upper Jurassic* paleochannel systems, which occupy the southwestern alluvial coastal plain of the Jurassic sea in the eastern foreland of the Caledonian Ural mountains. The channels were incised into a basement of *Devonian* felsic volcanics, continental and marine sediments (► Fig. 10.3).

Paleodrainage systems consist of 1–5 km wide channels filled with 30–120 m thick, permeable alluvial-fluvial sediments of *Bathonian-Kimmeridgian* age. Lithologies include beach gravel, conglomerate, sand, silt and mud containing

high amounts of plant debris (av. 0.5–3% C_{org}). Three sedimentary cycles are distinguished, which are attributed to attenuating movements during the final folding and uplift phase in the Ural mountains. Subsequent to the orogenic activity, the river valleys degraded to chains of drainage lakes into which proluvial and limnic sediments were deposited during *Late Jurassic – Early Cretaceous* (Volga stage and Berriasian) time. These sediments consist of 30–150 m thick impermeable, pink, carbonaceous silt, clay and sand, which contain 100–300 ppm U in form of syngenetic uranium associated with dispersed plant remains. 300–700 m thick *Cretaceous and Tertiary* sediments increasing to the east, north and south rest on the Jurassic rocks.

The northern limit of the uranium region is conterminous with the northern boundary of the Late Jurassic – Early Cretaceous pink sediments, which in turn coincides with the boundary between the late Jurassic semi-arid and humid climate zones to the south and north respectively.

Principal Host Rock Alteration

Oxidation and re-reduction altered the U-bearing grey alluvial-fluvial sediments. Both alteration facies do not contain either Fe-oxides or carbonaceous matter. A redox interface resulted from downstream influx of oxygenated waters. Re-reduction documented by bleaching is assumed to postdate the deposition of the overlying, impermeable pink facies. Reducing agent was plant debris originally present in high amounts of up to 3% C and more.

Principal Characteristics of Mineralization

Principal *U minerals* are colloform U-oxides and coffinite. *Associated minerals* include chalcopyrite, ferriselite, jordisite, marcasite, pyrite, sphalerite, native selenium, and rhenium and vanadium oxides. Additional elements in detrital minerals are Sc, Y, and lanthanides. The uranium and associated minerals occur in disseminated form along redox interfaces. Isotope dating of U minerals yield an age of 135 ± 7 Ma.

General Shape and Dimensions of Deposits

Individual deposits have resources from several hundreds to 12 000 t U mostly contained in several ore bodies. Ore grades range from 0.01 to 3% U and average 0.03–0.05% U.

Deposits are from less than 1 to 25 km long, 50–1 500 m wide and up to 50 m thick and occur at a depth in excess of 300 m. Individual ore bodies have dimensions of <1 to 7 km long, 50–700 m wide, and 1.5–20 m thick. Ore bodies display in plan view an elongated lens or ribbonlike configuration and in section predominantly a lenticular and, more rarely, a roll shape. Lenses occur singularly or en echelon stacked at several levels separated by aquicludes. Some of the ore bodies trend along and others oblique to channel axes (► Figs. 10.4, 10.5).

■ Fig. 10.2.

West Siberia. Paleogeomorphological map of the West-Siberian Platform illustrating the typical restriction of basal-channel sandstone-type U deposits of the Transural and West Siberian uranium regions to Jurassic (J_3) southern coastal alluvial plains (younger rocks not shown) of the Jurassic sea, which developed during a semiarid climate. Deposits of the Yenisey uranium regions occur within the Caledonian fold belt (after Loutchinin 1995a; Dolgushin et al. 1995; Laverov et al. 1992c). **U regions:** *TU* Transural, *WS* West Siberian, *YS* Yenisey. **Deposits:** *Bys* Bystroye, *Dob* Dobrovolnoye, *Dol* Dolmatovskoye, *Ked* Kedrovoye, *Kho* Kholovskoye, *Lab* Labyschkoye, *Mal* Malinovskoye, *Prg* Prigorodnoye, *Pri* Primorskoye, *San* Sanarskoye, *Smo* Smolenskoye, *Sol* Solonechnoye, *UU* Ust-Uyuk; in Kazakhstan: *Sem* Semizbayskoye, *Sen* Sensharskoye, *Tob* Tobolskoye

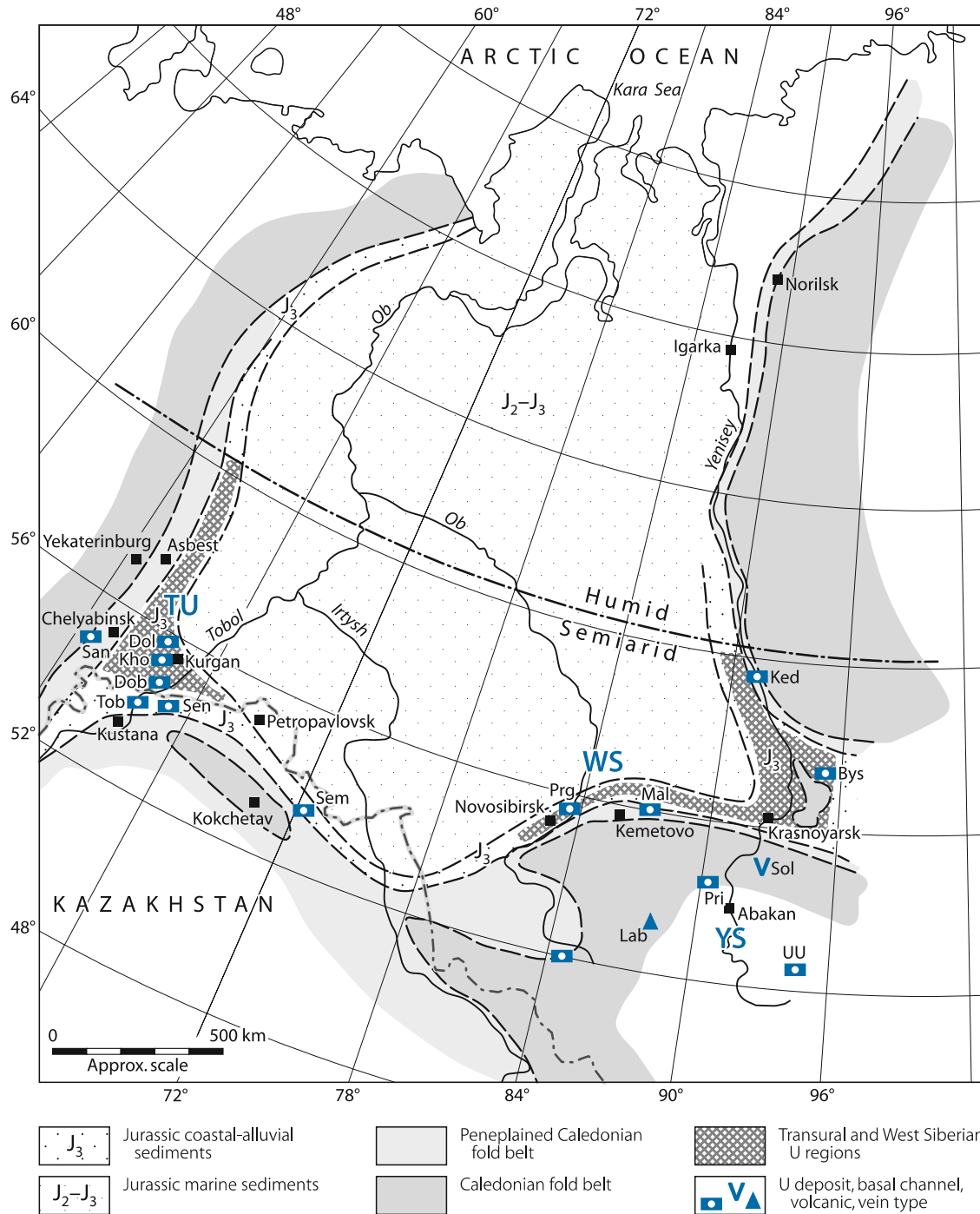
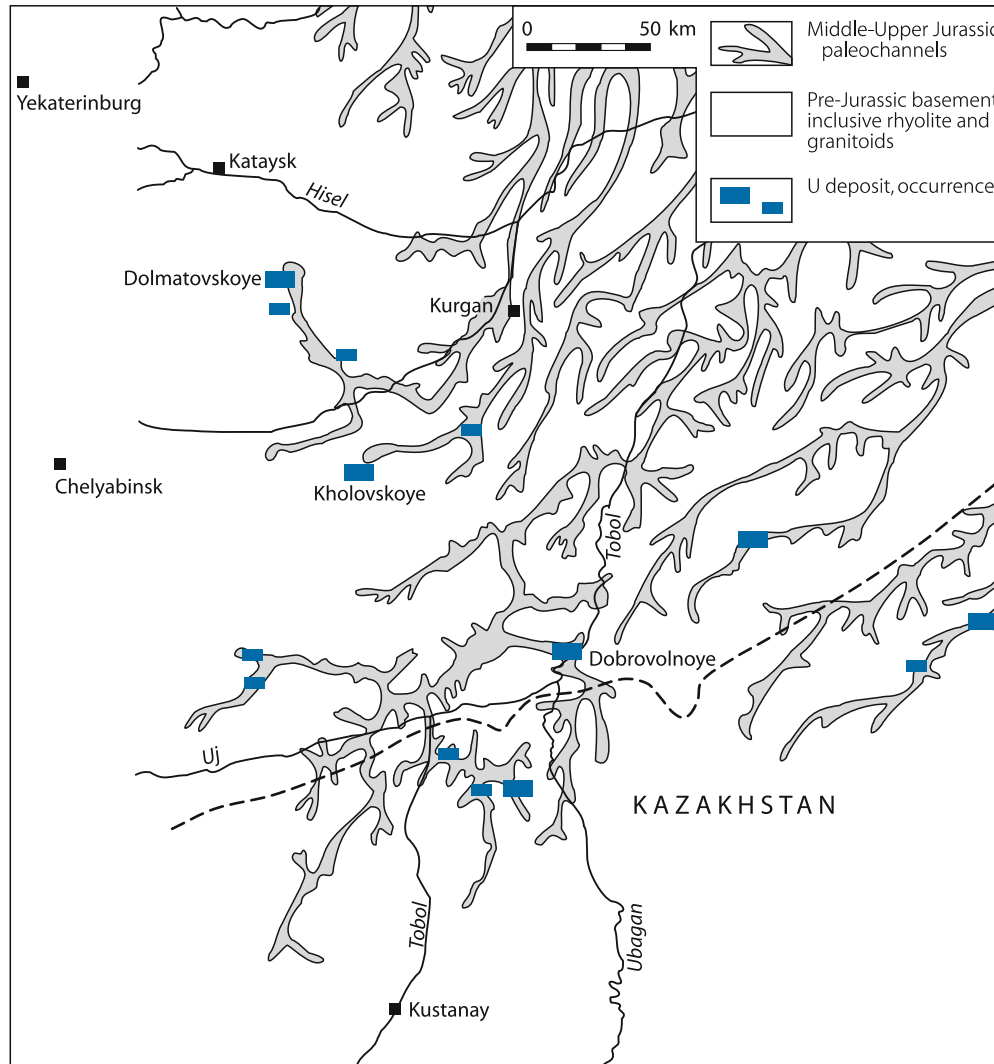


Fig. 10.3.

Transural region. Generalized paleogeological map of Middle to Late Jurassic paleochannel systems and related basal-channel sandstone-type U deposits and occurrences at the southwestern margin of the Middle-Upper Jurassic sea. Cretaceous to Quaternary cover not shown (after Loutchinin 1995a; Laverov 2000)



Principal Ore Controls and Recognition Criteria

Mineralization is primarily lithologically and geochemically controlled. Significant ore controlling parameters or recognition criteria of deposits of the Transural region include:

Host environment

- Basement of Devonian volcanics and continental and marine sediments
- Paleosurface weathered during semiarid climate
- Old peneplain incised by Middle to Late Jurassic paleodrainage systems
- Valleys filled with Middle to Late Jurassic continental clastic sediments
- Cover of Late Jurassic–Early Cretaceous impermeable, pink proluvial – limnic sediments overlain by thick Cretaceous to

Recent sediments providing protection against erosion of ore hosts

- Rhyolite with 4–5 times background U contents presumably provided potential U sources

Host rocks

- 30–150 m thick alluvial-fluvial sediments composed of well permeable beach gravel, conglomerate, sand, silt, and mud of Middle to Late Jurassic age
- Reduced facies of grey color and high content of carbonaceous matter (av. 0.5–3% C_{org}) and minor sulfides

Alteration

- Oxidation with formation of redox fronts
- Re-reduction reflected by bleaching

- Reduction potential provided predominantly by organic matter and subordinately by sulfides
- Redox fronts developed downstream by channel invading vadose waters

Mineralization

- U-oxides/sooty pitchblende and coffinite
- Large number of associated elements
- Disseminated texture of mineralization
- Elemental zoning
- Lens- and roll-shaped ore bodies
- Ore bodies trending along and oblique to channel axes
- Ore restricted to grey facies containing in excess of 0.2% C_{org}
- Regional distribution of deposits correlating with extension of pink proluvial-limnic cover facies

Principal Aspects of Metallogenesis

Deposits are of epigenetic origin derived from oxygenated meteoric waters. Loutchinin (1995) postulates that the solutions must have entered the permeable grey alluvial-fluvial horizon at the valley heads in the western uplands. Elsewhere impermeable sediments of the pink proluvial-limnic facies prohibited the downward percolation of mineralizing solutions. The oxygenated solutions oxidized the originally reduced grey facies and established redox fronts along which uranium and associated elements (Mo, V, Se, and Re) were fixed in a zonal distribution typical for these types of deposits. Ore concentration was restricted to lithological intervals containing 1.5–2.5% C_{org} .

Since the mineralizing solutions could have entered the alluvial horizon only at the exposed valley heads, the source of uranium must have been located in this region of the Ural foreland. Rocks in this region include rhyolite with 4–5 times background U values.

The main stage of uranium mobilization is attributed to an early weathering period under semiarid conditions affecting the peneplain formed during the waning stage of tectonic activity in the Ural region.

10.1.0.1 Dolmatovskoye

This deposit (Fig. 10.4) is located about 50 km S of the town of Dolmatovo. Original in situ resources amount to 10 200 t U (RAR). Ore grade is 0.039% U. A number of ore bodies occur at a depth of 360–500 m in an 11 km long main and an 8 km long tributary paleovalley. The valleys are locally up to 3 km wide. Channel facies are Middle-Upper Jurassic alluvial sediments composed of pink oxidized and grey reduced sandy gravel, sandstone and conglomerate interbedded with silty mudstone. Overburden consists of Cretaceous and younger sediments. The channels are incised for about 100 m deep into Upper-Middle Paleozoic slate, limestone and, towards the headwaters to the

SW, into Devonian rhyolite and rhyolite-porphphy. Faults trend E-W, NW-SE, and NE-SW.

Uranium is present as coffinite and pitchblende. Ore grades range from 0.01 to 3% U. High-grade U sections may contain Mo, Re, Sc, and REE minerals. Uranium distribution is controlled by redox boundaries in sand-gravel aquifers. In plan view, most ore bodies are lenticular in shape markedly elongated along the valley axis. In cross-section, they show a lenticular or roll-shape. Ore bodies occur individually or stacked at several levels separated by argillaceous aquicludes. Individually ore bodies are from 400 to 4 500 m long, 50–700 m wide, and 2–12 m thick. Rolls can be as much as 20 m thick (Naumov et al. 2005; Boitsov 1999).

10.1.0.2 Dobrovolnoye

Dobrovolnoye is located 100 km SW of Kurgan. RAR and EAR-I are estimated at 7 700 t U at an ore grade averaging 0.053% U. Dobrovolnoye is in the northern Turgai Basin where it covers a 17 km long stretch in the Ubagan paleovalley (Fig. 10.5). Middle-Upper Jurassic alluvial-fluvial sediments subdivided into three sedimentary cycles fill the valley. Each of the cycles contains uranium.

Four main ore bodies are delineated in three aquifers at a depth of 485–690 m with approximately 80% of the resources positioned at a depth of about 570 m. The ore bodies are of elongated lens or ribbonlike configuration but some display also rolls shapes. Some of the ore bodies trend along and others oblique to the channel axes. Individual ore bodies are from 1 to 7.5 km long, 50–800 m wide, and from 1.5 to 17.5 m thick. Ore grades range from 0.01 to 3% U (Loutchinin 1995a, 1995b; Boitsov 1999).

10.1.0.3 Khokhlovskoye

The deposit was discovered 1992 close to the Shumikha settlement. Speculative resources amount to 10 000 t U. Ore grade is 0.036% U. Host rocks are Upper Jurassic alluvial-fluvial sediments in a paleovalley incised into pre-Mesozoic shale, limestone, tuffite, and tuff-sandstone. A 10–50 m thick mineralized horizon occurs at a depth of 525–620 m. It was traced for 14 km along the paleochannel. Individual ore bodies are up to 12.8 m thick and average 6.2 m. Uranium tenors range from 0.01 to 0.3% U. Coffinite and pitchblende are the principal U minerals (Boitsov 1999).

10.2 West Siberian Region/Novosibirsk-Kemerov Area

The region extends as a relative narrow curvilinear belt along the southeastern edge of the West-Siberian Platform, from the south of Novosibirsk eastward for some 900 km to beyond Krasnoyarsk. The eastern portion around Krasnoyarsk adjoins with the Yenisey uranium region (see below). The belt coincides largely with the alluvial coastal plain of the Jurassic sea (Figs. 10.2, 10.6).

Known deposits are of basal channel sandstone type. Largest deposit is *Malinovskoye* (see below). The Malinovskoye area additionally includes the *Spirinskoye* and *Usmanskoye* U occurrences both hosted in the Jurassic Usmanskaya channel, and the *Novoalexandrovskoye* occurrence in the Tyshtymenskaya channel (► Fig. 10.7). Other, smaller deposits with resources on the order of 1 500–5 000 t U occur elsewhere in the region. They include *Prigorodnoye* located some ten kilometers to the NE of Novosibirsk, *Smolenskoye* in the southwestern part of the region both hosted in Tertiary paleochannels, and *Bystroye* in a Jurassic paleochannel near the eastern boundary of the region (► Fig. 10.6). Host rocks of many deposits are clastic sediments with limited permeability.

Total in situ resources of the West Siberian region in the up to \$80 per kg U cost category are estimated at approximately 40 000 t U. Ore grades of deposits are on the order of several hundreds ppm U.

Sources of information. Boitsov 1999; Boitsov and Nikolsky 2001; Dolgushin et al. 1995.

10.2.0.1 Malinovskoye

Malinovskoye is a basal channel sandstone-type deposit located 60 km SW of the town of Mariinsk. In situ resources are estimated at about 15 000 t U. Average ore grade is less than 0.06% U.

Malinovskoye is in the Jurassic, N-S-trending, 50 km long and 1–3 km wide Malinovskaya paleovalley (► Fig. 10.7). Depth increases from 70 m in the headwaters to 300 m in the downstream section. The channel is incised into a basement of Cambrian volcanic-sedimentary rocks into which granite and diorite were intruded, and Devonian terrestrial and continental volcanic sediments intruded by post-Devonian granite and syenite. Mesozoic sediments as much as 300 m thick rest on the

■ Fig. 10.4.

Transsural region, Dolmatovskoye deposit. **a** Schematic geological map at a level about 300 m below surface showing the distribution of alteration zones and U ore bodies in a Middle to Late Jurassic paleochannel. Overlying Cretaceous-Quaternary sediments not shown. **b** Geological SW-NE cross-section (after Naumov et al. 2005)

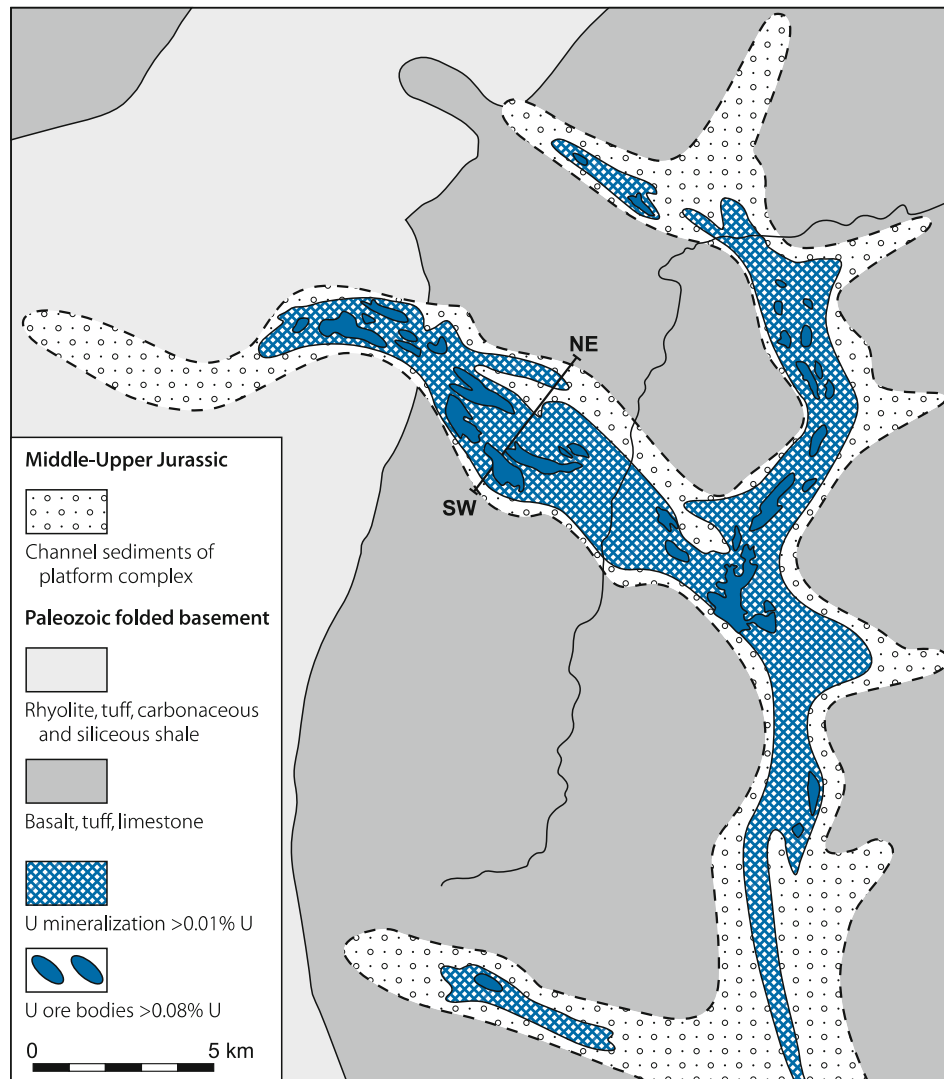
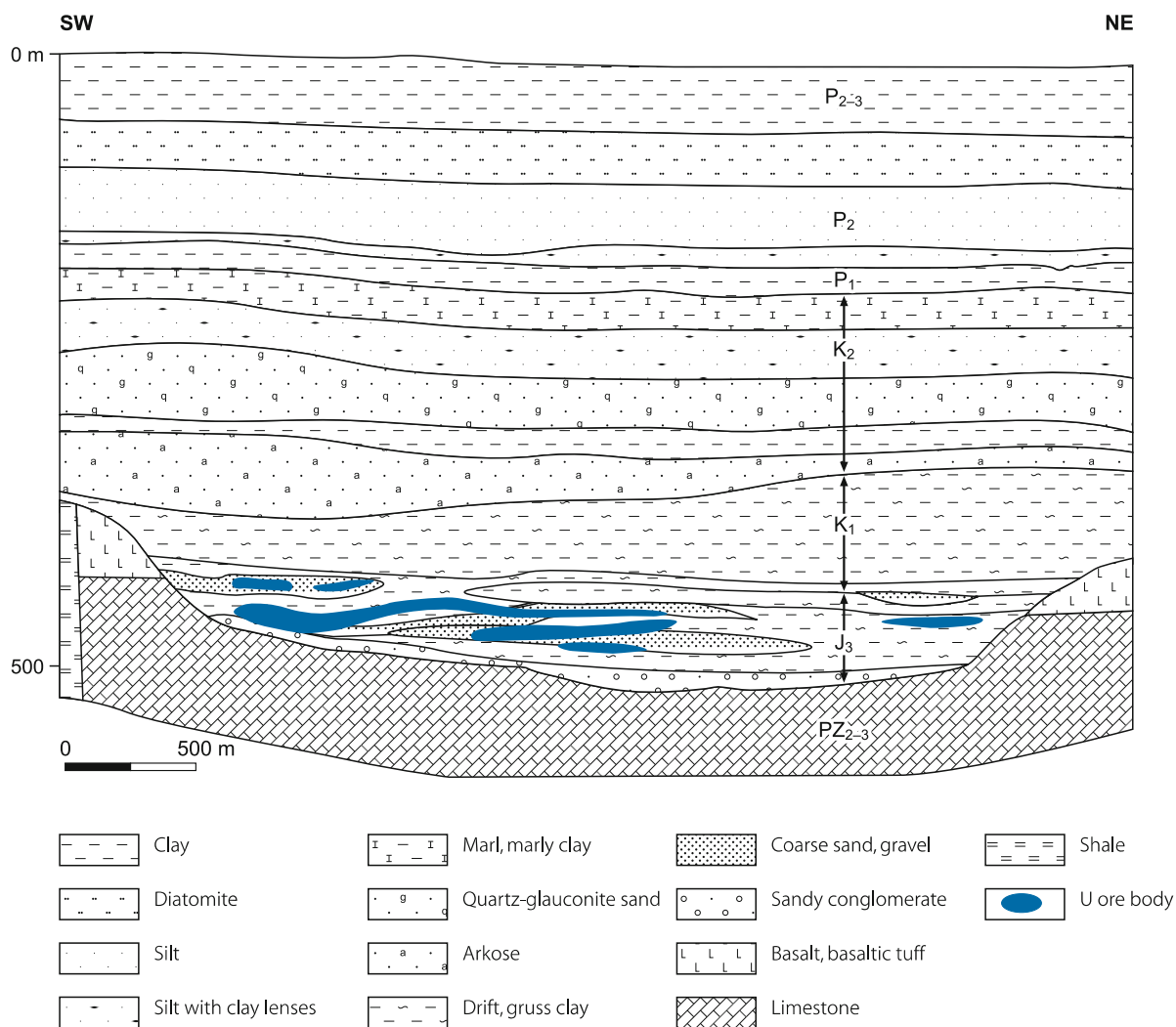


Fig. 10.4. (Continued)



channel facies. They start with 50–110 m thick, pink, Lower Cretaceous clays, which are overlain by up to 200 m thick Lower to Middle Cretaceous sands interbedded with kaolinic clays.

The paleovalley is filled with 70–120 m thick, alluvial sediments of the Late Jurassic–Early Cretaceous Bazhenovsky Horizon. Mineralized lithologic facies are grey, carbonaceous sands of variable grain size alternating with conglomerates, clay and silt beds. Coalified vegetal remains are abundant, particularly in the basal part of the channel. Thin, 0.1–0.5 m thick lignite seams are locally intercalated. The filtration factor varies in the aquifer between 0.65 and 17.

Mineralization is found over an 18.5 km long channel interval. It envelops a 2.6 km long, 100–300 m wide, and as much as 50 m thick ore zone at a depth of 100–300 m below surface. Ore occurs in lenticular and roll-shaped lodes within in two stratigraphic horizons, which are separated by an aquiclude. One horizon is 1.8 km long, 16–90 m wide, 1–15 m thick and occurs at a depth of 247–300 m in the eastern part of the paleochannel. The other horizon is 2.5 km long, 50–250 m wide, 0.7–20 m thick, and 277–300 m deep.

Mineralization consists primarily of disseminated sooty pitchblende. Pitchblende and coffinite occur subordinately.

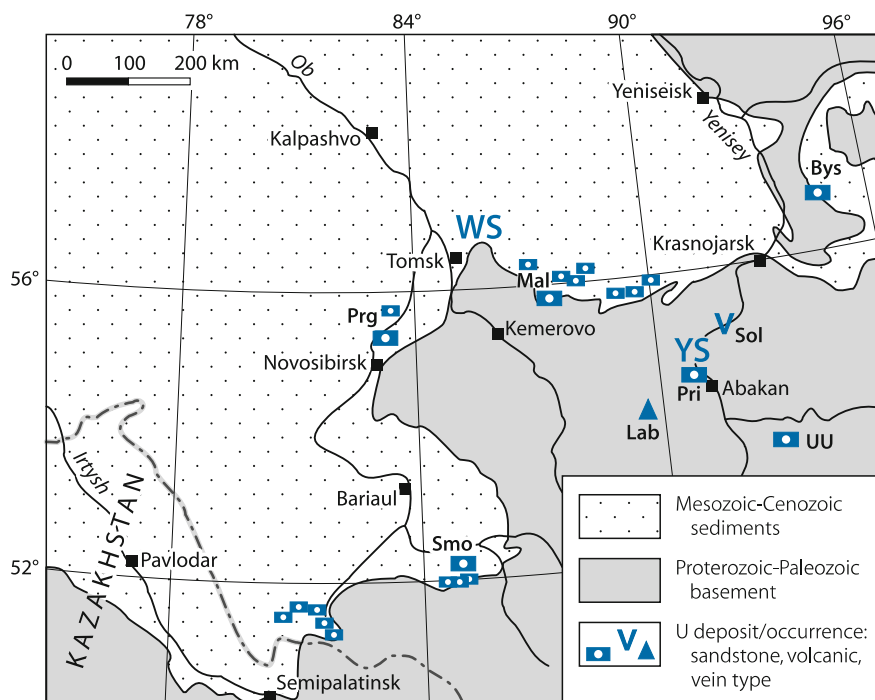
Ore grades vary between 0.013 and 0.139% U but go locally as high as 1.32% U. Associated elements average <0.045% Mo, <0.1% V, 0.01–0.15% Cu, 0.01–0.15% Pb, 0.01–0.15% Zn, <0.002 Sc, <0.015% Y, <0.02% Ge. Carbonate content is 0.5% CO₂. The clay fraction averages 17%.

10.3 Yenisey Region

The Yenisey uranium region occupies the upper Yenisey River–Altay–Sayan area, with the town of Abakan in its center. Early reports going back to 1925 report V–U mineralization in Permian carbonaceous or coal beds at Minussinsk and Abakan in the Paleozoic Minussinsk Depression, which covers over 16 000 km². Post-World War II exploration discovered a number of uranium occurrences. Ten occurrences of various types are reported (Figs. 10.2, 10.8). Representative occurrences of sandstone type include *Primorskoye* and *Ust-Uyuk*, of vein, type *Labyshkoye*, and of volcanic, type *Solonechnoye*. The first two occurrences have resources in excess of 5 000 t U and grades ranging from 0.1 to 0.3% U while the others contain between few hundreds to few thousands t U at grades of less than 0.1% U.

■ Fig. 10.6.

West Siberian (WS) and Yenisey (YS) regions. Regional geological map with location of U deposits and major occurrences. Deposits in the West Siberian region are typically of basal-channel type in Upper Jurassic alluvial-fluvial sediments whereas the Yenisey region contains deposits of various types in Paleozoic-Proterozoic rocks (after Dolgushin et al. 1995) *U regions*: WS West Siberian, YS Yenisey. *Deposits*: Bys Bystroye, Lab Labyshkoye, Mal Malinovskoye, Prg Prigorodnoye, Pri Primorskoye, Smo Smolenskoye; Sol Solonechnoye, UU Ust-Uyuk



Total resources of the Yenisey region are estimated at 40 000 t U in the \$130 per kg U cost category. They include 8 000 t U in the RAR + EAR-I class and 32 000 t U in the EAR-II class.

Source of information. Boitsov and Nikolsky 2001.

Regional Geology and Mineralization

The Yenisey uranium region is an orogenic terrane with uplifts and depressions. Proterozoic – Lower Paleozoic granite-metamorphic complexes constitute the cores of uplifts. They are locally mantled by early orogenic felsic and mafic continental volcanics of Lower Devonian age. Depressions are filled with late orogenic continental sediments, predominantly pink sandy siltstone of Upper Devonian-Carboniferous age. Jurassic sediments cover part of the older rocks. Major faults trend about ENE-WSW, N-S to NNW-SSE, and NNE-SSW.

10.3.0.1 Primorskoye

Primorskoye was discovered 75 km N of Abakan in 1970. It is a tabular sandstone-type deposit. Estimated resources are 7 600 t U. Ore grade averages 0.25% U.

Uranium occurs in an alternating sequence of Upper Devonian sandstone, siltstone, and claystone of lacustrine origin in the Minussinsk Basin. Mineralization is bound to 0.3–0.5 m thick lenses of grey, highly carbonaceous (up to few percent carbon) sediments. Ore bodies display two configurations, irregular tabular or lenticular associated with argillaceous limnic facies, and ribbon-like in fluvial sand and clay facies within channel systems (► Fig. 10.9). Principal U mineral is coffinite while pitchblende occurs in minor amounts. Texture of ore is finely disseminated. Ore grades range from 0.05 to 2% U. Isotope datings of ore minerals yield ages of 340–370 Ma (Mashkovtsev et al. 1995).

10.3.0.2 Ust-Uyuk

Ust-Uyuk is a basal-channel sandstone-type deposit located about 300 km SE of Abakan. Resources are in excess of 5 000 t U. Grades are on the order of several hundreds ppm U.

Ust-Uyuk is hosted in a paleochannel within the Tuvinsky Basin. Host rocks are Upper Devonian alluvial sediments composed of alternating sandstone, siltstone, mudstone, and tuff. U phases are dominated by finely disseminated coffinite. Pitchblende and sooty pitchblende are present in minor quantities. Mineralization occurs in form of elongated lenses but also of roll shaped bodies commonly positioned at the contact of pink and grey facies.

10.3.0.3 Labyshkoye

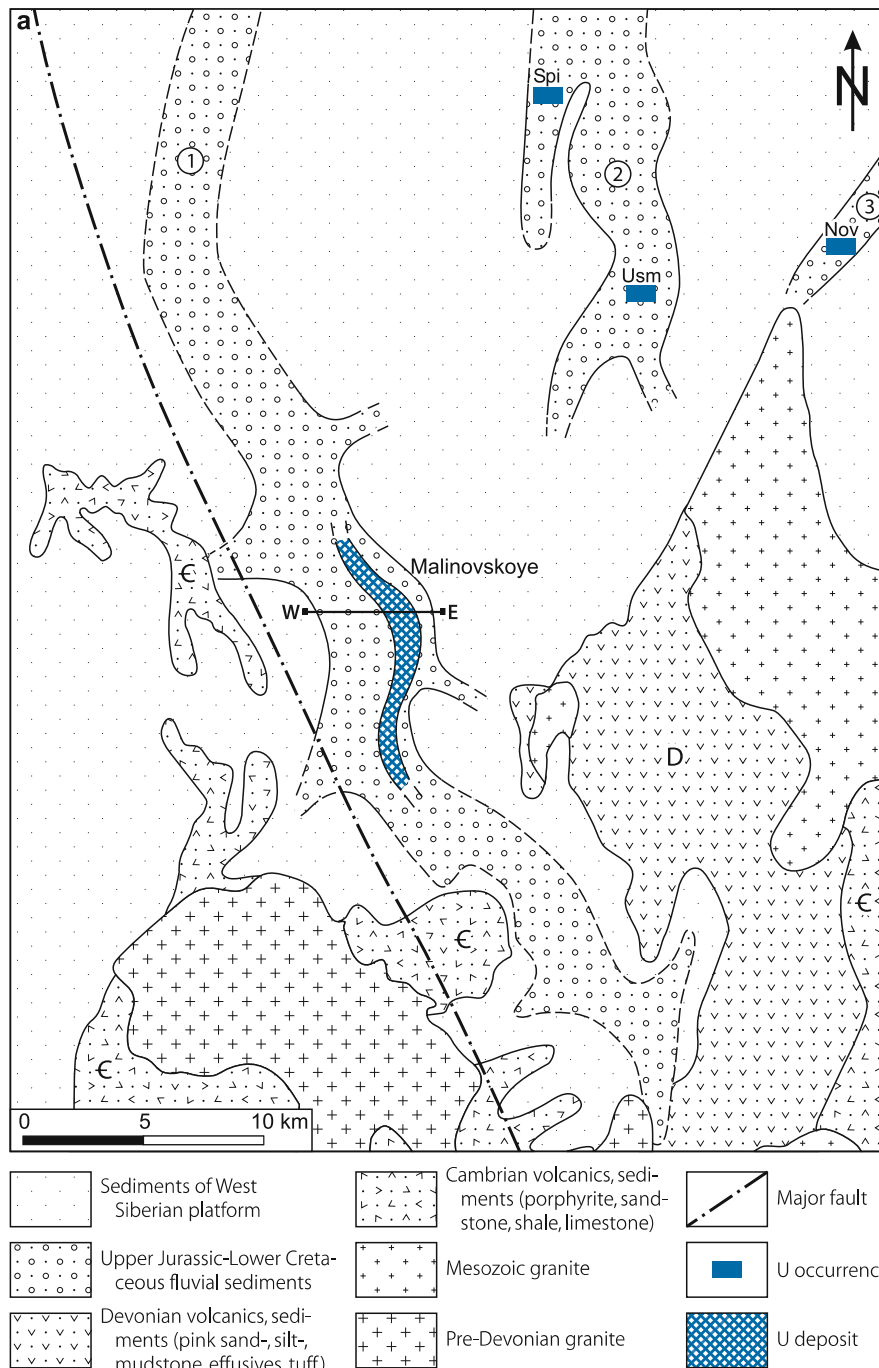
Labyshkoye was discovered about 250 km WSW of Abakan in 1960. The vein-type deposit is hosted in Cambrian marble, quartzite, and granite. Resources amount to some 1 500 t U. Grades are on the order of 0.1–0.3% U.

10.3.0.4 Solonechnoye

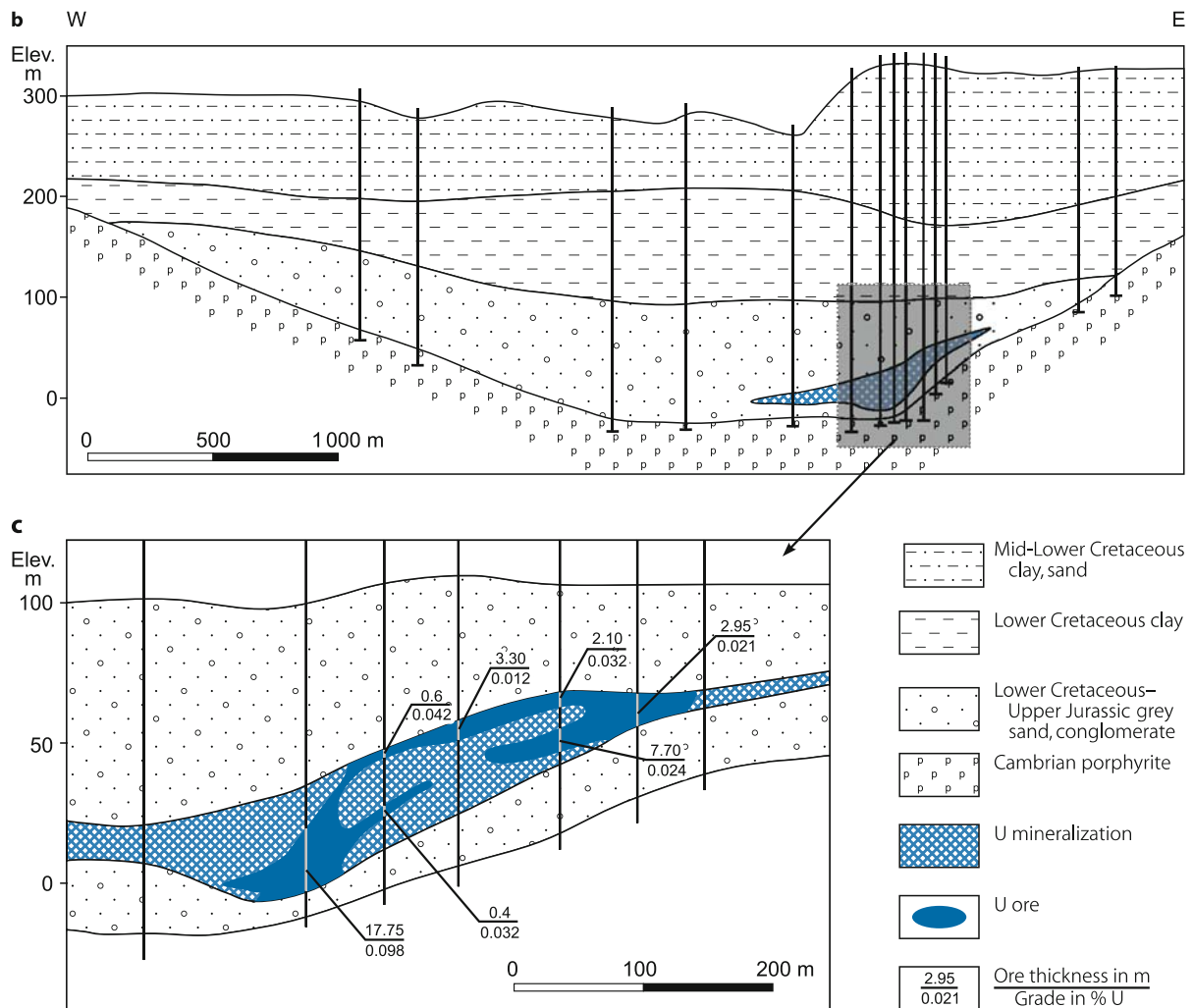
Solonechnoye is situated about 240 km NNE of Abakan and was discovered in 1961. It is a small (some 3 000 t U) volcanic-type deposit hosted by Lower Devonian felsic and mafic effusive rocks and tuff. Grades are several hundred ppm U.

Fig. 10.7.

West Siberian region, Malinovskoye deposit. **a** Generalized geological map; **b** W-E cross-section showing the position of the deposit at the basal eastern flank in the paleochannel; **c** Enlargement of the ore interval with U grade distribution along drill holes (after Dolgushin et al. 1995; Naumov et al. 2005; Boitsov and Nikolsky 2001). **Explanation for a Paleochannels:** 1 Malinovskaya, 2 Usmanskaya, 3 Tishtimskaya. **U occurrences:** Nov Novoaleksandrovskoye, Spi Spirinskoye, Usm Usmanskoye



■ Fig. 10.7. (Continued)



10.4 Transbaykal Region

A number of uraniumiferous areas are established in the Transbaykal region between Lake Baykal to the west and the Chinese-Mongolian border to the east and south. Most prominent are the *Streltsovsk* and *Vitim* districts (► Fig. 10.10); the first was the sole active mining district in Asian Russia during the 1990s and early 2000s while deposits in the Vitim District were tested for ISL mining in 2006. Other areas with numerous, mostly small uranium occurrences are mentioned by Pelmenev (1995) and Vishnyakov (1995) for the *Central Transbaykal subregion*.

10.4.1 Streltsovsk District, Asian Russia

The district is 12 km SE of the town of Krasnokamensk in eastern Transbaykalia, Chita Province, approximately 40 km to the west of the Chinese border formed by the middle course of the Argun River (► Figs. 10.10, 10.11). The Streltsovsk District is by reserves, grades, and production unique among volcanic-type U deposits of the world.

Mineralization is related to a volcanic caldera and largely controlled by structures. Deposits are therefore classified as

structure-bound volcanic type. Two principal ore varieties are distinguished, monometallic uranium and polymetallic uranium-molybdenum (-fluorite) ores.

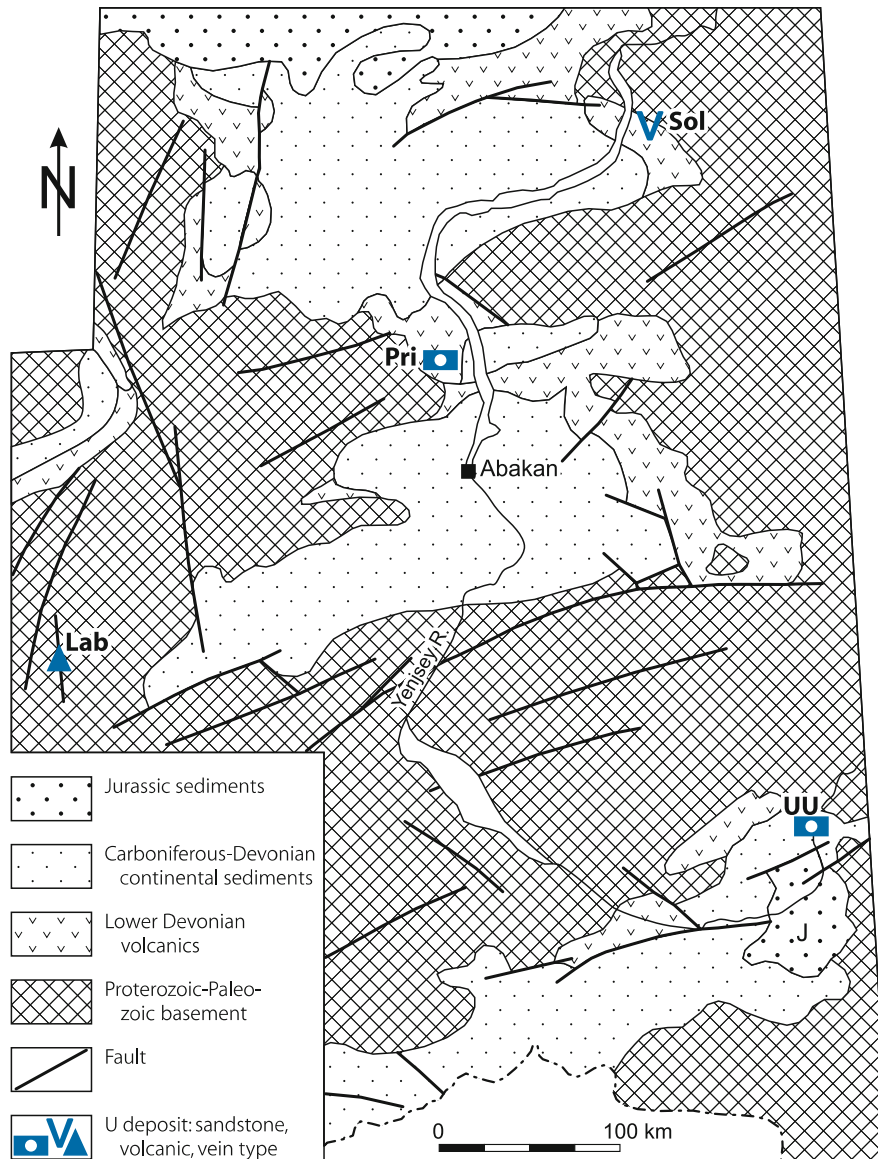
The first deposit was discovered in 1963 by drilling below fluorite veins that carried minor uranium mineralization. By 1979, nineteen uranium deposits had been found within an area of about 150 km² in size (► Fig. 10.11, ► Table 10.1). Largest deposits are *Streltsovskoye*, *Tulukuyevskoye*, and *Octyabrskoye* in Jurassic-Cretaceous volcanic-sedimentary rocks, and *Antei* and *Argunskoye* in Paleozoic granite and Proterozoic marble of the basement, respectively.

Original in situ resources of the district were estimated at some 280 000 t U (Laverov et al. 1992b, c). OECD-NEA/IAEA (2005) reports remaining reserves of 11 7120 t U RAR in the up to \$80 per kg U category including 42 900 t U in the less than \$40 per kg U cost category.

Since the begin of mining in 1968 (*Tulukuyevskoye*), ten deposits have produced uranium, eight by underground workings and two by open pits (► Table 10.1). Some of the mines produced also molybdenum and some fluorite. Open pit extraction was at *Tulukuyevskoye*, which was partly also mined underground, and at *Krasny Kamen*. Both deposits are depleted. Underground mining took place at *Streltsovskoye* (largely

Fig. 10.8.

Yenisey region, Abakan area/upper Yenisey river. Generalized geological map with location of U deposits (after Laverov et al. 1992c).
La Labyshkoye, Pr Primorskoye, So Solonechnoye, UU Ust-Uyuk



depleted), *Antei, Luchistoye, Martovskoye, Novogodneye, Shiron-dukuyevskoye, Vesennee, and Yubileinoye*. In situ ore grades of these deposits average 0.1–0.3% U at a cutoff grade of 0.039% U. In 2004 *Antei* and *Streltsovskoye* were in operation. The other six underground operations were on standby. *Antei*, the deepest mine with workings between 400 and 900 m below surface, is practically a depth extension of *Streltsovskoye*.

Cumulative production of the *Streltsovsk* District through 2005 is in excess of 100 000 t U. Annual production averaged almost 3 500 t U during the 1980s but dropped in the 1990s from 3 776 t U in 1990 to 2 160 t U in 1995. A turn around was achieved with 2 605 t U in 1996 rising to 2 880 t U in 2004. Mining capability is 6 700 t ore per day.

Most of the ore was and is recovered by conventional methods. Since the mid 1990s, some low-grade ore is also treated by

heap leaching and in place leaching methods. Open pit mining ceased in 1997.

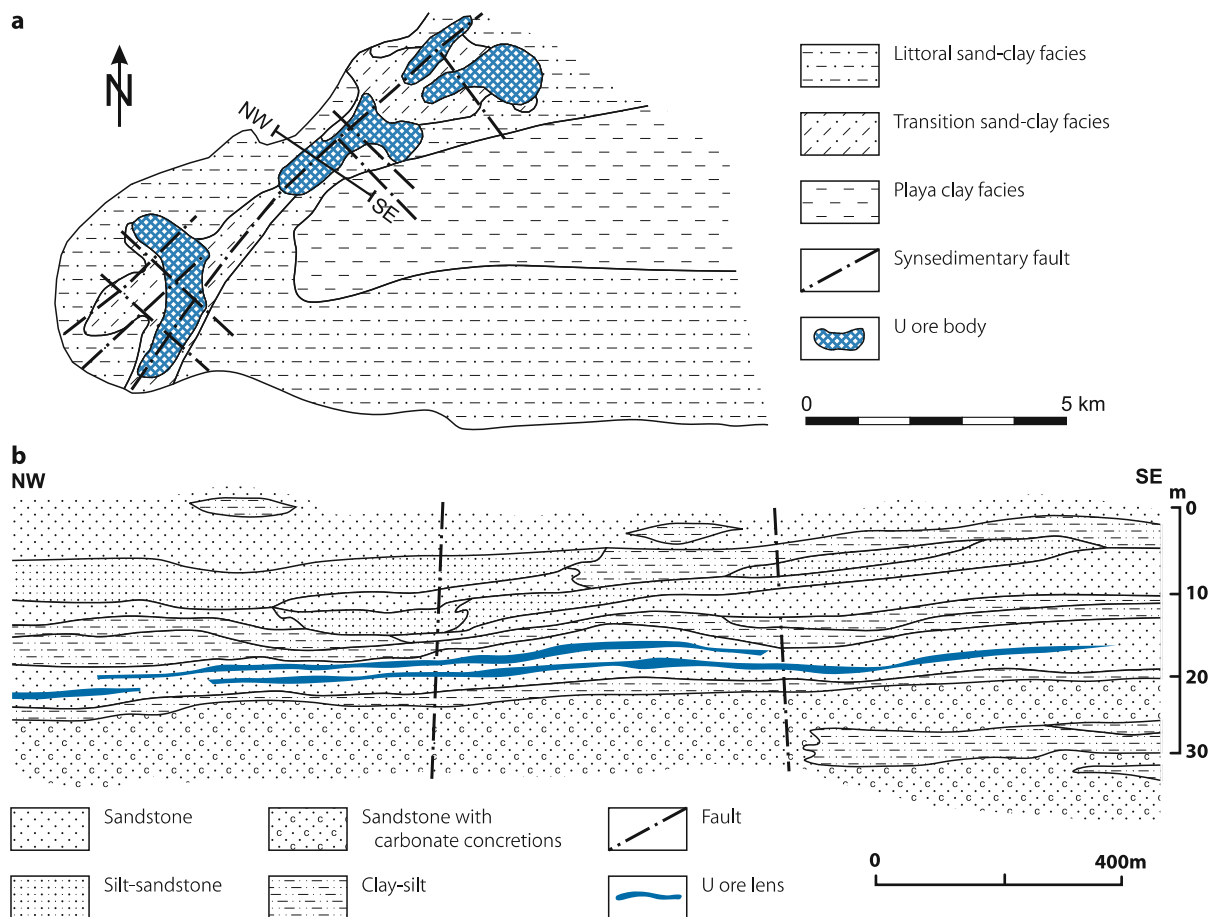
A hydrometallurgical plant with an sulfuric acid leach circuit is located 15 km from the town of *Krasnokamensk*. It started operation in 1974 and has a nominal capacity of about 3 500 t U yr⁻¹ and a daily throughput of 4 700 t ore. Up to 1995 the plant also treated ore from the *Dornod* uranium district located some 500 km to the southwest, in northeastern Mongolia.

Mining and milling operator is JSK “*Priargun Mining and Chemical Production Association*” (PPGHO) with headquarters at *Krasnokamensk*, a joint stock company owned by the state.

Source of information Aleshin et al. 2003a,b, 2005; Andreeva et al. 1990, 1996a,b; Boitsov et al. 1995; Chernyshev and Golubev

■ Fig. 10.9.

Yenisey region, Primorskoye deposit. **a** Schematic geological map illustrating the control of ore bodies by an intermediate sand-clay facies within an Upper Devonian lacustrine environment. **b** NW-SE lithologic-stratigraphic profile with position of ore lenses (after Mashkovtsev et al. 1995)



1996; Ischukova 1989, 1995, 1997; Laverov et al. 1992a–c, 1993, 2000; Kazansky 1995; Miguta and Modnikov 1993; OECD-NEA/IAEA 1993–2005; Nikolsky and Schulgin 2001; and other sources. Additional information is available in earlier papers cited by the here listed authors and more recent literature listed in Bibliography. Among new publications, which became available after finishing this manuscript, the interested reader is in particular referred to the book “Uranium deposits in volcanotectonic structures” by Ischukova et al. (2002).

Regional Geological Setting of Mineralization

The district coincides with the Tulukuyevsk (also referred to as Streltsovsk) Caldera, a Lower Cretaceous–Upper Jurassic volcanic-sedimentary complex composed of two joint calderas, a major eastern and a minor western caldera. The caldera measures some 15 km in diameter and 150 km² in size. The Tulukuyevsk Caldera is within the Mongol–Priargun continental volcanic belt. The belt has been traced for more than 1 000 km across Transbaykalia in Russia, northeastern Mongolia and

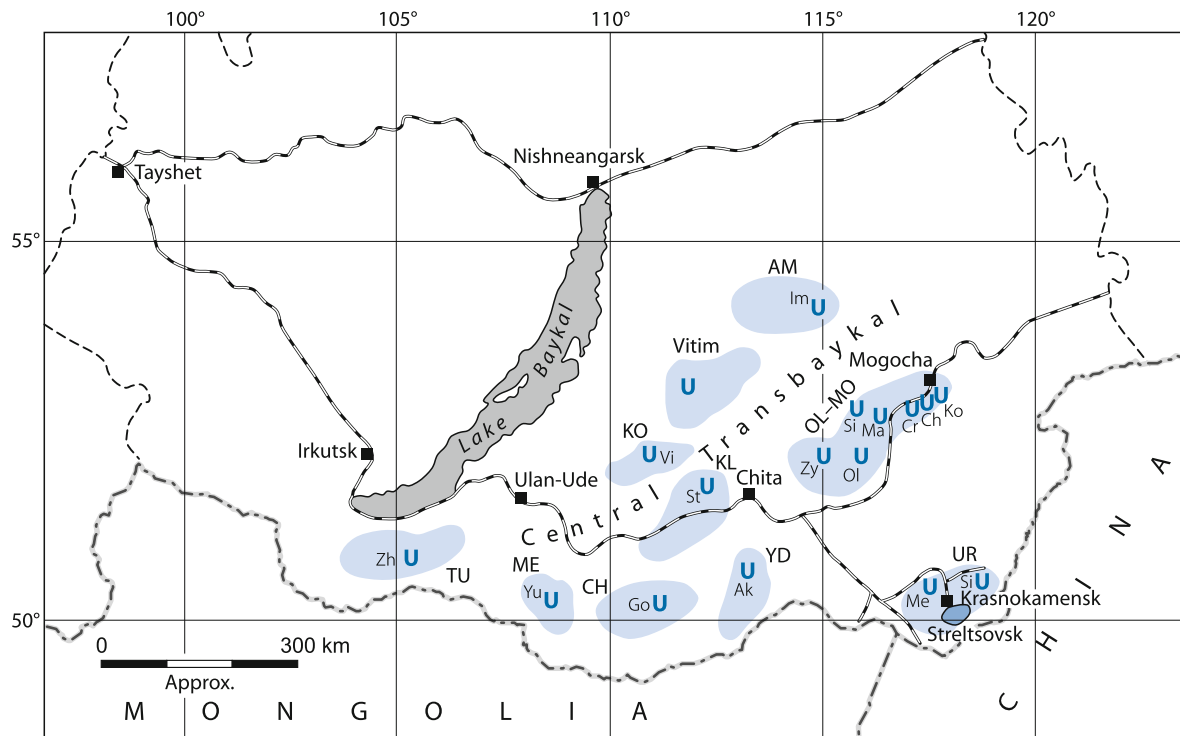
northeastern China where it contains the Dornod uranium district, and uranium showings in the Manzhouli area, respectively.

The position of the Tulukuyevsk Caldera is controlled by the conjugation and intersection of several repeatedly reactivated, deep reaching, submeridional and NE–SW-oriented shear zones (► Figs. 10.11, 10.12). The caldera tops a Paleozoic granite batholith of the Transbaykal Massif, a separate tectonic block of the Paleozoic Ural–Mongolian fold belt. Xenoliths of Proterozoic metamorphics (gneiss, amphibolite, dolomitic marble) and pegmatite occur in the granite.

Caldera lithologies include over 60 facies ranging from mafic to felsic volcanics and intercalated clastic sediments. The rocks are grouped into two volcano-sedimentary series: The upper *Turgin (Turginskaya) Series* is of Lower Cretaceous age and largely restricted to the central-eastern part of the caldera. It consists primarily of felsite, rhyolite with intercalated basalt and andesite sheets, and sandstone and conglomerate beds. The lower *Priargun (Priargunsky) Series* is of Upper Jurassic age and exposed almost all around the upper unit and occupies most of the western caldera. It includes three

Fig. 10.10.

Transbaykal region. Schematic map with location of the Streltsovsk, Vitim (details see Fig. 10.11 and Fig. 10.12, respectively) and other districts and related ore fields (OF) in Central Transbaikalia (after Pelmenev 1995; Vizhnyakov 1995a–c). Ore fields in Central Transbaikalia (deposits/occurrences in brackets): AM Amalat OF (*Im Ima* or *Imskoye*); OI-MO Olovo-Mogocha area: Olov OF (*OI Olovskoye, Zy Zylzinskoye*); Korolevo-Chasovo OF (*Cr Crystalnoye, Ch Chasovoye, Ko Korolevskoye*); Si Sigirlinskoye, Ma Mayak; UR Urulyunguevsky depression (*Me Meridionalnoye, Si Sirotininsk*) (overlaps N part of Streltsovsk/Tulukuyevsk Caldera) contains two stratiform U deposits in Lower Cretaceous argillized rocks; KO Kholoisky OF (*Vitlauskoye*); KL/Khiloksky OF (*Stepnoye*); YD Yuzhno Daursky OF (*Akuinskoye, Barun-Ulacha, Vostochnoye*); CH Chikoisky OF (*Gornoye, Berezovoye*); ME Mensensky OF (*Yugalskoye*); TU Tunguisky OF (*Zhuravlinoye*) (See Fig. 10.11 for details of the Streltsovsk and Fig. 10.20 for the Vitim ore fields)



alternating basalt and trachydacite sheets interbedded with thin horizons of dacitic tuff, ignimbrite, sandstone and conglomerate. A basal conglomeratic bed rests unconformably on the basement.

A generalized litho-stratigraphic column shows the following principal facies units (from top to bottom):

Lower Cretaceous Turgin (Turginskaya) Series

- Felsite sheet, up to 260 m thick: up to 10 m thick quartz porphyry and 1–15 m thick fluidal felsite horizons
- Plagioclase trachybasalt horizon, 30–140 m thick
- Pink conglomerate horizons, 40–90 m thick

(Three andesite horizons composed of andesite-basalt, plagioclase basalt, and andesite with trachybasalt are intercalated in the middle and lower sections of the Turgin Series.)

Upper Jurassic Priargun (Priargunskaya) Series

- Upper basalt sheet, up to 180 m thick: lava and lava breccia
- Upper fluidal trachydacite sheet, up to 75 m thick
- Middle basalt horizon, 10–240 m thick: massive basaltic lava, lava-breccia, and conglomerate; restricted to the southern part of the deposit

- Lower trachydacite sheet, 60–350 m thick: massive and fluidal trachydacite, tuff, lava, and ignimbrite horizons
- Lower basalt sheet, up to 400 m thick: lava sheets and conglomerate lenses, thickness depends on basement relief
- Basal conglomerate horizon, up to 50 m thick: paleoweathered conglomerate, sandstone, siltstone layers

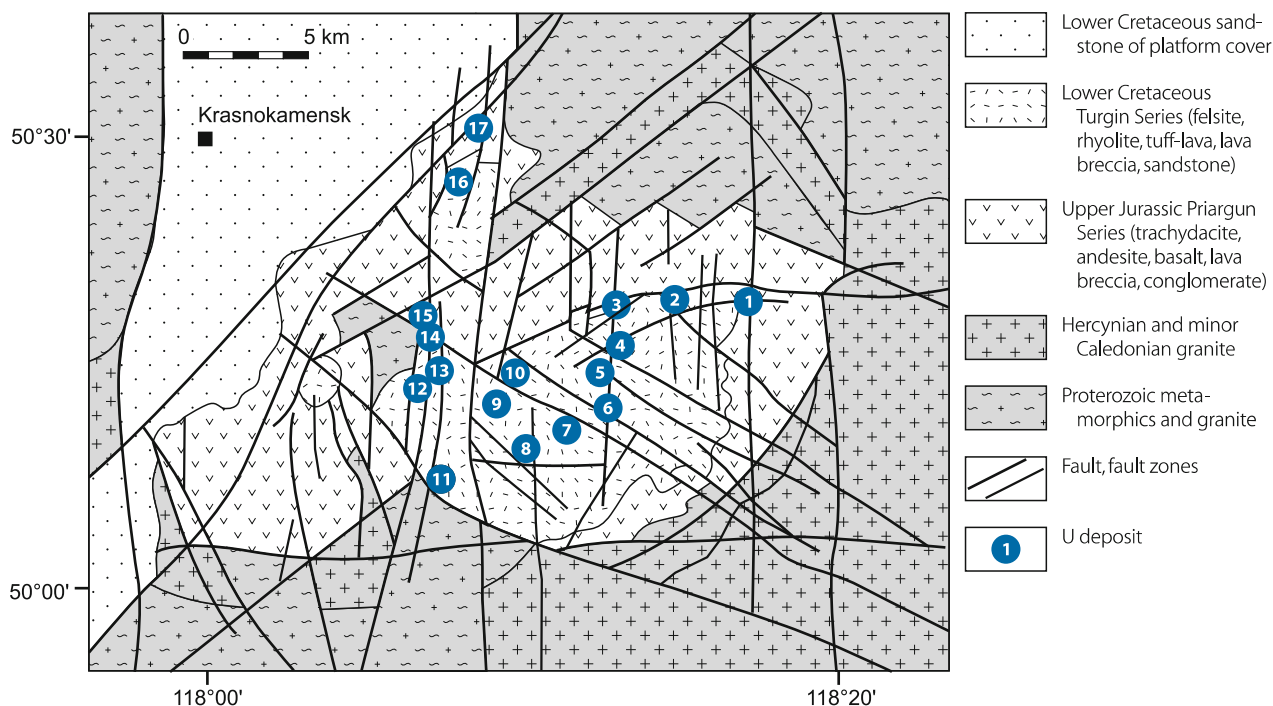
Total thickness of the caldera fill varies between 200 and 1 400 m, and averages 500–800 m. Intercalated sedimentary beds are from few meters to 100 m thick. Gently dipping stratified effusive sheets and sedimentary rocks dominate the eastern part of the caldera. Subvolcanic felsite, rhyolite and syenite-porphyry necks occur at intersections of major fault zones with crosscutting structures.

Numerous, about NE-SW-, N-S-, NW-SE-, and E-W-trending faults cut the caldera and adjacent terrane (Figs. 10.11, 10.12). Major faults persist into the basement. Late Cretaceous block faulting generated grabens adjacent to the caldera. Coal-bearing clastic sediments of Late Cretaceous and younger ages fill the grabens.

Ischukova (1997) alludes to the ore-controlling significance of major N-S-, NE-SW- and NW-SE-oriented, steeply inclined fault zones. N-S-oriented structures, such as the *Meridional Shear Zone*, are 500–900 m wide and consist of closely spaced

■ Fig. 10.11.

Streltsovsk region, generalized map showing the regional geological setting of the Lower Cretaceous-Upper Jurassic Tulukuyevsk (also named Streltsovsk) Caldera and location of uranium deposits (after Nikolsky and Schulgin 2001). *U*-deposits: 1 Shirondukuyevskoye and Vostochno-Shirondukuyevskoye, 2 Streltsovskoye and Antei, 3 Oktyabrskoye, 4 Martovskoye, 5 Luchistoye, 6 Malo Tulukuyevskoye, 7 Yubileinoye, 8 Novogodneye, 9 Vesennee, 10 Tulukuyevskoye, 11 Yugo Zapadnoye, 12 Krasny Kamen, 13 Pyatiletneye, 14 Zherlovoye, 15 Argunskoye, 16 Bezrechnoye, 17 Dalnee



faults. They control U deposits where they are intersected by NW-SE- or NE-SW-trending shear zones. A prominent representative of the NE-SW system is the 3–5 km wide *Argunskaya Shear Zone*. It consists of numerous NE-SW- and E-W-oriented faults associated with intervals of closely spaced fractures/joints, which developed in response to repeated reactivation throughout the Proterozoic and Paleozoic and during the Mesozoic sedimentary-volcanogenic activity.

Shallow dipping fault systems include gently pitching, gouge filled faults/fractures at the contact between the basement and overlying sedimentary-volcanogenic strata, and at the interface of the Priargun and Turgin series. In the latter case, the fault/fracture systems preferentially cut tuffaceous and sedimentary horizons in the footwall of felsite sheets.

Principal Host Rock Alteration

Proterozoic and Paleozoic (Pt₂-Pz₂) polychronic granitization and updoming were accompanied by silica-alkaline metasomatism (Ischukova 1997).

Late Paleozoic high-temperature metasomatism modified wall rocks along faults to K-feldspar (microcline) rocks, albitite (albite-1), greisen with fluorite, sulfides, and occasionally cassiterite, and, in the western Tulukuyevsk Caldera, skarn. Fine-scaled muscovite of these facies yield an age of 250–230 Ma (Arakelyants et al. in Andreeva et al. 1996).

Late Mesozoic tectonic events were linked with intense pneumatolytic-hydrothermal activity of acid nature and resulted in halos of silica-potassic-sodic alteration and greisens along reactivated shear zones. Principal alterations include albitization (albite-2), silicification, hydromicization, sericitization/beresitization, carbonatization, chloritization, argillization, and hematization. [Note: In Russian studies, the term *hydromica* is usually applied to mixed-layered minerals of the illite-smectite type with a low (<15%) content of swelling interlayers.] The mode of alteration depends on the lithology and displays a zoning. Silicification, sericitization/hydromicization prevail in the volcanic and sedimentary rocks while albitization is more typical for the crystalline basement. The types of wall rock alteration also correlate with the three types of ore mineral parageneses.

Pre-ore alteration phases are reflected by hydromica-carbonate-quartz, sericite-carbonate-quartz, and kaolinite-carbonate-quartz facies. Syn-ore alteration is manifested by linear albitization and hematitization, as well as silicification, carbonatization, and argillization. For more alteration-related information see Sect. 10.4.1.1: *Streltsovskoye-Antei*.

Principal Characteristics of Mineralization

Principal uranium mineral is pitchblende. Coffinite and branerite are less common. Associated ore minerals include molybdenite, jordisite, femolite, pyrite, marcasite, and galena.

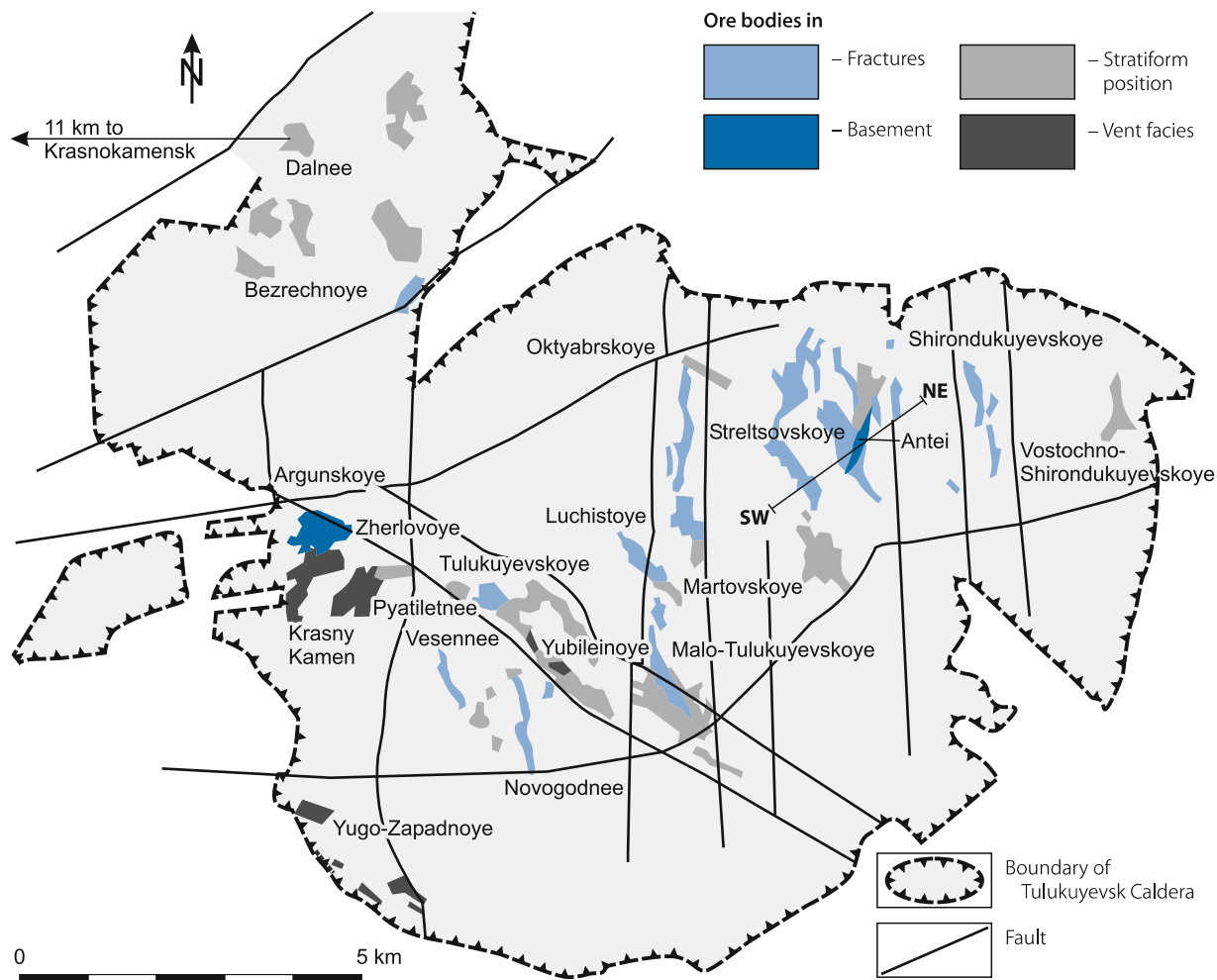
Table 10.1. Strel'tsovsk District, dimensions and status (2006) of individual deposits (after Ischukova 1997; Laverov et al. 1992; and other sources)

Deposit	Shape	Stratigraphy	Lithology	Length (m)	Width (m)	Depth interval (m a.s.l.)	Reserves (1 000 t U)	Grade (av.% U)	Co-/by-product	Status
Strel'tsovskoye	ve-stw	Jur-Cret	Bas, dac, fels, cgl	4 000	2 500	+720 to +300	71	0.19	Mo	Active UG
Antel	ve-stw	Up Pz	Grt	1 000	100	+350 to -700	40	0.30	Mo + F	Active UG
Argunskoye	stw	L Pt+Pz	Dol,grt	1 000	300	+550 to -350	30	0.17	Mo	Devel.prosp (UG)
Oktyabrskoye	stw-ve	Up Jur	Dac,bas	1 000	180	+600 to +250	23	0.25	Mo	Devel.prosp (UG)
Tulukuyevskoye	stw-ve	L Cret	Fels,ss, cgl	1 300	250	+720 to +450	37	0.24	Mo	Depleted OP,UG
Krasny Kamen	ve-stw	L Cret	Fels	400	100		0.25	0.14		Depleted OP,UG
Shirondukuyevskoye	stw-ve	Jur-Cret	Fels,ss, cgl, bas			+600 to +300	10	0.18		Standby UG
Luchistoye	stw	L Cret	Fels, cgl	1 000	200	+700 to +400	10	0.21	Mo	Standby UG
Martovskoye	ve-stw	L Cret	Fels, cgl	1 300	200	+700 to +480	5	0.17	Mo	Standby UG
Yubileinoye	tab, stw	L Cret	Fels, ss	1 000	250	+660 to +300	10	0.19		Standby UG
Vesennee	ve, tab	L Cret	Fels, ss				1.4	0.21		Standby UG
Novogodneye	ve, tab	L Cret	Fels, ss				4	0.25		Standby UG
Malo Tulukuyevskoye	stw-ve	Up Jur	Dac, bas				12	0.19	Mo	Devel.prosp (UG)
Zherlovoye	ve	L Cret	Fels, eff (rhy)	550	200	+450 to 0	?	0.07		Explored
Pyatiletneye	ve-stw	L Cret	Fels, rhy	500	250		7	0.10		Explored
Yugo Zapadnoye	ve-stw	L Cret	Fels, rhy	1 500		+600 to +200	5	0.10		Explored
Bezrechnoye	tab, stw	L Cret	Cgl, ss				1	0.09		Explored
Dalnee	tab, stw	L Cret	Ss, tuff, cgl, fels		<6 m thick	+600 to +400	7	0.12		Explored
Vostochno-Shirondukuyevskoye	tab, stw	L Cret ?	Cgl, ss?				1.5	0.11		Explored

Depth interval: a.s.l. = above sea level, surface is about 650–750 m a.s.l.; Reserves, Grade: estimated original in situ; Shape: stw stockwork, tab tabular/lensoid/stratiform, ve vein; Lithology: bas basalt, cgl conglomerate, dac dacite/trachydacite, dol dolomitic marble, eff effusive, fels felsic, grt granite, por porphyry, rhy rhyolite, ss sandstone.

■ Fig. 10.12.

Streltsovsk District, simplified map with surface projected contours of uranium deposits in the Lower Cretaceous-Upper Jurassic Tulukuyevsk Caldera (NE-SW section indicates position of ▶ Fig. 10.13) (after Krotkov et al. 1997)



In oxidized intervals, primary U minerals are predominantly altered to uranophane and sooty pitchblende, and molybdenite to ilsemannite and uranium-molybdates (iriginite, umohoite, mourite). Gangue minerals include albite, ankerite, calcite, dolomite, chlorite, fluorite, sericite, and quartz. Pitchblende and other ore and gangue minerals are present in several generations.

Ischukova (1997) established 6 ore-related mineral parageneses:

1. Kaolinite and hydromica (pre-ore argillization)
2. Cryptocrystalline quartz-carbonate-sulfide
3. Albite-brannerite (first ore phase)
4. Quartz-molybdenite-coffinite-pitchblende (major ore phase)
5. Quartz-molybdenum-sulfide phase
6. Calcite-fluorite-dickite (post-ore phase)

Boitsov et al. (1995) distinguish *three principal ore varieties*, from oldest to youngest: albite-coffinite-brannerite, quartz-molybdenite-pitchblende, and chlorite-carbonate-pitchblende. The first two assemblages contain less than 6% carbonate and

typically occur in the volcano-sedimentary suite and basement granite. The carbonate-bearing paragenesis has in excess of 25% carbonate when hosted in basement dolomite (Argunskoye), and 6–25% carbonate when it occurs in andesite, basalt, or conglomerate. Although the spatial distribution of the three varieties is primarily related to specific host rock lithologies, the assemblages often show telescoping.

These authors further subdivide mineralization according to the prevailing ore minerals into *four ore types*:

- *Pitchblende ore* is predominantly composed of pitchblende, with minor (commonly less than 20% of U components) coffinite, brannerite, and locally uranophane and sooty pitchblende. Associated Mo minerals are femolite, ilsemannite, iriginite, and molybdenite. Ore minerals fill voids and fissures. Pitchblende ore exhibits streaky, cocard, mottled, breccia, cement, and massive modes of aggregation. Predominant distribution is on upper levels of the volcano-sedimentary sequence. Pitchblende ore constitutes the bulk of reserves in most deposits. Ore grades vary between low and high ranging from <0.2 to >1% U. Mo content is from 0.01 to 0.03% Mo.

- *Complex molybdenite-pitchblende ore* contains the same mineral assemblage as pitchblende ore but differs from this by a higher Mo content. Ore textures correspond to those of pitchblende ore. Predominant distribution is in upper levels of the volcano-sedimentary sequence. The Argunskoye deposit contains substantial amounts of complex U-Mo ore in xenoliths of dolomitic marble in basement granite. This ore features a dolomite content ranging from 25 to 96%, averaging 70%. Reserves are second to pitchblende ore. Ore grades range from 0.2% to >1% U. Mo content is in excess of 0.03% Mo.
- *Coffinite ore* is dominated by coffinite. Other ore minerals occur in minor amounts. Ore textures are streaky, mottled, and disseminated. Prevailing distribution is in marginal parts of deposits. Reserves are of minor order. Grades are low to average (<0.2% U). Mo content is less than 0.015% Mo.
- *Brannerite ore* essentially consists of disseminated brannerite. Other ore minerals occur in subordinate quantity. Albite seems to be a characteristic gangue mineral of granite-hosted brannerite ore. Predominant distribution is at lower levels of deposits, particularly in basement granite and in trachydacite of the basal parts of the volcano-sedimentary sequence. Reserves are of minor order. Grades are low (<0.1% U). Mo content is less than 0.015%.

Fractures, cavities, pores, and metasomatic replacement features provided space for ore deposition. In result, mineralization has most commonly vuggy-disseminated, streaky-disseminated, and brecciated textures, but also occurs locally as veinlets and massive aggregates of ore minerals, which group to veins, stockworks, or stratiform-tabular lodes.

Mineralization occurs at several stratigraphic levels of the volcanic and sedimentary units and extends into the basement. Ore-hosting caldera lithologies range from felsic, intermediate and mafic effusive and neck volcanic facies to clastic sediments. Basement host rocks are granite and xenoliths of dolomitic marble in the apex part of the granite batholith.

Basement rocks host two large deposits, Argunskoye and Antei. Seventeen deposits occur in sedimentary-volcanogenic facies, thirteen of which in stratified effusive sheets and in sedimentary rocks, and four in volcanic neck facies.

According to Ischukova (1997), the majority of the deposits are associated with 500–900 m wide meridional shear zones at their junctions with NE-SW-oriented faults such as the Argunskaya Shear Zone. Segments of steeply dipping, NW-SE-striking fractures/joints in the sedimentary-volcanogenic strata characterize these sites. The steeply dipping fractures are best developed in effusive sheets and only to a minor degree in the less brittle sedimentary rocks. Basement-hosted ore bodies are controlled by either northeasterly or northwesterly striking faults.

General Shape and Dimensions of Deposits

Original in situ resources of the Strel'tsovsk District are estimated at approximately 280 000 t U contained in 19 deposits. Dimensions of the deposits are given in [Table 10.1](#).

Deposits are commonly composed of several ore bodies. Ore bodies are highly variable in shape, dimensions, internal structure, and grade. Ore bodies may extend intermittently over a vertical interval of about 800 m, a length of up to 300 m, and a width of up to 160 m. None of the ore bodies has a surface expression. Upper limit of ore lodes is between 50 m (Tulukuyevskoye) and 350 m (Antei) below surface. Most ore bodies start at a depth below 200 m.

Approximately 75% of the resources of the Strel'tsovsk District are at a depth interval from 200 to 600 m below surface where ore lodes are distributed at several levels in stratified sedimentary volcanogenic rocks. Largest deposits in this depth section include *Strel'tsovskoye*, *Tulukuyevskoye*, and *Octyabrskoye*. About 25% of the resources occur between 400 and 900 m deep. They are mainly contained in the two large and high-grade deposits *Antei* and *Argunskoye* hosted by granite and marble of the basement. Established depth of uranium ore is approximately 1 100 m but drilling intercepted also U mineralization down to a depth of 2 400 m in granitic basement.

The uranium content varies over a wide range, from the cutoff grade of 0.039% U to a few percent. [Note: 0.039% U is the normal cutoff grade used for conventional reserve estimation (i.e. non-in situ leach) in the CIS] The largest ore bodies have commonly the highest grades of up to between 0.6 and 3.0% U while most ore bodies average between 0.15 and 0.33% U. Several deposits contain additional to uranium molybdenum, while economic quantities of fluorite are rare.

Three principal configurations of ore bodies are discerned characterized by the following features:

- *Veins and veinlike* ore bodies are from several centimeters to about 25 m thick, from few meters to 700 m long, and 300 m high. Grades can be as high as 1% U. Dip is steep to shallow and may change abruptly. Greatest ore accumulations occur in highly fractured host rock intervals. Veins occur in almost all of the volcanic and sedimentary rocks and extend locally into the basement where it is heavily fractured. Veins extending into the basement are thickest near the contact to the overlying volcanics from where they rapidly thin downwards.
- *Stockwork* ore bodies are of complex linear or isometric configuration. Dimensions are on the order of up to 90 m wide, 300 long, and 600 m high. Grades can be as high as 0.6% U. Stockwork ore bodies are typically developed in favorable lithological units such as dacite and basement rocks.
- *Tabular/stratiform* ore bodies are from some tens of decimeters to a few meters thick, up to 1 400 m long and 1 000 m wide. Grades are on the order of 0.1 to several percent U. Reserves are small. Tabular ore lodes occur preferentially in cataclastic effusive sheets where these are overlain by felsite sheets and cut by both, shallow and steep dipping faults. Intercalated sandstone and conglomerate beds contain some stratiform mineralization. Minor tabular mineralization is found in sediments filling grabens peripheral to the Strel'tsovsk Caldera.

The bedded nature of the sedimentary-volcanogenic series and the repetition of brittle rocks at different levels caused a multi-layer distribution of ore lodes at six lithologic-structural

levels: Levels 1 to 5 are in the sedimentary-volcanogenic sequence. The 6th level is in basement rocks. As a general rule, the second level contains tabular lodes composed of gently dipping, mineralized fractures at the base of felsite sheets. The third and the fourth levels host the highest-grade ore contained in stockwork- or rarely vein-type lodes in trachydacite sheets. Smaller tabular lodes occur in sandstone of the basal horizon of the caldera fill.

Major deposits are predominantly of vein or stockwork configuration while stratiform deposits are commonly of smaller magnitude. But the various styles of mineralization may occur combined in a single deposit forming a complicated system of interlinked veins, stockworks, and stratiform lenses.

Stable Isotopes and Fluid Inclusions

Temperature deduced from stable isotopes and fluid inclusions data are 230–290°C for the pre-ore quartz-carbonate-sulfide stage, 200–150°C for the uranium, 150–50°C for the post-uranium stage (Ischukova 1995).

Regional Geochronology

Geochronologic data of rocks and ore minerals of the Streltsovsk District provided by Laverov et al. (1993) read as follows:

K-Ar rock dating (Laverov et al. 1985; Andreeva et al. 1991) of monomineralic fractions and whole rock samples from dacite of the lower volcanic-sedimentary sequence to syenite-porphyrries from subvolcanic stocks, yield K-Ar ages from 170 to 143 Ma. The various lithologies show a noticeable divergence in K-Ar data, except for the youngest rhyolite and syenite-porphyrries, the ages of which lie within a narrow span of 149–143 Ma (± 6 Ma) i.e. Upper Jurassic. The range of about 25 Ma is an approximate estimate of the duration of volcanism and the filling of the Streltsovsk depression.

K-Ar ages of mica of the pre-uranium hydromicization phase, which affected both, volcanics of the caldera and rocks of basement, range from 144 to 129 Ma. The youngest ages were found in finely dispersed micas of cataclastic and mylonitic zones and are thought the result of a “rejuvenation” by superimposed

processes. Micas outside the zones of dynamic metamorphism yield significantly narrower ranges of K-Ar ages, from 144 to 138 Ma. These values practically correspond to those of the youngest felsic volcanics. A Permian hydrothermal event is possibly indicated by K-Ar ages of 274–252 Ma obtained from biotite in granite below the caldera.

U-Pb ages of pure, massive pitchblende are within a narrow range of 136–134 Ma whereas massive pitchblende with coffinite inclusions give a 131–130 Ma age. The coffinite admixture probably causes the “rejuvenation”. Regenerated pitchblende yields a U-Pb age of 18–17 Ma indicating modification processes during the Neogene.

U-Pb systematics of disseminated uraninite mineralization in basement rocks yield concordant U-Pb data of 457 and 459 Ma for pure uraninite. Uraninite crystals with coffinite in microfractures and at the margin give lower, discordant values of 448–441 Ma. Samples that contained the impure uraninite also contained later molybdenite with inclusions of spherulitic pitchblende. U-Pb ages of the molybdenite-pitchblende aggregate vary between 156 and 150 Ma, which are close to the age of the principal U mineralization at the Streltsovsk deposits.

Several pre-, syn- and post-uranium generations of galena are noticed in the Streltsovsk deposits. Circumstantial evidence based on isotope data from polymetallic Pb-Zn mineralization in the Klichkinskoye ore field in the Transbaykal region suggest a formation at 140–130 Ma (Komarov et al. 1965), which practically coincides with the pitchblende age of the Streltsovsk deposits.

Potential Sources of Uranium

A variety of potential uranium sources are proposed including a magmatic, deep-seated crustal reservoir (Ischukova 1997), basement granite (e.g. Laverov et al. 1993) and felsic volcanics (rhyolite, particularly glassy phases). Volcanics are also thought to be the source of molybdenum. U and Th background values of selected lithologies of the sedimentary-volcanic caldera fill and caldera basement, which may be considered a potential U source, are given in [Table 10.2](#).

■ **Table 10.2.**

Streltsovsk District. Average U and Th background values of selected lithologies (Ischukova 1995)

Lithology	Number samples	U (ppm)	Th (ppm)	Th/U	Lithology	U (ppm)
Late Pz biotite granite	14	3.2	13.8	4.3	Early Pz amphibolite, amphibolite gneiss	2.1
Leucogranite	4	2.8	7.4	2.6	Quartz-mica-feldspar gneiss	4.4
Basalt	45	1.7	4.4	2.6	Granite-gneiss	3.7
Andesite-basalt	19	2.6	5.5	2.1	Porphyric granite	3.7
Trachydacite	15	7.7	22.8	3.0	Leucogranite	2.6
Trachydacite ignimbrite	39	7.2	21.6	3.0	Late Pz biotitic granite	2.8–4.46
Felsic ignimbrite	11	8.4	45.4	5.4		
Rhyolite	14	8.1	43.0	5.3		
Rhyolitic volcanic glass	14	19.0	40.2	2.1		

Granite below the caldera contains concentrations of accessory uraninite. Isotope data indicate this uraninite as one of the potential uranium sources for the uranium ore. A pre-Mesozoic source of the uranium is indirectly also supported by radiogenic lead in jordanite enclosed in pitchblende, the $^{207}\text{Pb}/^{206}\text{Pb}$ ratios of which suggest a 270–250 Ma old source for the lead (Laverov et al. 1993).

Principal Ore Controls and Recognition Criteria

Deposits are primarily of vein and stockwork and minor tabular configuration controlled primarily by structure and subordinately by lithology within a caldera. The marked difference in host lithologies – ranging from felsic, intermediate, and mafic effusives, to clastic sediments, granite and dolomitic marble – suggests that the petrochemical composition of the rocks had no significant influence neither on the depositional site nor on the quality and quantity of the ore. Physical or rock mechanical properties amenable to brittle deformation in reaction to tectonic stress primarily controlled the development of open spaces and as such provided the sites for ore deposition.

Significant ore controlling parameters or recognition criteria governing the position of deposits and style and distribution of mineralization include:

Host Environment

- Proterozoic metamorphic basement affected repeatedly by tectonic-magmatic events including the Caledonian and Hercynian Orogeny with intrusion of granites, and the Late Mesozoic Mongolian-Priargunian tectono-volcanic event
- Caldera of Upper Jurassic–Lower Cretaceous age largely composed of mafic to felsic volcanic sheets intercalated with terrestrial sediments
- Elevated U background values in basement granite (partly contained in uraninite)
- Elevated U background values in felsic volcanics particularly in vitreous facies
- Deep reaching regional faults
- Intense faulting, fracturing, brecciation along steep and shallow dipping N-S-, NW-SE- and NE-SW-oriented faults
- Grabens filled with terrestrial sediments
- Host rocks include
 - predominantly felsic to mafic volcanics, tuffs, and intercalated clastic sediments
 - exceptionally basement granite and enclosed xenoliths of metamorphites, particularly dolomitic marble
 - mainly silica-rich (<6% carbonate) and minor carbonate dominated (>6% carbonate) lithologies

Alteration

- Intense metasomatism of basement granite by albitization, microclinization, and greisens
- Polystage Mesozoic alterations of host rocks including albitization, silicification, sulfidization, carbonatization, chloritization, hydromicization, sericitization/beresitization, and argillization

- Vertical zoning of alteration reflected by silicification, hydromicization prevailing on upper and intermediate levels, sericitization and albitization on lowermost levels
- Correlation of types of wall rock alteration with types of ore mineral parageneses

Mineralization

- Monometallic U (<300 ppm Mo) and polymetallic U-Mo (>300 ppm Mo) mineralization
- Principal U minerals: U-oxide and minor U-silicate and U-Ti-phases
- Principal associated minerals: sulfides of Fe, Mo, Pb, carbonates, phyllosilicates, quartz, locally albite and fluorite
- Overprint of primary mineralization by deep reaching oxidation
- Disseminated, banded, streaky, and massive texture of ores
- Irregularly shaped vein, stockwork, and tabular-stratiform ore bodies, often interlinked in complicated fashion
- Locally vertical persistence of veins into basement (Strel'tsovskoye-Antei, Argunskoye)
- Position and configuration of ore bodies are related to
 - intersection of faults
 - intersection of transverse faults with volcanic dikes
 - sharp changes in dip of rock contacts cut by a fault
 - heterogeneous sections of volcanic rocks
 - intercalated pyroclastic and effusive sheets, and clastic layers cut by shallow and steeply inclined faults
 - unconformities between volcanic horizons

Principal Aspects of Metallogenesis

U-Mo deposits of the Strel'tsovsk District are – at least spatially – related to volcanics of the Strel'tsovsk Caldera. Although the U-Mo mineralization formed with a time gap of about 10 Ma after the youngest volcanics, a temporal hydrothermal link between volcanism and ore formation is documented by isotope ages of kaolinite and hydromica alteration that preceded the uranium deposition.

A number of metallogenetic hypotheses have been proposed with respect to the relationship of ore formation and volcanic processes. Some authors consider the felsic volcanism instrumental for the ore formation while others favor a magmatic, deep-seated crustal source as the main root for the ore-forming fluids. The origin of the ore metals still remains dubious. Was uranium, molybdenum concentrated as residues in final magmatic solutions or leached by such fluids from granite or felsic volcanics?

Laverov et al. (1993) summarize the principal views on the metallogenesis of uranium deposits in continental volcanic belts, which were formerly described as “uranium-molybdenum” or “uranium-fluorite” formations, or as “deposits in volcanic depressions” as follows:

1. The formation of the ore deposits was related to deep magmatic processes that occurred after volcanic activity ceased, and is chronologically discrete from continental volcanic processes (Smorchkov 1966).

2. The ore deposits were formed as a result of hydrothermal activity accompanying volcanic processes and are genetically linked with them (Kotlyar 1968).
3. Ore deposits formed at the final stage of volcanic activity under anomalous conditions of thermo-artesian systems of depressions. Metalliferous fluids of magmatic and meteoric origin were involved in ore formation (Anonymous/Usloviya Obrazovaniya 1972).

A substantial key for any genetic modeling of the Streltsovsk deposits is the age correlation between volcanism and ore formation, the duration of these processes, and the sources of ore forming elements. Laverov et al. (1993) address this matter based on isotopic geochronology of rocks and ore minerals and arrive at the following result. The Streltsovsk volcanic depression evolved over a period on the order of 25–30 Ma (± 5 Ma). The pre-ore and main ore stage hydrothermal processes were contiguous in time with the final phases of volcanism and lasted about 5 Ma. Later processes modified and partially redistributed the original uranium ore, at last during the late Cenozoic.

Mineralogical and geochronological evidence indicate an involvement of pre-Mesozoic uranium in the formation of the Streltsovsk deposits. Granite below the caldera contains concentrations of accessory uraninite that had crystallized at least 100 Ma earlier than the U-Mo ore. Isotope data indicate this uraninite as one of the potential uranium sources for the uranium ore. A pre-Mesozoic source of the uranium is also supported by radiogenic lead in 135 Ma old jordanite inclusions in pitchblende. $^{207}\text{Pb}/^{206}\text{Pb}$ ratios suggest an age of 270–250 Ma as source for the lead. A similar age was obtained from biotite in granite below the caldera, which yield K-Ar ages from 274 to 252 Ma and as such may possibly reflect a Permian hydrothermal event that may have concentrated uranium. Consequently, Laverov et al. (1993) postulate superimposed magmatic and postmagmatic processes to have played a significant role in the genesis of the Streltsovsk uranium deposits. (See also Sect. 10.4.1.1: *Streltsovskoye-Antei* for metallogenetic data.)

Ischukova (1997) elaborates on the evolution of the Streltsovsk District as follows: The geologic-metallogenetic history of the area started with polychronic granitization during the Proterozoic (Pt₂) and Paleozoic (Pz₂). During or after granite emplacement, the granite was affected by silica-alkaline metasomatism as reflected by local zones of quartz – K-feldspar – albite metasomatite and greisens along faults.

In Late Mesozoic time, the Streltsovsk Caldera evolved during a period of regional tectonic-volcanic reactivation. Associated hydrothermal processes include pronounced acidic leaching and silica-potassic-sodic alteration, and synchronous to subsequent ore formation along reactivated fault zones within and below the caldera. Greisens developed contemporaneously in the basement rocks. These processes are attributed to a deep seated, slowly evolving magmatic chamber. The chamber provided the material for the Paleozoic granite intrusions and Mesozoic volcanic extrusions, and generated the pneumatolitic-hydrothermal systems that metasomatized and altered the magmatic rocks, and, ultimately, the low temperature hydrothermal-metallogenetic system. A recurrent link in time between magmatic

differentiation and epigenetic processes is evidenced by superimposed, multi-stage alteration and mineralization imprints within the Streltsovsk Caldera and the basement.

The evolving magma chamber was capable of generating fluid flows, which introduced huge masses of ore-forming and other elements as well to form the present-day U-Mo deposits. The spatial distribution of products of magmatism and subsequent hydrothermal processes suggest a channeled fluid migration along deep-seated transcrustal faults. Steeply dipping faults that extend through basement rocks and the complete caldera fill fulfilled the channeling conditions for the percolation of the solutions.

Ischukova (1997) suggests that intersections of meridional faults and deep NE-SW faults such as the Argunskaya Shear Zone provided the main channels for magma and fluid invasion during the tectonic-volcanic event, and also acted as migration paths for the ore-forming solutions during the final period of activation.

The marked difference in host lithologies infers an only limited influence of the petrochemical composition of the rocks on the depositional site and the quality and quantity of the ore. Physical or rock mechanical properties favorable for brittle deformation in reaction to tectonic stress primarily governed the preparation of sites for ore accumulation.

Gently inclined fault/fracture zones composed of numerous gouge filled cracks exerted a screening effect on the percolation of the ore solutions. These structures are typical for the interface of the basement and overlying strata and between the Priargunskaya and Turginskaya series. These zones locally also host ore shoots. Consequently, Ischukova (1997) postulates that a combination of structural elements, that influenced, controlled and simultaneously provided the space for ore formation, combined with a few permeable faults and numerous screening fractures were the essential factor for the generation of favorable thermobaric conditions for ore deposition.

Six consecutive mineralization phases of a single hydrothermal event are documented by Ischukova (1997):

1. Argillization phase (facies of kaolinite and hydromica alteration)
2. Cryptocrystalline quartz-carbonate-sulfide phase
3. Albite-brannerite (the first ore) phase
4. Quartz-molybdenite-coffinite-pitchblende (the major ore) phase
5. Quartz-molybdenum-sulfide phase
6. Calcite-fluorite-dickite (post-ore) phase

In summary, metal mobilization and transport are attributed to hypogene(?) hydrothermal solutions. First hydrothermal processes are assumed to be contemporaneous with the final volcanic activity in the caldera. Mineralogical and geochronological evidence attest to repeated redistribution processes, which lasted into the Late Cenozoic.

Pathways for solutions and spaces for ore accumulation were provided by permeable faults and cataclastic volcanic sheets and sediments. They resulted from intense brittle deformation by multiple fault systems that generated a subvertical and

subhorizontal plumbing system for the migration of ore-forming solutions. The brittle deformation may possibly have been also instrumental in preparing source rocks for leaching of uranium and other metals. Structurally unaffected or otherwise impermeable rocks provided barriers for the fluids and as such contributed to the channeling of solutions to most favorable sites for ore deposition and enrichments.

Reducing conditions required for the reduction and arrest of uranium may have existed at sites where the host volcanics contained abundant sulfides and intercalated sediments plant remains. An additional reductant may have been ferric iron of mafic minerals as found in mafic and intermediate volcanics. Physico-chemical conditions, like effervescence with brake up of fluid components may have likewise contributed to uranium precipitation.

10.4.1.1 Streltsovskoye-Antei

The following presentation summarizes geological and metallogenetic characteristics of both, the Streltsovskoye and the Antei deposits because both are factually one deposit; Streltsovskoye is in the Mesozoic caldera-fill on top of the Paleozoic basement hosted Antei deposit.

The Streltsovskoye-Antei deposits are situated in the eastern part of the Tulukuyevsk Caldera, 18 km ESE of Krasnokamensk. Streltsovskoye, the largest deposit of the Streltsovsk U district, was discovered in 1963 and Antei in 1964. Exploitation is by underground methods and started at Streltsovskoye in 1969 and at Antei in 1976. Both deposits were in operation in 2006. Streltsovskoye had original in situ resources of 71 000 t U at an average grade of 0.185% U. Respective data for Antei are 40 000 t U and 0.2% U.

Sources of information. Andreeva et al. 1996a,b; Boitsov 1999; Boitsov et al. 1995; Chernyshev and Golubev 1996; Ischukova 1995, 1997; Laverov et al. 1992a,b; Nikolsky and Schulgin 2001; OECD-NEA/IAEA 1993–2005.

Geological Setting of Mineralization

The Streltsovskoye-Antei deposits occur at the intersection of the regional, NW-SE-oriented Argun and the N-S-trending Central fault zones in the eastern Tulukuyevsk Caldera (Fig. 10.12). The volcanic-sedimentary sequence, bipartite into the Lower Cretaceous Turgin and the Upper Jurassic Priargun series, is in the central part of the deposit up to 550 m thick and increases to 1 000 m thick in its southeastern part. Strata dip 5–10° SW. Principal lithologies are andesite-basalt lavas, dacite and rhyolite ignimbrites, trachydacite sheets, interbedded tuff, conglomerate-sandstone, cut by syenite-porphyry dikes. The caldera fill rests unconformably on Late Paleozoic basement composed of coarse-grained porphyry granite and medium-grained leucocratic biotite granite. Erosional incisions and tectonic arch-like uplifts deform the paleosurface (Fig. 10.13).

Intense tectonic activity conditioned four steeply dipping fault systems trending E-W, NE-SW, N-S, and NW-SE (from early to late). As a rule, these faults are represented by up to 12 m wide breccia and fracture zones. Although displacement of some tens of meters along major faults generated a block structure of the caldera fill, dislocations along most faults are small indicating a relative stable tectonic environment after the caldera formation. Shallow dipping faults occur intraformational within, and also separate the volcano-sedimentary suite from the basement granite.

Host Rock Alteration

Two prominent Phanerozoic alteration events, a Late Paleozoic and a Late Mesozoic, modified the host rocks at Streltsovskoye-Antei. Ischukova (1997) emphasizes the following features: Early pneumatolytic-hydrothermal activity metasomatized the ore-hosting Paleozoic granite by intense microclinization, albitization (albite-1), and greisens.

Late Mesozoic, *pre-ore*, low-temperature hydrothermal processes generated wide halos of hydromica, veinlets of quartz, siderite, and pyrite along faults. Mixed-layered hydromica-montmorillonite and chlorite occur in central parts of the halos. Fault controlled zones of early syn-ore sericitization and silicification contain polymetallic mineralization (galena with native silver, sphalerite, and molybdenite) mainly at deep levels.

Early *ore stage* phases include albite-2 veinlets, disseminated brannerite and ankerite veinlets, which prevail in the lower parts of the deposit. During the final ore stage, numerous veinlets of quartz and chlorite (chamosite-type) were formed. *Post-ore* alteration is only slightly developed in granite and restricted to faults. Veinlets of dickite, druses with quartz, calcite, pyrite, and fluorite attest to this stage.

Andreeva et al. (1996a) elaborate on the host rock alterations as summarized in the following (Fig. 10.14): *Late Paleozoic* metasomatism, dated at 250–230 Ma (Arakelyants et al. in Andreeva et al. 1996a), produced K-feldspar rocks, albitite, and greisen with fluorite, sulfides, and rare cassiterite along faults in Paleozoic granites. The K-feldspar zones expand with depth as documented by as much as 50 m long drill intersections of K-feldspar metasomatite below 1 500 m. Albitization, which is very rare at upper levels, becomes abundant below 2 100 m. Locally developed, narrow zones of fine-scaled muscovite unite to as much as several meters thick greisens with sulfide, quartz, and fluorite veinlets at a depth from 1 900 to 2 300 m. Though, no economic mineralization is associated with these processes.

Late Mesozoic tectonic and magmatic activation was associated with much more intense and widespread alteration than the Late Paleozoic process. Scope and intensity of the alteration activity can be estimated from the nearly total absence of fresh rocks within the Tulukuyevsk Caldera.

The Mesozoic hydrothermal event, which produced U(-Mo), base metals and fluorite mineralization, involves pre-, syn- and post-ore alterations with respect to the main U(-Mo) stage. The alterations imposed a differential, temperature-related vertical zoning upon the entire lithological section from the

Fig. 10.13.

Strel'tsovsk District, Strel'tsovskoye-Antei deposits, schematic geological SW-NE section across three ore zones of the two deposits. Antei is confined to Hercynian granite and contains ore primarily in an echelon arranged veins; major veins with paystreaks extend to over 1 000 m deep. Strel'tsovskoye ore bodies consist of anastomosing veins that grade into stockwork lodes hosted in Upper Jurassic-Lower Cretaceous volcanics and sediments. A basal conglomerate bed separates both deposits (after Krotkov et al. 1997) (see Fig. 10.11 for location)

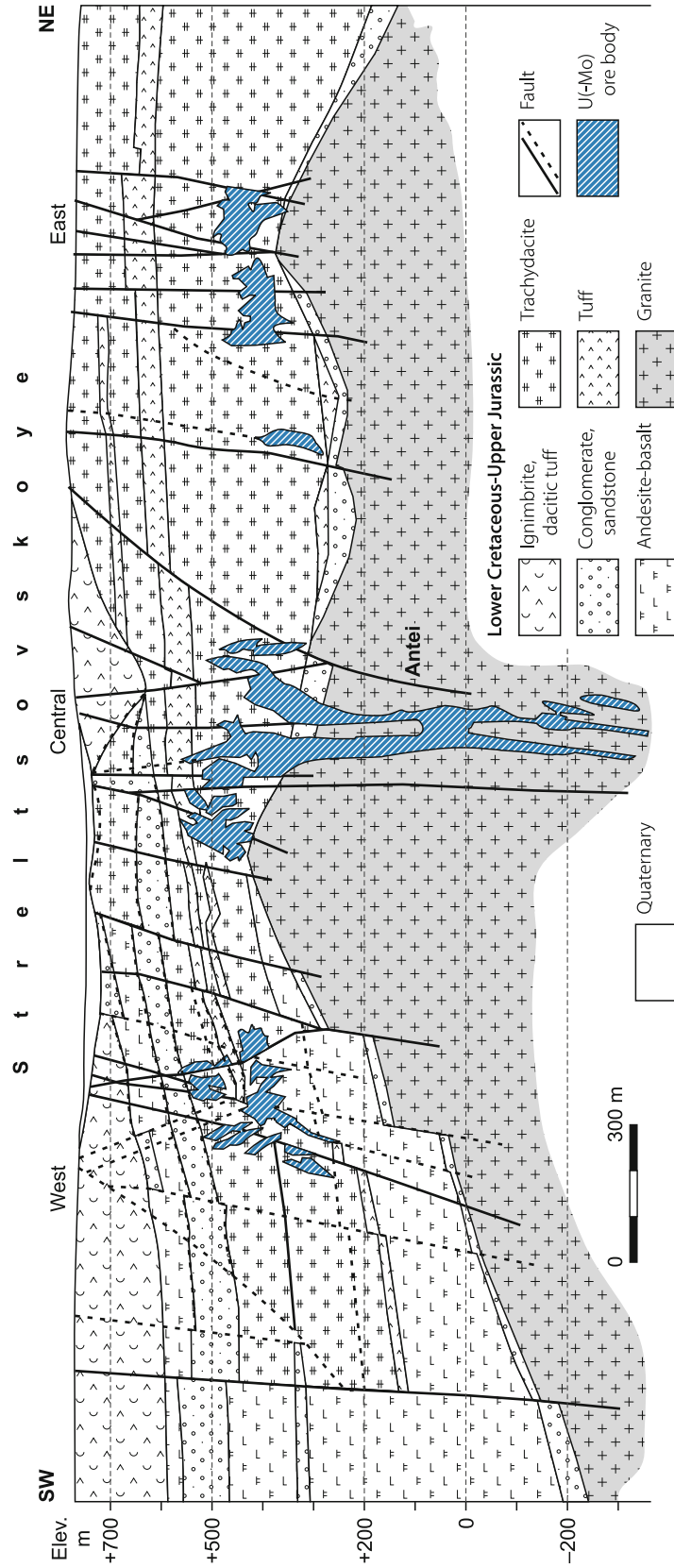
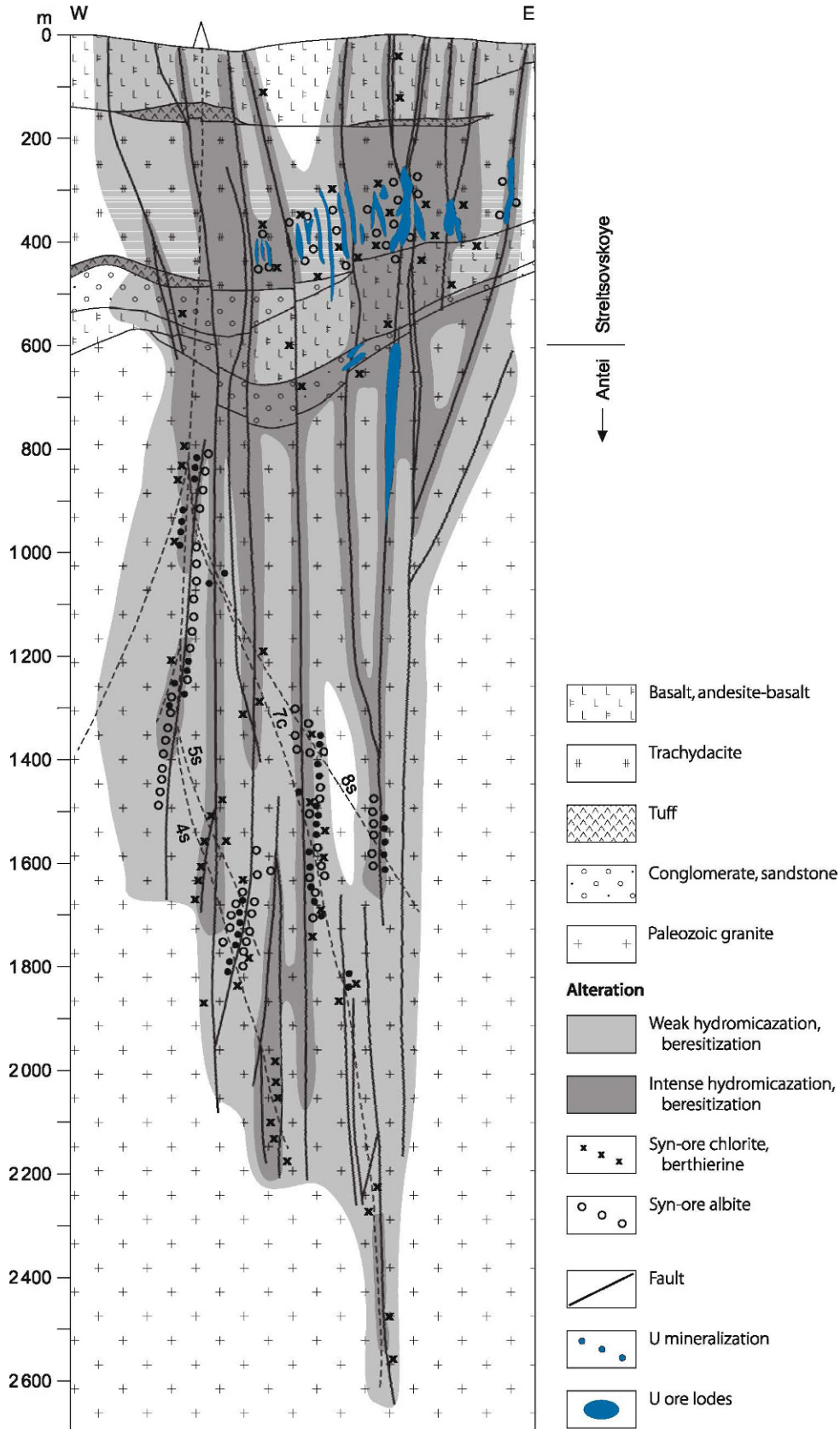


Fig. 10.14. Streltsovsk District, Streltsovskoye (Central)-Antei, schematic W-E section with distribution of wall rock alteration features (after Andreeva et al. 1996 based on data from Ischukova, Makushin, Evstratov and others)



Streltsovskoye into the Antei deposit. Hydromicaceous facies change gradually to sericite/beresite at a depth of 1 600–1 900 m, Fe-carbonates to Mg-Ca-carbonate at approximately 1 600 m, and berthierine to ferrous chlorites within 1 600–1 900 m deep. The alteration zoning is paralleled by modifications of the ore and gangue mineral assemblages. Pitchblende gives way to brannerite and other uranium titanates at a depth of about 1 100 m, ore-related albite disappears at about 1 800 m.

Pre-ore hydrothermal activity started with *low-temperature hydromica-sericite* formation, 139–130 Ma ago. Compared with the age of 144–143 Ma for the youngest rhyolite ignimbrites of the Tulukuyevsk Caldera, the alteration began shortly after subaerial volcanism waned. Faults, cataclastic zones, lithological contacts, and permeable rocks control the hydromica-sericite distribution. Intensely hydromica altered aureoles are from several centimeters to several tens of meters wide. The alteration phenomena tend to peter out only below 2.5 km.

Mixed-layer mica-smectite and hydromica are typical above a depth of 1 600–1 900 m. They grade downward into anhydrous sericite. The sericitized rocks are similar to beresite but differ from typical beresite by the lack of pyrite. A single process apparently formed both alteration facies as indicated by the gradual transition and identical K-Ar ages of 139–133 ±5 Ma for hydromica and sericite from different hypsometric levels (160–2 160 m deep). Temperature gradation is thought to have conditioned the facies change.

Carbonate composition also tends to rely on depth. Ferrous carbonate species, essentially ankerite and occasionally brannerite and siderite are typical for altered volcanic rocks and upper parts of granite above a depth of 1 600 m, while dolomite prevails below 2 000 m. The vertical zoning of carbonates is obscured, however, by superimposed later phase ankerite, siderite, and calcite veinlets.

Andreeva et al. (1996a) established the zonal pattern presented in Table 10.3 related to the development of hydromica and other alteration products, going from fresh rock to the core of an alteration halo (relict and neogenetic minerals listed together).

Table 10.3.

Zonal pattern related to the development of hydromica and other alteration products (Andreeva et al. 1996a)

Alteration assemblages in trachydacite	Alteration assemblages in granite
1. Slightly altered rocks: quartz, K-feldspar, plagioclase, biotite, calcite, hydromica, hematite, chlorite	1. Original granite: quartz, K-feldspar, plagioclase, biotite, titanomagnetite
2. Quartz, K-feldspar, plagioclase, hydromica, ankerite, hematite	2. Quartz, plagioclase, calcite, ankerite, chlorite, hematite, leucoxene, hydromica
3. Quartz, hydromica, ankerite, K-feldspar, siderite	3. Quartz, K-feldspar, hydromica, ankerite, hematite, siderite
4. Quartz, hydromica, ankerite	4. Quartz, K-feldspar, hydromica, leucoxene
	5. Quartz, hydromica

The main quantitative change in the authigenic mineral fraction is due to increasing hydromica and decreasing carbonate amounts in the intermediate and inner zones of the alteration aureole. Chlorite is scarce in rocks modified by the pre-ore alteration stage. On upper levels of the deposit, mafic minerals (biotite, amphibole, pyroxene) are often directly replaced by carbonate without intervening chloritization. This is notably true for trachydacite where ankerite completely pseudomorphs after biotite.

Andreeva et al. (1996a) postulate an acidic, low pH solution to have formed the beresitic-hydromicaceous alteration facies because in case of basic fluids, humbeite would have formed instead. Granite was much more altered than volcanic rocks. The discriminative alteration is attributed to more aggressive properties of the solutions presumably due to a low pH value conditioned by halide contribution, fluorine in particular, at the deep levels. Sericite and hydromica in pre-ore altered granite and volcanics contain up to 1 wt.-% fluorine, which may be regarded as indirect evidence for a fluorine involvement in early hydrothermal processes prior to the general deposition of vein fluorite.

Physico-chemical properties of the alteration minerals suggest that the thermal gradient and the total pressure hardly exceeded 100–120°C and 1 kbar, respectively, during the hydromicazation-beresitization event at the Streltsovskoye-Antei deposits. Maximum temperatures at deepest levels of the deposit were presumably in the order of 300°C as deduced from the beresite parageneses.

Hydromicazation was succeeded by the *quartz-carbonate-sulfide stage*. Thin ankerite and siderite veinlets with pyrite and arsenopyrite, and cryptocrystalline quartz with locally elevated uranium values of some tens of ppm U attest to this stage. The veinlets are usually restricted to the hydromica aureoles. They are rare in slightly altered and unaltered rocks.

The subsequent *albite-brannerite phase* produced up to 1.5 m wide zones composed of veinlets of fine-grained, untwinned albite, and disseminated brannerite and some unidentified uranium titanates. The albite contains irregularly distributed fine hematite, which imparts a pink color of varying intensity on the albitized rock. Albitization typically affected aluminous rocks, particularly granite, to a lesser extent trachydacite, scarcely basalt, and is absent in altered sediments and tuffs. A marked increase of albitization and brannerite intensity is noted around coffinite-brannerite-pitchblende ore close to the upper contact zones of granite. Veinlet albite persists over a vertical range of almost 1 600 m. It peters out at a depth of about 1 800 m and no albite is found below 1 880 m (Fig. 10.14).

Syn- to post-ore veinlets of berthierine, a ferrous chlorite-like mineral, developed simultaneously with and after the late pitchblende formation. In some volcanic rocks, for example basalt, berthierine persists beyond the hydromica aureoles.

Post-ore alteration along ore controlling faults include narrow argillization aureoles, and veins and veinlets of two fluorite generations, quartz of various habits, calcite, pyrite, marcasite, bertrandite, baryte, dickite, berthierine, zeolites, and some other minerals. Argillized aureoles are from fractions of a meter to several meters wide and appear as bleached rocks composed of smectite or smectite-kaolinite mixtures, which replace feldspar remnants or

ore-related albite. Coffinite veinlets emerge where argillization overprinted rich uranium ore. The post-ore alteration minerals are typical for upper levels down to a depth of 500 m. Their intensity, particularly that of fluorite and fluorite-calcite, decreases within the 500–1 000 m depth interval. Further below, these assemblages become rare, if not absent. The deepest argillized zone composed of to sudite-kaolinite was found at a depth of 2 307 m.

Mineralization

Pitchblende is the principal uranium mineral; coffinite and U-Ti phases (brannerite) are rare. Molybdenum occurs as Fe-molybdenite or jordisite, transformed into ilsemannite in oxidized sections. Uranium locally associates with pyrite; isolated quartz veinlets, and coarse flakes of molybdenite. Some ore lodes contain noticeable quantities of beryllium in form of bertrandite. As indicated in Fig. 10.15, over 30 minerals were formed in total by hydrothermal processes.

Uranium mineralization consists of several overprinted phases starting with albite-brannerite, followed by quartz-molybdenite-pitchblende, and finally quartz-coffinite. Quantitative relations between the uranium minerals vary widely, but pitchblende is always dominant particularly in high-grade ore. Host rocks of high-grade U ore are always intensely red colored by hematitization. Molybdenum mineralization consists of jordisite/molybdenite with cryptocrystalline quartz and fine-flaked molybdenite, which may associate with pitchblende and lath-like quartz. U-Ti phases occur predominantly as dissemination in trachydacite hosted low-grade ores.

Ore fabrics include fine disseminations, vug fillings, stringers, coatings of cracks and breccia fragments, and impregnations of breccia matrix.

Chernyshev and Golubev (1996) summarize characteristics of the main ore phase, the quartz-molybdenite-pitchblende paragenesis as follows. Pitchblende is the prominent ore mineral and occurs in three generations. *Pitchblende 1* forms small spherulites, crusts, pockets, up to 5 mm thick veinlets, and coats columnar quartz and rock fragments in breccia zones. Pitchblende aggregates are often broken and recemented by pitchblende 2 or feathery quartz with Fe-molybdenite. *Pitchblende 2* occurs as less than 0.1 mm large spherulites, intergrowths, veinlets, pockets, and overgrowths of lathlike quartz crystals, and nodules and fragments of pitchblende 1 spherulites. Feathery quartz and chalcopryrite cement broken pitchblende 2. *Pitchblende 3* constitutes the bulk (ca. 90%) of the Streltsovskoye ore. Pitchblende 3 occurs as up to 10 mm large spherulites and variably shaped nodular aggregates. Pitchblende 3 in veinlets and altered wall rocks is commonly associated with chlorite and hydromica.

First generation isotropic Fe-molybdenite (Fe-molybdenite 1) fills interstices between spherulites of pitchblende 1 and 2, or cracks within broken aggregates. Pitchblende 3 corrodes and cements fragments of Fe-molybdenite 1.

Galena crystallized during several stages. Galena of the quartz-sulfide-carbonate stage contained in quartz pockets and veinlets is closely associated with sphalerite and chalcopryrite. Galena of the quartz-molybdenite-pitchblende stage occurs in

thin quartz veinlets cutting pitchblende 1 and 2. In turn, this galena is corroded by pitchblende 3. Galena of a separate post-ore stage is associated with low-reflectance uranium oxides.

Redistribution of ore-forming metals is a common feature at Streltsovskoye. Redeposited coffinite and uranium oxides associated with post-ore galena occur in quartz and calcite veinlets and pockets, which cut early pitchblende. Black or dark violet, radioactive fluorite of the late quartz-fluorite-calcite phase contains minute pitchblende inclusions.

Andreeva et al. (1996a) report an alteration-related distribution of ore mineral assemblages from the Streltsovskoye into the Antei deposit (Fig. 10.16). Veins, veinlets, and disseminations of the quartz-molybdenite-pitchblende assemblage occur within and beyond the albitization zones, but they never extend beyond the boundaries of the hydromicaceous aureoles.

A vertical zoning of U mineralization is reflected by a distinct change of U mineral assemblages with depth. Pitchblende prevails on the upper levels of the deposits. It changes downward to brannerite-pitchblende and then to brannerite. Richest molybdenite-pitchblende ores with subordinate brannerite extend to a depth of 900 m. Mixed pitchblende-uranium titanate mineralization is typical for the 900–1 300 m depth interval, and uranium titanate mineralization below 1 300 m. Coffinite forming after pitchblende, and, to a lesser extent, brannerite, generally occurs on the upper levels of the Streltsovskoye-Antei deposits, although coffinite occasionally is also found at depths down to 1 200 m. Albite-brannerite ore persists to a depth of 1 880 m, and no more than a few narrow (several meters) high-radioactive zones in brecciated and fractured granite were encountered below this level (Ischukova 1995, 1997).

Shape and Dimensions of Deposits: *Streltsovskoye*

Streltsovskoye comprises six ore sectors, *Central*, *West*, *East*, *Glubinny*, *Golub*, and *Flangovy*, within a 4 km long and 2.5 km wide structural zone (Fig. 10.17). Fault zones and their intersections control their position. Mineralization occurs in the sedimentary-volcanic caldera fill over a vertical interval of 480 m. Upper limit of most ore bodies is several 10s of meters below surface. Only a single, steeply dipping uranium ore body occurs near surface, under 15 m of unconsolidated sediments. It is within the Streltsovsk fault near the same named fluorite vein. Approximately 80% of the reserves are concentrated between 300 and 550 m deep.

The *Central sector* is 2 300 m long and varies in width between 100 and 500 m; the *West sector* is 1 700 m long and 50–170 m wide; and the *East sector* 1 800 m long and 100–500 m wide. *Glubinny* is an isolated ore sector about 400 m to the NW of the Central and 500 m to the N of the West sector; ore occurs at deep levels in the lower trachydacite sheet. *Golub* is adjacent to the south of the East sector.

Sectors are composed of ore bodies of various shape ranging from variable large vein and stockwork to tabular stratiform lodes. Most ore bodies consist of a series of elongated and steeply inclined veins and stockworks in which ore occurs in contiguous, steeply dipping fractures that bifurcate from larger faults.

Fig. 10.15. Streltsovsk District, Streltsovskoye-Antei, paragenetic scheme of ore and related minerals. The symbol size reflects the mineral abundance and time interval of deposition (after Nikolsky and Schulgin 2001)

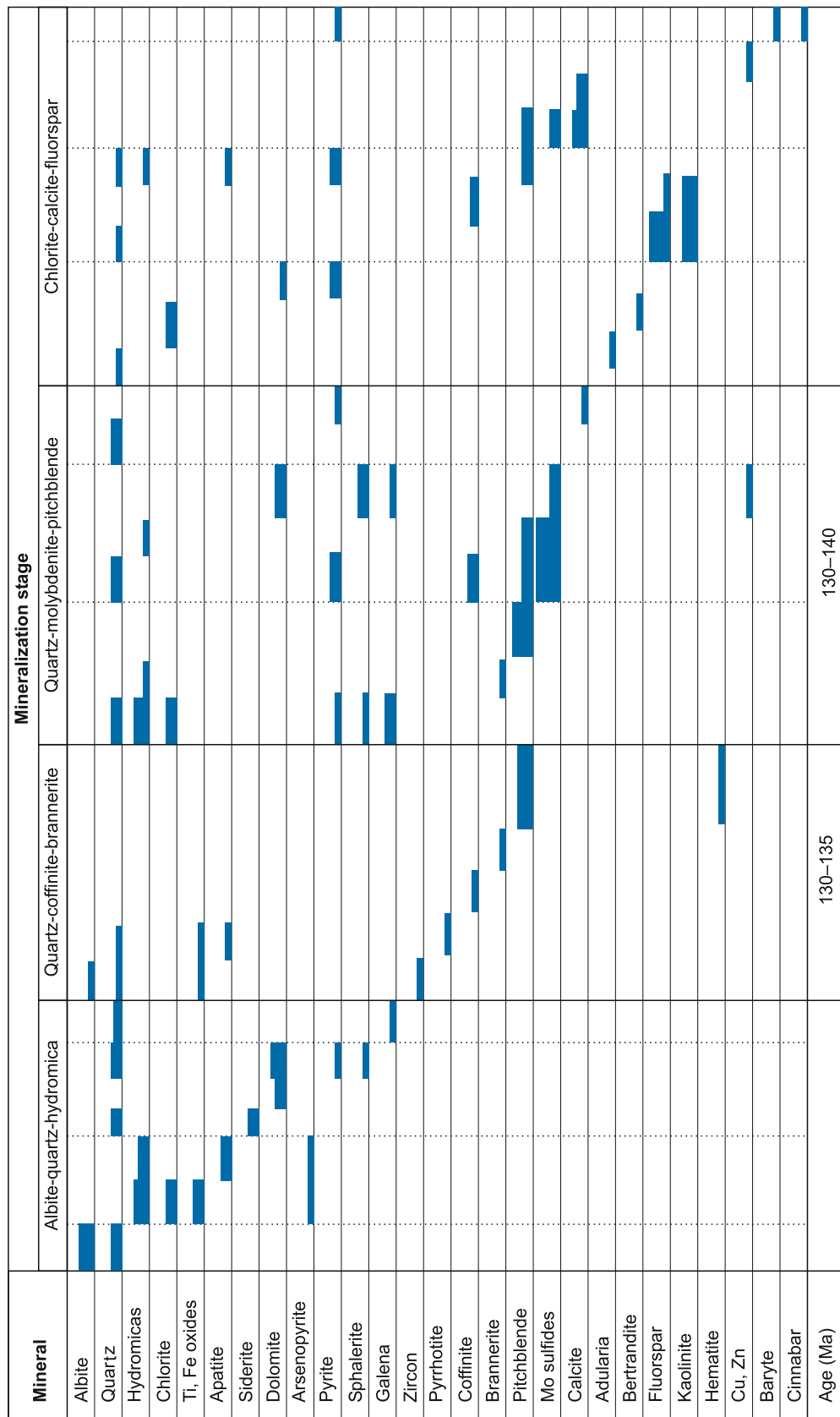
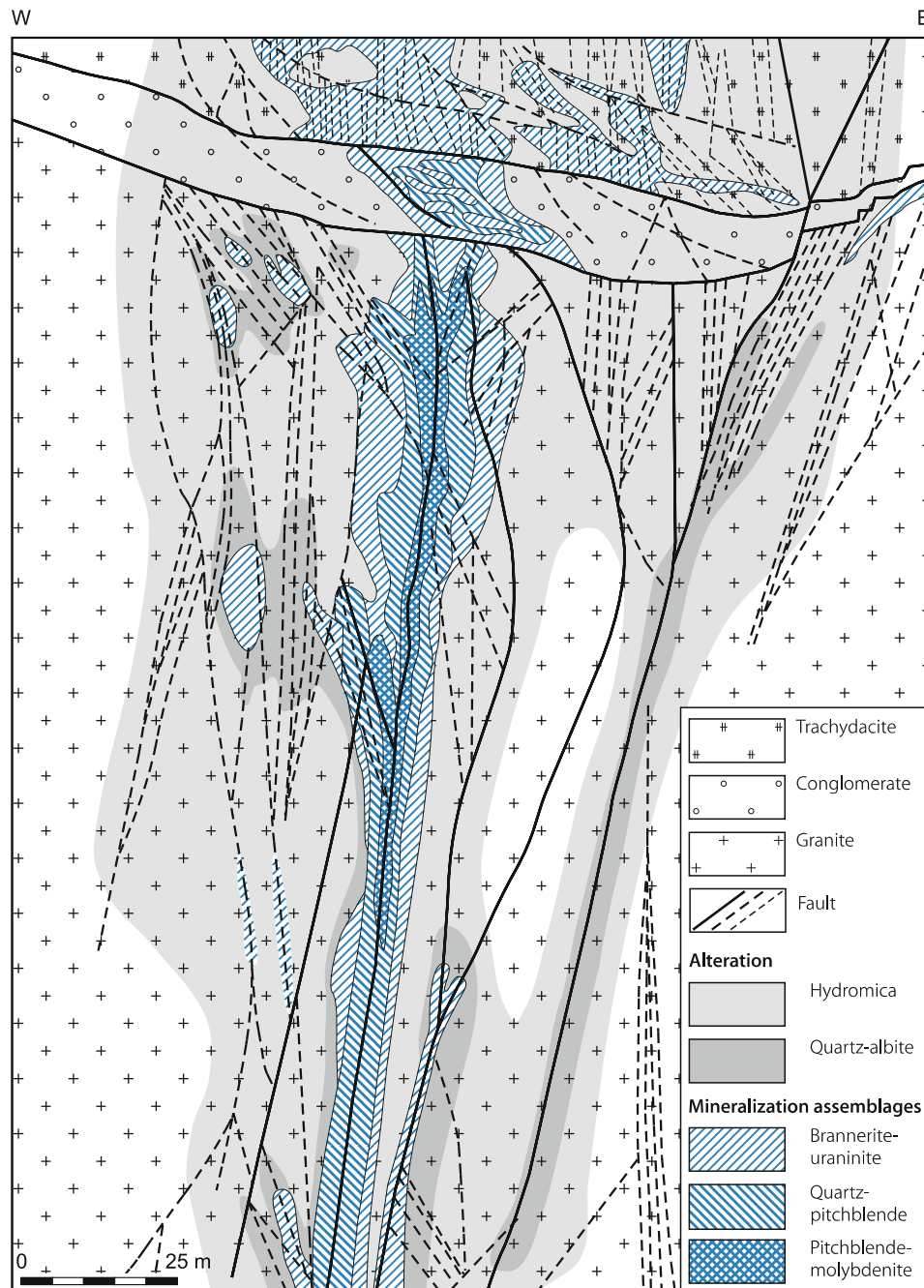


Fig. 10.16.

Streltsovsk District, Streltsovskoye-Antei, schematic W-E section with lateral and vertical distribution of uranium and molybdenum ore assemblages, and halos of major alteration facies in the basal Streltsovskoye and upper (about 200–300 m) Antei deposits (after Nikolsky and Schulgin 2001)

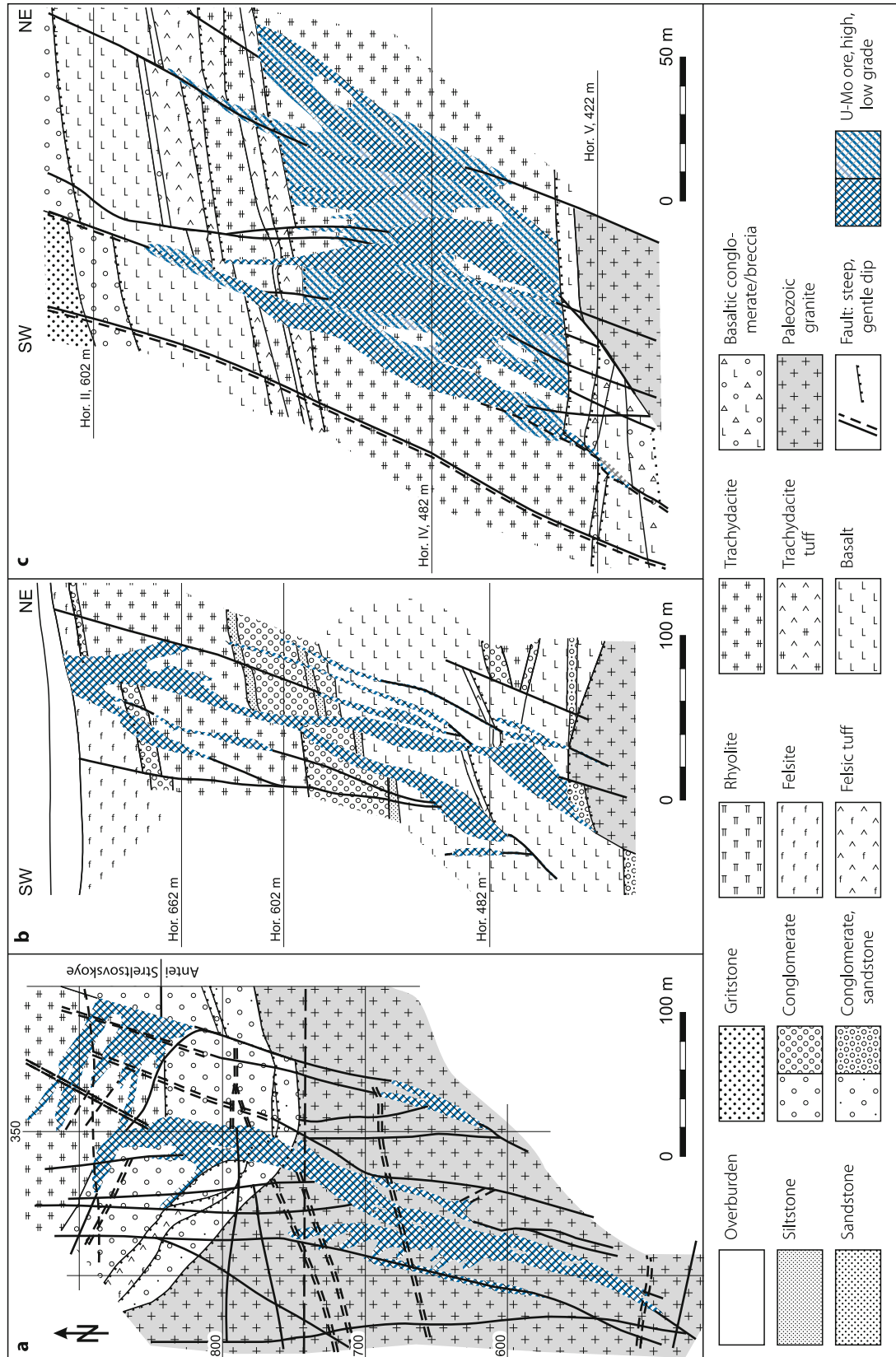


Stockwork lodes split at their periphery into short veins. Mineralization is distributed across all of the intersected rocks but in differential intensity. Length and width of ore bodies attains a few hundreds of meters. The vertical persistence of individual lodes commonly ranges from 30 to 90 m as a function of the thickness of the horizon cut by the ore controlling structure. Uranium grades of lodes vary between 0.15 and 0.5% U. Grades increase toward the lower or upper boundaries of ore bodies against gently dipping faults that transect tuff or conglomerate beds.

The bulk of reserves at Streltsovskoye is contained in relative narrow, 200–300 m wide, NE-SW-trending zones in the Central, West, and East sectors, which are terminated on the SE side by the NNE-SSW trending fault 13. The *Central sector* accommodates significant reserves in vein and stockwork ore lodes within the 3 km long Streltsovskaya (or N1) fault zone. The structure dips 65–80° and strikes NW-SE turning to N-S in the NW part where it joins the Central fault zone. The uranium mineralized section is 750 m long, averages 6 m thick, persists over a vertical interval of about 330 m, and averages a grade of 0.33% U.

Fig. 10.17.

Strel'tsovsk District, Strel'tsovskoye-Antei, plans and sections illustrating the shape and structural-lithological control of ore bodies. **a** Geological plan at level +302 m a.s.l. (ca. 400 m below surface) showing the shape of vein and stockwork ore lodes at and adjacent to the Paleozoic granite interface with overlying Late Jurassic conglomerate and trachydacite. **b** Geological SW-NE section (Central Zone, prospecting line 115 + 50) demonstrating the vein-stockwork system in the Strel'tsovskaya fault zone. Stockwork ore lodes prevail in basalt and trachydacite sheets. Their vertical extensions contract to veins particularly in conglomerate beds. **c** Geological SW-NE cross-section (prospecting line 113 + 50) illustrating the hanging and foot wall control of a stockwork ore body by shallow inclined faults along lithological contacts. **d** Geological plan at level 332 m and **e** W-E section (prospecting line 97) of the Glubinnyy sector of the Strel'tsovskoye deposit (after Ischukova 1997)



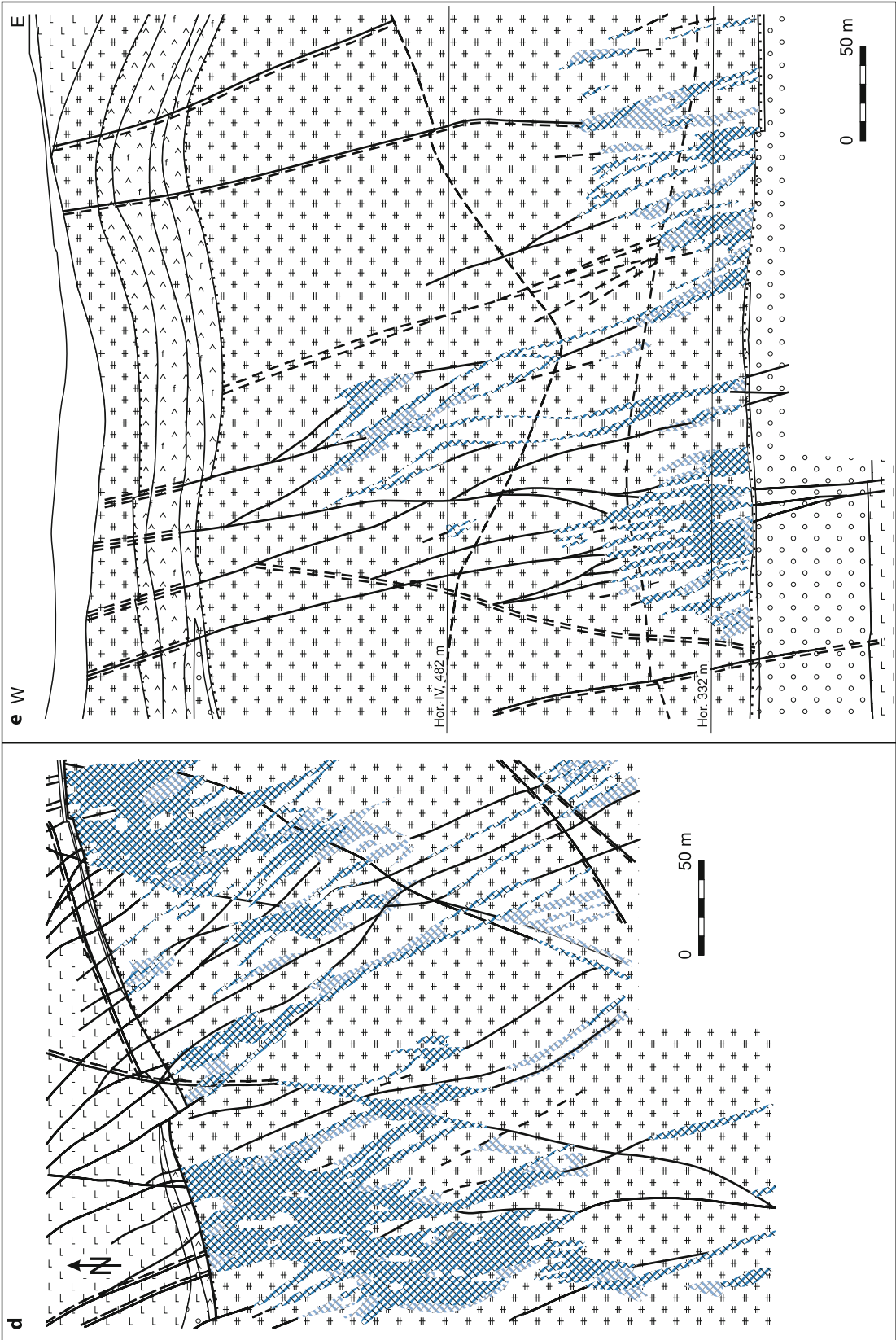


Fig. 10.17. (Continued)

The structure carries ore through all intersected lithologies, but the majority of reserves is concentrated in stockwork-like ore bodies in the lower trachydacite sheet whereas highest grades of up to 0.8% U and 0.4% Mo are restricted to basalt. 77% of the reserves occur in trachydacite, 16% in basalt, and the remainder in quartz porphyry and conglomerate. The N1 fault also contains the Streltsovskaya fluorite vein about 100 m to the NW of the uranium section.

The *Golub sector* holds in ore zone 2 the largest tabular stratiform ore body of Streltsovskoye. Ore is hosted by andesite and quartz porphyry conglobreccia (composed of almost equal amounts of pebbles and angular fragments) at the base of a felsic sheet, which is contiguous to the southern flank of the Eastern sector. The mineralized strata average 1.5 m thick, contain 0.2–0.24% U with local enrichments of as much as 2.2% U, and occur at a depth of 145–270 m below surface.

Shape and Dimensions of Deposits: *Antei*

Ore occurs over a depth interval from 350 to 1 400 m below surface, controlled by a bundle of steeply dipping, NE-SW-trending faults (Figs. 10.13, 10.16). Host rock is altered Late Paleozoic anatectic granite. Principal structures are faults number 13, 6A, 160 and 190. They control combined with a group of smaller faults the ore distribution. Most significant is the large, 30° NE-trending fault zone 6A that is between faults 13 and 160. As a function of the distance to these two faults, the width of zone 6A ranges from 10 to 50 m in the central part to 80–100 m at the flanks.

Fault 6A includes ore body 6A, which is 1 000 m long, extends 900 m down dip, has a grade of about 0.7–0.9% U locally with peaks of 4% U, and accounts for 94% of the *Antei* reserves. Molybdenum contents are less than 0.03%.

Ore body 6A is of complex vein-stockwork configuration. Up to 50 m wide swells with stockwork structure alternate with a few meters thick vein-like intervals. Its upper margin abuts against a gently dipping fault that follows the contact of disintegrated granite and overlying conglomerate and trachydacite. The trachydacite contains ore lodes of the Streltsovskoye deposit (Figs. 10.16, 10.17a). Most of the uranium is concentrated in the central part of the 6A body within a chimney shaped ore lode in cross-section. The lode is 200 m high, 300 m long, from 10 to 50 m thick, and averages 0.954% U (Ischukova 1997).

Geochronology

Age datings by Chernyshev and Golubev (1996) provide for massive, unaltered pitchblende concordant $^{206}\text{Pb}/^{238}\text{U}$ and $^{207}\text{Pb}/^{235}\text{U}$ ages within a narrow range of 136–134 Ma. Pitchblende impregnated by fine inclusions of chlorite and carbonate, and pitchblende with galena and Fe-molybdenite inclusions show a discordant age of 133 ± 4 Ma, but this is within a wide range of discordant U-Pb ages obtained from pitchblende with impurities. Pitchblende with coffinite inclusions is commonly rejuvenated presumably due to a loss of radiogenic lead (131–130 Ma for pitchblende with coffinite, and 83–52 Ma for hydrated uranium oxides and coffinite segregations associated with primary massive pitchblende). In contrast, higher ages than

those of the original pitchblende crystallization are usually obtained from pitchblende partially replaced by or intergrown with calcite or Fe-molybdenite. Massive nodular pitchblende, which is partially replaced by calcite and contains minute galena in the zones of replacement yield slightly discordant values of 142–138 Ma. Pitchblende intergrown with Fe-molybdenite shows a correlation between U-Pb age values and the content of Fe-molybdenite reflected by a roughly proportional increase of radiogenic ages of samples with an increase in Fe-molybdenite content, up to a geologically unrealistic value of 179–177 Ma.

K-Ar ages of mixed-layer micas formed during a pre-uranium hydromicazation process fall within a range of 144–129 Ma. Most samples of hydromica from altered granite yield Rb-Sr ages of 134 ± 1 to 131 ± 2 Ma, and K-Ar ages of 133 to 135 ± 5 Ma. Chernyshev and Golubev (1996) calculated an average Rb-Sr age of 133 ± 2 and a K-Ar age of 135 ± 3 Ma for these pairs and consequently propose a period between 139 and 131 Ma as a best estimate for the hydromicazation event, i.e. a time span, which only slightly exceeds that of the main ore-forming process of 135–133 Ma.

Monomineralic fractions and some whole rock samples of the volcanic-sedimentary suite, from trachydacite of the early lava unit to the youngest porphyritic syenite, give K-Ar ages from 166 to 142 Ma, and a Rb-Sr age of 139 Ma for the late porphyritic syenite and rhyolite.

Sources of Uranium

Various lithologies provide potential source rocks for the U deposits in the Streltsovsk District. Table 10.2 furnishes average U and Th background data for these and other rocks.

Circumstantial evidence based on isotope systematics provided by Chernyshev and Golubev (1996) indicates two discrete potential uranium sources in the basement of the Tulukuyevsk Caldera. Fe-molybdenite in a pitchblende-molybdenite ore sample contains 260–250 Ma old radiogenic lead. It is thought that the lead and presumably also uranium have originated from a Permian uranium protore in a 258–248 Ma old porphyry granite (biotite and K-Na feldspar dated by K-Ar method).

Another, still older uranium source is testified by dispersed uraninite mineralization in a granite-hosted Precambrian amphibolite xenolith. The uraninite yields an Ordovician U-Pb age of 459–457 Ma. The sample containing the uraninite also includes molybdenite crystals with small pitchblende spherulites. The pitchblende gives discordant U-Pb ages of 156 and 150 Ma, which point to a Mesozoic hydrothermal event that affected the Precambrian rocks below the caldera. The discordant U-Pb ages of pitchblende and their difference with the U-Pb ages of the Streltsovskoye ores proper may be caused by the significant amount of common lead in the sample (ca. 1.2% ^{204}Pb) and the excessive radiogenic lead mobilized by the alteration of the Ordovician uraninite.

A similar age as that of the afore mentioned uraninite is provided by isotopic data of common lead from galena of the Streltsovskoye deposit. The lead consists of a two-component mixture of lead with a model age of 460 Ma and lead similar in composition to radiogenic lead from the uranium ore.

Metallogenetic Aspects

The Streltsovskoye-Antei deposits originated in a relatively stable tectonic environment as indicated by only minor displacements along most faults. This and also the limited post-ore processes favored the conservation of the ore and pre-ore alteration assemblages.

Chernyshev and Golubev (1996) arrive at a metallogenetic model for the Streltsovskoye deposit that involves several hydrothermal events including two separate major phases of mineralization that formed uranium and fluorite ore. Strong hydromicization and relatively scarce quartzification-sulfidization preceded the uranium deposition. The bulk of uranium was deposited during the quartz-molybdenite-pitchblende stage, in which three generations of pitchblende are the predominant constituents. U-Pb ages of these three generations indicate that the principal ore-forming event took place 135–133 Ma ago, i.e. during the Hauterivian/Cretaceous and lasted less than 3 Ma. This episode coincides approximately with the age of 138–136 Ma for uranium deposition in the Dornod volcano-tectonic structure in eastern Mongolia, which is also within the Mongolian-Argun volcanic belt. The wide range of discordant U-Pb ages obtained from pitchblende with impurities is interpreted to testify to telescoping hydrothermal processes and related pitchblende modifications.

Chernyshev and Golubev (1996) also address the age relationship between volcanic rock and uranium ore formation. Compared with the 135–133 Ma ages of pitchblende, there is a formal time gap of 4 Ma between the intrusion of porphyritic syenite dikes, the latest magmatic facies at Streltsovskoye, and the principal uranium introduction. By including the pre-uranium hydrothermal event of hydromica formation, the time gap reduces to 3 Ma. Analytical error values and likewise the dispersion of ages signal an uncertainty of some 3–4 Ma, however, and thus the time gap could have been as long as a fraction of a million to several million years. The authors interpret the interval as the time it took for the major magma chamber, which existed below the Streltsovsk Caldera for a long time during the Late Jurassic and participated in the formation of the Tulukuyevsk volcano-tectonic structure, to cool to the point at which the mineralizing hydrothermal system began functioning that provoked the U-Mo ore formation. Consequently, they stipulate a contiguity of the final volcanic phases and the ore-forming process. The established hydromica ages, which overlap with those of the ore, are thought an additional argument to support the contiguity concept.

The metallogenesis of the large Streltsovskoye ore lodes involved repeated concentration processes that overlapped in time and space. Although a volcanogenic proper source of the uranium cannot be excluded, isotopic evidence attests to a uranium source in the basement granite. Excessive radiogenic lead, present in Fe-molybdenite and galena of the Streltsovskoye deposit and in the ore province as a whole, implies a contribution of lead and presumably uranium from precursor mineralization in basement rocks that had formed in at least two periods 460–450 and 260–250 Ma ago and was related to the granitization and granite emplacement processes.

The conclusions drawn by Chernyshev and Golubev (1996) with respect to the granitic uranium source are relativized by findings of Andreeva et al. (1996a,b) who studied the

redistribution of elements associated with the hydrothermal host rock alteration and who arrive at the following results: An increase of chalcophile elements (Li, Sb, Mo, Au, Zn, and Hg) in the volcanic and sedimentary rocks of the Tulukuyevsk Caldera at the upper levels of ore bodies and superjacent zones was already earlier established by Kozhevnikov (in Andreeva et al. 1996).

Average background values of trace elements in unaltered granite at Streltsovskoye-Antei are compared with those in hydromica/sericite-altered granite in Table 10.4. The calculated average of all analyzed samples yield a net gain of elements, such as Co, Mg, and Th in hydromica altered granite and a net loss for Mo, U, Pb, and other elements. Although the data in Table 10.4 provide a general picture of the geochemical (re-)distribution of trace elements, the factual situation is more complex. Altered granite and trachydacite display alternating gain and loss sections and a differentiated intensity of loss and gain patterns along the vertical profile. The intensity of the loss aureoles decreases towards the surface, while the gain aureoles become more pronounced.

In the granite, the loss of a number of components, including U, Mo, and Pb, is most pronounced in the lower, beresitized part

Table 10.4.

Streltsovsk District, Antei deposit. Average background values of trace elements and their ratios in hydromica altered and unaltered granites (Andreeva et al. 1996)

Element	Average content (ppm) Granite		Ratio 1/2
	Hydromicaceous (1)	Unaltered (2)	
Co+	4.6	4.1	1.121
Ti	1 958	1 805	1.085
Mg+	0.35	0.33	1.083
V	25	24	1.075
Th+	20	19	1.059
Mn	918	870	1.055
Sr	203	193	1.055
Fe	1.8	1.7	1.044
Be	4.4	4.3	1.030
Zn	62	60	1.029
P	326	318	1.022
Cr	53	52	1.014
Ba	734	729	1.006
Zr	145	149	0.978
Nb	9.5	9.7	0.977
La	56	58	0.967
Ni	22	23	0.960
Ga+	24	26	0.944
Cu	12	13	0.944
Y+	33	35	0.930
Yb+	3.3	3.7	0.913
Sc+	4.1	4.5	0.912
Sn+	3.8	4.1	0.910
Ca+	1.3	1.5	0.870
Pb+	24	28	0.861
U+	5.1	6.0	0.853
Mo+	6.2	8.2	0.750

Amount of samples: hydromicaceous granite: $N = 100$, unaltered granite $N = 136$; "+" marks the elements with significantly different average contents in the hydromicaceous and unaltered granites.

of the explored section. Other elements such as Co, Mg, and Th were accumulated at these levels, but a great number of the elements extracted at the lower levels (Yb, Mo, Sr, Y, Ni, Cr, Zr, Be, Nb, Mg, Fe, etc.) were transported to and redeposited at upper levels.

Hydromicization caused practically no loss of uranium from trachydacite, while the average uranium tenor of granite was reduced from 6.0 to 5.1 ppm but not in a uniform manner. A genuine U loss is documented for beresitized granite at deep levels below 1 500 m, whereas the upper, hydromica-altered levels show both, intervals of loss and partial gain of uranium as well, which, in sum, yielded a gain within the hydromica zone. Andreeva et al. (1996a) conclude from these data that the liberation of many elements, including uranium to some extent, from the basement granite in result of beresitization and hydromicization does not provide sufficient evidence to define the granite as a viable source for the uranium in the Streltsovsk deposits. The authors rather assume that the uranium leached during the pre-ore alteration was redeposited in subeconomic concentrations in cryptocrystalline quartz and siderite veinlets of the quartz-carbonate-sulfide assemblage.

10.4.1.2 Tulukuyevskoye

Tulukuyevskoye is a polymetallic U-Mo deposit in the central-western part of the Streltsovsk District, about 15 km SE of Krasnokamensk. Original in situ resources were some 37 000 t U. Ore averaged a grade of 0.24% U. The deposit also contained molybdenum ore with grades of 0.2% Mo. Molybdenum concentrate had an average rhenium content of 146 ppm. Mining was largely by open pit operation and lasted for almost 30 years from 1968 to 1998. The deposit is depleted.

Source of information. The subsequent description is summarized from Ischukova (1997) unless otherwise stated.

Geology, Alteration and Mineralization

Tulukuyevskoye is positioned at the intersection of the NW-SE-striking Tulukuyevskaya with the NE-SW-trending Argunskaya shear zone. Principal host rocks are stratified volcanics, predominantly Lower Cretaceous felsite/rhyolite and subjacent felsic tuff, and minor Upper Jurassic trachydacite and basalt (Figs. 10.12, 10.18a,b).

Wall rock alteration is well developed and includes hydromicization, carbonatization, silicification, hematitization, and chloritization. Banded silicification and chloritization are confined to large faults. Andreeva et al. (1996a) state, that, in contrast to the Streltsovskoye-Antei deposits, albitization is absent at Tulukuyevskoye.

Principal U mineral is pitchblende. Coffinite occurs in subordinate quantities and associates with pitchblende. Uraninite and U-Ti phases are rare. Molybdenite is present as finely flaked and cryptocrystalline (jordisite) varieties. Pyrite and loellingite occur locally. Trace amounts of beryllium, lead, and rhenium are associated with the U-Mo ore. Ore has disseminated and banded textures.

Shape and Dimension of Deposits

The deposit is 1 300 m long and up to 250 m wide. Ore starts 30–50 m below surface from where it extends for 180–270 m downward. The deposit includes several ore bodies of complex configuration composed of a series of contiguous, steeply dipping veins, stockworks, and gently pitching lodes (Figs. 10.18a,b).

Ore zone # 5 is the richest and largest ore zone. It persists for 400 m long and contains between 60 and 70% of the total Tulukuyevskoye reserves in ore bodies that are up to 60 m thick. Ore grades range from the cutoff grade to 7% U, and average in excess of 0.4% U. Some segments have grades of 30–40% U over a thickness of 5 m. Ore lodes of zone 5 are controlled by NW-SE-trending structures (Fig. 10.18c). Most favored host rocks are felsite, felsic lava breccias and tuffaceous sediments. Some lower grade ore is in underlying basalt and trachydacite.

Ore zone # 2 constitutes the central part of the deposit. Steeply dipping, N-S and NE-SW faults control the ore lodes; they are limited by NW-SE faults. Ore is particularly concentrated at fault junctions. Grades average about 0.3% U. A gently dipping tabular ore body occurs within a tuff-sandstone horizon below a felsite sheet. It averages 0.2% U. Where the tuffaceous horizon is intersected by steeply dipping faults, grades increase up to 10% U.

Recoverable molybdenum at Tulukuyevskoye is mainly concentrated in the lower part of rich uranium ore bodies. The average content is 0.2% Mo, but grades vary highly in different ore bodies, from a few hundreds ppm to 12% Mo. Highest Mo grades occur in basalt and felsite tuffs. Mo ore contains rhenium, which averages 146 ppm in molybdenum concentrate.

10.4.1.3 Argunskoye

Argunskoye is a polymetallic U-Mo deposit in the SW part of the Streltsovsk District, some 13 km SE of Krasnokamensk. It was discovered in 1979 and had original in situ resources in excess of 30 000 t U and 10 000 t Mo. Ore grades average 0.17% U and 0.18% Mo. The deposit is explored by underground methods (Mine 6).

Source of information. The subsequent description is largely derived from Ischukova (1995, 1997) amended by data from Nikolsky and Schulgin (2001).

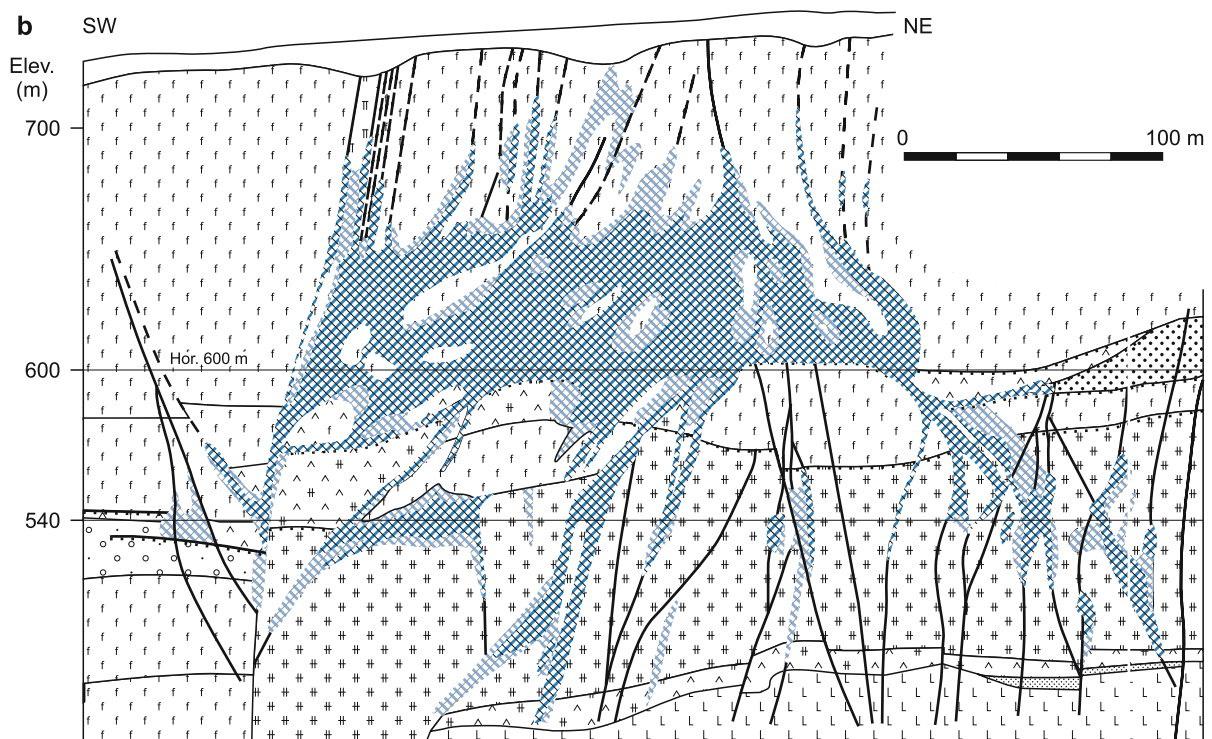
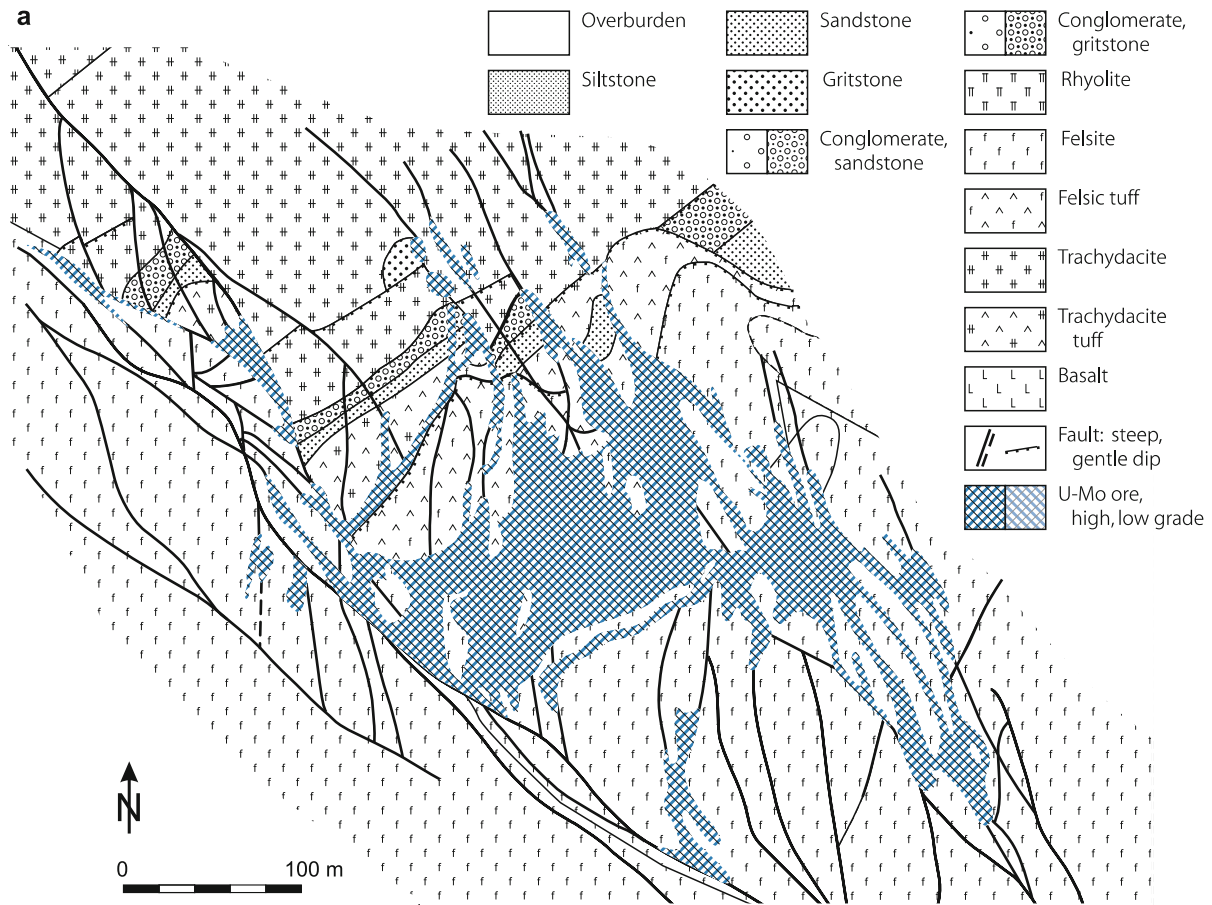
Geology and Alteration

Argunskoye is confined to the interjunction of NE-SW-, NW-SE-, and N-S-oriented deep shear zones intersecting the northern limb of an anticline of metamorphic basement rocks composed of steeply dipping, up to 200 m thick dolomitic marble with thin intercalations of quartz-mica-andalusite schist, and biotite-amphibole gneiss intruded by mafic magmatites (diabase, diorite) metamorphosed to amphibolite. The core and the southern limb of the anticline are composed of multiply metasomatized granite. A 140–300 m thick sequence of basalt and trachydacite sheets rests upon the basement. A volcanic neck occurs adjacent to the south of the deposit (Figs. 10.19a,b).

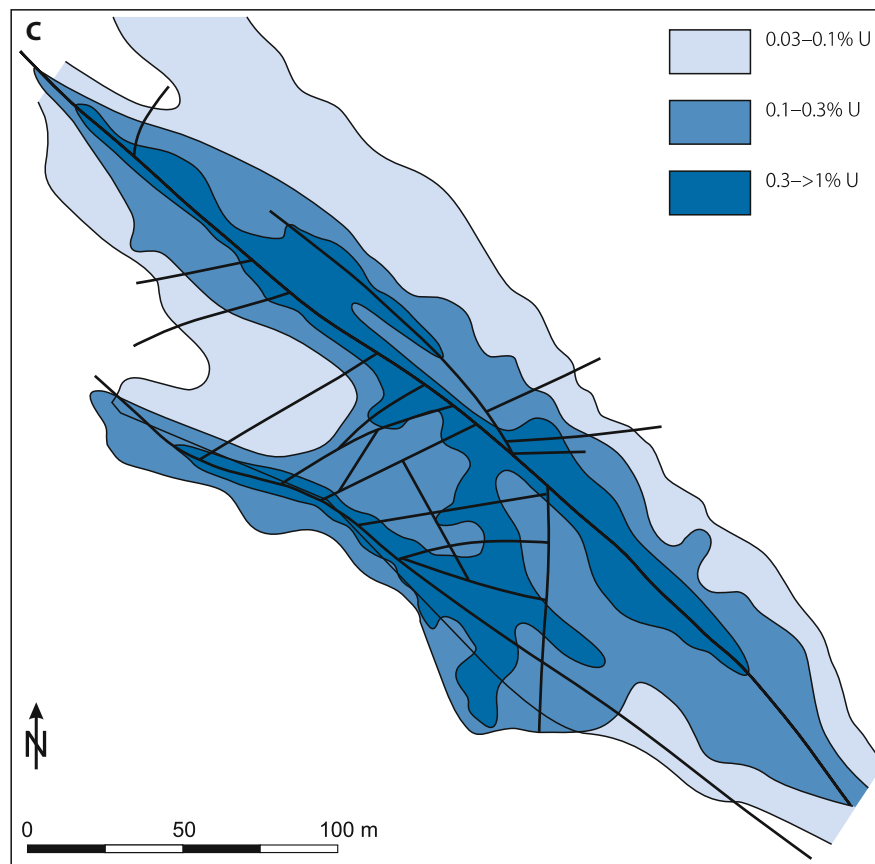
Pre-ore metasomatism produced microcline, albite, and phlogopite facies, skarn, and greisen. They tend to be particularly abundant within and near ore bodies. Low-temperature

Fig. 10.18.

Streltsovsk District, Tulukuyevskoye, **a** geological plan at level +600 m a.s.l.; **b** SW-NE section displaying the complex configuration of vein-stockwork-style U(-Mo) mineralization largely hosted in Lower Cretaceous felsite sheets and controlled by steeply dipping, NW-SE-trending structures. Shallow inclined faults act as ore boundaries; **c** grade distribution of uranium of a deposit segment at level 640 m a.s.l (after **a**, **b** Ischukova 1997; **c** Laverov et al. 1992b) (legend for **a** and **b** see Fig. 10.17)



■ Fig. 10.18. (Continued)



alteration includes argillization and silicification. Argillization displays a zoned pattern. Kaolinite prevails at upper levels. It is downwards replaced by montmorillonite and chlorite and, below 700 m, by hydromica. Chlorite and chlorite-montmorillonite assemblages, related to the post-uranium fluorite process, occur along faults to a drill intercepted depth of 2 500 m. Andreeva et al. (1996a) clarify, that in contrast to the Streltsovskoye-Antei deposits, albitization-2 is absent at Argunskoye.

Mineralization, Shape and Dimensions of Deposits

Principal U mineral is pitchblende. Coffinite occurs in minor amounts. Mo is present as coarse-flaked molybdenite and jordisite, associated with fluorite and sulfide-bearing quartz. The ore minerals form veinlets, fill cracks and cavities, and impregnate breccia cement and wall rocks. Three ore varieties are discerned, uranium and molybdenum proper, and a mixed U-Mo ore. Most of the ore is in the dolomitic marble unit. Some ore is in granite below the marble (► Figs. 10.19a,b).

Ore lodes are controlled by N-S-, NW-SE-, E-W- and, to a minor degree, NE-SW-trending structures. A 50–100 m thick breccia zone in the basal part of the marble horizon hosts the main ore lodes. The breccia body is isometric in plan view and has a steep dip conformable with the bedding.

Ore bodies consist of irregularly distributed mineralization contained in vertically elongated stockworks with apophyses, and veinlike lodes. Ore lodes are 200–300 m long, 16–70 m thick,

and occur over a vertical interval of more than 1 000 m. Uppermost ore is 140 m below surface. A fault contact between basement and overlying volcanics governs the upper boundary of the ore. Grades are highly variable ranging from the cutoff grade (0.039% U) to 3.5% U. Carbonatic ore contains about 0.15% Mo, and aluminosilicate (granite hosted) ore up to 0.26% Mo. Mo ore veins in syenite-porphyry contain between a few percent and 51% CaF_2 , and average 12.6% CaF_2 present as violet fluorite that fills veins and impregnates breccia cement.

Approximately one third of the reserves are concentrated in ore shoots of enlarged thickness and grade with more than 0.3% U.

10.4.2 Vitim District, Asian Russia

The Vitim (Vitimsky, also referred to as Khiagda) District is some 140 km north of the town of Chita at the upper course of the Vitim River on the Amalat Plateau in the Buryate Autonomous Republic (► Fig. 10.10). Although Vitim is located within the central Transbaykal subregion, it is treated separately due to its economic potential.

The district contains basal-channel sandstone-type U deposits; eight are grouped around the Khiagda ore field and form the Vitim District *sensu stricto*. In addition, several isolated deposits occur in some other fluvial systems in the Vitim area (► Fig. 10.20). Explored resources are estimated at 52 000 t U and total resources are speculated to be on the order of 100 000 t U (Naumov et al. (2005).

Sources of information. Boitsov 1999; Laverov et al. 1992b, c, 2000; Krotkov et al. 1997; Loutchinin 1995a; Naumov 1999; Naumov et al. 2005; Pelmenev 1995.

Regional Geological Setting of Mineralization

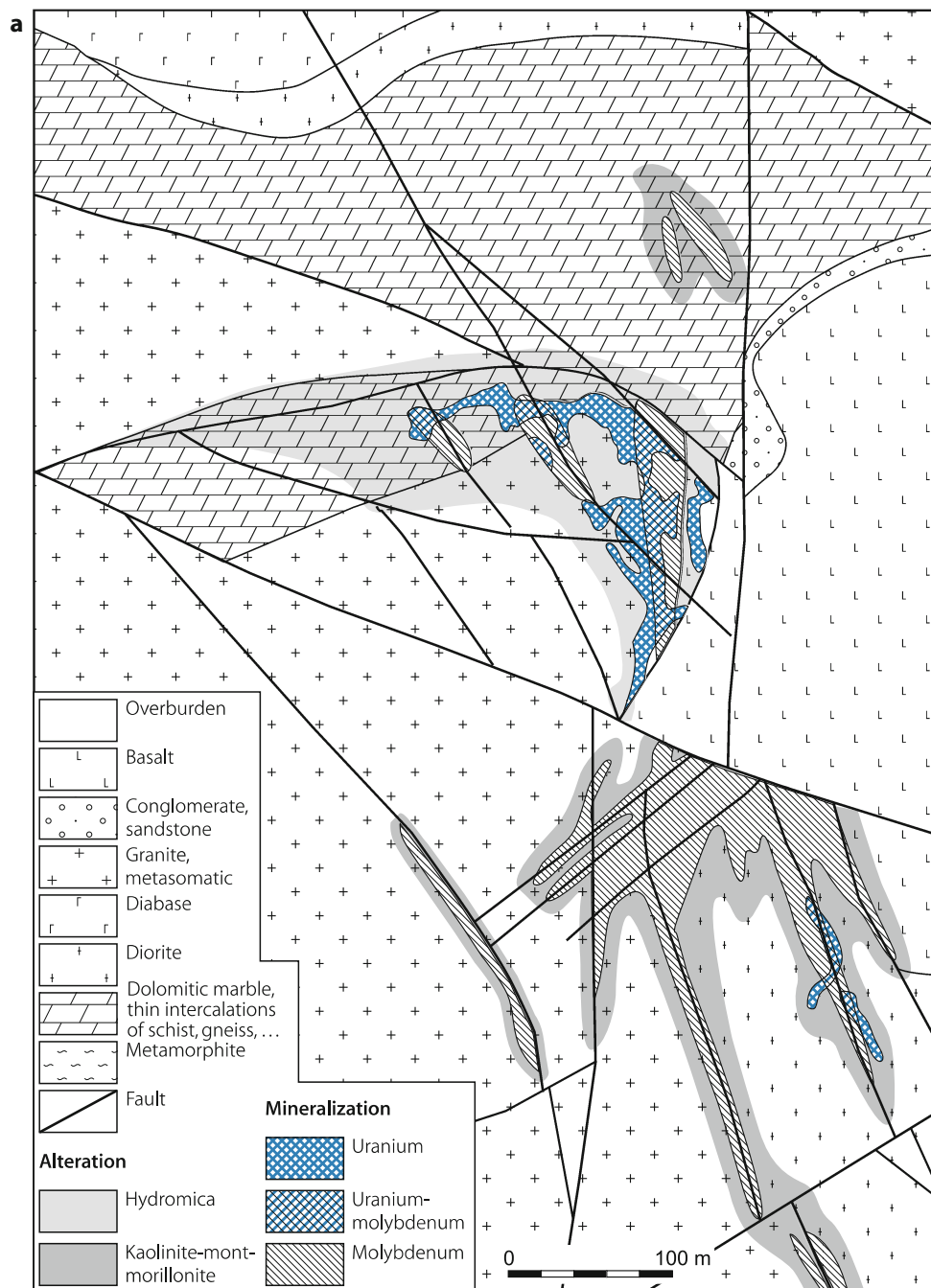
Paleoproterozoic metamorphic rocks (schist, gneiss, migmatite) intruded by Middle to Lower Paleozoic granite constitute the

basement of the Vitim District. The old peneplain was deeply weathered during a semiarid to arid climate and incised by a paleodrainage system. The system consists of tributary channels dewatering to two major ancestral rivers trending NE-SW at the margins of the Buysiuchan plain.

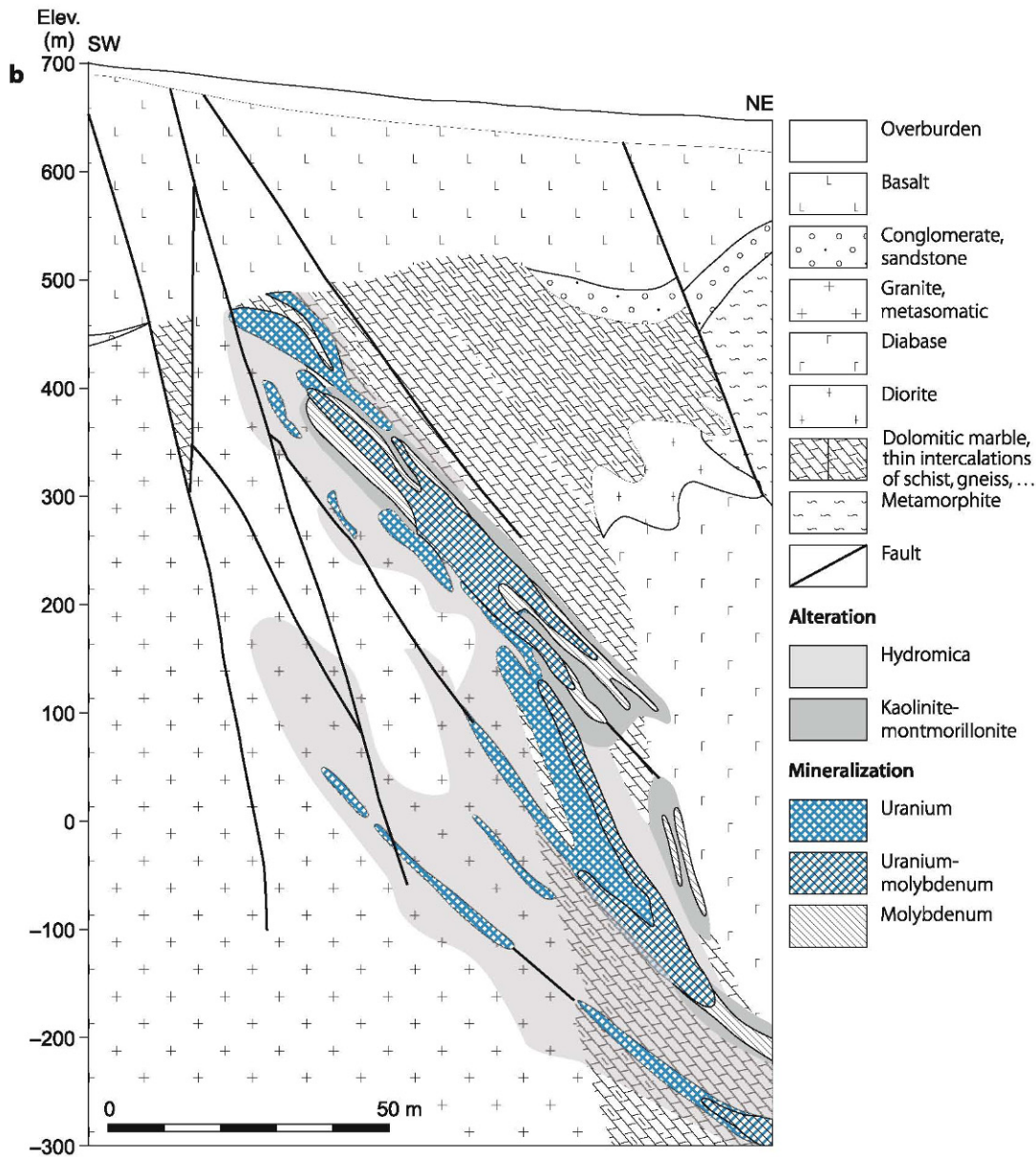
Up to 50 m thick or more Pliocene to Oligocene sediments predominantly of colluvial and, along thalwegs, of alluvial provenance fill the paleochannels. The sediments consist of grey and multicolored carbonaceous clay-siltstone, sandstone,

Fig. 10.19.

Streltsovsk District, Argunskoye, **a** geological plan at level +374 m a.s.l. and **b** SW-NE section illustrating the litho-stratigraphic position of ore lodes with U and/or Mo mineralization and related alteration aureoles in Proterozoic dolomitic marble xenolith in Late Paleozoic granite below a basalt sheet of the Tulukuyevsk Caldera (after Nikolsky and Schulgin 2001)



■ Fig. 10.19. (Continued)



conglomerate, and tuff with some intercalated lignite seams. Grey facies contain pyrite and are enriched in plant debris. Carbon content averages about 0.8% C_{org} . A cover of 10–30 m, locally up to 250 m thick Quaternary-Neogene tuff-bearing sand and gravel intercalated with or overlain by basalt lenses or sheets rests on the older rocks.

Principal Host Rock Alteration and Characteristics of Mineralization

Originally grey host rocks are oxidized to multicolored facies in which pyrite, siderite, and organic matter are replaced by Fe-hydroxides. The oxidation front developed from the sides of

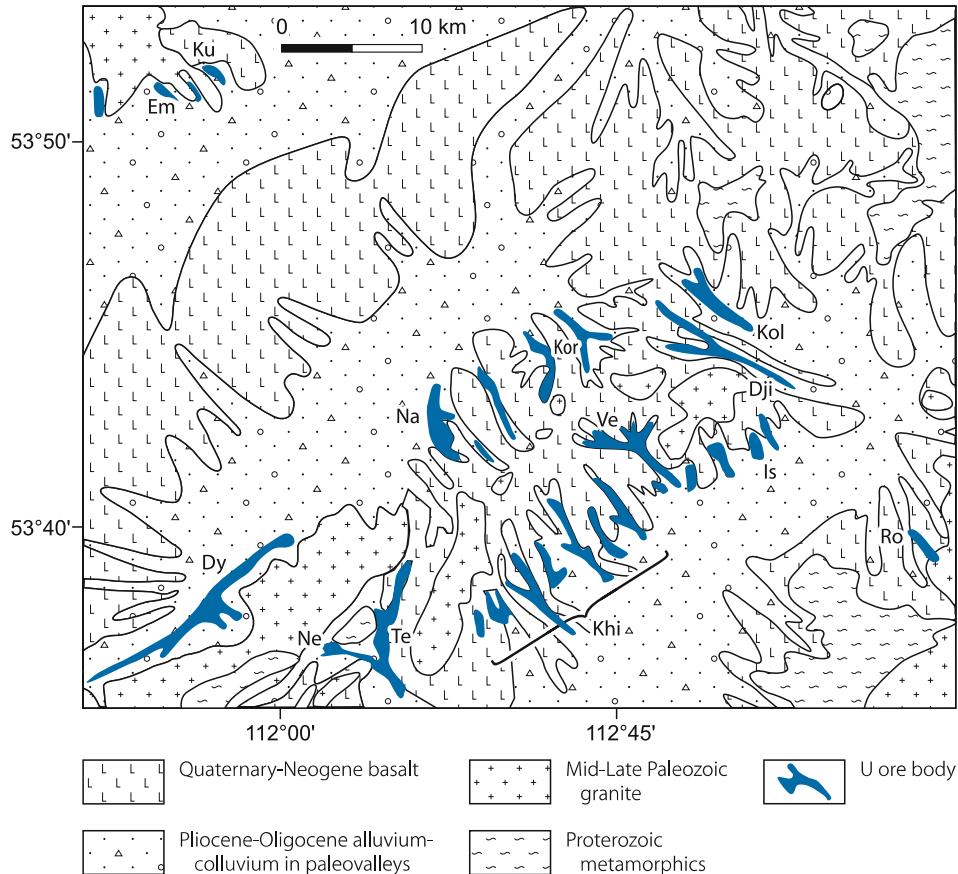
the paleovalleys. Bleaching produced a whitish facies along the interface of grey and multicolored rocks.

Principal U minerals are U-oxides and coffinite, and rare ningyosite. Uranium is also adsorbed on carbonaceous and clay matter. Associated minerals include arsenopyrite, galena, marcasite, pyrite, sphalerite, and hematite. In addition, the ore has elevated contents of Co, Cu, Mo, Sc, Y, Zn, and Zr. Their tenor ranges from 5 to 400 times of the Clarke figures. Dating of U minerals yields ages ranging from 25 Ma to Recent. The ore minerals occur finely dispersed mostly in sandstone and conglomerate in basal parts of paleochannels.

Uranium deposits are restricted to channel sections underlain by granite. Channels in metamorphic terrane are barren of

Fig. 10.20.

Vitim area, geological map with surface projected U deposits in contributory paleochannels filled with Oligocene-Pliocene alluvial-colluvial sediments. Quaternary plateau basalt sheets (not shown) cover most of the area (courtesy AV Boitsov based on Russian literature). U deposits: *Dji* Djilindinskoye, *Dy* Dybryn, *Em* Emkerse, *Is* Istochnoye, *Khi* Khiagdinskoye, *Kol* Kolichikan, *Kor* Koretkoide, *Ku* Kularinta, *Na* Namaru, *Ne* Nevskoye, *Ro* Rodionovskoye, *Te* Tetrakhskoye, *Ve* Vershinnoye



uranium but may contain gold. Ore minerals occur disseminated along the interfaces.

General Shape and Dimensions of Deposits

Mineralized paleochannels range commonly from 1 to 10 km in length and 0.5–1.5 km in width (Fig. 10.20). Individual deposits contain several hundreds to more than 5 000 t U. They consist of ore bodies, which are in plan view of ribbonlike configuration trending along channel axes, and in sections of elongated roll or lens shape (Figs. 10.21, 10.22). Ore bodies are up to 3 km long, 150–400 m wide, and from less than 1 m to a maximum of 23 m thick. They occur at a depth of 60–240 m. Grades range from 0.01 to 0.5% U.

Potential Sources of Uranium

Paleozoic granite exposed in the basement is favored as the most likely source of uranium. Granitic facies contain uraninite and have elevated uranium background values reportedly of up to 80 ppm U. Another uranium source is possibly provided by the tuffaceous constituents of the cover sediments.

Principal Ore Controls and Recognition Criteria

Mineralization is primarily of lithological and geochemical control. Significant ore controlling parameters or recognition criteria of deposits include:

Host Environment

- Basement of Proterozoic metamorphics intruded by Paleozoic granite
- Paleosurface deeply weathered during semiarid climate
- Old peneplain incised by Tertiary rivers
- Valleys filled with Tertiary continental clastic sediments
- Cover of Quaternary tuffaceous sediments and basalts providing protection against erosion of ore hosts
- Host rocks are characterized by
 - up to 50 m thick alluvial and proluvial sediments composed of sandstone, siltstone, and conglomerate of Oligocene-Miocene age
 - reduced facies of grey color and characterized by pyrite and high content of carbonaceous matter (1–8% C_{org})

- oxidized facies of multicolor containing Fe-hydroxides
- good permeability of ore hosting facies
- Potential U sources are primarily provided by granite

Alteration

- Oxidation with formation of redox fronts by vadose waters migrating downward from channel margins
- Re-reduction(?) -related bleaching along reduced and oxidized facies
- Reduction potential provided by organic matter and sulfide

Mineralization

- U-oxides and coffinite
- Large number of associated elements
- Disseminated texture of mineralization
- Ore bodies are
 - lens- and roll-shaped and elongated along channel axes
 - mostly in sandstone and conglomerate in the basal section of channels controlled by redox boundaries
 - restricted to channel sections underlain by granite
- Locally mineralization is in the weathering crust of granite

Principal Aspects of Metallogenesis

Uranium ore formation is considered of epigenetic origin resulting from the infiltration of oxygenated, U-bearing vadose water. The porous, predominantly sandstone channel facies served as

conduits through which the fluids migrated. Precipitation of uranium occurred where the pregnant solutions encountered sufficiently high carbonaceous matter to establish a redox front along which the dissolved hexavalent uranium was reduced and deposited. The ribbonlike configuration of ore bodies stretching along the axis of valleys suggests that the mineralizing fluids entered the valleys from their flanks.

Circumstantial evidence suggests that the uranium originated from basement granite. This hypothesis is supported by the fact that all deposits are restricted to channel sections underlain by granite and that oldest U minerals yield ages of 25 Ma i.e. they must have been formed prior to the deposition of the Quaternary tuffaceous cover rocks. The latter may perhaps have contributed uranium at a later stage.

Description of Selected Deposits in the Vitim District

10.4.2.1 Vitim District/Khiagda Ore Field

Eight basal-channel-type U deposits occur in several paleochannels, from 1.5 to 6 km apart, in a 250 km² large area: *Khiagda* (or *Khiagdinskoye*), *Tetrakhs koye*, *Vershinnoye*, *Dybryn*, *Istochnoye*, *Kolichikan*, *Koret kondinskoye*, and *Namaru* (Fig. 10.21). Distance between deposits varies between 1.5 and 6 km. Explored resources are estimated at 52 000 t U. Deposits consist partly of

Fig. 10.21.

Vitim District, geological subsurface map showing the location of ore bodies of the *Khiagdinskoye* (# 1–7) and other deposits. Oligocene-Pliocene colluvial sediments (conglomerate, sand silt, clay, mud, tuff) in contributory paleochannels incised into granite are the principal host to ore bodies. (Quaternary basalt sheets not shown) (after Loutchinin 1995a). U deposits: *Dji* Djilindinskoye, *Dy* Dybryn, *Is* Istochnoye, *Khi* Khiagdinskoye, *Kol* Kolichikan, *Kor* Koretkoide, *Na* Namaru, *Ne* Nevskoye, *Te* Tetrakhs koye, *Ve* Vershinnoye

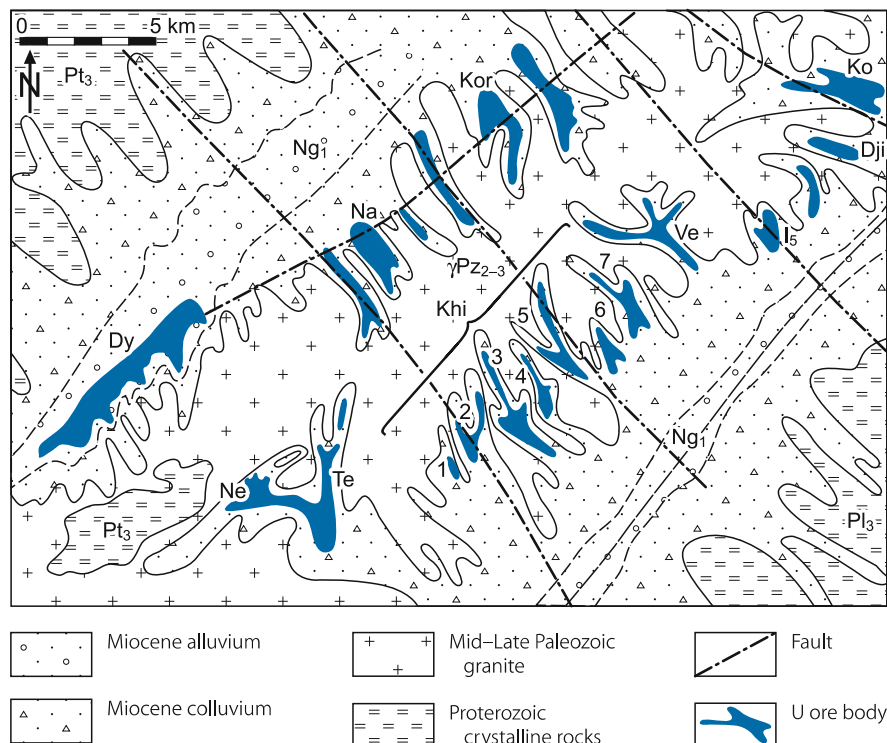
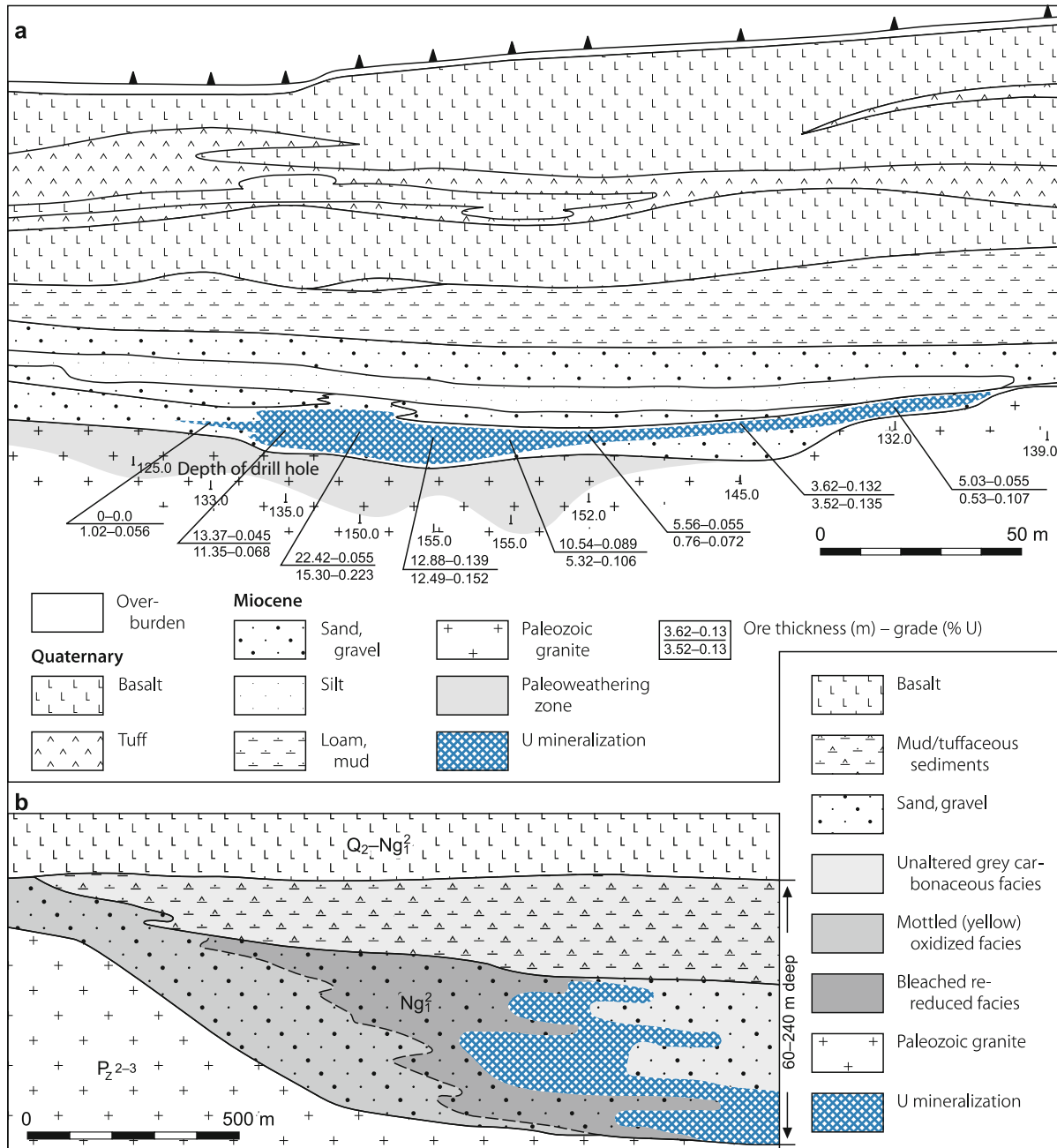


Fig. 10.22.

Vitim District, Khiagdinskoye (ore body VI?). **a** Geological SW-NE cross-section showing U mineralization along the upper contact of an oxidation zone, which has developed along the sediment-basement interface of a paleochannel incised into Paleozoic granite. Drill intercepted U grades are shown below the drill holes. (courtesy AV Boitsov based on Russian literature). **b** Schematic geological cross-section exhibiting alteration features associated with a roll-shaped U ore body in Miocene carbonaceous gravel and sand (after Boitsov and Nikolsky 2001; Loutchinin 1995a)



several ore bodies; their grades average between less than 0.05 and 0.3% U.

Khiagda is with 15 500 t U the largest deposit. This figure includes 6 900 t U RAR and 4 380 t U EAR-I in the <\$40 per kg U cost category (OECD-NEA/IAEA 2005). Average ore grade is 0.05% U. Resources of Tetrakhskoye are in excess of 5 000 t U, and of the others between 1 500 and 5 000 t U each. Khiagda is in the planning stage for exploitation by ISL methods at a

nominal production capacity of 1 000 t U yr⁻¹ (since 1999). Operator is JSC “Khiagda”.

Khiagda includes eight ore bodies in five neighboring paleochannels, which are incised into Paleozoic granite. The channels range from 5 to 7 km in length and from 0.5 to 1.5 km in width (Fig. 10.21), and are filled with slightly consolidated, from a few meters to 120 m thick, Neogene fluvial-colluvial sediments upon which Neogene to Quaternary basalt rests.

Host rocks contain abundant coaly debris and Fe-sulfides, and exhibit older sheet and soil-type oxidation zones from channel heads and from the slopes downward. In these oxidized zones pyrite, siderite, and coaly material are replaced by Fe-hydroxides that impose beige to tan hues on the sediments. A zone of secondary reduction reflected by lighter color and absence of Fe-hydroxides and coaly matter intervenes between oxidized and unaltered rocks.

Mineralization consists of finely dispersed pitchblende, coffinite, and sooty pitchblende. Ore bodies extend lenticular or ribbonlike along paleochannels and exhibit geological and alteration features as illustrated in [Fig. 10.22](#). Individual ore lenses are 800–4 100 m long, 15–800 m wide, and tens of centimeters to 26 m thick, and occur at a depth of 60–240 m.

10.4.2.2 Other Deposits in the Vitim Area

Zheglovskoye was discovered in 1998 in the Eravninsky area of the Buryatia A.R., some 100 km N of Chita. Total in situ resources amount to 7 900 t U contained within two tributary channels of the Khushida paleovalley. The channels are filled with 120–150 m and locally up to 250 m thick Neogene effusive-sedimentary rocks, from top to bottom composed of an as much as 170 m thick basalt sheet, which covers the commonly 5–20 m and locally up to 120 m thick, U-bearing horizon of badly sorted sand, gravel, and silt. A conglomerate horizon forms the basal channel unit.

The two channels contain lenticular ore bodies in two ore zones. Ore zone one is in the northern channel and ore zone two in a parallel channel 1.5 km to the south. Ore zone one is 5.8 km long, 70–300 m wide, averages 3.23 m thick, and occurs between 8 and 180 m deep. Ore zone two is 3.6 km long, 100–300 m wide, averages 3.4 m thick, and 10–180 m deep. Grades in both zones average 0.062% U.

Radinovskoye and *Vitlandskoye* are located in the Ingur and Kholoi areas, respectively. Both deposits occur in paleovalleys. Mineralization is in the permafrost zone and exposed on surface. Prognosticated resources of *Radinovskoye* amount to 5 300 t U and of *Vitlandskoye* to 8 980 t U.

Emkerse and *Kularinta* are small basal-channel U occurrences in another Tertiary fluvial system located about 30 km NW of the main part of the Vitim District.

10.4.3 Central Transbaykal Subregion, Asian Russia

The central Transbaykal subregion encompasses nine uranium areas distributed over an area extending for some 500 km from the northeast to the southwest of the town of Chita in central Transbaykalia, Buryatia Autonomous Republic. Each ore field contains several uranium deposits but none was mined to date (status 2006). Permafrost constitutes to some extent an obstacle to uranium recovery by ISL methods. [Figure 10.10](#) shows the distribution of uranium areas in the central Transbaykal subregion and a summary of available data of U deposits is given at the end of this chapter.

Deposits include volcanic vein-stockwork (referred to as Streltsovsk-type) and volcanic stratiform, sandstone, and granite-related vein types. Most deposits are small with resources of some hundreds to several thousands tonnes of uranium except for Olovskoye and Imskoye (see below). Ore grades generally average less than 0.1% U.

Total resources of the Central Transbaykal subregion are estimated at 40 000 t U, 24 000 t U of which are classified as RAR + EAR-I and 16 000 t U as EAR-II. All resources belong to the \$80–130 per kg U cost category (Laverov et al. 1992c).

Sources of information. Kislyakov and Shumilin 1996; Laverov et al. 1992b,c; Pelmenev 1995; Vizhnyakov 1995a–c.

General Geological Features and Metallogenetic Aspects of the Central Transbaykal Subregion

The central Transbaykal subregion covers part of the Mongolian-Okhotsk zone. The zone is situated at the boundary between Caledonian and Hercynian orogenic terrane and evolved by tectonic-magmatic reactivation in Mesozoic time during which Early Jurassic granite and volcanics were emplaced into crystalline rocks of Precambrian to Paleozoic age. Repeated tectonic events downfaulted NE-SW-oriented basins and grabens, which were filled with Middle to Upper Jurassic and Lower to Upper Cretaceous terrestrial carbonaceous sediments and mafic to felsic volcanics. Additional depressions filled with terrestrial sediments and basalt formed during the Quaternary.

Two significant metallogenetic episodes affected the Transbaykal subregion during the Late Jurassic and the Cretaceous. The former is the principal ore-forming event of U deposits associated with Jurassic calderas and the latter generated U mineralization in Lower Cretaceous depressions but also left traces in the volcanic-hosted deposits.

The Cretaceous event took place at the terminal stage of the Mesozoic tectonic-magmatic activation, independently of the Jurassic metallogenetic epoch from which it is separated by a substantial time span documented by the formation of grabens and deposition of the Lower Cretaceous coal-bearing sediments and intervening basalt flows.

More equivocal is the age relation of uranium deposits in the substantially sedimentary sequences of Middle-Late Jurassic depressions. Some of them, for instance, the Ozernoye deposit in the Zylzuya Depression, are close in age to the Olov and Ima deposits. Others, which probably include the Slantsevovoye and Zhuravlinovoye deposits of the western Transbaykal region, may be related to the Late Jurassic ore forming epoch (Kislyakov and Shumilin 1996).

In summary, uranium mineralization in the Mesozoic depressions of the central Transbaykal subregion is essentially related to three ore-forming processes and events:

1. Hydrothermal low- and medium-temperature processes of Late Jurassic age determined the formation of vein-stockwork and stratiform deposits in the Late Jurassic volcanogenic

structures of the Strel'tsovsk District and other districts as, for example, Dornod in Mongolia.

- Hydrothermal low-temperature processes of Cretaceous age were pronounced in the Early Cretaceous coal-bearing graben-syncline type depressions (Stepnoye, Kuka, Meridionalnoye, Sirotinsk deposits) and also in Jurassic volcanogenic-sedimentary depressions (deposits of the Olovsky area).
- Exogenic-epigenetic processes of Cretaceous age generated the ore-controlling oxidation zones in the Ima deposit and also, evidently, the pink coloration of Upper Jurassic and Lower Cretaceous coarse-clastic rocks in substantially grey-colored sequences (including coal-bearing strata). This event took place at the waning stage of block movements and related termination of sedimentation, and synchronous with the aridization of the climate during the Late Cretaceous. In result, the hydrodynamic regime of groundwater was changed from the former ascendant regime, determined by the squeezing of interstitial water, to the influx of oxygenated meteoric water.

10.4.3.1 Olovsky(-Mogochinsky) Area, Olovskoye Deposit

The Olovsky(-Mogochinsky) area is situated some 200 km to the NE of Chita. It includes the *Ozernoye* (also called *Zyulzinskoye*) and the large Olovskoye (or Olov) deposit described in the next

chapter. Additionally, more than fifteen, generally small and low grade, volcanic/sandstone-type U occurrences are established in the ore field. They are shown in [Fig. 10.23](#).

Sources of information. Kislyakov and Shchetochkin 2000; Kislyakov and Shumilin 1996; Vizhnyakov 1995a; unless otherwise stated.

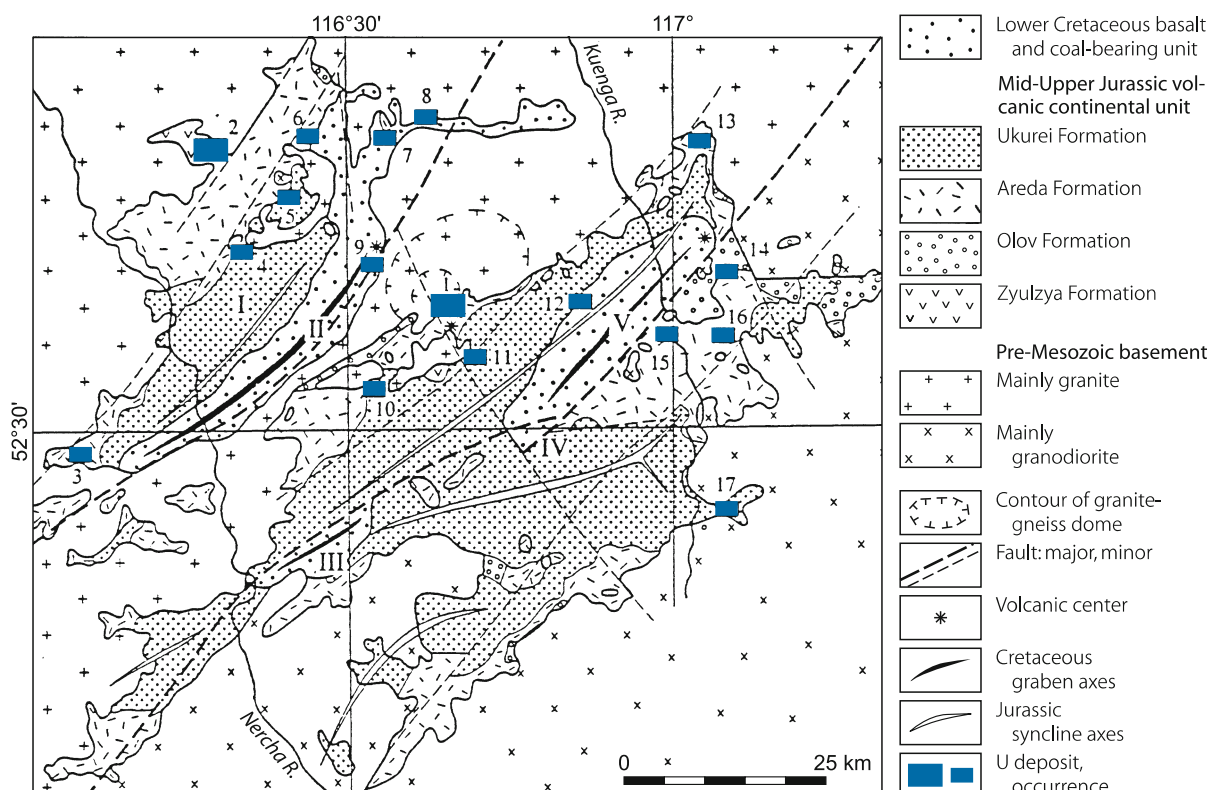
General Features of Geology

The Olov ore field covers two adjacent depressions filled with up to 3 000 m thick, subhorizontally dipping volcanic and sedimentary rocks of Middle Jurassic to Lower Cretaceous age. The basement consists of Paleozoic granite and Precambrian gneiss, and has a marked relief, which determines the thickness of the Jurassic deposits. The stratigraphic sequence includes from top to bottom ([Fig. 10.24](#)):

- Soktui Formation*, Lower Cretaceous, <800 m thick: Slightly indurated claystone, siltstone overlying sandstone, and sandy conglomerate, with intercalated lignite seams, and basalt flows.
- >Unconformity<
- Ukurai Formation*, Upper Jurassic, <700 m thick: An upper, as much as 500 m thick, alternating sequence of claystone, siltstone, sandstone and minor alluvial-deltaic conglomerate

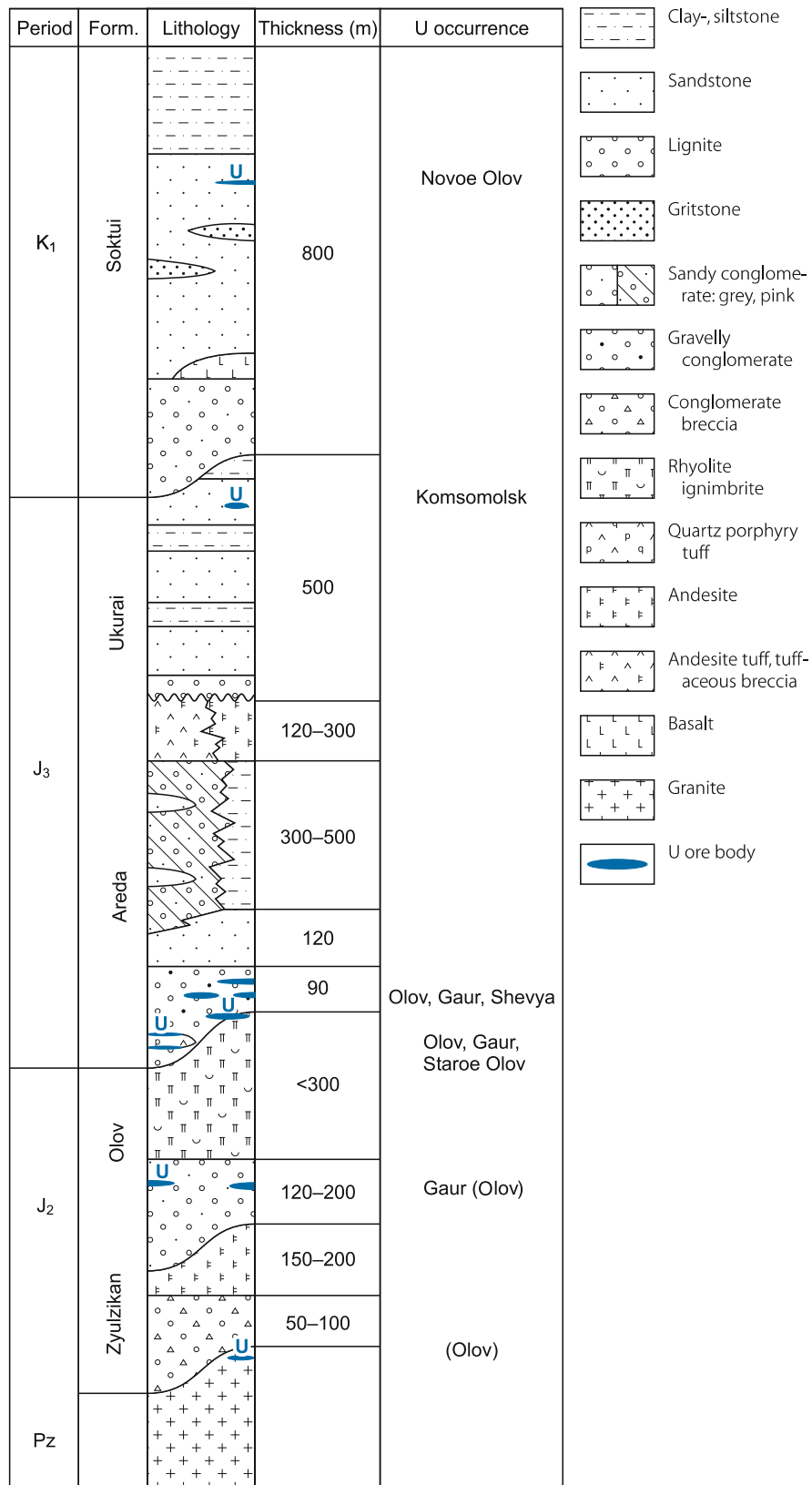
Fig. 10.23.

Central Transbaikalia, Olovsky (Olov) ore field, generalized geological map with location of U deposits and occurrences in Cretaceous-Jurassic volcanic-sedimentary depressions (after Kislyakov and Shumilin 1996). *Depressions: I Zyulzlya, II Southern Zyulzlya, III Kangil, IV Olov, V Utan. U deposits: 1 Olovskoye (Olov), 2 Ozernoye. U occurrences: 3 Olekan, 4 Zyulzlya, 5 Poiskovoye, 6 Severnoye, 7 Kalanga, 8 West Lukdun, 9 Novoe Olov, 10 Areda, 11 Staroe Olov, 12 Komsomolsk, 13 Aleur, 14 North Gaur, 15 West Gaur, 16 Gaur, 17 Shevya*



■ Fig. 10.24.

Central Transbaykalia, Olovsky ore field, litho-stratigraphic column of the Lower Cretaceous to Middle Jurassic volcanic-sedimentary sequence in the Olov area with stratigraphic position of U ore bodies (after Kislyakov and Shumilin 1996)



overlies a 120–300 m thick unit of andesite, basaltic andesite, and tuffaceous breccia with interbedded conglomerate, sandstone, and siltstone.

- *Areda Formation*, Upper Jurassic, 500–700 m thick: The upper, 120 m thick member consists of lacustrine, grey claystone, siltstone and sandstone, which grade laterally into up to 500 m thick, deltaic and proluvial, pink conglomerate with intercalated grey sand- and siltstone beds. The middle member is as much as 120 m thick and composed of alluvial gritstone, sandstone, siltstone, and tuffite. The lower, up to 90 m thick member consists of proluvial, grey conglomerate with intercalated sandstone and deluvial breccia lenses, and, in the basal part, a single bed of quartz porphyry tuff.
- >Unconformity<
- *Olov Formation*, presumably Middle Jurassic, <500 m thick: An upper, up to 300 m thick suite of rhyolitic ignimbrite with black volcanic glass sheets rests upon an 120–200 m thick suite of gritstone with sandstone and carbonaceous shale interlayers, and a basal grey conglomerate of granitic and andesitic provenance.
- >Unconformity<
- *Zyulzikan Formation*, presumably Middle Jurassic, <250 m thick: Two units are distinguished, an upper, 150–200 m thick andesite unit that rests on 50–100 m thick conglomerate and conglomeratic breccia with granite and gneiss fragments.

Deposition of the various sedimentary formations was preceded by general uplifts, followed by subsidence and erosion. Early sediments accumulated along the axial zone of the paleovalleys and abut against the granitic sidewalls. Major, NE-SW-oriented dislocation zones in the basement control the paleovalleys. Tectonic features are reflected by about NE-SW-, NW-SE- and E-W-trending, steeply dipping faults and closely spaced fractures, and by gently inclined faults. Mafic dike swarms follow the fault systems.

Host rock alteration features at U occurrences in the Zyulzya Depression include kaolinitization, hydromicazation, carbonatization (calcite veinlets), and, locally, silicification (dark grey and pink cryptocrystalline quartz veinlets). Hydrobiotitization is related to the ore-forming process (for alteration features in the Olov Depression see Sect. *Olovskoye*).

Principal Characteristics of Mineralization

Mineralization of U occurrences in the Zyulzya Depression consists of disseminated sooty pitchblende and other U-oxides associated with metacolloid and crystalline pyrite. U occurrences in the Olov Depression may additionally contain pitchblende and native arsenic (see Sect. *Olovskoye*).

Uranium deposits/occurrences of the Olovsky ore field are structurally controlled and hosted by terrestrial, grey, carbonaceous sandstone and siltstone predominantly of the Areda and Olov Formations, and to a minor degree of the Suktui and Ukurai Formations. Only a few occurrences are in rhyolitic volcanics of the upper Olov Formation and the granitic basement. Ore bodies are controlled by shallow dipping, intraformational

faults and occur most commonly at or adjacent to the intersection of these structures with steep faults.

General Shape and Dimensions of Deposits

U occurrences of the Zyulzya Depression consist of stratiform, up to 0.5 m thick lenses. The lenses are conformable with the bedding and display irregularly shaped tabular and curvilinear bandlike configurations in plan view. Lateral dimensions of ore bodies range from less than 100 m wide and long to 1 000–1 500 m long and 200–400 m wide. Ore grades average 0.05–0.08% U. Grades increase up to 0.2% U close to steep faults and granitic channel walls.

Olovskoye

Olovskoye (or Olov) was discovered in the central-north part of the Olovsky area in 1957. In situ resources are estimated at some 15 000 t U. at a grade of less than 0.1% U.

Sources of information. The subsequent description is summarized from Kislyakov and Shumilin (1996) and Vizhnyakov (1995a).

Geology and Alteration

The Olov deposit is on the northwestern flank of the Olov Depression (Fig. 10.23). Middle(?) and Upper Jurassic sediments and volcanics of several paleovalleys fill the depression. The channels are incised into a basement of Paleozoic granite. Proterozoic gneiss forms the basement to the south. Andesite and microdiorite dikes and sills cut the sedimentary-volcanic sequence. Host strata dip 10–12° SE. Structures include shallow inclined faults, and steeply dipping, NE-SW-, NW-SE- and E-W-trending faults (Fig. 10.25).

Alteration phenomena include argillization, carbonatization, silicification, sulfidization, and hematitization. *Pre-ore alteration* is represented by clay minerals (kaolinite after feldspar), carbonate (ankerite), and sulfide (pyrite) the distribution of which is controlled by the original rock permeability. These alteration products encompass the entire uranium mineralized litho-stratigraphic segment and display their strongest development within the uranium dispersion halo. Hematitization is presumably also a pre-ore process. Hematitization postdates argillization and is best developed in some parts of the deposit in unmineralized, basal conglomerate and subjacent granite imposing a dark red color on the rocks over up to 30 m thick intervals. Other parts of the Olov deposit display less pronounced hematitization, which is thought the result of a partial reduction of hematitized rocks. *Syn-ore alteration* is reflected by hydrobiotite and restricted to ore bodies, where it imposed a dark green color upon the host rocks. *Post-ore alteration* produced fissure fillings of dickite, realgar, and orpiment over a large vertical extent.

Mineralization – Shape and Dimensions of Deposits

The ore is monometallic. Uranium minerals include finely dispersed pitchblende, sooty pitchblende, and minor hydro-pitchblende and coffinite. Associated minerals are cryptocrystalline pyrite and native arsenic.

Uranium mineralization extends bandlike for more than 10 km in curvilinear E-W direction along the main paleochannel trend with diversions into tributary valleys. The band is composed of numerous, mostly ribbonlike ore bodies of low grade (<0.1% U) stacked along intraformational inhomogeneities. Better grade ore occurs as pockets characterized by grades of 0.1–1% U and a dark green color due to abundant hydrobiotite along steeply and gently dipping fractures filled with post-ore dickite. Position, size and shape of ore bodies are controlled by shallow inclined, often strata-peneconcordant faults composed of densely spaced fracture systems, and particularly at their intersection with steeply dipping NE-SW, NW-SE and E-W faults (Fig. 10.25).

Paleovalleys filled with the Upper Jurassic Areda Formation provide the preferential host sites. Some mineralization occurs in the Middle Jurassic Olov Formation and in granite. Mineralized horizons occur at several litho-stratigraphic levels. *Ore horizons 1 and 2* are confined to thin carbonaceous silt- and sandstone beds of the gritstone member of the Olov Formation. The Areda Formation contains *ore horizons 3 and 3a* in both tuff and grey sediments at the base and top, respectively, of the quartz porphyry tuff intercalation within the basal

gritstone-conglomerate member, and *ore horizons 4, 4a, and 4b* in the upper part of the same gritstone-conglomerate member. Most extensive ribbonlike ore bodies are found in ore horizons 3 and 3a. Largest ore bodies in horizons 4, 4a, and 4b occur as up to 30 m thick, elongated lenses in tributaries to the main paleovalley on the northern flank of the Olov deposit. Ore lenses may laterally cross litho-stratigraphic contacts of overlapping channels, and may also persist into granite.

In a general way, ore bodies are preferentially localized in the basal part of the volcanogenic-sedimentary sequence close to the granitic basement. Ore bodies are enveloped and interconnected by an up to 100 m thick halo of elevated uranium tenors; the lower boundary of which largely coincides with the basal volcanogenic-sedimentary contact but locally also penetrates into the underlying granite. The upper limit corresponds to the roof of the gritstone-conglomerate member of the Areda Formation. Arsenic, mainly as realgar and orpiment, forms an even larger aureole than the uranium.

Metallogenetic Aspects

Both hydrothermal and exogenic-epigenetic ore-forming processes of Cretaceous age left their prints in the Olov deposit. The leading role is attributed to the hydrothermal activity.

Kislyakov and Shumilin (1996) suggest a hydrothermal model for the origin for the Olov deposit, which includes four mineral stages:

■ Fig. 10.25.

Central Transbaykalia, Olovskoye (Olov) deposit. **a** Generalized structural map outlining the distribution of U lenses in the Olov and basal Areda Formations, and granite; **b** schematic geological NW-SE cross-section at the western flank and **c** at the northern appendix of the deposit. The latter exhibits the spatial relationship between hematitized and U mineralized zones. U mineralization (Fig. a) extends over a NW-SE width of several 100s of meters and is hosted in grit of the Olov Formation (# 1 and 2 Fig. b), and in quartz porphyry tuff (# 3, 3a) and grit-conglomerate (# 4, 4a, 4b) of the Areda Formation (after Kislyakov and Shumilin 1996)

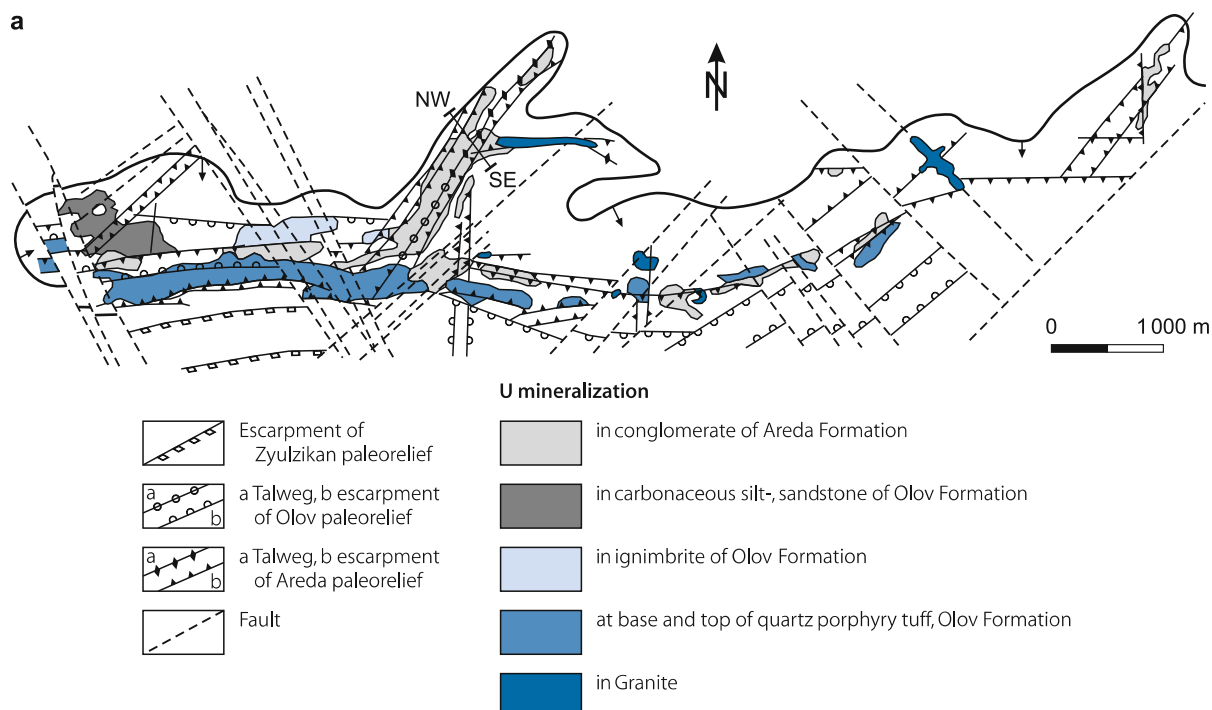
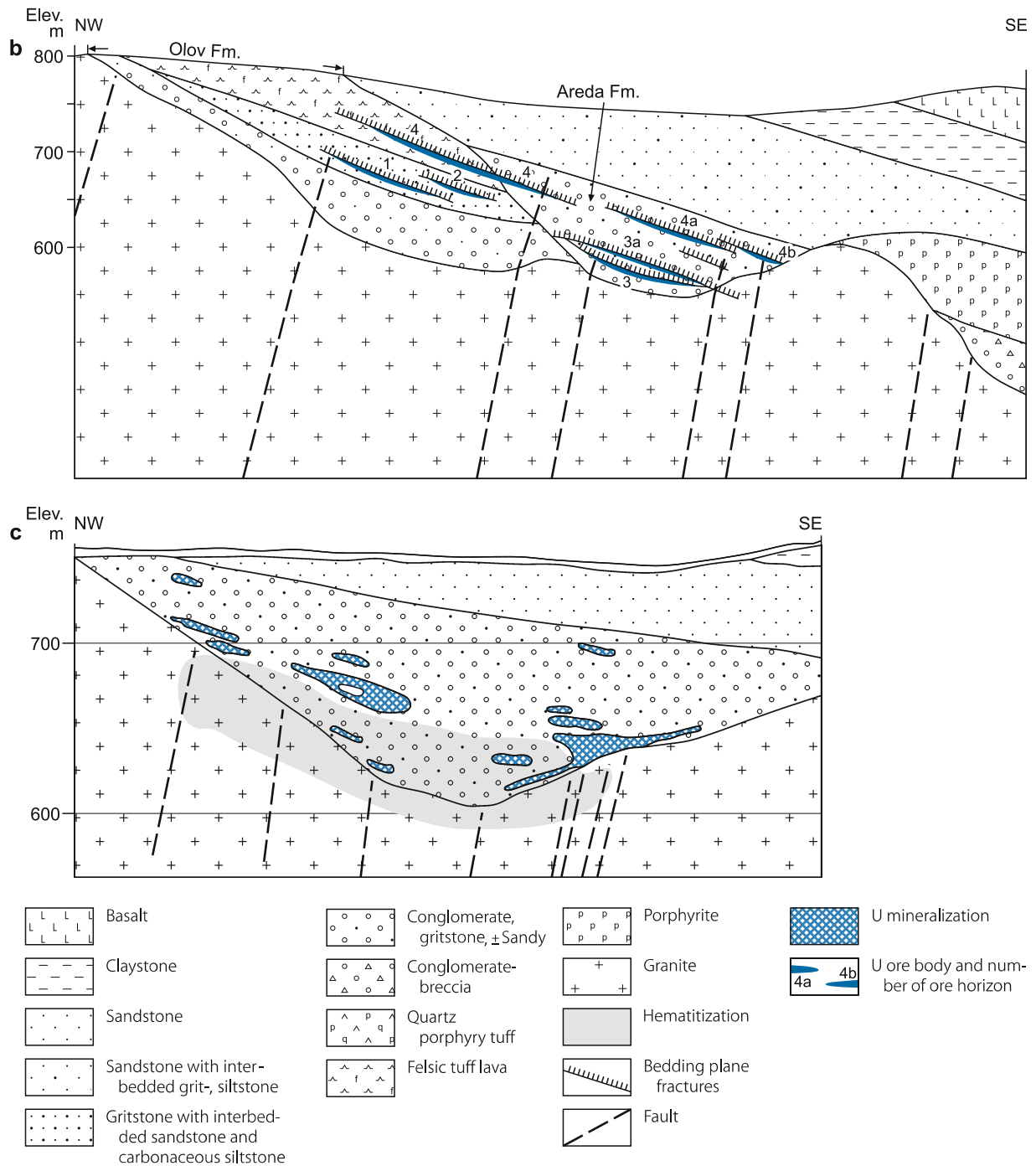


Fig. 10.25. (Continued)



1. pre-ore acidic leaching stage reflected by argillic, siliceous, and carbonate alterations
2. pre-ore carbonate-sulfide (ankerite, pyrite) stage
3. ore stage represented by disseminated U minerals, native As, pyrite, and hydrobiotite; and
4. post-ore stage marked by fissures filled with dickite, realgar, and orpiment

Radiometric datings yield ages of 110–100 Ma for the ore formation (Rozentsvit in Kislyakov and Shumilin 1996).

A hydrothermal origin of the Olov deposit is favored due to circumstantial evidence provided by the

- a spatial relationship with vein-stockwork uranium mineralization in claystone of the Ukurei Formation at the Komsomolsk occurrence southeast of the Olov deposit and that in granitoids of the Mayak, Korolevsk, and Chasovoye deposits southeast of the Olov ore field,
- b localization of the U mineralization mostly near the contact to the basement granitoid,

- c predominance of stratiform ore bodies,
- d structural features of ore localization, and
- e wide development of hydrothermal low-temperature ferromagnesian alteration and hematitization.

The low grade of the Olov ore can be partially explained by a low uranium concentration in the granitoid basement.

10.4.3.2 Amalat Area, Imskoye Deposit

The Amalat area is some 300 km N of Chita in the northern Buryatia A.R. It includes with the 1964 discovered Imskoye (or Ima) deposit a large but low-grade tabular sandstone-type uranium deposit in the western section of the Malaya Amalat Depression (Fig. 10.26). Kislyakov and Shumilin (1996) report that Ima is larger in size than Olov (= 15 000 t U). Ore grades are low, ranging between 0.01–0.1% U.

Source of information: Kislyakov and Shumilin 1996 unless otherwise stated.

Geological Setting of Mineralization

The Malaya Amalat Depression is a graben structure down-faulted along NE-SW and NW-SE faults into Precambrian and Early Paleozoic metamorphites intruded by Proterozoic, Paleozoic, and Mesozoic granitoids. Sediments of the Lower

Cretaceous Gusinoe Ozero Series fill the graben. There are three deepened segments within the depression, one of which, the Ima “syncline”, hosts the Ima deposit.

The Gusinoe Ozero Series is partitioned into three lithostratigraphic formations; only the lower of which, the 1 500–1 800 m thick Ima Formation, occupies the area of the Ima deposit. The Ima Formation is dominated by polymictic, unsorted clastic sediments and proluvial conglomerate alternating, in the mineralized upper section, with sandstone, gritstone, siltstone, and single claystone and lignite beds. Granite-derived clastic material with elevated uranium tenors of 5–20 ppm U constitutes a large fraction of the rocks at the deposit. Basal, coarser clastic facies of the Ima Formation are pink colored, while the upper, U mineralized part consists of alternating grey and pink beds. Host rocks dip 20–25° NNW. Transverse strike-slip faults separate the deposit area into several blocks while linear normal faults generated numerous slices (Figs. 10.26, 10.27).

Alteration

Host rock alteration phenomena include argillization, carbonatization, sulfidization, silicification, chloritization, sericitization, zeolitization, and oxidation and reduction processes. Argillic alteration distribution is controlled by structures and elevated permeability of slightly lithified sediments and shows zoning as exemplified from the eastern flank of the Ima deposit where mineralization occurs in the lower part of the grey unit near the interface with pink sediments:

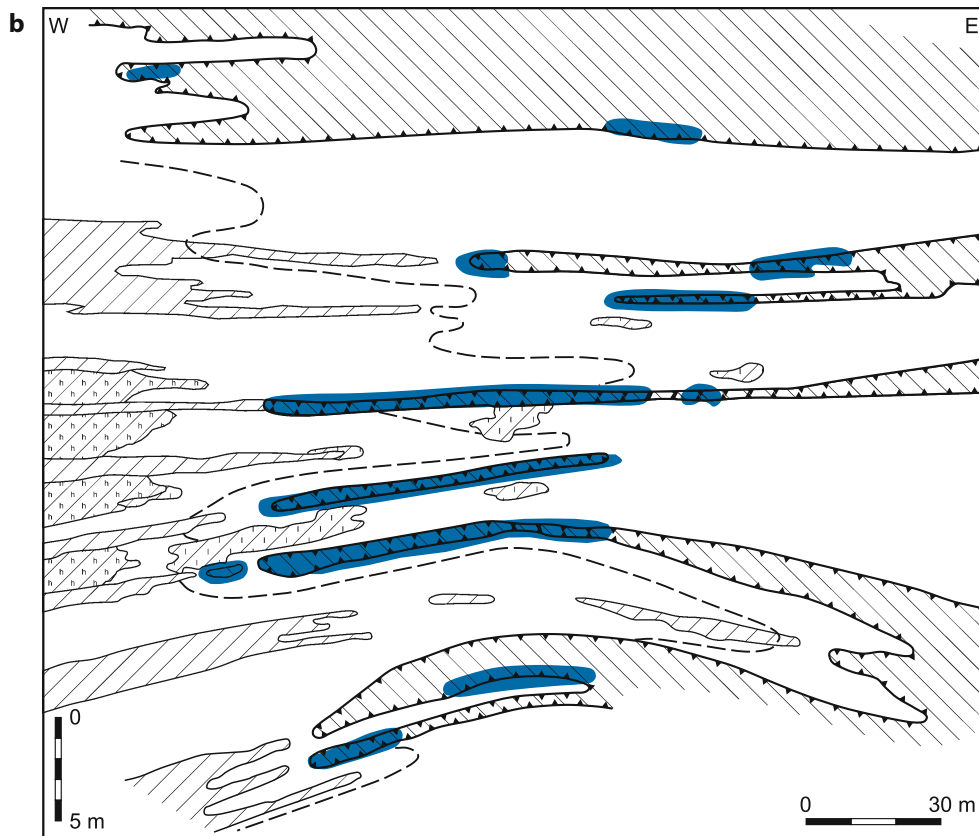
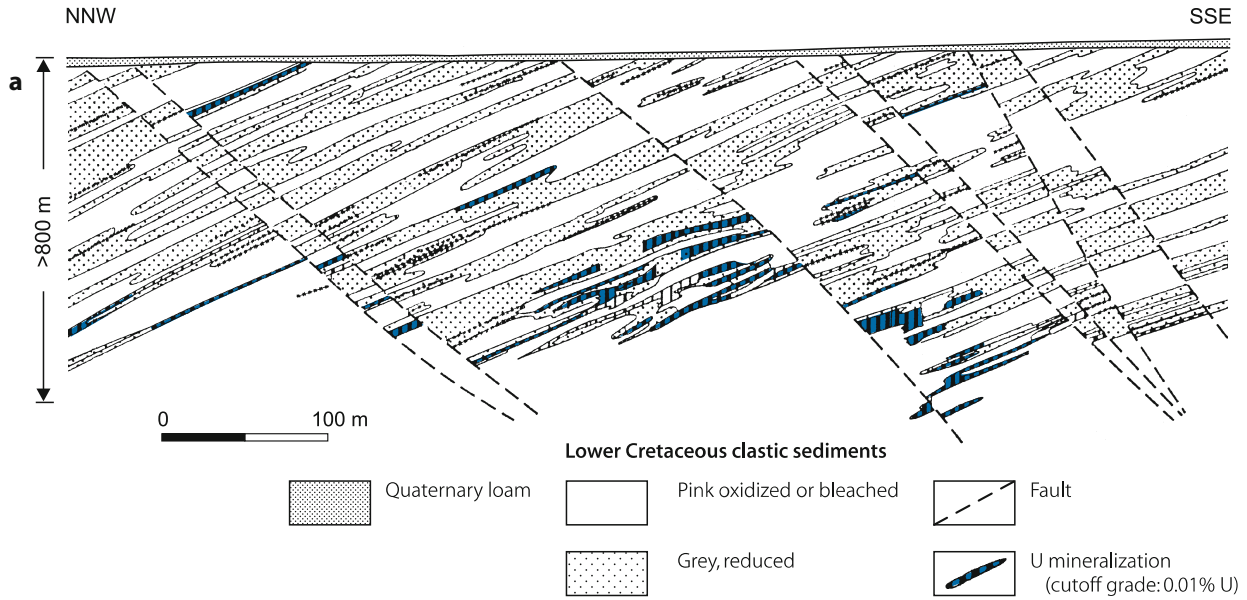
Fig. 10.26.

Central Transbaykalia, Malyi Amalat area, generalized geological map of the Lower Cretaceous Malo Amalat Basin with delineation of the Ima (or Imskoye) deposit (after Kislyakov and Shumilin 1996 based on Korobenko, Ilichev, and others)



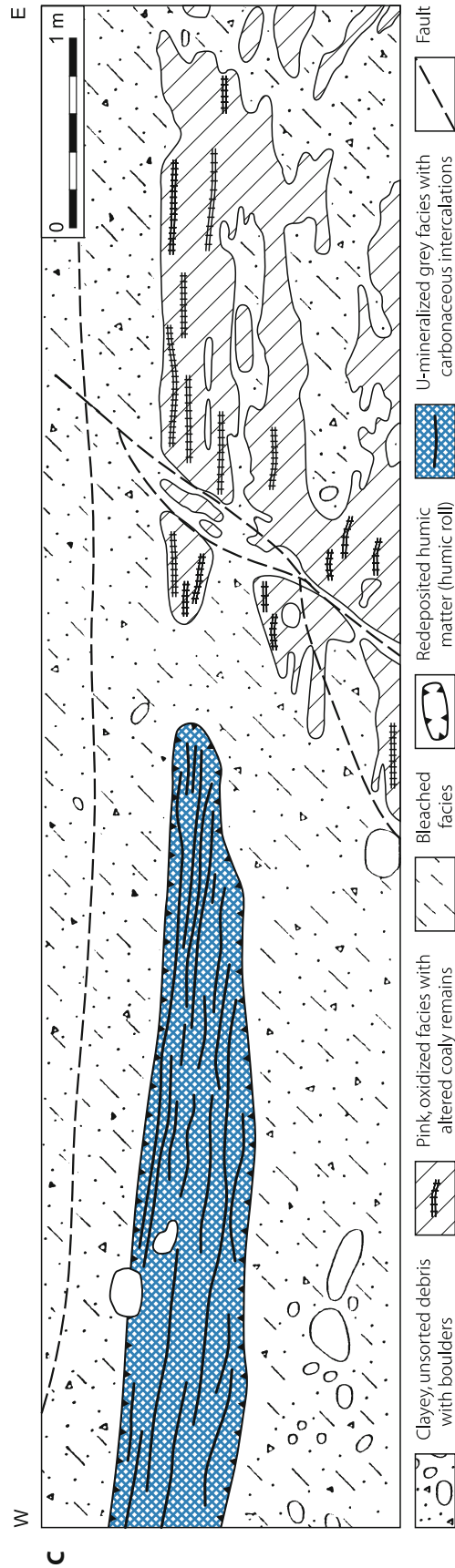
Fig. 10.27.

Central Transbaykalia, Ima deposit. **a** NNW-SSE cross-section through part of the sandstone-type deposit showing the superjacent stacked U lenses in the Lower Cretaceous Ima Formation/Gusinoye Ozero Series; **b** schematic W-E section illustrating alteration features of the mineralized segment; **c** sketch of a drift wall demonstrating the relationship of oxidized pink, reduced grey and bleached alluvial facies, humic accumulations, and U mineralization (after Kislyakov and Shumilin 1996)



Lower Cretaceous clastic sediments

Fig. 10.27. (Continued)



W

E

C

1 m

0

Clayey, unsorted debris with boulders

Pink, oxidized facies with altered coaly remains

Bleached facies

Redeposited humic matter (humic roll)

U-mineralized grey facies with carbonaceous intercalations

Fault

Outer, uppermost zone, divided into two subzones: (a) a kaolinite-carbonate subzone where kaolinite replaces the ground mass and clastic plagioclase, and carbonate biotite; and (b) a carbonate-quartz-pyrite subzone where authigenic kaolinite is replaced by carbonate, biotite by both carbonate and pyrite; and cryptocrystalline quartz has formed.

Inner hydromicaceous-chlorite zone: hydromicas replace plagioclase, orthoclase, biotite, newly formed kaolinite, and carbonate. Chlorite replaces biotite. Sericite and adular replace orthoclase. Zeolites developed locally.

Ore zone: composed of complex mineral associations including organic matter (rich in U, Mo, As, and, less commonly, Pb and Cu), pyrite, chlorite, hydromicas, and cryptocrystalline quartz.

Vein carbonate is widespread in the outer and inner zones but almost absent in the ore zone. Siderite is typical for the inner and ore zones, dolomite and calcite in the outer zone.

The hydrodynamic regime, which was from west to east during the oxidation event, later reversed its direction and redox potential. Mild reducing conditions evolved and generated in the formerly pink facies an irregular dimensioned bleached zone. The zone is up to several hundreds of meters wide in permeable rocks and narrows to fractions of a meter in impermeable beds. Traces of former oxidation are retained in bleached rocks as relic pink patches in clayey nests and lenses and in the interior of boulders and pebbles, and as pink speckled argillized feldspar due to Fe-hydroxides pigmentation. The bleaching of oxidized rocks was accompanied by a partial Fe loss, and Fe redeposition in pink facies. In the latter, the total iron content makes up 1.5–2 wt.-% whereas in bleached rocks it does commonly not exceed 0.4 wt.-%. The adjacent grey rocks also show low iron contents (0.3–1%) suggesting a Fe loss due to carbonate solution.

During a later event, bleached rocks near the contact with pink facies experienced locally a re-introduction of iron of up to 0.4–0.6 wt.-% associated with a pink re-coloration. There are also local areas of manganese and calcite accumulation with the formation of a coarse-grained poikilitic rock matrix. Calcite veinlets occur locally. Calcite contains fluid-gas inclusions with a homogenization temperature of 200 °C.

An unusual feature of redox activity is reflected by a narrow, 1–20 cm thick zone of redeposited organic matter (humic roll), whose appearance is related not only to the abundance of organic matter in primary grey rocks (3–5% C_{org}), but, evidently, also to the elevated alkalinity of the stratum waters. In mineralized horizons, the humic roll is universally traced along the boundary between primarily grey and bleached rocks. The humic roll does generally not differ in uranium content and radioactivity from uraniferous but ore-free grey rocks. Despite the influence of later reducing processes, the rear segment of the humic roll still reveals subzones of both weak oxidation with relics of coalified debris and more intense rock transformations up to complete oxidation of chlorites and ferruginous hydromicas. At some distance from the humic roll, the green color of clayey layers in bleached facies turns to pale.

A late yellowish limonitization is essentially confined to the present-day surface and probably originated during the Neogene-Quaternary prior to the development of permafrost. Permafrost persists to a depth of 120 m. At deep levels, limonitized rocks are partially reduced presumably by reaction with locally formed oxygen-free carbonic acid waters.

Mineralization

Principal uranium minerals are pitchblende and coffinite, and subordinate hydrous pitchblende and ningyoite. The uranium minerals associate with carbonaceous debris, redeposited humate, globular pyrite, and jordisite (Kochenov et al. 1995).

Most ore samples yield a radiometric age of 80–50 Ma, i.e., they formed not earlier than the Late Cretaceous whereas low-grade mineralization distant from stratum oxidation zones gives an age of 130 Ma (Malyshev in Kislyakov and Shumilin 1996).

U mineralization is controlled by an asymmetric, strata intersecting redox zoning. Four zones are distinguished: (1) primarily grey, intensely argillized host rocks with an elevated uranium content of several 100 ppm U; (2) rocks with redeposited organic matter (humic roll); (3) bleached reduced rocks with relics of preceding oxidation; and (4) pink oxidized rocks with pseudomorphoses of Fe-hydroxides after coalified remains, pyrite, and siderite. Ore occurs primarily in the grey facies and, to a lesser extent, in humic rolls and adjacent bleached rocks.

Ore lodes are essentially arrested at the interface of oxidized and reduced facies, and they are noticeably associated with zones of spatially continuous pink oxidized facies, which are typical for weakly permeable horizons. Within these zones, ore bodies are commonly confined to intervening grey rocks, which are marked by a bleached aureole. Some ore bodies occupy the hanging and footwall of ancient stratum oxidation zones whereas a few others show in cross section a reversed roll shape.

In the heavily disrupted SW segment of the deposit, numerous pink oxidation tongues penetrate permeable sand-gravel horizons from E to W and control the ore locus. Pseudomorphoses of Fe-hydroxides after abundant coaly debris and, less commonly, pyrite and siderite imposed the pink hue. The tongues join in the westernmost part of the deposit to a single, thick, pink unit.

Shape and Dimensions of Deposits

The Ima deposit consists of numerous, commonly tabular uranium lodes. Ore lodes are defined by a cutoff grade of 0.01% U. Ore lodes are from 0.2 to 12 m thick, tens of meters wide, and hundreds of meters long, and occur multiply stacked over a vertical range of more than 800 m. In the northern flank of the deposit, as much as 60 ore bodies were intercepted by deep drilling.

Conterminous, but fault separated blocks and beds differ, in spite of equal lithology with ore-hosting rocks and apparent uniform epigenetic alterations, in grade and size of ore lodes.

The difference is tentatively explained by a screen provided by gouge filled faults during ore formation.

Metallogenetic Aspects

The origin of the Ima deposit is debatable; a favored concept involves a multistage provenance during Cretaceous time. In a *first* stage, permeable granitoid clastic material with elevated uranium contents was accumulated. The *second* stage involves a low-temperature hydrothermal event that resulted in carbonatic-argillaceous alteration, chloritization, and zeolitization of the sediments, and an additional uranium influx into grey rock facies. During the subsequent *third* stage, exogenic-epigenetic processes produced the ancient (Late Cretaceous?) stratum oxidation tongues and related ore bodies at their basinward interfaces.

It is assumed that the hydrothermal and exogenic-epigenetic events most likely occurred during the terminal phase of the Malyi Amalat Basin development and prior to a denudation period, which eroded substantial parts of the Ima deposit. Some uranium was redistributed by Cenozoic redox processes, which produced young “augen” ores composed of round aggregates of finely dispersed coffinite fringed by light rims within limonitized rocks.

10.4.3.3 Other Uranium Deposits/Occurrences in the Central Transbaykal Subregion

The Korolevo-Chasovo ore field is to the north of Chita and contains the vein-type *Crystalnoye*, *Chasovoye*, and *Korolevskoye* occurrences (each <5 000 t U, <0.1% U) in Middle-Upper Paleozoic granites (Vizhnyakov 1995b).

Chikoisky-Yuzhno-Daursky ore field, situated to the south of Chita, contains a number of U occurrences of various type, all of them are of low grade. Reported occurrences include: *Gornoye* (>5 000 t U): vein-type hexavalent U mineralization in highly radioactive Mesozoic granite; *Berezovoye* (>500 t U): vein-type hexavalent U mineralization in Mesozoic highly radioactive granite; *Akhutinskoye*; *Barun-Ulacha*; and *Vostochnoye* (Vizhnyakov 1995c).

Khiloksky area, close to SW of Chita, includes the *Stepnoye* deposit in the Beklemishev Depression/Graben structure. *Stepnoye* has estimated resources in excess of >5 000 t U at ore grades of <0.1% U, contained in tabular, basal channel sandstone-type ore bodies. Host rocks are Lower Cretaceous lignite-bearing sandstone and conglomerate altered by argillization and intense zeolitization (Pelmenev 1995).

Mensensky area in the southern Transbaykal region contains the *Yugalskoye* vein-type deposit in highly radioactive granite (>1 500 t U, approximately 0.2% U).

Tunguiskey area in the southwestern Transbaykal region hosts the tabular *Zhuravlinoye* F-Mo-U deposit (>5 000 t U, <0.1% U) in Lower Cretaceous pyroclastics and clastic sediments.

Urulyunguevsky depression (overlaps the north part of the Streltsovsk/Tulukuyevsk Caldera) includes the *Meridionalnoye* and *Sirotininsk* deposits (each <5 000 t U, <0.1% U) with stratiform U mineralization in Lower Cretaceous argillized arenaceous sediments.

10.5 Aldan Shield Region

The Aldan Shield is an Archean-Lower Proterozoic crystalline massif in the Aldan River region in southern Yakutiya. Major towns are Aldan and Tommot. The massif is known for gold and uranium deposits. Gold is mined from recent placers and stratiform concentrations in basal Jurassic? beds. Uranium was explored in the Elkon District, an uplifted basement block in the central part of the Aldan Shield. Boitsov and Nikolsky (1997) in agreement with Naumov and Shumilin (1994) consider the uranium potential of the shield as the largest in Russia.

10.5.1 Elkon District

This district is located some 100 km ENE of the town of Aldan in the Sakha Republic, eastern Asian Russia. After the discovery of the first uranium occurrence in the early 1960s, about eighty more Au-U(-Ag)-bearing occurrences including nine deposits of vein-stockwork-type were found along distinct structural zones. Most significant deposits were identified along the Yuzhnaya structure. Figure 10.28 shows the location of major ore zones and deposits.

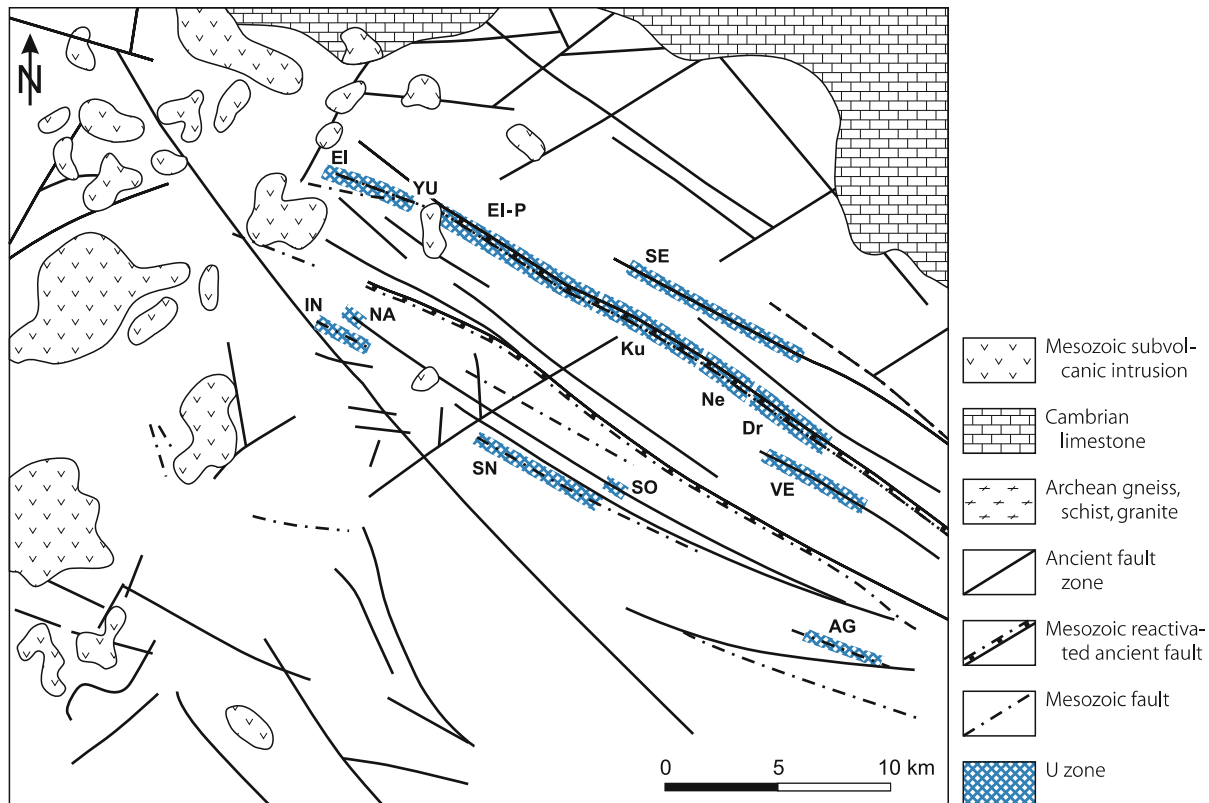
Four deposits were investigated by underground workings and five by drill holes to a depth of 2 000 m from the 1960s to the early 1980s. Some uranium was presumably produced during the underground investigations.

Total resources of the Elkon District are estimated in excess of 200 000 t U in the high cost category. Ore grades average 0.1–0.15% U while gold values range from less than 1 ppm to several ppm. (According to a press release of the Russian Natural Resources Ministry in 2006, “proven” resources amount to 342 000 t U; planned production capacity is 3 000 t U yr⁻¹ in ten years time.)

Sources of information. Birka et al. 2005; Boitsov and Nikolsky 1997; Boitsov 1989, 1996; Boitsov and Pilipenko 1998; Gotman et al. 1979; Kazansky 1995; Kazansky and Laverov 1977; Kazansky and Maksimov 2000; Kirillov and Berdinkov 1998; Kochetkov et al. 1986; Korolev et al. 1979; Miguta 1997; Miguta and Modnikov 1993; Naumov and Shumilin 1994. Miguta (1997) provides a comprehensive synopsis of alteration and ore-related mineralogical and geochemical features while Boitsov and Pilipenko (1998) address the typical geological settings of deposits and ore types.

Fig. 10.28.

Aldan region, Elkon District, generalized geological map with location of principal U zones and deposits. Small intrusive bodies and dikes (not shown) of Mesozoic age are particularly abundant in the western part of the region (after Boitsov AV and Nikolsky 2001 based on Akhapkin EV). **Au-brannerite zones:** AG Agdinskaya (Agda), SE Severnoye, SN Snezhnoye, SO Sokhsolookhsk, VE Vesennyaya, YU Yuzhnaya; **deposits:** Dr Druzhnoye(-Mineyevsky), EI Elkon, EI-P Elkon Plateau, Ku Kurung, Ne Neprokhodimoye. **Au-uraninite zones/deposits:** IN Interesnaya, NA Nadezhda



Regional Geological Setting of Mineralization

The core of the Aldan Shield consists of an Archean-Lower Proterozoic crystalline basement, which is exposed in several uplifts including the Au and U-bearing Elkon Horst. As much as 700 m thick, subhorizontally bedded Vendian-Lower Cambrian limestone and dolomite cover the basement to the north while Lower Jurassic coal-bearing continental sediments and pyroclastics fill grabens.

The Elkon Horst is a NW-SE-elongated, 60 km long and up to 40 km wide uplift in the central Aldan Shield. Principal lithologies are Archean granulite, amphibolite, gneiss, schist, quartzite, and marble. Intense Late Archean-Early Proterozoic granitization generated leucocratic biotite-microcline granite and migmatite. Only remnants of gneiss and schist are found in the granitized rocks.

Small laccolithic bodies, stocks, sills, and dikes of alkaline and calc-alkaline rocks of the Aldan volcano-plutonic complex were intruded into the afore mentioned units during three periods in the Jurassic and Cretaceous. Their abundance is most prominent in the western part of the Elkon Horst.

Brittle deformation affected repeatedly the region, particularly during the Early Proterozoic and Mesozoic and resulted in

three prominent fault sets: *ancient*, NW-SE- and NW-SE-trending faults formed during the Early Proterozoic, ancient faults *reactivated* during the Mesozoic, and *neotectonic* NW-SE and submeridional oriented faults of Mesozoic age. The latter caused block movements and resulted in horst and graben structures.

Principal Host Rock Alterations

Several kinds of alteration are documented by Miguta (1997). They include from oldest to youngest:

Post-granitization potassium-siliceous metasomatism is developed in zonal distribution in the Early Proterozoic granitoids. These metasomatites contain local concentrations of disseminated uraninite, cleveite, bröggerite, orthite, thorite, malaccon, and sphene.

Multistage Mesozoic, *pre-uranium* (brannerite) alteration is reflected by various mineral assemblages (Table 10.5), which are superimposed on each other in ore-bearing zones. All of them are controlled by Mesozoic neotectonic and reactivated ancient fault zones. Oldest is an *albite-sericite-chlorite* facies that zonally overprinted former rock constituents and formed microveinlets for up to a few tens of meters from faults. In the *outer*

■ Table 10.5.

Aldan region, Elkon District. Mineral assemblages of uranium-bearing zones (Miguta 1997)

Mineral assemblage	Minerals	Mode of occurrence
Albite-sericite-chlorite	Actinolite-tremolite, biotite, talc, chlorite, epidote, sericite, albite, calcite, magnetite, hematite, rutile, leucoxene	Metasomatite replacement, microveinlets
Pyrite-carbonate-K-feldspar	Pyrite, marcasite, calcite, dolomite, ankerite, brown K-feldspar, adularia, sericite, sphene, apatite, fluorite, and dispersed gold	Metasomatite replacement, microveinlets
Pyrite-carbonate	Pyrite, marcasite, dolomite, calcite, dispersed gold	Veinlets, breccia cement
Baryte-quartz	Quartz, baryte, tennantite, pyrite, chalcopyrite, enargite, sphalerite, galena	Veins, veinlets
Brannerite	Brannerite, pyrite, marcasite	Microveinlets, breccia cement
Micrograined quartz	Quartz, sagenite, recrystallized brannerite	Metasomatic replacement
Brookite-molybdenite	Finely dispersed molybdenite, brookite, uranium oxide	Veinlets, gouge
Coffinite-carbonate	Dolomite, ankerite, pyrite, marcasite, coffinite, hematite, anatase, gold	Metasomatic replacement
Fluorite-quartz-carbonate	Quartz, carbonate, baryte, fluorite, pyrite, marcasite, galena, sphalerite	Veinlets
Oxidized phases	Fe and Mn hydroxides, clay minerals, opal, chrysocolla, malachite, azurite, jarosite, carbonates, products of brannerite decomposition, utanyl minerals	Crusts, films, dispersed inclusions

zone, only mafic minerals were replaced by actinolite, tremolite, and talc imposing a greenish color on the rocks. An *intermediate zone* is characterized by chlorite development and locally hematite giving a green or pinkish-green color to the rocks. An *inner zone* is only locally developed. Where present, all leucocratic minerals were replaced by albite or albite-oligoclase, and mafic minerals by hematite and chlorite, which imposed a greenish-pink or reddish color on the rocks. Sericite and carbonates occur in the latter two zones. The process is considered of Mesozoic age since it affected Jurassic minette dikes.

A younger and the most prominent pre-uranium alteration assemblage consists of *pyrite-carbonate-potassium feldspar* with dispersed gold. It is of tan, greenish-brown, or dark grey color and surrounds all ore-bearing structures. This facies overprinted particularly the albite-sericite-chlorite aureoles, and formed micro-veinlets for several hundreds of meters along strike and dip of reactivated ancient faults and commonly persists for 6–10 m and locally up to 20 m into the wall rocks. A vague zoning is reflected by an outer halo of *pyrite-carbonate-sericite* that developed along fractures and an inner zone where *pyrite-carbonate-orthoclase* with *adularia* subzones overprinted brecciated rocks. In the *outer zone*, mafic minerals are completely substituted by dolomite, ankerite, pyrite, and marcasite while plagioclase is replaced by sericite and carbonate, magnetite by pyrite, and quartz by calcite. Proportions of carbonate and pyrite are highly variable. Carbonate can amount to 50% as found in the Yuzhnaya zone. The *inner halo* is characterized, besides the above mentioned replacements, by a markedly increased K-feldspar content. Microgranular orthoclase formed first and was subsequently more or less recrystallized to translucent adularia over tens of centimeters to few meters thick intervals. In result, a dense, dark grey, fine-grained alteration facies evolved composed of 40–75% K-feldspar, 35–50% carbonate, 5–15% pyrite and minor sericite, sphene, and apatite. Pyrite concentrates carry as much as 80 g t⁻¹ of gold.

Boitsov VE and Pilipenko (1998) consider the pyrite-carbonate-feldspar alteration facies to have originated from three sequential mineral formations: (1) pyrite-ankerite-orthoclase, (2) pyrite-dolomite-orthoclase, and (3) calcite-adularia. Pyrite of the first and second assemblages contains significant amounts of gold and silver.

Subsequent to brecciation, a *pyrite-carbonate* assemblage developed within the older pyrite-carbonate-orthoclase/adularia facies. Dolomite is the prevailing mineral associated with subordinate calcite, pyrite, and marcasite. The assemblage cements breccias and forms up to 0.5 cm thick veinlets. Pyrite contains dispersed gold with values of up to 4.5 g t⁻¹ Au in pyrite concentrate.

A *baryte-quartz* assemblage associated with minor Fe-, Cu-, Zn-, and Pb-sulfides is restricted to the Druzhnoye deposit in the Yuzhnaya zone where these minerals form up to 2 m thick and 30 m long and deep veins. Quartz occurs in several generations.

Late and post-ore alteration includes carbonatization, silicification, fluoritization, sulfidization, and oxidation. The post-ore emplacement of Mesozoic alkaline intrusions caused fenitization of earlier facies.

Geochemical changes by the alteration processes include removal and introduction of elements. Desilicification is documented by replacement of quartz by calcite and the destruction of mafic minerals both causing removal of SiO₂ from the altered zones. The SiO₂ content of quartz-rich gneissic granite and massive granite was depleted by about 40% while gneiss and schist lost on the order of 12% SiO₂. Redeposition of the liberated SiO₂ occurred as quartz along structurally prepared sites in form of segregations, stockworks of thin veinlets, up to 3 cm thick veins, and cement of breccias. Quartz was preferentially deposited at the upper levels of deposits where it formed “quartz caps”.

Removal of alumina is typical for wall rocks in the vicinity of mineralized zones. Al₂O₃ depletion is strongest in extremely

altered rocks immediately adjacent to ore veins where the original alumina content decreased by up to 25%.

Ca, Mg, Mn, P, and Ti were dissolved and redeposited over the whole section as constituents of authigenic mafic minerals, apatite, carbonates, rutile, sphene, and other minerals.

Potassium was introduced and sodium removed during the pyrite-carbonate-potassium feldspar alteration process. Altered rocks show an addition on the order of 10–20% K_2O and a loss of 80–90% Na_2O .

Addition of carbon dioxide and sulfur occurred all along the metallogenetic evolution. It was distinctively intense during the pre-ore stage when calcite replaced quartz while ankerite, dolomite, marcasite, and pyrite substituted mafic minerals. In addition, carbonates and sulfides developed as disseminations along fissures, and in the matrix of breccias. Carbonates also constitute late stage gangue minerals. Miguta (1997) estimates that during the alteration processes about 130 kg of CO_2 and 60 kg sulfidic sulfur per m^3 was added to the precursor rocks.

Fluorine was locally introduced into peripheral parts of alteration zones where it occurs as fluorite veinlets and matrix constituents of breccias. The fluorine grade increases here up to 0.6% as compared with background values of 0.05–0.1 wt.-% F.

Principal Characteristics of Mineralization

The only *primary uranium mineral* is a medium to low temperature U-Ti-phase defined as brannerite-A by Korolev et al. (1979). It commonly occurs in massive, colloform aggregates that enclose small fragments of host rocks, and more rarely as up to 0.08 mm high prismatic crystals. *Associated minerals* are pyrite and marcasite. They largely predate brannerite. Only a small fraction of them is contemporaneous with brannerite. Alteration products of brannerite include secondary brannerite, more or less uraniumiferous TiO_2 -phases, U-oxides and, in oxidized intervals, hexavalent U minerals, which formed after renewed deformation interludes.

Gold is a common constituent of most of the ores but it tends to be not syngenetically related to U. Au mineralization predates and postdates the brannerite formation.

Brannerite was significantly decomposed during a carbonatization event to amorphous TiO_2 -phases containing variable amounts of uranium and admixtures of Nb, W, and Zr. A part of the liberated uranium migrated into the host metasomatites where it recrystallized as coffinite during a silicification event that generated microgranular quartz in up to a few meters wide, lenticular, brecciated intervals. Corroded primary brannerite survived as relics in the quartz mass and as recrystallized prismatic crystals. Titanium was redeposited as acicular rutile crystals. Coffinite typically replaces pyritized mafic minerals, and coats Fe-sulfides contained in fissures and voids. This silicification affected all deposits where it prevails in the upper sections and decreases with depth.

Aggregates of subhedral to rounded uraninite and Ti-oxide phases with or without brannerite occur in the vicinity of Mesozoic magmatic intrusions in the NW segment of the Elkon District. Their generation is attributed to the destruction of brannerite by contact metamorphism.

Fenitization related to Mesozoic alkaline intrusions caused alteration of brannerite and its decay products up to a complete replacement of the uranium ore by biotite, aegirine, and albite.

At the Druzhnoye deposit and adjacent sections of the Yuzhnaya zone, a brookite-molybdenite assemblage with a uranium mineral that was tentatively defined as a uranium oxide was found. The minerals form a few centimeters to 2.5 m wide, flattened stockworks of veinlets, and black earthy masses, crusts, and coatings in breccias.

Post-ore breccias are cemented by dolomite and ankerite with disseminated marcasite, pyrite, rare anatase, and native gold. Rock fragments contain intensely corroded brannerite. Small grains and rare veinlets of coffinite, which always associate with pyrite or marcasite, occur in the breccia matrix. Up to 36 μm large grains and leaflets of native gold are enclosed in fine-grained carbonates. The gold accumulates in pockets, which locally can contain up to 100 $g\ t^{-1}$ Au.

A final generation of endogenic mineralization consists of dark veinlets of calcite, dolomite, fluorite, marcasite, pyrite, quartz, and minor baryte, chalcopyrite, galena, and sphalerite.

Oxidation of primary ore persists to a depth of some tens of meters below the current surface in most deposits of the Elkon District but may extend to 600 m deep in some ore-bearing structures. Characteristic minerals include Fe- and Mn-hydroxides, azurite, carbonates, chrysocolla, clay minerals, jarosite, malachite, opal, various products of decomposed brannerite, uranyl-phosphates, and U adsorbed by Fe-hydroxides and other minerals.

Textures of uraniumiferous mineralization are dominated by fine- to microclastic breccia and veinlet-breccia. Stringer and dissemination textures are less frequent.

Breccia-type ore includes the primary brannerite-pyrite-marcasite paragenesis and occurs along mylonites, quartz vein contacts and similar structural elements within deformed pyrite-carbonate-potassium feldspar altered rocks. Primary brannerite, pyrite, and marcasite occur as up to 3 mm thick and several centimeters long veinlets and disseminated grains or aggregates within the matrix of breccias. Both textural varieties coexist commonly and constitute together with their alteration products the bulk of the veinlet-breccia-type uranium ore.

Miguta (1997) reports as major *geochemical ore components* 1.5–10 wt.-% CO_2 and 1–4 wt.-% sulfidic sulfur, and distinguishes four characteristic geochemical groups of minor elements in the various ore zones (in wt.-%):

Group 1 elements are 0.1–0.3% As, 0.01–0.1% Tl, 1–10 ppm Ag, and 0.2–2 ppm Au, which are concentrated in finely dispersed pyrite of pre-ore potassium metasomatite. The host pyrite replaced mafic minerals or occurs in the matrix of pyrite-carbonate breccias.

Group 2 elements are As, Bi, Cd, Cu, Ge, Pb, Sb, Sn, Tl, and Zn. They typically occur in chalcopyrite, fahlore, sphalerite, and other sulfides associated with pre-ore quartz-baryte veins.

Group 3 is composed of minor constituents of brannerite and includes Nb, W, Zr, radiogenic Pb, and some REE. Their tenor in ore correlates well with that of uranium.

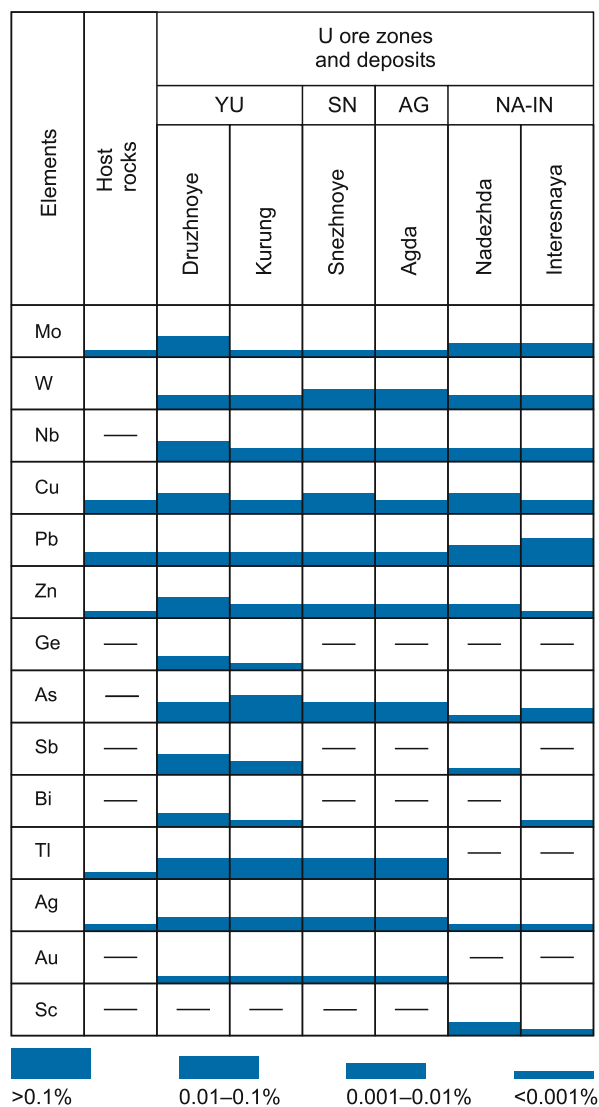
Group 4 includes Ag, As, Hg, Pb, and Tl that occur with finely dispersed molybdenite. The abundance of the various elements in selected deposits is shown in [Fig. 10.29](#).

Boitsov VE and Pilipenko (1998) distinguish three *uranium ore varieties*: gold-brannerite, gold-uraninite, and brannerite-silver-gold mineralization, and, additionally, three gold ore types, which may or may not contain minor uranium.

Gold-brannerite mineralization is typical for deposits at the Yuzhnaya, Severnoye, Sokhsolookhsk, Pologaya, Vesennaya, and Agdinsk zones. Ore control is by reactivated ancient and

Fig. 10.29.

Aldan region, Elkon District, abundance of minor and trace metallic elements in selected U deposits and host rocks (after Miguta 1997). U ore zones: AG Agdinskaya, NA-IN Nadezhda-Interesnaya, SN Snezhnoye, YU Yuzhnaya



neotectonic NW-SE-oriented and steeply SW dipping faults of Mesozoic age and by pyrite-carbonate-potassium feldspar altered rocks. Mineralized zones are traced by blastomylonites imposed on Early Proterozoic metadiorite dikes. Country rocks are Archean-Early Proterozoic ultrametamorphic lithologies. Gold-brannerite mineralization is of veinlet-disseminated-type and commonly located within gold-bearing pyrite-carbonate-potassium feldspar altered zones. Brannerite is the only primary U mineral. Appreciable amounts of gold and silver are bound in two, pre-brannerite pyrite generations of the pyrite-carbonate-potassium feldspar facies. Pyrite I occurs as 0.001–0.1 mm large grains and contains most of the gold but only minor silver, thallium, vanadium, and, more rarely, arsenic. Together with ankerite, pyrite I profoundly replaced magnetite and feric minerals. It constitutes up to 20 vol.-% of altered mafic and 0.5–7 vol.-% of other host rocks. Monomineralic concentrates of pyrite I yield 60–90 ppm of gold. Pyrite II occurs as 0.01–0.15 mm large grains. Contents of pyrite II in altered rocks compare with those in pyrite I, but pyrite II contains much less gold (2–5 ppm in concentrate) whereas it is enriched in arsenic (up to 0.5 wt.-%), silver, vanadium, lead, and zinc. Native gold occurs locally and is associated with the calcite-adularia alteration facies.

Gold-uraninite mineralization is known from the Nadezhda and Interesnaya zones in the northwestern sector of the Elkon District where Mesozoic stocks and dikes are abundant ([Tables 10.6, 10.7](#)). Ore control and geological setting are similar to those of the gold-brannerite deposits except that the uraninite is restricted to zones of thermal metamorphism. In contrast to the gold-brannerite assemblage, the gold-uraninite mineralization has higher uranium grades. Early pyrite tends to be the essential host of native gold. Concentrates of the early pyrite have contents from 9.1 to 24.5 ppm Au.

Brannerite-silver-gold mineralization is reported from the Fedorov, Marsovaya, Mramornaya, and Zvezdnaya zones in the southwestern Elkon District. Ore control and geological setting are similar to those of the gold-brannerite deposits. Ore lodes consist of gold-bearing metasomatic rocks intersected by thin brannerite stringers and a younger generation of small quartz and carbonate veinlets with acanthite, native gold, native silver, and pyrite (for ore grades see next section).

General Shape and Dimensions of Deposits

Location, shape, dimensions, and internal structure of uranium-gold and uranium-gold-silver deposits are primarily controlled by NW-SE-oriented and steeply SW dipping faults ([Fig. 10.30](#)).

Deposits consist of one or several intermittently distributed ore bodies composed of veinlike or columnar ore lodes with an internal stockwork or network structure of closely spaced brannerite stringers and impregnations ([Fig. 10.31](#)). Ore shoots within these lodes may carry also gold, silver, and locally molybdenum in variable amounts ([Fig. 10.32](#)). Ore lodes are usually 0.2–5 m wide in neotectonic Mesozoic faults but achieve a width of up to 10 m in rejuvenated Proterozoic faults. Lodes group to

Table 10.6. Aldan Shield, Elkton District. Types of Mesozoic gold-uranium and gold mineralization (Boitsov and Pilipenko 1998)

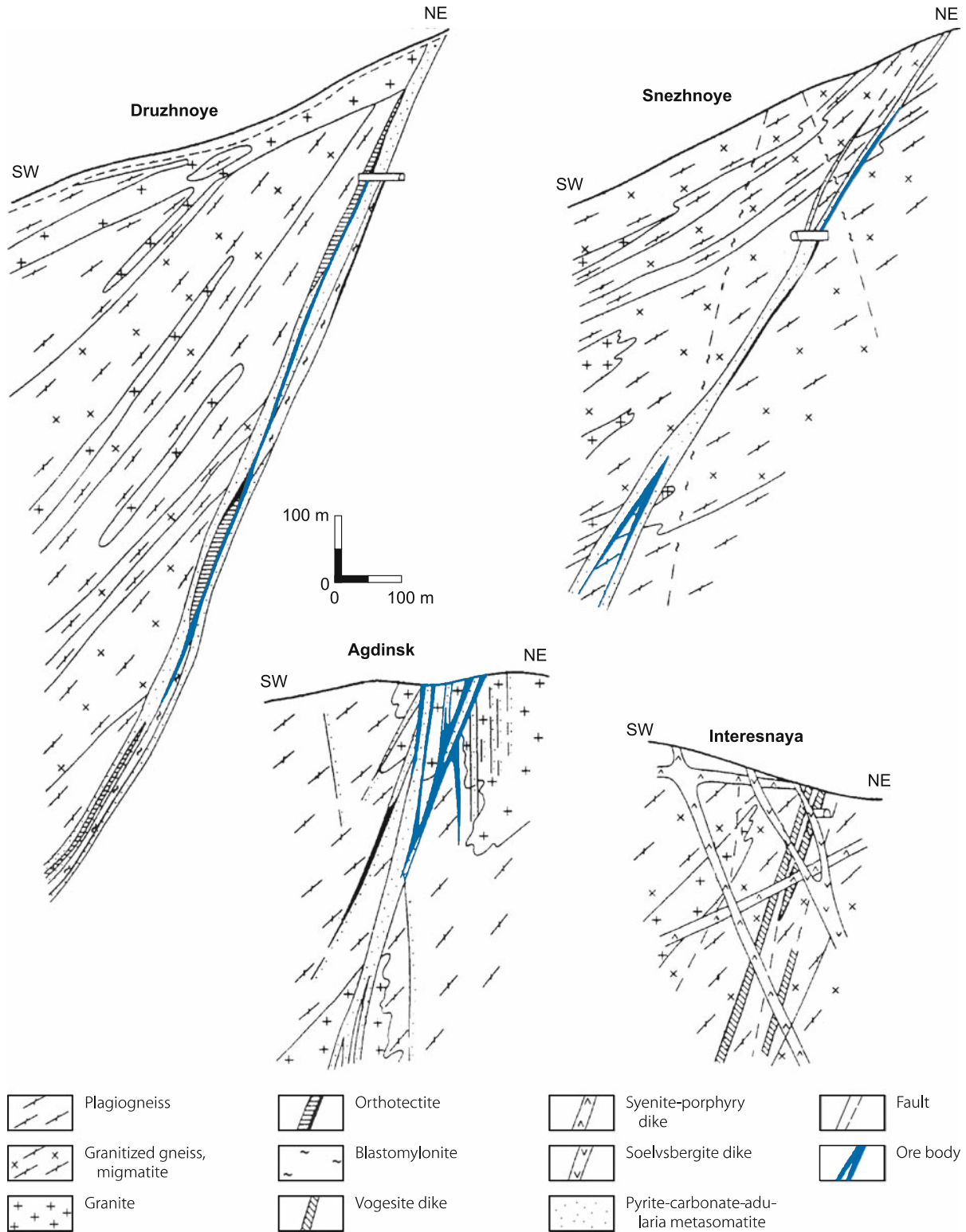
Ore zone/deposit	Ore types	U phases	Au and Ag phases	Geological setting	Ore-controlling structures	Morphology of ore bodies	Average mineral composition of ore (vol.-%)					Average content (ppm)	
							F	Q	C	S	Au	Ag	
Yuzhnaya, Sokhsolookhsk, Pologaya, Vesennyaya, Agdinsk zones	Au-brannerite	Brannerite	Au-bearing pyrite, native Au	Crystalline basement	Reactivated old faults, Mesozoic fractures	Large lodes	65	10	20	5	1-2	8-15	
Interesnaya, Nadezhda zones	Au-uraninite	Uraninite	Native Au	Crystalline basement	Mesozoic fractures	En echelon lenses	60	15	15	10	0.5-1	10-20	
Fedorovsk, Zvezdnaya, Marsovaya zones	Brannerite Ag-Au	Brannerite	Native Au, Ag, Au-Ag-bearing pyrite, acanthite	Crystalline basement	Reactivated old faults, Mesozoic fractures	En echelon veins	50	10	30	10	3-10	15-200	
Ryabinovsk, Novoye deposits	Porphyry Au	-	Native Au, Au-Ag-bearing pyrite	Crystalline basement	Mesozoic intrusions contact zones of intrusive phases	Linear, ring, and pipe-like	75	5	10	10	2-5	2-10	
Lebedinsk, Kolytkon, Samodumovsk deposits	Au-sulfide	-	Native Au and Ag, Au-Ag-bearing sulfides	At base of platform cover	Bedding-plane and cross-cutting fractures	Ribbon-shaped lodes and veins	5	10	10	75	10-80	20-90	
Bokovoye, Delbe, Centralnoye, Porfirovoye, Severnoye deposits; Nizhne-Yakokit ore field	Au redeposited in karst	Uraninite	Native Au, Au-bearing pyrite	At contact of platform carbonate rocks with Jurassic terrestrial sediments	Linear karst zones	Ribbon- and lens-shaped	5	80	5	10	2-10	2-10	

F feldspar, Q quartz, C carbonate, S sulfide. Note: For the mineralization type of redeposited gold, the table shows an average mineral composition of primary ores.

Table 10.7. Aldan region, Elkon District. Characteristics and dimensions of uraniferous zones (Miguta 1997)

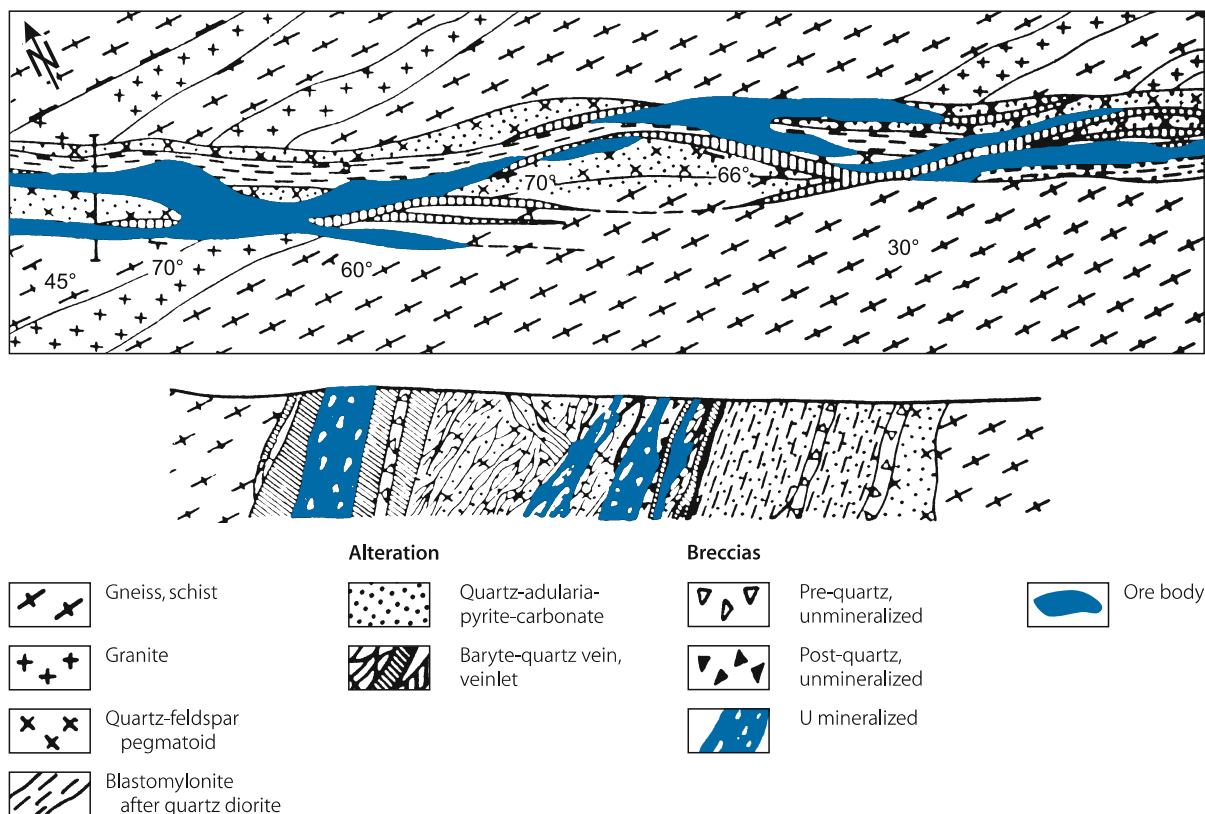
Ore zone	Structural characteristics						Ore bodies	
	Type of zone	Length (km)	Width (m)	Strike and dip	Inherited older structural elements	Mesozoic structure	Shape and size	Depth extension
Yuzhnaya, Sokhsolokhst	Rejuvenated ancient regional faults	Sev.10	Sev. 100	300–330°, 65–90° SE	Ancient structural elements: orthotectonite, metamorphosed dikes, blasto- and ultramylonite	Elongated subparallel cataclastic and breccia zones, <10 m wide, commonly in the footwall of ancient faults	Large tabular bodies, 1.5–10 m thick, sev. 100s m long along strike and dip	~2 km
Pologaya, Fedorov, Centralnaya, Nevskaya	Large fault zones of relative simple structure	2–15	2–10	280–330°, 45–80° SE	Some, extended intervals at contacts of metamorphosed rocks and dikes	Extended cataclastic and breccia zones, 1–3 m wide	Elongated, flat lensoid bodies, 1–2 m thick, several 10s to sev. 100s m long, elongated along dip	1–1.2 km
Agda, Veselaya, Marsovaya, Kurumkan	Variably oriented, complex fault zones	1–8	2–3, in bulges 10–15	Variable strike and dip with 65–80°	–	En echelon cataclastic and breccia zones, sev. 10s cm to 3 m wide, at fault junctions <15 m wide	Flat lensoid bodies, sev. 10s cm to 2 m thick, sev. 10s to sev. 100s m long, complex bodies at fault junctions	700 m
Interesnava, Udachnaya	Fault zones at contact with Mesozoic dikes	0.3–2	1–5	280–310°, 65–80° SE	Contact of pre-ore dikes	Cataclastic zones with breccias at contact with dikes	Small individual lodes with complex morphology, sev.m long along strike and dip	100–300 m

Fig. 10.30. Aldan region, Elkon District, geological sections across deposits in the four principal U zones (after Miguta 1997)



■ Fig. 10.31.

Aldan region, Elkon District, **a** Plan and **b** SW-NE cross-section across a U mineralized structure illustrating the distribution of alteration zones and U mineralization along rejuvenated blastomylonite intervals (after Kazansky and Laverov 1977 based on Krupenikov et al. 1968)



en echelon arranged, linear, 500–700 m long and 0.5 to more than 10 m wide ore bodies. Ore bodies are separated by barren or erratically mineralized ground composed of variably mineralized fractures, joints, and disseminations, the distribution, intensity, and dimensions of which are a function of the brecciation degree of the host rock.

Ore bodies are rarely exposed on surface. Upper limit of most ore bodies is at a depth below 200 m. Ore was drill intercepted to a depth of 2 000 m. No depth-related change in ore mineralogy was noticed over the whole vertical interval suggesting that mineralization probably continues into greater depth.

Brannerite-gold ore has uranium contents ranging from 0.02% to 0.2% U and more, and averages about 0.1–0.15% U. Gold tenors average 1–2 g t⁻¹, silver 8–15 g t⁻¹. Molybdenum grades vary between 0.01 and 0.1%. *Uraninite-gold ore* averages 0.5–1 g t⁻¹ Au, 10–20 g t⁻¹ Ag and has U contents exceeding that of the brannerite-gold ore. *Brannerite-gold-silver ore* has average tenors of 3–10 g t⁻¹ Au and 15–200 g t⁻¹ Ag but locally the Au and Ag grades can be substantially higher. U grades are between 0.02 and 0.2% but can exceed 0.5% U. The carbonate content of ore varies between 1.5 wt.-% in silicified ore and 10 wt.-% in other ore types, and the sulfidic sulfur content between 1 and 4 wt.-% but can be up to 20% S and more. For more details see Sect. *Description of Individual Ore Zones*.

Stable Isotopes and Fluid Inclusions

Fluid inclusion studies suggest the following approximate crystallization temperatures (Miguta 1997): Calcite formed at the end of the albite-sericite-chlorite alteration stage: 250 °C, pre-ore quartz of quartz-baryte veins: 230–290 °C, post-ore quartz: 160–200 °C, and late post-ore fluorite: 115–140 °C.

Decreepitization tests on pyrite of the main pyrite-carbonate-potassium feldspar, pre-ore alteration stage indicate a formational temperature of about 300 °C. Circumstantial evidence provided by adularia recrystallization suggests that subsequently the temperature dropped markedly since adularia typically crystallizes at temperatures of 150–200 °C.

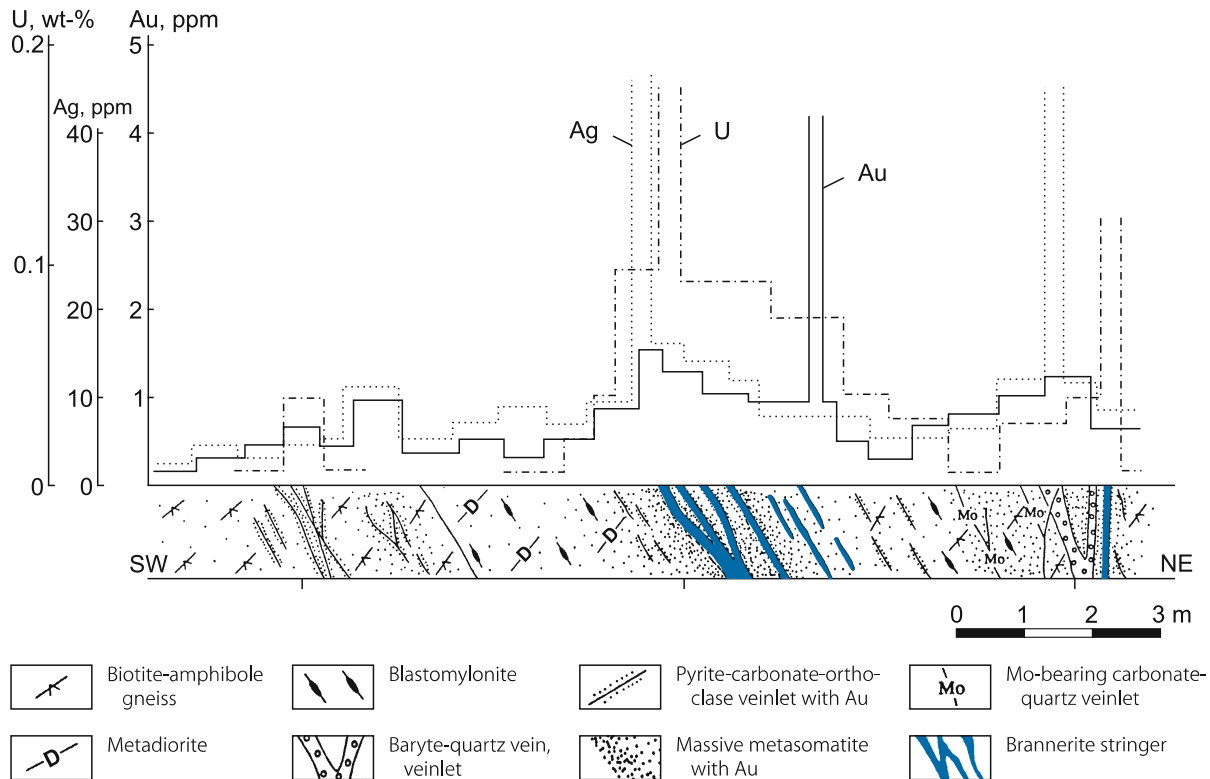
Thermobarometric studies indicate pronounced variations of temperatures during the entire metallogenetic evolution of the Elkon ores and its individual stages. Successive mineral stages started constantly with higher temperatures than those at the end of the previous stage suggesting a multiphase influx of ore-forming fluids.

Regional Geochronology

Three major episodes of Mesozoic magmatism are recorded: Syeno-diorite porphyry, minette, bostonite, kersantite, and

Fig. 10.32.

Aldan region, Elkon District, schematic section of a trench floor across a blastomylonite interval with vein and disseminated gold, silver, and brannerite mineralization (after Boitsov VE and Pilipenko 1998)



calcalkaline rocks yield a *Middle Jurassic* age of 188–158 Ma; monzonite, nepheline syenite etc. an *Early Cretaceous* age of 140–130 Ma; and aegirine granite, sölvbergite, tinguaita a *Middle Cretaceous* age of 120–107 Ma.

U/Pb isotope dating gives an age of 135–130 Ma for primary brannerite, which correlates with the emplacement of the Early Cretaceous intrusions (Boitsov VE and Pilipenko 1998).

Potential Sources of Uranium and Gold

Archean-Lower Proterozoic granitized rocks are considered the most likely source of uranium. Miguta (1997) reports the following uranium contents of these rocks from the Druzhnoye deposit. Unaltered granite contains 10 ppm U, pyrite-carbonate altered apo-granite 270 ppm U, and pyrite-carbonate-potassium feldspar metasomatite 1980 ppm U. At the Agda deposit, granitized plagiogneiss contains less than 2 ppm U, metasomatized apo-gneiss <620 ppm U, and ore-bearing breccia of altered apo-gneiss <3 800 ppm U (Table 10.8).

The assumption of uranium derivation from Archean-Lower Proterozoic granitoids is supported by Tugarinov's studies (in Miguta 1997), which identified a lead isotope composition in galena associated with uranium ore similar to that of galena in Archean rocks.

The pre-uranium gold is considered to have a source related to Mesozoic magmatic chambers of mantle material while the

post-uranium gold and silver, and the porphyry gold derived from shallower magmatic chambers (Boitsov VE and Pilipenko 1998).

Principal Ore Controls and Recognition Criteria

Location, shape, and dimensions of uranium-gold and uranium-gold-silver deposits are primarily controlled by reactivated ancient and neotectonic NW-SE-oriented and steeply SW dipping faults of Mesozoic age and surrounding pyrite-carbonate-potassium feldspar alteration zones. Significant ore-controlling parameters or recognition criteria of the major deposits in the Elkon District include:

Host Environment

- Archean-Early Proterozoic metamorphic and granitoid lithologies
- Granitoids with elevated uranium background
- Reactivated ancient and neotectonic NW-SE-oriented, steeply SW dipping faults of Mesozoic age

Alteration

- Pre-uranium multistage Mesozoic alteration processes are dominated by silicification, carbonatization, desilicification, feldspathization, and sulfidization and include from oldest to youngest:
 - Albite-sericite-chlorite
 - Pyrite-carbonate-potassium feldspar with dispersed gold

■ Table 10.8.

Aldan region, Agda deposit. Minor and trace element tenors in % of unaltered plagiogneiss, metasomatite, and ore-bearing breccias of apogneiss metasomatite (Miguta 1997)

Component	Granitized plagiogneiss	Apogneiss metasomatite	Ore-bearing breccia	Component	Granitized plagiogneiss	Apogneiss metasomatite	Ore-bearing breccia
U	<0.0002	0.062	0.38	FeO	4.15	2.04	1.33
TiO ₂	0.90	1.02	1.27	Fe ₂ O ₃	2.81	4.95	5.23
Pb	Traces	<0.01	<0.01	S _{total}	0.26	–	–
V ₂ O ₅	0.02	0.07	0.06	SO ₃	–	0.24	0.43
Nb ₂ O ₅	n.d.	0.005	0.011	S _{sulf}	–	2.48	3.36
ZrO ₂	0.01	0.01	0.02	F	0.16	0.08	0.06
As	<0.005	0.03	0.051	CO ₂	1.37	5.34	5.56
W	n.d.	n.d.	<0.04	P ₂ O ₅	0.44	0.53	0.43

- Locally baryte-quartz with minor Fe-, Cu-, Zn- and Pb-sulfides
- Late and post-ore alteration includes carbonatization, silicification, fluoritization, sulfidization, and oxidation
- Finitization related to Mesozoic alkaline intrusions

Mineralization

- Principal ore assemblages are gold-brannerite, gold-uraninite and brannerite-silver-gold
- Early gold is dispersed in pyrite of the pyrite-carbonate-potassium feldspar alteration facies
- Brannerite, the only primary U mineral, is superimposed on earlier gold mineralization
- Uraninite substituted brannerite in contact-metamorphic aureoles
- Late veinlets of native gold and silver overprint locally earlier mineralization
- U ore is restricted to pyrite-carbonate-potassium feldspar alteration zones intersected by NW-SE-oriented, steeply SW dipping faults
- Location, shape, dimensions of deposits is largely defined by brecciated intervals of faults
- Deposits consist of intermittently distributed ore bodies separated by barren or erratically mineralized ground
- Distribution, dimensions, and internal structure of ore bodies is defined by the brecciation degree of the host rock
- Ore bodies are of veinlike or columnar shape
- Internal structure of ore bodies is of stockwork or network nature composed of variably mineralized breccias, fractures, joints, and disseminations

Metallogenetic Concepts

A multistage metallogenetic evolution for the gold-uranium deposits of the Elkon District may be deduced from the work of Miguta (1997), Boitsov VE and Pilipenko (1998), and other authors.

The ore-forming process started with the gold-bearing pyrite-carbonate-orthoclase alteration event with most of the gold contained in pyrite. Subsequently, uranium was introduced into the previously altered rocks by hydrothermal fluids. Both processes occurred during the Mesozoic tectono-magmatic activation of the Aldan Shield. Uranium was deposited as brannerite under medium to low temperature conditions at medium to shallow depth and formed structurally controlled deposits in rejuvenated ancient and neotectonic Mesozoic fault zones. Due to the association of deposits and intrusions in space and time, it can be assumed that the hydrothermal process was initiated by the Mesozoic magmatic activity. Uranium probably derived from the Archean granitized rocks, which have an elevated uranium content. Uranium dissolution resulted from the interaction of ascending medium temperature, sulfide-carbonate-bearing solutions with granitized rocks. Posterior, the Au-Ag mineralization with native gold and silver minerals developed in some of the formerly generated U-Au zones in areas with Mesozoic intrusions as exemplified by the Fedorov zone.

It is noteworthy that there is no vertical zoning in the uranium zones of the Elkon District except for an immense quartz accumulation in the upper parts of the deposits. Mineralogical and chemical composition of ores are rather uniform over the drill intercepted interval, in the Yuzhnaya zone down to about 2000 m, which indicates relative stable conditions of ore deposition over a large vertical section presumably due to a homogenous environment.

Thermobarometric studies indicate pronounced variations of temperatures during the entire metallogenetic evolution of the Elkon ores and its individual stages as well. Successive mineral stages started constantly with higher temperatures than those at the end of the previous stage suggesting a multiphase influx of ore-forming fluids.

Where thermal metamorphism related to Mesozoic magmatic intrusions affected the brannerite mineralization, uraninite and Ti-oxide phases replaced the original brannerite. All post-brannerite processes only altered the original brannerite and redistributed uranium to form coffinite but they did not furnish new uranium.

10.5.1.1 Yuzhnaya Zone

The Yuzhnaya (southern) zone is by underground workings and up to 2 000 deep drill holes the best explored uranium zone in the Elkon Horst. Five large, more or less continuous gold-brannerite deposits are established, spread over a distance of about 20 km along the central section of the zone. They are arbitrarily defined as separate deposits, namely – from NW to SE – the *Elkon*, *Elkon Plateau*, *Kurung*, *Neprokhodimoye*, and *Druzhnoye* deposits. Each deposit consists of several north-westerly plunging ore bodies (Fig. 10.33).

Ore control is by the NW-SE-trending and steeply SW dipping, approximately 30 km long and several hundreds of meters wide, ancient Yuzhnaya fault, which was reactivated during the Mesozoic, and by pyrite-carbonate-potassium feldspar altered rocks. Country rocks are Archean-Early Proterozoic ultrametamorphic lithologies. Mineralized sections are traced by blastomylonite imposed on Early Proterozoic metadiorite dikes.

The bulk of the ore is composed of brannerite and gold and related alteration products contained in breccias and, more rarely, in fractures cutting the altered host rocks. Ore bodies

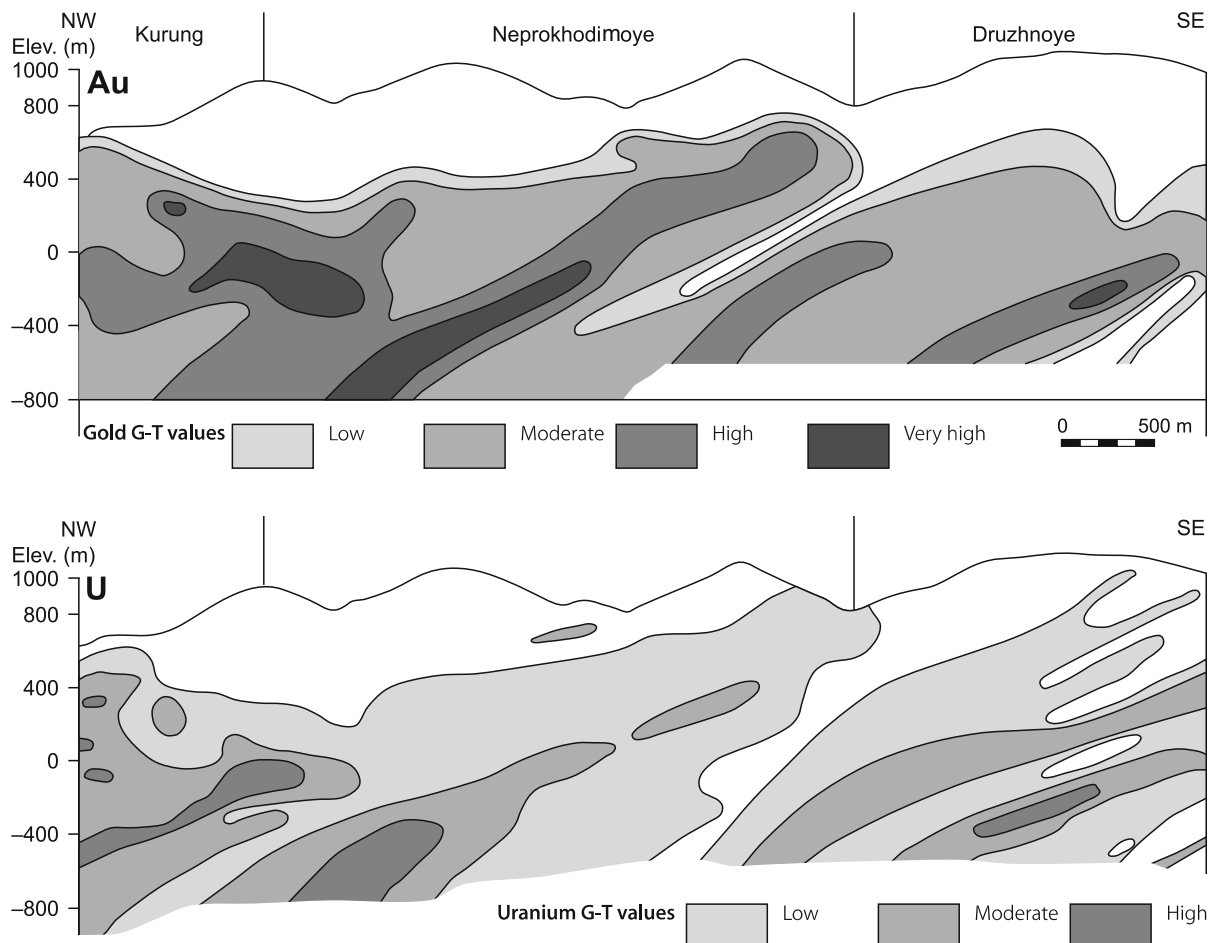
consist of closely spaced brannerite stringers and impregnations that group to an echelon arranged, linear, 500–700 m long along strike and dip, and 0.5–10 m wide ore bodies.

Upper limit of ore is at a depth between 200 m and 500 m. Depth persistence exceeds 2 000 m. Low ore grades of up to about 0.1% U prevail in upper levels, down to about 500–600 m. Grades increase downwards to 0.2% U and more at about 1 000 m and further below. Uranium and gold are spatially closely associated both along strike and dip, and show no signs of mineral changes and pinch out at explored depth suggesting that mineralization probably continues into greater than the drill intercepted depth. The spatial association is also documented by the fact that massive pyrite-carbonate-orthoclase alteration facies hold 72% of the whole gold of the Yuzhnaya zone and 62% of which is contained in uranium ore.

Late baryte-quartz and carbonate-quartz veins and veinlets accompanied by molybdenite mineralization occur in the upper, near-surface, low gold and uranium intervals at the southeastern flank of the Yuzhnaya zone. The here situated Druzhnoye deposit contains elevated amounts of molybdenite associated with a uranium mineral that was tentatively defined as a uranium oxide.

Fig. 10.33.

Elkon District, Yuzhnaya zone, NW-SE longitudinal section along the southeastern part of the structural zone with projection of grade-thickness values (or productivity) of gold (Au, upper section) and uranium (U, lower section) (after Boitsov VE and Pilipenko 1998 based on Prilensk PGO)



The ore minerals occur in few centimeters to 2.5 m wide, flattened stockworks composed of veinlets, and black, earthy masses, crusts and coatings within breccias (Boitsov VE and Pilipenko 1998).

10.5.1.2 Sokhsolookhsk Zone

The Sokhsolookhsk zone is several tens of kilometers long and contains gold-brannerite deposits including *Konkulaakh*. It parallels the Yuzhnaya zone at a distance of 5–6 km to the southwest. Similar to the Yuzhnaya, the Sokhsolookhsk zone is a reactivated old fault, but of an echelon nature and, in consequence, the gold-uranium mineralization is less continuous, although the mineral composition is the same. Ore bodies are roughly of the same size as those of the Yuzhnaya zone (Boitsov VE and Pilipenko 1998).

10.5.1.3 Severnoye, Pologaya, Vesennaya, and Agdinsk (or Agda) zones

The Severnoye, Pologaya, Vesennaya and Agdinsk (or Agda) zones contain gold-brannerite occurrences similar to those of the Yuzhnaya and Sokhsolookhsk zones. Ore bodies at Pologaya, Vesennaya, and Agdinsk have a lenticular shape, are several tens of centimeters to 2 m thick and from several tens to several hundreds of meters long. Pologaya ore bodies are elongated down dip. Vesennaya and Agdinsk have complexly shaped ore bodies at fault intersections (Boitsov VE and Pilipenko 1998).

10.5.1.4 Nadezhda and Interesnaya Zones

The Nadezhda and Interesnaya zones are in the northwestern sector of the Elkon District where Mesozoic intrusive stocks and dikes are abundant (Fig. 10.34). Both zones trend parallel,

about 2 km apart, in NW-SE direction and are located close to the NW of a 700 m wide and 2 500 m long, alkaline intrusion. Gneiss around the intrusion is intensely fenitized. The Interesnaya zone is 1–5 m wide and largely controlled by displaced contacts of a vogesite dike. The Nadezhda zone is situated on the northwestern extension of the Sokhsolookhsk zone. At some distance from the intrusion, both zones are characterized by gold-bearing pyrite-carbonate-orthoclase altered facies with superimposed brannerite mineralization. This facies grades within the fenitization aureole, at a distance of about 500 meters from the intrusion, into narrow, up to 2 m wide, en echelon arranged bodies of fine-grained orthoclase-biotite-aegirine-augite-amphibole-magnetite rock cut by pyrite-bearing carbonate stringers. The pyrite contains grains of native gold and is locally accompanied by galena, chalcopyrite, pyrrhotite, and valleriite. Uraninite occurs associated with biotite, orthoclase, sphene, and pyrite in superimposed younger fractures.

Post-uraninite processes are testified by less than 1 m wide grorudite or sölvbergite dikes, which cut the gold-uraninite ores. In turn, the dikes are traversed by veinlets composed of oligoclase, aegirine with Fe- and Cu-sulfides, pectolite, adularia, quartz, baryte, calcite, fluorite with sphalerite and galena. Gold was not found in the veinlets.

Ore bodies are small and of irregular configuration. They extend for several tens of meters along strike and dip but have better uranium grades than the brannerite-gold deposits. Early pyrite tends to be the essential host of native gold. Concentrates of the early pyrite yield values from 9.1 to 24.5 ppm Au (Boitsov VE and Pilipenko 1998).

10.5.1.5 Fedorovsk Zone

The Fedorovsk zone in the southwestern Elkon District carries brannerite-silver-gold mineralization. It occurs in an area with multiphase Mesozoic dikes. The structural zone is of Mesozoic

Fig. 10.34.

Elkon District, Interesnaya zone, geological sketch illustrating the relationship between U mineralization along the tectonic contact of a pre-ore vogesite dike; both are cut by syenite porphyry and grorudite dikes (after Miguta 1997)

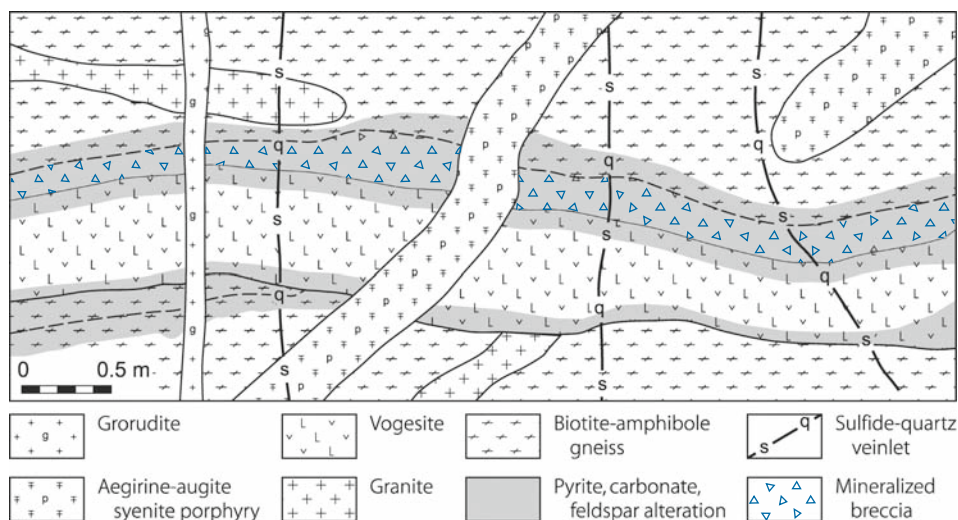
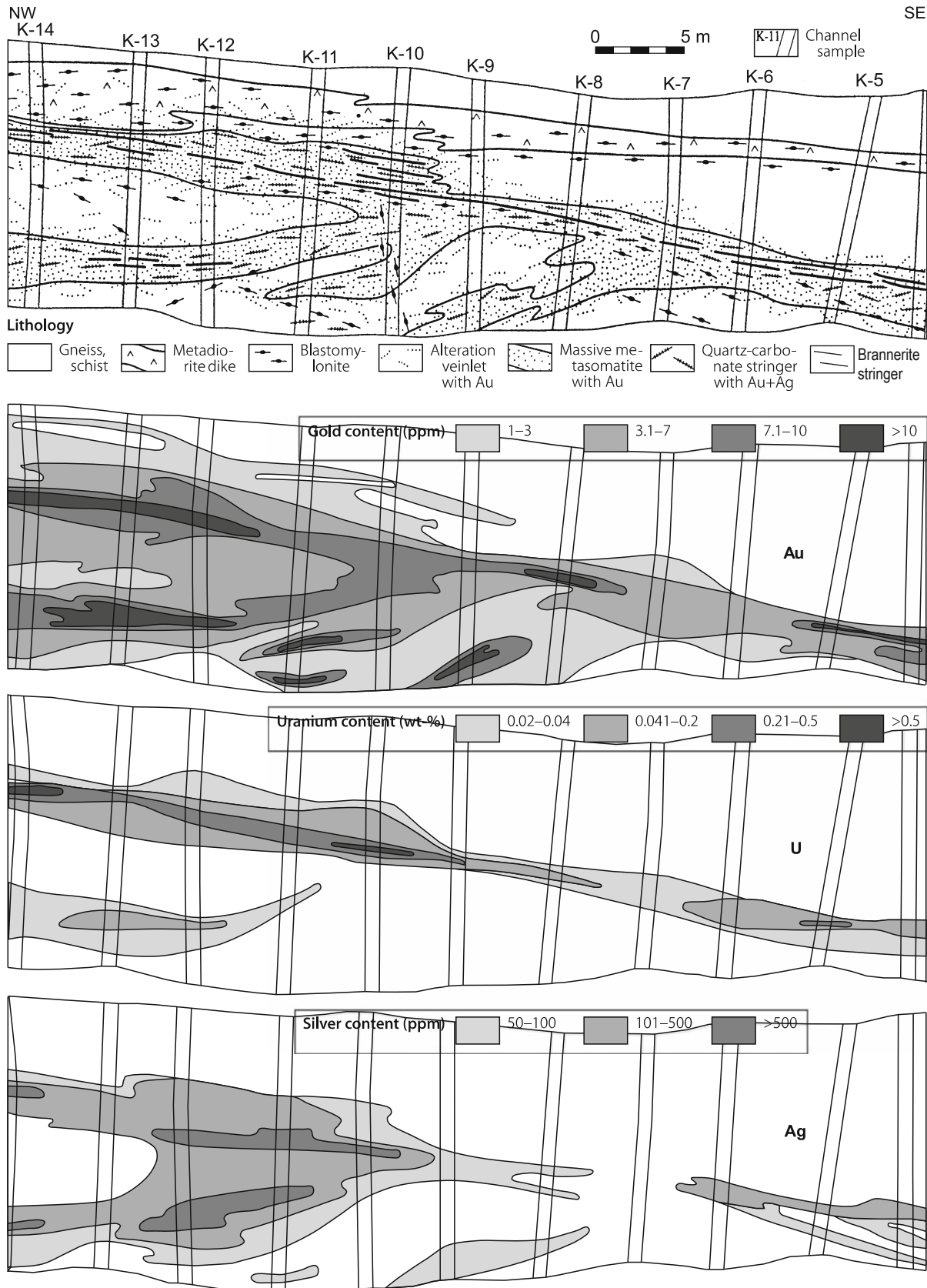


Fig. 10.35.

Elkon District, Fedorovsk zone, geological plan of a trench floor along a blastomylonite zone with distribution of gold (Au), uranium (U) and silver (Ag) grades (after Boitsov VE and Pilipenko 1998)



age, trends NW-SE for 10 km long and dips steeply to the SW. It largely follows metadiorite dikes and blastomylonites. Wall rocks are overprinted by post-fault gold-bearing pyrite-carbonate-orthoclase alteration. Massive metasomatic rocks are well developed. Structure controlled oxidation persists to a depth in excess of 300 m.

As far as established, mineralized sections can be as much as 30 m wide and persist at least to a drill indicated depth of about 1 000 m. Ore bodies are 1–2 m thick, several tens of meters long, and elongated down dip. They consist of gold-bearing metasomatic rocks intersected by thin brannerite stringers and a younger generation of small quartz and carbonate veinlets with pyrite, native gold, native silver, and acanthite. Although there is widely a close spatial coincidence of uranium, gold, and silver in the Fedorov zone, there are also some intervals where the late gold-silver-paragenesis prevails.

The altered melanocratic host rocks carry up to 15 vol-% of gold-bearing pyrite and up to 35 vol-% of carbonate. Due to the increased amount of gold-bearing pyrite coupled with the presence of the late gold-silver assemblage, the Fedorov zone carries markedly elevated tenors of gold and silver. Gold values commonly range from 3 to 10 ppm and silver from 15 to 200 ppm but local maxima can be in excess of 10 ppm Au and up to 1 400 ppm Ag. Most of the ore has U grades between 0.02 and 0.2% U but local enrichments exceed 0.5% U (Boitsov VE and Pilipenko 1998) (Fig. 10.35).

10.5.1.6 Marsovaya, Mramornaya, and Zvezdnaya Zones

Some additional zones with brannerite-gold-silver mineralization were discovered to the southwest of the Fedorov zone. They include the Marsovaya and Mramornaya zones in neotectonic Mesozoic faults and the Zvezdnaya zone controlled by a reactivated ancient blastomylonite structure. Mineralization of these zones consists of native gold- and silver-bearing carbonate veinlets and an erratic distribution of both, early gold-bearing pyrite-carbonate-orthoclase alteration and brannerite mineralization. Ore bodies at Marsovaya have a lenticular shape, are several tens of centimeters to 2 m thick and from several tens to several hundreds of meters long and elongated down dip (Boitsov VE and Pilipenko 1998).

10.6 Amur and Ussuri Rivers Region/Far East Region

Several small uranium deposits and occurrences are reported from this region. They are grouped in two U districts as described below.

10.6.1 Khankaisky District

The Khankaisky District is situated to the northeast of the town of Vladivostok. Estimated total resources of the district are reportedly 25 000 t U. Four small deposits have been explored. Resources of individual deposits range from several hundreds to

several thousands tonnes of uranium. Grades are less than 0.1% U.

Sinegorskoye and *Fenix* are volcanic vein-type deposits. They contain U-Mo mineralization in quartz-sericite-hydromica/beresite altered Devonian rhyolite close to a leucogranite body. *Lipovskoye* is a metasomatite vein-stockwork deposit hosted by an up to 50 m wide albitized cataclastic zone within skarn-altered Cambrian continental carbonate rocks adjacent to Devonian granite. *Rakovskoye* is of basal-channel sandstone type. It consists of elongated, up to 1 km long, 100 m wide, and 5–10 m thick ore lenses in Cenozoic lignite-bearing sandstone that fills a paleo-channel incised into granite. Coffinite and sooty pitchblende are the principal ore minerals.

10.6.2 Bureinsky District

This district is located to the northwest of the town of Khabarovsk. Nine small uranium deposits are reported. Five of which, *Lastochka*, *Kamenushinskoye*, *Skalnoye*, *Svetloye*, and *Tigrovaya Pad*, are of volcanic vein-stockwork type associated with Cretaceous felsic volcanics (rhyolite and felsite) similar to deposits in the Streltsovsk District. Four deposits, *Molodezhnoye*, *Osenneye*, *Sentyabrskoye*, and *Sularinskoye*, are of metasomatite vein-stockwork type hosted in Upper Paleozoic rocks altered to beresite and albitite.

Total resources of the Bureinsky District are estimated at 29 000 t U in the high cost category. Ore grades range from 0.03 to 0.2% U. 3 900 t U (RAR + EAR-I) of the Bureinsky resources are contained in the underground explored *Lastochka* deposit. *Lastochka* was discovered in 1965 in the southern part of the Bureinsky Massif, to the north of the Amur River. Nearest town is Khabarovsk in 100 km distance to the SE of the deposit. Vein-stockwork lodes occur in felsite of a small Upper Cretaceous caldera. Paleozoic granites form the basement. U minerals include pitchblende, sooty pitchblende, β -uranotile, and uranophane. In situ ore grade is 0.1–0.2% U.

10.7 Okhotsk Region

The Okhotsk U region is located to the west and northwest of the town of Okhotsk on the Sea of Okhotsk. Exploration in this region began in the early 1950s (by Dalstroj organization) and led to the discovery of U occurrences, e.g. *Tas-Kastabyt* and *Butuguchag*, in granite massifs in the Magadan District. Subsequent exploration in neighboring terrane resulted in the discovery of volcanic-type U occurrences associated with the Uliya and Kuidusun volcanogenic depressions in Khabarovsk territory and the adjacent Sakha-Yakutia Republic and Magadan territory.

Source of information: The subsequent description is a synopsis of the paper by Kirillov and Goroshko (1997), who elaborate on the geological environment and mineralogy of U occurrences in the Okhotsk region but do not give any data on resources and grades. They note, however, that most occurrences are small, of limited vertical and lateral extent, and of low grade except for some deposits with economic potential.

Regional Geological Setting of Mineralization

The U-hosting *Uliya* and *Kuidusun* volcanogenic depressions are situated in the western Okhotsk segment of the Okhotsk-Chukotka marginal continental volcanic belt. Tuffaceous sediments, lavas, subvolcanic intrusions, and intrusive rocks constitute the principal lithologies. These rocks are grouped into four volcano-plutonic complexes, which were emplaced during four main episodes of igneous activity.

The Khakarin Complex is made up of Paleogene basalt and basaltic andesite.

The Urak Complex consists of Late Cretaceous tuffs, ignimbrites, and felsic lavas. These rocks differ from the Amka rocks (see below) by the presence of glass, larger amounts of subvolcanic and extrusive formations, and a considerable abundance of comagmatic intrusive rocks. In addition, the volcanics of this complex are more silicic and contain more alkalis, especially potassium, as compared to the Amka volcanic rocks.

The Amka Complex comprises the Late Cretaceous Khetanin Formation (andesite, basaltic andesite, and basalt) and the Amka Formation (tuff, ignimbrite, and minor dacitic andesite, dacite, rhyodacite, and rhyolite lavas intercalated with tuffaceous sediments as well as scarce subvolcanic and extrusive bodies).

The Okhotsk Complex includes the Early Cretaceous Alan Formation (mainly continental tuffaceous sediments) and the Ulberikan Formation (andesite, basaltic andesite, and related tuffs).

The Cretaceous volcanics rest upon Archean metamorphic rocks, Proterozoic quartzose or quartz-feldspar sandstones, and Devonian volcanogenic lithologies of the Okhotsk Massif. Major faults trend NNW to NNE, and NW-SE.

Principal Host Rock Alteration

Alteration phenomena relate to the wide variety of lithologies and presumably also to variations in hydrothermal solutions. Prominent alteration features include early stages of greisenization, followed by propylitization, beresitization, argillization, and silicification. Albitization and carbonatization developed locally. Beresitization (particularly of sericite-hydromica facies) and argillization reflect the most typical alteration of wall rocks associated with U mineralization. (For more details see description of individual types.)

Principal Characteristics and Types of U Mineralization

Most U occurrences are hosted in uraniumiferous felsic intrusive and extrusive volcanic rocks of the Cretaceous *Urak Complex*. One U occurrence was found in Devonian volcanics. U mineralization is structurally controlled and occurs preferentially in large, submeridional fault zones that border volcanogenic depressions in the Okhotsk Massif.

U minerals include pitchblende, nasturan (sooty pitchblende?), uraninite, brannerite, uranothorianite, and a great variety of uranyl hydroxides, silicates, phosphates, arsenides, and molybdates. U-bearing minerals are thorite, fergusonite, beta-fite, samiresite (U-bearing pyrochlore). U is also concentrated in goethite (0.2–0.3% U), pyrite (up to 0.3%), fluorite (up to 0.3%), orthite (0.7%), sphene (0.05%), wolframite (0.1%), and plant remains (up to 0.4%). Arsenic (<2%) is the most abundant accessory element. Other frequently-associated elements (present in fractions of a percent) are Cu, Pb, and Zn. Other metals that may or may not be locally present include Ag, As, Au, Bi, Mo, Nb, Sb, Th, V, Y, and Zr.

Uraniferous mineral assemblages can be grouped into two principal ore types:

1. U mineralization in mostly beresitized and/or argillized rocks. Based on predominant minerals, this assemblage can be subdivided into three subtypes: (a) pitchblende (nasturan)-sulfide, (b) pitchblende-quartz, and (c) pitchblende-hydromica; and
2. REE-Th-U mineralization in apatite-orthite metasomatite and pegmatites.

Geotectonic Setting of U mineralization

Kirillov and Goroshko (1997) recognized four geotectonic settings of U mineralization: (1) superimposed terrigenous basins, (2) volcano-tectonic depressions, (3) extrusive volcanic domes, and (4) intrusive domes, in which the authors identified the following fourteen types of U mineralization based on lithological setting, wall rock alteration, and mineralogy. Types 1–5 are enveloped by clay-altered wall rocks and types 6–11 by beresitized wall rocks.

Type 1: Argillized sections in superimposed terrigenous depressions

The *Atandzhakan* occurrence is the only known example for this environment. It is a U-V occurrence located on the western side of the Uliya Basin in argillized, carbonaceous tuffogenic sediments of the Early Cretaceous Alan Formation. The tuffaceous unit is intercalated with siltstone, sandstone, and greywacke and rests upon Precambrian granite. Host rock alteration is reflected by argillization that was superimposed on propylitization. Altered facies are characterized by chlorite, chalcedony, hydrosericite, kaolinite, montmorillonite, quartz, and limonite. Sulfides are scarce.

Mineralization occurs in several stratiform bodies, up to 20 m in thickness, in the lower Alan Formation. Mineralized horizons typically contain up to 10% organic matter. Better grade mineralization is concentrated at ore intersecting faults. U minerals include pitchblende (nasturan) and more abundant U⁶⁺ minerals. Some U is in apatite, pyrite, limonite, and plant remains. U minerals form nests, veinlets, and elongated masses. Ag, Cu, Mo, Pb, V, and Zn occur in elevated concentrations. U mineralization was dated at 89–119 Ma.

Atandzhakan mineralization may be to some extent comparable with U-V mineralization of the Salt Wash Formation on the Colorado Plateau.

Type 2: Argillized sections in volcano-tectonic depressions

Rocks of volcano-tectonic depressions that are altered by argillization (kaolinite and hydrosericite) contain locally small occurrences of pitchblende (nasturan) associated with galena.

Type 3: Argillized sections in volcanic domes and extrusive viscous-lava bodies

Felsic lava sheets and extrusive bodies of the Urat Complex contain structurally controlled small U occurrences in poorly eroded areas of the *Uliya Basin*. Mineralization is related to argillized sections (kaolinite, hydrosericite, and colloform quartz) that often occur in zones of fumarolic and solfataric alteration.

An exception with economic potential is the *Mulachen* deposit. This deposit is controlled by NE-SW-trending faults cutting brecciated felsite, trachydacite, dacite, and rhyolite tuff. In mineralized zones, host rocks exhibit an alteration succession from adularization to argillization (kaolinite, hydrosericite), and to extensive silicification (quartz, opal, chalcedony). Mineralization consists of U⁶⁺ minerals, dominated by uranophane, which often occur in opal masses in association with jarosite. Associated minerals are sulfides and, less commonly, cornwallite, scorodite, and fergusonite. Ore has elevated contents of Ag, As, Au, Mo, Pb, and Sb. U-Pb isochronal ages range between 127 and 72 Ma.

Type 4: Argillized sections in intrusive domes

Intrusive domes of the Tas-Kastabyt granite massif at the NE margin of the Okhotsk Massif host U occurrences in argillized intervals. Gabbro and granodiorite constitute the main petrographic phase of the massif while porphyry-like quartz diorite and subalkaline leucocratic granite with xenoliths of metamorphic rocks form a later phase. Uranium is mainly concentrated in porphyry-like granite. This granite was intruded into Triassic clastic sediments and contains up to 9 ppm U in subparallel NW-SE-trending extensive fault zones that enclose belts of glassy rhyolite and felsite dikes.

Type 5: Argillized contact zones of dikes cutting sandstone

Contact zones between sandstone and intrusive dikes host locally linear zones with strike-persistent U mineralization. U minerals occur as disseminated particles and veinlets. Brecciated ore textures are also noted. Axial parts of mineralized zones are dominated by argillic (mainly kaolinite), while margins are dominated by beresitic alteration (sericite-hydromica with minor chlorite and carbonate locally). Argillization is superimposed on tourmaline-muscovite greisens and beresites. Uranium mineralization is more abundant in beresitized than in argillized rocks.

Pitchblende is the principal primary U mineral. U⁶⁺ minerals include uranyl arsenates and phosphates, enriched in copper and lead. Age dating yields 60–50 Ma for U mineralization. Ore contains sulfides and elevated concentrations of As, Cu, F, Sn, and Zn but these minerals/elements are of pre-uranium origin and presumably are related to the greisenization phase.

Type 6 and 7: Beresitized sections in volcanic domes and extrusive lava

Beresite-altered sections in or at (sub)volcanic domes and extrusive, low-viscosity lava bodies of felsite or rhyolite composition

with elevated background U concentrations are favorable sites for many U occurrences. Denominated U occurrences include *Vinto-Khalyya*, *Druzhnoye*, *Raduzhnoye*, and *Zergan* in the *Kuidusun Basin*, and *Amagaran*, *Iskra*, and *Kotla* in the *Uliya Basin*.

U mineralization is commonly bound to small domal edifices situated within larger volcanic structures, mainly within volcano-tectonic depressions. Ore bodies are fault controlled and occur within and adjacent to these subvolcanic and extrusive bodies.

In spite of similar structural settings and identical wall rock alteration, ore bodies have variable ore compositions: The *Zergan* occurrence is characterized by abundant fluorite; *Druzhnoye* by chloritization and diverse non-radioactive minerals; *Raduzhnoye*, *Kotla*, and *Vinto-Khalyya* by the almost absence of non-radioactive minerals. These differences are believed to be the result of geochemical different hydrothermal solutions. Accordingly, some occurrences contain complex U mineralization, whereas others consist of practically monometallic uranium. In more detail:

Type 6: Mineralization associated with intrusive domes

Numerous U showings have been discovered in beresitized Devonian volcanic rocks around the Uliya Basin, and north of the Verkhnemaiskiy intrusion, where Devonian volcanics occur in the central part of an intrusive dome of Mesozoic diorites and leucogranites.

Most uranium is hosted by the Taabyrdaakh Formation (felsic lava, ignimbrite, and tuff) in which it occurs in breccias with a hematite-quartz matrix. NW-SE, NE-SW and W-E faults control mineralized sections. These faults are located in a major NE-SW-trending fault zone, which is characterized by dike swarms and a large area (12 × 2 km) of beresitic alteration.

Wall rocks are altered by beresitization that developed after greisens. The beresite assemblage includes quartz, sericite, hydromica (schilkinite), ankerite, calcite, goethite, hydrogoethite, chlorite, baryte, and rutile. Uranium was deposited as pitchblende when the beresitization stage changed from sericitization to hydromicazation. Pitchblende occurs as thin veinlets, nests, or disseminated particles in cryptocrystalline quartz aggregates. Secondary U minerals include silicates, and uranyl phosphates and arsenates. Ag, As, Cu, Pb, Sb, and Zn occur in substantial amounts (samples contain more than 3% As, Pb, and Sb, and more than 1% Cu). Mo ranges locally up to 0.05%. Sulfides, mainly galena and pyrite, are common ore constituents.

U-Pb dating indicates three episodes of U deposition: 390–370 Ma (Devonian), 215 Ma (Triassic), and 150–110 Ma (Cretaceous). K-Ar dating of micas in altered wall rocks yields ages of 332 and 110 Ma. Mesozoic tectonomagmatic reactivation fragmented the original ore and fragments were transported into Triassic sediments and Lower Cretaceous tuffogenic sediments of the Alan Formation. U ore pebbles in Triassic deposits evidence the Paleozoic age of initial U deposition.

Type 7: Mineralization in extrusive viscous lava bodies

The *Druzhnoye* occurrence provides an example for Mesozoic U mineralization for this environment. *Druzhnoye* is located in

the Nyut volcanic-tectonic depression, which is filled with volcanic and volcanogenic-sedimentary rocks of the Arnka and Urak complexes. NW-SE and NE-SW faults control the position of ore bodies. Wall rocks consist of beresitized volcanics of the Amka Complex and rhyolite extrusions of the Urak Complex. Three beresite facies are identified: muscovite-sericite, sericite, and sericite-hydromica. Higher-temperature products are replaced by low-temperature phases. Uranium associated with chamosite and carbonate was deposited during the late alteration stage. U minerals are pitchblende and, less commonly, uraninite; they occur as disseminated particles and intermittent veinlets. U⁶⁺ minerals are mainly silicates and minor hydroxides and phosphates as well as uranyl molybdates. Uranium is closely correlated with Co and Ni, which are concentrated in chlorite, and with Ba and Sn as well. Associated minerals include sulfides of As, Pb, Mo, Sb, and Zn; commonly formed in pocket-like masses. Emplacement of Mo and U mineralization was not coeval as indicated by a lack of U and Mo correlation. Mo minerals crystallized during a feldspathization event, whereas U minerals formed during beresitization dated at 90–100 Ma.

Type 8: Beresite overprinted by hornfels contact metamorphism

U occurrences in hornfels adjacent to subvolcanic intrusions of the Urak Complex (e.g. *Tarakan* and *Ketanda*) derived by contact metamorphism that locally overprinted progenitor U mineralization in beresitized rocks similar to that noted under types 6 and 7. As a result, ore was locally redistributed; pitchblende recrystallized to uraninite, and hornfels-related minerals, mainly biotite, were formed.

At *Tarakan*, mineralization is controlled by N-S-trending faults that cut beresitized rhyolites and their tuffs in a volcanic dome with widespread subvolcanic rhyolite intrusions. Neoformed minerals are andalusite, actinolite, muscovite, and garnet of an early stage, and chlorite, biotite, hydrobiotite, spinel, and sulfides of a later stage. Pitchblende and uraninite are associated with hydrobiotite and spinel. Late stage (?) sulfides are abundant. As, Bi, Cu, F, Pb, Th, and Y occur in elevated concentrations.

Type 9: Beresitized volcanogenic sediments in volcanotectonic depressions

The central Kuidusun volcanotectonic depression hosts U mineralization in beresitized volcanogenic sediments. An example is the *Astra* occurrence; it is hosted in tuffaceous siltstone with carbonized plant remains that is cut by a N-S-trending fault zone. Beresites are of hydromica facies and contain fluorite, chlorite, carbonate, and hematite. Small pitchblende grains are enclosed in plant remains. Ore has elevated concentrations of As, Mo, Pb, and Zn. Age dating gives 110–90 Ma for the ore formation.

Types 10 and 11: Beresitized intrusive rocks

Beresitized intrusive rocks of the Arkhimed and Pestraya complexes in the eastern *Nyut-Ulbei batholith* contain numerous small U occurrences. The eastern part of the *Arkhimed Massif* consists of medium-grained biotite granite and small stocks or sheets of fine-grained subalkaline granite dated at 76–74 Ma (K-Ar). Beresitic alteration is concentrated along fissures that

accompany major NW-SE- and N-S-trending faults. U minerals include pitchblende, U-silicates, and metatorbenite. Ag, Bi, Cu, Pb, Sn, and Zn occur in elevated concentrations. In the *Pestraya Massif*, U mineralization occurs at the contact of xenoliths of sediments in granodiorite or subalkaline quartz diorite, and in NE-SW- and N-S-trending fault zones. Wall rocks are altered by beresitization that overprinted earlier greisens. U mineralization comprises only U⁶⁺ minerals that form nests and veinlets, and was dated at 70–60 Ma.

Type 12: Albitized felsic volcanics

This type is scarce and is characterized by prominent albitization with some hematite, chlorite, and apatite alteration of felsic volcanics along steeply dipping faults. The *Bulakag* U occurrence is an example. It is controlled by a NE-SW fault that transects ignimbrites of the Urak Formation in the central Kuidusun Basin. Alteration phases include extensive early propylitization followed by a later event with significant removal of potassium (from 4–5% to roughly 0%) and addition of sodium (from 2 to 6%). Mineralization forms a lenticular, steeply dipping ore body. Masuyite is the principal U mineral. Hematite contains up to 0.3% U. Mo, Pb, and As occur in high concentrations. Age dating yields 132–104 Ma for the ore formation.

Type 13: Metasomatized syenite porphyry

Syenite porphyry intrusions of the *Nyut-Ulbei batholith* that were modified by orthite-apatite metasomatism host U mineralization in the form of closely spaced, subparallel veinlets within cataclastic zones. Uraniferous minerals include apatite, orthite, and minor monazite, zircon, and Y-rich uranothorianite.

Type 14 Alaskitic gneiss-granites and pegmatites

Alaskitic gneiss-granite and pegmatite of the crystalline basement contain numerous small occurrences of U and, more commonly, Th or U-Th mineralization. Uranothorianite is the prevailing U-bearing mineral. It occurs as disseminated grains that are locally concentrated to loosely packed accumulations. Zones of these accumulations usually show evidence of high-temperature quartz-microcline metasomatism.

Metallogenetic Aspects

In summary, Kirillov and Goroshko (1997) provide the following metallogenetic concept:

U occurrences in the Kuidusun and Uliya Basins are of volcanic type and are associated with intrusive and extrusive volcanic rocks of variable age. U-Pb dating documents repeated mineralizing events during Devonian, Cretaceous, and Paleogene episodes of tectonomagmatic activity; but the most productive episode of U mineralization was related to Late Mesozoic revival of tectonomagmatic activity in the Okhotsk Massif.

The mode of U mineralization and wall rock alteration suggest that most of these U occurrences were generated by metasomatism. Residual melts of shallow magma chambers are thought to have served as a U source. Uranium transport, deposition, and wall rock alteration resulted from low temperature residual

hydrothermal solutions. These fluids were active during the waning emplacement phase of magmatic bodies, and commonly affected autometasomatised zones of previous greisenization and propylitization.

10.8 Southern Kalyma River Region

One deposit, *Butugichag* (Butygychagskoye), is reported from the southern Kalyma River, about 250 km NW of the town of Magadan on the north coast of the Okhotsk Sea. This vein-type U deposit was hosted in Mesozoic granite and formerly mined. It is depleted. Reserves were reportedly between 1 500 and 5 000 t U.

10.9 Chukotsky Region

The region is between the Arctic Ocean and the Bering Sea in the extreme northeast of Asian Russia. Five deposits are recorded, four of volcanic vein-stockwork type associated with Jurassic calderas (*Severnoye*, *Katumskoye*, *Chaika*, and *Keef*) and one of lignite type (*Chaplinskoye* at the Bering Sea) hosted in Jurassic continental sediments. All deposits have low grades of less than 0.1% U, and are small in size containing few hundreds to few thousands tonnes of high cost uranium. *Severnoye*, located 80 km

to the east of the settlement of Pevok at the East Siberian Sea, was formerly mined and is depleted.

References and Further Reading for Chapter 10 • Russian Federation – Asian Territory

For details of publications see Bibliography.

Aleshin et al. 2003a,b, 2005; Andreeva et al. 1990, 1991, 1996a,b; Andreeva and Golovin 1999; Arzruni 1885; Birka et al. 2005; Blondeau 1827; Boitsov 1999; Boitsov et al. 1995, 2002; Boitsov and Nikolsky 2001; Boitsov 1989, 1996; Boitsov and Pilipenko 1998, 2000; Chabiron 1999; Chabiron et al. 2002, 2003; Chernyshev and Golubev 1996; Chervinsky 1923, 1925; Chudnyavtzeva and Samonov 2003; Dolgushin et al. 1995; Gavrilin et al. 2000; Gotman et al. 1979; IAEA 1995, 2007; Ischukova 1989, 1995, 1997; Ischukova et al. 1991, 1998, 2002; Kazansky 1995; Kazansky and Laverov 1977; Kazansky and Maksimov 2000; Khalezov 2000a,b; Kirikov 1928; Kirillov and Berdinkov 1998; Kirillov and Goroshko 1997; Kislyakov and Shchetochkin 2000; Kislyakov and Shumilin 1996; Kochenov et al. 1995; Kochetkov et al. 1988; Komarov et al. 1965; Korolev et al. 1979; Kotlyar 1968; Kotlyar et al. 1973; Krotkov et al. 1997; Krylova et al. 2003; Laverov 1995; Laverov et al. 1985, 1992a–c, 1993, 1995, 2000; Leymerie 1859; Loutchinin 1995a,b; Mashkovtsev et al. 1995a,b, 1998; Miguta 1997; Miguta and Modnikov 1993; Moltchanov 2003a,b; Naumov 1993, 1999; Naumov and Shumilin 1994; Naumov et al. 2005; Nikolsky and Schulgin 2001; OECD-NEA/IAEA 1993–2005; Pelmenev 1995; Petrov et al. 2005, 2006; Sherih et al. 1999; Smorchkov 1966; Terentyev and Kazansky 1999; Varnavsky and Shevchenko 2000; Vishnyakov 1995a–c. Boitsov AV, Boitsov VE, and Kazansky pets. Commun.

Chapter 11

South Korea

Several U occurrences that may be defined as modified black shale-type U deposits are reported from the *Okchon* (Okch'on, or Ogcheon) area, Chung-Cheong-do Province, in central-western Korea. They were explored by drilling and tunneling and reportedly have U resources of 14 800 t U (OECD-NEA/IAEA 1993). Grades are on the order of 200–400 ppm U, locally up to 600 ppm U.

These occurrences (*Goesan*, *Geumsan*, *Kolnami*) are located within the Ogcheon fold belt that trends NE-SW across S Korea and includes weakly regionally metamorphosed, \pm uraniferous marine black shales in the Early Paleozoic Ogcheon System. Better grade U concentrations are confined to discontinuous, highly deformed graphitic black slate intervals, tens of meters thick and hundreds of meters long. The bulk of the uranium tends to be adsorbed on clay minerals except for rare uraninite cubes and U^{6+} minerals in weathered material. These U accumulations are obviously controlled by fault/shear zones, which may

suggest that tectonic activity was a critical factor to promote a localized redistribution and reconcentration of uranium along structures within the normal black shale.

In metamorphic terrane of the *Gyeonggi* (Kyonggi) Massif, the *Jungwonsan*, *Yumyeongsan*, and *Bonapsan* prospects, located some 50 km NW of Seoul, consist of small, fracture-controlled U concentrations (pitchblende, U^{6+} minerals) associated with strong chloritization at the contact of highly deformed quartzite (Jangrag Formation or equivalent) and gneiss or schist of Proterozoic age.

Small sandstone-type U mineralization in continental sediments of the Cretaceous Gyeongssang System is known from (a) the *Onjeong* occurrence in the Youngyang Basin, south of the town of Pyeoghae on the east coast, and (b) the *Gongju-Ooseong* occurrence (with U in sandstone at Echeonri and in shale at Jaijigri) in a graben structure in central Chungcheongnam-do, western Korea.

All national uranium exploration activities were in the hands of the Atomic Energy Bureau of the Ministry of Science and Technology.

Sources of information. Jong Hwan Kim 1988; OECD-NEA/IAEA 1979, 1983, 1986, 1993.



Chapter 12

Tajikistan

Uranium occurrences are known in the Kuramin Range, southwestern Tien Shan mountains, in NW Tajikistan (Figs. 7.1, 7.2). First reports on the presence of uranium in this area date back to the 1920s and include the *Taboshar* and *Andrasman* deposits; both were mined. Other occurrences are known in the southern Tien Shan.

A uranium mill, known as *Leninabad mill*, was built at Chkalovsk, 15 km SE of Khudzhand (formerly Leninabad) in NW Tajikistan in 1945. It was originally operated by Combine # 6 and at last by Vostochny (eastern) Rare Metal Industrial Complex. Uranium ore processing started in 1946 and ceased in 1993. Since then, the mill has been modified to treat Pb-Zn-Ag ores. Mill feed derived at the beginning from ores of the Karamazar region and – between 1946 and 1950 – also by U concentrates from Bulgaria, ČSSR, East Germany, and Poland. The capacity was eventually expanded to 2 000 t U yr⁻¹ when the mill began processing ISL slurries from the Kyzylkum region in Uzbekistan.

Sources of information. See at end of Chap. 12 *Tajikistan*.

12.1 Kuramin Range, SW Karamazar Region

The Kuramin Range is located in the southwestern part of the Karamazar uranium region that covers parts of Tajikistan, Uzbekistan, and Kyrgyzstan. Three U deposits are reported in the Tajikistan part of this range, from NE to SW: *Adrasman*, *Taboshar*, and *Keektal* (Fig. 7.2). Chapter *Uzbekistan* provides geological characteristics of the Karamazar region.

12.1.0.1 Taboshar

Taboshar is located near Sarimsakli, on the southern slope of the Kuramin Range, about 40 km N of Khudzhand. The deposit was discovered in 1927 and exploited in the 1930s for radium. Along with Tyuya-Muyun, Taboshar delivered the first production of radium in the Soviet Union. Radium was extracted at a special plant in the settlement of Taboshar established in 1934. Underground mining for uranium resumed in 1943 (6 mining levels) and Taboshar was the first deposit mined purely for uranium in the former USSR during World War II. The deposit yielded some 500 t U and is now depleted. Ore averaged 0.06% U and was processed at the Leninabad mill.

Geology and Mineralization

The Kuramin Range is part of the Chatkal-Kuramin uplift, a segment of the Ural-Mongolian orogenic belt of Hercynian age. Country rocks at Taboshar are granite and granodiorite of the second Hercynian phase, which were intruded into Proterozoic

metamorphites. Deep rooted baryte veins up to 1 m wide and 2 km long cut the crystalline complex at intervals ranging from tens to hundreds of meters. Some of the baryte veins are mineralized by uranium and other metals. Wall rocks of such mineralized veins and fracture zones are altered by sericitization, silicification, and hydromicazation.

Primary mineralization of ore veins is rare and consists of a polymetallic paragenesis of pitchblende, bismutinite, chalcopyrite, galena, pyrite, sphalerite, tungsten minerals, and other sulfarsenides associated with a quartz-pyrite-baryte matrix. Uranium occurs essentially as hexavalent U minerals such as sooty pitchblende, autunite, fritscheite, torbernite, uranotile, and zeunerite. Gangue minerals are mainly radiobaryte and/or quartz.

Secondary ore minerals constituted the bulk of mined ore. They occurred over a length of up to 1 km and a depth of about 250 m in several subparallel radiobaryte veins, some 10 cm to 1 m (av. 30–40 cm) wide, as well as in fracture zones in granite and granodiorite. A high-grade U zone existed at a depth of about 120 m.

12.1.0.2 Adrasman

This polymetallic deposit was discovered some 70 km NE of Khudzhand in 1934 but uranium was only identified in 1940. It was first mined for copper and bismuth in 1945. Uranium mining by underground methods began in 1946 and lasted to the 1950s, yielding 103 t U. Ore grades averaged 0.053% U. Adrasman occurs in a geological setting similar to that at Taboshar and consists of vein-stockwork mineralization composed of a Bi-Cu-U association.

12.2 Other Uranium Occurrences in Tajikistan

A number of U occurrences are reported from the *Gissar* and *Karetegin Ranges* of the southern Tien Shan. They are associated with Paleozoic complexes and include: (1) pitchblende mineralization in Permian volcanics at *Khanaka*, *Paridan*, *Rafikon*, *Mumin*, and in granite at *Yakhob* and *Moscovskoye*; (2) pitchblende-brannerite-fluor apatite mineralization in granite at *Lugur* and *Farkak*; (3) pitchblende-fluor-apatite mineralization in Middle Paleozoic carbonatic rocks at *Vaidara*; and (4) bitumen-pitchblende as well as fluor apatite-bitumen pitchblende mineralization in metasediments at *Karategin* and *Kamaroy*.

Early known occurrences mentioned by Bain (1950) include *Ayni/Zakhamatabad* and *Dzhirgashal* where a 10–14 m thick horizon contains thin bands of roscoelite mineralization with intervals enriched in carnotite. This horizon could be traced for 25–30 km. Bain suggests a surficial origin of the ore.

References and Further Reading for Chapter 12 · Tajikistan

For details of publications see Bibliography.

Bain 1950; IAEA 1995; Laverov et al. 1992a–c; Kohl 1954; Mashkovtsev and Naumov 1999; OECD-NEA/IAEA 2001; Shcherbakov 1937; Boitsov AV and Kazansky pers. commun.



Chapter 13

Turkey

A number of small sandstone-type uranium deposits have been found mainly in the Menderes Massif, western Turkey, and in northeastern and central Turkey. They contain up to several hundred tonnes of uranium each at grades on the order of 0.03–0.05% U. A few small, vein or veinlike-type U occurrences are reported from the South Menderes Massif.

13.1 Menderes Massif

Sandstone-type U occurrences are known from the *Köprübasi-Salihli* and *Fakili* areas in the northern and the *Koçarli* area in the southern Menderes Massif.

Sources of information. Kaplan et al. 1974; King et al. 1976; Komura and Ziehr/IUREP 1985; OECD-NEA/IAEA 1977, 1983, 1986, 2005; Yilmaz 1981.

Regional Geologic Features of the Menderes Massif

The Menderes Massif comprises domes of Precambrian to Lower Paleozoic augengneiss mantled by Lower Paleozoic phyllite, quartzite, marble, and mica schist, which have evolved by several episodes of metamorphism. Some vein or veinlike uranium occurs in these crystalline rocks.

Intramontane basins are filled with Tertiary to Quaternary sediments and host U occurrences preferentially in Neogene sediments. Lower Neogene strata are chiefly of fluvial origin and consist of alternating beds of conglomerate, sandstone, mudstone, and minor tuff. Upper Neogene strata are of lacustrine provenance and contain extensive limestone, locally intercalated with tuff and other pyroclastics.

13.1.1 Köprübasi-Salihli Basin

Located in the North Menderes Massif, this basin extends for about 25 km in NE-SW direction and 10 km in width. It contains ten uranium ore bodies ranging in size from some 10 t U (*Tüllüce*) to 700 t U (*Tasharman*) at grades averaging 0.03–0.05% U (cutoff grade 0.025% U). Total in situ resources of the basin are estimated at 2 850 t U (OECD-NEA/IAEA 2005). Host rocks are predominantly loosely consolidated Lower Neogene fluvial conglomerates with a matrix of abundant silt and clay, interbedded in sandstone. Carbonaceous material is rare. Dip of the strata is commonly less than 5°.

Both oxidized and unoxidized mineralization occurs. Oxidized mineralization is most abundant. It forms lenses a few meters thick of uranium disseminated through the sand or clay

matrix of conglomerate and sandstone. Unoxidized mineralization is composed of U associated with authigenic pyrite and siderite in the clay matrix of sandstone below the water table and is only found in the *Ecinlitas* deposit (ca. 500 t U). Higher grade intervals are restricted to zones enriched in pyrite whereas zones in which siderite is the dominant matrix mineral have low uranium values (Yilmaz 1981). The *Kasar* deposit (ca. 500 t U) averages 4 m thick and is covered by 8 m overburden.

Two U occurrences are identified in Upper Neogene lacustrine sediments in which U is associated with carbonate and phosphate minerals (Komura and Ziegler/IUREP 1985).

13.1.2 Fakili-Güre Basin

Located 70 km E of Köprübasi, the sandstone-type *Fakili* deposit contains some 500 t U at a grade of 0.04% U in a single lens as much as 9 m thick within lacustrine sediments at the base of the Neogene sequence. The mineralized interval includes clay-rich and tuffaceous beds with gypsum and authigenic pyrite. Uranium is present as sulfate minerals (Kaplan et al. 1974).

13.1.3 Koçarli Basin

This small Neogene basin in the South Menderes Massif contains the *Küçükçavdar* U occurrence. Mineralization consists of U⁶⁺ minerals that occur at a depth of 60 m in host rocks similar to those of the Köprübasi Basin. Resources are estimated at about 200 t U at a grade of 0.04% U (Komura and Ziehr/IUREP 1985).

13.1.4 Southern Menderes Massif

Located 35 km SW of Aydin in the southern Menderes Massif, the *Demirtepe-Cavdar* vein or veinlike-type deposit contains some 1 700 t U at a grade of 0.06–0.07% U hosted in a hematitic-limonitic, silicified breccia zone at the contact between gneiss and mica schist.

Similar mineralization occurs at *Kisir-Osmankuy*, 25 km SE of Söke, where shallow dipping fissures in coarse granitic gneiss contain siliceous, pyritic pitchblende veins and hexavalent U minerals (ca. 20 t U, 0.2% U) (Komura and Ziehr/IUREP 1985).

13.2 Other U Occurrences in Turkey

Sebinkarahisar, NE Turkey: Uranium is contained in paleochannels at the base of marine sediments of Eocene age. These sediments overlie uraniumiferous Paleozoic granite and uraniumiferous rhyolite, felsic tuff, dacite and andesite of various ages. Resources are some 250 t U at a grade of 0.03–0.04% U (OECD-NEA/IAEA 1983).

Küçükkuyu, NW Turkey: Uranium bound to phosphorite is hosted in tuff and tuffite embedded in sandstone of Miocene age. Phosphorite constitutes up to 30% of the host rock. Thorium is also abundant. Resources are about 200 t U at a grade of ca. 0.06% U (Komura and Ziehr/IUREP 1985).

Yozgat-Sorgun/Temvezli Basin, central Anatolia: U mineralization occurs in stratiform mode in several silty horizons within Lower Eocene deltaic-lagoonal sediments in the southwestern part and in Lutetian channel-type conglomeratic to silty sandstones of littoral-marine provenance in the northeastern section of the small Temvezli Basin. Mineralization tends to be controlled by basement morphology (paleovalleys), sedimentology (facies change), and structures (faults and warps). Resources

total 3 850 t U at a grade of 0.08% U (OECD-NEA/IAEA 2005) the bulk of which is situated in the northeastern section of the basin. Mineralization is in strong disequilibrium supposedly caused by an active groundwater regime. Minor U concentrations occur in thin coal seams in the southwestern part of the small basin (Komura and Ziehr/IUREP 1985).

References and Further Reading for Chapter 13 · Turkey

For details of publications see Bibliography.

Kaplan et al. 1974; King et al. 1976; Komura and Ziehr/IUREP 1985; OECD-NEA/IAEA 1977, 1983; 1986, 2005; Yilmaz 1981.

Chapter 14

Turkmenistan

Uranium occurrences have been identified at the Taurkyr (or Kaplankyr-Tauryuk) Dome near the settlement of Kizyl-Kaya at the western margin of the Karakum Desert in NW Turkmenistan. Kizyl-Kaya is located some 230 km ENE of the town of Turkmenbashi (formerly Krasnovodsk) on the Caspian Sea. U localities include *Cernoye*, *Novodgodny*, and *Amanbulak*, which are of structurally controlled volcanic (or sandstone?) type; and the black shale-type *Bailik* occurrence (► Figs. II-1, 14.1). *Cernoye* was the only deposit mined (see further below).

Sources of information. Pers. commun. by Blaise JR/Cogema 2002 and Boitsov 2000.

14.1 Taurkyr Dome, Western Karakum Desert

Regional Geological Setting of Mineralization

The Taurkyr Dome is a Paleozoic anticline exposed for 17 km in NW-SE direction and 5 km wide. Steeply dipping Permian and Triassic rocks form the core of the anticline. Jurassic and Cretaceous sediments drape around the core; they unconformably overlie the older strata.

A complete litho-stratigraphic section of the Taurkyr region includes the following units from top to bottom:

- *Cretaceous*: Mudstone, sandstone, silt, and carbonates
- *Upper-Middle Jurassic*: Marine sediments
- *Lower Jurassic*: Continental sediments with coal seams
- >Major unconformity<
- *Triassic*: Molasse
- >Slight unconformity<
- *Permian* (some 2 500 m in thickness, uranium host): Mudstone, siltstone, sandstone, conglomerate, tuff
- >Unconformity<
- *Carboniferous* (4 units): C4 carbonates, C3 sandstone, C2 black shale, and C1 basal volcanics (basalt, dacite, rhyolite); basalt interfingers laterally with the black shale unit
- *Devonian*: Volcano-sedimentary schists
- *Silurian*: Carbonates
- *Precambrian*: Schist, amphibolite

Ultrabasic (gabbro, dunite, peridotite) and minor granite and granodiorite intrusions cut the Silurian, Devonian, and Carboniferous units.

A regional NW-SE fault system dominates the region. It consists of steeply dipping, repeatedly reactivated major faults, which have put the Permian formations into a horst position. Numerous E-W faults dissect the dome into multiple blocks. Several submeridional faults complete this tectonic framework.

In addition, abundant NE-SW faults in the SE part of the Permian horst indicate another tectonic regime.

14.1.0.1 Cernoye (Sernoye) Deposit

This U deposit (in Soviet time labeled as sulfur deposit) is located about 1 km S of the village of Kizyl-Kaya. Mineralization is of the structurally controlled volcanic type. Discovered in 1952, the deposit was mined by open pit (100 m deep) and underground (to depths of 245 m) methods from 1952 to 1967. Ore was pre-concentrated on site by radiometric sorting and the concentrate was processed in the Aktau/Mangyshlak mill, Kazakhstan.

Production was reportedly 5 000–7 000 t U at (preconcentrated?) grades averaging 0.4–0.5% U (other estimates are 7 000–10 000 t U but without giving grades).

Geology and Mineralization

Cernoye consists of U mineralized structures/veins, which cut basal Permian facies on the NE flank of the Taurkyr Dome (► Fig. 14.2). Permian host rocks comprise reddish-brown and violet-brown mud-siltstone, sandstone, and conglomerate that rest upon a tuffaceous horizon. This basal tuff-mudstone section contains high quantities of pyroclastic material and effusives, and the conglomerate beds contain numerous pebbles of felsic volcanics (ignimbrite, rhyolite etc.). Host rocks are altered more or less by albitization, chloritization, silicification, carbonatization, and hematitization.

The deposit is associated with a cluster of subvertical faults oriented NNW-SSE that are particularly intense along the contact of the upper tuffaceous suite with sandstone-conglomerate and tuff-mudstone beds (► Fig. 14.2c). Flexures and junctions of subsidiary faults branching off a central fault provide the most favored sites for U concentrations. High-grade ore (<5% U) prevails in the central part of the deposit in the form of veined mineralization; it is enveloped by low-grade, streaky-disseminated mineralization. These features suggest ore control by structure and volcanic lithologies.

Pitchblende and sooty pitchblende associated with arsenopyrite, galena, marcasite, pyrite, and sphalerite are the principal ore minerals in the reduced zone. Coffinite, schoepite, tyuyamunite, and uranophane are typical for the weathering zone, which persists to depths of 60–100 m.

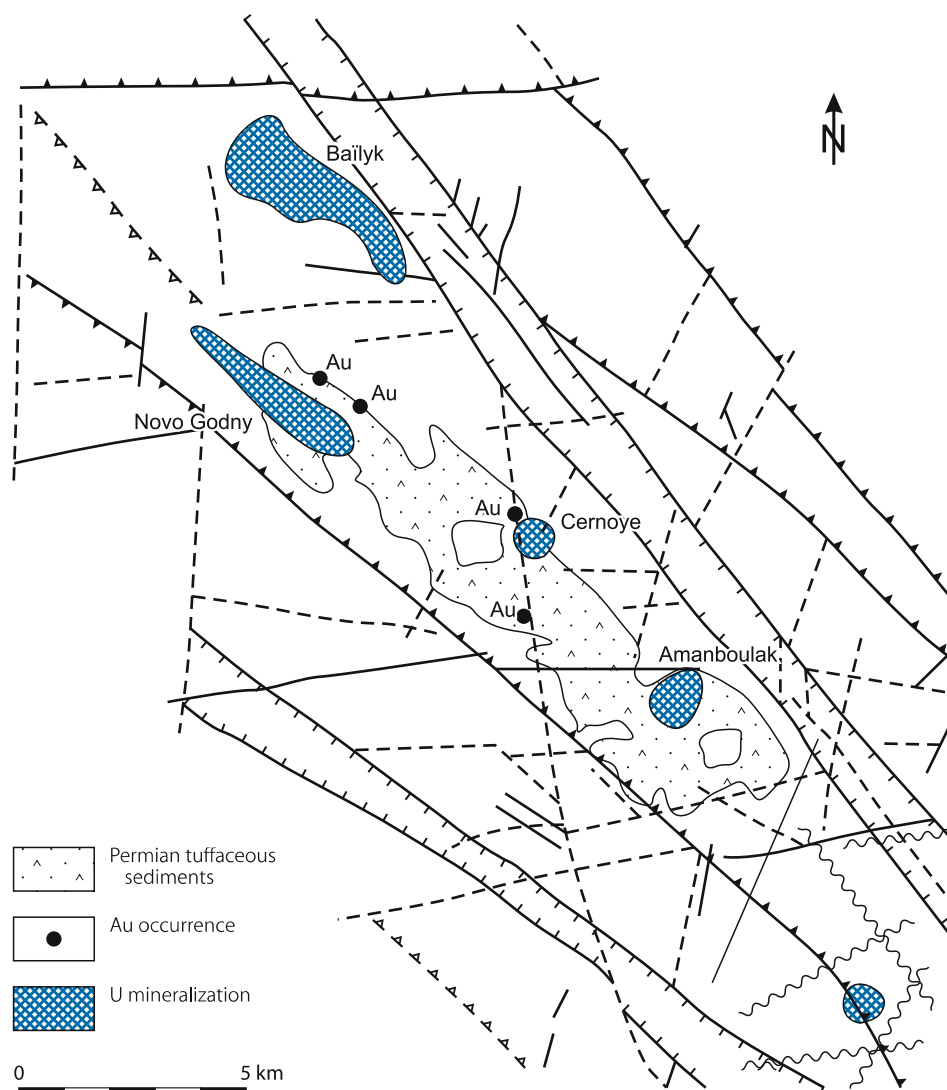
Mineralization extends for a length of 130 m in the upper, near-surface section and 200 m at depths of 245 m. Maximum width is some 50 m at depths of 80 m. Depth persistence is almost 300 m.

14.1.0.2 Novodgodny

Novodgodny is located 6 km NW of *Cernoye* in the northwestern part of the Taurkyr Dome. U showings occur on surface in a zone almost 2 km in NW-SE length and 200 m wide. U mineralization extends to depth of some 300 m and is

■ Fig. 14.1.

Turkmenistan, Taurkyr dome, structural map with location of U deposits and Au showings hosted in Permian tuffaceous sediments (courtesy of J.R. Blaise/Cogema)



confined to reduced Permian facies of the basal (PK2) horizon in the upper conglomeratic mega-sequence. Reduced beds are interbedded with and enveloped by oxidized beds. The strata dip 40–60° SW and consist of alternating sandstone-conglomerate-mudstone beds. Organic matter that is transformed into bitumens characterizes reduced horizons.

Mineralization is of tabular sandstone-volcanic(?) type. Grades are low (0.01–0.1%, av. 0.03% U). Mineralization is composed of U-vanadates associated with Mo (1.0%) in the form of jordisite, Zn, Pb, and Ag. Resources are estimated at 2 000–2 500 t U at 0.03% U and 10 000–15 000 t Mo.

14.1.0.3 Amanbulak

Located in the southeastern part of Taurkyr Dome, about 5 km SE of Cernoje, Amanbulak contains lithologic-tectonic sandstone-volcanic(?) type U mineralization. Surface U anomalies

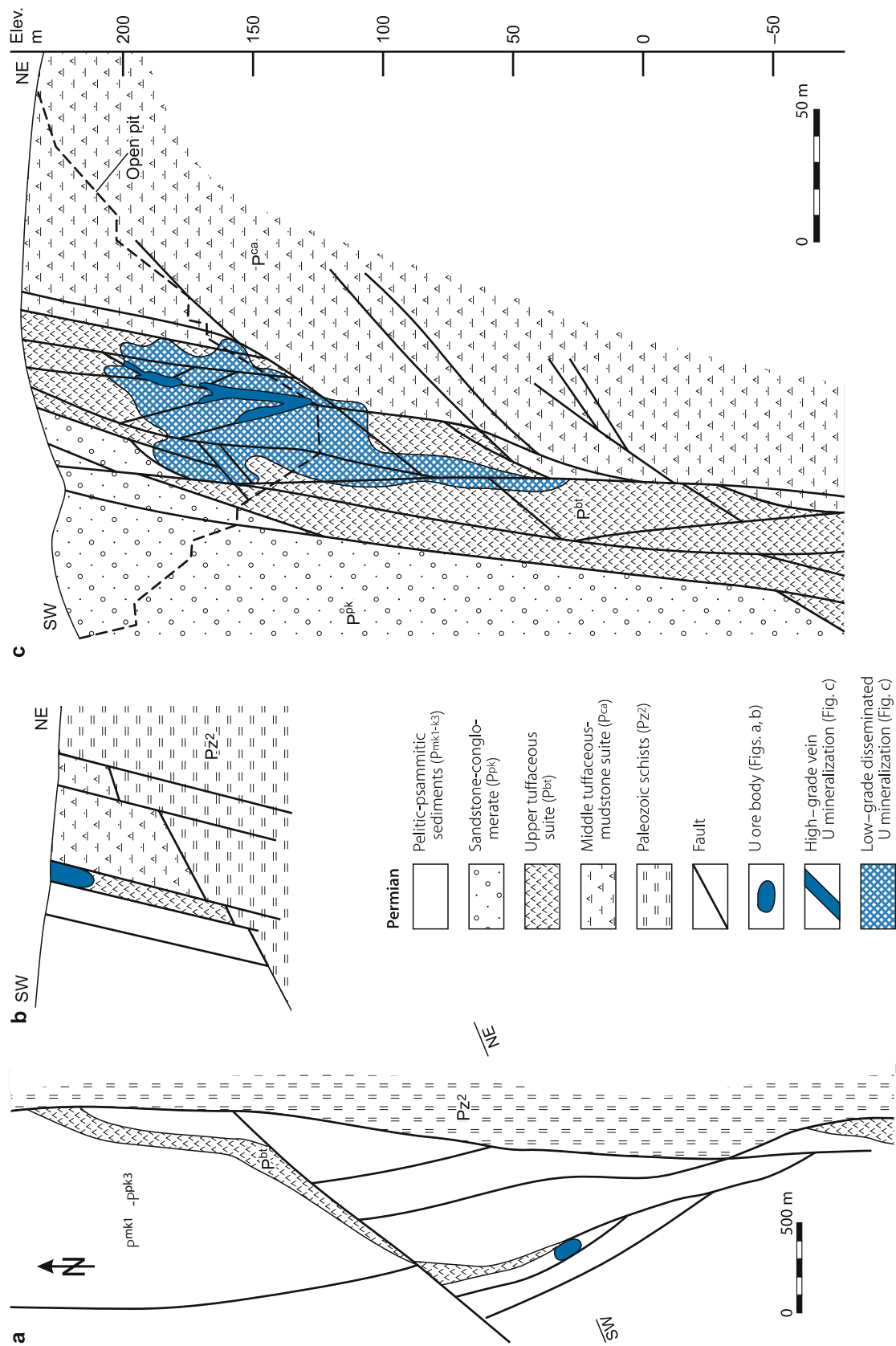
are found over a NW-SE distance of 1.6 km along the interface between two Permian units: a basal sequence of alternating sandstone-mudstone (PnA) and an overlying mudstone (PBA). U mineralization is concentrated where this interface is dislocated by E-W faults.

Some mineralization was mined in a trench on surface; it averaged 0.12% U (with maxima up to 5% U) over a width up to 13 m and a length of 35–40 m. This mineralization is known to occur to a depth of 150 m and follows the intersection of an E-W fault with the host sandstone.

14.1.0.4 Baïlik

This U occurrence of black shale and partly black shale-related stockwork type is situated in a Carboniferous pelite sequence to the NE of the Permian Taurkyr Dome, some 10 km NNW of Cernoje. Carboniferous beds consist of almost flat-lying black

Fig. 14.2. Taurkyr dome, Cernoye deposit, **a** litho-structural map of the volcanic-type deposit area; **b** and **c** SW-NE sections illustrating the structural control and setting of the deposit in basal Permian tuffaceous rocks below a sandstone-conglomerate horizon (after **a**, **b** courtesy of J.R. Blaise/Cogema, **c** A.V. Boitsov selected from Russian literature)



and grey pelites within a NW-SE-oriented complex that extends for some 5 km in NW-SE direction with an average width of 400 m. Jurassic clastic sediments with intercalated lignite seams rest unconformably upon the carbonaceous pelites. Major NW-SE faults bound and submeridional faults dissect the complex.

Uranium mineralization occurs in two sectors, north and south, at depths from 130 to 180 m. The north sector is said to contain about 5 000 t U. U is concentrated immediately below the pre-Jurassic unconformity and hosted in weakly metamorphosed black and grey shales with variable contents of organic matter. U-hosting shales are partly brecciated. U is essentially present as coffinite. Associated elements include Ag, Co, Mo, Ni, Pb, V, and traces of Au and Pt. Pyrite amounts to 2–5%. Siderite and phosphates complete the mineral assemblage.

Grades range from 140 to 690 ppm U over thicknesses from 1 to 32 m (cutoff grade 100 ppm U) and average 260 ppm over 18 m for the Bailik occurrence. These intervals include

narrow better-grade sections where black shale has enhanced organic matter contents; but here also grades are mostly less than 1 000 ppm U over commonly less than 1 m thickness (maximum 1 600 ppm over 0.3 m). Fault zones are reportedly enriched in U but no data are available (due to only vertical drilling).

Since U mineralization is restricted to a zone immediately below the Jurassic unconformity, it is thought that U was concentrated by oxidation processes that affected the uppermost section of the Carboniferous pelite sequence in pre-Jurassic time. Jurassic sediments laid down upon the Carboniferous strata protected this U mineralization against destruction.

References and Further Reading for Chapter 14 · Turkmenistan

For details of publications see Bibliography.

Pers. commun. by Blaise JR/Cogema 2002 and Boitsov AV 2000.

Chapter 15

Uzbekistan

Uranium deposits have been identified in the *Kyzylkum* region in central Uzbekistan and the *Karamazar* region in eastern Uzbekistan (Fig. 7.1). The former contains sandstone-type U mineralization in sedimentary basins as well as carbonaceous (or black) shale-related stockwork-type mineralization in basement uplifts. Volcanic vein-stockwork-type deposits are typical for the *Karamazar* region.

Remaining in situ resources (status: January 1, 2005) are confined to the *Kyzylkum* region and amount to 165 000 t U RAR + EAR-I and 220 000 t U EAR-II + SR recoverable at costs of up to \$130 per kg U (OECD-NEA/IAEA 2005). (Note: mining and processing losses of 30% have to be deducted to convert from in situ to recoverable resources.)

Mining took place in the *Kyzylkum* and *Karamazar* regions. Conventional mining had ceased, however, by 1994. Continued exploitation was restricted to ISL operations in the *Kyzylkum* basins.

From 1946 through 2004, cumulative production in Uzbekistan amounted to between 105 000 and 110 000 t U (OECD-NEA/IAEA 2003, 2005). The bulk of production came from the *Kyzylkum* region and an estimated few thousand tonnes U from the *Chatkal Range* of the *Karamazar* region (total production from the *Karamazar* region, including *Kyrgyzstan* and *Tajikistan*, was reportedly 20 000 t U). Annual production reached a peak of 3 700–3 800 t U in the 1980s. Since the mid-1990s, production has been on the order of 1 500–2 200 t U yr⁻¹. A production of 2 300 t U was expected for 2005.

A hydro-metallurgical plant started operation at *Navoi* in 1964/1965. It has a nominal annual production capacity of 2 300 t U. Molybdenum, vanadium, selenium, rhenium, scandium, yttrium, and REE were recovered as, or are considered potential by-products. Ore from the *Karamazar* region and *Nurabad District* was shipped to the *Chkalovsk* mill near *Khodzhand* (*Khudzhand*, *Chudzand*, formerly *Leninabad*) in *Tajikistan*.

As of January 2005, uranium production is in the responsibility of three mining divisions of the “*Navoi Mining and Milling Integrated Works*” (NMMIW) headquartered in *Navoi* [formerly “*Navoi Mining and Milling Combine*” (NMMC) established in 1958 that became a subsidiary of the state corporation “*Kizilkumredmetzoloto*” upon independence in 1991]. A fourth mining division was closed for economic reasons.

The “*State Committee of Geology and Mineral Resources of the Republic of Uzbekistan*” formerly carried out uranium exploration. This responsibility is now segmented. Exploration in areas with established deposits is in the hands of the geological divisions of local mining companies, whereas the search for new deposits is the duty of the “*State Geological Company Kyzyltepageologia SGE*”, successor to the “*Krasnokholmgeologia*” in the late 1990s.

The following description is based on *Laverov et al. (1992b, c)*, *OECD-NEA/IAEA (1993–2005)*, amended by data of other authors cited in the sections of the various uranium regions and districts.

Historical Review

Several expeditions into the *Karamazar* region, which extends from eastern Uzbekistan into *Tajikistan* and *Kyrgyzstan*, were organized by *Vernadsky* between 1914 and 1940. These expeditions discovered several U deposits including *Taboshar* in 1927 (*Tajikistan*), and *Mailuu-Suu* in 1933 (*Kyrgyzstan*); thus establishing the first uranium region in the former USSR.

Systematic exploration for uranium started at the end of World War II. Discoveries in the *Uzbekistan* sector of the *Karamazar* region include U-Mo deposits *Kattasay* and *Alatanga* in 1949, *Chauli* in 1952, and *Maylikatan* and *Rizak* (*Rezak*) in 1954–1955. At *Adrasman*, in nowadays *Tadjikistan*, a base metal deposit discovered in 1934, uranium associated with bismuth mineralization was found in 1950.

Uranium indications in the *Kyzylkum* region were first reported in the early 1950s and the first deposit, *Uchkuduk*, was confirmed in 1952. Subsequent exploration resulted in the discovery of additional deposits in the region including *Ketmenchi* in 1956, *Tokumbet* and *Bakhaly* in 1958, *Bukinai* in 1959, *Sabyrsai* in 1960, *South Bukinai*, *Sugraly*, *Lyavlyakan* and *Meilylsay* in 1961, and *North Kenimekh* in 1980.

Taboshar (*Tajikistan*) and *Tyuya-Muyun* (*Kyrgyzstan*) provided U ore for the first Soviet radium production in a special plant close to *Taboshar* during the 1930s. Actual mining for uranium started in the *Karamazar* region in 1946, first at *Shakaptar* (mined to 1958) and again at *Taboshar* in 1952; in the early years the ore was leached in *pachucas* close to the mines and the leachate was treated at the mill at *Leninabad* (now *Chkalovsk*) formerly called *Combine # 6*. Mining of the U-Mo deposits in *Karamazar* and other parts of the former USSR served as the prime source of uranium in the Soviet Union until the mid 1960s.

Development of open pit and underground mines commenced in the *Kyzylkum* region at *Uchkuduk* in 1958. Ore was initially stockpiled until the new mill at *Navoi*, located some 300 km SE of *Uchkuduk*, became operational in 1964/1965. Conventional underground mining operations began at the *Sabyrsai* and *Sugraly* deposits in 1966 and 1977, respectively. All conventional mining ceased in the *Kyzylkum* region in 1994, and only ISL operations continued. Testing of ISL techniques was carried out first in 1961 at the *Uchkuduk* deposit. Commercial ISL U production followed in 1965. ISL methods were subsequently applied at nine deposits (see next chapter).

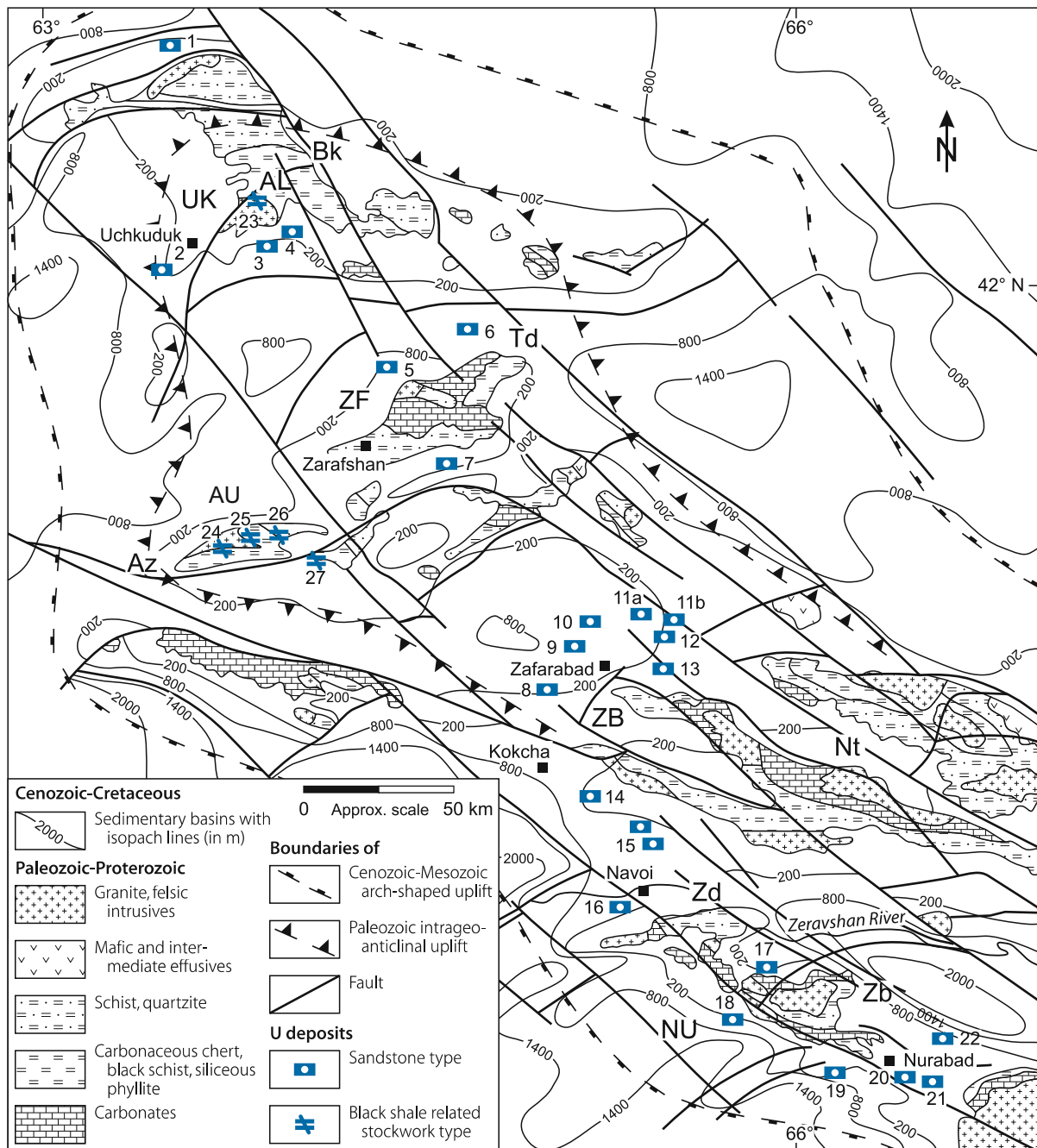
Four mining towns, *Uchkuduk*, *Zarafshan*, *Zafarabad*, and *Nurabad* were established to serve the four mining districts of the *Kyzylkum* region.

15.1 Kyzylkum Region

The *Kyzylkum* region is located in arid country of the *Kyzylkum Desert* in central Uzbekistan. U deposits occur in a 125 km wide belt, which extends for about 400 km from *Uchkuduk* in the northwest to *Nurabad* in the southeast. *Navoi* is the largest town in the region and is located about 65 km NE of *Bukhara*. A basin and range morphology as reflected by broad valleys separated by ranges of low relief characterizes the landscape.

■ Fig. 15.1.

Uzbekistan. Kyzylkum uranium region, generalized geological map with location of sandstone-type U deposits in Tertiary-Cretaceous basins and black shale-related stockwork-type U deposits in uplifted blocks of the Paleozoic-Proterozoic basement (after Shchetchkin and Kislyakov 1993 amended from OECD-NEA/IAEA 1995). **Mountain ranges:** *Az* Auminzatau, *Bk* Bukintau, *Nt* Nuratau, *Td* Tamdytau, *Zd* Ziatdin, *Zb* Zirabulak. **U districts/deposits in Tertiary-Cretaceous basins:** *UK* Uchkuduk District: 1 Bakhaly, 2 Meylisa, 3 Uchkuduk, 4 Kendyktyube; *ZF* Zarafshan District: 5 Sugrally, 6 Aktau, 7 Amantai. *ZB* Zafarabad District: 8 Bukinai (North) and Tokumbet, 9 Alendy, 10 Beshkak, 11a Lyavlyakan, 11b Aulbek, 12 Terekuduk, 13 Varadzhan, 14 Bukinai South, 15 Kenimekh North and South. *NU* Nurabad District: 16 Maizak North, 17 Ketmenchi, 18 Tutly, 19 Agron, 20 Sabyrtsai, 21 Shark, 22 Nagornoye. **Kyzylkum basement area:** *AL* Altyntau ore field: 23 Khodzhaakhmet. *AU* Auminza-Beltau ore field: 24 Dzhanuar, 25 Rudnoye, 26 Kostcheka, 27 Voskhod



Four districts with 25 sandstone- and 6 black shale-related stockwork deposits have been established in the region since the discovery of uranium at Uchkuduk in 1952. These districts group around four mining towns (mentioned as second names) and include – from NW to SE: *Bukantau* or *Uchkuduk*,

Auminza-Beltau or *Zarafshan*, *West-Nuratau* (*Nurantinsky*) or *Zafarabad*, and *Zirabulak-Ziatdin* or *Nurabad* (Fig. 15.1). Deposits are often closely spaced, a circumstance, which permits a grouping of, deposits into ore fields in which the deposits exhibit similar structural and litho-geochemical features.

Prominent uranium deposits are of *rollfront sandstone type* hosted in small Tertiary-Cretaceous basins at depths from 50 to 610 m on the western and southwestern side of the Bukantau-Aristantau-Nuratau Ranges of the northwestern spur of the Tien Shan mountains. Most deposits occur in Upper Cretaceous and a few in Lower Cretaceous and Upper Eocene strata.

Uranium grades of sandstone deposits are highly variable ranging in average from 0.026 to 0.18% U. Associated elements include Se, V, Mo, Re, Sc and lanthanides in potentially economic concentrations.

Two modes of deposits are distinguished. Deposits of lower grade such as Beshkak, Bukinai, Lyavlyakan and others are controlled by “normal” redox fronts that were presumably exclusively generated by the reaction of oxygenated groundwater with syndimentary organic debris reductants. Better grade ore bodies with an average of several tenths of a percent U and more are typically associated with zones, which have been additionally affected by epigenetic extrinsic reductants. Such ore bodies are known from Uchkuduk, Sugraly, and Sabysai where the higher grade and tonnage permitted conventional mining as outlined further below.

Compared with sandstone-type U deposits in the USA, the Kyzylkum rollfront deposits resemble in their regional geological setting those in the Wyoming Basins while at some locations hydro-geochemical processes related to the influx of extrinsic reductants tend to be more similar to those in the South Texas U region.

Basement uplifts contain small *stratiform and stockwork-type* U or U-V-phosphate deposits in tectonically deformed carbonaceous and siliceous metasediments of Precambrian to Lower Paleozoic age (locally referred to as “black shale” type). Deposits of this type are reported from two ore fields: *Altyntau* in the Bukantau/Uchkuduk and *Auminza-Beltau* in the Zarafshan District. The average U grade is between 0.06 and 0.132%. Associated metals occur in concentrations of 0.1–0.8% V, 0.1–0.2 g Au t⁻¹, and up to 0.024% Mo and 68 g Y t⁻¹.

Remaining *in situ* U resources (status: January 1, 2005) contained in *sandstone-type deposits* amount to 118 000 t U RAR + EAR-I and 166 000 t U EAR-II + SR in the up to \$130 per kg U cost category. Combined with past production of some 100 000 t U from sandstone deposits, the original uranium endowment of the Kyzylkum basins would total almost 400 000 t U or some 280 000 t U of recoverable uranium based on mining and processing losses of ca. 30%. Resources of black *shale-related stockwork deposits* total 47 000 t U RAR + EAR-I and 54 000 t U EAR-II + SR (OECD-NEA/IAEA 2001–2005).

Only sandstone-type ore bodies were or are exploited. *Conventional mining* methods have been used at three deposits: open pit methods at Uchkuduk beginning in 1958, and underground methods at Sugraly and Sabysai beginning in 1966 and 1977, respectively. Nine deposits were subject to *ISL exploitation* since 1961 including ore bodies at the aforementioned deposits. In 1975, the ISL technique began to replace underground mining at Sabysai; conventional mining came to a complete halt in 1983. All conventional mining ceased in the Kyzylkum region when the mines at Uchkuduk and Sugraly were added to the closure list in 1994. Also in this same year, ISL operations at Sugraly were terminated.

In 2005, nine *ISL operations* were active in three districts: at Uchkuduk and Kendyktube in the Uchkuduk District (operated by the Northern Mining Division); at Bukinai North, Bukinai South, Beshkak, Lyavlyakan, and Tohumbet in the Zafarabad District (Mining Division # 5); and at Ketmenchi and Sabysai in the Nurabad District (Southern Mining Division). The maximum depth of ISL extraction is 700 m.

Total uranium production of the Kyzylkum region is some 103 000 t through 2004. The three conventional mines at Uchkuduk, Sugraly and Sabysai delivered almost 56 000 t U for the years between 1958 and 1994 while ISL operations produced about 47 000 t U from 1961 through 2004. Annual production peaked in the 1980s when 3 700–3 800 t U yr⁻¹ were recovered. Current ISL production is on the order of 2 000 t U yr⁻¹ (2 087 t U in 2004) (OECD-NEA/IAEA 2001–2005). Mo, Se, Re, and Sc were recovered as by-products, whereas V, Y, and REE are considered potential by-products at some deposits. Final processing is centralized at the Navoi mill. Mining and milling operations are the responsibility of NMMIW.

Sources of information. Karimov et al. 1996; Kislyakov and Shchetochkin 2000; Kuchersky 1997; Laverov et al. 1992a-c; Mashkovtsev et al. 1979; OECD-NEA/IAEA 1995–2005; Shchetochkin and Kislyakov 1993; Venatovsky 1993; and other sources as noted. Note Worthy is the work by Karimov et al. (1996) who describe the known geology of the Kyzylkum uranium region adequately and present on comprehensive synopsis of the regional and local geological setting and characteristic features of all known uranium deposits.

Regional Geological Setting of Mineralization

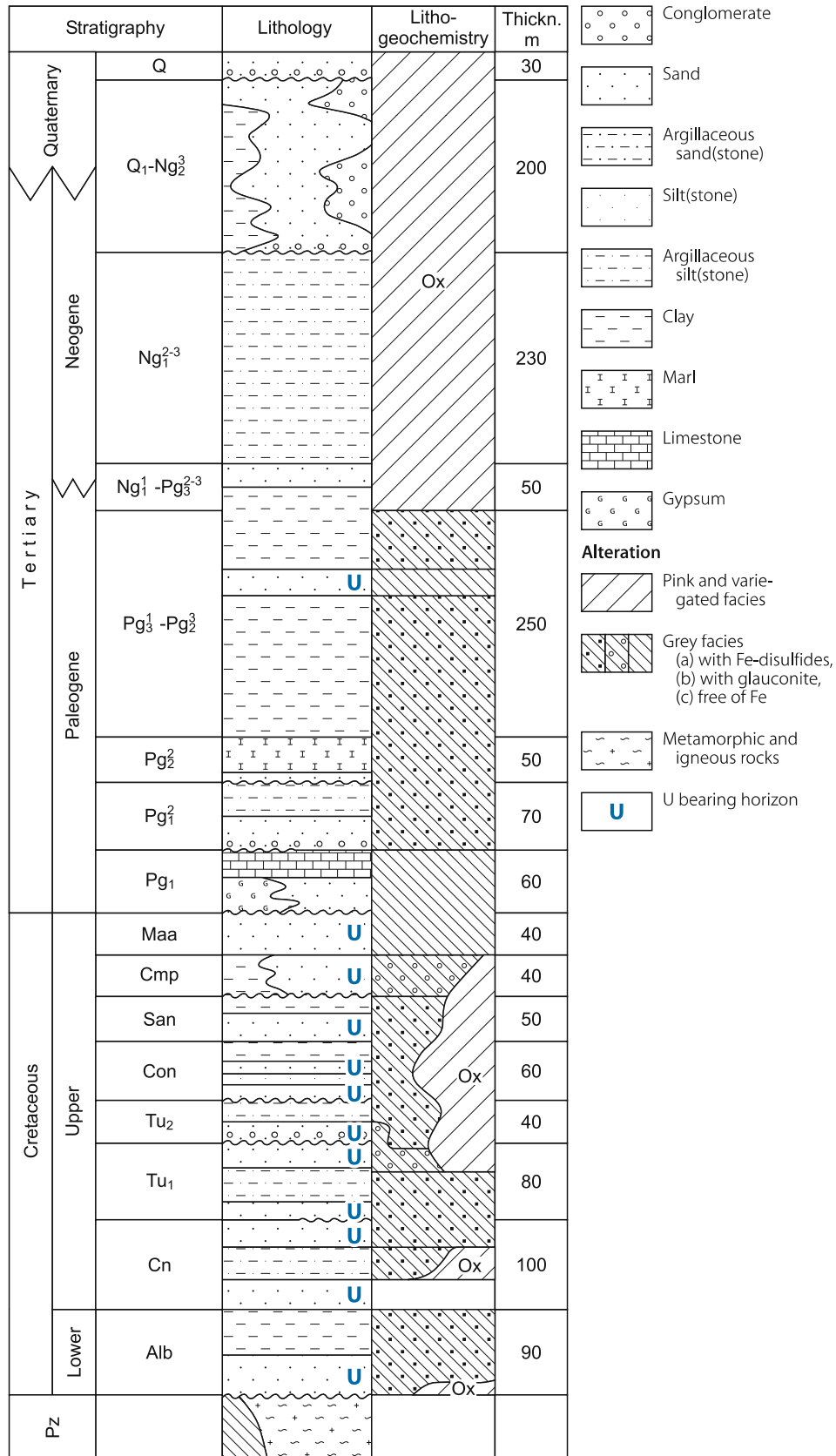
The Kyzylkum uranium region occupies the Central Kyzylkum Uplift, an arch-shaped structure raised by Hercynian and Alpine tectogenesis within the SE section of the post-Hercynian Turan Platform. Several large and deep Cenozoic-Mesozoic basins border the Kyzylkum Uplift: the Northern Kyzylkum Basin to the N, the Syr-Darya Basin (see Chap. 6: *Kazakhstan*) to the N, NE and E, and the oil- and gas-bearing Bukhara-Khivin and Bukhara-Karsha Basins to the W and SW.

Block faulting during the Paleozoic and Mesozoic-Quaternary related to the Hercynian and Alpine orogenies, respectively, generated a horst and graben structure in the Kyzylkum Uplift. Folded Proterozoic-Paleozoic rocks are exposed in uplifted blocks while subhorizontally bedded continental clastic sediments of Cretaceous and Cenozoic age fill the basins.

Two stratigraphic-structural units are distinguished in the Kyzylkum Uplift. The *upper unit* (► Fig. 15.2) consists of a Paleogene-Cretaceous sequence, from less than 100 m to about 1 000 m thick, of un- to slightly-lithified platform sediments covered by Miocene to Quaternary pink and tan molasse-type deposits, 0 to about 500 m thick. The latter developed in response to the general rise of the Kyzylkum Uplift. Compared with other sedimentary basins adjacent to the Kyzylkum Uplift, the assemblage of Tertiary-Cretaceous sediments in the Kyzylkum Basins has a reduced thickness and an increased and highly differentiated lithologic variation. This sequence evolved by multiple cycles of

Fig. 15.2.

Kyzylkum Basins, generalized litho-stratigraphic column (thickness figures give order of magnitude, deviations are given in deposit descriptions) (after Shchetchkin and Kislyakov 1993)



transgression and regression reflected by rhythmic development of alternating beds of grey, pink, or variegated, partly carbonaceous sand or weakly cemented sandstone, minor conglomerate, argillaceous, and/or silty facies. The basal Paleogene sediments also include limestone, marl, and gypsiferous horizons.

The *lower or basement unit* is composed of Proterozoic and Lower Paleozoic geosynclinal facies metamorphosed and folded during the Hercynian Orogeny. It includes Cambrian-Ordovician sandstone/quartzite, schists, siliceous phyllite, carbonaceous chert, carbonaceous black shale/slate and carbonates. Magmatic lithologies include felsic intrusives, and intermediate and mafic effusives. The “black shale” contains markedly elevated U values.

The structural framework of the Kyzylkum Uplift, as it is reflected to day by downfaulted, small artesian basins separated by basement horsts, had its root in Late Paleozoic tectonism associated with the Hercynian Orogeny and in tectonic reactivation during the Late Mesozoic and Quaternary. Orogenic activity from the end of the Oligocene onward caused a general rise to form the arch-like uplift, and a subsequent dissection of the uplift into an intricate block structure with horst and graben development. Major faults trend NW-SE. They cut faults oriented about E-W and are displaced by WNW-ESE structures (Fig. 15.1).

Uranium ore bodies occur in twelve arenaceous horizons embedded within argillaceous, silty beds of Upper Eocene, Maastriichtian, Campanian, Santonian, Coniacian, and Turonian age. Mineralized lithologies are of fluvial or shallow marine origin and consist predominantly of sand, minor conglomerate as in parts of Sabyrsai and Ketmenchi, and sandstone cemented by clay (part of Lyavlyakan) and/or carbonate as in sections of Sugraly and Ketmenchi. Quartz (65–80%), feldspar (6–22%), chlorite, biotite, muscovite, and fragments of siliceous (1–5%) and aluminosilicate (5–16%) rock fragments are the dominant detrital constituents of mineralized facies. Clay minerals such as hydromica with admixtures of kaolinite and montmorillonite make up between 1 and 15%. Authigenic minerals are mainly calcite and dolomite (up to 10%), pyrite and marcasite (up to 3.5%) or hematite and limonite, and locally siderite, ankerite, glauconite, and others. The sulfides and glauconite are typical for reduced facies whereas hematite and limonite are characteristic for oxidized facies.

Chemically, host rocks are predominantly silicic as reflected by a content of 63–85% SiO₂. Carbonate, sulfide, organic debris, and phosphate contents are quite variable (Table 15.1). Some ore bodies are carbonate free while others may contain substantial amounts of up to 5% carbonate. Sulfur contained in pyrite ranges from 0.05 to 3% with maximum values occurring at some sites in Sugraly and Sabyrsai. Organic carbon commonly amounts to 0.03–0.1% C in alluvial sediments but can be up to 10% locally as in Sabyrsai and Ketmenchi. Shallow marine sediments have lower organic carbon contents, on the order of a few hundredths of a percent. Some uraniferous horizons are barren of carbonaceous debris, e.g. the Kendyktube Horizon at Uchkuduk. Bitumen is a common constituent at Sabyrsai but also occurs at Sugraly and elsewhere. Phosphorous ranges generally from 0.03 to 0.4% but can be up to 6% as at Ketmenchi.

Rock temperatures range from 20 to 40°C. Lowest temperatures occur at Beshkak, Lyavlyakan, and in parts of Bukinai and Ketmenchi. Maximum values are recorded from Kenimekh North and the NE section of Sugraly.

Groundwater flow rate is 1–10 m per year in mineralized beds. The filtration coefficient of sand, which is a critical factor for ISL operations, varies between 2 and 10 m d⁻¹ but can locally be as low as between 0.1 and 1 m d⁻¹ as, e.g. at Sugraly. Depths to groundwater vary between less than 50 m and 100 m and locally more. Water contained in the ore-bearing strata is artesian and, chemically, mostly slightly saline but locally neutral (Table 15.1).

Principal Host Rock Alterations

Aquifers around uplifted basement blocks commonly exhibit a bipartitioned oxidation zone generated by differential, oxygenated groundwaters that produced either hematitization or limonitization and, as such, imposed a pink or yellow hue, respectively, on the originally grey strata. The inner oxidation aureole is marked by pink facies and extends from a few to several tens of kilometers from an uplifted core into the basin. It grades into the yellow facies, which persists further downdip for a short distance and terminates at the interface with reduced, grey, pyrite and/or glauconite containing arenites. Locally, the limonitic zones enclose pink, hydro-hematitic alteration intervals that are thought to be the product of thermal solutions.

Reduced sediments are characterized by pyritization, bituminization, carbonatization, and aureoles of hydrogen and hydrogen-sulfide. At least two modes of reducing media generated the reducing environments. The first is widespread and derived diagenetically from synsedimentary carbonaceous matter. The second is locally restricted (e.g. at Uchkuduk, Sugraly, Bukinai, Sabyrsai) and is the result of extrinsic reducing thermal solutions that percolated along faults and invaded the aquifers. It is reflected by pyritized, bitumenized, carbonatized and silicified complex, column-like segments with tongues and lenses extending tree-like into adjacent permeable horizons (Mashkovtsev et al. 1979) (for more details see Sect. *Sugraly*).

Principal Characteristics of Mineralization

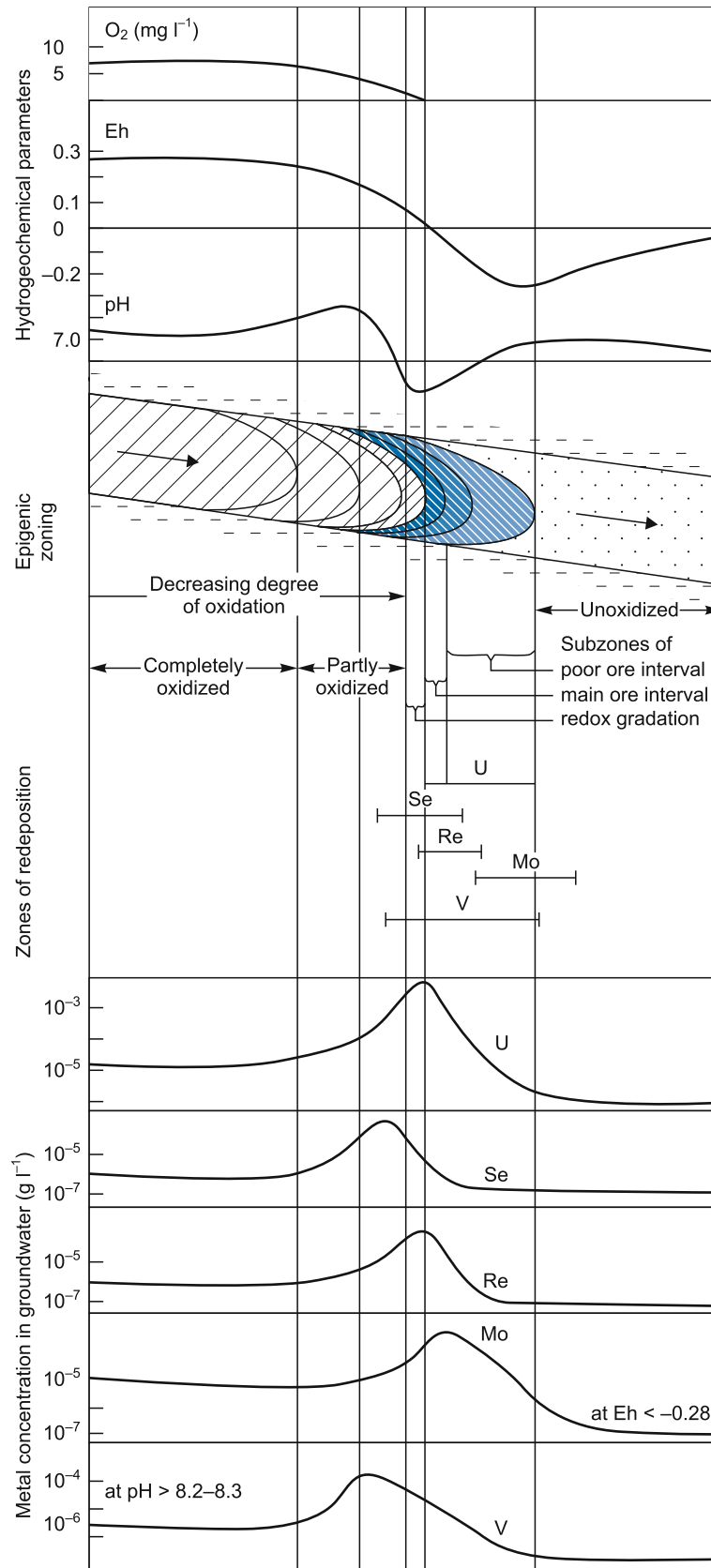
Venatovsky (1993), amended by data from Shchetochkin and Kislyakov (1993) and Kislyakov and Shchetochkin (2000), provides the following information on ore composition: Pitch-blende, black products (sooty pitchblende) and coffinite are the principal uranium minerals in unoxidized ore, whereas uranophane and rarely U-vanadates are typical for oxidized ore. Associated minerals/elements include pyrite, minor marcasite, carbonates (mainly calcite), hematite, molybdenum in the form of jordisite and minor ilse-mannite and femolite, vanadium as V-oxides and, more rarely, as U-vanadates, selenium as native Se and selenides, rhenium in form of ReS₂ and ReO₂, and scandium as Sc-hydroxide and Sc-bearing apatite. Yttrium and lanthanides (cerium, dysprosium, erbium, thulium, ytterbium, europium, samarium, gadolinium, terbium) contained in detrital accessories of ore-bearing sands are reported from the Bukinai-Kenimeth ore field.

There is a transitional overlapping of elemental assemblages downdip across an ore roll starting on the rear side with native Se or V-Se, followed by Se-Y-lanthanides-U, Sc-Y-lanthanides-U-Re, and Mo-Re on the convex side. Re, V, and locally Mo halos may extend markedly beyond the uraniferous interval (Fig. 15.3).

Table 15.1. Uzbekistan, Kyzylkum Basins. Geochemical and groundwater characteristics of selected sandstone-type uranium deposits (after Karimov et al. 1996; Kisiyakov and Shchetochkin 2000; Kuchersky 1997; Shchetochkin and Kisiyakov 1993; Venatovsky 1993) (m b.s.l. = meter below sea level)

District/deposit	Ore chemistry				Groundwater				Temperature (°C)
	Fe-sulfide S-content (%)	Carbonate CO ₂ content (%)	Phosphate P-content (%)	Organic carbon (%)	Metallic components	Table (m b.s.)	Flow rate (m yr ⁻¹)	Chemistry	
General					U, Se, Mo, V:0.x%				
• range	0.05–3	0–>5	0.03–6	0.03–10	Re, Sc, Y, REE: ppm	<50–>100	1–10	Neutral or saline	
• average			0.03–0.4	0.03–0.1		>100		Slight saline	
Uchkuduk Dist									
• Meylilai		<5+				<50			
Zarafshan Dist									
• Sugraly	<3	<5+				100+			<40
Zafarabad Dist									
• Kenimekh		<2				100+			40
• Bukinai S		<2–5				<50–100			20
• Bukinai N						<50			
• Alendy						<50			
• Beshkak		<2				<50			20+
• Lyavlyakan		<2				<50–100			20
Nurabad Dist									
• Ketmenchi		<2–5	<6	<10					
• Tutly									20+
• Sabyrsai	<3	<5+							

Fig. 15.3. Kyzylkum Basins, schematic section across a redox front documenting typical hydrogeochemical conditions and related differentiated oxidation zones as well as the concentration of U, Se, Re, Mo, and V in groundwater and distribution of these elements across the redox interface (after Karimov et al. 1996)



Three main ore types and several subtypes are distinguished based on mineralogical composition and U grade:

- a **Ordinary, low to medium-grade, unoxidized ore** composed predominantly of black U products (sooty pitchblende). This type is typical for most U deposits in the Kyzylkum region and occurs at a redox front of a stratum oxidized tongue with diagenetically reduced ground derived from intrinsic reducing agents, essentially detrital carbonaceous matter.
- b **High in grade, unoxidized (or partially oxidized) ore** consisting of pitchblende-hematite-sulfide or pitchblende-coffinite-sulfide assemblages. This ore variety is related to redox interfaces controlled by locally reduced or re-reduced ground caused by extrinsic reducing thermal solutions that migrated along faults. Ore bodies of this type do not exhibit the mineralogical and elemental features and zoning that are characteristic of normal rollfront deposits (typical ore bodies of this type are identified e.g. in the Sugraly, Bukinai, and Sabyrtsai deposits).
- c **Oxidized, commonly uranophane dominated ore**, which is rare and commonly positioned updip behind unoxidized lodes and represents relics of former high grade ore bodies.

Host rocks, as mentioned earlier (see Regional Geological Setting of Mineralization) are arenaceous, permeable horizons interbedded with impermeable beds. Most deposits are hosted

by Upper Cretaceous sediments. A few, like Aktau, Beshkak, and Lyvlyakan, occur in Eocene strata. Mineralization at Bakhaly and Ketmenchi occurs in Tertiary and Lower and Upper Cretaceous sediments as well.

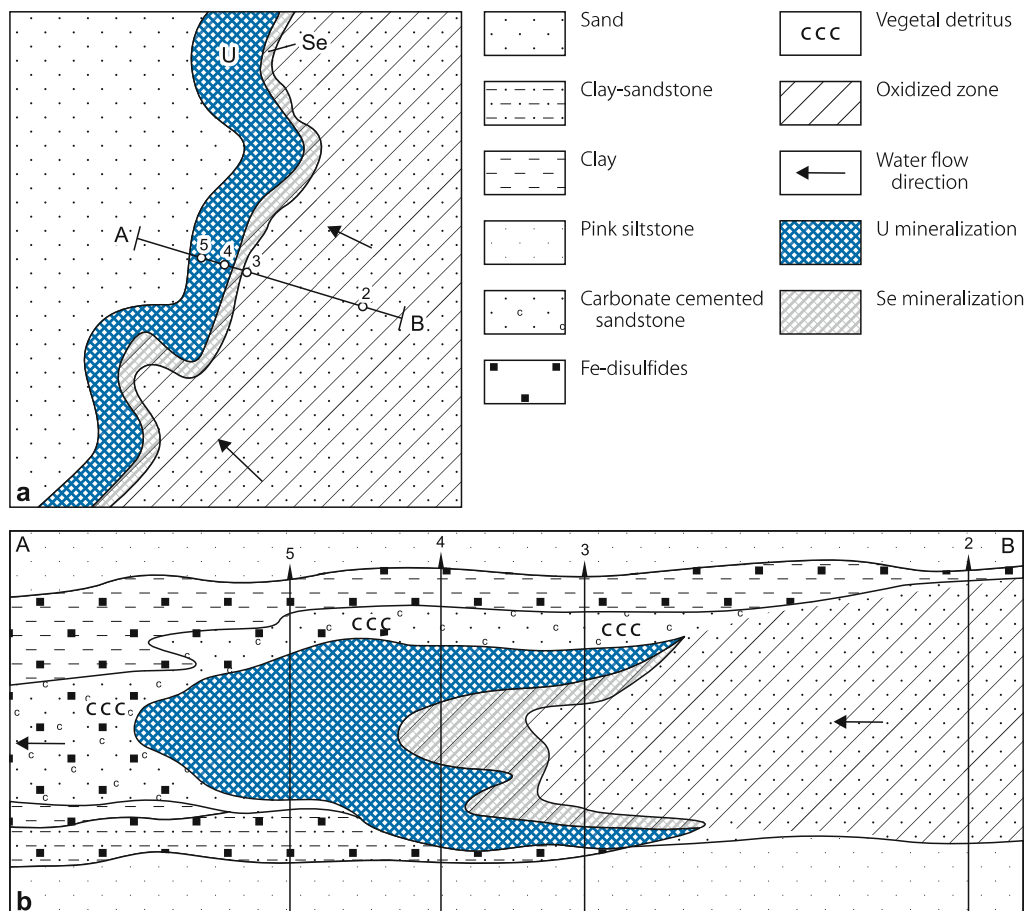
General Shape and Dimensions of Deposits

Deposits consist, in planview, of a number of discontinuous, elongated ore lodes controlled by highly twisted redox boundaries. These redox fronts can be traced for up to several hundreds of kilometers bending around basement highs. In cross-section, mineralization occurs as simple crescent-shaped (▶ Fig. 15.4) or complex rolls stacked in up to six superjacent horizons; cumulative thicknesses of which range from 8 to 30 m but are generally less than 20 m. Depths vary from less than 50 m to about 700 m. Individual ore bodies are from less than one meter to almost 20 m but mostly between 3 and 5 m thick, from about 50 m to more than 300 m wide perpendicular to the roll, and up to several kilo-meters long. The two thickness parameters give a ratio of ore body thickness to host bed thickness ranging from 1:2 to 1:10 with most common values between 1:3 and 1:7.

Individual deposits have in situ resources from a few 1 000 to more than 50 000 t U and average grades usually of less than 0.1% U.

■ Fig. 15.4.

Kyzylkum Basins, schematic **a** map and **b** section of rollfront-type (Uchkuduk-type) U deposits. (Scale vertical to horizontal 1–10) (after Karimov et al. 1996)



Grades of ore bodies within a deposit range from 0.01–3% U. Common tenors of associated elements include: 0.001–0.3% Mo; 0.03–0.5% V; 0.05–0.07% Se but with ranges from 0.01 to 0.2% Se; 0.5–2 ppm and occasionally up to 15 ppm Re; 3–20 ppm Sc; and locally, as in the Bukinai-Kenimekh ore field, <120 ppm Y, <150 ppm Ce, and <50 ppm other lanthanides, [dysprosium, erbium, thallium, ytterbium (<10 ppm), europium, samarium (<3 ppm), gadolinium and terbium (<1.5 ppm)]. In terms of a productivity coefficient, values range from 1 to 20 kg U m⁻² and average between 2 and 6 kg U m⁻². Respective Mo, Se, and V values range from less than 1 to more than 5 kg m⁻² while Sc, Re, and REE values vary from less than 1 to more than 5 g m⁻².

Stable Isotopes and Fluid Inclusions

Kislyakov and Shchetochkin (2000) report results of stable isotopes and fluid inclusions studies mainly but not exclusively from the Sugrally deposit and arrive at the following conclusions. Decrepitation of inclusions in pitchblende and paragenetic calcite in high-grade ore suggests increased temperatures of 120–200°C for this mineralizing process. Homogenization of gaseous-fluid inclusions in gangue minerals of the various alteration stages indicates a temperature of not less than 120°C during mineral crystallization. Fluid inclusions in vein quartz correspond to gaseous-aqueous brines with very high tenors of (in mol kg⁻¹ H₂O) 0.3–2.4 total sulfur, 0.9–4.3 Ca and 0.4–1.7 CO₂.

Sulfur isotopes in pyrite derived from thermal solutions and associated with pitchblende-hematite-sulfide ore have different ratios than sulfur isotopes of sulfate-ions in present-day groundwater in the Cretaceous aquifers and in near surface deposited gypsum (► Table 15.2). This indicates a sulfur source for the pyrite different to that of the groundwater. Otherwise, pyrite in black U ores has a wide range of $\delta^{34}\text{S}\text{‰}$ values, which may be attributed to the isotopic fractionation during biogenic

reduction of sulfate in groundwater and incorporation of sulfur from earlier sulfides including those of thermal fluid origin. The isotopic composition of sulfur in pyrite and baryte in unaltered aquiclude clays, except for diagenetic mineral phases, is thought to be due to early diagenetic fractionation of the sulfur of marine waters.

Principal Ore Control or Recognition Criteria

Host Environment

- Horst and graben structural pattern
- Relatively small artesian basins separated by uplifted basement ranges
- Basins are filled with
 - Quaternary and Upper Tertiary molasse-type sediments, 0–500 m thick resting upon
 - Lower Tertiary to Cretaceous clastic sediments, from less than 100 m to about 1 000 m thick, of fluvial, deltaic, and shallow marine provenance
- Alternating sedimentary cycles are reflected by permeable arenaceous horizons intercalated with impermeable argillaceous or silty beds
- Subhorizontal dip of strata except for flexures along faults
- Widespread faulting by repeated tectonism
- Potential source rocks for U and other metals are provided by basement lithologies particularly black slate

Alteration

- Principal pre-ore alteration includes oxidation and reduction
- Oxidation is reflected by hematitization and limonitization
- Oxidation zones often occur as relatively narrow aureoles around basement uplifts
- Reduction is documented by sulfidization (mainly pyritization) and bitumenization

► Table 15.2.

Kyzylkum Basins. Sulfur isotope composition of sulfide and sulfate minerals and sulfate in present-day groundwater (Shchetochkin and Kislyakov 1993 including data from other authors)

Specimen	Sampling site/ deposit	$\delta^{34}\text{S}\text{‰}$; Fe-disulfide (pyrite)			$\delta^{34}\text{S}\text{‰}$; sulfates		
		Range	Average	No. of samples	Range	Average	No. of samples
Thermal veins in ore bearing beds	Uchkuduk	–33.7 to –37.1	–35.4	3	+50.4 to +24.0 (baryte)	+37.2	12
Pitchblende-hematite-sulfide ore	Sugrally, Sabysai	–28.2 to –46.2	–37.2	25			
Black U products ore	Uchkuduk, Sugrally, Lyavlyakan	+17.9 to –46.2	–14.0	40			
Surficial oxidation zone	Uchkuduk				+9.1 to +4.1 (gypsum)	+6.6	12
Groundwater	Uchkuduk, Sabysai				+8.2 to +1.4 (sulfate-ion)	+4.8	11
Unaltered aquiclude clays of U-hosting strata with diagenetic minerals	Uchkuduk	–13.2 to –40.3	–26.7	10	+28.8 to +27.0 (baryte)	+27.9	3

- Reducing agents are of twofold origin
 - Synsedimentary carbonaceous matter and/or epigenetic sulfides and bitumens, and
 - Extrinsic reducing thermal solutions ascending along faults
- Syn-ore alteration includes sulfidization, locally hematitization, carbonatization, silicification, and argillization

Mineralization

- Ore bodies are predominantly of rollfront type
- Mineralization is polymetallic and may include U, Mo, Se, V, Re, Sc, Y, and/or REE
- Various ore types exist due to redox fronts of different origin and
- Repeated reworking of older mineralization
- High-grade pitchblende-hematite-sulfide and pitchblende-sulfide ores are associated with redox fronts generated by extrinsic reducing thermal solutions
- Low-grade (ordinary) black U ore is related to redox fronts generated by diagenetically reduced environments based on carbonaceous matter and/or sulfides
- Uranophane mineralization is locally developed due to oxidative replacement of high-grade U-oxide ore
- Zoning of ore-related elements across roll-shaped ore bodies
- Simple and multiply stacked ore rolls in superjacent aquifers
- Relatively close position of most deposits to basement uplifts
- Favorable host rocks include un- to weakly-lithified sands, clay- or carbonate-cemented sandstone, and minor conglomerate with or without organic debris and with Fe-sulfides, -oxides, -hydroxides, phosphates, and carbonates as minor constituents

Principal Aspects of Metallogenesis

In conclusion from descriptions of the various researchers, uranium deposits in the Kyzylkum Basins were formed and are still in the process of modification by epigenetic hydrodynamic processes, which dominated the hydrodynamic regime in the Kyzylkum Basins from the Pliocene onward. Oxygenated groundwater and intrinsic reductants such as organic matter and diagenetically derived sulfides and bitumens as well as locally active extrinsic reducing thermal solutions ascending along faults are the salient ingredients in the metallogenesis. The hydrodynamic regime is the result of local recharge of oxygenated waters from basement uplifts and their down-gradient migration in permeable strata. U and other ore-forming metals were supposedly leached by meteoric waters from fertile source rocks in the basement complex such as black slates and then incorporated into the groundwater. The basinward migrating oxygenated waters generated an aureole of oxidized aquifers up to few tens of kilometers wide around basement highs. These solutions also transported the ore-forming elements down-dip the hydrogenic gradient to redox interfaces where chemical reactions caused their deposition in roll-shaped ore lodes.

Redox interfaces were generated at sites where the oxygenated waters encountered reduced ground. Reducing conditions were provided by two principal sources of reductants. The first was provided by synsedimentary carbonaceous matter and/or diagenetically derived sulfides, and the second by locally upwelling, extrinsic thermal fluids. These reducing thermal solutions percolated along faults, invaded adjacent aquifers and generated locally-restricted reducing environments (Mashkovtsev et al. 1979). Perevozchikov (2000) identified liquid hydrocarbons and hydrogen in the reducing thermal solutions that control the uranium in the glauconite sands of the Kendykube Horizon of the Uchkuduk deposit (these sands are barren of carbonaceous debris); and he could trace the migration paths of hydrocarbons concentrations in groundwater from the discharge area back to the oil-bearing Amudarya Basin.

Consequently, two varieties of redox fronts were formed. Strata inherent reductants commonly produced only a weak redox front along which only low-grade, ordinary black U mineralization developed. The magnitude or intensity of this type of mineralization is inversely proportional to the width of “young” limonitic subzones in aquifers and in the zone of oxidized strata in general. Extrinsic reducing thermal fluids provided a more powerful reductant. Where they intervened with oxygenated groundwater, a geochemical interface was established that provided the required geochemical conditions for deposition of relatively high-grade U mineralization.

Periodically repeated tectonic activity from the Late Pliocene into Quaternary exerted a strong influence on the metallogenetic evolution by triggering multiple alternations and variably intense processes of oxidation and reduction. During more quiet interludes, ore deposition accelerated. In contrast, periods of increased tectonism were accompanied by not only a rapid advance of oxygenated waters but also by a renewed influx of reducing thermal solutions, which resulted in redistribution of U and other metals. During these processes older mineralization was repeatedly reworked and high-grade pitchblende-hematite-sulfide and pitchblende-sulfide ores were transformed into ordinary black U ores and locally, in zones of oxidation, into uranophane mineralization.

A more detailed metallogenetic model for an individual deposit, namely Sugrally, is forwarded by Shchetochkin and Kislyakov (1993) for which the reader is referred to Sect. *Sugrally*.

15.1.1 Uchkuduk or Bukantau District

Four U deposits are reported from the Uchkuduk District; *Bakhaly* is situated to the north and *Uchkuduk*, *Meilysai*, and *Kendyktyube* to the south of the Bukantau Range. A mining town, Uchkuduk, was established 250 km NNW of Navoi to serve the district. Remaining in situ resources amount to 17 900 t U RAR + EAR-I and 21 200 t U EAR-II + SR (OECD-NEA/IAEA 2005).

Conventional mining produced on the order of 30 000 t U between 1958 and 1994 when conventional mining was terminated. An estimated additional quantity of about 15 000 t U was recovered by ISL operations between 1964 and 2001, all from the Uchkuduk deposit. In 2005 production was restricted to ISL

operations at the Kendyktube deposit. The Northern Mining Division, a subsidiary of NMMIW, is the mining operator.

Source of information. Karimov et al. 1996; unless otherwise cited.

15.1.1.1 Bakhaly

Bakhaly is an explored deposit located ca. 65 km N of the town of Uchkuduk. It contains in situ resources of some 3 000 t U. Three horizons of Albian, Turonian, and Cenomanian age are mineralized and contain several ore bodies, 0.1–1.5 m thick, of roll and lenticular shape. Ore occurs at depths from 160 to 430 m. Ore grades vary between 0.03 and 0.5% U. Ore body # 3 is the largest. It is 2 700 m long, 200 m wide, and hosted by an Albian carbonaceous sand and clay sequence with lignite intercalations.

15.1.1.2 Meilysai

This explored deposit was discovered 30 km SW of the town of Uchkuduk in 1959. Lenticular U mineralization occurs in three Upper Cretaceous arenaceous beds at depths from 160 to 350 m. Paleogene clay and marl overly the ore-bearing unit, while siltstone of the Taikarshin horizon forms the footwall. Some U mineralization is also found in the latter. A stratum of sand with argillaceous intercalations, 10–30 m thick, within the lower section of the 130 m thick Aitymsky Horizon is the principal ore-bearing unit. Four ore bodies are identified in this unit. Ore bodies consist of 3–10 ore lenses separated by barren ground. Ore body # 1 is the largest; it measures 6 km long, from 50 to 1 300 m wide, from 3 to 4 m thick, and accounts for 60% of the resources of Meilysai. Grades range from 0.01 to 0.05% U and average 0.026% U. The ore contains from 2 to 4% CO₂ contained in carbonate.

15.1.1.3 Uchkuduk

Uchkuduk is located 25 km E of the same named town. Discovered in 1952, it was exploited by open pit mining from 1958 to 1994. ISL tests started in 1961 and lasted until 2001/2002. Original total resources amounted to more than 50 000 t U at grades averaging about 0.04% U except for some higher grade ore bodies. Remaining resources (RAR + EAR-I high cost category) are about 12 000 t U.

Geology and Mineralization

Bedrock geology consists of a slightly SE dipping Upper Cretaceous-Paleogene sequence covered by an up to some 10 m thick veneer of Quaternary alluvium. The sediments rest on Upper Carboniferous siliceous schists intruded by granite. The basement crops out to the north and plunges to 400 m deep to the south of the deposit. Major faults trend curvilinear NNW-SSE, NE-SW, and E-W (Fig. 15.5). The Cretaceous-Tertiary litho-stratigraphic column includes from top to bottom:

Lower Oligocene-Upper Eocene: 0 to >20 m thick, clay

Middle Eocene: <40 m thick, marl

Lower Eocene: 2–8 m thick, calcareous clay.

>Unconformity<

Senonian, Aitymsky Horizon: 20–60 m thick, alluvial fine-grained grey sand and carbonatic sandstone

Upper Turonian, Taikazhinsky Horizon: 90–105 m thick, separated into

- upper unit: proluvial pink siltstone with interbedded pink sandstone
- lower unit: alluvial carbonate cemented sand

Lower Turonian

- Kendyktube Horizon (U): 20–25 m thick, marine green-grey glauconite sand and muddy sand (barren of organic debris)
- Dzheirantyi Horizon: 40 m thick, blue-grey mudstone and montmorillonite-hydromica-bearing clay
- Uchkuduk Horizon (U): 10–35 m thick, alternating fine-grained sandstone and clay

Cenomanian: <30 m thick, variegated kaolinitic clay.

U minerals are mainly pitchblende and coffinite with minor uranophane, β -uranotile, and uraniferous phosphatic fish detritus. Associated elements include small concentrations of Se, Mo, and others.

Uchkuduk encompasses 93 roll-type ore bodies within a triangular area with a NNE-SSW-oriented base line, about 30 km long, that forms the SE boundary, and slightly shorter southwestern and northwestern limbs. These ore bodies are distributed over five Senonian, Turonian and Cenomanian aquifers with an aggregate thickness of 150–160 m. Fifty percent of Uchkuduk's resources, however, are contained in the two Lower Turonian Uchkuduk and Kendyktube Horizons; the former contains major lodes. A clay and silty clay aquiclude up to 40 m thick of the Dzheirantyi Horizon separates both horizons. Ore lodes have lengths from 100 to 6 000 m, widths from 25 to 2 000 m and occur at depths from 10 to 110 m in the north and as much as 280 m in the southern Aitinski sector of the deposit. Ore grades average 0.03% U but can be as much 0.4% U. Se and Mo values are commonly on the order of 0.01%.

15.1.1.4 Kendyktyube

This deposit is located ca. 40 km E of the town of Uchkuduk and contains about 1 000 t U RAR + EAR-I in three horizons of Santonian, Turonian, and Coniacian strata; about half of which is contained in the central sector and the rest in the eastern and western segments of the deposit.

15.1.2 Zarafshan or Auminza-Beltau District

This district contains the *Aktau* and *Sugrally* deposits on the northern side and the *Amantei* occurrence on the southern side

■ Fig. 15.5.

Uchkuduk District, Uchkuduk deposit, **a** geological map with surface projected ore bodies in the Turonian Kandyktube and Uchkuduk Horizons, and **b** NNW-SSE section (explanations and legend see below) (after Karimov et al. 1996)

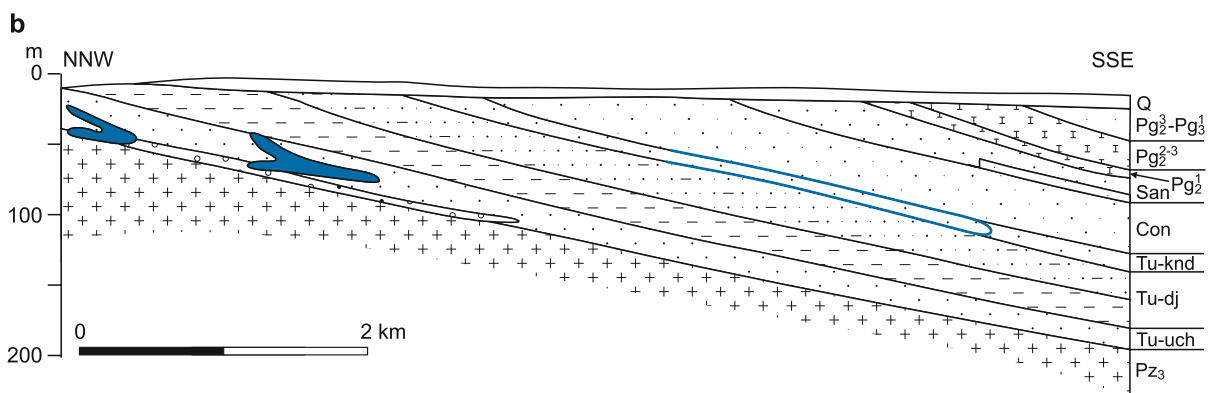
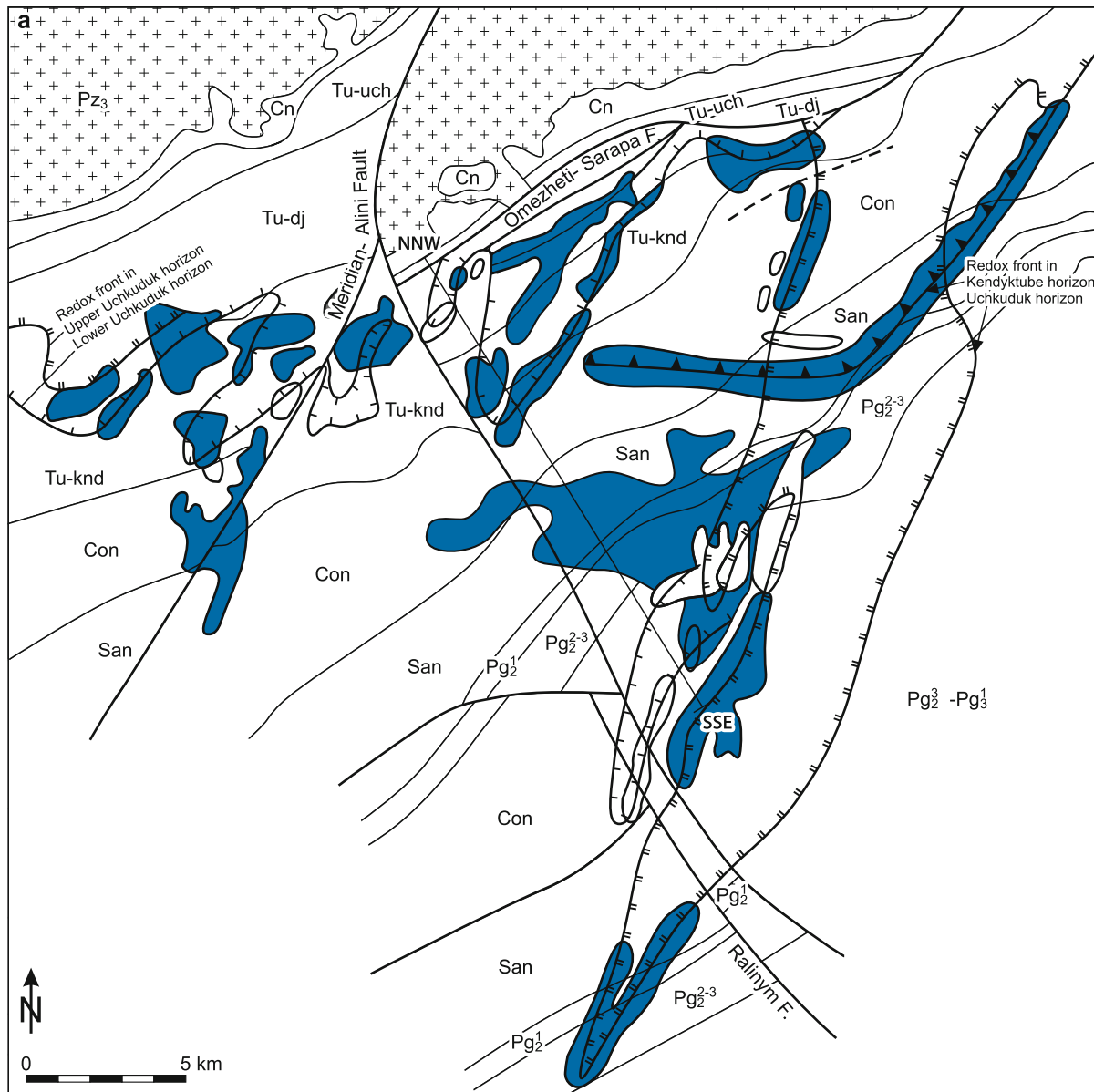


Fig. 15.5. (Continued)

Explanations and legend for figures of Kyzylkum sandstone-type U deposits (Figs. 15.5 to 15.8 and 15.10 to 15.15)

Ph Phanerozoic	Tertiary-Cretaceous sediments		Ultramafics (gabbro-peridotite)	
Q Quaternary		Conglomerate		Marble
Cz Cenozoic		Sand(stone)		Quartzite, schist
Mz Mesozoic		Silt(stone)		Slate, schist, quartzite, marble
K Cretaceous		Clay, mudstone		Basement
J Jurassic		Marl		Anticline axis
Tr Triassic		Limestone		Syncline axis
Pz Paleozoic		Dolomite		Fault
P Permian		Sand(stone), gravel, conglomerate		Direction of groundwater flow
C Carboniferous		Silt, sand(stone), conglomerate	Alteration	
D Devonian		Sand(stone), silt(stone)		Pyritic grey facies
S Silurian		Clay, silt(stone), sand(stone), conglomerate		Re-reduced greenish-grey facies
O Ordovician		Carbonatized sand(stone)		Pink oxidized facies
€ Cambrian		Argillaceous sand(stone)		Pink oxidized and whitish facies
Pt Proterozoic (Pt ₃ Pt ₂ Pt ₁)		Carbonaceous argillaceous silt		Yellow limonitized facies
Ar Archean		Calcareous silt		Variegated facies
TT Tertiary		Clay, silt(stone), sand(stone)		Boundary of yellow limonitic and grey reduced facies
Ng Neogene		Sandy clay and sand(stone)		Center of epigenetic reducing thermal activity
Pli Pliocene		Clay, marl, sand(stone)		Epigenetic thermal alteration in U hosting sediments
Mio Miocene		Clay, marl, sand(stone), limestone	Mineralization	
Pg Paleogene		Limestone with sandstone		U ore body
Oli Oligocene		Shell		Ordinary ore (black U products, jordisite, native Se)
Eoc Eocene	Paleozoic basement			High grade pitchblende-sulfide
Pal Paleocene		Metamorphic and igneous rocks (porphyry etc.)		High grade pitchblende-hematite-sulfide
K ₂ Upper Cretaceous		Granite, granodiorite		Uranophane
Sen Senonian				
Maa Maastrichtian				
Cmp Campanian				
San Santonian				
Con Coniacian				
Sn ₁ Lower Senonian (San + Con)				
Tu Turonian				
Cn Cenomanian				
K ₁ Lower Cretaceous				
Al Albian				
Apt Aptian				
Brm Barremian				
Ncm Neocomian				
U mineralized horizons				
Eoc-I Lyavlyakan horizon				
Upper Turonian				
Tu-ul Ulus horizon				
Tu-sb Sabyrsai horizon				
Lower Turonian				
Tu-knd Kendykube (Kendyk) horizon				
Tu-dj Dzheirantyi horizon				
Tu-uch Uchkuduk horizon				

of the Tamdytau Range. A mining town, Zarafshan, was established about 170km NNW of Navoi to serve the district. Remaining in situ resources are 36 000t U RAR + EAR-I and 48 000t U EAR-II + SR. Sugrally was the only deposit exploited to date. The Eastern Mining Division (also referred to as Central Ore Division), a subsidiary of NMMIW, is in charge of mining operations (OECD-NEA/IAEA 2005).

15.1.2.1 Sugrally

Sugrally was discovered to the north of the Tamdytau Range, ca. 30 km NNE of the town of Zarafshan in 1961. Underground mining started in 1977 but was suspended in 1994, as was the ISL operation. Two mines were active, the *Kyzylkumskaya* (lodes 1 and 7?), and the *Oktyabrskaya mine* (lode 8). With an average

mining grade in excess of 0.2% U, Sugraly belongs to the better grade U deposits of the Kyzylkum Basins. Original resources amounted reportedly to almost 60 000 t U.

Source of information: Shchetochkin and Kislyakov (1993) provide well-documented geological coverage of the Sugraly deposit which is largely used for the following presentation amended by data from Karimov et al. (1996), Kislyakov and Shchetochkin (2000) and other sources.

Geological Setting of Mineralization

Sugraly is situated on the southern limb of the large artesian Beshbulak Basin. Quaternary, Tertiary, and Upper Cretaceous sediments fill the basin and rest unconformably on a basement of Paleozoic metamorphics (\pm metamorphosed limestone, dolomite, sandstone, mudstone; porphyry, granite,) and Hercynian felsic and ultramafic (gabbro, peridotite) igneous rocks of the northern slope of the Tamdytau Uplift (► Figs. 15.6, 15.7).

The Cenozoic-Cretaceous litho-stratigraphic column includes the following units:

Cenozoic (total thickness 400–600 m)

- *Quaternary*: 1–50 m thick, alluvium (sandy rubble)
- *Quaternary-Pliocene*: 10–150 m thick, pink, coarse-fragmented proluvial and yellowish-tan argillaceous-arenaceous alluvium
- *Upper-Middle Miocene*: 80–320 m thick, monotonous pink calcareous siltstone
- *Lower Miocene-Middle Oligocene*: 40–50 m thick, pink arenite of marine and continental origin
- *Lower Oligocene-Eocene*: 140–150 m thick, grey marly-argillaceous sediments

Upper Cretaceous (total thickness 100–120 m)

- *Maastrichtian* (main U-bearing unit): 10–25 m thick, micaceous-quartzose sand, calcareous sandstone, conglomerate, and shell beds of shallow marine-lagoonal origin. Carbonaceous matter is absent. The Maastrichtian is continuous over the entire area. It rests upon Campanian in the E, Lower Senonian in the W, and on Turonian sediments elsewhere.
- *Campanian*: 0–30 m thick, variegated clay, argillaceous and calcareous sandstone, with fragments of pelecypod shells, quartz gravel, and phosphorite of marine origin. Campanian strata are only present in the eastern section of the deposit where the Campanian unconformably transgressed upon Lower Senonian, Turonian, and Cenomanian sediments, and further eastward upon the crystalline basement.
- *Lower Senonian* (Santonian-Coniacian) (minor U-bearing unit with few U lodes in grey facies): up to 40 m thick, pink, light grey and grey crossbedded sands alternating with clay, silt, and variegated argillaceous sandstone beds of proluvial, fluvial, and flood plain provenance. The sequence pinches out in the central part of the deposit and increases to the west and south where it rests on Turonian sediments and attains its greatest thickness.

- *Turonian* (some U): 10–45 m thick, argillaceous-arenaceous sediments of marine origin, variegated in upper section and grey in lower section. The Turonian overlies Cenomanian strata in the western, and transgressed over basement in the eastern area.
- *Cenomanian*: 2–12 m thick, pink conglomerate and grit-stone, variegated clay, silt, argillaceous sandstone, and sand of proluvial, fluvial, and flood plain provenance forming the basal unit of the Mesozoic sediments resting on Paleozoic basement rocks.

The Mesozoic and Tertiary strata have a monoclinical dip of 1–3° N to NW. Low-angle drag folds occur along faults. Faults are of normal and reverse nature and trend about NE-SW, NW-SE, and E-W. Inclination is commonly steep. The first two fault systems generated three major blocks in the area of the Sugraly deposit: (a) a NE-SW-elongated graben structure along the northwestern slope of the Tamdytau Uplift, (b) a horst structure (later referred to as “SW block or sector” containing ore lodes # 1–6 and others) situated to the SW of the Charyktin fault and subparallel to the NW the afore mentioned graben, and (c) a downfaulted block (“NE block/sector” with ore lodes # 7, 8, 9, 15 and others) located to the NE of the two aforementioned blocks (a) and (b) but separated from them by the NW-SE-trending Charyktin fault.

The Charyktin fault also constitutes the boundary between two independent groundwater regimes. The first is contained in the NE block where it is restricted to the Maastrichtian aquifer and the second in the SW blocks in form of a hydraulically integrated water regime in Lower Senonian to Maastrichtian aquifers.

Groundwaters in the Cretaceous and Tertiary aquifers are artesian and flow toward the N and NW. Local recharge is from fracture and karst waters in the Tamdytau Uplift. Discharge of stratum water manifested by springs, lakes, and salt marshes occurs along faults on the N flank of the Beshbulak Basin. Chemically, the groundwater is slightly saline and has a pH value of 7.1–7.8. Constituents include Na and Ca sulfate-hydrocarbonates, Na sulfate-chloride, and 0.7–2.5 g l⁻¹ solid residues. The content of dissolved U, Se, and V varies between 2 and 30 ppb in oxygenated waters. These elements decrease markedly to 0.1 ppb in non-oxygenated waters associated with an Eh drop from +140 mV in oxygenated to –180 mV in non-oxygenated waters.

A hydrogeochemical anomaly is noted at the NE margin of the deposit near ore lode 8. Here, present-day groundwater contained in stratum-oxidized rocks is non-oxygenated, has negative Eh values and contains up to 4 mg l⁻¹ H₂S and up to 2.8 mg l⁻¹ hydrocarbons.

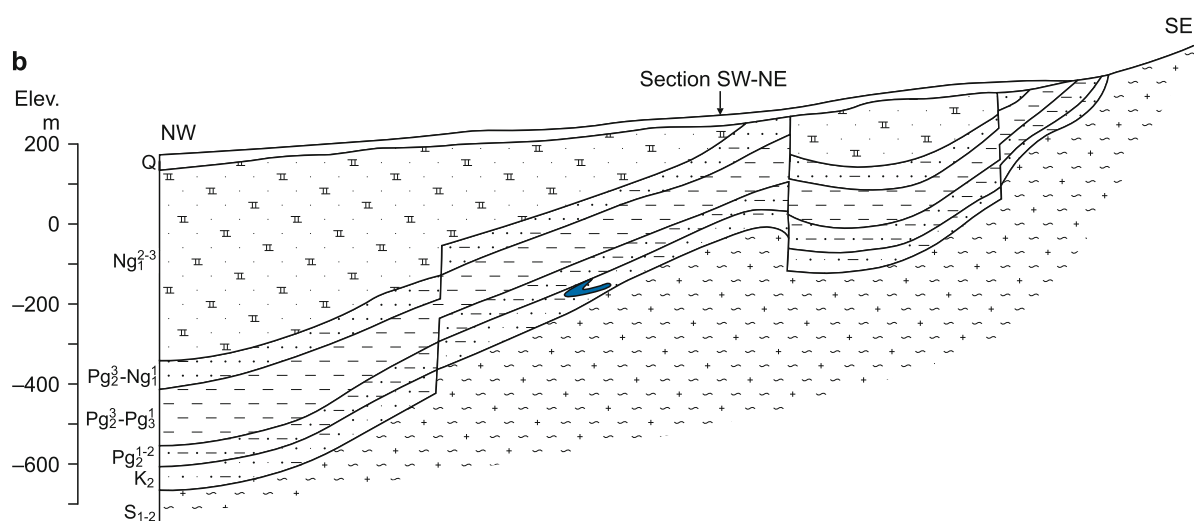
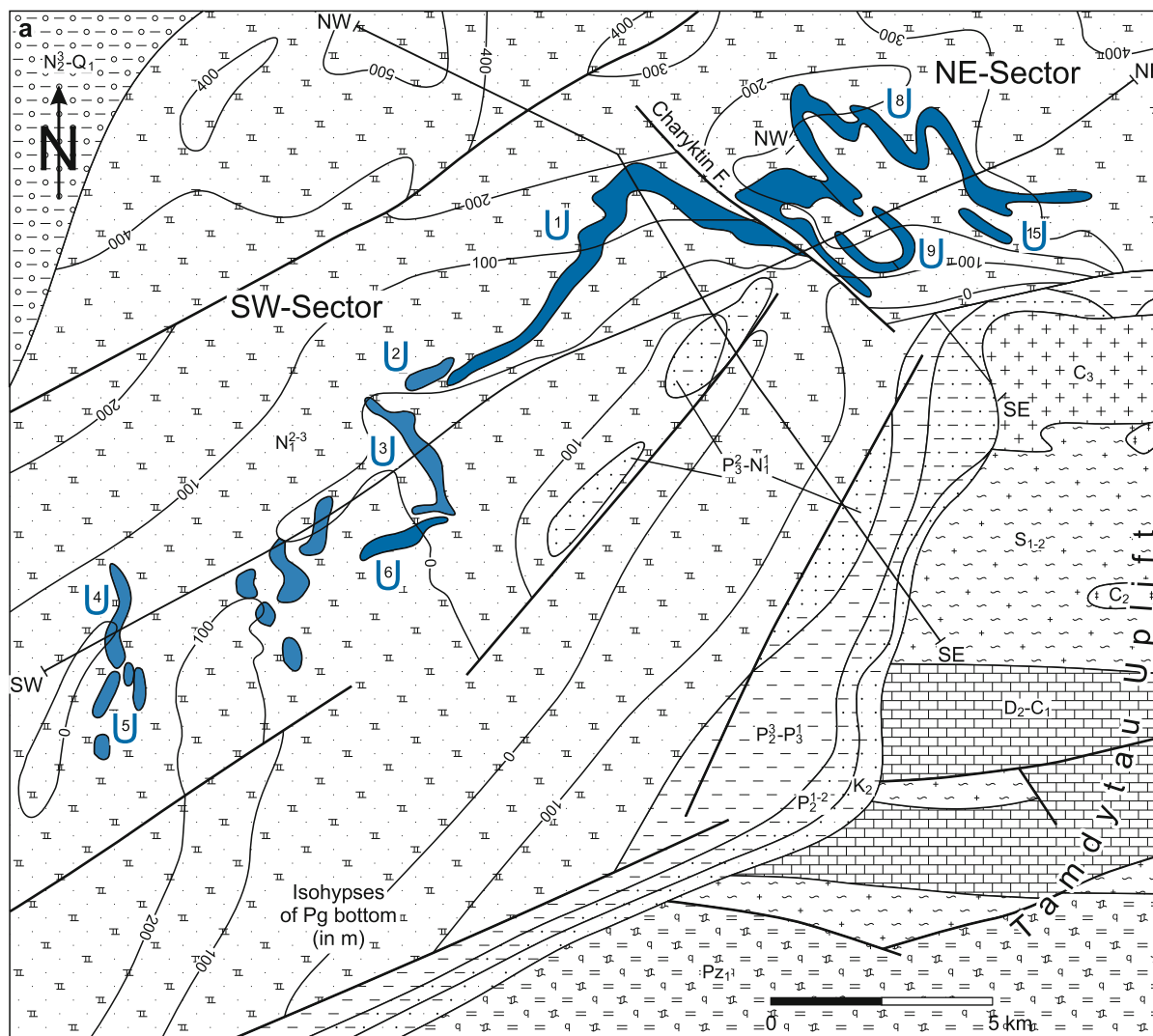
Temperatures in the deposit range from 50°C in the NE to 40°C in the SW part. The high temperatures result from a large geothermal anomaly with a 6.5°C per 100 m gradient centered to the NE of the deposit.

Host Rock Alteration

Repeated oxidation and reduction related to diagenetic events and multiple epigenetic hydrogeochemical processes of extrinsic and intrinsic provenance generated the alteration features in

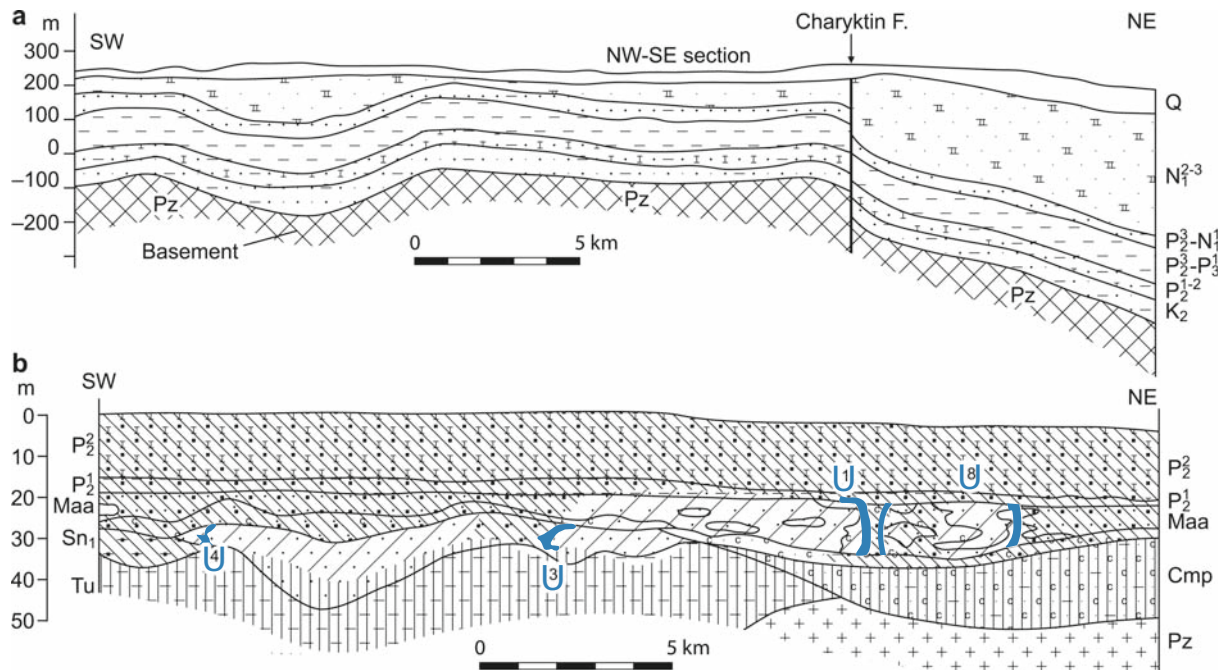
Fig. 15.6.

Zarafshan District, Sugrally deposit. **a** Geological map with surface projection of ore bodies in Maastrichtian and Senonian strata; **b** NW-SE section with intersection of ore body #1 (explanations and legend see Fig. 15.5) (after Shchetchkin and Kislyakov 1993, amended by data from Sikorskii, Kazarinov, and Ponomarev)



■ Fig. 15.7.

Zarafshan District, Sugrally deposit, SW-NE longitudinal sections (for location see Fig. 15.6) showing **a** the geological profile and **b** the lithologic-geochemical characteristics of the uranium-bearing Maastrichtian and Senonian Horizons (explanations and legend see at Fig. 15.5) (after Shchetchkin and Kislyakov 1993)



the U-hosting Maastrichtian and Lower Senonian strata. Early stratum alteration by oxygenated groundwaters percolating downdip the hydrological gradient from the Tamdytau Uplift toward N-NW imposed a 3–12 km wide differentiated oxidation tongue on aquifers ending in redox fronts at the interface of diagenetically reduced grey facies in the blocks mentioned earlier.

Subsequent processes, however, as noted by Shchetochkin and Kislyakov (1993), generated different modes of alteration in the two blocks situated to the SW and NE, respectively, of and separated by the Charyktin fault. In the SW block, early oxidation imposed a pink hue on the permeable Maastrichtian beds, which was overprinted downdip by a frontal zone of yellow limonitization. The limonitized zone is 25–100 m wide in the NE and increases to 4–6 km in the SW. The limonitic oxidation apparently replaced diagenetically (?) reduced pyritic facies, which prevail further basinward. Underlying Lower Senonian strata are primarily pink but also white colored in an up to about 5 km wide belt adjacent to the Paleozoic basement outcrop of the Tamdytau Range. Limonitization affected the belt to some extent but was strongest further downdip to the N and NW where it generated a yellow limonitic alteration facies. The yellow facies ends basinward at the updip boundary of a narrow, NE-SW-oriented reduced pyritic zone. In contrast to the Maastrichtian sequence, the Lower Senonian sediments are oxidized towards the center of the basin. (Fig. 15.8a,b). In the NE block, the U-hosting Maastrichtian aquifer, colored pink or red brown due to traces of finely dispersed hematite, became locally re-reduced to a greenish-grey facies, which was subsequently partially re-oxidized as reflected by neogenic yellowish goethite-hydrogoethite as found at lodes 9 and 15.

Re-reduction is a prominent feature in the NE sector and occurred in response to reducing thermal fluids ascending along faults. These fluids caused alterations proceeding through several stages including:

1. Early acidic alteration associated with argillization and silicification reflected by kaolinite, illite, montmorillonite, quartz, chalcedony, and opal formation;
2. Carbonatization documented by dolomite and calcite associated with pyrite crystallization;
3. Low-grade bitumenization of hydrocarbons resulting in bitumens associated with calcite, pyrite, and marcasite; and finally
4. Sulfidization expressed by pyrite and marcasite associated with calcite derived by secondary reduction of stratum oxidized facies.

Silicic alteration of the first stage is restricted to the immediate vicinity of faults and fractures. Second stage carbonatization persists in a significantly wider aureole (Fig. 15.9) while bitumenization and sulfidization of the last two stages display the widest spreading. The total amount of Fe-sulfides in reduced zones is approximately 1% or more while that of bitumens soluble in chloroform is as much as 0.15%.

Fracture controlled reduced ground within sandy horizons is conspicuous by greenish-grey colored, lenticular, tabular or patchy bodies altered by silicification, argillization, carbonatization, sulfidization, and/or bitumenization. In aquicludes over- and underlying such horizons, reduction-related minerals include disseminated carbonates and sulfides, and veinlets or stringers of quartz-carbonate-sulfide.

Re-reduction in the SW sector of the Sugrally deposit occurred along contact faults of the horst block where primarily pink Lower Senonian sediments were altered to grey pyritic facies.

Mineralization

Mineralization is polymetallic composed primarily of U, Se, Mo, Re, and traces of other elements. The principal U minerals are pitchblende, black U products (sooty pitchblende?), and locally uranophane. Additional ore constituents include native γ -Se, jordisite, minor ilsemannite and femolite, and rhenium-bearing minerals. Associated minerals are pyrite, minor marcasite, hematite-hydrohematite, carbonates (mainly calcite), and locally zeolites.

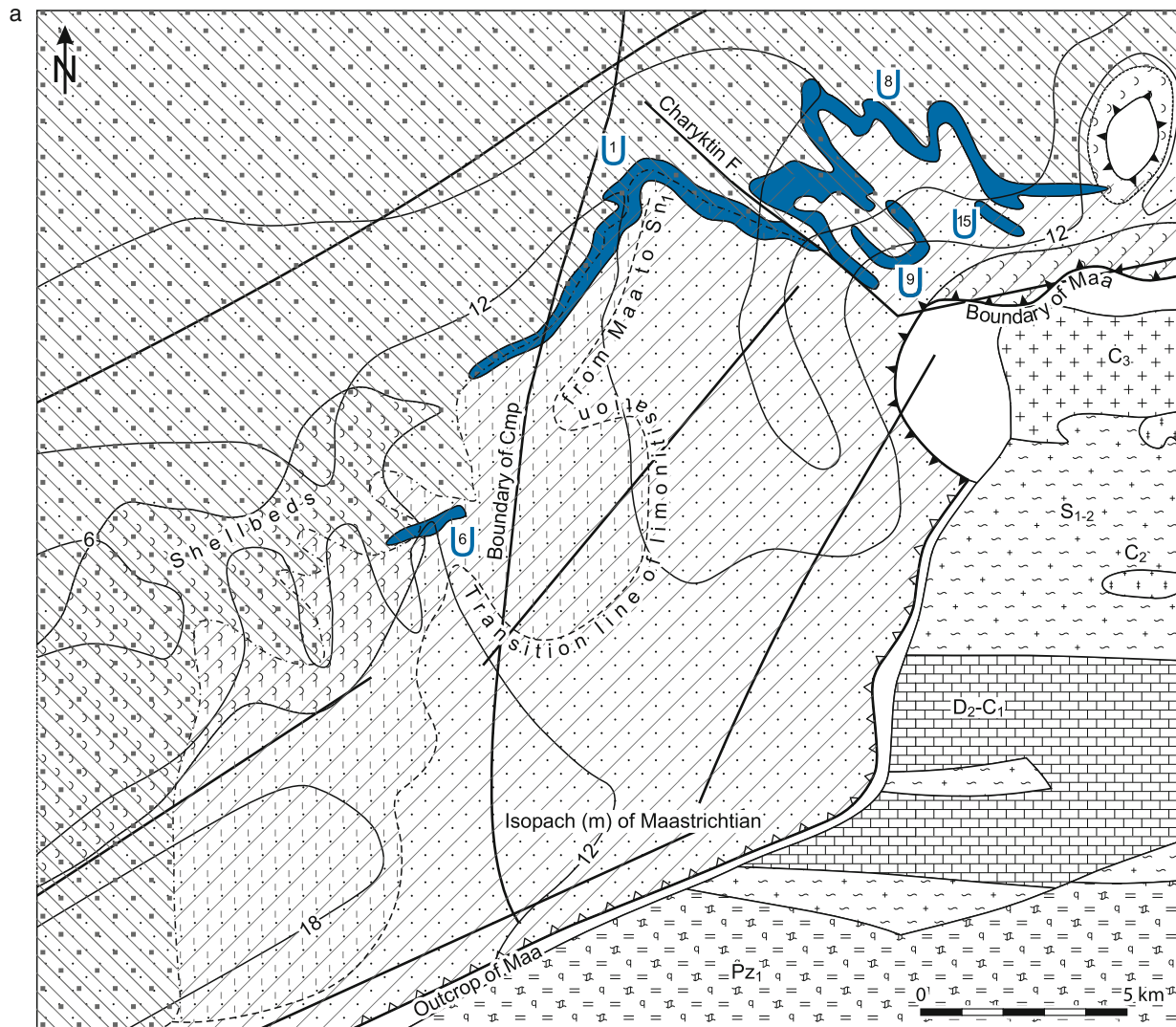
Several mineral assemblages are noted: black U products associated with jordisite and native selenium, pitchblende-hematite-sulfide, pitchblende-sulfide, and uranophane. The first

assemblage is typical for ordinary ore while the latter three are typical for high-grade ore (for more details see further below).

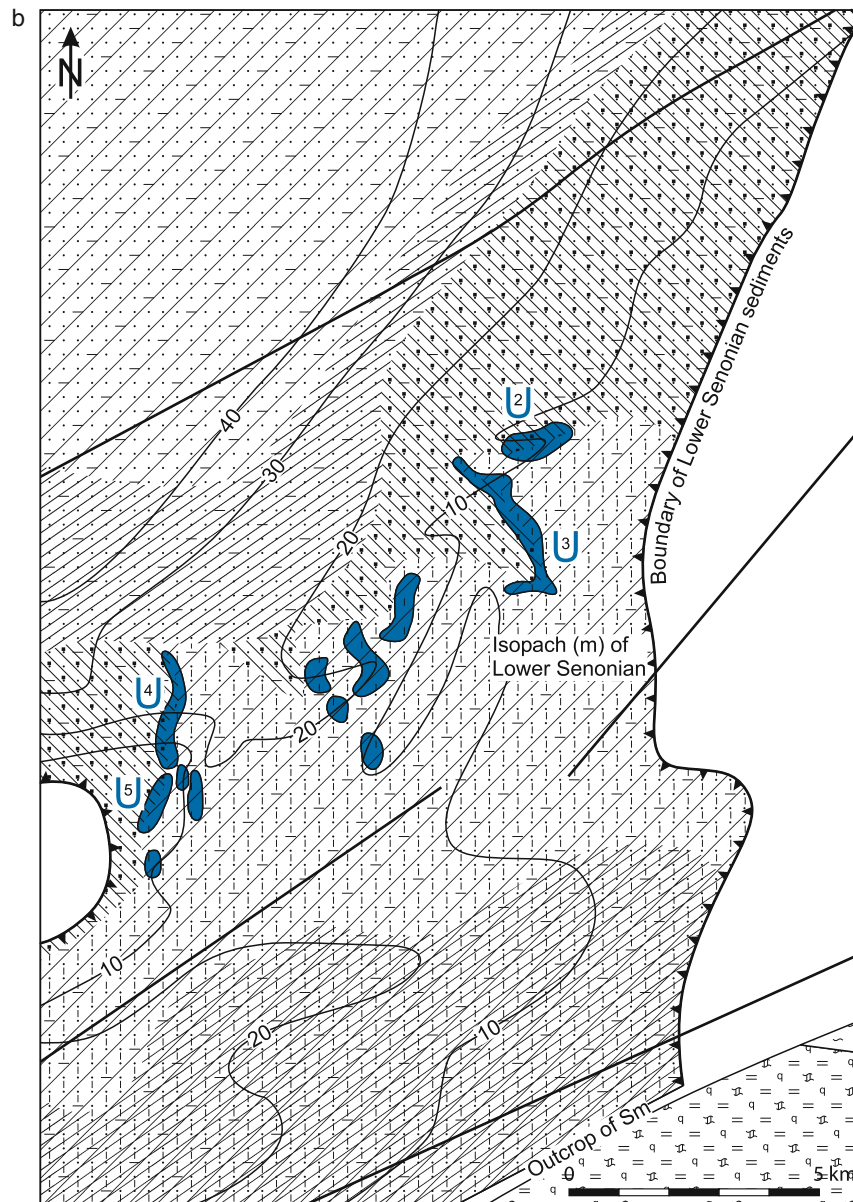
Ore minerals occur in the matrix of sandy beds as powdery black U products together with jordisite, fine colloform pitchblende, acicular native selenium, and other minerals. Uranophane occurs as cone-shaped and radiated-fibrous particles or spherulites finely disseminated in oxidized, pink and reddish-brown sand and sandstone. It is also present in spheric aggregates up to few millimeters in size that consist of detrital minerals cemented by uranophane and calcite.

In the few cases where pitchblende-sulfide and uranophane mineralizations are overlapping, dark grey sandstone with U-oxides and Fe-sulfides may be dotted with disseminated yellow uranophane spherulites. U-oxides of this assemblage are clearly superimposed on the uranophane as documented by finely dispersed pitchblende coating not only sand grains but also uranophane. Uranophane spherulites as well as massive carbonate intercalations often contain relics of Fe-hydroxides

Fig. 15.8. Zarafshan District, Sugrally deposit, geological map illustrating the distribution of alteration facies **a** in Maastrichtian and **b** in Lower Senonian sediments and the related position of U ore bodies (explanations and legend see at **Fig. 15.5**) (after Shchetchkin and Kislyakov 1993)



■ Fig. 15.8. (Continued)



representing traces of an earlier pre-uranophane rock oxidation. In most permeable zones, Fe-hydroxides underwent reduction during the co-precipitation of U-oxides and pyrite. The reduction also affected Fe-hydroxides along the margins of massive aggregates of uranophane spherulites. A younger oxidation effect is reflected by a hematitic aureole occasionally found around uranophane aggregates, and is likewise noted adjacent to pitchblende-sulfide segregations.

Three principal *types of ore* and several subtypes are distinguished based on mineralogical composition and U grade: (a) ordinary (unoxidized) low- to medium-grade ore composed predominantly of black U products; (b) high-grade (unoxidized or partially oxidized) ore consisting of pitchblende-hematite-sulfide and/or pitchblende-sulfide assemblages; and (c) uranophane dominated (oxidized) ore.

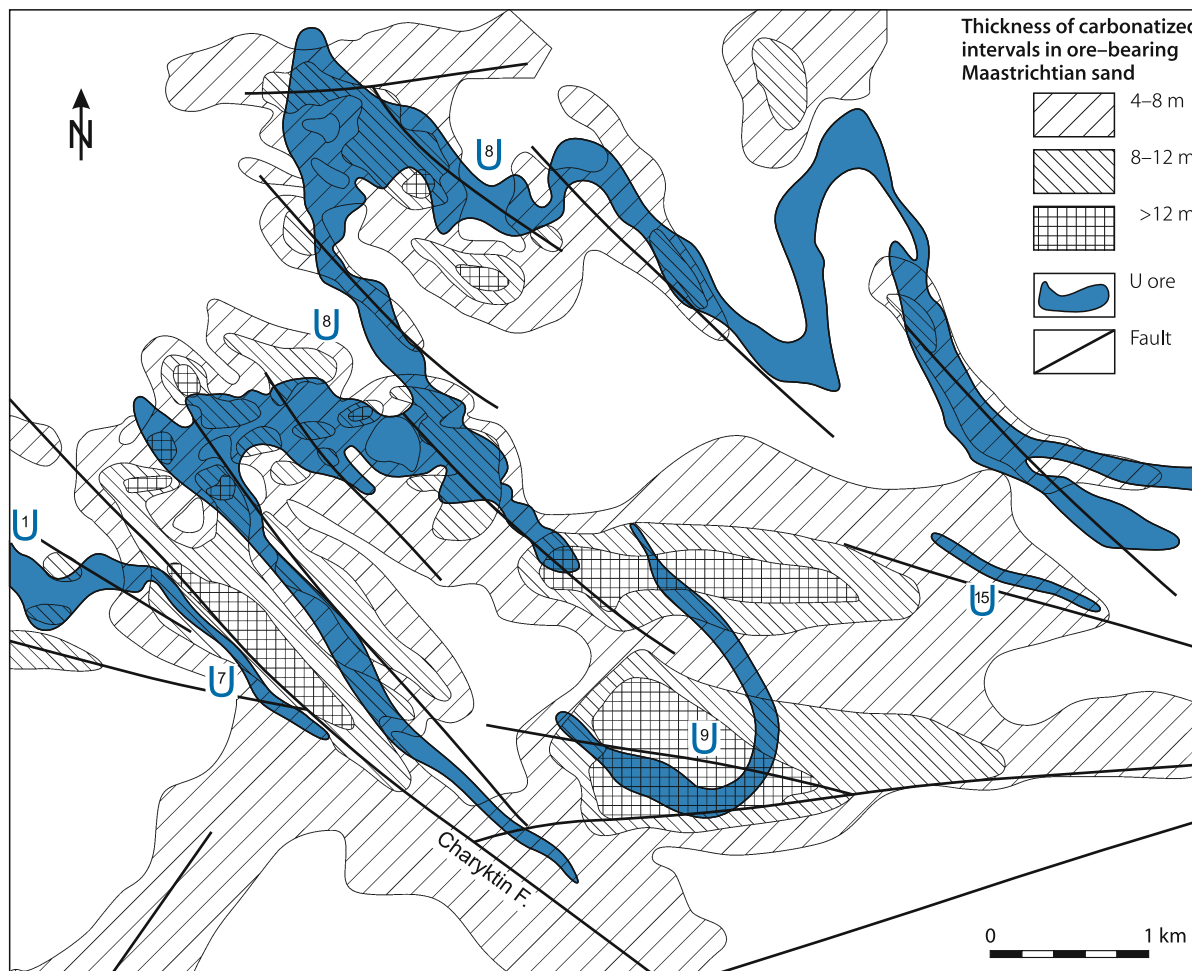
Ordinary U ore, the typical ore of most U deposits in the Kyzylkum region, is characteristic at Sugraly for all ore lodes in the block SW of the Charyktin fault and for some lodes to the

NE thereof. Ore bodies are roll-shaped and positioned at a redox front at the downdip head of yellow limonitic oxidation zones. Ore constituents are predominantly black U products, jordisite, and native selenium. The NE block contains ordinary ore lodes updip behind the main oxidation front, which is controlled by redox interfaces between locally developed yellow limonitization and greenish-grey reduction intervals as exemplified in lodes 9 and 15 (● Figs. 15.10a–c).

High-grade U ore with grades up to 3% U is restricted to the block NE of the Charyktin fault where it is found in lode 8. Three reduced mineral assemblages of high-grade ore are distinguished by mineralogical composition and redox front-related setting: pitchblende-sulfide, pitchblende-hematite-sulfide, and pitchblende-U black products-sulfide. A fourth subtype of uranophane is typical for oxidized ore (see below). The pitchblende-sulfide assemblage typically occurs in grey lithologies at the frontal part of the redox interface. Mineral phases include aggregates of colloform pitchblende (lattice constant $a_0 = 5.370 \pm 0.007 \text{ \AA}$),

Fig. 15.9.

Zarafshan District, Sugrally deposit, planview of distribution and thickness of carbonatization in ore-bearing Maastrichtian sands and its spatial relationship to U ore zones/bodies (after Shchetkin and Kislyakov 1993)



pyrite, calcite, and locally zeolites. The pitchblende-hematite-sulfide assemblage is commonly restricted to the rear part of a roll. Mineral phases include pitchblende, pyrite, and calcite associated with neogenic hematite-hydrohematite, and pink color-altered goethite. Ore has a patchy texture and a bright-variegated pinkish-black hue. Occasionally, pitchblende and black products coat or cement Fe-hydroxides in oxidized ores, and fill cracks therein. Dark ore aggregates are up to 1 cm in size and are successively rimmed by bleached and hematitic lamellae superimposed on pink rocks. Locally, hydrohematite replaces completely pink or reddish-brown goethite associated with a marked increase of U to the highest ore grades. The pitchblende-black U products-sulfide assemblage occurs in grey rocks at some distance from oxidized rocks and is controlled by the interface of secondarily reduced greenish-grey with originally grey sands and sandstones.

Uranophane ore of lode 8 occurs in a few, discontinuous bodies on the rear side of the redox front in oxidized ground. Uranophane is thought to be the replacement product derived by secondary oxidation of high-grade pitchblende ores.

The spatial distribution of associated elements in lode 8 corresponds in principle to that in other lodges. An exception is the

replacement of Mo- and Fe-sulfides in the rear, updip part of the grey Mo-bearing zone by black, pitchblende-dominated ore. In this case, the pitchblende ore is developed in pink oxidized sand and sandstone that are locally re-reduced by secondary processes. The halo of native selenium is displaced updip and partially overlaps the interval of variegated, pinkish-black U mineralization, and oxidized U poor rocks.

A Maastrichtian arenaceous horizon is the principal U-hosting unit at Sugrally. It contains the largest lodges, # 1 and 8, and likewise all other ore bodies in the NE sector like lodges 9 and 15, and several lodges in the SW sector of the deposit such as lode 6. Lower Senonian sands are mineralized to a minor extent in the SW sector (lodges 2–5) (► Figs. 15.6, 15.7).

High-grade lodges to the NE of the Charyktin fault, such as lode 8, are associated with a redox front at the head of a pink, hematitic oxidation tongue while a few small lodges with ordinary mineralization, like lodges 9 and 15, hang isolated behind this redox front and are positioned at the contact of a localized yellowish, limonitic zone with re-reduced facies. In contrast, lodges in the SW sector occur at a redox interface at the front of a yellowish, limonitic zone forming and replacing the frontal part of a pink hematitic tongue in both Maastrichtian and

Lower Senonian aquifers. An exception occurs with a few lodes in the SW sector in which U mineralization, as in lodes 4 and 5, is also found in grey facies several hundreds of meters ahead of the redox boundary of the limonitized tongue as a result of post-ore reduction of originally oxidized strata (► Figs. 15.7, 15.8a,b).

Host rocks are fine-grained sand and sandstone with 3–6% silt and 10–15% clay fractions. Allogenic rock constituents

comprise 60–80% quartz, 5–15% feldspar, 5–7% muscovite, 10–20% illite, and fragments of basement rocks. Sand grains are predominantly slightly rounded and range in diameter from 0.05 to 0.25 mm. Locally the sands contain biotite, chlorite, ilmenite, leucoxene, and other minerals in accessory amounts. Carbonaceous plant remains are absent in mineralized strata of the Sugrally deposit. Mineralized and adjacent sands have a filtration coefficient of approximately 1 m d^{-1} and

■ Fig. 15.10.

Zarafshan District, Sugrally deposit, **a** planview, **b** NW-SE section, and **c** sections across ore bodies illustrating the distribution of U mineralization and adjoining alteration zones as well as morphology and quality of ore lodes in ore body #8 and adjacent ore bodies in Maastrichtian sediments (explanations and legend see at ► Fig. 15.5) (after Shchetchkin and Kislyakov 1993)

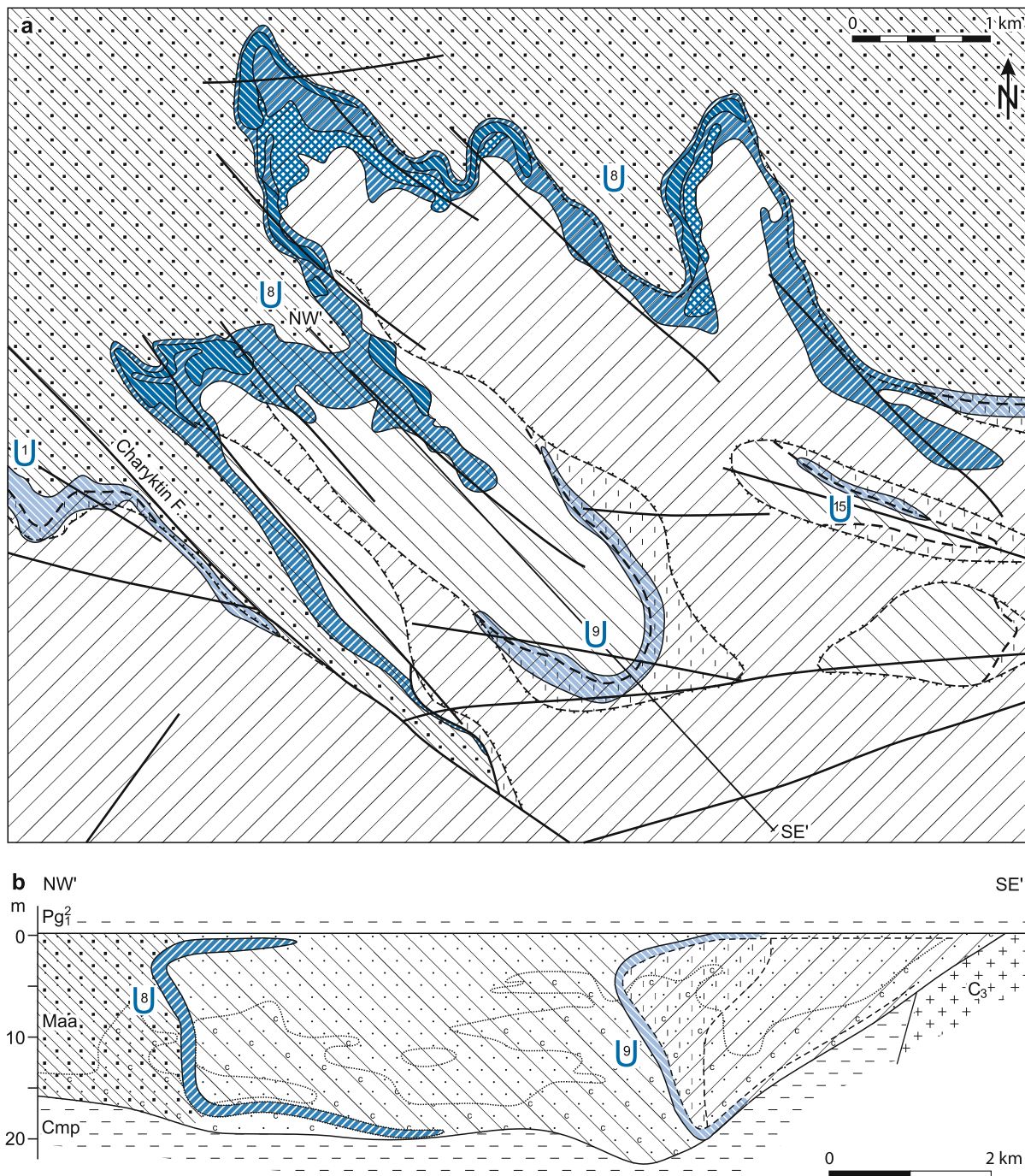
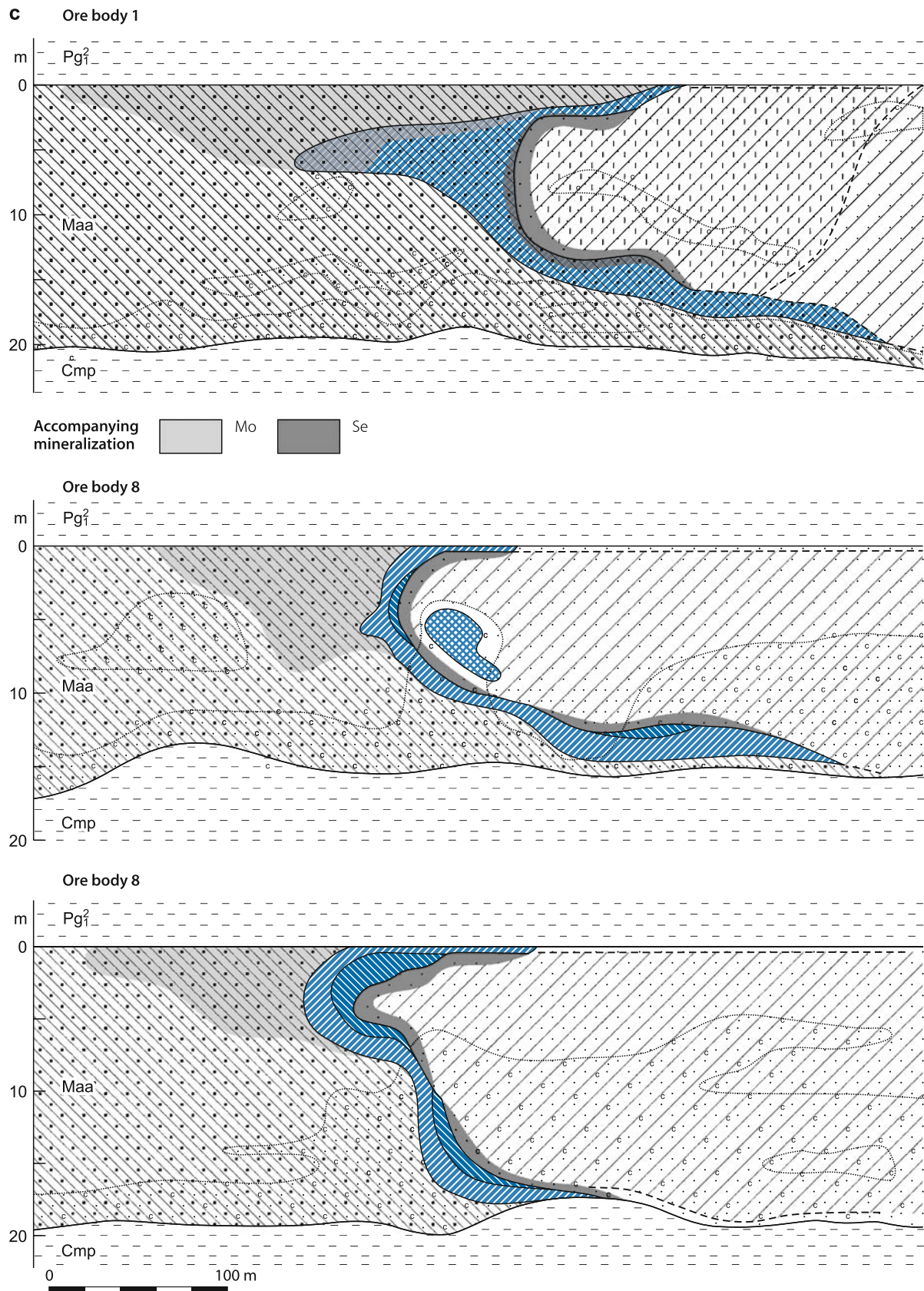


Fig. 15.10. (Continued)



more but the permeability is sharply reduced in highly carbonated sandstone.

Shape and Dimensions of Deposits

Sugrally consists of a number of ore lodes (Karimov et al. 1996 show 25 lodes on their Fig. 2.2). These ore lodes are distributed over an area in excess of 30 km long in NE-SW direction and few hundred meters to more than 5 km wide in which they occur elongated along partly highly twisted redox fronts. U mineralization occurs at depths from 260 to 580 m but minable ore is confined to depths averaging 450–500 m. Lodes # 1 and 8 are the largest and are separated by the Charyktin fault.

Uranium lodes consist of sinuous bands from several 100 m to 20 km long (Fig. 15.6a). In cross-section, most ore bodies exhibit a crescent-like shape whereas lodes of lenticular configuration are rare. Roll-shaped ore bodies have an elemental zoning, starting with Mo at the downdip head followed by U, and then by Se at the rear of the roll. The Mo interval ranges from 0.03 to 4 m and locally up to 8 m thick and may be as much as 600 m wide (perpendicular to strike) persisting into grey facies. U extends over widths from 100 to 500 m and thicknesses between 0.2 and a few meters, rarely up to almost 20 m. The Se-bearing segment is less than 150 wide and from several tens of centimeters to 4 m thick (Fig. 15.10c).

The in situ U content commonly varies between 0.03 and 0.27% U, but increases to 3% in parts of lode 8. Due to the high-grade sections, the average grade of lode 8 is twice that of lode 1, which contains only ordinary ore. The principal associated elements include: Se (0.06–0.12%), Mo (0.004–0.26%), and Re (10–15 ppm). Increased amounts of carbonates are noticed in some lodes, e.g. in lodes 8 and 9.

Geometric characteristics of the three principal ore types and their distribution in the Sugrally deposit are as follows:

Ordinary U ore forms wedge- or C-shaped rolls with tails up to more than 200 m long (Fig. 15.10c). The grade is generally low to medium (0.03–0.3% U). The magnitude or productivity coefficient of the mineralization in the SW sector is inversely proportional to the width of the limonite zone i.e. increasing width of the oxidation zone correlates with a decreasing productivity coefficient.

High-grade U ore as found in lode 8 typically exhibits the following characteristics: Mineralization occurs along an up to 400 m wide (perpendicular to the redox front) and almost 20 km long sinuous, highly indented ribbon. In cross-section, the ribbon shows a crescent-shaped roll and mostly a longer and thicker lower tail. The roll has a vertical dimension of 10–20 m, variable widths perpendicular to the strike of a few meters to 60 m or more, and a lower tail from 20 to more than 100 m long and as much as 3 m thick. Grades and reserves of the three mineral assemblages, which constitute the unoxidized high-grade ore of lode 8 are as follows: pitchblende-sulfide ore has a grade of up to few percent U and constitutes the bulk of the U reserves of this lode; pitchblende-hematite-sulfide ore is of high grade and constitutes about 10–15% of the reserves;

while pitchblende-U black products-sulfide ore is commonly of lower grade than the former. The spatial distribution of associated elements in lode 8 corresponds, in principle, to that in lodes of ordinary ore except for differences in the radium distribution.

Uranophane ore occurs in a few discontinuous lenses in oxidized Maastrichtian strata on the rear side of lode 8. Ore lenses are from a few tens of meters to 400 m wide, up to 4 m thick, and from less than 100 m to as much as 2 000 m long elongated parallel to the redox front as shown in Figs. 15.10a,c. Grades range from few hundredths to about 2% U.

Radioactive disequilibrium is common for all ores. Ordinary ore has a higher Ra/U ratio at the backside of a roll than at the frontal side. High-grade ore of lode 8 has symmetric and very weak halos of radium on the downdip and updip side of the roll and a radioactive disequilibrium in favor of uranium (av. $K_1 = 79\%$). Uranophane ore is in radioactive disequilibrium in favor of radium ($K_1 = 110\text{--}290\%$).

Ore Controls and Recognition Criteria

Sugrally is defined as a rollfront sandstone-type U deposit characterized by the following ore controlling or recognition criteria:

Host Environment

- Tertiary-Upper Cretaceous artesian basin of relative small size separated by basement uplifts
- 400–600 m thick Quaternary-Tertiary and 100–120 m thick Upper Cretaceous strata
- Alternating permeable and impermeable beds of continental and marginal marine origin
- Widespread block faulting with horst and graben structures along NW-SE-, NE-SW-, and E-W-trending faults
- Separation of the deposit area into two principal blocks by a NW-SE-trending, steep fault
- Separate groundwater regimes in the two main blocks
- Host Rocks consist of
 - two mineralized horizons in Maastrichtian and Lower Senonian aquifers, 10–25 m and <40 m thick, respectively,
 - fine-grained sand and sandstone with minor silt and clay fractions
 - no carbonaceous matter in the Maastrichtian host beds
- A Campanian aquiclude, up to 30 m thick, separates the two host horizons
- Hanging wall and footwall lithologies consist of argillaceous beds
- Potential U and other metal sources exist in basement uplifts

Alteration

- Several phases of oxidation and reduction with corresponding redox fronts
- Oxidizing conditions due to differential, repetitive influx of oxygenated groundwaters along aquifers to form
 - hematite altered zones and
 - zones of limonite overprinting the hematite facies

- Early diagenetic stratum reduction reflected by sulfidized grey lithologies
- Epigenetic (re-)reduction by extrinsic reducing thermal solutions percolating along faults
- Reduction-related alterations include sulfidization (pyrite, marcasite), and bitumenization of hydrocarbons
- Carbonatization (calcite, dolomite), silicification, and argillization

Mineralization

- Polymetallic U, Mo, Se, Re mineralization present in several generations
- Three varieties of ore, unoxidized ordinary (low-grade) and high-grade ore, and oxidized ore
- Both unoxidized ore types form roll-shaped ore bodies
- Ordinary ore is composed of black U products associated with jordisite and native Se
- Ordinary ore associates with redox fronts at the front end of yellow limonitized rocks
- High-grade ore associates with redox fronts of pink hematitized rocks
- High-grade unoxidized ore includes three parageneses/assemblages
 - Pitchblende-sulfide assemblage occurs in grey lithologies at the frontal part of a rollfront
 - Pitchblende-hematite-sulfide assemblage is mainly distributed on the up dip side of a rollfront
 - Pitchblende-U black products-sulfide assemblage is positioned in grey rocks distant from oxidized rocks and controlled by an interface of secondarily reduced greenish-grey sands and sandstones
- Oxidized ore consists of uranophane and occurs as lenses on the rear side of a redox front in oxidized ground
- Spatial distribution of associated elements corresponds to the standard pattern of rollfront-type mineralization
- Radioactive disequilibrium is common for all ore but of different nature in ordinary and high-grade ores

Metallogenetic Aspects

Rollfront-type U lodes at Sugraly have evolved in a complex manner. Critical ingredients are various and episodically repeated oxidizing events and reducing processes of two different modes. The principal hydrogeochemical activities involved are diagenetic stratum reduction, near surface oxidative leaching of ore-forming elements from basement rocks, low temperature stratum oxidation of different kinds and intervening reducing processes by extrinsic thermal solutions.

Shchetochkin and Kislyakov (1993) elaborate on the genetic implications of the various processes and suggest a metallogenetic model, which may be summarized as follows. Two principal reducing environments and associated processes were involved in the metallogenetic system at Sugraly and originated from diagenetic and extrinsic epigenetic actions, respectively. These two modes are documented by reducing barriers caused by (a) rock constituents with reducing potential of supposedly diagenetic origin (see below) and (b) upwelling extrinsic

reducing thermal solutions. The latter are reflected by a remarkable spatial relationship of ore lodes with sites of authigenic minerals generated by such fluids, in spite of the fact that the fluids by themselves are free of U, Mo, and Se.

Sulfur isotopes provide a clue to the origin of the different reducing sources. Diagenesis-related reduction of Upper Cretaceous sediments is deduced from the isotopic composition of sulfur in pyrite and baryte in diagenetically altered but otherwise unaltered aquiclude clays. The present isotope values are thought to be the product of early diagenetic fractionation of the sulfur of marine waters. The existence of an additional reducing source is supported by different groups of sulfur isotopes in pyrites in high-grade ore versus those in ordinary ore (Table 15.2). These isotopes indicate different sulfur sources and, as such, a distinct contrast in origin between the extrinsic thermal solutions involved as reductants in the formation of the high-grade pitchblende(-hematite)-sulfide ores and reductants involved in the formation of ordinary ore.

A sequence of ore-forming events may read as follows. After the early diagenetic reduction stage, block faulting exposed Cretaceous strata heads on surface at uplifted blocks permitting oxygenated meteoric waters to enter into the aquifers. Permeable horizons were oxidized as reflected by hematite development associated with pink coloration. The oxygenated, fertile groundwaters descended basinward until they encountered reducing barriers of either mineralogical or fluidal nature as outlined further below. Interaction of the oxygenated waters with the reducing media produced favorable redox prerequisites for deposition of uranium and other ore constituents.

Downflow of oxygenated groundwater was not everywhere a simple process. It was repeatedly interrupted not only by tectonic activity but also by locally restricted re-reducing interventions of fault ascending thermal reducing solutions. Consequently, new redox fronts were successively established at variable fault-controlled places and governed the formation of high-grade ore lodes.

Tectonic reactivation apparently played a significant role in the metallogenesis by episodic initiation or reactivation of thermal processes. Each such event presumably promoted the percolation of extrinsic reducing thermal fluids and likewise that of near-surface hot solutions. When the latter contained carbonic acid and were incorporated into meteoric groundwater, the oxidative leaching potential of these waters was notably boosted to liberate ore-forming elements from source rocks in basement uplifts. Favorable source rocks were provided by Paleozoic lithologies such as black slates.

The bulk of the high-grade ore was presumably deposited during relatively short periods of tectonic activity that triggered the postulated thermal reducing processes. These intervals of intense ore formation alternated with calm periods associated with remodification and minor dilution of mineralization formed earlier.

Studies of fluid inclusions in gangue minerals of the various alteration stages indicate a temperature of at least 120°C during alteration processes and an involvement of brines with very high tenors of total sulfur, Ca, and CO₂.

Redox processes related to diagenetically derived reducing conditions produced ordinary, low to medium-grade mineralization dominated by black U products along a simple redox boundary at the interface between a reducing environment characterized by Fe-sulfides and bitumens, and basinward migrating oxygenated groundwater. Pyrite in these black U ores displays a wide range of $\delta^{34}\text{S}\%$. Isotopic fractionation during biogenic reduction of sulfate in groundwater and incorporation of sulfur from earlier sulfides, locally including those of thermal fluid origin, are considered the reason for this variation.

The inverse proportionality of the concentration of mineralization in ordinary ore to the width of the younger limonitic oxidation zones suggests that under a weak reducing potential a redistribution of ore constituents takes place along the flow path. If this assumption is correct, present-day ordinary mineralization can hardly be considered a product of an independent metallogenetic event but instead it resulted from continuous or repetitive events that presumably reworked and incorporated constituents of preexisting mineralization.

Metallogenesis-related criteria or actions associated with the reducing process(es), which produced high-grade ore in lode 8 of the Sugrally deposit are reported by Shchetochkin and Kislyakov (1993) as follows:

- Pre-ore pink recoloration of yellow limonitized arenite
- Close paragenetic relationship of pitchblende and black U products with neogenic Fe-sulfides, calcite, hematite, and locally zeolites derived from extrinsic thermal solutions
- Partial superposition of U-oxides upon oxidized rocks contradicting any link between the geochemical nature of the host rock and the cause for the precipitation of uranium
- Deposition of U-oxide ore in pink oxidized rocks suggests an involvement of a reductant of fluid nature
- Oxidized ore phases are enveloped in a reduced halo, which became concentrically pyritized, bleached, and hematitized
- Decrepiation of inclusions in calcite paragenetic with pitchblende suggests increased temperatures of 120–200°C for this mineralizing process
- Pitchblende-sulfide mineralization was repeatedly reworked and transformed into ordinary black ore or, at some sites, into uranophane ore, the latter marks the original position of sulfidic high-grade ore
- Post-ore reducing activity caused an isolation of ore zones from the oxidation tongue

Given evidence suggests that the high-grade ore is related to the redox interface that evolved at sites of interaction of oxygenated, fertile groundwater with extrinsic reducing thermal solutions ascending along faults and spreading into aquifers. These solutions consequently generated a mobile hydraulic screen that complicated the general hydrodynamics and produced a highly effective hydrogeochemical barrier.

Mineral relationships suggest a formation of the ordinary ore and ore-controlling limonitization zones postdating that of mineral phases such as Fe-sulfides and bitumens derived from extrinsic reducing solutions. Also, ordinary ore is in radioactive disequilibrium with a higher Ra/U ratio at the rear side of a roll than on the frontal side suggesting a relatively recent

if not ongoing formation by redistribution of uranium and other metals.

With respect to processes prior to or following the uranophane formation, relics of Fe-hydroxides often found in uranophane spherulites and massive carbonate inclusions as well document an earlier rock oxidation that was superimposed by reduction. The reducing event is attributed to the contemporaneous precipitation of U-oxides and pyrite in most permeable zones. Reduction of Fe-hydroxides is also noted along the margins of massive uranophane spherulites. These relationships attest to a uranophane formation during an oxidation stage that remodified earlier pitchblende-hematite-sulfide mineralization, which existed slightly updip of the present ore site. On the other hand, uranophane coated by finely dispersed pitchblende documents a post-uranophane generation of U-oxide.

The existence of at least two generations of U-oxides is furthermore supported by rare cases of their telescoping in which an early, finely dispersed pitchblende is restricted to the inner zone of low-permeable intercalations of carbonatized lithologies while the margins of the intercalations are oxidized and colored pink by Fe-hydroxides. The carbonatic intercalations occur in loose, dark grey sands that contain younger U-oxides and pyrite. A bleached rim has formed along the contact of the intercalations attesting to a complete or partial reduction of pink Fe-hydroxides.

A late stage in the evolution of the Sugrally deposit is documented at the far eastern margin of lode 8 where the yellow limonitization zone reappears and oxygenated groundwater remodified high-grade pitchblende ore to ordinary black U ore. Apparently, the same process also generated the small roll-shaped ore bodies of ordinary black U ores of lodes 9 and 15 situated as much as several thousands meters updip behind lode 8. These lodes are controlled by a secondary redox front at the contact between re-reduced ground and confined younger, narrow intercalations of yellow limonitization, which were overprinted upon pink stratum oxidation (Figs. 15.10a,b).

15.1.2.2 Aktau

This explored deposit is situated ca. 60 km NE of the town of Zarafshan and 20 km E of Sugrally. It was discovered in 1967. U occurs in Tertiary arenites. The Tertiary stratigraphic column at Aktau includes, from top to bottom: Miocene gravel, Oligocene pink sediments, and the Upper Eocene Lyavlyakan Horizon. This lower horizon is subdivided into three units: an upper unit, 0.2–0.5 m thick, of silty sandstone with pyrite and phosphate nodules; a middle unit, 10–15 m thick, of unconsolidated quartz sand with U mineralization; and a lower unit, up to 15 m thick, of silty sandstone with clay intercalations. U mineralization of rollfront-type occurs in sands of the middle unit for a length of 13 km in a N-S direction and at depths from 400 to 500 m. The main part of a roll is 1–4.2 m (av. 2.8 m) thick and 25 to 100 m wide while tails are from some ten meters to 250 m long. About 50% of Aktau's resources are in the lower tail, which is 0.2–1.0 m thick and 50–250 m long. Resources are estimated at 5 000 t U at an average grade of 0.08% U calculated on average thickness of 1.56 m. U is associated with Se and Mo (Karimov et al. 1996).

15.1.3 Zafarabad or West-Nuratau District

This district includes ten deposits (📍 Fig. 15.1): *Kenimekh* and *Bukinai South* (also referred to as *Kenimekh-Bukinai South* ore field) are located to the southwest of the Nuratau Range, while *Bukinai (North)*, *Alendy*, *Terekuduk*, *Varadzhnan*, and *Tokhumbet*, which form the *Bukinai* ore field (📍 Fig. 15.11a), are situated to the north of the range, and *Beshkak*, *Lyavlyakan*, and *Aulbek* to the north of this ore field. U mineralization occurs in six horizons within Upper Turonian to Maastrichtian strata. A mining town for the district, Zafarabad, was established by the Soviet government about 40 km NNW of Navoi. Remaining in situ sources amount to 51 500 t U RAR + EAR-I and 46 800 t U EAR-II + SR. Four deposits, *Bukinai (North)* and *South*, *Beshkak*, and *Lyavlyakan* were being exploited by ISL techniques in 2005 and *Tokumbet* was in ISL testing stage. Mining Division # 5, a subsidiary of NMMIW, is the mining operator (OECD-NEA/IAEA 2005).

Source of information: The subsequent descriptions are largely derived from Karimov et al. (1996) unless otherwise noted.

15.1.3.1 Kenimekh

Kenimekh is located in the southwestern foothills of the Nuratau Range, ca. 5 km S of Zafarabad and about 20 km N of Navoi. *Kenimekh* includes the adjacent ore zones *Kenimekh North* and *South*, which occur in the southern part of the *Kenimekh-Bukinai South* ore field. (see also *Bukinai South*). Resources at *Kenimekh North* (RAR + EAR-I) amount to about 2 000 t U RAR in the <40\$/kg U cost category. Grades are about 0.07%U.

Sources of information. Laverov et al. 1992b; Venatovsky 1993.

Geology and Mineralization

The *Kenimekh-Bukinai South* ore field occurs in the artesian *Kuldzhyktau* Subbasin of the *Kenimekh* Basin. The latter is bounded to the NE by the Nuratau Range and the regional *Kokcha* fault, and to the SW by a Paleozoic basement uplift. Upper Cretaceous-Tertiary sediments covered by 0–30 m thick Quaternary alluvium fill the basin.

Ore zones at *Kenimekh South* are hosted by Cretaceous strata, which are overlain by Tertiary sediments and rest unconformably on Devonian-Carboniferous bituminous limestone. The Tertiary-Cretaceous stratigraphic column is over 800 m thick and includes from top to bottom:

Tertiary

- *Neogene*: up to 300 m thick, sediments with intercalated, 15–20 m thick, quartz sand beds
- *Paleogene*: 80–200 m thick, argillaceous sediments

Cretaceous

- *Upper Cretaceous* (U): more than 300 m thick, alluvial and marine sand, and clay
- *Lower Cretaceous* (some U): 20–70 m thick, sand, conglomerate, and clay

Six ore-bearing horizons, 8–22 m thick, occur within a 130–190 m thick section of Upper Cretaceous sediments. Invariably, there is 1 horizon each in Maastrichtian, Campanian, and Coniacian aquifers, and 3 horizons in Santonian aquifers. Some uranium also occurs in Turonian, Cenomanian, and Lower Cretaceous strata. Permeable sand beds altered by carbonatization, kaolinitization, and pyritization host the ore.

The ore-bearing zone is 15 km long and 3–7 km wide but its southeastern margin is not yet delineated due to an increased depth of the ore horizons to 900–1 000 m. Explored ore bodies occur at depths from 400 to 680 m. Ore bodies are curvilinear ribbon-like in planview and roll- or lenticular-shaped in section. They are from 25 to 150 wide and from 0.5 to 7 m thick. Ore grades range from 0.01 to 0.5% U, 0.01–0.1% Se, 0.005–0.05% Mo, and up to 15 ppm Re. Scandium (<30 ppm) occurs locally. Carbonate content averages 1.54% CO₂, but in excess of 30% of the resources average over 2% CO₂.

At *Kenimekh North*, rollfront-type ore lodes occur stacked in five arenaceous horizons of Upper Turonian age. They are distributed along highly twisted redox fronts along the foothills of the *Karatau* Range. Lode depth is in excess of 300 m.

15.1.3.2 Bukinai South

This deposit was discovered 30 km N of Navoi in 1961. The deposit was being mined by ISL techniques in 2005 and had remaining resources (RAR + EAR-I) of some 7 000 t U at a grade of ca. 0.06%U.

Geology and Mineralization

At *Bukinai South* (📍 Fig. 15.12), Tertiary-Upper Cretaceous strata are covered by up to 30 m thick Quaternary alluvium. The sediments dip slightly NE and rest on Silurian metamorphic rocks. The Tertiary-Cretaceous profile includes from top to bottom:

Tertiary

- *Pliocene*: 120 m thick, reddish-brown sand, silt, marl
- *Miocene*, 2–140 m thick, tan silt, and at the base, 80 m thick, greenish-grey sand and pink silt
- *Eocene-Oligocene*, 150 m thick, greenish-grey clay-marl and silt with calcareous intercalations
- *Lower Eocene*, 80 m thick, marl with interbedded clay

Cretaceous

- *Maastrichtian* (U): up to 25 m thick, sand with dolomitic intercalations
- *Campanian* (U): up to 35 m thick, sand with intercalations of shell beds
- *Santonian* (3 U horizons): up to 90 m thick, yellow-green sand

- *Coniacian* (U): <70 m thick, green, grey and pink sand
- *Turonian*: 10–90 m thick, clay
- *Cenomanian*: 5–12 m thick, silt

Ore is polymetallic composed of U, Mo, and Se and consists of finely dispersed aggregates of U oxides (pitchblende, sooty pitchblende). Jordisite, pyrite, and native selenium are the principal associated minerals. Uranium grades can be as high as 0.5% U. Carbonate content is commonly less than 2.5% CO₂ but can locally be as high as 5% CO₂. In addition to authigenic mineralization, uraniferous sands also contain yttrium and lanthanides in detrital heavy minerals. Tenors of these trace elements are <120 ppm Y, <150 ppm Ce, <50 ppm other lanthanides, [dysprosium, erbium, thulium, ytterbium (<10 ppm), europium, samarium (<3 ppm), gadolinium and terbium (<1.5 ppm)].

Main ore bodies occur discontinuously along sinuous redox fronts contained in a zone that varies from a few hundred meters to more than 1 000 m wide. It extends in a linear NNE-SSW direction for about 25 km bordered to the south by the steeply dipping WNW-ESE-oriented Kokzhin fault zone and dissected in the northern part by the likewise oriented North and South Muyunkum faults. Other faults in the area trend NE-SW.

Roll-shaped ore lodes occur in six arenaceous horizons within Maastrichtian, Campanian, Upper Santonian (e.g. ore zone 4), Lower Santonian (ore zones 3, 5, and 6), and Coniacian strata. Depths vary from less than 150 m to 200 m in the southern part to 450 m in the northern segment.

Fazlullin et al. (2002) provide some details on an ore body – lode 10 – that was exploited by ISL from 1968 to 1975. The lode had a lateral extension of 70 000 m², occurred in a 15.5 m thick aquifer at depths from 150 to 165 m, and contained 1 733 000 t of ore at a grade of 0.024% U. Total in situ U reserves were 500 t U, 420 t U were recovered corresponding to a recovery rate of 84%.

15.1.3.3 Bukinai North

Bukinai North (► Fig. 15.11a,b) was discovered some 10 km W of Zafarabad in 1959 and has been mined by Mining Division # 5 using ISL techniques since 1969. Remaining resources (RAR + EAR-I) amount to about 5 000 t U. grading about 0.06% U. Selenium resources were on the order of 20% of the U resources.

Geology and Mineralization

U is hosted in a Cretaceous sequence, 170–320 m thick, composed of – from top to bottom:

- *Maastrichtian* (U): 25 m thick, marine quartz sand
- *Campanian* (U): 15–35 m thick, marine sand
- *Santonian* Karasazyg Horizon (U): 160 m thick, alluvial sand and clay
- *Upper Turonian* Tokumbet Horizon: 35–40 m thick, sand and silt
- >Unconformity<
- *Lower Turonian*
 - Kendyktyubinsky Horizon: 3–8 m thick, sand and clay

- Dzheyrantiysky Horizon: 20–30 m thick, grey marine clay
- Uchkuduk Horizon: 5–12 m thick, marine sand and clay
- *Cenomanian*: up to 12 m thick, conglomerate, sand, and silt

The Cenomanian sediments rest unconformably upon weathered Paleozoic basement rocks composed of sediments and metamorphics intruded by Late Paleozoic granite, granodiorite, and diorite.

Pitchblende and sooty pitchblende are the principal U minerals, with minor coffinite. Associated elements include Se (<0.1%), Mo (<0.1%), and Re (<5.5 ppm).

The Bukinai North ore zone is up to 400–500 m wide and extends for a length of some 20 km in a submeridian direction. It contains ore lodes in four Upper Cretaceous arenaceous horizons. The Karasazyg Horizon is the principal ore host: 87% of Bukinai's resources are contained in its lower section, positioned at depths from 150 to 200 m. Ore bodies are of a roll shape, which exhibits a complex configuration at sites where the oxidation zone is split by argillaceous intercalations. Ore bodies have a length from 0.5 to 7.8 km along NW-SE-oriented redox fronts, a thickness from 1.05 to 3.22 m, and grades from 0.028 to 0.09% U. The ore is in radioactive disequilibrium with a Ueq to Uchem coefficient of 53%.

15.1.3.4 Alendy

This explored deposit is situated at the northern extension of the Bukinai North ore zone and ca. 10 km NW of Zafarabad and contains estimated in situ resources of 14 000 t U at an average grade of ca. 0.05% U. U is hosted by Lower Senonian continental sands and by Campanian and Maastrichtian marine sandy horizons and occurs at depths from 300 to 600 m. Total thickness of the mineralized strata is 80–90 m. Alendy occupies a 20 km long stretch that encompasses – in planview – discontinuous, ribbon-like ore bodies, 50–100 m wide and up to several kilometers long along sinuous redox fronts. In cross-section – ore bodies are of lenticular or roll shape, ranging in thickness from 0.5 to 3 m. Mineralized zones occur in close proximity, arranged in an echelon fashion. The ore is of low grade, generally less than 0.04% U. Ore lodes in the lower horizon of the Lower Senonian strata contain up to 3 ppm Re. Some mineralization contained in oxidized sediments has tenors of as much as 0.2% Se.

15.1.3.5 Terekuduk

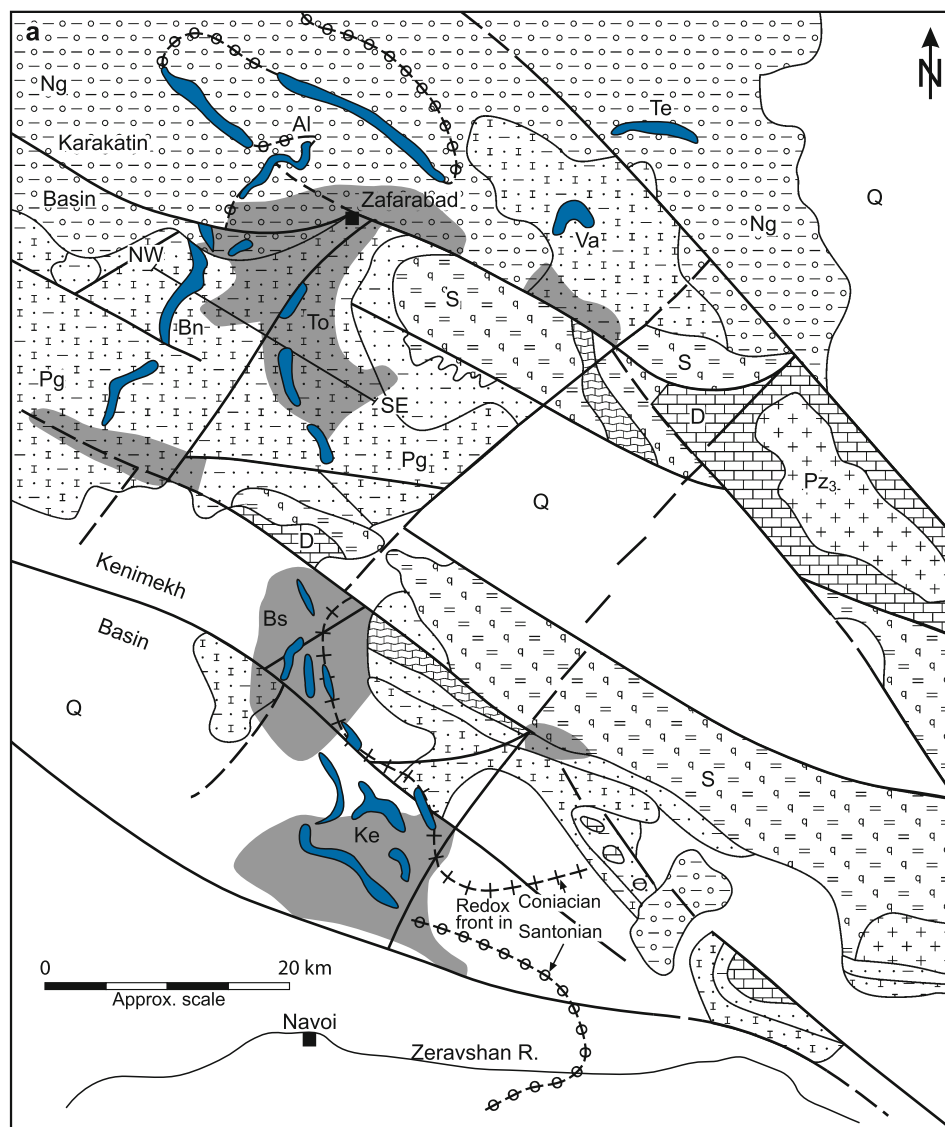
This explored deposit is located ca. 25 km NE of Zafarabad, a few kilometers to the south of the Aulbek deposit. U is hosted in two arenaceous horizons of Senonian age and occurs at depths of 135–340 m. Resources amount to some 2 000 t U at grades of 0.02–0.03% U.

15.1.3.6 Varadzhnan

This explored deposit is located ca. 20 km E of Zafarabad, about 10 km S of Terekuduk. U mineralization is found over a length of

Fig. 15.11.

Zafarabad District/Bukinai ore field, **a** generalized geological map with location of U deposits; **b** NW-SE section showing the litho-stratigraphic sequence and alteration zones at the Bukinai (North) and Tokhumbet deposits (explanations and legend see at Fig. 15.5). (Courtesy of Boitsov A.V. based on Russian literature). **U deposits** in a: *Al* Alendy, *Bn* Bukinai (North), *Bs* Bukinai South, *Ke* Kenimekh, *Te* Terekuduk, *To* Tokhumbet, *Va* Varadzhan



15 km along the front of a gulf-like tongue of limonitized strata within Upper Cretaceous marine sediments. Explored resources are estimated at 500t U. Individual ore bodies are up to 5 km long and consist of rolls or lenses, a few meters thick, and occur at depths from 160 to 200m. Ore bodies have low U grades, commonly less than 0.04% U and contain in sections, up to 1 m thick, as much as 0.1% Mo.

15.1.3.7 Tokhumbet

Tokhumbet is an explored deposit located ca. 10 km SW of Zafarabad, 8 km E of Bukinai North. It contains about 700t U in Upper Cretaceous strata.

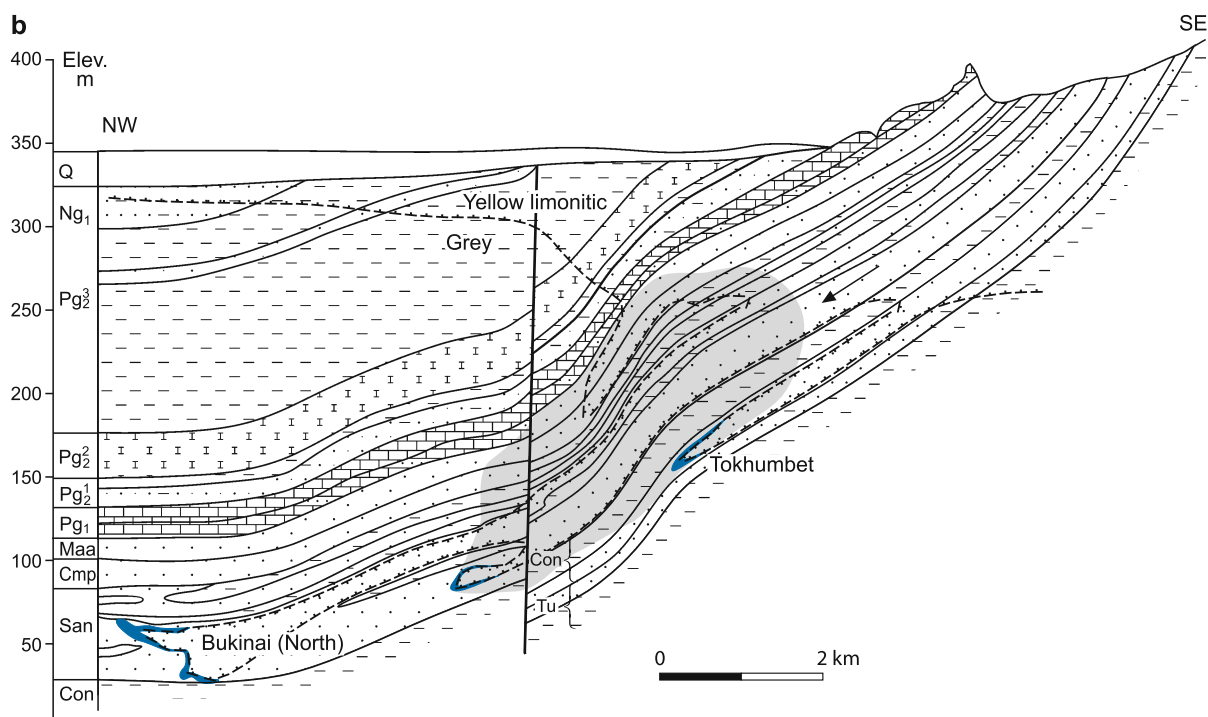
15.1.3.8 Beshkak

Discovered in 1969, Beshkak is situated about 40 km NNE of Zafarabad. Exploitation by ISL started in 1978 and was on going in 2005 operated by Mining Division # 5. Remaining resources (RAR + EAR-I) amount to about 5 000t U including almost 3 000t U of high cost resources.

Geology and Mineralization

Bedrock consists of a slightly SW dipping Tertiary-Upper Cretaceous sequence covered by a 0–50 m thick sheet of

■ Fig. 15.11. (Continued)



Quaternary alluvium and resting on Paleozoic schists (Fig. 15.13a,b). The Tertiary-Cretaceous litho-stratigraphic column includes – from top to bottom:

Tertiary

- *Pliocene-Miocene*(Ng_2^{3-1}): 0–90 m thick, gypsiferous, carbonatic sandstone and marly clay
- *Miocene*
 - upper unit: (Ng_1^{2-3}) 0–200 m thick, brown-red clay and silt
 - lower unit (Ng_1^1) 40 m thick, grey and tan sand and argillaceous sandstone
- *Eocene*(Pg_2^3):
 - 0–65 m thick, greenish-grey silty clay
 - 30 m thick, sand, clayey sandstone, Lyavlyakan Horizon (U)
 - 100–120 m thick, greenish-grey clay, silt
 - 40 m thick, marl
 - 30 m thick, sand
- *Paleocene*(Pg_1): 20 m thick, limestone

>Unconformity<

Upper Cretaceous

- *Maastrichtian-Campanian*: 30 m thick, sand containing shells
- *Coniacian-Santonian*: 80 m thick, sand
- *Turonian*
 - upper unit: 30 m thick, clay, sand, sandstone
 - lower unit: 60 m thick, silty clay
- *Cenomanian*: 5 m thick, silt and intercalated gritstone

Major faults trend about NNW-SSE, the Aktau fault for example, and NW-SE, as the Lyavlyakan fault. The sediments are bent into wide-amplitude folds along E-W-trending axes to the

W of the Aktau fault where the Beshkak deposit is located. These axes turn NW-SE in the area to the NE of that fault.

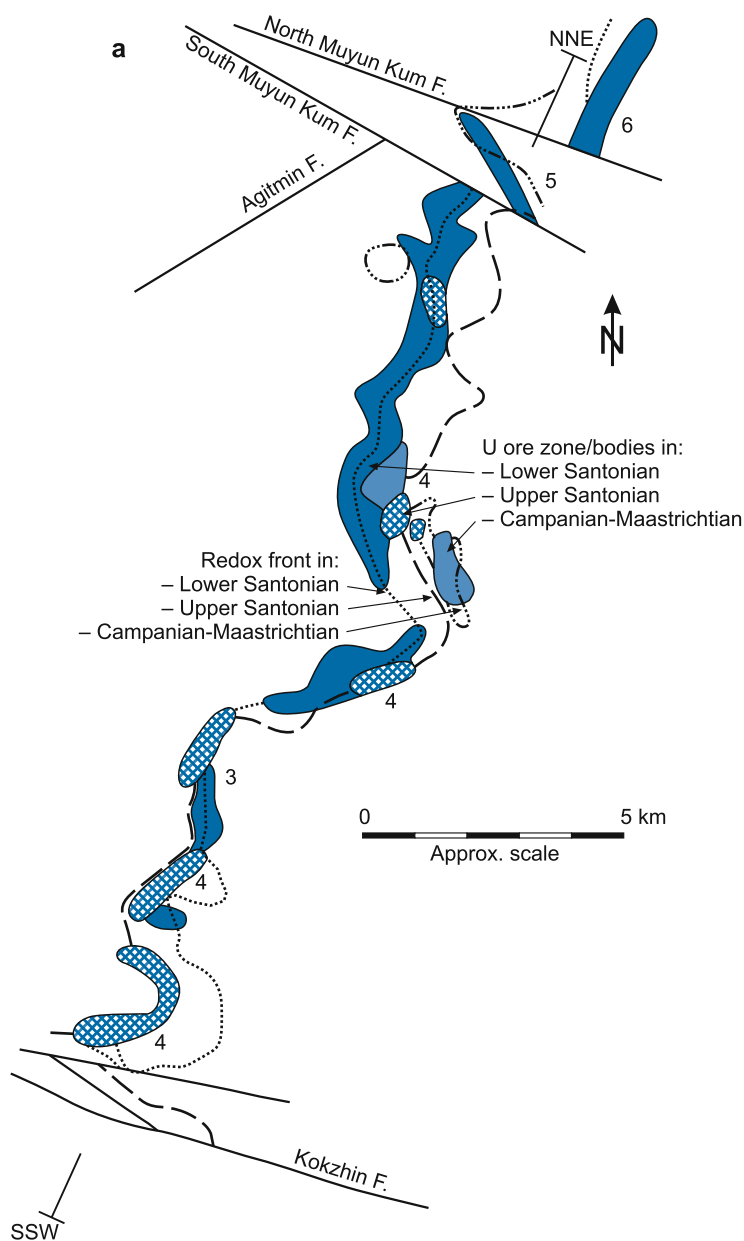
Mineralization consists of U oxides associated with Se. U grades are low. Carbonate content is up to 2.5% CO_2 . Ore lodes are of roll shape hosted in the Upper Eocene, ca. 30 m thick, Lyavlyakan Horizon. Host rocks are partly clay-cemented sands sandwiched between clayey-silty aquicludes. The strata have a slight southerly dip. Two ore zones occur in a NE-SW-trending zone, some 20 km long, and join in the southern part of the deposit. Ore depths range from about 50 m in the north to almost 400 m below surface in the southwest (Fig. 15.13b). *Ore zone 1*, located in the SW segment of the deposit, has a length of more than 6 km along a redox front in the lower Lyavlyakan Horizon, and occurs at depths from 250 m in the NE part to more than 350 m in the SW part. *Ore zone 2* forms the eastern part of the deposit and accounts for 87% of Beshkak's resources. Ore in this zone is up to 500 m wide, 6 km long, and occurs at depths from 30 m in the north to 250 m in the south. In planview, it shows a crescent-shaped configuration open to the east. The northern two thirds of the lode contains U mineralization along a redox front in the upper Lyavlyakan Horizon while mineralization in the southern third is contained in both the upper and lower Lyavlyakan Horizon. Ore grades range from 0.015 to 0.2% U (av. 0.045% U) and up to 0.03% Se.

15.1.3.9 Lyavlyakan

This deposit is located about 20 km to the east of Beshkak. It was being mined by ISL techniques in 2005 and had remaining resources (RAR + EAR-I) of some 7 000 t U (including ca. 5 000 t U low cost resources) contained in three ore lodes in Eocene strata. The litho-stratigraphic setting of the Lyavlyakan deposit

Fig. 15.12.

Zafarabad District, Bukinai (South) deposit, **a** schematic plan and **b** SSW-NNE section showing the distribution of ore bodies hosted in Senonian sediments; **c** simplified profile across a rollfront ore body in Santonian-Coniacian sands with grade-thickness values of ore intervals (explanations and legend see at Fig. 15.5) (after **a**, **b** Karimov et al. 1996; **c** Laverov et al. 1992b)



corresponds largely to that of the westerly located Beshkak deposit (see previous chapter, Fig. 15.13a,c). The two deposits are separated by the NNW-SSE oriented Aktau fault. This fault coincides with the SW boundary, and the NW-SE-trending Lyavlyakan fault with the N boundary, of the Lyavlyakan deposit. Sediments in the Lyavlyakan area are folded along NW-SE-trending axes into wide-amplitude folds.

Three roll-type ore zones occur along a slightly sinuous section, about 25 km long, of an approximately N-S-oriented redox front at depths from 50 to 200 m. The northern # 1 ore zone is 6.5 km long, the central # 2 ore zone 1.5 km, and the southern # 3 ore zone 4 km long. The ore has grades of about 0.06 U and contains as much as 2.5% CO₂.

15.1.3.10 Aulbek

Aulbek is located a few kilometers from Lyavlyakan. The deposit is only partly explored since exploration was interrupted in 1995. U is hosted in five arenaceous strata of Maastrichtian to Upper Turonian age and occurs at depths from 60 to 520 m. Resources are speculated at 2 000 t U at grade averaging ca. 0.035% U.

15.1.4 Nurabad or Zirabulak-Ziaetdin District

Seven U deposits occur in the Nurabad District. *Maizak North* is situated to the northwest, *Ketmenchi* to the central west, and *Agron*, *Sabyrsai*, *Shark*, *Tutly*, and *Nagornoye* to the south and

■ Fig. 15.12. (Continued)

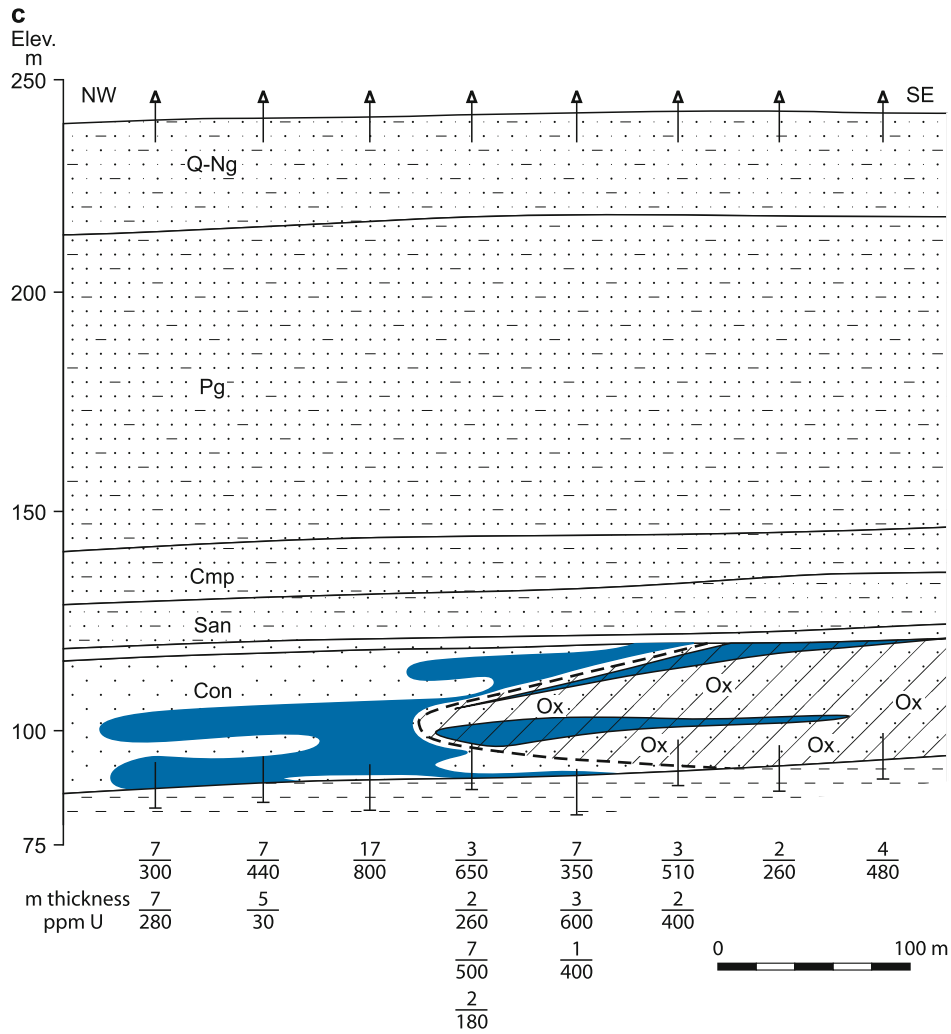
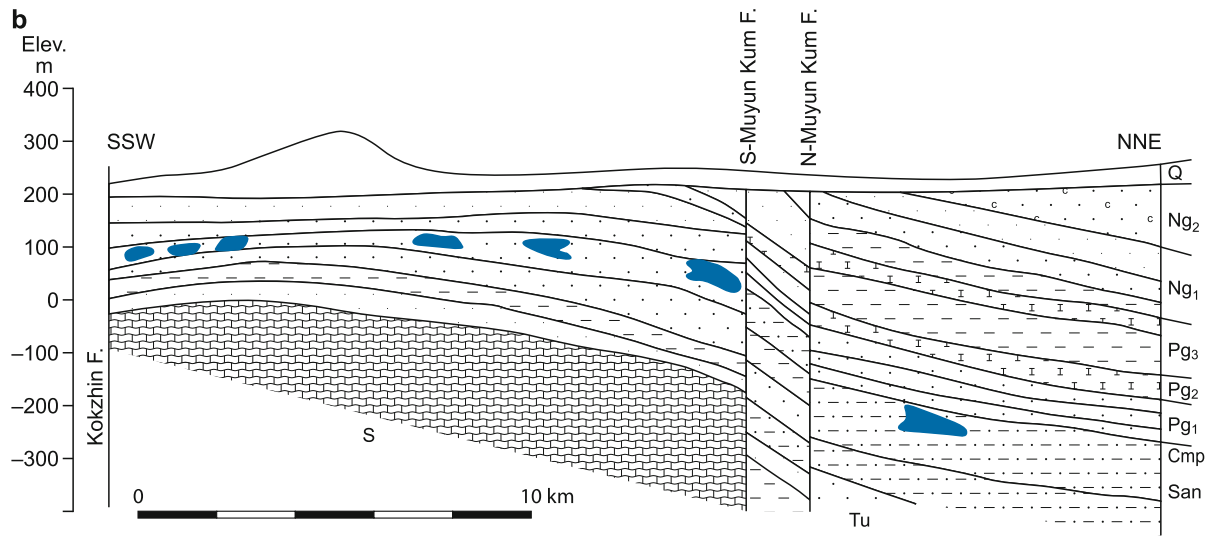
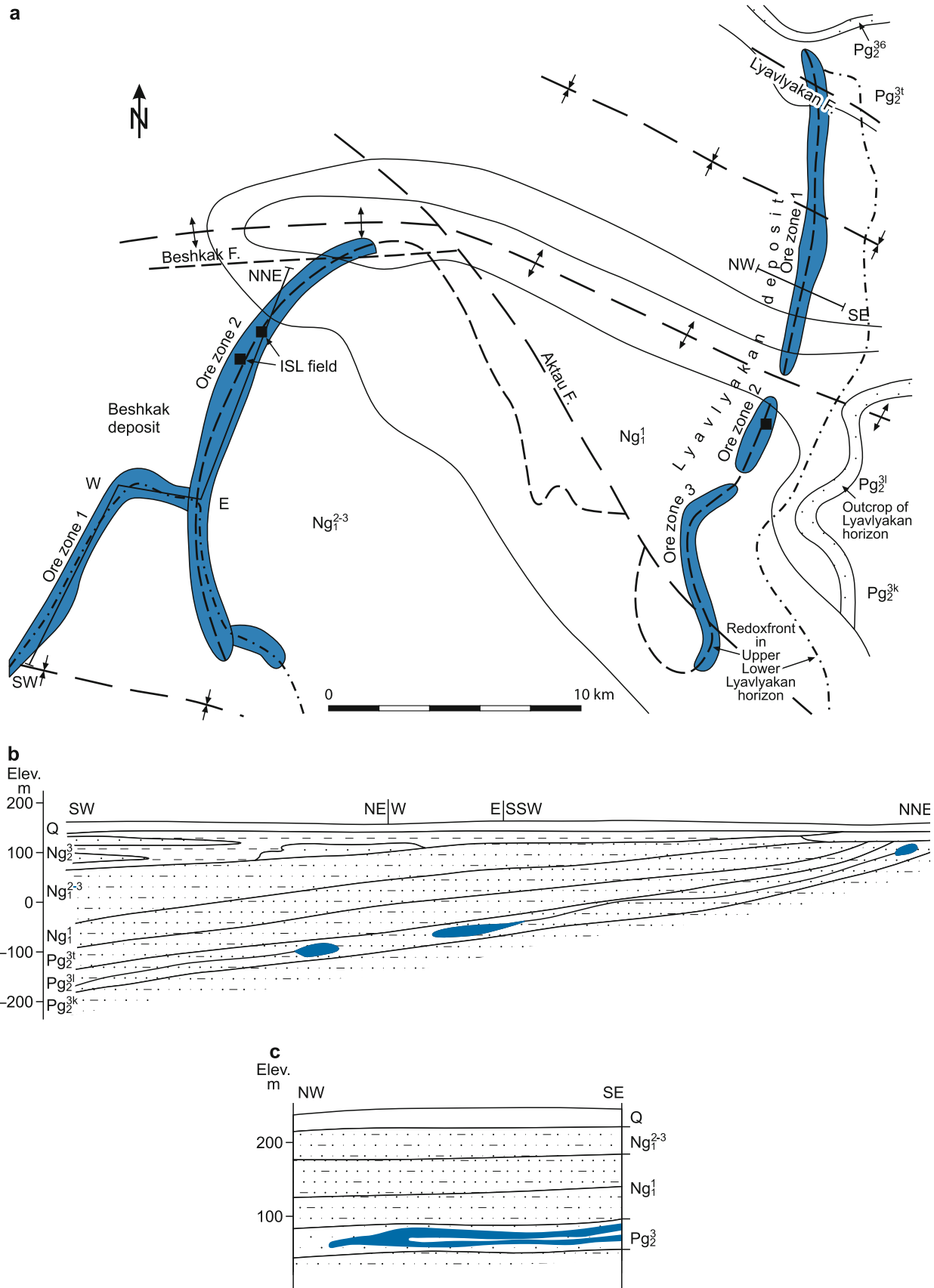


Fig. 15.13.

Zafarabad District, Beshkak and Lyavlyakan deposits, **a** schematic plan of the ore field, **b** SW-NNE section along the Beshkak and **c** across the Lyavlyakan deposit. Ore bodies are controlled by two redox fronts in the upper and lower Lyavlyakan Horizon, Eocene (explanations and legend see at **Fig. 15.5**) (after Karimov et al. 1996)



southeast of the Zirabulak Range. A mining town, Nurabad, was established about 70 km SE of Navoi to serve the district (Fig. 15.1). Remaining in situ sources amount to 12 600 t U RAR + EAR-I and 50 100 t U EAR-II + SR. Operating ISL facilities are located at Ketmenchi and Sabyrsai; they are under the direction of the Southern Mining Division, a subsidiary of NMMIW (OECD-NEA/IAEA 2005).

Source of information: Karimov et al. (1996) amended by data from other sources.

15.1.4.1 Maizak North

This explored deposit is situated ca. 110 km NW of Nurabad and about 8 km W of Navoi. Resources (RAR + EAR-I) amount to some 2 500 t U. Stacked U mineralization occurs at depths from 250 to 500 m and locally down to 600 m in a 5 km long and 50–150 m wide, sinuous string. U hosts are four sand horizons, 20–38 m thick, of Maastrichtian, Campanian, and Santonian age. Grades are on the order of 0.03–0.04% U. Carbonate content is less than 2% CO₂.

15.1.4.2 Ketmenchi

Ketmenchi is situated ca. 60 km NW of Nurabad and about 40 km SE of Navoi (Fig. 15.1). The deposit was discovered in 1967, ISL tested between 1973 and 1977. Zone II of this deposit was subsequently exploited by ISL methods (Fig. 15.14). Remaining in situ resources (RAR + EAR-I) amount to about 12 000 t U at about 0.07% U.

Geology and Mineralization

Bedrock consists of a Tertiary-Cretaceous sequence covered by 2–200 m thick Quaternary alluvium (loam, conglomerate). These sediments rest unconformably upon a Paleozoic basement composed of Ordovician to Carboniferous metamorphic rocks intruded by Upper Carboniferous-Permian granite. The Tertiary-Cretaceous litho-stratigraphic profile includes – from top to bottom:

Neogene: 20–40 m, thick proluvial sand-silt.

Paleogene: marine carbonate-clay facies including

- *Oligocene:* 5–15 m thick, sand-mudstone
- *Upper Eocene:* up to 80 m thick, clay
- *Middle Eocene:* 10–15 m thick, marl
- *Lower Eocene:* 15–20 m thick, clay with shale beds
- *Paleocene:* 10–15 m thick, limestone

>Unconformity<

Upper Cretaceous

- *Maastrichtian-Campanian* (U): 40–80 m thick, marine sand underlain by alternating sand and mud beds,

- *Santonian-Coniacian* Tepalik Horizon: 40–50 m thick, alluvial-lacustrine clay, silt, and sand
- Upper Turonian
 - Ulus Horizon: 25–45 m thick, marine clay and mudstone
 - Sabyrsai Horizon (U): 5–15 m thick, alluvial sand and grit
- Lower Turonian
 - Kandyktube Horizon (U): 25–40 m thick, marine clay-carbonate interbedded with dolomitic sandstone
 - Dzhezantyi Horizon: 30–50 m thick, marine clay
 - Uchkuduk Horizon (U): 5–15 m thick, marine sand, clay, basal conglomerate (U at base extending into Cenomanian)
- *Cenomanian* (U): 50–70 m thick, silt, gravel, conglomerate, basal claystone

Lower Cretaceous

- *Albian* (U): 5–50 m thick, upper clay with intercalated lignite seams underlain by sand, grit, and basal silt
- *Aptian-Neocomian* (two U horizons): 15–20 m thick, continental proluvial conglomerate, sandstone with intercalated carbonaceous clay, and basal gritstone

The Tertiary-Cretaceous beds exhibit a shallow monoclinical dip to the SW from basement outcrops situated in the E-NE. Faults trend NNW-SSE, NW-SE, and curvilinear ENE-WSW to E-W. The latter offset the two former systems.

Ore is polymetallic essentially composed of U, Mo, and Se. U occurs primarily as U-oxides (pitchblende, sooty pitchblende) and to a minor degree adsorbed on phosphate and vegetal matter. Mineralization occurs in eight Cretaceous horizons but minable ore bodies are confined to two horizons in Cenomanian and three horizons in Lower Cretaceous strata. Mineralized horizons consist mainly of sand and some of gravel or gritstone facies (see above), which are partly cemented by carbonate with CO₂ contents commonly less than 2.5% but locally up to 5%. Some 40 ore lodes have been identified. They are essentially of roll shape and occur at depths from less than 100 m to as much as 500 m discontinuously distributed along sinuous redox fronts within a NW-SE-elongated zone, about 35 km long and as much as 10 km wide.

15.1.4.3 Tutly

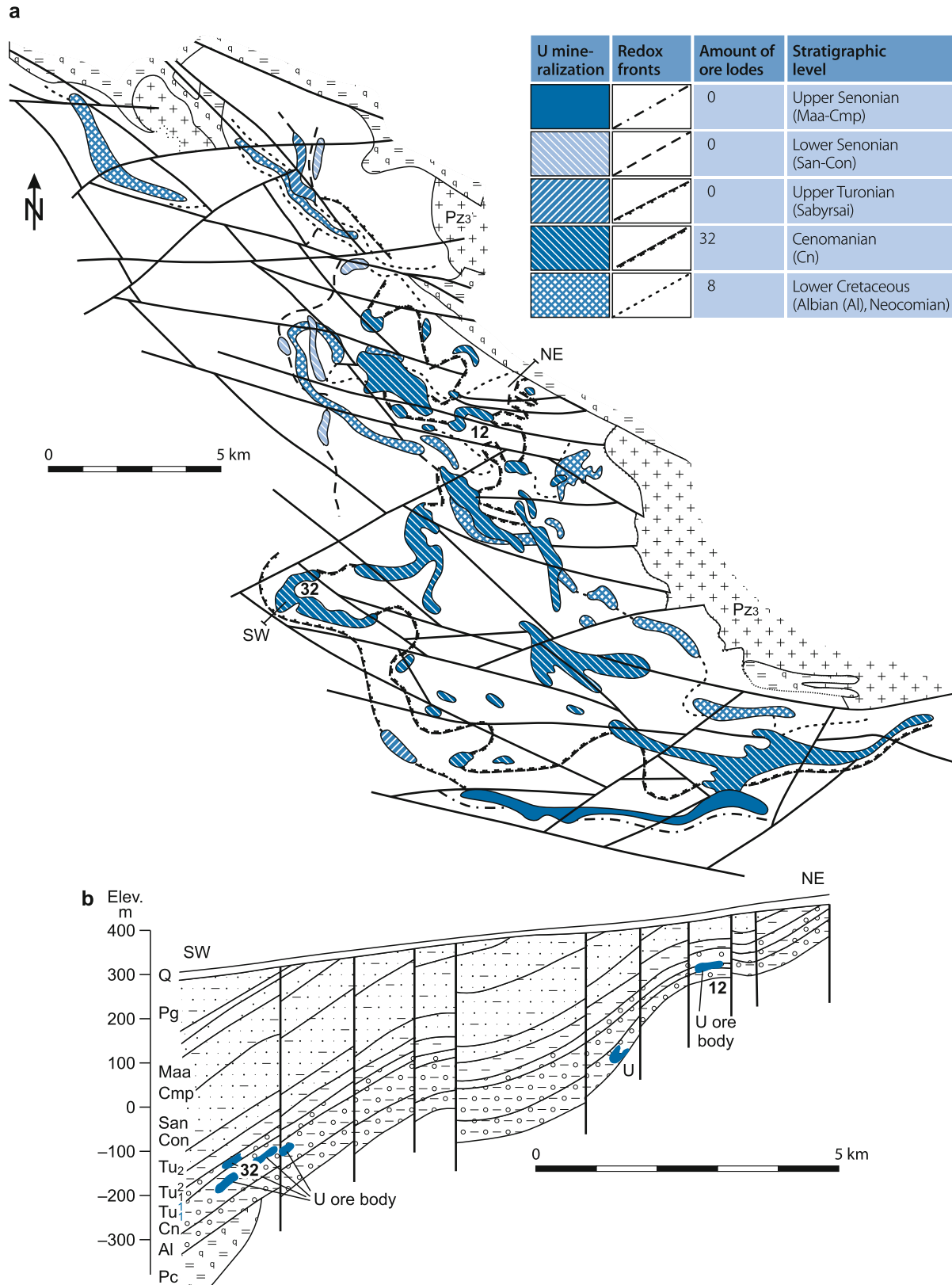
This deposit is located ca. 50 km WNW of Nurabad. In situ resources amount to some 3 000 t U at ca. 0.1% U, hosted in Campanian-Maastrichtian strata at depths from 220 to 700 m.

15.1.4.4 Agron

This deposit was discovered ca. 20 km SSW of Nurabad and 20–30 km W of Sabyrsai in 1980 (Fig. 15.1). In situ resources are estimated at some 5 000 t U at a grade of about 0.1% U.

U mineralization occurs in a N-NE to S-SW-oriented trend some 15–25 km long, at depths from 220 to 700 m in Upper Cretaceous arenaceous horizons intercalated with argillaceous beds. Tertiary sediments achieve a cover thickness from 700

Fig. 15.14. Nurabad District, Ketmenchi deposit, **a** schematic plan and **b** SW-NE-NNE section showing the distribution of ore bodies in Upper and Lower Cretaceous sediments (explanations and legend see at **Fig. 15.5**) (after Karimov et al. 1996)



to 900 m to the S and SW of the deposit. Maastrichtian and Campanian sand beds with an aggregate thickness of 100–140 m provide the main ore hosts. Six ore-bearing horizons, 4–40 m thick, are identified. Ore bodies are from 0.3 to 2.8 m thick, up to 100 m wide, and have grades between 0.01 and, 0.1% U.

15.1.4.5 Sabyrsai

Sabyrsai was discovered 8 km SE of Nurabad in 1960. U was extracted by underground mining between 1977 and 1983 and by ISL techniques since 1975. The latter was active in 2005 and was operated by the Southern Mining Division. Remaining resources (RAR + EAR-I, status 1999) amount to about 2 300 t U.

Geology and Mineralization

Paleogene-Cretaceous sediments are covered by Quaternary-Neogene sediments up to 200 m thick. The sediments rest on Silurian schist and marble intruded by Upper Paleozoic granite (Fig. 15.15). The Paleogene-Cretaceous stratigraphic column includes – from top to bottom:

Paleogene: 140–230 m thick, limestone intercalated with dolomitic sandstone layers

Maastrichtian: 3–10 m thick, calcareous sandstone

Campanian: 20–40 m thick, calcareous sandstone on top, underlain by sorted sand with rare clay lenses

Coniacian-Santonian Telalik Horizon: 25–40 m thick, silt, silty clay with interbeds of calcareous sandstone

Upper Turonian

- Ulus Horizon: 25–40 m thick, silty clay with interbedded silt and sand
- Sabyrsai Horizon (U): 5–20 m thick, sand, silt, basal conglomerate

Lower Turonian

- Kendik Horizon: 30–35 m thick, sand, silt, with basal dolomite
- Azhenrantui Horizon: 22–44 m thick, finely laminated clay
- Upper Uchkuduk Horizon: 4–9 m thick, sandstone, gritstone, and conglomerate
- Basal Uchkuduk Horizon: 0–1.2 m thick, sandstone and siltstone

Albian: 5–13 m thick, carbonaceous sand and clay.

In the deposit area, strata are downwarped to form the Ulus-Dzhamoky Depression between two basement outcrops situated to the east and west within a distance of approximately 20 km from each other. The depression is bordered or transected, from N to S, by the curvilinear WNW-ESE-trending and steeply inclined Borikly, Khodzhalik, Bakalysay, and South Bakalysay faults. Other major faults such as the Uikir trend E-W.

Some 15 ore lodes are delineated within a WNW-ESE-elongated area, about 13 km long and 8 km wide, which covers

part of the Ulus-Dzhamoky Depression. Most of the lodes are controlled by a redox front on the northern and southern flank of the depression. The basal Upper Turonian Sabyrsai Horizon, from 5 to 20 m thick, and composed of alternating lenses of sand, conglomerate, and silt is the principal ore-hosting unit. Parts of the host lithologies are cemented by carbonate in amounts up to as much as 5% CO₂. Argillaceous-silty aquicludes several meters thick of the Upper Turonian Ulus and Lower Turonian Kendik Horizons overly and underlay, respectively, the mineralized horizon.

U mineralization consists predominantly of sooty pitchblende and minor pitchblende and coffinite that form roll- and tabular-shaped ore lodes. Roll-shaped ore bodies extend ribbonlike from 400 to 3 000 m long, are from 100 to 350 m wide, and up to 8 m thick. Tabular ore bodies range in length from 1 000 to 3 000 m and in width from 450 to 700 m. Ore lodes occur at depths from 50 to 150 m in the western part, and from 200 to 250 m in the eastern part of the deposit. Ore grades vary between 0.03 and 0.2% U.

15.1.4.6 Shark

Shark is located about 5 km E of Sabyrsai and ca. 15 km ESE of Nurabad. It was discovered in 1978 and contains resources of about 1 500 t U grading ca. 0.08% U. Three ore bodies, from 2.5 to 8 km long, are delineated in two Upper Cretaceous horizons within a zone up to 250 m wide. The bulk of resources occurs in sand and gravel beds of the 10–17 m thick upper Cenomanian horizon. One ore body is in gravel-sand intercalated with sandstone, siltstone, and clay beds of the Turonian, 10–15 m thick Sabyrsai Horizon. Ore bodies are 0.2–4 m thick, 25–250 m wide, grade up to 0.1% U and occur at depths from 150 to 300 m except at the S and SE margin where ore is as much as 500 m deep.

15.1.4.7 Nagornoye

Nagornoye is located ca. 20 km NE of Nurabad (Fig. 15.1). In situ resources are estimated at to some 3 000 t U, hosted in Senonian strata at depths from 550 to 700 m.

15.1.4.8 Ulus

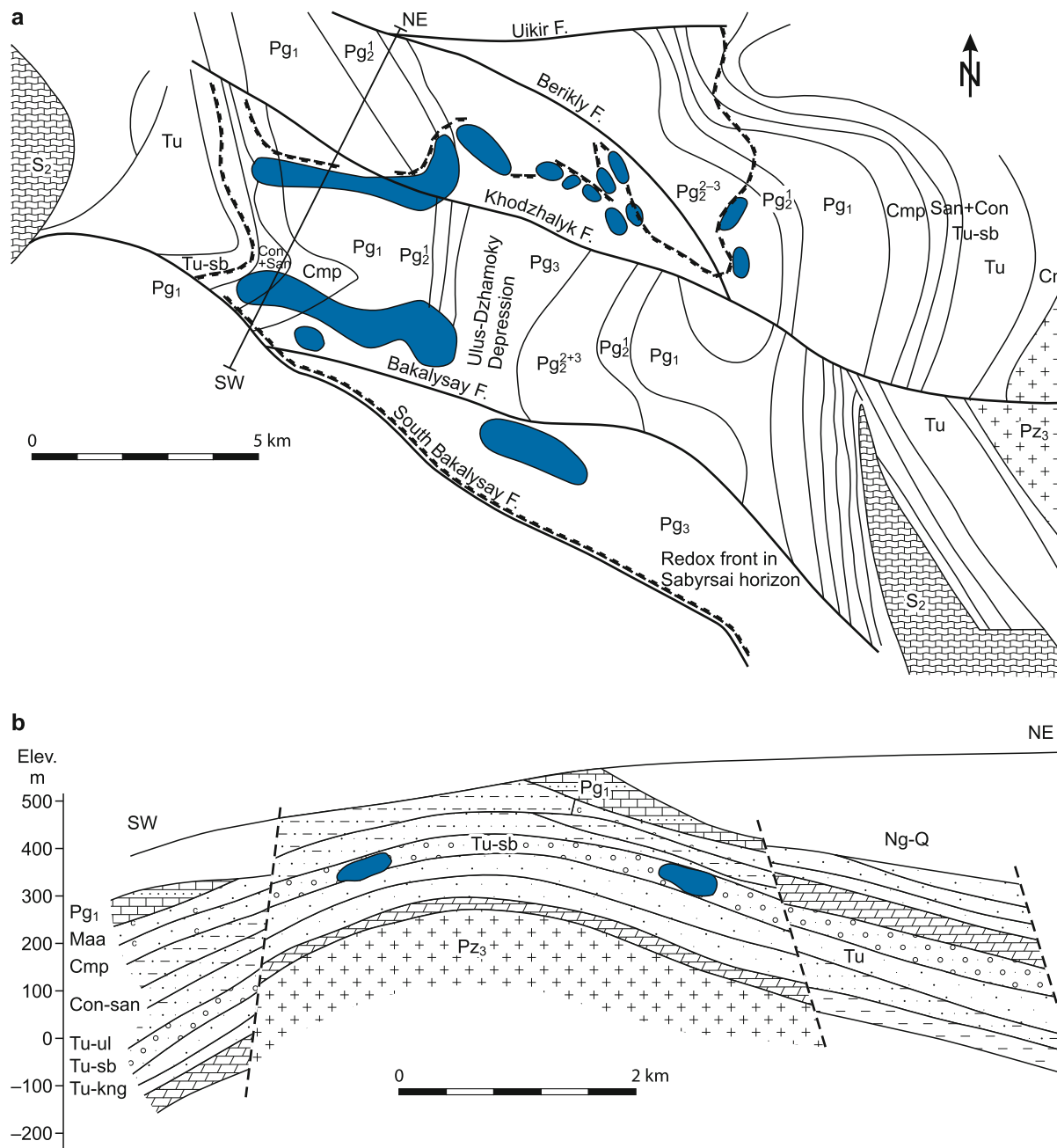
Discovered in the late 1990s, a first drilling phase identified some 800 t U in Coniacian and Santonian strata at depths from 170 m to 220 m.

15.2 Kyzylkum Basement Areas

Geologic data is available for two ore fields, *Altyntau* and *Auminza-Beltau*, in Precambrian-Paleozoic basement ranges of the Kyzylkum region (Fig. 15.1). Resources for these fields total 47 000 t U in the RAR + EAR-I and 54 000 t U in the EAR-II + SR categories (OECD-NEA/IAEA 2005). Deposits/ore bodies

Fig. 15.15.

Nurabad District, Sabysai deposit, **a** schematic plan and **b** SW-NE section showing the distribution of ore bodies hosted in Upper Turonian Sabysai Horizon (explanations and legend see at Fig. 15.5) (after Karimov et al. 1996)



consist of stratiform and/or complex stockwork mineralization contained in graphitic slate and phyllite (siliceous and carbonaceous shale metamorphosed to greenschist grade facies). Both deposit configurations are strata-controlled, structure-bound and therefore tentatively assigned to the carbonaceous shale-related stockwork deposit type (locally referred to as “black shale type”).

Ore bodies occur at depths from 20 to 600 m and consist of uranium oxides (pitchblende, black U products) and/or uranium-vanadium/uranium-phosphate minerals, which may be accompanied by appreciable tenors of other elements such as Au, Mo, and Y. Uranium grades range from 0.02 to 0.132%.

Metallogenetic considerations favor a multistage evolution with roots in the Hercynian Orogeny. Hydrothermal ore-forming processes continued periodically through the Alpine Tectogenesis. Present-day deposits/ore bodies are thought to have derived by redistribution of uranium and other ore components from older mineralization during the Neogene-Quaternary as suggested by ages ranging from 400 Ma to Recent. Extrinsic hydrocarbons provided the reducing conditions required for ore mineral precipitation (see Dzhamantuar). Final activities were of supergene nature and resulted in the formation of U^{6+} minerals down to considerable depths.

Sources of information. Gorlov et al. 2005; Laverov et al. 1992a,b; OECD-NEA/IAEA 1995, 1999, 2005.

15.2.1 Altyntau or Bukantau Ore Field

The Altyntau (also referred to as Bukantau) ore field is located in the Bukantau Range, about 30 km NE of the town of Uchkuduk (Fig. 15.1). In situ resources are 33 100 t U RAR + EAR-I and 11 200 t U EAR-II + SR. Several deposits including *Khodzhyakhmet* and *Novoye* were explored to the development stage. Underground mining associated with heap leaching is considered to be the potential extraction method. Estimated resources of *Khodzhyakhmet* are between 500 and 1 500 t U at grades ranging from 0.02 to 0.1% U.

The ore field occupies the northern flank of the Altyntau anticline and is bordered by the approximately N-S-trending Altym and Taikarshi fault zones. Country rocks are folded Proterozoic (Vendian-Riphean) black slate and phyllite. Mineralization consists of uranium and vanadium associated with yttrium and REE, and occurs in stockwork ore bodies within brecciated black slate.

15.2.2 Auminza-Beltau or Auminzatau Ore Field

This ore field is located in the Auminzatau Range, centered about 50 km SW of Zarafshan (Fig. 15.1). In situ resources are 13 900 t U RAR + EAR-I and 42 700 t U EAR-II + SR (OECD-NEA/IAEA 2005). Reported U deposits include *Dzhantuar*, *Dzitym*, *Kostcheka*, *Rudnoye*, and *Voskhod*. Grades range from 0.02 to 0.13% U and average about 0.05% U.

Regional Characteristics of Mineralization

Country rocks consist of metamorphosed and tectonically deformed black carbonaceous and siliceous slates/schists, phyllite, quartzite, and diabase dikes of the Proterozoic Taskazgan and Auminza Formations. Increased tenors of U, V, Mo, Zn, and other elements are typical accessories of the carbonaceous black slate. The metasediments were intruded by granite during the Carboniferous. Regional weathering imprinted a kaolinite-type crust on the rocks during Triassic-Jurassic time. Numerous faults transect the crystalline complex and were repeatedly reactivated until the Quaternary.

Structurally controlled U deposits occur in the exocontact zone of granite plutons. These deposits consist of discontinuous ore bodies of complex stockwork or lensoid/stratiform configuration. Primary mineralization is represented by pitchblende and coffinite associated with several generations of sulfides. Unoxidized ore minerals are restricted to lower levels of the deposits, downward from 250–300 m below present-day surface. Mineralization above the 300 m level consists exclusively of uranyl vanadates and phosphates. Some deposits, like *Rudnoye*, contain appreciable amounts of vanadium while vanadium tenors in other deposits are low.

Wall rock alteration includes an early quartz, chlorite, and sericite stage that accompanies early pitchblende while later pitchblende generations are associated with argillization. Uranyl-type mineralization may, in addition, be accompanied by limonitization.

15.2.2.1 Dzhantuar

Dzhantuar is located ca. 60 km SW of Zarafshan and has been investigated by an exploratory mine. Mineralization is of stockwork and stratiform type hosted by graphitic slate and phyllite of Proterozoic age. Rocks are folded into an about NW-SE oriented syncline, which is complicated by faults oriented about NW-SE and steeply inclined to the SW and NE (Fig. 15.16). Wall rocks are altered by silicification and kaolinitization.

Uranyl vanadates and uranyl phosphates are typical for upper levels, to depths of about 250 m. Pitchblende and sooty pitchblende occur in the southern part of the deposit, but only at depths from 250 to 600 m.

The deposit is NE-SW elongated and almost 600 m wide. Most ore bodies occur intermittently over depth intervals from 60 to 300 m. In the southern part of the deposit, some ore persists to 600 m deep. Ore bodies are placed at or near faults but in unpredictable distribution. The preferential position is in black slate at the fault contact with siliceous phyllite. Ore lodes commonly have an irregular strata-peneconcordant to -discordant configuration. Better grade lodes (>0.03% U) are a few meters to about 30 m thick and extend from a few meters to approximately 200 m down-dip. Lower grade mineralization (<0.03% U) forms semi-continuous haloes around and interconnects better-grade lodes.

Perevozchikov (2000) documents the presence of extrinsic gaseous and liquid hydrocarbons and hydrogen that form geochemical haloes around ore-controlling structures. These geochemical haloes show a close spatial relationship to the uranium ore bodies; consequently, the author postulates the involvement of hydrocarbons and hydrogen in the formation of ore. Liquid hydrocarbons and hydrogen provided a reducing environment and, as such, were instrumental in the concentration of uranium and in the preservation of ores.

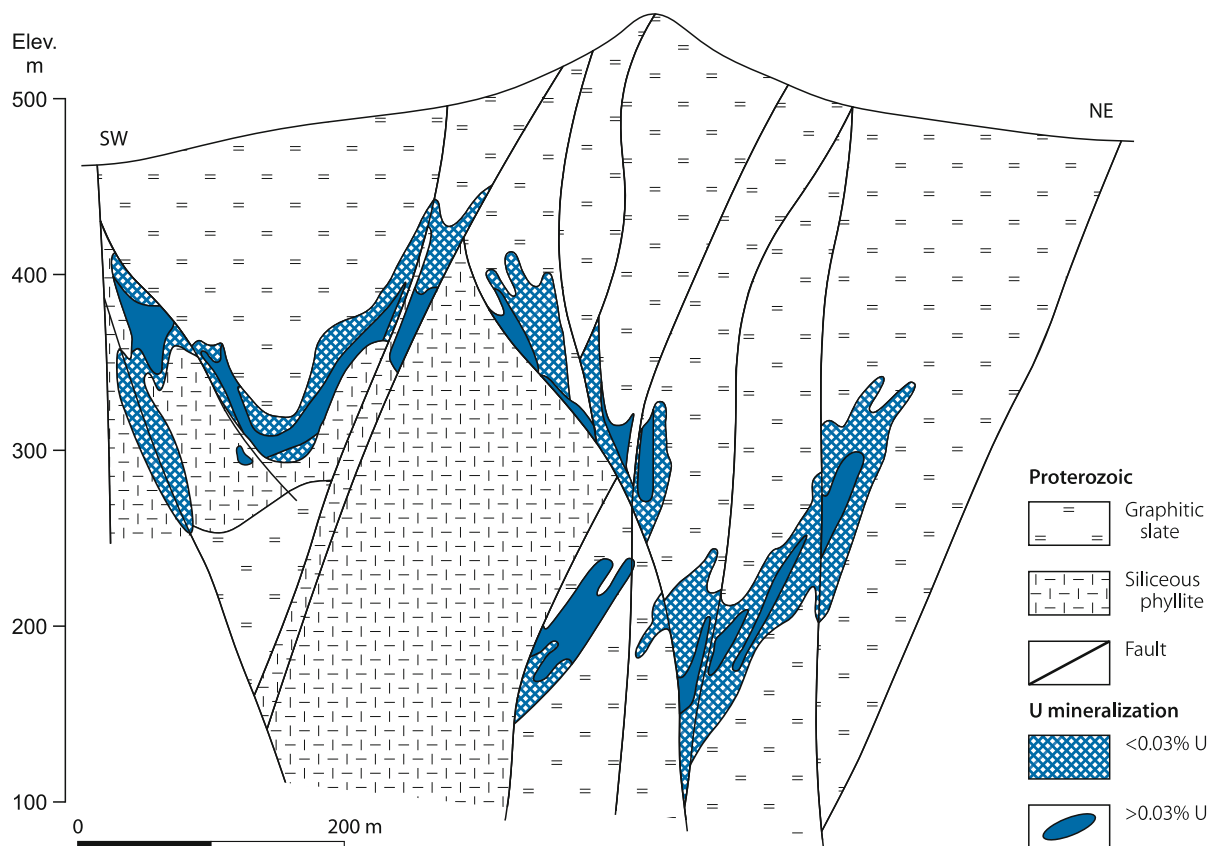
15.2.2.2 Rudnoye

Rudnoye was discovered ca. 50 km SW of Zarafshan in the early 1960s. The deposit is of polymetallic U-V-Mo stockwork-type mineralization. Grades range from 0.06 to 0.132% U, 0.1–0.8% V₂O₅, up to 0.024% Mo, 6–8 ppm Y, and 0.1–0.2 ppm Au (OECD-NEA/IAEA 1995, 1997). In situ resources amount to 2 900 t U (RAR + EAR-I).

U occurs in the oxidation zone of weathered Proterozoic carbonaceous, siliceous slate, quartzite, and microquartzite. The metasediments are folded into a NW-SE-oriented syncline and are transected by faults in 40–50 m intervals. Ore lodes are of stratiform shape controlled by interformational fracture zones that follow lithology contacts. Wall rocks are altered by kaolinitization and montmorillonitization. Ore lodes are composed of minute veinlets, specks, and disseminations of autunite, carnotite, torbernite, tyuyamunite, and zeunerite. Associated gangue

Fig. 15.16.

Kyzylkum basement area, Auminza-Beltau ore field, Dzhantuar deposit, geological SW-NE section illustrating the setting of stockwork and stratiform U mineralization controlled by faults in Proterozoic graphitic slate and siliceous phyllite (after Laverov et al. 1992b)



minerals include alunite, baryte, calcite, gypsum, kaolinite, and montmorillonite. A lithologic affinity of various mineral parageneses is noticed. Uranium-vanadium mineralization prevails in siliceous slate and uranium-phosphate-vanadium mineralization prevails in carbonaceous, siliceous slate.

15.2.2.3 Kostcheka

Kostcheka was discovered about 40 km SW of Zarafshan in 1973. Mineralization is of polymetallic U-V-Mo lenticular stockwork type. Grades are from 0.03 to 0.224% U, up to 0.3% V, and up to 0.012% Mo (OECD-NEA/IAEA 1995, 1997). In situ resources are reportedly almost 2 000 t U averaging a grade of 0.07-0.08% U.

Two horizons of black slate intercalated with phyllite of the Riphean-Vendian Taskazgan and Auminza Formations are mineralized and are cut by NW-SE-trending faults. Wall rock alteration includes silicification, montmorillonitization, and limonitization. Ore bodies consist of structurally controlled lenses and saddle-back lodes intermittently distributed over a depth interval of 50–200 m below surface. U minerals include carnotite, tyuyamunite, autunite, torbernite, saleite, minor pitchblende, coffinite, and ningyoite. A vertical zoning of ore minerals is noticed. Uranyl vanadates prevail at depths from 50 to 80 m; uranyl phosphates dominate between 100 and 120 m while uranyl vanadates, uranyl phosphates and minor U silicates and

pitchblende are typical for the 150–200 depth interval. Gangue minerals compare largely with those at Rudnoye.

15.3 Karamazar Uranium Region, Uzbekistan-Tajikistan-Kyrgyzstan

The Karamazar U region (also referred to as Chatkal-Kuramin region or district) is located to the north and northeast of the town of Khudzhand, Tajikistan (formerly Leninabad). It covers parts of the Chatkal and Kuramin Ranges of the western Tien Shan mountains in eastern Uzbekistan and northwestern Tajikistan, respectively, as well as an adjoining area in western Kyrgyzstan, to the NW of the Fergana Valley (see Chap. 7: *Kyrgyzstan*, 12: *Tajikistan* and Fig. 7.1). The region is known for uranium as well as for gold, silver, base metals, and fluorite deposits. Laverov et al. (1992a,b) report original resources of 20 000 t U for the entire Karamazar region.

U deposits in the Uzbekistan part of the Karamazar region occur in the Chatkal mountains. Deposits are of volcanic vein-stockwork type [in Russian literature termed deposits of “uranium-molybdenum”, “uranium-fluorite”, or “deposits in volcanic depressions”: Vlasov et al. (1966), Volfson (1978), Kazansky and Laverov (1977)]. Mineralization is polymetallic and classified either as U-Mo, U-Bi, or U-Cu-Pb-Zn mineral assemblages. The principal deposits are *Adrasman* (U-Bi), *Chauli*, *Alatanga*,

Kattasay, *Dzhekindek* (U-Mo), and *Maylikatan* (U-Cu-Pb-Zn). Resources of these deposits were on the order of a few hundred to a few thousand tonnes U except for the two largest deposits Alatanga and Chauili, which contained 4 500 t U each. Additional, but small, deposits are *Aksay*, *Dzheekamae*, *Kazakhat*, and *Tary-Ekan* in the vicinity of Adrasman, and *Rizak* (Rezak). A small sandstone-type deposit, *Uigar Sai*, is known from the Papsk region in the northern Fergana area. Ore grades averaged 0.1–0.3% U. All known deposits are depleted. Mining was by underground means and lasted from the late 1940s to the early 1960s. Ore processing was at the Chkalovsk mill near Khudzhand, the former Leninabad.

Source of information: Kazansky and Laverov (1977); Laverov et al. (1992a,b, 1993); Melnikov et al. (1996) unless otherwise cited.

Regional Geological Setting of Mineralization

The Karamazar uranium region is within the Chatkal-Kuramin metallogenetic zone located in the Chatkal-Kuramin Uplift, a section of the Ural-Mongolian Hercynian orogenic belt in central Asia. Precambrian to Early Paleozoic metasediments intruded by Early Paleozoic granite (with xenoliths of schists and marble), Early to Middle Paleozoic continental carbonates, and Ordovician-Silurian schists constitute the basement. Early orogenic mafic to intermediate and late orogenic intermediate to felsic volcanics of the Beltau-Kuramin volcanic-structural belt were intruded and extruded during the Hercynian Orogeny. The Carboniferous and Permian volcanic suite consists of alternating rhyolite to dacite and andesite lava sheets intercalated with pyroclastic and clastic rocks. Multiphase subvolcanic stocks and dikes of rhyolitic to andesitic composition and various types of granitic, syenitic, and silicic porphyries were intruded into this suite and the older basement. The volcanics occupy structural depressions represented by calderas and linear troughs. Deep-seated lineaments control the position of volcanic structures. Mesozoic-Paleogene continental- to shallow-marine sediments overlain by Neogene-Quaternary coarse-grained clastics fill the adjacent intermontane Fergana Basin.

Principal Host Rock Alteration

Beresitization is ubiquitous in all lithologies but is more pronounced at depth. Felsic host rocks are altered on upper levels by albitization and carbonatization, and on lower levels by quartzitization and sericitization. Other types of alteration include argillization, chloritization, and fluoritization. More details are given below and in Sect. *Alatanga-Kattasay OF*.

Principal Characteristics of Mineralization

Pitchblende is the principal U mineral while coffinite and/or U-Ti-phases occur locally. Associated metallic minerals may

include Bi, Cu, Mo, Pb, and Zn-phases giving rise to three ore mineral parageneses: U-Mo (Alatanga, Kattasai, Dzhekindek, and Chauili), U-Cu-Pb-Zn (Maylikatan), and U-Bi (Adrasman). Gangue minerals include quartz, sericite, carbonates, and some minor minerals as listed below. Pitchblende is present in three generations. Major quantities formed together with galena, molybdenite, and calcite. Molybdenite and jordisite occur in some deposits in considerable amounts. Ore exhibits a disseminated, stringer or veinlet, and locally a massive texture.

Kazansky and Laverov (1977) distinguish four stages of mineralization and alteration:

- Pre-uranium stage 1: Beresitization
- Pre-uranium stage 2: Predominantly ankerite and dark sphalerite veinlets and veins, associated with arsenopyrite, chalcopyrite, fahlore, galena, hematite, magnetite, pyrite, pyrrhotite, chlorite, dolomite, and sericite
- Uranium stage: Pitchblende, carbonate, chlorite, jordisite, molybdenite, quartz, sericite, as well as bournonite, chalcopyrite, cleiophane (= white sphalerite), fahlore, and galena
- Post-uranium stage: Calcite, baryte, fluorite, and quartz veins and veinlets that may contain cleiophane, cinnabar, galena, hematite, magnetite, marcasite, pyrite, pyrrargyrite, chlorite, and dickite

[A more differentiated mineral suite is provided by Melnikov et al. (1996) for the Alatanga-Kattasay deposits mentioned further below]

Deposits exhibit a distinct vertical and lateral mineral zoning. Phases of the earlier stages and a wider aureole of beresitization are typical for lower levels but gradually decrease upwards. On upper levels of stockworks and on their flanks, specimens of the post-uranium stage and late pitchblende prevail.

Ore lodes are controlled by steeply to gently dipping faults and highly fractured zones. Particularly favored sites of ore concentrations are cataclastic zones at the contact of intrusions and at the paleounconformity of the basement. Favorable host rocks include leucocratic, mainly rhyolitic volcanics, preferentially in form of subvolcanic bodies and, to a lesser extent, pyroclastic and clastic sheets, and locally basement rocks.

General Shape and Dimensions of Deposits

Deposits are highly variable in magnitude and grade. Original reserves range from a few hundred to 4 500 t U and grades from 0.03 (= cutoff grade) to about 2% U averaging 0.1–0.3% U. Deposits are composed of several ore bodies separated by barren or weakly mineralized ground. Such intermittently mineralized zones may be up to 2 km long, 250 m wide, and in excess of 300 m deep as exemplified by the Alatanga-Kattasay ore field (see later). Ore is rarely exposed at surface.

The shape, dimensions, grade, and internal structure of ore bodies are highly irregular due to heterogeneous systems of interlinked veins, stockworks, and stratiform lenses. Lateral dimensions range from a few meters to about 200 m, while vertical persistence is from a few meters to about 100 m. Reserves vary between a few tonnes and a few hundred tonnes U.

As may be derived from Kazansky and Laverov (1977) (they do not give names and dimensions but the deposits they describe can be tentatively identified as situated in the Karamazar region), ore bodies may simplistically be grouped into two principal geometric-structural types: gently dipping lodes (the most significant variety from an economic point of view) and steeply dipping veins, lenses, and shoots. Gently dipping lodes have a stockwork structure. Their position in multiphase extrusions and intrusions is controlled by lithologic boundaries along which they preferentially occur at those interface sections that vary in attitude and are intersected by major faults. Steeply dipping ore lenses and shoots are composed of interlinked veinlets and disseminated ore minerals. They prevail in latest dike-like bodies of granite porphyry. Locally, the contour of an ore body coincides entirely with that of the host intrusion; but most commonly, the lenses or shoots occupy the intrusive endocontact zone where the rock interface is markedly irregular. In essence, the morphology of ore bodies hosted by intrusive bodies tends to be conditioned, to some extent at least, by the shape and internal structure of the intrusive edifice. The internal structure is reflected by stockworks of complex fracture systems that served as receptacles for ore veinlets. Stockworks are widest in the upper parts while they taper substantially at depth where the host intrusions acquire a narrow stock-like form. In the latter case, mineralization is essentially restricted to complexly arranged, closely spaced, cm to dm thick veins positioned in the contact zone between intrusion and country rocks.

Uranium distribution in lodes is extremely irregular. The largest U accumulations are typical for gently inclined segments of a stockwork. With increasing depth, the quantity and grade of ore decreases gradually.

Deposits hosted in multiphase extrusive domes consist of ore bodies of a particularly complex structure with marked variations in position and configuration due to the irregular shape of the subvolcanic bodies and numerous steeply and gently dipping faults. Ore frequently occurs in these deposits at several vertical levels and concentrates at major tensional faults.

Regional Geochronology and Fluid Inclusions

Laverov et al. (1993) and Melnikov et al. (1996) report geochronological data from the Chauli deposit in the Karabash Caldera and the Alatanga-Kattasay ore field, respectively, which may also be considered representative for the other uranium deposits in the Karamazar region. Basement granitoids range in age from 410 to 385 Ma; K-Ar dating of rhyolite effusives that fill the Karabash depression yields ages from 305 to 270 Ma, while felsic extrusives and dikes that contain ore bodies date from 279 to 264 Ma. Sericite from the Chauli U deposit and the nearby Chiborgata fluorite deposit give K-Ar ages of 274 ± 8 and 278 ± 8 Ma, respectively. U-Pb dating yields concordant or close to concordant ages of 275–267 Ma for pitchblende-I (calcite-coffinite-pitchblende association) and strongly discordant ages ranging from 259 to 212 Ma for admixtures of coffinite and pitchblende-II (sulfide-pitchblende associations). Similar ages are obtained for the Alatanga-Kattasay ore field as

documented by $280\text{--}270 \pm 10$ Ma for third phase granite porphyry and latest dikes, and 270 ± 10 Ma for pitchblende and beresite.

Fluid inclusion and stable isotope data are reported from the Alatanga-Kattasay ore field and presented in Sect. *Alatanga-Kattasay*.

Principal Ore Controls or Recognition Criteria

Ore control is by a combination of structural and lithologic elements. Primary control of deposits is by extrusive and intrusive felsic volcanics of rhyolitic composition with alkaline tendency and major faults. The position and shape of ore lodes tend to be a function of shallow- and steeply-dipping faults with their associated fracture and breccia zones as well as with their intersection with youngest magmatic bodies or with interfaces of different lithologies.

Principal Aspects of Metallogenesis

Polymetallic uranium deposits of the Karamazar region are of epigenetic hydrothermal origin. Circumstantial evidence suggests a genetic relation to felsic volcanics as indicated by a distinct spatial association of mineralization with near surface emplaced felsic (sub-)volcanic lithologies, which formed during the waning episode of the Hercynian Orogeny. Critical ingredients for deciphering the metallogenesis of the volcanic-type U deposits include the age correlation between volcanism and ore formation, the duration of these processes, the composition and source of mineralizing solutions, and the potential sources of uranium and other ore constituents.

A variety of metallogenetic concepts has been proposed by various geoscientists. Early models on the evolution of the Karamazar U deposits are summarized by Laverov et al. (1993) as follows:

1. The formation of the deposits was related to deep-seated magmatic processes that occurred after volcanic activity ceased, and is chronologically discrete from continental volcanic processes (Smorchkov 1966).
2. The ore deposits were formed as a result of and are genetically linked with hydrothermal activity accompanying volcanic processes (Kotlyar 1968).
3. Ore deposits formed at the final stage of volcanic activity in the anomalous conditions of thermo-artesian depression systems. Metalliferous fluids of magmatic and meteoric origin were involved in ore formation (Barsukov et al. 1972).

Laverov et al. (1993), largely based on their studies of the Chauli deposit, arrive at the following conclusion: The Karamazar U deposits are spatially closely linked to paleovolcanos that extruded a subplatform environment on an ancient, consolidated basement. The position of paleovolcanos, and of volcanic depressions in continental volcanic belts in particular, is controlled by deep fault zones. Uranium mineralization is associated with differentiated intrusive and extrusive volcanic lithologies, for the most part of andesite-rhyolite composition

and increased alkalinity. The deposits formed by postvolcanic polyphase hydrothermal activity. Ore minerals were predominantly deposited in form of stringer-disseminations, stringers, and breccia fillings in discharge areas of the hydrothermal systems. These areas are essentially confined to faults and fracture zones in volcanic rocks, necks, deep morphological depressions that existed at the time of ore formation, and most-permeable sections of lithologic horizons. Associated wall rock alterations are dominated by argillization and beresitization.

The principal U mineral, pitchblende, occurs in several generations and various mineral associations, which formed within a fairly wide range of temperature from 200 to 90°C. The most reliable age of the original uranium ore formation, represented by pitchblende I, is 275–267 Ma as established for the Chauli deposit. This age correlates fairly well with the 280–270 Ma value obtained from intrusive dikes of the final magmatic stage, and with the isotopic ages of wall rock alterations (e.g. 270 Ma for beresite of the Alatanga-Kattasay ore field).

According to Kazansky and Laverov (1977) the isotopic composition of lead and sulfur and the geochemical signatures of rocks and mineralization as well indicate a polygenetic origin of the ore-forming elements. Uranium, fluorine, and heavy metals most likely derived from a deep seated, possibly magmatic source while other ore components have a different provenance. Ore-forming hydrothermal fluids had a temperature of about 200–120°C. Mineral deposition occurred at shallow depth, about 500–3 000 m below surface during Permian time.

Melnikov et al. (1996) established four metallogenetic cycles in the Alatanga-Kattasay ore field, and related fluid inclusions data suggest a decrease of solution temperatures from 290°C at the onset to 160°C at the final stage of the metallogenetic evolution. For more details see Sect. *Alatanga-Kattasay Ore Field*.

With the above given time span of primary pitchblende formation in the Karamazar region, this metallogenetic event in the Hercynian Belt of the western Tien Shan correlates well with the period of 280–260 Ma established for the formation of hydrothermal uranium vein deposits in the Hercynian Orogen in central and western Europe.

15.3.0.1 Chauli

Chauli is located at the western margin of the Chatkal Range, about 80 km SE of the town of Tashkent (Fig. 7.2). Discovered in 1952, the U-Mo deposit was mined by underground methods and delivered about 4 500 t U. Ore grade was similar to deposits in the Alatanga-Kattasay ore field.

Sources of information. Barsukov et al. 1972; Laverov et al. 1972, 1985, 1992b, 1993.

Geology and Mineralization

Chauli occurs in the Karabash Caldera (Fig. 15.17). Crystalline schists intruded by granite and granodiorite (410–385 Ma old) with xenoliths of schists and marble constitute the basement. The caldera is filled with a bipartite volcanic-sedimentary

complex, 500–1 000 m thick. The upper, rhyolitic *Ravashskaya Formation* consists of three Lower Permian horizons of felsic effusives, quartz porphyry and pyroclastic sheets of tuff, tuffaceous breccia, and ignimbrite, intersected by Upper Permian felsite, granite porphyry and lamprophyre dikes, rhyolite and granite porphyry extrusions, and felsite and quartz porphyry domes. The lower *Akchinskaya Formation* is composed of Middle Carboniferous mafic volcanics, 70–250 m thick, including – from top to bottom – dacitic tuff and tuffite, clastic andesite lava 15–80 m thick, and andesitic lava agglomerate 20–150 m thick. Lower Permian dacite and andesite dikes cut these rocks.

Uranium mineralization is confined to felsic extrusions, domes, and dikes of the youngest volcanic formations. Host rocks are altered by argillization, chloritization, and carbonatization. Ore consists of pitchblende, coffinite, and molybdenite associated with galena, chalcopyrite, and pyrite. Gangue minerals include calcite and chlorite. At least two mineral associations are identified: pitchblende I-coffinite-calcite and pitchblende II-sulfides.

Fourteen ore lodes are identified in a 2 km long and 700 m wide zone controlled by the NW-SE-trending Chaulisai fault and bordered by the Pologi and Sushizotny faults. The position of ore lodes is controlled by cataclastic zones and faults cutting volcanic sheets above felsic intrusions. Four geometric-textural configurations of ore lodes are recognized: steeply dipping veins in pyroclastic rocks, pipe- and lens-shaped stockworks, flat lenses composed of veinlets, stringers and disseminated mineralization, and lensoid and pipelike bodies of disseminated mineralization. Veins prevail on upper levels and stockworks on lower levels. Ore lodes are from 50 to 160 m long and 5–60 m wide or thick, respectively.

15.3.0.2 Alatanga-Kattasay Ore Field

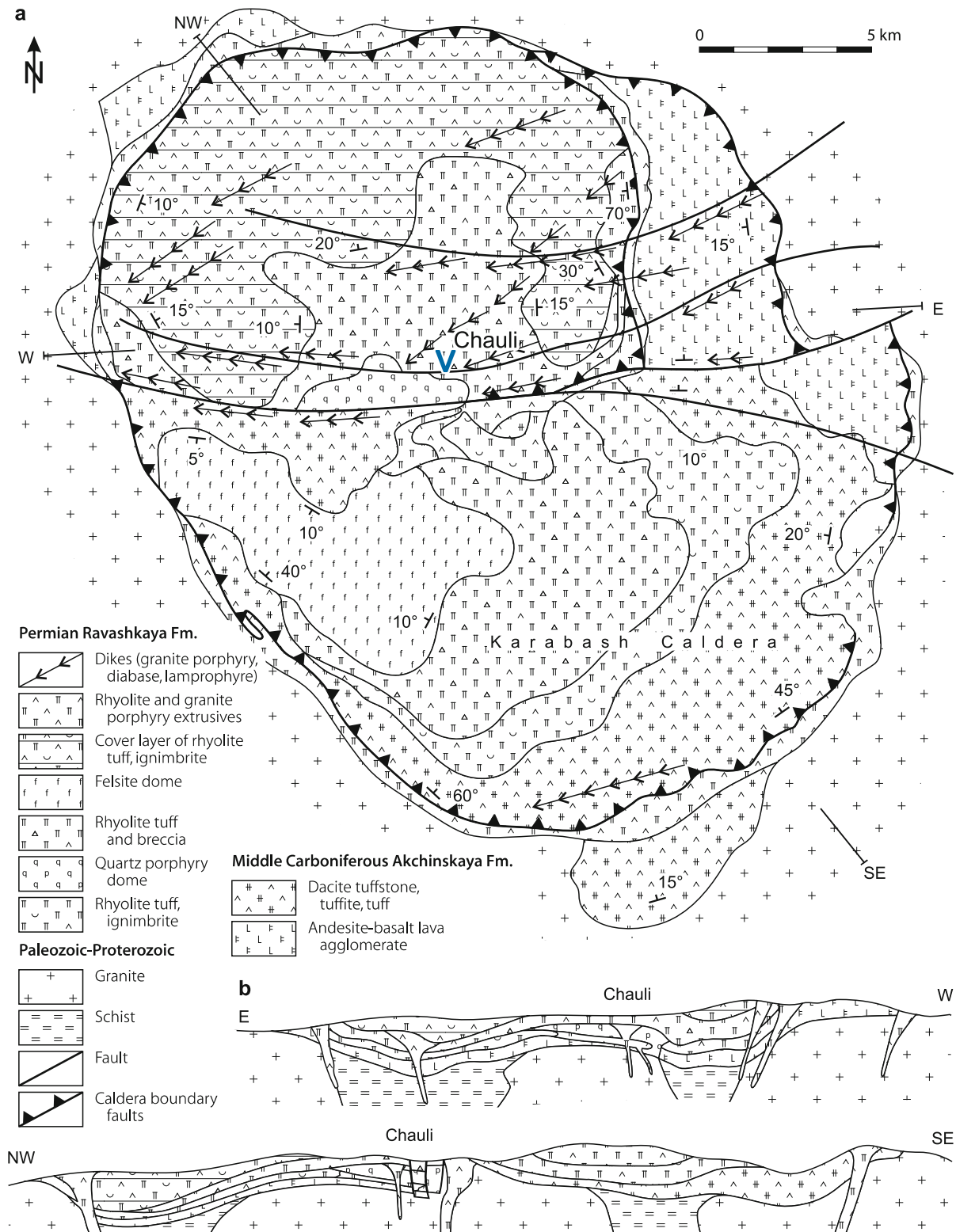
This ore field, located in the SW part of the Chatkal Range, 120 km E of Tashkent, is the largest U ore field in the Karamazar region. It includes a number of polymetallic U-Mo deposits and occurrences including *Alatanga*, centered approximately 3 km to the NW and *Dzhekindek* about 3 km to the SE of *Kattasai*, plus several Pb-Zn occurrences (Figs. 15.18, 15.19). Underground mining of the U deposits started shortly after discovery in 1948–1949 and ceased after their depletion in the early 1990s after yielding some 4 500 t U (from 6 000 t U reserves). Mining grades ranged from 0.03 to 2% U and 0.03–0.5% Mo. In addition to uranium and molybdenum, some tin was recovered at Kattasai.

Source of information: Melnikov et al. (1996) unless otherwise cited.

Geological Setting of Mineralization

The Alatanga-Kattasay ore field is situated at the NW margin of the large mushroom-shaped Babaitaudor intrusive massif composed of Upper Permian, multiphase, felsic subvolcanic

Fig. 15.17. Karamazar region, Chauli deposit, **a** geological map of and **b** sections across the Karabash Caldera showing the lithologic-structural setting of the volcanic-type deposit (see Fig. 7.2 for location) (after Laverov et al. 1993)



■ Fig. 15.18.

Karamazar region, Alatanga-Kattasay ore field, geological map with position of volcanic-type U deposits and occurrences (see Fig. 7.2 for location) (after Melnikov et al. 1996 based on Laverov, Rybalov, Korotaev)

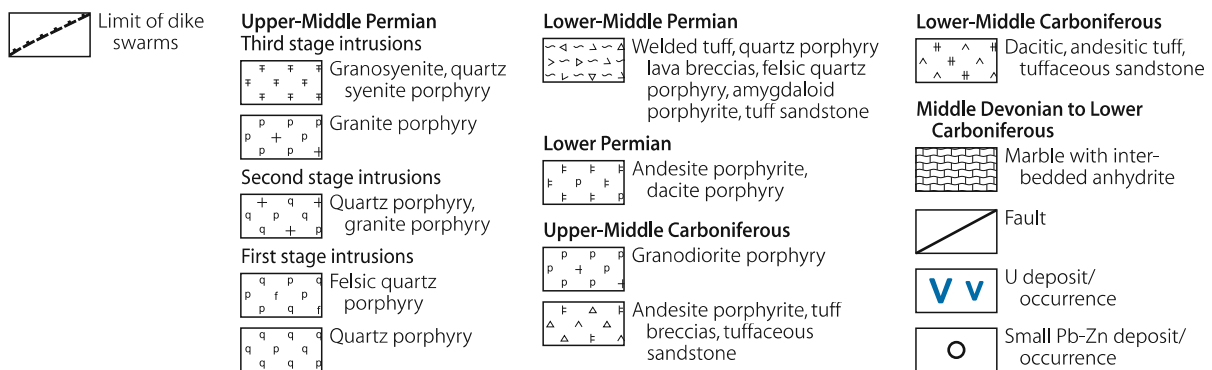
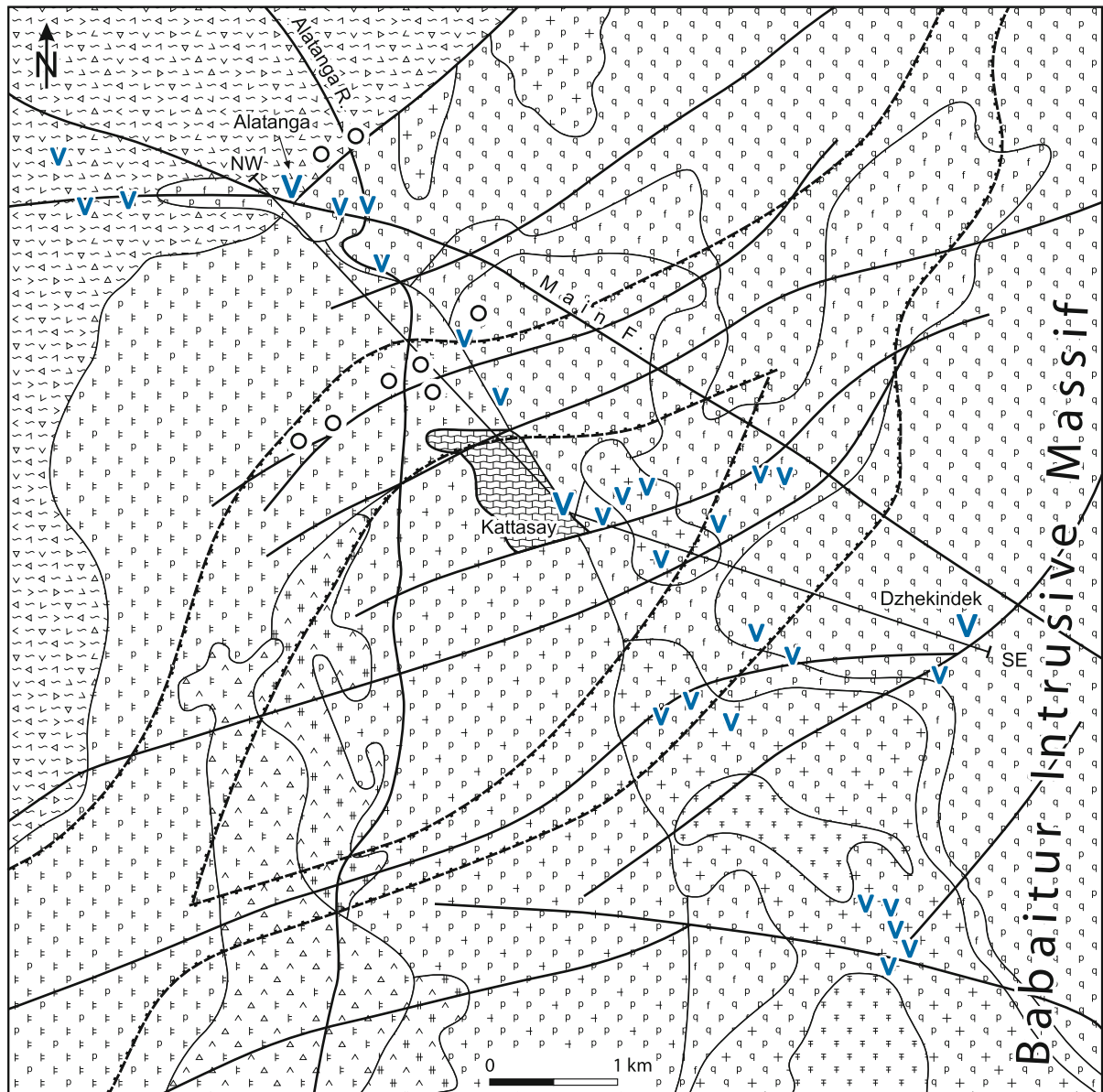
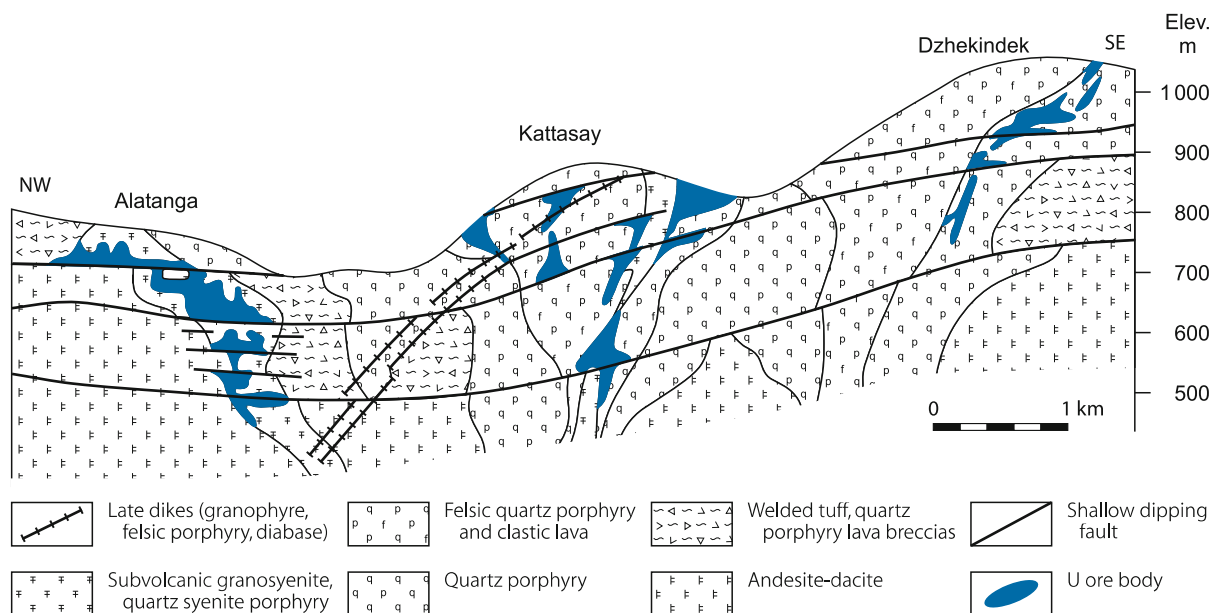


Fig. 15.19.

Karamazar region, Alatanga, Kattasay, and Dzhekindek deposits, geological NW-SE section documenting the irregular shape of stockwork-type U ore lodes and their structurally controlled position in late orogenic felsic volcanic and subvolcanic rocks of Permian age (after Laverov et al. 1992b, Melnikov et al. 1996 based on Tolkunov 1986)



rocks. The bulk of the massif consists of a first phase core facies of quartz porphyry and a marginal facies of felsite and welded felsitic tuff at the periphery of the massif. In a second phase, quartz porphyry and granite porphyry were intruded along the western fault contact with older volcanics. Granite porphyry, granosyenite, and quartz syenite porphyry constitute the youngest phase of the massif.

The Babaitaudor Massif was emplaced into a variety of older rocks. Xenoliths of Middle Devonian-Lower Carboniferous marble with intercalated anhydrite beds are the oldest. Volcanic lithologies start with a thick sheet of Middle to Upper Carboniferous dacitic and andesitic porphyries, tuff breccias, and tuffaceous sandstone intruded by a N-S-elongated granodiorite porphyry body. Lower Permian andesite porphyry and dacite porphyry rest unconformably upon the Carboniferous rocks, followed by Lower to Middle Permian predominantly felsic pyroclastics and porphyry. Two large, about NE-SW-oriented dike swarms transect the ore field (Fig. 15.18).

The leucocratic magmatites have U and Th background values increasing from 6.4 ppm U and 20.1 ppm Th in older rocks to 13.5 ppm U and 40.5 ppm Th in younger facies but retain the same U/Th ratios. Sn values are commonly 10 ppm in granitoid rocks while the youngest quartz syenite porphyry contains as much as 40 ppm Sn. According to Laverov et al. (1992b) these facies also contain distinctly elevated tenors of syngenetic Be, Y, and REE.

Intense faulting and heavy fracturing deformed the terrane. Major faults trend NW-SE to WNW-ESE and NE-SW and dip steeply. They include the large, NW-SE-oriented "Main Fault". Shallow and steeply dipping secondary faults of variable directions are abundant.

Host Rock Alterations

Host rock alterations are reflected – in sequential order – by pre-ore albitization, greisenization, and beresitization, followed by widespread, presumably syn-ore, crystallization of phyllosilicates, albite, quartz, Fe-Mg carbonates, calcite, chlorite, and fluorite.

Albitization resulted in linear bodies, as much as 15 m thick, of white, massive albitite restricted to faults or tectonic interfaces of intrusive bodies. Albite replaces all pre-existing minerals except quartz. Geochemically, albitization resulted in an increase in the central segments of albitite bodies of the Na₂O content of up to 7.8 wt.-% as compared to between 3.8 and 4.2 wt.-% in unaltered felsic precursors, and of FeO from 1.1 to 2.8 wt.-%. Simultaneously K₂O was decreased from between 4.9 and 6.1 wt.-% originally to 0.4 wt.-%, Fe₂O₃ from 1.6 to 0.7 wt.-%, CaO from 1.2 to 0.3 wt.-%, and MgO from 0.25 to 0.08 wt.-%. Tenors of SiO₂, Al₂O₃, TiO₂, CO₂, and S₂– remained practically unchanged.

Greisenization was found at Kattasai below a depth of 680 m where it affected not only granite and late dikes but also albitite at some sites. Down to about 720 m, greisen consists of green veins and lenses, 3–5 cm thick, which widen to over 3 m further down. Common greisen constituents are quartz, muscovite, siderophyllite, and cassiterite. With increasing depth, siderophyllite decreases while muscovite and cassiterite increase, and topaz, zircon, and pyrite appear. Sn tenors range from 0.05 to 1 wt.-% but are commonly between 0.1 and 0.5 wt.-%. Other typomorphic phases include Mo, La, Li, and to a lesser extent W and Bi minerals.

occurrence in the western part of the ore field. Wall rocks are altered by sericitization and/or ankeritization.

2. **Quartz-fluorite-baryte assemblage** is present as veins, veinlets, coatings of rock fragments and cement of breccias. Associated minerals include cleiophane, galena, and ankerite. Wall rocks are altered by sericitization and/or carbonatization.
3. **Pitchblende-sulfide assemblage** occurs as veinlets and disseminations. The richest ore lodes occur where this assemblage is superimposed on the quartz-sulfide-carbonate assemblage or where it cuts carbonaceous (kerite, anthraxolite) tuffite intercalations. Four parageneses are discerned: (a) albite-hematite-U titanates (including brannerite); (b) pitchblende I-molybdenite I + II-quartz-hydromica; (c) pitchblende II-sulfide (bournonite, fahlore, galena); (d) pitchblende III-Fe-chlorite-calcite (with galena and minor cleiophane). The second and third parageneses are most abundant. The three pitchblende varieties have the following lattice constants and impurity contents (in wt.%). Pitchblende I: $a_0 = 5.39\text{--}5.42 \text{ \AA}$; several% Mo and Pb, 0.4–0.5 Mn, 0.05–0.5 Sb and Tl, 0.05–0.1 Zr, 0.005–0.04 Be, and 0.003 Ag. Pitchblende II: $a_0 = 5.43\text{--}5.46 \text{ \AA}$; several% Zr, Pb, Zn, and Ca, 0.5–2 Sb, 0.2–0.3 As and Si, 0.02–0.05 Cu, Cd, Ag, and Mn, 0.0003–0.0005 Be. Pitchblende III contains up to 3% Zr. Fe content in ferrous molybdenite is 5.50–6.72 wt.%. Wall rock alterations relate to the various parageneses. Paragenesis (a) is accompanied by albitization and hematitization, (b) by hydromicization and silicification, (c) and (d) by hematitization, and (d) additionally by carbonatization and chloritization. The hematitic halo around pitchblende-bearing veinlets and aggregates is commonly up to 15 cm and locally up to 2 m wide; it contains dispersed fine-grained, reniform pitchblende and galena.
4. **Post-ore quartz-baryte-fluorite-calcite assemblage** forms veinlets and up to 10 cm thick and as much as 80 m long veins. Associated minerals are partly present in several generations and include chalcopyrite, cleiophane, galena, hematite, marcasite, pyrite, siderite, ankerite, chlorite, and, rarely, cinnabar, pyrrargyrite, and whewellite. Alteration imposed an about 10 cm to a few meters wide aureole on wall rocks by sericitization, silicification, chloritization, and carbonatization. Plagioclase is replaced by sericite, biotite successively by chlorite, sericite and ore minerals, and hornblende by chlorite, quartz, and sericite.

Replacement and recrystallization of various minerals typically occurred where younger assemblages were superimposed on older ones.

Four ore types are distinguished by minero-chemical composition and economic value as outlined further below. *U ores proper* consist essentially of pitchblende. *U-Mo* ore is composed of ferruginous molybdenite and pitchblende associated with hematite, albite, and sericite. *U-Mo-Sn* ore (restricted to Kattasai) has a mineral assemblage of galena, ferruginous molybdenite, pitchblende, and greisen minerals such as cassiterite, fluorite, muscovite, siderophyllite, quartz, topaz, and zircon as a

result of superimposition of U-bearing assemblages on greisens. *U-Ti-Na* ores were found only at great depth and consist of U-Ti phases including brannerite, Ti hydroxides, hematite, and albite.

A combination of structural and lithologic elements provided the sites for deposits and ore lodes. Deposit position and extension are primarily controlled by major structures while ore lode position and shape tend to be a function of shallow and steeply dipping faults and their intersection with youngest magmatic facies, or with interfaces of different lithologies. The largest ore bodies and better ore concentrations occur particularly at heavily fractured intervals.

Shape and Dimensions of Deposits

The Alatanga-Kattasay ore field contains three minable U deposits and some 25 U and almost 10 Pb-Zn occurrences within an area 10 km long in NW-SE direction and up to 2 km wide. Deposits consist of irregularly shaped, variably-sized ore lodes (Fig. 15.19), which may have breccia, stringer, and/or disseminated textures.

The earlier mentioned four ore types differ by economic value. *U ores proper* are of limited distribution and have grades (in wt.-%) from 0.03 to 5% U. *U-Mo* ore is the most extensive type and has grades from 0.03 to 2% U and 0.03–0.5% Mo. *U-Mo-Sn* ore is found at Kattasai at a depth below 680 m; grades range from 0.03 to 5% U, 0.03–0.5% Mo, 0.2–1% Sn and Pb. *U-Ti-Na* ore with grades between 0.03 and 0.08% U were drill intercepted at depths below 1 000 m of present-day surface.

Alatanga: The location of this deposit is controlled by the intersection of the “Main Fault” with the northwestern tectonic contact of the Babeitador Massif. Ore lodes are controlled by gently dipping faults that transect various volcanics including the youngest facies. U ores have predominantly stringer and disseminated, and minor breccia textures. The quartz-sulfide-carbonate assemblage occurs as disseminations in bodies from 20 to 30 cm thick and 6–8 m long. Minerals of the pitchblende-sulfide assemblage occur predominantly as dispersed grains and aggregates and, rarely, as veinlets.

Kattasay: Ore lodes are separated from those of Alatanga by about 1.5 km of barren ground. The deposit is positioned at and controlled by the western tectonic contact of the Babeitador Massif. Ore lodes occur in veins, stockworks, and breccias controlled by intersections of shallow and steeply inclined faults within the youngest magmatic facies. Ore textures are dominated by breccia, stringer, and dissemination styles. The quartz-sulfide-carbonate assemblage occurs as veins, from 20–30 cm thick and 6–8 m long, and the quartz-fluorite-baryte assemblage as veinlets and up to 2 m thick veins. Minerals of the pitchblende-sulfide assemblage form veins, 2–3 cm and, locally, up to 15 cm thick.

Dzhekindek: This deposit is separated from Kattasay by barren ground about 1.5 km wide. The position of the deposit is controlled by a marked NE-SW fault while the size and configuration of ore lodes tend to be a function of gently and steeply dipping faults, which cut the contact of the youngest subvolcanics with rocks of the core facies of the Babeitador Massif. Ore texture is predominantly of stringer and disseminated, and minor breccia nature. The quartz-sulfide-carbonate assemblage is present as disseminations in elongated bands, from 20 to 30 cm thick and 6–8 m long. Veinlets and up to 2 m thick veins are typical for the quartz-fluorite-baryte assemblage whereas minerals of the pitchblende-sulfide assemblage occur predominantly as dispersed grains and aggregates and, rarely, as veinlets.

Fluid Inclusions, Stable Isotopes, and Geochronology

Primary fluid inclusions in quartz, baryte, fluorite, calcite, and ankerite give homogenization temperatures equivalent to temperatures (after correction for pressure) of ore-forming hydrothermal solutions of 290–230°C for the quartz-sulfide-carbonate stage, 280–210°C for the quartz-fluorite-baryte stage, 215–180°C for the pitchblende-sulfide stage, and 220–160°C for the quartz-baryte-fluorite-calcite stage.

Sulfur isotopes of pyrite, chalcopyrite, galena, and sphalerite of the quartz-ankerite-sulfide stage found at Kattasai and Alatanga yield $\delta^{34}\text{S}$ values of +4.5 to +7.4‰ and for Fe-molybdenite $\delta^{34}\text{S}$ values of +6.5 to +8.0‰. Pyrite, chalcopyrite, and molybdenite of the post-pitchblende stage at Alatanga have $\delta^{34}\text{S}$ values of +3.4 to +5.3.

U-Pb age datings yield 270 ± 10 Ma for beresite and pitchblende. Third phase granite porphyry and latest dikes give ages of $280\text{--}270 \pm 10$ Ma.

Ore Controls and Metallogenetic Aspects

Ore controls and/or recognition criteria correspond to those mentioned earlier for the other volcanic-type U deposits in the Karamazar region. A metallogenetic model forwarded for the Alatanga-Kattasay ore field by Melnikov et al. (1996) includes the following events and processes. Ore formation was generated by a hydrothermal system related to late volcanism in which hypogene and supergene solutions were involved. Variable fluid inclusion compositions in ore-related mineral assemblages suggest that the ore forming process was not a single event but consisted of periodic pulsations of solutions of variable compositions, which deposited and/or reworked ore minerals in cyclic intervals interrupted or triggered by episodes of intensified tectonic activity.

Melnikov et al. (1996) established four metallogenetic cycles separated from each other by culminating tectonic activity. As deduced from stable isotopes and fluid inclusions, the authors suggest that crystallization of minerals of each stage started at higher temperatures than those at the end of the preceding stage documenting a temperature inversion between stages. A cyclic inversion is also indicated by anion tenors of fluid inclusions.

Cl/CO₂ ratios in solutions were higher at the beginning than at the termination of each stage. As a result, the initial phases of each stage had higher Cl and lower CO₂ contents than the preceding stage. Temperatures of solutions dropped from 290°C at the onset of the metallogenetic evolution to 160°C at its final stage. Minerals of the pitchblende-sulfide stage deposited at 215–180°C.

Ore and associated minerals were deposited predominantly as veins and breccia fillings at Kattasai suggesting the availability of larger open spaces whereas at Alatanga and Dzhekindek, stringer- and dissemination-type ore textures reflect the absence of such openings. Instead, ore deposition was restricted to small pores and fractures.

The time of ore formation was during the Permian, roughly contemporaneous with the intrusion of third phase granite porphyry and the latest dikes as indicated by ages of 270 ± 10 Ma for beresite and pitchblende, which overlaps with the age of $280\text{--}270 \pm 10$ Ma for these intrusions.

Three sources are postulated for components in the mineralizing solutions. Anions, alkali and calc-alkali elements, Sn, REE, Th, U?, and some water are thought to be of magmatic origin. Sulfur isotope ratios of sulfides in various ore-forming mineral assemblages correspond to those of granitoid magma and, as such, they support a derivation from a magmatic source. A non-magmatic source is accepted for the bulk of the solutions. The principal sources for U and Mo as well as for Ca, Mg, and K were presumably felsic volcanics from which these elements were leached by circulating solutions. Leaching of uranium from host rocks is evidenced by a thick zone depleted in uranium at the U-Mo Chauli deposit located some 40 km to the west of the Alatanga-Kattasay ore field.

15.3.0.3 Maylikatan

Maylikatan is a U-Cu-Pb-Zn deposit situated at the SW margin of the Chatkal Range (Fig. 7.2). Ore lodes are associated with an 80–400 m wide, 65–70° N dipping granite porphyry dike. The dike occupies the Naugarzan fault zone at the southern exocontact of the Babaytag subvolcanic massif. Middle Carboniferous granodiorite occurs in the footwall and Paleozoic tuff in the hanging wall of the dike. Ore lodes occur at the contact and at flexures in the interior of the dike controlled by NE-SW- and E-W-oriented faults. Ore lodes at the dike contact consist of up to 10 m wide, up to 150 m long, and up to 80 m deep veins and lenses. Dike interior lodes are up to 20 m wide, up to 60 m long, and up to 60 m steeply dipping column-like bodies.

15.3.0.4 Rezak

Rezak is located at the southern slope of the Kuramin Range close to the Uzbek-Tadjik borderline. U-Mo mineralization is confined to breccias and fractured intervals at the contact, which separates a Middle Permian rhyolite/felsite porphyry stock from Carboniferous granite and Lower Permian volcanics. Ore lodes consist of columnar stockworks and lenses emplaced in fracture

and breccia zones. Linear networks prevail at depth; they bifurcate upwards into fans of radially arranged veins.

15.3.0.5 Uigar Sai

The *Uigar Sai* (or Yuigar Sai or Atbash) deposit in the Papsk region in the northern Fergana area, discovered 1923, consists of lenses of carnotite disseminations, cavity linings, and coatings of minor faults in continental Miocene sandstone. U is concentrated near fossil logs and organic trash associated with interbedded mudstone lenses. Some ore lenses have cores of higher-grade material. Mineralization is similar to that in deposits of the Colorado Plateau.

References and Further Reading for Chapter 15 • Uzbekistan

For details of publications see Bibliography.

Aleksandrov 1922; Barsukov et al. 1972; Vlasov et al. 1966; Volfson (chief ed) 1978; Bain 1950; Boitsov AV pers. commun.; Chervinsky 1925; Fazlullin et al. 2002; Fersman 1927, 1930; Gorlov et al. 2005; IAEA 1995, 2007; Ischukova et al. 2002; Karimov et al. 1996; Kazansky 1955, 1970; Kazansky and Laverov 1977; Kislyakov and Shchetochkin 2000; Kohl 1954; Komischau 1927; Kotlyar 1968; Kuchersky 1997; Laverov 1972; Laverov et al. 1985, 1992a–c, 1993; Mashkovtsev et al. 1979; Mashkovtsev and Naumov 1999; Melnikov et al. 1996; Minerals Yearbook 1946, 1949; OECD-NEA/IAEA 1993–2005; Perevozchikov 2000; Shcherbakov 1924; Shchetochkin and Kislyakov 1993; Shimkin 1949; Smorchkov 1966; Venatovsky 1993.



Chapter 16

Vietnam

Sandstone-type U occurrences are known from the Nong Son Basin in central Vietnam. A few U occurrences of various types are reported in northern Vietnam. Total in situ U resources in Vietnam amount to some 8 500 t U in the high cost RAR plus EAR-I categories (OECD-NEA-IAEA 2005).

U exploration began by the French Geological Department of Indochina prior to 1955. It was succeeded by Vietnamese governmental institutions in northern Vietnam since 1955. Systematic exploration was initiated in 1978. Presently (2004), U exploration is in the hands of geological and geophysical departments of the Ministry of Industry.

Sources of information: Nguyen Van Hoai and Phan Van Quynh 1992; OECD-NEA/IAEA 1992, 1997, 2001, 2005.

16.1 Nong Son Basin, Central Vietnam

The Nong Son Basin is located in Quang Nam Province, central Vietnam, some 20 km and more to the south and southwest of the city of Da Nang. U mineralization is predominantly of sandstone type.

Reported sandstone-type U deposits include *Khe Hoa-Khe Cao* located some 10 km to the east of the town of Tnamh Afg in the central basin; *Nong Son* to the SE of Khe Hoa-Khe Cao at the southern margin of the basin; *An Diem* to the north of Tnamh Afg in the northern basin; *Dong Nam Ben Giang* (= southeastern Ben Giang) in the southwestern basin, to the SE of the town of Ben Giang; *Pa Rong* to the west of this town; and *Pa Lua* adjacent and to the west of Pa Rong.

Geology and Mineralization

The Nong Son Basin is 50 km long in an E-W direction and 15–20 km wide. It is thought to be the product of rifting in Late Paleozoic-Early Mesozoic time. The basin is filled with Mesozoic sediments 1 500–2 000 m in thickness the bulk of which consists of Upper Triassic continental sediments that are separated into (from top to bottom): Lignite-bearing sediments, 100–200 m thick, a sequence of alternating grey and pink sandstones, mudstones, and shales, 500–1 000 m thick; grey and pink sandstones with carbonaceous matter and intercalated limestone, 300–600 m thick; and conglomerate, 30–50 m thick. These Mesozoic sediments rest unconformably upon Paleozoic sediments in the north and Proterozoic metamorphics in the south. Paleozoic granites with 12–15 ppm U occur at the rims of the basin.

Sandstone-type U mineralization is hosted by Upper Triassic clastic sediments and consists of pitchblende, uraniferous arsenates and vanadates, as well as autunite and carnotite. Ore bodies are mainly of lenticular configuration but roll-shaped ore bodies controlled by redox fronts also occur. Cao HT et al. (2002) report grades of 0.104% U in unweathered, 0.169% U in semi-weathered, and 0.06% U in weathered sandstone ore. Lignite seams are also uraniferous, but the grades are very low.

Khe Hoa-Khe Cao with in situ resources (RAR + EAR-I) of 6 744 t U is the largest deposit discovered so far in the Nong Son Basin. It consists of U mineralization distributed over an area 10 km long and 5 km wide, and positioned within a 150 m thick interval below a depth of 300 m.

An Diem contains 500 t U EAR-I at a grade of 0.034% U and some 1 000 t U EAR-II. Additional resources (EAR-II) of 6 860 t U are reported from the *Tabhing* area (OECD-NEA-IAEA 2001, 2005).

16.2 Other U Deposits/Occurrences in Vietnam

Tien An is a metamorphic-type U occurrence in east-central Vietnam. U mineralization is associated with irregular graphite bodies on the flanks of an anticline of Proterozoic metamorphics.

Nam Xe is a vein-type, uranium-bearing REE occurrence in Lai Chau Province in NW Vietnam. Mineralization occurs in Paleozoic marble forming the core of an anticline. The marble overlies metamorphic and volcanic rocks. Primary mineralization is both in massive veins with 8–10% REO and in impregnations with 1–2% REO. Due to the tropical weathering, the REE content is enriched in weathered material that resembles dark brown soil with 4–5% REO. Ore minerals include pyrochlore, bastnaesite, and parisite. Pyrochlore is the main U host; it contains up to several percent U as well as 2.7–12.4% Nb, some Ta at a Nb:Ta ratio of 5:1, and REE.

Other uraniferous REE occurrences located in northern Vietnam are *Muong Hum* and *Dong Pao*, which are located in vicinity of Nam Xe and *Yon Phu*.

Sinh Quyen is a vein-type Cu-U occurrence in Hoang Lien Son Province, N Vietnam. Ore lodes occur in silicified zones within metasomatized Proterozoic metamorphics. Chalcopyrite, pyrite, and uraninite are the principal ore minerals.

Tule is a volcanic-type U occurrence in Sonla Province in NW Vietnam. Mineralization comprises pitchblende, uranophane, uranium molybdates, and molybdenite contained in felsic to intermediate volcanogenic sediments within a sequence composed of subvolcanic rhyolite, trachyte-liparite porphyry, granitic porphyry, tuffaceous sandstone-mudstone, tuffaceous shale with organic matter, and conglomerate with volcanic components.

Binh Duong is a surficial U deposit in Cao Bang Province in north Vietnam. Mineralization consists of small irregular nests and lenses with autunite and torbernite within Early

Quaternary-Neogene sediments, which cover the contact between a Cretaceous two-mica granite and Devonian limestones.

Low-grade U occurrences similar to the uraniferous lignite in the Nong Song Basin are also known from a number of high-grade coal deposits (anthracite, semi-anthracite) elsewhere in Vietnam.

References and Further Reading for Chapter 16 · Vietnam

For details of publications see Bibliography.

Cao et al. 2002; Nguyen Van Hoai and Phan Van Quynh 1992; OECD-NEA-IAEA 1992, 1997, 2001, 2005.

Chapter 17

Middle East Countries with Uraniferous Phosphorite

The Late Cretaceous Mediterranean phosphorite belt, which extends from southwestern Turkey to Morocco, is represented by a number of minero-chemical uraniumiferous phosphorite deposits in Iraq, Israel, Jordan, and Syria. Published figures of phosphorite resources in these countries are often not clearly defined and/or in discord in various papers. The figures given below are estimates that may have changed since their publication. For precise data, the interested reader is therefore referred to the respective government authorities or phosphate mining companies.

Iraq: Phosphorite resources are located at *Akashat* between the town of Rutba (Al Rutbah) and the Jordanian border. Several phosphate beds occur within a Lower Eocene to Upper Cretaceous sequence of limestone, marl, shale, and siltstone up to 45 m thick. De Voto and Stevens (1979) estimate an amount of recoverable phosphate product of 579 million t containing on average 130 ppm U. Pool (1993) calculated from these figures potentially recoverable uranium resources of some 58 000 t (based on a U recovery rate of 77%). Krauss et al. (1984) report 500 million t ore resources at grades ranging from 17.5 to 22.5% P_2O_5 for the open pit mining area at Akashat.

Israel's phosphorite deposits are all located in the Negev Desert. About twenty phosphorite ore fields/deposits have been identified. Deposits, which have been mined, include *Hor Harar*, *Maktesh* (Mactesh) *Qatan*, *Mishor Rotem?*, *Nahal Zin*, *Oron*, and *Zefa E'fe* (Arad). All are situated in the northern Negev Desert to the south and east of the town of Beersheba and the Jordanian border.

The Negev phosphorites occur in relatively narrow synclines, trending NE-SW, hosted by the Late Campanian Upper Mishash Formation. This formation consists of alternating beds, one to two meters thick each, of one to four phosphorite beds intercalated with chert, chalk and, limestone horizons. The lowest phosphorite bed commonly rests upon a massive chert horizon. Marl and chalk, locally with a basal oil shale horizon of the Maastrichtian Ghareb Formation, rest upon the Mishash Formation while chalk of the Santonian Menuha Formation underlies the Mishash Formation.

In the *Zefa* deposit, as described by Avital et al. (1983), mineralization consists of phosphorite composed of small bone fragments, oolitic, and coprolitic grains mixed with clay and marl. Carbonate-fluorapatite (francolite) constitutes the principal phosphate mineral. Calcite or apatite forms the matrix – if present. Bone phosphorite is the main type in the *Zefa* deposit.

Zefa has one of the highest-grade phosphate (24–32% P_2O_5) and uranium (<225 ppm) ores in the Negev deposits. Samples of the upper and lower phosphorite beds average 138 ± 32 ppm U and 173 ± 18 ppm U, respectively.

Bartels and Gurr (1994) give a figure of 600 million t for Israel's phosphate rock resources (including 300 million t of economic resources). Krauss et al. (1984) report 428 million t ore resources at grades ranging from 20 to 33.9% P_2O_5 for deposits at *Zefa E'fe* (Arad), Beersheva, *Maktesh* (Mactesh), *Nahal Zin*, and *Oron*. Nathan and Shiloni (1976) report reserves of 292 million t phosphorite for nine ore fields/districts in the northern Negev Desert with grades ranging from 22–26% in the *Oron* to 28–32% P_2O_5 in the *Maktesh Qatan* District. The U concentration varies in the nine phosphorite districts; average contents range from 91 (Saraf) to 159 ppm U (*Zefa*), and U/ P_2O_5 ratios (normalized mean) from 3.54 (Saraf) to 5.89 ppm U per 1% P_2O_5 (*Zefa*). Based on the data provided by Nathan and Shiloni (1976), these nine districts would contain about 33 000 t U in situ resources.

Jordan: Phosphorite deposits are found over a distance of some 250 km in a N-S-oriented belt in western Jordan, from Ras en Naqb in SW Jordan to the north of Amman. The Wadi Araba-Jordan Graben forms the western boundary of this belt. Deposits, which have been mined include, *Al Hasa-Al Qatrana*, *Al Shediya*? and *Ruseifa*.

Phosphorite beds occur in the relatively flat-lying Belga Series of Maastrichtian-Danian age. The Belga Series comprises an alternating sequence, up to 45 m thick at *Ruseifa*, of limestone, oyster beds, marl, some chert, and four phosphorite layers 1–3 m thick. *Al Hasa* contains two phosphorite beds with a cumulative thickness of about 2.5 m. P_2O_5 contents in phosphorite range from 15 to 33%.

Krauss et al. (1984) report P_2O_5 contents of 28–33% in ore mined at *Ruseifa*, 29.7% at *Al Hasa*, and 26.5% at *Al Shediya*, and cumulative resources of 1 678 million t phosphorite ore for these three deposits. Bender et al. (1970) reports U concentrations of 80–120 ppm in phosphorite ore for *Ruseifa* and *Al Hasa*. Samples with over 30% P_2O_5 analysed by Reeves and Saadi (1971) contained 120 ppm U. De Voto and Stevens (1979) estimate an amount of recoverable phosphate product of 3 000 million t containing an average of 120 ppm U. From these figures, Pool (1993) calculated potentially recoverable resources of some 277 000 t U.

Syria: Phosphorite deposits occur in the general area of the oasis town of Palmyra in the central part of the country. Deposits are located in the *Eastern A* and *B* and *Kneifiss* (Kneifes) areas in the *Ghadir el Hamel* region, some 50–80 km SW of Palmyra; the *Al Haberi* (Maberi) area, about 100 km SE of Palmyra; and the *Wadi al Rakheime* area to the NW of Palmyra.

Phosphorite beds are intercalated in a relatively flat-lying Campanian sequence, from 30 to 150 m in thickness, composed of fine-grained, argillaceous limestone, marl, and chert. The

phosphorite beds are from 1 to 20 m thick with abrupt lateral changes in thickness.

De Voto and Stevens (1979) estimate an amount of recoverable phosphate product of 405 million t containing in average 130 ppm U. Pool (1993) calculated from these figures potentially recoverable resources of some 40 000 t U. Krauss et al. (1984) report 431 million t ore resources at grades ranging from 27.5 to 29.6% P_2O_5 for the open pit mining areas at Kneifiss and Eastern A and B.

References and Further Reading for Chapter 17 · Middle East Countries with Uraniferous Phosphorite

For details of publications see Bibliography.

Avital et al. 1983; Bartels and Gurr 1994; Bender et al. 1970; Cathcart 1978; De Voto and Stevens 1979; Krauss et al. 1984; Nathan and Shiloni 1976; Pool 1993; Reeves and Saadi 1971; Saadi and Shaaban 1981.

Bibliography

- Abakumov AA (1995) Uranium raw material base of the Republic of Kazakhstan. TECDOC-823, IAEA, Vienna, pp 163–176
- Abakumov AA, Zhelnov VP (1997) Short geological description of the Inkai uranium deposit in south Kazakhstan. *In: Changes and events in uranium deposit development, exploration, resources, production and the world supply-demand relationship*. TECDOC-961, IAEA, Vienna, pp 201–202
- Achar KK, Pandit SA, Natarajan V, Kumar MK, Dwivedy KK (2001) Bhima Basin, Karnataka, India, uranium mineralisation in the Neoproterozoic. *In: Assessment of uranium deposit types and resources – A worldwide perspective*. TECDOC-1258, IAEA, Vienna, pp 129–140
- Adams SS, Saucier AE (1981) Geology and recognition criteria for uraniferous humate deposits, Grants mineral region, New Mexico. US-DOE, GJBX-2(81), 225 p
- Adams SS, Smith RB (1981) Geology and recognition criteria for sandstone uranium deposits in mixed fluvial-shallow marine sedimentary sequences, south Texas. Final report, US-DOE, GJBX-4(81), 145 p
- Aleksandrov S (1922) Die Radiumexpedition nach Tyuya-Muyun. *Berg-Journal, Moskau*, Nr. 22, pp 415–416
- Aleshin AP, Rassulov VA, Velichkin VI, Cuney M (2003a) X-ray, cryo-photo and laser luminescence of fluorite as typomorphic feature indicating uranium ore grade at the Mo-U deposits of the Streltsovskaya Caldera (Eastern Transbaikalia). *In: Cuney et al. (eds) Uranium geochemistry*. Univ Henri Poincaré, Vandoeuvre les Nancy, pp 29–32
- Aleshin AP, Velichkin VI, Krylova TL, Golubev VN, Cuney M, Poty B (2003b) Unique Mo-U deposits of the Streltsovskaya Caldera (eastern Transbaikalia, Russia): Geological settings, mineralization and formation conditions. *In: Cuney et al. (eds) Uranium geochemistry*. Univ Henri Poincaré, Vandoeuvre les Nancy, pp 33–36
- Aleshin AP, Velitchkin VI, Cuney M, Dymkov YM (2005) Polyphase coffinite-like V-Si Gel and its role in uranium redistribution in the Mo-U deposits of the Streltsovsky ore field (Transbaikalia, Russia). *In: Symposium on uranium production and raw materials for the nuclear fuel cycle – Supply and demand, economics, the environment and energy security*. Extended synopsis. CN-128, IAEA, Vienna, pp 255–259
- Alexander RL (1986) Geology of Madawaska Mines Limited, Bancroft, Ontario. *In: Evans EL (ed) Uranium deposits of Canada*. CIM Spec v 33, pp 62–69
- Altschuler ZS, Clarke RS, Jr, Young EJ (1958) Geochemistry of uranium in apatite and phosphorite. US Geol Surv Prof Paper 314-D, pp 45–90
- Andreeva OV, Golovin VA (1999) Uranium deposits and alteration processes at the Late Mesozoic Tuluevskoe Caldera, Transbaikalia, Russia. *In: Mineral Deposits: Process to processing*. Balkema, Rotterdam, pp 467–470
- Andreeva OV, Volfson FI, Golovin VA, Rossman GI (1990) Uranium behavior in the processes of low-temperature alteration of wall rocks. *Geokhimiya*, no 2, pp 21–31, (in Russian)
- Andreeva OV, Arakelyants MM, Golovin VA, Golubev VN (1991) K-Ar dating of low-temperature metamorphites for dispersed micas. *Iz AN SSSR, Geol Ser*, no 8, pp 95–102, (in Russian)
- Andreeva OV, Aleshin AP, Golovin VA (1996a) Vertical zonality of wall rock alterations at the Antei-Streltsovsk uranium deposit, eastern Transbaykal region, Russia. *Geol Ore Deposits*, v 38, no 5, pp 353–366
- Andreeva OV, Golovin VA, Kozlova PS, Seltsov BM, Chernyshev IV, Arakelians MM, Goltzman IV, Bairova ED (1996b) Evolution of Mesozoic magmatism and ore-metasomatic processes in southeast Transbaykalia. *Geol Rudn Mestorozhd*, v 38, no 6, pp 115–130, (in Russian)
- Anhaeusser CR, Maske S (eds) (1986) Mineral deposits of southern Africa. *Geol Soc S Afr*, v 1, 2, 2340 p
- Arakel AV (1988) Carnotite mineralization in inland drainage areas of Australia. *In: Gabelman JW (ed) Unconventional uranium deposits*. *Ore Geol Rev*, v 3, pp 289–311
- Arzruni A (1885) Untersuchung einiger granitischer Gesteine des Urals. *Z dt geol Ges*, Nr. 37
- Aubakirov KB (1998) On the deep origin of ore-forming solutions in the uranium deposits in platform sequence of depressions (with Chu-Sarysu Province as an example). *Geology of Kazakhstan* 2(354), pp 40–47
- Avital Y, Starinsky A, Kolodny Y (1983) Uranium geochemistry and fission-track mapping of phosphorites, Zefa Field, Israel. *Econ Geol*, v 78, pp 121–131
- Avrashov A (1980) Albitized uranium deposits: Six articles translated from Russian literature. US-DOE, GJBX-193(80), 114 p
- Awati AB, Grover RB (2005) Demand and availability of uranium resources in India. *In: Recent developments in uranium exploration, production, and environmental issues*. TECDOC-1463, IAEA, Vienna, pp 7–16
- Azhar AM, Qamar NA, Butt KA (2003) Study of radioactive occurrences in middle Siwalik molasse of Khisor Range, Bannu Basin, Pakistan. *In: Cuney et al. (eds) Uranium geochemistry*. Univ Henri Poincaré, Vandoeuvre les Nancy, p 62
- Baig MSA (1990) Recognition of remobilized uranium deposition environments in Dhok Pathan Formation of Siwalik Group, District Bannu, Pakistan. *In: Uranium Provinces in Asia and Pacific*. IAEA Techn Com Meetg, Beijing, 17 p, 17 figs, 3 tables
- Bain GW (1950) Geology of the fissionable materials. *Econ Geol*, v 45, no 4, pp 273–323
- Bakarzhiyev ACh, Makhivchuk OF, Nizovsky VN, Popov NI (1995a) The Kirovograd uranium ore bearing district, Ukraine. *Otechestvennaya Geologia*, no 9, pp 45–55, (in Russian)
- Bakarzhiyev ACh, Makhivchuk OF, Komarov AN, Popov NI, Lovinyukov VI, Koval VB, Kramar OA (1995b) Deposits of sodium-uranium formation. *In: Belevtsev YN, Koval VB (eds) Genetic types and regularities of the location of uranium deposits in Ukraine*. Navkova, Dumka, Kiev, pp 94–125, (in Russian)
- Bakarzhiyev (also spelled *Bakarzhiev* or *Bakarjiev*) ACh, Makhivchuk OF, Popov NI (1997) The industrial types of uranium deposits of Ukraine and their resources. *In: Changes and events in uranium deposit development, exploration, resources, production and the world supply-demand relationship*. TECDOC-961, IAEA, Vienna, pp 35–42
- Banerjee AK (1975) On the evolution of the Singhbhum nucleus, eastern India. *Geol Min Met Soc India, Quat J*, v 47, pp 51–60
- Banerjee DC (2005) Uranium exploration in the Proterozoic Basins in India – Present status and future strategy, India. *In: Developments in uranium resources, production, demand and the environment*. TECDOC-1425, IAEA, Vienna, pp 81–94
- Banerjee AK, Talapatra AK, Shankaran AV, Bhattacharyya TK (1972) Ore genetic significance of geochemical trends during progressive migmatization within part of the Singhbhum shear zone, Bihar. *J Geol Soc India*, v 13, pp 39–50
- Barsukov VL, Gladisher GD, Kosirev VN et al. (1972) Conditions of uranium ore deposit formation in volcanic depressions. *Atomizdat, Moscow*, (in Russian)
- Bartels JJ, Gurr TM (1994) Phosphate rocks. *In: Carr DD (sen ed) Industrial minerals and rocks*, 6th edn. Soc Mining, Metall, Expl, Littleton, Colorado, pp 751–764
- Barthel F, Dahlkamp FJ, Fuchs H, Gatzweiler R (1986) Kernenergieerohstoffe. *In: Bender F (ed) Angewandte Geowissenschaften*. Ferd. Enke Verlag, Stuttgart, pp 268–298
- Barthel FH (1988) Sandstone uranium deposits in central Sumatera, Indonesia, and northern Thailand. *In: Uranium deposits in Asia and the Pacific: Geology and exploration*. IAEA, Vienna, pp 179–192
- Basham IR, Matos Dias JM (1986) Uranium veins in Portugal. *In: Vein type uranium deposits*. TECDOC-361, IAEA, Vienna, pp 181–192
- Basham IR, Rice CM (1974) Uranium mineralization in Siwalik sandstones from Pakistan. *In: Formation of uranium ore deposits*. IAEA, Vienna, pp 405–417
- Basham IR (1980) Charged-particle track analysis in the assessment of sandstone-type uranium ore from Pakistan. *Nucl Tracks*, v 4, pp 33–40
- Batbold T (2001) Uranium favourability and evaluation in Mongolia (Phase II), recent events in uranium resources and production in Mongolia. *In: Assessment of uranium deposit types and resources – a worldwide perspective*. TECDOC-1258, IAEA, Vienna, pp 93–100
- Belevtsev YN, Koval VB (eds) (1995) Genetic types and regularities of the location of uranium deposits in Ukraine. Navkova, Dumka, Kiev, 395 p (with contributions by Bakarjiev et al., Grechishnikov, Koval et al., Shumlyansky et al., Syrodov et al. and others), (in Russian)

- Belevtsev YN, Batashov BG, Koval VB (1984a) The Zholtve Vody uranium deposit and the iron ore deposits of Krivoi Rog. 27th Intern Geol Congr, Guidebook, Excursion 108, Moscow, pp 21–32
- Belevtsev YN, Koval VB, Stryghin AI (1984b) Genetic pattern for the deposits of uranium-albite formation. *In: Metallogenesis and uranium deposits*. 27th Intern Geol Congr, abstr, v IX, pt 1, Moscow, pp 332–333
- Belevtsev YN, Barkarzhiev AKh, Koval WB, Makivchuk OF, Popov NI, Lovinyukov VI, Sykov EA (1992) Uranium deposits of Ukraine. *Geol Zhur* 5, pp 28–44, (in Russian)
- Bell KG (1963) Uranium in carbonate rocks. *US Geol Surv Paper* 474-A, 29 p
- Bell RT (1978) Uranium in black shales: A review. *In: Kimberley MM* (ed) Short course in uranium deposits: Their mineralogy and origin. *Miner Ass Can, Short Course Handbook* no 3, pp 207–329
- Bender F, Eckhardt FJ, Heimbach W (1970) Rohstoffe zur Düngemittelherstellung auf Phosphatbasis in Jordanien. *Ber Bundesanst Bodenforsch, Hannover*, 31 p
- Berning J (1986) The Rössing uranium deposit, South West Africa/Namibia. *In: Anhaeusser CR, Maske S* (eds) Mineral deposits of Southern Africa. *Geol Soc S Afr*, v 2, pp 1819–1832
- Berning J, Cooke R, Hiemstra SA (1976) The Rössing uranium deposit, SWA. *Econ Geol*, v 71, pp 351–368
- Berzina IG, Yeliseyeva OP, Popenko DP (1974) Distribution relationships of uranium in intrusive rocks of Northern Kazakhstan. *Intern Geol Rev*, v 16, 11, pp 1191–1204
- Bhasin JL (1997) Uranium mining and production of concentrates in India. *In: Changes and events in uranium deposit development, exploration, resources, production and the world supply-demand relationship*. *TECDOC-961*, IAEA, Vienna, pp 307–322
- Bhattacharyya AK et al. (1992) Chhotanagpur granite-gneiss complex, Rihand Valley, Sonbhadra District, Uttar Pradesh. *Ind J Geol*, v 64, no 2, pp 259–276
- Bhattacharyya DS, Sanyal P (1988) The Singhbhum orogen – Its structure and stratigraphy. *In: Mukhopadhyay D* (ed) Precambrian of the Eastern Indian Shield. *Geol Soc Ind, Bangalore*, pp 85–111
- Bhola KL (1965) Radioactive deposits in India. *Symp uranium prospecting and mining in India*. DAE, Jaduguda, pp 1–45
- Bhola KL (1972) Uranium deposits in Singhbhum and their development for use in the nuclear power programme in India. *Proc Ind Nat Sci Acad*, 37A, pp 277–296
- Bhola KL, Rama Rao YN, Surrastry C, Mehta NR (1966) Uranium mineralization in Singhbhum thrust belt, Bihar, India. *Econ Geol*, v 61, pp 162–173
- Binns R, McAndrew J, Sun SS (1980) Origin of uranium mineralization at Jabiluka. *In: Ferguson J, Goleby A* (eds) Uranium in the Pine Creek Geosyncline. IAEA, Vienna, pp 543–562
- Birka GI, Dubinchuk VT, Pogibelny AA, Khorosova OL, Artyukhina AI (1995) Natural U-Mo-containing zirconium-siliceous glasses and Glass-crystalline materials from Kazakhstan. *Science*, pp 62–70
- Birka GI, Osipov BS, Khorosova OD, Goleva RV, Dubinchuk VT, Raudonis PA (2003) U-Mo-containing Zr-Si glasses in hydrothermal U ore formation. *In: Cuney M* (ed) Uranium geochemistry 2003. Nancy, France, pp 69–74
- Birka GI, Nikolsky AL, Tarkhanov AV, Shulgin AS (2005) Zoning of ore fields with brannerite mineralization. *In: Symposium on uranium production and raw materials for the nuclear fuel cycle – Supply and demand, economics, the environment and energy security*. Extended synopsis. CN-128, IAEA, Vienna, pp 241–244
- Blondeau CF (1827) *Manuel de minéralogie*. II éd., Paris
- Bohse H, Rose-Hansen J, Sørensen H, Steenfelt A, Løvborg L, Kunzendorf H (1974) On the behaviour of uranium during crystallization of magmas – With special emphasis on alkaline magmas. *In: Formation of uranium ore deposits*. IAEA, Vienna, pp 49–60
- Boitsov VE (1996) Geology of uranium deposits. *MGGa*, Moscow, 72 p, (in Russian)
- Boitsov VE (1989) Geology of uranium deposits. *NEDRA*, Moscow, 302 p, (in Russian)
- Boitsov AV (1999) Uranium districts and deposits in Russian Federation. Manuscript for IAEA Atlas/UDEPO, 39 p
- Boitsov AV, Nikolsky AL (2001) Characteristics of uranium districts of the Russian Federation. *In: Assessment of uranium deposit types and resources – A worldwide perspective*. *TECDOC-1258*, IAEA, Vienna, pp 61–76
- Boitsov VE, Pilipenko GN (1998) Gold and uranium in the Mesozoic hydrothermal deposits of the central Aldan region. *Geol Ore Dep*, v 40, no 4, pp 315–328
- Boitsov VE, Pilipenko GN (2000) Accumulation and localization regularities of complex uranium-gold ores. *In: Gavrilin VI et al.* (eds) Uranium at the turn of the century: Resources, production, demand. *Abstr Intern Symp Uran Geol*, Moscow, All-Russian Sci Res Inst Mineral Resources NM Fedorovsky, pp 90–91
- Boitsov AV, Birka GI, Nicolsky AL, Shulgin AS (1995) Application of mineralogical-technological mapping for ores: Qualitative evaluation of endogenic uranium deposits of Streltsovsk and Kokchetavsk uranium ore regions. *TECDOC-823*, IAEA, Vienna, pp 213–224
- Boitsov AV, Nikolsky AL, Chernigov VG, Ovseichuk VA (2002) Uranium production and environmental restoration at the Priargunsky Centre, Russian Federation. *In: The uranium production cycle and the environment*. *CandS Papers Series 10/P*, IAEA, Vienna, pp 199–204
- Boyle DR (1984) The genesis of surficial uranium deposits. *In: Surficial uranium deposits*. *TECDOC-322*, IAEA, Vienna, pp 45–52
- Briot P (1978) Phénomènes de concentration de l'uranium dans les environs évaporitiques intercontinentaux: les calcrètes de l'Yilgarn Australien. *Essai de comparaison avec les calcrètes de Mauritanie et de Namibie*. Thèse Orsay, 167 p
- Bruneton P (1987) Geology of the Cigar Lake uranium deposit, Saskatchewan, Canada. *In: Gilboy CF, Vigrass LW* (eds) Economic minerals of Saskatchewan. *Sask Geol Soc Spec Publ* 8, pp 99–119
- Bruneton P (1993) Geological environment of the Cigar Lake uranium deposit. *Can J Earth Sci*, v 30, pp 653–673
- Brynard HJ, Andreoli MAG (1988) The overview of the regional, geological and structural setting of the uraniferous granites of the Damara Orogen, Namibia. *In: Recognition of uranium provinces*. IAEA, Vienna, pp 195–212
- Budunov AA (2002) Hydrogenic uranium deposits of Mongolia. *In: Proceedings of geology of uranium, rare-metal, and rare-earth-metal deposits*, VIMS, Inform Zbornik no 144 Moscow, pp 84–89, (in Russian)
- Bureau of Geology, CNNC (1990) Uranium provinces in China. *Bur Geol, CNNC*, Beijing, China
- Bureau of Geology, CNNC (2002) Sandstone-type uranium deposits in China: Geology and exploration techniques. *Atomic Energy Press*, Beijing, 217 p
- Butt KA (1989a) Uranium occurrences in magmatic and metamorphic rocks of northern Pakistan. *In: Uranium deposits in magmatic and metamorphic rocks*. IAEA, Vienna, pp 131–154
- Butt KA (1989b) Release of uranium through cataclastic deformation of Manehra granite gneiss and its precipitation in the overlying intramountain basin in northern Pakistan. *In: Uranium deposits in magmatic and metamorphic rocks*. IAEA, Vienna, pp 155–166
- Butt CRM, Mann AW, Horwitz RC (1984) Regional setting, distribution and genesis of surficial uranium deposits in calcretes and associated sediments in Western Australia. *In: Surficial uranium deposits*. *TECDOC-322*, IAEA, Vienna, pp 121–127
- Button A, Adams SS (1981) Geology and recognition criteria for uranium deposits of the quartz-pebble conglomerate type. *US-DOE, GJBX-3(81)*, 390 p
- Bykadorov VA, Bush VA, Fedorenko DA, Filipova IB, Miletenko NV, Puchkov VN, Smirnov AV, Uzhekenov BS, Volozh AV (2003) Ordovician-Permian palaeogeography of Central Eurasia: Development of Palaeozoic petroleum-bearing basins. *J Petrol Geol*, v 26, pp 325–350
- CAMECO, Annual report 2000
- Cameron E (1984) The Yeelirrie calcrete uranium deposit, Western Australia. *In: Surficial uranium deposits*. *TECDOC-322*, IAEA, Vienna, pp 157–165
- Camisani-Calzolari FAGM, Ainslie LC, Van Der Merwe PJ (1986) Uranium in South Africa (1985). *AEC-S Afr*, Pretoria, 27 p
- Cao HT, Le QT, Dinh MT, Than VL, Le KD (2002) Uranium leaching and recovery from sandstone ores of Nong Son Basin, Viet Nam. *In: The uranium production cycle and the environment*. *CandS Papers Series 10/P*, IAEA, Vienna, pp 547–549
- Carlisle D (1983) Concentration of uranium and vanadium in calcretes and gypcretes. *In: Wilson RCL* (ed) Residual deposits: Surface-related weathering processes and materials. *Geol Soc, London*, pp 185–196
- Carlisle D, Merifield PM, Orme RR, Kohl MS, Kolker O (1978) The distribution of calcretes and gypcretes in southwestern United States and their uranium

- favourability based on a study of deposits in Western Australia and South West Africa (Namibia). US-DOE, GJBX-29(78), 274 p
- Carlsson D, Nojd LA (1977) Uranium production from low-grade Swedish shale. Paper (IAEA-CN 36/277), Intern Conf Nuclear Power and its Fuel Cycle, Salzburg, 12 p
- Carroll PA (1997) The reconstruction of the uranium industry in Kazakstan. *In: Uranium and nuclear energy: 1997*. Uranium Institute, London, pp 91–98
- Catchpole G (1997) The Inkay ISL uranium project in Kazakstan. 22nd Annual Symposium, Uranium Institute, London, manusc 6 p
- Cathcart J (1978) Uranium in phosphate rock. US Geol Surv Prof Paper 988-A, pp A1–A6
- Cathelineau M (1984) Uranium veins in western France, mineralogy and geochemistry of uranium deposition. *In: Proc ICAM 84 Congr*, Los Angeles, TMS AIME, pp 1083–1094
- Cavaney RJ (1984) Lake Maitland uranium deposit. *In: Surficial uranium deposits*. TECDOC-322 IAEA Vienna, pp 137–140
- CEA (1976–1977) Overseas Mineral Exploration: Indonesia, Project Kalan, Kali 14.44 (final report)
- Chabiron A (1999) Les gisements d'uranium de la caldeira de Streltsovka (Transbaikalie, Russie), PhD thesis UHP, 266 p
- Chabiron A, Alyoshin AP, Cuney M, Deloule E, Golubev VN, Velitchkin VI, Poty B (2001) Geochemistry of the rhyolitic magmas of the Streltsovka Caldera (Transbaikalia, Russia): A magmatic – inclusion study. *Chem Geol*, v 175, pp 273–290
- Chabiron A, Cuney M, Poty B (2003) Possible uranium sources for the largest uranium district associated with volcanism: The Streltsovka Caldera (Transbaikalia, Russia). *Mineral Deposita*, v 38, pp 127–140
- Chaki A, Panneerselvam A, Chavan SJ (2006) Uranium exploration in the Upper Proterozoic Bhima Basin, Karnataka, India: A new target area. *In: Symposium on uranium production and raw materials for the nuclear fuel cycle*. Proceedings Series, IAEA, Vienna, pp 183–194
- Chapot G, Couprie R, Dumas J, Leblanc P, Kerouanton JL (1996) L'uranium vendéen. *Cahiers du Patrimoine*, no 45, Dir Rég Affaires Cult Pays de la Loire, Nantes, 221 p
- Chemillac R (2004) Caractéristiques géochimiques originelles et transferts de matière lors de altération des roches volcaniques acides associées aux minéralisations uranifères. Thèse Dr., Univ Henri Poincaré, Nancy, France, 494 p
- Chemillac R (2004) Géochimie des magmas associés aux gisements d'uranium intravolcaniques. PhD thesis, Nancy Université, 383 p
- Chemillac R, Cuney M, Zhou W, Liu X (2005a) The Xiangshan uraniferous caldera, Southeast China: Geochemistry and melt inclusions. *In: Symposium on uranium production and raw materials for the nuclear fuel cycle – supply and demand, economics, the environment and energy security*. Extended synopsis. CN-128, IAEA, Vienna, 231–234
- Chemillac R, Cuney M, Petrov VA, Golubev VN, Pujol M (2005b) Uranium deposit favourability estimation from pristine rhyolitic magma composition of the Dornot uranium ore field, Mongolia. *In: Symposium on uranium production and raw materials for the nuclear fuel cycle – supply and demand, economics, the environment and energy security*. Extended synopsis. CN-128, IAEA, Vienna, pp 96–99
- Chen Anping, Wu Rengui, Miao Aisheng, Zhu Minqiang, Yu Dagan (2002) Mineralization characteristics of Dongsheng uranium mineralized area, Ordos Basin. *In: Bureau of Geology, CNNC (ed) Sandstone-type uranium deposits in China: Geology and exploration techniques*. Atomic Energy Press, Beijing, pp 88–97
- Chen Ranzhi, He Gaiyi (1996) Metallogenetic conditions of volcanic-type uranium deposits in South China. *In: Chen Zhaobo et al. (eds) Galaxy of research achievements of uranium geology in China*. Uranium geol, Beijing, pp 66–74
- Chen Yifeng (1996) Discussion on uranium metallogenic regularities in Lu-Zong region. *In: Chen Zhaobo et al. (eds) Galaxy of research achievements of uranium geology of China*. Uranium Geol, Beijing, pp 75–85
- Chen Youliang, Zu Xiyang (2002) Sandstone type uranium deposits in Western Yunnan, Southwest China: Geological setting of mineralization and comparison with those in Trans-Baikal, Russia. *In: Bureau of Geology, CNNC (ed) Sandstone-type uranium deposits in China: Geology and exploration techniques*. Atomic Energy Press, Beijing, pp 119–126
- Chen Yuehui (1995) The metallotectonic stress field in the west of the Xiangshan uranium ore field and its relations to uranium mineralization. *Mineral Deposits*, v 14, no 3, pp 250–259
- Chen Yuqi et al. (1996) An introduction to the regional geology of China. Publ House Geol, Beijing, 517 p, (in Chinese) (Chapter Five (Regional geological characteristics of S. China region by Yang Minggui et al.), Section Five: Geological structure by Yang Minggui, pp 369–377
- Chen Zhaobo (1981) “Double mixing” genetic model of uranium deposits in volcanic rocks and the relationship between China's Mesozoic vein-type uranium deposits and Pacific plate tectonics. (Metallogenesis of Uranium) Proc 26th Intern Geol Congr (1980), Geoinstitut, Beograd, pp 65–97
- Chen Zhaobo, Fang Xiheng (1985) Main characteristics and genesis of Phanerozoic vein-type uranium deposits. *In: Uranium deposits in volcanic rocks*. IAEA, Vienna, pp 69–82
- Chen Zhaobo et al. (1982) Uranium deposits in Mesozoic volcanics in southeast China. *Acta Geol Sin*, v 56, no 3, pp 235ff
- Chen Zhaobo, Zhang Weixing, Liu Xingzhong, Zhao Fengmin (hon. chief eds); Du Letician, Huang Shijie, Chen Zuyi, Jiang Yongyi (chief eds) (1996) Galaxy of research achievements of uranium geology of China. Uranium geol, Beijing, 393 p
- Chen Zhaobo, Zhao Fengmin, Xiang Weidong, Chen Yuehui (2000) Uranium provinces in China. *Acta Geol Sinica*, v 74, no 2, pp 587–594
- Chen Zuyi (2002) Regional distribution of uranium deposits in northern Asia. *In: Bureau of Geology, CNNC (ed) Sandstone-type uranium deposits in China: Geology and exploration techniques*. Atomic Energy Press, Beijing, pp 24–32
- Chen Zuyi, Huang Shijia (1993) In-situ leachable sandstone uranium resources in Yili Basin, Xinjiang AR, China. NEA/IAEA Uranium Group meeting, Paris, 11 p
- Chen Zuyi et al. (1983) The stages of the development of fault-block movement and continental red beds with respect to the regional uranium mineralization in South China. *Acta Geol Sin*, v 57, no 3, pp 294ff, (in Chinese)
- Chenoweth WL, Holen HK (1980) Exploration in the Grants Uranium Region since Memoir 15. *In: Rautman CA (ed) Geology and mineral technology of the Grants uranium region 1979*. New Mex. Bur Mines Mineral Res Mem. 38, pp 17–21
- Chenoweth WL, Malan RC (1973) The uranium deposits of northeastern Arizona, in Monument Valley and vicinity, Arizona and Utah. *New Mex Geol Soc Guidebook*, 24th Field Conf, pp 139–149
- Chernyshev IV, Golubev VN (1996) The Streltsovskoye deposit, eastern Transbaikalia: Isotope dating of mineralization in Russia's largest uranium deposit. *Geochem Intern*, v 34, no 10, pp 834–846
- Chervinsky N (1925) Tyuyamunit from the Tyuya-Muyun radium mine in Fergana. *Mineral Mag*, v 20, pp 287–295
- Chudnyavtzeva II, Samonov AE (2003) Uranium geochemistry in landscapes of Streltsovsky U-Mo ore field (Russia). *In: Cuney et al. (eds) Uranium geochemistry*. Univ Henri Poincaré, Vandoeuvre les Nancy, pp 119–122
- Chuluun O, Oyunbaatar O (1994) Hydrogenic and metasomatic types of uranium ore mineralization in Mongolia. Report IAEA TCM, Ottawa, pp 171–182
- Collot B (1981) Le granite albitique hyperalcalin de Bokan Mountain (SE Alaska) et ses minéralisations U-Th. Sa place dans la Cordillère Canadienne. USTL, Montpellier, 3^o cycle thesis, 238 p
- Crew ME (1981) NURE Uranium deposit model studies. *In: Uranium industry seminar proceedings*. US-DOE, GJO-108(81)
- Cuney M (1982) Processus de concentration de l'uranium et du thorium au cours de la fusion partielle et de la cristallisation des magmas granitiques. *In: Les méthodes de prospection de l'uranium*. OCDE (ed), Paris, pp 277–292
- Cuney M (2009) The extreme diversity of uranium deposits. *Miner Deposita*, v 44, pp 3–9
- Cuney M, Brouand M, Cathelineau M, Derome D, Freiberger R, Hecht L, Kister P, Lobae V, Lorilleux G, Peiffert C, Bastoul A (2003) What parameters control the high grade-large tonnage of the Proterozoic unconformity related uranium deposits? *In: Cuney M (ed) Uranium geochemistry 2003*. Nancy, France, pp 123–126
- Cuney M, Friedrich M (1987) Physicochemical and crystal chemical controls on accessory mineral paragenesis in granitoids. Implications for uranium metallogenesis. *Bull Minéral* 110, pp 235–247

- Cuney M, Kyser K (2008) Recent and not-so-recent developments in uranium deposits and implications for exploration. Short Course Vol 39, Mineral Ass Can (MAC) and Soc Geol Applied to Mineral Deposits (SGA), 272 p
- Dahlkamp FJ (1993) Uranium ore deposits. Springer-Verlag, Berlin, 460 p
- Dahlkamp FJ (1989) Classification scheme of uranium deposits. *In: Metallogenesis of uranium deposits*. IAEA, Vienna, pp 1–31
- Dahlkamp FJ, Scivetti N (1981) IUREP/International uranium resources evaluation project: Austria. OECD-NEA, Paris, 87 p
- Dai Jiemín (1990) Regional metallogenic geological conditions and recognition criteria of Dianxi sandstone-type uranium deposit. *In: Bureau of Geology, CNCC (ed) Uranium provinces in China*. Beijing, China, pp 162–175
- Dai Jiemín (1996) Regional metallogenic geological conditions and recognition criteria of sandstone-hosted uranium deposit in western Yunnan. *In: Chen Zhaobo et al. (eds) Galaxy of research achievements of uranium geology of China*. Uranium Geol, Beijing, pp 112–121
- Danchev VI, Lapinskaya TA (1966) Deposits of radioactive raw materials. Nedra, Moscow, (in Russian)
- Danchev VI, Strelyanov NP (1979) Exogenic uranium deposits. Atomizdat, Moscow, 245 p, (in Russian)
- Dayvault RD, Castor SB, Berry MR (1985) Uranium associated with volcanic rocks of the McDermitt Caldera, Nevada and Oregon. *In: Uranium deposits in volcanic rocks*. IAEA, Vienna, pp 379–410
- De Voto RH (1978) Uranium geology and exploration: Lecture notes and references. Col Sch Mines, Golden, 396 p
- De Voto RH, Stevens DN (eds) (1979) Uraniferous phosphate resources and technology and economics of uranium recovery from phosphate resources, United States and the free world. US-DOE, GJBX-110, v 1, 686 p, v 2, 606 p
- Den Ping et al. (2002) Mesozoic tectonomagmatic activity and uranium metallogenetic sequence in Mid-Nanling tectonic belt. *Uranium Geol*, v 18, no 5 pp 257–263, (in Chinese)
- Denson NM, Gill JR (1965) Uranium-bearing lignite and carbonaceous shale in the southwestern part of the Williston Basin. *US Geol Surv Prof Paper* 463, 75 p
- Derricks JJ, Vaes JF (1956) The Shinkolobwe uranium deposit. Current status of our geologic and metallogenetic knowledge. 1st Intern Conf Peaceful Uses of Atomic Energy, UN, Geneva, Proc, v 6, Geology of uranium and thorium, pp 94–128
- Dhana RR, Panneer Selvam A, Virnave SN (1989) Characterisation of the Upper Cretaceous Lower Mahadek sandstone and its uranium mineralization in the Domiasiat-Gomaghat Pdenghakap area, Meghalaya. *Expl Res Atom Minerals*, v 2, pp 1–17
- Dhana RR, Roy M, Madhuparna R, Vasudeva SG (1993) Uranium mineralisation in the south-western part of Cuddapah Basin: A petromineralogical study. *J Geol Soc India*, v 42, pp 135–149
- Dhana RR, Mary KK, Babu EVSSK, Pandit SA (2002) Uranium mineralization in the Neoproterozoic Bhima Basin at Gogi and near Ukinal – Ore petrology and mineral chemistry. *J Geol Soc India*, v 59, pp 299–321
- Diouly-Osso P, Chauvet RJ (1979) Les gisements d'uranium de la région de Franceville (Gabon). *In: Uranium deposits in Africa, geology and exploration*. IAEA, Vienna, pp 123–148
- Doi K, Hirono S, Sakamaki Y (1975) Uranium mineralization by ground water in sedimentary rocks, Japan. *Econ Geol*, v 70, pp 628–646
- Dolgushin PS, Bazhenov MI, Rubinov IM, Zadorin LI (1995) The Malinovskoye uranium deposit. *Otech Geol*, no 9, pp 42–45, (in Russian)
- Du Letian (1982) Contributions of granite-hosted uranium deposits. Atomic Energy Publ House, Beijing, pp 238–252
- Du Letian (1986) Granite-type uranium deposits of China. *In: Vein type uranium deposits*. TECDOC-361, IAEA, Vienna, pp 377–394
- Du Letian et al. (1990) The regional distribution of granite-type uranium deposits in China and their criteria of prognosis and evaluation. *In: Bureau of Geology, CNCC (ed) Uranium provinces in China*. Bur Geol, CNCC, Beijing, China, pp 35–53
- Dwivedy KK (1995a) Possibility of new uranium discoveries in the environs of Domiasiat, Meghalaya, India. *In: Recent developments in uranium resources and supply*. TECDOC 823, IAEA, Vienna, pp 145–162
- Dwivedy KK (1995b) Economic aspects of the Cuddapah Basin with special reference to Uranium – An overview. Seminar on Cuddapah Basin. Abstract volume, Geol Soc India, pp 116–138
- Dwivedy KK, Sinha KK (1997) Uranium exploration target selection for Proterozoic iron oxide/breccia complex type deposits in India. *In: Changes and events in uranium deposit development, exploration, resources, production and the world supply-demand relationship*. TECDOC-961, IAEA, Vienna, pp 163–176
- Eldorado Resources Ltd. (1986, updated 1987) The Eagle Point uranium deposits, northern Saskatchewan. Manuscr, 56 p
- Espahbod MR (1985) Uranium mineralization in relation to alteration and sulfide paragenesis in the polymetallic zones of Iran and new uranium discoveries in Zagros Mountain. Concentration mechanisms of uranium in geological environments. Intern Meeting, Nancy, pp 323–328
- Espahbod MR (1986) Metaltectonic control of the uranium mineralization in vein-type deposits of central Iran (Anarak District). *In: Vein type uranium deposits*. IAEA-TECDOC-361, IAEA, Vienna, pp 415–422
- Ewers GR, Ferguson J (1980) Mineralogy of the Jabiluka, Ranger, Koongara uranium deposits. *In: Ferguson J, Goleby AB (eds) Uranium in the Pine Creek geosyncline*. IAEA, Vienna, pp 363–374
- Ewers GR, Ferguson J, Needham RS, Donnelly TH (1984) Pine Creek geosyncline, NT. *In: Proterozoic unconformity and stratabound uranium deposits*. TECDOC-315, IAEA, Vienna, pp 135–206
- Fan Honghai, Ni Pei, Wang Dezi et al. (2002) Genetic mechanism of cryptoexplosive breccia pipe at depth of Zoujiashan uranium deposit and its relationship to uranium mineralization. *Mineral Deposits* 21 (supplement issue), pp 857–860, (in Chinese)
- Fan Honghai, Ling Hongfei, Wang Dezi et al. (2003) Study on metallogenetic mechanism of Xiangshan uranium ore-field. *Uranium Geology*, 19(4), pp 208–213, (in Chinese)
- Fayek M, Kyser TK (1997) Characterization of multiple fluid events and rare-earth-element mobility associated with formation of unconformity-type uranium deposits in the Athabasca Basin, Saskatchewan. *The Canadian Mineralogist*, v 35, pp 627–658
- Fazlullin MI, Novoseltsev, VV, Farber, VJ, Solodov IN, Nesterov JV (2002) Restoration experience on uranium ore-bearing aquifers after in situ leach via hydrogeochemical methods. *In: In situ leach uranium mining (Working material)*. IAEA, Vienna, pp 132–140
- Feather CE, Glatthaar CW (1987) A review of uranium-bearing minerals in the Dominion and Witwatersrand placers. *In: Uranium deposits in Proterozoic quartz-pebble conglomerates*. TECDOC-427, IAEA, Vienna, pp 355–386
- Feng Mingyue, Rong Jiashu, Sun Zhifu (1996) Formation mechanism and prospect prognosis of pegmatite type uranium deposits in eastern Qinling, China. *In: Chen Zhaobo et al. (eds) Galaxy of research achievements of uranium geology of China*. Uranium Geol, Beijing, pp 174–181
- Ferguson J, Goleby AB (eds) (1980) Uranium in the Pine Creek Geosyncline. IAEA, Vienna, 760 p
- Ferguson J, Rowntree JC (1980) Vein-type uranium deposits in Proterozoic rocks. *Rev Inst Français Pétrole*, v 35, pp 485–496
- Fersman A (1927) Zur Morphologie und Geochemie von Tuja Mujun. *Beiträge Radiumforschung, Akad Wiss, III, Leningrad*, pp 1–93
- Fersman A (1930) Geochemische Migration der Elemente. Teil II, *Abh prakt Geol*, Nr. 19, pp 1–32
- Fersman A, Shcherbakov DI (1925) Tyuya-Muyun radium ore deposit in Fergana. *VSNKH*, no 74, (in Russian)
- Filonenko YD et al. (1993) Uranium deposits in basalt sheets (Eastern Mongolia). *Geol Ore Deposits*, v 35, no 5, pp 351–361
- Finch WI (ed) (1985) Geological environments of sandstone-type uranium deposits. TECDOC-328, IAEA, Vienna, 408 p
- Finch WI, Davis JF (1985) Sandstone-type uranium deposits – An introduction. *In: Finch WI (ed) Geological environments of sandstone-type uranium deposits*. TECDOC-328, IAEA, Vienna, pp 11–20
- Finch WI, Shen Feng, Chen Zuyi, McCammon RB (eds) (1993) Descriptive models of major uranium provinces in China. *Nonrenewable Resources*, v 2, no 1, pp 39–48
- Fogwill WD (1985) Canadian and Saskatchewan uranium deposits: Compilation, metallogeny, models, exploration. *In: Sibbald, TII, Petruk W (eds) Geology of uranium deposits*. CIM Spec, v 32, pp 3–19

- Fouques JP, Fowler M, Knipping HD, Schimann K (1986) Le gisement d'uranium de Cigar Lake: Découverte et caractéristiques générales. *CIM Bull*, v 79, no 886, pp 70–82
- Freiberger R, Cuney M (2003) New evidence for extensive fluid circulation within the basement in relation to unconformity type uranium deposits genesis in the Athabasca Basin, Saskatchewan, Canada. *In: Cuney M (ed) Uranium geochemistry 2003. Proc Unité Mixte Rech, Univ Henri Poincaré, Nancy, France*, pp 151–154
- Frey M, Saager R, Buck S (1987) Heavy mineral distribution and geochemistry related to sedimentary facies variation within the uraniferous intermediate reefs placers, Witwatersrand Supergroup, South Africa. *In: Uranium deposits in Proterozoic quartz-pebble conglomerates. TECDOC-427, IAEA, Vienna*, pp 313–334
- Fritsche R (1986) Natrium-Metasomatose und Urananreicherung am Beispiel Kitongo-Granit/Kamerun und vergleichbare Uranvorkommen. Univ Heidelberg, PhD thesis, 190 p (unpubl)
- Fritsche R, Dahlkamp FJ (2001) Contribution to characteristics of uranium oxides. *In: Assessment of uranium deposit types and resources – A worldwide perspective. TECDOC-1258, IAEA, Vienna*, pp 223–238
- Fritsche R, Amstutz GC, Dahlkamp FJ (1988) Primäre Uranerzminerale und ihre lagerstättengenetische Stellung. Deutsche Forschungsgemeinschaft, final report, DFG Project Am 23/65, 212 p
- Fuchs H (ed) (1986) Vein-type uranium deposits. TECDOC-361, IAEA, Vienna, 423 p
- Fyodorov GV (2001) Industrial types of uranium deposits in Kazakhstan. *In: Assessment of uranium deposit types and resources – A worldwide perspective. TECDOC-1258, IAEA, Vienna*, pp 77–83
- Fyodorov GV (2002a) A comparative description of the geological-technological description of the sandstone hosted uranium deposits in Wyoming and southern Kazakhstan. *In: In situ leach uranium mining. T1-TC-975, IAEA, Vienna*, pp 42–48
- Fyodorov GV (2002b) Uranium production and the environment in Kazakhstan. *In: The uranium production cycle and the environment. Cands Papers Series, IAEA, Vienna*, pp 191–198
- Fyodorov GV (2005) Uranium deposits of the Inkay-Mynkuduk ore field (Kazakhstan). *In: Developments in uranium resources, production, demand and the environment. TECDOC-1425, IAEA, Vienna*, pp 95–112
- Fyodorov GV, Bayodilov E, Zhelnov V, Akhmetov M, Abakamov A (1997) Uranium and environment in Kazakstan. *In: Changes and events in uranium deposit development, exploration, resources, production and the world supply-demand relationship. TECDOC-961, IAEA, Vienna*, pp 115–122
- Galloway WE (1985) The depositional and hydrogeologic environment of Tertiary uranium deposits, south Texas uranium province. *In: Geological environments of sandstone type uranium deposits. TECDOC-328, IAEA, Vienna*, pp 215–228
- Gauthier-Lafaye F, Weber F, Naudet R, Pfiffelmann JP, Chauvet R, Michel B, Reboul JC (1980) Le gisement d'Oklo et ses réacteurs de fission naturels. *In: Ferguson J, Goleby AB (eds) Uranium in the Pine Creek geosyncline. IAEA, Vienna*, pp 663–673
- Gavrilin VI, Dmitrieva IE, Pechonkin IG (eds) (2000) Uranium at the turn of the century: Resources, production, demand. *Abstr Intern Symp Uran Geol, Moscow, All-Russian Sci-Res Inst Mineral Resources NM Fedorovsky*, 156 p
- Geoffroy J (1973) Les gites uranifères dans le Massif Central français. *In: Géologie, géomorphologie et structure profonde du Massif Central français. Symposium J Jung, 1971, Plein Air Service Edit., Clermont-Ferrand*, pp 541–579
- George E, Pagel M, Dusausoy Y, Gauthier JM (1986) Formation conditions of a tetragonal uranium oxide: U_3O_7 in the Brousse-Broquiès Basin (Aveyron France). *Uranium*, v 3, pp 69–89
- George-Aniel B, Leroy J, Poty B (1991) Volcanogenic uranium mineralizations in the Sierra Peña Blanca District, Chihuahua, Mexico: Three genetic models. *Econ Geol*, v 86, no 2, pp 233–248
- Goodell PC (1985) Classification and model of uranium deposits in volcanic environments. *In: Uranium deposits in volcanic rocks. IAEA, Vienna*, pp 1–16
- Gorlov IG, Korsakov YF, Golshtein RI (2005) Uranium mineral base of Republic Uzbekistan. *In: Developments in uranium resources, production, demand and the environment. TECDOC-1425, IAEA, Vienna*, pp 147–150
- Gotman YD, Eremeev AN (eds) (1976) Genesis of uranium deposits. Nedra, Moscow, (in Russian)
- Gotman YD, Miguta AK, Petrosyan EV, Pruss AK, Smilkstyn AO (1979) The main types of uranium deposits on the shields of ancient platforms. *Sov Geol*, no 11, pp 65–78, (in Russian)
- Granger HC, Finch WI (1988) The Colorado Plateau uranium province, (with contributions by Bromfield CS, Duval JS, Grauch VJS, Green MW, Hills FA, Peterson F, Pierson CT, Sanford RF, Spirakis CS, Wahl RR. *In: Recognition of uranium provinces. IAEA, Vienna*, pp 157–193
- Grenthe I, Fuger J, Konings M et al. (1992) Chemical thermodynamics of uranium. Elsevier, New York
- Grushevoi GV, Pechonkin IG (2002) Localization of hydrogenic uranium deposits in the Pamir and Himalayan sectors in the Neogene and Quaternary region. *Geol Metallogeny*, no 16, pp 69–79
- Gu Kangheng, Wang Baoqun (1996) Uranium metallogenetic geological characteristics of deposit no 512 in interlayer oxidation zone in Yili Basin, Xinjiang. *In: Chen Zhaobo et al. (eds) Galaxy of research achievements of uranium geology of China. Uranium Geol, Beijing*, pp 196–204
- Guiollard PC, Milville G (2003) l'Uranium de deux "Privés". Edit PC Guiollard, Fichous-Riumayou, France, 141 p
- Guo Zhitian, Zhong Jiarong, Wang Zongying (1996) Geological conditions of uranium ore formation and recognition criteria in the east Liaoning uranium metallogenic region. *In: Chen Zhaobo et al. (eds) Galaxy of research achievements of uranium geology of China. Uranium Geol, Beijing*, pp 86–94
- Gupta RK (2002) Present status of uranium exploration in India. *Manuscr IAEA TC Meeting, Beijing*, 8 p
- Gupta R, Sarangi AK (2006) Emerging trend of uranium mining: The Indian scenario. *In: Symposium on uranium production and raw materials for the nuclear fuel cycle. Proceedings Series, IAEA, Vienna*, pp 47–56
- Gupta RK, Perumal NVA, Sagar S, Upadhyaya LD, Verma HM (1989) Uranium mineralization in some typical igneous-metamorphic environments of India. *In: Uranium deposits in magmatic and metamorphic rocks. IAEA, Vienna*, pp 113–130
- Hallbauer DK (1986) The mineralogy and geochemistry of Witwatersrand pyrite, gold, uranium, and carbonaceous matter. *In: Anhaeusser CR, Maske S (eds) Mineral deposits of Southern Africa. Geol Soc S Afr*, v 1, pp 731–752
- Hambleton-Jones BB (1976) The geology and geochemistry of some epigenetic uranium deposits near the Swakop River, South West Africa. *Univ Pretoria, DSc thesis*, 306 p (unpubl)
- Hambleton-Jones BB (1984) Surficial uranium deposits in Namibia. *In: Surficial uranium deposits. TECDOC 322, IAEA, Vienna*, pp 205–216
- Han Zhaeong, Rong Jiashu, Wang Yanting, Feng Mingyue, Sheng Zhuyong (1985) A possible origin of uranium deposits in granites with special reference to the formation of SL deposit. *Geochem*, v 4, no 2, pp 127–140
- Hancock MC, Maas R, Wilde AR (1990) Jabiluka uranium gold deposits. *In: Hughes FE (ed) Geology of the mineral deposits of Australia and Papua New Guinea. Australasian Inst Mining and Metallurgy*, pp 785–793
- Harshman EN, Adams SS (1981) Geology and recognition criteria for roll-type uranium deposits in continental sandstones. *US-DOE, GJBX-1(81)*, 185 p
- Häusser I, Kruse, BM, Parchmann J (1997) Übersicht über die mineralischen Rohstoffe von Kasachstan, Kirgisistan, Tadschikistan, Turkmenistan, Usbekistan. BGR, Hannover/Berlin, 104 p
- Hayashi S (1970) Uranium occurrences in small sedimentary basins in Japan. *In: Uranium exploration geology. IAEA, Vienna*, pp 233–242
- Hegge MR, Mosher DV, Eupene GS, Anthony PJ (1980) Geologic setting of the East Alligator uranium deposits and prospects. *In: Ferguson J, Goleby AB (eds) Uranium in the Pine Creek Geosyncline. IAEA, Vienna*, pp 259–272
- Heine TH (1986) The geology of the Rabbit Lake uranium deposit, Saskatchewan. *In: Evans EL (ed) Uranium deposits of Canada. CIM Spec*, v 33, pp 134–143
- Heinrich EW (1958) Mineralogy and geology of radioactive raw materials. McGraw Hill, New York Toronto London, 654 p
- Hoeve J, Qurt D (1984) Uranium mineralization and host-rock alteration in relation to clay mineral diagenesis and evolution of the Middle Proterozoic Athabasca Basin, northern Saskatchewan. *Sask Res Counc Tech Rep no 187*, 187 p

- Hoeve J, Sibbald TH (1978) On the genesis of Rabbit Lake and other unconformity-type uranium deposits in northern Saskatchewan, Canada. *Econ Geol*, v 73, pp 1450–1473
- Hoeve J, Sibbald TH, Ramaekers P, Lewry JF (1980) Athabasca Basin unconformity-type uranium deposits: A special class of sandstone-type deposits. *In: Ferguson J, Goleby A (eds) Uranium in the Pine Creek Geosyncline*. IAEA, Vienna, pp 575–594
- Hou YQ, Wang QH, Liu LJ (1993) Genesis and prospecting direction of the no 320 uranium deposit. *Uranium Geol*, v 9, pp 6–13, (in Chinese with English abstract)
- Huang Guangrong, Pang Yuhui (1987) Organic matter and its relation with uranium mineralization in carbonate-type uranium deposits in South China. *Mineral Deposits*, v 4, pp 63–71, (in Chinese)
- Huang Shijie (1996) Formation conditions and prospecting criteria for interlayered oxidation type of sandstone uranium deposits. *In: Chen Zhaobo et al. (eds) Galaxy of research achievements of uranium geology of China*. Uranium Geol, Beijing, pp 57–65
- Huang Xianfang, Liu Dechang, Du Letian, Zhao Yingjun (2005) A new sandstone type uranium metallogenetic type - structure-oil, gas type. *In: Jingwen Mao & Bierlein FP, eds., Mineral deposit research: meeting the global challenge*. Proc Eighth Biennial SCA meet, Beijing, China, pp 265–268
- Huang Zhizhang, Li Xinzhen, Cai Genqing (2002) Alteration geochemistry of interlayer oxidation zone, Shihongtan uranium deposit. *In: Bureau of Geology, CNCC (ed) Sandstone-type uranium deposits in China: Geology and exploration techniques*. Atomic Energy Press, Beijing, pp 136–144
- Hutchinson RW, Blackwell JD (1984) Time, crustal evolution and generation of uranium deposits. *In: deVivo B, Ippolito F, Capaldi G, Simpson PR (eds) Uranium geochemistry, mineralogy, geology, exploration and resources*. IMM, London, p 89–100
- IAEA (1982a) Vein-type and similar uranium deposits in rocks younger than Proterozoic. IAEA, Vienna, 391 p
- IAEA (1983b) Age, sedimentary environments, and other aspects of sandstone and related host rocks for uranium deposits, Tech Rep Series no 231. IAEA, Vienna, 62 p
- IAEA (1984a) (Ferguson J ed) Proterozoic unconformity and stratabound uranium deposits. TECDOC-315, IAEA, Vienna, 338 p
- IAEA (1984b) (Toens D ed) Surficial uranium deposits. TECDOC-322, IAEA, Vienna, 252 p
- IAEA (1985a) Uranium deposits in volcanic rocks. IAEA, Vienna, 468 p
- IAEA (1985b) (Finch W ed) Geological environments of sandstone-type uranium deposits. TECDOC-328, IAEA, Vienna, 408 p
- IAEA (1986) (Fuchs H ed) Vein-type uranium deposits. TECDOC-361, IAEA, Vienna, 423 p
- IAEA (1987) (Pretorius D ed) Proterozoic quartz-pebble conglomerates. TECDOC 427, IAEA, Vienna, 459 p
- IAEA (1988) Uranium deposits in Asia and the Pacific: Geology and exploration. IAEA, Vienna, 341 p
- IAEA (1989a) Uranium deposits in magmatic and metamorphic rocks. IAEA, Vienna, 253 p
- IAEA (1989b) Uranium resources and geology of North America. TECDOC-500, IAEA, Vienna, 529 p
- IAEA (1989c) Metallogenesis of uranium deposits. IAEA, Vienna, 489 p
- IAEA (1991) Assessment of uranium resources and supply. TECDOC-597, IAEA, Vienna
- IAEA (1992) New developments in uranium exploration, resources, production and demand. TECDOC-650, IAEA, Vienna, 258 p
- IAEA (1993) Uranium in situ leaching. TECDOC-720, IAEA, Vienna, 245 p
- IAEA (1995a) World distribution of uranium deposits. IAEA, Vienna, map, first edition
- IAEA (1995b) Recent developments in uranium resources and supply. TECDOC-823, IAEA, Vienna, 266 p
- IAEA (1996) Innovations in uranium exploration, mining and processing techniques, and new exploration target areas. TECDOC-868, IAEA, Vienna, 148 p
- IAEA (1997) Changes and events in uranium deposit development, exploration, resources, production and the world supply-demand relationship. TECDOC-961, IAEA, Vienna, 343 p
- IAEA (2000) International symposium on the uranium production cycle and the environment. Book of extended synopses, SM-362, IAEA, Vienna, 251 p
- IAEA (2001a) Manual of acid in situ leach uranium mining technology. TECDOC-1239, IAEA, Vienna, 283 p
- IAEA (2001b) Impact of new environmental and safety regulations on uranium exploration, mining, milling and management of its waste. TECDOC-1244, IAEA, Vienna, 244 p
- IAEA (2001c) Assessment of uranium deposit types and resources – A worldwide perspective. TECDOC-1258, IAEA, Vienna, 253 p
- IAEA (2002) Annex II: Description of the Number 6 Mining Company in situ leach uranium operations, Chiili, Kyzl Orda Oblast, Kazakhstan. *In situ leach uranium mining*. T1-TC-975, IAEA, Vienna, pp 174–175
- IAEA (2002) *In situ leach uranium mining (Working material)*. TCM Almaty, Kazakhstan, 1996, IAEA, Vienna, 179 p
- IAEA (2007) Database on world distribution of uranium deposits (UDEPO). IAEA, Vienna, (in preparation)
- Ischukova LP (1989) Geological setting of southern Priargun area in Eastern Transbaikalia. *News Acad Sci USSR, geology*. Moscow, pp 102–118
- Ischukova LP (1995) Strel'tsovskoye ore field. *In: Laverov NP (ed) Deposits of Transbaykal*. Geoinformmark, Chita-Moscow, v 1, book 2, pp 130–156, (in Russian)
- Ischukova LP (1997) The Strel'tsovskoye uranium district. *In: Changes and events in uranium deposit development, exploration, resources, production and the world supply-demand relationship*. TECDOC-961, IAEA, Vienna, pp 237–250
- Ischukova LP, Naumov SS et al. (1998) Geology of Urulyungui ore district and molybdenum-uranium deposits of Strel'tsovsk ore field. *Geoinformmark*, Moscow, pp 524ff, (in Russian)
- Ischukova LP, Modnikov IS, Sychev IV (1991) Uranium ore-forming systems in areas of continental volcanism. *Geol Rudn Mestorozhd*, no 3, pp 16–25, (in Russian)
- Ischukova LP, Ashikhmin AA, Konstantinov AK, Kostikov AT, Modnikov IS, Sychoy IV, Tolkachev AE, Chesnokov LV, Shumilin MV (Mashkovtsev GA, Naumov SS, Shumilin MV eds) (2002) Uranium deposits in volcano-tectonic structures. Moscow, (in Russian)
- James O, Hamani M (1999) L'uranium nigérien de la découverte à l'exploitation, les modèles et les potentiel exploration (manusc, 40 p)
- Jefferson CW, Delaney G (eds) (2007) EXTECH IV: Geology and uranium exploration technology of the Proterozoic Athabasca Basin, Saskatchewan and Alberta. *Geol Surv Canada, Bull 588*, 644 p (also *Sask Geol Soc, Spec Publ 18; Geol Ass Canada, Mineral Deposits Div, Spec Publ 4*)
- Jefferson CW, Thomas D, Quirt D, Mwenifumbo CJ, Brisbin D (2007) Empirical models for Canadian unconformity-associated uranium deposits. *In: B Milkereit (ed) Exploration in the New Millennium. Proceedings of Exploration 07, Fifth Decennial Intern Conf Mineral Exploration*, Toronto, Canada, Sept 9–12, 2007, 27 p
- Jeyagopal AV, Dhana Raju R (1998) Recognition criteria and sedimentology of dolostone-hosted stratabound uranium mineralisation in Vempalle Formation, Cuddapah Basin, Andhra Pradesh, India. *In: Tiwari RN (ed) Proc Nat Symp on "Recent Researches in Sedimentary Basins"*. Indian Petroleum Publishers, Dehra Dun, pp 172–179
- Jiaron Z, Zhitian G (1984) The Liangshanguan uranium deposit, northeast China: Some petrological and geochemical constraints on genesis. *In: Proterozoic unconformity and stratabound uranium deposits*. TECDOC-315, IAEA, Vienna, pp 115–134
- Jiashu R, Zehong H (1984) Form of uranium occurrence and its distribution in uraniferous granites. *In: Geology of granites and their metallogenetic relations*. Proc Symp Nanjing, 1982, Univ Press, Beijing, pp 621–635
- Jiashu R, Zehong H, Yuliang X (1989) Uranium metallogenesis of coarse-grained granite in Area H, China. *In: Uranium deposits in magmatic and metamorphic rocks*. IAEA, Vienna, pp 93–112
- John EC (1978) Mineral zones in the Utah copper orebody. *Econ Geol*, v 73, pp 1250–1259
- Johnson SY, Otton JK, Macke DL (1987) Geology of the Holocene surficial uranium deposit of the north fork of Flodelle Creek, northeastern Washington. *Geol Soc AM Bull*, v 98, no 1, pp 77–85
- Jon Hwan Kim (1988) Uranium geology of the Republic of Korea. *In: Uranium deposits in Asia and the Pacific: Geology and exploration*. IAEA, Vienna, pp 141–154
- Jones CA (1978) Uranium occurrences in sedimentary rocks exclusive of sandstone. *In: Mickle DG, Mathews GW (eds) Geologic characteristics of*

- environments favorable for uranium deposits. US-DOE, GJBX 67(78), pp 1–86
- Jong Hwan Kim (1988) Uranium geology of the Republic of Korea. *In: Uranium deposits in Asia and the Pacific: Geology and exploration*. IAEA, Vienna, pp 141–154
- Ju Yejun, et al. (1985) On the sedimentary environments of the Late Sinian and Early Cambrian carbonaceous formation in South China and their relations with uranium mineralization. *Sci Papers on Geology for Intern Exchange*, Beijing, 5, pp 181ff
- Ju Yejun, Li Shunchu, Fang Shiyi (1990) Geological characteristics of the carbonate-siliceous-pelitic uranium ore belt in the Xuefeng-Jiuling region and analysis of its ore-forming conditions. *In: Bureau of Geology, CNNC (ed) Uranium provinces in China*. Bur Geol, CNNC, Beijing, China, pp 104–116
- Kamiyama T, Kubo K, Shimazaki Y (1976) Geologic aspects of uranium resources of Japan. *In: Circumpacific energy and mineral resources*. AAPG Memoir no 25, pp 451–455
- Kaplan H, Uz S, Çetintürk I (1974) Le gîte d'uranium de Fakih (Turguie) et sa formation. *In: Formation of uranium ore deposits*. IAEA, Vienna, pp 453–465
- Karimov et al. (1996) Uranium deposits of the Uchkuduk type in the Republic of Uzbekistan. *Publ House Fan of Acad Sci of Rep Uzbekistan*, Tashkent, 334 p, (in Russian)
- Katayama N (1958) Genesis of the uranium deposits in Tertiary sediments in the Ningyo-toge area, western Japan. *Proc 2nd UN Int Conf, Peaceful Uses of Atomic Energy*, v 2, Geneva, pp 402–406
- Katayama N, Fukuoka I (1970) Ningyo-toge uranium deposits. *Intern Mineral Assoc Proc, 7th Gen Meeting*, Tokyo and Kyoto, Guidebook v 8, pp 24–48
- Katayama N, Kamiyama T (1977) Favourable conditions for the formation of basal type uranium deposits. *Min Geol (Japan)*, v 27, pp 1–8
- Katayama N, Kubo K, Hirono S (1974) Genesis of uranium deposits of the Tono Mine, Japan. *In: Formation of Uranium Ore Deposits*. IAEA, Vienna, pp 437–452
- Kaul R, Varma HM (1990) Geological evaluation and genesis of the sandstone-type uranium deposit at Domiasiat, West Khasi Hills District, Meghalaya, India. *Expl Res Atom Minerals*, v 3, pp 1–16
- Kazansky VI (1970) Geology and structure of the Tyuya Muyun ore deposit. *In: Essays on geology and geochemistry of ore deposits*. Nauka, Moscow, pp 34–57
- Kazansky VI (1995) Uranium deposits of the Asian sector of the Pacific ore belt. *Geol Ore Dep*, v 37, no 4, pp 303–316
- Kazansky VI, Laverov NP (1977) Deposits of uranium. *In: Smirnov VI (ed) Ore deposits of the USSR – Vol. II*. Pitman Publ, London, pp 349–424
- Kazansky VI, Maksimov EP (2000) Geological setting and development history of the Elkon uranium ore district (Aldan Shield, Russia). *Geol Ore Dep*, v 42, no 3, pp 189–204
- Kazansky VI, Laverov NP, Tugarinov AI (1978) Evolution of uranium deposits. *Atomizdat*, Moscow, 208 p
- Khalezov AB (2000a) On the different productivity of uranium-bearing oxidation zones in the buried river channels, the Transural area. *In: Gavrilin VI et al. (eds) Uranium at the turn of the century: Resources, production, demand*. *Abstr Intern Symp Uran Geol*, Moscow, All-Russian Sci Res Inst Mineral Resources NM Fedorovsky, pp 68–70
- Khalezov AB (2000b) Presumable stages of uranium accumulation in sedimentary rocks of the central and eastern parts of the Russian platform. *In: Gavrilin VI et al. (eds) Uranium at the turn of the century: Resources, production, demand*. *Abstr Intern Symp Uran Geol*, Moscow, All-Russian Sci Res Inst Mineral Resources NM Fedorovsky, pp 70–71
- Kim (1988) *See* Jon Hwan Kim (1988)
- King J, Tauchid M, Frey D, Basset M, Çetintürk I, Aydonoz F, Keçeli B (1976) Exploration for uranium in southwestern Anatolia: A Case History. *In: Exploration for uranium ore deposits*. IAEA, Vienna, pp 501–529
- Kirikov AP (1928) To the knowledge of radioactiveness in Sewiretschie. *Bull Committee Geol, Leningrad*, v 47, no 6, pp 637–652, (in Russian)
- Kirikov AP (1929) Tyuya-Muyun radium deposit. *Papers Geol Committee*, new series, issue 181, (in Russian)
- Kirillov VY, Berdinkov NV (1998) Ore potential of Precambrian unconformity zones in stratabound basins of the Aldan Shield, Russia. *Intern Geol Rev*, v 40, no 2
- Kirillov VE, Goroshko MV (1997) Uranium metallogeny of the Uliya and Kuidusun volcanogenic basins, western Okhotsk region. *Geol Pac Ocean*, v 13, pp 567–582
- Kislyakov YM, Shchetochkin VN (2000) Hydrogenic ore formation. *ZAO Geoinformark*, Moscow, 608 p
- Kislyakov YM, Shumilin MV (1996) Olov and Ima uranium deposits in Mesozoic depressions of the Transbaikalian region (Russia). *Geol Ore Dep*, v 38, no 6, pp 478–493
- Kochetkov AY, Kravchenko SM, Lezebnik KY (1988) New aspects of the Mesozoic metallogeny in the Aldan Shield. *In: Distribution pattern of mineral resources*. *Metallogeniya Sibiri (Metallogeny of Siberia)*, v 15, Nauka, Moscow, pp 91–99, (in Russian)
- Kochenov AV, Kruglova VG, Khaldei AE, Khalezov AB (1995) Factors controlling the concentration and content of trace elements of ores in the infiltration uranium deposits in paleovalleys and intermontane depressions. *In: Kholodov VN, Mashkovtsev GA (eds) Rare-metal-uranium ore formation within sedimentary rocks*. Nauka, Moscow, pp 59–75, (in Russian)
- Kohl E (1954) *Uran*. *Die metallischen Rohstoffe*. 10. Heft, Enke Verlag, Stuttgart, 234 p
- Kolektiv (CSSR) (1984) Czechoslovakian uranium deposits. *Nakl technické literatury*, Prague, 365 p, (in Czech)
- Kolektiv (CSSR) (2003) *Rudné a uranové hornictví České Republiky (Uranium mining industry, Kafka J (ed))*. DIAMO/ANGRAM, 647 p, (in Czech)
- Komarova PV, Komarova GN, Goltzman YV, Arakelyants MM (1965) Age of intrusive rocks and mineralization of the Klichkinskoye ore field in the eastern Transbaikalian region. *Izv AN SSSR, Geol Ser*, no 12, pp 12–19, (in Russian)
- Komínek J (1997) An overview of the distribution of hydrothermal veins and uranium mineralization in Příbram uranium deposit. *Uhli-rudy 45, geologický průzkum 39/U-R-GP 1, 4*, pp 6–11, (in Czech)
- Komínek J, Veselý T (1986) Uranium deposit of Jáchymov, CSSR. *In: Vein type uranium deposits*. *TECDOC-361*, IAEA, Vienna, pp 293–306
- Komischau MS (1927) *Die Lagerstätte Almalysk der Region Tuja-Mujun*. *Westn d Geol Kom*, Nr 6, pp 17ff, and *Geol Zentralbl*, Nr. 38/1928–29, pp 569ff
- Komura, Ziehr (1985) IUREP orientation phase mission: Turkey. *Summary report*. IAEA, Vienna, 21 p
- Korolev KG, Miguta AK, Polyakova VM et al. (1979) Mineralogy, geological and physicochemical features of uronotitanate formation. *Nedra*, Moscow, pp 144ff, (in Russian)
- Korolev KG, Belov VK, Putilov GS (1983) Phosphoric-uranium ore deposits. *Anergoatomizdat*, Moscow, (in Russian)
- Kotlyar VN (1968) Volcanogenic, hydrothermal ore deposits. *In: Genesis of endogenous ore deposits*. *Nedra*, Moscow, (in Russian)
- Kotlyar VN et al. (1973) Deposits of radioactive and rare metals. *Atomizdat*, Moscow, (in Russian)
- Kotzer TG, Kyser TK (1995) Petrogenesis of the Proterozoic Athabasca Basin, northern Saskatchewan, Canada, and its relation to diagenesis, hydrothermal uranium mineralization and paleohydrogeology. *Chem Geol*, v 120, pp 45–89
- Kovalenko and Yarmolyak (1995) Endogenous rare metal ore formations and metallogeny of Mongolia. *Econ Geol*, v 90, no 5, pp 520–529
- Krauss UH, Saam HG, Schmidt HW (1984) International strategic minerals inventory summary report – phosphate. *US Geol Surv Circ 930-C*, 41 p
- Krotkov VV, Vetrov VI, Naumov SS, Tarkhanov AV, Birka GI (1997) Uranium production in Russian Federation (manuscript). *IAEA Symposium: Developments in uranium resources, production, demand and the environment*. IAEA, Vienna
- Krylova TL, Aleshin AP, Velichkin VI, Cuney M, Pironon J, Chabiron A, Poty B (2003) Physico-chemical conditions of uranium ore formation at the Strel'tsovskoye and Antei deposits (Eastern Transbaikalia, Russia). *In: Cuney et al. (eds) Uranium geochemistry*. *Univ Henri Poincaré, Vandoeuvre les Nancy*, pp 205–208
- Kuchersky NI (1997) Providing radiation safety for the environment and people at uranium ore mining and primary processing operations and treatment of radioactive wastes in the Navoi Mining and Metallurgy Combinat, Uzbekistan. *In: Changes and events in uranium deposit development, exploration, resources, production and the world supply-demand relationship*. *TECDOC-961*, IAEA, Vienna, pp 107–114

- Kumar S, Singh R, Bahuguna R, Sengupta B, Kaul R (1990) Geological environment of the sandstone-type uranium deposit, Domiasiat area, West Khasi Hills District, Meghalaya, India. *Expl Res Atom Minerals*, v 3, pp 17–26
- Kunzendorf H, Nyegaard P, Nielsen BL (1982) Distribution of characteristic elements in the radioactive rocks of the northern part of Kvanefjeld, Ilimaussaq Intrusion, South Greenland. *Geol Surv Greenl, Copenhagen, Rep 109*, pp 1–32
- Lainé R, Alonso D, Svab M (eds) (1985) The Carswell Structure uranium deposits, Saskatchewan. *Geol Ass Can Spec Paper 29*, 240 p
- Lange G, Freyhoff G (1991) Geologie und Bergbau in der Uranlagerstätte Ronneburg, Thüringen. *Erzmetall 44*, Nr. 5, pp 264–269
- Langmuir D (1978) Uranium solution–mineral equilibria at low temperatures with applications to sedimentary ore deposits. *Geochim Cosmochim Acta*, v 42, pp 547–569
- Lanier G, John EC, Swensen AJ, Reid J, Bard CE, Caddey SW, Wilson JC (1978) General geology of the Bingham Mine, Bingham Canyon, Utah. *Econ Geol* v 73, pp 1228–1241
- Laverov NP (1972) Conditions of the formation of hydrothermal deposits in continental volcanic belts. *In: Mineralnye mestorozhdeniya (Mineral Deposits). Proc 24th Intern Geol Congr, Nauka, Moscow*, pp 35–45, (in Russian)
- Laverov NP (ed) (1995) Deposits of Transbaykal. *Geoinformmark, Moscow*, v 1, book 2, 244 p, (in Russian)
- Laverov NP (chief ed) (2000) Atlas: Uranium of Russia. The Russian Federation Ministry of Natural Resources a.o., Moscow, 40 p
- Laverov NP, Zaporozhets AN, Kantsel AV et al. (1965) Geology of uranium-molybdenum deposits confined to acid subvolcanic intrusive bodies. *Geol Rudn Mestorozhd*, no 6, pp 34–48, (in Russian)
- Laverov NP, Volfson FI, Seltsov BM, Chernyshev IV, Ivanov IB (1985) Geochronology of continental volcanism of the Phanerozoic (Exemplified by the eastern Transbaykal area and central Asia). *In: Isotope dating of the process of volcanism and sedimentation. Nauka, Moscow*, pp 116–124
- Laverov NP, Velichkin VI, Shumilin MV (1992a) Uranium ore deposits of the Commonwealth states. The main economic and genetic types. *Geol Ore Deposits*, no 2, pp 3–18, (in Russian)
- Laverov NP, Velichkin VI, Vetrov VI, Krotkov VV, Lapin AL, Naumov SS, Pelmenev MD, Shumilin MV (1992b) Ex-USSR uranium raw material resources. *Nucl Soc Intern, Moscow*, 60 p
- Laverov NP, Velichkin VI, Vetrov VI, Krotkov VV, Lapin AL, Naumov SS, Pelmenev MD, Shumilin MV (1992c) Uranium resources of the Union of Soviet Socialist Republics. *TECDOC-650, IAEA, Vienna*, pp 172–186
- Laverov NP, Chernyshev IV, Golobev VN (1993) Isotope constraints on the age and genesis of hydrothermal uranium ore deposits in volcanic belts. *Geol Ore Deposits*, v 35, no 0, pp 22–30
- Laverov NP, Naumov SS, Smyslov AA, Terentiev VM, Kharlamov MG (1995) Map of uranium deposits of Russia – 1:10000000. *In: Smyslov AA (ed) Geological Atlas of Russia, Section III, Economic minerals and their distribution patterns. Geologorazvedka Concern/AP Karpinsky All-Russian Geol Inst, Russian Federation Committee Geology Use Mineral Resources and GV Plekhanov Tech Univ/St. Petersburg State Mining Inst, State Russian Federation Committee Higher Education*
- Leroy J (1978a) Métallogénèse des gisements d'uranium de la Division de la Crouzille (COGEMA – Nord Limousin – France). *Sci Terre, Nancy, Mém no 36*, 276 p
- Leroy J (1978b) The Margnac and Fanay uranium deposits of the La Crouzille District (western Massif Central, France): Geologic and fluid inclusion studies. *Econ Geol*, v 73, pp 1611–1634
- Leroy J (1982) Le gisement du Bernardan, Études minéralogiques chimiques et des inclusions fluides de lépisyénitisation. *Rapport CREGU 82–01*, 93 p
- Leroy J, Cathelineau M (1982) Les minéraux phylliteux dans les gisements hydrothermaux d'uranium I. *Christalochimie des micas hérités et néoformés. Bull Minér*, v 105, pp 99–109
- Leroy J, George-Aniel B, Pardo-Leyton E (1985) Deposits and radioactive anomalies in the Sevaruyo region (Bolivia). *In: Uranium deposits in volcanic rocks. IAEA, Vienna*, pp 289–300
- Leroy J, Aniel B, Poty B (1987) The Sierra Peña Blanca (Mexico) and the Meseta Los Frailes (Bolivia): The uranium concentration mechanisms in volcanic environment during hydrothermal processes. *Uranium*, 3, pp 211–234
- Leymerie A (1859) *Cours de minéralogie. II pt, Paris and Toulouse*
- Li Jian-Wei (1998) The NNE-trending strike slip faulting, fluid flow and uranium mineralization in the border area between Hunan and Jiangxi Provinces, southern China. *China Univ Geosci, PhD thesis*, (in Chinese with English summary)
- Li Jian-Wei, Zhou Mei-Fu, Li Xian-Fu, Fu Zhao-Ren, Li Zi-Jin (2001) The Hunan-Jiangxi strike-slip fault system in South China: Southern extension of the Tan-Lu fault. *J Geodyn*, v 32, pp 333–354
- Li Jian-Wei, Zhou Mei-Fu, Li Xian-Fu, Li Zi-Jin, Fu Zhao-Ren (2002) Origin of a large breccia-vein system in the Sanerlin uranium deposit, southern China: A reinterpretation. *Mineral Deposita*, v 37, no 2, pp 213–225
- Li Shengxiang, Zhao Fengmin, Cai Yuqi (2000) Analysis of uranium resources prospect in the region of northeastern China and inner Mongolia. *In: Gavrilin VI et al. (eds) Uranium at the turn of the century: resources, production, demand. Abstracts Intern Symp Uran Geol, Moscow, All-Russian Sci Res Inst Mineral Resources NM Fedorovsky*, pp 84–85
- Li Shengxiang, Chen Daisheng, Cai Yuqi (2002) Geologic evolution and uranium metallogenic regularity of Yili Basin. *In: Bureau of Geology, CNNC (ed) Sandstone-type uranium deposits in China: Geology and exploration techniques. Atomic Energy Press, Beijing*, pp 53–64
- Li Shengxiang, Wang Baoqin, Cai Yuqi, Li Xigen, Han Xiaozhong, Zheng Enjiu et al. (2005) The discovery and prospecting potential of ISL sandstone-type uranium deposit in Xishanyao Formation, Middle Jurassic in Yili Basin. *In: Symposium on uranium production and raw materials for the nuclear fuel cycle – Supply and demand, economics, the environment and energy security. Extended synopsis. CN-128, IAEA, Vienna*, pp 284–288
- Li Tiangang, Huang Zhizhang (1986) Vein uranium deposits in deposits of Xiaozhuang ore field. *In: Vein type uranium deposits. TECDOC-361, IAEA, Vienna*, pp 359–376
- Li Tiangang, Tong Hangshou, Feng Mingyue (1996) Geological characteristics and formation conditions of rich ore in granitic type uranium deposits. *In: Chen Zhaobo et al. (eds) Galaxy of research achievements of uranium geology of China. Uranium Geol, Beijing*, pp 122–131
- Li Wenxing (1990) Characteristics of radioactive hydrochemistry in Gan-Hang uranium metallogenic belt in volcanics and its significance in regional evaluation. *In: Bureau of Geology, CNNC (ed) Uranium provinces in China. Bur Geol, CNNC, Beijing, China*, pp 88–103
- Li Ziyang, Dong Wenming, Guo Qingyin (2002) Metallogenetic features and perspective evaluation of sandstone-type uranium mineralization in Hailaer Basin, NE China. *In: Bureau of Geology, CNNC (ed) Sandstone-type uranium deposits in China: Geology and exploration techniques. Atomic Energy Press, Beijing*, pp 110–118
- Li Ziyang, Chen Anping, Fan Xiheng, Xia Yuliang, Jiao Yangquan, Zhang Ke, Xiao Xinjian, Sun Ye (2005) Metallogenetic conditions and exploration criteria of Dongsheng sandstone type uranium deposit in Inner Mongolia, China. *In: Symposium on uranium production and raw materials for the nuclear fuel cycle – Supply and demand, economics, the environment and energy security. Extended synopsis. CN-128, IAEA, Vienna*, pp 270–274
- Liebenberg WR (1955) The occurrence and origin of gold and radioactive minerals in the Witwatersrand System, the Dominion Reef, the Ventersdorp Contact Reef and the Black Reef. *Trans Geol Soc S Afr*, v 58, pp 101–254
- Lin Shuangxin, Wang Baoqin, Li Shengxiang (2002) Characteristics of uranium mineralization and ore-controls of Kujieertai Deposit, Yili Basin, Xinjiang Autonomous Region. *In: Bureau of Geology, CNNC (ed) Sandstone-type uranium deposits in China: Geology and exploration techniques. Atomic Energy Press, Beijing*, pp 65–76
- Liu Ruzhou (1995) Magmatic evolutionary sequence and uranium enrichment in Xiaozhuang ore field. *Research rep, Research Inst no 290, Bur Geol, CNNC*, (in Chinese)
- Liu Xiadong, Zhou Weixun (2005) Felsic magma-related uranium deposits in Southeast China. *In: Symposium on uranium production and raw materials for the nuclear fuel cycle – Supply and demand, economics, the environment and energy security. Extended synopsis. CN-128, IAEA, Vienna*, pp 214–217
- Liu Xingzhong (1982) The types of uranium deposits and characteristics of geological mineralization in China. *Chinese J Nuclear Sci Eng*, v 2, 1, 81 p
- Liu Xingzhong, Zhou Weixun (1990) Uranium provinces in China and their distribution patterns. *In: Bureau of Geology, CNNC (ed) Uranium provinces in China. Beijing, China*, pp 1–16
- Liu Yifa, Xue Zhian, Meng Xianyu, He Gaiyi, Wan Senru, Feng Bida, Li Wengsing (1990) Metallogenesis of uranium metallogenetic belt in the Gan-Hang

- volcanic rocks. *In: Bureau of Geology, CNNC (ed) Uranium provinces in China*. Beijing, China, pp 69–87
- Loutchinin IL (1995a) Valley-type uranium deposits in Russia. TECDOC-823, IAEA, Vienna, pp 235–242
- Loutchinin IL (1995b) Uranium perspectives of the Uralian region. *Otech Geol*, no 9, pp 39–42, (in Russian)
- Luo Yi, Wang Zhenban, Zhou Dean (1996) Study on the structure-mineralization zoning and the metallogenetic model for volcanics type molybdenum-uranium deposit No. 460. *In: Chen Zhaobo et al. (eds) Galaxy of research achievements of uranium geology of China*. Uranium Geol, Beijing, pp 189–195
- Luo XZ, Du GS, He BA, Campbell AR (1999) Mineralogical and geochemical constraints on the genesis of the granite-hosted Huangao uranium deposit, SE China. *Ore Geol Reviews*, 14, pp 105–127
- Magnuson S, Stover DE (2006) Commercial development of the Inkai ISL uranium project. *In: Symposium on uranium production and raw materials for the nuclear fuel cycle*. Proceedings Series, IAEA, Vienna, pp 212–224
- Mahadevan TM (1988) Characteristics and genesis of the Singhbhum uranium province, India. *In: Recognition of Uranium Provinces*, IAEA, Vienna, pp 337–370
- Maksimova MF, Brovin KG, Goldstein RI, Natalchenko BI (1995) Rare earth elements concentration in the areas of grey rocks and thinning out oxidation zones. *In: Rare metal-uranium ore formation within sedimentary rocks*. Nauka, Moscow, pp 90–106, (in Russian)
- Malan RC (1980) Volcanogenic uranium-molybdenum deposits in Russia and China. US-DOE Country File CN-14, 17 p
- Mangas J, Arribas A (1984) Características físico-químicas de los fluidos asociados con las mineralizaciones de uranio de mina Fé (Salamanca). VII Congr Intern Min Met, Barcelona, I, pp 435–451
- Mann AW, Deutscher RL (1978a) Genesis principles for the precipitation of carnotite in calcrete drainages in Western Australia. *Econ Geol*, v 73, pp 1724–1737
- Mann AW, Deutscher RL (1978b) Hydrogeochemistry of a calcrete-containing aquifer near Lake Way, Western Australia. *J Hydrol*, 38, pp 357–377
- Mansoor M, Ali M, Jafri SSH (2002) In situ leach mining operations at Qabul Khel, Pakistan. *In: In situ leach uranium mining*. T1-TC-975, IAEA, Vienna, pp 64–73
- Maruejol B, Cuney M (1985) Xihuashan tungsten-bearing granites (Jiangxi, China): Mineralogical controls on REE, Y, Th, U mobility during magmatic evolution and hydrothermal alteration (abstr). K 54, EUG III, Strasbourg
- Mashkovtsev GA, Naumov SS (eds) (1999) (Map of) Uranium resources, production, consumption. Russia and CIS countries. Ministry Natural Resources Russia and Fedorovsky Scientific-Research Inst.
- Mashkovtsev GA, Kislyakov YM, Miguta AK, Modnikov IS, Shchetochkin VN (1995b) Prerequisites for the formation of large hydrothermal and exogenic-epigenetic uranium deposits. *Geol Rudn Mestorozhd*, v 37, no 6, pp 467–482
- Mashkovtsev GA, Kochenov AV, Khaldey AE (1995a) On hydrothermal sedimentary formation of stratiform uranium deposits in Phanerozoic depressions. *In: Kholodov VN, Mashkovtsev GA (eds) Rare-metal-uranium ore formation within sedimentary rocks*. Nauka, Moscow, pp 37–52, (in Russian)
- Mashkovtsev GA, Kislyakov YM, Miguta AK, Modnikov IS (1998) Commercial genetic types of uranium deposits. *Otechestvennaya Geologia*, no 4, pp 13–20, (in Russian)
- Mathews GW, Jones CA, Pilcher RC, D'Andrea RF Jr (1979) Preliminary recognition criteria for uranium occurrences: A field guide. US-DOE, GJBX-32(79), 41 p
- Matos Dias JM, Soares de Andrade AA (1970) Uranium deposits in Portugal. *In: Uranium exploration geology*. IAEA, Vienna, pp 129–252
- Maurice YT (ed) (1982) Uranium in granites. *Geol Surv Canada P 29* 81–23, 173 p
- Mazimhaka PK, Hendry HE (1989) Uranium deposits in the Beaverlodge area, northern Saskatchewan: Their relationship to the Martin Group (Proterozoic) and the underlying basement. *In: Uranium resources and geology of North America*. TECDOC-500. IAEA Vienna, pp 297–320
- McKay AD, Miezitis Y (2001) Australia's uranium resources, geology and development of deposits. AGSO-Geoscience Australia, Mineral Resource Report 1, 200 p
- McKelvey VE, William JS, Sheldon RP, Cressman ER, Cheney TM, Swanson RW (1956) Summary descriptions of Phosphoria, Park City, and Sheshhorn Formations in western phosphate field. *Amer Assoc Petrol Geol Bull*, v 40, pp 2326–2363
- Mellinger M, Quirt D, Hoeve J (1987) Geochemical signatures of uranium deposition in the Athabasca Basin of Saskatchewan, Canada. *Uranium*, 3, pp 187–209
- Melnikov IV, Streltsov VA, Timofeev AV (1996) Mineralogical and geochemical features of the molybdenum-uranium deposits in the Kattasai-Alatanga ore field (Uzbekistan). *Geol Ore Dep*, v 38, no 3, pp 227–246
- Mickle DG, Mathews GW (1978) Geologic characteristics of environments favorable for uranium deposits. US-DOE, GJBX-67(78), 250 p
- Miguta AK (1997) Composition and mineral assemblages of uranium ores in the Elkon District, Aldan Shield (Russia). *Geol Ore Deposits*, v 39, no 4, pp 275–293
- Miguta AK (2000) Peculiarities of the uranium deposits in the Elkonsky area, the main uranium producers in Russia. *In: Gavrilin VI et al. (eds) Uranium at the turn of the century: Resources, production, demand*. Abstracts Intern Symp Uran Geol, Moscow, All-Russian Sci Res Inst Mineral Resources NM Fedorovsky, pp 57–58
- Miguta AK (2001) Uranium deposits of the Elkon ore district in the Aldan shield. *Geol Ore Deposits*, v 43, no 2, pp 117–135
- Miguta AK, Modnikov IS (1993) Uranium mineralization of the Mesozoic activated regions in the southeastern Siberian Platform. *Otechestvennaya Geol*, no 5, pp 15–21, (in Russian)
- Miguta AK, Tarkhanov AV (1998) Mineral types of uranium ores in sodic metasomatites, Ukrainian Shield. *Geol Ore Deposits*, v 40, no 6, pp 429–444
- Mikhailov VV, Petrov NN (1998) Age of exogene uranium deposits in south and south-east Kazakhstan according to the lead-isotope study. *Geology of Kazakhstan* 2(354), pp 63–70 (in Russian)
- Min M (1991) Mineral paragenetic associations and textural patterns in the uranium deposits of granite-type in China. *In: Cuney M (ed) Primary radioactive minerals: The textural patterns of radioactive mineral paragenetic associations*. Theophrastus, Zographou, Athens, pp 75–104
- Min M (1995) Carbonaceous-siliceous-pelitic rock type uranium deposits in southern China: Geologic setting and metallogeny. *Ore Geol Reviews*, v 10, pp 51–64
- Min M, Wang XY, Shen BP (1996) Mechanics of the mineralized breccias in no 320 uranium deposit. *Uranium Geol*, v 12, pp 24–28, (in Chinese with English abstract)
- Min M, Zheng D, Shen B, Wen G, Wang X, Gandhi SS (1997) Genesis of the Sanbaqi deposit: A paleokarst-hosted uranium deposit in China. *Mineral Deposita*, v 32, pp 505–519
- Min M, Luo XZ, Du GS, He BA, Campbell AR (1999) Mineralogical and geochemical constraints on the genesis of the granite-hosted Huangao uranium deposit, SE China. *Ore Geol Review*, v 14, no 2, pp 105–127
- Min M, Luo XZ, Mao SK, Zheng DY, Shen BP (2002) The Saqisan Mine – A paleokarst uranium deposit, South China. *Ore Geol Reviews*, v 19, no 1–2, pp 79–94
- Mineeva IG (1984) Mineralogisch-geochemische Aspekte der Bildung uranförender Albitite. 27th Intern Geol Congr, Moscow, manuscript, 15 p
- Minter WEL, Hill WCN, Kidger RJ, Kingsley CS, Snowden PA (1986) The Welkom Goldfield. *In: Annhaeusser CR, Maske S (eds) Mineral deposits of southern Africa*. *Geol Soc S Afr*, v 1, pp 497–539
- Minerals Yearbook (1946) pp 1205–1231
- Minerals Yearbook (1949) pp 1257ff
- Mironov YB (2002) Formation conditions and localization of endogenic ore mineralization of the Dornod ore cluster. DSc (Geol-Mineral) Diss, VSEGEI, St. Petersburg, (in Russian)
- Mironov YB (2003) Uranium in Mongolia. St. Petersburg, 326 p, (in Russian) (English version NHM-CERCAMS, London 2005, 241 p)
- Mironov YB, Rogov YG (1992) Geological information on uranium deposits of Mongolia including geological-economical passports of deposits. Irkutsk
- Mironov YB, Rogov YG (1993) Data on uranium deposits of Mongolia (manuscript for IAEA World Uranium Atlas)
- Mironov YB, Davidenko VM, Petrov VA (1991) Structural and petrophysical localization conditions of uranium ore mineralization in volcanotectonic edifices. *Geol Rudn Mestorozhd*, v 33, no 4, pp 49–57, (in Russian)

- Mironov YB, Filonenko YD, Solovov NS, Petrov VA, Golovin VA, Streltsov VA (1993) Lead-zinc, uranium, and fluorite deposits in the Dornot volcano-tectonic structure (East Mongolia). *Geol Rudn Mestorozhd.*, v 35, no 1, pp 16–30, (in Russian)
- Mironov YB, Naumov SS, Jamsrandorj G, Chuluun O (1995) The uranium resources of Mongolia. *In: Recent developments in uranium resources and supply*. TECDOC 823, IAEA, Vienna, pp 177–192
- Miyoda H (2001) The current uranium exploration activities of the Power Reactor and Nuclear Fuel Development Corporation (PNC), Japan. *In: Assessment of uranium deposit types and resources – A worldwide perspective*. TECDOC-1258, IAEA, Vienna, pp 53–60
- Modnikov IS, Chesnokov LV, Lebedev-Zinovyev AA, Khaldey AY, Frolov GI (1978) Distribution patterns of uranium-molybdenum mineralization in volcanic-tectonic complexes of regions of continental volcanism. *Intern Geol Rev*, 21(1), pp 11–24
- Moghal MY (1974a) Uranium in Siwalik sandstones, Sulaiman Range, Pakistan. *In: Formation of uranium ore deposits*. IAEA, Vienna, pp 383–400
- Moghal MY (1974b) Exploration of uranium deposits in Dera Ghazi Khan District (Punjab), Pakistan. *Geol Surv Pak, Geonews, Quetta*, v 5, no 4, pp 72–78
- Moghal MY (1992) Field test for in situ leach mining of uranium in Pakistan. *In: New developments in uranium exploration, resources, production and demand*. TECDOC-650, IAEA, Vienna, pp 214–224
- Moghal MY (2001) Current uranium activities in Pakistan. *In: Assessment of uranium deposit types and resources – A worldwide perspective*. TECDOC-1258, IAEA, Vienna, pp 101–115
- Molinas E, Dardel J (1985) Mission d'expertise Cogéma en Indonésie, (internal report)
- Moltchanov A (2003a) The Toporican uranium deposit (Aldan shield, Russia) – Geological and mineral-geochemical aspects of the model unconformity type-deposit. *In: Cuney et al. (eds) Uranium geochemistry*. Univ Henri Poincaré, Vandoeuvre les Nancy, pp 251–253
- Moltchanov A (2003b) Metallogeny of the Aldan and the Annabar shields. *In: Cuney et al. (eds) Uranium geochemistry*. Univ Henri Poincaré, Vandoeuvre les Nancy, pp 254–255
- MSRandD/Mountain States Research and Development (1978) Engineering assessment and feasibility study of the Chattanooga Shale as a future source of uranium. US-DOE, GJBX-4(79), v 1, 257 p, v 2, 365 p, v 3, 216 p
- Muto T (1961) Parageneses of the minerals of the Ningyo-toge Mine. *Mineral J*, Tokyo, v 3, pp 195–222
- Muto T, Meyrowitz R, Pornmer AM, Murano T (1959) Ningyoite – A new uranium phosphate mineral from Japan. *American Mineral*, v 44, pp 633–650
- Mutschler PH, Hill JJ, Williams BB (1976) Uranium from the Chattanooga Shale. *US Bur Mines Inform Circ* 8700, 85 p
- Nagabhushana IC, Vasudeva Rao M, Sahasrabudhe GH, Krishnamoorthy B, Suryanarayana Rao C, Rama Rao YN (1976) Geology and structure of major uranium-bearing zones in India and their exploration. *In: Exploration for uranium deposits*. IAEA, Vienna, pp 625–643
- Nakoman E (1979) Geology of radioactive deposits, Maden Tetik ve Arama Enst Vayinl. *Egit Ser* no 20, Ankara, 575 p, (in Turkish)
- Nash JT, Granger HC, Adams SS (1981) Geology and concepts of genesis of important types of uranium deposits. *Econ Geol*, 75th Anniversary Vol, pp 63–116
- Nathan Y, Shiloni Y (1976) Exploration for uranium in phosphorites: A new study on uranium in Israel phosphorites. *In: Exploration for uranium ore deposits*. Proc Series, IAEA, Vienna, pp 645–656
- Naumov SS (1993) Mineral-resource base of uranium in Russia. *Razved Okhr Nedr*, no 8, pp 11–13, (in Russian)
- Naumov SS (1999) Uranium raw material base. *Gorny Journal*, no 12, pp 12–18, (in Russian)
- Naumov SS, Shumilin MV (1992) The classification, cost categories and the system accounting of uranium resources in Russia and CIS countries. Consultative meeting, IAEA, Vienna, 12 p
- Naumov SS, Shumilin MV (1994) Uranium deposits of Aldan. *Otech Geol*, no 11–12, pp 20–23, (in Russian)
- Naumov SS et al. (1996) Mineralogy, zonality and ore types of hydrothermal uranium deposits of northern Kazakhstan (abstr). 30th Intern Geol Congr, Beijing, China, v 2, p 701
- Naumov SS, Tarkhanov AV, Birka GI (2005) Future development of uranium industry in Russia. *In: Developments in uranium resources, production, demand and the environment*. TECDOC-1425, IAEA, Vienna, pp 43–49
- Needham RS, Ewers GR, Ferguson J (1988) Pine Creek Geosyncline. *In: Recognition of uranium provinces*. IAEA, Vienna, pp 235–262
- Nenadkevich KA (1912) Tyuyamunitite – A new mineral. *Izv Akad Nauk SSSR, Ser* 6, 6, pp 945–946, (in Russian)
- Nenadkevich KA (1917) Deposit Tyuya-Muyun. *KEPS Russia*, 4, issue 14, (in Russian)
- Nguyen Van Hoai, Phan Van Quynh (1992) Main types of uranium mineralization and uranium exploration in Viet Nam. *In: New developments in uranium exploration, resources, production and demand*. TECDOC-650, IAEA, Vienna, pp 115–117
- Nikolsky A, Schulgin A (2001) Regularities of mineral and commercial ore types: Location in uranium deposits of Streltsovsky District (Russia). *In: Assessment of uranium deposit types and resources – A worldwide perspective*. TECDOC-1258, IAEA, Vienna, pp 239–250
- NUKEM (1999) The Chinese approach to mining, milling and management. *Nukem Market Report July 1999*, NUKEM, Stanford, Ct, pp 7–20
- OECD/NEA (2006) Forty years of uranium resources, production and demand in perspective. *OECD/NEA*, Paris, 270 p
- OECD-NEA, IAEA (1978) IUREP/International uranium resources evaluation project: Pakistan. *OECD-NEA*, Paris, 7 p
- OECD-NEA, IAEA (1980) World uranium geology and resource potential. IUREP, report on phase I. *OECD-NEA*, Paris, Miller Freeman Public. Inc., San Francisco, 524 p
- OECD-NEA, IAEA (1973–2008) Uranium: Resources, production and demand. Biannual publications
- Okada S, Hashimoto Y, Itoh K (1988) Historical review of uranium exploration in Japan. *In: Uranium deposits in Asia and the Pacific: Geology and exploration*. IAEA, Vienna, pp 193–206
- Omelyanenko BI (1978) Wall rock hydrothermal alteration. *Nedra*, Moscow, (in Russian)
- Omelyanenko BI, Gorshkov AA, Kambolin AE, Raudonis PA (1993) Geological characteristics of the Grachevskoye uranium deposit. *Geol Ore Deposits*, v 35, no 5, pp 386–404
- Orajaka IP (1981) Mineralogy and uranium geochemistry of selected volcanoclastic sediments in the western United States – an exploration model. *Univ Texas, El Paso, DGSc diss*, 365 p
- Otton JK (1981) Geology and genesis of the Anderson Mine, a carbonaceous lacustrine uranium deposit, western Arizona: A summary report. *US Geol Surv Open File Report* 81–780, 24 p
- Otton JK (1986) Geological environment of uranium in lacustrine host rocks in the western United States. *In: Geological environments of sandstone-type uranium deposits*. TECDOC-328, IAEA, Vienna, pp 229–241
- Otton JK, Zielinski RA, Johnson SY (1989) The Flodelle Creek surficial uranium deposit, Stevens County, Washington, USA. *In: Uranium resources and geology of North America*. TECDOC-500, IAEA, Vienna, pp 241–262
- Page M (1984) Petrology, mineralogy and geochemistry of surficial uranium deposits. *In: Surficial uranium deposits*. TECDOC-322, IAEA, Vienna, pp 37–44
- Page M, Pironon J (1986) Un modèle de formation de gisements d'uranium dans les shales noirs continentaux. *Sci Géol Bull*, 39, pp 277–292
- Page M, Halter G, Ruhlmann F, Tona F (1988) Évolution polycyclique de la province uranifère Athabasca (Saskatchewan-Canada) et genèse des gisements liés spatialement à la discordance du Proterozoïque moyen dans la structure de Carswell. *In: Johan Z, Ohnenstetter D (eds) Gisements métallifères dans leur contexte géologique*. *Bur rech géol minières, Document* 158, pp 389–414
- Page M, Forbes P, Mondy J, Oumarou J, Vergely P, Wollenberg P (2003) The uranium deposits from the Arlit area (Niger): Field observations, laboratory data, questions. *In: Cuney M (ed) Uranium geochemistry*, Nancy, pp 277–280
- Palabora Mining Company Limited Mine Geological and Mineralogical Staff (1976) The geology and economic deposits of copper, iron and vermiculite in the Palabora Igneous Complex: A brief review. *Econ Geol*, v 71, pp 177–192
- Pan Yongzheng, Zhang Jianxin (1996) Discussion on the relationship between extensional tectonics and U metallogenesis in the southern part of the Zhuguang granite massif. *In: Chen Zhaobo et al. (eds) Galaxy of research achievements of uranium geology in China*. *Uranium Geol*, Beijing pp 132–137
- Pardo-Leyton E (1985) Uranio en rocas igneas: Intrusivas sub-efusivas y piroclásticas del Orogeno Andino boliviano. *In: Uranium deposits in volcanic rocks*. IAEA, Vienna, pp 255–274

- Pavlenko DM (1933) New data on geology and genesis of the Tyuya-Muyun deposit in Uzbekistan. *Problems of Soviet geology*, no 10, (in Russian)
- Pavlenko VM (2005) Status and perspective developments of uranium production in Ukraine. *In: Developments in uranium resources, production, demand and the environment*. TECDOC-1425, IAEA, Vienna, pp 51–72
- Peiffert C, Nguyen Trung C, Cuney M (1996) Uranium in granitic magmas. Part II: experimental determination of uranium solubility and fluid–melt partition coefficients in the UO_2 –haplogranite– H_2O –halides system at 720–770°C, 200 MPa. *Geochim Cosmochim Acta*, v 60, pp 1515–1529
- Pelmenev MD (1995) Essential regularities of formation and conditions of marking out uranium ore-bearing districts in East Siberia. *Otechestvennaya Geologia*, no 9, pp 32–38, (in Russian)
- Peng Xinjian, Min Maozhong, Luo Xingzhang, Qiao Haiming, Jiang Shaoyong, Zhang Guanghui (2002) Elemental and isotopic geochemistry of modern ore-forming fluids in Shihongtan uranium deposit, NW China. *In: Bureau of Geology, CNNC (ed) Sandstone-type uranium deposits in China: Geology and exploration techniques*. Atomic Energy Press, Beijing, pp 153–165
- Perelman (ed) (1980) Hydrogenic uranium deposits. Atomizdat, Moscow, 270 p, (in Russian)
- Perevozchikov GV (2000) Petroleum hydrocarbons and uranium deposits. *In: Gavrilin VI et al. (eds) Uranium at the turn of the century: resources, production, demand*. Abstracts Intern Symp Uran Geol, Moscow, All-Russian Sci Res Inst Mineral Resources NM Fedorovsky, pp 87–88
- Petroš R, Prokeš S, Komínek J (1986) Uranium deposits of Pojbram, CSSR. *In: Vein type uranium deposits*. TECDOC-361, IAEA, Vienna, pp 307–318
- Petrov NN (1998) Epigenetic stratified-infiltration uranium deposits of Kazakhstan (in Russian). *Geology of Kazakhstan* 2(354), pp 22–39 (in Russian)
- Petrov NN, Yazikov VG, Aubakirov HB, Plekhanov VN, Vershkov AF, Lukhtin VF (1995) Uranium deposits of Kazakhstan (exogenous). *Gylym Almaty*, 264 p, (in Russian)
- Petrov NN, Yazikov VG, Berikbolov BR, Vershkov AF, Egorov SA, Zhelnov VP, Karelin VG, Kravtsov EG, Nikolaev SL, Ostrokom IM, Shishkov IA (2000) Uranium deposits of Kazakhstan (endogenous). *Gylym Almaty*, 523 p, (in Russian)
- Petrov VA, Golubev VN, Golovin VA (2002) Structural, geochemical and isotopic evolution of uranium deposits in the Domot ore field, Mongolia. *In: Kribek B, Zeman J (eds) Uranium deposits: from their genesis to their environmental aspects*, Czech Geol Surv, Prague, pp 103–106
- Petrov VA, Golubev VN, Golovin VA (2003) A unique uranium mineralization in pillow lavas, Dornot ore field, Mongolia. *In: Cuney et al. (eds) Uranium geochemistry*. Univ Henri Poincaré, Vandoeuvre les Nancy, pp 289–292
- Petrov VA, Poluektov V, Golubev VN, Andreeva OV, Kartashov PN, Lespinasse M, Sausse J, Cuney M, Lichtner PC, Perry FV, Galinov YN, Ovseichuk VA, Schukin SI (2005) Uranium mineralization in oxidized fractured environment of the giant volcanic-related uranium field from the Krasnokamensk area. *In: Uranium production and raw materials for the nuclear fuel cycle – Supply and demand, economics, the environment and energy security*. CN-128, IAEA, Vienna, pp 260–264
- Petrov VA, Poluektov V, Hammer J, Wittenberg A, Kocks H, Lespinasse M (2006) Process of uranium migration and fixation in fractured volcanic environment of the Tuluevskoe deposit, Transbaikalia, Russia (abstr.). *Berichte DMG*, no 1, p 104
- Polito PA, Kyser TK, Thomas D, Marlatt J, Drever G (2005) Re-evaluation of the petrogenesis of the Proterozoic Jabiluka unconformity-related uranium deposit, Northern Territory, Australia. *Mineral Deposita*, v 40, pp 257–288
- Polyarshinov GP, Pigulski VM (1995) Geological prospecting experience resulting in discovery of workable uranium deposits of various genetic types in north Kazakhstan ore province. TECDOC-823, IAEA, Vienna, pp 243–256
- Pool TC (1993) Uranium resources for long-term, large-scale nuclear power requirements (manusc). Nuclear Energy Workshop, Oak Ridge National Laboratory, 5 p
- Poty B, Leroy J, Cathelineau M, Cuney M, Friedrich M, Lespinasse M, Turpin L (1986) Uranium deposits spatially related to granites in the French part of the Hercynian Orogen. *In: Vein type uranium deposits*. TECDOC-361, IAEA, Vienna, pp 215–246
- Pretorius DA (1976a) Gold in the Proterozoic sediments of South Africa: Systems, paradigms and models. *In: Wolf KH (ed) Handbook of strata-bound and stratiform ore deposits*. v 7, Elsevier, Amsterdam, pp 1–27
- Pretorius DA (1976b) The nature of the Witwatersrand gold-uranium deposits. *In: Wolf KH (ed) Handbook of strata-bound and stratiform ore deposits*. v 7, Elsevier, Amsterdam, pp 29–88
- Pretorius DA (1981) Gold and uranium in quartz-pebble conglomerates. *Econ Geol*, 75th Anniversary Vol, pp 117–138
- Qin Fei, Hu Shaokang (1980) Present exploration status of the Lianshangan uranium deposit, northeast China. *In: Uranium in the Pine Creek Geosyncline*. IAEA, Vienna, pp 655–661
- Ramdohr P (1958a) Die Uran- and Goldlagerstätten Witwatersand-Blind River District-Dominion Reef-Serra de Jacobina. *Abh Deutsch Akad Wiss, Berlin, Klasse Chem Geol Biolog*, no 3, pp 1–35
- Ramdohr P (1958b) New observations on the ores of the Witwatersrand in South Africa. *Geol Soc S Afr*, v 71, pp 67–100
- Ramdohr P (1980) The ore minerals and their intergrowths. Pergamon Press, 1207 p
- Ramezani J, Tucker RD (2003) The Saghand region, Central Iran: U-Pb geochronology, petrogenesis and implications for Gondwana tectonics. *American J Sci*, v 303, pp 622–665
- Rao NK (1977) Mineralogy, petrology and geochemistry of uranium prospects from parts of Singhbhum shear zone, Bihar. Ph.D. thesis, Banaras Hindu Univ, 335 p
- Rao BV, Ramo (1975) Discovery of the uraniumiferous Precambrian conglomerates at Chikmagalur, Karnataka, India. *Current Sci*, v 44, p 174
- Rao NK, Rao GVU (1983) Uranium mineralization in Singhbhum shear zone, Bihar. *J Geol Soc India*, v 24, pp 615–627
- Rao NK, Aggarwal SK, Rao GVU (1979) Lead isotope ratios of uraninites and the age of uranium mineralization in Singhbhum shear zone, Bihar. *J Geol Soc India*, v 20, pp 124–127
- Rao NP, Kumar P, Srivastava SK, Sinha RM (2001) Uranium mineralisation in Kurnool sub-basin Cuddapah Basin, Andhra Pradesh. *J Geol Soc India*, v 57, no 5, pp 462ff
- Rautman CA (ed) (1980) Geology and mineral technology of the Grants Uranium Region 1979. *New Mex Bur Mines Mineral Res Mem* 38, 400 p
- Reeve JS, Cross KC, Smith RN, Oreskes N (1990) The Olympic Dam copper-uranium-gold silver deposit, South Australia. *In: Hughes F (ed) Geology of mineral deposits of Australia and Papua New Guinea*. AIMM Monogr 14, pp 1009–1035
- Reeves MJ, Saadi TA (1971) Factors controlling the deposition of some phosphate-bearing strata from Jordan. *Econ Geol*, v 66, pp 451–465
- Rich RA, Holland HD, Petersen U (1977) Hydrothermal uranium deposits. Elsevier Scientific Publ Co, Amsterdam Oxford New York, 264 p
- Robertson JA (1989) The Blind River (Elliot Lake) uranium deposits. *In: Uranium resources and geology of North America*. TECDOC-500, IAEA, Vienna, pp 111–147
- Roscoe Postle Associates Inc. (1996) Technical audit of uranium, phosphate and diamond reserves of Tselinny Gorno-Khimicheskii Kombinat, Northern Kazakhstan. Unpubl rep, 79 p + appendix
- Roslyi AI (1975) Concentration of uranium ores in carbonatic rocks. *Litologiya I, Iskopnaemye*, no 1, pp 84–97, (in Russian)
- Roubault M (1958) Géologie de l'uranium. Masson et Cie, Editeurs, Paris, 462 p
- Roubault M et al. (1969) La géologie de l'uranium dans le massif granitique de Saint-Sylvestre (Limousin, Massif Central Français). *Sci Terre, Mém* no 15, 213 p
- Roy M, Dhana Raju R (1997) Petrography and depositional environment of the U-mineralized phosphatic siliceous dolostone of Vempalle Formation, Cuddapah Basin, India. *J Geol Soc India*, v 50, pp 577–585
- Roy C, Halaburda J, Thomas D, Hirsekorn D (2006) Millennium Deposit – Basement-hosted derivative of the unconformity uranium model. *In: Symposium on uranium production and raw materials for the nuclear fuel cycle – Supply and demand, economics, the environment and energy security*. Proc Series, IAEA, Vienna, pp 111–121
- Rubinov IM, Bazhenov MI, Udovik VV, Brednihin IF (2000) The Malinovskoye uranium deposit in the Westsiberian uranium belt. *In: Gavrilin VI et al. (eds) Uranium at the turn of the century: resources, production, demand*. Abstracts Intern Symp Uran Geol, Moscow, All-Russian Sci-Res Inst Mineral Resources NM Fedorovsky, p 59
- Ruhrmann G (1986) The Gaertner uranium orebody at Key Lake (northern Saskatchewan, Canada) after three years of mining: An update of the geology.

- In: Gilboy CF, Vigrass LW (eds) Economic minerals of Saskatchewan. Sask Geol Soc Spec Publ no 8, pp 120–137*
- Rui-Zhong Hu, Xian-Wu Bi, Mei-Fu Zhou, Jian-Tang Peng, Wen-Chao Su, Shen Liu, Hua-Wen Qi (2008) Uranium metallogenesis in South China and its relationship to crustal extension during the Cretaceous to Tertiary. *Econ Geol*, v 103, no.3, pp 583–598
- Ruzicka V (1971) Geological comparison between East European and Canadian uranium deposits. *Geol Surv Can Paper* 70–48, 196 p
- Ruzicka V (1988) Geology and genesis of uranium deposits in the Early Proterozoic Blind River–Elliot Lake Basin, Ontario, Canada. *In: Recognition of uranium provinces. IAEA, Vienna, pp 107–130*
- Saadi TA, Shaaban MR (1981) Uranium in Jordanian phosphates and its distribution in the beneficiation processes. *Arab Mining J*, v 1, no 3, pp 70–79
- Safonov YG, Bortnikov NS, Zlobina TM, Chernyshev VF, Dzainukov AB, Prokofev VY (2000a) Polymetal (Ag, Pb, U, Cu, Bi, Zn, F) Adrasman-Kanimansur ore field (Tajikistan), and its ore-forming system. I: Geology, mineralogy, and structural conditions of the ore deposition. *Geol Ore Dep*, v 42, no 3, pp 175–188
- Safonov YG, Bortnikov NS, Zlobina TM, Chernyshev VF, Dzainukov AB, Prokofev VY (2000b) Polymetal (Ag, Pb, U, Cu, Bi, Zn, F) Adrasman-Kanimansur ore field (Tajikistan), and its ore-forming system. II: Physico-chemical, geochemical and geodynamic formation conditions. *Geol Ore Dep*, v 42, no 4, pp 317–327
- Saima Deposit Research Group (1976) Uranium deposits in the Saima Alkaline Massif, northeast China. *Peking Inst Uranium Geol*, pp 1–18
- Saima Scientia Sinica (anonymous) (1977) Uranium deposit in the Saima alkaline massif, northeast China. *Scientia Sinica*, v 21, no 9
- Sakamaki Y (1986) Geologic environments of Ningyo-toge and Tono uranium deposits, Japan. *In: Geological environments of sandstone type uranium deposits. TECDOC-328, IAEA, Vienna, pp 135–154*
- Samama JC (1984) Uranium in lateritic terranes. *In: Surficial uranium deposits. TECDOC-322, IAEA, Vienna, pp 53–59*
- Samani B (1988a) Metallogeny of the Precambrian in Iran. *Precambrian Research*, v 39, pp 85–106
- Samani B (1988b) Recognition of uraniferous products from the Precambrian of Iran. *Krystalinikum*, v 19, pp 147–165
- Samani B (1998) Precambrian metallogenic in Central Iran. *AEOI Scientific Bull*, v 17, pp 1–16, (in Persian with English abstr.)
- Saraswat AC, Mahadevan TM (1989) Genetic aspects of uranium mineralization in the Himalaya. *In: Metallogenesis of uranium deposits. IAEA, Vienna, pp 369–397*
- Saraswat AC, Rishi MK, Gupta RK, Bhaskar D (1977) Recognition of a favourable uraniferous area in sediments of Meghalaya, India: A case history. *In: Recognition and evaluation of uraniferous areas. IAEA, Vienna, pp 165–181*
- Saraswat AC, Krishnamoorthy P, Mahadevan TM (1988) Uranium provinces of the Indian subcontinent and surroundings. *In: Uranium deposits in Asia and the Pacific: geology and exploration. IAEA, Vienna, pp 39–58*
- Sarbini SA, Wirakusumah W (1988) Uranium deposit model for estimation of ore reserves in the Remaja area, west Kalimantan. *In: Uranium deposits in Asia and the Pacific: geology and exploration. IAEA, Vienna, pp 155–166*
- Sarkar SC (1982) Uranium (nickel-cobalt-molybdenum) mineralization along the Singhbhum copper belt, India and the problem of ore genesis, *Mineral Deposita*, v 17, pp 257–278
- Sarkar SC (1984) Geology and ore mineralisation of the Singhbhum copper-uranium belt, Eastern India. *Jadavpur Univ, Calcutta*, 263 p
- Sarkar SC (1986) The problem of uranium mineralization in Precambrian metamorphic shear tectonites – With particular reference to the Singhbhum copper-uranium belt Eastern India. *In: Vein type uranium deposits. TECDOC-361, IAEA, Vienna, pp 9–20*
- Sarkar SN, Saha AK (1983) Structure and tectonics of the Singhbhum iron ore craton. *In: Sinha Roy S (ed) Structure and tectonics of Precambrian rocks of India. Recent Researches Geol*, 10, Hindusthan Publ Corp, Delhi, pp 1–25
- Sarkar SN, Chakravarti A, Basu S, Gangopadhyay A (1988) Structural control and geochemistry of sulfide bodies in Mosabani-Badia area, Singhbhum copper-belt. *In: Mukhopadhyay D (ed) Precambrian of the Eastern Indian Shield. Geol Soc Ind*, pp 217–228
- Savchenko GA, Zubkov VP, Malyukova NN (2003) General condition and perspectives for development of U mineral-raw material in Kyrgyz Republic. *In: Cuney et al. (eds) Uranium geochemistry. Univ Henri Poincaré, Vandoeuvre les Nancy, pp 327–330*
- Saxena VP, Sinha RM, Yadav OP, Sessa Rao RVS (2006) Geochemical modelling for the unconformity-related uranium mineralization. A case study from Baskati area, Madhya Pradesh, India. *In: Symposium on uranium production and raw materials for the nuclear fuel cycle. Proceedings Series, IAEA, Vienna, pp 141–151*
- Schmitt JM, Clement JY (1989) Triassic regolithization: A major stage of pre-enrichment in the formation of unconformity-related deposits in southern France. *In: Metallogenesis of uranium deposits. IAEA, Vienna, pp 93–114*
- Sengupta PR (1972) Studies on mineralisation in the southeastern part of the Singhbhum copper belt. *Mem Geol Surv Ind*, p 101
- Sengupta B, Bahuguna R, Kumar S, Singh R, Kaul R (1991) Discovery of a sandstone-type uranium deposit at Domiasiat, West Khasi Hills District, Meghalaya, India. *Current Sci*, v 61, pp 46–47
- Seo T, Ochiai Y, Takeda S, Nakatsuka N (1989) Natural analogue study on Tono sandstone-type uranium deposit in Japan. *In: Proc 1989 Joint Int Waste Management Conf, Kyoto, Japan. pp 353–358*
- Shakhverdov V (2003) Major mechanism of uranium behaviors in modern oxidizing epigenetic process in exogenetic epigenetic deposits of the Chusarysuskay Province (Southern Kazakhstan). *In: Cuney et al. (eds) Uranium geochemistry. Univ Henri Poincaré, Vandoeuvre les Nancy, pp 339–342*
- Shankaran AV, Bhattacharyya TK, Dar KK (1970) Rare earth and other trace elements in uraninites. *Jour Geol Soc India*, v 11, pp 205–216
- Sharma UP, Gajapathi RR, Pandit SA, Mary KK (1998a) A note on uranium mineralization in the Neoproterozoic calcitic phosphorite from Ramthirth, Bhima Basin, Gulbarga Dist., Karnataka. *Current Sci*, v 75, no 4, pp 357–358
- Sharma UP, Panda A, Pandit SA, Gangadharan GR, Roy M (1998b) Proterozoic stratabound dolostone-hosted uranium mineralization in the Komantula-Reddypalle area, Cuddapah Basin, Anantapur District, Andhra Pradesh, India. *Expl Res Atom Minerals, AMD, India*, v 11, p 45–53
- Sharma M, Rawat TPS, Sharma YC, Swarnkar BM, Jagmer Singh (2001) Sandstone-type uranium mineralisation in the early Tertiary sedimentary sequence in Tarol-Maltu area, Solan District, Himachal Pradesh. *J Geol Soc India*, v 57, no 5, pp 459–461
- Shayakubov TS, Karimov KK, Bobonarov NS, Demina TY, Goldshtein RI (1995) Uranium geology and uranium ore base of Uzbekistan. *Otech Geol*, no 9, pp 55–61, (in Russian)
- Shcherbakov DI (1924) Deposits of radioactive ores and minerals in Fergana and tasks for their study. *Materials for study of natural resources in Russia*, no 47, (in Russian)
- Shcherbakov DI (1937) The rare elements of central Asia (abstr). *Intern Geol Congr, Moscow*, pp 171–172
- Shcherbakov DI (1941) Searching for radium. *Gosgeoltechizdat*, (in Russian)
- Shcherbakov DI (chief ed) (1966) *Geology of hydrothermal uranium deposits. Nauka, Moscow*, 443 p, (in Russian)
- Shchetochkin VN, Kislyakov YM (1993) Exogenic-epigenetic uranium deposits of the Kyzylkums and adjacent areas. *Geol Ore Deposits*, v 35, no 3, pp 199–220
- Shen J (1991) Isotope geochemistry of granitoid in the middle Zhuguang, south China. *Petrol Acta Sinica*, v 2, pp 38–43, (in Chinese, with English abstr)
- Shen Feng (1991) Uranium exploration and resources in China. *In: Assessment of uranium resources and supply. TECDOC-597, IAEA, Vienna, pp 91–97*
- Shen Feng (1995) Some new uranium exploration areas in China. *In: Recent developments in uranium resources and supply. TECDOC-823, IAEA, Vienna, pp 69–74*
- Shen Feng, Pan Yongzheng, Gong Zhigen, Rong Jiashu (1992) Geological features and new development of the Xiashuang uranium ore field in South China. *In: New developments in uranium exploration, resources, production and demand. TECDOC-650, IAEA, Vienna, pp 169–172*
- Sherborne JE Jr, Buckovic WA, Dewitt DB, Hellinger TS, Pavlak SJ (1979) Major uranium discovery in volcanoclastic sediments, basin and range province, Yavapai County, Arizona. *Amer Ass Petrol Geol Bull* v 63/4, pp 621–645
- Sherih AS, Mihailo GN, Lopatkin AA (1999) Euro-Asian transcontinental uranium metallogenic belt. *Russ Geophys J*, v 25, 16, pp 144–148
- Shi Wenjin, Hu Junzhen (1996) Metallogenic regularities and genetic models of Longshoushan uranium metallogenic belt. *In: Chen Zhaobo et al. (eds)*

- Galaxy of research achievements of uranium geology of China. *Uranium Geol*, Beijing, pp 95–102
- Shikazono N, Utada M (1997) Stable isotope geochemistry and diagenetic mineralization associated with the Tono sandstone-type uranium deposit in Japan. *Mineral Deposita*, v 32, no 6, pp 596–606
- Shimkin DB (1949) Uranium deposits in the USSR. *Science*, v 109, pp 58ff
- Shimkin DB (1953) *Minerals, a key to Soviet power*. Univ Harvard press, 149 p
- Shiqing YU (1989) Characteristics and regional geological environments of uranium deposits in Mesozoic volcanics in east China. *In: Uranium deposits in magmatic and metamorphic rocks*, IAEA, Vienna, pp 77–92
- Shor GM, Markov SN (2002) Paleochannel type uranium deposits in western Siberia and Transbaikalian regions. *Uranium Geol*, v 18, no 2, pp 65–76
- Shor GM, Afanasyev AM, Alekseyenko VD, Koudryovtsev VE, Rousinova LG (2000) The state and prospects for development of the uranium industry base in the West-Siberian platform cover. *In: Gavrilin VI et al. (eds) Uranium at the turn of the century: Resources, production, demand. Abstracts Intern Symp Uran Geol, Moscow, All-Russian Sci Res Inst Mineral Resources NM Fedorovsky*, pp 77–79
- Sibbald TII (1988) Geology and genesis of the Athabasca uranium deposits. *In: Recognition of uranium provinces*. IAEA, Vienna, pp 61–106
- Sibbald TII, Petruk W (eds) (1985) *Geology of uranium deposits*. CIM Spec Vol. 32, 268 p
- Sibbald TII, Quirt D (1987) Uranium deposits of the Athabasca Basin. *Sask Res Council Publ no R-855-1-G-87*, 72 p
- Simpson PR, Yu Shiqing (1989) Uranium metallogeny, magmatism and structure in southeast China. *In: Metallogenesis of uranium deposits*. IAEA, Vienna, pp 357–368
- Singh H (2002) Uranium processing in India: In situ leach prospects. *In: In situ leach uranium mining*. IAEA, Vienna, pp 116–119
- Singh G, Banerjee DC, Dhana Raju R, Saraswat AC (1990) Uranium mineralization in the Proterozoic belts of India. *Expl Res Atom Minerals, AMD, India*, v 3, pp 83–101
- Sinha KK et al. (1992) U mineralization in granitic rocks of Binda-Nagnaha area, Palamau District, Bihar. *Ind J Geol*, v 64, no 1, pp 61–95
- Sinha RM, Srivastava VK, Sharma GVG, Parthasarathy TN (1995) Geological favourability for unconformity-related uranium deposits in the northern parts of Cuddapah Basin; Evidence from Lambapur uranium occurrence, Andhra Pradesh, India. *Expl Res Atom Minerals*, v 8, pp 111–126
- Sinha RM, Parthasarathy TN, Dwivedy KK (1996) On the possibility of identifying low cost, medium grade uranium deposits close to the Proterozoic unconformity in Cuddapah Basin, Andhra Pradesh, India. *In: Innovations in uranium exploration, mining and processing techniques, and new exploration target areas*. TECDOC-868, IAEA, Vienna, pp 35–56
- Smirnov VI (1947) *Geology of mercury deposits in central Asia*. Gosgeolizdat, (in Russian)
- Smirnov VI (1977) *Ore deposits of the USSR*. Pitman, London, 1258 p
- Smorchkov IE (1966) The role of magmatic processes in forming hydrothermal uranium deposits. *In: Geology of hydrothermal uranium deposits*. Nauka, Moscow, pp 119–147, (in Russian)
- Sørensen H, Rose-Hansen J, Nielsen BL, Løvborg L, Sørensen E, Lundgaard T (1974) The uranium deposit at Kvanefeld, Ilimaussaq intrusion, South Greenland. *Rapp Grønlands geol Unders* 60, 54 p
- Stoikov HM, Bojkov IB (1991) *Geology and exploration of uranium deposits*. Spector, Sofia, 148 p, (in Bulgarian)
- Stolyarov AS, Ivleva EI (1995) Uranium-rare metal deposits related to stratum concentrations of fish bone detritus. *In: Kholodov VN, Mashkovtsev GA (eds) Rare-metal-uranium ore formation within sedimentary rocks*. Nauka, Moscow, pp 200–223, (in Russian)
- Sulovsky P (1994) Occurrences of radioactive mineralization associated with salt plugs in the southeastern Zagros fold belt, Iran. PhD thesis, Masaryk University, Czech Rep., (in Czech)
- Swanson VE (1961) *Geology and geochemistry of uranium in marine black shales, a review*. US Geol Surv Prof Paper 356-C, pp 67–112
- Terentyev VM, Kazansky VI (1999) Elkon uranium ore district in the Aldan Shield. *Region Geol Metallogeniya*, no 8, pp 47–58, (in Russian)
- Thamm JK, Kovschak AA, Adams SS (1981) *Geology and recognition criteria for sandstone uranium deposits of the Salt Wash type, Colorado Plateau Province*. US-DOE, GJBX-6(81), 136 p
- Thompson TB, Lyttle T, Pierson JR (1980) *Genesis of the Bokan Mountain, Alaska, uranium-thorium deposits*. US-DOE, 80-38, 237 p
- Thompson TB, Pierson JR, Lyttle T (1982) *Petrology and petrogenesis of Bokan granite complex, southeastern Alaska*. *Geol Soc Amer Bull*, 93, pp 898–908
- Thoste V (1999) *Decommissioning of Mailuu-Suu uranium production combinat (manuscr)*. TCM Developments in uranium resources, production, demand and the environment. IAEA, Vienna, June 1999
- Tjokrokardono S, Sastratenaya AS (1988) *Rich mineralized boulders of the Rirang River, west Kalimantan*. *In: Uranium deposits in Asia and the Pacific: geology and exploration*. IAEA, Vienna, pp 79–96
- Toens PD, Corner B (1980) *Uraniferous alaskitic granites with special reference to the Damara orogenic belt*. S Afr Atomic Energy Board Res PER 55, 18 p
- Toens PD, Hambleton-Jones BB (1984) *Definition and classification of surficial uranium deposits*. *In: Surficial uranium deposits*. TECDOC-322, IAEA, Vienna, pp 9–14
- Tremblay LP (1982) *Geology of the uranium deposits related to the sub-Athabasca unconformity, Saskatchewan*. *Geol Surv Can Paper* 81-20, 56 p
- Tu Guangzhi (1990) *The SW Qinling and SW Guizhou uranium and gold metallogenic belts and their similarities to the Carlin-type gold deposits in the Western States*. *In: Bureau of Geology, CNNC (ed) Uranium provinces in China*. Nat Nuclear Corp, Beijing, China, pp 28–34
- Turner-Peterson CE, Santos ES, Fishman NS (eds) (1986) *A basin analysis case study: The Morrison Formation, Grants Uranium Region, New Mexico*. Amer Ass Petrol Geol, *Studies in Geology*, no 22, 391 p
- Umamaheswar K, Himadri Basu, Patnaik JK, Mir Azam Ali, Banarjee DC (2001) *Uranium mineralisation in the Mesoproterozoic quartzites of Cuddapah Basin in Gandi area, Cuddapah District, Andhra Pradesh: A new exploration target for uranium*. *J Geol Soc India*, v 57, no 5, pp 405–442
- Underhill DH (2005) *Uranium production in the Commonwealth of Independent States, China and Mongolia*. *In: Developments in uranium resources, production, demand and the environment*. TECDOC-1425, IAEA, Vienna, pp 19–42
- US-AEC (1959) *Guidebook to uranium deposits of the western United States*. US-AEC, Grand Junction, Colorado, 1-1 to 7-14 p
- Varnavsky V, Shevchenko B (2000) *The lithologic and facial peculiarities of the uranium-coal deposits in the upper Amur River area*. *In: Gavrilin VI et al. (eds) Uranium at the turn of the century: resources, production, demand. Abstracts Intern Symp Uran Geol, Moscow, All-Russian Sci Res Inst Mineral Resources NM Fedorovsky*, p 42
- Vasudeva RM, Nagabhushana JC, Jeyagopal AV (1989) *Uranium mineralisation in the Middle Proterozoic carbonate rock of the Cuddapah Supergroup, Southern Peninsular India*. *Expl Res Atom Minerals*, v 2, pp 29–38
- Venatovsky IV (1993) *Study of the geotechnical conditions of uranium deposits in Uzbekistan during exploration work*. TECDOC-720, IAEA, Vienna, pp 95–104
- Vishnyakov VE (1995a) *Olovskoye uranium deposit*. *In: Laverov NP (ed) Deposits of Transbaykal*. Geoinformmark, Moscow, v 1, book 2, pp 157–164, (in Russian)
- Vishnyakov VE (1995b) *Uranium deposits of the Korolevo-Chasovo ore field*. *In: Laverov NP (ed) Deposits of Transbaykal*. Geoinformmark, Moscow, v 1, book 2, pp 165–168, (in Russian)
- Vishnyakov VE (1995c) *Uranium deposits of the Daurisky ore district*. *In: Laverov NP (ed) Deposits of Transbaykal*. Geoinformmark, Moscow, v 1, book 2, pp 169–178, (in Russian)
- Viswanath RV, Mahadevan TM (1988) *Uranium exploration in India: An overview*. *In: Uranium deposits in Asia and the Pacific: Geology and exploration*. IAEA, Vienna, pp 213–228
- Vlasov BP, Volovikova IM, Glagyshev GD (1966) *Geology of deposits of uranium-molybdenum ore formation*. Atomizdat, Moscow, 183 p, (in Russian)
- Volfson FI (chief ed) (1978) *Hydrothermal uranium deposits*. Nedra, Moscow, (in Russian)
- Von Backström JW (1975) *Uranium and the generation of power, South Africa perspective*. *Trans Geol Soc S Africa*, v 78, pp 275–292
- Von Backström JW (1976) *Uranium*. *In: Coetzee CB (ed) Mineral resources of the Republic of South Africa*. Rep S Afr Geol Surv, pp 233–239
- Von Backström JW, Jacob RE (1979) *Uranium in South Africa and South West Africa (Namibia)*. *Phil Trans Royal Soc, London*, A291, pp 307–319

- Wallace AR (1986) Geology and origin of the Schwartzwalder uranium deposit, Front Range, Colorado, USA. *In: Vein-type uranium deposits*. TECDOC-361, IAEA, Vienna, pp 159–168
- Wang Chuanwen, Chen Zhaobo, Xie Youxin (1980) The uranium deposits in Shenyuan volcanic basin, South China. Beijing U Geol Research Inst, pp 93–100, (in Chinese with English abstract)
- Wang Jian, Dai Yuan Ning (1993) In-situ leaching of uranium in China. *In: Uranium in situ leaching*. TECDOC-720, IAEA, Vienna, pp 129–132
- Wang Jinping, Li Zhanshuang, Li Zhanyou (2002) Geological-geochemical characteristics of Shihongtan uranium deposit, SW Turfan-Hami Basin, Xinjiang Autonomous Region. *In: Bureau of Geology, CNNC (ed) Sandstone-type uranium deposits in China: Geology and exploration techniques*. Atomic Energy Press, Beijing, pp 77–87
- Wang Yusheng, Li Wenjun (1996) Metallogenetic regularity and exploration model and prospecting potential for Meso-Cenozoic volcanics type uranium deposits in the east of southern China. *In: Chen Zhaobo et al. (eds) Galaxy of research achievements of uranium geology of China*. Uranium Geol, Beijing, pp 182–188
- Wenrich KJ, Sutphin HB (1989a) Grand Canyon caves, breccia pipes and mineral deposits. *Geology Today*, v 10, no 3, pp 97–104
- Wenrich KJ, Sutphin HB (1989b) Lithotectonic setting necessary for formation of uranium-rich solution collapse breccia-pipe province, Grand Canyon region, Arizona. *In: Metallogenesis of uranium deposits*. TECDOC-542, IAEA, Vienna, pp 307–344
- Wilde AR 1988. On the origin of unconformity-type uranium deposits. PhD thesis, Monash University (unpubl)
- Wismut (1999) Chronik der Wismut. Wismut GmbH, Chemnitz, 2738 p
- Xia Yuliang, Lin Jinrong, Liu Hanbin, Fan Guang, Hou Yanxian (2002) Research on geochronology of sandstone-hosted uranium ore-formation in major uranium-productive basins, Northern China. *In: Bureau of Geology, CNNC (ed) Sandstone-type uranium deposits in China: Geology and exploration techniques*. Atomic Energy Press, Beijing, pp 166–177
- Xiang Weidong, Chen Zhaobo, Chen Zuyi, Yin Jinshuang (2000) Discussion on organic matter and mineralization of sandstone-type uranium deposits – Taking Shihongtan uranium deposit, Turfan-Hami Basin as an example. *Uranium Geol*. v 16, no 2 pp 65–73, (in Chinese with English abstract)
- Yamamoto I, Shiota T, Harashima F, Fujimoto J, Koinuma M, Hirono S (1974) Uranium exploration in the Tono District, Gifu Prefecture, Japan. *Min Geol*, v 24, pp 123–132
- Yao Zhenkai, Liu Yuanhou, Zhu Rongbin, Yang Shanghai, Li Deping (1989) Uranium metallogenesis in southeast China. *In: Metallogenesis of uranium deposits*. IAEA, Vienna, pp 345–356
- Yazikov VG (2000) Uranium potential of the Republic of Kazakhstan and the prospects for its development. *In: Gavrilin VI et al. (eds) Uranium at the turn of the century: resources, production, demand*. Abstracts Intern Symp Uran Geol, Moscow, All-Russian Sci Res Inst Mineral Resources NM Fedorovsky, pp 39–40
- Yazikov VG (2002) Uranium raw material base of the Republic of Kazakhstan and prospects of using in situ leach mining for its development. *In: In situ leach uranium mining*. T1-TC-975, IAEA, Vienna, pp 22–31
- Yazikov VG, Zabaznov VU (2002) Experience with restoration of ore-bearing aquifers after in situ leach uranium mining. *In: The uranium production cycle and the environment*. CandS Papers Series 10/P, IAEA, Vienna, pp 396–403
- Yermolayev NP, Zhidikova AP (1966) Behaviour of uranium in progressive metamorphism and ultrametamorphism as observed in the western part of the Aldan Shield. *Geochem Intern*, v 3, pp 716–731
- Yilmaz H (1981) Genesis of uranium deposits in Neogene sedimentary rocks overlying the Menderes metamorphic massif, Turkey. *Chem Geol*, v 31, pp 185–210
- Yin Di (1990) YZPX-1 uranium resource evaluation system and its applications in the north of China. *In: Bureau of Geology, CNNC (ed) Uranium provinces in China*. Bur Geol, CNNC, Beijing, China, pp 176–190
- Yu Dagan, Chen Anpin, Wu Rengui, Zhu Mingqiang, Xu Jianzhang (2002) A regional evaluation model for the basal-channel-type sandstone uranium deposits. *In: Bureau of Geology, CNNC (ed) Sandstone-type uranium deposits in China: Geology and exploration techniques*. Atomic Energy Press, Beijing, pp 43–52
- Zabaznov VU (2002) Special characteristics of ISL mining from deep-seated sandstone uranium deposits. *In: In situ leach uranium mining*. T1-TC-975, IAEA, Vienna, pp 39–41
- Zagruzina IA, Smyslov AA (1978) Uranium and thorium in rocks of the Soviet Northeast. *Intern Geol Rev*, v 20, no 10, pp 1230–1238
- Zakaulla S, Tripathi BK, Thirupathi PV, Umamaheshwar K, Dhana Raju R (1998) Alterations in the basement fracture zones and their bearing on uranium mineralisation in the southwestern environs of the Cuddapah Basin, Andhra Pradesh, India. *Expl Res Atom Minerals, AMD, India*, v 11, pp 13–24
- Zhang Bantong (1990) On geochemical recognition criteria and genesis of two kinds of granite-type uranium deposits in South China. *In: Bureau of Geology, CNNC (ed) Uranium provinces in China*. Bur Geol, CNNC, Beijing, China, pp 54–66
- Zhang Rong (2001) New development stage of China's uranium industry. *In: Assessment of uranium deposit types and resources – A worldwide perspective*. TECDOC-1258, IAEA, Vienna, pp 39–43
- Zhang Ruliang, Ding Wanlie (1996) Discussion on geologic characteristics of NHT type uranium deposit and the relationship between oil and gas-bearing water and uranium metallogenesis. *In: Chen Zhaobo et al. (eds) Galaxy of research achievements of uranium geology of China*. Uranium Geol, Beijing, pp 205–214
- Zhang Zuhuan (1990) On the geological characteristics of SE China uranium province and the distribution of uranium belts. *In: Bureau of Geology, CNNC (ed) Uranium provinces in China*. Bur Geol, CNNC, Beijing, China, pp 17–27
- Zhang Zuhuan (1991) On the uranium-bearing granites and their uranium deposits in south China. Atomic Energy Publish House, Beijing, pp 234–248
- Zhong Jiarong, Guo Zhitian (1984) The Lianshangan uranium deposit, Northeast China: Some petrological and geochemical constraints on genesis. *In: IAEA/Ferguson J (ed) Proterozoic unconformity and stratabound uranium deposits*. TECDOC-315, IAEA, Vienna, pp 115–134
- Zhou Weixun (1988) Uranium deposits in south China: Ore forming features and tectonic environments. *In: Uranium deposits in Asia and the Pacific: geology and exploration*. IAEA, Vienna, pp 59–78
- Zhou Weixun (1996) Continental tectonics and uranium province of south China. *In: Chen Zhaobo et al. (eds) Galaxy of research achievements of uranium geology of China*. Uranium Geol, Beijing, pp 26–34
- Zhou Weixun (1997) Uranium deposits in China (manusc.). IAEA training course on uranium resource inventories and ore reserve calculations, Central South Bureau of Geology, Changsha, China, 33 p
- Zhou Weixun (2000) Uranium provinces in China. Manuscript for IAEA atlas/ UDEPO, 18 p (unpubl)
- Zhou Weixun, Chen Anping (2001) Sandstone-type uranium deposits and deposits amenable to in situ leach mining: Review and prospect. *In: The scientific and technical status at the turn of century*. Bur Geol, CNNC, Beijing, pp 1–42, (in Chinese)
- Zhou Weixun, Teng R (2003) Tianshan sandstone-type uranium province and its principal characteristics. *In: Cuney et al. (eds) Uranium geochemistry*. Univ Henri Poincaré, Vandoeuvre les Nancy, pp 393–395
- Zhou Weixun, Chen Zuyi, Li Jianhong, Guan Taiyang, Fan Liting, Li Wuwei (2002) ISL-amenable sandstone-type uranium deposit: Global aspects and recent development in China. *In: Bureau of Geology, CNNC (ed) Sandstone-type uranium deposits in China: Geology and exploration techniques*. Atomic Energy Press, Beijing, pp 1–23
- Zhou Weixun, Zhang Bantong, Wu Jianhua (2003) Granite types uranium deposits in South China Uranium Province. *In: Cuney et al. (eds) Uranium geochemistry*. Univ Henri Poincaré, Vandoeuvre les Nancy, pp 396–399
- Zhou Weixun, Liu S, Wu J, Wang Z (2006a) Sandstone type uranium deposits in NW China. *In: Symposium on uranium production and raw materials for the nuclear fuel cycle*. Proc Series, IAEA, Vienna, pp 152–159
- Zhou Weixun, Liu Xiaodong, Yu Dagan, Wu Rengui (2006b) Xiangshan Caldera (SE China): Magmatism and uranium mineralization. (manusc. 18 p, 8 figs)
- Zhou Wenbin, Li Mangen, Zhang Zhanshi, Shi Xiaoping, Luo Mingbiao (2002) Organic geochemistry of sandstone type uranium deposits in Yili Basin,

- Northwest China. *In*: Bureau of Geology, CNNC (ed) Sandstone-type uranium deposits in China: Geology and exploration techniques. Atomic Energy Press, Beijing, pp 127–135
- Zhu Jiechen, Zheng Maogong, Ying Junlong (1996) Study on geological characteristics in Dalongshan and Kunshan uranium deposits. *In*: Chen Zhaobo et al. (eds) Galaxy of research achievements of uranium geology of China. Uranium Geol, Beijing, pp 234–241
- Zhu Minqiang, Wu Rengui, Yu Dagan, Chen Anping, Shen Kefeng (2002) Geologic characteristics of sandstone-type uranium deposits and depositional system of host sediments, Bayantala Sag, Tengge'er Depression, Eren Basin, Inner Mongolian Autonomous Region. *In*: Bureau of Geology, CNNC (ed) Sandstone-type uranium deposits in China: Geology and exploration techniques. Atomic Energy Press, Beijing, pp 98–109
- Ziegler V (1974) Essai de classification métallotectonique des gisements d'uranium. *In*: Formation of uranium ore deposits. IAEA, Vienna, pp 661–677
- Ziegler V, Dardel J (1984) Uranium deposits in Europe. *In*: de Vivo F et al. (eds) Uranium geochemistry, mineralogy, geology, exploration and resources. IMM, London, pp 140–161
- Zinchenko VM, Stoliarenko NN (2002) Extraction of uranium by in situ leaching method under the conditions of Kanzhugan deposit. *In*: In situ leach uranium mining. TCM Almaty, 1996, T1-TC-975, IAEA, Vienna, pp 32–38



Subject Index

(Note: *Italics* refer to chapters or sections describing uranium districts and deposits, while normal letters refer to other terms in the index)

A

- Alaskite, alaskitic 19, 75, 76, 221, 304, 306
Albitite 12, 51, 76, 109, 112, 126, 172, 177, 210, 336, 343, 386, 443
 facies (characteristic co-mineral assemblages), aegirine 12, 49, 54–58, 375, 381, 384
Alteration/metasomatism viii (see Sect. *Alteration*)
 albitization 48, 50, 52, 54, 55, 57, 59, 76, 80, 83, 95, 97, 101, 109, 117, 118, 120, 123–126, 172, 199–202, 205, 210–212, 216, 217, 219, 255, 257, 260, 336, 341, 343, 346, 347, 354, 356, 389, 397, 438, 443–445
 analcimization 55
 argillization 36, 60, 62, 65, 66, 85, 94, 97, 101, 113, 117, 120, 146, 149, 178, 255, 257, 258, 266, 267, 272, 277, 290, 291, 316, 336, 338, 341, 346, 356, 365, 368, 372, 387, 388, 410, 416, 423, 436, 438, 440
 beresitization ix, 195, 199, 201–203, 205, 207, 208, 216, 224, 255, 257, 258, 260, 266, 336, 341, 346, 354, 387–389, 438, 440, 443, 444
 bleaching 7, 21, 134, 144, 149, 178, 179, 221, 224, 259, 272, 275, 277, 323, 325, 360, 371
 calcitization 148, 273, 316, 317
 cancrinitization 55
 carbonatization 36, 48, 52, 54, 55, 57, 60, 76, 80, 83–86, 92, 97–99, 109, 114, 118, 123, 125, 126, 143, 146, 149, 177, 199–202, 205, 207, 210, 212, 216, 217, 219, 221, 224, 258–260, 266, 291, 293, 297, 305, 306, 310, 336, 341, 354, 365, 368, 374, 375, 381, 387, 397, 405, 410, 416, 419, 425, 438, 440, 445
 chloritization 48, 52, 54, 55, 60, 62, 76, 84, 92, 95, 97–99, 101, 102, 105, 109, 113, 117, 118, 120, 123, 125, 134, 148, 199, 200, 202, 205, 207, 210, 212, 217, 219, 221, 258, 266, 293, 297, 336, 341, 346, 354, 368, 372, 388, 391, 397, 438, 440, 445
 damouritization 60, 92, 113
 decomposition, destruction, corrosion of rock constituents 8, 57, 65, 101, 178, 221, 224, 233, 234, 263, 264, 282, 374, 375, 400
 desilicification 65, 92, 316, 317, 381 (see also *episyenitization*)
 dickitization 60, 120, 123, 127
 dolomitization 147, 199, 213
 episyenitization 9, 49, 55, 57, 58, 102
 Fe-Mg metasomatism 13
 fentization 55, 374, 384
 greisenization 95, 195, 209, 387, 388, 390, 443, 444
 hematitization 7, 21, 36, 42, 59, 62, 66, 76, 80, 84, 92, 95, 97–99, 101, 102, 104, 105, 109, 114, 117, 118, 120, 123, 129, 131, 133, 136, 143, 148, 161, 178, 199, 200, 202, 205, 210, 212, 219, 266, 267, 272, 273, 277, 291, 293, 297, 302, 309, 310, 336, 347, 354, 365, 368, 397, 405, 409, 445
 hydrogoethitization 55
 hydromicazation 35, 55, 59, 62, 64, 80, 83, 84, 92, 94, 97, 99, 102, 105, 117, 118, 120, 123–125, 129, 131, 132, 149, 199, 210, 272, 277, 291, 293, 297, 303, 305, 306, 309, 310, 336, 340, 341, 346, 352–354, 365, 388, 393, 445
 illitization 60, 95, 99, 127
 kaolinitization 62, 69, 76, 123, 148, 293, 297, 305, 306, 309, 310, 365, 425, 436
 K feldspathization 92, 95, 97, 99, 101, 102, 109, 134
 K metasomatism 19, 65
 limonitization 36, 42, 62, 133, 136, 178, 245, 246, 272, 274, 277, 305, 306, 309, 371, 405, 409, 416, 418, 424, 436, 437
 Mg metasomatism 279
 microclinization 55, 341, 343
 montmorillonitization 59, 60, 62, 92, 97, 99, 123, 290, 291, 293, 297, 436, 437
 muscovitization 50, 95, 97, 101, 102, 117, 120
 Na metasomatism 13, 177, 201, 202, 257 (see also *albitization*)
 natrolitization 55, 57
 nephelinization 55
 orthite-apatite metasomatism 389
 oxidation x, 7, 17, 20, 21, 34, 36, 57, 60, 69, 73, 74, 132–134, 136, 169, 187, 221, 222, 224, 231, 233, 234, 236, 239, 241, 243, 245, 246, 250, 258, 261, 263–266, 272, 273, 277, 278, 287, 299, 304–310, 316, 341, 358, 361–363, 368, 371, 372, 374, 382, 386, 400, 405, 407, 409, 410, 414, 416, 418, 419, 422–424, 426, 436
 phlogopitization 177
 potassium-siliceous metasomatism 373
 propylitization 195, 255, 257, 259, 291, 387, 389, 390
 pyritization 8, 54, 59, 62, 76, 80, 85, 92, 97, 99, 101, 109, 117, 120, 139, 143, 146, 147, 149, 177, 200, 202, 205, 207, 258, 266, 272, 273, 277, 302, 405, 409, 425
 quartz-microcline metasomatism 389
 reduction x, 21, 69, 74, 83, 101, 132, 135, 187, 221, 224, 233, 261, 263–265, 272, 277, 287, 292, 309, 310, 323, 325, 343, 360, 362, 365, 368, 409, 410, 414, 416–418, 420, 422–424
 sericitization 48, 50, 52, 54, 76, 85, 86, 92, 97, 99, 143, 146, 203, 205, 207, 210, 258, 316, 336, 341, 343, 368, 388, 393, 438, 445
 silicification 13, 48, 52, 54, 55, 57, 59, 62, 65, 66, 76, 80, 83–85, 92, 95, 97, 99, 101, 102, 105, 109, 114, 120, 123, 127, 132, 140, 141, 146, 147, 149, 177, 200, 202, 203, 207, 212, 258, 267, 297, 302, 305, 306, 316, 336, 341, 343, 354, 356, 365, 368, 374, 375, 381, 387, 388, 393, 397, 410, 416, 423, 436, 437, 445
 smectitization 69
 sulfidization 52, 224, 305, 306, 308–310, 316, 317, 341, 353, 365, 368, 374, 381, 409, 416, 423
 tourmalinization 101
 zeolitization 62, 64, 316, 317, 368, 372
Alum shale 25
Anatectic (environment, processes) 19, 92, 104, 116, 118, 352
Annular ring (fracture) 15
Anthraxolite 203, 445
Apatite 10, 12, 13, 23, 57, 101, 109, 113, 116, 117, 120, 125, 126, 129, 160–164, 167, 176, 188, 199–202, 210, 212, 216–219, 259, 287, 304, 320, 374, 375, 387, 389, 393, 405, 451
Aquiclude 181, 183, 221, 252, 261, 264, 328, 409, 411, 422, 423
Aquifer/solution conduit 42, 183, 252, 328, 414, 416, 426
Atmosphere 16
 oxyatmoversion 16
 oxygenated 65, 68, 70, 73–75, 98, 113, 118, 135, 144, 169, 183, 224, 231, 233, 263, 264, 323, 326, 360, 363, 403, 405, 410, 414, 416, 422–424
Autochthonous 130
- ## B
- Bacteria species 183, 234, 247
Bacteriogenic (bacterial, biogenic) 167, 183, 187, 233, 234, 246, 409, 424
Basins (general)
 Cenozoic 46, 47, 108, 153, 154
 continental, intermontane, intracratonic 7, 29, 34, 46, 48, 65, 133, 135, 148, 149, 264, 304
 limnic 24

- Mesozoic 98, 286
 Neoproterozoic 157, 170
 Paleoproterozoic 16
 Paleozoic 31, 199, 202
 Paleozoic 175
 paralic 24
 Tertiary (-Cretaceous) 29, 33, 101, 117, 118, 137, 144, 147, 167, 181, 183, 188, 287, 304, 402, 403
- Basins, depressions etc. (geographic locations)
- Amalat Basin, Russia 368, 372
 Amudarya Basin, Uzbekistan 410
 Aravalli Basin, India 30, 157, 172
 Aravalli-Delhi Basin, India 30, 157, 172
 Athabasca Basin, Canada 4, 5
 Balkhash Basin, Kazakhstan 260–262
 Bangmai Basin, China 154, 155
 Bannu Basin, Pakistan 30, 313, 318, 319
 Baoyong Depression, China 149
 Barthi Basin, Pakistan 315, 318
 Bayantala Sag Depression, China 32, 65, 68–71
 Bhima Basin, India 30, 157, 171
 Brousse-Broquiès Basin, France 5
 Burqin Basin, China 43
 Chaling-Yongxing Basin, China 140, 141, 143, 144
 Chattisgarh Basin, India 30, 157, 172
 Chelaomiao Basin, China 65
 Chistopol Basin, Kazakhstan 205
 Choibalsan Basin, Mongolia 287
 Choir Basin, Mongolia 285, 304–306, 309
 Chu-Sarysu Basin, Kazakhstan 7, 30, 191–194, 228, 231, 233–245, 247–250, 257
 Cuddapah Basin, India 30, 157, 170–172
 Dazhou Basin, China 129
 Delhi Basin, India 157, 172
 Döhlen Basin, Germany 24
 Eastern Gobi Basin, Mongolia 286, 287, 304
 Erdos Basin, China 72
 Eren (Erlian) Basin, China 33, 34, 46, 47, 65–71
 Erennaoer Depression, China 66–68
 Erlian Basin, China (see *Eren Basin*)
 Fergana Basin, Uzbekistan 321, 438
 Franceville Basin, Gabon 9
 Gangou Basin, China 59–61
 Ganzhou Basin, China 147
 Gaoligong Basin, China 148–151, 153
 Gurvansaikhan Basin, Mongolia 285, 286
 Hailar Basin, China 46, 47
 Hami Basin, China 31, 36, 40, 41
 Hengyang Basin, China 147
 Heyuan Basin, China 95
 Huichang Basin, China 132
 Ily Basin, Kazakhstan 29, 36, 191–193, 260, 264, 265, 270
 Irtysh Basin, Kazakhstan 220, 221
 Iwamura Basin, Japan 183
 Jianchang Basin, China 33, 34, 59
 Jilantai Basin, China 46
 Jingan (Shiwandashan?) Basin, China 34, 147, 148
 Junggar Basin, China 34, 36, 40
 Kalan Basin, Indonesia 175
 Kangil Depression, Russia 363
 Kani Basin, Japan 183
 Kashi Depression, China 34, 43
 Kenimekh Basin, Uzbekistan 425
 Khairkhan Basin, Mongolia 285, 286
 Koçarli Basin, Turkey 395
 Kokshetau Basin, Kazakhstan 194, 216, 218
 Köprübasi Basin, Turkey 395
 Krivoy Rog Basin, Ukraine 13
 Kuidusun Basin, Russia 388, 389
 Kyzylkum Basin, Uzbekistan 29, 270, 401, 403, 404, 406–410, 414, 434
 Lianghe Basin, China 150, 153
 Liaohe Basin, China 30, 35, 46, 48–52, 54
 Liaoning Basin, China 33, 35, 46–51, 54, 59
 Lincang Basin, China 151, 154, 155
 Longchuanjiang (Longchuan) Basin, China 149–154
 Lower Liaohe Basin, China 46
 Luxi Basin, China 100, 101
 Mabugang Basin, China 147
 Malaya Amalat Depression, Russia 368
 Mengtuo Basin, China 153, 154
 Mengwang Basin, China 153–155
 Minussinsk Basin 328, 330
 Misasa Basin, Japan 187, 188
 Mizunami Basin, Japan 184
 Nanxiong Basin, China 107
 Naryn Basin, Kyrgyzstan 270, 282
 Ningan Basin, China 46
 Ningdu Basin, China 147
 Nong Son Basin, Vietnam 30, 449
 Nujiang Basin, China 148
 Olov Depression, Russia 365
 Ongiingol Basin, Mongolia (see *Undurshil*)
 Ordos Basin, China 29, 31, 34, 47, 71–73
 Powder River Basin, USA 7
 Qaidam Basin, China 34, 75
 Qinglong Basin, China 30, 33, 34, 46, 59–61
 Rencha (Renchai) Basin, China 132
 Sainshand Basin, Mongolia 285, 287, 308, 310
 Salihli Basin, Turkey 395
 Sanjiang Basin, China 46
 Shiwandashan? Basin, China (see *Jingan Basin*)
 Songliao Basin, China 46
 Southern Zylzya Depression, Russia 363
 Syr Darya Basin, Uzbekistan 29, 229, 230
 Tarim Basin, China 34, 35, 43
 Tavansuveet Basin, Mongolia 285, 286
 Temvezli Basin, Turkey 396
 Tengchong Basin, China 150, 153, 154
 Tenggeer Depression, China 65, 68, 69
 Tim Mersoï Basin, Niger 8
 Toki Basin, Japan 183
 Turgai Basin, Russia 326
 Uliya Basin, Russia 387–389
 Ulziit Basin, Mongolia 285, 286, 303
 Undurshil (Ongiingol) Basin, Mongolia 285–287
 Urulyunguevsky Depression, Russia 335, 372
 Utan Depression, Russia 363
 West Siberian Basin, Russia 29
 Williston Basin, USA 24
 Witwatersrand Basin, South Africa 16, 17
 Xianggui Basin, China 35, 139, 141, 145
 Xinjiang Basin, China 31, 34–36, 40, 43, 44, 261, 264
 Xinwu Basin, China 147, 148
 Yili Basin, China 31, 34, 36–42
 Yingshan Basin, China 71
 Yongxing Basin, China 140, 141, 143, 144
 Youngyang Basin, South Korea 391
 Zaisang Basin, Kazakhstan 43
 Zuunbayan Basin, Mongolia 286, 287, 289, 303, 304, 306, 308–310
 Zylzya Depression, Russia 362, 365
- Batholiths (see *Intrusive complexes*)
 Bentonite, bentonitic 318
 Bitumen, bituminous (see *Black shale, Organic material*)
 Bituminous-cataclastic limestone (see *Uranium deposits – types: Type 14*)
 Black shale 24–25, 29, 72, 86, 88, 132, 136, 140, 144, 201, 278, 282, 283, 391, 397, 398, 400, 402, 403, 435

bituminous-sapropelic- 24–25
deposits (see Uranium deposits – types: Type 19)
humic, coaly, kolm 24–25
Bog (see Organic material)
Bone (see Organic material)
Brannerite (see Index U and U-bearing minerals)
Breccia(s) (see Sect. *Shape and Dimensions of Deposits*, and Uranium deposits – types: Types 8 and 9)

C

Calcrete 17, 18, 178
Caldera (see Volcano-tectonic structures)
Carbonaceous (see Organic material)
Carbonaceous-carbonate-siliceous-pelite (C-Si-pelite) (see Uranium deposits – types: Type 13)
Carbonatite 19, 166, 320 (see also Uranium deposits – types: Type 12)
Channel, paleochannel 6, 8, 17, 29, 34, 36, 40, 46, 58–60, 66, 68–72, 148, 153, 154, 167–169, 176, 181–185, 187, 188, 193, 194, 220–222, 224, 245, 246, 255, 260, 263, 264, 266, 267, 279, 282, 287, 306, 316, 317, 323–332, 342, 356–362, 365, 366, 372, 386, 395, 396
Climate, paleoclimate 17, 18, 65, 72, 98, 113, 135, 144, 187, 224, 263, 317, 323–325, 357, 359, 363
Closed system 118
Coal (see Organic material)
Coffinite (see Index U and U-bearing minerals)
Conglomerate, oligomictic, Proterozoic (see Uranium deposits – types: Type 10)
Contact metamorphism, contact metamorphic viii, 25, 55, 82, 109, 114, 185, 187, 209, 375, 389

D

Deposit
dimensions, grades, resources/reserves ix, x, 3 [see *uranium districts and deposits (introductory section)*, and Sect. *Shape and Dimensions*]
types (see Uranium deposits – types)
Deuteric 113
Diabase/dolerite 92, 94, 98, 99, 101, 102, 105, 107, 109, 132, 158, 167, 175, 178, 200, 205, 212, 217, 219, 258–260, 265, 266, 278, 289, 309, 354, 436, 444
Diagenesis, diagenetic 16, 20, 35, 69, 82, 118, 134, 135, 146, 167, 169, 185, 187, 226, 231, 233, 306, 316–318, 409, 414, 423
Disequilibrium (radioactive) 422, 424
Duricrust, duricrusted 17, 18, 178, 179
nonpedogenic
calcrete 17
calcrete (groundwater-, valley-) 17
dolocrete 17
gypcrete 17
silcrete 17
pedogenic
calcrete 18
ferricrete 18
gypcrete 18
laterite 18

E

Effusive/extrusive rocks (see Volcanic)
Endogenic/endogenetic 10, 11, 200, 375
Endogranitic 9, 31, 92, 95, 114, 139 (see also Uranium deposits – types: Type 4)
Episyenite 9, 49, 55, 57, 58, 102
Eugeosynclinal 48, 49
Evaporite, evaporitic, evaporative 178
Exocaldera (see Uranium deposits – types:) Type 5
Exogenic/exogenetic 7, 8, 17, 21, 224, 366, 372
infiltration 7, 8, 17, 21
Exogranitic 95, 110, 114 (see also Uranium deposits – types: Type 4)

F

Faults, lineaments, structures (see Sect. *Geological Setting*)
Ferro-uranium formation 13

Fluid inclusions (see Sect. *Stable Isotopes and Fluid Inclusions*)
Fossil (fish) bone, wood, plant debris (see *Organic material*)

G

Gangue minerals (see Sect. *Mineralization*)
albite 48, 50, 51, 76, 92, 94, 109, 116, 125, 126, 143, 177, 199, 202, 205, 210, 212, 217, 218, 258, 260, 336, 338, 339, 341–343, 346, 347, 354, 373–375, 381, 443–445
alunite 80, 81, 116
ankerite 80, 83, 86, 146, 199, 203, 216–218, 258, 290, 293, 343, 346, 367, 374–376, 388, 405, 438, 444, 446
anthraxolite 203, 445
baryte 76, 125, 139, 146, 278–283, 290, 293, 346, 374, 375, 382–384, 388, 393, 409, 423, 438, 445, 446
calcite 34, 36, 49, 54, 57, 66, 68, 74, 76, 78, 80, 86, 90, 92, 94–96, 99, 102, 109, 111, 112, 114, 125, 126, 131–134, 141, 143, 145–147, 176, 185, 187, 199, 201, 217, 224, 232, 236, 255, 258, 260, 273, 279–281, 283, 290, 293, 300, 316–318, 338, 342, 346, 347, 352, 365, 371, 374–376, 380, 384, 388, 405, 416, 417, 419, 423, 424, 438–440, 443–446, 451
carbonates 5, 6, 12, 52, 61, 81, 85, 120, 135, 144, 177, 199, 202, 224, 233, 253, 255, 257, 309, 341, 346, 374, 375, 397, 405, 410, 416, 417, 422, 438, 443, 444
chalcedony 57, 62, 65, 92, 116, 151, 387, 388, 416
chlorite 6, 42, 48, 49, 54, 57, 74, 76, 80, 92, 94, 102, 109, 111, 112, 116, 126, 131, 132, 139, 140, 144, 145, 161, 163, 164, 175, 176, 183, 188, 199–202, 204, 208, 210, 212, 217, 219, 224, 255, 258, 290, 300, 301, 338, 343, 346, 347, 352, 356, 371, 373, 374, 381, 387–389, 405, 420, 436, 438, 440, 443–445
collophane 116, 117, 120, 128, 171, 172
dolomite 20, 21, 36, 65, 66, 68, 80, 86, 94, 95, 133, 134, 139, 144–147, 178, 185, 199–202, 209, 212, 250, 254, 271, 338, 339, 346, 371, 373–375, 405, 414, 416, 423, 434, 438
fluorite 10–12, 34, 36, 49, 54, 57, 60, 62, 65, 78, 80, 92–97, 99, 101, 102, 108, 109, 111–118, 120, 125, 129, 131, 132, 134, 135, 139, 143, 145, 146, 172, 255, 257, 290, 292, 293, 300, 302–304, 332, 336, 338, 341–343, 346, 347, 352, 353, 356, 375, 384, 387, 437–439, 443–446
gibbsite 143
gypsum 66, 80, 81, 175, 176, 178, 181, 185, 187, 189, 395, 409
hydromica 36, 62, 66, 74, 76, 80, 101, 102, 125, 126, 129, 131, 132, 143, 199–202, 210, 217, 255, 260, 290, 293, 300, 301, 303, 309, 336, 338, 341–343, 346, 347, 352, 353, 356, 386, 388, 389, 405, 444, 445
illite 42, 57, 66, 92, 94, 113, 116, 140, 143, 336, 416, 420
kaolinite 42, 76, 94, 143, 167, 185, 236, 255, 300, 301, 303, 336, 338, 341, 342, 346, 356, 365, 371, 387, 388, 405, 416, 436
lanthanides 225, 403, 405, 409, 426
montmorillonite 62, 76, 92, 101, 185, 236, 290, 293, 300, 301, 343, 356, 387, 405, 416
opal 94, 133, 375, 388, 416
phyllosilicates 341, 443, 444
quartz ix, 5, 6, 16, 17, 19, 35, 42, 46, 48–52, 54, 57, 59, 60, 65, 66, 69, 74, 76, 78, 80–85, 88, 92–97, 99, 101–105, 107–109, 111–114, 116, 117, 122, 125, 129, 131–135, 139–141, 143–149, 151, 161, 163, 164, 167, 172, 175, 176, 185, 188, 194, 195, 199–203, 205–210, 212, 234, 236, 244, 246, 254, 255, 257, 258, 260, 265, 280, 281, 289–293, 296, 299–301, 304, 309, 310, 315–318, 335, 336, 338, 341–343, 346, 347, 352–354, 356, 365, 371, 374–376, 382–384, 386–389, 393, 405, 409, 414, 416, 420, 424–426, 436, 438, 440, 443–446
radiobaryte 232, 233, 263, 393
sericite ix, 6, 52, 80, 92, 143, 146, 175, 199, 202, 203, 210, 245, 255, 257, 290, 292, 316, 336, 346, 353, 371, 373, 374, 381, 386, 388, 389, 436, 438, 439, 444, 445
Gas (natural) 6, 66, 68, 71, 403
Geochemistry, geochemical ix, 58, 82, 83, 93, 149, 224, 247, 263, 264, 278, 290, 293, 297, 300, 301, 353, 359, 372, 374, 375, 402, 406, 410, 416, 424, 436, 440
Geochronological (age) data 58, 99, 439 (see Sect. *Geochronology*)
Glass, glassy 185, 187, 291, 296, 299, 340, 365, 387, 388
volcanic 185, 187, 291, 296, 299, 365
Grade (of uranium deposits and ore bodies) (see Sect. *Shape and Dimensions*)
Granite viii, 3, 4, 9–13, 15, 24, 29, 31–35, 47–52, 54, 59, 60, 68, 75, 76, 79, 84, 86–102, 104–109, 111–117, 122, 125, 126, 129–137, 139, 140, 144, 151, 153,

155, 157–172, 181–189, 194, 195, 200–202, 205, 209, 210, 213, 216, 217, 221, 249, 250, 253, 255, 257, 260, 277, 286, 287, 289, 299, 301–304, 308, 309, 320, 327, 331, 332, 334, 338–343–356, 357–368, 372–374, 381, 386–390, 393, 395, 397, 411, 414, 426, 436, 438–443, 446, 450
 batholiths, plutons (see Intrusive complexes)
 leucocratic 195, 201, 302, 304, 388
 metasomatized 12, 48, 51, 59, 94, 109, 112, 113, 354
 peraluminous (leucocratic, two-mica) 195, 201, 302, 304, 388
 subalkaline 389
 two-mica 94–96, 99–101, 105, 109, 114, 115, 450
 Graphite, graphitic 4, 5, 51, 134, 201, 212, 391, 435–437, 449
 Ground-oxidation 17
 Groundwater 7, 17, 36, 65, 68–70, 73, 74, 98, 104, 108, 113, 151, 169, 181, 183, 187, 231, 263, 281, 282, 284, 316, 317, 363, 405, 406, 409, 410, 414, 423, 424
 table 17, 281, 282, 284, 316–318
 Growth faults 66, 68

H

Halo/aureole 10, 21, 34, 75, 80, 85, 91, 92, 95, 97, 99, 101, 108, 109, 115, 130, 149, 179, 260, 274, 277, 290, 291, 293, 296, 297, 300, 301, 336, 343, 346, 349, 353, 357, 358, 365, 366, 371, 374, 382, 405, 409, 410, 416, 418, 419, 422, 424, 438, 445
 wall rock alteration 13, 48, 83, 92, 93, 97, 120, 129, 134, 144, 164, 205, 207, 219, 273, 336, 341, 345, 388, 436, 437, 440, 445
 Halokinesis, halokinetic 178, 179
 Host environments, -rocks (see Sect. *Geological Setting*, and Sect. *Ore Controls and Recognition Criteria*)
 Humate, humic 7, 8, 21, 24, 25, 134, 183, 318, 369–371 (see also Organic material)
 Hydrocarbon(s) 8, 68–70, 74, 104, 231, 233, 274, 278, 310, 319, 414, 416, 423, 435, 436
 Hydrogen sulfide (H₂S) 6, 149, 183, 226, 234, 261, 264
 Hydrogenic/hydrothermal solutions/systems 65, 81–83, 97, 98, 104, 113, 118, 135, 144, 151, 292, 342, 353, 387, 440, 446
 brines 143, 409, 423
 connate 104, 134, 135, 169
 convective 98
 endogenic hydrothermal 10, 11
 hydrothermal-reworked 20, 133, 137, 140
 hypogene 98, 134, 202, 342, 446
 magmatic 341
 metamorphic 146
 metasomatic ix, 4, 12, 48–52, 54, 55, 58, 80, 95, 97, 102, 107, 109, 125, 162, 177, 304, 339, 376, 386
 phreatic infiltration 20, 133
 springs (thermal) 151
 supergene, meteoric, phreatic groundwater 118, 133, 282, 446

I

Impermeable, impervious 6, 36, 68, 69, 75, 117, 144, 181, 183, 201, 236, 239, 241, 263, 310, 323, 326, 343, 371, 409

Intergranular, interstitial 109, 187, 363 (see also Sect. *Mineralization*)

Intrinsic 8

Intrusive 10, 19, 29, 31, 32, 35, 46, 47, 49, 54, 55, 57, 58, 65, 75, 76, 78–81, 83, 84, 96, 98, 101, 102, 116, 130, 158, 200, 209, 257, 259, 260, 285, 303, 373, 384, 387–389, 439, 440, 443

complexes (batholith, belt, pluton, massif etc.)

Aldan pluton, Russia 29, 30, 321, 322, 372–374, 376–382
 Arkhimed Massif, Russia 389
 Babaitaudor Massif, Uzbekistan 443
 Babaytag Massif, Uzbekistan 446
 Baksan Massif, Kazakhstan 224
 Baoshan Massif, China 148, 149, 153
 Bokan Mountain Granite, USA 13
 Bureinsky Massif, Russia 386
 Central Bohemian pluton, Czech Republic 9
 Chengshan pluton, China 79–82, 84
 Dalongshan Massif, China 79
 Dalongshan pluton, China 79–84

Dasi Massif, China 148

Guidong Massif, China 96, 99, 100

Huangmeijian Massif, China 83

Jinjiling batholith, China 90, 91, 95, 98, 99, 114

Jiuyishan batholith, China 96, 114

Jiuyishan Massif, China 114

Khasi batholith, India 157, 164–169

Kokshetau (Kokchetav) Massif, Kazakhstan 191, 194, 195, 216, 220, 221, 224

Legaevskii Massif, Kazakhstan 209

Longhuashan batholith, China 105

Lujing batholith, China 109

Luxi pluton, China 101

Mao'ershan Massif, China 114

Massif Central, France 4, 5, 9

Menderes Massif, Turkey 30, 395

Motianling batholith, China 115

North China Massif, China 47, 48

Okhotsk Massif, Russia 387, 388

Pestraya Massif, Russia 389

Qinling Massif, China 30, 75, 76, 79, 84, 85

Rössing Alaskite, Namibia 19

Saima Massif, China 54, 55, 58

Sambalpur Massif, India 157, 172

Sanerer pluton, China 109

Sanfang batholith, China 86, 88, 89, 91, 96, 98, 114, 136

Shantobe Massif, Kazakhstan 206

Shaziling pluton, China 114

Singhbhum batholith, India 30, 157–162

Siqian pluton, China 100

Southern Zhuguang batholith, China 106

Taima batholith, China 148

Transbaykal Massif, Russia 334

Ulutau Massif, Kazakhstan 229

Xiazhuang pluton, China 96, 99–102, 104, 105

Yangtze Granite Belt, China 34, 79

Yangtze Massif, China 29, 86, 120, 146

Yongchen Massif, China 84

Yuechengling batholith, China 95, 114, 137, 139

Yuechengling Massif, China 114

Zhuguang Massif, China 105, 107, 108, 114

Zongyang Massif, China 79, 84

deposits (see Uranium deposits – types: Type 12)

rocks 54, 58, 65, 83, 387, 389 (see also Intrusive complexes, Uranium contents, and Uranium deposits – types: Types 4 and 12)

Iron-uranium formation (associated with sodic and carbonate metasomatites) 13

Isotopes (stable) 82, 85, 112, 116, 409, 423, 446 (see also Stable isotopes, and Sect. *Stable Isotopes and Fluid Inclusions*)

K

Karst (cavern) 15, 17, 18, 140, 144, 146, 269, 278, 279, 281, 282, 414 (see also Uranium deposits – types: Types 8, 11, and 14)

Kerogen 134

Kolm 25

L

Lacustrine 8, 11, 18, 21, 39, 65, 66, 72, 79, 82, 121, 149, 166, 167, 178, 179, 181, 184, 185, 187, 229, 231, 250, 261, 264, 289, 304, 306, 308, 313, 315, 317, 330, 334, 365, 395, 432 (see also Sediments, and Uranium deposits – types: – Type 15)

Lagoon, lagoonal 133, 135, 396, 414 (see also Sediments)

Lamprophyre 92–94, 99, 101, 102, 109, 175, 203, 219, 224, 440

Land-pebble phosphate (see Uranium deposits – types: – Type 17)

Laterite, lateritic 4, 18

Leaching-accumulative (see Uranium deposits – types: – Type 13)

Lignite 21, 24, 29, 31, 34, 35, 37, 42, 140, 148, 151, 153, 155, 187, 191, 192, 242, 243, 245, 248, 261, 263–265, 269, 282, 283, 285, 287, 304, 305, 358, 368, 372,

386, 390, 400, 411, 432, 449 (see also Organic material, and Uranium deposits – types: Type 18)

Limestone 15, 20, 21, 24, 29, 33, 50, 54, 55, 81, 85, 86, 88, 94, 109, 133, 134, 137–147, 166, 171, 172, 199, 202, 209–215, 217, 218, 220, 228, 231, 245, 249, 250, 253, 259, 269, 271–278, 279–284, 309, 310, 316, 326, 373, 395, 405, 414, 450, 451 (see also Uranium deposits – types: – Type 14)

Lineaments 13, 49, 109, 117, 119, 160, 175, 201, 255, 304, 438 (see also Sect. *Geological Setting*)

Lujavrite 19

Lutite 21

M

Magmatic (igneous) environment, processes 341, 439

Magmatic differentiation 55, 57, 82, 104, 202, 342

Massif (see Intrusive complexes)

Metallic elements (associated with U)

Ag 15, 16, 22, 34, 124–126, 131, 132, 134, 161, 171, 199, 263, 288, 290, 300, 302, 303, 343, 372, 374–376, 380–382, 384, 386–389, 393, 398, 445

As 6, 15, 22, 31, 47, 55, 58, 62, 64–66, 75, 82, 84, 85, 88, 95, 115, 116, 120, 122, 130, 135, 141, 143, 144, 146, 151, 157, 179, 181, 183, 199–203, 207, 208, 210, 221, 224, 231–234, 244, 251, 257, 258, 270, 274, 277, 278, 285, 290, 291, 293, 297, 300, 301, 303, 310, 317, 340, 343, 347, 352, 365–367, 371, 373, 375, 376, 386–389, 397, 401, 439, 445, 446

Au ix, 15–17, 29, 79–81, 84–86, 104, 131, 132, 146, 161, 189, 195, 216, 269, 283, 302, 303, 321, 353, 359, 372–377, 380–384, 386–388, 402, 403, 435, 436, 444

Be 76, 125, 151, 221, 254, 258, 263, 264, 323, 347, 354, 445

Bi 29, 86, 95, 97, 161, 188, 258, 375, 387, 389, 401, 437, 438, 443

Cd 125, 263, 375, 445

Ce 16, 23, 92, 111, 306, 405, 409, 426

Co 9, 14, 15, 18, 19, 26, 55, 79–81, 151, 161, 162, 171, 199, 225, 228, 241, 244, 246, 249, 258, 263, 274, 277, 278, 353, 354, 358, 389

Cu 6, 14–16, 19, 21, 24, 29, 48, 55, 79–81, 84, 86, 91, 92, 95, 97, 111, 120, 125, 130–132, 134, 140, 143, 146, 148, 157, 159–162, 164, 177, 179, 181, 188, 189, 199, 201–203, 216, 258, 263, 269, 278–280, 283, 310, 317, 328, 358, 371, 374, 375, 382, 384, 387–389, 437, 438, 445, 446, 449

Fe 6, 11–15, 42, 48, 54, 55, 57, 68, 74, 79–81, 83, 84, 92, 95, 111, 133, 134, 144, 158–160, 167, 169, 172, 177, 178, 188, 195, 199, 201–203, 212, 216, 221, 233, 234, 257, 263, 265, 272–275, 277, 278, 281, 283, 292, 304, 310, 316, 322, 323, 341, 343, 346, 347, 352, 354, 358, 360, 362, 371, 374, 375, 382, 384, 410, 416, 417, 419, 424, 443–446

Ga 22, 42, 60, 66, 158–160, 162, 258, 263

Ge 22, 37, 148, 150, 154, 155, 224, 232, 246, 250, 251, 263, 303, 306, 310, 328, 375

Mo ix, 8, 10, 11, 14, 15, 19, 21, 24, 29, 34, 37, 42, 59, 61, 62, 64–66, 69, 79–81, 86, 91, 95, 97, 116, 120, 124, 125, 128, 134, 143, 146, 161, 162, 164, 176–179, 194, 195, 199–203, 205–208, 216, 217, 219–221, 225, 232, 246, 255, 257–261, 263–265, 274, 277, 290, 291, 293, 297, 300–304, 306, 308, 313, 314, 317, 318, 320, 326, 328, 332, 338–343, 347, 349, 352–358, 371, 372, 380, 386–389, 398, 401, 403, 405, 409–411, 417, 419, 422–427, 435–438, 440, 443, 445, 446

Ni 5, 9, 14, 15, 21, 23, 46, 74, 86, 125, 134, 146, 151, 161, 162, 164, 171, 199, 225, 263, 274, 277, 283, 354, 389

Pb 5, 6, 11, 12, 14, 15, 29, 36, 48, 49, 52, 55, 57, 62, 69, 79–82, 86, 92, 95–97, 105, 107, 111–113, 116, 120, 124–126, 129, 131, 134, 139, 143, 145, 146, 148, 151, 161, 179, 181, 188, 189, 199–203, 207, 216, 233, 258, 263, 274, 277, 288, 290, 291, 293, 297, 300–303, 328, 340–342, 352–354, 371, 374–376, 381, 382, 387–389, 393, 398, 437–440, 444–446

Pt 6, 199

Rare elements 57, 58

Re 37, 42, 69, 224, 232–234, 246, 247, 250, 251, 261, 263, 265, 266, 270, 306, 308, 323, 325, 326, 354, 401, 403, 405, 409, 410, 416, 417, 422, 423, 425, 426

REE ix, 8, 12, 15–17, 19, 23–25, 29, 48–50, 57, 58, 76, 80, 86, 92, 95, 124, 125, 134, 161, 176, 177, 194, 200, 201, 217, 225, 226, 228, 232, 234, 236, 246, 263, 264, 283, 287, 292, 304, 306, 308, 326, 376, 401, 403, 409, 410, 436, 446, 449

Sb 15, 85, 146, 151, 258, 353, 375, 387–389, 445

Sc 23, 37, 42, 69, 194, 217, 221, 224–226, 233, 234, 236, 246, 263, 306, 308, 309, 326, 328, 358, 401, 403, 405, 409, 410, 425

Se 36, 37, 42, 69, 192, 193, 195, 224, 232–234, 236, 246–248, 250, 251, 253, 263, 266, 306, 308, 309, 317, 326, 401, 403, 405, 407, 409–411, 414, 417–419, 422–426, 428

Sn ix, 19, 29, 86, 91, 95, 97, 125, 188, 195, 221, 258, 304, 375, 388, 389, 443, 445, 446

Sr 57, 80–82, 92, 107, 115, 116, 125, 218, 220, 292, 310, 352, 354

Th ix, 12, 17, 19, 48–50, 55–58, 80, 92, 105, 111, 112, 117, 118, 120, 123–125, 157, 161, 176, 177, 179, 200, 201, 210, 212, 217, 221, 228, 287, 292, 317, 340, 352–354, 387, 389, 396, 408, 443, 446

Ti 17, 22, 37, 42, 57, 58, 151, 172, 177, 200, 203, 212, 217, 292, 341, 347, 354, 375, 382, 445

Tl 85, 146, 263, 375, 376, 409, 445

V 7, 8, 15, 17, 21, 24, 37, 38, 66, 69, 72, 74, 79, 81, 82, 86, 112, 143, 212, 228, 232, 248, 250, 251, 253, 263, 265, 269, 274, 277–279, 282, 310, 317, 318, 326, 328, 359, 361, 363, 376, 387, 399, 401, 403, 405, 409, 410, 414, 435–437

Y 17, 23, 46, 177, 189, 194, 200, 221, 224, 225, 232, 234, 236, 246, 263, 264, 283, 292, 306, 308–310, 328, 354, 358, 387, 389, 401, 403, 405, 409, 410, 426, 435, 436

Yb 80, 92, 306, 354, 409, 426

Zn 8, 11, 14, 15, 29, 48, 55, 79–81, 86, 92, 95, 97, 111, 124–126, 131, 134, 143, 146, 148, 179, 181, 188, 189, 203, 216, 233, 258, 263, 288, 302, 303, 310, 328, 340, 353, 358, 374–376, 382, 387–389, 393, 398, 436–438, 440, 444–446

Metallogenesis 3 (see Sect. *Metallogenetic Concepts/Aspects*)

Metallogenetic province/domain 86–88, 115, 285, 286

Metamorphic environment

amphibolite grade viii, 160, 175

greenschist grade 209, 435

Metasomatism, metasomatic alteration 12, 13, 15, 19, 48–50, 54, 55, 65, 75, 76, 80, 92, 95, 97, 99, 101, 109, 113, 162, 177, 199, 201, 202, 210, 257, 279, 336, 341–343, 373, 389 (see also Alteration)

Metasomatite facies 57

aegirinite 12

albitite (see Albitite)

carbonate metasomatite 13

Fe-Mg metasomatite 13

Methane 68, 234, 261, 263, 264

Migmatite, migmatitic, migmatization 6, 12, 50–54, 59, 61, 107, 108, 162, 167, 175, 205, 287, 357, 373

Mineral assemblage/paragenesis (see Sect. *Mineralization*)

Mineralization [see Sect. *Mineralization*, and Uranium (deposit) mineralization]

Miogeosynclinal 48, 49, 88, 89

Modified paleoconglomerate 16

Monazite (see Index U and U-bearing minerals)

Monometallic viii, 5, 6, 9, 10, 13, 16, 49, 155, 194, 233, 296, 302, 332, 341, 366 (see also Uranium (deposits) mineralization)

Monzonite (see Quartz monzonite)

N

Nappe 125–127, 129

Nasturan (pitchblende) (see Index U and U-bearing minerals - Pitchblende)

Nenadkevite (see Index U and U-bearing minerals)

O

Oil 66–68, 71, 274, 277, 308, 310, 403, 410

Oligomictic (paleo)conglomerate 16

Open system 118, 146

Ore viii

bodies (see Sect. *Shape and Dimensions*)

shape/configuration (see Sect. *Shape and Dimensions*)

composition/metal associations

U, Cu 84, 160, 162

U, Fe 277

U, Mo 34, 162, 308, 353, 371, 410, 423, 426

U, REE 226

U, Th ix, 19, 50, 55, 57, 111, 177

U, Th, REE ix

U, Th, Ti, Nb, Zr, REE 177

U, V 436

- controls (see Sect. *Ore Controls and Recognition Criteria*)
 fields (see Locality Index)
- Organic material
 algae 6, 24, 140
 bitumen, bituminous 8, 21, 24, 25, 29, 129, 167, 269, 271, 274, 277, 278, 309, 310, 393, 405, 425
 bog, marsh, muskeg, paludal, peat, swamp 18, 21, 24, 39, 40, 66, 72, 154, 261, 264, 304, 414
 bones 23, 191, 224–226, 228, 244, 282, 316, 451
 carbonaceous 7, 8, 20, 21, 24, 29, 32, 34, 35, 42, 49, 59–61, 66, 69, 80, 81, 85, 88, 99, 102, 109, 112–114, 120, 128, 129, 133, 135–137, 139, 140, 144–146, 148, 154, 156, 166–170, 172, 181, 183, 185, 199–201, 209, 213, 220, 221, 231, 234, 242, 246, 250, 259, 260, 263, 264, 278, 296, 301, 303, 304, 306, 309, 310, 315, 317, 318, 323, 328, 330, 357–362, 365, 371, 387, 400, 401, 403, 405, 410, 411, 422, 432, 434–436, 445
 coal, coaly, coalified 21, 24, 29, 30, 34–38, 40, 41, 54, 66, 71, 72, 75, 88, 120, 122, 140, 147, 151, 167, 191, 205, 264, 269, 282, 328, 335, 362, 363, 371, 373, 397
 fish bones, scales (fossil, phosphatic) 23, 191, 224–226, 228, 244
 humate, humic 7, 8, 21, 24, 25, 134, 183, 318, 369–371
 kerogen 134
 kolm 25
 lignite 21, 24, 29, 31, 34, 35, 37, 42, 140, 148, 151, 153, 155, 187, 191, 192, 242, 243, 245, 248, 261, 263–265, 269, 282, 283, 285, 287, 304, 305, 358, 368, 372, 386, 390, 400, 411, 432, 449
 organic (not differentiated) 7, 8, 18, 20, 21, 24, 25, 29, 36, 37, 60, 66, 69, 72, 74, 75, 83, 95, 133–135, 140, 144, 147, 148, 151, 154, 167–169, 181, 183, 185, 187, 188, 191, 192, 199, 221, 224, 231, 234, 236, 261, 263, 264, 266, 271, 289, 305–309, 316–318, 320, 323, 326, 358, 360, 371, 387, 400, 405, 410, 447, 449
 organic phosphorous (see Uranium deposits – types: Type 16, and above - fish bones)
 plant, detrital carbon, vegetal debris/trash 6–8, 22, 24, 34, 35, 66, 68, 74, 157, 164, 169, 170, 175, 177, 184, 185, 187, 232, 236, 246, 266, 278, 283, 290, 291, 292, 299, 304, 306, 310, 313, 316, 317, 323, 333, 343, 358, 387, 389, 393, 401, 408, 420
 tree logs/trunks 314
 uraniferous (see Uranium ab-, adsorbing agents/material/minerals, and Urano-organic complexes)
- Orogeny, orogen, orogenic belt, system, zone
 Alpine, Alpidic 29, 282, 403, 435
 Caledonian 29, 44, 75, 76, 78, 84, 86–89, 91, 95, 96, 98, 106, 107, 109, 114, 115, 122, 125, 127, 129, 130, 133, 137, 139, 191, 194, 195, 199–203, 209, 211, 217, 222, 229, 254, 255, 287, 304, 308, 323, 324, 341, 362
 Cathaysian fold system 88, 99, 109, 115, 120
 Central Mongolian fold belt (Caledonian) 287, 304
 Grenville 19
 Guangxi (see below Yangtze)
 Hercynian (Variscan) 5, 9, 29, 35, 65, 68, 75, 84, 88, 106, 107, 120, 139, 155, 271, 282, 341, 362, 393, 403, 405, 414, 435, 438–440
 Himalayan (Xishanian) 29, 62, 65, 96, 113, 133, 135, 149, 313, 319
 Indosinian 29, 48–50, 80, 83, 84, 87–89, 91, 95, 98, 106–109, 111–115, 120, 122, 130, 133, 137, 139, 144, 155
 Iron Ore (Older Metamorphic) 158–160
 Jinning (Xuefeng) 35, 86–88, 91, 96, 98, 114, 115, 120, 132, 136, 138, 139
 Luliangian 48, 49
 Nanhua metallogenetic zone (South China Caledonian fold belt) 29, 86–89, 115
 North Tien Shan fold belt (Caledonian) 44
 Ogcheon fold belt (Early Paleozoic) 46, 76, 88, 107, 117, 129, 289, 299, 301, 303, 368, 391, 438
 Older Metamorphic (see above Iron Ore)
 Sibao 86, 115
 Singhbhum 30, 157–162
 South China Caledonian fold belt (see above Nanhua metallogenetic zone)
 South Gobian fold belt 308
 South Mongolian fold belt (Caledonian) 29, 75, 76, 78, 84, 86–89, 91, 95, 96, 98, 106, 107, 109, 114, 115, 122, 125, 127, 129, 130, 133, 137, 139, 191, 194, 195, 199–203, 209, 211, 217, 222, 229, 254, 255, 287, 304, 308, 323, 324, 341, 362
 Ural-Mongolian fold belt or orogenic system (Hercynian/Variscan) 5, 9, 29, 35, 65, 68, 75, 84, 88, 106, 107, 120, 139, 155, 271, 282, 341, 362, 393, 403, 405, 414, 435, 438–440
 Xianggui fold belt 35, 88, 132, 133, 139, 141
 Xishanian (see above Himalayan)
 Xuefeng (see above Jinning)
 Yangtze (Guangxi) 29, 31, 34, 35, 79, 84, 86–89, 98, 99, 114, 115, 120, 132, 136, 139, 140, 146–148
 Yanshanian 29, 48, 50, 59, 61, 62, 65, 68, 76, 79, 80, 83, 85, 87–89, 91, 93, 95, 96, 98, 99, 106–109, 111, 112, 114, 115, 118, 120, 130, 131, 133, 135, 137, 139, 140, 146, 155
- Oxidized deposits/mineralization (see Sect. *Mineralization*)
 Oxidized environment, zone (see Sect. *Alteration*)
- P**
 Paleosol viii
 Paragenesis, paragenetic mineral assemblage (see Sect. *Mineralization*)
 Peat (see Organic material)
 Pechblende (see Index U and U-bearing minerals: Pitchblende)
 Pegmatite, pegmatitic viii, 19, 31, 35, 55, 76, 78, 79, 92, 109, 167, 175, 176, 287, 313, 323, 334, 389
 deposits (see Uranium deposits – types: Type 12)
 Peralkaline (nepheline) syenite 19, 35, 49, 54–58, 381 (see also Uranium deposits – types: Type 12)
 Permeability, transmissivity 6–8, 15, 36, 65, 68–70, 154, 168, 169, 175, 231, 233, 252, 263, 293, 311, 318, 319, 327, 360, 365, 368, 422
 Petroleum 274, 278
 Phosphatic, phosphorous 24, 29, 118, 171, 172, 194, 202, 224, 225, 405, 411
 Phosphorite deposits (minerochemical) 23, 191, 451–452 (see also Uranium deposits – types: – Type 17)
 Phosphorite, phosphate 11, 20, 23, 24, 29–31, 35, 135, 157, 191, 192, 217, 225, 226, 285, 287, 375, 387–389, 395, 396, 403, 405, 410, 414, 435–437, 451–452
 Phosphorous deposits, organic 218, 224–228 (see also Uranium deposits – types: Type 16)
 Phreatic, groundwater/infiltration 7, 17, 20, 34, 36, 65, 68–70, 73–75, 81, 94, 98, 104, 108, 113, 133, 135, 136, 151, 169, 181, 183, 187, 231, 263, 281, 282, 284, 316, 317, 363, 405, 406, 409, 410, 414, 416, 422–424
 Pitchblende viii (see also Index U and U-bearing minerals)
 Placer, paleoplacer 16, 157 (see also Uranium deposits – types: – Type 10) modified 16
 Platform, paraplatform 29, 33, 34, 47, 86, 140, 191, 194, 195, 203, 228, 233, 253, 254, 288, 323, 324, 326, 403
 Playa (see Uranium deposits – types: Type 11)
 Pluton (see Intrusive complexes)
 Pneumatolytic 55, 58, 118, 130, 181, 336, 343
 Polymetallic, polygenetic, polyphase, viii, 5, 9, 10, 13, 14, 16, 17, 57, 62, 75, 79–82, 86, 91, 92, 99, 114, 115, 130, 135, 140, 162, 177, 194, 195, 201, 224, 233, 255, 257, 258, 261, 263, 265, 302, 303, 306, 308, 332, 340, 341, 343, 354, 393, 410, 417, 423, 426, 436, 437, 439, 440 (see also Sect. *Mineralization*)
 Potassium, potassic 15, 48–50, 52, 54, 58, 61, 109, 116, 120, 336, 342, 373–376, 381–383, 387 (see also Alteration: – K metasomatism)
 Precipitation (deposition, fixing) of uranium (see Uranium - deposition)
 Production of uranium [see *Uranium districts and deposits (introductory section)*, and Part I, Uranium deposits – types and subtypes]
 Province, uranium (see also Uranium province) 29–32, 35, 36, 47, 75, 79, 86, 88, 89, 96, 98, 115, 287
 Pyroclastic rocks 10, 34, 292, 440 (see also Tuff, and Volcanic)
- Q**
 Quartz-monzonite 19, 86, 95, 175
 deposits (see Uranium deposits – types: – Type 12)
- R**
 Radium 269, 278, 280, 393, 401, 422
 Rare
 earth elements (REE) ix (see Metallic elements)
 elements (see Metallic elements)
 Recognition criteria (see Sect. *Ore Controls and Recognition Criteria*)

- Redox conditions, reduction-oxidation interfaces 5, 7, 65, 108, 168, 233, 239, 250, 266, 306, 308–310, 318, 323, 408, 410, 418, 419, 424 (see also Sections *Alteration* and *Metallogenetic Aspects/Concepts*)
- Reducing agents, reduction (see Uranium, and Sections *Alteration* and *Metallogenetic Aspects/Concepts*)
- Regolith (paleosol) viii
- Reserves/resources (of uranium) [see *Uranium districts and deposits (introductory section)*]
 cost categories ix
 definitions, categories ix, x
 estimated additional (EAR) (= inferred) x
 in situ x
 inferred ix
 reasonably assured (RAR) ix, x
 recoverable x
- Rhyolite, rhyolitic (see also Volcanic) 10, 11, 24, 51, 59, 62, 99, 116–132, 166, 175, 178, 179, 195, 201, 202, 208, 255, 257, 259, 260, 267, 289–293, 296, 303, 308, 326, 335, 340, 343, 352, 354, 365, 386–389, 395, 397, 438–440, 449
- Rollfront, roll-shaped, roll-type 6, 7, 36, 68, 193, 228, 239, 241, 243, 248, 253, 255, 260, 265, 266, 310, 403, 408, 410, 422–425 (see also Sect. *Shape and Dimensions*, and Uranium deposits – types: Type 3)
- ## S
- Salt domes/diapirs 178
- Sand/sandstone (arkose, arkosic, feldspathic) (see Uranium deposits – types: Type 3)
 carbonaceous (organic-bearing) 20, 102, 120, 139, 148, 154, 156, 231, 259, 306, 323, 365, 405, 411, 434
 continental, fluvial-alluvial 8, 36, 43, 127, 234, 236, 245, 250, 253, 304, 330, 426, 432
 marginal marine, fluvial, littoral 8, 36, 43, 127, 330
 redbed 122, 127, 201 (see also Sediments)
 tuffaceous, tuff/acid volcanic interbeds 35, 66, 120, 123, 126–128, 151, 185, 266, 302, 308, 443, 449
- Sandstone uranium deposits (see Uranium deposits – types: Type 3)
- Saprolite, saprolitic viii
- Sediments, sedimentary environment (see Sections *Geological Setting* and *Ore Controls and Recognition Criteria*)
 continental/terrestrial 11, 21, 36, 65, 114, 144, 148, 155, 219, 233, 245, 250, 253, 261, 264, 271, 303, 304, 313, 330, 341, 362, 373, 390, 391, 397 (see also Sand/sandstone)
 delta, deltaic 70
 fluvial, alluvial 7, 71, 153, 183, 184, 195, 201, 224, 232, 245, 304, 308, 323, 326, 328, 330, 405
 lacustrine 79, 149, 179, 187, 229, 289, 313, 315, 395
 lagoonal 135, 396
 limnic 308, 310, 323
 marginal marine 6, 8, 36, 43, 127, 168, 330
 marine 6, 16, 168, 178, 187, 224, 229, 245, 249, 277, 323, 325, 395, 397, 438
 playa 18
 redbed 88, 97, 98, 113, 118, 122, 127, 201, 205
 shallow marine (near-shore platform) 229, 245
 terrestrial (see above continental)
 volcanogenic (ignimbrite, tuff) 10, 11, 22, 24, 46, 51, 59, 62, 66, 116, 121, 123, 127, 128, 132–134, 148, 153, 166, 175, 177, 178, 181, 185, 195, 205–207, 212, 217, 218, 220, 258, 259, 265–267, 278, 290, 291, 296, 299–302, 309, 315, 316, 326, 331, 335, 341, 343, 346, 349, 354, 358, 360, 365, 387–389, 395–397, 440, 443, 446, 449
- Sedimentary-diagenetic (see Uranium deposits – types: – Type 13)
- Shape/configuration/texture of ore bodies/shoots, style of uranium (mineral)
 distribution (see Sect. *Shape and Dimensions*)
 dimensions (see Sect. *Shape and Dimensions*)
 lens, lensoid, lenticular 116, 125, 127, 154, 213, 218, 220, 233, 246, 251, 263, 267, 275, 276, 311, 362
 linear 9, 200
 peneconcordant 7, 21, 99
 stack, stacked 8, 23, 151, 153, 232
 stockwork 11, 14, 20, 203–205, 211, 213, 216, 259, 266, 290, 299–301, 339, 350, 351, 436
 tabular, blanket, trend 7, 11, 38, 68, 75, 130, 131, 232, 265, 296, 299, 302, 304, 308, 311, 434
- Silicolite 20, 133, 136, 139, 147
- Skarn 25, 49, 54, 55, 57–59, 80, 81, 97, 199, 304, 336, 354, 386
- Sodium, sodic 12–13, 15, 47–49, 52, 54, 58, 76, 80, 109, 336, 342, 375 (see also *Alteration/metamorphism*)
- Soil 17, 18, (see also Duricrust: – pedogenic)
- Solution (see Hydrogenic, hydrothermal)
- Source(s) of uranium (see Sect. *Sources of Uranium*)
- Stable isotopes 49, 97, 104, 116, 118, 135, 143, 187, 409, 446 (see also Sect. *Stable Isotopes and Fluid Inclusions*)
- Strata-bound, -controlled mineralization 6, 10, 11, 17, 34, 49, 122, 133, 135, 137, 146, 161, 162, 170, 171
- Strata oxidation 7
- Stratigraphy (see Sect. *Geological Setting*)
- Stratigraphic units
 A Fm 66
 Aershan Fm 68
 Akchinskaya Fm 440
 Akeyo Fm 185, 186
 Aktau Fm 265
 Alan Fm 387, 388
 Alatanheli Gp 66
 Amka Fm 387
 Andreevskaya Mbr 199, 209, 210
 Anshan Gp 48, 50, 51
 Areda Fm 365–367
 Arkasani Granophyre/Gneiss 159, 160
 Arkharlin Fm 267
 Baghal Chur Sand 315
 Banganapalle Fm 170
 Bangmai Fm 155
 Baogedewula Fm 68, 69
 Bayanhua Gp 66, 68, 69
 Bayanshiree Fm 308
 Bhima Gp 30, 157, 171
 Bone Valley Fm 23
 Borovsk Fm 199
 Chaibasa Fm 161
 Chakradharpur Granite Gneiss 159, 160
 Chattanooga Shale 24, 25
 Chengapara Fm 166
 Chotanagpur Gneiss 158, 159
 Cuddapah Supergp 171
 Daguding Fm 120, 126, 129
 Dalma Volcanics 159
 Dangchong Fm 140, 143
 Dhanjori Fm 159–162
 Dhanjori Gp 159
 Dhok Pathan Fm 314, 315, 318
 Dongsheng Fm 75
 Dornod Fm 289–294, 296, 299–302
 Dusinobin Fm 309
 Dzheirantyi Hor 411
 E'huling Fm 122
 Erendabusu Fm 66, 67
 Erliandabusu Fm 68
 Fushan Fm 81
 Fuxian Fm 72
 Garo Gp 166
 Gassaway Mbr 25
 Ghareb Fm 451
 Gulcheru Fm 171
 Gunbayan Fm 309
 Gurvansaihan Fm 309
 Gusinoeye Ozero Series 369, 370

- Haifanggou Gp 59, 60
 Hongqiyingsi Gp 61
 Hormoz Fm 178
 Huashanling Fm 122
 Ikan Fm 254
 Ily Fm 265, 266
 Ima Fm 368–370
 Inkuduk Fm 231, 236, 239
 Inkuduk Hor 231, 232, 234–236, 239, 241, 243
 Iron Ore Gp 158–160
 Jadukata Fm 166, 170
 Jaintia Gp 166
 Jangrag Fm 391
 Jianchang Fm 33, 34, 59
 Jiuling Gp 35, 86–88, 114, 132, 133, 135, 136
 Kamlial Fm 320
 Kanzhugan Fm 232, 241, 246
 Kanzhugan Hor 245
 Karagiin Mbr 225–227
 Karamolin Hor 217
 Karasay Fm 259
 Kendyktube (Kendyk) Hor 405, 411, 432
 Keregetas Fm 267
 Khasi Gp 166
 Khetanin Fm 387
 Kijalin Fm 221
 Kokshetau Fm 199, 209
 Koktaus Fm 259
 Kombolgie Fm 6
 Kurnool Gp 170
 Lancang Gp 155
 Langpar Fm 166, 170
 Lanqi Gp 60
 Liaoho Gp 54
 Luoling Fm 81, 84
 Lyavlyakan Hor 424, 428, 431
 Mahadek Fm 166, 169, 170
 Maikop Fm 225, 227
 Manchar Fm 320
 Mangbang Fm 151
 Mangbanzu Fm 153
 Mayurbhanj Granite 159, 160, 162
 Menuha Fm 451
 Misasa Gp 187, 188
 Mishan Fm 178, 179
 Mizunami Gp 185, 186
 Moshishan Fm 120
 Mynkuduk Fm 232, 234, 236, 239
 Mynkuduk Hor 235, 236, 239, 241
 Nagri Fm 314
 Nakatsugo Fm 183, 187–189
 Oidawara Fm 185, 186
 Older Metamorphic Gneiss 158
 Older Metamorphic Gp 158
 Older Metamorphic Tonalite Gneiss 158
 Olov Fm 365
 Orlov Fm 366, 367
 Papaghi Gp 171
 Phosphoria Fm 23
 Priargun Series 343
 Qabul Khel Sandstone Hor 318, 319
 Qabul Khel Shale Hor 319
 Qinling Gp 76
 Ravashskaya Fm 440
 Sabyrsai Hor 432, 434, 435
 Saihan Fm 66, 68, 286
 Saihantala Fm 69–71
 Semizbay Fm 221, 224
 Seto Gp 184, 186
 Sharlin Fm 309
 Sharykskaya Mbr 209
 Shella Fm 170
 Shidengzi Fm 144
 Shillong Gp 166
 Shuixigou Gp 38–41
 Singhbhum Gp 158–162
 Singhbhum Granite 158–160, 162
 Siwalik Div 313–316, 318
 Siwalik Gp 313, 318
 Soda Granite 159–161, 164
 Suktui Fm 363
 Srisailam Fm 170
 Sylhet Trap 166
 Taabyrdaakh Fm 388
 Tashk Fm 177
 Tenggeer Fm 68–71
 Todusken Fm 229, 244
 Toki Fm 185, 187
 Tsagaant 308
 Turgin Series 335, 336
 Uchkuduk Hor 411–413, 426, 432, 434
 Ukurai (Ukurei) Fm 363, 367
 Ulberikan Fm 387
 Ulus Hor 432, 434
 Ulziin Fm 303
 Undurud Fm 309
 Urak Fm 387, 389
 Uvanas Fm 241, 243
 Uyuk Fm 231, 242, 244, 246, 248, 249, 254, 324, 328, 330, 333
 Uyuk Hor 248, 249
 Vempalle Fm 171
 Witwatersrand Supergp 16, 17
 Witwatersrand Syst 17
 Xiangshan Gp 79, 81, 82, 84
 Xishanyao Fm 41
 Yan'an Fm 74
 Yanchang Fm 72
 Yujiang Gp 119
 Zerendin Fm 199
 Zhalpak Fm 232, 234, 236, 241
 Zhalpak Hor 236
 Zhangjiakou Gp 62
 Zhidan/Liupanshan Gp 72
 Zhiluo Fm 72–75
 Zuunbayan Fm 303, 304, 306, 309, 310
 Zyzulikan Fm 365
 Zyzulya Fm 362, 363, 365
- Structures, faults, lineaments etc. (see Sect. *Geological Setting*)
 Supergene 62, 65, 75, 94, 97, 113, 133, 135, 136, 144, 149, 153, 264, 277,
 282, 287, 435, 446 (see also Hydrogenic, and Sect. *Metallogenetic Concepts/Aspects*)
 Surficial 10, 17, 18, 149, 178, 179, 191, 193, 269, 285, 287, 316, 323, 393, 449
 deposits (see Uranium deposits – types: Type 11)
 Syngenetic 23, 24, 25, 135, 139, 217, 221, 323, 443
 Synmetamorphic deposits (see Uranium deposits – types: – Type 20)
- T**
 Taphrogeny, taphrogenic tectonics 85
 Thorium (in uraniferous rocks and minerals) (see Metallic elements)
 U–Th minerals (see Index U and U-bearing minerals)
 Tuff, tuffaceous units 10, 11, 22, 24, 46, 51, 59, 62, 66, 116, 121, 123, 127,
 128, 132, 148, 153, 166, 175, 177, 178, 181, 185, 195, 205–207, 212, 217,
 218, 220, 258, 259, 265–267, 278, 290, 291, 296, 299–302, 309, 315, 316,
 326, 331, 335, 341, 343, 346, 349, 354, 358, 360, 365, 387–389, 395–397,
 440, 443, 446
 Types of deposits vii, 3, (see also Uranium deposits – types)

U

- Unconformity, paleounconformity 4–6, 50, 51, 69, 157, 166, 167, 169–172, 179, 185, 188, 194, 200, 203–205, 229, 231, 233, 236, 239, 244, 250, 264, 293, 299, 301, 304, 308, 310, 365, 397, 400, 411, 426, 428, 432, 438
- intraformational 21, 99, 117, 135, 138–140, 161, 222, 239, 290–292, 296, 301, 302, 306, 310, 318, 366
- Paleoproterozoic/Carpentarian 6
- Proterozoic 4
- Uraniferous lignite/coal deposits (see Uranium deposits – types: Type 18)
- Uraninite viii (see Index U and U-bearing minerals)
- Uranium
- ab-, adsorbing agents/material/minerals (see also Sect. *Mineralization*)
- bitumen 8, 167, 274, 309, 310, 393
- clay minerals, particles 17, 24, 99, 306, 310
- goethite 94, 112, 145, 167, 200, 212, 232, 246, 277, 280, 316, 317, 387, 388, 416, 419
- hematite 6, 7, 15, 16, 22, 60, 62, 75, 76, 80, 81, 92, 94, 99, 102, 109, 111, 112, 114, 125, 126, 129, 132, 134, 139, 143, 145, 148, 151, 164, 176, 178, 185, 210, 213, 246, 255, 272, 274–277, 281, 290, 292, 293, 299, 300, 316, 317, 346, 358, 374, 388, 389, 405, 408–410, 416–418, 422–424, 438, 445
- hydroxides of Al, Fe, Mn, Mo, Si, Ti, Zr 445
- kerite 274, 310, 445
- martite 178, 316
- organic matter 8, 18, 24, 72, 74, 133–135, 140, 147, 148, 151, 154, 167–169, 181, 183, 187, 224, 234, 236, 261, 266, 289, 306, 308, 309, 318, 320, 323, 326, 358, 360, 371, 387, 400, 410, 449
- plant remains 232, 290, 292, 306, 310, 316, 323, 343, 387, 389, 420
- silica 22
- zeolites 57, 183, 185, 316
- contents (background values) 24, 50, 58, 66, 85, 92, 94, 102, 104, 105, 112, 176, 178, 199, 224, 234, 263, 264, 316, 339, 371, 372, 380, 381, 422 (see also Sect. *Sources of Uranium*)
- deposition/fixing/precipitation 7, 58, 82, 83, 98, 104, 118, 144, 179, 183, 187, 231, 234, 263, 264, 273, 290, 292, 317, 319, 341, 343, 353, 360, 388, 418, 424, 435 (see also Sect. *Metallogenetic Concepts/Aspects*)
- deposits vii, viii, 3, 4 (see also Uranium deposits: – examples and Locality Index)
- districts vii, 3, (see also Locality Index)
- hexavalent (U⁶⁺) ion 36, 52, 74, 112, 114, 133, 135, 148, 181, 187, 188, 208, 264, 299–301, 387–389, 391, 395, 435
- magmatic (igneous)/anatectic environment/origin 9, 10, 15, 19, 55, 116, 446
- metallogenesis vii, 3 [see Uranium (deposits) mineralization, and Sect. *Metallogenetic Concepts/Aspects*]
- mineralization (see Sect. *Mineralization*)
- minerals (see Index U and U-bearing minerals, and Sect. *Mineralization*)
- mobilization, mobility (see Sect. *Metallogenetic Concepts/Aspects*)
- production [see *Uranium districts and deposits (introductory section)*]
- province 29–32, 35, 36, 47, 75, 79, 86, 88, 89, 96, 98, 115, 287 (see also Locality Index)
- redistribution, recrystallization (see Sect. *Metallogenetic Concepts/Aspects*)
- reduction, reducing agents 83, 183, 224, 231, 261, 317, 323, 408, 410 (see also Sect. *Metallogenetic Concepts/Aspects*)
- reserves/resources [see *Uranium districts and deposits (introductory section)*, and Uranium deposits – types]
- source (rocks) (see Sect. *Sources of Uranium*)
- transport (see Sect. *Metallogenetic Concepts/Aspects*)
- Uranium (deposits) mineralization (general) (see Sect. *Mineralization*)
- authigenic/authigenous (see Sections *Alteration, Mineralization, and Metallogenetic Concepts/Aspects*) 426
- complex (or polymetallic) viii
- metallogenesis/mode of origin vii, 3 (see Sect. *Metallogenetic Concepts/Aspects*)
- mineral assemblages/parageneses (see Sect. *Mineralization*) 82, 84, 94, 95, 101, 102, 107, 111, 118, 123–125, 136, 161, 162, 199, 200, 202, 219, 273, 277, 301, 304, 310, 336, 339, 341, 346, 347, 373, 374, 387, 417, 418, 422, 437, 438, 444–446
- monometallic (or simple) viii
- ore composition/metal associations (see Ore composition, Metallic elements, and Sect. *Mineralization*)
- oxidized (see Sect. *Mineralization*)
- polymetallic (or complex) viii
- redistributed, recrystallized, remobilized, reworked (see Sect. *Metallogenetic Concepts/Aspects*)
- shape, configuration (see Sect. *Shape and Dimensions*)
- supergene (see Hydrogenic/hydrothermal solutions/systems)
- surficial (see Uranium deposits – types: – Type 11)
- syngenetic (see Uranium deposits – types: – Types 10, 12, 16, 17, 18, 19, 20)
- Uranium and uraniferous minerals (see Index U and U-bearing minerals)
- Uranium deposits – types (bold numbers in headings and subheadings refers to descriptions in Part II)
- collapse breccia pipe, type 8 15
- type examples 15
- grades 15
- locality 15
- resources/reserves 15
- granite-related, type 4 9, 34, 75ff, 79ff, 89ff, 170, 172, 390, 393
- contact-granitic 9
- endogranitic 9, 89f
- episyenite-hosted 9
- exogranitic (= perigranitic) 9, 10, 89f
- perigranitic
- in contact-metamorphosed rocks 10
- monometallic 9, 10
- polymetallic 9
- type examples 9, 10
- grades 9, 10
- locality 9, 10
- resources/reserves 9, 10
- intrusive, type 12 19, 54ff, 75ff, 79
- alaskite 19, 76
- carbonatite Cu-U 19, 320
- pegmatite 19, 79
- peralkaline syenite 19, 54ff
- quartz-monzonite/copper-porphyry Cu-U 19
- type examples 19
- grades 19
- locality 19
- resources/reserves 19
- metasomatite-related, type 6 12, 50ff, 172, 177–178
- ferro-uranium formation 13
- iron-uranium formation associated with sodic and carbonate metasomatites 13
- metasomatized
- granite 12
- metasediments/metavolcanics 13
- type examples 12, 13
- grades 12, 13
- locality 12, 13
- resources/reserves 12, 13
- Paleoproterozoic quartz-pebble conglomerate, type 10 16
- Lower Proterozoic conglomerate 16
- modified paleoconglomerate 16
- monometallic (or U-dominant with REE) 16
- oligomictic conglomerate 16
- paleoconglomerate 16
- polymetallic Au with U 17
- type examples 17
- grades 17
- locality 17
- resources/reserves 17
- polymetallic hematite-breccia-complex, type 9 15
- type examples 16
- grades 16
- locality 16
- resources/reserves 16

- Proterozoic subunconformity-epimetamorphic, type 2 6
 - type examples 6
 - grades 6
 - locality 6
 - resources/reserves 6
- sandstone, type 3 6, 34, 35ff, 59ff, 65ff, 147ff, 164ff, 181ff, 220ff, 228ff, 248ff, 260ff, 304ff, 313ff, 318ff, 323ff, 356ff, 368ff, 386, 395–396, 402ff, 449
 - basal-channel 8, 59ff, 68ff, 148ff, 220ff, 260ff, 323ff, 356ff, 386
 - blanket 7
 - continental basin, U associated with intrinsic reductant 7
 - continental fluvial
 - U associated with (extrinsic) humate/bitumen 8
 - U associated with intrinsic reductant 8
 - vanadium-uranium 8
 - continental to marginal marine, U associated with intrinsic reductant 7
 - exogenic infiltration 7, 8
 - marginal marine 7
 - rollfront 7, 35ff, 59–60, 71ff, 228ff, 248ff, 402ff
 - strata-oxidation 7
 - tabular/peneconcordant 7, 35ff, 59–60, 65ff, 154ff, 164ff, 304ff, 313ff, 318ff, 368ff, 449
 - tectonic-lithologic 8
 - type examples 7–9
 - grades 7–9
 - locality 7–9
 - resources/reserves 7–9
 - U associated with extrinsic reductant 7
 - U-REE in erosive paleovalley 8
 - valley
 - on plain 8
 - on plateau 8
 - valley or paleovalley 8
- surficial, type 11 17, 178, 278ff
 - calcrete 17–18
 - duricrusted sediments 17–18
 - exogenic infiltration 17
 - fluvial valley-fill 18
 - ground-oxidation 17
 - groundwater-calcrete 17
 - karst cavern 18, 278ff
 - lacustrine/playa 18
 - peat-bog 18
 - playa 18
 - silcrete 17
 - structure fill 18
 - surficial pedogenic 18
 - type examples 18, 19
 - grades 18, 19
 - locality 18, 19
 - resources/reserves 18, 19
 - valley-calcrete 17
- unconformity-contact, type 1 4, 6,
 - Proterozoic unconformity-contact 4
 - clay-bound 5
 - fracture-bound 5
 - Phanerozoic unconformity 5
 - type examples 5
 - grades 5
 - locality 5
 - resources/reserves 5
- undifferentiated (meta-)sediment hosted (in veins and shear zones), type 7
 - 6, 13, 157ff, 170–171, 175–176, 194ff, 372ff, 449
 - monometallic shear zone fillings 13, 14
 - monometallic veins 13, 194ff
 - polymetallic veins, stockworks 14, 157ff, 194ff, 372ff
 - type examples 14, 15
 - grades 14, 15
 - locality 14, 15
 - resources/reserves 14, 15
- uraniferous bituminous-cataclastic limestone, type 14 21, 146–147, 269ff
 - exogenic epigenetic infiltration 21
 - type examples 21
 - grades 21
 - locality 21
 - resources/reserves 21
 - vanadium-uranium deposits in carbonate sediments 21
- uraniferous carbonaceous lutite (lacustrine), type 15 21
 - type examples 23
 - grades 23
 - locality 23
 - resources/reserves 23
- uraniferous carbonaceous shale-related stockwork, type 13 20, 34, 85, 86, 132ff, 391, 398, 434
 - carbonaceous-carbonate-siliceous-pelite (C-Si-pelite) 20, 34, 85, 86, 132ff
 - hydrothermal-reworked 20, 133, 137, 140
 - leaching-accumulative 20, 133
 - phreatic infiltration 20, 133
 - sedimentary-diagenetic 20, 133
 - silicolite 20, 133, 136, 139, 147
 - type examples 21
 - grades 21
 - locality 21
 - resources/reserves 21
- uraniferous lignite/coal, type 18 24, 36, 191, 261ff, 269, 282, 390
 - mixed stratiform/fracture-controlled epigenetic 24
 - stratiform-syngenetic 24
 - type examples 24
 - grades 24
 - locality 24
 - resources/reserves 24
- uraniferous minerochemical phosphorite, type 17 23, 451–452
 - bedded phosphorite 23
 - land-pebble phosphate 23
 - type examples 23
 - grades 23
 - locality 23
 - resources/reserves 23
- uraniferous organic phosphorous, type 16 23, 224ff
 - exogenic sedimentational-diagenetic 23
 - rare-earth – uranium deposits in clays with fish remains 23, 224ff
 - type examples 23
 - grades 23
 - locality 23
 - resources/reserves 23
- uraniferous stratiform black shale, type 19 24, 398
 - bituminous/sapropelic black shale 25
 - humic/kolm in alum shale 25
 - type examples 25
 - grades 25
 - locality 25
 - resources/reserves 25
- uraniferous synmetamorphic and contact-metamorphic, type 20 25
 - type examples 25
 - grades 25
 - locality 25
 - resources/reserves 25
- volcanic, type 5 10, 34, 60ff, 115ff, 178–179, 254ff, 266–267, 287ff, 331, 332ff, 386ff, 390, 393, 397ff, 437ff, 449
 - apatite-uranium 10
 - associated with felsic volcanic complexes 11, 60ff, 115ff, 387ff, 437ff
 - associated with mafic-felsic volcanics in calderas underlain by granite 11, 287ff, 332ff
 - deposits in volcanic depressions 10
 - diatreme hosted 11
 - endo(intra)caldera 11
 - endogenic hydrothermal 10, 11
 - exocaldera 12

- fluorite-uranium 10
deposits associated with andesite-rhyolite in erosional-tectonic basins 11
- molybdenum-uranium 10
- strata-bound 11, 12
exocaldera 12
intracaldera 11
- structure-bound 10, 11
- surficial fracture fills 10
- surficial veinlike 11
- tabular-stratiform 11
- type examples 11, 12
grades 11, 12
locality 11, 12
resources/reserves 11, 12
- vein-stockwork 11
- Uranium deposits types by type number
type 1 unconformity-contact 4
type 2 Proterozoic subunconformity-epimetamorphic 6
type 3 sandstone 6
type 4 granite-related 9
type 5 volcanic 10
type 6 metasomatite-related 12
type 7 undifferentiated (meta-)sediment hosted (in veins and shear zones) 13
type 8 collapse breccia pipe 15, 389
type 9 polymetallic hematite-breccia-complex 15
type 10 Paleoproterozoic quartz-pebble conglomerate 16
type 11 surficial 17
type 12 intrusive 19
type 13 uraniferous carbonaceous shale-related stockwork 20
type 14 uraniferous bituminous-cataclastic limestone 21
type 15 uraniferous carbonaceous lutite (lacustrine) 21
type 16 uraniferous organic phosphorous 23
type 17 uraniferous minerochemical phosphorite 23
type 18 uraniferous lignite/coal 24
type 19 uraniferous stratiform black shale 24
type 20 uraniferous synmetamorphic and contact-metamorphic 25
- Uranium province 29–32, 35, 36, 47, 75, 79, 86, 88, 89, 96, 98, 115, 287 (see also Locality Index)
- Urano-organic complexes
anthraxolite 203, 445
humate 7, 8, 21, 24, 369–371
kerogen 134
thucholite 6, 17
- Uranpecherz (see Index U and U-bearing minerals -Pitchblende)
- Uranyl minerals (see Index U and U-bearing minerals)
- U-Ti compounds/phases 17, 37, 172, 200, 202, 203, 212, 216, 217, 341, 347, 354, 375, 438, 445
- V**
- Valley (on plain, plateau) (see Uranium deposits – types: – Type 3)
- Vanadium (see also Metallic elements and Ore composition/metal associations) 7, 8, 21, 66, 248, 250, 251, 269, 278, 279, 317, 318, 376, 401, 405, 435, 436
- Vegetal matter (see Organic material)
- Vein viii, 3–4, 9–14, (see also Sect. *Shape and Dimensions*)
- Volcanic, volcanite 4, 5, 10–11, 16, 25 (see also Uranium deposits – types: – Type 5)
belt 10, 11, 31, 46, 86, 88, 89, 115, 119, 122, 129, 257, 285, 288, 334, 341, 353, 439 (see also Volcanic structures)
caldera 10, 11, 34, 116–118, 120–123, 125, 126, 131, 259, 266, 285, 291, 292, 332, 334–336, 338–343, 347, 352, 353, 357, 358, 372, 386, 390, 438–441
deposits (see Uranium deposits – types: Type 5)
- depression/basin 5, 7–11, 13, 16–18, 24, 29–43, 46–50, 59–62, 65–73, 75, 79, 80, 82, 87–89, 95–99, 101, 105, 107–109, 113, 116–122, 126–129, 132, 133, 135, 137, 139–141, 143, 144, 147–155, 157, 167, 169–172, 175, 179, 181, 183, 184, 187, 188, 191–194, 199, 202, 203, 205, 206, 216, 221, 228–239, 241, 243, 244, 247–253, 255, 257, 258, 260, 261, 263–266, 269, 270, 278, 282, 283, 285–287, 289, 296, 303–306, 308–310, 313, 315, 318, 321, 326, 328, 330, 335, 340, 341, 362, 363, 365, 368, 372, 386–389, 391, 395, 396, 401–407, 409, 410, 414, 416, 425, 434, 437–439, 449
diatreme 131
- Volcanic structures – localities (basin, caldera, depression, subvolcanic massif, volcanic-tectonic structure etc.) 116, 122, 199, 208, 353, 388, 438
Babaitaudor subvolcanic massif, Uzbekistan 440, 443
Babaytag subvolcanic massif, Uzbekistan 446
Batnorov volcanic structure, Mongolia 303
Berkh region, Mongolia 30, 303
Botaburum Caldera, Kazakhstan 191–193, 254, 255, 259, 260
Bureinsky district, Russia 322, 386
Chatkal Mountains, Uzbekistan 248–250, 271, 277, 278, 393, 401, 437, 440, 446
Chukotsky region, Russia 30, 321, 322, 390
Dornod (Mardai) volcanic-tectonic structure, Mongolia 10, 285–296, 299–303, 308, 333, 334, 353, 363
Eastern Gobi region, Mongolia 286, 287
Engershand volcanic-tectonic complex, Mongolia 286, 303
Gan-Hang volcanic belt, China 115–129
Karabash Caldera, Uzbekistan 439–441
Karamazar region, Uzbekistan 30, 269–272, 393, 401, 437, 439–444, 446
Kendykta-Chuily-Betpak Dala (Pribalkash region), Kazakhstan 260
Kokshetau Massif, Kazakhstan 191, 194, 195, 216, 220, 221, 224
Kuidusun volcanic depression, Russia 386, 388, 389
Manzhouli volcanic-tectonic area, China 334
Mardai (see Dornod)
Mongol-Priargun (Argun) volcanic belt, Mongolia-Russia 288, 304, 332, 343, 353
North Choibalsan region, Mongolia 30, 285–289, 302, 303
Niyut volcanic-tectonic depression, Russia 389
Pribalkash (Kendykta-Chuily-Betpak Dala region), Kazakhstan 191, 233, 254, 260
Sasyrlyk volcanic basin, Kazakhstan 257, 258
Shengyuan (Shunyuan) volcanic-tectonic basin, China 119, 122, 127, 129
Tulukuyevsk (Streltsovsk) Caldera, Russia 334–336, 338, 343, 346, 352, 353, 357, 358, 372
Turgen volcanic-tectonic complex, Mongolia 288, 302
Ugtam volcanic-tectonic complex, Mongolia 288, 302
Uliya volcanic depression, Russia 386–389
Wuyishan (Wuyi) volcanic-tectonic belt, China 11, 86, 88, 89, 115–117, 129–131
Xiangshan Caldera, China 122
Xiaoqiuvuran volcanic-tectonic basin, China 122, 129
Yakshin volcanic structure, Kazakhstan 208
- W**
- Wall rock alteration (see Halo/aureole, and Sect. *Alteration/metasomatism*)
- Weathering/paleoweathering 4, 6, 49, 72, 94, 151, 155, 175, 221, 263, 290, 293, 299, 301, 305, 308, 309, 360, 397, 436
- X**
- Xenolith 54, 55, 76, 81, 83, 84, 91, 95, 96, 109, 217, 293, 334, 339, 341, 357, 358, 388, 389, 438, 440, 443
- Z**
- Zircon 57, 58, 62, 76, 81, 92, 101, 109, 188, 210, 287, 290, 292, 300, 389, 443, 445
- Zoning/zonation 37, 42, 62, 65, 92, 102, 108, 199, 213, 234, 255, 263, 326, 336, 341, 343, 346, 347, 368, 374, 382, 408, 410, 422, 437, 438, 444



Geographical Index

A

Abakan, Russia 328, 330, 331, 333
Abayskoye, Kazakhstan 216
Academic Hill, Kyrgyzstan 280
Adrasman, Tajikistan 271, 393, 401, 437, 438
Agashskoye, Kazakhstan 192, 193, 195, 216, 217
Agda zone, Russia (see *Agdinsk*)
Agdinsk (Agdinskaya, Agda) zone, Russia 373, 376, 379, 384
Agdinskaya zone, Russia (see *Agdinsk*)
Agron, Uzbekistan 402, 429, 432
Agulak, Kyrgyzstan 282
Akashat, Iraq 30, 451
Akdala, Kazakhstan 192–194, 228, 234, 236, 239, 257
Akhutinskoye, Russia 372
Akkon-Burluiskoye, Kazakhstan 205
Aksay, Uzbekistan 438
Aksu, Kazakhstan 192, 193, 195, 218, 220
Aktau, Kazakhstan 191–194, 224, 226, 228, 261, 264–266, 270, 397, 402, 408, 411, 424, 428, 429
Akuinskoye, Russia 335
Al Haberi (Maberi) area, Syria 451
Al Hasa-Al Qatrana, Jordan 451
Al Shediya, Jordan 451
Alai Range, Kyrgyzstan 269, 278, 279, 282, 283
Alatanga, Uzbekistan 271, 401, 437–440, 442–446
Alatanga-Kattasay ore field, Uzbekistan 438–440, 442, 444–446
Aldan region, Russia 321, 322, 373, 374, 376, 378–382
Aldan Shield, Russia 29, 30, 372, 373, 377, 382
Alendy, Uzbekistan 402, 425–428
Aleur, Russia 363
Alligator Rivers ore field, Australia 6
Almalyk, Kyrgyzstan 283
Altai-Hinggan fold system, China 46, 59
Alto Alentejo, Portugal 10
Altybaysky ore field, Kazakhstan 192, 193, 195, 199, 216
Altyntau ore field, Uzbekistan 270, 402, 403, 434, 436
Amagaran, Russia 388
Amalat Basin, Russia 368, 372
Amalat ore field/area, Russia 335
Amalat Plateau, Russia 356
Amanbulak, Turkmenistan 397, 398
Amantai, Uzbekistan (see *Amantei*)
Amantei (Amantai), Uzbekistan 402, 411
Ambrosia Lake, USA 8, 9
Amka Complex, Russia 387, 389
Amudarya Basin, Uzbekistan 410
An Diem, Vietnam 449
Anderson Mine, USA 21, 23
Andhra Pradesh State, India 157
Anhui Province, China 75, 79
Antei, Russia 11, 332, 333, 336, 339, 341–354, 356
Arad (Zefa E'fe), Israel 451
Arai, Indonesia 176
Aravalli Basin, India 30, 157, 172
Aravalli-Delhi Basin, India 30, 157, 172
Arbulag, Mongolia 288

Ardakan, Iran 177
Areda, Russia 363, 365–367
Argasan, Uzbekistan 445
Argunskoye, Russia 11, 332, 336, 338, 339, 341, 354, 356–358
Arizona Strip, USA 15
Arkhimed Massif, Russia 389
Arlit, Niger 8
Astra, Russia 389
Atandzhakan, Russia 387
Atbash (Uigar Sai, Yuigar Sai), Uzbekistan 438, 447
Athabasca Basin, Canada 4, 5
Aulbek, Uzbekistan 402, 425, 426, 429
Auminsa-Beltau (Zarafshan) ore field/district, Uzbekistan 270, 402, 403, 411, 415–421, 434, 436, 437
Auminzatau ore field/Range, Uzbekistan 436
Aurora, USA 11, 12
Avdar-Tolgoy, Mongolia 288
Ayni/Zakhamatabad, Tajikistan 393

B

Babaitaudor Massif, Uzbekistan 443
Babaytag Massif, Uzbekistan 446
Badain Jaran Desert, China 35
Badia-Mosabani, India 157, 164
Badielskoye, Russia 322
Bafq district, Iran 177
Bafq-Posht-e-Badam zone, Iran 30, 177
Bagazos-nuur, Mongolia 287
Baghal Chur (Baghal Chor) district, Pakistan 313–318
Bagjata-Moinajharia, India 157, 164
Baiderin Uplift, Mongolia 287
Baiklik, Turkmenistan 397, 398, 400
Baimadong, China 132, 133, 146
Baimeishi (Baimianshi), China 130, 148
Baishun, China 105–107
Baishun/Longhuashan ore field, China 106, 107
Baiti (Baitu, Baitou), China 133, 136, 137
Baitou, China (see *Baiti*)
Baitu, China (see *Baiti*)
Baiyanghe, China 31, 44
Bakhaly, Uzbekistan 401, 402, 408, 410, 411
Baksan Massif, Kazakhstan 224
Balillu Plains, Pakistan 313
Balkashinsky (Balkashinskoye) ore field, Kazakhstan 191–193, 195, 199, 203, 205–208
Balkhash Basin, Kazakhstan 260–262
Balkhash Lake, Kazakhstan 191, 254, 259–262, 267
Baluchistan, Pakistan 313
Bancroft, Canada 19
Bandar Abbas region, Iran 30, 178
Banduhurang, India 157, 164
Bangmai Basin, China 154, 155
Bannu Basin, Pakistan 30, 313, 318, 319
Baofengyuan (Baoyan), China 133, 136
Baoshan Massif, China 148, 149, 153
Baoyan, China (see *Baofengyuan*)

- Baoyong Depression, China 149
 Baquan (617), China 122, 123, 125, 126
 Bars, Kazakhstan 192, 193, 228, 241, 246
 Barthi Basin, Pakistan 315, 318
 Barun-Ulacha, Russia 335, 372
 Baruun-Hooloi, Mongolia 302, 303
 Baruun-su, Mongolia 288
 Baryte Hill, Kyrgyzstan 280
 Bashibulak, China 43
 Bat, Mongolia 302
 Bataw-Borghat, India 170
 Batnorov volcanic structure, Mongolia 286, 303
 Bayan-bulag, Mongolia 287
 Bayandun, Mongolia 288
 Bayantala deposit, China 46, 65, 66
 Bayantala Sag, China 32, 65, 68–71
 Beaverlodge, Canada 6, 202
 Bedre sector, Kyrgyzstan 269, 271, 273–276
 Beishan Range, China 35
 Belskoye, Russia 322
 Beltau ore field, Uzbekistan 270, 402, 403, 411, 434, 436–438
 Beltau-Kuramin volcanic-structure belt, Uzbekistan 30, 393, 437, 438, 446
 Benti (Bentou or Sanbaqi), China 35, 132–134, 139, 144, 145
 Bentou, China (see *Benti*)
 Benxi City, China 50
 Benxi Mine, China 47, 50, 51
 Berezovoye, Russia 335, 372
 Berkh, Mongolia 30, 285, 286, 303
 Bernardan, France 9
 Beshkak, Uzbekistan 402, 403, 405, 408, 425, 427, 428, 431
 Bezrechnoye, Russia 336
 Bezymyannoye, Kazakhstan 192, 193, 254, 258
 Bhalki-Kanyaluka, India 157, 164
 Bhatin, India 157, 161, 164
 Bhima Basin, India 30, 157, 171
 Bihar State, India (see *Jharkand*)
 Bingham, USA 19
 Binh Duong, Vietnam 449
 Bokan Mountain, USA 13
 Bokarda, India 172
 Bolotinskii, Mongolia 302
 Bolotny, Kazakhstan 212, 213
 Bonapsan, South Korea 391
 Borovskoye, Kazakhstan 192, 193, 218
 Bor-Undur, Mongolia 304, 306
 Botaburum Caldera, Kazakhstan 191–193, 254, 255, 259, 260
 Botaburum ore field, Kazakhstan 259
 Briketno/Zheltukhinskoye, Russia 322
 Brousse-Broquiès Basin, France 5
 Budenovskoye, Kazakhstan 192, 193, 228, 234, 239
 Bukantau, Uzbekistan (see *Uchkuuduk*)
 Bukhara-Karsha Basin, Uzbekistan 403
 Bukhara-Khivin Basin, Uzbekistan 403
 Bukinai North, Uzbekistan 402, 425, 427, 428
 Bukinai ore field, Uzbekistan 408, 425, 427, 428
 Bukinai South, Uzbekistan 402, 403, 425, 427, 428
 Bukintau Range, Uzbekistan 402
 Bulakag, Russia 389
 Bureinsky district, Russia 322, 386
 Bureinsky Massif, Russia 386
 Burlukskoye, Kazakhstan 192, 193, 205
 Burqin, China 35, 36, 43
 Burqin Basin, China 43
 Butugichag (Butygychagskoye), Russia 321, 322, 386, 390
 Butygychagskoye, Russia (see *Butugichag*)
 Bystroye, Russia 324, 327, 330
- C**
 Cao Bang Province, Vietnam 449
 Caotaobei (6722), China 117, 130–132
 Cathaysian (Huanan) fold system, China 120
 Cave Hills, USA 24
 Central Asian Mobile Belt 29
 Central Bohemian pluton, Czech Republic 9
 Central Chuily area, Kazakhstan 259
 Central Kyzylkum Uplift, Uzbekistan 249, 403
 Central Mongolian fold system, Mongolia 287, 304
 Central (or Nanling) granite-dominated U domain, China 87
 Central region, Mongolia 286
 Central Transbaykal subregion, Russia 322, 332, 362, 372
 Central Zhuguang batholith, China 95, 105
 Cernoye (Sernoye), Turkmenistan 397–399
 Chaglinskoye, Kazakhstan 192, 193, 195, 216
 Chaigan (279), China 130, 132
 Chaika, Russia 322, 390
 Chaling-Yongxing Basin, China 140, 141, 143, 144
 Changjiang, China 105, 107, 108
 Changjiang ore field, China 105, 107
 Chanpi (Chanziping), China 31, 95, 114, 132–134, 136, 139
 Chanziping, China (see *Chanpi*)
 Chaplinskoye, Russia 322, 390
 Charkasar, Kyrgyzstan 269, 271, 278
 Chasovoye, Russia 335, 367, 372
 Chatkal Mountains/Range, Kyrgyzstan-Uzbekistan 248–250, 271, 277, 278, 393, 401, 437, 438, 440, 446
 Chatkal-Kuramin Uplift, Tajikistan-Uzbekistan 248–250, 271, 393, 437, 438
 Chattanooga, USA 24, 25
 Chattisgarh Basin, India 30, 157, 172
 Chauli, Uzbekistan 271, 401, 437–441, 446
 Chelaomiao Basin, China 65
 Chelyabinsk, Russia 322, 323
 Chemindyn, Mongolia 303
 Chen Massif, China 36, 37, 43, 72–74, 78–84, 86, 88, 115–121, 127–130, 148, 150, 156
 Chengkou, China 105, 106, 108
 Chengkou ore field, China 106, 108
 Chengshan, China 79–82, 84
 Chengshan Massif, China 79
 Chengshan pluton, China 81
 Chengzishan (381), China 150, 151, 153, 154
 Chenjiashuang Massif, China 78, 79
 Chenxian-Hengyang region, China 141
 Cherepanoskoye, Russia 323
 Cherrapunji, India 170
Chienxian (mine), China 146
 Chikoisky-Yuzhno-Daursky ore field, Russia 372
 Chilavaripalle, India 170
 China, Peoples Republic vii, 3, 10, 11, 29ff
 Chistopol Basin, Kazakhstan 205
 Chistopolsky ore field, Kazakhstan 192, 193, 195, 199, 205
 Chita, Russia 322, 332, 356, 362, 363, 368, 372
 Chita Province, Russia 332
 Chitakhol, India 172
 Chkalovsk, Tajikistan 270, 393, 401, 438
 Choibalsan, Mongolia 285, 287, 293, 296, 299, 300, 303
 Choibalsan Basin, Mongolia 287
 Choir Basin, Mongolia 285, 304–307, 309
 Chongyi Mine, China 34, 122
 Chu (Tshu) Valley, Kyrgyzstan 7, 29, 30, 191–194, 228–245, 247–250, 255, 257, 270, 283
 Chudzand, Tajikistan (see *Khodzhent*)
 Chukotsky Peninsula, Russia 321
 Chukotsky region, Russia 30, 322, 390
 Chuluut region/area, Mongolia 286, 287
 Chung-Cheong-do Province, Korea 391

Chu-Sarysu Basin, Kazakhstan 7, 30, 191–194, 228, 231, 233–245, 247–250, 257
 Chuulun-Khuriete, Mongolia 288
 Cigar Lake, Canada 5
 Colorado Plateau, USA 8, 387, 447
 Cotaje, Bolivia 11
 Cottonwood Creek, USA 12
 Crystalnoye, Russia 335, 372
 Cuddapah Basin, India 30, 157, 170–172
 Cuddapah district, India 170

D

Da Hinggan Range, China 35, 46, 47, 59, 60
 Da Hinggan-Ergun zone, China 35
 Da Hinggan-Yanshan region, China 46, 47, 59
 Daba, Kazakhstan 192, 193, 254, 257, 259
 Dabao, China (see *Wangjiachong*)
 Dabu, China 31, 34, 90, 115
 Dachayuan (661), China 129
 Daladi (509), China 31, 34, 36, 40
 Daliang, China 115
 Dalmatovskoye, Russia 8, 191
 Dalnee, Russia 336
 Dalongshan (4360), China 79–84
 Dalongshan Massif, China 79–84
 Dalongshan pluton, China 79–84
 Damaofeng (331), China 99, 100
 Damaogou, Massif, China 78
 Danfeng, China 35, 76, 78, 79
 Danfeng-Shangnan area, China 78
 Danfeng-Zhuyangguan-Shangnan area, China 35, 76, 78, 79
 Daping, China (see *Daxing*)
 Dapujie, China (see *Wangjiachong*)
 Daqinggou, China 40
 Dashuzhuang, China 84
 Dasi Massif, China 148
 Date Creek Basin, USA 23
 Davaan, Mongolia 302
 Dawan (382), China 90, 114
 Daxin (Daxing) (373), China 34, 46, 59, 132–134, 146, 147
 Daxing (Daping), China 34, 46, 59, 133, 134
 Daxing-anling-Yanshan volcanic belt, China 34
 Daxing-anling Range, China 34, 46, 59, 133, 134, 146
 Daybreak Mine, USA 19
 Dazhai (301), China 154, 155
 Dazhou ore field, China (see *Xiaoqiuyuan*)
 Dazhou Basin, China 129
 Dazhou ore field, China 120, 122
 Dazhou-Furongshan, China 119
 Delger-Haan, Mongolia 303
 Delger-nuur, Mongolia 287
 Delhi Basin, India 157, 172
 Demirtepe-Cavdar, Turkey 395
 Dendang, Indonesia 176
 Dera Ghazi Khan district, Punjab 30, 313, 314, 318
 Dergachevskoye, Kazakhstan 205, 208
 Dianxi (Sandstone) U belt, China 148, 149
 Djekindek, Uzbekistan 271
 Djilindinskoye, Russia 359, 360
 Dobrovolnoye, Russia 323, 324, 326, 329
 Döhlen Basin, Germany 24
 Dolmatovo, Russia 326
 Dolmatovskoye, Russia 323, 324, 326–328
 Domiasiat, India 157, 164, 167–170
 Domiasiat-Gomaghat area, India 164
 Dong Nam Ben Giang, Vietnam 449
 Dong Pao, Vietnam 449
 Dongka (Dongkeng) (361), China 90, 105, 106, 108, 133, 136
 Dongkeng (361), China (see *Dongka*)

Dongsheng area, China 31, 47, 71–75
 Doos, Mongolia 302
 Dorno Gobi (Dornogovi), Mongolia 30, 285, 287, 304, 306, 308, 310
 Dornod (Mardai), Mongolia 29, 285–289, 291, 292, 294, 295, 302, 303
 Dornod (Mardai) volcanic-tectonic structure, Mongolia 10, 29, 285–296, 299–303, 308, 333, 334, 353, 363
 Dornod Aimag, Mongolia 287, 308
 Dornogovi (Dorno Gobi, Eastern Gobi) Aimag, Mongolia 30, 285, 287, 304, 306, 308, 310
 Dorozhnoye, Mongolia 302
 Dorozhny, Kazakhstan 212, 213
 Druzhnoye, Russia 373–375, 381, 383, 388
 Druzhnoye-Mineyevsky, Russia 373
 Dubrovskoye, Kazakhstan 192, 193, 195, 205
 Durbulja, Mongolia 308, 309
 Dybryn, Russia 359, 360
 Dzhanantuar, Uzbekistan 402, 435–437
 Dzheekamae, Uzbekistan 438
 Dzhekindek, Uzbekistan 438, 440, 443, 446
 Dzhideli, Kazakhstan 192, 193, 254, 255, 257, 258
 Dzhideli ore field, Kazakhstan 257
 Dzhigda, Russia 322
 Dzhihsikoye (Tuyuk-Suu), Kyrgyzstan 282, 283
 Dzhirgashal, Tajikistan 393
 Dzhitym (Dzitym), Uzbekistan 436
 Dzhusandalinskoye, Kazakhstan 192, 193, 254, 255, 260
 Dzitym, Uzbekistan (see *Dzhitym*)

E

Eagle Hill, Pakistan 318
 Eagle Point, Canada 5
 East Khasi Hill, India 164, 165, 169
 East Liaoning block, China 46
 East Liaoning Massif, China 46
 East Tastykolskoye, Kazakhstan 217, 218
 East Xinqiao (332), China 99, 100
 Eastern A & B areas, Syria 451, 452
 Eastern Gobi Basin, Mongolia 286, 287, 304
 Eastern Gobi region, Mongolia 286, 287, 304
 Eastern Qinling, China 76
 Ebisu, Japan 188
 Echeonri, South Korea 391
 Ecinlitas, Turkey 395
 Efta, Indonesia 176
 Eko, Indonesia 175, 176
 Eko-Remaja area, Indonesia 176
 Elkon (district), Russia 29, 372–385
 Elkon Horst, Russia 373, 383
 Elkon Plateau, Russia 373, 383
 Elliot Lake, Canada 16, 17
 Emkerse, Russia 359, 362
 Engershand (area), Mongolia 286, 287, 302, 303
 Engershand volcanic-tectonic structure, Mongolia 303
 Erdos Basin, China 72
 Eren (Erlian) Basin, China 33, 34, 46, 47, 65–71
 Eren-Hailar subdomain, China 46
 Erennaoer Depression, China 66–68
 Ergun fold system, China 35, 46
 Ergun-Da Hinggan-Yanshan subdomain, China 46
 Erlian Basin, China (see *Eren*)
 Erzgebirge, Germany-Czech Republic 9, 10

F

Fakili, Turkey 395
 Fakili Güre Basin, Turkey 395
 Fanay, France 9
 Far East region, Russia 30, 322, 386
 Farkak, Tajikistan 393

Fedorovsk zone, Russia 384, 385
 Fengcheng Complex, China 48–51
 Fenix, Russia 386
 Fergana, Uzbekistan 29, 269, 277, 278, 283, 321, 322, 437, 438, 447
 Fergana Basin, Uzbekistan 321, 438
 Fergana Valley/region, Kyrgyzstan 269, 278, 283, 437
 Fevral'skoye, Kazakhstan 192, 193, 195, 209, 213
 Flodelle Creek, USA 18
 Forstau, Austria 25
 Franceville Basin, Gabon 9
 Freital-Gittersee, Germany 24
 Front Range, USA 14
 Fujian (Fujiang) Province, China 11, 115, 129–132
 Fukazawa, Japan 183
 Fuxi Complex, China 107
 Fuzhou ore field, China (see *Xiangshan*)

G

Gachin salt plug, Iran 177, 178
 Gadankipalle, India 170
 Gangou, China 59–61
 Gangou Basin, China 59–61
 Gangue deposit, China 60
 Gan-Hang volcanic-tectonic belt, China 10, 34, 86, 88, 89, 115–124, 127–130
 Gansu Province, China 35, 75, 76
 Ganzhou Basin, China 147
 Gaoligang Uplift, China 148
 Gaoligong Basin/region, China 148–151, 153
 Gaoxi (326), China 109, 111
 Garo Hills, India 164, 169
 Gaur, Russia 363
 Gawler Craton, Australia 16
 Gejiazhai (382), China 150–153
 Gera-Ronneburg, Germany 21
 Geumsan, South Korea 391
 Ghadir el Hamel region, Syria 451
 Ghat domain, India 166
 Ghateshwar, India 172
 Gifu Prefecture, Japan 181, 183
 Gissar Range, Tajikistan 393
 Glubbinnoye, Kazakhstan 192, 193, 195, 216, 217
 Glubninny (sector), Russia 347, 350, 351
 Glukhariny, Kazakhstan 212, 213
 Gobi Altai Mountains, Mongolia 308
 Gobi Desert, China 29, 46, 65, 285
 Gobi-Tamtsag U province, Mongolia 285
 Goesan, South Korea 391
 Gogi, India 171, 172
 Golub, Russia 347, 352
 Gomaghat, India 164, 167
 Gongchangling, China 48–50
 Gongju-Ooseong, South Korea 391
 Gornoye, Russia 335, 372
 Grachevskoye, Kazakhstan 191–193, 195, 199, 200, 202, 209–211
 Grachevsky ore field, Kazakhstan 192, 193, 195, 200, 209
 Granitnoye ore field, Kazakhstan 255, 260
 Granitnoye region, Kazakhstan 270
 Grants Uranium Region, USA 8, 9
 Greenbushes, Australia 19
 Guangdong Province, China 31, 33, 86, 89, 99, 105, 115, 130, 132
 Guangshigou, China 78, 79
 Guangxi A.R., China 31, 35, 86–89, 98, 99, 114, 115, 132, 136, 139, 146–149
 Guangxi-Hunan-Jiangxi carbonate U subdomain, China 86, 87, 139
 Guangxi-Hunan-Jiangxi U region, China 139
 Guangzitian, China 114
 Guidong Massif, China 96, 99, 100
 Gujjara State, India 158
 Guixi (65), China 126, 129

Guizhou Province, China 35, 86, 146
 Gulbarga district, India 171
 Guntur district, India 170
 Gurvanbulag, Mongolia 285, 287–290, 296–299, 302
 Gurvansaikhan Basin, Mongolia 285, 286
 Guyuan (460), China 61
 Guyuan area, China 61, 63, 64
 Guyuan-Duolun area, China 59, 60
 Guyuan-Duolun volcanic belt, China 46
 Gyeonggi (Kyonggi) Massif, South Korea 391

H

Hack Canyon, USA 15
 Hailar Basin, China 46, 47
 Hami Basin, China 31, 36, 40, 41
 Hebei Province, China 33, 59, 61
 Hecaokeng, China 130
 Henan Province, China 75
 Hengfeng, China 119
 Hengjian (611), China 122, 123, 125
 Hengyang Basin, China 147
 Henxi, China 119
 Heyuan Basin, China 95
 Highland Mine, USA 7
 Himachal Pradesh State, India 158
 Himalayan foothills, Pakistan 313
 Hinggan fold system, China 46, 59
 Hireiwa, Japan 183
 Hoang Lien Son Province, Vietnam 449
 Hongor, Mongolia 304
 Hongshiquan, China 75, 76
 Hooloi, Mongolia 302
 Hope (Xiwang, 330), China 31, 99, 100, 105
 Hor Harar, Israel 451
 Huanan fold system, China (see *Cathaysian*)
 Huanfengling (325), China 109
 Huanfengling-Gaoxi, China 110
 Huangao, China 109, 111–113
 Huangcai (Huangcu), China 133, 136, 138
 Huangcu, China (see *Huangcai*)
 Huanglongmiao Massif, China 78
 Huangmeijian Massif, China 79–84
 Hubbulag, Mongolia 288
 Huhe, China 65, 66, 68–71
 Huichang Basin, China 132
 Huichi Massif, China 78
 Hunan Province, China 31, 34, 114, 139, 140, 144, 147

I

Iberian Meseta, Spain-Portugal 10
 Idaho, USA 23
 Idupulapaya, India 171
 Ikh-bulag, Mongolia 303
 Ikh-Khet, Mongolia 304
 Illimaussaq, Greenland 19
 Ily Basin, Kazakhstan 29, 36, 191–193, 260, 264, 265, 270
 Ily region, Kazakhstan 30, 260, 261
 Ima (Imskoye), Russia 335, 362, 363, 368–372
 Imskoye, Russia (see *Ima*)
 India 29–30, 157ff, 313
 Indonesia 29–30, 175–176
 Indus Valley, Pakistan 313
 Ingin, Mongolia 309–311
 Ingur area, Russia 362
 Inkay, Kazakhstan 7, 192–194, 228, 232, 234, 237–241
 Inner Mongolia A.R., China 35, 46, 59, 60, 65, 66
 Inner Mongolian-Yanshan Uplift, China 46
 Interesnaya zone, Russia 376, 384

- Iran, Islamic Republic 29–30, 177ff
Iraq 30, 451
Irkol ore field, Kazakhstan 250, 253
Irtys Basin, Kazakhstan 220, 221
Ishimskoye, Kazakhstan 191–193, 195, 199, 200, 202, 203
Ishimsky ore field, Kazakhstan 192, 193, 195, 202
Iskra, Russia 388
Israel 30, 451
Issa Khel, Pakistan 313
Istochnoye, Russia 359, 360
Iwamura Basin, Japan 183
Iwate Prefecture, Japan 181, 189
- J**
- Jabiluka, Australia 6
Jáchymov, Czech Republic 10
Jaduguda, India 157, 159, 161–164
Jaijigri, South Korea 391
Jaintia Hills, India 164, 165
Jammu State, India 158
Janchivlan Massif, Mongolia 286, 287
Japan 29, 30, 181–183, 188, 189
Jharkand (formerly Bihar) State, India 157, 158, 162
Jianchang, China 33, 34, 59
Jianchang Basin, China 33, 34, 59
Jiangnan Uplift, China 86–89, 91, 114, 115, 132, 133, 135
Jiangxi granite belt, China 95
Jiangxi Province, China 34, 35, 88, 109, 112, 120, 122, 125, 126, 129, 132, 148
Jiaoping (362), China 106, 107
Jilantai Basin, China 46
Jiling, China 75, 76
Jingan (Shiwandashan?) Basin, China 34, 147, 148
Jinjiling batholith, China 99
Jinjiling Massif, China 91, 95, 98, 99, 114
Jinyinza, China 132, 133
Jiuwandaishan-Xuefeng area, China 136
Jiuyishan batholith, China 96, 114
Jiuyishan Massif, China 114
Jiuyishan-Jinjiling Massif, China 90
Jordan 30, 451
Jorinji, Japan 183
Jumbang, Indonesia 176
Junggar Basin, China 34, 36, 40
Junggar-Tien Shan U province, China 30, 35, 36
Jungwonsan, South Korea 391
- K**
- Kadzhi-Say, Kyrgyzstan 283
Kagoshima Prefecture, Japan 181, 188
Kaha Nalo, Pakistan 313
Kalan Basin, Indonesia 175
Kalan district, Indonesia 30, 175, 176
Kalanga, Russia 363
Kalkan, Kazakhstan 192, 193, 261, 264, 266
Kallar Kahar, Pakistan 313, 320
Kamaroy, Tajikistan 393
Kamenushinskoye, Russia 386
Kamyshevoye, Kazakhstan 191, 193, 195, 199, 200, 203, 204
Kangil Depression, Russia 363
Kani Basin, Japan 183
Kannokura, Japan 183, 187
Kanzhugan, Kazakhstan 192–194, 228, 231, 232, 234, 241–246, 248, 249
Kaplankyr-Tauryuk Dome, Turkmenistan (see *Taurkyr*)
Kara Balta, Kazakhstan 191, 193, 255, 269, 270, 283
Karabash Caldera, Uzbekistan 439–441
Karagiin ore field, Kazakhstan 23, 192, 193, 224–226
Karaktau district, Kazakhstan 248, 250, 253
Karakum Desert, Turkmenistan 397
Karamazar region, Kyrgyzstan-Tajikistan-Uzbekistan 21, 30, 257, 269–272, 277, 393, 401, 437, 439–444, 446
Karamurun district, Kazakhstan 248, 250
Karamurun-Kharasan ore field, Kazakhstan 250–252
Karategin, Tajikistan 393
Karetegin Range, Tajikistan 393
Karnataka State, India 171
Karunuk-Sehwan, Pakistan 320
Kasar, Turkey 395
Kashi Depression, China 34, 43
Kashka-Suu, Kyrgyzstan 282
Kashmir, India-Pakistan 158, 313
Kassan-Varzykskoye ore field, Kyrgyzstan 278
Katanga Copper Belt, Congo, Democratic Republic 14
Kattasay, Uzbekistan 271, 401, 438–440, 443, 445, 446
Katumskoye, Russia 390
Kavly, Russia 322
Kazakhat, Uzbekistan 438
Kazakhstan ix, 7, 23, 29–30, 36, 43, 191ff, 269, 270, 321, 323, 324, 397, 403
Kedrovoye, Russia 324
Keef, Russia 390
Keektal, Tajikistan 393
Kendyktas area, Kazakhstan 260
Kendyktas-Chuily-Betpak Dala (Pribalkash) region, Kazakhstan 191, 233, 254, 260
Kendyktyube, Uzbekistan 402, 410, 411
Kenimekh Basin, Uzbekistan 425
Kenimekh North, Uzbekistan 402, 405, 425
Kenimekh South, Uzbekistan 425
Kenimekh-Bukinai South ore field, Uzbekistan 425
Kenzan, Japan 188
Kenze-Budenovskaya district, Kazakhstan 228, 234
Kerala State, India 157, 158
Keruvadungri, India 157, 164
Ketanda, Russia 389
Ketmenchi, Uzbekistan 401–403, 405, 408, 429, 432, 433
Key Lake, Canada 5
Khabarovsk, Russia 322, 386
Khadandungri, India 157, 164
Khadandungri-Purandungri, India 157, 164
Khairkan Basin, Mongolia (see *Khairkhan*)
Khairkhan (Khairkan) Basin, Mongolia 285, 286
Khakarin Complex, Russia 387
Khalchin, Mongolia 302
Khanaka, Tajikistan 393
Khangai region, Mongolia 287
Khankaisky district, Russia 322, 386
Kharaat, Mongolia 285, 304–309
Kharasan, Kazakhstan 192, 193, 250, 252, 253
Khara-Tolgoi, Mongolia 304
Khashaat, Mongolia 287
Khasi batholith, India 168
Khavtgai, Mongolia 303
Khe Hoa-Khe Cao, Vietnam 449
Khentei Aimag, Mongolia 303
Khentei-Daur metallogenetic province, Mongolia 285–287
Khentei-Daur U province, Mongolia 287
Khiagda (Khiagdinskoye), Russia 8, 321, 356, 359–361
Khiagda (Vitim, Vitimsky) ore field/district, Russia 8, 30, 321, 322, 332, 356, 357, 360–362
Khiagdinskoye, Russia (see *Khiagda*)
Khiloksky ore field/area, Russia 335, 372
Khisor Range, Pakistan 318
Khodzhaakmet (Khodzhyakhmet), Uzbekistan 402, 436
Khodzhent (Khudzhand, Chudzand), Tajikistan 269, 270, 322, 393, 401, 437, 438
Khodzhyakhmet, Uzbekistan (see *Khodzhaakmet*)
Khokhlovskoye, Russia 323, 326
Kholoi area, Russia 362

- Kholoisky ore field, Russia 335
 Kholovskoye, Russia 324
 Khooloy, Mongolia 288
 Khoshoumi, Iran 177
 Khudzhand, Tajikistan (see *Khodzhent*)
 Kichgine, Uzbekistan 444
 Kirovograd, Ukraine 12
 Kirthar Range, Pakistan 313, 320
 Kisir-Osmankuy, Turkey 395
 Kneifiss (Kneifes) area, Syria 451, 452
 Koçarli area, Turkey 395
 Koçarli Basin, Turkey 395
 Koitass, Kazakhstan 191–193, 266
 Kokchetav Basin, Kazakhstan (see *Kokshetau Basin*)
 Kokchetav Massif, Kazakhstan (see *Kokshetau Massif*)
 Kokchetav region, Kazakhstan (see *Kokshetau region*)
 Koksengirsky ore field, Kazakhstan (see *Zaozernoye*)
 Kokshetau (Kokchetav) Basin, Kazakhstan 194, 216, 218
 Kokshetau (Kokchetav) Massif, Kazakhstan 191, 194, 195, 216, 220, 221, 224
 Kokshetau (Kokchetav) region, Kazakhstan 29, 30, 191–196, 199–202, 204–206, 208, 209, 211–213, 216–218, 220, 222, 224, 270
 Koksorskoye, Kazakhstan 192, 193, 217, 218
 Koksorskoye South, Kazakhstan 192, 193, 218
 Koldzhat, Kazakhstan 191–193, 261, 264, 265
 Kolichikan, Russia 359, 360
 Kolnami, South Korea 391
 Konkulaakh, Russia 384
 Kopalysay (Kopalysayskoye), Kazakhstan 192, 193, 254, 255, 260
 Kopalysayskoye, Kazakhstan (see *Kopalysay*)
 Koppunuru, India 170
 Köprübasi Basin, Turkey 395
 Köprübasi-Salihli area, Turkey 395
 Korba district, India 172
 Koretkoide, Russia 359, 360
 Koretkondinskoye, Russia 360
 Kormsomolsk, Russia 363
 Korolevo-Chasovo ore field, Russia 335, 372
 Korolevskoye, Russia 335, 372
 Kosachinoye, Kazakhstan 192, 193, 195, 199, 200, 202, 203, 209, 212, 213
 Kostcheka, Uzbekistan 402, 436, 437
 Kostobe, Kazakhstan 192, 193, 254, 257–259
 Kotla, Russia 388
 Kovalev, Mongolia 303
 Krasnokamensk, Russia 285, 288, 321, 332, 333, 343, 354
 Krasnoyarsk, Russia 326
 Krasny Kamen, Russia 332, 336
 Kremnistoye, Russia 322
 Krivoy Rog Basin, Ukraine 13
 Kuangji (Kuangshanjiao), China 95, 114, 133, 134
 Kuangshanjiao, China (see *Kuangji*)
 Kuanshan area, China (see *Kunshan*)
 Kubul Khel, Pakistan (see *Qabul Khel*)
 Küçükçavdar, Turkey 395
 Küçükkuuyu, Turkey 396
 Kuidusun Basin, Russia 388, 389
 Kuidusun volcanic depression, Russia 386–389
 Kujiertai (Kujieertai) (512), China 36
 Kuka, Russia 363
 Kularinta, Russia 359, 362
 Kumhamahar, India 172
 Kunshan (8411), China 79–84
 Kunshan (Kuanshan) area, China 79, 81, 83
 Kuramin Range, Tajikistan 248, 393, 437, 446
 Kuray, Kazakhstan 192, 193, 267
 Kurday, Kazakhstan 191–193, 254–256, 260
 Kurgan area, Russia 323, 326
 Kurmanchite, Kazakhstan 192, 193, 254, 259
 Kurokawa, Japan 188
 Kuroko, Japan 181, 189
 Kurung, Russia 373, 383
 Kutuzovskiy, Kazakhstan 212, 213
 Kvanefeld, Greenland 19
 Kyishu island, Japan 181, 188
 Kyonggi Massif, South Korea 391
 Kyrgyzstan 18, 21, 29–30, 191, 193, 248, 250, 254, 255, 259, 269ff, 321, 393, 401, 437
 Kyzyl, Kazakhstan 192, 193, 250, 253, 267, 283
 Kyzyl-Dhzar, Kyrgyzstan 283
 Kyzylkol-Chayan district, Kazakhstan 248, 250, 253, 254
 Kyzylkum Basin, Uzbekistan 29, 270, 401, 403, 404, 406–410, 414, 434
 Kyzylkum basement area 402, 437
 Kyzylkum Desert, Uzbekistan 401
 Kyzylkum region, Uzbekistan 30, 393, 401, 403, 408, 418, 434
 Kyzylkum Uplift, Uzbekistan 29, 403, 405
 Kyzylkumskaya Mine, Uzbekistan 413
 Kyzylsay ore field, Kazakhstan 259
 Kyzyltas, Kazakhstan 191–193, 254, 259
- L**
 L'Écarpière, France 9
 La Crouzille, France 9
 La Marche, France 9
 Labrador, Canada 10
 Labyshkoye, Russia 324, 328, 330, 331, 333
 Lai Chau Province, Vietnam 449
 Lake Maitland, Australia 18
 Lambapur, India 157, 170, 172
 Lambapur outlier, India 172
 Lambapur-Peddagattu, India 157
 Lancang Uplift, China 149
 Land Pebble district, USA 23
 Lanhe (201), China 90, 96, 105–108
 Lantian, China 34, 76, 77, 79
 Lantian Mine, China 79
 Laowulong (Yaxi), China 133, 136, 138
 Larma (510), China 35, 85, 86
 Lastochka, Russia 386
 Le Roube, France 4, 5
 Lean-Dongxiang, China 119
 Legaevskii Massif, Kazakhstan 209
 Leigongdian (663), China 129
 Lemajung, Indonesia 175
 Leninabad, Tajikistan 269, 278, 393, 401, 437, 438
 Les Sagnes, France 9
 Liadong Block, China 47
 Lianghe Basin, China 150, 153
 Lianshanguan (3075), China 34, 35, 46–54
 Lianshanguan Dome, China 34, 35, 47, 50–52
 Lianshanguan-Gongchangling area, China 48
 Liaohe Basin, China 30, 35, 46, 48–52, 54
 Liaoning Basin, China 33, 35, 46–51, 54, 59
 Liaoning Province, China 33, 35, 47, 50, 51, 59
 Liaoning U region, China 46, 47
 Lincang Basin, China 151, 154, 155
 Lincang region, China 148, 153, 154
 Lingtou, China 59–61
 Lipovskoye, Russia 386
 Little Mountains, USA 18
 Liuchen batholith, China 91
 Liuchen Massif, China 89, 91, 95, 115
 Liujiaao, China 81
 Longchuan Basin, China (see *Longchuanjiang*)
 Longchuanjiang (Longchuan) Basin, China 149–154
 Longhuashan batholith, China 105
 Longhuashan Complex, China 108
 Longhuashan ore field/zone, China 106

- Longshoushan fold belt, China 75
 Lower Liaohe Basin, China 46
 Luchistoye, Russia 333, 336
 Lugur, Tajikistan 393
 Lujing (322), China 75, 105, 109–111, 113, 139
 Lujing batholith, China 109
 Lujing ore field, China 105, 109, 111, 113, 139
 Lulitang, China 147
 Luojungou (512), China 85, 86
 Luxi Basin, China 100, 101
 Luxi pluton, China 101
 Lyavlyakan, Uzbekistan 401–403, 405, 408, 424, 425, 428, 429, 431
 Lyubotinsky, Kazakhstan 212, 213
- M**
- Ma'andu (Mada), China 115, 133
 Maberri area, Syria (see *Al Haberi*)
 Mabugang Basin, China 147
 Machizai, China 133
 Mactesh Qatan, Israel (see *Maktesh*)
 Mada, China (see *Ma'andu*)
 Madawaska, Canada 19
 Madhya Pradesh State, India 157, 158, 172
 Magadan, Russia 322, 386, 390
 Magadan territory/district, Russia 386
 Maharashtra State, India 158
 Maili-Sai, Kyrgyzstan (see *Maylisay*)
 Mailisu, Kyrgyzstan (see *Mailuu-Suu*)
 Mailuu-Suu (Mailisu), Kyrgyzstan 21, 269, 271, 275, 401
 Maizak North, Uzbekistan 402, 429, 432
 Maktesh (Mactesh) Qatan, Israel 451
 Malai Sary, Kazakhstan 266
 Malaya Amalat Depression, Russia 368
 Malinovskoye (area), Russia 324, 327, 330–332
 Malo Tulukuyevskoye, Russia 336
 Malyi Amalat area, Russia 368
 Mangheite, China 65, 66, 68–71
 Mangyshlak Peninsula, Kazakhstan 23, 224
 Mangyshlak U region, Kazakhstan (see *Pricaspian*)
 Manybayskoye, Kazakhstan 191–193, 199, 218–220
 Manybaysky ore field, Kazakhstan 192, 193, 195, 218
 Manzhouli volcanic-tectonic area, China 34, 334
 Maoershan batholith, China 91, 98, 158, 335
 Maoershan-Yuechengling Massif, China 114, 137
 Maoyantou (Maoyantou) (570), China 11, 117, 130, 131
 Maoyantou (570), China (see *Maoyantou*)
 Maraghzar area, Pakistan 320
 Mardai, Mongolia (see *Dornod*)
 Mardai volcanic-tectonic structure, Mongolia (see *Dornod volcanic-tectonic structure*)
 Mardaingol, Mongolia 285, 287–290, 299, 302
 Margaritas, Mexico 12
 Martovskoye, Russia 333, 336
 Mary Kathleen, Australia 25
 Massif Central, France 4, 5, 9
 Mawkyrwat, India 164, 170
 Mawsynram, India 170
 Mayak, Russia 335, 367
 Maylikatan, Uzbekistan 271, 401, 438, 446
 Maylisay (Maili-Sai), Kyrgyzstan 269, 271, 278
 Mayluu-Suu, Kyrgyzstan 269, 271–276
 McDermitt, USA 10, 11
 McMullen County, USA 7
 Mediterranean phosphorite belt 30, 451
 Meghalaya Plateau, India 30, 157, 164–166, 169
 Meghalaya State, India 157, 164
 Meilysai (Meylisai), Uzbekistan 402, 410, 411
 Melovoye, Kazakhstan 23, 191–193, 224–228
 Menderes Massif, Turkey 30, 395
 Mengqiguer (510), China 31, 34, 36, 40
 Mengtuo Basin, China 153, 154
 Mengwang Basin, China 153–155
 Mensensky ore field/area, Russia 335, 372
 Meridionalnoye, Russia 335, 363, 372
 Meylisai, Uzbekistan (see *Meilysai*)
 Mezhozernoye, Kazakhstan 192, 193, 217, 218
 Mianhuakeng (305), China 105
 Mianwali district, Pakistan 313
 Michelin, Canada 10
 Michurinskoye, Russia 12
 Middle-Gobi region, Mongolia 286
 Mikouloungou, Gabon 9
 Min-Kush, Kyrgyzstan (see *Turakavak*)
 Minussinsk, Russia 322, 328, 330
 Minussinsk Basin/Depression, Russia 328, 330
 Misano, Japan 183
 Misasa Basin, Japan 187, 188
 Mishor Rotem, Israel 451
 Miso, Mongolia (see *Mys*)
 Mitoya, Japan 188
 Miyoshi, Japan 181, 188
 Mizunami Basin, Japan 184
 Mogochinsky area, Russia (see *Olov*)
 Moinajharia, India 157, 164
 Molodezhnoye, Kazakhstan 192, 193, 195, 196, 205, 386
 Mongolia 10, 29–31, 33–35, 46, 59, 61, 71, 285ff, 321, 333, 334, 353, 363
 Mongol-Priargun (Argun) metallogenetic province, Mongolia 285–287, 303, 334
 Mongol-Priargun (Argun) volcanic belt, Mongolia-Russia 287, 353
 Mongol-Transbaykal fold belt, Mongolia-Russia 287
 Monument Valley, USA 8
 Moonlight, USA 11
 Mosaboni, India 157, 164
 Moscovskoye, Tajikistan 393
 Motianling batholith, China 115
 Motianling Massif, China 86, 88, 89, 96, 98, 114, 115, 136
 Motianling ore field, China 86, 88, 89, 96, 98, 114, 115, 136
 Motochudag Complex, Mongolia 293, 301
 Moynkum, Kazakhstan 192–194, 228, 232, 241, 243–247
 Mramornaya zone, Russia 386
 Mufu Shan area, China 136, 137
 Muhar, Mongolia 288, 302
 Mulachen, Russia 388
 Mumin, Tajikistan 393
 Muong Hum, Vietnam 449
 Mynkuduk, Kazakhstan 192–194, 228, 231, 232, 234–241, 243
 Mys (Miso), Mongolia 309–311
- N**
- Nadezhda zone, Russia 384
 Nadezhda-Interesnaya zone, Russia 379
 Nagornoye, Uzbekistan 402, 429, 434
 Nahal Zin, Israel 451
 Nairin, Mongolia 302
 Nakatsugo, Japan 183, 187–189
 Nalgonda district, India 157, 170
 Nam Xe, Vietnam 449
 Namaru, Russia 359, 360
 Nangar Nai, Pakistan 313, 318
 Nanhua mobile zone, China 89, 115
 Nanling granite belt, China 98, 99
 Nanling granite-dominated U domain, China 87
 Nanling metallogenetic zone, China 31, 34, 86–89, 98, 99, 105, 114, 115, 129, 132, 148
 Nanling tectonic-magmatic belt/zone, China 88, 98, 99, 132
 Nanxiong Basin, China 107

Naomugen (110), China 65, 68
 Narigan, Iran 177
 Nars, Mongolia 287, 308–311
 Nars 2, Mongolia 308
 Narwahaapar, India 164
 Naryn Basin, Kyrgyzstan 270, 282
 Navoi, Uzbekistan 270, 322, 401, 403, 410, 413, 425, 432
 Negev Desert, Israel 30, 451
 Nemer, Mongolia 285, 287, 289, 290, 300, 301
 Neprokhodimoye, Russia 373, 383
 Nevskoye, Russia 359, 360
 Ningan Basin, China 46
 Ningdu Basin, China 147
 Ningxia Huizo A.R., China 84
 Ningyo-Toge Mine, Japan 30, 181, 183, 187–189
 Ningyo-Toge ore field, Japan 30, 183, 187–189
 Nisa, Portugal 10
 Niutoushan, China 123, 125, 126
 Niuweiling (324), China 109
 Nizhne Ilyskoye, Kazakhstan 192, 193, 261, 263, 265
 Nizhny-Ily Subbasin, Kazakhstan 261, 263, 265
 Nodatamagawa, Japan 181, 189
 Nong Son, Vietnam 30, 449, 450
 Nong Son Basin, Vietnam 30, 449
 Nongmalang, India 164, 169
 Nopal, Mexico 10, 11
 North China Massif, China 46–48, 75, 76
 North Choibalsan region, Mongolia 30, 285–289, 302, 303
 North Gaur, Russia 363
 North Huanglongmiao Massif, China 78
 North Kerulen tectonic zone, Mongolia 303
 North Kherlen Uplift, Mongolia 287
 North Mongolian fold belt, Mongolia 287
 North Qilian fold belt, China 35, 84
 North Qinling U zone, China 76, 79
 North Tien Shan, China 44, 194
 North Tien Shan fold belt, Kazakhstan 194
 Northeast Asian Plate, China 46
 Northern Betpak Dala area, Kazakhstan 257
 Northern Kyzylkum Basin, Uzbekistan 403
 Northern Mongolian U province, Mongolia 285
 Northwest Frontier Province, Pakistan 320
 Novoalexandrovskoye (Novoaleksandrovskoye), Russia 327, 331, 332
 Novodgodny, Turkmenistan 397
 Novogodneye, Russia 333, 336
 Novosibirsk, Russia 322, 326, 327
 Novosibirsk-Kemerov area, Russia 326
 Novoye, Uzbekistan 436
 Novyi Olov, Russia 363
 Nuheting, China 34, 46, 65–68
 Nujiang Basin, China 148
 Nurabad (Zirabulak-Ziatdin) district, Uzbekistan 270, 401–403, 429, 433, 435
 Nurantinsky district, Uzbekistan (see *Zafarabad*)
 Nuratau Range, Uzbekistan 403, 425
 Nyut volcanic-tectonic depression, Russia 389
 Nyut-Ulbei batholith, Russia 389

O

Obara, Japan 183
 Octyabrskoye, Russia 332, 339
 Ogamo, Japan 189
 Ogcheon area, South Korea (see *Okchon*)
 Ogcheon fold belt, South Korea 391
 Oguni, Japan 181, 188
 Okayama Prefecture, Japan 181
 Okchon (Okch'on, Ogcheon) area, South Korea 30, 391
 Okhotsk, Russia 30, 322, 362, 386–390
 Okhotsk Complex, Russia 387

Okhotsk Massif, Russia 387–389
 Okhotsk region, Russia 30, 322, 386
 Okhotsk-Chukotka volcanic belt, Russia 387
 Okoshiri (Okujiri), Japan 188
 Oktyabrskaya Mine, Uzbekistan 413
 Oktyabrskoye, Russia 336
 Okujiri, Japan (see *Okoshiri*)
 Okutango, Japan 181, 183, 188
 Olekan, Russia 363
 Olenty-Seletinsk area, Kazakhstan 220
 Olginskoye, Kazakhstan 192, 193, 195, 205, 206, 208
 Olov (Olovsky, Olovskoye, Mogochinsky), Russia 335, 362–368
 Olov Depression, Russia 365
 Olov ore field, Russia 335, 363, 367
 Olovo-Mogocha area, Russia 335
 Olovskoye, Russia (see *Olov*)
 Olovsky, Russia (see *Olov*)
 Olympic Dam, Australia 15, 16
 Onbara, Japan 187
 Ongiingol Basin, Mongolia (see *Undurshil*)
 Onjeong, South Korea 391
 Ordos Basin, China 29, 31, 34, 47, 71–73
 Orissa State, India 158
 Oron, Israel 451
 Osenneye, Russia 386
 Osh Province, Kyrgyzstan 18, 269, 278
 Oshiin-nuur Basin, Mongolia 285, 286
 Ozeroye, Russia 362, 363

P

Pa Lua, Vietnam 449
 Pa Rong, Vietnam 449
 Pakistan 29–30, 179, 313ff
 Panfilovskoye, Kazakhstan 192, 193, 266
 Papsk region, Uzbekistan 438, 447
 Paridan, Tajikistan 393
 Pdengshakap-Tarangblang, India 170
 Peddagattu, India 157, 170
 Peña Blanca (Sierra de), Mexico 10–12
 Pestraya Massif, Russia 389
 Phalaborwa, South Africa 19, 26
 Phlangdiloin, India 164, 170
 Phosphoria region/Montana, USA 23
 Piaoichi Massif, China 78
 Pjatigorsk, Kazakhstan 191–193, 266
 Plateau domain, India 164, 166–168
 Příbram, Czech Republic 9
 Pologaya, Russia 376, 384
 Potwar Plateau, Pakistan 313
 Powder River Basin, USA 7
 Pribalkash region, Kazakhstan (see *Kendyktas-Chuily-Betpak Dala*)
 Pricaspian (Mangyshlak) region, Kazakhstan 23, 30, 191–194, 224–227, 270, 397
 Prigorodnoye, Russia 324, 327, 330
 Primorskoye, Russia 324, 328, 330, 333, 334
 Promeshutochnoye, Kazakhstan 192, 193, 195, 205–207
 Pryor Mountains, USA 280
 Pukuitang (Puquitang), China 31, 89, 147
 Punjab Province, Pakistan 313
 Puquitang, China (see *Pukuitang*)
 Purandungri, India 157, 164
 Pyatiletneye, Russia 336

Q

Qabul Khel (Qubul, Kubul Khel), Pakistan 313, 314, 318, 319
 Qaidam Basin, China 34, 75
 Qiaozhuang area, China 79
 Qiaozhuang, China 79, 84

Qilian, China 30, 35, 75, 79, 84, 85
 Qilian-Qinling U province, China 75, 79, 85
 Qinghai Province, China 33, 34
 Qinglong Basin, China 30, 33, 34, 46, 59–61
 Qinglong ore field/area, China 30, 34, 59–61
 Qinling Massif, China 30, 75, 76, 79, 84, 85
 Qinling, China 30, 75, 76, 79, 84, 85
 Quang Nam Province, Vietnam 449
 Qubul, Pakistan (see *Qabul Khel*)
 Quirke Lake, Canada 17

R

Rachakuntapalle, India 170, 171
 Radinskoye, Russia 362
 Radium Hill, Kyrgyzstan 280
 Raduzhnoye, Russia 388
 Rafikon, Tajikistan 393
 Rajanpur, Pakistan 313
 Rajasthan State, India 157, 158, 172
 Rakha, India 157, 164
 Rakhi Munh, Pakistan 313
 Rakovskoye, Russia 386
 Rakuchur, Pakistan 313
 Rangjadong, India 164, 170
 Ranstad, Sweden 24, 25
 Rehman Dhora, Pakistan 320
 Remaja, Indonesia 175
 Rencha (Renchai) Basin, China 132
 Renkhol, India 172
 Rhodes Ranch, USA 7
 Rirang River area, Indonesia 175, 176
 Rizak (Rezak), Uzbekistan 401, 438, 446
 Rodionovskoye, Russia 359
 Rohil (Rohili), India 172
 Rongcheng Plateau, India 164, 169
 Rongdinala, India 164, 169
 Ronneburg, Germany 20
 Ross Adams, USA 13
 Rössing, Namibia 19
 Rožná, Czech Republic 14, 15
 Rudnoye, Uzbekistan 402, 436, 437
 Ruoergai district, China 85
 Ruseifa, Jordan 451
 Russia/Russian Federation ix, 8, 10, 11, 23, 29, 30, 191, 224, 257, 266, 269, 285, 287, 288, 291, 292, 321ff

S

Sabyrsai, Uzbekistan 401–403, 405, 408, 429, 432, 434, 435
 Sadyrnyn, Kazakhstan 192, 193, 224–226, 228
 Saghand ore field, Iran 177
 Saikhan-Uul, Mongolia 303
 Saima Complex, China 35, 46–50, 54–58, 156
 Saima Massif, China 49, 54, 55, 58
 Sainshand, Mongolia 285, 286, 304, 308–311
 Sainshand Basin, Mongolia 285, 287, 308, 310
 Salihli Basin, Turkey 395
 Sallai Patti, Pakistan 320
 Salt Range, Pakistan 313, 320
 Sambalpur granite massif, India 157, 172
 Sanarskoye, Russia 321, 323, 324
 Sanbaqi, China (see *Benti*)
 Sanerer ore field/district, China (see *Lujing*)
 Sanerer pluton China 109
 Sanfang ore field, China 88, 114, 115
 Sanin, Japan 181, 188
 Sanjiang Basin, China 46
 Saquisan Mine (373), China 146
 Sartubek, Kazakhstan 212, 213

Sarykamys, Kyrgyzstan 282
 Sarytas, Kazakhstan 257, 258
 Sasyktash, Kyrgyzstan 282
 Sasyrlyk volcanic basin, Kazakhstan 257, 258
 Sateek, India 164, 170
 Schwartzwalder, USA 13, 14
 Sebinkarahisar, Turkey 395
 Semizbay, Kazakhstan 191–193, 195, 199, 220–222, 224
 Semizbayskoye, Kazakhstan 324
 Sensharskoye, Kazakhstan 192, 193, 266, 324
 Sentyabrskoye, Russia 386
 Seripally, India 157, 170
 Sernoje, Turkmenistan (see *Cernoje*)
 Sevaruyo, Bolivia 11
 Severnoye, Russia 206, 321, 322, 363, 373, 376, 384, 390
 Shaanxi Province, China 34, 71, 79
 Shabazi (Shabon), China 95, 109, 133–135, 139
 Shabon, China (see *Shabazi*)
 Shakaptar (Shakoptar), Kyrgyzstan 269, 271, 278, 401
 Shakhtny, Kazakhstan 212, 213
 Shakoptar, Kyrgyzstan (see *Shakaptar*)
 Shanawah, Pakistan 318, 320
 Shangangning Basin, China 35
 Shantobe Massif, Kazakhstan 206
 Shanxi Province, China 71
 Shapo (602), China 150, 153
 Shark, Uzbekistan 402, 429, 434
 Shatskoye-1, Kazakhstan 195, 216, 217
 Shatskoye-2, Kazakhstan 216, 217
 Shatsky ore field, Kazakhstan 192, 193, 195, 216
 Shazhou (615), China 123, 125, 126
 Shazhou Yu, China 123, 125, 126
 Shaziling pluton, China 114
 Shengyuan (Shunyan, Yingtan), China 119, 120, 122, 126–129
 Shengyuan (Shunyan, Yingtan) volcanic-tectonic basin, China 127, 129
 Shenyang, China 47, 50, 51, 54
 Shevchenko (now Aktau), Kazakhstan 191–194, 224, 226, 228, 261, 264–266, 270, 322, 390, 397, 402, 408, 411, 424, 428, 429
 Shevya, Russia 363
 Shigaizi, China 59
 Shihongtan, China 31, 34, 36, 40–45
 Shijiao (339), China 99, 100, 102, 103
 Shimane Prefecture, Japan 181, 188
 Shinebulag, Mongolia 287
 Shinkolobwe, Congo, Democratic Republic 14
 Shirondukuyevskoye, Russia 333, 336
 Shituling (337), China 99, 100
 Shiwandashan Basin, China (see *Jingan*)
 Shiyuanlong, China 130, 131
 Shokay zone, Kazakhstan 199, 220
 Shokpak, Kazakhstan 199, 200, 203, 204
 Sholak Espe, Kazakhstan 192, 193, 228, 232, 241
 Shorly, Kazakhstan 192, 193, 254, 256–258
 Shuiyingsi (108), China 150, 153
 Shunyan, China (see *Shengyuan*)
 Sibbeichong, China 147
 Siberian Plate, China 46
 Sichuan Province, China 35
 Sierra de Peña Blanca, Mexico (see *Peña Blanca*)
 Sigirlinskoye, Russia 335
 Sind Province, Pakistan 320
 Sinegorskoye, Russia 386
 Singhbhum batholith, India 158
 Singhbhum region, India 157–160
 Singhbhum Thrust Belt, India 157, 159–162
 Sinh Quyen, Vietnam 449
 Sino-Korean Paraplatform, China 46
 Sinokorean Plate, China 46

- Siqian pluton, China 100
 Sirotininsk, Russia 335, 363, 372
 Skalnoye, Russia 386
 SL deposit, China 115
 Slantsevoye, Russia 362
 Slavyanskoye, Kazakhstan 192, 193, 195, 216
 Smolenskoye, Russia 324, 327, 330
 Snezhnoye zone, Russia 373, 379
 Sogut-Issyk-Kul Basin, Kyrgyzstan 270, 283
 Sogut Basin, Kyrgyzstan 269, 270, 282, 283
 Sokhsolookhsk zone, Russia 384
 Solonechnoye, Russia 324, 328, 330, 331, 333
 Songliao Basin, China 46
 Songnen Massif/block, China 46
 Sonla Province, Vietnam 449
 South China U province, China 29, 35, 86, 88, 89, 91, 96, 98, 115, 147
 South Gobian fold belt, Mongolia 308
 South Korea 29–30, 391
 South Lancang River fold belt, China 155
 South Manybayskoye, Kazakhstan 219
 South Mongolian fold belt, Mongolia 287, 308
 South Qinling fold belt, China 75
 South Texas Coastal Plains, USA 7
 Southeast Zhuguang Massif, China 105, 106
 Southern Kalyma River region, Russia 30
 Southern Menderes Massif, Turkey 395
 Southern Xuefeng Shan area, China 138, 139
 Southern Zyluzya Depression, Russia 363
 Southwest Guangxi area, China 146
 Southwest Guizhou region, China 146
 Southwest Qinling metallogenetic zone, China 30, 75, 76, 79, 84, 85
 Spirinskoye, Russia 327, 331, 332
 Staryi Olov, Russia 363
 Stavropol, Russia 321, 322
 Stepnogorsk, Kazakhstan 191, 193, 194, 219, 220, 270, 322
 Stepnoye, Russia 228, 241, 335, 363, 372
 Stevens County, USA 18
 Streltsovsk (Tulukuyevsk) Caldera, Russia 11, 291, 292, 334–336, 338, 339, 341–343, 346, 352, 353, 357, 358, 372
 Streltsovsk, Russia 10, 11, 29, 30, 257, 287, 288, 291, 292, 321, 322, 332–345, 347–358, 362, 363, 372, 386
 Streltsovsk district, Russia 30, 257, 287, 288, 321, 322, 332, 333, 337–342, 344, 345, 348–358, 363, 386
 Streltsovskoye, Russia 11, 332, 336, 339, 341–354, 356
 Stuart Shelf, Australia 16
 Subeng (861), China 34, 65, 66, 68
 Sugraly, Uzbekistan 401–403, 405, 408–411, 413–424
 Suichang area, China 119, 122
 Suimin gol Basin, Mongolia 287
 Sulaiman anticline, Pakistan 315
 Sulaiman Range, Pakistan 30, 313–315
 Sularinskoye, Russia 386
 Suluchekinskoye, Kazakhstan 192, 193, 261, 264–266
 Sumsar, Kyrgyzstan 278, 283
 Surda, India 157, 161, 164
 Surda-Rakha, India 157, 164
 Surghar Range, NW Pakistan 318
 Sverdlovsk (now Yekaterinburg), Russia 321, 322
 Sverdlovsk Province, Russia 323
 Svetloye, Russia 386
 Syr Darya Basin, Uzbekistan 29, 229, 230
 Syria 30, 451
- T**
 Taboshar, Tajikistan 271, 278, 393, 401
 Taima batholith, China 148
 Tajikistan 29–30, 269–271, 393, 401, 437
 Takashimizu, Japan 187
 Talmesi, Iran 177
 Tamdytau Range, Uzbekistan 413, 416
 Tamil Nadu State, India 158
 Tamtsag Basin, Mongolia 30, 285–287, 308
 Tanah Merah, Indonesia 176
 Tanai, Mongolia 303
 Tanwang, China 106
 Taohuashan, China 84
 Taoshan, China 89–91, 98, 105, 115
 Taoshan Massif, China 89–91, 98, 105, 115
 Tarakan, Russia 389
 Tarim Basin, China 34, 35, 43
 Tarumizu, Japan 181, 188
 Tary-Ekan, Uzbekistan 438
 Tasharman, Turkey 395
 Tas-Kastabyt, Russia 386, 388
 Tasmurun, Kazakhstan 192, 193, 224–226, 228
 Tastykolskoye, Kazakhstan 192, 193, 195, 199, 217, 218
 Tastykolskoye East, Kazakhstan 218
 Tatsumitoge, Japan 187
 Taunsa, Pakistan 313, 318
 Taurkyr (Kaplankyr-Tauryuk) Dome, Turkmenistan 397, 398
 Tavansuveet Basin, Mongolia 285, 286
 Taybagar, Kazakhstan 192, 193, 224–226, 228
 Temvezli Basin, Turkey 396
 Tengchong, China 150, 153, 154
 Tengchong Basin, China 150, 153, 154
 Tengchong Mine, China 150, 153, 154
 Tengchong-Lianghe Basin, China 150, 153
 Tenger, Mongolia 302
 Tenggeer Depression, China 65, 68, 69
 Terekuduk, Uzbekistan 402, 425–428
 Tetrakhskoye, Russia 359–361
 Thajistan (511), China 36, 38, 40, 44
 Tianhuashan, China 119
 Tien An, Vietnam 449
 Tien Shan Mountains 34, 228, 229, 231, 233, 248, 250, 269, 278, 279, 282, 393, 403, 437
 Tigrovaya Pad, Russia 386
 Tim Mersoï Basin, Niger 8
 Tobolskoye, Kazakhstan 192, 193, 266, 324
 Toge, Japan 30, 181, 187, 188
 Tokhumbet, Uzbekistan 425, 427, 428
 Toki Basin, Japan 183
 Tokumbet, Uzbekistan 401, 402, 425, 426
 Tomak, Kazakhstan 192, 193, 224–226
 Tono Mine, Japan 30, 181, 183, 184, 187
 Tono ore field, Japan 181, 183
 Torfjanoye, Kazakhstan 191–193, 266
 Tottori Prefecture, Japan 187
 Toyoda, Japan 181, 188
 Transbaykal Massif, Russia 334
 Transbaykal region, Russia 30, 321, 322, 332, 335, 340, 362, 372
 Transbaykalia, Russia 29, 285, 287, 288, 321, 332, 334, 335, 362–364, 366–370
 Transural region, Russia 30, 266, 321–323, 325, 327–329
 Tsagaan-Chuluut, Mongolia 302
 Tsagaan-nuur, Mongolia 302
 Tsav, Mongolia 288, 303
 Tsever, Mongolia 302
 Tshu Valley, Kyrgyzstan (see *Chu Valley*)
 Tsukiyoshi, Japan 181, 183–187
 Tuantian (506), China 150, 153
 Tule, Vietnam 449
 Tüllüce, Turkey 395
 Tulukuyevsk Caldera, Russia (see *Streltsovsk*)
 Tulukuyevskoye, Russia 332, 336, 339, 354–356
 Tumen-Haan, Mongolia 303

Tummalapalle, India 170, 171
 Tungusky ore field/area, Russia 335, 372
 Tunling (Tunlin), China 89, 148
 Turakavak (Min-Kush), Kyrgyzstan 269, 270, 282
 Turamdih ore field, India 164
 Turan Platform, Uzbekistan 29, 228, 229, 403
 Turgai Basin, Russia 326
 Turgai-Priyrtish region, Kazakhstan 30, 266
 Turgen area/district, Mongolia 302
 Turkey 29–30, 395–396, 451
 Turkmenistan 29–30, 397ff
 Turpan-Hami Basin, China 29, 31, 36, 40, 41, 44, 45
 Tushinskoye, Kazakhstan 192, 193, 195, 205–207
 Tutly, Uzbekistan 402, 429, 432
 Tuvinsky Basin, Russia 330
 Tuyuk-Suu, Kyrgyzstan (see *Dzhilskoye*)
 Tynai, India 164, 170
 Tyuya-Muyun, Kyrgyzstan 30, 269, 270, 278–280, 282, 321, 393, 401
 Tyuya-Muyun district, Kyrgyzstan 30, 269, 278

U

Uchkuduk (Bukantau), Uzbekistan 270, 401–403, 405, 408, 410–413, 426, 432, 434, 436
 Uchkuduk (Bukantau) Range, Uzbekistan 410, 436
 Ugtam, Mongolia 286–288, 302
 Ugtam district, Mongolia 286
 Uigar Sai, Uzbekistan (see *Atbash*)
 Ukrainian Shield, Ukraine 12, 13, 202
 Ulaan, Mongolia 285, 287, 288, 302–304, 306, 308, 310
 Ulaan-nuur-2, Mongolia 285
 Uliya Basin, Russia 387–389
 Uliya volcanic depression, Russia 386–389
 Ulken Akzhal, Kazakhstan 192, 193, 266
 Ulus, Uzbekistan 432, 434
 Ulus-Dzhamoky Depression, Uzbekistan 434
 Ulutau Massif, Kazakhstan 229
 Ulziit-Saikhan-uul area, Mongolia 303
 Ulziit-Saikhan-uul volcanic structure, Mongolia 303
 Ulziit Basin, Mongolia 285, 286, 303
 Undurshil (Ongiingol) Basin, Mongolia 285, 286
 Urak Complex, Russia 387, 389
 Ural-Mongolian fold belt 255, 334
 Ural-Mongolian orogenic system 194, 255, 334, 393, 438
 Uravan Mineral Belt, USA 8
 Urlinobin, Mongolia 288
 Urulyunguevsky Depression, Russia 335, 372
 Usmanskoye, Russia 327, 331, 332
 Ussuri River region, Russia 386
 Ust-Uyuk, Russia 324, 328, 330, 333
 Uta Pradesh State, India 158
 Utan Depression, Russia 363
 Utozaka, Japan 183
 Uvanas, Kazakhstan 191–194, 228, 231, 232, 234, 241–246
 Uvanas-Kanzhugan district, Kazakhstan 228, 241, 242
 Uzbekistan ix, 29–30, 248, 250, 257, 269–271, 321, 393, 401ff

V

Vaidara, Tajikistan 393
 Varadzhan, Uzbekistan 402, 425–428
 Vendée, France 9
 Vershinnoye, Russia 359, 360
 Vesennee, Russia 333, 336
 Vesennyaya (zone), Russia 373, 376, 384
 Victorovskoye, Kazakhstan 192, 193, 195, 205
 Vietnam 29–30, 148, 449–450
 Vinogradovskoye, Russia 323
 Vinto-Khalyya, Russia 388
 Vitim ore field/district, Russia (see *Khiagda*)

Vitimsky ore field/district, Russia (see *Khiagda*)
 Vitlandskoye, Russia 362
 Vladivostok, Russia 386
 Voskhod, Kazakhstan 224
 Voskhod, Uzbekistan 402, 436
 Vostochno-Shirondukuyevsk, Russia 336
 Vostochnoye, Russia 207, 335, 372
 Vostochny, Kazakhstan 212, 213, 228, 251, 393
 Vostok, Kazakhstan 191–195, 199, 205–208

W

Wadi al Rakheime area, Syria 451
 Wahi Pandi area, Pakistan 320
 Wahkyn, India 164
 Wangjiachong (Dapujie, Dabao), China 89, 147
 Wenduerming Uplift, China 69
 West Bengal State, India 158
 West Gaur, Russia 363
 West Khasi Hill, India 157, 164, 166–169
 West Lukdun, Russia 363
 West Siberian Basin, Russia 29
 West Siberian region, Russia 30, 322, 326, 327, 330–332
 West Xinqiao (332), China 99, 100
 West Yunnan U province, China 29, 30, 32–35, 148–150, 153
 Western Karakum region, Turkmenistan 30
 Western Moravia, Czech Republic 15
 West-Nuratau district, Uzbekistan (see *Zafarabad*)
 West-Siberian Platform, Russia 323, 324, 326
 Williston Basin, USA 24
 Witwatersrand Basin, South Africa 16, 17
 Wodgina, Australia 19
 Wujiashai (384), China 150, 153
 Wukulqi (513), China 38
 Wukulqi upwarp, China 38
 Wuyi magmatic/volcanic-granite belt, China (see *Wuyishan*)
 Wuyishan (Wuyi) magmatic/volcanic-granite belt, China 11, 34, 86, 88, 89, 115–117, 129–132
 Wuyishan (Wuyi) ring structure, China 130, 131

X

Xiangca (Xiangcao), China 95, 114, 133, 135, 136
 Xiangcao, China (see *Xiangca*)
 Xianggui Basin, China 35, 139, 141, 145
 Xianggui fold system, China 88
 Xiangshan Caldera, China 118, 122–124, 126
 Xiangshan (Fuzhou) ore field (660, 670, 681), China 122, 124
 Xianrenzhang (338), China 99, 100
 Xiaojiang (Xudou), China 133
 Xiaoqiuvuran (Dazhou, Xiaoqiuyuan) ore field, China 119, 120, 122, 129
 Xiaoqiuvuran (Dazhou, Xiaoqiuyuan) volcanic-tectonic basin, China 122, 129
 Xiaoqiuyuan ore field, China (see *Xiaoqiuyuan*)
 Xiazhuang (336), China 96, 99–102, 104, 105
 Xiazhuang ore field, China 96, 99–102, 104, 105
 Xiazhuang pluton, China 96, 99–102, 104, 105
 Xiguitu fold belt, China 46
 Xincun, China 115, 136
 Xinfengjiang Massif, China 95
 Xinjiang Basin, China 31, 34–36, 40, 43, 44, 261, 264
 Xinjiang Uygur A.R., China 35, 36, 43
 Xinjiao (Xinqiao) (332), China 99, 100, 102
 Xinqiao (332), China (see *Xinjiao*)
 Xinwu Basin, China 147, 148
 Xiushui ore field, China 132, 133, 136, 137
 Xiwang (Hope) (330), China 31, 99, 100, 105
 Xiwang ore field, China 31, 99, 100, 105
 Xiwuzhumuxin fold belt, China 46
 Xudou, China (see *Xiaojiang*)
 Xuefeng Motianling batholith, China 91

Xuefeng Shan area, China 136
 Xuefeng-Jiuling region, China 35, 135
 Xuefeng-Jiuling U belt/zone, China 86, 88, 114, 132, 136
 Xuefeng-Jiuling U subdomain, China 35, 86–88, 114, 132, 135, 136

Y

Yakhob, Tajikistan 393
 Yakshin volcanic structure, Kazakhstan 208
 Yakutia, Russia 29, 386
 Yallaguchi Prefecture, Japan 181
 Yamagata Prefecture, Japan 181, 188
 Yamaguchi Prefecture, Japan 181, 188
 Yangtze granite belt, China 34, 75, 79, 84–86, 120, 140, 146, 149
 Yangtze Massif (Platform), China 29, 75, 85, 86, 120, 146
 Yanshan Mountains, China 46
 Yant, Mongolia 308, 309
 Yanzitou (50), China 150, 153
 Yaxi, China (see *Laowulong*)
 Yeelirrie, Australia 18
 Yekaterinburg (former Sverdlovsk), Russia 321, 322
 Yellapur-Peddagattu, India 170
 Yenisey region, Russia 29, 30, 321, 322, 328, 330, 333, 334
 Yenisey River-Altay-Sayan area, Russia 328
 Yilgarn Block, Australia 18
 Yili Basin, China 31, 34, 36–44
 Yingshan Basin, China 71
 Yingtan, China (see *Shengyuan*)
 Yining, China 34, 36, 41
 Yinshan-Liaohu U province, China 30, 35, 46
 Yon Phu, Vietnam 449
 Yongchen Massif, China 84
 Yongxing Basin, China 140, 141, 143, 144
 Yotsugi, Japan 187
 Youngyang Basin, South Korea 391
 Yozgat-Sorgun, Turkey 396
 Yubileinoe, Russia 11, 333, 336
 Yuechengling batholith, China 95, 114, 137, 139
 Yuechengling Massif, China 114
 Yugalskoye, Russia 335, 372
 Yugo Zapadnoye, Russia 336
 Yuhuashan, China 119
 Yuigar Sai, Uzbekistan (see *Atbash*)
 Yujiang-Qianshan, China 119
 Yumyeongsan, South Korea 391
 Yunji (628), China 122, 123, 125, 126
 Yunnan Province, China 33, 148, 154
 Yuya, Japan 181, 188
 Yuzhnaya zone, Russia 374, 375, 382–384
 Yuzhno Daursky ore field, Russia 335

Z

Zafarabad, Uzbekistan 270, 401–403, 425–431
 Zafarabad (West-Nuratau, Nurantinsky) district, Uzbekistan 270, 402, 403, 425, 427–431
 Zaisang Basin, Kazakhstan 43
 Zaozernoie (Koksengirsky), Kazakhstan 191–193, 195, 199, 217, 218
 Zapadny, Kazakhstan 212, 213
 Zarafshan, Uzbekistan (see *Auminza-Beltau*)
 Zarechnoye, Kazakhstan 193, 248, 253
 Zefa E'fe, Israel (see *Arad*)
 Zergan, Russia 388
 Zhaixia (335), China 99, 100
 Zhalanshiksky region, Kazakhstan 30, 191, 266
 Zhalpak, Kazakhstan 191–193, 228, 231, 232, 234–236, 239, 241, 242
 Zhaman-Kotass Massif, Kazakhstan 221
 Zhaohuohao area, China 72, 74
 Zharaahai, Mongolia 302
 Zhargalant, Mongolia 302
 Zheglvskoye, Russia 362
 Zhejiang Province, China 31, 86, 115, 119, 120, 122, 129
 Zheltorechenskoye, Ukraine 13
 Zheltye Vody, Ukraine 13, 322
 Zherlovoe, Russia 336
 Zhifangou Massif, China 78
 Zhilanshiksky region, Kazakhstan 192, 193, 270
 Zhongchun (238), China 106, 108
 Zhuguang (Zhuguanshan) Massif, China 96, 98, 105, 107, 108, 114, 139
 Zhuguang fold belt, China 88, 91, 96, 98, 105–110, 114, 139
 Zhuguanshan Massif, China (see *Zhuguang*)
 Zhuravlinoye, Russia 335, 362, 372
 Zhushanxia (333), China 96, 98–101, 103
 Zhutongjian, China 96, 98, 99
 Ziatdin Range, Uzbekistan 402
 Zijinshan, China 117, 130, 132
 Zinda Pir anticline, Pakistan 315
 Zirabulak Range, Uzbekistan 432
 Zirabulak-Ziatdin district, Uzbekistan (see *Nurabad*)
 Ziyuan ore field, China 114, 136, 139
 Zongyang Massif, China 79, 84
 Zongyang Massif, China 79, 84
 Zoujiashan (612), China 122, 123, 125
 Zurkhin, Mongolia 304
 Zuunbayan Basin, Mongolia 286, 287, 289, 303, 304, 306, 308–310
 Zvezdnaya zone, Russia 376, 386
 Zvezdnoye, Kazakhstan 192, 193, 195, 205–207
 Zyulzinskoye (Ozernoie), Russia 335, 362, 363
 Zylzya Depression, Russia 362, 365
 Zylzya, Russia 362, 363, 365
 Zyunigawa, Japan 187

U Minerals Index

Th-U-bearing minerals

Ferrithorite 210
Monazite 16, 76, 109, 157, 161, 176, 181, 188, 287, 389
Nenadkevite ix, 13, 55
Thorianite 120, 125
Thorite 12, 57, 58, 120, 125, 287, 387
Thucholite 6, 17
Uranothorianite 12, 16, 19, 177, 387, 389
Uranothorite 12, 16, 19, 55, 57, 116
Wisaksonite 125
Zirtolite 210

U oxides, oxide hydrates, molybdates, phosphates, silicates, U-Ti phases, etc.

Black products 224, 303, 306, 309, 310, 405, 418, 422, 423
Brannerite/U-Ti phases 4, 6, 12, 13, 16, 17, 29, 36, 37, 116, 117, 120, 125, 126, 129, 161, 172, 175, 176, 200, 204, 205, 212, 216, 217, 219, 260, 290, 292, 293, 336, 338, 339, 342, 343, 346, 347, 354, 373, 375, 376, 380–384, 386, 387, 393, 445
Broeggerite (see *Uraninite*)
Cleveite (see *Uraninite*)
Coffinite 4, 6, 8, 11–17, 21, 34, 36, 37, 42, 48, 52, 66, 80, 92, 99, 102, 116, 117, 120, 125, 126, 129, 132–136, 148, 151, 167, 170–172, 179, 181–183, 185, 187, 188, 199, 200, 202, 203, 210, 212, 216, 217, 219, 224, 234, 236, 243, 245, 251, 253–255, 257, 258, 260, 265, 266, 290, 292, 293, 299–301, 304, 309, 310, 316–318, 326, 328, 330, 336, 338–340, 342, 346, 347, 352, 354, 356, 358, 360, 362, 366, 371, 372, 375, 382, 386, 397, 405, 408, 411, 426, 434, 437, 439, 440
Metaschoepite 160
Nasturan (see *Pitchblende*)
Nenadkevite ix, 13, 55
Ningyoite 182, 183, 187, 358, 371, 437
Nivenite 273–277
Pechblende (see *Pitchblende*)
Pitchblende (nasturan, pechblende, uranpecherz) viii, 4, 6, 8, 9, 11, 13–16, 21, 25, 34–37, 42, 48–50, 52, 54, 55, 57–60, 62, 65, 66, 74–76, 80–85, 92, 94, 95, 97, 99, 102, 104, 107, 108, 111–117, 120, 124–126, 129, 132–136, 139, 140, 143–148, 151, 154, 160, 167, 169, 171, 172, 179, 182, 183, 185, 187, 189, 199–204, 210, 212, 216, 217, 219, 221, 224, 234, 236, 245, 251, 253–255, 257–261, 265–267, 273–277, 281, 290, 293, 299–301, 303, 304, 306, 308–310, 316–318, 320, 326, 328, 330, 336, 338–342, 346, 347, 352–354, 356, 362, 365, 366, 371, 386–389, 391, 393, 397, 405, 408–411, 417–419, 422–424, 426, 434–440, 444–446, 449
lattice constants 445
oxidation coefficients 136
sooty/earthy 11, 85, 143, 146, 224, 234, 258, 265, 266, 274, 303, 309, 310, 326, 328, 338, 362, 365, 366, 386, 387, 393, 397, 405, 408, 417, 426, 434, 436
unit cell dimensions 136
Schoepite 160, 397
Ulrichite (see *Uraninite*)
Uraninite (ulrichite, broeggerite, cleveite) viii, 4, 6, 12–14, 16, 19, 25, 48, 49, 52, 54, 75, 76, 78–80, 92, 96, 101, 104, 105, 109, 113, 130, 160–162, 164, 172, 175–178, 181, 199, 200, 205, 218, 221, 260, 266, 287, 340–342, 352, 354, 359, 373, 375, 376, 380, 382, 384, 387, 389, 391, 449

lattice constants 445
oxidation coefficients 136
unit cell dimensions 136
Uranpecherz (see *Pitchblende*)

Uranium-bearing/refractory minerals (niobates, phosphates, tantalates titanates etc.)

Allanite 101, 109, 161
Arshinovite 199, 217–219
Chevkinite 55
Davidite 161, 170, 177
Fergusonite 181, 387, 388
Lovchorrite 55
Malacon 13
Monazite 16, 76, 109, 157, 161, 176, 181, 188, 287, 389
Pyrochlore 49, 54, 55, 57–59, 387
Rinkite 49, 54, 55, 57–59
Samarskite 181
Samiresite 387
Thorianite 120, 125
Thorite 12, 57, 58, 120, 125, 287, 387
Zirtolite 210

Uranyl minerals

Autunite 52, 74, 94, 99, 112, 133, 160, 172, 175, 181, 185, 188, 189, 208, 258, 303, 306, 308, 309, 393, 436, 437, 449
Bassetite 133
Bergenite 306, 308
Beta-uranophane (old term lambertite) 52
Billietite 52
Carnotite 22, 317, 320, 393, 436, 437, 447, 449
Clarkeite 161, 293
Cuprosklodowskite 188
Curite 290, 300, 320
Irginite 338
Kasolite 52, 188, 290, 301
Lambertite (see *Beta-uranophane*)
Masuyite 293
Metaschoepite 160
Phurcalite 320
Saleeite 320
Schoepite 160, 397
Schroëckingerite 306, 309
Tyuyamunite 94, 133, 251, 279–282, 317, 397, 436, 437
Uranocircite 94, 133, 185
Uranophane (old term uranotile) 52, 94, 99, 112, 133, 143, 160, 172, 258, 266, 290, 293, 299–301, 309, 318, 338, 386, 388, 393, 397, 405, 408, 410, 411, 417–419, 422–424, 449
Uranopilite 143
Uranospathite 133
Uranospinite 266
Uranotile (see *Uranophane*)
Zeumerite 133, 143, 181, 188, 393, 436
Zippeite 62

